Joint AKTU-AICTE Short-Term Training Program

Faculty Development Programme (FDP)

on

Advances in Microwave Engineering (AME-19)

(Sponsored by AKTU-AICTE)

08th – 12thJune 2019

Organised by:

Dr. A. P. J. Abdul Kalam Technical University, Lucknow

COMPENDIUM OF LECTURES DELIVERED BY THE RESOURCE PERSONS

Edited by

Rajiv Kumar Singh *is Assistant Professor, Department of Electronics Engineering, Institute of Engineering & Technology, Lucknow, and Associate Dean (Postgraduate Studies & Research), Dr. APJ Abdul Kalam Technical University, Uttar Pradesh. He is the Convener of FDP-AME-19. (email: rajivinbhu@gmail.com).*

Raktim Guha *is with CSIR-Central Elctronics Engineering Research Institute (CEERI), Pilani, Rajasthan. He took part with Dr. N. Purushothaman of CEERI in a live demonstration of electromagnetic simulation using CST Microwave Studio Suite, besides giving a deliberation on recent advances in metamaterial assistance in microwave tubes, at FDP-AME-19. (e-mail: raktim.guha01@gmail.com).*

B. N. Basu *is superannuated as Professor & Head of Electronics Engineering Department and Coordinator of Centre of Research in Microwave Tubes (CRMT), IIT-BHU), Varanasi and is now Adjunct Professor, Sir JC Bose School of Engineering, Supreme Knowledge Foundation Group of Institutions, Mankundu, West Bengal. He is one of the resource persons of the present Faculty Development Programme. (email: bnbasu.india@gmail.com).*

CONTENTS

CONTENTS

CONTENTS

MESSAGE

Professor Pradip Kumar Saha
Professor (Superannuated)
Institute of Radiophysics and Electronics
Calcutta University, Kolkata

It's with deep regret that I have to miss the FDP due to an unforeseen situation. I must, however, express my gratitude to the Organising Committee, Professor B. N. Basu and Dr. R. K. Singh specially, for the kind invitation.

I had thought of an introductory lecture on Microwaves for familiarization with microwave energy through examples of applications. This probably would have been elementary for the attending faculty members. However, I have observed sadly that even the teachers teaching microwave engineering do not always have very clear concepts about various aspects of microwaves. And for understanding microwave engineering, the most essential pre-requisite is a thorough knowledge of circuit theory, engineering electromagnetics and computational electromagnetics. With proper background, research in the field of microwaves can be managed more comfortably. The present trend, in fact for quite a few years, is to launch the research career with simulation tools. The more powerful tools you have at your disposal, more the number of papers you would be able to churn out, regrettably, often without understanding the problem or digging deep into it. To an old-fashioned old-timer like me, the pleasure that is obtained from solving a problem analytically or semi-analytically using elegant mathematical techniques is immense. Powerful simulation software is always welcome as additional supporting tools, particularly when a problem is not easily amenable to theoretical formulation. But understanding the basics is paramount to solving a problem; otherwise, the paper produced from the results may be just a paper to add to the list of publications but not treated as a 'contribution'.

I am sure, this FDP will go a long way towards encouraging the faculty to build up a solid knowledge base and conduct fruitful SDP in microwave engineering.

I convey my regards and best wishes to all the resource scientists who are contributing to this grand ambitious programme. I wish all the participants to derive maximum benefit from the resources made available to them.

Professor Pradip Kumar Saha
Professor (Superannuated)
Institute of Radiophysics and Electronics
Calcutta University, Kolkata

PROLOGUE

As Indians we all feel proud that it was Jagadis Chunder Bose in India to establish the first ever radio link in 1895 by publicly demonstrating the transmission of electromagnetic waves (described by him as "Adrisya Alok", or "Invisible Light" at around 60 GHz operating frequency) to ring a bell remotely and explode some gunpowder, before Marconi carried out his wireless signalling experiment on Salisbury Plain in England in 1897. (See D. T. Emerson, "The work of Jagadis Chunder Bose: 100 years of mm-wave research," *IEEE Trans. Microwave Th. Tech.* December 1997, 45, No. 12 (2267-2273)). On this landmark is based the area of microwave engineering and its advances¾the theme of the present Faculty Development Programme. We are happy that we could present the experts from the different corners of the country before the participants of the programme to listen to and interact with, in this area. The Programme was inaugurated by Professor Vinay Kumar Pathak, Vice-Chancellor, Dr. APJ Abdul Kalam Technical University, Lucknow in the Lecture Hall of Centre of Advanced Study of the University (CAS). Professor Pathak welcomed the participants and resource persons of the programme. He congratulated Dr. Rajiv Kumar Singh, the convener of the programme for inviting the experts from the national laboratories and premier academic institutions of the country. Professor Manish Gaur, Director, CAS of the University also welcomed and greeted the participants, resource persons. Dr. S. U. M. Reddy, the Director of DRDO-Microwave Tube Research and Development, Bengaluru, was the Chief Guest of the inauguration programme, who congratulated the University for organising the faculty development programme in such an important area of national relevance. The Guests of Honour of the inauguration programme, who also have presented their respective lectures at the various stages of the faculty development programme, were: Professor B. N. Basu, Professor Subal Kar, Professor L. M. Joshi, Professor A. K. Sinha, and Dr. S. K Datta. Professor Basu read out an encouraging message befitting to the programme from the renowned scientist in the area of microwave engineering: Professor P. K. Saha who could not attend the programme due to unforeseen reasons.

ABSTRACTS OF LECTURES AND LIVE DEMONSTRATION OF SIMULATION

The eminent microwave engineer ***Professor P. K. Saha***, who is internationally acclaimed for his research contributions in the areas of corrugated waveguides and corrugated horn antenna and recipient of the Eminent Teacher Award of the University of Calcutta and Lifetime Achievement Award of the AP-MTT Chapter of IEEE Calcutta Section, and who missed the FDP under unforeseen circumstances, in his 'Message' (presented in the present compendium of lectures) emphatically believed that this FDP would go a long way towards encouraging the faculty participating in the programme to build up a solid knowledge base in microwave engineering and derive maximum benefit from the resources made available to them. However, Professor Saha emphasized that, above all, the participants of the programme should develop the prerequisite understanding of circuit theory, engineering electromagnetics and computational electromagnetics. He cautioned the participants against depending on only the simulation tools for their research without digging deep into the problem analytically or semi-analytically.

The resource persons whose lecture notes have been included in this compendium are: Professor B. N. Basu, Professor P. K. Saha, Professor Subal Kar, Professor L. M. Joshi, Professor A. K. Sinha, Dr. S. U. M. Reddy, Dr. S. K Datta, Dr. Vishal Kesari, Dr. Vishant Gahlaut, Dr. N. Purushothaman, Mr. Subhradeep Chakraborty, Mr. Raktim Guha and Dr. Rajiv Kumar Singh (convener of the present FDP).Some of the resource persons delivered more than one lecture. Out of the resource persons listed, Professor Saha could not deliver his lecture under unforeseen circumstances. However, for the benefit of the participants of the programme, we have presented his lecture note here. Very importantly, Dr. Dr. N. Purushothaman and Mr. Raktim Guha with the accompaniment of Dr. Vishal Kesari, in a dedicated session, presented the life demonstration of CST Microwave Studio. Further, the resumes of the resource persons have also been appended in this compendium.

Professor B. N. Basu delivered two lectures. At the outset of his *first lecture* that is on the national scenario of microwave tubes, Professor Basu has motivated the participants of the programme by pointing out the pioneering contribution of JC Bose as mentioned in the beginning of this prologue. He has narrated the applications of microwaves and discussed why vacuum electron devices in the form of microwave tubes are so important and continue to remain so despite the competitive incursions from solid state devices. He has classified microwave tubes and the wide range of their applications and narrated the global trends in their development. He has given a picture of the entire range of microwave tubes in which the laboratories, universities and industries of the country are involved in R&D/ production encompassing the civil, defence, space, science, medical, industry, and environment sectors. He has emphasized on the renewal of the position paper on the national requirement of microwave tubes. He has discussed how the different organisations of the country can work together in the development of microwave tubes in consortia and mentioned the role of Vacuum Electronic Devices and Applications Society already established in the country in this regard. In his *second lecture*, Professor Basu has reiterated the need of developing the base of electromagnetic theory as has also been mentioned by Professor PK Saha in his 'Message' to the participants of the programme. At the outset of this second lecture he has suggested that the teachers may explain to their students the beauty of the

symmetry of the expressions in curvilinear coordinates of the gradient, curl and Laplacian of a scalar/vector and how these expressions could be very easily got by heart by an easy permutation of the first term of any of these expressions and subsequently easily read for the desired system of coordinates (rectangular, spherical and spherical-polar). He has explained the concept of the relaxation time of a medium in terms of its conductivity and permittivity. He has also explained its role in reading the general electromagnetic boundary conditions at a point on the interface between two media (expressed in terms of a unit vector at the point directed from one medium to another) for the special cases of the boundary conditions at the dielectric-dielectric and conductor-dielectric interfaces for both the time-independent and time-dependent situations. He has suggested that the teachers could make the topic interesting by showing that the circuit laws are manifestations of electromagnetic field concepts; for instance, he has explained how one can appreciate the circuit law of parallel resistances from the electromagnetic boundary condition that the electric field is continuous at the interface between two media.

From the lecture note of ***Professor P. K. Saha*** the participants of the programme would get an introductory glimpse of the different aspects of microwave propagation and communication as well as microwave antennas. He has described in this note the rectangular and circular horns and discussed the various aspects of reflector antennas (plane-corner reflector, 3D retro-reflector, parabolic and spherical reflectors) and their feeds (Gregorian and Cassegrain). He has also discussed radar before taking up the topics of biological effects of microwaves and active denial system. He has also discussed the mechanism of interaction of microwave with matter before going into microwave heating and its historical development. He has concluded his note of presentation with the salient features of microwave cooking oven thereby arousing the interest in the subject of microwave engineering in common public.

Professor Subal Kar has delivered two lectures. In his *first lecture* Professor Kar has emphasized on the need for paradigm shift in teaching the subject of microwave engineering to make the students truly capable and professionally employable thereby meeting the present-day need of industry and R&D sectors. He has insisted on revisiting the essential elements of electromagnetic theory as required for studying microwave engineering. He has suggested that the basic concepts of dielectric heating should be developed before taking up the application of microwave for heating purposes. He has explained how the teaching of high frequency behaviour of transmission line has to be taken up to develop the relevant concepts such as the return loss for load reflection and the reflection loss for load absorption as relevant from the designer's point of view. He has suggested that the planar transmission line concepts should be developed for understanding the principles of microwave integrated circuit (MIC). The need for being conversant with the Smith chart, which is one of the screen options in network analyser, has been reiterated. He has dealt with the problem of impedance matching in depth. He has also discussed how the concepts of scattering matrix and signal-flow graph have to be used in the study of microwave circuits. His lecture has uncovered the concepts of microwave guided structures, passive circuit components, filters, antennas and wave propagation, measurement, monolithic MIC, hybrid MIC, and EMI and EMC. He has also given the glimpse of the various applications of microwave engineering. Finally, he touched upon the potential of metamaterial in microwave engineering, which has taken up in depth in his second lecture. He has also discussed with the participants of the programme the features of the second edition of his book: Microwave Engineering (see the biography of Professor Kar in this compendium). In his *second lecture* Professor Kar, to whom and to the team led by him at Institute of Radiophysics & Electronics of Calcutta University, SAMEER, Kolkata and BARC, Mumbai goes the credit of developing the

first ever metamaterial crystal in India as displayed on 17th August, 2009 at BARC (see the lecture of Mr. Raktim Guha included in this compendium), has taken up more elaborately the subject of metamaterial—initially developed in the microwave frequency domain—which he had touched upon in his first lecture. The subject of photonic metamaterials has also been introduced by him. While explaining the basics of metamaterial in this second lecture he has shown the difference between left handed material (LHM) and right handed material (RHM). He has elaborated the applications of metamaterial such as the development of the cloaking and stealth technology, super-lens/sub-wavelength imaging (overcoming the conventional diffraction limit), metamaterial assisted accelerator based on reversed Cherenkov radiation, metamaterial based CNT, transparent metamaterial based fast data processing, metamaterial fuelled sparser (surface plasmon amplification by stimulated emission of radiation), and so on, besides the commonplace applications such as the size reduction of antennas, filters and other passive components.

Professor L. M. Joshi has presented in his lecture the R&D scenario of multi-cavity klystrons vis-à-vis their applications in charged particle accelerators based on his profound experience in the area. At the outset he has introduced different kinds of accelerators, namely, cyclotron, pelletron, synchrotron, and linear accelerator (linac). He has brought out the advantages and drawbacks of the linacs for electrons, protons and heavy ions. He has also discussed the applications of linacs in medical, industrial, national security, and scientific research sectors. Professor Joshi has further outlined the principle of particle acceleration and the role of RF sources therein, before introducing the solid state devices(silicon bipolar transistor, silicon MOS-FET, and silicon carbide static induction transistor (SIT))and vacuum electron devices (tetrode, inductive output tube (IOT), magnetron, klystron and gyrotron)as the RF sources(frequency range: 50 MHz–50 GHz, power: 10 kW–2 MW CW or moreup to 150 MW peak)for the linac. He has chosen to focus on one of these devices, namely, the multi-cavity klystron and went into the details of its working principle as well as its design and development. He has discussed a pertinent issue of the design of the klystrons, namely, the enhancement of their peak power, efficiency and reliability. He has also apprised the participants of the programme of the various design software simulation tools, namely, EGUN, TRAK, OPERA, FEMAG, and POISSON for electron optics as relevant to the design of the electron gun and that of the magnetic focussing stricture; MAFIA, CST Microwave Studio, and HFSSfor the design ofthe cavity interaction structures; AUTOMDC for the design of the depressed collector; KL1D, MAGIC 2D/3D, CST PARTICLE STUDIO for beam-wave interaction simulation predicting the device power output and efficiency; and ANSYS, SOLID WORKS for the thermal and structural design. He has displayed and explained the typical results based on the simulation of the klystron. Furthermore, he has presented before the participants of the programme all the relevant tube fabrication and processing cycle leading to the practical development of a klystron. He has also discussed the characterization of the parts of the klystron involving both the cold and hot measurements. His vivid photographic display of the facilities round the laboratories of CSIR-CEERI gave the participants the amazing feeling of the actual visit to these laboratories. Further, Professor Joshi has introduced to the participants the relatively recent version of the klystron, namely, the multi-beam klystron which operates at low beam voltage and compactness due to reduced plasma wavelength, the latter being equal to the beam velocity divided by the plasma frequency, in which the individual low-perveance well-focused beamlets in a PPM stack transmit through a common RF interaction cavity structure rendering an overall enhancement of the beam current and perveance. He has concluded his presentation with the narration of the activities of particle accelerators at the different organisations abroad, for instance, at Stanford and DESY,

Hamburg, as well as in the country, for instance, at BARC, RRCAT, SAMEER and IPR, and the specific R&D contribution of CSIR-CEERI to these activities.

Professor A. K. Sinha has delivered three lectures. In his *first lecture* Dr. Sinha presented the national and global scenarios of microwave tube development before taking up the prospects of microwave tubes in the 21st century. He brought out the various applications of microwave tubes in the designated frequency ranges. He classified microwave tubes and the basis for making such classifications. He took care to present historical timeline of the development of microwave tubes including gyrotrons. He explained the functions of the different parts of a gyrotron. He narrated the role of the magnetron in thermonuclear power generation and the role of India in the international consortium ITER. He presented the range of magnetrons for fusion plasma heating and other technological applications manufactured developed by the various companies and institutes throughout the globe. He motivated the participants of the programme by narrating the success account of the development of the first ever gyrotron in the country the credit of which goes to a consortium of five Indian organisations working together in a multi-institutional DST-sponsored project, in which CSIR-CEERI, Pilani played the role of the nodal centre. He displayed the various parts of the gyrotron fabricated at CEERI as well as the colourful picture of the gyrotron development facilities established at CEERI. In his *second lecture*, Professor Sinha has reported the R&D efforts in gyrotrons in different frequency ranges for different applications such as ADS, ITER, material processing, radioactive material detection, and NMR beyond the development of the first ever gyrotron for fusion plasma heating in the country. In particular, he emphasized on the applications of terahertz gyrotrons and the global status of their development. He also apprised the participants of the results obtained by CEERI on terahertz gyrotrons. He has also reported the R&D effort of CEERI in double-beam gyrotrons and triple-frequency gyrotrons. He concluded this lecture with the present state-of-the-art capability of the country in the development of gyrotrons. In his *third lecture*, Professor Sinha has demonstrated how one can make a scientific approach to solving a problem. He gave the example of the electromagnetic field analysis of a helical slow-wave structure that can be approximated by a physical model of the structure to obtain the dispersion relation of the structure. He showed how to model the actual helix by a sheath helix and how to model the discrete dielectric helix-supports deviating from a simple wedge geometry by a number of adjacent dielectric tubes of an effective permittivity that is found by the material permittivity and geometry of the supports. He has discussed the method of taking into account effect of finite helix thickness in the field analysis. Furthermore, he has also presented the equivalent circuit analysis of the helical slow-wave structure that can yield one and the same dispersion relation of the structure as obtained by the field analysis. The equivalent circuit analysis also yields the characteristic impedance of the structure that finds relevance in the design of the couplers for coupling RF power in and out of the structure. Furthermore, since the sheath-helix model cannot take into the effect of space harmonics generated due to the axial periodicity of the structure he has presented another improved model namely the tape-helix model that is capable of accounting for the space-harmonic effects. Similarly, he has in this lecture another example of the theoretical approach leading to the design of a magnetic injection gun of a gyrotron. He concluded this lecture with a note that the participants of the programme as a way of life should inculcate the scientific temperament in their research.

Dr. S .U. M. Reddy through his lecture has given the definition of high power microwave (HPM) and exposed the exciting field of HPM sources to the participants of the programme.At the outset he has explained the features of high power electromagnetic pulse (EMP), high

altitude electromagnetic pulse (HEMP), nuclear electromagnetic pulse (NEMP), non-nuclear electromagnetic pulse (NNEMP) and their respective roles as weapons in defence while explaining the difference between lethal and non-lethal weapons. He has also defined the category of directed energy weapon (DEW) and the belonging of high energy laser (HEL) to this category. The advantages and disadvantages of DEW have been explained and their offensive applications, in general, and specific applications in Army, Air Force and Navy, in particular, have been discussed. His lecture also uncovered the RF effects of HPM DEW on a defined 5-level scale and the upset and damage caused by these effects on the electronic systems. He has also narrated the mechanism of HPM coupling to electronic systems. Further, in order to evoke interest in the mind of the participants of the programme, Dr. Reddy suggested that they should see the literature available in public domain for some weapons such as laser-DEW weapon developed by Lockheed Martin; SHF (3-30 GHz) weapon developed by Russia unveiled in the classified area of an international military forum; high energy laser (HEL) DEW developed for Navy Bay systems; Raytheon-USA-developed anti-UAV HPM-DEW system, non-lethal active denial system (ADS) for crowd dispersal, which is an option between 'shouting' and 'shooting' complying with the International Law of Armed Conflict; vigilant eagle airport security system providing aircraft protection against shoulder fired missiles; and so on. While presenting Indian HPM scenario, Dr. Reddy has referred to DRDO laboratories, namely, Microwave Tube Research and Development Centre, Centre for High Energy Systems and Sciences (CHESS), Hyderabad, Terminal Ballistics Research Laboratory (TBRL), Chandigarh, and Research Centre Imarat(RCI), Hyderabad. Hence, he has apprised the participants of the relevant activities in Laser-DEW by CHESS; UWB DEW by RCI; electrically driven HPM-DEW by MTRDC; and explosively driven HPM-DEW by both MTRDC and TBRL. Before describing the HPM source development activities of DRDO-MTRDC (of which he himself is the Director), Dr. Reddy presented the capabilities of VIRCATOR, MILO, RELTRON, relativistic magnetron, relativistic BWO and gyro-devices with respect to the frequency, efficiency, output power, size, external magnetic field requirement, construction complexity, and spectral purity. Dr. Reddy concluded his lecture by presenting the glimpses of HPM activities of MTRDC in the development of relativistic magnetron, relativistic BWO and MILO. He has commented that the Marx generator commissioned at MTRDC with the help of the vendor from Ukraine would prove to be the workhorse for developing intensive relativistic electron beam (IREB) driven HPM sources in the country. Last but not least, Dr Reddy has considered it appropriate to give a glimpse of the effort of MTRDC in developing explosive electron emission.

Dr. S. K. Datta in his lecture has taken up a topic of very much relevance to microwave engineering, namely, microwave radiation safety standard vis-à-vis biological effects of microwaves. In order to deal with the subject, he has considered it appropriate to introduce the relevant enabling concepts. Thus, he has explained the concept of ionizing radiation and non-ionizing radiation and introduced hazards of electromagnetic radiation to personnel (HERP) and hazards of electromagnetic radiation to ordnance (HERO). He has also discussed the other relevant concepts such as the physics of microwave heating that helps to understand microwave biological effects and homeostasis which is basically the state of steady internal physical and chemical conditions maintained by human body and which need be kept within certain pre-set limits (homeostatic range) for the optimal functioning of the body, and, moreover, which is controlled solely by the hypothalamus of the human brain which in turn controls the variables of the body such as temperature, blood glucose, iron level, copper regulation, blood gases, blood oxygen content, calcium level, sodium and potassium concentration, arterial blood pressure and

fluid balance, blood pH, neuro-endocrine balance, gene regulation, energy balance, etc. Based on this conceptual background, Dr. Datta has then defined the safety standards, as stipulated typically by IEEE, American National Standards Institute (ANSI), International Commission on Non-Ionizing Radiation Protection (ICNIRP), and Internal Radiation Protection Association (IRPA) vis-à-vis biological effects of microwaves, the two quantities, namely, specific absorption rate (SAR) and basal metabolic rate (MBR) being found to be of relevance in such definition. He has thus stated the exposure limits for professionals and common people in terms of Roentgen equivalent in mammal (rem) (100 rem being 1 J/kg = 1 Sievert) as well as mW/cm^2 at specified duration of exposure. In parallel, the electric field (V/m) and magnetic field (A/m) safe limits vis-à-vis the radiation frequency have also been stated. He has also stated the SAR safe limit for specified duration for cell phone users. The radiation limits for telephone/cell phone and radio station towers and Bluetooth at specified frequencies have also been discussed. His discussion on biological effects has further included the role of microwave radiation in causing cancer. He has also cautioned the radiation hazards around the installations ofmilitary radars. His presentation has also included the biological hazards of HPM-DEW such as ocular, cardiac and neurological disorders. The need for being aware of the biological effects on pacemakers, hearing aids, ornaments, vascular and prostatic stents put on human bodies has also been emphasized by him.

Dr. Vishal Kesari has delivered two lectures. In his *first lecture*, from first principles he has developed electromagnetic analysis of a disc-loaded circular waveguide which has potential application in widening the bandwidth of a gyro-TWT which is essentially a gyro-device like the gyrotron. However, before discussing such analysis Dr. Kesari has aroused interest among the participants of the programme where in historical timeline of the development of microwave tubes and in their average power versus frequency capability the gyro-device, namely, the gyrotron stands. Dr. Kesari has, with the help of the schematic of a gyro-TWT, explained the working principle of a gyro-TWT. He has shown the operating point of a gyro-TWT as the point of intersection between two dispersion characteristics, namely, the beam-mode dispersion line of the gyro-TWT and the waveguide-mode dispersion hyperbola of the waveguide interaction structure of the device. He has hence explained how one can widen the bandwidth of the coalescence between the beam-mode and waveguide dispersion characteristics for broad-banding a gyro-TWT. Further, he has enumerated the different approaches to the analysis of a disc-loaded waveguide reported in literature. He has chosen the field matching approach and elaborated it giving the different steps involved in the approach. He has not only taken up for analysis the conventional disc-loaded waveguide but also a number of variants there of that has taken into account the space harmonics in the propagating wave in the disc-free region as well as in the standing wave in the disc-occupied region of the structure, and discussed the method of deducing the structure dispersion relation. Plotting the dispersion characteristics with the help of his analysis he has shown how the disc parameters controls the shape of the structure dispersion characteristics and hence can provide the desired wideband coalescence between the beam-mode and waveguide-mode dispersion characteristics as required for widening the gyro-TWT bandwidth. For each of the variants of the disc-loaded waveguide studied, he has shown that the structure periodicity proves to be the most sensitive controlling parameter. Further, he has discussed how the gain reduction in the method of broad-banding the device bandwidth by tapering the cross section of the disc-free interaction waveguide could be compensated for by disc-loading the waveguide. In his *second lecture*, Dr. Kesari has presented ANSYS-HFSS simulation of the interaction structures and also such simulation of the RF input and output

couplers/windows of slow-wave and fast-wave microwave tubes. The results of modelling and simulation have typically encompassed the helix and coupled-cavity and folded-waveguide slow-wave structures of TWTs and their couplers, and also the beam tunnel, interaction cavity, nonlinear taper and RF window of a gyrotron. (The pdf of this second lecture has, however, not been included in this compendium due to its non-availability in public domain under proprietary constraints).

Dr. Vishant Gahlaut in his lecture has raised a very pertinent issue of the thermal and structural behaviours of a device that is otherwise successfully designed electrically. He has discussed the capability of the software ANSYS in this regard. For instance, one has to check if the device parts get destroyed due to excessive heating or if the changes in the dimensions of the device due to heating are approvable from the standpoint of electrical design. Further, the designer of a device, for instance, a space-TWT should ensure that the device could withstand mechanical shocks and resonances during its launching. He has exemplified the issue with particular reference to a space-TWT and a gyrotron with and without cooling. To be more specific he has presented his own thermal-structural ANSYS analyses of the subassemblies/parts of a TWT, namely, electron gun, helical slow-wave structure, RF couplers and also those of a gyrotron, namely, its cavity and collector.

Dr. N. Purushothaman has delivered a lecture on metamaterial and metamaterial based microwave tubes. (Besides, along with Mr. Raktim Guha, he has presented a live demonstration of electromagnetic simulation using CST Microwave Studio Suite). In his lecture, Dr. Purushothaman has uncovered the general design studies as well as case studies on split-ring resonators (SRRs) and fishnet structures, and also the use of optimization methods in designing metamaterial based devices. Obviously, he has introduced the introductory basics of metamaterial for the benefit of the participants of the programme. He has given the methods of extraction of the parameters of the metamaterial treating it as equivalent to a homogenous material. He has then introduced the SRR+TW metamaterial (TW standing for thin wire) in which one of the edge-faces of the slab is provided with the SRR while the other with the TR. How the simulated dispersion characteristics of the SRR+TW metamaterial, taking the typical structure parameters (substrate relative permittivity, substrate loss tangent, unit cell size, ring width, thin wire width, inter-ring gap, intra-ring gap, and metallic inclusion thickness) compare with the corresponding dispersion characteristics of the SRR metamaterial has also been discussed by him. He has further discussed how to simulate the S-parameter versus frequency response of the metamaterial with particular reference to the SRR metamaterial. He has also reviewed the various methods of extracting the effective permittivity and the effective permeability of the metamaterial. He has also discussed how to develop the bulk medium model starting from the unit cell of the metamaterial. Finally, Dr. Purushothaman has shared some of his exciting experiences of practically developing metamaterials with respect to SRR, vane-type fishnet metamaterial and characterizing them with respect to the S-parameters. The comparison with respect to refractive index and FoM of the vane-type fishnet metamaterial developed by Dr. Purushothaman, with the cross-circle fishnet, cut-wire pair, 3D fishnet, octagon-shaped patch, and I-shaped patch metamaterials developed elsewhere and reported in literature has immensely cheered the participants of the programme.

Mr. Subhradeep Chakraborty has delivered two lectures. His *first lecture* is divided in two parts, the first part dealing with some enabling basics of antennas and the second part with some relevant concepts in microstrip antennas. He has apprised the participants of the "IEEE

Standards Definitions of Terms" as well as of the four perspectives of antennas: transducers, transformers, radiators and energy converters. His historical timeline mentioning the first antenna (arial) proposed by Dr. Mahlon Loomis, the historical Heinrich Hertz's experiment, and of course the first ever public demonstration of communication of radio waves by Sir. J. C. Bose has immensely inspired the participants of the programme. He has also mentioned the first ever research paper from India entitled "Radiation field of a conical antenna" by Professor J. S. Chatterjee of Institute of Radiophysics and Electronics, Calcutta University. He has concluded the first part of this lecture by the explanation of major lobes, minor lobes, HPBW, and FNBW of a typical antenna in three-dimensional radiation pattern. His description of ADS with the antenna used therein has evoked interest among the participants of the programme. The second part of this lecture has begun with the discussion on the advantages and disadvantages of microstrip patch antenna. He has presented the design approach to rectangular and circular microstrip patch antennas with examples. Further, Mr. Chakraborty has discussed the various causes of cross-polarized radiation from microstrip antennas and the methods of reducing such radiation more so in H-plane in which it is more pronounced than in E-plane. He has elaborated such interesting issues as the effect of the location of the probe position on the radiation pattern. He has also elaborately explained the use of the defected—for instance, in dumbbell shape—ground structure in rectangular or circular patch antenna in reducing the cross-polarized radiation.In his *second lecture,* Mr. Chakraborty has taken up a more specialized problem of obtaining flat-top antenna radiation pattern which is useful in base station for mobile communication services and which can be used as an efficient feed for a parabolic reflector for the sake of uniform aperture illumination. The problem has stimulated very much interest especially among those participants of the programme who are actively involved in research in the area of microstrip antennas. Mr. Chakraborty has added more rigour to the problem by posing the requirement of reduced cross-polarized radiation while obtaining flat-top radiation. In this context, he has brought out the role of an antenna array and presented topical concepts, namely, the interleaving array, the beam-switching array, and the method of maximum power transmission efficiency (MMPTE). He has also discussed the challenge of obtaining flat-top antenna radiation pattern from a unit antenna and hence discussed the features of reduced-size double-shell lens antenna, dual-patch antenna, and compact smooth horn antenna. Mr. Chakraborty has concluded his presentation with the description of the contribution of him and his team in designing a quasi-planar composite microstrip antenna that has yielded flat-top radiation with high gain and low cross polarization.

Mr. Raktim Guha has delivered a lecture on recent advances in metamaterial assistance in microwave tubes. (Besides, along with Dr. N Purushothaman, he has presented a live demonstration of electromagnetic simulation using CST Microwave Studio Suite). Mr. Guha has begun his presentation with his salutation to the pioneersofmetamaterials(Professors Victor G. Veselago, John B. Pendry, David R. Smith, Nader Engheta, Richard W. Ziolkowski and Subal Kar). In fact, he has thrilled the participants of the programme informing them that Professor Kar, who is one of the resource persons of the present programme, along with his team at Institute of Radiophysics & Electronics of Calcutta University, SAMEER, Kolkata and BARC, Mumbai, has first ever developed the metamaterial crystal in India and displayed it on 17th August, 2009 at BARC. Mr. Guha has quoted Dr. David R. Smith to describe metamaterial as "any material composed of periodic, macroscopic structures so as to achieve a desired electromagnetic response" ('meta' meaning 'altered/changed/beyond' and 'macroscopic' meaning 'large enough to be visible with the naked eye'). In quadrant classification of material,

in which the quadrant is formed by the relative permeability on the ordinate (y-axis) and the relative permittivity on the abscissa (x-axis), he has enumerated (i) double positive (DPS) material in which epsilon (ε) or permittivity and mu (μ) or permeability are each positive, and which supports propagating wave-mode; (ii) epsilon (ε) negative (ENG) material such as plasma and metal at optical frequencies in which epsilon (ε) or permittivity is negative, and which supports evanescent wave-mode, (iii) double negative (DNG) material, also known as left-handed material (LHM), in which epsilon (ε) or permittivity and mu (μ) or permeability are simultaneously each negative, and which supports propagating wave-mode; and (iv)mu (μ) negative (MNG) material in which mu (μ) or permeability is negative, and which supports evanescent wave-mode. Further, Mr. Guha has uncovered Lorentz model for a dielectric, Drude model for a metal, the concepts of DNG material, the method of parameter retrieval of metamaterial, and the techniques of fabricating metamaterials. He has explained how the simultaneous possession of negative permeability and negative permittivity makes the DNG metamaterial exhibit negative refractive index and makes it left-handed material (LHM), too. He has discussed how the metamaterial exhibits some other exotic properties, namely, reverse Snell's law, reverse Cherenkov radiation, and reverse Doppler effect. He has also discussed the metamaterial application in microwave engineering, namely, antennas, microwave tubes, power dividers/combiners, phase shifters, directional couplers, near-field imaging/microscopy, filters, absorbers, transmission lines, radars/cloaking, etc. He has further explained the physics of split-ring resonator (SRR) and complementary split-ring resonator (CSRR) and also mentioned how ENG property could be achieved by metallic wire lattice at relatively low frequencies and similarly MNG property by SRR. He has also explained even though the metal like silver, gold and aluminium exhibits ENG property at optical frequencies and similarly the ferromagnetic system at resonance exhibits MNG property, and even though one cannot obtain DNG material in nature, one can realise DNG property in a metamaterial. He has also given the method of practically implementing DNG material or LHM. Further, the presentation of Mr. Guha has included the studies reported in literature on waveguides loaded with SRRs and CSRRs, folded waveguide slow-wave structure with metamaterial insert, and metamaterial parameter retrieval using CST Microwave Studio simulation and MATLAB. He has concluded his lecture by presenting a brief account of the recent effort in the country in theoretical and experimental research in the area of metamaterial inspired microwave tubes. For instance, he has mentioned how a slow-wave structure consisting of a helix supported by wedge-shaped DNG-metamaterial support rods, symmetrically arranged a around the helix in a metal envelope, has been analyzed by both field and equivalent circuit analyses to obtain one and the same dispersion relation of the structure. He has discussed how the earlier oversimplified analysis ignoring the frequency dependence of the permittivity and permeability of DNG metamaterial has been improved by him by taking into account this frequency dependence in the analysis and how he has validated his analysis against CST Microwave Studio simulation with respect to both dispersion and interaction impedance versus frequency characteristics of the structure. He has also commented that such a DNG metamaterial supported helical slow-wave structure has high interaction impedance as compared to its traditional counterparts promising its use for enhancing the device efficiency and miniaturization. He has also discussed the tunability of the structure over multiple-frequency bands and hence the potential of the structure to be used as a multi-band structure without requiring any alteration in the helix and envelope dimensions while giving the advantage of reduced dimensions as compared to the other structures used individually in different bands. Furthermore, the analysis of Mr. Guha has shown that the structure provides a

negative value of interaction impedance indicating backward-wave interaction due to backward energy flow and thus enjoys the potential application in backward-wave amplifiers and backward wave oscillators. He has also suggested the possible means of metal MTM layering of the radial faces of the discrete helix-support rods in a more realistic structure configuration from the standpoint of its practical implementation. Finally, in his lecture, Mr. Guha has outlined the effort of his colleagues at CSIR-CEERI in practically developing metamaterial; he has also acknowledged the collaboration he has received from his colleagues at CSIR-CEERI-Pilani (his present affiliation), DRDO MTRDC-Bengaluru and SKFGI-Mankundu (his almamater) in his investigation into metamaterial inspired microwave tubes.

Dr. Rajiv Kumar Singh (convener of the present programme) before presenting his lecture on the electromagnetic field analysis of interaction structures has reiterated the concern of Professor Saha expressed in his Message already mentioned in this compendium that the participants of the programme should not merely depend on simulation tools for their research and that they should dig deep into the problem analytically as well. In fact, in his lecture he has shown how to develop electromagnetic analysis of a periodically loaded cylindrical waveguide. He has discussed the working principles and applications of two gyro-devices, namely, the gyrotron and the gyro-TWT in which such a waveguide can be used as the resonating and propagating interaction structures, respectively. He has also explained the operating points of the gyrotron and the gyro-TWT as the points of intersection between the beam-mode and waveguide-mode ω-β dispersion plots. He has discussed why the operating point of a gyrotron should be close to the waveguide cut-off to reduce the effect of beam velocity spread and enhance the diffractive quality factor of the waveguide resonator and why the operating point of s gyro-TWW should be slightly off from the waveguide cutoff for wideband coalescence between the beam-mode and waveguide-mode dispersion characteristics. He has also given the steps of his analysis leading to the dispersion relation of the structure starting from the field expressions in the different regions of the structure and electromagnetic boundary conditions at the different interfaces and the metallic waveguide wall of the structure. He has also validated his electromagnetic analysis against his CST simulation and the effect of the structure parameters such as vane and disc parameters on the control of dispersion characteristics of the structure. He has also presented his eigenmode analysis using CST simulation typically with reference to a disc-loaded cylindrical waveguide. Dr. Singh has shown that the tapered cross-section waveguide exhibits more controlled dispersion characteristics for its potential application in widening a gyro-TWT. He has further shown that the vane angle is more effective than the vane depth and number of vanes of a vane-loaded waveguide and that the disc periodicity is more effective than the disc-hole radius of a disc-loaded waveguide in controlling the structure dispersion characteristics.

Dr. N. Purushothaman and Mr. Raktim Guha, besides delivering their respective lectures as reported above, have also presented together a live demonstration of electromagnetic simulation using CST Studio Suite, taking the typical example of a split-ring resonator (SRR) combined with a thin wire (TW) metamaterial unit cell. The key steps have been shown for the initial simulation setup while explaining the step-by-step procedure to evolve the model by creating basic 3D building blocks, carrying out the Boolean operations, loading the material from material library, defining a new material and using global and local coordinate systems. The other key settings for simulation such as the frequency range, background material, relevant electromagnetic boundary conditions and excitation ports have been discussed pointing out the importance of global and local mesh settings and the various available mesh types. The method

has also been given to carry out the simulation using time domain solver after setting up the simulation environment. The participants have also been shown the progress of the simulation and, following the solver run, the display of the electric and magnetic fields at the waveguide ports while relating it with the type of excitation necessary for the SRR and the TW; the S-parameter results have also been shown to them. The procedure to extract the constitutive electromagnetic properties of the SRR+TW unit cell, namely, permittivity, permeability and refractive index using the in-built postprocessor have also been demonstrated. Dr. Purushothaman and Mr. Guha have further remarked that the basic steps of this demonstration of simulation using CST Studio Suite continue to be the same for the simulation using any other computational electromagnetic (CEM) software package as well.

EPILOGUE

It is hoped that the lecture material presented in this compendium should be useful to not only the participating faculty but also the expert resource persons. The compendium has provided the abstracts of the lectures delivered besides 14 pdf's of the lecture material including the one due to Professor P. K. Saha who due to unforeseen reason could not attend the FDP. We have also included a Message from him in the compendium. Further, we have provided the biographies of the resource persons. In this FDP, the participants and the expert resource persons from universities and national laboratories interacted with one another on the subject matter of the FDP. It is hoped that the participants would utilize the acquaintance developed by them with the expert resource persons in the development of their own teaching and research career.

ACKNOWLEDGMENT

We have from time to time taken suggestions from Professor P. K. Saha and Professor Subal Kar while preparing this document. To them go our sincere thanks. We sincerely express our gratitude to Professor Vinay Kumar Pathak, Vice-Chancellor, Dr. APJ Abdul Kalam Technical University, Lucknow for extending all his support. We also keep in record our sincere acknowledgment to Professor Manish Gaur Director, Centre of Advanced Study, Dr. APJ Abdul Kalam Technical University, Lucknow and Professor H. K. Paliwal, Director, Institute of Engineering and Technology, Lucknow for their constant encouragement.

BIOGRAPHIES OF THE RESOURCE PERSONS

Professor B. N. Basu (B. Tech, M. Tech, Ph. D): Superannuated as Professor & Head of Electronics Engineering Department and Coordinator of Centre of Research in Microwave Tubes (CRMT) at Institute of Technology, Banaras Hindu University (BHU), (now known as Indian Institute of Technology (IIT)-BHU), India, Professor Basu is now Adjunct Professor at Sir JC Bose School of Engineering, Supreme Knowledge Foundation Group of Institutions, Mankundu, West Bengal, India. Earlier, besides IIT-BHU and SKFGI-Mankundu, he served several other organizations in India: National Institute of Technology, Jamshedpur; CSIR-Central Electronics Engineering Research Institute (CEERI), Pilani; DRDO-Defence Electronics Research Laboratory, Hyderabad; College of Engineering and Technology, IFTM, Moradabad. He was in the team responsible for the development of the first ever travelling-wave tube (TWT) in the country. He was one of the members of the DST Steering Committee of the multi-institutional project in which the first ever gyrotron in the country for fusion plasma heating was developed. He was Distinguished Visiting Scientist of CSIR at CEERI-Pilani and Consultant to DRDO-MTRDC-Bangalore. He at present co-chairs with ISRO Director a committee that monitors a project at CEERI-Pilani for the indigenous development of a class of space-qualified TWTs for ISRO-SAC-Ahmedabad. He played a pivotal role in establishing MOUs (i) between Department of Electronics Engineering, IIT-BHU and CSIR-CEERI, Pilani; (ii) between Seoul National University and CSIR-CEERI, Pilani; and (iii) between SKFGI, Mankundu and CSIR-CEERI, Pilani. He is Golden Reviewer of IEEE Transactions on Electron Devices. He is on the Editorial Board of the Journal of Electromagnetic Waves and Applications and he guest-edited Special Issue on Microwave Tubes and Applications: Issue 17, Vol. 31, 2017 of the Journal of Electromagnetic Waves and Applications (Taylor and Francis).Professor Basu took visiting assignments abroad at Lancaster University, UK; Seoul National University, Korea; Karlsruhe Institute of Technology, Germany; and University of Electronic Science and Technology of China, Chengdu. Professor Basu has authored (or co-authored) >125 research papers in journals of international repute (including >40 in IEEE Transactions) and 6 monograph chapters in the area of vacuum electron devices (microwave tubes). He has authored 4 books: (i) Electromagnetic Theory and Applications in Beam-Wave Electronics (World Scientific, Singapore/New Jersey/London/Hong Kong, 1996) (ii) Technical Writing (Prentice-Hall of India, New Delhi, 2007), (iii) Engineering Electromagnetics Essentials (Universities Press, Hyderabad, 2015) (distributed by Orient Blackswan, India) and (iv) High Power Microwave Tubes: Basics and Trends (Vol. 1 and Vol. 2), Morgan & Claypool Publishers, California, USA with IOP Publishing, Bristol, UK 2018) (with Vishal Kesari as the co-author). He is on the Editorial Board of the Journal of Electromagnetic Waves and Applications and he guest-edited Special Issue on Microwave Tubes and Applications: Issue 17, Vol 31, 2017 of the Journal of Electromagnetic Waves and Applications (Taylor and Francis publication). He was President of Vacuum Electronic Devices and Application Society, India. He served on the Technical Committee on Vacuum Electronic Devices of the IEEE Electron Devices Society. He is recipient of the SVC Aiya Memorial Award of IETE, India; Lifetime Achievement Award of the Vacuum Electronic Devices and Application Society, India; and Microwave Pioneer Award of International Symposium of Microwaves, India.

Professor P. K. Saha (B. Tech, M. Tech, Ph. D): Well known for the hybrid-mode analysis of corrugated waveguides and horns by modelling the groove of a corrugated wall as a parallel resonant circuit, which Professor Saha developed while he was working with Professor P. J. B. Clarricoats, it is possible to develop high quality antenna systems for communication/satellite industry, for instance, corrugated horn feeds providing wideband high level cross-polar isolation. After completing his doctoral work at University of Leeds and postdoctoral work at Queen Mary College, University of London, he joined University of Calcutta as Lecturer in 1971 and retired as Professor in 2008 from the same university. Professor Saha is Fellow of IETE (India), Fellow of West Bengal Academy of Science and Technology, and Senior Member of IEEE (USA). He received the Eminent Teacher Award of University of Calcutta. The AP-MTT Chapter of IEEE Calcutta Section conferred on him the Lifetime Achievement Award for his pioneering contributions on corrugated horn antennas. At present, he teaches antennas and microwaves as visiting professor in Swami Vivekananda Institute of Science and Technology, Maulana Abul Kalam Azad University of Technology.

Professor Subal Kar (B. Tech, M. Tech, Ph. D): Acclaimed for his pioneering contribution in developing the first ever plasmonic metamaterial in India having led his team at Institute of Radiophysics and Electronics of Calcutta University, SAMEER, Kolkata Centre and BARC, Mumbai—the achievement displayed on 17th August, 2009 at BARC and reported online in Nature (India) article on 20thAugust, 2009—Professor Kar served Institute of Radiophysics and Electronics of Calcutta University for 33 years as Professor and also as Head of Department for a stipulated period. His field of specialization encompasses electromagnetics of metamaterials, microwave and millimeter-wave engineering, THz imaging, optical communication, and high energy physics. He has published a large number of research papers in peer reviewed international journals and presented invited papers/talks in France, Japan, China, Switzerland, Italy, U.K and U.S.A. He has three patents to his credit for innovative developments of IMPATT oscillators, amplifiers and power combiners at microwave frequency. Professor Kar received the Young Scientist Award of URSI and IEEE MTT and he is also the recipient of Fulbright Award of U.S Government. He worked as Visiting Scientist at Kyoto University, Japan in 1997 and as a Visiting Fulbright Scientist at Lawrence Berkeley National Laboratory, University of California at Berkeley, U.S.A during 1999-2000 and also at Oxford University, U.K in 2013. He also served as Visiting Scientist at NASA, Houston, U.S.A, 2004; Kyushu University, Japan in 2007; Warsaw University, Poland in 2010; University of Western Australia, Australia in 2011; Oxford University, U.K in 2013; Oxford University, U.K in 2013; Cockcroft Institute, UK in 2013; and Microtechnique Centre, EPFL, Switzerland in 2014. Professor Kar is also famous for the book authored by him entitled "Microwave Engineering—Fundamentals, Design, and Applications" (Universities Press, Hyderabad, 2016). Professor Kar is a Senior Member, IEEE; Fellow, IETE; and Fellow, VEDA Society. He is currently Adviser to SAMEER, Government of India.

Professor L. M. Joshi (M. Sc, Ph. D): Mapping Central Electronics Engineering Research Institute (CEERI), Pilani as one of the top labs of CSIR, largely for his contribution in designing and developing klystrons for defence and accelerator applications, Professor Joshi served CEERI for nearly 38 years before superannuating as Chief Scientist in 2015 and making his services available even thereafter as Emeritus Scientist until 2018. He executed sponsored projects of national relevance running into the budgetary of over Rs. 12 crores during the last decade. The project leading to the development of 6-MW peak power and 24-kW average power

klystron, which Professor Joshi has led as Chief Investigator/Project Coordinator, has been adjudged the best 70 products in CSIR's history. He also served CEERI as Alternate Nodal Officer for CSIR Network Program on high power microwave devices X^{th} and XI^{th} plan-periods, leading to the creation of specialized infrastructural facilities catering to the need of the present and future requirements of laboratories and equipment at CEERI. He also served Academy of Scientific and Innovative Research (AcSIR) of CSIR by serving it as its Professor and Coordinator of M. Tech and Ph. D programmes in the area of High Power Microwave Devices and System Engineering. Further, he served the academia and manpower training by supervising a large number of M. Tech projects and Ph. D theses. He also authored/co-authored more than 60 research papers and delivered a number of keynote and invited lectures at conferences in the country and abroad. Professor Joshi also took the various assignments abroad as Scientist Fellow/Visiting Scientist at University of Lancaster, UK); FZK, Karlsruhe, Germany; DESY, Hamburg, Germany; Stanford University & SLAC, USA; and ScandiNova Electronics, Uppsala, Sweden. Professor Joshi served a large number of national review committees and also served several academic research degree committes and management/executive boards of universities such as Graphic Era University, Dehradun and IFTM University, Moradabad. He has also been active in the activities of professional societies. He is member, Indian Physics Association; member, Indian Vacuum Society; Fellow, Institution of Electronics and Telecommunication Engineers (IETE); Fellow, Vacuum Electron Devices and Applications Society (VEDAS); and Fellow, Indian Society of Particle Accelerators. He also served as Chairman, IETE, Pilani Chapter and President, VEDAS.

Professor A. K. Sinha (M. Sc, Ph. D):Gifted with profound competence in electromagnetic analysis of periodically loaded interaction structures of microwave tubes, Professor Sinha has served CSIR-Central Electronics Engineering Research Institute (CEERI), Pilani since 1989 before superannuating as Chief Scientist in 2014 and continuing to serve CEERI thereafter as Consultant/Emeritus Scientistuntil 2018. He first led the activities of designing and developing helix TWTs as member/project leader/activity coordinator/head of a number of DRDO/ISRO/DST/CSIR sponsored projects at CEERI. He spearheaded the activities as CEERI Group Leader of the DST-sponsored multi-institutional project, in which CEERI was the Nodal Centre, on the design and development of the first ever gyrotron in the country for fusion plasma heating. He played a pivotal role in establishing the first ever Gyrotron Lab in the country at CEERI, which is capable of designing, fabricating and tube-processing gyrotrons of various ranges of power and frequency. He, as Visiting Scientist/Visiting Professor, extensively visited the premier institutions abroad: Lancaster University, UK; Seoul National University, South Korea; PAL, Pohang, South Korea; KERI, Changwon, South Korea; UNIST, Ulsan, South Korea; Massachusetts Institute of Technology (MIT), USA; and Karlsruhe Institute of Technology, Germany. He also attended IEEE-IVEC abroad at Monterey, USA; Rome, Italy; and Paris, France. He also contributed to PIERS-12 at Kuala Lumpur as Session Coordinator of one of its sessions. He was recipient of JC Bose award for best research paper in JIETE, Brain-pool Fellowship of South Korea and Senior DAAD Fellowship of Germany. He has to his credit >250 research papers in peer-reviewed national and international journals and conference proceedings. He served Academy of Scientific and Innovative Research (AcSIR) of CSIR as Professor. He served IETE at its Pilani Centre as Secretary and also as Executive Body Member. He was National Executive Body Member of Indian Vacuum Society. He is reviewer of journals such as IJPAP (CSIR) and IEEE Transactions: ED; PS; MTT. Further, he served the academia and manpower training by supervising a large number of M. Tech/ M. Sc projects and 12 Ph. D

theses. He also served academic/executive/review bodies, for instance,as Chairman of Ad-Hoc Board of Physical Science, Swami Ramanand Teerth Marathwada University, Nanded, Maharashtra and gyrotron projects at DRDO-MTRDC. He is life fellow/member of professional societies such as IETE, IPA, ISCA, IFTA, IVS, CSI, PSI, SSMI and VEDA.

Dr. S. U. M. Reddy (M. Tech, Ph. D): Well acclaimed for his immense contribution in designing and developing both helix and coupled-cavity TWTs and MPMs/transmitters, Dr. Reddy is the Director of DRDO-Microwave Tube Research and Development Centre (MTRDC), Bangalore beginning his career there in 1987. He discharged his responsibilities at MTRDC as Project Manager, Group Head, Divisional Head and Project Director contributing to a number of projects and technologies and spearheading the activities in the development of HPM tubes for strategic defence applications. Dr. Reddy is Fellow of Vacuum Electronics Devices and Applications Society (VEDAS), member of IEEE, member of Magnetic Society of India and member of Society of EMC Engineers. He is the recipient of the DRDO AGNI Award for Self-reliance in 2003 and 2013. He has also received DRDO Scientist of the Year award in 2001 for his significant contribution in the field of microwave tubes. He has to his credit a large number of papers in national/international journals and conferences.

Dr. S. K. Datta (B. E, M. Tech, Ph. D): Leading a number of defence projects and contributing to the technology development for different classes of TWTs and compact transmitters at DRDO-Microwave Tube Research and Development Centre (MTRDC), Bangalore while beginning his career there in 1995, Dr. Datta is now Scientist-G and Associate Director of MTRDC. Dr. Datta is internationally acclaimed for his nonlinear hydrodynamic analysis of a TWT that gives the microwave tube community a clear understanding of harmonic generation and intermodulation distortion in the device. Dr. Datta has authored/co-authored a large number of research papers and filed 3 patents. He is also Golden Reviewer of IEEE-EDS, USA (2009, 2010, 2011, 2012, 2014, 2015, 2016, and 2017). He has contributed to the management and promotion of science and technology by monitoring and upgrading the teaching and curriculum of electronics engineering in the country, for instance, as member of the Board of Studies of Defence Institute of Advanced Technology, Pune and Pune and that of Motilal Nehru National Institute of Technology (MNNIT), Allahabad; bringing together the vacuum electronic devices (VED) fraternity of the country and founding Vacuum Electronic Devices and Applications Society (VEDAS), India as its Founder General Secretary; and being instrumental as the Head of Facilities Division and the Chief Implementer of ISO Standards while implementing the ISO 9001:2000 and ISO 9001:2008 at DRDO-MTRDC. Dr. Datta is Life member, National Academy of Sciences, India; Life Member, Magnetic Society of India; Life Member, Society of EMC Engineers, India; Life Member, Astronautical Society of India; Life Member, Indian Science Congress Association; Life Member, Indian Vacuum Society; Senior Member, IEEE, USA; Life Fellow, IETE, India; Life Fellow, Institution of Engineers India; and Fellow, Vacuum Electronic Devices and Applications Society (VEDAS), India. Dr. Datta is recipient of a number of awards: Sir C. Ambashankaran Award for Best Paper of Indian Vacuum Society (IVS) (1998); INAE Young Engineer Award of Indian National Academy of Engineering (2001); Sir C. V. Raman Award for Young Scientists, Government of Karnataka (2002); Agni Award for Excellence in Self Reliance of DRDO (2003); Science Day Silicon Medal of DRDO (2004); Technology Day Titanium Medal of DRDO (2007); Laboratory Scientist of the Year of DRDO (2009); B. V. Baliga Memorial Award for Innovations of Institution of Electronics & Telecommunications Engineers (IETE) (2010); and DRDO Scientist of the Year of DRDO (2015).

Dr. Vishal Kesari (M. Sc, Ph. D): Applauded for the electromagnetic analysis of periodically loaded waveguide interaction structures developed by him, Dr. Kesari has significantly contributed to R&D in TWTs and gyro-devices in India while being employed as Scientist at DRDO-Microwave Tube Research and Development Centre (MTRDC), Bangalore since 2008 after beginning his professional career as faculty of first Birla Institute of Technology, Mesra, Ranchi and then Indian Institute of Information Technology, Allahabad. Dr. Kesari has to his credit numerous research papers published in peer-reviewed journals and conference proceedings. He is reviewer for more than 15 international journals of IEEE, Springer, Taylor and Francis, Elsevier, IET, Progress in Electromagnetic Research, etc. He has also been recognized as Golden Reviewer of IEEE Electron Device Letters and IEEE Electron Devices for several years.The credit also goes to Dr. Kesari for authoring4 books: (i) Analysis of Disc-loaded Circular Waveguides for Wideband Gyro-TWTs, LAP - Lambert Academic Publishing AG & Co., Germany, 2009; (ii) High Power Microwave Tubes: Basics and Trends, Volume 1, IOP Concise Physics, Morgan & Claypool Publishers, CA, USA. IOP Publishing, UK, 2018 (co-authored by B. N. Basu); (iii) Ibid., Volume 2; and (iv) सूक्ष्मतरंगऔरमिलीमीटर-तरंगनिर्वातइलेक्ट्रॉनिकयुक्तियांएवंसम्बंधिततथ्य, डी.आर.डी.ओ. विशेषप्रकाशनश्रृंखला**,** रक्षाविज्ञानसूचनाएवंप्रलेखनकेन्द्र (डेसीडाक),रक्षाअनुसंधानएवंविकाससंगठन, रक्षामंत्रालय, नईदिल्लीद्वारामुद्रणएवंप्रकाशन, जनवरी**,**2019. Dr. Kesari is recipient of a number of international, departmental and city-level awards, medals and prizes including German DAAD Fellowship award, DRDO Technology Day Titanium Medal-2019, and DRDO Young Scientist Award 2012.

Dr. Vishant Gahlaut (M. Sc, Ph. D): Specialist in the thermal and structural analysis of microwave tubes, Dr. Vishant Gahlaut is sought after always by microwave tube designers for the certification of their electrical design. He has been Assistant Professor at Banasthali University, Banasthali, Rajasthansince 2014.Besides the thermal management of microwave tubes, Dr. Gahlaut has also extended his research contribution to the area of microwave engineering encompassing microstrip antennas, for instance, for cognitive radio applications, and microwave measurement, besides the electrical designs of microwave tube components such as the electron gun, multi-stage depressed collector, helical slow-wave structure, RF coupler, and window. He has to his credit a good number of papers published in peer-reviewed journals. He is in the editorial board of International Journal of Advanced Research in Physical Science. He has presented his papers in the country and abroad, for instance, in Prague, Czech Republic (Progress in Electromagnetics Research Symposium PIERS-2015, July 06-09, 2015) and in Monterey, California (IEEE International Vacuum Electronics conference IVEC-2012, April 24-26, 2012). Dr. Gahlaut is the recipient of Best Oral Presentation award in National Conference on Recent Trades in Microwave Techniques and Optical Communication, IIS University, Jaipur, in February 2015. He has also received the Best Participant certificate of appreciation in Staff Development Programme on 'Analysis of Interaction Structures for Wideband Travelling-Wave Tubes' in June 2010 at CET, IFTM (now IFTM University), Moradabad. He has the experience of organising the conferences and short-term courses for faculty development in his university. He has a group of students working with him in the doctoral research programme of the university, one of his students having passed out with the Ph. D degree. In the sponsored DST-TARE scheme he has established an experimental set up for the validation of the analytical modal and simulation of thermal analysis of a TWT for space applications. Dr. Gahlaut is Associate member of Vacuum Electronic Devices and Applications (VEDA) Society and Life time member of Thermophysical Society of India.

Dr. N. Purushothaman (B. E, M. Tech, Ph. D): Justifying his selection in the master's degree programme of Academy of Scientific and Innovative Research (AcSIR) of CSIR at Central Electronics Engineering Research Institute (CEERI), Pilani, within a small span of time Dr. Purushothaman has proved him to be a successful scientist facing the challenges of indigenously developing satellite communication space-TWTs for ISRO in the country. He joined CEERI as Scientist after obtaining his M. Tech degree in the postgraduate degree programme of AcSIR in 2012. In the same programme he teaches now a theory subject 'Numerical Analysis and Techniques for Microwave Applications' as Instructor. Further, he has also obtained his Ph. D degree in the doctoral degree programme of AcSIR in 2019. In the original innovative research front, he is one of the few scientists in the country to appreciate the potential of metamaterial assistance in improving the performance of microwave tubes. He has given the methods of extraction of the parameters of the metamaterial treating it as equivalent to a homogenous material. He has also developed the theory of metamaterial assisted helical slow-wave structure of a TWT and experienced the primary success in the practical development of metamaterial in the laboratory. Dr. Purushothaman is Student Member of IEEE. He is recipient of CSIR-CEERI Research Excellence Award in 2018 for the successful development of Ku-band TWT as a project team member. Dr. Purushothaman played a lead role in setting up a Digital India Lab in Gyan Vihar, Pilani as a case study to understand the grassroots level problem in implementing the Digital India Initiative of the country.

Mr. Subhradeep Chakraborty (B. Tech, M. Tech, Ph. D): Developing the acumen for doing research in microwave engineering while he was a post graduate student and carrying out his M. Tech project work at CSIR-Central Electronics Engineering Research Institute (CEERI), Pilani in 2014 on the antenna compatible with the gyrotron of an active denial system,and publishing thereafter quite a good number of papers in the area of microstrip antennas, Mr. Subhradeep Chakraborty joined CEERI in March 2016 as Scientist in the Device Technology Group, MWD area, CSIR-CEERI, Pilani. At CEERI, he is at present devoted to the CAD and development of space-TWTs. His papers in journals/conference proceedings deal with microstrip antennas and TWTs. He has also to his the credit of co-authoring a book chapter with Professor Sudipta Chattopadhyay. Mr. Chakraborty is member of IEEE (USA); member of Antenna Propagation Society of IEEE (USA); member of European Microwave Association (EuMA) (EU); and Overseas Member of Institute of Electronics, Information and Communication Engineers, Japan. He serves as reviewer committee member of a number of international conferences such as RFM-2018, Malaysia, ACES-2019, Miami, USA, and TENCON-2019, Kochi, India. He also serves as the reviewer of IEEE Access, IET Electronic Letters, IET Microwave, Antennas and Propagation, International Journal of RF and Microwave, Computer-Aided Engineering, Progress in Electromagnetic Researches, Applied Computational Electromagnetic Society Journal, AEÜ-International Journal of Electronics and Communications, Turkish Journal of Electrical Engineering & Computer Sciences, etc.He, along with his other team members, received the CSIR-CEERI Foundation Day Award 2018 for Excellence in Research in TWTs.

Mr. Raktim Guha (B. Tech, M. Tech, Ph. D): Working on "coaxial coupler and waveguide transition for Ka-band helix TWT" in his M. Tech project at CSIR-Central Electronics Engineering Research Institute (CEERI) in 2015 and subsequently getting an opportunity to work at CEERI in two spans as Project Assistant—one from 01/04/2016 to 31/3/2017 in the area of multi-beam klystron and the other from 26/11/2017 till date in the area

of Ku-band helix TWT—Mr. Raktim Guha has inculcated in him research interest in the area of microwave tubes. He co-authored, with others, 4 journal papers and 6 conference papers in the area of TWTs. In one of these papers, of which Mr. Guha is the progenitor and which is published in IEEE Transactions on Electron Devices, and which is written during the period between the above two spans of his being Project Assistant at CEERI, he has developed the analysis of a helix supported by double negative metamaterial (DNG-MTM) rods, symmetrically arranged around the helix, in a metal envelope. He has extracted the parameters of the metamaterial treating it as equivalent to a homogenous material and considered the frequency dependence of the permeability and permittivity of the DNG-MTM following Lorentz and Drude models. He has studied the effects of the DNG-MTM parameters on the dispersion and interaction impedance of the structure. He has shown the tunability of the structure over multiple-frequency bands suggesting that the structure can be used as a multi-band structure without requiring any alteration in the helix and envelope dimensions. A negative value of interaction impedance obtained by him suggests that the structure provides backward energy flow and thus enjoys the potential application in backward-wave amplifiers and backward wave oscillators. A high value of the interaction impedance obtained promises the enhanced device efficiency and miniaturization of the structure. He has also suggested the possible means of metal MTM layering of the radial faces of the discrete helix-support rods in a more realistic structure configuration from the standpoint of its practical implementation. Mr. Guha is conversant with MATLAB, CST-Microwave Studio, CST-Particle Studio, TRAK (2D), HFSS, Solid Works, and AJ-Disk. He has validated his results of electromagnetic analysis of helical structures against CST simulation.

Dr. Rajiv Kumar Singh (B. E, M. Tech, Ph. D): Well versed in the electromagnetic analysis of periodically loaded waveguide taking into account the space-harmonic effects and validating his analytical results against CST simulation, Dr. Rajiv Kumar Singh has given the methods of rarefying the modes of a gyrotron using a vane-loaded circular waveguide and broad-banding a gyro-TWT using a disc-loaded circular waveguide by the optimization of structure parameters. After serving Department of Electronics and Communication Engineering, UNS Institute of Engineering and Technology, VBS Purvanchal University, Jaunpur as Lecturer; carrying out his doctoral research at Electronics Engineering Department, IIT-BHU, Varanasi; and serving Bharat Sanchar Nigam Ltd., Ludhiana, Punjab as Junior Telecom Officer, Dr. Singh is nowAssistant Professor, Department of Electronics Engineering, Institute of Engineering & Technology, Lucknow, and Associate Dean (Postgraduate Studies and Research),Dr. APJ Abdul Kalam Technical University, Uttar Pradesh. Dr. Singh contributed significantly to WiMAX services in Ludhiana, Punjab for BSNL and is carrying out CST sponsored R&D project on electromagnetic analysis of RF interaction structures of gyrotron devices. He was convener of Short-Term Training Programme jointly organized by Dr. APJ Abdul Kalam Technical University (AKTU), Lucknow and AICTE and held at AKTU. Dr. Singh is C. Eng (IEI) and Fellow of IETE, Fellow of IEI.

PDF'S OF LECTURES AND NOTE ON LIVE DEMONSTRATION OF SIMULATION

National Scenario of the Development of Microwave Tubes

B N Basu

Sir J. C. Bose School of Engineering
Hooghly-712139, West Bengal, India

Superannuated from Electronics Engineering Department, Banaras Hindu University, Varanasi-221 005, India

"What man 'learns' is really what he discovers by taking the cover off his own soul, which is a mine of infinite knowledge."

Microwave and Communication

Wireless communication depending on microwaves:

- **Direct broadcast satellite (DBS)**
- **Personal communication system (PCS)**
- **Wireless local area networks (WLANS)**
- **Worldwide interoperability for microwave access (WIMAX)**
- **Cellular video (CV)**
- **Global positioning satellite (GPS)**

High power Microwave sources and amplifiers constitute the backbones of

- **Point-to point communication with more channel capacity**
- **Satellite-to-home communication (TVBS)**
- **Radar**
- **Electronic warfare**
- **Missile tracking and guidance**
- **Remote sensing**
- **Material processing**
- **Imaging**

Exploration of millimeter-wave regime includes:

- **Extension of radio range**
- **High information density communication**
- **Deep-space and specialized satellite communication**
- **High resolution radar**

Magnetron was the key element in RADAR that significantly controlled World War II.

Synthetic Aperture Radar (SAR) has made it possible to simulate electronically an extremely large antenna or aperture that provides

- **high-resolution remote sensing imagery at night or during inclement weather**
- **reconnaissance and targeting information to military operations**
- **reconnaissance terrain structural information to geologists for mineral exploration**
- **oil spill boundaries on water to environmentalists**
- **sea state and ice hazard maps to navigators**

Civilian radars are used for

- weather detection
- highway collision avoidance
- air-traffic control
- burglar alarm
- garage door opener
- speed detectors (law enforcement)
- air-traffic control
- mapping of ground terrain
- ground probing (for the detection of underground materials like gun emplacements, bunkers, mines, geological strata, pipes, voids, etc.)
- remote sensing
- imaging in atmospheric and planetary science
- space debris phased-array mapping, analysis of cloud (as a sensor in environmental research), etc.
- microwave life detection for sensing heart beats and breathing, for instance, under earth-quake rubbles

Industrial heating applications:

Industries: paper, leather, textile, plastic, wood, forest, food, printing, pharmacy, chemical, photographic, measurement, etc.

- **Drying of leather, rubber, pharmaceuticals, tea, coffee, tobacco, textiles, film, etc.**
- **Food: precooking, cooking, pasteurizing, sterilizing, dough proofing, thawing, tempering, pasta drying, roasting of food grains/beans**
- **Plastic: sealing/ bonding, bulk heating, molding plastic foam, plastic laminate production, drying**
- **Forest: hardwood drying, plywood-veneer drying, pulp/wood-chip drying, destruction of fungi, and insects in wood**
- **Rubber: vulcanization, curing sponge rubber tubing, curing and foaming polyurethane bulk heating**
- **Chemical: drying paint and varnish, refractory processes, polymerizing**

- **Photographic: film processing requiring selective coating: polyesters and acetates of low dielectric loss and emulsions of high dielectric loss (photographic)**
- **Measurement: thickness monitoring of metal/dielectric sheets in rolling mills**
- **Medical: medical diagnosis and treatment using the phenomenon of dielectric heating**

  - **orthopedics: arthritis, sciatica, rheumatism**
  - **internal medicine: asthma, bronchitis, urology**
  - **dermatology: boils, carbuncles, sores, chilblains.**
  - **oto-rhyno-laryngology: abscesses, laryngitis, etc.**
  - **dental care and ophthalmology**

◊ **hyperthermia implemented by using phased-array antenna that locally heats the tumor cells selectively and raptures their membrane leading to the destruction of cancerous cells, without harming healthy ones, thus enabling such heated tissues to receive more nutrients and antibodies thereby speeding up the healing process**

◊ **ablation that dries up or desiccates the tumor with localized application of heat for the removal unwanted tissues, for example, liver and lunge tumors of patients with poor surgical condition**

Typical antenna applicator at 2.45 GHz (ISM band) can provide powers from100 mW/cm^2 to ~1 W/cm^2 for 15 to 30 minutes.

Other peaceful applications:

- **industrial heating**
- **material processing**
- **waste remediation**
- **civil, mining and public health engineering—including breaking of rock, breaking of concrete, tunnel boring and soil treatment**
- **plasma heating for a controlled thermonuclear reactor (electron cyclotron resonance heating of fusion plasmas) involving heating of hydrogen isotopes typically at ignition temperature of 108 K at 200 GHz**
- **scientific applications including RF linear accelerators, plasma diagnostics and chemistry, nonlinear spectroscopy, etc.**

- **Material processing providing volumetric and selective heating millimeter-wave frequencies using gyrotrons**

  → ceramic sintering and joining

  → production of new composite ceramics—stronger and less brittle—that can retain their high strength under high temperature and corrosive conditions

Consequently, this has made it possible to develop lightweight ceramic engines for aircraft and automobiles as well as strong, long-lived ceramic walls for thermonuclear power reactors.

Terahertz-regime applications:

- **imaging**
- **security inspection**
- **enhanced sensitivity spectroscopy**
- **dynamic nuclear polarization enhanced nuclear magnetic resonance**

Other unconventional applications:

- **satellite power station**
- **artificially created ionized layers for the extension of radio range**
- **city lighting**
- **nitrogen fertilizer raining on the earth**
- **environmental control by both ozone generation and atmospheric purification of admixtures that destroy ozone layer**

SSD versus VED/ Microwave Tube

Issue	SSD	VED/ Microwave tube
Collisional heat produced by electron stream	Throughout volume	At the collector
Operating temperature	Lower temperature operation for a longer life (lower mobility — a greater drag or inertial forces due to collision) Degradation at a higher temperature due to dopant migrating excessively, lattice becoming imperfect, mobility getting reduced impairing high frequency performance Wide-band-gap semiconductors like SiC and GaN to be used for high temperature operation	Higher temperature operation

SSD versus VED/ Microwave Tube (*continued*)

Issue	SSD	VED/ Microwave tube
Breakdown limit on maximum electric field inside the device	Lower	Higher
Base plate size Determined by cooling efficiency increasing with (i) the temperature difference between the hot surface and the cool environment and (ii) the surface area of the hot surface	Larger	Smaller (higher collector temperature)
Peak pulsed power	Lower Calls for power combining by multiple transistors and proportionate increase in package size	Higher Beam may be pulsed in the region separated from the interaction region
Ultra-bandwidth performance (Three-plus-octaves)	Possible below 1 GHz Corresponding to longer wavelengths ensuring negligible phase difference, for instance, in the voltage between the emitter and base	Usually not possible Controlling the structure dispersion is a challenging problem

Microwave tubes enjoy superiority over their solid state counterparts with respect to having

- **lesser heat generated due to collision in the bulk of the device**
- **higher breakdown limit on maximum electric field inside the device**
- **smaller base-plate size (determined by the cooling efficiency)**
- **higher peak pulsed-power operability**
- **ultra-bandwidth (three-plus octave) performance above a gigahertz**
- **inherently hardened against radiation and fairly resistant to temperature and mechanical extremes (being fabricated out of metals and ceramics)**

In fact, attempts were made to replace space-TWTs with SSDs however with limited success in view the required $5X10^6$ hr MTBF (mean time before failure) in satellite qualified devices.

Thus, although SSDs were tried out in satellite communication system during the last decade of the twentieth century, for instance, replacing ~50% TWTs with SSDs in 1995, such replacements declined beyond 1998 to only ~10% making space TWTs more relevant than their SSD counterparts.

Microwave tubes continue to be important despite competitive incursion from solid state devices (SSDs).

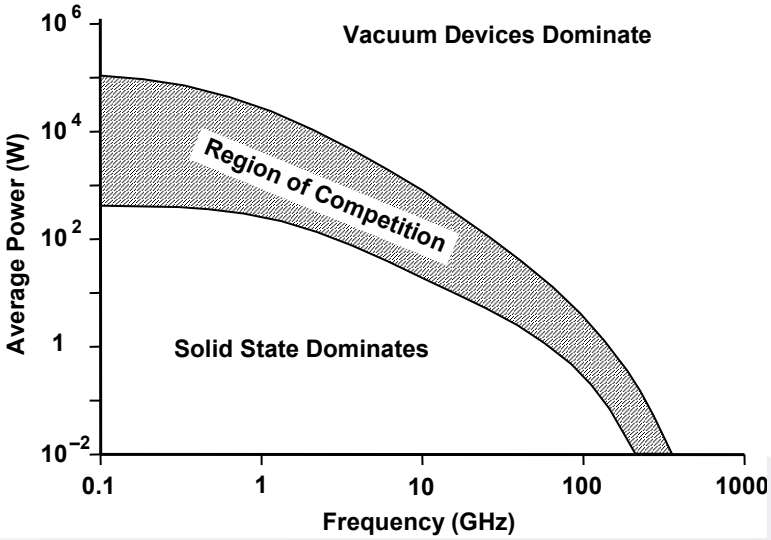

Solid state and vacuum device average power capabilities

Why use a thousand mice when one horse can do the job? (From Rodney Vaughan, Litton?

◊ **Both wideband helix-TWTs and coupled-cavity TWTs (CC-TWTs) are used in radars.**

◊ **Wideband helix-TWTs are used for**

∘ **electronic warfare (EW)**

→ **Electronic countermeasure (ECM), for both brutal jamming and deceptive jamming of radars in order to reduce the effectiveness of radars**

→ **electronic counter countermeasure (ECCM) to protect radars from ECM**

→ **electronic support measure (ESM) by detecting, intercepting, identifying, locating, recording, and analyzing sources of radiated electromagnetic energy for the purposes of immediate threat recognition and thus providing a source of information required for decisions involving electronic protection (EP), electronic attack (EA), avoidance, targeting, and other tactical employment of forces.**

◊ **Narrow-band helix TWTs are used for missile tracking that has revolutionized the armored corps by enabling tanks and fighter jets to hit a target at a greater distance.**

◊ **Klystrons are used for**

- **radars**
- **satellite communication**
- **TV transmitters**
- **particle accelerators (considered the *sine qua non* of such accelerators)**

◊ **Gyrotrons are used in the millimeter-wave regime for long-distance radar, high resolution radar imaging and precision tracking.**

◊ **High power microwave (HPM) tubes (using intensive relativistic electron beam) are used in information warfare (IW) involving directed energy weapon (DEW) such as electromagnetic bomb.**

Microwave tubes vis-à-vis applications

Microwave tube	System of application
Wideband helix-TWT	ECM, ECCM, ESM
Narrow-band helix-TWT	Radar; satellite and ground-based communication; telemetry and tele-command; missile seeker; astronomy/telescope
CC-TWT (narrow-band)	Radar
Klystron	Radar, particle accelerator; TV transmitter; satellite communication; microwave relay; astronomy/telescope
Magnetron	Radar; broadcasting; microwave heating

Microwave tubes vis-à-vis applications *Contd.*

Microwave tube	System of application
CFA (crossed-field amplifier)	Buffer/driver for an amplifying tube such as klystron or CC-TWT
MILO	HPM/DEW
Relativistic tubes: magnetron, BWO, klystron	HPM/DEW
VIRCATOR/reflex triode	HPM/DEW
Gyrotron	Millimeter-wave radar; long-range radar; high resolution radar; high information density communication; plasma heating; material processing; low intensity conflict; active denial system (ADS)
Gyro-TWT	Millimeter-wave radar
Gyro-klystron	Millimeter-wave radar

Designation of frequency ranges/bands

Frequency ranges/bands (MHz/kHz/GHz)	Terminology
Radio waves: 3 kHz-3 GHz	ISM: Industrial, Scientific and Medical ELF: Extremely low frequency VLF: Very low frequency LF: Low frequency VHF: Very high frequency UHF: Ultra high frequency SHF: Super high frequency
Microwaves: 3-300 GHz	
ISM band: 6.765-6.795 MHz; 13.553-13.567 MHz; 26.957-27.283 MHz; 40.66-40.7 MHz; 433.05-434.79 MHz; 902-928 MHz; 2.4-2.5 GHz; 5.725-5.875 GHz, 24-24.25 GHz	
ELF: <3 kHz; VLF: 3-30 kHz; LF: 30-300 kHz; MF: 0.3-3 MHz; HF: 3-30 MHz (short radio wave); VHF: 30-300 MHz (FM radio, TV); UHF: 300-3000 MHz (TV, mobile phone, GPS); SHF: 3-30 GHz (radar); EHF: 30-300 GHz (millimetre-wave); Terahertz: 300-3000 GHz (sensing and imaging)	
L: 1.12-1.70 GHz; S: 2.60-3.95 GHz; C: 3.95-5.85 GHz; X: 8.20-12.40 GHz; Ku: 12.40-18.00 GHz; K: 18.00-26.50 GHz; Ka: 26.50-40.00 GHz; V: 40.00-60.00 GHz; E: 60.00-90.00 GHz; F: 90.00-140.00 GHz; W: 75-110 GHz (satellite communications, targeting, tracking, active denial system)	

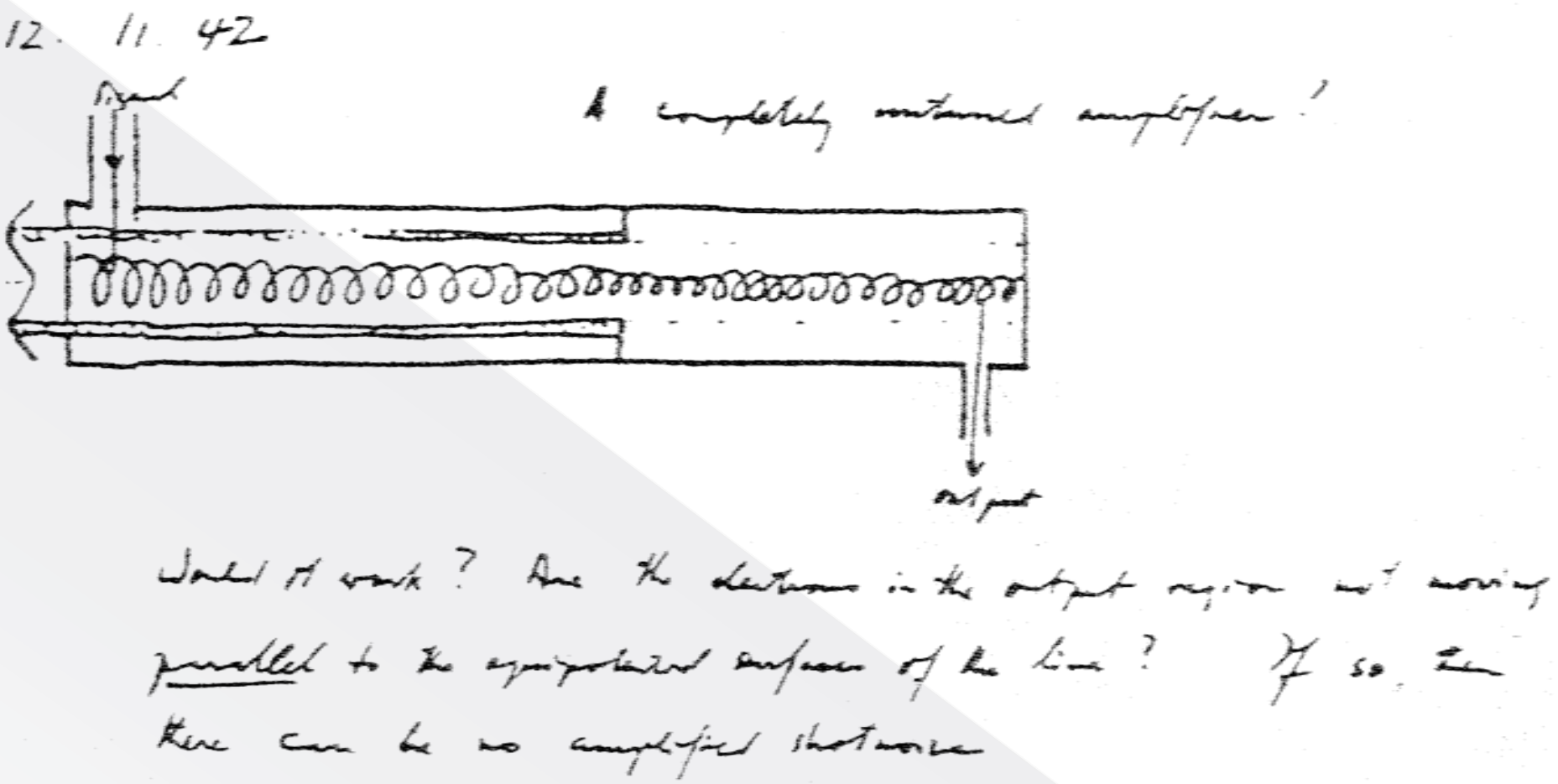

Sketch of the travelling-wave tube from R. Kompfner's note book

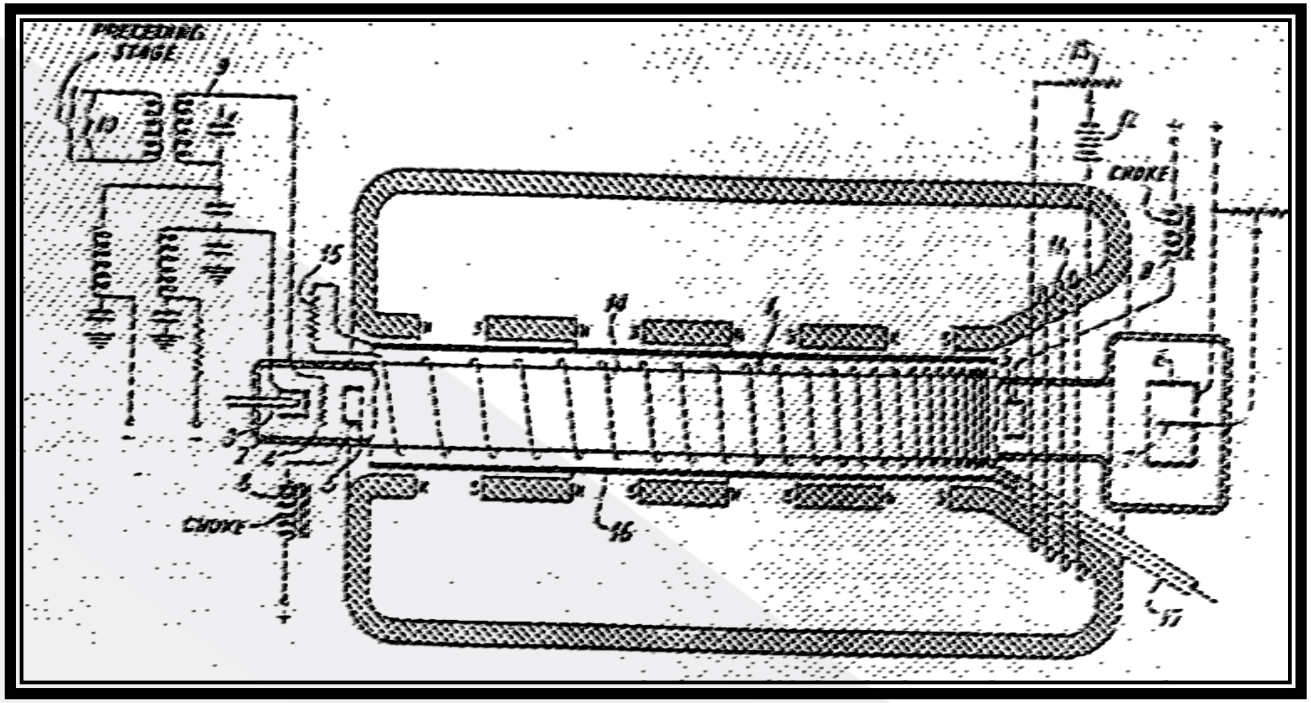

N. E. Lindenblad's travelling-wave tube amplification at 390 MHz over a 30 MHz band (U. S. Patent 2,300,052, filed on May 4, 1940 issued on October 27, 1942)

Helix wound around the outside the glass envelope. Signal applied to the grid of the electron gun (also applied to the helix in other experiments). Series of permanent magnets (non-periodic). Pitch tapered for velocity re-synchronization

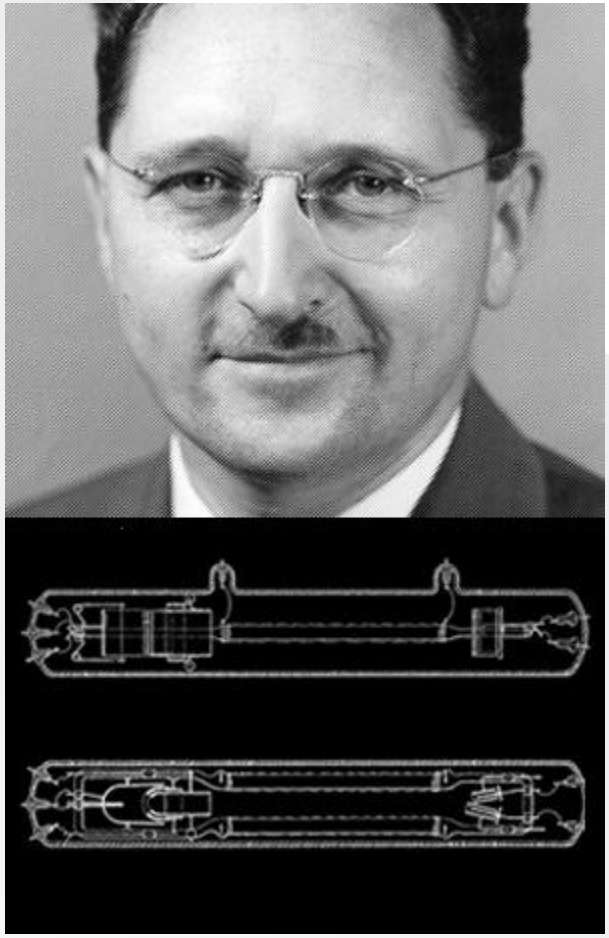

The patent Andrei Haeff filed in 1933 for a primitive type of traveling-wave tube has been largely ignored.

J.C. Bose (1858-1937) at the Royal Institution, London, 1897

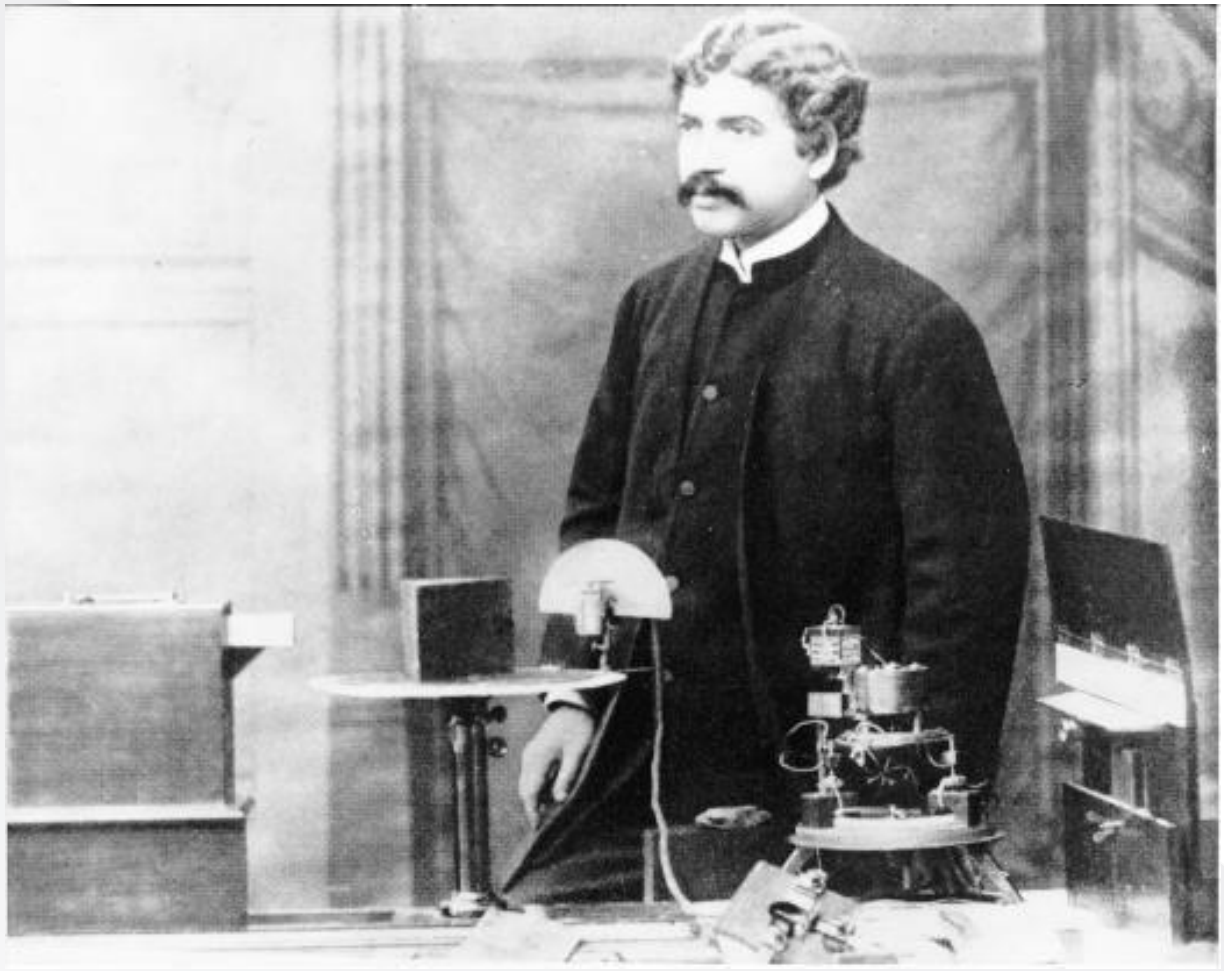

In 1895 Bose gave his first public demonstration of electromagnetic waves, using them to ring a bell remotely and to explode some gunpowder. In 1896 the Daily Chronicle of England reported: ***"The inventor (J.C. Bose) has transmitted signals to a distance of nearly a mile and herein lies the first and obvious and exceedingly valuable application of this new theoretical marvel."***

"Popov in Russia was doing similar experiments, but had written in December 1895 that he was still entertaining the hope of remote signaling with radio waves."

"The first successful wireless signaling experiment by Marconi on Salisbury Plain in England was not until May 1897."

Source: D. T. Emerson, "The work of Jagadis Chunder Bose: 100 years of mm-wave research," *IEEE Trans. Microwave Th. Tech.* December 1997, 45, No. 12 (2267-2273)

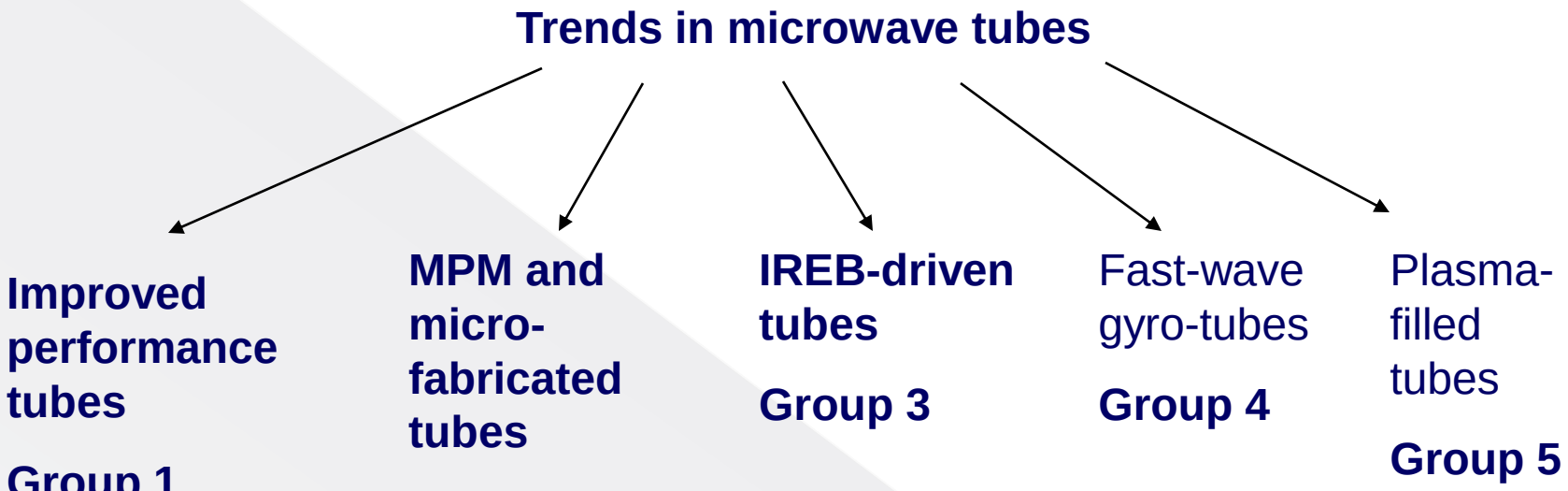
Trends in microwave tubes
Improved performance tubes
Group 1
MPM and micro-fabricated tubes
Group 2
IREB-driven tubes
Group 3
Fast-wave gyro-tubes
Group 4
Plasma-filled tubes
Group 5

Grouping of microwave tubes

Group 1	**Improved performance tubes: TWT (ultra-wide bandwidths, high efficiency); Klystron (high-power klystron, EIK— wider bandwidths, higher power, EIO — millimeter-wave, low-power, MBK (large beam current, low effective beam perveance, low beam voltage, tube compactness at higher RF powers)**
Group 2	**MPM and microfabricated tubes: MPM: (ground and air-borne platforms, ECM and towed decoys, phased-array and power-combined EW, mobile and satellite communication, missile seeker and surveillance radar); Microfabricated tubes: Triode, Klystron, Klystrino, FW-TWT (folded waveguide TWT), etc.**
Group 3	**HPM tubes driven by IREB: VIRCATOR (no magnetic fields), BWO, Orotron (RDG), MWCG (multi-wave Cerenkov generator), MWDG (multi-wave diffraction generator), MILO (magnetically insulated line oscillator (no external magnetic field, magnetic insulation), Relativistic klystron, RELTRON, relativistic BWO, etc.**
Group 4	**Fast-wave gyro-tubes: Gyrotron (High-harmonic, low magnetic fields, Large-orbit, Vane-loaded, Coaxial-cavity, Quasi-optical, etc.); Gyro-TWT (dielectric-loaded, disc-loaded, frequency multiplying, etc.); Gyro-klystron; Gyro-twystrons, PHIGTRON (phase-coherent, harmonic multiplying, inverted gyro-twystron); Gyro-BWO; CARM; SWCA; Peniotron, etc.**
Group 5	**Plasma-filled tubes: Pasotron (BWO) (IREB-driven Group 3), Coupled-cavity TWT (Group 2), Helix TWT, Gyrotron (Group 4) (Plasma filling for large beam transport, relaxation of magnetic field, larger structure cross section, etc.)**

Trend	Tubes	Some Features/Comments
Improved performance conventional microwave tubes	Wideband electronic warfare TWTs, high efficiency, long-life, light-weight space-TWTs, high power compact multi-beam klystrons,etc.	Innovative tube-envelope/tapered dielectric helix-support/pitch profiling/depressed collection Multi-beam electron gun
Tubes accruing the advantages of both vacuum and solid-state devices/electronics	Micro-fabricated tubes: folded-waveguide TWT, reflex klystron, etc. Microwave power module (MPM)	Terahertz generation/ batch production
IREB driven tubes for HPM/DEW/ Information warfare applications	VIRCATOR, MILO, relativistic backward-wave oscillator, relativistic klystron (RELTRON), OROTRON, etc.	Bremsstrahlung of electrons in electrostatic field (VIRCATOR) E-bomb using a magnetic flux compression generator (FCG) in conjunction with a VIRCATOR Self focussing (MILO)

Fast-wave tubes	**Gyrotron, gyro-TWT, gyro-klystron, etc.**	**Filling up of mm-wave technology gap in high power domain Bremsstrahlung of electrons in magnetic field, Periodic beam Coaxial structure, PBG structure for mode selection/rarefaction**
Plasma-filled tubes	**Plasma-assisted TWT, pasotron, gyrotron, etc.**	**Space-charge neutralization for enhanced beam current transport/relaxed focussing Development of PCE gun**

Organisation	Activity areas and status
Institute of Radiophysics and Electronics (Calcutta University), Kolkata	Establishment of the facilities for the development of magnetrons in late 1950's (since discontinued) Significant contribution to understanding the non-linear theory of electron beam parametric amplifiers by N. B. Chakrabarti Subsequently motivated study on nonlinear effects in multi-beam and beam-plasma devices and in TWTs, elsewhere in the country
National Physical laboratory (NPL), New Delhi (CSIR)	Development of magnetrons initiated at National Physical laboratory (NPL), New Delhi (CSIR) by Amarjit Singh and N. C. Vaidya Subsequent shifting of activities to Central Electronics and Engineering Research Institute (CEERI), Pilani (CSIR)

Central Electronics and Engineering Research Institute (CEERI), Pilani (CSIR)	**Magnetron, Carcinotron, TWT (wide bandwidth, high efficiency), klystron, multi-beam technology, high emission density cathode, gyrotron, plasma-assisted tubes, HPM tubes (initiated)**
Centre of Research in Microwave Tubes (CRMT), Banaras Hindu University (BHU), Varanasi	**Established at the Banaras Hindu University (BHU) in 1979 by N. C. Vaidya Analysis of helical structures, broadbanding of TWTs, nonlinear Eulerian dynamics for harmonic and inter-modulation effects in TWTs, analyses of gyro-TWTs and gyrotrons, broadbanding of gyro-TWTs**
Microwave Tube Research and Development Centre (MTRDC), Bangalore (DRDO)	**Established in 1984 Helix and coupled-cavity TWTs, high emission density cathodes, gyro-TWTs, HPM tubes (initiated)**

Electronics and Radar Development Organisation (LRDE), Bangalore (DRDO)	**Vulnerability of electronic systems to HPM generated, for instance, by the VIRCATOR in collaboration with MTRDC and BARC**
Bhaba Atomic Research Centre, Mumbai (DAE)	**Vulnerability of electronic systems to HPM generated, for instance, by the VIRCATOR in collaboration with MTRDC and LRDE**

Bharat Electronics (BE) Limited, Bangalore	**Manufacturer of microwave tubes such as magnetrons, klystrons and TWTs**
Pilani Electron Tubes, Sangrur	**Established by G. S. Sidhu Manufacturer of high power transmitting tubes having potential for manufacturing magnetrons**
Indian Institute of Technology (IIT), Roorkee	**Gyrotron theory due to M. V. Kartikeyan (with support from Karlsruhe Institute of Technology) Participation in a multi-institutional project for the development of the first ever gyrotron with CEERI, Pilani as the nodal centre**
Devi Ahalya Vishwa Vidyalaya (DAVV), Indore	**Initiated by K. P. Maheshwari and Y Choyal in the development of relativistic microwave tubes (TWTs and oscillators)**

Wideband multi-octave TWTs for EW applications

Zero-to-slightly-negative-dispersion structure for wideband performance:

- **Negative dispersion ensures the constancy of Pirece's velocity synchronization parameter *b***
  - **Anisotropically loaded helix:**
  - **Metal vane/ segment loaded envelope**
  - **Inhomogeneously loaded helix:**
    - **Helix with tapered geometry dielectric supports such as half-moon-shaped and T-shaped supports**
- **Multi-dispersion, multi-section helix for wideband performance:**
  - **The value of *N* in the gain parameter *CN* depends on both the frequency and the interaction helix length.**
  - **One positive-dispersion helix section of length l_1 is synchronous only at lower frequencies and the other no-dispersion helix section of length l_2 is synchronous both at lower and higher frequencies.**
  - **Causes an increase in effective length to $l_1 + l_2$ at lower frequencies and a decrease in effective length to l_2 at higher frequencies**
  - **Reduction of length at higher frequencies prevents oscillation at higher frequencies**

MBK — multi-beam klystron

A parallel arrangement of low-perveance beamlets within a common RF structure for

- **Large beam current and RF output power**
- **Low beam voltage and compactness due to reduced plasma wavelength (= beam velocity/ plasma frequency)**
- **PPM-stacked device**

Each beam propagates in its own channel and then interacts with the field of a common interaction structure.

The space-charge effects and correspondingly the efficiency are the same as that of a single-beam tube but the beam current, beam perveance and power increase with the number of beamlets.

Typical SLAC MBK

- **10 individual 500 kV, 500 A (1.5 microperv) beams**
- **Output: 1 GW, 1 μs, 1.5 GHz, 36 dB gain, 40% efficiency**

Typical L-3 Communications Electron Devices MBK

- **10 individual 115 kV, 13 A (1.6 microperv) beams**
- **Output: 10 MW, 1.5 μs, 1.3 GHz, 47 dB gain, 70% efficiency**

Advantages of MBKs over conventional klystrons

The space-charge effects and correspondingly the efficiency are the same as that of a single-beam tube but the beam current, beam perveance and power increase with the number of beamlets.

- **Reduced cathode voltage (40 to 50% less)**
- **Possible increase in pulse length**
- **Increased reliability of the HV power supply**
- **Fewer risks of gun arcing**
- **Smaller size at a given power level**
- **Easier protection against X-rays**
- **Higher efficiency**
- **Wider bandwidth**

Devices accruing the advantages of solid-state devices and technology

- **Microwave power module (MPM)**
- **Vacuum microelectronic tubes**

MPM Capitalizes relative strengths of both the solid-state and vacuum-electronic technologies
Utilises miniature, high-efficiency electronic power conditioner (EPC) technology to build a compact power amplifier

Vacuum-microelectronic (microfabricated) tube fundamental advantages: (i) electron velocity in vacuum about a thousand times grater than that in semiconductor solids, and higher signal processing speeds, (ii) less collisions of moving electrons with atoms and less associated energy loss as heat, (iii) precision dimensioning of parts/ electromagnetic structures in the millimeter-wave and terahertz regimes, (iv) cold field-emission arrays cathodes (such as carbon nanotubes), batch production, etc.

Microwave Power Module (MPM)

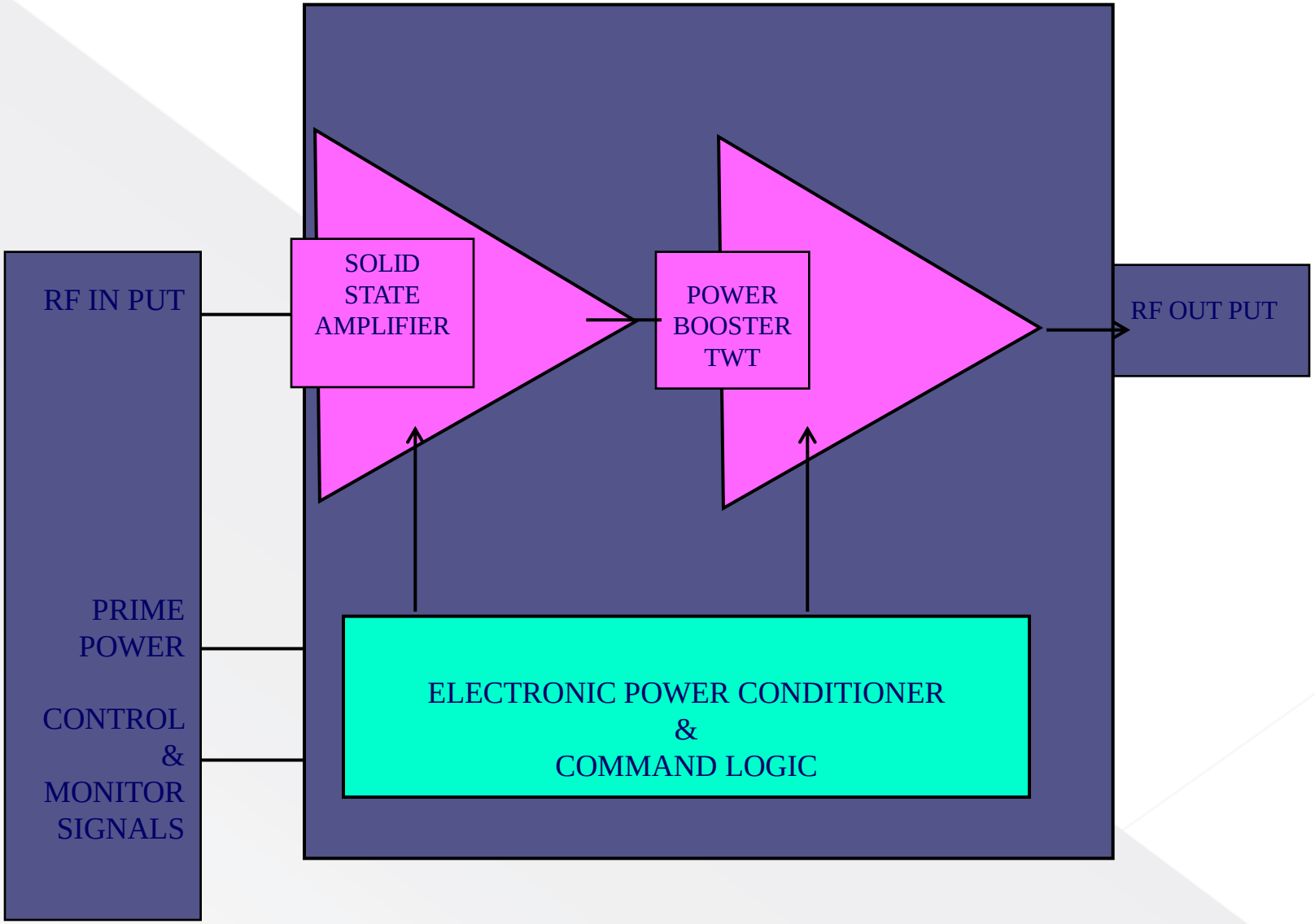

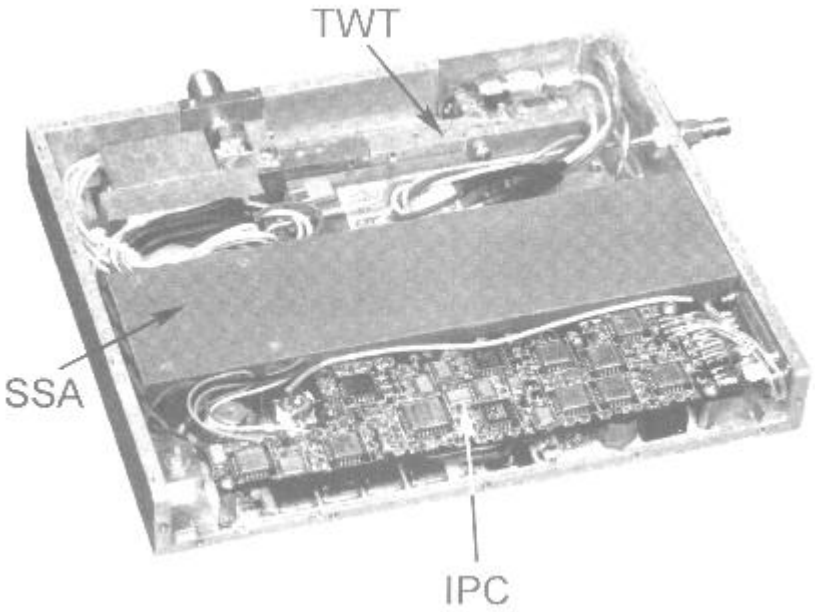

An 80-W, 6- to 8-GHz wideband MPM

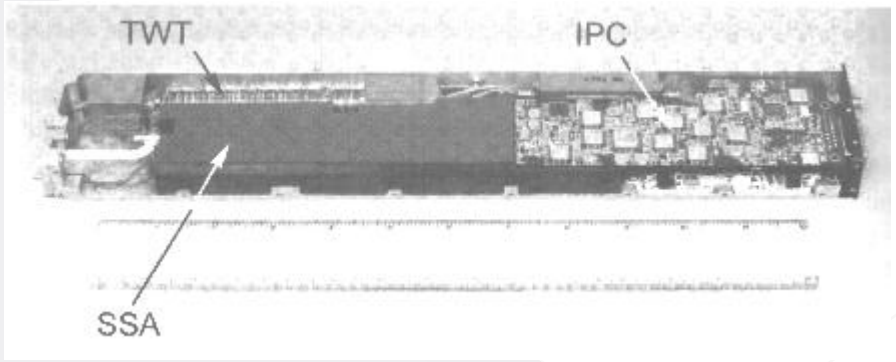

Ka-band MPM

MPM in power versus frequency domain

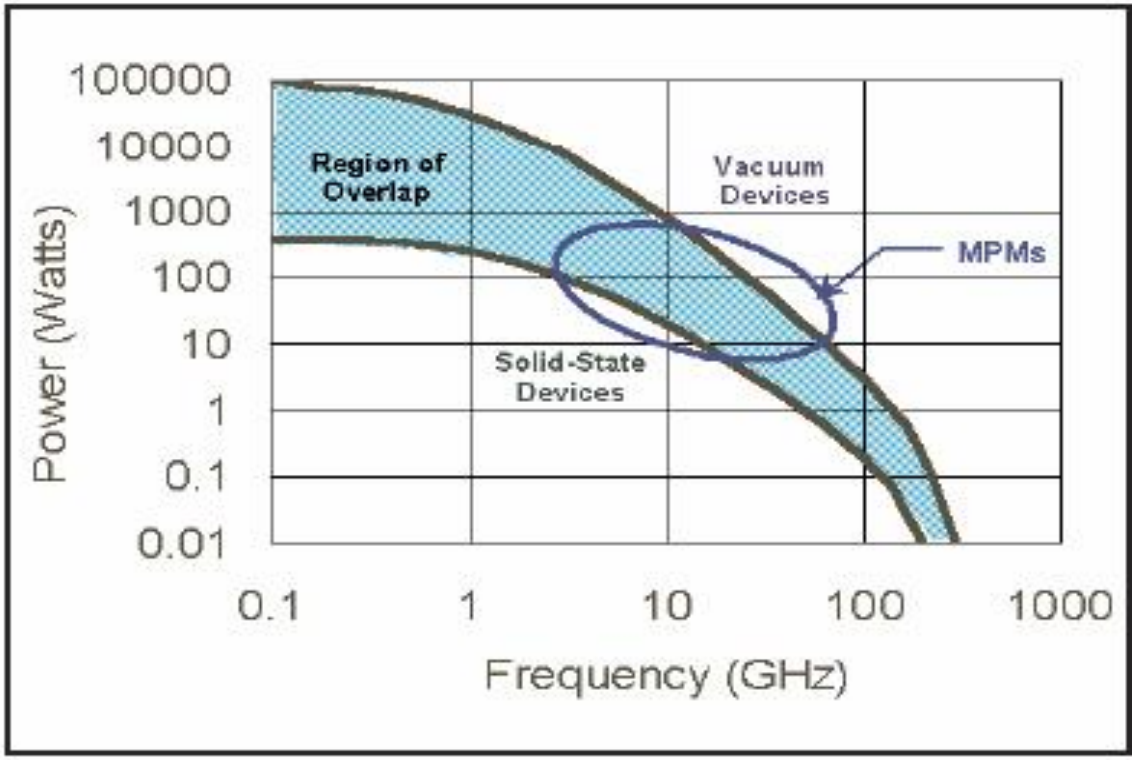

Vacuum microelectronic tubes in terahertz regime

Micro-fabricated TWTs

Folded waveguide slow-wave structure using microfabrication techniques like

- **EDM — electric discharge machining**
- **DRIE — deep reactive ion etching**
- **LIGA — lithographie, galvanoformung, abformung**

Example: A folded (serpentine) trench is etched in silicon with a DRIE tool, and then gold-plated. Two such trenches bonded together form a folded waveguide

Field emission array cathode

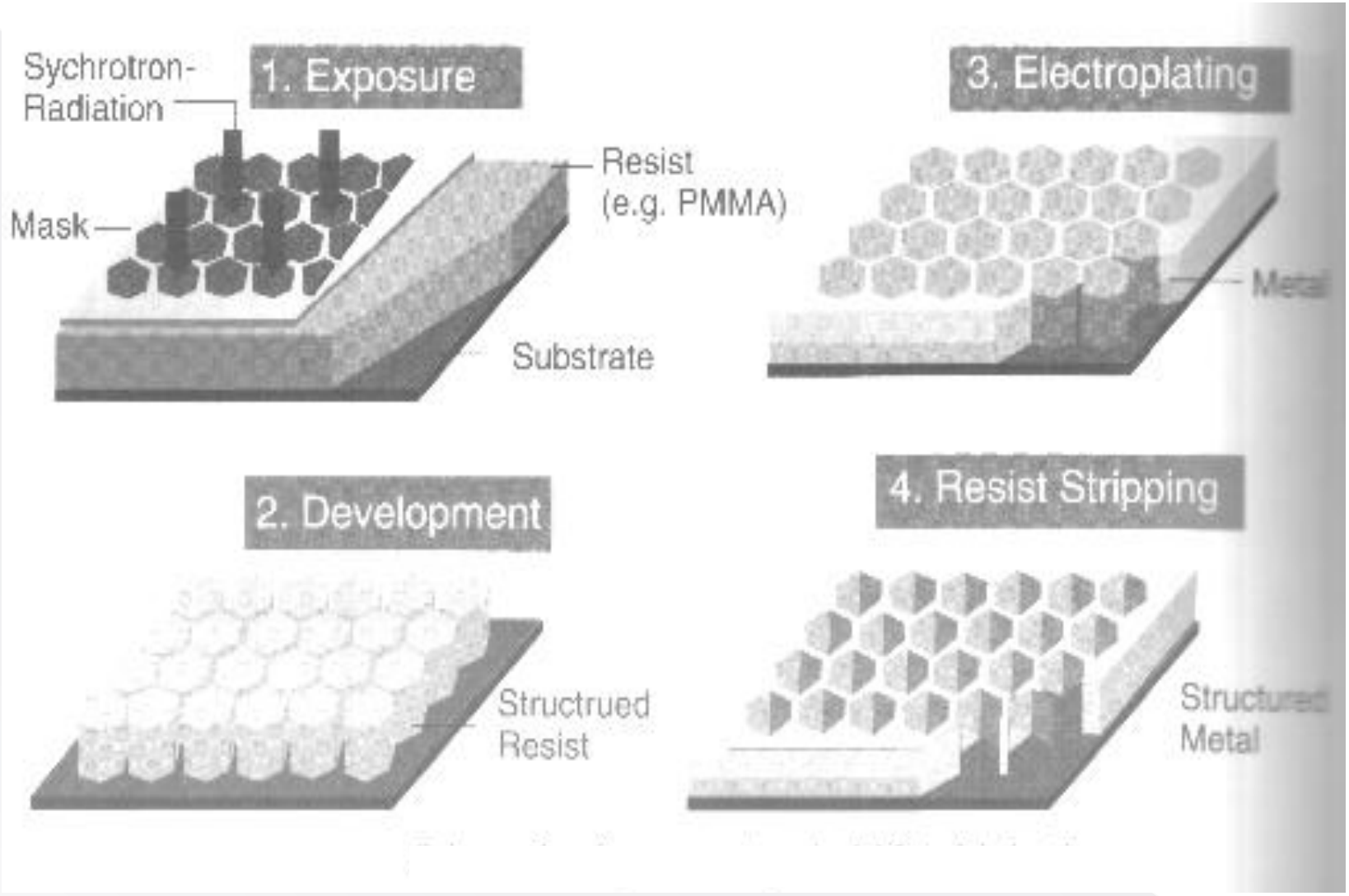

Schematic of process steps in LIGA fabrication

Gold-plated chrome mask
Polymethyl metahacrylate resist
Aluminum substrate (low atomic number to reduce back scattering)

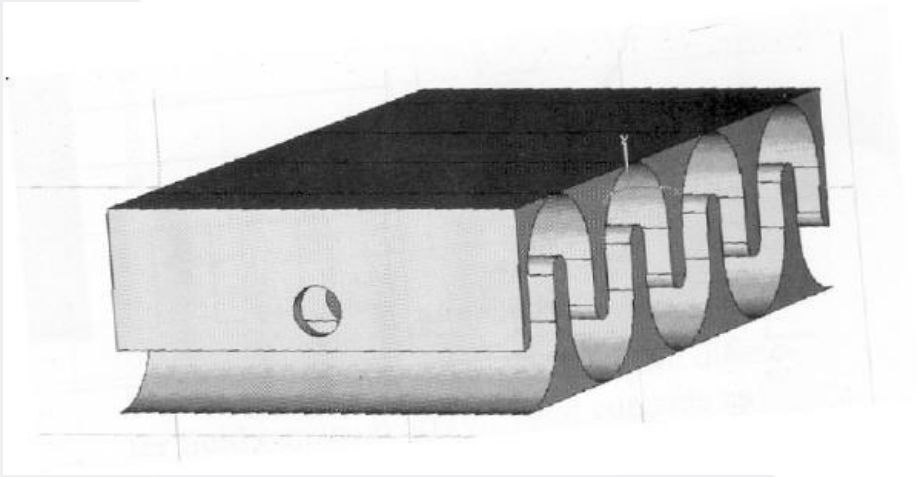

Folded waveguide for a TWT

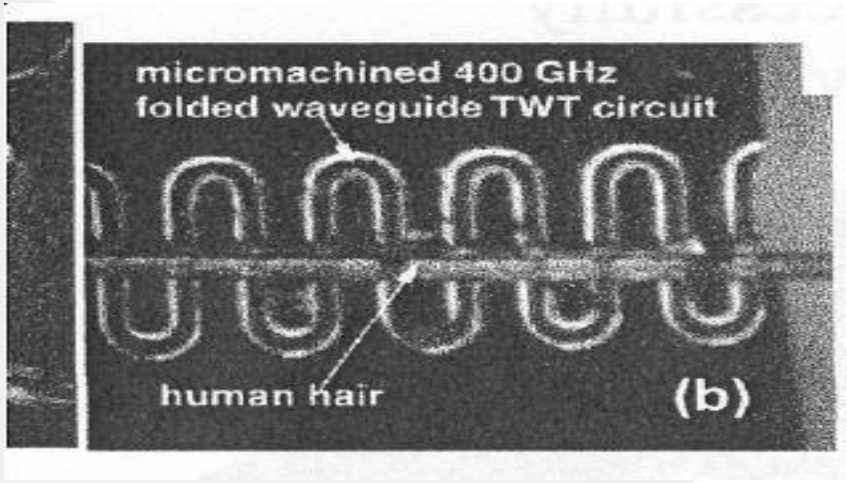

Vacuum microelectronic klystrino

W band (~3 mm wavelength) Klystrinos in a klystron module
Dimensioning of conventional klystrons difficult in the millimeter-wave band
Lightweight PPM focusing possible in a klystrino
LIGA microfabrication technique for W-band klystrino cavity features with 2-3 μm tolerances and excellent surface finish

A typical klystron module, with 6 klystrinos in parallel, has separate electron guns 0.6 microperv each, cavities and PPM stacks, but a common vacuum and beam dump
Typical W-band klystrino parameters: 120 kV, 15 A; 0.5 MW peak, and 5 kW average; 6 inch dia, 12 inch length, < 20 lbs weight.

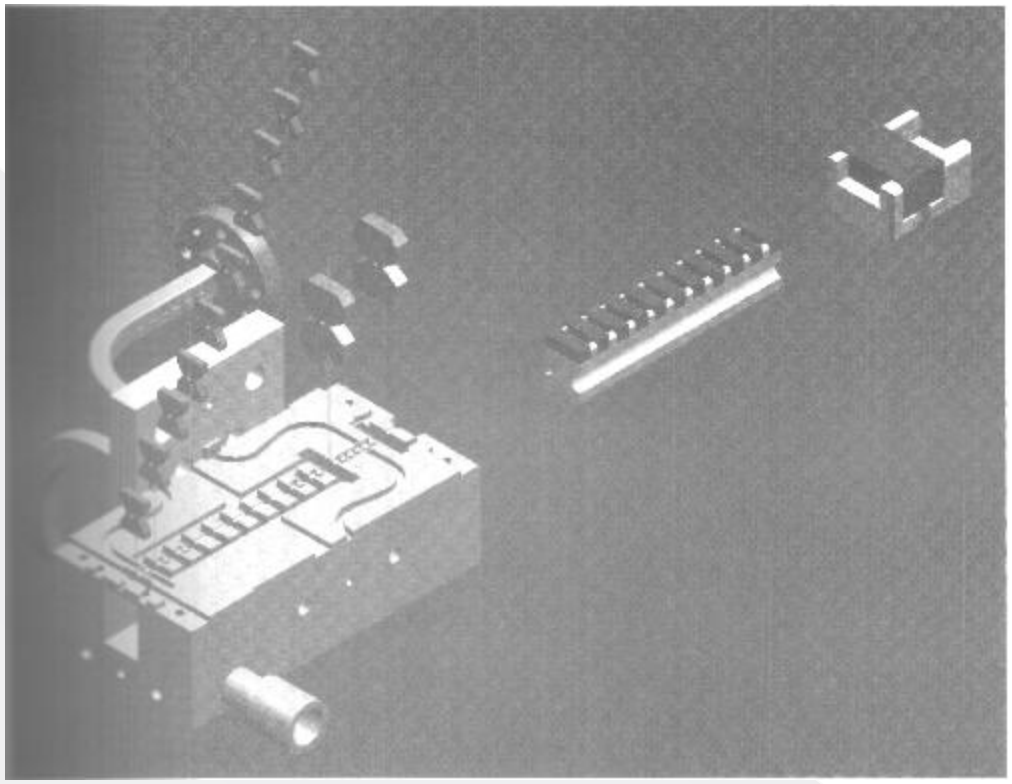

Explored model of klystrino circuit assembly with PPM pole pieces and magnet.

Nanoklystron: a monolithic terahertz reflex klystron

Carbon nanotube field emitter

The structure is formed monolithically from two thermo-compression bonded silicon wafers processed using deep reactive ion etching (DRIE) technique and using carbon nanotube field emitter

~mW power at 1.2 THz

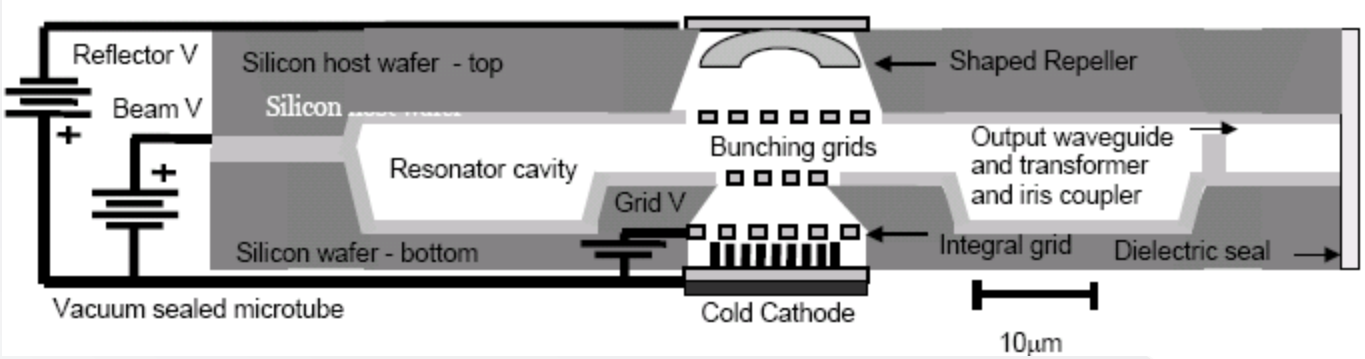

PH Siegel, and others: 12th Int. Conf. Space THz Technology, San Diego, Feb 14-16, 2001

HPM (1-100GHz)

Refers to:

i) long pulse duration, high-prf, or CW

ii) high-peak power, short-pulse duration, low-prf or single-shot

Both military and civilian applications:

Military — Conventional electronic warfare (EW) in the high power level Directed energy weaponry (DEW) of both the hard-kill type (physical destruction of targets), and the soft-kill type (making enemy's mission critical components either inoperative or faulty)

Civilian — Satellite power stations (SPS), Artificially ionised layer (AIL): remote radio and TV communication, remote spectroscopy of atmosphere, city lighting and nitrogen fertiliser generation, Environmental control: repair of ozone hole, atmospheric purification of admixtures that destroy the ozone layer, etc.

… HPM–DEW

Hard-kill type:

Physical destruction of targets, burnout of or lethal damage to enemy electronic systems

Soft-kill type:

Making enemy's mission-critical components either inoperative or faulty

10^{-7} Jcm^{-2} is good enough to cause bit error in computers and computer-aided equipment!), deception or spoofing of enemy systems into mission failure, temporary upset or disruption of enemy electronic systems, jamming of enemy microwave or RF receivers or radar sets to disrupt detection, communication and control systems

… HPM–DEW

Non-lethal weaponry

provides 'friendly' troops with the ability to remotely neutralise the communication systems of 'aggressive' forces without loss of life on either side

Energy, instead of matter, to be directed on targets

Attacks at high speed

Ammunition

Relies on power supply rather than on magazines of explosives

Spreading of microwaves by diffraction

Accommodates lack of tracking precision requiring no pinpointing of a target, as in laser warfare

Coarse pointing of targets

Large image zone

All-weather performance

Exploits the vulnerability of small-size electronic components

Effective even if the enemy system is switched off

… HPM-DEW

Typical parameters of HPM tubes:

Frequency: 10 MHz – 100 GHz

Power: 100 MW – 100 GW

Pulse width: Up to 1 msec

Duty factor: Single shot to 0.002

Intense electromagnetic pulse (EMP) of peak powers ~10's of TW of very short duration ~100's of ns (shock-wave) can be used for a directed energy weapon (DEW) may be generated typically by 'Electromagnetic Bomb' made out of an HPM tube and a flux compression generator

Coupling Mechanisms:

Front door : through transmitting /receiving antennas

Back door : Power connector cables, grills/holes in enclosures, display screens of computers, etc.

Effect of HPM on systems

- Dielectric heating
- High voltage transients
- High voltage breakdown
- Deception or spoofing of target to mission failure
- Jamming of radar, communication or control systems
- Temporary upset or disruption of electronic systems
- Burn-out of electronic devices

Breakdown voltage ratings of electronic devices

Silicon high frequency bipolar transistor: 15 V – 65 V
Gallium arsenide FET: ~ 10V
Dynamic random access memories (DRAM) ~ 7 V
CMOS logic: 7 V – 15 V
Microprocessor: ~ 5 V

Upset levels for electronic devices

Type	Power (W)	Energy(J) @ 1msec
Operational amplifier	0.0009	9×10^{-10}
TTL device	0.008	8×10^{-9}
CMOS device	0.001	10^{-9}
Voltage regulators	0.09	9×10^{-8}
Comparator (output switches)	0.008	8×10^{-9}
VHSIC (pulsed exposure)	0.1	10^{-7}

Courtesy: SUM Reddy/S Kamath

Electronic device burnout thresholds

Component	Energy (J)
GaAs MESFET	10^{-7} – 10^{-6}
MMIC	7 x 10^{-7} –5 x 10^{-6}
Microwave diodes	2 x 10^{-6} –5 x 10^{-4}
VLSI	2 x 10^{-6} –2 x 10^{-5}
Bipolar transistor	10^{-5} –10^{-4}
CMOS RAM	7 x 10^{-5} – 10^{-4}
MSI	10^{-4} –6 x 10^{-4}
SSI	6 x 10^{-4} –10^{-3}
Operational amplifiers	2 x 10^{-3} –6 x 10^{-3}
Courtesy: SUM Reddy/S Kamath	

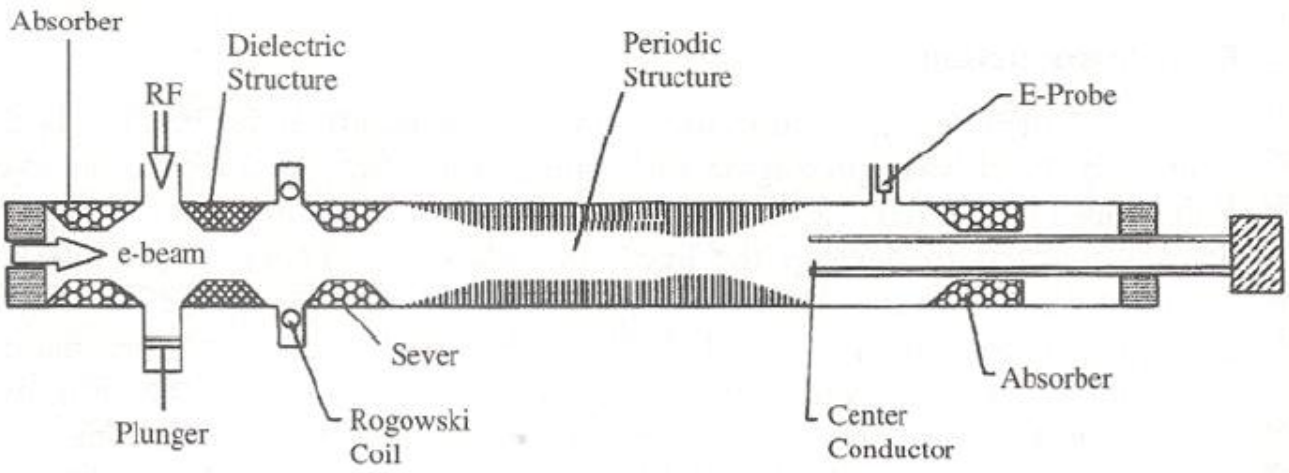

Relativistic TWT

Capable of delivering large RF power due to high beam voltage/ high beam power

Larger dimensions due to high beam voltage

Synchronisation is maintained even if significant reduction in beam kinetic energy takes place

VIRCATOR

Virtual Cathode oscillator (vircator): Simple, no magnetic field required, single-shot device, low cost, tunable by controlling the space-charge density

Bremsstrahlung device in an electrostatic field realised in a waveguide resonator

Virtual cathode forms beyond the anode at a distance equal to the anode-cathode spacing

Beam current > Space-charge limiting current

Space-charge limiting current in a metal drift tube:

Radial space-charge electric field (potential gradient) gives a radial electron velocity at the expense of longitudinally directed electron velocity. At the space-charge limiting current, the electrostatic potential energy corresponding to the potential difference between the beam and the drift tube equals the electron kinetic energy, and the beam electrons cannot propagate forward Analogous to an *LC* oscillator generating microwaves, the virtual cathode acting as a capacitor *C* in storing the beam kinetic energy, and the beam current itself being like a time- varying current through an inductor *L*

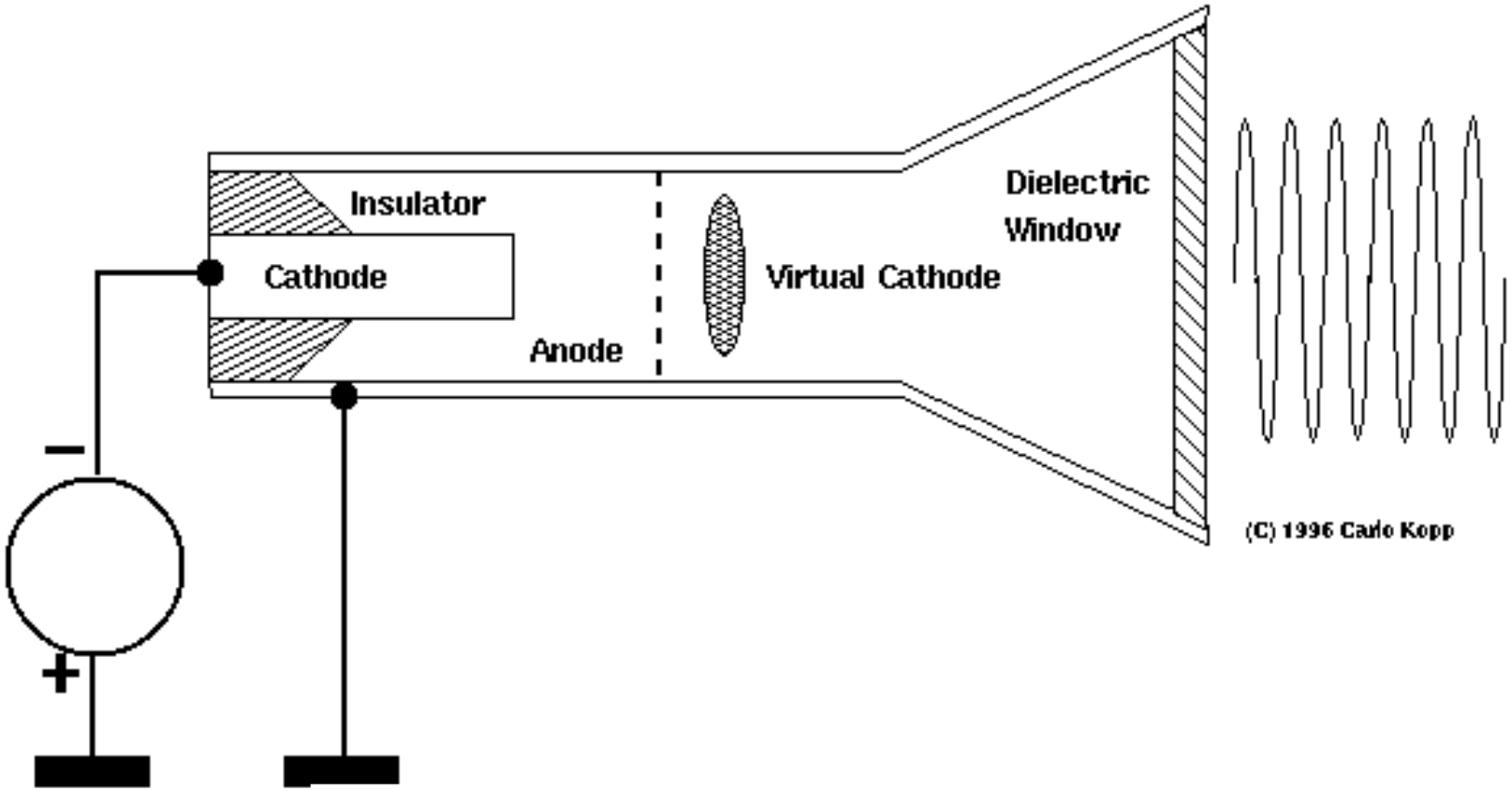

Virtual cathode oscillator (VIRCATOR)

VIRCATOR

Types:

Axial extraction (TM mode)

Transverse extraction (TE mode)

Coaxial structure

Reditron (with the anode foil replaced by a thick metal anode with large holes)

Typical output parameters:

1 GW, 400-800 MHz, 75-125 ns, 100 J, single shot (220 lb)
400 MW, 435-544 MHz, ≤140 ns, 56 J, single shot (500 lb)
1GW, 2-4 GHz, 30 ns, 50 J, single shot (220 lb)

Typical beam voltage and current: 200 kV-6.5 kV; 10-100 kA (25 ns-1.7 μs)

Other typical reported specifications:

20 GW below 1 GHz; 7.5 GW at 1.7 GHz; 4 GW in C-band;
1 GW in X-band; 0.5 GW at 17 GHz

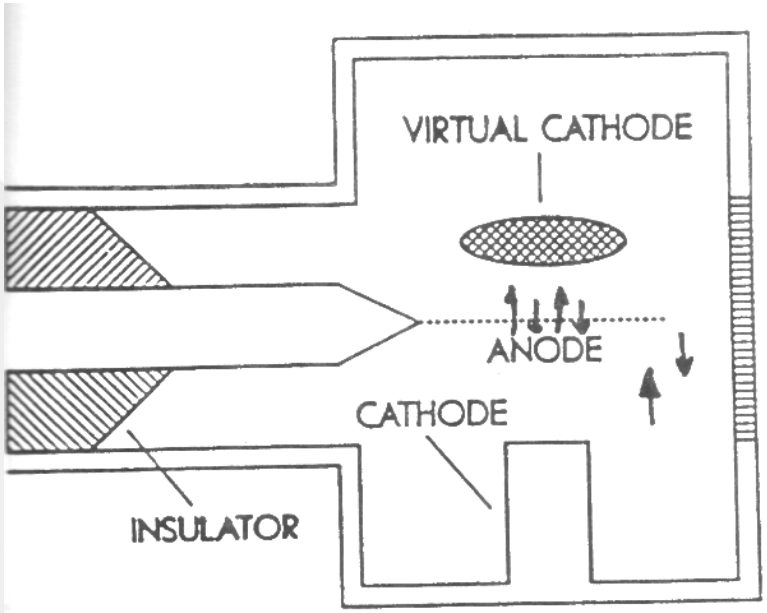

SIDE
EXTRACTION

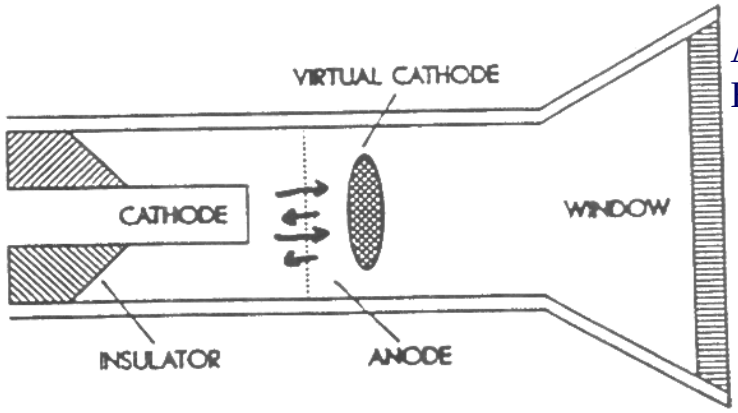

AXIAL
EXTRACTION

HPM system configuration

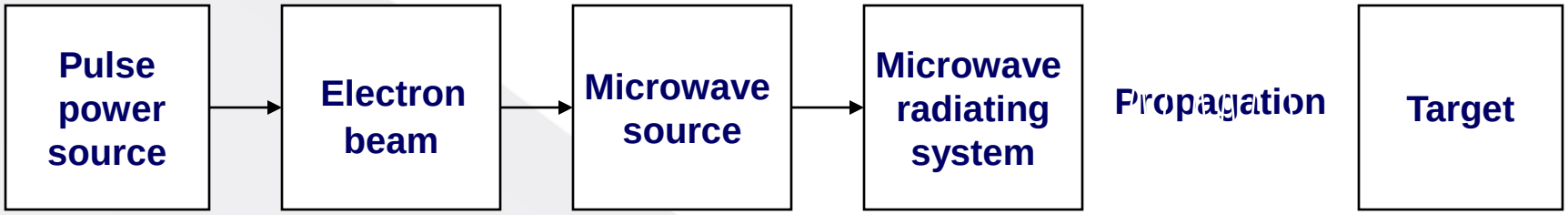

Typical vircator-antenna assembly

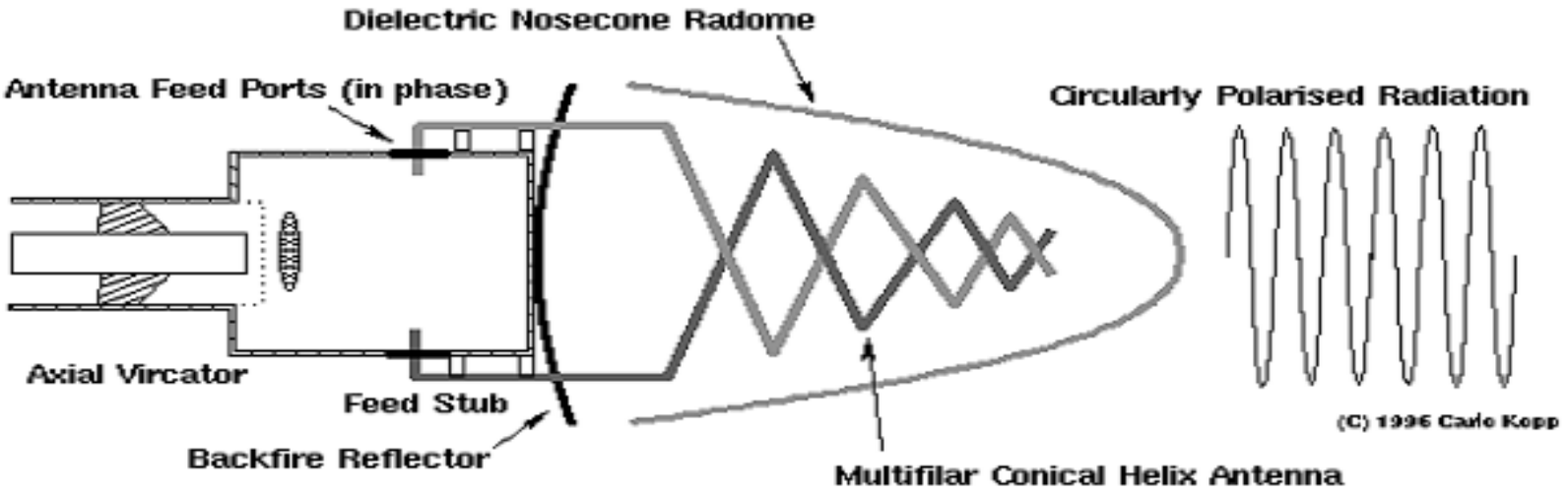

HPM E-bomb warhead

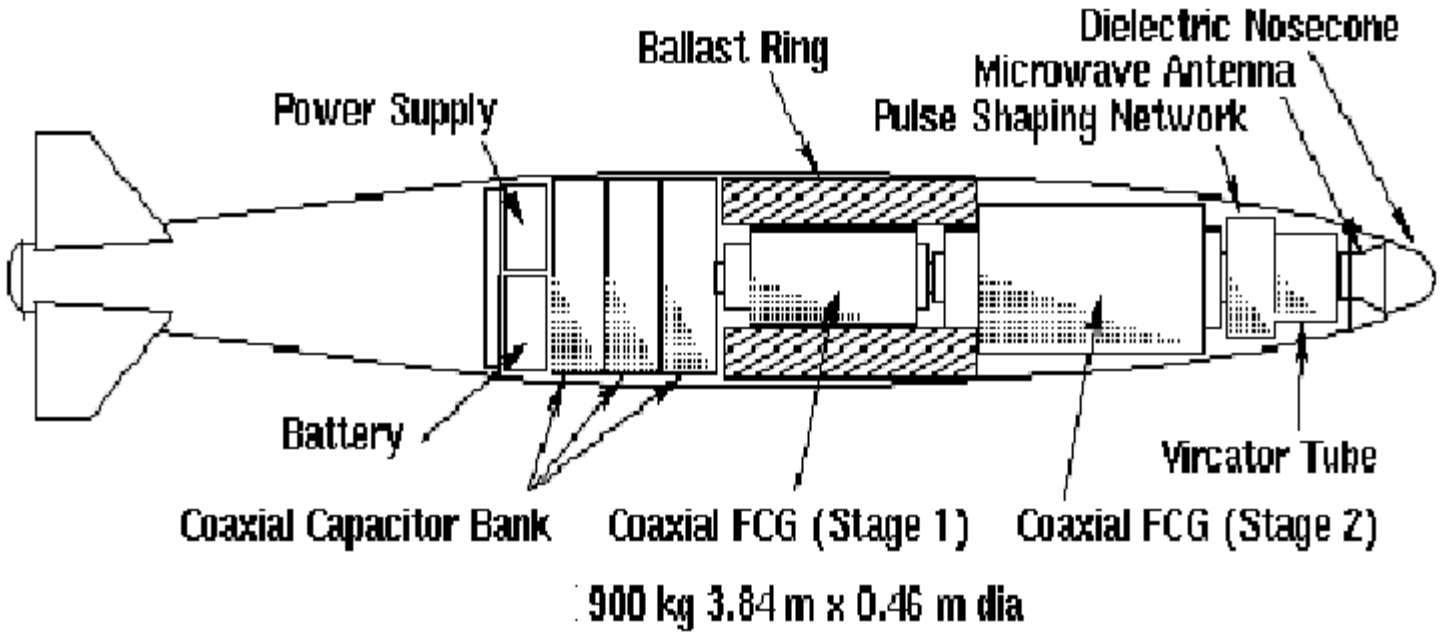

E-bomb

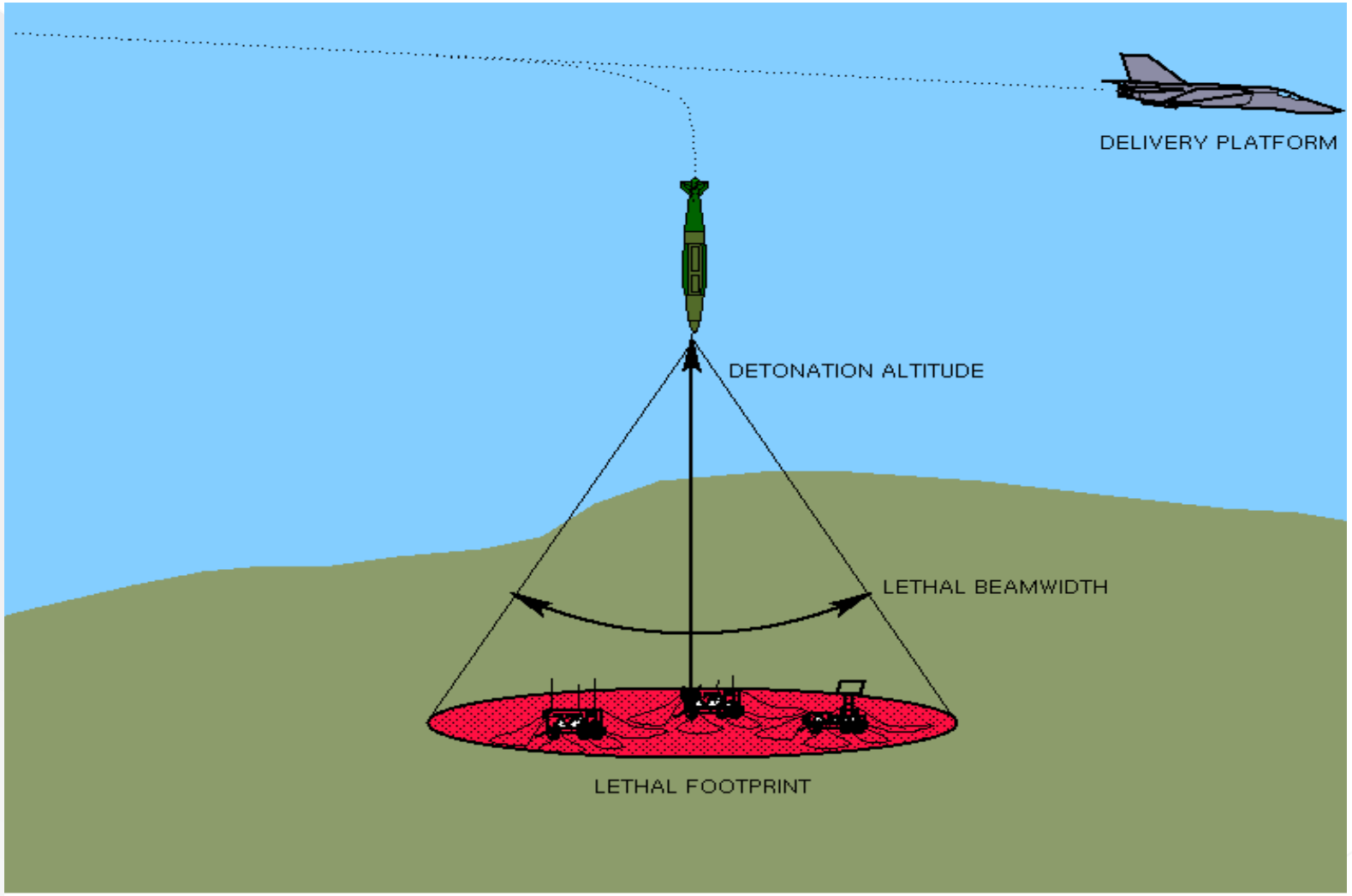

Lethal footprint of an E-bomb in relation to altitude

MILO

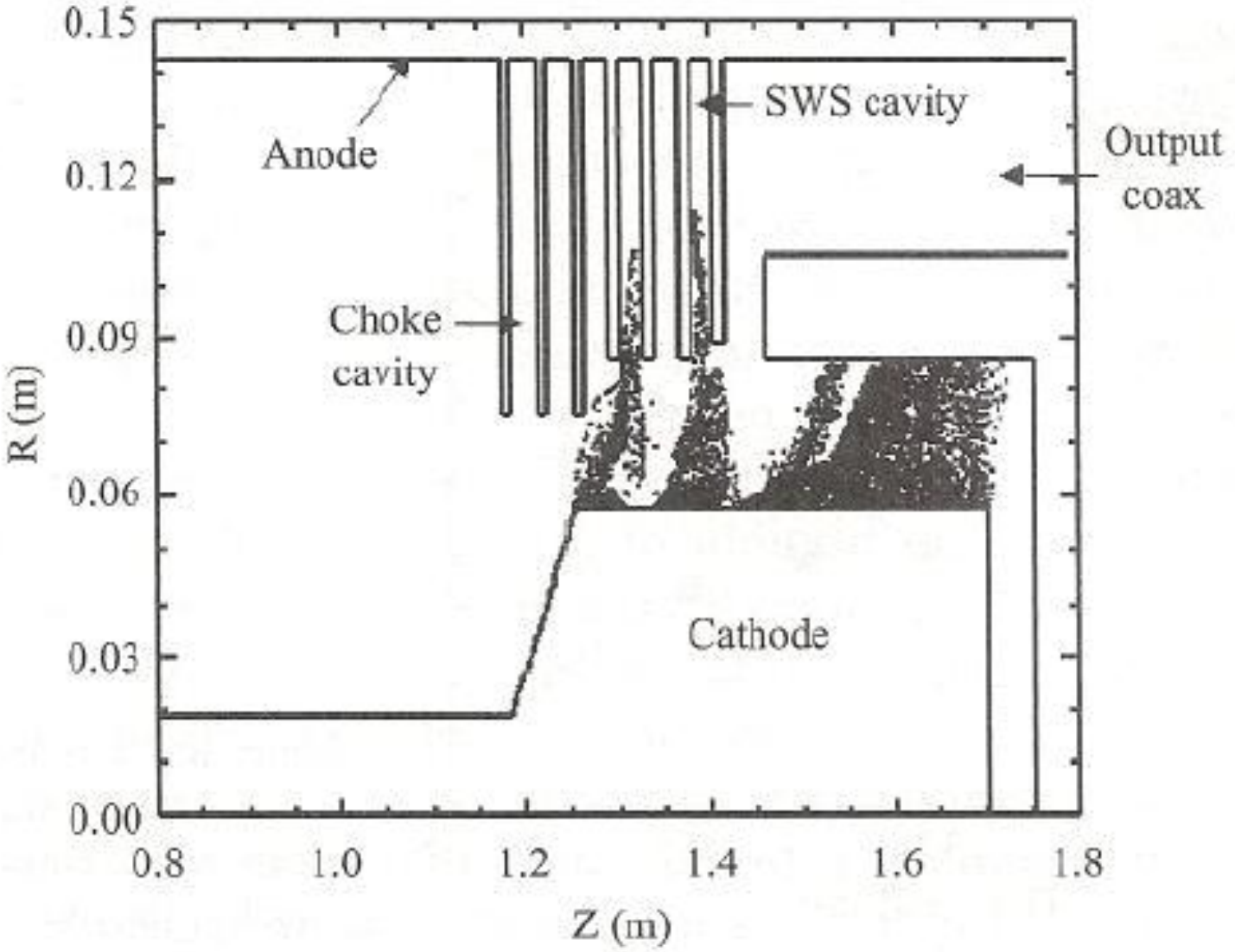
0.15
0.12
0.09
0.06
0.03
0.00
R (m)
0.8
1.0
1.2
1.4
1.6
1.8
Z (m)
Anode
SWS cavity
Output coax
Choke cavity
Cathode

…MILO

Magnetically insulated line oscillator — MILO

A crossed-field device but requires no external magnetic field

- unlike a magnetron

Self-generated magnetic field

Intrinsic electron current generates azimuthal magnetic field

Azimuthal magnetic field inhibits electron flow from reaching the anode prior to oscillation (provides self insulation)

Self-insulating property inhibits electrical breakdown of the anode-to-cathode gap

- Can handle 10-100's of GW at a voltage of 100's of kV.

Typical MILO experimental parameters:

- 50 MW, 75 ns; 300 MW, 10 ns

Tapered MILO for better efficiency and output power

- First group (4-5) uniform cavities define the oscillation frequency
- Second group of tapered cavities increase the group velocity, amplifies microwave signal and transforms into a travelling-wave mode in the output line.
- Placement of the diode within the slow-wave region allows for energy recovery from the diode circuit.

Plasma-assisted tubes

- **Neutralization of the space-charge by the plasma (denser the beam) allowing higher electron current transport (50-1000 A cm^{-2})**
- **Beam transport is provided by ions produced by the impact of the electron beam on neutral gas molecules**
- **Ions causing the partial compensation of beam space-charge forces, causing the beam to pinch (ion channeling) resulting in self focussing known as the Bennett effect**
- **Higher frequencies for a given tube size since the phase velocity of electromagnetic waves in a plasma is higher than in vacuum [size~ λ; $v_{ph} = f\lambda$)]**
- **Performance improvement with respect to**
  - **bandwidth (~30%)**
  - **efficiency (>70%)**
  - **power output**
  - **long-pulse operation (~120 μs)**
  - **high-prf operation**

….

....

- **Larger interaction area as the beam could be placed far from the metal envelope**
- **No or less externally required magnetic field**
- **Passage of the electron beam → production of neutralizing ions → prevention of space charge blowup**
- **Axial electron beam current → azimuthal magnetic field → radially inward force on the beam (magnetic confining force)**
- **Allowance for misalignment of the magnetic field if any applied externally**

....

Plasma-filled TWTs

Robert W. Schumacher et al. 1990: U.S. Pat. No. 4,912,367 (assigned to Hughes Aircraft Company)

A plasma-cathode electron gun coupled to a gas-filled, slow-wave structure (SWS) in the form of a rippled-wall waveguide

Space-charge waves on the beam resonantly coupled to rippled waveguide modes→ transfer of energy from the electron beam to RF waves → coupling to space through an output horn antenna

Zero cutoff frequency of the helix → reduction of the tube diameter → reduction of the tube size and weigh and tighter coupling with the beam

Helix-waveguide coupling structure that facilitates a flow of cooling liquid through the helix to remove heat generated during high-power operation

TEM mode of operation of the helix and its surrounding housing → conversion into the TE_{10} mode in input and output waveguides by the helix-waveguide coupling structure

S. K. Datta, Lalit Kumar, and B. N. Basu, "Pierce-type one-dimensional Eulerian hydrodynamic analysis of a plasma-filled helix TWT," *IEEE Trans. Plasma Science,* March, 882-890 (2011).

Effect of plasma filing in CC-TWT

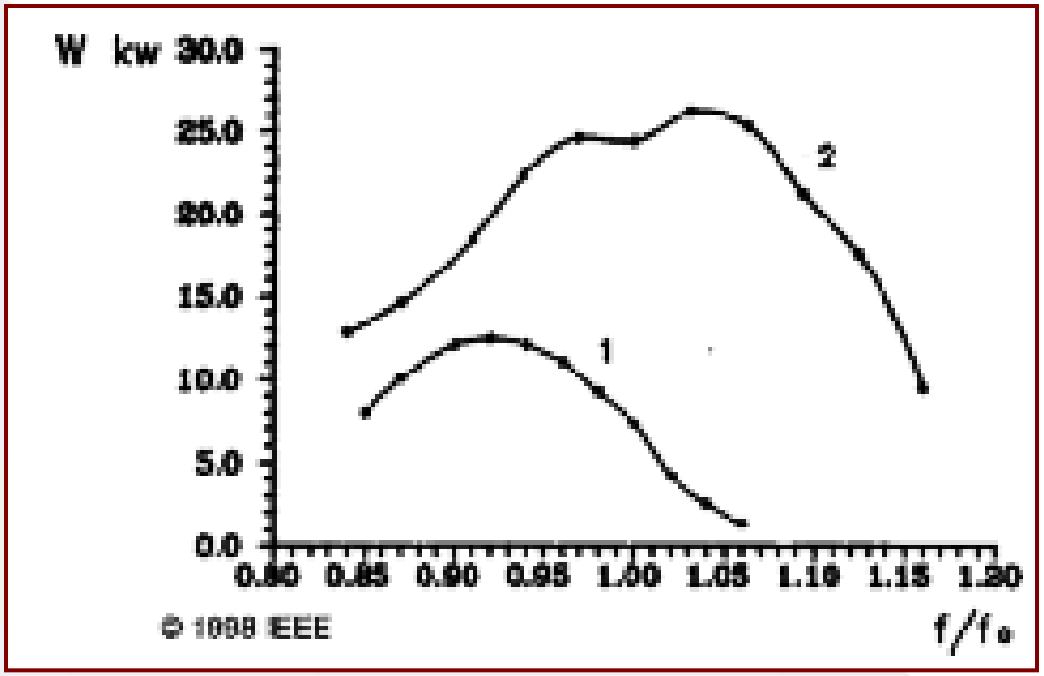

Output power vs frequency characteristics of a typical vacuum (1) and plasma-filled (2) coupled cavity TWT showing increased power and bandwidth with plasma filling

Nusonovich et al.: *IEEE-PS* 26 628-644 (1998)

Rippled-walled pasotron (plasma-assisted slow-wave oscillator)

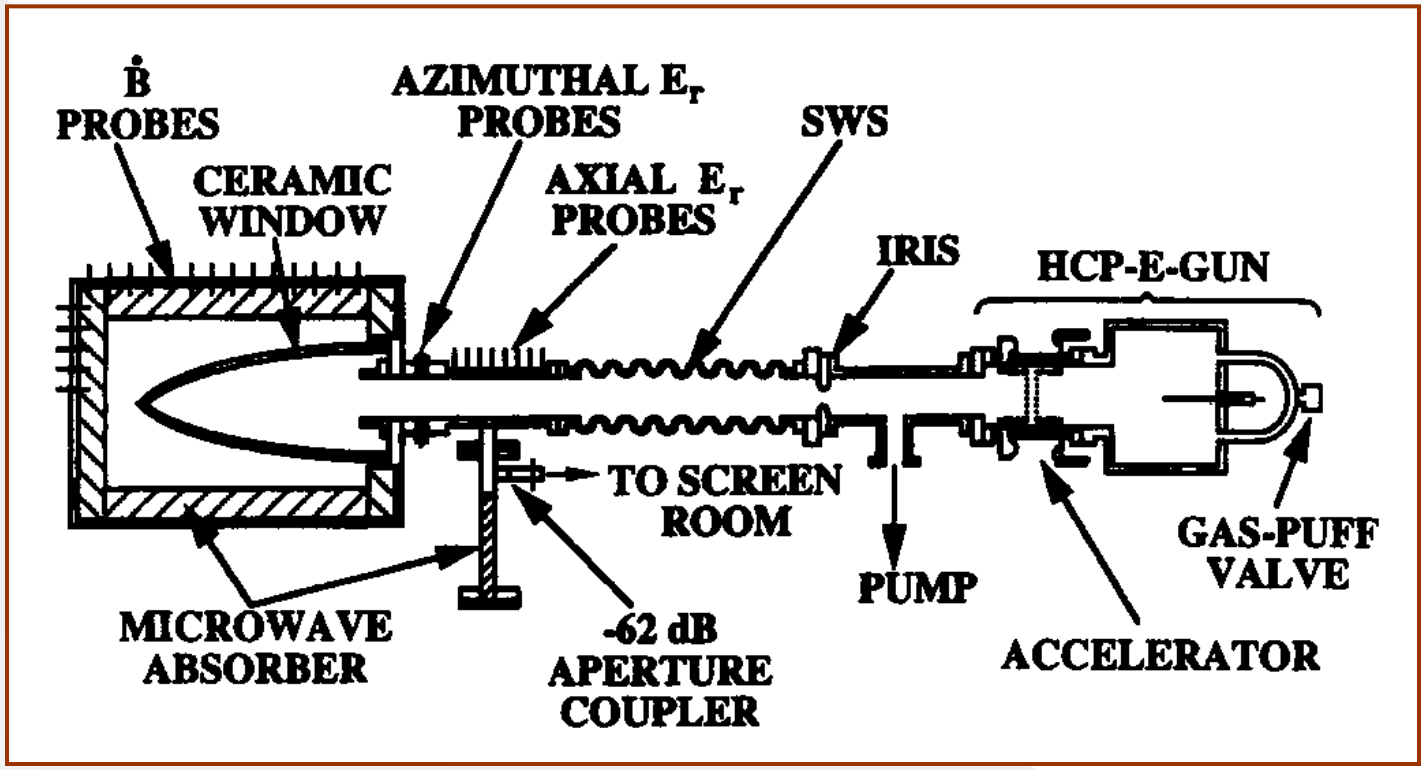

Pasotron schematic (Hughes make: JM Butler, RL Eisenhart, and AJ Schneider, *IEEE MTTT-S Digest*, 511-513 (1992)

Pasotron: a plasma-filled BWO

- **Plasma aids electron beam transport through the interaction region**
- **Plasma contributes to the improvement of coupling of the beam to the structure yielding higher efficiency**
- **Capable of repetitively fired operation and exceptionally reproducible shot-to-shot characteristics**
- **Plasma-cathode electron gun to create a plasma-fill through impact ionization of the background gas, typically, 5-50 mTorr helium or hydrogen for high-current density (50-1000 A/cm^2) and long-pulse operation (>100 μsec)**
- **No magnetic field required: beam confined by its own magnetic field**
- **Compact, lightweight**
- **Slow-wave structure: typically, 3.25 cm average radius, 0.715 cm ripple-depth, and 2.4 cm periodicity**
- **A reflective iris positioned upstream for forward-wave RF extraction**

Output: A typical L-band 200 kV PASOTRON produced 20 MW peak power (1 kJ per pulse)

Effect of plasma filing a typical gyrotron

Parameters	Without plasma	With plasma
Power	100-200MW	~1GW
Beam Current	1-3kA	~10kA
Frequency	35GHz	35GHz
Beam Voltage	0.60-1.35MV	0.60-1.35MV
Plasma Density	——	$>10^{13}$ cm^{-3}

(Source: Udit N Pal)

R&D Initiatives in India in the areas of microwave tubes

- India is one among ~ 10 countries engaged in microwave tubes development
- Pulsed magnetron activity in early 50's at NPL, CSIR, New Delhi
- Magnetron activity was shifted to CEERI, CSIR, Pilani in 1957
- Theoretical and experimental activities in 50's at Institute of Radio Physics and Electronics, Kolkata in the area of electron tubes including magnetrons
- S-band klystron activities initiated at TIFR, Mumbai in 60's (related technologies established)

  Later on this technology utilized for developing linear accelerators
- Centre of Research in Microwave Tubes (CRMT) at Banaras Hindu University (BHU) was established in 1979 with the support of the erstwhile DOE
- Microwave Tube Research and Development Centre (MTRDC), Bangalore was established by DRDO in 1985

Courtesy: Dr. SN Joshi

Global list of typical companies manufacturing microwave tubes

USA: Litton, CPI

Germany: Siemens, AEG, Philips

Russia: ISTOK, ALMAZ

France: Thales (Formerly Thompson CSF)

Italy : Electronica

Japan: Toshiba, NEC

China: BVEDRI

India: Bharat Electronics

Courtesy: Dr. SN Joshi

Major users of microwave tubes in India

- RR-CAT, Indore
- IPR, Gandhinagar
- BRAC, Mumbai
- ISRO
- DLRL
- DRDL
- RCI
- LRDE
- P&T
- Doordarshan
- Defence

Courtesy: Dr. SN Joshi

User	System	Microwave tube type
ISRO	INSAT/ GSLV	Space TWT
Defence and DRDO	Radar, EW	TWT, klystron magnetron, MPM
RR-CAT (DAE), SAMEER	Particle accelerator, pulsed system	Magnetron, klystron, GDT switches (thyratron)
IPR	Plasma heating (ECRH)	Gyrotron, long-pulsed klystron
IPR, BARC, LRDE, MTRDC	HPM	Vircator

Courtesy: Dr. SN Joshi

Organizations involved in microwave tube research, development and production in India

Industries

- Bharat Electronics (BE) Limited (a public-sector organisation earmarked for defence production)
- Pilani Electron Tubes and Devices Pvt. Limited , Sangrur (a private industry)
- Central Electronics Limited, Sahibabad (a public sector organisation, which once used to manufacture magnetrons for defence application)

Laboratories

- Central Electronics Engineering Research Institute (CEERI), Pilani (CSIR)
- Microwave Tube Research and Development Centre (MTRDC), Bangalore (DRDO)
- Society for Applied Microwave Electronics Engineering and Research (SAMEER), Mumbai
- Electronics Radar Development Establishment, Bangalore (LRDE) (DRDO)
- Bhaba Atomic Research Centre (BARC), Mumbai
- Institute for Plasma Research (IPR), Gandhinagar
- Raja Ramanna Centre for Advanced Technology (RRCAT), Indore

Universities

- Banaras Hindu University, Centre of Research in Microwave Tubes (CRMT), Burdwan University, IIT-Roorkee, Devi Ahilya Vishwa Vidyalaya (DAVV), Indore

- **Bharat Electronics (BE), Bangalore started prducing magnetrons in 1969. It had a major collaboration in 1985 with M/s Varian, USA. It also has collaboration with EEV, Thales, Philips, MTRDC and CEERI**

- **Central Electronics Limited (CEL), Sahibabad established magnetron production facilities in 1977 and continued for a decade**

- **Pilani Electron Tubes and Devices Private Limited. Sangrur was established in early 90s**

Courtesy: Dr. SN Joshi

Centre of Research in Microwave Tubes (CRMT), Department of Electronics Engineering, Banaras Hindu University (BHU), Varanasi

Slow-wave tubes

- **Field and equivalent circuit analyses of helical slow-wave structures for travelling-wave tubes**
- **Modelling of helix thickness, discrete dielectric helix-support rods, and metal envelope of helical slow-wave structures of TWTs**
- **Anisotropic helix loading (metal vane/segment loading) for widening the bandwidth of a TWT**
- **Inhomogeneous helix loading (using tapered-geometry dielectric helix-support rods) for widening the bandwidth of a TWT**
- **Nonlinear hydrodynamic analysis of helix TWTs for the estimation of harmonic content and intermodulation distortion**
- **Synthesis of Pierce electron guns**

Fast-wave tubes

- Cold and hot (small-signal) analysis of a vane-loaded gyrotron for mode selectivity
- Analysis of a tapered-cross section, corrugated coaxial-cavity gyrotron for rarefaction
- Cold and hot (small-signal) analysis of a dielectric-loaded gyro-TWT for wide bandwidths
- Analysis of a tapered cross-section gyro-TWT for wide bandwidths
- Analysis of a disc-loaded gyro-TWT for wide bandwidths
- Simulation of gyrotron cavities
- Large-signal analysis and simulation of gyrotrons, gyro-TWTs, and gyro-klystrons, gyro-twystrons, relativistic BWO and MILO

Recent work at CRMT, IIT-BHU

MILO

Gyrotron

Gyro-Twystron

Gyro-TWT

Relativistic BWO

Non-conventional microwave tubes R&D in the country

HPM devices like the virtual cathode oscillator

BARC, Mumbai

MTRDC (DRDO), Bangalore

LRDE (DRDO), Bangalore

DAVV, Indore

Gyro-devices like the gyro-TWT and the gyrotron

Basic research in the area of gyro-TWTs initiated at CRMT, BHU (evidenced by publications of papers, theses and reports by B. Tech, M. Tech and Ph. D students)

A multi-institutional project funded by DST to develop a 42-GHz, 200-kW gyrotron forthe IPR Tokomak (with CEERI, IPR, SAMEER, BHU, and IIT-Roorkee as the participants), which is further important in view of India participating in the programme ITER (International Thermonuclear Experimental Reactor) aiming at demonstrating the scientific and technical feasibility of fusion power (the other participants being the European Union, USA, Japan, China, and South Korea)

The first ever TWT built in India (1977) at CEERI, Pilani 2 W (CW) S-band helix TWT

The first TWT developed by MTRDC (1993): 200 W X-Ku-band helix TWT

Subsequently, other helix TWTs developed in India such as

- **C-band 20 W (CW) TWT (CEERI) for satellite communication**
- **S-band 30 W (pulsed) TWT (CEERI) 3D radar of Air force**
- **X-Ku-band 40 W (CW) Mini-TWT (CEERI) for EW**
- **X-Ku band 2 kW (Pulsed) TWT (MTRDC-BEL) for EW**
- **X-Ku band 300 W (CW) TWT (MTRDC-BEL) for EW**
- **C band 60 W (CW) TWT (CEERI-BEL) for space communication**

Some other helix TWTs under development such as

- **Ku-band 140 W (CW) TWT (CEERI-BEL) for communication**
- **K-Ka band 40 W (CW) TWT (MTRDC) for EW**
- **C-X-Ku band 100 W (CW) TWT (MTRDC) for EW**
- **C-X-Ku band 200 W (CW) TWT (MTRDC) for EW**
- **C-X-Ku band 1.5 kW (CW) TWT (MTRDC) for EW**

CEERI

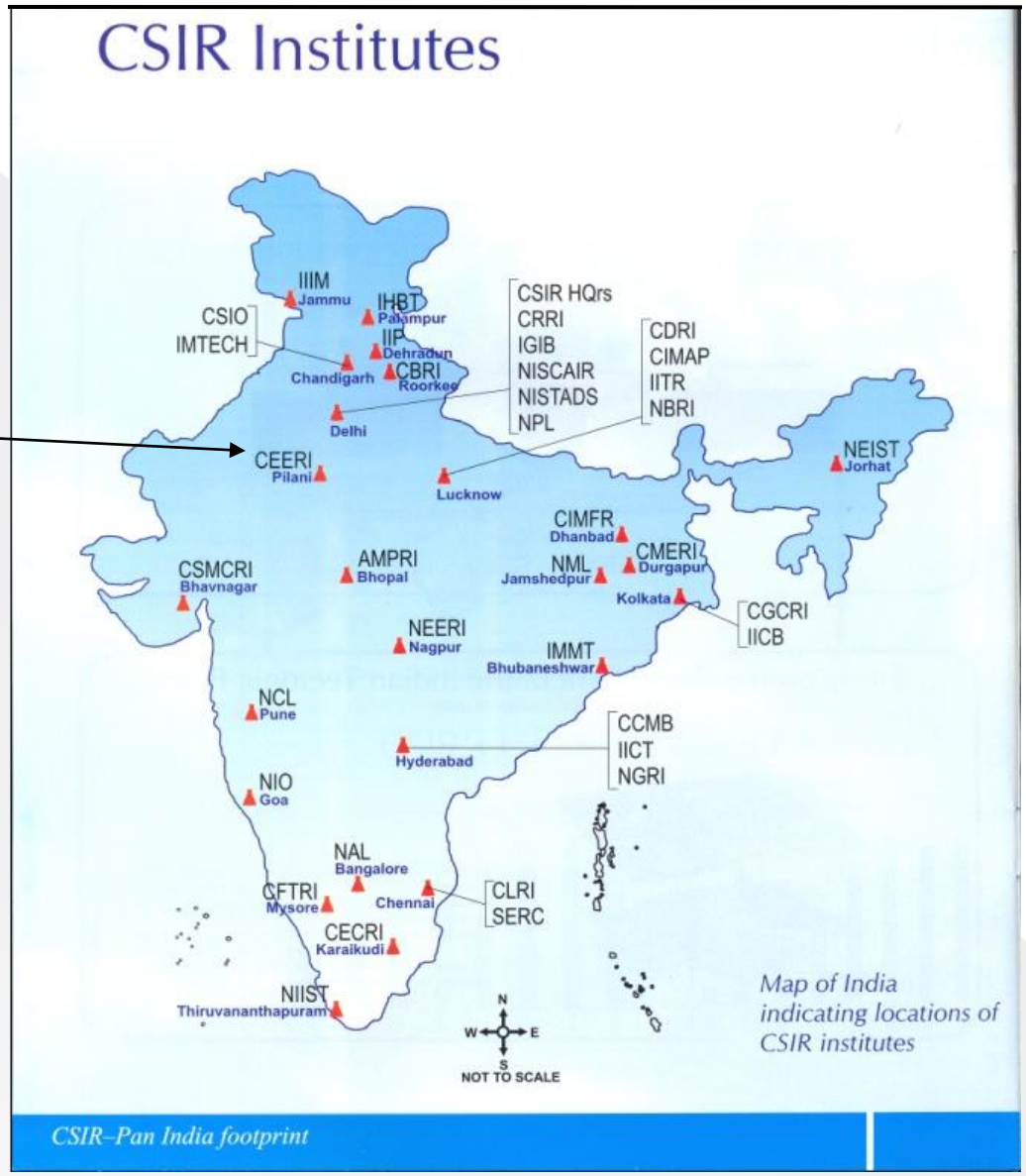

Information to be updated

CSIR Institutes

CBRI - Central Building Research Institute, Roorkee CCMB - Centre for Cellular & Molecular Biology, Hyderabad CDRI - Central Drug Research Institute, Lucknow CECRI - Central Electrochemical Research Institute, Karaikudi CEERI - Central Electronics Engineering Research Institute, Pilani CFRI - Central Fuel Research Institute, DhanbadCFTRI - Central Food Technological Research Institute, Mysore CGCRI - Central Glass & Ceramic research Institute, CalcuttaCIMAP - Central Institute of Medicinal & Aromatic Plants, LucknowCLRI - Central Leather Research Institute, Chennai CMERI - Central Mechanical Engineering Research Institute, Durgapur C-MMACS - CSIR Centre for Mathematical Modelling and Computer Simulation, Bangalore CMRI - Central Mining Research Institute, Dhanbad CRRI - Central Road Research Institute, New Delhi CSIO - Central Scientific Intruments Organisation, Chandigarh CSMCRI - Central Salt & Marine Chemicals Research Institute, Bhavnagar IICB - Indian Institute of Chemical Biology, Calcutta IICT - Indian Institute of Chemical Technology, Hyderabad IIP - Indian Institute of Petroleum, Dehradun IGIB - (Institute of genomics and Integrative Biology) formerly Centre for Biochemical Technology (CBT)IHBT - Institute of Himalayan Bioresource Technology, PalampurIMT - Institute of Microbial Technology, ChandigarhITRC - Industrial Toxicology Research Centre, Lucknow NAL - National Aerospace Laboratories, Bangalore NBRI - National Botanical Research Institute, Lucknow NCL - National Chemical Laboratory, PuneNEERI - National Environmental Engineering Research Institute, Nagpur NGRI - National Geophysical Research Institute, Hyderabad NIO - National Institute of Oceanography, GoaNISCAIR - National Institute of Science Communication and Information Resources, New DelhiNISTADS - National Institute of Science, Technology & Development Studies, New Delhi NML - National Mettalurgical Laboratory, Jamshedpur NPL - National Physical Laboratory, New DelhiRRL,BHO- Regional Research Laboratory, Bhopal RRL, BHU - Regional Research Laboratory, Bhubaneshwar RRL, JM - Regional Research Laboratory, Jammu RRL, JT - Regional Research Laboratory, Jorhat RRL, TVM - Regional Research Laboratory, Thiruvananthapuram SERC, M - Structural Engineering Research Centre, Madras

CSIR labs

Information to be updated

Information to be updated

Research laboratories under CSIR

AMPRI - Advanced Materials and Processes Research Institute, Bhopal
C-MMACS - CSIR Centre for Mathematical Modelling and Computer Simulation, Bangalore
CBRI - CSIR-Central Building Research Institute, Roorkee
CCMB- Centre for Cellular and Molecular Biology, Hyderabad
CDRI - Central Drug Research Institute, Lucknow
CECRI- Central Electro Chemical Research Institute, Karaikudi
CEERI - Central Electronics Engineering Research Institute, Pilani
CFTRI - Central Food Technological Research Institute, Mysore
CGCRI - Central Glass and Ceramic Research Institute, Kolkata
CIMAP - Central Institute of Medicinal and Aromatic Plants, Lucknow
CIMFR - Central Institute of Mining and Fuel Research, Dhanbad
CLRI - Central Leather Research Institute, Chennai
CMERI - Central mechanical engineering research institute, Durgapur
CRRI - Central Road Research Institute, New Delhi
CSIO - Central Scientific Instruments Organisation, Chandigarh

Information to be updated

CSMCRI - Central Salt and Marine Chemicals Research Institute, Bhavnagar
IGIB - Institute of Genomics and Integrative Biology, Delhi
IHBT - Institute of Himalayan Bioresource Technology, Palampur
IICB - Indian Institute of Chemical Biology, Kolkata
IICT - Indian Institute of Chemical Technology, Hyderabad
IIIM, Jammu - Indian Institute of Integrative Medicine, Jammu
IIP - Indian Institute of Petroleum, Dehradun
IMMT - Institute of Minerals and Materials Technology, Bhubaneswar
IMTECH - Institute of Microbial Technology, Chandigarh
IITR - Indian Institute of Toxicology Research, Lucknow (formerly known as Industrial Toxicology Research Centre)
NAL - National Aerospace Laboratories, Bangalore
NBRI - National Botanical Research Institute, Lucknow
NCL - National Chemical Laboratory, Pune
NEERI - National Environmental Engineering Research Institute, Nagpur
NEIST (RRL), Jorhat - North East Institute of Science and Technology, Jorhat , Jorhat

Information to be updated

NGRI - National Geophysical Research Institute, Hyderabad
NIIST - National Institute for Interdisciplinary Science and Technology - Thiruvananthapuram
NIO - National Institute of Oceanography, Goa
NISCAIR - National Institute of Science Communication and Information Resources, New Delhi
NISTADS - National Institute of Science, Technology and Development Studies, New Delhi
NML - National Metallurgical Laboratory, Jamshedpur
NPL - National Physical Laboratory, New Delhi
OSDD - Open Source Drug Discovery
SERC - Structural Engineering Research Centre, Chennai
URDIP Unit for Research and Development of Information Products, Pune

Courtesy: Mr. Uttam Goswami

Contribution of CEERI

- Started with pulse magnetrons: batch produced them and supplied to Indian Navy
- Developed various specifications of magnetrons, klystrons, TWTs, BWOs, and thyratrons
- Carried out limited production of S-band, 2 MW magnetron and supplied them to RRCAT and BARC
- Developed in India the first ever space-qualified TWT in collaboration with BE, Bangalore and handed over the flight models to ISRO
- Has created a design and technology base

Courtesy: Dr. SN Joshi

- **Has established required infrastructure with the support of CSIR and other funding agencies**
- **Has collaboration with various national and international organisations**
- **Has taken up various R&D programmes with support from CSIR and other sponsors like DRDO, ISRO, DAE and DST**
- **Has been involved in developing various critical technologies for multi-beam electron gun, high power RF window, very high power (~ 250 KW CW) and high frequency (120 – 170 GHz) devices, multi-stage collectors, large geometry dispenser cathodes, THz and plasma devices**
- **Has adopted a multi-institutional approach for three major programmes with the support of CSIR, DST, and ISRO.**

Courtesy: Dr. SN Joshi

Achievement of CSIR-CEERI, Pilani

Crossed-field (M-type) tube develoment at CEERI:

Dr. Shivendra Maurya
<shivendra.ceeri@gmail.com>

- 500 kW (S-band) magnetron
- 1.0 MW (S band) magnetron
- 800 kW (tunable S band) magnetron
- 2 MW/3 MW (S band) magnetron
- 10 kW CW magnetron
- Limited production of S-band, 2 MW magnetron (completed in 2005)
- Technology development for 170 GHz, 1 MW, long-pulse RF windows (completed in 2017)
- Development of glass sealed RF window for 4 MW S-band tunable pulse magnetron
- 200 W and 400 W (S band), BWO (Carcinotron)

The major earlier work on the development of magnetrons was in S-band for pulsed operation using the hole-and-slot-type cavities and either the echelon or ring-type strapping.

Some experimental work was also carried out during 1980-1990 in coaxial magnetrons at 9.5 GHz (using the rising-sun structure).

<u>Recent work on magnetron has focused on</u>:

- **Design and development of high power pulsed magnetron with hole-and-slot type cavities and echelon type strapping with higher powers (S band, ~5-7.5 MW peak)**

- **Design and development of CW magnetron (S-band,15 kW) using the vane-type, double-ring, strapped structure for magnetron in S-band (the first version having been already developed)**

- **Design and development of S-band 10-kW CW magnetron**

- **Theoretical work on spatial-harmonic magnetron with cold cathode in other such as planer configurations for higher frequencies**

- **Design and development of coaxial magnetrons from C-to-Ku-to Ka band as per requirements of users**

Klystron development at CEERI:

Dr. LM Joshi <lmj1953@gmail.com>
Dr. Ayan Kumar Bandyopadhyay
<ayan.bandyopadhyay@gmail.com>

- **1 kW CW (D/E band) klystron**
- **5 MW (peak), 5 kW (average) (S band) klystron**
- **6 MW peak, 24 kW average power klystron (for cargo scanning application)**
- **300 W CW (KU/J-band) klystron for missile seekers**
- **100 kW CW, 350 MHz klystron (prototype developed)**
- **250 kW CW, 5 GHz klystron (for ITER lower hybrid current drive) (parts fabricated as per indigenous design)**

Specifications of typical klystron developed at CEERI

Peak output power	6	MW
Average power	24	kW
Pulse width	10	μS
Frequency	2856	MHz
PRF	400	Max
Gain	45	dB
Efficiency	45	%
-1 dB bandwidth	±4	MHz
Beam voltage	130	kV
Beam current	95	A
Focussing	Electromagnet	

Courtesy: Dr. LM Joshi, Dr. SN Joshi

In addition, the klystron group of CEERI has carried out related activities such as:

- **Foundation of the development of multi-beam klystron (MBK) encompassing the design of a 19-beam gun and other parts and fabrication of piece parts of MBK**

- **Low-power air-cooled RF coupler (for low energy high-intensity proton accelerator)**

- **High power water-cooled coaxial RF coupler (for low-energy high-intensity proton accelerator)**

- **High-power water cooled iris coupled RF coupler (for low-energy high-intensity proton accelerator)**

- **Eight channel rectangular RF window (for IPR-Aditya TOKAMAK, lower hybrid current drive)**

TWT development at CEERI:

Dr. Sanjay Kumar Ghosh <ghoshskdr@gmail.com>
Dr. purushothaman <purushothaman.n@gmail.com>

- **2 W CW (S-band) helix TWT**
  (first ever indigenous TWT in India in 1977)
- **20 W (C band) helix TWT (for ISRO)**
- **30 W (S band) helix TWT**
- **40 W CW (X-Ku band) mini-TWT (for DRDO)**
- **60 W (CW) (C-band) space-TWT for ISRO) (jointly with BEL, Bangalore)**
  (first ever indigenous space-TWT in India)
- **140W (Ku-Band/10.9-11.7) GHz short length space-TWT (for ISRO)**

- **60 W (CW) (C-band) space-TWT for ISRO) (jointly with BEL, Bangalore) — the country's first ever indigenous space-TWT**

- **70kW pulsed (C-band) CC-TWT (for DRDO)**

- **140 W (CW) (Ku-band) state-of-the-art space-TWTs for on-board satellite application (under development for ISRO-SAC)**

- **100 W (CW) (Ka-band) state-of-the-art space-TWTs for on-board satellite application (under development for ISRO-SAC)**

- **Development of lab prototype of W-band (94 GHz) folded-waveguide TWT (underway)**

Dr. Ranjan Barik <ranjan.ceeri@gmail.com>

Activities in the development of cathodes at CEERI:

- **20 A/cm2, >8 yr (extrapolated) B-type dispenser cathode**
- **> 100 A/cm2, >12 yr (extrapolated) alloy-coated dispenser cathode**
- **Technology development for reliable long-life dispenser cathodes**
- **Surface analytical studies on dispenser cathode using**
- **Development of large-area dispenser cathodes for high-power microwave tubes: M-type cathode, ~3.1 mm cathode diameter, >20 A per square cm current density, 1000 C operating temperature**
- **Development contract for triple-alloy coating**

- **Development of graphene-based field emitters**

- **Design and development of high current density (> 100 A/cm^2) thermionic cathode for terahertz devices application**

- **Design and development of the work function measurement setup at elevated temperatures of thermionic cathode**

- **Design and development of thermionic emitter for ISRO electric propulsion (ion-thruster) system**

- **Design and development of multi-beam cathode for multi beam klystron**

- **Design of sheet beam electron gun for THz vacuum electron devices**

- **Numerical design of vacuum micro-electronics devices using AI algorithm**

Cathode Activity at CSIR-CEERI

Dr. Ranjan Barik (CSIR-CEERI)

Cathode parts developed at CSIR-CEERI

Small Φ3.1 mm for TWT, Klystron, J> 50A/cm^2

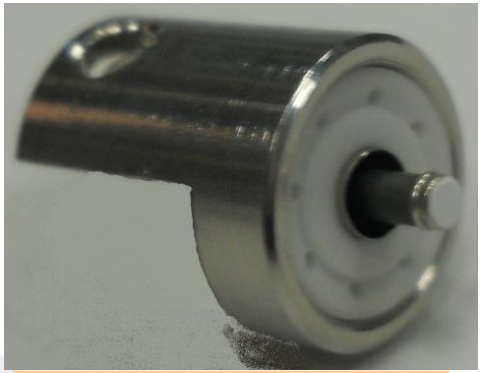

Nanoparticle-based cathode, J>100A/cm^2

CPD cathode, J>50A/cm^2

MBK Cathode

S-Band Klystron cathode
Φ 50 mm diameter

Gyrotron cathode

Gyrotron cathode under hot condition

Space Qualified Cathode

Future Plan

Ongoing Project: Development of high current density cathodes

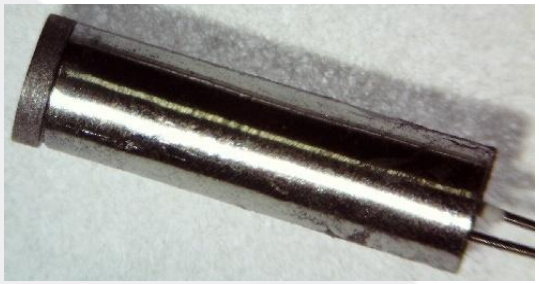

Optical photograph of Cathode

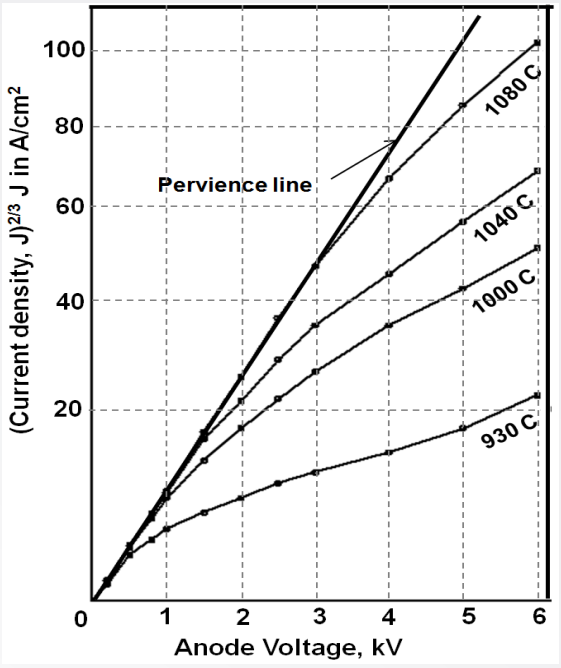

I-V characterization in diode mode

User Specifications:

- Device Dimension: Φ 0.8 mm
- Current Density @1050 C > 100 A/cm^2
- Heater Power @ 1050 C= 6.5 W
- Cathode life = 1000 hours

Application Potential:

- THz Vacuum Electron Devices

Sponsoring Agency:
ER & IPR, DRDO, New Delhi

Sponsoring Agency:
Microwave Tube Research and Development Centre – DRDO, Bangalore

Ongoing Project: Technology development for small-size cathodes

Cathode mounted inside electron gun

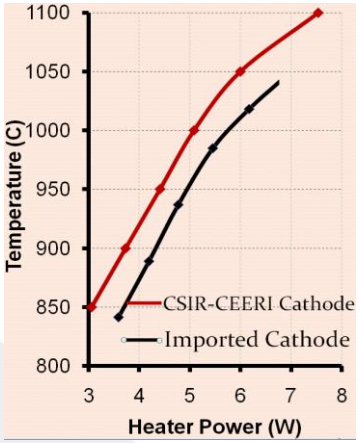

I-V characterization inside electron gun

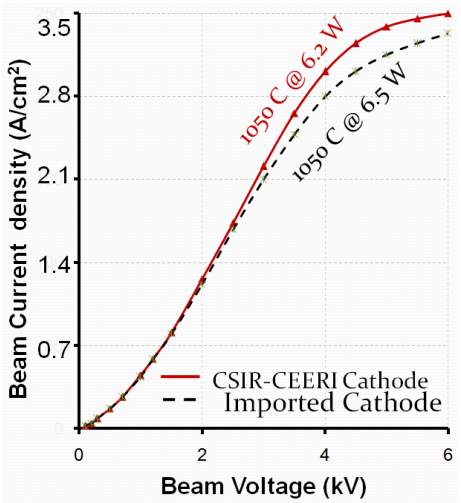

Thermal characterization inside electron gun

User Specifications:

- Device Dimension: Φ 3mm
- Current Density @1050 C > 10 A/cm^2
- Heater Power @ 1050 C= 6.5 W
- Cathode life = 10000 hours

Application:

- Microwave & mm wave Vacuum tubes

Sponsoring Agency: CSIR

User Agency: Bharat Electronics Limited, Bangalore

Ongoing Project: Development of thermionic emitters for electric propulsion system

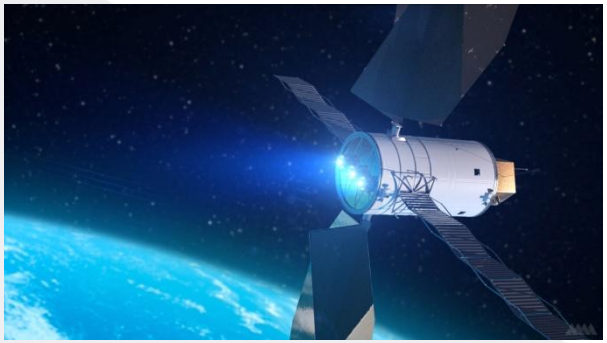

Electric propulsion system for satellite

Optical image of thruster pellet

User Specifications:

- Dimension: Φ 5 mm, Length-15 mm
- Current Density > 12 A/cm^2 @1200 ^{0}C
- Cathode life = 1000 hours @1100 ^{0}C

Application Potential:

- Electric propulsion system for satellite

Sponsoring Agency: VSSC, ISRO

Advance Research Activities in Cathodes

Graphene based Field Emitter

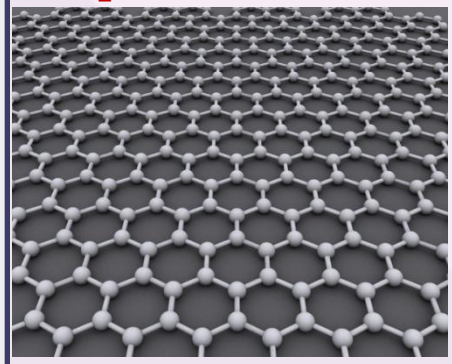

Graphene lattice structure

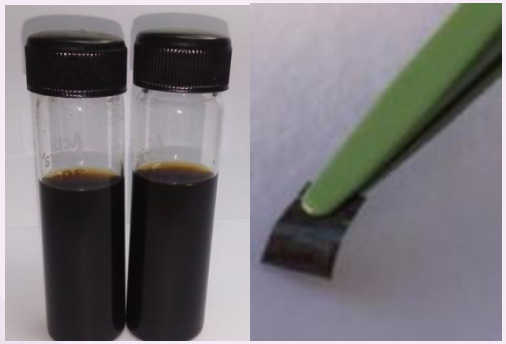

Synthesis of Graphene Oxide using Modified Hummers Method

Promise:

- ✓Very High Current Density
- ✓Micro-fabrication possible
- ✓No warm up time required

Field Emitter based vacuum transistor

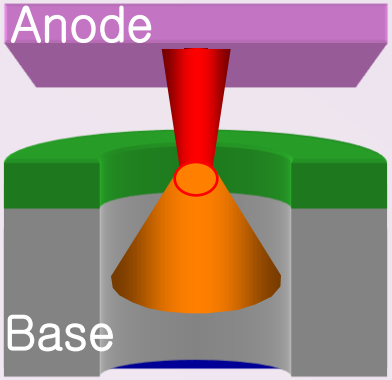

- ➢ Low voltage operation
- ➢ Increased life time.
- ➢ Device can be scaled to nm dim.
- ➢ Future transistor for electronic warfare

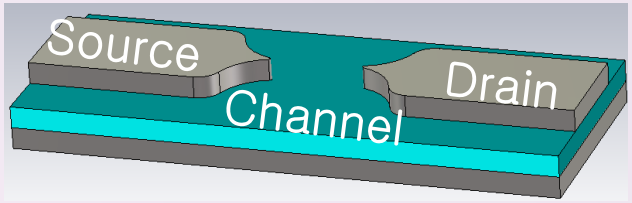

Dr. ashok sinha <aksinha.ceeri@gmail.com>
Dr. Anirban Bera <bera.anirban@gmail.com>

Gyrotron development at CEERI:

- **Design and development of 42 GHz, 220 kW CW gyrotron (for fusion plasma heating) (carried out under a DST-sponsored multi-institutional project)**
- **Design and development of 170 GHz, 1MW (short pulse) gyrotron**
- **EM simulator for gyrotron**

Development of plasma based/ion source based devices and systems at CEERI:

- **VUV/UV excimer sources based on DBD** *Dr. Udit Pal <paludit@gmail.com>*
  - **Biomedical applications**
  - **Surface treatment**
  - **Water purification (jointly with CSIR-NEERI)**

- **High power plasma switches**
- **Thyratron (25 kV/1 kA and 40 kV/3 kA) (for RRCAT, Indore) and pseudospark switches (40 kV/5 kA and 20 kV/20 kA)**
- **Plasma cathode electron guns**
- **Electron and ion sources (40 kV/200 A, ~200 A/cm^2)**
- **Plasma assisted microwave sources**
- **PASOTRON (X-band, 0.5 MW) and THz sources**
- **Penning discharge devices**
- **Ion beam sources and VUV spectroscopy**

DRDO operates through a network of around 47 laboratories and establishments located nationwide and manned by over 34,000 personnel, including about 16,000 scientific technical persons

Information to be updated

47 DRDO laboratories

1. AERIAL DELIVERY RESEARCH AND DEVELOPMENT ESTT. (AIRDEL) Station Road, Post Box No.51, Agra Cantt. 28,.1 001

2. VEHICLE RESEARCH &;DEVELOPMENT ESTABLISHMENT (VAHANVIKAS), Ahmednagar 414 001

3. DEFENCE AGRICULTURAL. RESEARCH LABORATORY Almora 263 601

4. COMBAT VEHICLES RESEARCH AND DEVELOPMENT ESTT. (VEHICLEDEV) Avadi, Madras 600 054

5. **PROOF AND EXPERIMENTAL ESTT. (PROOF)**
   PO Chandipore, Balasore 756 025

6. **AERONAUTICAL DEVELOPMENT ESTT. (LABAIR)**
   Suranjan Dass Road, Jiwan Bima Nagar PO, Bangalore 560 075

7. **GAS TURBINE RESEARCH ESTT. (TURBINE)**
   Suranjan Das Road, CV Raman Nagar PO, Bangalore 560 093

8. **ELECTRONICS & RADAR DEVELOPMENT ESTT. (DEVELECTRONICS)**
   DRDO Complex, Byrasandra Village, Jivan Bima Nagar, Bangalore 560 075

9. **DEFENCE BIO-ENGINEERING AND ELECTRO-MEDICAL LABORATORY (DEBEL)**
   High Grounds, Bangalore 560 001

10. CENTRE FOR AERONAUTICAL SYSTEM STUDIES AND ANALYSIS (CASSA)Suranjan Das Road, Jivan Bima Nagar, Bangalore 560 075

11. MICROWAVE TUBE R & D CENTRE (MTRDC)
Ministry of Defence, BEL Complex, PO Jalahaiii, Bangalore 560 013

12. CENTRE FOR ARTIFICIAL INTELLIGENCE
LRDE Campus, Jivan Bima Nagar, Bangalore 560 075

13. NAVAL CHEMICAL &;METALLURICAL LABORATORY (NAVYLAB)
Naval Dockyard, Bombay 400 023

14. DEFENCE RESEARCH AND DEVELOPMENT UNIT (DEFUNIT)
S-212, Commissariat Road, Hastings, Calcutta 700 022

15. TERMINAL BALLISTICS RESEARCH LABORATORY (BALLISTICS)
Sector 30, Chandigarh

16. NAVAL PHYSICAL & OCEANOGRAPHIC LABORATORY (INPHYLAB)
Naval Base, Cochin 682 004

17. DEFENCE SCIENCE CENTRE (DEFSCCENT)
Metcalfe House, Delhi 110 054

18. SOLIDSTATE PHYSICS LABORATORY (SOLIDSTATE)
Lucknow Road, Delhi 110 007

19. INSTITUTE OF NUCLEAR MEDICINE AND ALLIED
SCIENCE (DEFSCIENCE) Lucknow Road, Delhi 110 007 NMAS

20. DEFENCE INSTITUTE OF PHYSIOLOGY AND ALLIED SCIENCES (DEFSCIENCE/DIPAS) Delhi Cantt. I 10 010

21. INSTITUTE OF SYSTEMS STUDIES &;ANALYSIS
Metcalfe House, Delhi 110 054

22. DEFENCE INSTITUTE OF FIRE RESEARCH
(FIRERESCH) Probyn Road, Delhi 110 007

23. DEFENCE SCIENTIFIC INFORMATION AND DOCUMENTATIONS CENTRE (DESIDOC) Metcalfe House, Delhi 110 054

24. DEFENCE TERRAIN RESEARCH LABORATORY (DEFSCIENCE/DTRL)
Metcalfe House, Delhi 110 054

25. SCIENTIFIC ANALYSIS GROUP (DEFSCIENCE/SAG) Metcalfe House, Delhi 110 054

26. DEFENCE INSTITUTE OF PSYCHOLOGICAL RESEARCH (DEF SCIENCE/DIPR)
West Block No. 8, Wing No. 1, R.K. Puram, New Delhi 110 066

27. INSTRUMENTS RESEARCH AND DEVELOPMENT ESTABLISHMENT (IRDE)
Rajpur Road, Dehradun 248 008

28. DEFENCE ELECTRONICS APPLICATION LAB (RAKESHELECTRONIK)
Rajpur Road, Dehradun 248 008

29. DEFENCE RESEARCH &;DEVELOPMENT ESTT. (DEFRES)
Tansen Road, Gwalior 474 002

30. DEFENCE RESEARCH &;DEVELOPMENT LAB (MISLAB)
Kanchanbagh PO, Hyderabad 500 258

31. DEFENCE METALLURGICAL RESEARCH LAB (DEFMETLAB)
Kanchanbagh PO DMRL, Hyderabad 500 258

32. DEFENCE ELECTRONICS RESEARCH LAB (DEFELECTRONICS)
Chandrayanguntta Lines, Hyderabad 500 005

33. DEFENCE LABORABTORY (DEFLAB)
Ramada Palace, Jodhpur 342 001

34. DEFENCE MATERIALS AND STORES RESEARCH AND DEVELOPMENT ESTT. (LABDEV)
DMSRDE Post Office, G.T. Road, Kanpur 208 013

35. DEFENCE INSTITUTE OF WORK STUDY (WORKSTUDY)
Landour Cantt., Mussoorie 240 179

36. DEFENCE FOOD RESEARCH LAB (RAKSHAKHADYA)
Jyotinagar, Mysore 570 011

37. ARMAMENT RESEARCH & DEVELOPMENT ESTABLISHMENT (AYODH &;ARMAMENTS)
Armament Post Pashan, Pune 411 021

38. EXPLOSIVE RESEARCH AND DEVELOPMENT LABORATORY (MEXDEV PASHAN)
Pashan Pune 411 021

39. RESEARCH AND DEVELOPMENT ESTT. {ENGRS} (ENGIVIKAS)
Pioneer Lines, Dighi, Pune 411 021

40. INSTITUTE OF ARMAMENT TECHNOLOGY (ARMINST {E})
Simhagad Road, Girinagar, Pune 411 025

41. DEFENCE RESEARCH LABORATORY (TEZLAB)
Post Bag No. 2, Tezpur, Assam 784 001

42. NAVAL SCIENCE &;TECHNOLOGICAL LABORATORY (ENESTIEL)
Vigyan Nagar, Visakhapatnam 530 006

43. SNOW AVALANCHE STUDY ESTT (MANALIEX CHANGE)
C/o 56 APO

44. FIELD RESEARCH LABORATORY
C/o 56 APO

45. RANGE CENTRE &;INTERIM TEST RANGE
Balasore

46. ADVANCE SYSTEMS INTEGRATION EVALUATION ORGANISATION (ASIEO)
Bangalore

47. DRDO COMPUTER CENTRE
Metcalfe House, Delhi 110 054

Information to be updated

Microwave Tube Research and Development Centre (MTRDC) (DRDO)

MTRDC is a constituent R&D laboratory of Defence Research & Development Organisation (DRDO), Ministry of Defence. It was established in 1984, with an aim to develop advanced types of microwave tubes to meet the present and futuristic needs of the country and establish self-reliance in this strategic area.

MTRDC initially started in CASSA, Bangalore and moved to a small accommodation in the Bharat Electronics Complex, Bangalore. It was housed in its own building in 1992 near the Microwave Tube Division of Bharat Electronics in order to facilitate continuous interaction between the R&D and production teams. MTRDC has built a residential complex in HMT Township just 4 km away from the laboratory.

It has a team of 125 highly qualified and dedicated scientists, technologists and office staff.

MTRDC, Bangalore (DRDO)

Information to be updated

Achievement of MTRDC (typical)

200W (CW) X-Ku band helix TWT (for airborne jammer)

2 kW (pulsed) X-Ku band helix TWT (for airborne ECM, TEMPEST)

10 kW (pulsed), Ku-band CC-TWT (for AKASH missile seeker/DRDL, DRDO)

6.5 kW (pulsed), X-band CC-TWT (for LCA radar/ADA, DRDO)

Ongoing activities of MTRDC (typical)

130 kW (pulsed), S-band CC-TWT (for AWACS system, DRDO)

300 W (CW) X-Ku band helix TWT (for EW SANYUKTA / DLRL, DRDO)

40 W (CW) mm-wave helix TWT (for EW SANGRAHA/ DLRL, DRDO)

100 W, X-Ku band microwave power module (MPM) (for EW) SANYUKTA / DLRL, DRDO) (~4 kg; <85 ns EPC throughput delay)

Initial work/enabling technologies for gyro-TWTs, Vacuum microelectronic devices (with SSPL as a partner), Transmitters using MPMs, VIRCATOR, Relativistic devices (magnetrons and BWO) (with LRDE, BARC, and DAVV as partners)

Microwave Power Module (MPM)

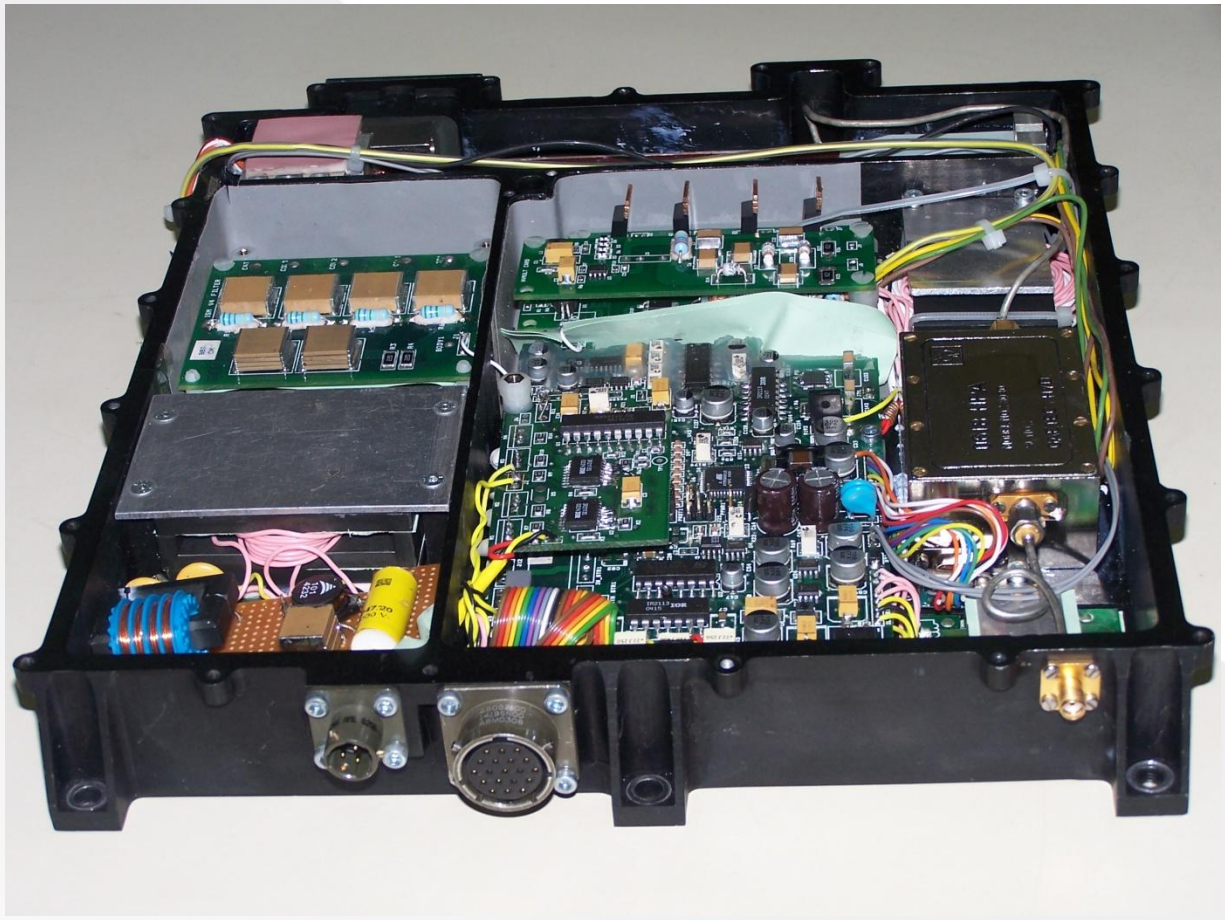

- Ship/Air borne EW
- Data-Link
- Command & Guidance
- Towed Decoy
- Seekers
- SAR

MPM/ Transmitters for EW & communication

Information to be updated

Microwave Power Modules (MPM)

- **100 W(CW) Ku-band for SATCOM Data-link (ADE/DEAL)**
- **100 W X-band for FLR for AKASH (LRDE/DRDL)**

- **MPM based Tx. For EWSFA (DARE)**
- **100W(CW) C-Ku band**
- **200 W(CW) C-Ku band**
- **1500W(P) C-Ku band**

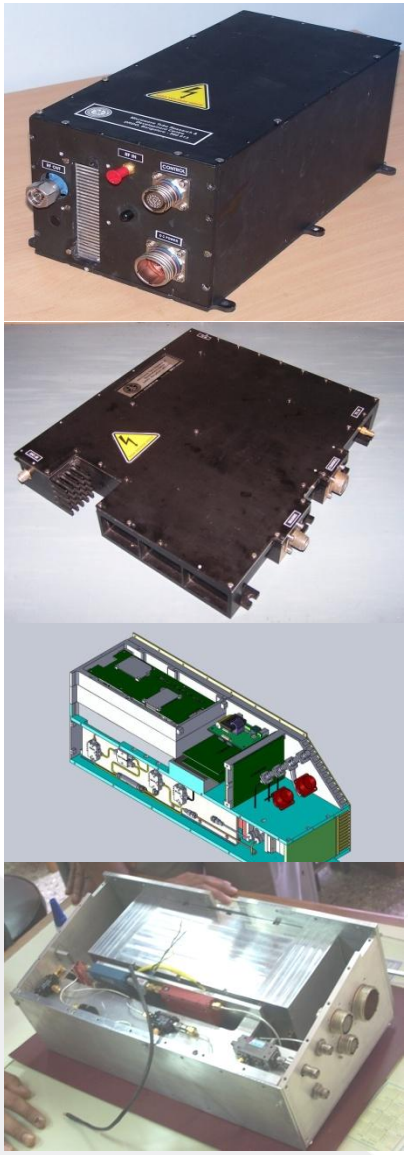

Power Booster TWTs for MPMs Developed by MTRDC

Information to be updated

	MCH-3550	MCH-3553	MPH-4052	MPH-5055
Band	C-Ku	C-Ku	X	Ku
Bandwidth (GHz)	12	12	1	2
Duty	CW/Pulsed	CW/Pulsed	Pulsed	Pulsed
Peak power (W)	100	200	180	375
Focussing	PPM	PPM	PPM	PPM
Cooling plate	Cold plate	Cold plate	Cold plate	Cold
Weight (gm)	540	800	500	500

In 1993, MTRDC developed its first TWT: 200W X-Ku-band helix TWT

Information to be updated

Some other helix TWTs developed in India:

- **C-band 20 W (CW) TWT (CEERI) for satellite communication**
- **S-band 30 W (pulsed) TWT (CEERI) 3D radar of Air force**
- **X-Ku-band 40 W (CW) Mini-TWT (CEERI) for EW**
- **X-Ku band 2 kW (Pulsed) TWT (MTRDC-BEL) for EW**
- **X-Ku band 300 W (CW) TWT (MTRDC-BEL) for EW**
- **C band 60 W (CW) TWT (CEERI-BEL) for space communication**

Some other helix TWTs under development:

- **Ku-band 140 W (CW) TWT (CEERI-BEL) for communication**
- **K-Ka band 40 W (CW) TWT (MTRDC) for EW**
- **C-X-Ku band 100 W (CW) TWT (MTRDC) for EW**
- **C-X-Ku band 200 W (CW) TWT (MTRDC) for EW**
- **C-X-Ku band 1.5 kW (CW) TWT (MTRDC) for EW**

Dispenser cathodes at MTRDC:

> 50 A/cm^2 Os-coated; 30 A/cm^2, >20,000 hr Lithium oxide MM; > 50 A/cm^2, >45,000 hr W-Ir MM; > 40 A/sq cm, >40,000 hr W-Re MM; 35,000 hr Scandate cathode; >360 A/cm^2 PZT based ferroelectric

CC-TWT development at MTRDC

CC-TWT development taken up in1993: S, X and Ku bands at MTRDC; C-band subcontracted to CEERI

New relevant technologies developed and critical areas addressed:

- **Fabrication of shadow-gridded electron gun**
- **Distributed-loss and resonant-loss loading of cavities**
- **Development of samarium cobalt magnets with good homogeneity**
- **Thermal management were some of the key areas addressed under this project**
- **Collaboration with ISTOK, Russia on joint development of X- and Ku-band CC-TWTs**

Qualified tubes delivered for multimode radar of LCA to HAL/ADA

- **Technology for production of the X-band and S-band CC-TWTs transferred to BE resulting in limited series production**

Design of miniaturized MBKs is also one of the key areas at MTRDC

Multi-Beam Klystrons Developed at MTRDC

150W, Ku band

400W, 60MHz, Ku band

250W, 90MHz, Ku band

Information to be updated

The KALI series (KALI 80, KALI 200, KALI 1000, KALI 5000 and KALI 10000) of accelerators are described as "Single Shot Pulsed Gigawatt Electron Accelerators“

Under consideration of DRDO:

Single shot devices, using water filled capacitors to build the charge energy (0.4-40 GW; pulse time~60 ns)

KALI-5000:

3-5 GHz radiation range, pulsed accelerator of 1 MeV electron energy, 50-100 ns pulse time, 40 kA current and 40 GW power level; bulky 10 tons: power hungry, requiring a cooling tank of 12,000 liters of oil; too long recharging time to make it a viable weapon in its present form

X-rays emitted are used in Ballistics research as an illuminator for ultrahigh speed photography by the Defence Ballistics Research Institute (DBRL), Chandigarh

Microwave emissions for EM research

KALI microwave version used by DRDO for testing the vulnerability of the electronic systems such as those of LCA

Helped in designing electrostatic shields to "harden" the LCA and missiles from microwave attack by the enemy as well as protecting satellites against deadly Electromagnetic Impulses (EMI) generated by nuclear weapons and other cosmic disturbances, which "fry" and destroy electronic circuits

(Electronic components currently used in missiles can withstand fields of approx. 300 V/cm, while the fields in case of EMI attack reach thousands of V/cm)

Axial VIRCATOR

- **LRDE/BARC: 5 MW, 1-4 GHz**
- **BARC/MTRDC/LRDE 100 MW KALI-200**
- **BARC/MTRDC: >500 MW, 2-4 GHz, KALI-5000**

Cavity VIRCATOR

- **MTRDC/LRDE/BARC 2 MW, KALI-1000**
- **MTRDC/LRDE 0.2 MW, KALI-200**

BWO

- **BARC/LRDE: 2 MW, 11 GHz**
- **BARC/DAVV: 1 MW, KALI-200, X-band**

Plasma-filled REB device

- **BARC/LRDE: 10-20 MW, 7-10 GHz**

Bharat Electronics Limited (BEL) was established at Bangalore, India, by the Government of India under the Ministry of Defence in 1954 to meet the specialised electronic needs of the Indian defence services. Over the years, it has grown into a multi-product, multi-technology, multi-unit company serving the needs of customers in diverse fields in India and abroad.

"Good service is when the customers come back and the goods don't."

Bharat Electronics (BE), Bangalore (public sector)

- Conventional and coaxial magnetrons (L-, C-, K- and Ku-band), power levels from 400 W to 1.0 MW (pulsed)
- TWT (helix type: L-, S-, C-, X- and Ku-band), power levels from 1.0 W to 400 W (CW); 1 kW to 6 kW (pulsed) and coupled cavity type: X-, S band)
- Power triodes and tetrodes
- Klystrons (L-, S-, and C- band)

Technology know-how, when necessary, taken from CEERI, Pilani, MTRDC, Bangalore,
Philips, EEV, UK, VARIAN (now CPI), USA, Thomson-CSF (now Thales), France, ISTOK, Russia, etc.

Pilani Electron Tubes and Devices Pvt. Ltd., Sangrur (private industry)

Power triodes up to 80 kW (typical)

CEL, Sahibabad (public sector)

Magnetrons for Defence (since suspended)

Bharat Electronics (BE) Tubes

TWT (BE) :

BEL6242: 2 GHz, 200 W (CW), 35 dB (3.9 kV, 525 mA)

BEL6252: 2-4 GHz, 200 W (CW), 37 dB (4.2 kV, 430 mA)

BTC401: 5.5-6.5 GHz, 400 W (CW), 50 dB (9.6 kV, 350 mA)

BTC6262: 4-8 GHz, 200 W (CW), 37 dB (9.0 kV, 300 mA)

BTU5191 (under production): 8-18 GHz, 1 kW (pulsed; 4% duty), 50 dB (11.5 kV, 1.8 A)

BEL mini-TWT (under production): 7.5-18 GHz, 80 W (CW), 50 dB (4.2 kV, 175 mA)

BEL CC-TWT (BCCT 2000X) (under production): 9.2-9.5 GHz, 120 kW(pulsed; 0.5% duty), 50 dB (45 kV, 14 A)

BTC60 (Space-TWT under development); 3.6-4.2 GHz, 60 W (CW), 50 dB (3.2 kV, 80 mA)

BTU140 (Space-TWT under development): 10.9-11.7 GHz, 140 W (CW), 50 dB (6.2 kV, 120 mA)

Klystron (BE):

BEL 4K3SL3 (under production): 1.7-2.4 GHz, 1 kW (CW) (7 kV, 650 mA)

BEL 4K3SL3 (under production): 1.7-2.4 GHz, 12 kW (CW) (20 kV, 3 A)

BEL 888E (under production): BEL 888E (under production): 4.4-5.0 GHz, 1.4 kW (CW) (8.5 kV, 600 mA)

Magnetrons (BE):

5J26 (under production): 1.22-1.35 GHz, 600 kW (pulsed, 0.25%) (34 kV, 55 A)

BEL 200 MX (under production): 8.54-8.94GHz, 200 kW (pulsed, 0.11%) (23 kV, 12 A)

BEL 512 cm (under production): 9-9.6 GHz, 200 kW (pulsed, 0.11%) (23 kV, 30 A)

Requirement of microwave tubes in the country for the coming ten years

Requirement of microwave tubes has been estimated by CEERI, Pilani (CSIR) based on the deliberation at the Technical Meet of all concerned R&D, academia, production, and user organisations held on April 10, 2006 at CSIR Vigyan Kendra, New Delhi to generate 'Position Paper on the Requirement of Microwave Tubes and their Development for the coming ten years'.

Consolidated requirement of travelling-wave tubes in coming ten years (number of tubes required is shown in parenthesis)

ISRO: CW space TWTs: Ka-band, 100 W (60); X-band, 40 W (15); L-band, 200 W (20); S-band, 230 W (40); C-band, 60 W(120); Ku-band, 140 W (150) Pulsed space TWTs: Ku-band, 150 W (12); X-band, 200 W (25)

RCI: Pulsed miniature TWTs: Ku-band, 300 W (300); X-band, 50-100 W (300); Ka-/ W-band; 50-100 W (300-500)

LRDE: Pulsed TWTs: X-band, 8/4 kW (20); X-band, 1 kW (20); C-band, 75 kW (20); S-band, 120 kW (20)

DLRL: CW TWTs: S-band, 500 W (09); S-C-band, 600 W (09); C-X-Ku-band, 350 W (15); K-Ka-band, 100 W (10); CW miniature TWTs: C-X-Ku-band, 100 W (80)

MTRDC: CW TWTs: K-Ka band, 40 W (04); X-Ku band, 300 W (04)

DEAL: CW TWTs X-band, 100 W (300)

ADA: CC-TWTs: X-band (100)

Consolidated requirement of klystrons in coming ten years (number of tubes required is shown in parenthesis)

RCI: CW miniature MBKs: Ku-band, 400 W (250)

RRCAT: Pulsed klystrons: S-band, 5 MW (05); CW MBKs: S-band, 64 kW (10); CW klystrons: 350 MHz and 700 MHz, 250 kW (07)

RRCAT/BARC: Pulsed klystrons: S-band (14)

IPR: CW klystrons: 3-10 GHz, 500 kW (22)

SAMEER: Pulsed klystrons: S-band, 5 MW (05)

BEL: Pulsed klystrons: S-band, 1.5 MW (15); for military communication: (150); for missiles: (150); for laboratory LINACS: (20)

Consolidated requirement of magnetrons in coming ten years (number of tubes required is shown in parenthesis)

BARC: CW magnetrons: 2.45 GHZ, 3 kW (10)

SAMEER: Pulsed magnetrons: S-band, 2.6 MW (20)

BEL: Pulsed magnetrons: X-band, 25 kW (200)

Pulsed magnetrons (coaxial): Ka-band, 80 kW (1000)

Consolidated requirement of gyrotrons in coming ten years (number of tubes required is shown in parenthesis)

BARC: CW gyrotrons: 24 GHz, 5 kW (02)

IPR: CW gyrotrons: 140 GHz, 500 kW (01); 170 GHz, 500 kW (01); 210 GHz, 500 kW (01); multi-frequency, 500 kW; 42 GHz, 200kW (02)

BEL: ITER gyrotrons: (50)

Consolidated requirement of 'electron tubes other than microwave tubes' in coming ten years (number required is shown in parenthesis)

IPR: CW triodes/ tetrodes: 20-100 MHz, 20 kW (10); 20-100 MHz, 200 kW (10); 20-100 MHz, 1.5 MW (10)

BEL: Thyratrons: 20-25 kV, 100 A (peak) (100)

Consortium for the development of the first ever gyrotrons in the country for the IPR tokamak executed in a multi-institutional DST-sponsored project

42 GHz, 200 kW (CW or long pulse); 1.6-1.62 Tesla; 65-70 kV, 10-15 A; TE_{03} mode

Participating organizations:

1. CEERI, Pilani — Electron gun and beam tunnel, Collector, Fabrication of all parts, Assembly/Integration of parts, Processing, Testing, and Coordination with the other participants of the project working as the Nodal Centre

2. SAMEER, Mumbai — Window

3. IPR, Gandhinagar — Magnetic focusing structures, Thermal management, Power supply and Plumbing line

4. BHU — Cavity and Nonlinear taper

5. IIT-Roorkee — Providing assistance to the other participants in the design of the device and its parts

Bharat Electronics is one the members of the steering committee of the project with the understanding that the production of the gyrotron would be eventually taken up once it is designed and developed

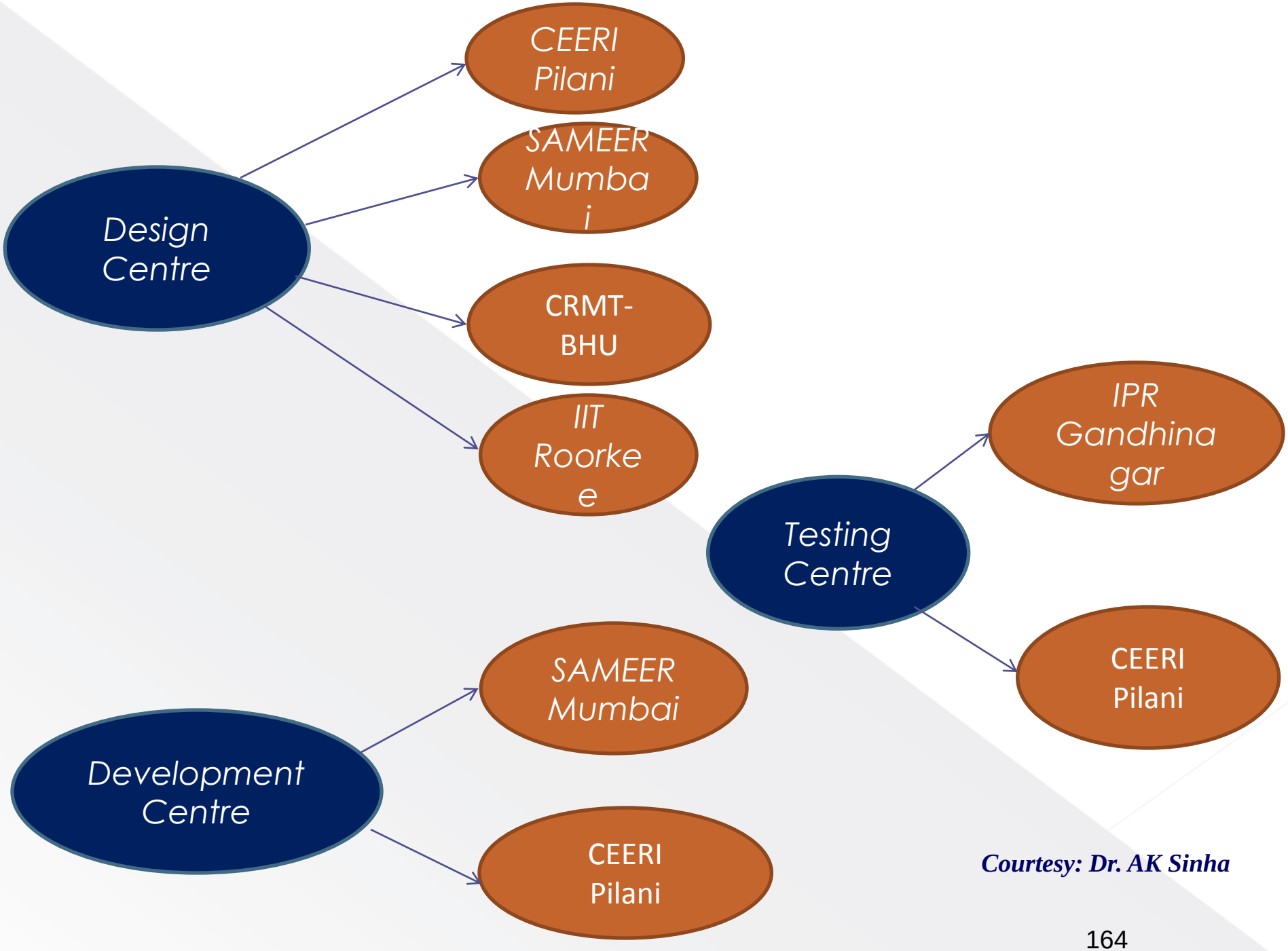

Courtesy: Dr. AK Sinha

Vacuum Electron Devices and Applications (VEDA) Society

Organises either a workshop or a symposium usually every alternate year in the country

VEDA 2004 Symposium: MTRDC, Bangalore (30 & 31 October 2004)
VEDA 2005 Workshop: CRMT-BHU, Varanasi (18 & 19 January 2006)
VEDA 2006 Symposium: CEERI, Pilani (CSIR) (11-13 October 2006)
VEDA 2007 Workshop: SAMEER, Mumbai (22 & 23 November 2007)
VEDA 2008 Workshop: MTRDC, Bangalore (DRDO) (8-10 January 2009)
VEDA 2009 Symposium: CRMT-BHU, Varanasi (30 & 31 October 2009)
VEDA 2010 Workshop: CET, Moradabad (18 & 19 November 2010)
VEDA 2011 Workshop: RKGIT, Ghaziabad (18 & 19 November 2011)
IEEE-EDS IVEC-2011: Organized in Bangalore jointly with VEDA Society
VEDA 2012 Symposium: CEERI, Pilani (CSIR) (21-24 September 2012)
VEDA 2013 Workshop: IIT-R, Roorkee (18-20 October 2013)
VEDA 2014 Workshop: DAVV, Indore (20 & 21 March 2015)
VEDA 2015 Conference: MTRDC-DRDO, Bangalore (3-5 December 2015)
VEDA 2016 Conference: IPR-DAE, Gandhinagar (16-18 March 2017)
VEDA 2017 Symposium: IIT-R, Roorkee (17-19 November 2017)
VEDA 2018 Symposium: IIT-G, Guwahati (22-24 November 2018)
VEDA 2019 Workshop/ Symposium: NIT-Patna (dates yet to be announced)

List of M. Tech students of Burdwan University who have completed their thesis work at CEERI, Pilani in the areas of microwave tubes

1. Debojoity Chaudhary (1996)
2. Mrinal (1997)
3. Arindam Chakraborty (1998)
4. Sivendra Maurya (1999)
5. Gautam Sarkar (1999)
6. Ayan Banerjee (2000
7. Hasibur Rahaman (2000)
8. Anirban Bera (2001)
9. Shiv Chadan (2001)
10. Raudra Gatak (2001)
11. Amitavo Roy Chaudhary (2002)
12. Promod Kumar (2002)
13. Shalabh Gunjan (2002)
14. Maifuz Ali (2002)
15. Sarbani Basu (2002)
16. Shiv Kumar (2003)
17. Shubhamaya Bose (2003)
18. Intekhab (2004)
19. Indrajit Banerjee (2004)
20. Asim Biswas (2004)
21. Anal Hembram (2004)
22. Aritra Bhaumik (2004)
23. Pranab (2004)
24. Raju Manna (2005)
25. MitraBarun Sarkar(2005)
26. Naru Gopal Nayek (2005)
27. Narendranath Mukherjee (2005)
28. Pampa Debnath (2005)
29. Deblina basudhar (2005)
30 Debashish Pal(2005)
31. Tanuja (2005)
32. Santanu Mandal (2006)
33. Partha sarathi Nandi (2006)
34. Anirban Karmakar (2006)
35. Tanima Giri (2006)
36. Maria Rosi
37. Jyotirmoy Koner (2007)
38. Rezoul Karim (2007)
39. Joydeep Banerjee (2007)
40. Dipankar Mondal (2007)
41. Anujit Adhikari (2007)

Incomplete list to be updated

Thank you

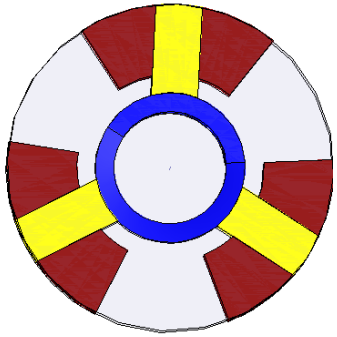

Embedded rod

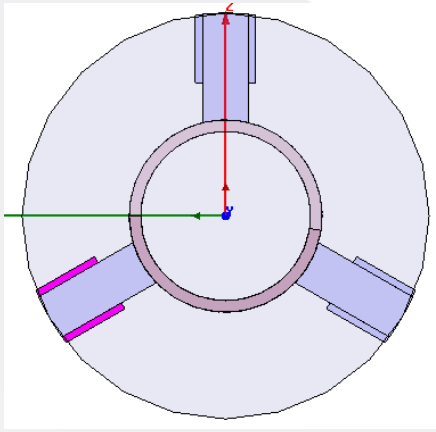

Source: MTRDC (DRDO)

Metal-coated support rods

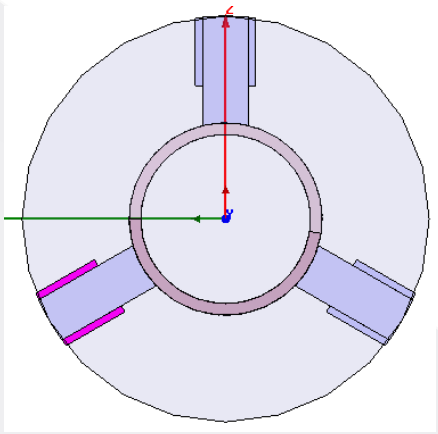

Provides negative dispersion with quite high interaction impedance compared to other segment variants

Source: MTRDC (DRDO)

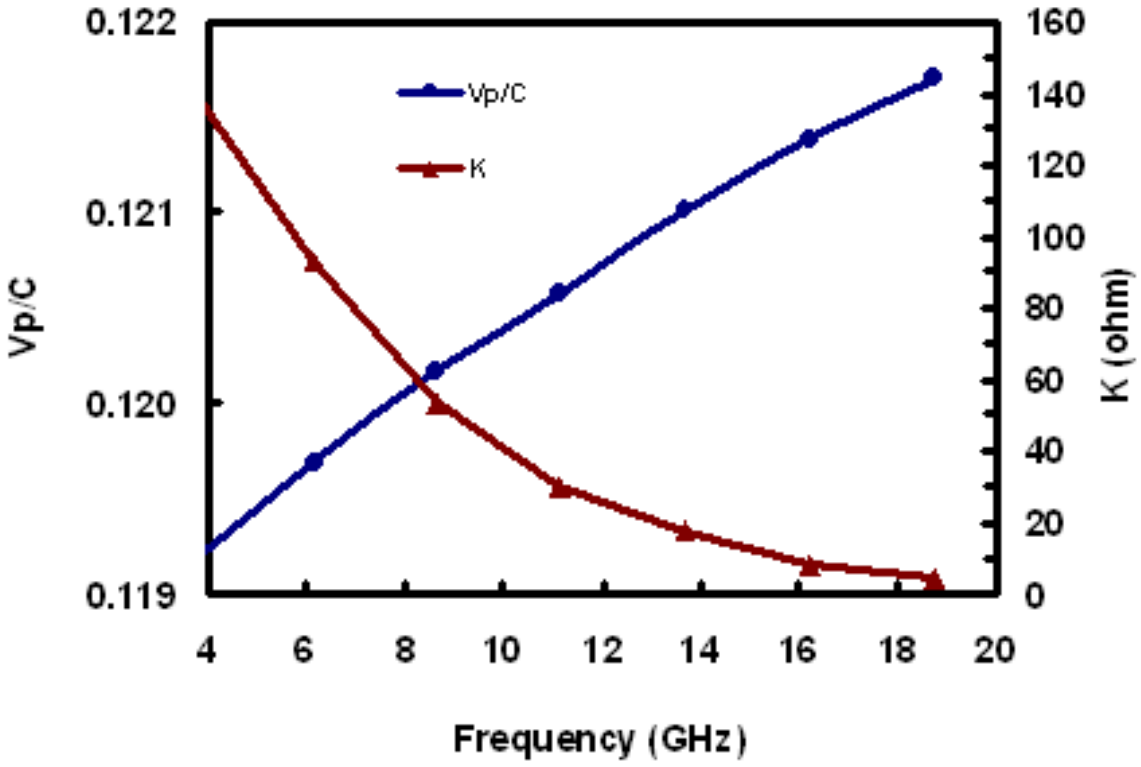

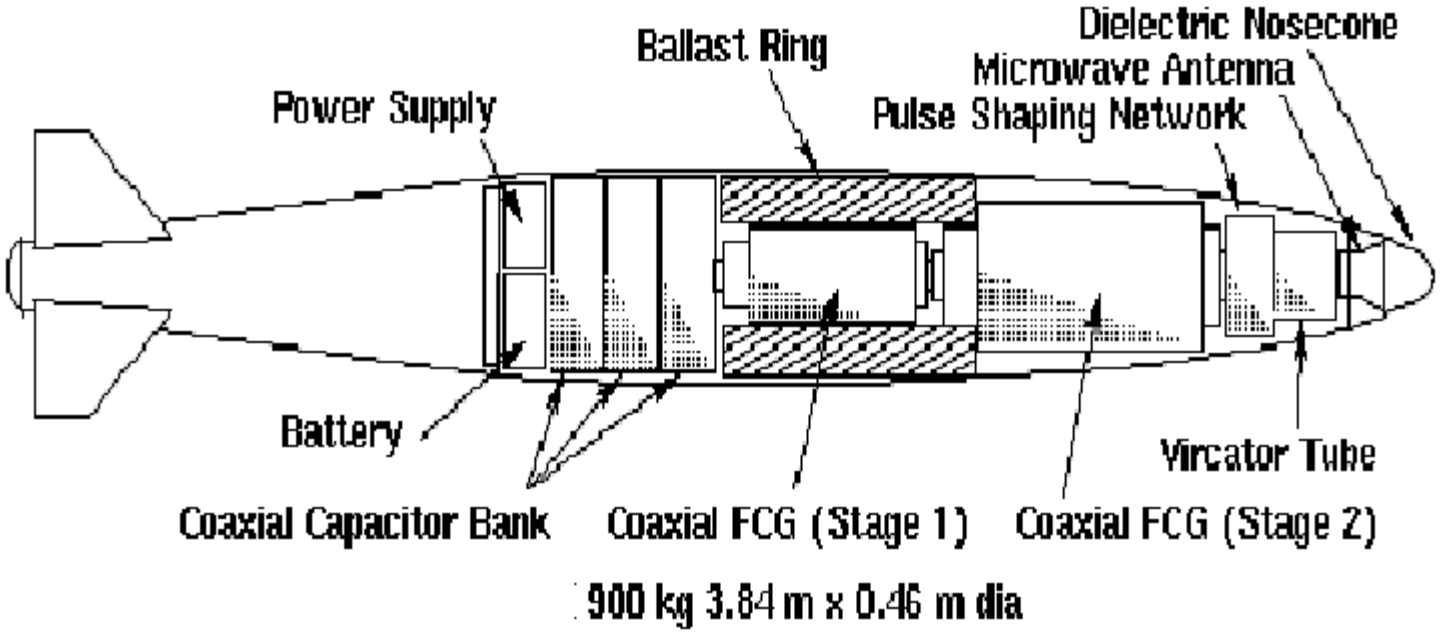

E-bomb warhead using vircator and two-stage FCG

Flux compression generator (FCG)

FCG is a single-shot device delivering ~ 10's of MJ of energy, TW – 10's of TW of peak power in 100's of μs of time

Used as a single device
- **as a pulse power supply for HPM tubes**
- **in cascade — a smaller FCG priming a larger FCG for smallest possible start current source in application where space and weight are at a premium**

Operation is based on transfer of energy from the explosive to the magnetic field

A copper tube (armature), filled in typically by PBX-9501 explosive, is surrounded typically by a helical winding coil of heavy wire typically of copper (stator), the armature tube and the stator coil being separated by an insulator block

Initial magnetic field prior to explosion is produced by a start current in helical coil supplied by an external source like Marx generator — an assembly of capacitors that are charged in parallel and then quickly switched into a series circuit (discharged in series), allowing the original charging voltage to be multiplied by the number of capacitor stages

Explosion breaks the insulation and shorts the turn, the short moving with time

Coaxial FCG ⟶

(Explosively pumped)

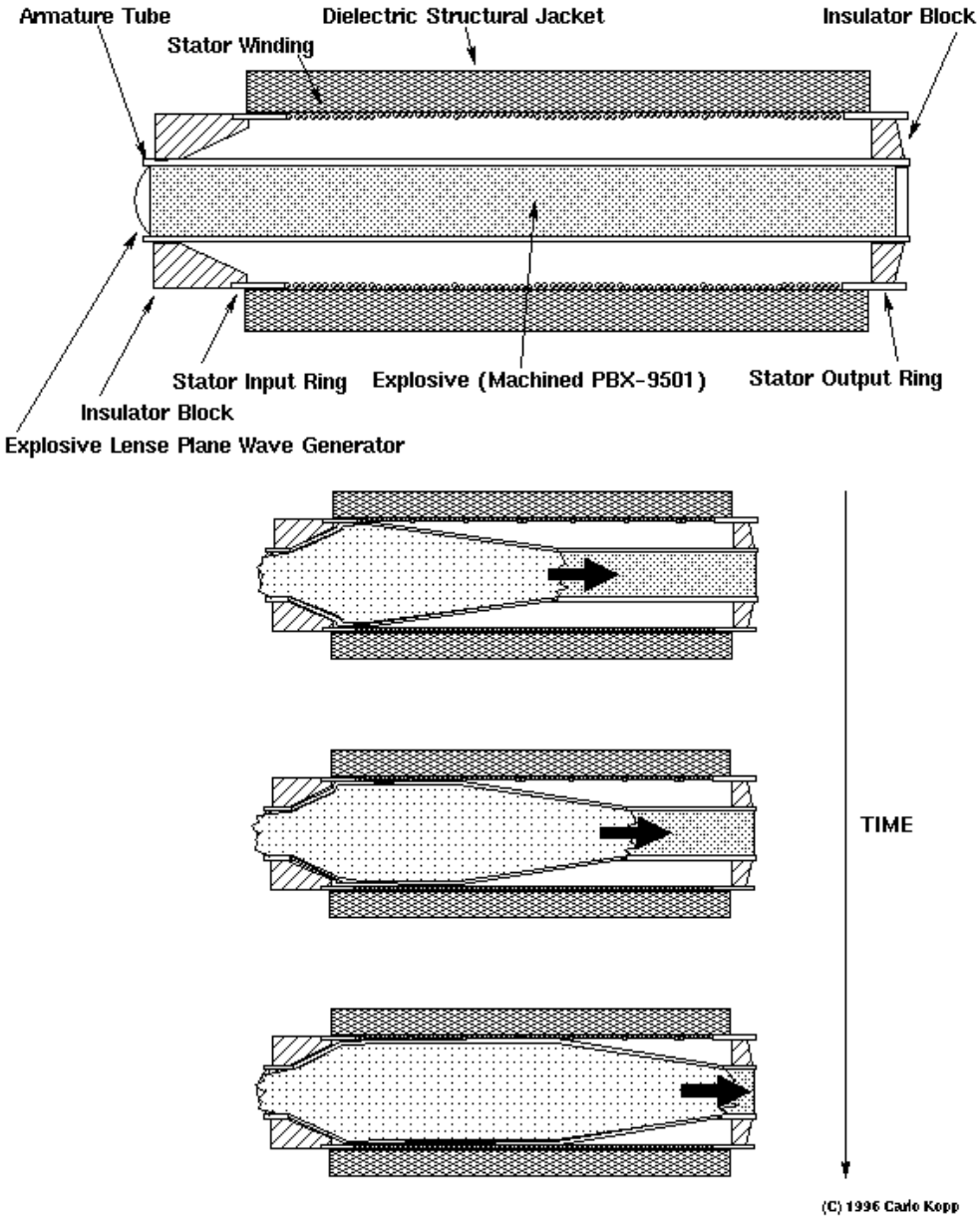

Flux compression generator (FCG) (*continued*)

Explosive is initiated when the start current peaks
Accomplished with an explosive lens plane wave generator producing a uniform plane wave detonation front in the explosive

Armature tube distorts and expands into conical shape to the full diameter of the stator coil winding thereby causing a short circuit between the coil ends isolating the start current source and trapping the current within the device

The propagating short results in magnetic flux compression and reduction in the inductance of the helical winding, and hence a ramping current (current multiplication ~60, typically) that peaks before the final disintegration of the device

10's of MA's peak current in 10's-100's μs and 10's of MJ (typical)

LANL and AFWL demonstrated the viability of FCG

Ramping current pulse

$$H = ni$$

$$B = \mu_0 H = \mu_0 ni$$

$$\phi_B = NAB = NA\mu_0 ni$$

$$L = \frac{\phi_B}{i} = \frac{NA\mu_0 ni}{i}$$

$$= \mu_0 AnN$$

Energy of the coil

$$= 1/2 Li^2$$

With the propagation of the detonation wave, the short propagates

Number of turns N **decreases**

Length of the coil l **also decreases in the same proportion**

Number of turns per unit length $n = N / l$ **remains constant**

Area of the coil A **remains constant**

Inductance of the coil L **decreases**

Energy of the coil $1/2 Li^2$ **remains constant**

Current ***i*** **increases (spikes) (ramping current)**

Marx generator

— an assembly of capacitors that are charged in parallel and then quickly switched into a series circuit (discharged in series), allowing the original charging voltage to be multiplied by the number of capacitors

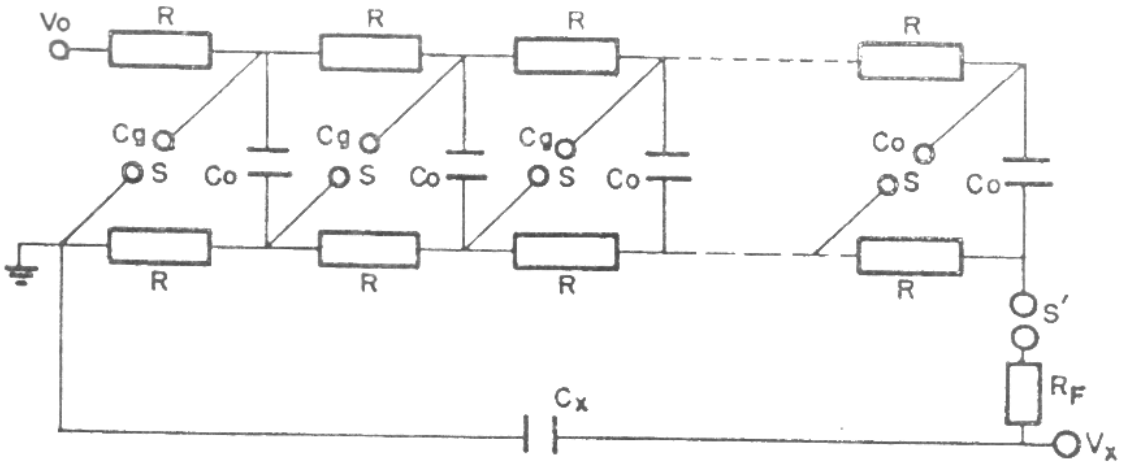

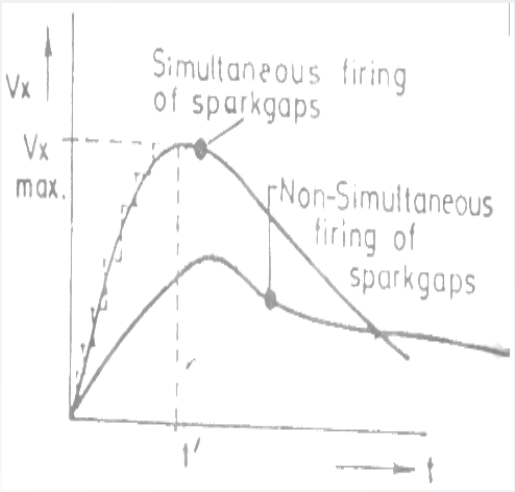

Capacitors C_0 are charged in parallel and discharged through spark gaps S initiated by triggering the first one or more spark gaps by an external triggering source, as a consequence of which the remaining gaps get overloaded thus causing their self-breakdown

Reduction and distortion of output voltage for non-simultaneous triggering

Spark gap S' is used to reduce the charging current though the external load, for instance C_x.

Maximum pulse voltage is NV_0.

Front resistor R_F, tail resistor R and number of stages used adjust the pulse duration

Improvised Marx generator with pulse forming network (PFN)

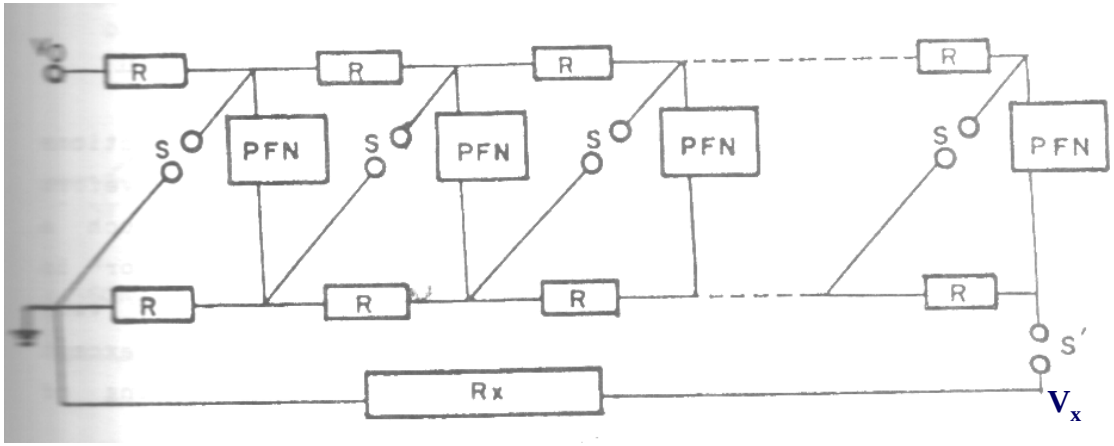

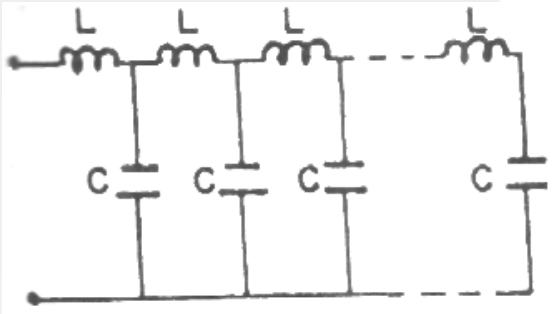

PFN

Characteristic impedance $R' = \sqrt{L/C}$

Load resistance $= NR'$

Output voltage $V_x = NV_0/2$

Pulse duration $= n\sqrt{LC}$

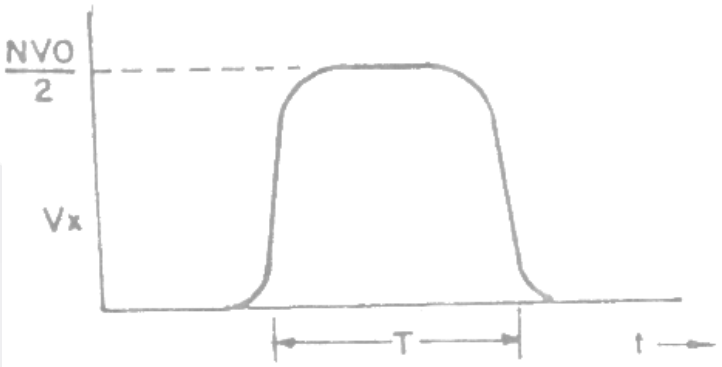

Flat-top pulse

Some MTRDC-developed tubes

S-band CCTWT

X-band CCTWT

Ku-band CCTWT

X-Ku-band 2 kW Helix TWT

X-Ku-band 300W Helix TWT

100W (CW) C-X-Ku band MPM

Courtesy: SK Datta, MTRDC

2 kW pulsed X-Ku band helix TWT for airborne ECM system

10 kW pulsed Ku band coupled-cavity TWT for airborne radar

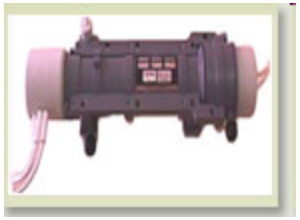

6.5 kW pulsed X-band coupled-cavity TWT for airborne radar

S-band 130 kW (pulsed) coupled -cavity TWT

M-type cathode

Microwave power module

Microwave tube components developed at MTRDC

MTRDC: Courtesy: SK Datta

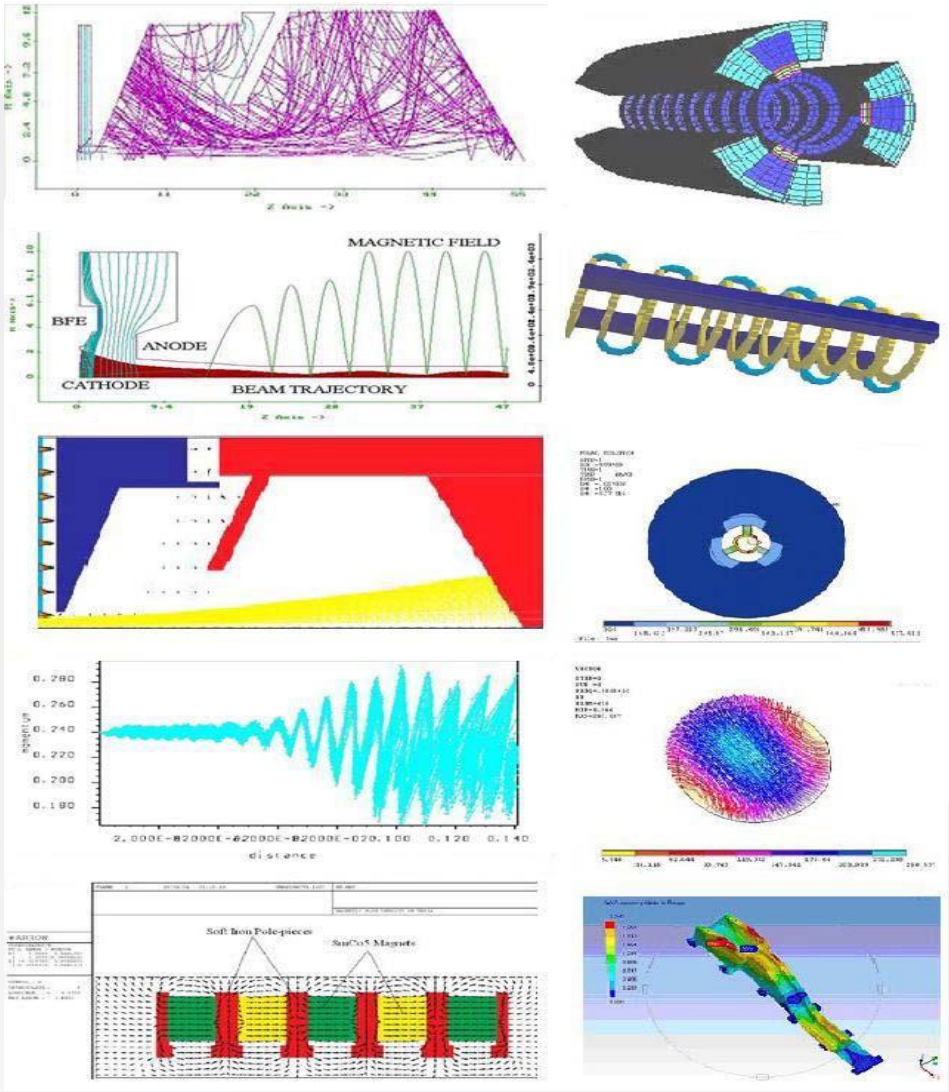

← **Typical CAD models of MTRDC**

Courtesy: SK Datta

Electron-optic & Electromagnetic Simulation

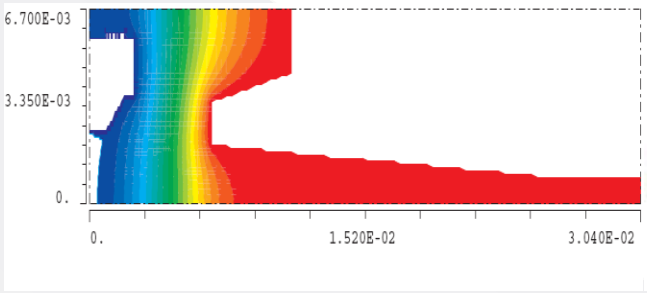

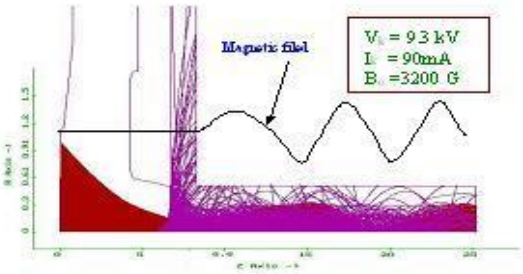

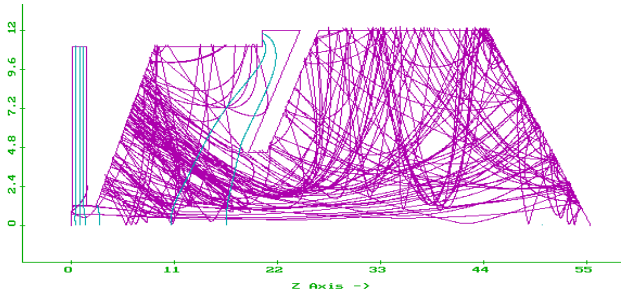

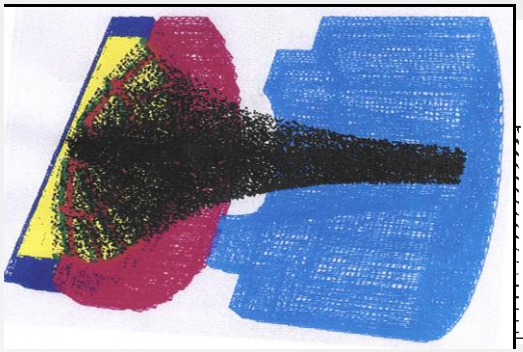

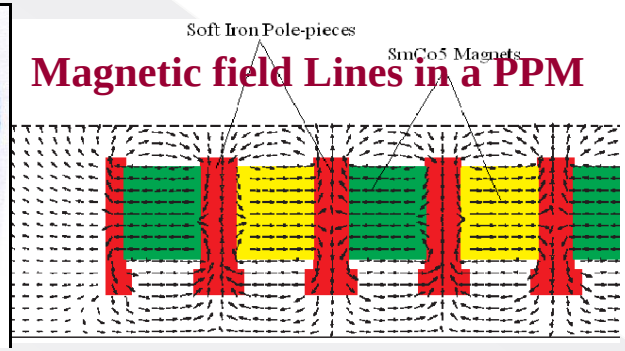

Magnetic field Lines in a PPM

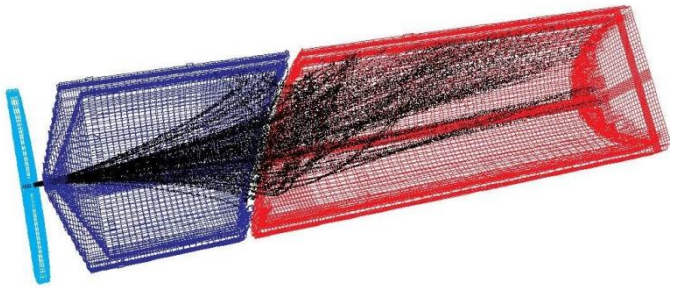

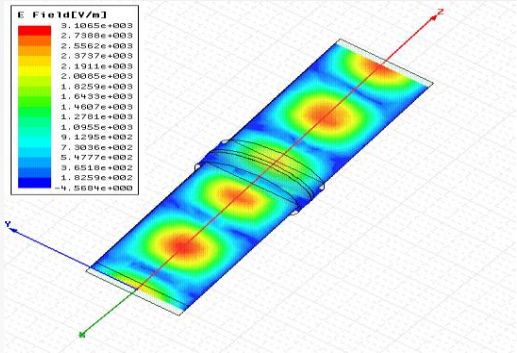

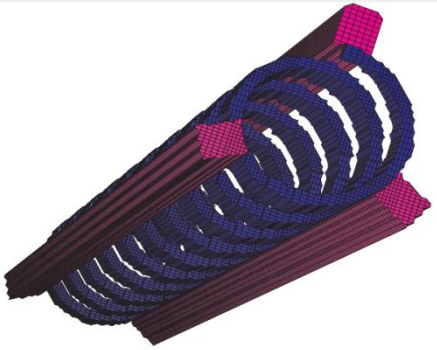

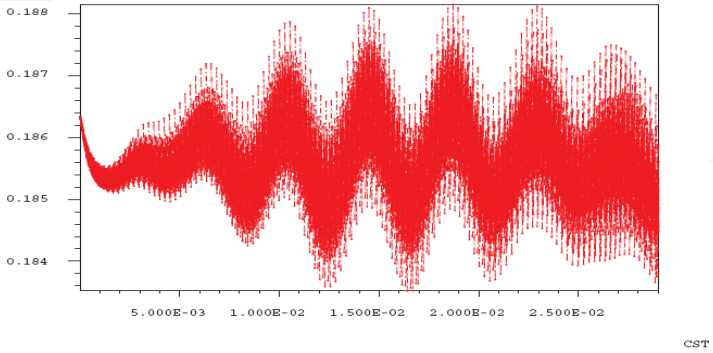

Helix Slow-wave Structure

Thermal Analysis of sub-systems of TWT & EPC

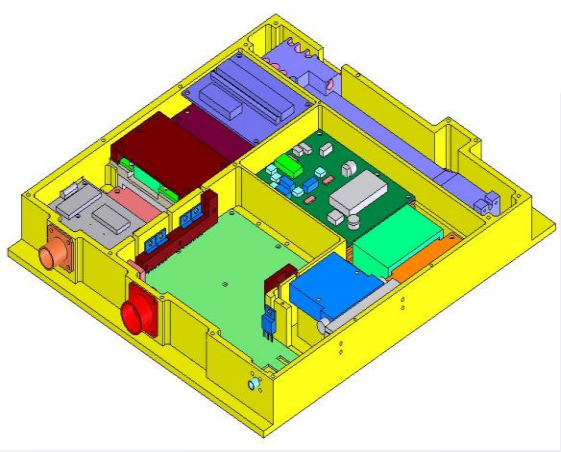

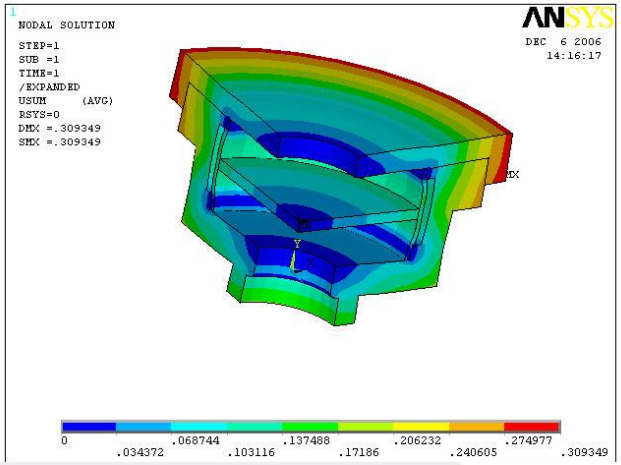

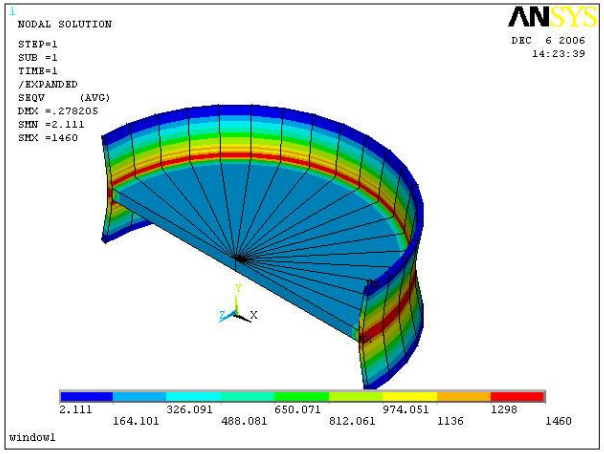

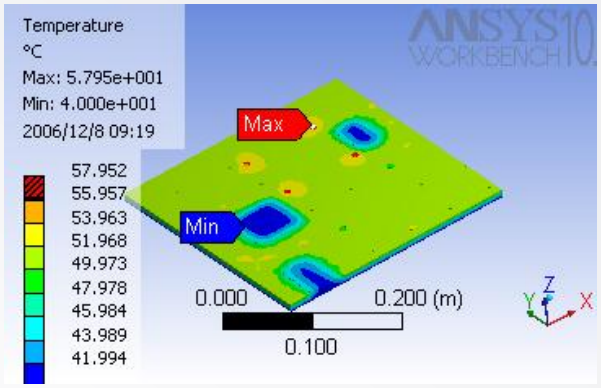

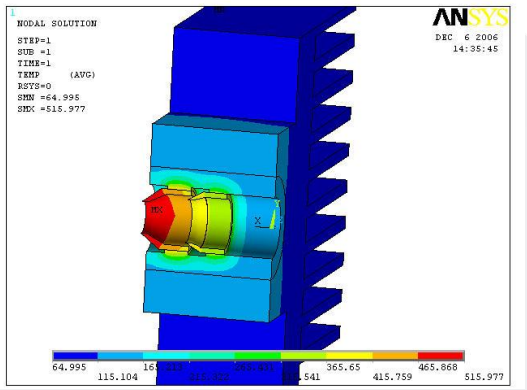

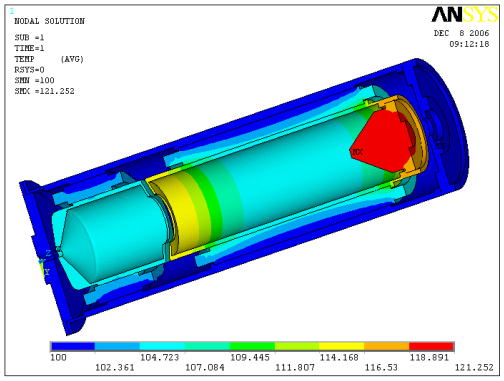

Pulsed magnetrons developed at CEERI

400 W Ka-band

500 kW S-band

800 kW S-band

1 MW S-band

2 MW S-band

3 MW S-band

Courtesy: Dr. SN Joshi

Ground-based TWTs developed by CEERI for communication and EW Systems

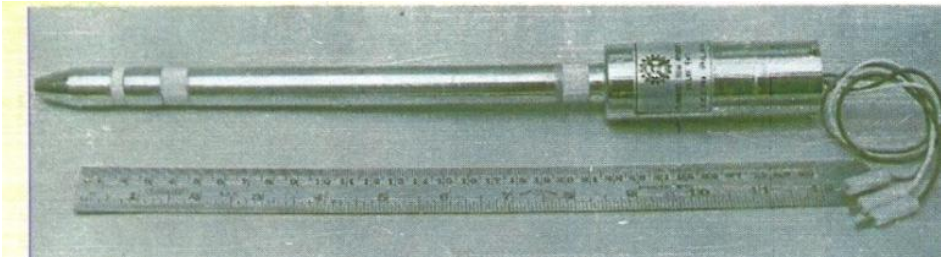

Courtesy: Dr. SN Joshi

Space TWTs for communication systems developed by CEERI

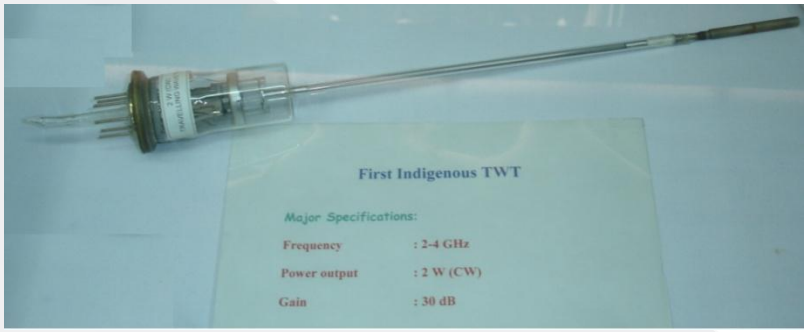

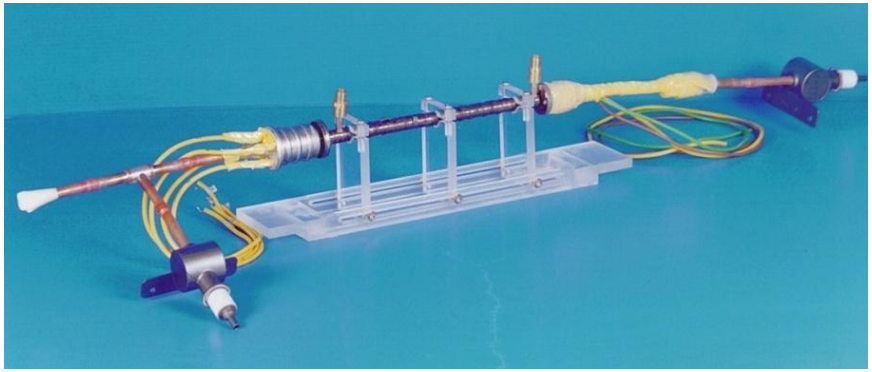

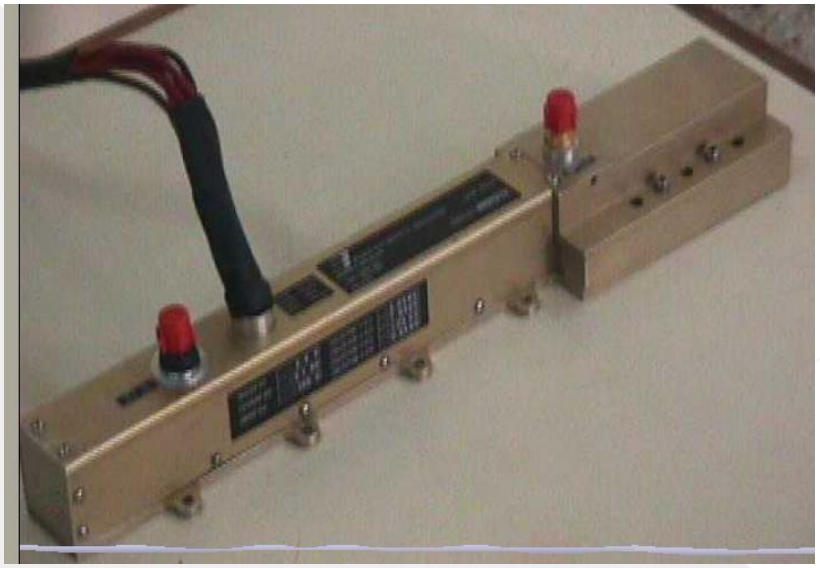

Courtesy: Dr. SN Joshi

C-band 60W CEERI space-TWT
(developed jointly with Bharat Electronics)

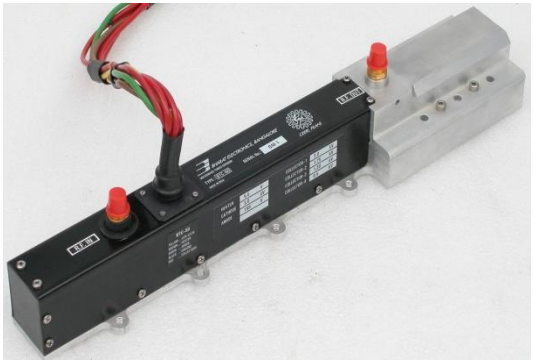

C-Band 60W conduction cooled
Frequency: 3.6-4.2 GHz
Power: 60 W (CW)
Gain: 50 dB
Efficiency: >55%
AM/PM: < 5^0/dB
IMP: <-10 dBc @ 3 dB BO
Noise figure: 30 dB
Gain flatness: 1.0 dB p-p over 200 MHz
Group delay: <1 nS in any 40 MHz BW
2^{nd} harmonics: < -16 dBc
Spurious: < -60 dBc

Courtesy: Dr. S. Ghosh and Dr. RK Sharma

Ku-band 140W CEERI space-TWT
(developed jointly with Bharat Electronics)

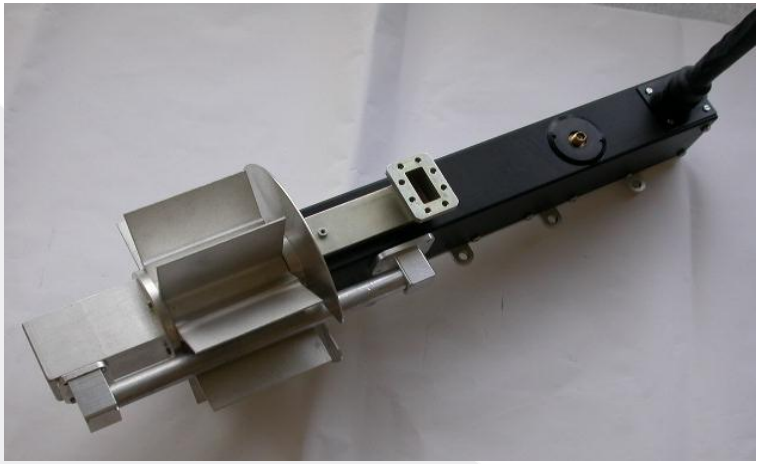

Ku-band 140W radiation cooled
Frequency: 10.9-11.7 GHz
Power: 140 W (CW)
Gain: 50 dB
Efficiency: >55%
AM/PM: < 5^0/dB
IMP: <-10 dBc @ saturation
Noise figure: 30 dB
Gain flatness: 1.0 dB p-p over 200 MHz
Group delay: <1 nS in any 40 MHz BW
2^{nd} harmonics: < -16 dBc
Spurious: < -60 dBc

Courtesy: Dr. S. Ghosh and Dr. RK Sharma

Ka band 100W CEERI helix TWT (Under CSIR Network Project)

Beam stick on pump station
Frequency: 20.6-21.2 GHz
Power: 100 W (CW)
Gain: 50 dB
Efficiency: 55%

Courtesy: Dr. S. Ghosh and Dr. RK Sharma

CEERI klystrons

1 kW CW L/S-band Klystron

5 MW (P) 5 kW (Avg)
S-band Klystron

Courtesy: Dr. SN Joshi, Dr. LM Joshi

Klystron vacuum processing

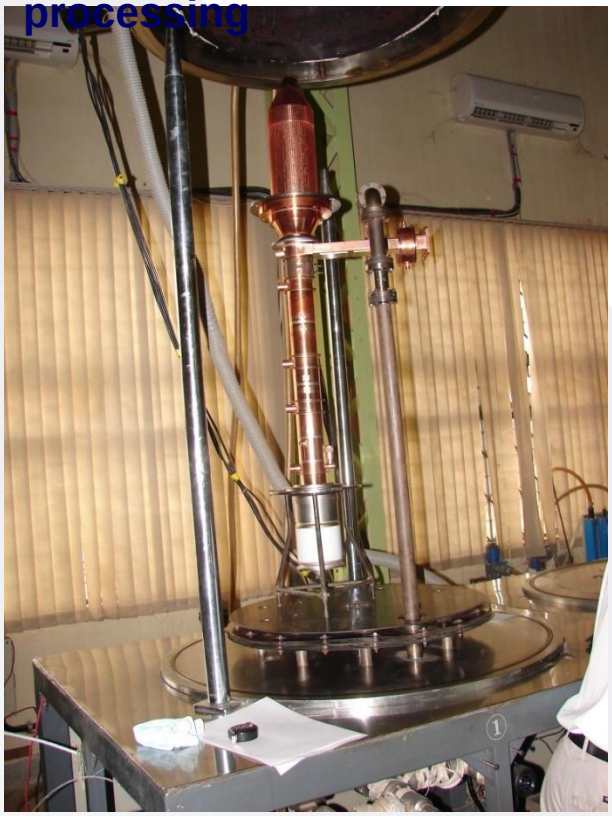

Klystron hot testing

Courtesy: Dr. SN Joshi, Dr. LM Joshi

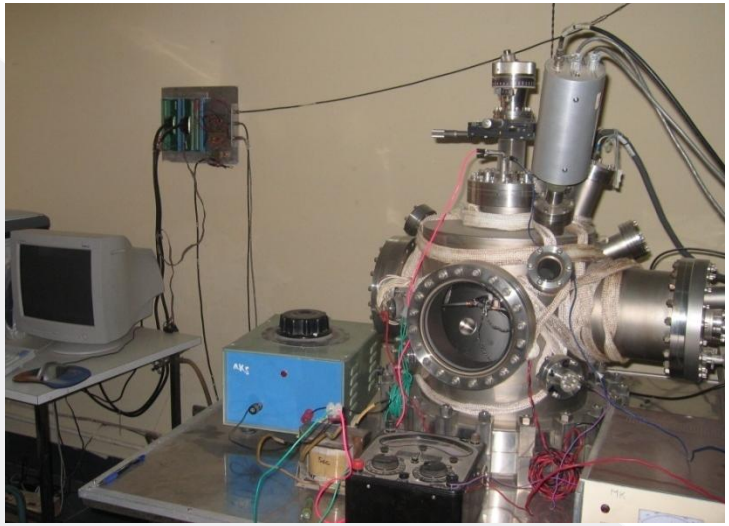

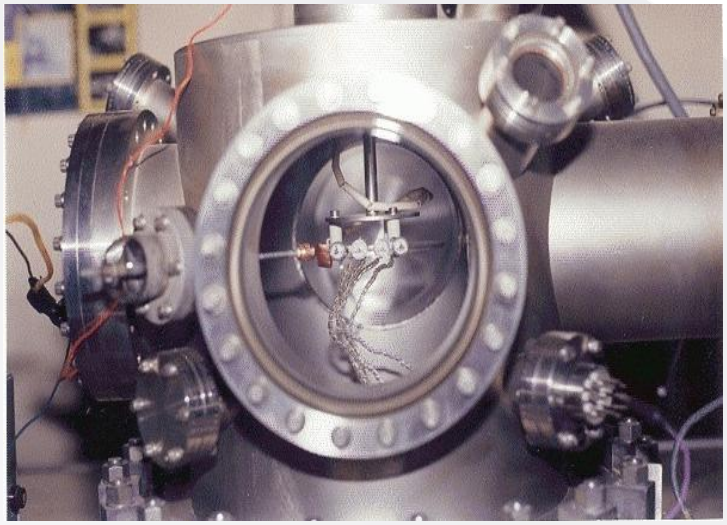

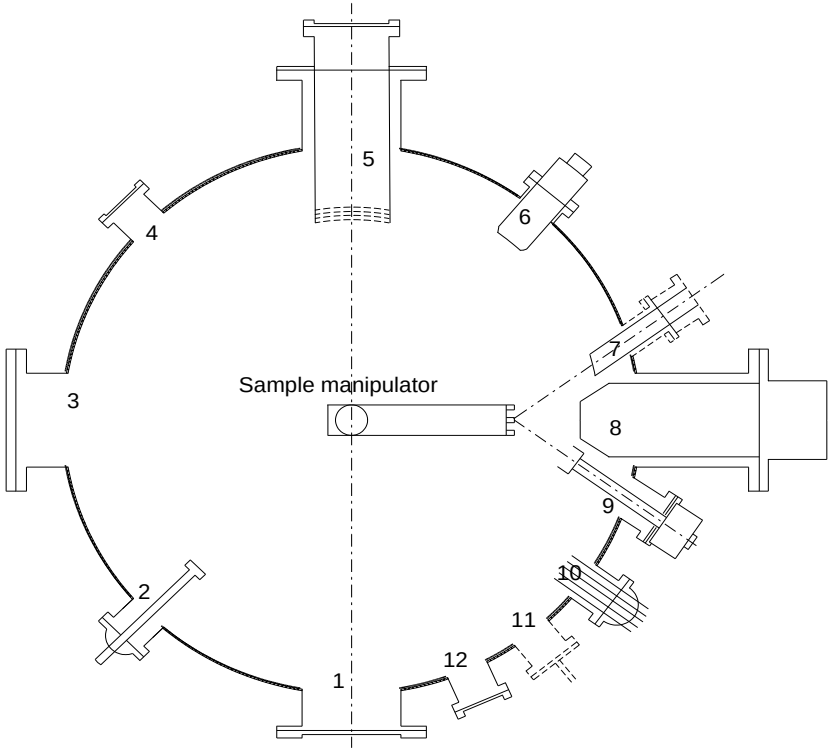

Chamber of Analytical System

1. Viewing window
2. Anode
3. Access flange
4. Viewing window
5. ErLeed
6. Mass spectrameter
7. Ion Gun
8. CMA
9. Sec. El detector
10. El. feed through
11. Leak valve
12. Viewing window

Cathode assembly in UHV chamber

Courtesy: Dr. RS Raju

CEERI thyratron

25 kV, 1kA, Hydrogen thyratron

Pulse duration: 500 nsec
Rate of current rise: 20kA/µsec
Jitter: 5 nsec
PRR: 8kHz
➢ Copper vapour laser system (tested at RRCAT, Indore).

- **40 kV, 3kA, Deuterium thyratron**

Pulse duration: 3-5 µsec
Rate of current rise: 5kA/µsec
Jitter: 2 nsec
PRR: 300 kHz
➢ BARC happy with the performance and want to test at their setup.

Courtesy: Mr. Udit N Pal

CEERI pseudospark high power plasma switch

40 kV/5kA pseudospark
Pulse duration: 3-5 μsec
Rate of current rise: 5kA/μsec
Jitter: 5 nsec
PRR: 300 kHz

Courtesy: Mr. Udit N Pal

CEERI VUV/UV excimer dielectric barrier discharge source

Wave length: 120-270 nm (Germicidal range)
Energy conversion efficiency: 30-40 %
Input power: up to 100 watt

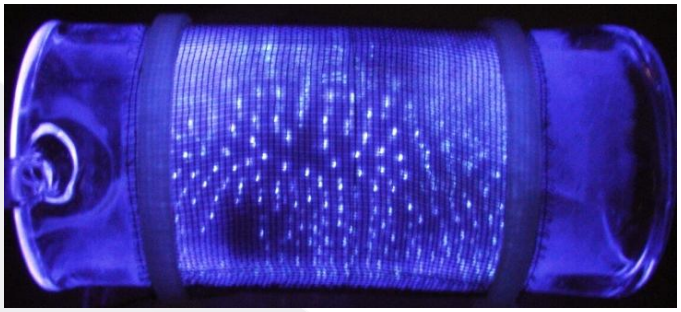

Different types of environment friendly, efficient VUV/UV source (Xenon, Ar, and N_2)
have been developed.

Courtesy: Mr. Udit N Pal

Plasma cathode electron (PCE) gun for plasma-filled devices like the pasotron

Specifications

Beam current ≥ 30 A
Beam density ≥20 A/cm^2
Duration of beam current pulses ≥ 10 microsecond
Beam voltage: 50 kV ± 50%
Pulse repetition frequency: 0.1-10 Hz

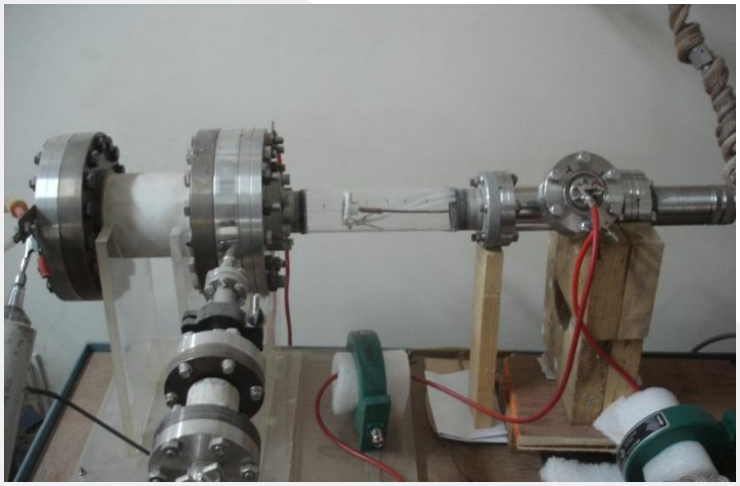

PCE gun preliminarily developed (20 kV/ 200 A at 0.5 mbar Argon)

Courtesy: Mr. Udit N Pal

Magnetron injection gun (MIG)

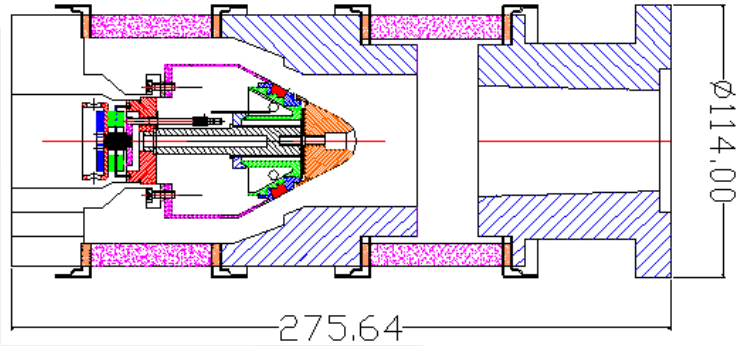

Parameters	Design values	Tolerance
Cathode radius	22.55 mm	± 0.05 mm
Cathode angle	28^0	± 1^0
Slant length	7 mm	± 0.1 mm
Modulating anode voltage	29 kV	± 0.5 kV
Beam voltage	65 kV	± 1 kV
Alpha (α)	1.26	± 5%
Magnetic field at interaction	1.61 Tesla	± 1%
Cathode anode distance	9 mm	±0.1mm
Beam current	10.3 A	±0.01 A
Larmor radius	0.42 mm	±0.02 mm
Avg. velocity spread	2.65%	±0.15%
Distance from cavity centre	330 mm	±0.05 mm
Cavity radius	11.57 mm	±0.03 mm

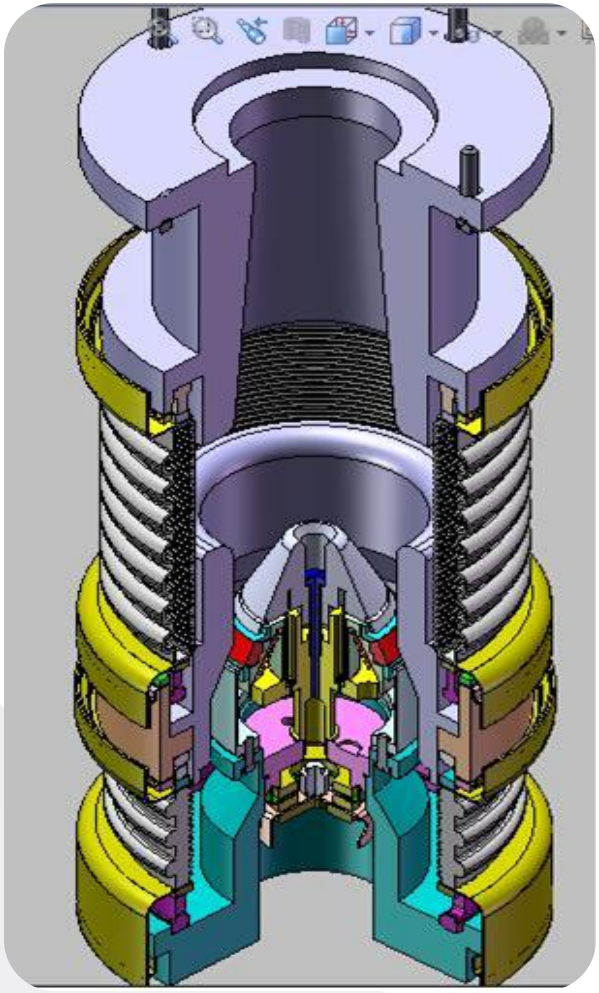

Courtesy: Dr. AK Sinha

MIG with the electron beam and the magnetic firld profiles

Magnetic field at cathode centre	0.11 Tesla
Magnetic field at interaction region	1.65/ 1.61 Tesla
Variation of B field around Zcav+/-20mm	20 Gauss

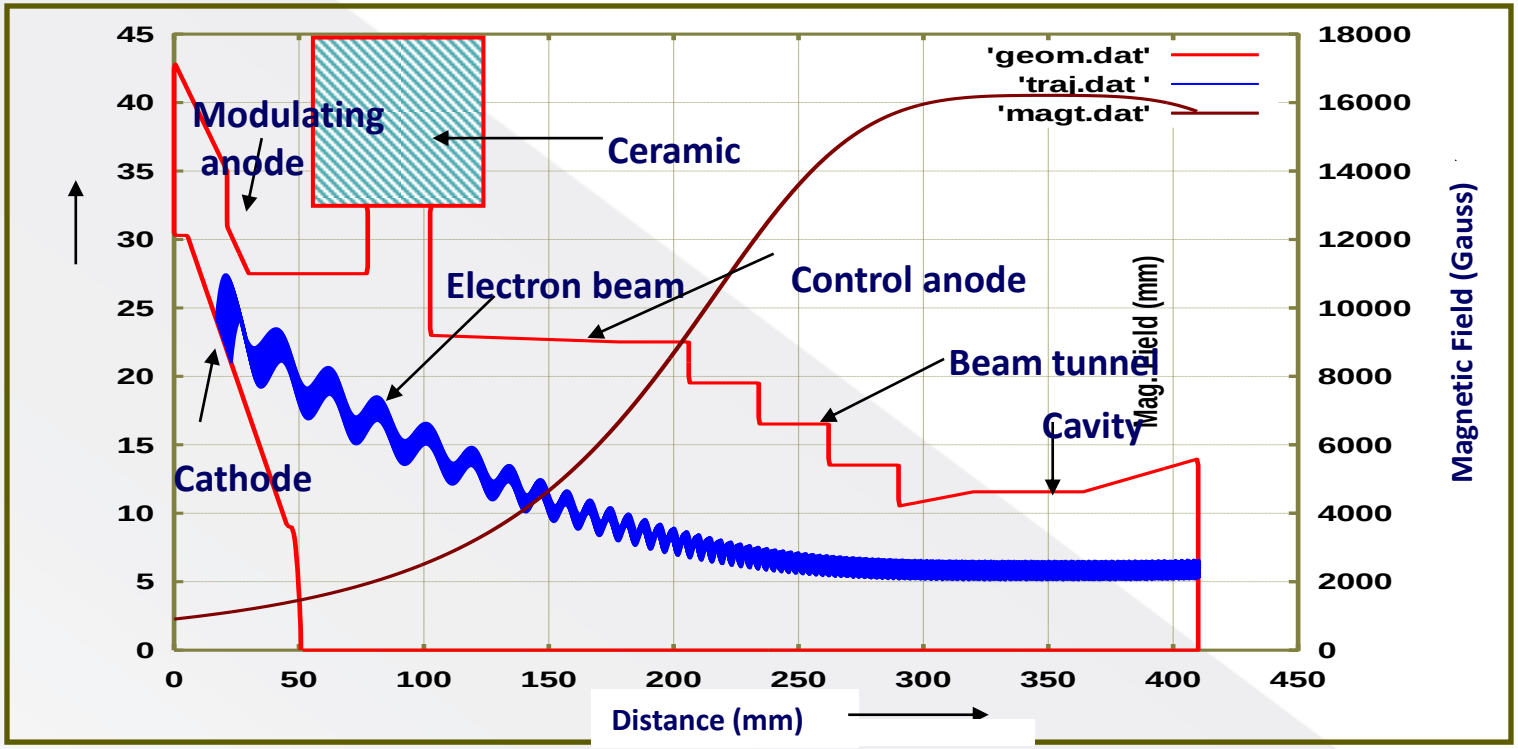

Courtesy: Dr. AK Sinha

Gyrotron beam tunnel

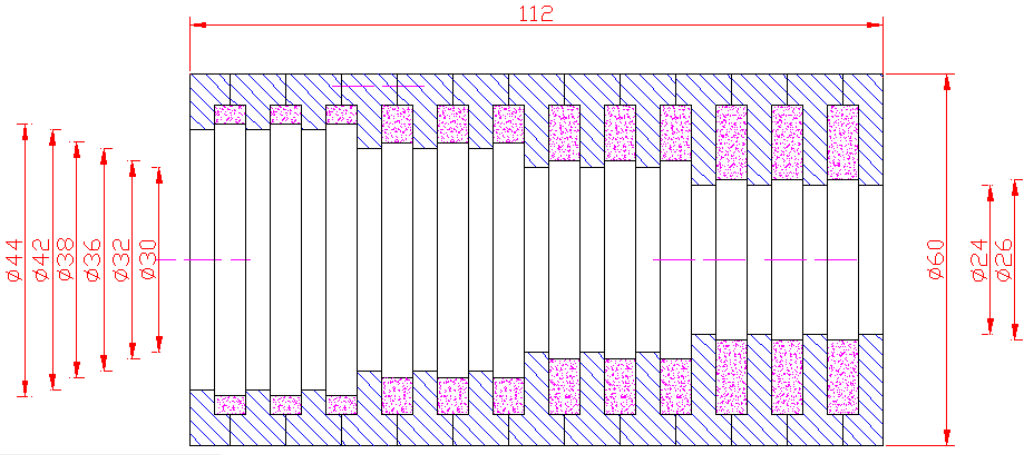

(Diameter in mm)

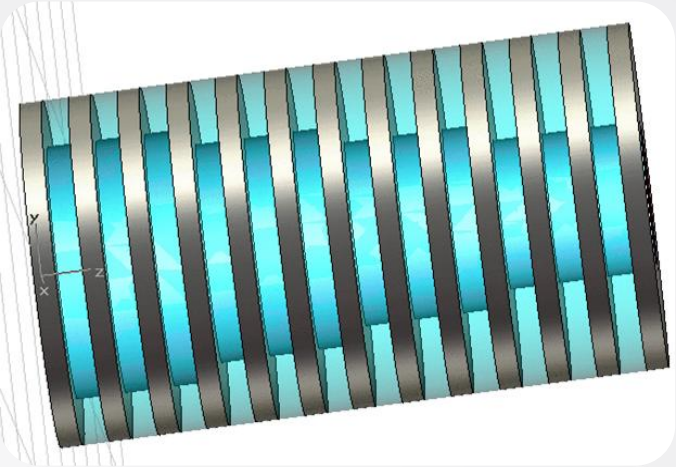

CST model

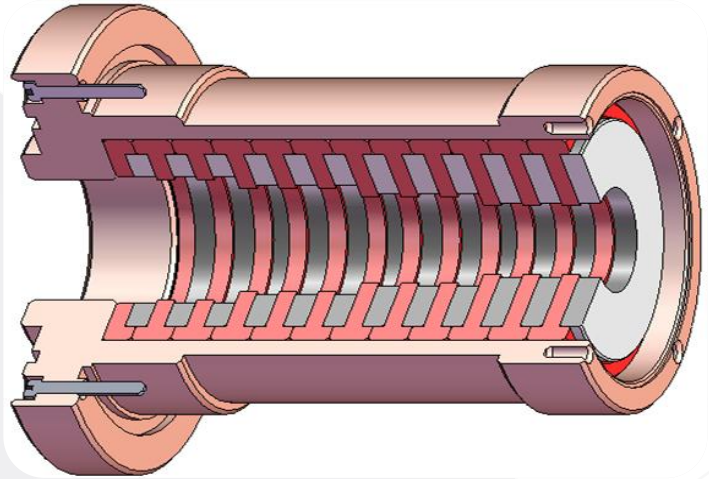

3D view

Courtesy: Dr. AK Sinha

Gyrotron interaction cavity

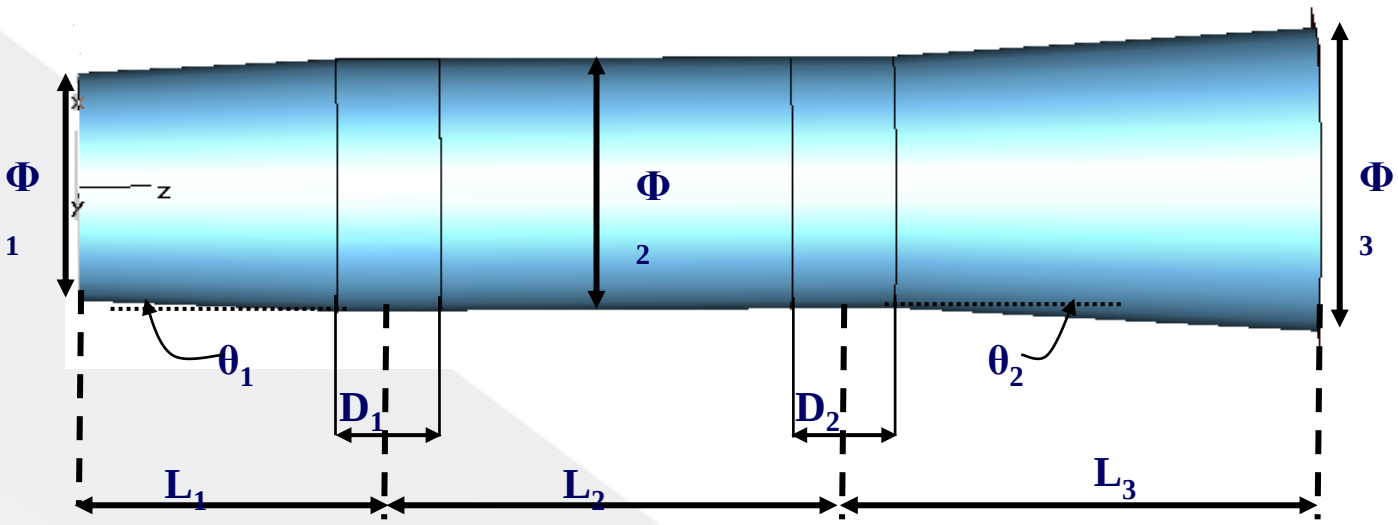

Dimensions	
Length $L_1/L_2/L_3$ (mm)	30/44/46
Taper angle $\theta_1/\theta_2/\theta_3$ (degree)	2º/0º/3º
Parabolic smoothing D_1/D_2 (mm)	10/10
Cavity diameter $\Phi_1/\Phi_2/\Phi_3$ (mm)	21.14/23.14/28

Courtesy: Dr. AK Sinha

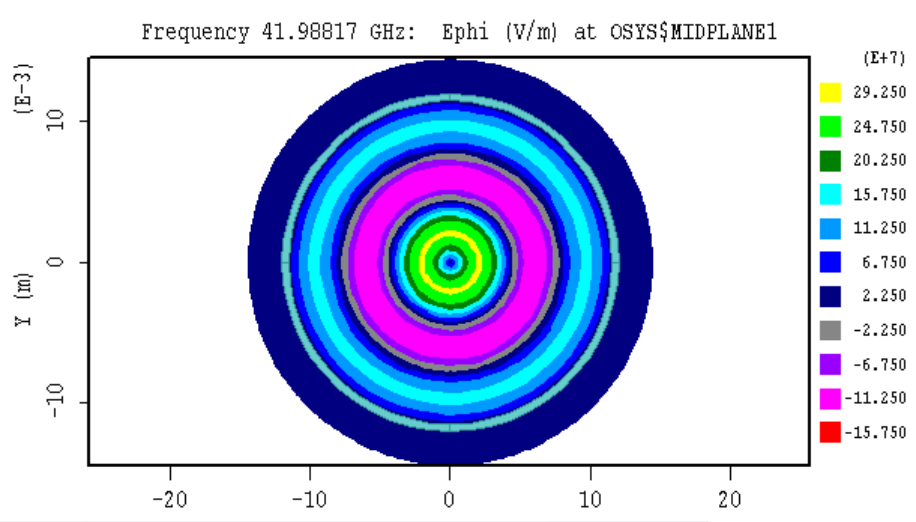

Field contour

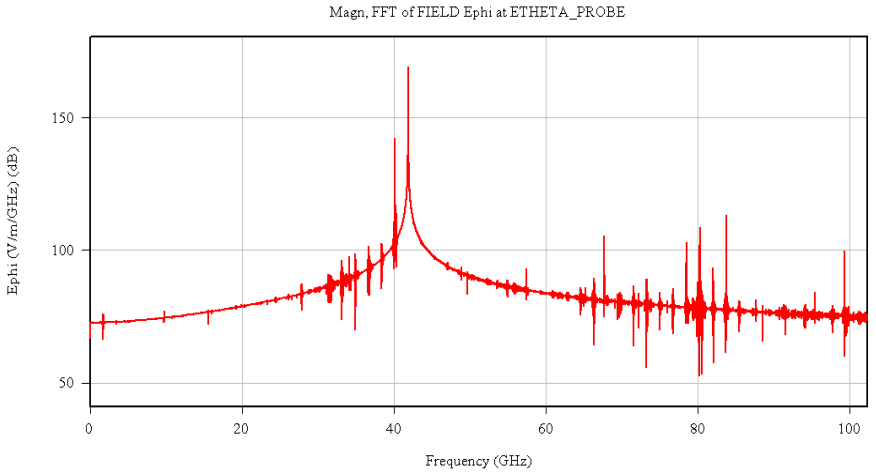

Field versus frequency

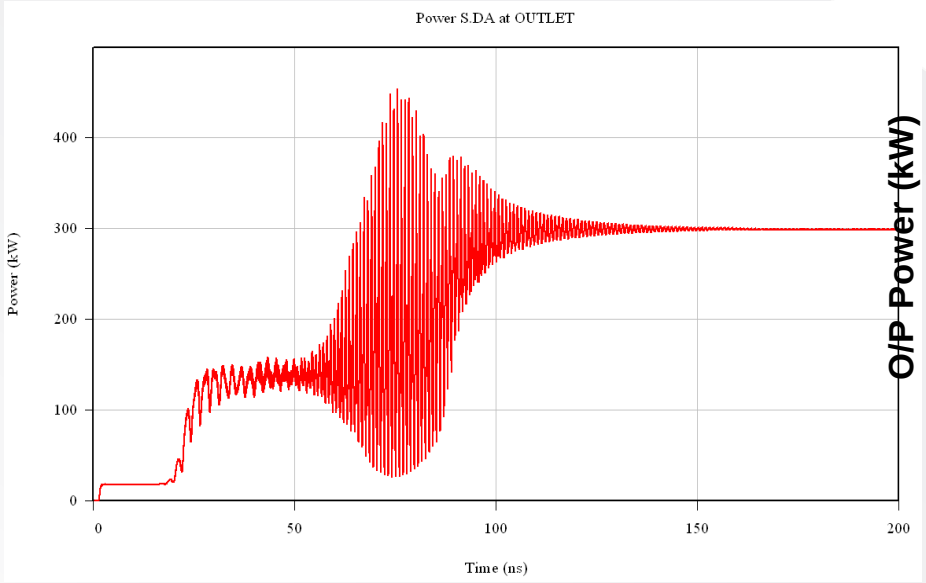

Output versus time

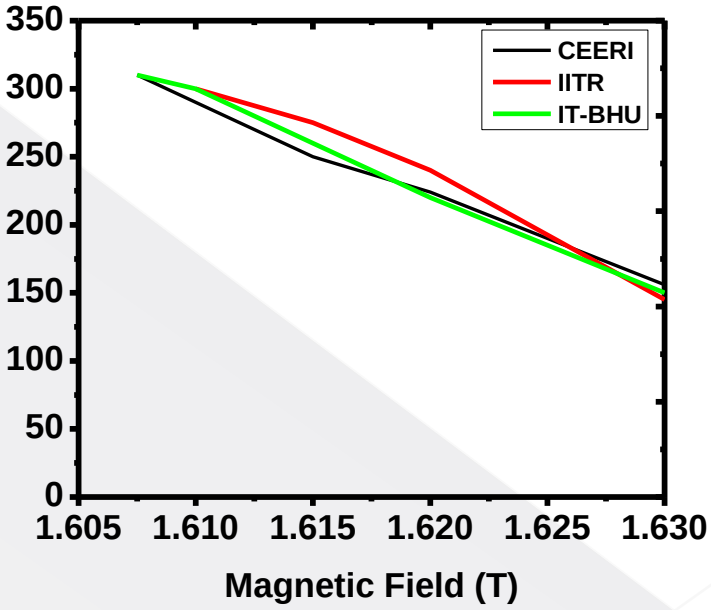

Output power versus time

Courtesy: Dr. AK Sinha

Gyrotron nonlinear taper

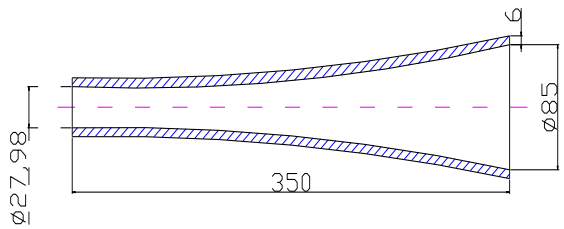

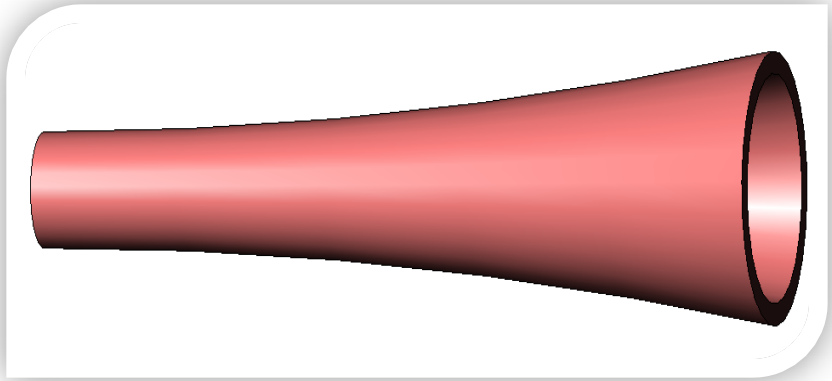

2D view

3D view of Non linear taper

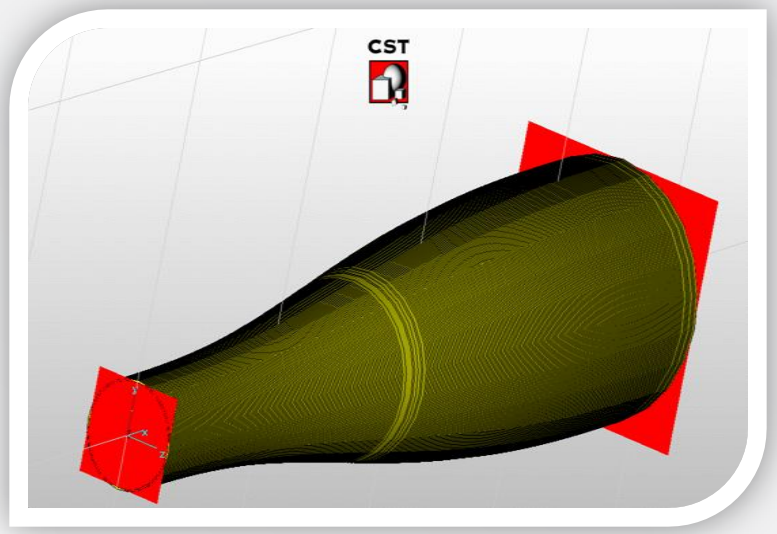

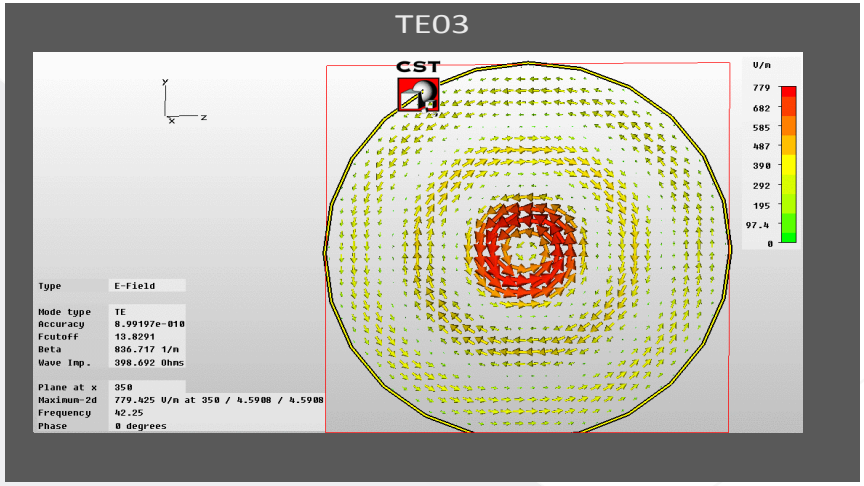

Simulated model

Field pattern at the taper output port

Courtesy: Dr. AK Sinha

Radius (mm)	Nonlinear taper length (mm)	Transmission coefficient S_{21}
35.0	300.0	99.8299 %
35.0	350.0	99.7418 %
35.0	400.0	99.8376 %
40.0	300.0	98.9202 %
40.0	350.0	99.4713 %
40.0	400.0	99.8643 %
45.0	300.0	96.5986 %
45.0	350.0	98.9727 %
45.0	400.0	98.4444 %

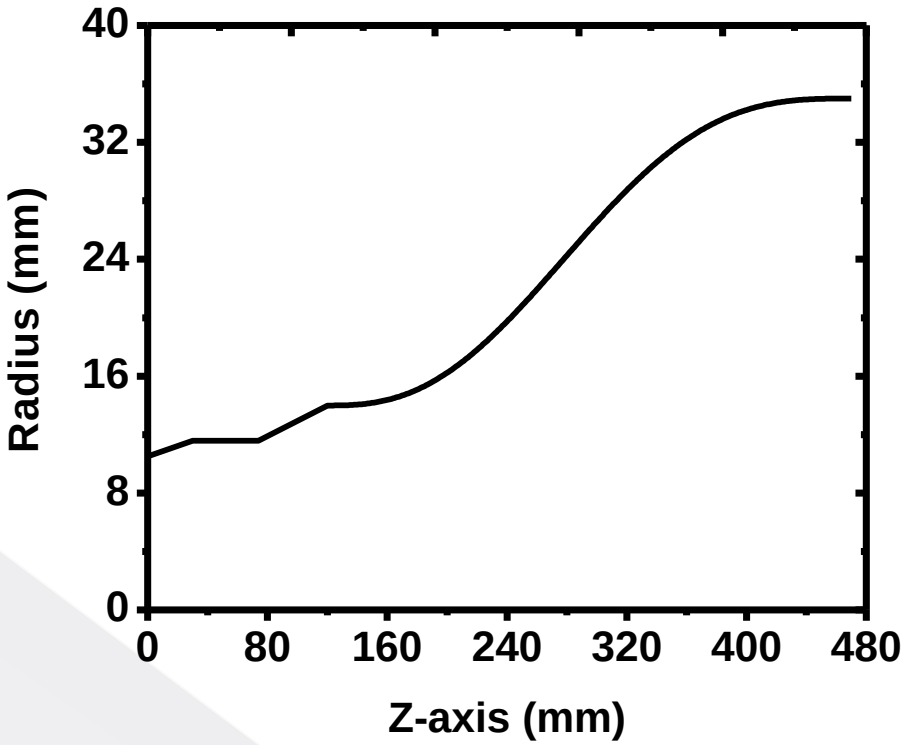

Mode purity at the end of the taper	Better than 92%

Courtesy: Dr. AK Sinha

CEERI folded-waveguide TWT in collaboration with TUB,Germany

3D modeling

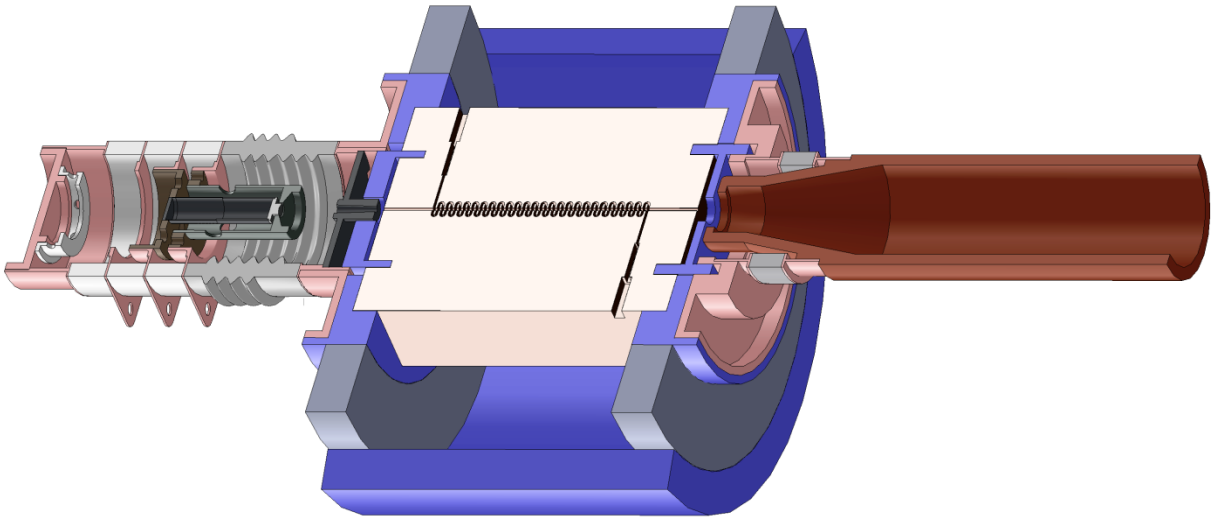

Courtesy: Ms. Isha Rathi, Dr. RK Sharma

Optimized dimensions

Parameter	Dimension (µm)
Depth ‘a’	1800
Gap Width ‘b’	300
Pitch ‘p’	550
Straight Height ‘h’	600
Tunnel Radius ‘r’	200

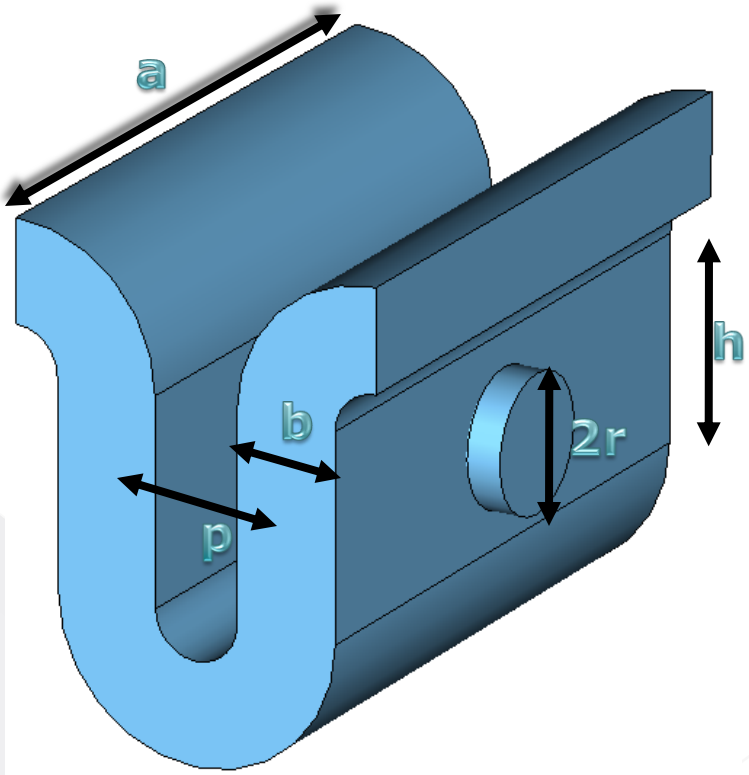

Courtesy: Ms. Isha Rathi, Dr. RK Sharma

Electric field pattern
(CST)

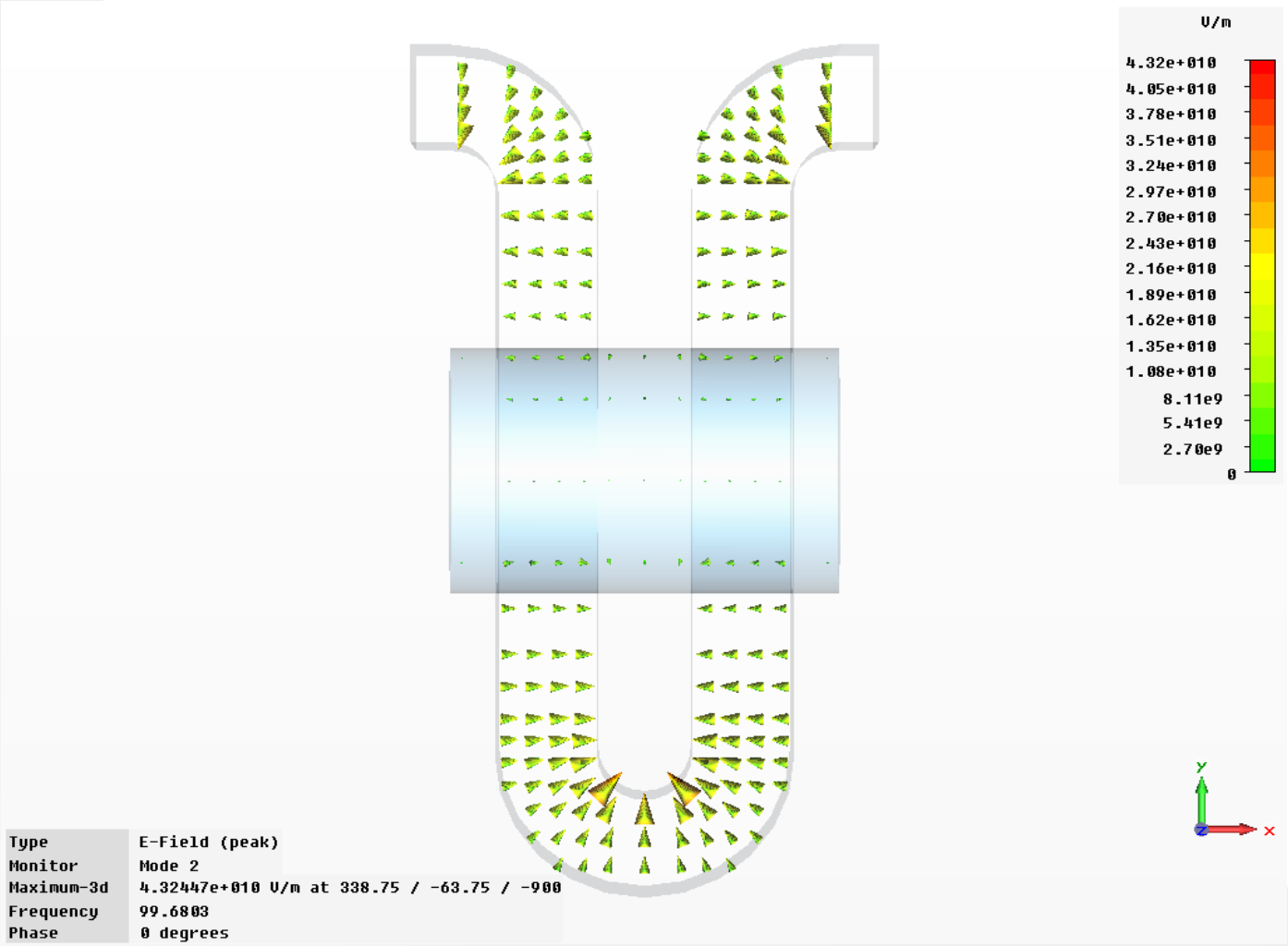

Courtesy: Ms. Isha Rathi, Dr. RK Sharma

Electric field pattern (using GdfidL at TUB)

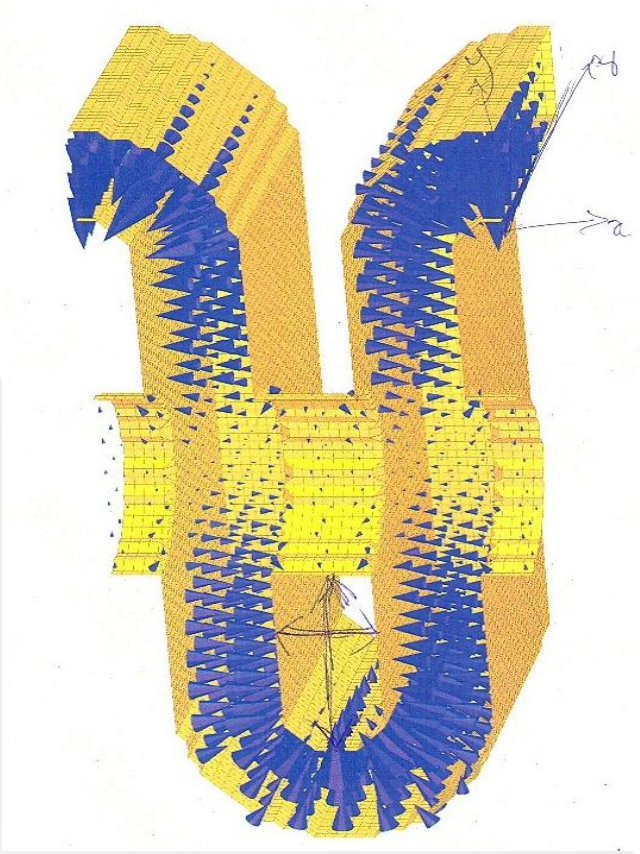

Courtesy: Dr. A. Grede, Prof. Dr. H. Henke (TUB)

Dispersion plot

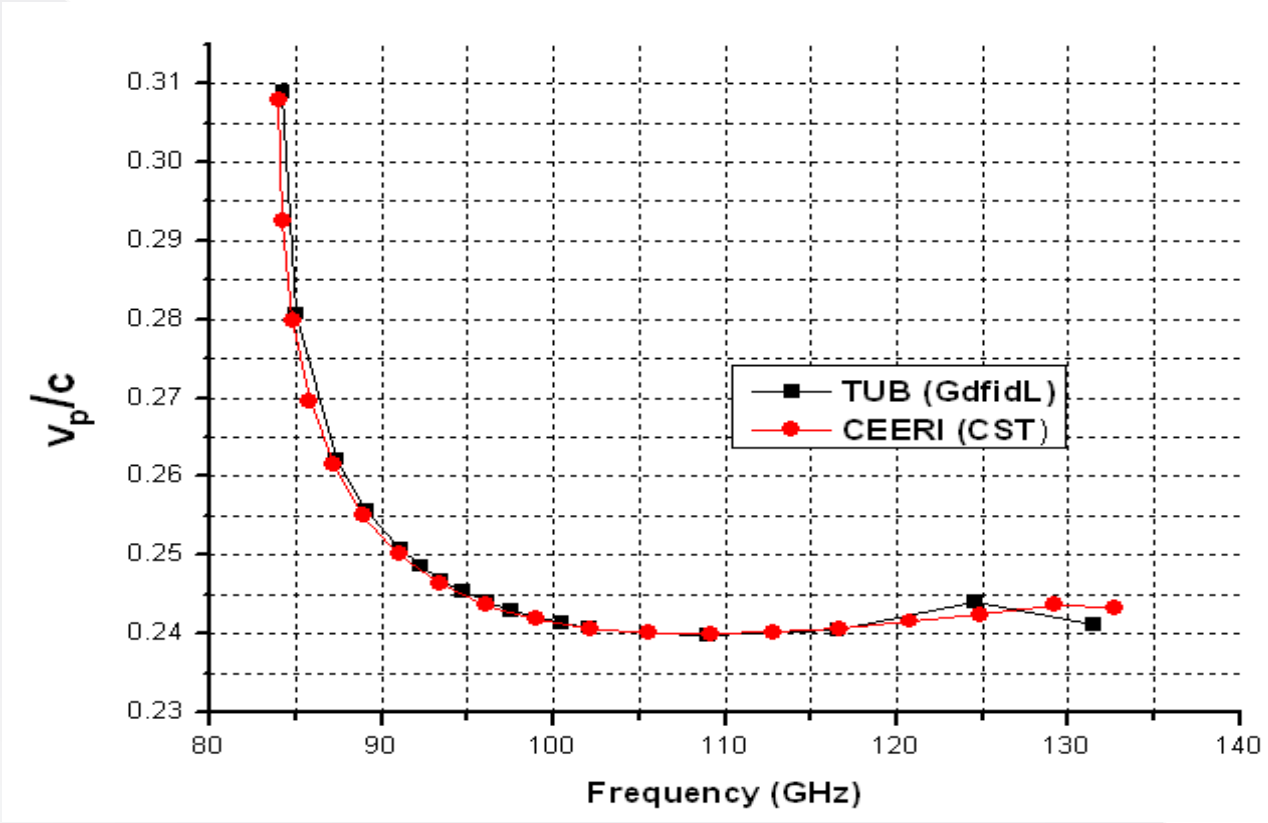

Courtesy: Ms. Isha Rathi, Dr. RK Sharma

Dispersion plot

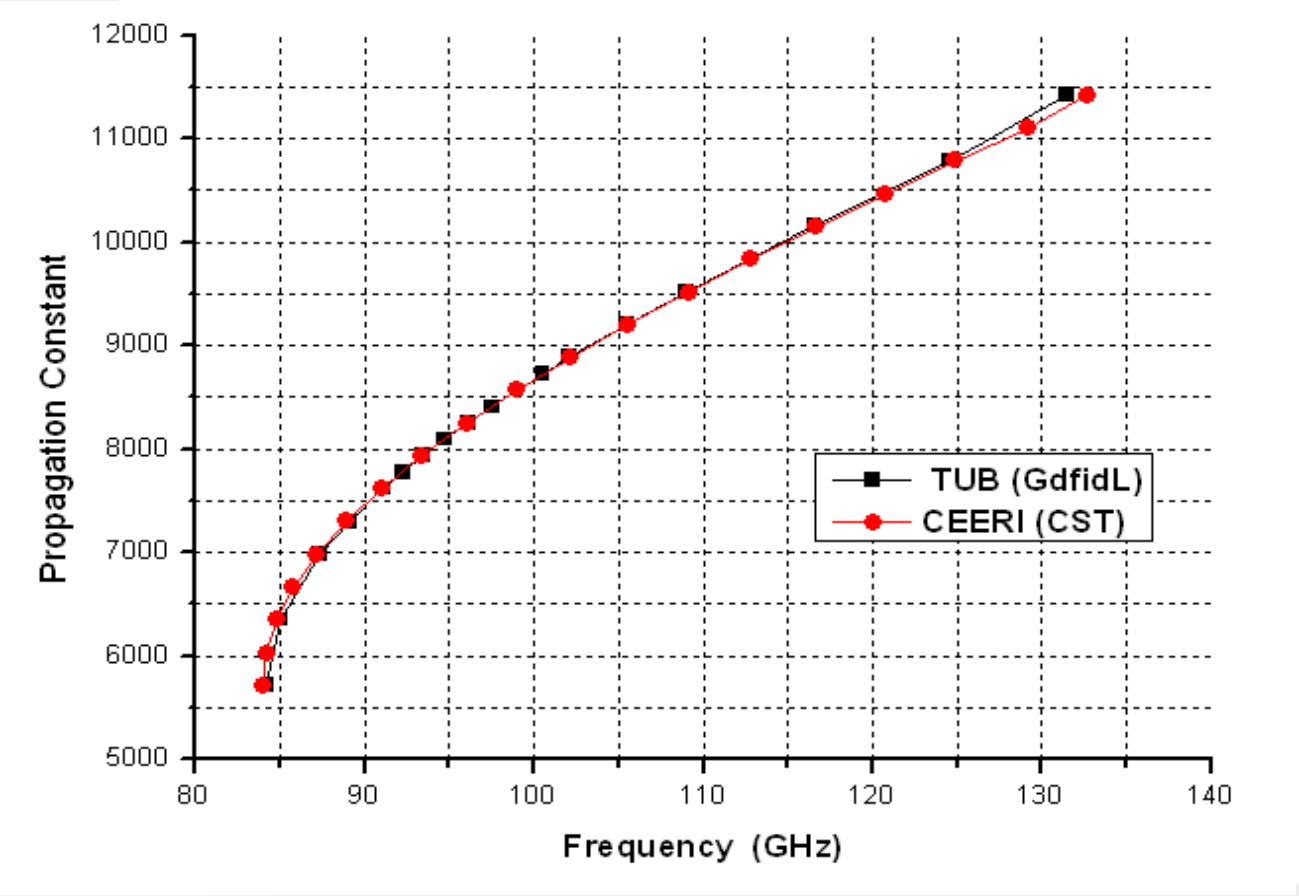

Courtesy: Ms. Isha Rathi, Dr. RK Sharma

Quality factor

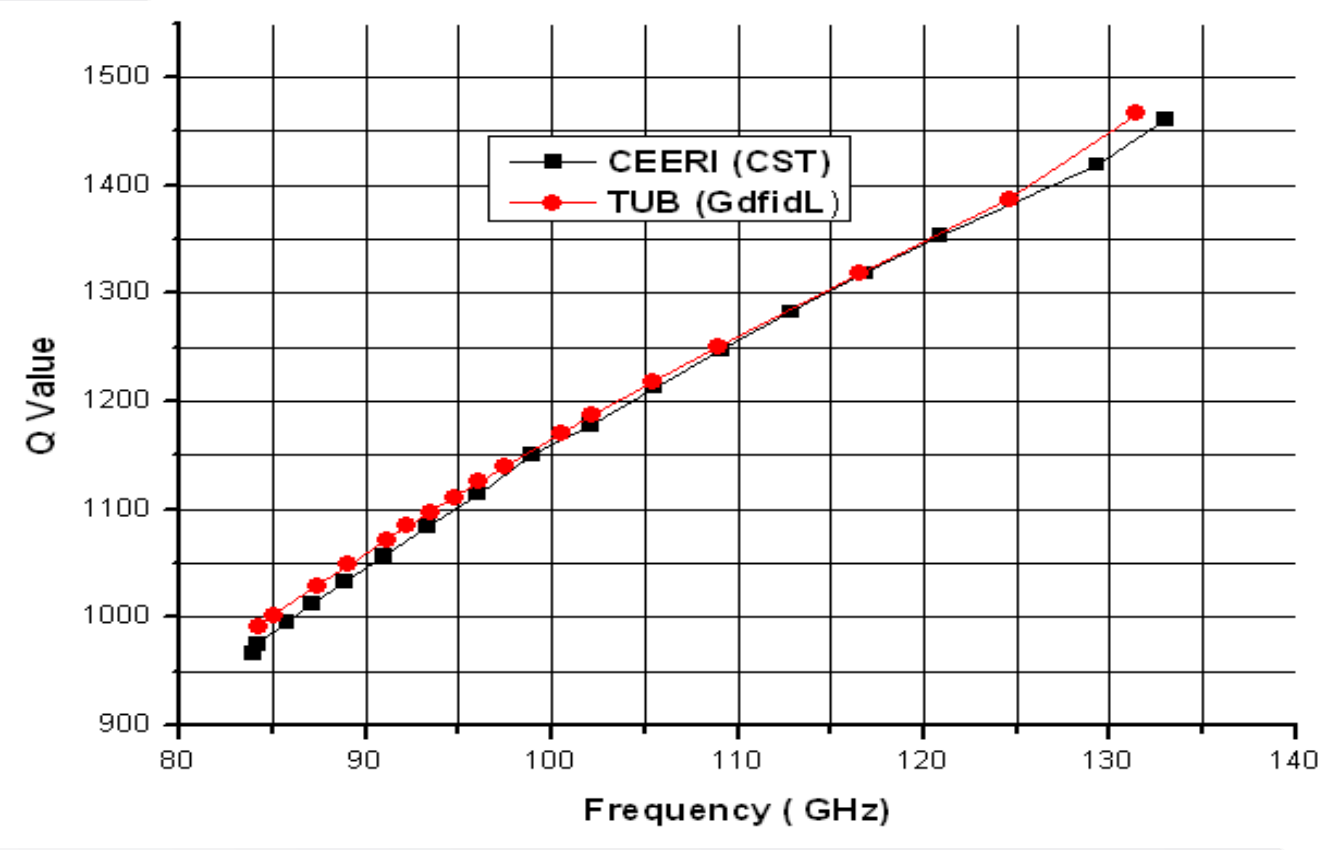

Courtesy: Ms. Isha Rathi, Dr. RK Sharma

Loss characteristics

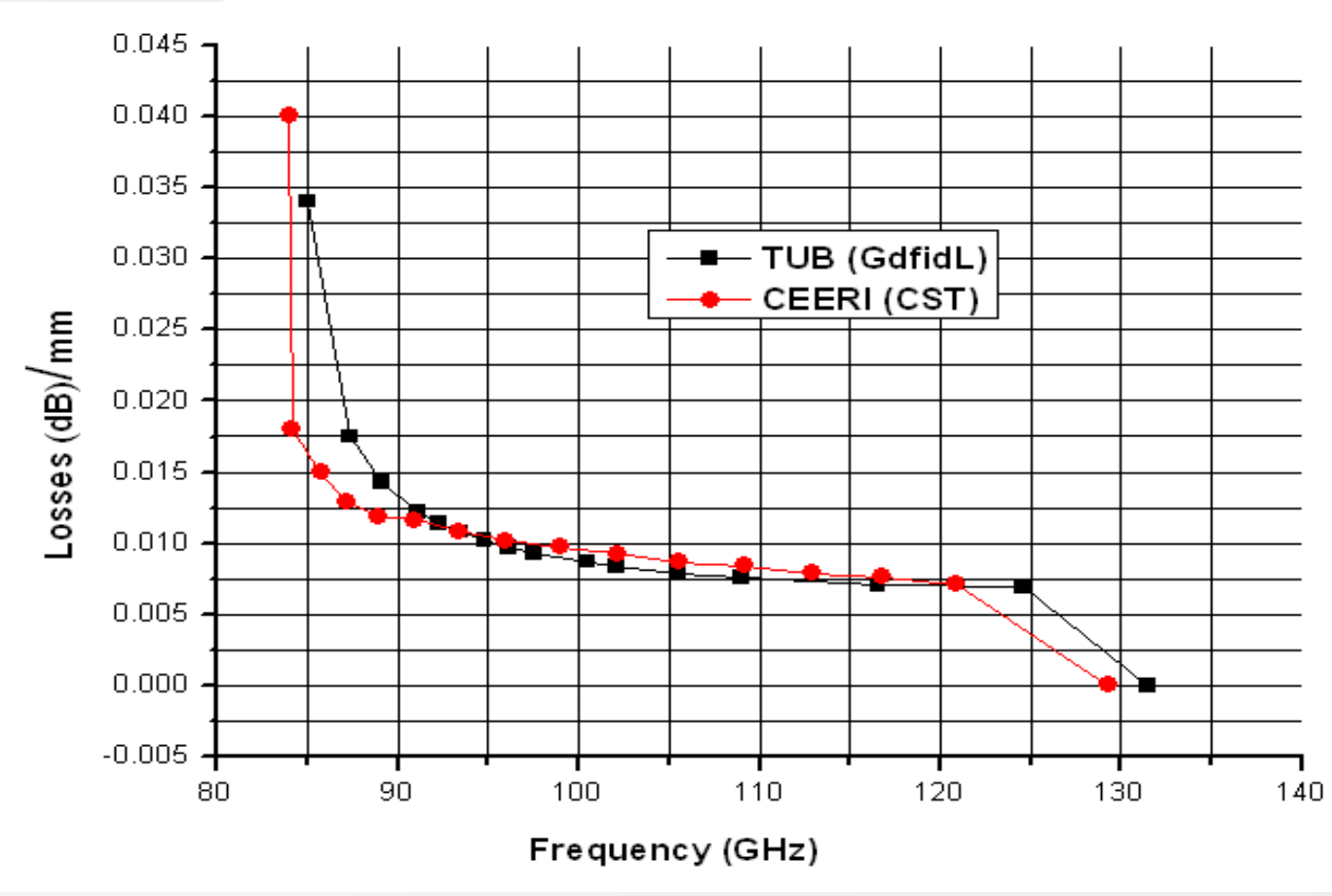

Courtesy: Ms. Isha Rathi, Dr. RK Sharma

Dispersion plot

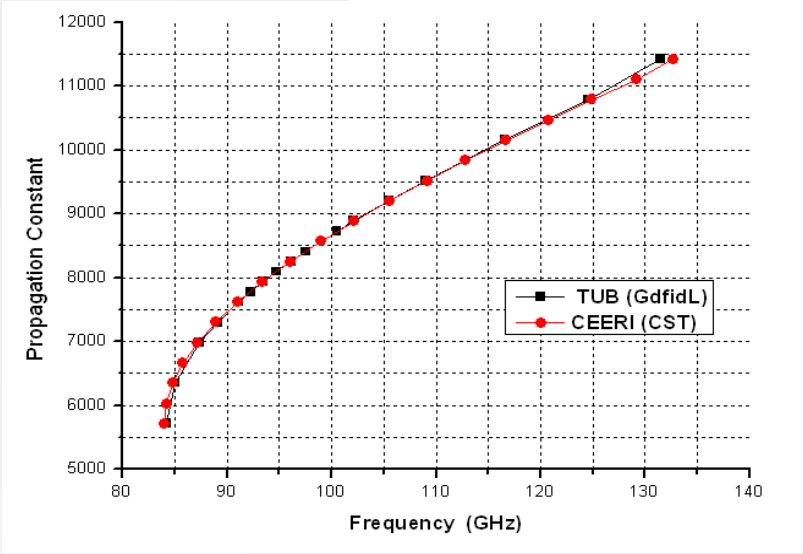

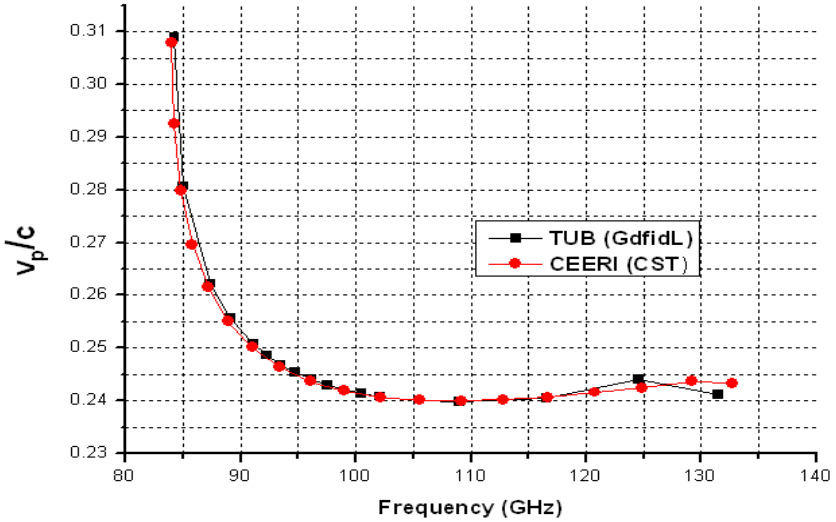

Courtesy: Ms. Isha Rathi, Dr. RK Sharma

Quality factor

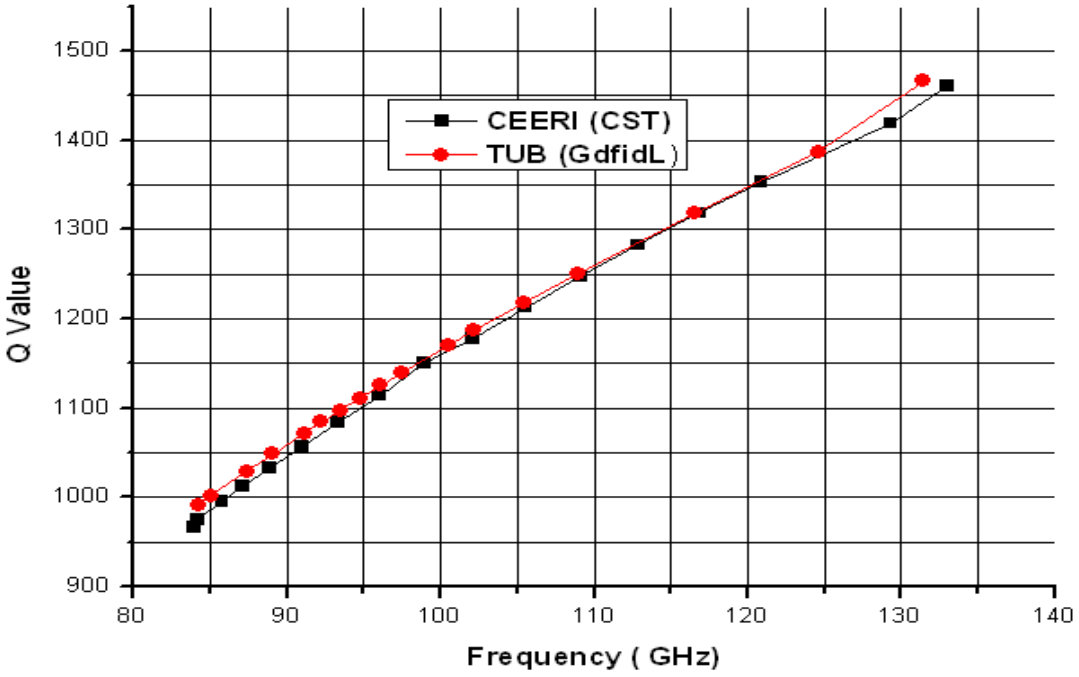

Courtesy: Ms. Isha Rathi, Dr. RK Sharma

Circuit loss

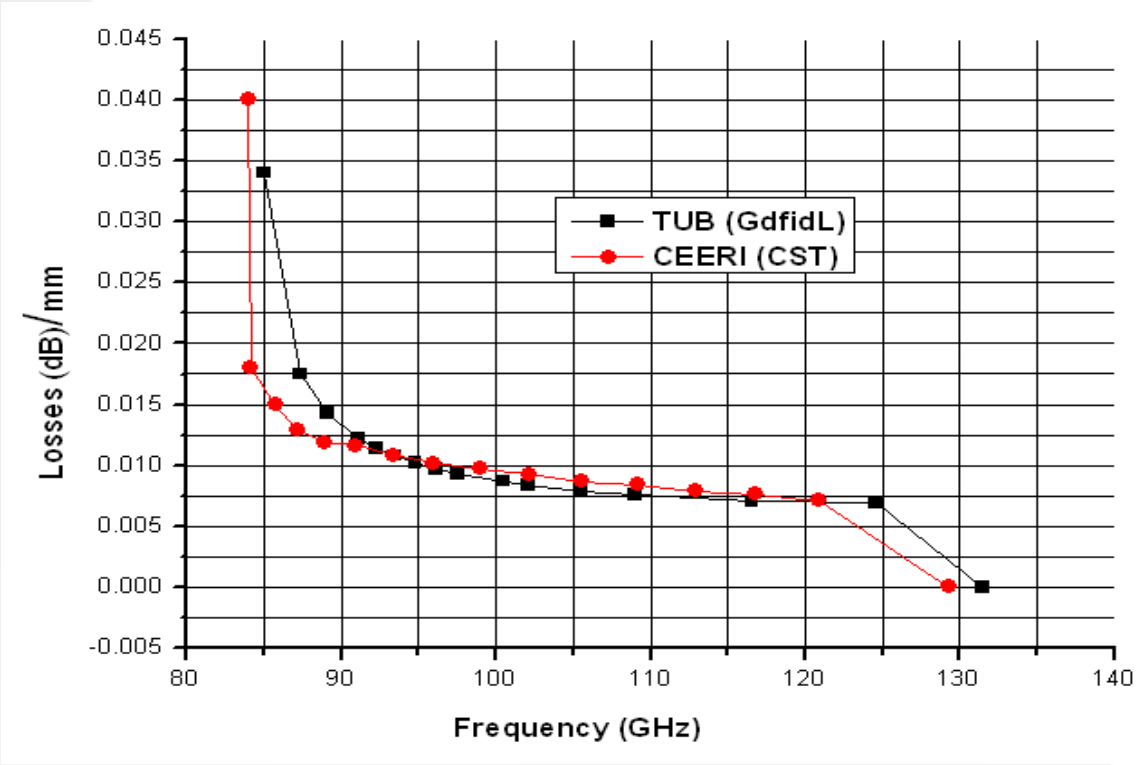

Courtesy: Ms. Isha Rathi, Dr. RK Sharma

Small signal gain using SUNRAY-1D for circuit length 55mm

Frequency in GHz	Gain in dB
85.02	-0.24
87.36	0.16
89.07	-1.87
91.11	-6.03
92.25	-5.93
93.46	2.19
94.74	11.14
96.10	15.85
97.50	17.79
100.52	17.06
102.11	15.43
105.45	11.63
108.98	8.73
116.54	7.55

Courtesy: Ms. Isha Rathi, Dr. RK Sharma

PIC-simulation using Gdfid (TUB)

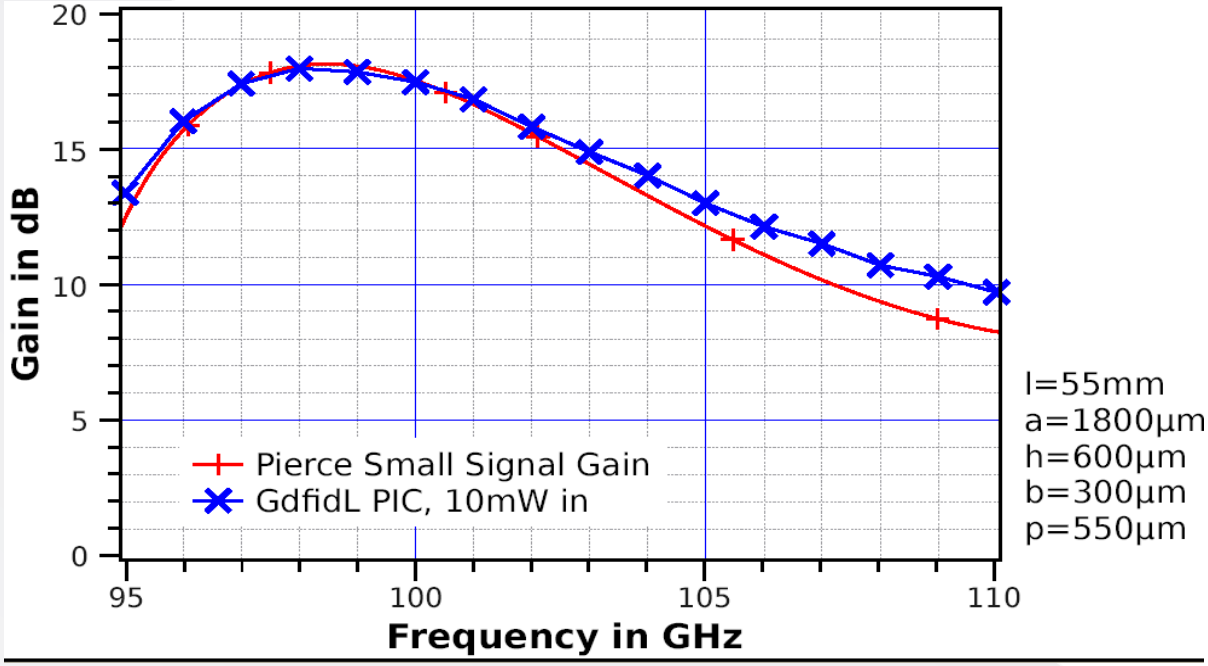

Courtesy: A. Grede, H. Henke (TUB)

Helix Slow-wave Structure – 3D Simulation

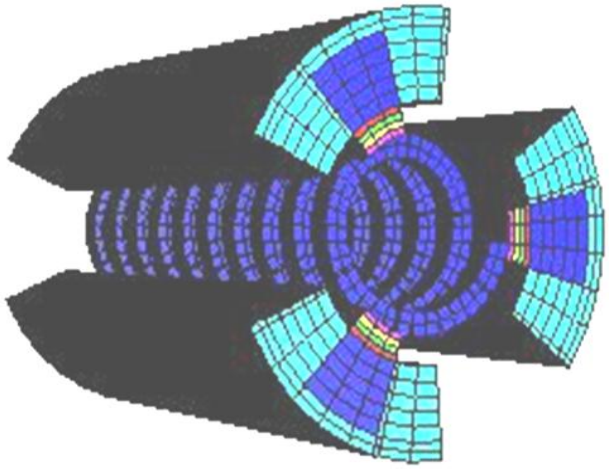

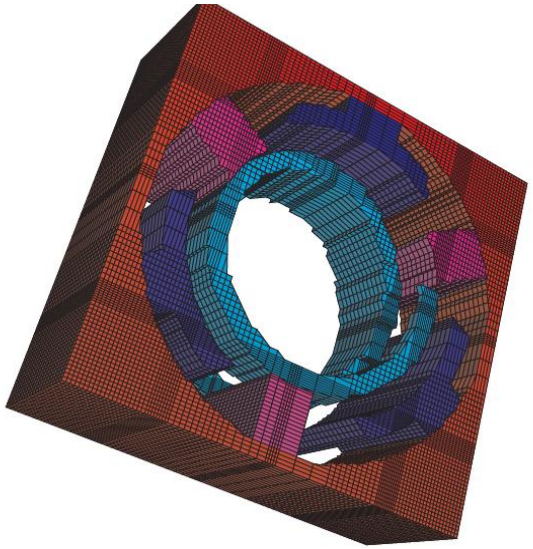

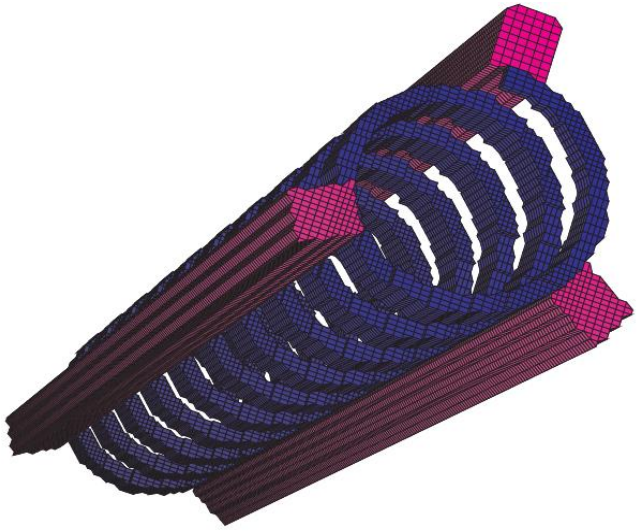

Dispersion Characteristics

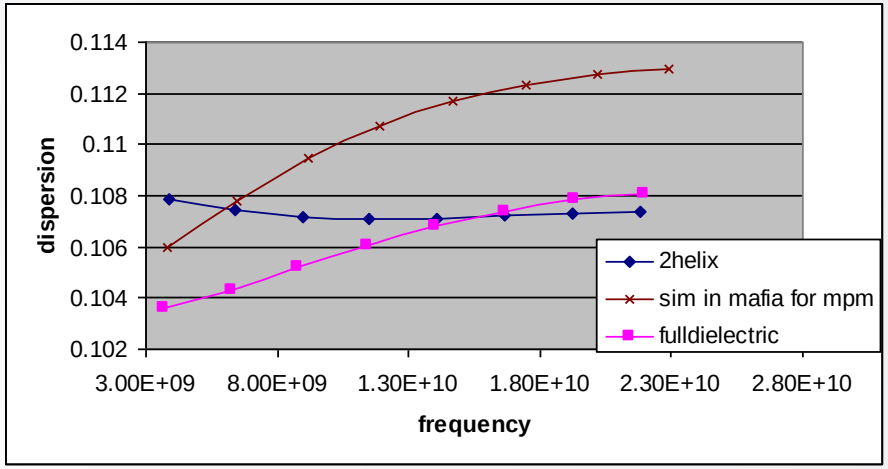

Impedance Characteristics

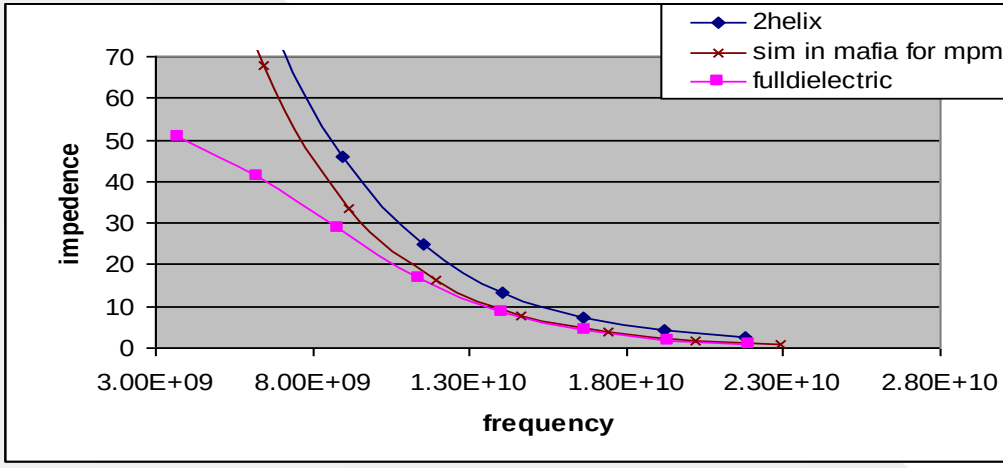

Trial fabrication at CMRI in liaison with CEERI

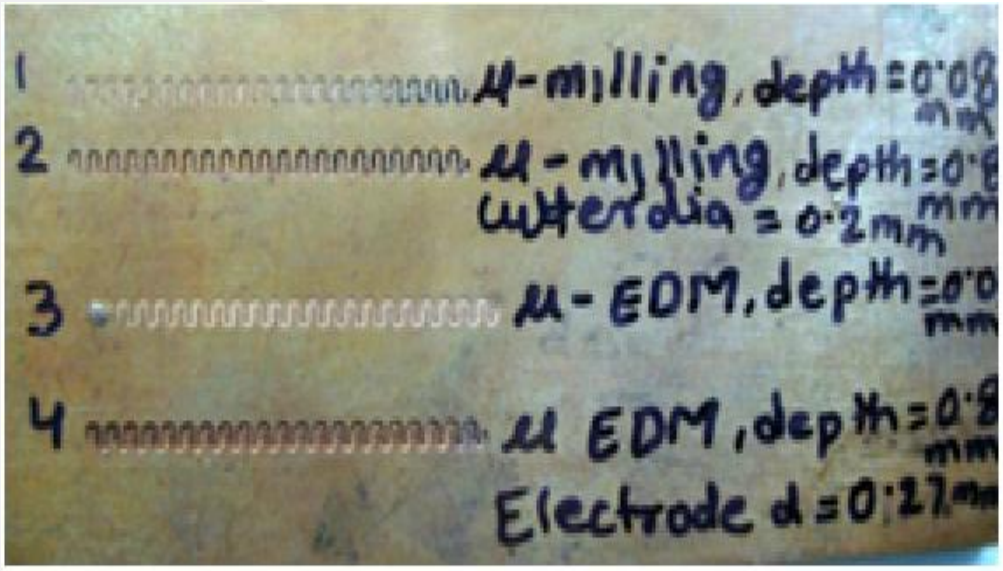

Trial using laser technology

Courtesy: Ms. Isha Rathi, Dr. RK Sharma

Electron Gun for mm-wave TWT

Electron Gun for mm-wave TWT

- Ion barrier Anode
- Beam diameter : 350μm
- Beam current : 100mA
- Highly thermal beam

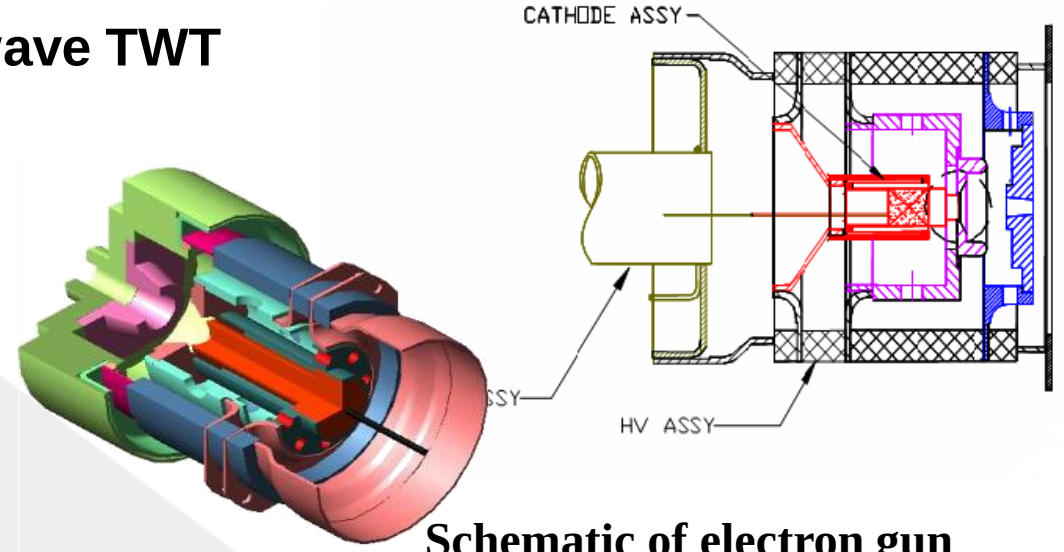

Schematic of electron gun

Ion effects in mm-wave gun

- Ion generation major problem in mm wave guns
- Causes neutralization of electron beam
- Causes problems in beam focusing
- Cathode poisoning

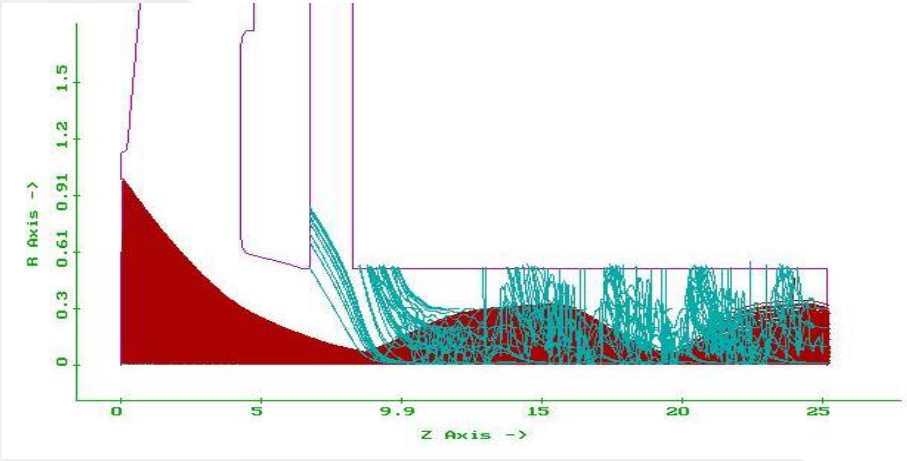

Ion anode barrier restricting ions to go to cathode

Advanced Technology for TWTs

- *Brazed helix SWS.*

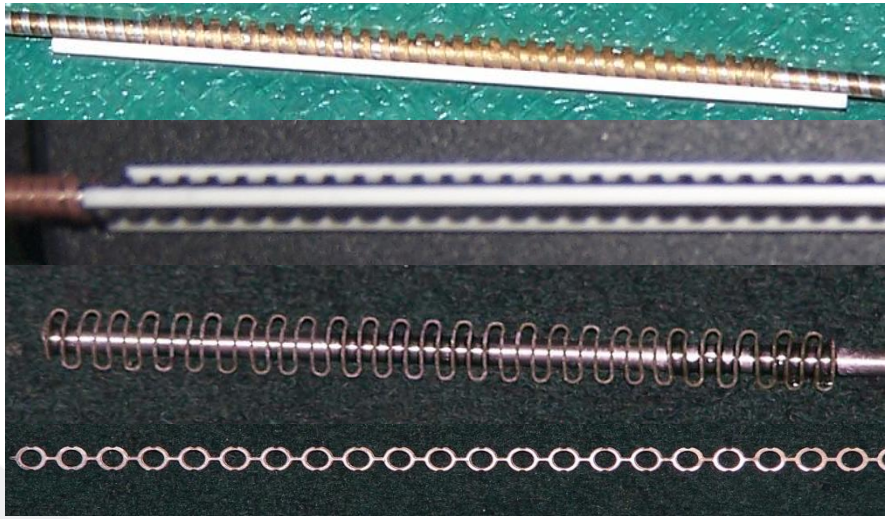

- *Ring-loop SWS*

- *Folded-waveguide*

Ka-band FWS

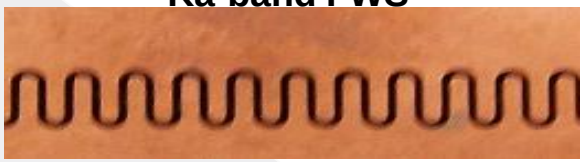

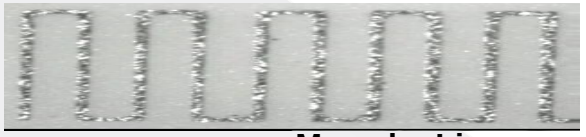

Meander Line

W-band

- *Resonant loss (meander line) for BWO suppression*

- *Coated Vane SWS*

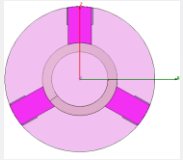

Depressed Collectors

Tilted Electric Field (TEF) Collector for mm-wave helix TWT

- **Higher efficiency collector (Typical Collector Efficiency ~ 70-80%**
- **Better Thermal Handling**

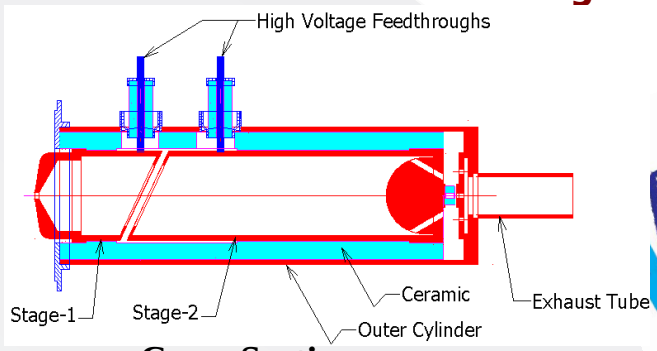

Cross Section

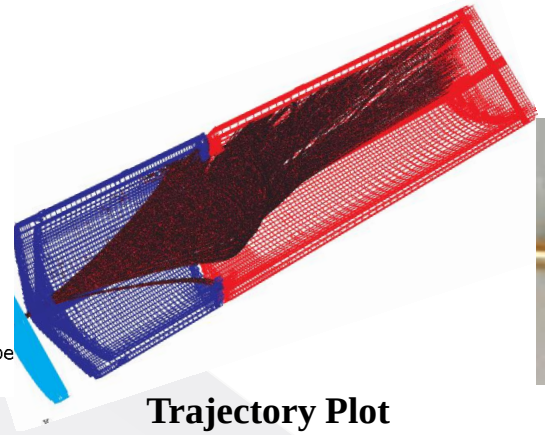

Trajectory Plot

Final Collector

Collector Piece Parts

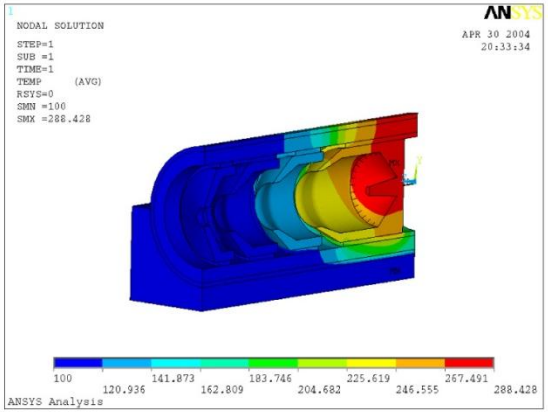

Thermal Analysis

Multiple Beam Klystrons (MBK)

Specifications:

- **Frequency : Ku-Band**
- **Power Output : 400W (Min)**
- **Gain : 39 dB (min)**

Electron Gun Simulation

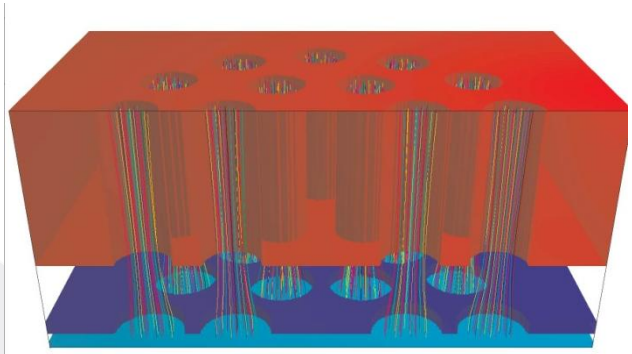

Solid model of Gun

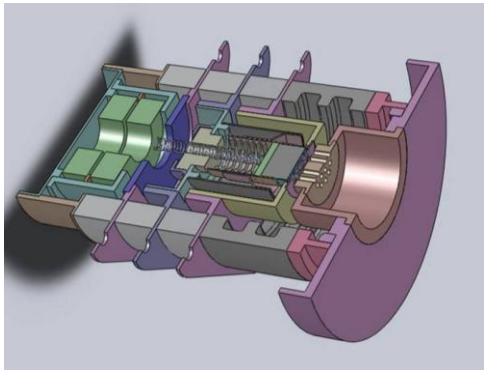

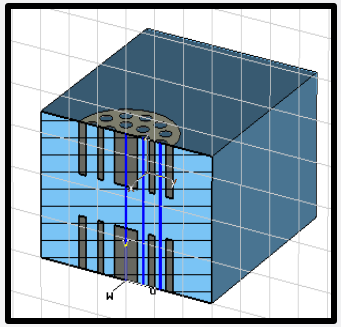

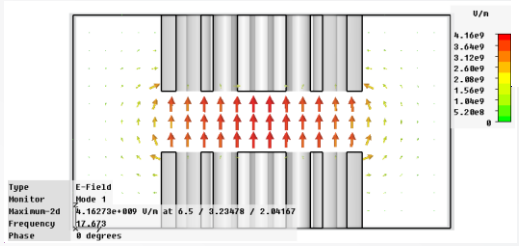

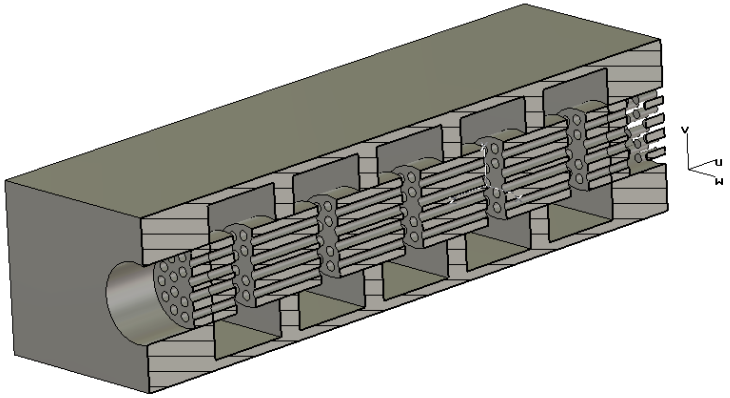

Cavity Simulation

Solid Model of Collector

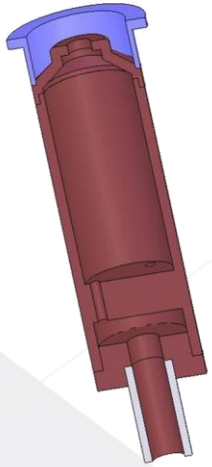

Multiple Beam Klystrons (MBK)

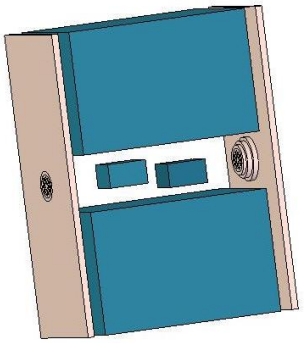

Magnetic Field Simulation

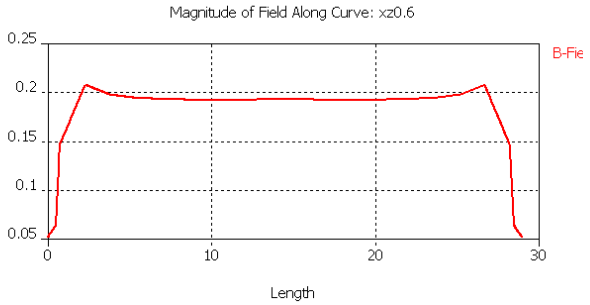

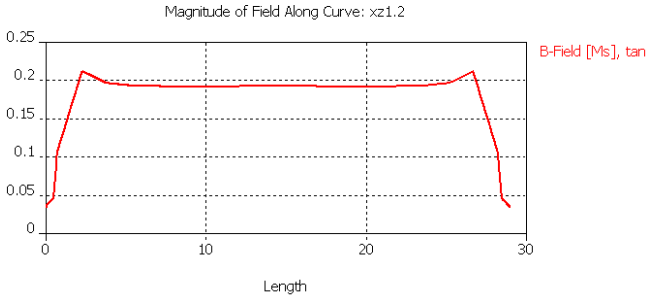

Off-axis magnetic fields

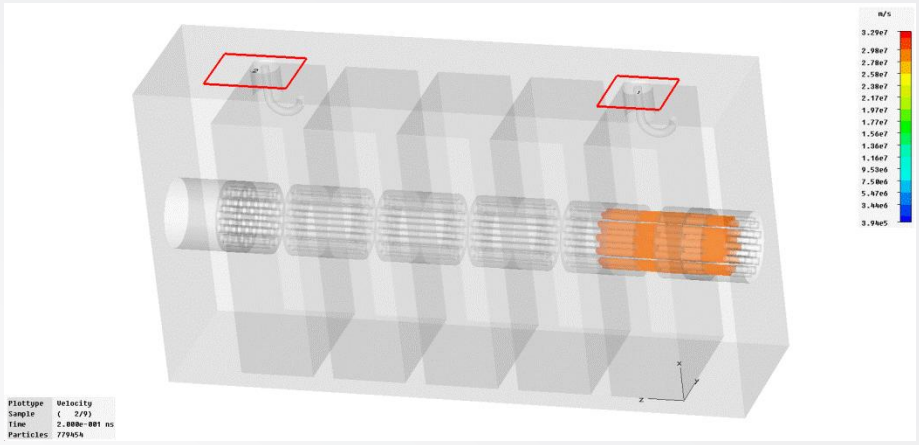

Magnetostatic Focusing

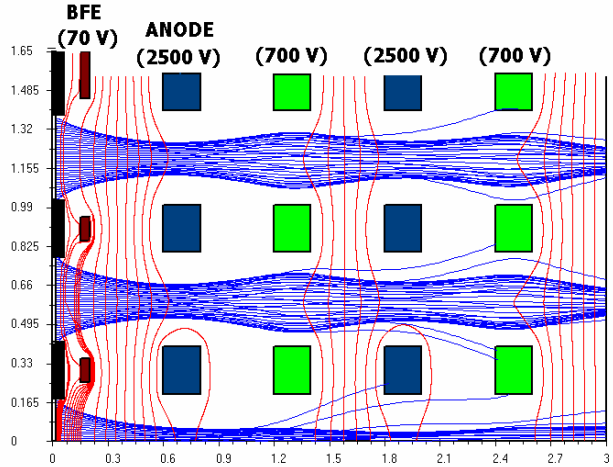

Electrostatic Focusing


Thank You!

Maxwell's Equations
and
Electromagnetic Boundary Conditions

B N Basu
<bnbasu.india@gmail.com>

Gradient of a scalar quantity

$$\left.\begin{aligned}(\nabla V)_1 &= \frac{1}{h_1}\frac{\partial V}{\partial u_1}\\ (\nabla V)_2 &= \frac{1}{h_2}\frac{\partial V}{\partial u_2}\\ (\nabla V)_3 &= \frac{1}{h_3}\frac{\partial V}{\partial u_3}\end{aligned}\right\} \longleftarrow \left\{\begin{aligned}\frac{\partial V}{\partial u_1} &= (\nabla V)_1 h_1\\ \frac{\partial V}{\partial u_2} &= (\nabla V)_2 h_2\\ \frac{\partial V}{\partial u_3} &= (\nabla V)_3 h_3\end{aligned}\right\}$$

$$\nabla V = (\nabla V)_1 \vec{a}_1 + (\nabla V)_2 \vec{a}_2 + (\nabla V)_3 \vec{a}_3$$

$$\nabla V = \frac{1}{h_1}\frac{\partial V}{\partial u_1}\vec{a}_1 + \frac{1}{h_2}\frac{\partial V}{\partial u_2}\vec{a}_2 + \frac{1}{h_3}\frac{\partial V}{\partial u_3}\vec{a}_3$$

(Gradient of scalar *V* in generalized curvilinear system of coordinates)

$$\nabla V = \frac{1}{h_1}\frac{\partial V}{\partial u_1}\vec{a}_1 + \frac{1}{h_2}\frac{\partial V}{\partial u_2}\vec{a}_2 + \frac{1}{h_3}\frac{\partial V}{\partial u_3}\vec{a}_3$$ **(Curvilinear system of coordinates)**

$$\nabla V = \frac{\partial V}{\partial x}\vec{a}_x + \frac{\partial V}{\partial y}\vec{a}_y + \frac{\partial V}{\partial y}\vec{a}_y$$ **(Rectangular system of coordinates)**

$$(h_1 = 1, h_2 = 1, h_3 = 1;\ u_1 = x, u_2 = y, u_3 = z)$$

$$\nabla V = \frac{\partial V}{\partial r}\vec{a}_r + \frac{1}{r}\frac{\partial V}{\partial \theta}\vec{a}_\theta + \frac{\partial V}{\partial z}\vec{a}_z$$ **(Cylindrical system of coordinates)**

$$(h_1 = 1, h_2 = r, h_3 = 1;\ u_1 = r, u_2 = \theta, u_3 = z)$$

$$\nabla V = \frac{\partial V}{\partial r}\vec{a}_r + \frac{1}{r}\frac{\partial V}{\partial \theta}\vec{a}_\theta + \frac{1}{r\sin\theta}\frac{\partial V}{\partial \phi}\vec{a}_\phi$$ **(Spherical system of coordinates)**

$$(h_1 = 1, h_2 = r, h_3 = r\sin\theta;\ u_1 = r, u_2 = \theta, u_3 = \phi)$$

Divergence of a vector quantity

The divergence of a vector quantity such as electric field $\vec{E}$ at a point is a scalar quantity.

The divergence of a vector quantity such as electric field $\vec{E}$ at a point is the outward flux of $\vec{E}$ through the surface of an elemental or differential volume $\Delta\tau$ enclosing the point (closed surface integral of $\vec{E}$ over the surface of the enclosure) divided by the volume element $\Delta\tau$ in the limit the volume element $\Delta\tau$ tending to zero, thereby the volume element shrinking to the point.

$$\mathrm{div}\vec{E} = \nabla \cdot \vec{E} = \underset{\Delta\tau \to 0}{Lt} \frac{\oint_S \vec{E} \cdot \vec{a}_n \, dS}{\Delta\tau}$$

Divergence of a vector quantity in curvilinear system

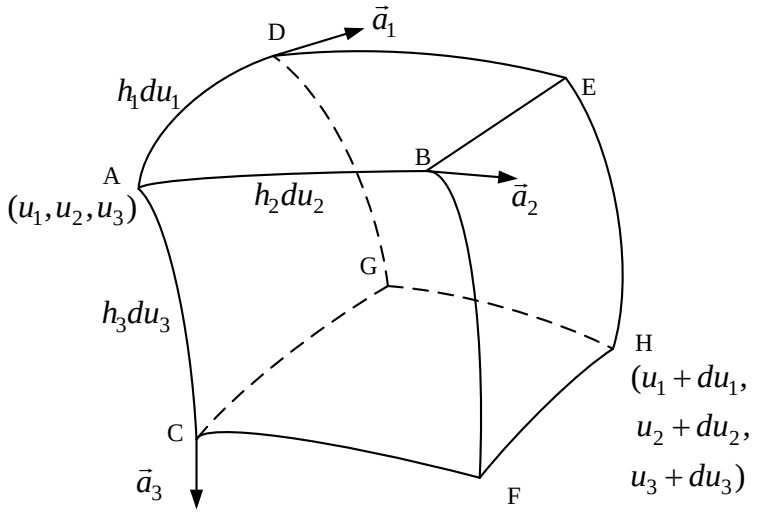

$$\operatorname{div}\vec{E} = \nabla \cdot \vec{E} = \lim_{\Delta\tau \to 0} \frac{\oint_S \vec{E} \cdot \vec{a}_n \, dS}{\Delta\tau}$$

$$\nabla \cdot \vec{E} = \frac{1}{h_1 h_2 h_3}\left[\frac{\partial(h_2 h_3 E_1)}{\partial u_1} + \frac{\partial(h_3 h_1 E_2)}{\partial u_2} + \frac{\partial(h_1 h_2 E_3)}{\partial u_3}\right]$$

(Curvilinear system of coordinates)

$$\nabla \cdot \vec{E} = \frac{\partial E_x}{\partial x} + \frac{\partial E_y}{\partial y} + \frac{\partial E_z}{\partial z}$$

(Rectangular system of coordinates)

$$(h_1 = 1, h_2 = 1, h_3 = 1;\ u_1 = x, u_2 = y, u_3 = z)$$

$$\nabla \cdot \vec{E} = \frac{1}{r}\left[\frac{\partial(rE_r)}{\partial r} + \frac{\partial E_\theta}{\partial \theta} + \frac{\partial(rE_z)}{\partial z}\right] = \frac{1}{r}\frac{\partial(rE_r)}{\partial r} + \frac{1}{r}\frac{\partial E_\theta}{\partial \theta} + \frac{\partial E_z}{\partial z}$$

(Cylindrical system of coordinates)

$$(h_1 = 1, h_2 = r, h_3 = 1;\ u_1 = r, u_2 = \theta, u_3 = z)$$

$$\nabla \cdot \vec{E} = \frac{1}{r^2 \sin\theta}\left[\frac{\partial(r^2 \sin\theta\, E_r)}{\partial r} + \frac{\partial(r \sin\theta\, E_\theta)}{\partial \theta} + \frac{\partial(rE_\phi)}{\partial \phi}\right]$$

$$= \frac{1}{r^2}\frac{\partial(r^2 E_r)}{\partial r} + \frac{1}{r\sin\theta}\frac{\partial(\sin\theta\, E_\theta)}{\partial \theta} + \frac{1}{r\sin\theta}\frac{\partial(E_\phi)}{\partial \phi}$$

(Spherical system of coordinates)

$$(h_1 = 1, h_2 = r, h_3 = r\sin\theta;\ u_1 = r, u_2 = \theta, u_3 = \phi)$$

Curl of a vector quantity

The curl $\nabla \times \vec{E}$ of a vector quantity such as electric field $\vec{E}$ at a point is a vector quantity.

$$\nabla \times \vec{E} = (\nabla \times \vec{E})_1 \vec{a}_1 + (\nabla \times \vec{E})_2 \vec{a}_2 + (\nabla \times \vec{E})_3 \vec{a}_3$$

$(\nabla \times \vec{E})_1, (\nabla \times \vec{E})_2, (\nabla \times \vec{E})_3$ **: Components in the directions of** $\vec{a}_1, \vec{a}_2, \vec{a}_3$ **respectively**

$$(\nabla \times \vec{E})_3 = \lim_{\Delta S_3 \to 0} \frac{\oint_l \vec{E} \cdot d\vec{l}}{\Delta S_3}$$

$$\Delta S_3 = h_1 du_1 h_2 du_2$$

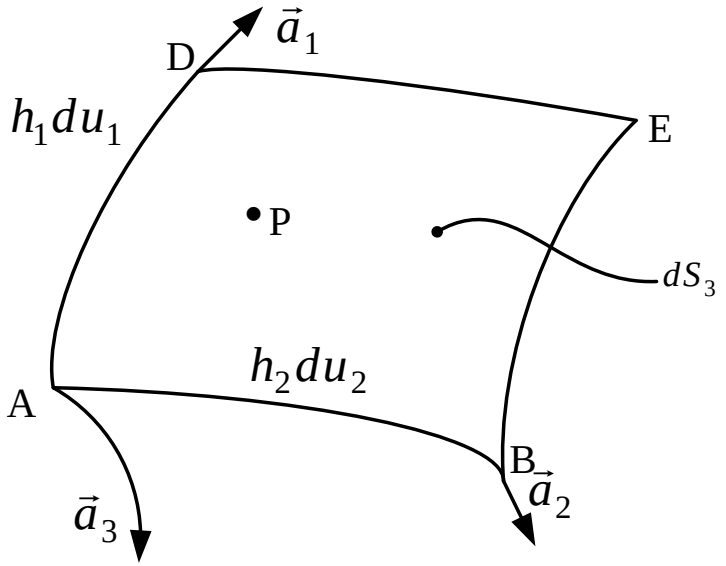

$$\nabla\times\vec{E}=\frac{1}{h_2h_3}\left(\frac{\partial(h_3E_3)}{\partial u_2}-\frac{\partial(h_2E_2)}{\partial u_3}\right)\vec{a}_1+\frac{1}{h_3h_1}\left(\frac{\partial(h_1E_1)}{\partial u_3}-\frac{\partial(h_3E_3)}{\partial u_1}\right)\vec{a}_2+\frac{1}{h_1h_2}\left(\frac{\partial(h_2E_2)}{\partial u_1}-\frac{\partial(h_1E_1)}{\partial u_2}\right)\vec{a}_3$$

(Curvilinear system of coordinates)

$$\nabla\times\vec{E}=\left(\frac{\partial E_z}{\partial y}-\frac{\partial E_y}{\partial z}\right)\vec{a}_x+\left(\frac{\partial E_x}{\partial z}-\frac{\partial E_z}{\partial x}\right)\vec{a}_y+\left(\frac{\partial E_y}{\partial x}-\frac{\partial E_x}{\partial y}\right)\vec{a}_z$$

(Rectangular system of coordinates)

$$(h_1=1,h_2=1,h_3=1;\ u_1=x,u_2=y,u_3=z)$$

$$\nabla\times\vec{E}=\frac{1}{r}\left(\frac{\partial E_z}{\partial\theta}-\frac{\partial(rE_\theta)}{\partial z}\right)\vec{a}_r+\left(\frac{\partial E_r}{\partial z}-\frac{\partial E_z}{\partial r}\right)\vec{a}_\theta+\frac{1}{r}\left(\frac{\partial(rE_\theta)}{\partial r}-\frac{\partial E_r}{\partial\theta}\right)\vec{a}_z$$

$$=\left(\frac{1}{r}\frac{\partial E_z}{\partial\theta}-\frac{\partial E_\theta}{\partial z}\right)\vec{a}_r+\left(\frac{\partial E_r}{\partial z}-\frac{\partial E_z}{\partial r}\right)\vec{a}_\theta+\frac{1}{r}\left(\frac{\partial(rE_\theta)}{\partial r}-\frac{\partial E_r}{\partial\theta}\right)\vec{a}_z$$

(Cylindrical system of coordinates)

$$(h_1=1,h_2=r,h_3=1;\ u_1=r,u_2=\theta,u_3=z)$$

$$\nabla\times\vec{E}=\frac{1}{r\sin\theta}\left(\frac{\partial(\sin\theta\,E_\phi)}{\partial\theta}-\frac{\partial E_\theta}{\partial\phi}\right)\vec{a}_r+\frac{1}{r}\left(\frac{1}{\sin\theta}\frac{\partial E_r}{\partial\phi}-\frac{\partial(rE_\phi)}{\partial r}\right)\vec{a}_\theta+\frac{1}{r}\left(\frac{\partial(rE_\theta)}{\partial r}-\frac{\partial E_r}{\partial\theta}\right)\vec{a}_\phi$$

$$(h_1=1,h_2=r,h_3=r\sin\theta;\ u_1=r,u_2=\theta,u_3=\phi)$$

(Spherical system of coordinates)

$$\nabla \times \vec{E} = \frac{1}{h_1 h_2 h_3} \begin{vmatrix} h_1 \vec{a}_1 & h_2 \vec{a}_2 & h_3 \vec{a}_3 \\ \frac{\partial}{\partial u_1} & \frac{\partial}{\partial u_2} & \frac{\partial}{\partial u_3} \\ h_1 E_1 & h_2 E_2 & h_3 E_3 \end{vmatrix}$$

(Curvilinear system of coordinates)

$$\nabla \times \vec{E} = \begin{vmatrix} \vec{a}_x & \vec{a}_y & \vec{a}_z \\ \frac{\partial}{\partial x} & \frac{\partial}{\partial y} & \frac{\partial}{\partial z} \\ E_x & E_y & E_z \end{vmatrix}$$

(Rectangular system of coordinates)

$$(h_1 = 1, h_2 = 1, h_3 = 1;\ u_1 = x, u_2 = y, u_3 = z)$$

$$\nabla \times \vec{E} = \frac{1}{h_1 h_2 h_3} \begin{vmatrix} h_1 \vec{a}_1 & h_2 \vec{a}_2 & h_3 \vec{a}_3 \\ \frac{\partial}{\partial u_1} & \frac{\partial}{\partial u_2} & \frac{\partial}{\partial u_3} \\ h_1 E_1 & h_2 E_2 & h_3 E_3 \end{vmatrix}$$

(Curvilinear system of coordinates)

$$\nabla \times \vec{E} = \frac{1}{r} \begin{vmatrix} \vec{a}_r & r\vec{a}_\theta & \vec{a}_z \\ \frac{\partial}{\partial r} & \frac{\partial}{\partial \theta} & \frac{\partial}{\partial z} \\ E_r & rE_\theta & E_z \end{vmatrix}$$

(Cylindrical system of coordinates)

$$(h_1 = 1, h_2 = r, h_3 = 1;\ u_1 = r, u_2 = \theta, u_3 = z)$$

$$\nabla \times \vec{E} = \frac{1}{h_1 h_2 h_3} \begin{vmatrix} h_1 \vec{a}_1 & h_2 \vec{a}_2 & h_3 \vec{a}_3 \\ \frac{\partial}{\partial u_1} & \frac{\partial}{\partial u_2} & \frac{\partial}{\partial u_3} \\ h_1 E_1 & h_2 E_2 & h_3 E_3 \end{vmatrix}$$

(Curvilinear system of coordinates)

$$\nabla \times \vec{E} = \frac{1}{r^2 \sin\theta} \begin{vmatrix} \vec{a}_r & r\vec{a}_\theta & r\sin\theta\, \vec{a}_\phi \\ \frac{\partial}{\partial r} & \frac{\partial}{\partial \theta} & \frac{\partial}{\partial \phi} \\ E_r & rE_\theta & r\sin\theta\, E_\phi \end{vmatrix}$$

(Spherical system of coordinates)

$$(h_1 = 1, h_2 = r, h_3 = r\sin\theta;\ u_1 = r, u_2 = \theta, u_3 = \phi)$$

Laplacian of scalar and vector quantities

Laplacian of a scalar quantity

The gradient of a scalar quantity is a vector quantity.

The divergence of a vector quantity is a scalar quantity.

Then if we take V as the scalar quantity then

$$\text{grad}\, V = \nabla \vec{V}$$

becomes a vector quantity and its divergence a scalar quantity.

In other words, $\nabla \cdot \nabla V = \nabla^2 V$

is a scalar quantity called the Laplacian of the scalar quantity here V .

Let us take the following two vector quantities:

$$\vec{E} = E_1\vec{a}_1 + E_2\vec{a}_2 + E_3\vec{a}_3$$

$$\nabla V = (\nabla V)_1\vec{a}_1 + (\nabla V)_2\vec{a}_2 + (\nabla V)_3\vec{a}_3$$

Interpreting $\vec{E}$ as ∇V in the following expression

$$\nabla \cdot \vec{E} = \frac{1}{h_1 h_2 h_3}\left[\frac{\partial(h_2 h_3 E_1)}{\partial u_1} + \frac{\partial(h_3 h_1 E_2)}{\partial u_2} + \frac{\partial(h_1 h_2 E_3)}{\partial u_3}\right]$$

we get

$$\nabla \cdot \nabla V = \nabla^2 V = \frac{1}{h_1 h_2 h_3}\left[\frac{\partial(h_2 h_3 \nabla V_1)}{\partial u_1} + \frac{\partial(h_3 h_1 \nabla V_2)}{\partial u_2} + \frac{\partial(h_1 h_2 \nabla V_3)}{\partial u_3}\right]$$

$$\nabla \cdot \nabla V = \nabla^2 V = \frac{1}{h_1 h_2 h_3}\left[\frac{\partial(h_2 h_3 \nabla V_1)}{\partial u_1} + \frac{\partial(h_3 h_1 \nabla V_2)}{\partial u_2} + \frac{\partial(h_1 h_2 \nabla V_3)}{\partial u_3}\right]$$

$$\left.\begin{aligned}(\nabla V)_1 &= \frac{1}{h_1}\frac{\partial V}{\partial u_1}\\ (\nabla V)_2 &= \frac{1}{h_2}\frac{\partial V}{\partial u_2}\\ (\nabla V)_3 &= \frac{1}{h_3}\frac{\partial V}{\partial u_3}\end{aligned}\right\}$$

$$\nabla^2 V = (\nabla \cdot \nabla V =) \frac{1}{h_1 h_2 h_3}\left[\frac{\partial}{\partial u_1}\left(\frac{h_2 h_3}{h_1}\frac{\partial V}{\partial u_1}\right) + \frac{\partial}{\partial u_2}\left(\frac{h_3 h_1}{h_2}\frac{\partial V}{\partial u_2}\right) + \frac{\partial}{\partial u_3}\left(\frac{h_1 h_2}{h_3}\frac{\partial V}{\partial u_3}\right)\right].$$

$$\nabla^2 V = (\nabla \cdot \nabla V =) \frac{1}{h_1 h_2 h_3}\left[\frac{\partial}{\partial u_1}\left(\frac{h_2 h_3}{h_1}\frac{\partial V}{\partial u_1}\right)+\frac{\partial}{\partial u_2}\left(\frac{h_3 h_1}{h_2}\frac{\partial V}{\partial u_2}\right)+\frac{\partial}{\partial u_3}\left(\frac{h_1 h_2}{h_3}\frac{\partial V}{\partial u_3}\right)\right].$$

(Curvilinear system of coordinates)

$$\nabla^2 V = \frac{\partial}{\partial x}\left(\frac{\partial V}{\partial x}\right)+\frac{\partial}{\partial y}\left(\frac{\partial V}{\partial y}\right)+\frac{\partial}{\partial z}\left(\frac{\partial V}{\partial z}\right)=\frac{\partial^2 V}{\partial x^2}+\frac{\partial^2 V}{\partial y^2}+\frac{\partial^2 V}{\partial z^2}$$

(Rectangular system of coordinates)

$$(h_1 = 1, h_2 = 1, h_3 = 1;\ u_1 = x, u_2 = y, u_3 = z)$$

$$\nabla^2 V = \frac{1}{r}\left[\frac{\partial}{\partial r}\left(r\frac{\partial V}{\partial r}\right)+\frac{\partial}{\partial \theta}\left(\frac{1}{r}\frac{\partial V}{\partial \theta}\right)+\frac{\partial}{\partial z}\left(r\frac{\partial V}{\partial z}\right)\right]=\frac{1}{r}\frac{\partial}{\partial r}\left(r\frac{\partial V}{\partial r}\right)+\frac{1}{r^2}\frac{\partial^2 V}{\partial \theta^2}+\frac{\partial^2 V}{\partial z^2}$$

$$(h_1 = 1, h_2 = r, h_3 = 1;\ u_1 = r, u_2 = \theta, u_3 = z)$$

(Cylindrical system of coordinates)

$$\nabla^2 V = \frac{1}{r^2 \sin\theta}\left[\frac{\partial}{\partial r}\left(r^2 \sin\theta \frac{\partial V}{\partial r}\right)+\frac{\partial}{\partial \theta}\left(\sin\theta \frac{\partial V}{\partial \theta}\right)+\frac{\partial}{\partial \phi}\left(\frac{1}{\sin\theta}\frac{\partial V}{\partial \phi}\right)\right]$$

$$= \frac{1}{r^2}\frac{\partial}{\partial r}\left(r^2 \frac{\partial V}{\partial r}\right)+\frac{1}{r^2 \sin\theta}\frac{\partial}{\partial \theta}\left(\sin\theta \frac{\partial V}{\partial \theta}\right)+\frac{1}{r^2 \sin^2\theta}\frac{\partial^2 V}{\partial \phi^2}\ .$$

(Spherical system of coordinates)

$$(h_1 = 1, h_2 = r, h_3 = r\sin\theta;\ u_1 = r, u_2 = \theta, u_3 = \phi)$$

Laplacian of a vector quantity

Laplacian of the vector is the vector sum of the Laplacian of the vector components. For the vector $\vec{E}$

$$\nabla^2 \vec{E} = (\nabla^2 E_1)\vec{a}_1 + (\nabla^2 E_2)\vec{a}_2 + (\nabla^2 E_3)\vec{a}_3$$

where $\nabla^2 E_1, \nabla^2 E_2, \nabla^2 E_3$

are obtained by replacing V **by** E_1, E_2, E_3 **in the expression for** $\nabla^2 V$

.

Maxwell's Equations

Simple enough to imprint on a T-shirt and yet rich enough to provide new insights throughout a lifetime of study — **J.R. Whinnery**

"The teaching of electromagnetics", *IEEE Trans. Education* ED-33 (1990) p.327

Several disciplines hang as gems on one priceless necklace which it was Maxwell's privilege and honour to recognize as capricious Nature's enduring ornament

— **P. Khastagir**

"Apologia," *Seminar on Electromagnetics and their applications*, 22-23 December 1988, Varanasi, India

***James Clerk Maxwell* originally gave as many as twenty equations in twenty variables; it was Oliver Heaviside, who is one of the founders of vector calculus, who reduced these equations to four equations.**

We may recall the following four equations in their integral and differential forms; they have already been derived and are known as Maxwell's equations.

Maxwell's equations

Integral form	Differential form
$\oint_S \vec{D}\cdot d\vec{S} = \oint_S \vec{D}\cdot\vec{a}_n\, dS = \int_\tau \rho\, d\tau$	$\nabla\cdot\vec{D} = \rho$
$\oint_S \vec{B}\cdot d\vec{S} = \oint_S \vec{B}\cdot\vec{a}_n\, dS = 0$	$\nabla\cdot\vec{B} = 0$
$\oint_l \vec{E}\cdot d\vec{l} = -\int_S \frac{\partial\vec{B}}{\partial t}\cdot\vec{a}_n\, dS$	$\nabla\times\vec{E} = -\frac{\partial\vec{B}}{\partial t}$
$\oint_l \vec{H}\cdot d\vec{l} = \int_S \left(\vec{J} + \frac{\partial\vec{D}}{\partial t}\right)\cdot\vec{a}_n\, dS$	$\nabla\times\vec{H} = \vec{J} + \frac{\partial\vec{D}}{\partial t}$

Maxwell's four equations are used extensively to develop concepts of electromagnetic theory and their applications.

Relaxation time

Relaxation time is a measure of how fast or slow a medium of uniform conductivity and permittivity approaches electrostatic equilibrium.

Continuity equation → **Relaxation time** ← **Poisson's equation** ← **Ohm's law**

$$\nabla . \vec{J} + \frac{\partial \rho}{\partial t} = 0 \quad \longleftarrow \quad \vec{J} = \sigma \vec{E}$$

↓ **Conductivity is uniform in the medium**

$$\sigma(\nabla . \vec{E}) + \frac{\partial \rho}{\partial t} = 0 \quad \longleftarrow \quad \nabla \cdot \vec{E} = \frac{\rho}{\varepsilon}$$

↓

$$\sigma\left(\frac{\rho}{\varepsilon}\right) + \frac{\partial \rho}{\partial t} = 0$$

↓

$$\frac{\partial \rho}{\partial t} = -\frac{\sigma}{\varepsilon}\rho$$

$$\frac{\partial \rho}{\partial t} = -\frac{\sigma}{\varepsilon}\rho$$

$$\downarrow$$

$$\int \frac{d\rho}{\rho} = -\frac{\sigma}{\varepsilon}\int dt$$

$$\downarrow$$

$$\ln \rho = -\frac{\sigma}{\varepsilon}t + \text{constant}$$

$$\downarrow$$

We tacitly choose constant in terms of ρ_0

$$\text{constant} = \ln \rho_0$$

$$\ln \rho = -\frac{\sigma}{\varepsilon}t + \ln \rho_0$$

$$\downarrow$$

$$\ln \rho - \ln \rho_0 = -\frac{\sigma}{\varepsilon}t$$

$$\downarrow$$

$$\ln \frac{\rho}{\rho_0} = -\frac{\sigma}{\varepsilon}t$$

$$\ln\frac{\rho}{\rho_0} = -\frac{\sigma}{\varepsilon}t$$ **(rewritten)**

$$\downarrow$$

$$\frac{\rho}{\rho_0} = \exp\left(-\frac{\sigma}{\varepsilon}t\right)$$

$$\downarrow$$

$$\rho = \rho_0 \exp\left(-\frac{\sigma}{\varepsilon}t\right)$$

$$\downarrow$$

$$\rho = \rho_0 \exp\left(-\frac{t}{\mathrm{T}}\right) \longleftarrow \text{Relaxation time } T = \frac{\varepsilon}{\sigma} = \frac{\varepsilon_r \varepsilon_0}{\sigma}$$

For very large values of relaxation time *T*

$$-\frac{t}{\mathrm{T}} \to 0$$

$$\exp\left(-\frac{t}{\mathrm{T}}\right) \to 1$$

$$\rho \to \rho_0$$

For very small values of relaxation time *T*

$$-\frac{t}{\mathrm{T}} \to -\infty$$

$$\exp\left(-\frac{t}{\mathrm{T}}\right) \to 0$$

$$\rho \to 0$$

For very large values of relaxation time T

(dielectric medium)

$$\mathrm{T} = \frac{\varepsilon}{\sigma} = \frac{\varepsilon_r \varepsilon_0}{\sigma}$$

$$-\frac{t}{\mathrm{T}} \to 0$$

$$\exp\left(-\frac{t}{\mathrm{T}}\right) \to 1$$

$$\rho \to \rho_0$$

For very small values of relaxation time T

(good condutor)

$$\mathrm{T} = \frac{\varepsilon}{\sigma} = \frac{\varepsilon_r \varepsilon_0}{\sigma}$$

$$-\frac{t}{\mathrm{T}} \to -\infty$$

$$\exp\left(-\frac{t}{\mathrm{T}}\right) \to 0$$

$$\rho \to 0$$

For a dielectric medium, the value of conductivity σ is very small that renders *T* a very large value. This makes the volume charge density ρ in the bulk of the dielectric tend to ρ_0 (equilibrium volume charge density). Therefore, within a time of interest *t*, the bulk of a dielectric medium can be charged with the equilibrium volume charge density (ρ_0).

On the other hand, for a medium of good conductivity, the value of conductivity σ is very large that renders *T* a very small value. This makes the volume charge density ρ in the bulk of the dielectric tend to 0. Thus, the bulk of a medium of a good conductor cannot be charged; any charge injected into such a medium of good conductivity will not stay long within the bulk of the conductor only to reappear at the outer surface of the conducting medium in compliance with the requirement of the conservation of charge.

Conductivity, permittivity, and relaxation time of typical medium materials

Medium material	σ (mho/m)	ε_r	$T = \varepsilon_r \varepsilon_0 / \sigma$
Copper	5.8×10^{7}	1	1.5×10^{-19} s
Sea-water	4	81	2×10^{-10} s
Corn oil	5×10^{-4}	3.1	0.55 s
Mica	10^{-15}	5.8	~1/2 a day
Quartz (fused)	10^{-17}	5	~50 days

The concept of the relaxation time is very useful in understanding the electromagnetic boundary conditions at the interface between two dielectrics as well as those at the interface between a conductor and a dielectric.

Surface charge density is defined as the product of the volume charge density and the infinitesimal thickness over which the charge is spread at the interface, in the limit of the infinitesimal thickness tending to zero. (This definition emerges in course of the deduction of general electromagnetic boundary conditions).

Definition of surface charge density ρ_s

$$\rho_s = \lim_{dh \to 0} \int_{Lt} \rho \, dh \quad \text{(C/m}^2\text{)}$$

Surface current density is defined as the product of the current density and the infinitesimal thickness at the interface over which the current density is significant, in the limit of the infinitesimal thickness tending to zero. (This definition emerges in course of the deduction of general electromagnetic boundary conditions).

Definition of surface current density $\vec{J}_S$

$$\vec{J}_S = \lim_{dh \to 0} \int_{Lt} \vec{J}\, dh \quad \text{(A/m}^2\text{)}$$

Electromagnetic boundary conditions

Maxwell's equation in integral form		Electromagnetic boundary conditions
$\oint_S \vec{D}\cdot\vec{a}_n dS = \int_\tau \rho\, d\tau$	$\longrightarrow$	$(\vec{D}_2 - \vec{D}_1).\vec{a}_n = \rho_s$
$\oint_S \vec{B}\cdot d\vec{S} = \int_S \vec{B}\cdot\vec{a}_n\, dS = 0$	$\longrightarrow$	$(\vec{B}_2 - \vec{B}_1).\vec{a}_n = 0$
$\oint_l \vec{H}\cdot d\vec{l} = \int_S \left(\vec{J} + \frac{\partial \vec{D}}{\partial t}\right)\cdot\vec{a}_n\, dS$	$\longrightarrow$	$\vec{a}_n \times (\vec{H}_2 - \vec{H}_1) = \vec{J}_S$
$\oint_l \vec{E}\cdot d\vec{l} = -\int_S \frac{\partial \vec{B}}{\partial t}\cdot\vec{a}_n\, dS$	$\longrightarrow$	$\vec{a}_n \times (\vec{E}_2 - \vec{E}_1) = 0$

Electromagnetic boundary condition	Meaning	At a point on the interface between two media
$(\vec{D}_2 - \vec{D}_1).\vec{a}_n = \rho_s$	⟶	Normal component of electric displacement is discontinuous, the amount of discontinuity being equal to the surface charge density
$(\vec{B}_2 - \vec{B}_1).\vec{a}_n = 0$	⟶	Normal component of magnetic flux density is continuous
$\vec{a}_n \times (\vec{H}_2 - \vec{H}_1) = \vec{J}_S$	⟶	Tangential component of magnetic field is discontinuous, the amount of discontinuity being equal to the surface current density
$\vec{a}_n \times (\vec{E}_2 - \vec{E}_1) = 0$	⟶	Tangential component of electric field is continuous

Electromagnetic boundary conditions at the dielectric-dielectric interface

Electromagnetic boundary conditions at the dielectric-conductor interface

We can interpret general electromagnetic boundary conditions for dielectric-dielectric interface and conductor-dielectric/free-space interface. For this purpose, it is worth reviewing some of the basic behaviours of conductor and dielectric media with regard to relaxation time, existence of a free charge in the bulk of the media, surface resistance, surface current density, and electric field and magnetic in the media.

Dielectric	Conductor
Relaxation time of is very large	Relaxation time is very small
A charge can stay longer inside the bulk of a dielectric without appearing at its surface and a finite volume charge density can be established inside the bulk resulting in a zero surface charge density at the surface of a dielectric for both time-independent and time-dependent situations.	A charge inside the bulk of a good conductor decays very fast to appear with a large volume charge density concentrated over a thin layer on the surface of the conductor, resulting in a finite surface charge density on the conductor surface for both time-independent and time-dependent situations.

$$\rho_s = \lim_{dh \to 0} \rho \, dh \quad \text{(C/m}^2\text{)}$$

$$\vec{J}_s = \lim_{dh \to 0} \vec{J} dh \quad \text{(A/m}^2\text{)}$$

Continued

In continuation

Dielectric	Conductor
The electric field and the electric displacement can be established inside a dielectric for both time-independent and time-dependent situations.	The bulk of a conductor cannot be electrically charged, resulting in no electric field or electric displacement inside the conductor for both time-independent and time-dependent situations.
A finite magnetic field or magnetic flux density can be established inside a dielectric independently of electric field, for both time-independent and time-dependent situations.	A finite magnetic field or magnetic flux density can be established inside a conductor independent of electric field for time-independent situations. However, for time-dependent situations, the magnetic field or magnetic flux density is nil inside a conductor since it is coupled to the electric field which is nil inside the conductor for such situations.

$$\rho_s = \lim_{dh \to 0}^{Lt} \rho \, dh \quad (C/m^2)$$

$$\vec{J}_s = \lim_{dh \to 0}^{Lt} \vec{J} dh \quad (A/m^2)$$

Continued

In continuation

Dielectric	Conductor
No current flows through a dielectric and therefore the surface current density becomes zero at the dielectric surface for both time-independent and time-dependent situations.	A finite current can be made to flow through the bulk of a conductor for time-independent situations, resulting in zero surface current density. However, for time-dependent situations a large current density can be concentrated over a thin layer on the conductor surface resulting in a finite surface current density.

$$\rho_s = \lim_{dh \to 0} \int_{Lt} \rho \, dh \quad (\text{C/m}^2)$$

$$\vec{J}_s = \lim_{dh \to 0} \int_{Lt} \vec{J} dh \quad (\text{A/m}^2)$$

The above behaviours of the dielectric and conductor help in the interpretation of general electromagnetic boundary conditions for dielectric-dielectric interface and conductor-dielectric/free-space to be taken up next in our study, which is of practical relevance.

dielectric-dielectric interface

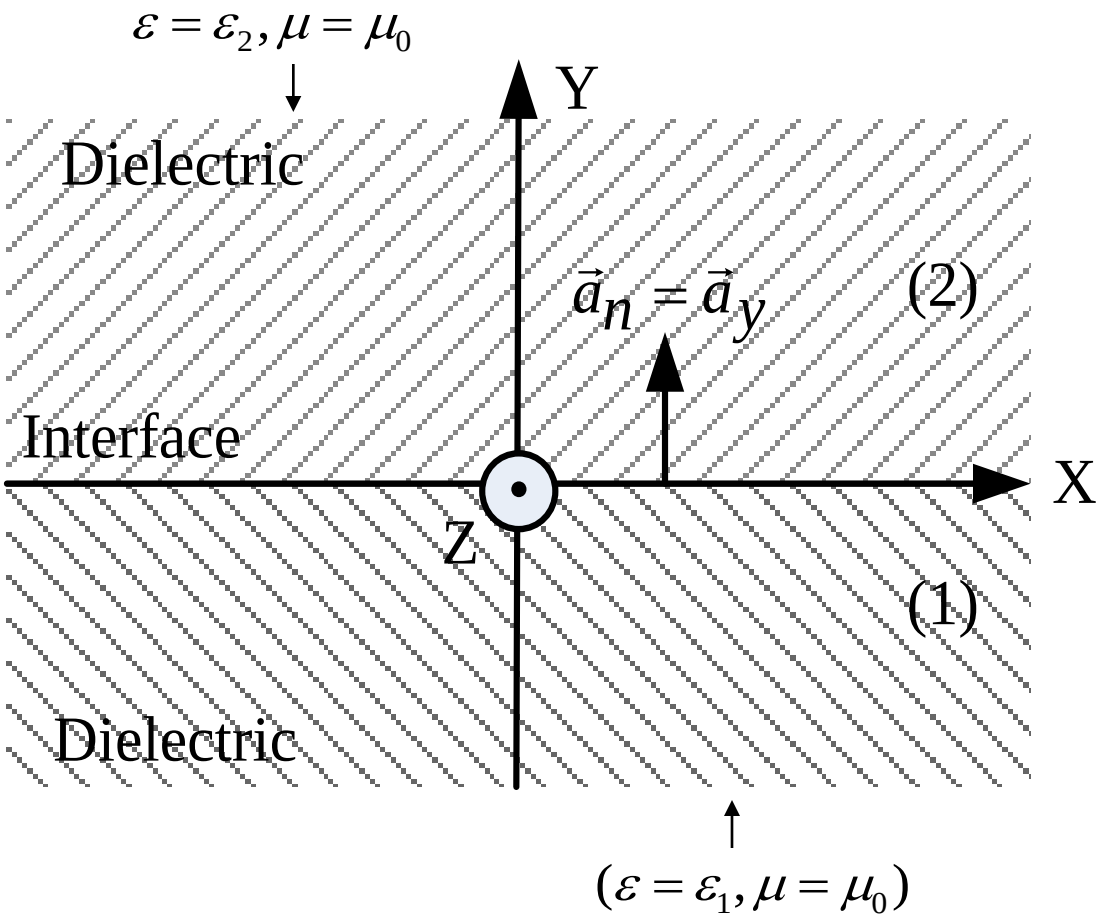

conductor-dielectric interface

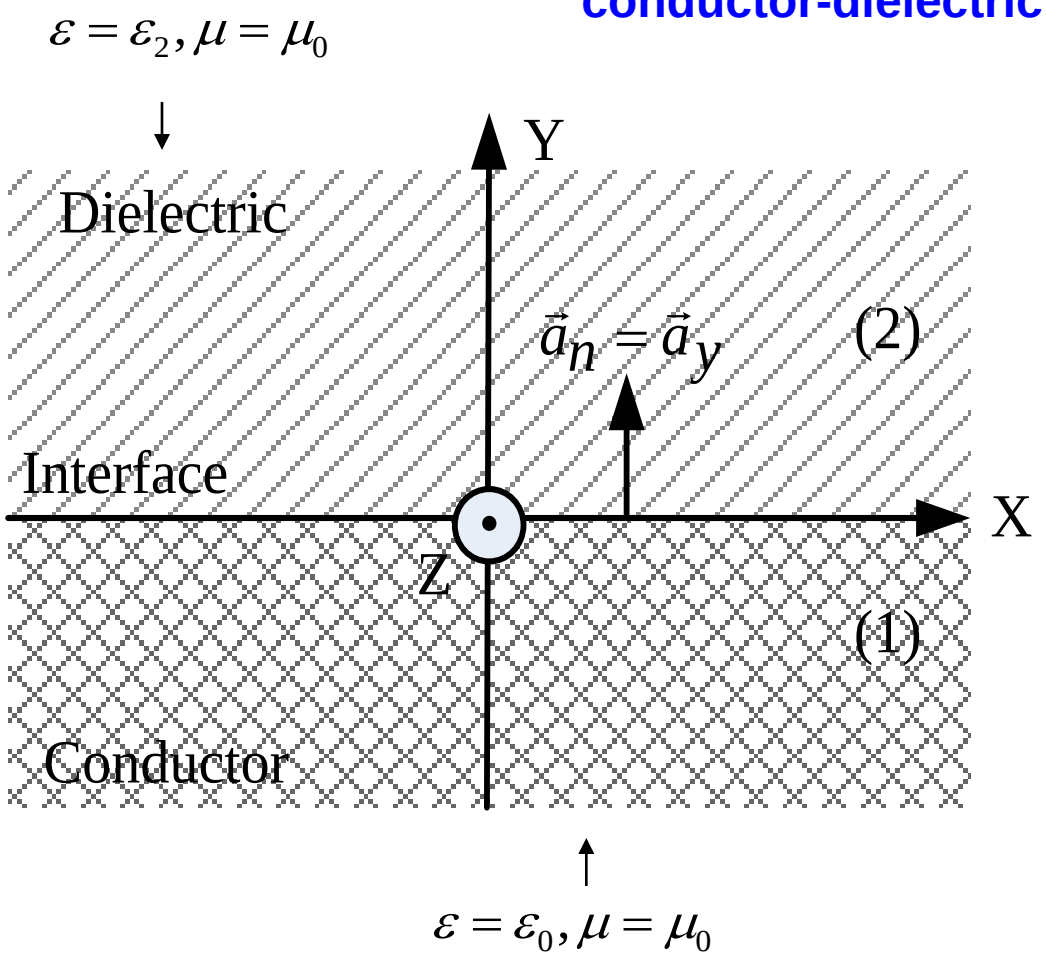

Electromagnetic boundary conditions at dielectric-dielectric interface

$$\rho \neq 0 \rightarrow \rho_s = \lim_{dh \to 0} \rho\, dh = 0$$

$$\vec{E}_{1,2} \neq 0, \vec{D}_{1,2} \neq 0$$

$$\vec{H}_{1,2} \neq 0, \vec{B}_{1,2} \neq 0$$

Subscripts 1 and 2 refer to quantities in region1 and 2 respectively

$$(\vec{D}_2 - \vec{D}_1).\vec{a}_n = \rho_S$$
$$(\vec{B}_2 - \vec{B}_1).\vec{a}_n = 0$$
$$\vec{a}_n \times (\vec{H}_2 - \vec{H}_1) = \vec{J}_s$$
$$\vec{a}_n \times (\vec{E}_2 - \vec{E}_1) = 0$$

(general electromagnetic boundary conditions)

$$(\vec{D}_2 - \vec{D}_1).\vec{a}_n = 0$$
$$(\vec{B}_2 - \vec{B}_1).\vec{a}_n = 0$$
$$\vec{a}_n \times (\vec{H}_2 - \vec{H}_1) = 0$$
$$\vec{a}_n \times (\vec{E}_2 - \vec{E}_1) = 0$$

(electromagnetic boundary conditions at dielectric-dielectric interface)

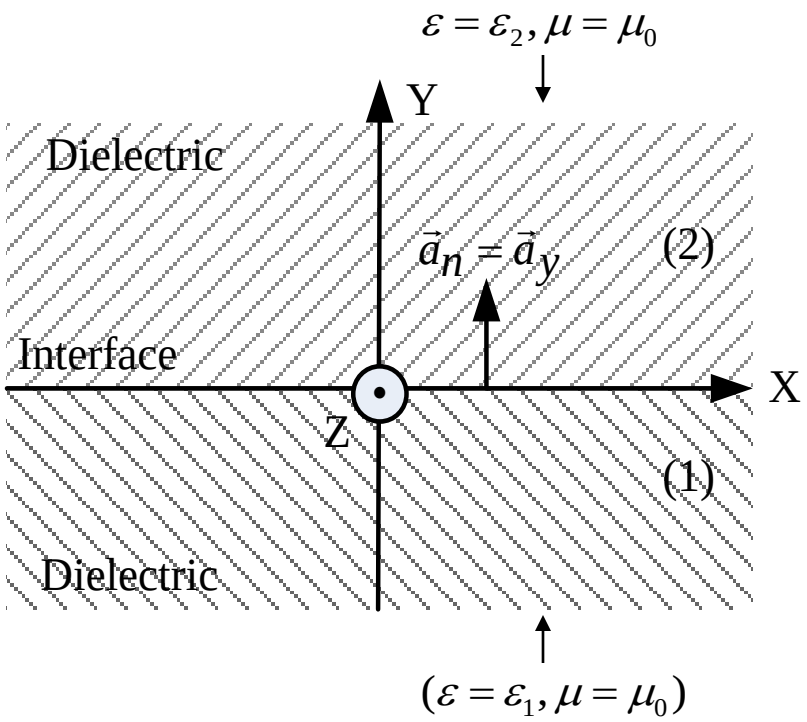

Electromagnetic boundary conditions at conductor-dielectric interface

$$\vec{J}_S = \lim_{dh \to 0} \int_{Lt} \vec{J}\,dh$$

$$\vec{E}_1 = 0, \vec{D}_1 = 0$$

$$\vec{H}_1 \neq 0,\ \vec{B}_1 \neq 0 \ \text{(for time-independent situations)}$$

$$\vec{H}_1 = \vec{B}_1 = 0 \ \text{(for time-dependent situations)}$$

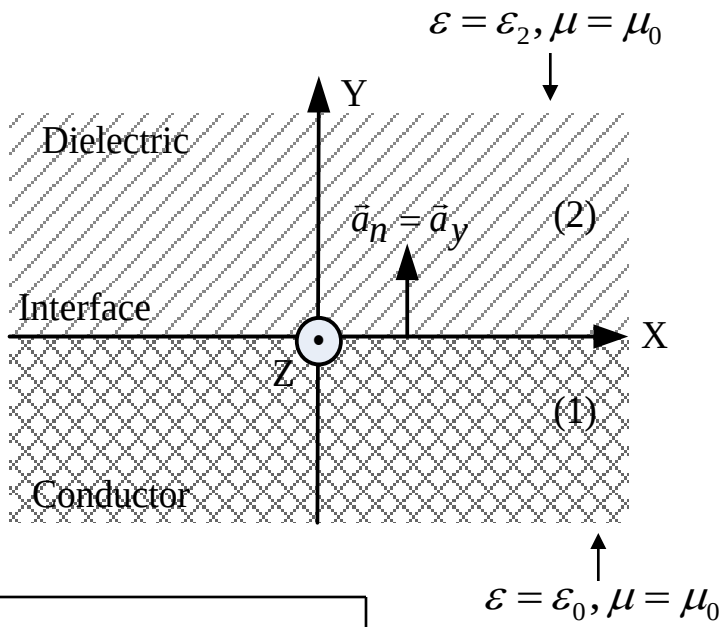

$$(\vec{D}_2 - \vec{D}_1).\vec{a}_n = \rho_S$$

$$(\vec{B}_2 - \vec{B}_1).\vec{a}_n = 0$$

$$\vec{a}_n \times (\vec{H}_2 - \vec{H}_1) = \vec{J}_s$$

$$\vec{a}_n \times (\vec{E}_2 - \vec{E}_1) = 0$$

(general electromagnetic boundary conditions)

$$\vec{D}_2.\vec{a}_n = \rho_S$$

$$(\vec{B}_2 - \vec{B}_1).\vec{a}_n = 0$$

$$\vec{a}_n \times (\vec{H}_2 - \vec{H}_1) = 0$$

$$\vec{a}_n \times \vec{E}_2 = 0$$

(electromagnetic boundary conditions for time-independent situations)

$$\vec{D}_2.\vec{a}_n = \rho_S$$

$$\vec{B}_2.\vec{a}_n = 0$$

$$\vec{a}_n \times \vec{H}_2 = \vec{J}_s$$

$$\vec{a}_n \times \vec{E}_2 = 0$$

(electromagnetic boundary conditions for time-dependent situations)

Let us illustrate the application of the boundary conditions at a dielectric-dielectric interface by taking up the problem of finding the electric displacements in region 1 ($x>0$) containing a dielectric of relative permittivity $\varepsilon_{r1} = 3$ and region 2 ($x<0$) containing another dielectric of relative $\varepsilon_{r2} = 5$, the two regions forming an interface at $x = 0$ if the electric field in region 2 is given as:

$$\vec{E}_2 = 40\vec{a}_x + 60\vec{a}_y - 80\vec{a}_z \text{ V/m.}$$

$\downarrow$ **(given)**

$$\vec{D}_2 = \varepsilon_2\vec{E}_2 = \varepsilon_0\varepsilon_{r2}\vec{E}_2 = 5\varepsilon_0\vec{E}_2$$
$$= 5\varepsilon_0 \times (40\vec{a}_x + 60\vec{a}_y - 48\vec{a}_z) \text{ V/m}$$

$\downarrow$

$$\vec{D}_2 = (200\vec{a}_x + 300\vec{a}_y - 400\vec{a}_z)\varepsilon_0 \text{ C/m}^2$$

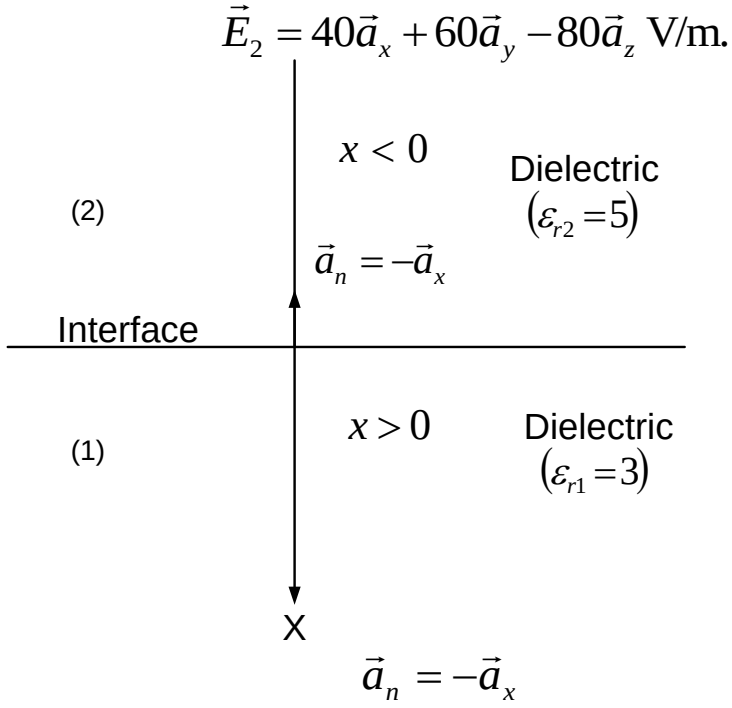

Let us recall the boundary condition

$$(\vec{D}_2 - \vec{D}_1).\vec{a}_n = 0 \quad \textbf{(recalled)}$$

$\downarrow$

$$[(D_{2x} - D_{1x})\vec{a}_x + (D_{2y} - D_{1y})\vec{a}_y + (D_{2z} - D_{1z})\vec{a}_z].[-\vec{a}_x] = 0$$

$\downarrow$

$$-(D_{2x} - D_{1x}) = 0$$

$$\vec{D}_2 = (200\vec{a}_x + 300\vec{a}_y - 400\vec{a}_z)\varepsilon_0 \text{ C/m}^2 \quad \textbf{(recalled)}$$

$\downarrow$

$$D_{1x} = D_{2x} = 200\varepsilon_0 \text{ C/m}^2$$

$\vec{a}_n \times (\vec{E}_2 - \vec{E}_1) = 0$ **(boundary condition recalled)**

$\downarrow$

$-\vec{a}_x \times [(E_{2x} - E_{1x})\vec{a}_x + (E_{2y} - E_{1y})\vec{a}_y + (E_{2z} - E_{1z})\vec{a}_z)] = 0$

$\downarrow$

$-(E_{2y} - E_{1y})\vec{a}_z + (E_{2z} - E_{1z})\vec{a}_y = 0$

$\downarrow$

$E_{1y} = E_{2y}$ and $E_{1z} = E_{2z}$ $\leftarrow$ $\vec{E}_2 = 40\vec{a}_x + 60\vec{a}_y - 80\vec{a}_z$ V/m. **(given)**

$\downarrow$ $\qquad$ $\downarrow$

$E_{1y} = 60$ V/m and $E_{1z} = -80$ V/m $\qquad$ $E_{2y} = 60$ V/m and $E_{2z} = -80$ V/m

$\downarrow$

$D_{1y} = \varepsilon_1 E_{1y} = \varepsilon_0 \varepsilon_{r1} E_{1y} = (\varepsilon_0)(3)E_{1y} = (\varepsilon_0)(3)(60) = 180\varepsilon_0$ C/m^2

$D_{1z} = \varepsilon_1 E_{1z} = \varepsilon_0 \varepsilon_{r1} E_{1z} = (\varepsilon_0)(3)E_{1z} = (\varepsilon_0)(3)(-80) = -240\varepsilon_0$ C/m^2 $\leftarrow$ $E_{1z} = -80$ V/m **(recalled)**

$\downarrow$

$\vec{D}_1 = D_{1x}\vec{a}_x + D_{1y}\vec{a}_y - D_{1z}\vec{a}_z)\varepsilon_0$ $\leftarrow$ $D_{1x} = D_{2x} = 200\varepsilon_0$ C/m^2 **(recalled)**

$\downarrow$ $\qquad$ $D_{1y} = 180\varepsilon_0$ C/m^2 **(recalled)**

$\vec{D}_1 = (200\vec{a}_x + 180\vec{a}_y - 240\vec{a}_z)\varepsilon_0$ C/m^2 $\qquad$ $\vec{D}_2 = (200\vec{a}_x + 300\vec{a}_y - 400\vec{a}_z)\varepsilon_0$ C/m^2

(recalled)

,

Take up another similar problem as an exercise to illustrate the application of boundary conditions at a dielectric-dielectric interface in which to find the electric field in region 2 ($y>0$) containing a dielectric of relative permittivity ε_{r2} separated at the interface ($y = 0$) from region 1 ($y<0$) containing another dielectric of relative permittivity ε_{r1} if the electric field in region 1 is given as:

The approach to getting the solution to the problem has already been elaborated in the preceding illustration. Some of the steps are provided as a hint as follows.

$$\vec{E}_1 = l\vec{a}_x + m\vec{a}_y - n\vec{a}_z.$$

$$\vec{D}_1 = \varepsilon_1\vec{E}_1 = \varepsilon_0\varepsilon_{r1}(l\vec{a}_x + m\vec{a}_y + n\vec{a}_z) \longleftarrow \vec{E}_1 = l\vec{a}_x + m\vec{a}_y - n\vec{a}_z$$

(electric field in region 1) (given)

$$\downarrow$$

$$\left.\begin{aligned} D_{1x} &= \varepsilon_0\varepsilon_{r1}l \\ D_{1y} &= \varepsilon_0\varepsilon_{r1}m \\ D_{1z} &= \varepsilon_0\varepsilon_{r1}n \end{aligned}\right\}$$

$$(\vec{D}_2 - \vec{D}_1).\vec{a}_n = 0 \quad \textbf{(boundary condition)} \longleftarrow \vec{a}_n = \vec{a}_y$$

$$\downarrow$$

$$[D_{2x}\vec{a}_x + D_{2y}\vec{a}_y + D_{2z}\vec{a}_z - (D_{1x}\vec{a}_x + D_{1y}\vec{a}_y + D_{1z}\vec{a}_z)]\cdot\vec{a}_y = 0$$

$$\downarrow$$

$$D_{2y} - D_{1y} = 0$$

$$\downarrow$$

$$\left.\begin{aligned} \vec{a}_x\cdot\vec{a}_y &= 0 \\ \vec{a}_y\cdot\vec{a}_y &= 1 \\ \vec{a}_z\cdot\vec{a}_y &= 0 \end{aligned}\right\}$$

$$\vec{E}_1 = l\vec{a}_x + m\vec{a}_y - n\vec{a}_z \quad \textbf{(given)}$$

$$\downarrow$$

$$E_{1y} = m \longrightarrow D_{2y} = D_{1y} = \varepsilon_1 E_{1y} = \varepsilon_0\varepsilon_{r1}E_{1y} = \varepsilon_0\varepsilon_{r1}m$$

,

$$\vec{a}_n \times (\vec{E}_2 - \vec{E}_1) = 0 \quad \longleftarrow \quad \left.\begin{array}{l} \vec{a}_n = \vec{a}_y \\ \vec{E}_1 = l\vec{a}_x + m\vec{a}_y - n\vec{a}_z \end{array}\right\}$$

$$\downarrow$$

$$\vec{a}_y \times [(E_{2x}\vec{a}_x + E_{2y}\vec{a}_y + E_{2z}\vec{a}_z) - (l\vec{a}_x + m\vec{a}_y + n\vec{a}_z)] = 0 \quad \longleftarrow \quad \left.\begin{array}{l} \vec{a}_y \times \vec{a}_x = -\vec{a}_z \\ \vec{a}_y \times \vec{a}_y = 0 \\ \vec{a}_y \times \vec{a}_z = \vec{a}_x \end{array}\right\}$$

$$\downarrow$$

$$-(E_{2x} - l)\vec{a}_z + (E_{2z} - n)\vec{a}_x = 0$$

$$\downarrow$$

$$\left.\begin{array}{l} E_{2x} - l = 0 \\ E_{2z} - n = 0 \end{array}\right\}$$

$$\downarrow$$

$$\left.\begin{array}{l} E_{2x} = l \\ E_{2z} = n \end{array}\right\}$$

$$D_{2y} = \varepsilon_0 \varepsilon_{r1} m \quad \textbf{(recalled)}$$

$$\downarrow$$

$$E_{2y} = \frac{D_{2y}}{\varepsilon_2} = \frac{D_{2y}}{\varepsilon_0 \varepsilon_{r2}} = \frac{\varepsilon_{r1} m}{\varepsilon_{r2}}$$

$$\vec{E}_1 = l\vec{a}_x + m\vec{a}_y - n\vec{a}_z$$

$$\vec{E}_2 = E_{2x}\vec{a}_x + E_{2y}\vec{a}_y + E_{2z}\vec{a}_z = l\,\vec{a}_x + m\frac{\varepsilon_{r1}}{\varepsilon_{r1}}\vec{a}_y + n\,\vec{a}_z$$

Law of parallel resistances

Let us begin the study with the appreciation of the circuit law of parallel resistances with the help of the boundary condition that the tangential component of electric field is continuous at the interface between two media.

For this purpose, the said boundary condition is applied at the interface between two rectangular conducting slabs in contact of the same length *l*, conductivities σ_1 and σ_2 and cross-sectional areas A_1 and A_2 respectively.

Current densities J_1 and J_2 are related to electric fields E_1 and E_2 in the slabs through Ohm's law while the current *I* fed into the slabs in contact is divided in currents I_1 and I_2 through the slabs.

$$J_1 = \sigma_1 E_1 \qquad J_2 = \sigma_2 E_2$$

$$E_1 = \frac{J_1}{\sigma_1} \qquad E_2 = \frac{J_2}{\sigma_2}$$

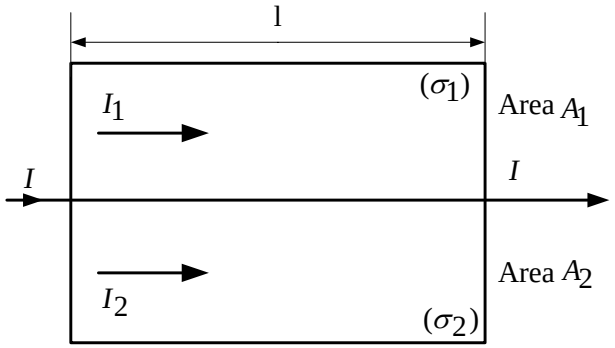

E_1 and E_2, which are tangential at the interface, are continuous at the interface:

$E_1 = E_2$ **(boundary condition)**

$$\downarrow$$

$$\frac{J_1}{\sigma_1} = \frac{J_2}{\sigma_2}$$

$$\downarrow$$

$$\frac{I_1}{A_1\sigma_1} = \frac{I_2}{A_2\sigma_2}$$

$$\downarrow$$ **Multiplying by /**

$$I_1 \frac{l}{A_1\sigma_1} = I_2 \frac{l}{A_2\sigma_2}$$

$$\downarrow \leftarrow$$

$$I_1 R_1 = I_2 R_2$$

$$R_1 = \frac{1}{\sigma_1}\frac{l}{A_1}$$

$$R_2 = \frac{1}{\sigma_2}\frac{l}{A_2}$$

$I = I_1 + I_2 \longrightarrow$

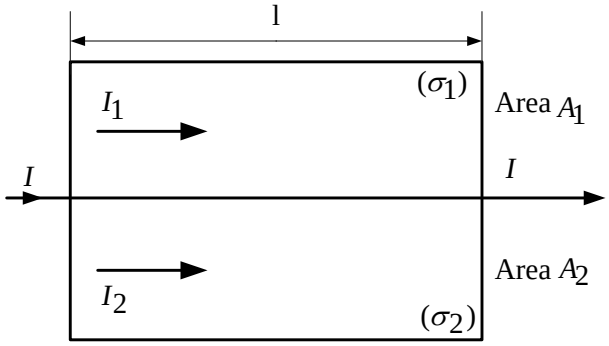

$I = I_1 + I_2 \longrightarrow$

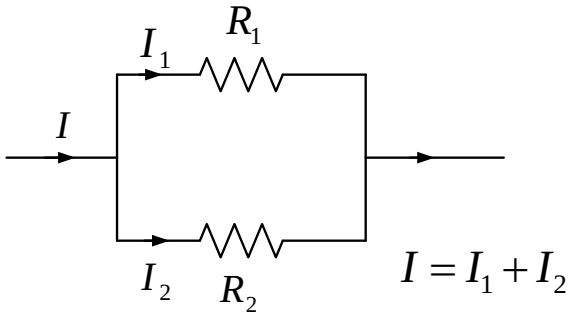

$$I_1 R_1 = I_2 R_2 \longrightarrow \frac{I_1}{I_2} = \frac{R_2}{R_1}$$

$$\downarrow$$

$$\frac{I_1}{I_1 + I_2} = \frac{R_2}{R_2 + R_1} = \frac{R_2}{R_1 + R_2}$$

$$\downarrow$$

$$\frac{I_1}{I} = \frac{R_2}{R_1 + R_2}$$

$$\downarrow$$

$$I_1 = \frac{R_2}{R_1 + R_2} I$$

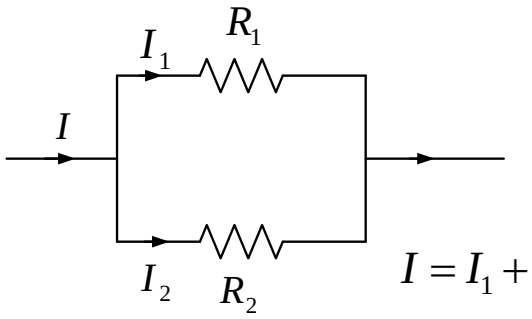

$I = I_1 + I_2$

Multiplying by R_1

$$\longrightarrow I_1 R_1 = I \frac{R_1 R_2}{R_1 + R_2} = I R_{\text{equivalent}}$$

$$\downarrow$$

$$R_{\text{equivalent}} = \frac{R_1 R_2}{R_1 + R_2}$$

$$\downarrow$$

$$\frac{1}{R_{\text{equivalent}}} = \frac{1}{R_1} + \frac{1}{R_2}$$

(Law of parallel resistances)

UNDERSTANDING MICROWAVE ENERGY THROUGH APPLICATIONS

PRADIP KUMAR SAHA

saha.pradipk@gmail.com

Microwave Window in Electromagnetic Spectrum

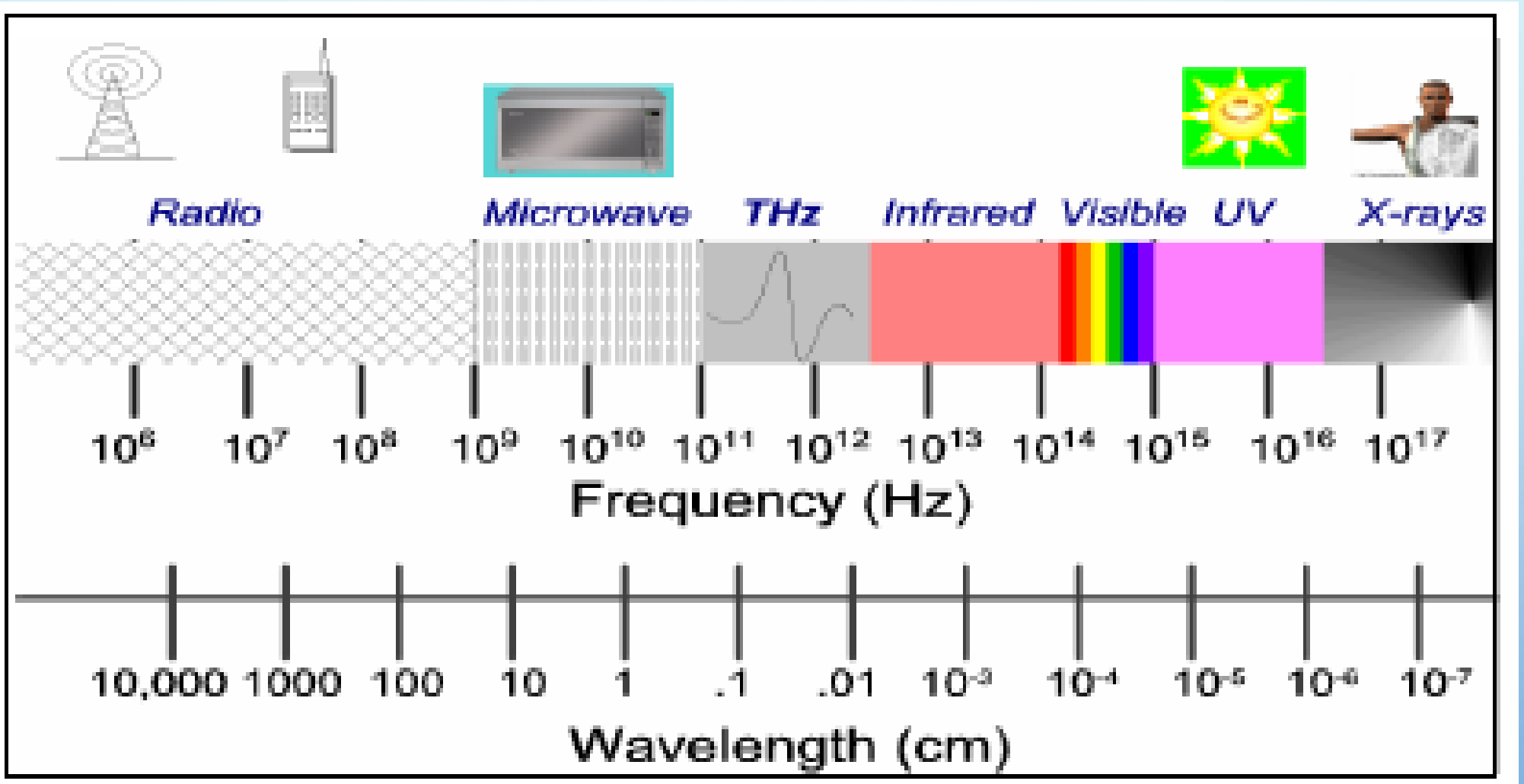

From Radio Waves to X-rays

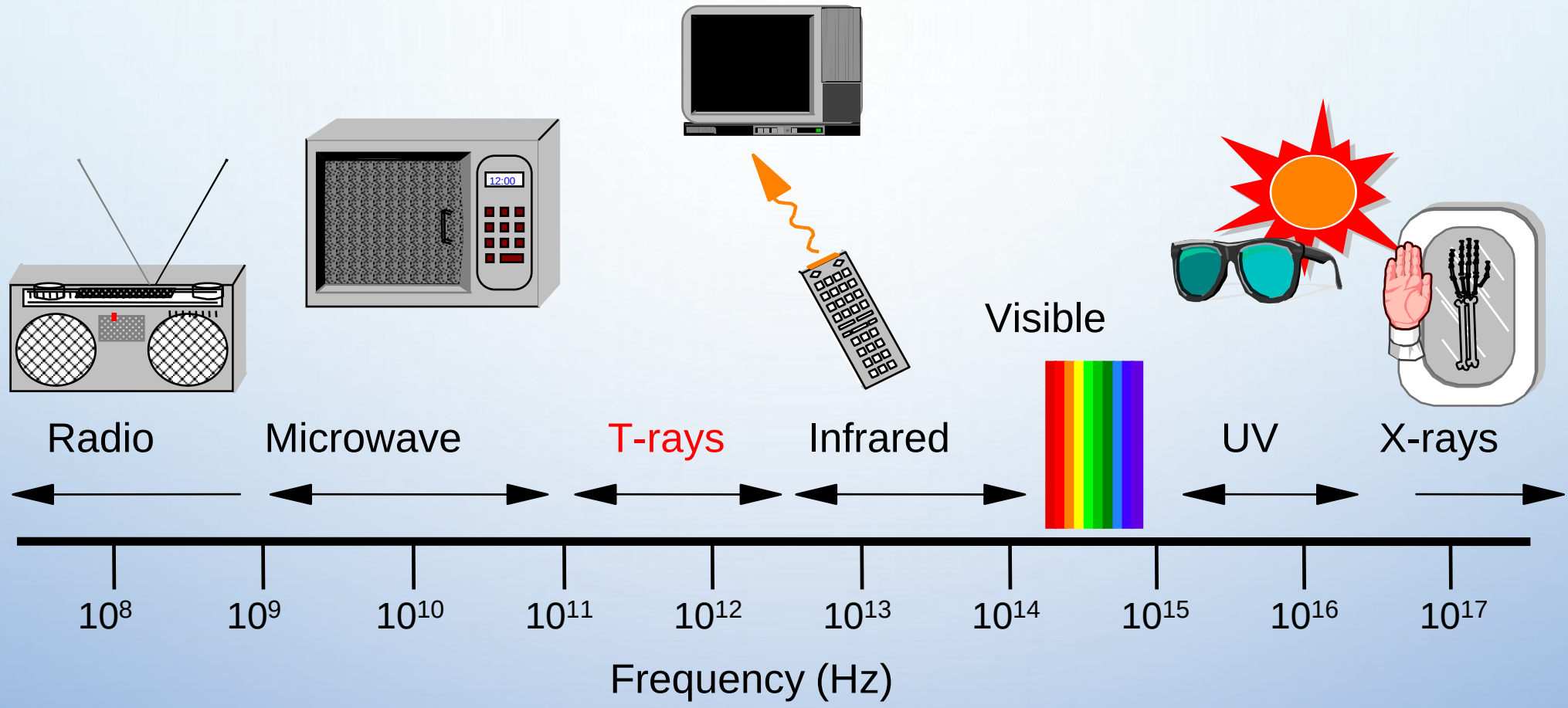

Application of Microwaves
Some Areas

- Communication
- Radar
- Biological Effects of Microwaves
- Microwave Heating

Communication Frequency Bands

Bands	Frequency Range	Wavelength Range
VLF	3 KHz – 30 KHz	100 Km – 10 Km
LF	30 KHz – 300 KHz	10 Km – 1 Km
MF	300 KHz – 3000 KHz	1000 m – 100m
HF	3 MHz – 30 MHz	100 M – 10 m
VHF	30 MHz – 300 MHz	10 m – 1 m
UHF	300 MHz – 3000 MHz	100 cm – 10 cm
MW	3 GHz – 30 GHz	10 cm – 1 cm
MMW	30 GHz – 300 GHz	10 mm – 1 mm

The term ‘Microwaves’ is loosely used to cover both MW & MMW bands

COMMUNICATION WITH MICROWAVES

FROM SOURCE (MICROWAVE GENERATOR) → **DESTINATION (RECEPTION)**

GENERATION	TRANSMISSION	RECEPTION
ELECTRON TUBE DEVICES	FREE SPACE (ANTENNA) (WHY DO WE NEED ANTENNA)	ANTENNA IN FREE SPACE
SEMICONDUCTOR DEVICES	GUIDED WAVES TRANSMISSION LINES (CABLES, WAVEGUIDES)	MICROWAVE RECEIVER

Some Microwave Communication Systems

- **FM transmission ~ 100 MHz**
- **Cellular Communication ~ 900 MHz**
- **Cordless Phone ~ 2.4 GHz**
  (Industrial, Scientific and Medical-ISM- band)
- **Satellite Communication ~ 4 & 6 GHz (Geo-stationary communication satellites are at about 36000 Km above Earth).**

Propagation

- **Ionosphere (*ionized layers of electron plasma)* surrounds the Earth like a shell from about 50 Km to 10,000 Km.**
- **Signals lower than about 40 MHz are partially or totally reflected by the layer.**
- **Frequencies in the GHz range, up to about 10 GHz are not significantly affected by the ionosphere. This frequency range is utilised for satellite and deep-space communication.**
- **Higher frequencies – tens of GHz – show bands of high and low absorption loss. This feature is utilised in 'secure communication'.**

Benefits of using microwaves for communication

- Higher *Information Capacity* with microwaves than available with lower frequency bands.
- 'Large' antennas (typically, dish antennas of many wavelengths in diameter) become practically realizable with centimetric wavelengths.
- Line – of – Sight (LOS) communication becomes feasible (Diagram)
- Power output requirement on the generator/transmitter is substantially reduced.
- Frequency range of about 100 MHz to 10 GHz in the microwave band constitute a transparent 'window' in the atmosphere allowing almost free propagation – suitable for radio astronomical studies, communication with artificial satellites and space vehicles. Lower frequencies are reflected partially or almost totally.

Line of Sight Communication

Transmission Link

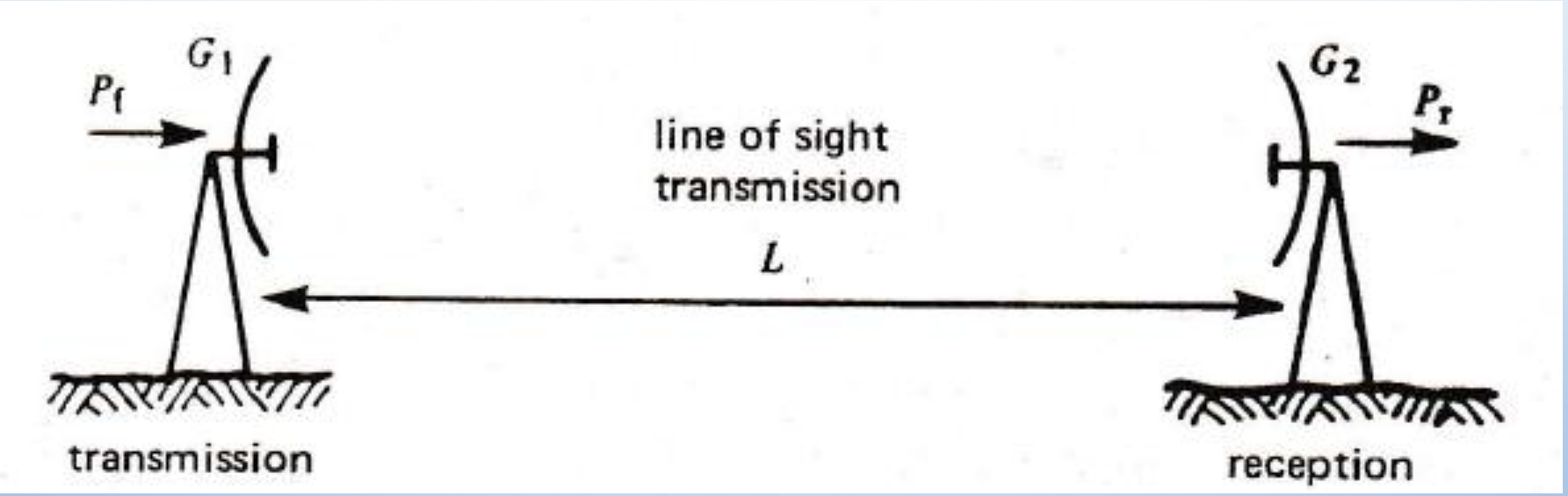

Microwave Antennas

Rectangular Horns

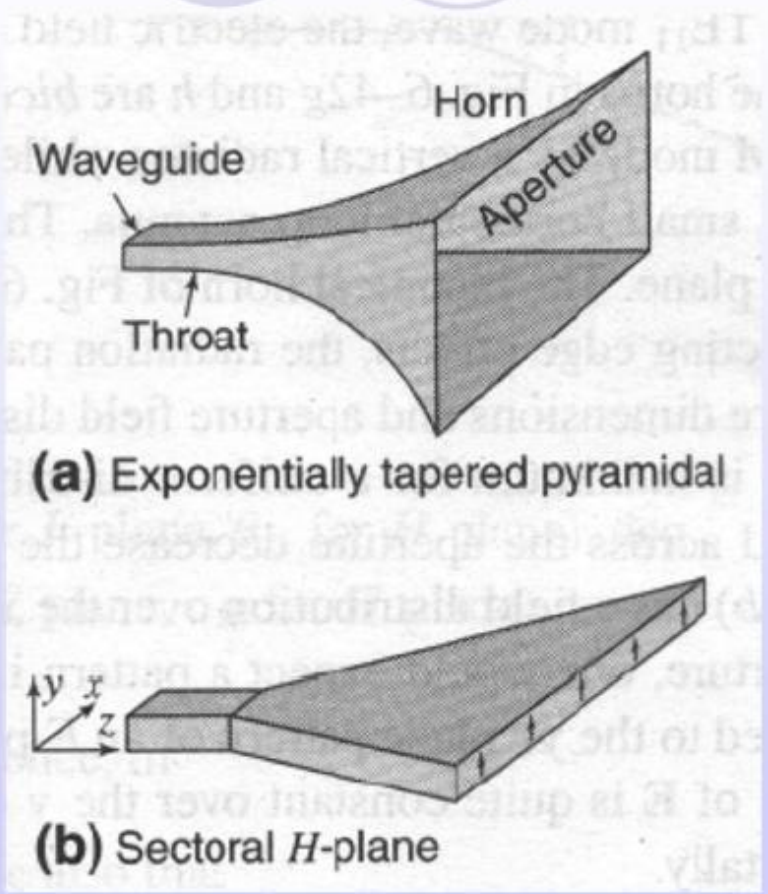

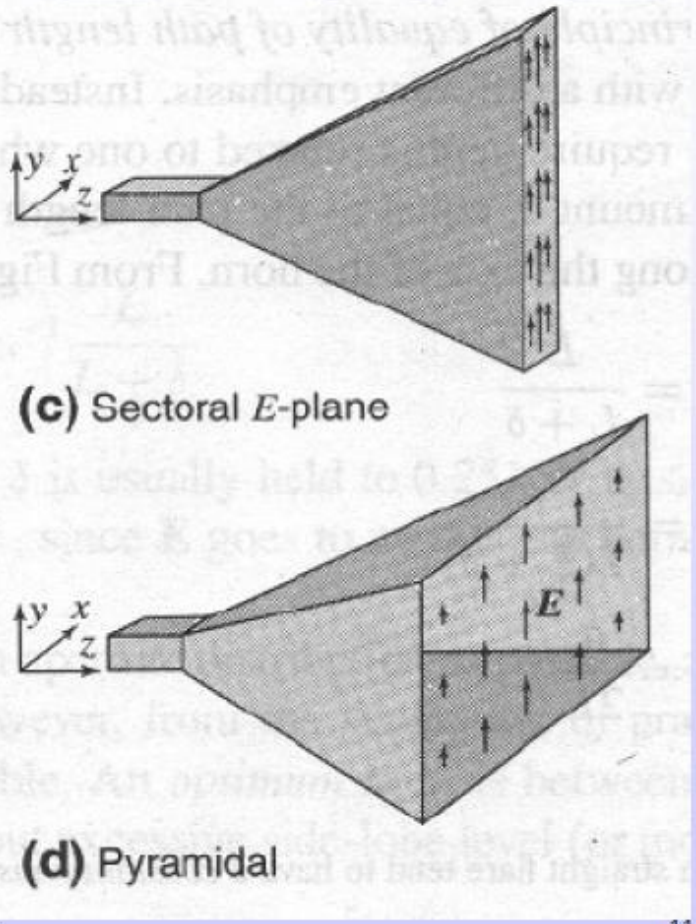

Circular Horns

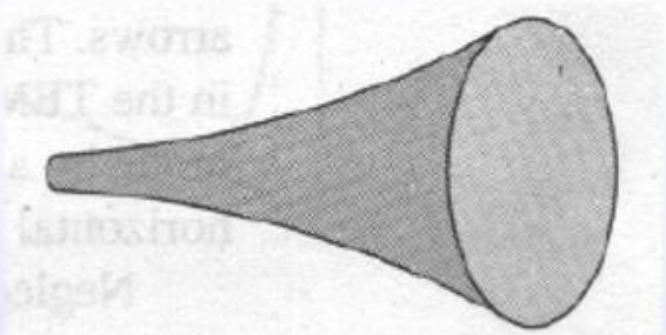

(e) Exponentially tapered

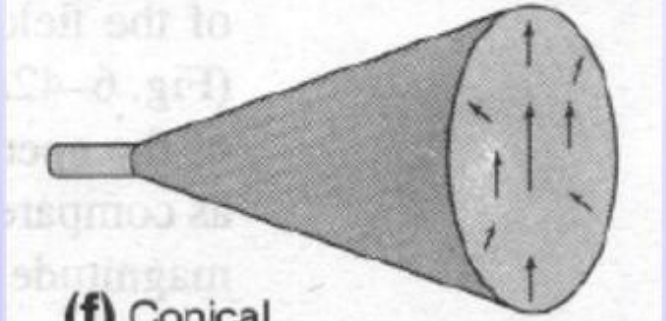

(f) Conical

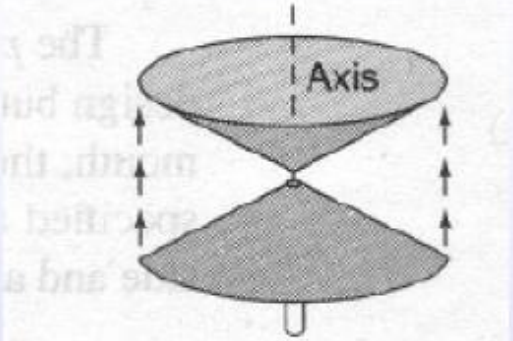

(g) TEM biconical

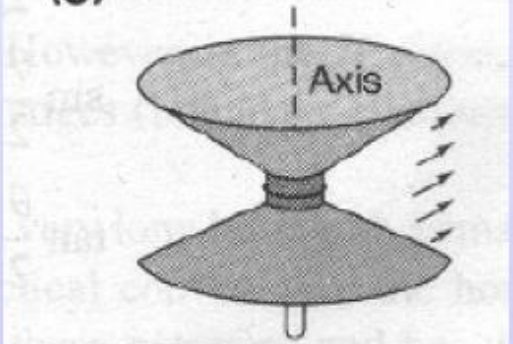

(h) TE_{01} biconical

Reflector Antennas

Corner Reflector

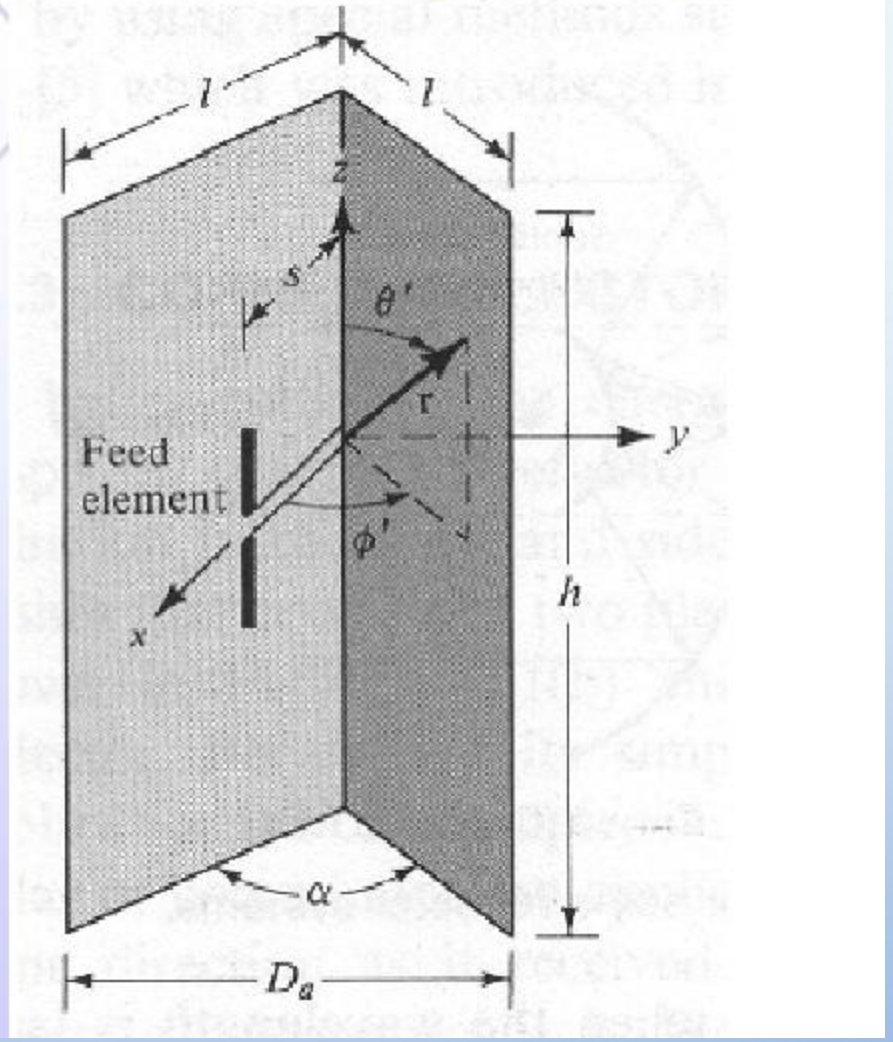

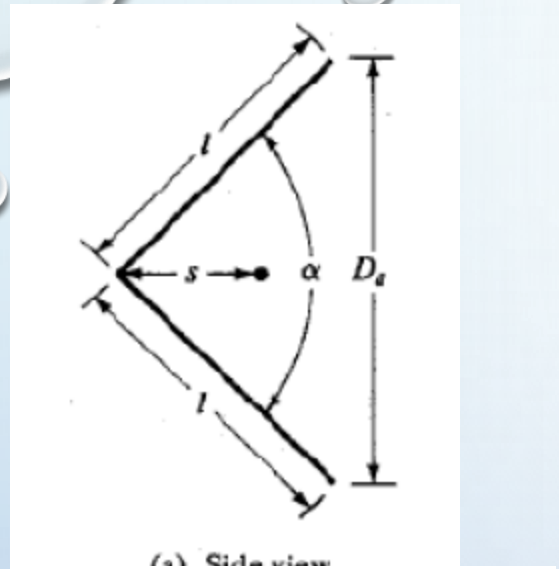

(a) Side view

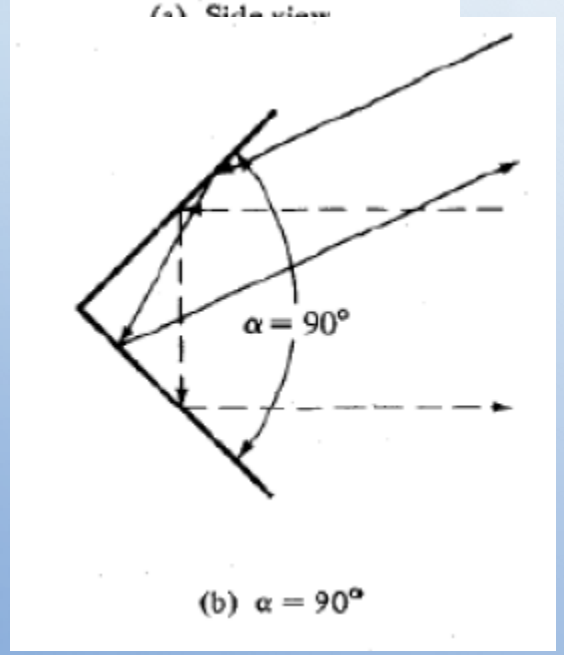

(b) $\alpha = 90°$

Plane reflectors cannot collimate energy. A divergent beam from a source becomes more divergent after reflection from a flat sheet. Corner reflectors are better collimators. Figure shows the corner reflector geometry. Because of its simplicity in construction, it has many applications. A 90º CR is used as a passive target for radar applications. Because of its unique feature, military ships and vehicles are designed to have minimum such sharp corners to evade detection by enemy radars. CRs are also widely used as receiving element for home television.

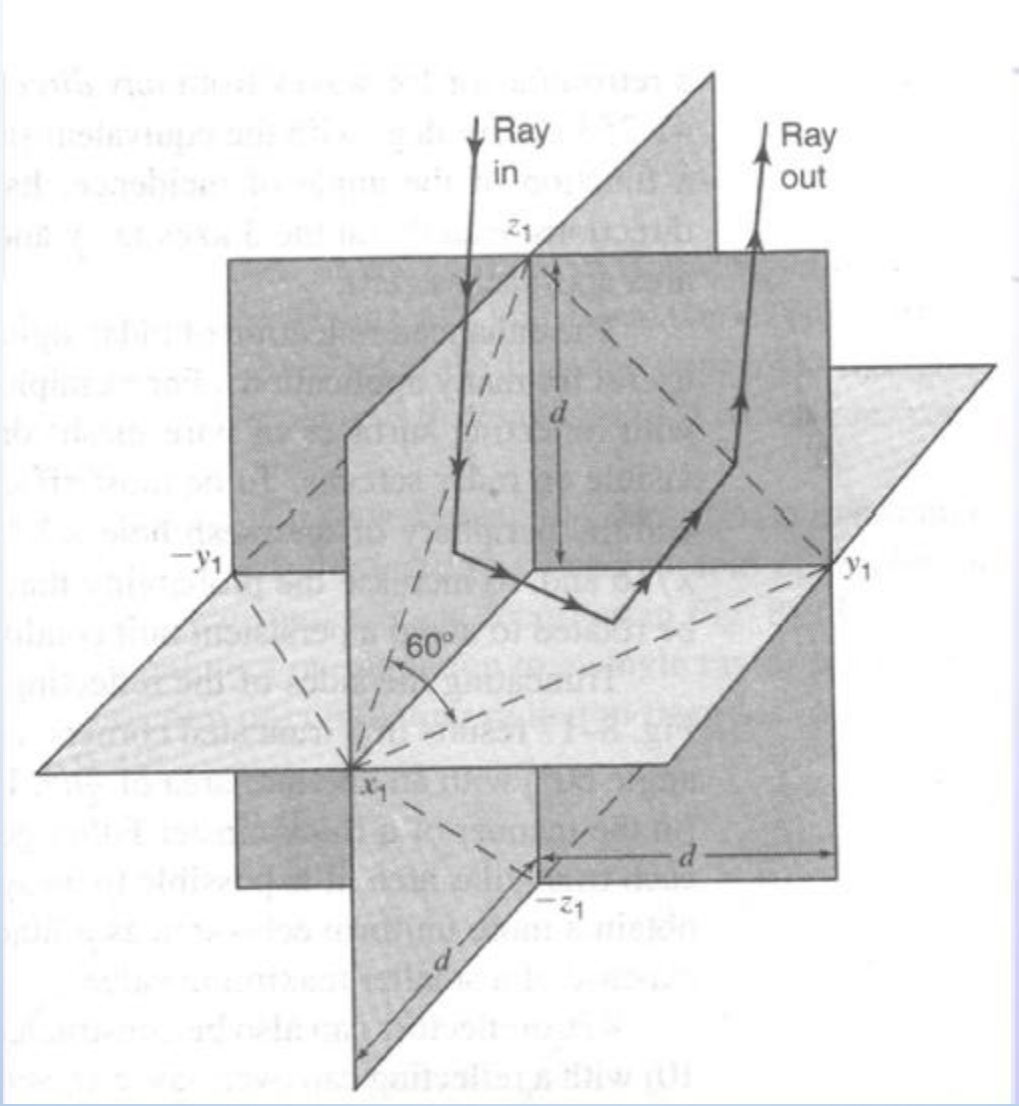

3D Retro Reflector

Parabolic Reflector

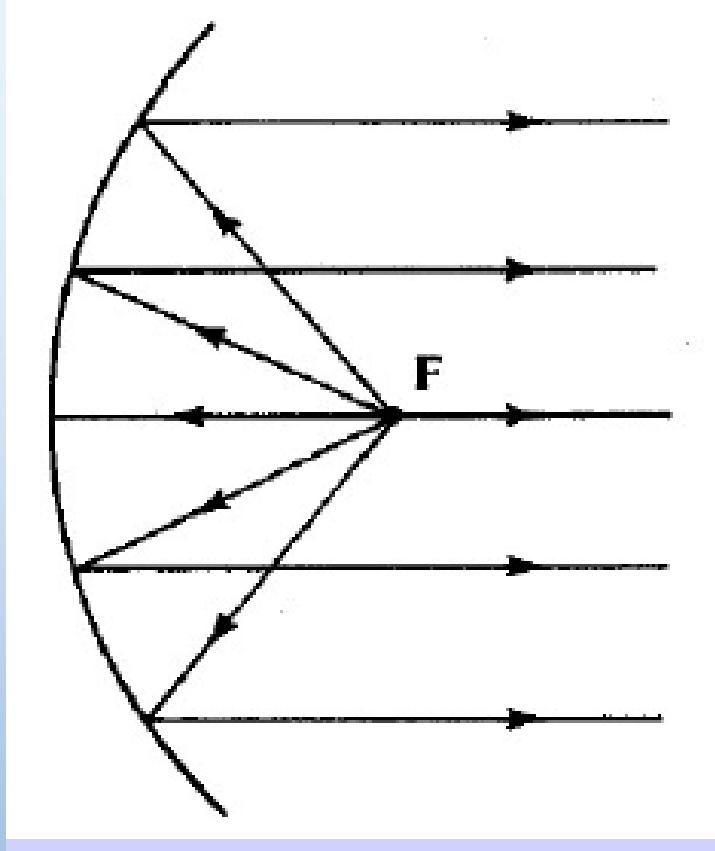

Spherical Reflector

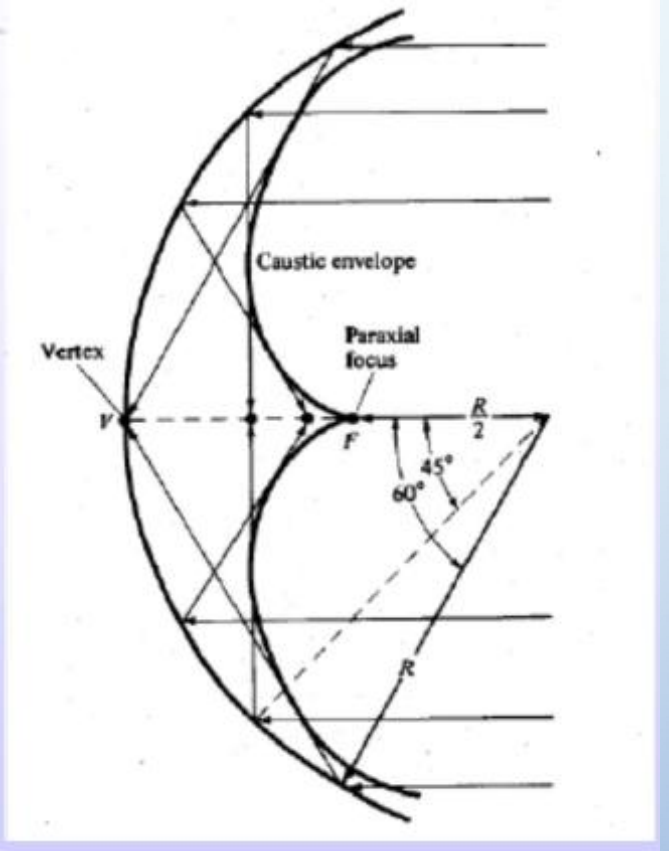

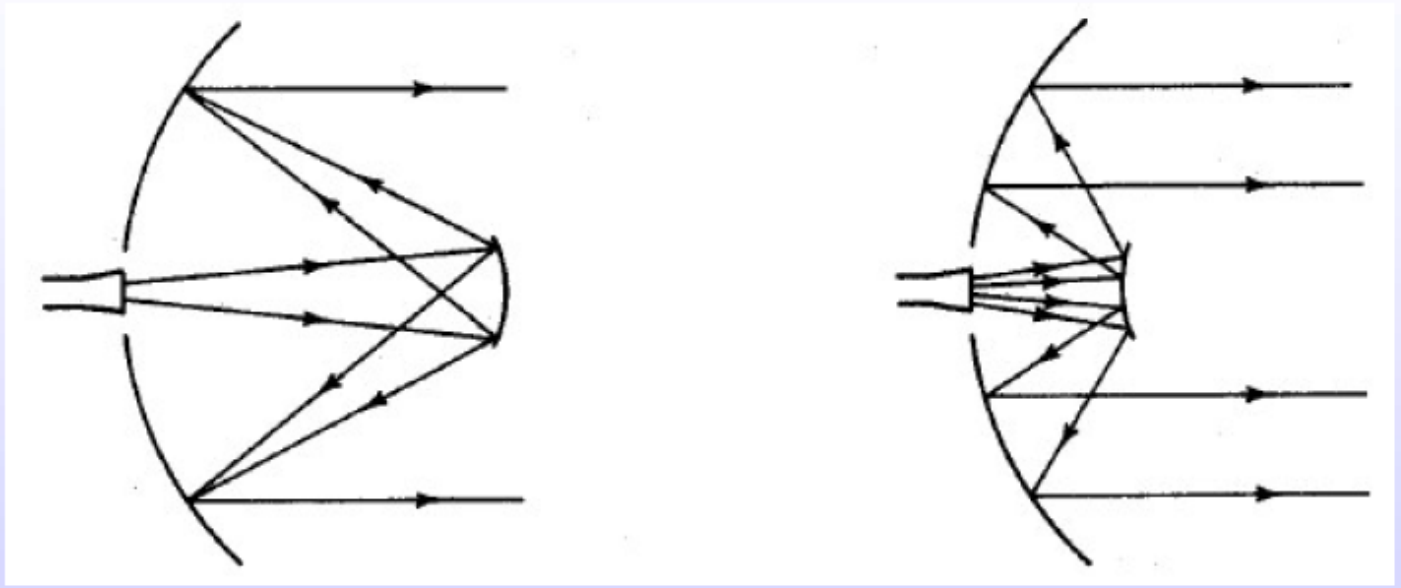

Gregorian System

Cassegrain System

These systems were derived conceptually from optical telescopes

RADAR

Block Diagram of Basic Radar

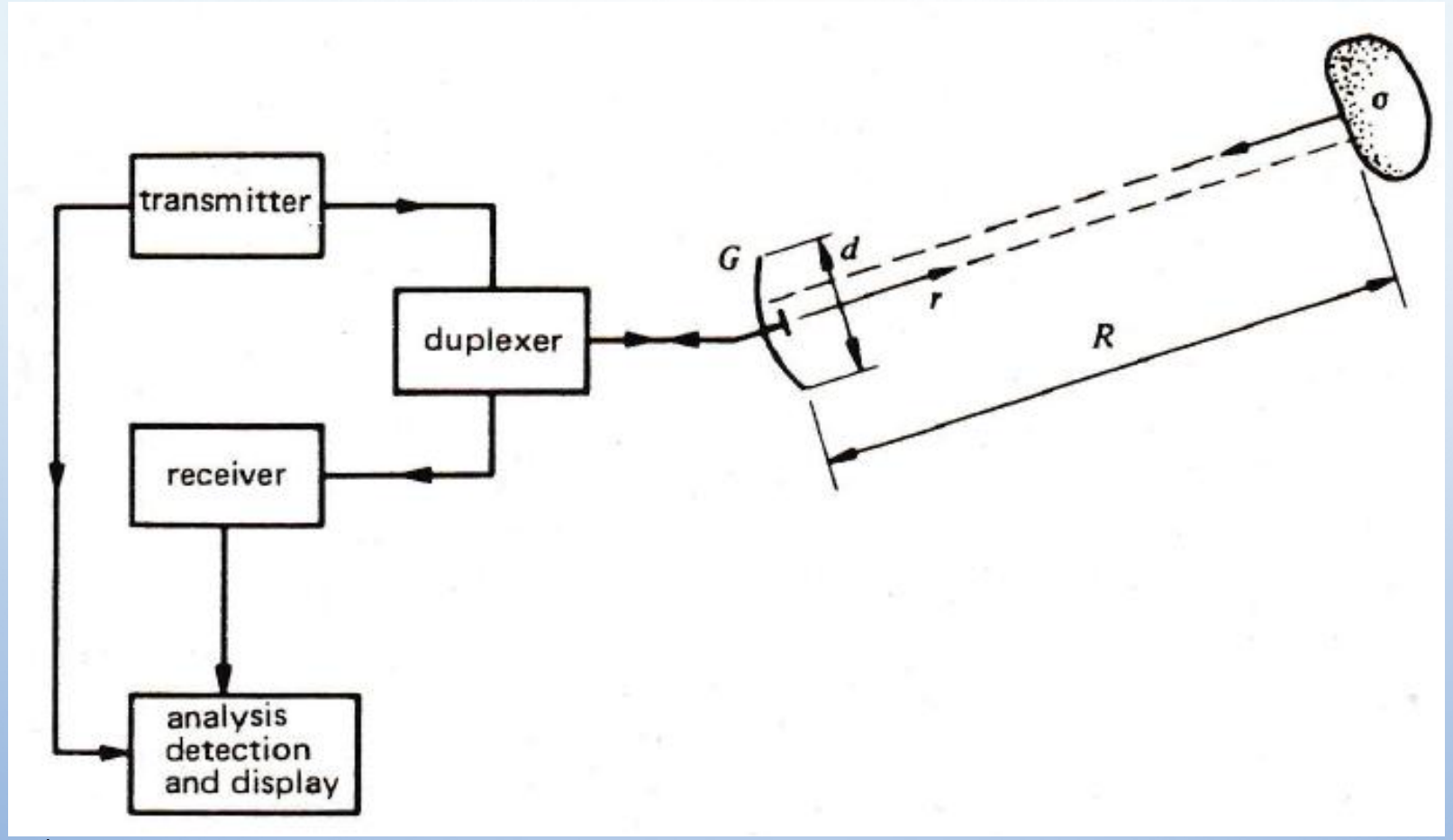

Biological Effects of Microwaves

Thermal Effects

- **Microwave radiation is non-ionizing, its main effect being of a *thermal nature*, used in medical applications (Hyperthermia).**
- **The body absorbs radiation and automatically adapts to the resulting temperature rise, excess heat being removed by the blood flow.**
- **However, should the radiation become too intense, the thermal balance could no longer be restored by the body processes, and burns would then occur.**
- **As microwaves tend to heat deeply into the body, one might fear deep burns would occur while the surface remains at an acceptable temperature. There exists a radiation threshold, beyond which irreversible (cumulative) changes do occur.**

- **In a number of studies, no permanent effect was observed for power levels lower than 100 mW/cm^2.**
- **The most sensitive organ, the eye, was found to possess a threshold around 150 mW/cm^2 for development of cataracts after a 1 ½ hr continuous exposure.**
- **The Sun provides us with the level of 100 mW/cm^2 in the Infra-Red range at noon on a sunny summer day. Introducing a safety factor of 10, the value of 10 mW/cm^2 was adopted as the upper limit tolerable for microwave irradiation of indefinite length.**

An Application of Thermal Effect: Active Denial Systems (ADS)

Biological Effects of Microwaves

Non-Thermal Effects

- The upper limit for long-term microwave exposure, prescribed in different countries varies in the range of 10 $\mu w/cm^2$ to 10 mw/cm^2 .
- A somewhat higher level is tolerated for short-term exposures.
- Very low limits are justified by the existence of non-thermal effects, produced by other interactions of microwave radiations with the organism, even at very low signal levels.
- Health problems attributed to microwaves include nervousness, hormonal imbalance, malformation, anomalous brain activities etc.

Observation

One cannot say anything conclusively about the possible hazards arising out of non-thermal effects because, (a) the effects observed and reported by some researchers could not be duplicated by others under supposedly identical conditions, and (b) in experiments, unless 'spurious mechanisms' (for example: X-ray emission from poorly shielded magnetron) are eliminated, possibilities always will remain that some symptoms attributed to microwave exposure are actually produced by some other mechanism.

Active Denial Technology (ADT)

WEAPON OF THE 21st CENTURY

In March 2001, a representative of the United States Air Force made a short statement at the press conference about existence of a new weapon called Active Denial Technology (ADT).

- The bullet of this weapon is the microwave electromagnetic radiation.
- ADT should be operating at the frequency of 95 GHz (wavelength $\lambda = 3.16$ mm) and its transmitter power should be 100 kW.
- The microwave electromagnetic radiation should penetrate 0.4 mm (1/64 inch) deep into the skin and cause such a pain sensation that the radiated person should run away to avoid it.
- The weapon is intended to control the crowds.
- The weapon should be humane, nonlethal, invisible and inaudible.
- No ballistic correction is needed and its bullet, i.e. the microwave electromagnetic radiation spreads with the velocity of light.
- The effective range of ADT is made approximately 700 yards.
- The scientists and sponsors, participating in the project, declared it to be the most revolutionary weapon since the atom bomb.

Skin Depth

$$\delta_s = \frac{1}{\sqrt{\pi f \mu_0 \sigma}}$$

As an example, for copper (conductivity σ = 5.8 x 10^7 S/m), commonly used in microwave applications, δ_S = 8.6 mm, 0.066mm and 0.002mm at 60 Hz, 1 MHz and 1 GHz, respectively.

Active Denial System

Figure 1: ADS Systems

System 1

System 2

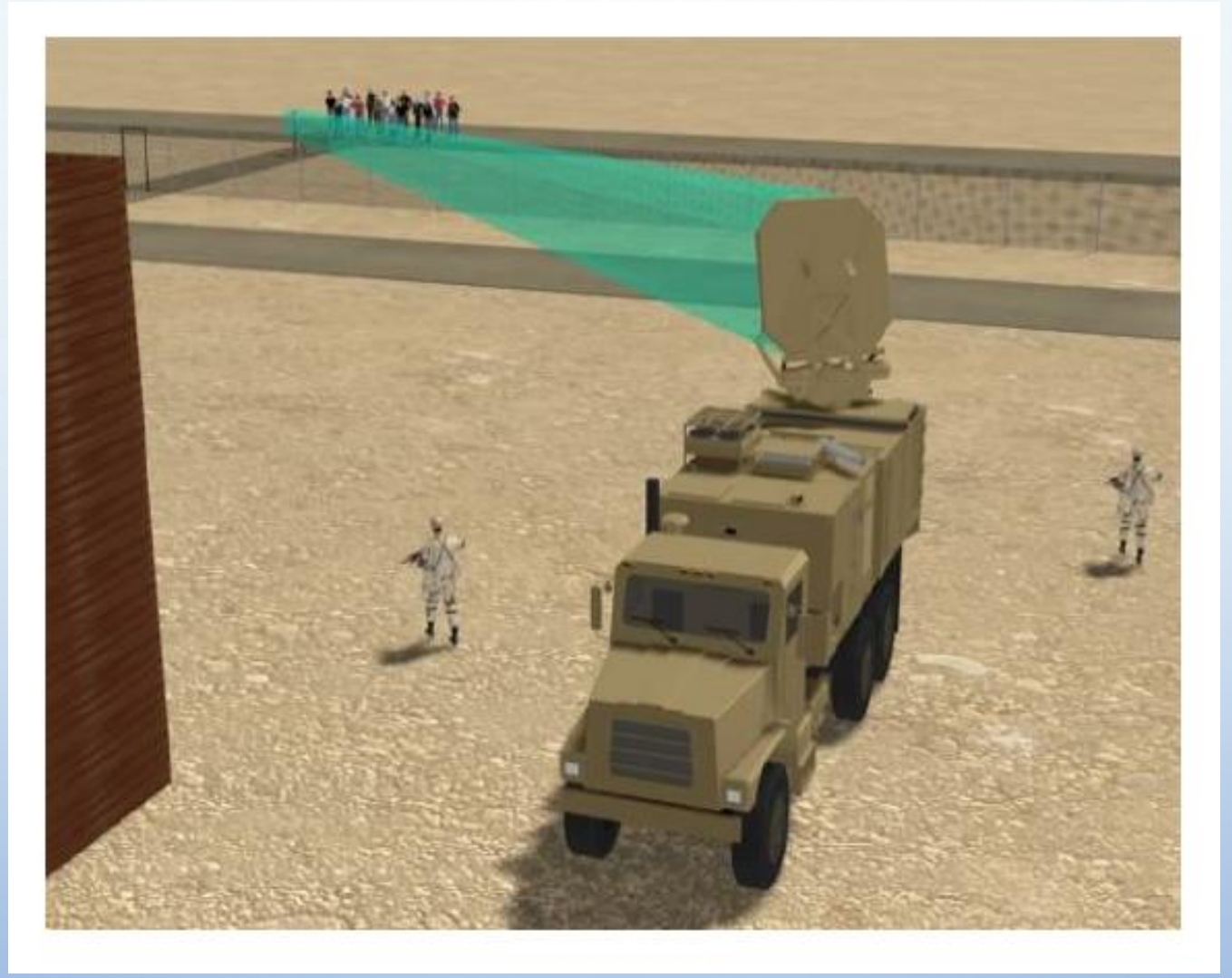

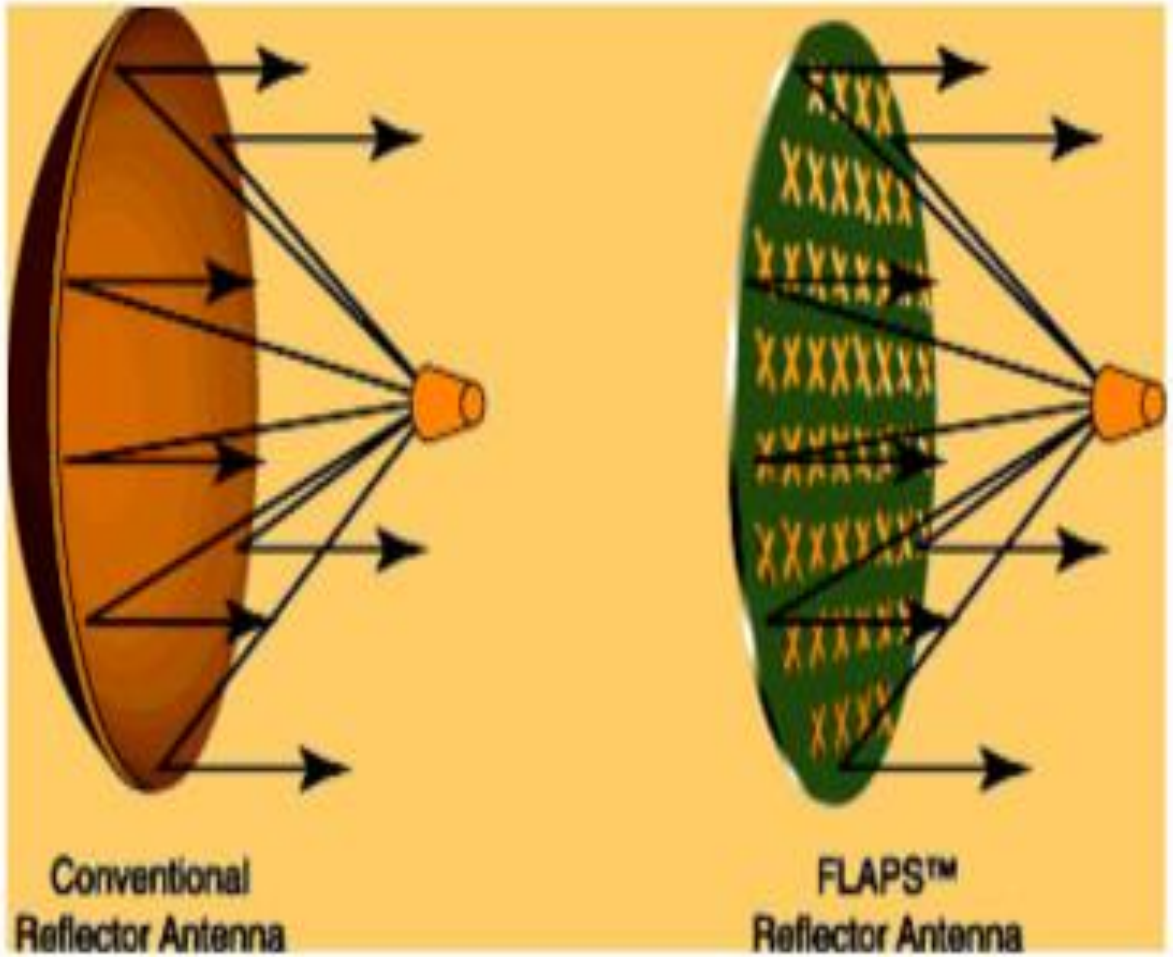

Conventional parabolic antenna and FLAPS antenna

Efficiency of a conventional circular parabolic antenna is 50 - 60 %. The efficiency mainly depends on roughness of its surface. The roughness should not exceed 1/16 of its wavelength. At 95 GHz this about 0.2 mm. Development and construction of a 2m or 3m circular parabolic antenna with that roughness would entail huge costs and require special tools to be developed.

To avoid high costs of construction FLAPS (flat parabolic surfaces) technology was used in constructing the ADT antenna. On its flat surface little dipoles are set in groups.

Efficiency of a FLAPS antenna is 95 %; it is also possible to scan its main beam to a certain extent so that mechanical rotation is not necessary.

For ADT mobile construction a folding FLAPS antenna is used, which is its great advantage when transport in strong wind is required.

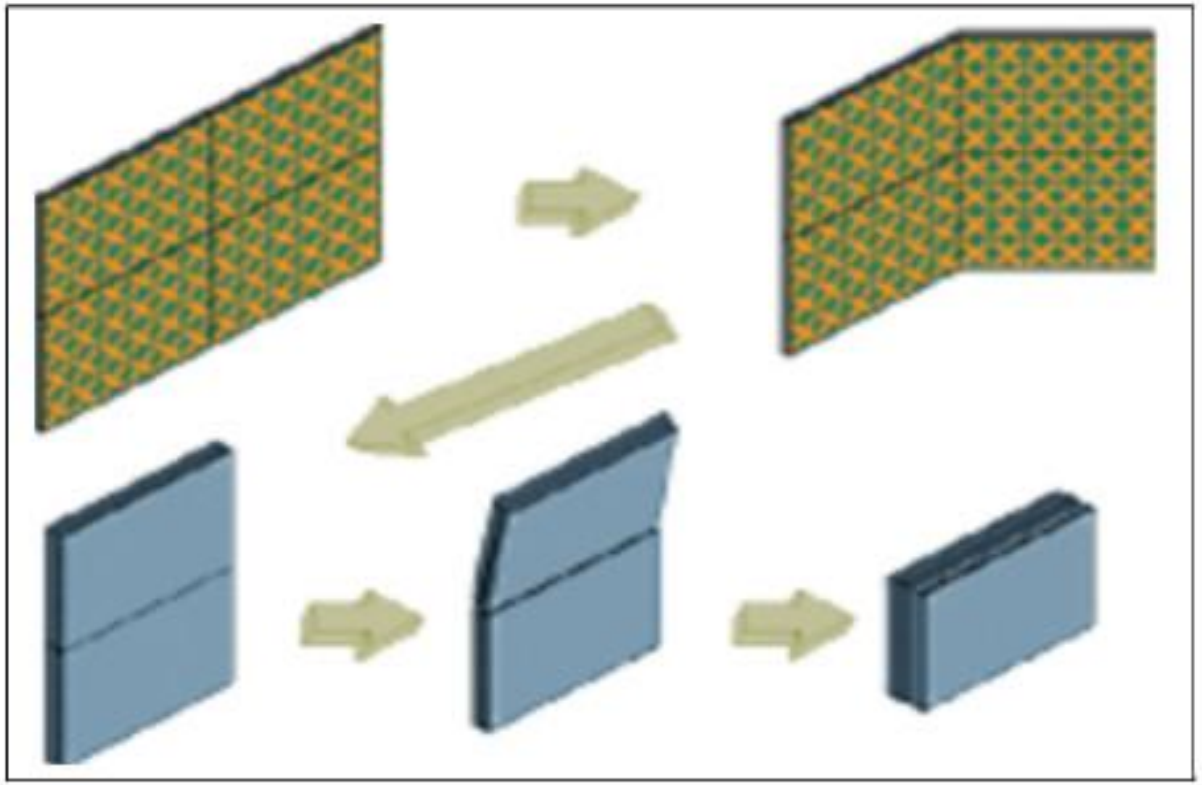

Mobile construction of FLAPS antenna

Interaction of Microwaves with Matter
Microwave Heating
Physics of Microwave Oven

saha.pradipk@gmail.com

Interaction With Matter

- When an EM wave impinges on a material sample, it is preferentially absorbed at particular frequencies, which are the resonant frequencies of the material.
- The resonances observed at microwaves depend on the molecular composition of matter. This effect is put to good use in chemical and physical analysis.
- In particular, water strongly absorbs all microwaves, a specific property which leads to two types of applications:
  - Microwave heating, utilised for cooking of food, drying and thermal processing of numerous materials, and the medical treatment of a number of ailments by hyperthermia.
  - Detection and measurement of moisture content in materials.

Microwave Heating: Characteristics (1)

- EM waves at microwave frequencies can produce heating that is utilized in heating or drying various (non-metallic materials): food, wood, paper, plastics, chemicals, textiles, etc.
- Microwave energy is a very convenient and versatile source of heat, quite flexible, reacting instantaneously to control.
- It is clean as no combustion products appear under proper operating conditions.
- Microwave heating is completely different from the conventional processes. In conventional heating, heat is generated outside the object to be heated (by flame, resistive heater) and conveyed by conduction or convection (hot air). The surface of the object is heated first and the heat then flows inward by conduction only. The inside of the object always remains colder than the surface. The heating process may become long if one wishes to bring the inside up to a cooking temperature without charring the surface.

Microwave Heating (2)

- Microwave radiation penetrates an object very deeply and the EM energy is transformed to heat by various complex mechanisms.
- The heat is thus generated in a distributed manner inside the material, allowing for a more uniform and faster heating.
- The surface in contact with the surrounding remains cooler than in the other heating techniques. The surrounding air (or the oven) is not heated up. So, little heat is lost to the environment.
- Average efficiency of conversion of electrical energy drawn from the network into heat within the body is on the order of 40 to 50%.
- A comprehensive study has shown that a MW oven used 60 to 70% less energy than conventional stoves.

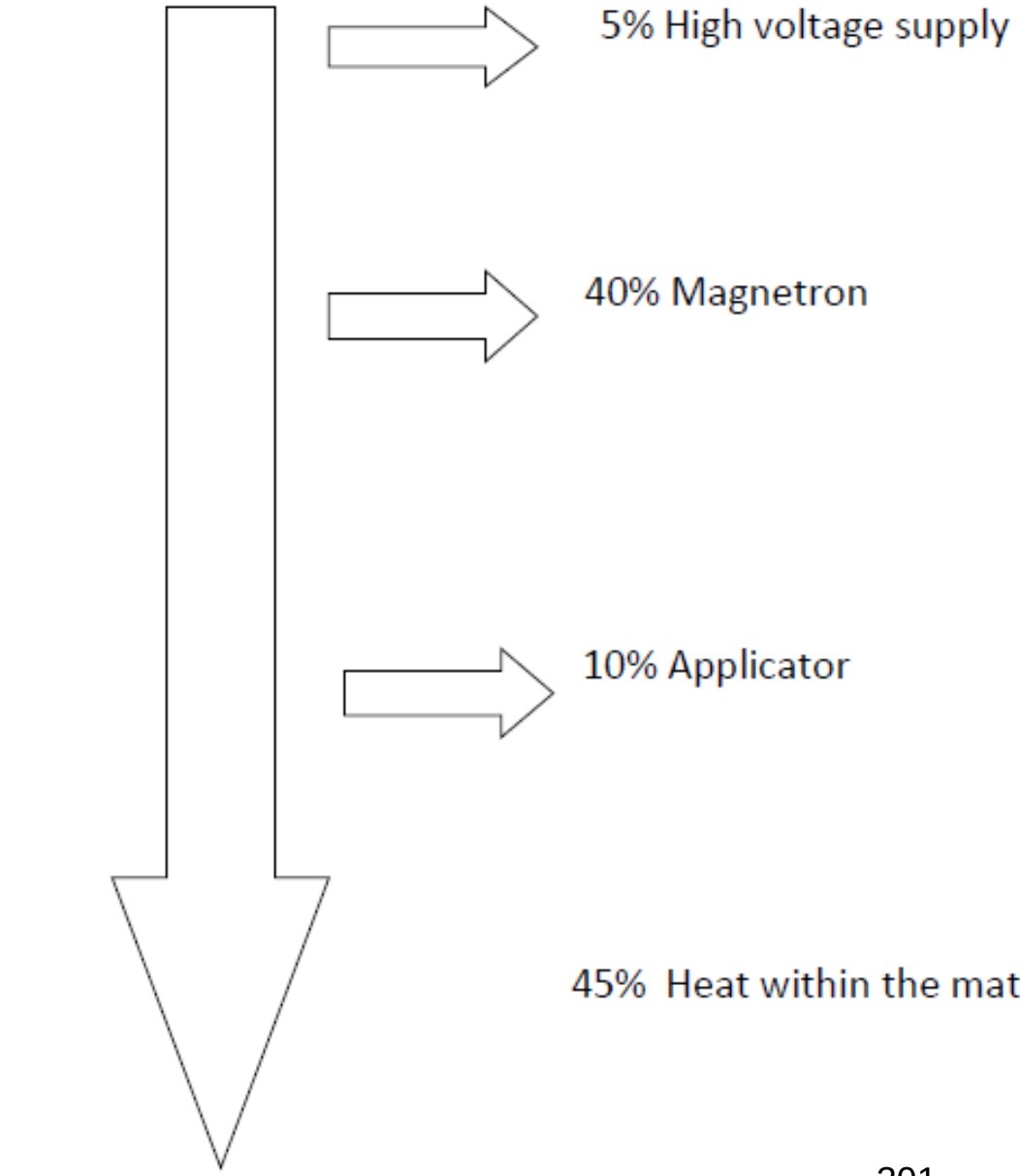
From Network 100%
Losses
5% High voltage supply
40% Magnetron
10% Applicator
45% Heat within the material

Microwave Oven

Discovery and Development of Microwave Cooking

Microwave oven is perhaps the most used kitchen appliance for heating and cooking food. A 'magnetron', operating in the 2.45 GHz band (Industrial, Scientific and Medical –ISM- band) generates microwave power typically 600 – 800 Watt.

1. Microwave oven

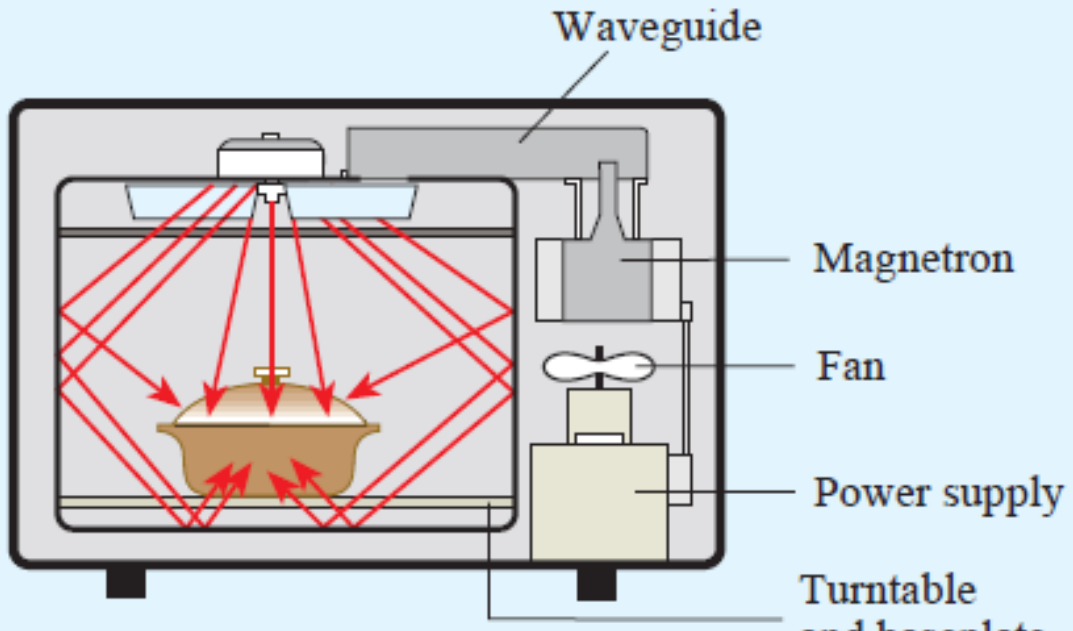

2. The magnetron

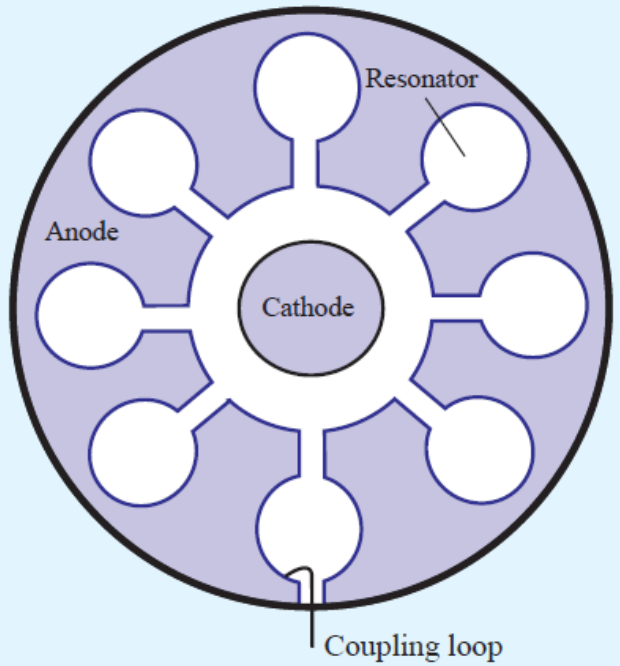

In 1945 Percy L Spencer was a man renowned for his insatiable curiosity about everything and already a Second World War hero for his development of the proximity fuse and his work in radar. One day, working with a high intensity magnetron microwave generator, he noticed a strange feeling as he walked past a magnetron and he noticed that a chocolate bar in his pocket had melted. Sending the message boy out for some popcorn, he did a few quick experiments and soon demonstrated the cooking effect of the microwaves. According to one account, the next day Spencer decided to put the magnetron tube near an egg. He and a colleague "watched as the egg began to tremor and quake. Evidently the curious colleague moved in for a closer look just as the egg exploded and splattered hot yolk all over his amazed face."

The Raytheon company, Spencer's employers, took only a year to develop the discovery into a demonstration model: the Raytheon RadaRange.

The first commercial models were housed in refrigerator-sized cabinets – standing 5'6" tall, weighing over 750 pounds and costing about 5000USD. The first microwave ovens to arrive in UK were described in the language of the time: 'as tall as a woman and took four men to move'. These early models required installation of water supply system for cooling the magnetron. At those prices and cooking tasteless and soggy food, the early microwave oven was not an instant hit. It was not until 1967 that a real contender for domestic market emerged: a 100-volt oven, which cost just under 500USD and was smaller, safer and more reliable.


© Spencer Family Archive

Some Practical Features of Microwave Oven

Necessity of a turntable

Once the microwaves have been fed into the cooking chamber, they are effectively reflected by the metallic walls. The waves resonate in the cavity and form *standing waves*. An ideal microwave oven cooks all food evenly but the nodes and antinodes of the standing waves can cause the food to burn in some places but to remain cool in others. The thermal image of intensity distribution shows that this would lead to uneven heating of food. This is the reason for having a rotating turntable: the rotation will move the food in and out of the hot spots.

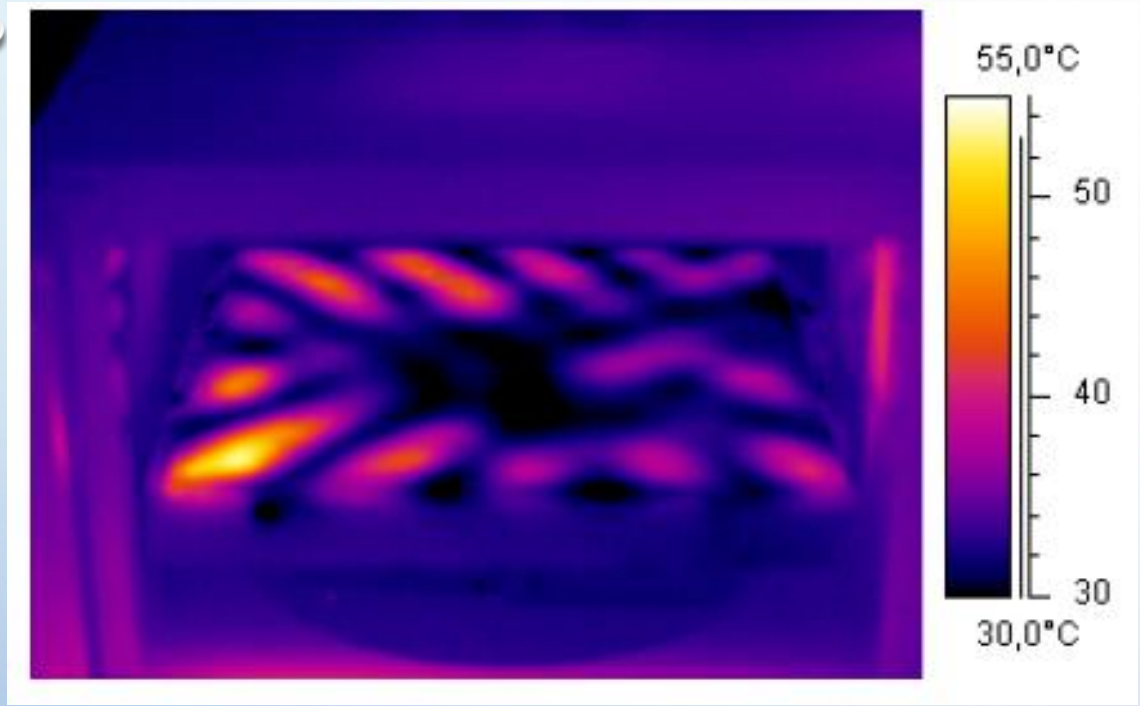

Visualization of the horizontal mode structure in a microwave oven using infrared thermal imaging. A glass plate with a thin water film was placed at a height of 8 cm and heated for 15 s with a microwave power of 800Wwithout using the turntable.

Leakage of microwaves from the oven

There are very strict regulations governing how much radiation is allowed to be emitted from microwave ovens: they could be a health risk and they could interfere with other electronic apparatus. Because a microwave oven is a *Faraday cage* little radiation is expected to escape. The most crucial part is the door, which is equipped with additional radiation traps. The radiation level close to the surface of most ovens amounts to about 1% of the allowed limit of 5 $mWcm^{-2}$. As you get further from the oven the intensity rapidly decreases, such that the usual radiation dose is well below 1/1000 of the maximum permitted value. Since a small amount of radiation does escape from the oven, it is also possible for microwaves to enter the closed oven. This may be demonstrated by putting a cell phone into the oven (turned off!) and calling it.

Metal in microwave oven

Most ordinary cooks are very confused about the effect of metals in a microwave oven. The rule ‘don’t put anything metal in a microwave oven’ is well known, and but not well- understood. Metals essentially reflect microwaves, but the process means that small pieces of metal can become hot and also spark and arc. The heating effect can be demonstrated very impressively by placing an ordinary tungsten filament bulb in the microwave. A standard 60 W bulb in a 700 W oven will explode in about 30 s, so one should only switch on microwaves for a few seconds and should put a glass of water in the microwave with the bulb to absorb some of the microwave energy. The bulb lights (with ‘no power supply’!) and it does so even if the filament is broken.

Microwave ovens have been around for more than 50 years and many millions of them are being routinely used. No major accidents have been reported to date.

Perhaps no other consumer appliance can offer such high safety record.

American physicist James Van Allen remarked – "in my judgment, [the oven's] its hazard is the same as the likelihood of getting a skin tan from moonlight".

Teaching of Microwave Engineering
— Needs a Paradigm Change

Dr. Subal Kar

Former Professor and Head

Institute of Radio Physics and Electronics (IRPE)

University of Calcutta

E-mail: subal.kar@fulbrightmail.org

Introduction

- Microwave Engineering research *First* started at the Radiation Laboratory of MIT, U.S, during Word War II and in following years—resulting in MIT Radiation Lab series (28 volumes).
- In India, *First* magnetron (at S-band) was successfully designed and developed in 1959 at IRPE, C.U.
- IRPE started microwave teaching at P.G level again *First* time in India. I have taught microwave engineering at IRPE, C.U for 33 years (1983 - 2016); every year trying to update myself in terms of content and techniques of teaching.
- *First* successful Metamaterial (plasmonic-type) at Ka-band in India was designed, fabricated and tested in 2009 by our group at IRPE,C.U in collaboration with SAMEER, Kolkata Centre and BARC, Mumbai.
- Incidentally, pioneering millimetre-wave research was done by Sir J.C. Bose of Calcutta University during 1895 - 1897; for which we all Indians are proud of.

Introduction (contd ....)

- Starting from World War II microwave engineering has seen scorers of developments:

  Tubes: Klystron, Magnetron, TWT etc.; latest inclusion: Gyrotron.

  Semiconductor Devices: Latest ones being HEMT, HBT etc.

  Circuits: Co-axial lines, Waveguides, planer transmission-line etc.

  Antennae: Latest ones being microstrip, DR antenna etc.

  Materials: Ferrites, Meatamterials etc.

  Instruments: Spectrum analyser, Network analyser etc.

  Simulation tools: 3D EM-simulator (HFSS), EDA-simulation tool (ADS) etc.

Introduction (contd ....)

- From the beginning of 21st century, especially during last one decade, a new change is felt by the teaching community of microwave engineering.
- How to teach microwave engineering to make our students "***truly capable***" and "***professionally employable***" to meet the present-day needs of R&D sector and industry?
- Today we are here to exchange our views regarding a very challenging question of "***how to teach microwave engineering today***" so that our future generation students are genuinely benefitted.

Introduction (contd ....)

- The traditional view of microwave teaching has been generating a fear-psychosis in the mind of students that '***microwave learning demands too much of mathematics***'.
- In my view, "***some essential mathematics is definitely required***", however, such mathematics need to be used to that extent and with that end in view which will lead to the meaningful physical insight of the subject and would give guidance to application view points.
- My book on "Microwave Engineering" has been written with that spirit in mind.

RE-VISIT TO ELECTROMAGNETICS

• Elecromagnetics is in the soul of microwave engineering. A re-visit to the essential elements of electromagnetism is a must for getting insight into the study of microwave engineering.

• Though electromagnetics is being taught as a core subject in the curriculum of ECE in a previous semester at least two lectures in the beginning should try to summarize the essential elements of electromagnetics before entering into the actual content of microwave engineering.

• Recapitulation of Maxwell's equations, electromagnetic wave propagation in space, principle of dielectric heating and microwave oven need to be addressed.

• Wave propagation in interfacing media, boundary conditions, oblique incidence on plane boundaries—from which the concept of parallel-plate waveguide comes, need to be touched.

• Basic concept of radiation mechanism in antenna and various antenna characteristic parameters including Friss' transmission equation and the concept of antenna noise temperature should be addressed—which are essential for microwave system designer.

HF Behavior of Transmission Lines

- ***RF transmission lines*** and waveguides are the transmission medium for RF and microwave signal (unlike power transmission lines at 50/60 Hz).
- RF transmission lines are analysed with "***distributed***" circuit concept (unlike "***lumped***" circuit concept at power line frequency). Here current, voltage and impedance varies all along the length of the line.
- Not only the telegrapher's equation and terminated transmission line including transmission line circuit elements be taught but the designer's clues like ***return loss*** (for load reflection), ***reflection loss*** (for load absorption) are to be addressed with practical view points.
- ***Smith chart***, which is one of the primary screen options in network analyzer and are used in solving stub matching problem and also in impedance measurement in microwave frequency need to taught in details with practical design problems.
- ***Planer transmission lines*** which is in the heart of MICs need to be covered with physical principle and field patterns which help to get insight for design with such transmission lines.

Guided structures: Waveguide and Cavity Resonators

- ***Waveguides*** are single conductor guiding structures with mode of signal propagation in TE or TM mode (unlike TEM mode in coaxial/twin-wire lines).
- A waveguide supports travelling waves; when closed along its length at two the ends with short circuit (placed $\lambda_g/2$ apart) we have ***cavity resonator*** supporting standing waves in which e.m. energy can be stored at its resonant frequency.
- In addition to boundary value solution of wave-guiding phenomena in rectangular and circular waveguide; from designer's point of view one must understand that ***circular waveguide becomes two times larger in size than rectangular waveguide for same cut-off frequency (both operating in dominant mode).***
- ***Strip/disc resonator*** and dielectric resonators are important for planer transmission line based design.
- ***Mode chart*** aids in the design of cavity resonators. ***Coupling and tuning of microwave resonators*** are also important for a microwave design engineer.

Microwave Network and Scattering Matrix

- ***Scattering parameters*** are used for microwave circuit/device analysis and design, just as Z, Y, and h parameter are used for low-frequency device/circuit characterization.
- S-parameters are defined in terms of the wave variables. ***The square of any wave variable is proportional to the average power in the wave***, which are directly measurable quantities at microwave frequency.
- A network analyser characterizes the microwave circuit in terms of S-parameters: S_{11} → input reflection coefficient, S_{21} → forward transmission coefficient, S_{22} → output reflection coefficient, S_{12} → reverse transmission coefficient.
- ***Signal flow graph***, ***decomposition rule/ Mason's rule*** are used to find the transfer function of complex microwave circuits.
- ***Microwave amplifier gains*** like: transducer gain, available power gain etc***. are expressed in terms of S-parameters***.

Microwave Passive Circuit Components

- ***Passive components*** are inseparable part of any system design—microwave system is no exception. Both waveguide based and planer transmission line based passive components including the lumped-element and distributed-element components are to be known and also optimum design with simulators.

Terminations	Matched load.
	Variable short.
Tee-junctions and hybrids	*E*-plane tee, *H*-plane tee.
	Hybrid tee (magic tee), hybrid ring (rat-race). Wilkinson power divider/combiner, branch-line qudrature hybrid, short-slot hybrid.
Tuners	*E-H* tuner.
	Slide screw tuner.
Directional coupler	Multi-hole directional coupler, Schwinger reversed-phase coupler, Bethe-hole coupler.
	Coupled-line directional coupler, Lange coupler.
Attenuator	Flap attenuator.
	Rotary vane attenuator.
Isolator	Faraday rotation isolator.
	Resonance absorption isolator.
Circulator	Faraday rotation circulator—SPDT switch, power divider.
	Y/*T*-junction circulator.
Phase shifter	Ferrite type, reflection and transmission type.
	Rotary phase shifter (waveguide type).
Bends and corners	
Waveguide twist, transitions and adaptor	
Flanges and connectors	

Impedance Matching in transmission lines and Waveguides

- ***Impedance matching*** is a very important issue related to the design of a microwave system.
- A transmission line or waveguide is said to be ***matched*** to a load if the load impedance is equal to the characteristic impedance of the line. Similarly, if the line impedance is equal to the generator impedance, the two are matched.
- ***Stub matching***: single, double, triple stub matching depending on situation. *Smith chart solution of stub matching problem is given in the book*.
- ***Quarter-wave transformer*** is for ***narrow-band*** matching. *For* ***broad-band*** *matching* use ***stepped-impedance*** **transformer** (binomial or Tchebyscheff response) or ***tapered*** (exponential/triangular/Klofenstein) ***impedance transformer***.
- Impedance matching in microwave system is also done with ***Windows (iris)*** and ***matching screws in wave guide***. *Lumped component and planer distributed line reactive line elements* are also used *for impedance matching in amplifier design*.

Microwave Filters

- ***Microwave filter*** is realized by replacing all inductors and capacitors of low-frequency prototype by suitable microwave circuit elements (length of transmission line with suitable termination/ lumped microwave components).

- ***Insertion-Loss Method*** is commonly used for Low-pass Prototype Design which is then transformed to the required filter type (low-pass, high-pass, band-pass, and band-stop) with proper scaling of the prototype circuit elements in terms of impedance and frequency.

- ***Richard's transformation*** is used for microwave implementation of the filter, ***Kuroda's identity*** and ***impedance/ admittance inverters*** are used to convert series to parallel stub and vice versa, the latter technique being used for band-pass and band-stop design.

- Design of ***Stepped impedance low-pass filter***, ***Coupled-line band-pass filter***, ***band-stop filter*** using ***analytical synthesis process*** *and also using* ***EDA (Electronic design Automation) tool*** *has been given in the book which is used for practical engineering design of such filters required in* in any type of communication, radar and test/measurement

Microwave Active Devices

- **Microwave active devices:** For Signal generation, Amplification, Mixing. switching etc.

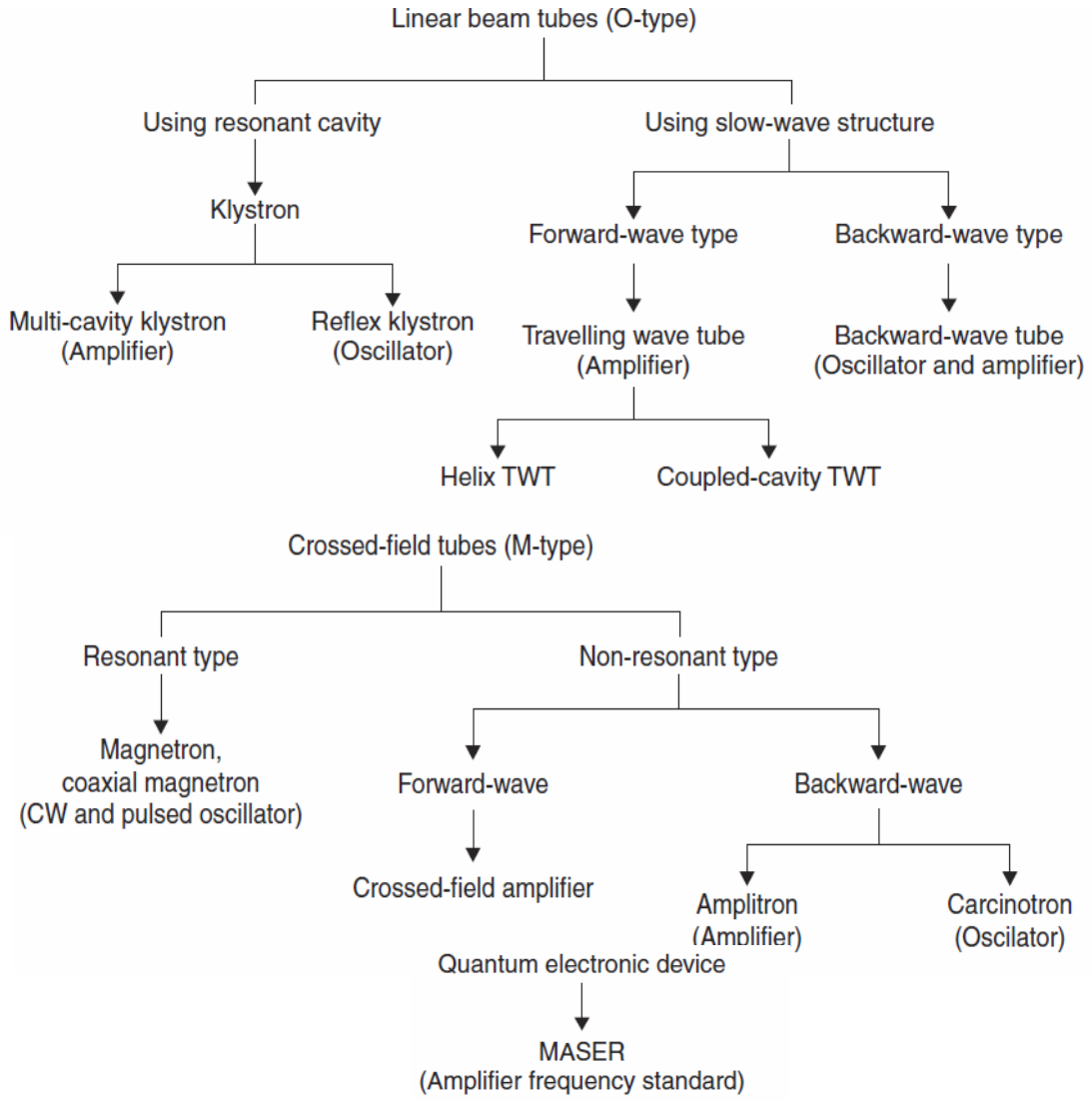

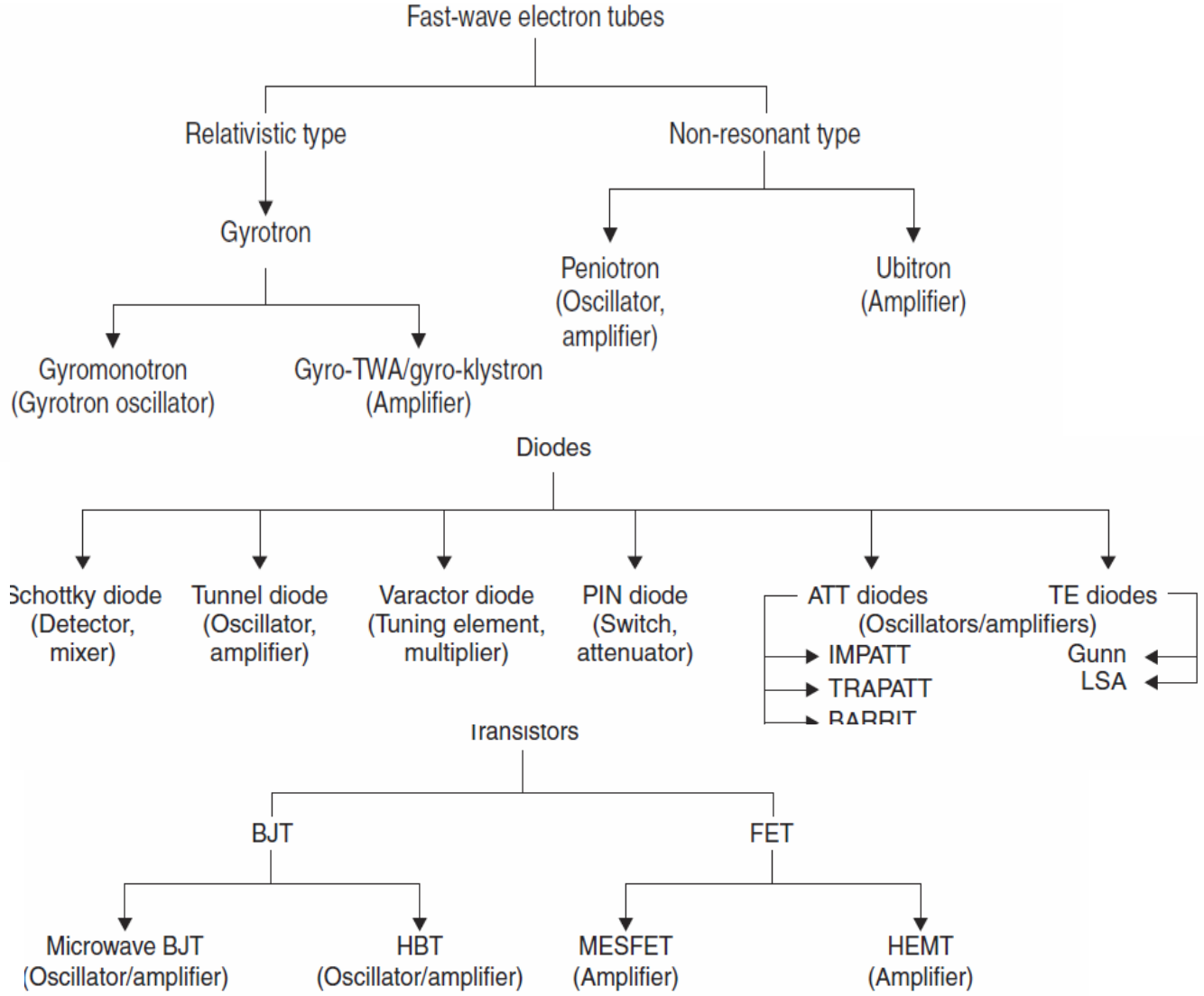

Microwave Antennae and Wave Propagation

- At present many different forms of ***microwave antennae*** are used whose principle of operation is more or less similar (i.e. dependent on diffraction principle) and differ significantly from antennae operating at lower radio frequencies.

- In general, there are six types of conventional microwave antennas viz. ***horn, reflector, slot, lens, dielectric, and surface-wave***. Each of these types has several sub-types with large number of variants.

- Apart form these conventional diffraction-type microwave antennas many civil and military applications demand planer (printed) antennas like ***microstrip patch antenna*** and its variants which are useful for low power applications. In recent times, ***dielectric resonator antenna*** is also gaining importance for millimeter-wave applications.

- ***Microwave signal propagation*** normally takes place by ***LOS***. ***Troposcatter microwave communication*** possible in difficult geographical terrain using tropospheric scattering of radio signal. In subtropical region, the phenomena of super-refraction allows the propagation of microwave signal through ***atmospheric ducts*** to very long distance. Further, microwave signal propagation around the globe is done these days popularly and elegantly via ***communication satellites***.

Microwave Measurement Techniques

- The techniques of ***measurement at microwave frequency*** is expected to be different from lower frequency radio waves because here the operating wavelength is comparable to and even becoming smaller than the component size.

- ***Primary measurable quantities*** at microwave frequency are ***standing wave ratio/reflection coefficient, power and frequency***. Measurement of ***microwave impedance and quality factor (Q)*** of a microwave cavity can be done ***in terms of standing wave ratio measurement***. ***S-parameters*** of a microwave network *can be* ***determined in terms of microwave power measurement***. Smith Chart aids in impedance measurement at microwave frequency.

- ***Antenna measurement*** *(in brief)*, ***measurement of dielectric constant*** and ***noise figure and phase noise measurements*** have been discussed in this book.

- Fundamentals of ***Spectrum Analyzer*** and ***Network Analyzer*** has also been discussed.

Microwave Integrated Circuits

- The integrated circuit realized at microwave frequencies with microwave active device and passive components including the interconnecting transmission lines are known as ***microwave integrated circuit* (MIC)** which may be either hybrid microwave integrated circuit (***HMIC***) or monolithic microwave integrated circuit (***MMIC***).

- In ***HMIC***, distributed microstrip line is formed with metallization on some dielectric substrate while packaged active devices like transistor, diode etc. and passive components like, inductor, capacitor etc. (either in distributed or lumped form) are soldered or bonded on to the substrate.

- In ***MMIC***, active devices (in un-capsulated/un-packaged form), passive components and interconnections are fabricated on a single semiconductor material that allows to keep the parasitic capacitance and inductance to a minimum permitting mm-wave performance.

- Fabrication processes of HIMC/MMIC demands ***diffusion, Ion-implantation and Epitaxial techniques, masked Lithography and mask-less lithography, thick and thin-film technology***.

EMI and EMC

- ***EMI*** is the phenomena that originates the problem of electromagnetic interference while ***EMC*** is the characteristic with which equipment should be designed so that it is not being affected or disturbed by EMI and do not also generate EMI above a specified limit.

- Mitigation of electromagnetic interference (EMI) and to comply with electromagnetic compatibility (EMC) at radio frequencies (RF) is commonly realized with ***electromagnetic shielding*** **(i.e. RF shielding)**.

- The RF testing of a prototype is most often carried out in a radio-frequency ***anechoic chamber*** (an-echoic meaning non-echoing or non-reflecting, or totally absorbed).

- For mobile phones ***SAR (Specific Absorption Rate)*** value limit for European standard is a maximum of 2 W/kg averaged over 10g of human tissue while the U.S standard is 1.6 W/kg averaged over 1g of human tissue. In India, as per 2012 regulation US standard is adopted.

An Emerging Topic of Microwave Engineering: Metamaterials

- ***Metamaterials*** are engineered composite media that exhibit counter-intuitive phenomena like ***reversal of Snell's law and hence negative refractive index, reversed Doppler Effect and reversed Cherenkov Effec***t not observed in nature.

- Apart from these exotic properties metamaterial-inspired microwave components like couplers, phase-sifters and efficient antenna design is a very thriving domain of research in microwave engineering.

- There are two types of metamaterials: ***plasmonic type*** and ***transmission-line type***; the latter being useful for microwave components design to realize broad-band operation.

- Apart from its traditional use as meta-material the meta surfaces can be used for improving the functionalities of microwave and even photonic devices.

- Fundamentals of metamaterials and simulator-based design of microwave components like antenna, filter etc. has been discussed in the book.

Applications of Microwave Engineering

- ***RADAR*** is the primary application of microwaves engineering and both of them started their journey from World War II onwards.

- In recent times, a large fraction of the world's international and other long, medium, and short-haul telephone, data and television transmissions use ***microwave communication systems***. Broad-band Microwave Access for ***Mobile Communications*** use microwave for *last mile access connectivity.*

- ***Microwave heating*** is unquestionably the first fundamentally new heating technique since the discovery of fire and it has become familiar to the general public because of the ubiquitous domestic cooking/heating appliance—the ***microwave oven***. In addition to that ***drying***, ***vulcanization*** are also important application of microwave heating in industry.

- Microwave in ***Medical Applications*** is very important these days. ***Microwave hyperthermia and microwave ablation*** are important for recent day cancer treatment.

NEW INCLUSIONS IN THE SECOND EDITION OF THE BOOK

- In the chapter on ***Microwave Active Devices*** a number of new inclusions have been done. **(i)** Here the necessary ***analytical derivations for two-cavity klystron amplifier and reflex klystron, TWT, magnetron, gyrotron, Gunn diode, IMPATT diode, and MESFET/HEMT has been included***.
  (ii) ***Microwave power amplifier and its simulation based design has been newly included*** and also **(iii) A** new section on ***Microwave Mixer and its design using simulator has been incorporated*** in the same chapter.

- The chapter on Radar has been renamed and ***a new section on Radio-aids to Navigation has been included which also covers global positioning system (GPS).***

- New emerging applications like ***RFID, MEMS for microwave components, microwave and THz imaging has been discussed briefly***.

- The ***'recapitulation' part*** in all chapters have ***been re-written to make them short and crisp*** in order to imbibe only the snap-shot points to be kept in mind after completing the study of a chapter.


Thank You

Metamaterials: An Emerging Field of Research in Microwaves and Photonics

Dr. Subal Kar

(Subal.Kar@fulbrightmail.org)

Former Professor and Head

Institute of Radio Physics and Electronics

University of Calcutta

92, A. P. C. Road

Kolkata-700009, India

Introduction

- Metamaterials are the watchword of 21st century.
- In the year 2001 first successful metamaterial was experimentally demonstrated in UCSD, U.S.A that could exhibit negative refractive index, a counter-intuitive phenomena (not available in Nature).
- Initial developments in metamaterials was in the microwave frequency domain, limited by the fabrication technology available in those days. Most of the proof of principle for metamaterials developed at microwave frequency with many novel applications.
- However, with the advent of nano fabrication technology of today the photonic metamaterials (i.e. metamaterial at optical frequency) are now possible to fabricate which opened up an excitingly new vista of applications of metamaterials in photonics.

Organization of the Talk

This presentation will discuss:

- The basics of metamaterial including its significant developments covering both exotic applications (like cloaking and stealth technology, sub-wavelength imaging, super-lens etc.) and commonplace applications (like size-miniaturized and efficient antennae, filters and other passive components), including negative refractive index, at microwave frequency.
- Photonic metamaterials and other metamaterial-assisted photonic applications with astonishing and unprecedented capabilities.

METAMATERIAL
AND ITS APPLICATIONS
AT MICROWAVE FREQENCY

Normal Crystal, Photonic Crystal, and Metamaterial

Normal Crystal (λ >> p)

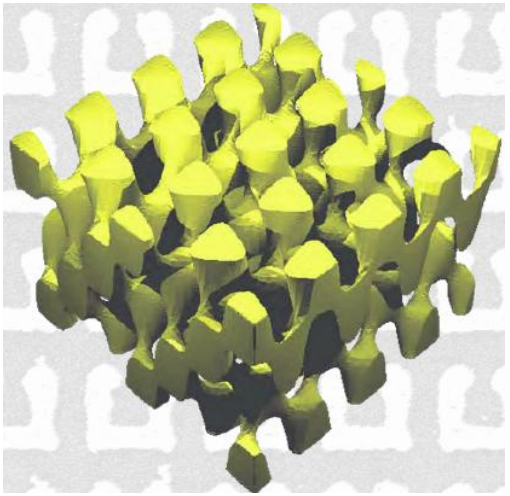

Photonic crystal (λ ≈ p)

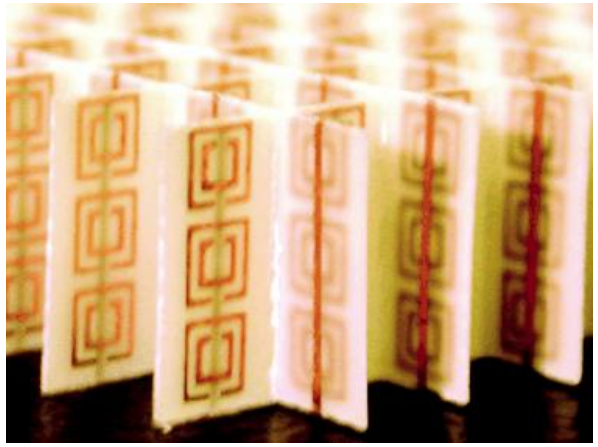

Metamaterial (λ > p)

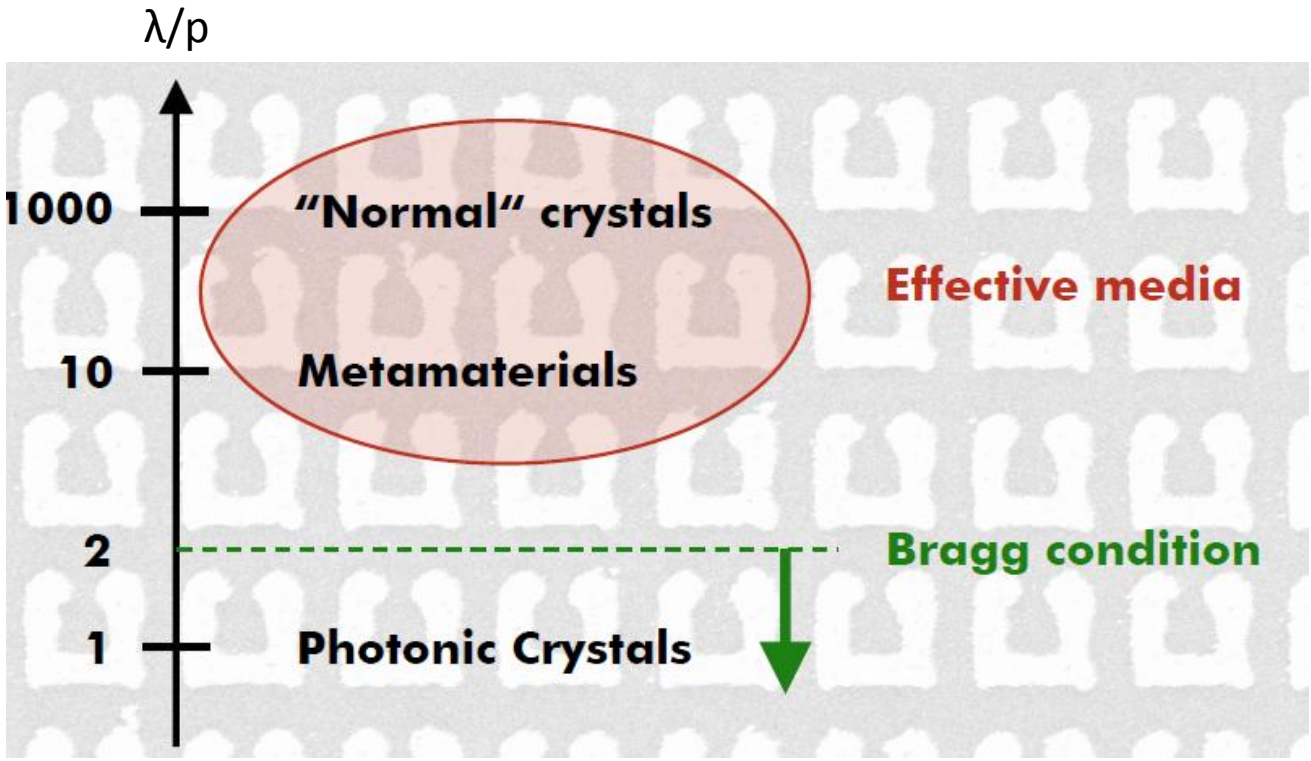

Ratio of wavelength (λ) to lattice constant (p)
for different types of crystals

Metamaterial

- Metamaterial, or phenomenologically the Left-Handed Material (LHM), is popularly known to make things “invisible”.

- Technically speaking LHM is artificially structured material (commonly metal-dielectric composite) having extrinsic inhomogeneity but to an incident e.m. wave it is effectively homogeneous. The structural properties, rather than the chemistry (of the material with which it is designed), determine the characteristics of LH materials.

- LHMs are realized with unit cells in periodic structure having unit cell dimensions commensurate with small-scale physics [$h << \lambda$, where h is the characteristic dimension of a unit cell (i.e the elementary motif size) and λ is the operating wavelength].

- In recent years, the R&D in metamaterials is very active in realizing exotic functionalities not available in nature including commonplace applications.

Right Handed vs Left Handed Materials

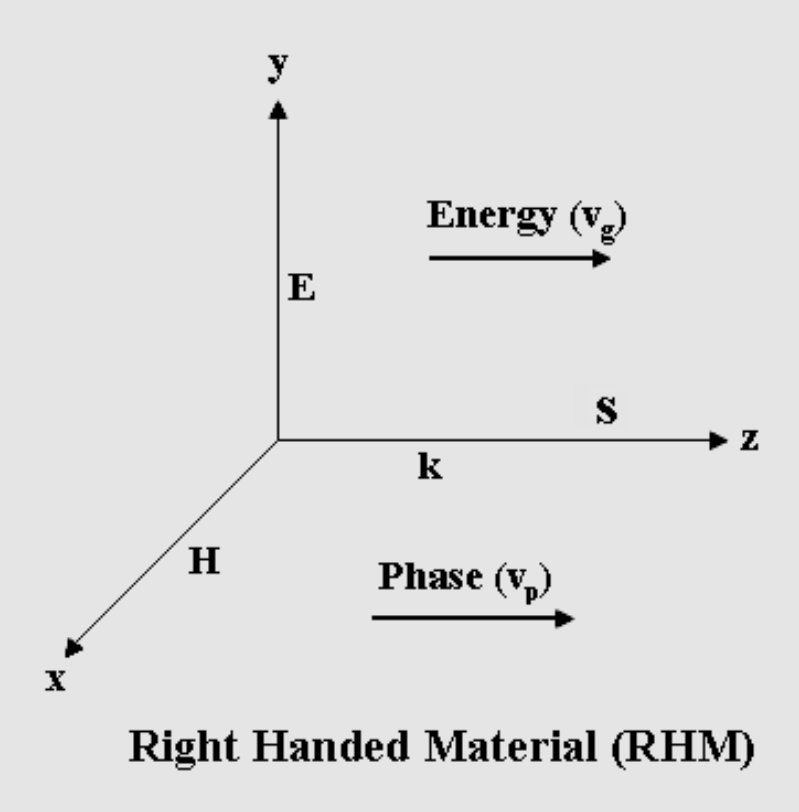

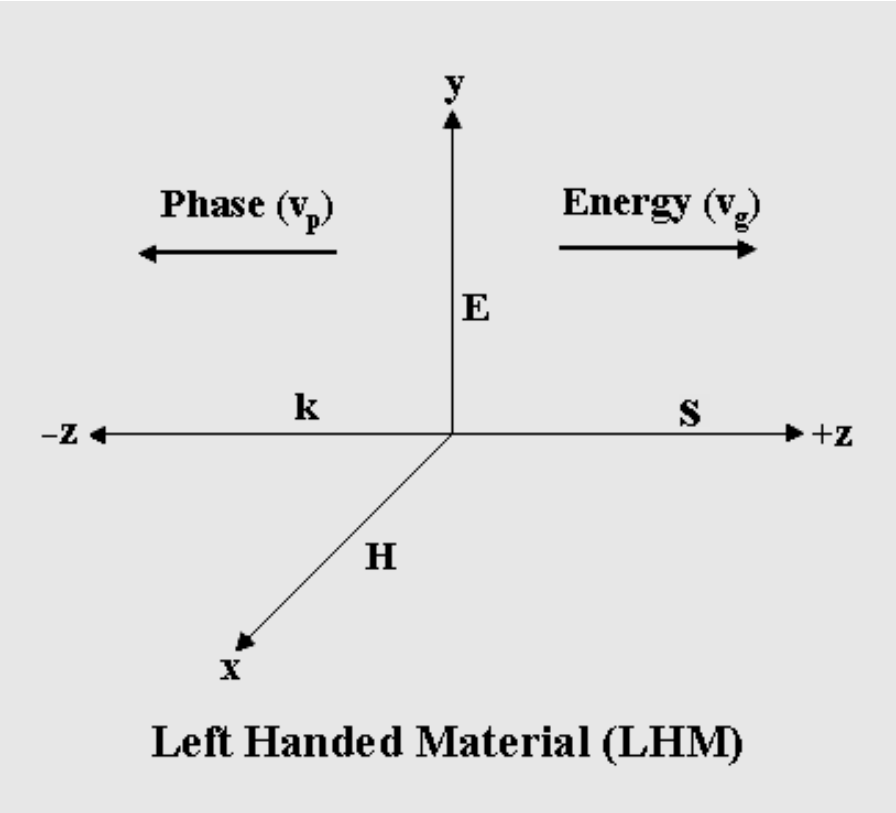

- RHM (Natural Materials)
- LHM (Metamaterial)

Plot of Constitutive Parameters

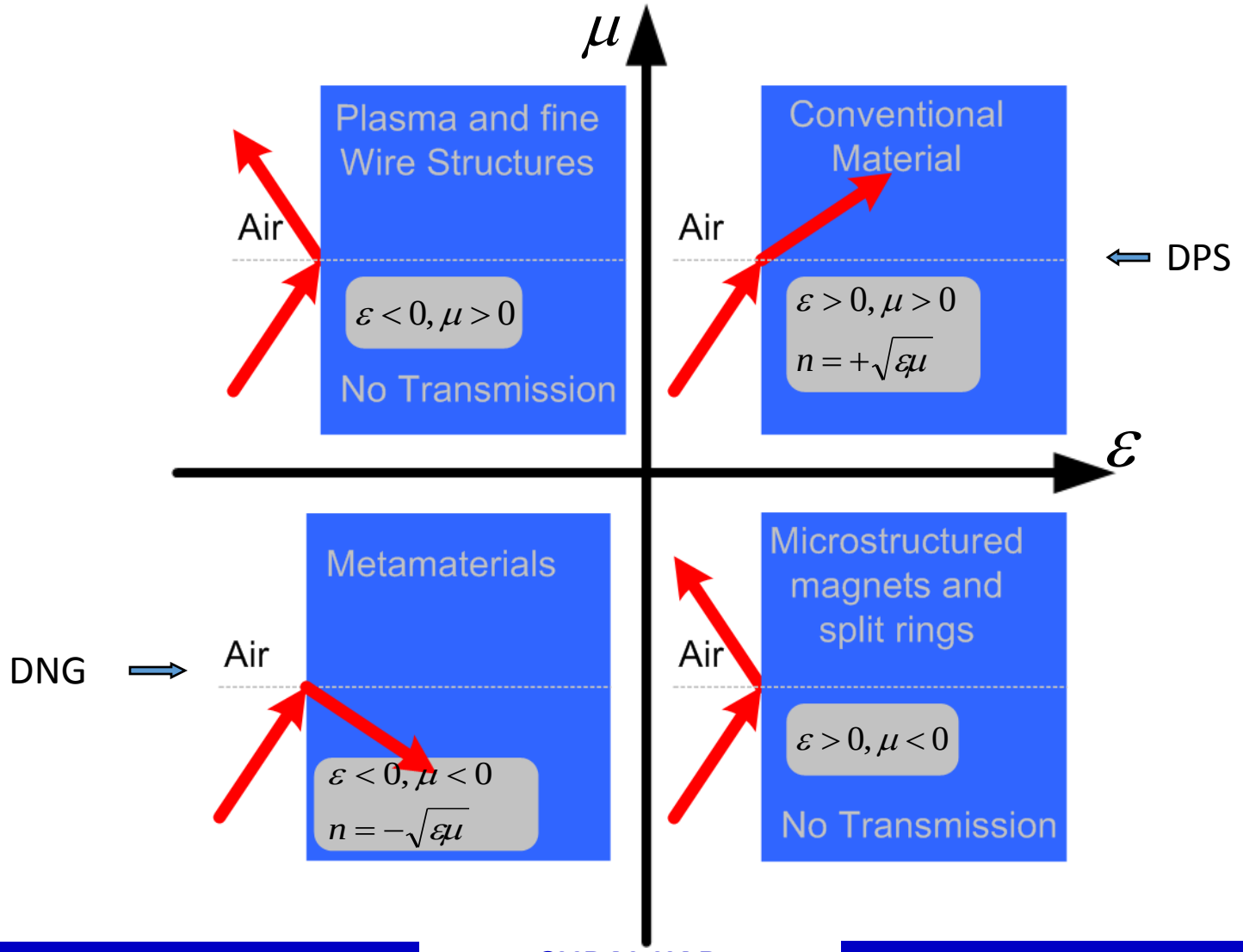

THE VISIONARIES

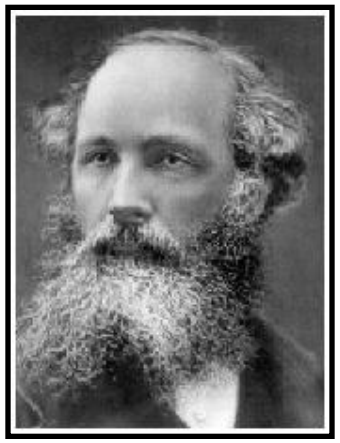

J. C. Maxwell

$$\nabla^2\Psi + n^2\frac{\omega^2}{c^2}\Psi = 0$$

$$n^2 = \varepsilon_r\mu_r$$

➢ *Maxwell's wave equation is equally valid for signal propagation both in case of RHM and LHM.*

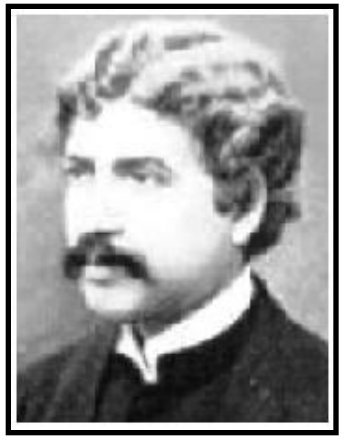

J. C. Bose

His research on twisted structures (1898) as polarizer was essentially artificial 'Chiral materials' we know in today's terminology.

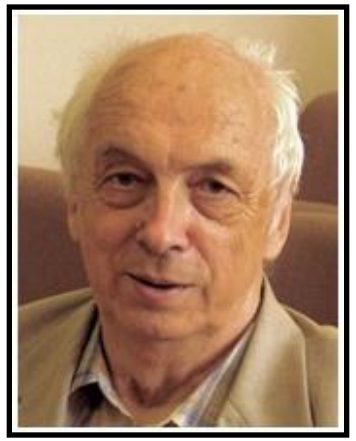

V. G. Veselago

His theoretical investigations indicated the reversibility of Snell's law, reversed Doppler effect, and reversal of Cherenkov radiation *for materials with ε and μ simultaneously negative.*

J. B. Pendry

***John Pendry made the real breakthrough*: showed the possibility for practically realizing the electric and magnetic plasma at microwave frequency using an array of thin metallic wires (1996) and an array of split-ring resonators (1999) respectively to realize negative ε_{reff} and negative μ_{reff} below the plasma frequency.**

Plasmonic Metamaterial

- First metamaterial developed at UCSD, U.S.A in 2000 was of plasmonic type.

- Negative permittivity realized with an array of metallic thin wires (TW), below its electric plasma frequency, and negative permeability with a matrix of C-shaped split-ring resonators (SRR), below its magnetic plasma frequency.

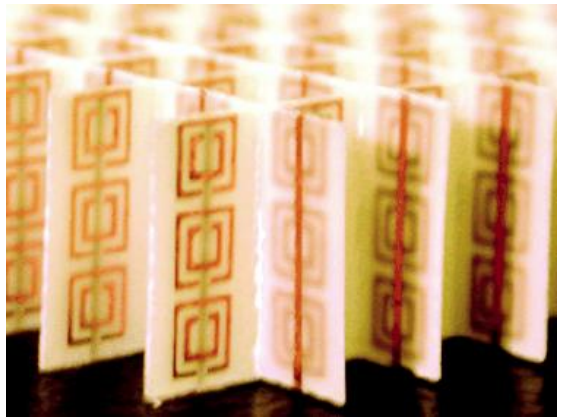

First metamaterial

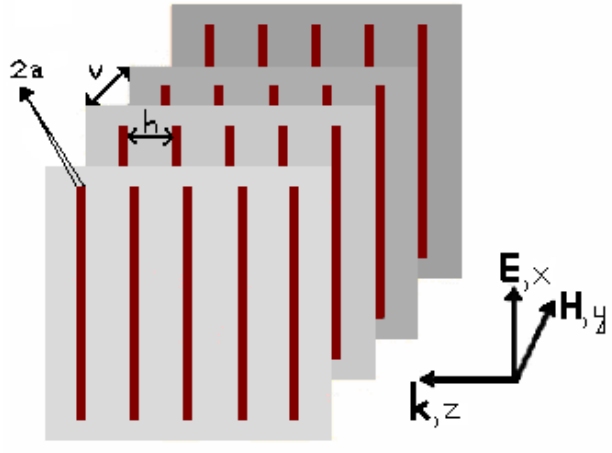

TW Array

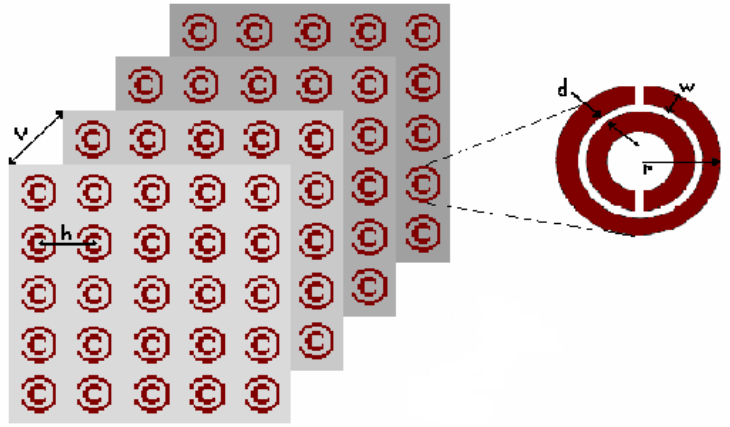

SRR Matrix

- *Each unit cell* in such periodic array of TW and SRR when irradiated with an e.m. signal *acts respectively as an 'electric atom' and 'magnetic atom' mimicking the atomic arrangements as in the lattice of natural material*.

Transmission Line Metamaterial

- Recognizing the analogy between the LH waves possible with the dual of the normal transmission line and similar backward wave already known to exist in periodic structures, Eleftheriades et. al, Olnier, and Caloz et. al almost simultaneously proposed in 2002 an alternative way to realize LHM property using transmission lines.

- The practical implementation *is done by periodically loading a host transmission line with series capacitance and shunt inductance*. Effective metamaterial property is realizable only when the *unit cell dimension (p) satisfies the condition*: $p << \lambda$.

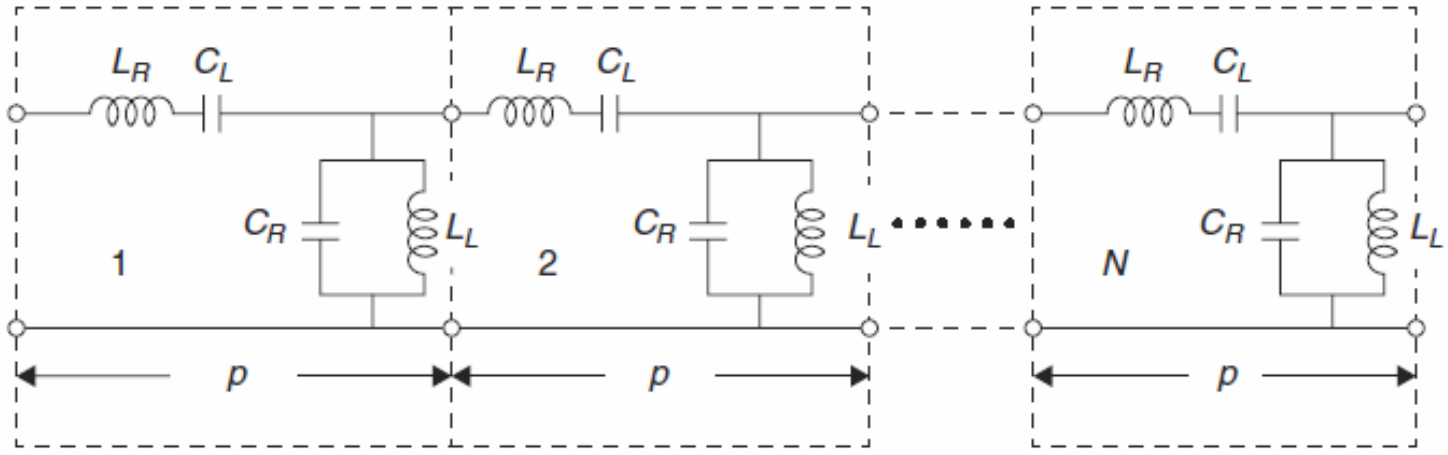

Transmission Line Metamaterial (contd…)

Parameters	β	Z_C	v_p	v_g	n
RHM 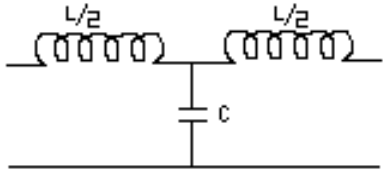	$\omega\sqrt{LC}$	$\sqrt{\frac{L}{C}}$	$\frac{1}{\sqrt{LC}}$	$\frac{1}{\sqrt{LC}}$	$\frac{\sqrt{LC}}{\sqrt{\mu_0\varepsilon_0}}$
LHM 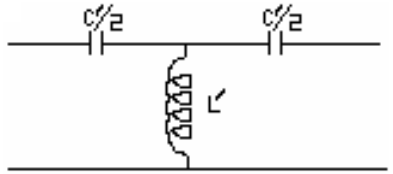	$-\frac{1}{\omega\sqrt{L'C'}}$	$\sqrt{\frac{L'}{C'}}$	$-\omega^2\sqrt{L'C'}$	$+\omega^2\sqrt{L'C'}$	$-\frac{1}{\omega^2\sqrt{L'C'\mu_0\varepsilon_0}}$

- For frequency dispersive ε and μ, from Poynting's theorem the expression for energy:

$$W = \frac{\partial(\varepsilon\omega)}{\partial\omega}|E|^2 + \frac{\partial(\mu\omega)}{\partial\omega}|H|^2$$

- Even when ε, μ < 0, their spectral derivatives remain positive. Hence, causality is not violated.

Transmission Line Metamaterial (contd…)

➢ Negative refraction at microwave frequency with PLTL was reported by G. V. Eleftheriades *et. al.* of the University of Toronto, Canada (2002).

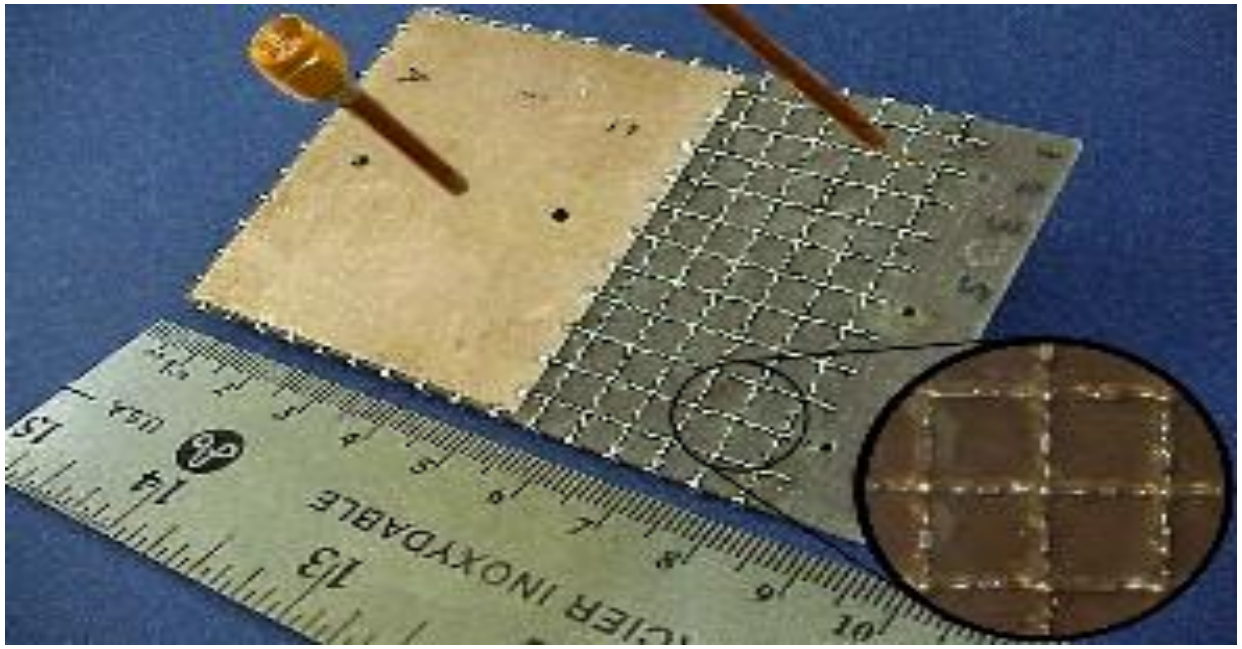

PLTL Metamaterial

➢ Being non-resonant , PLTL exhibit simultaneously low loss and broad bandwidth and are thus well suited for RF and microwave circuit applications.

Our Metamaterial Research—A Glimpse

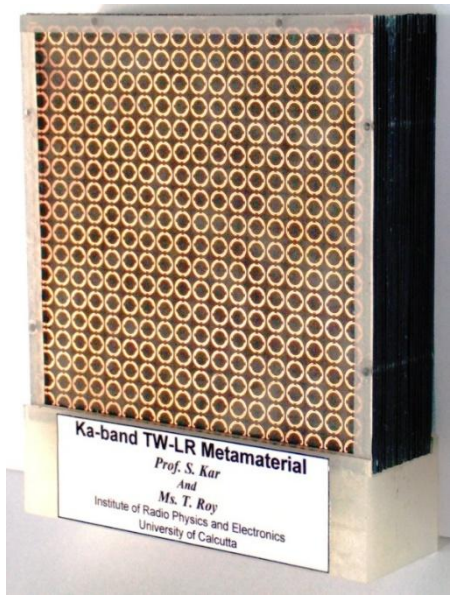

Plasmonic Metamatrial

{Showcased at the National Theme Meeting at BARC, Mumbai, on 17th August 2009}

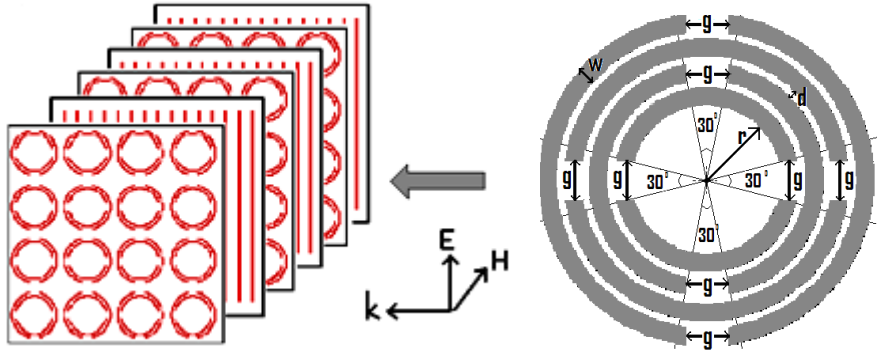

[Analytical Result: n = - 1.84 at 31.25 GHz]

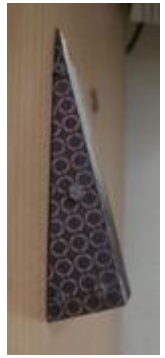

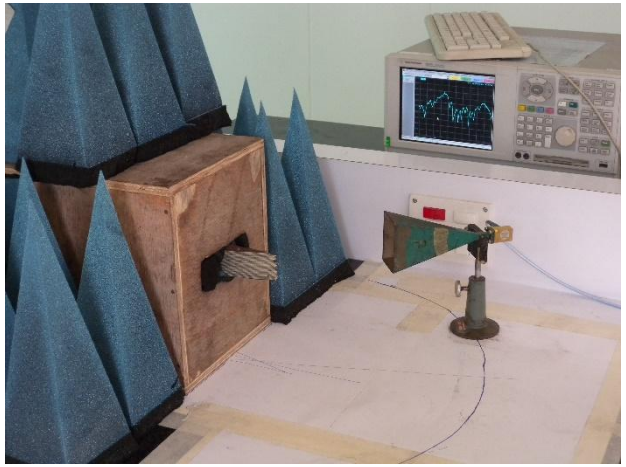

[Experimental Result: n = – 1.89 at 30.858 GHz]

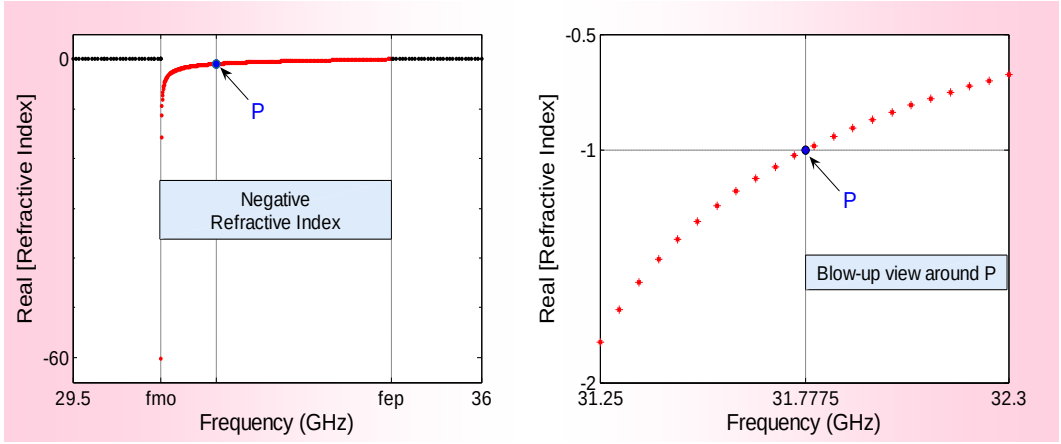

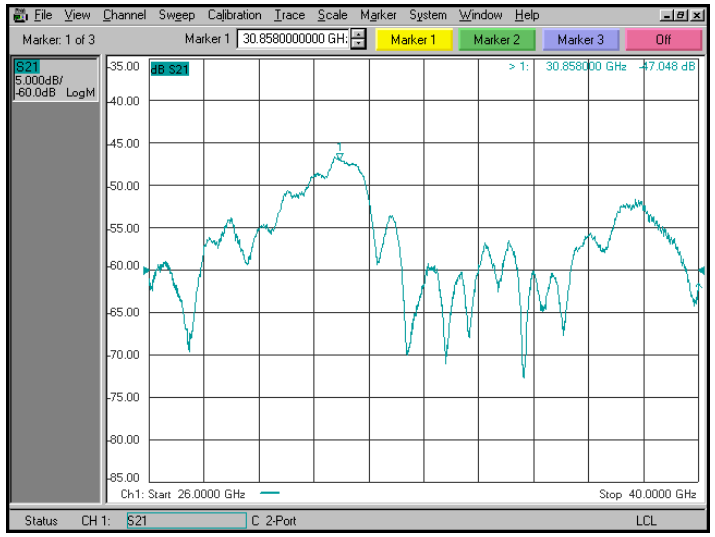

(Documented as on-line news article in *Nature* (India) on 20th August 2009)

[http://www.nature.com/nindia/2009/090820/full/nindia.2009.273.html]

Our Metamaterial Research—A Glimpse (contd …) [BPF]

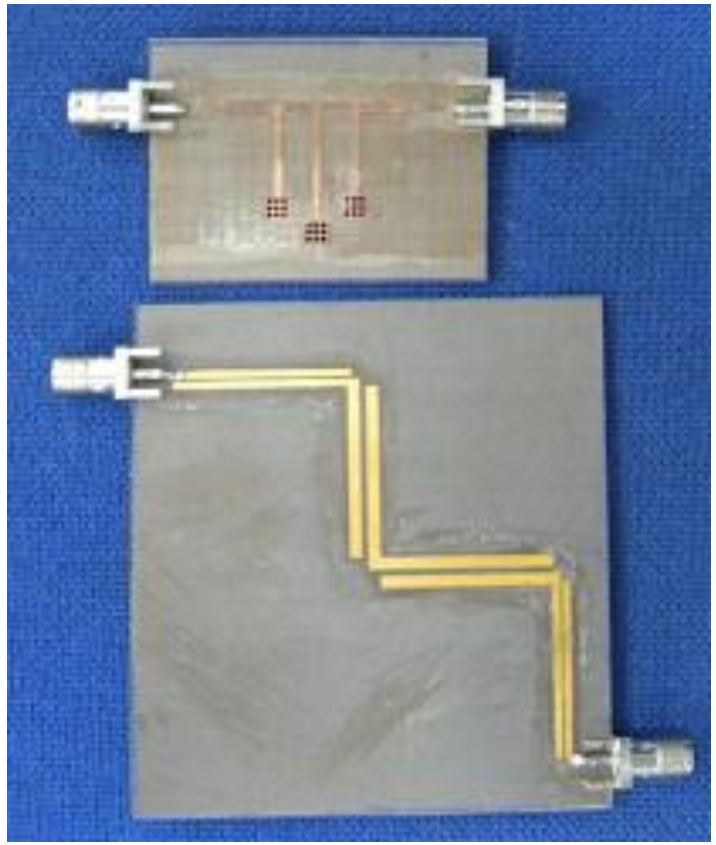

Comparison of fabricated CRLH and conventional edge-coupled BPF at 2.45GHz (67% Size reduction)

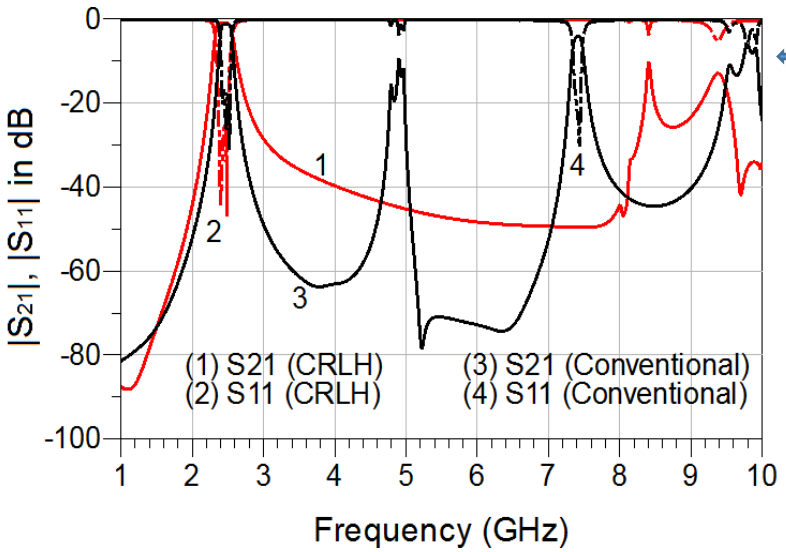

Simulated performance Ch.

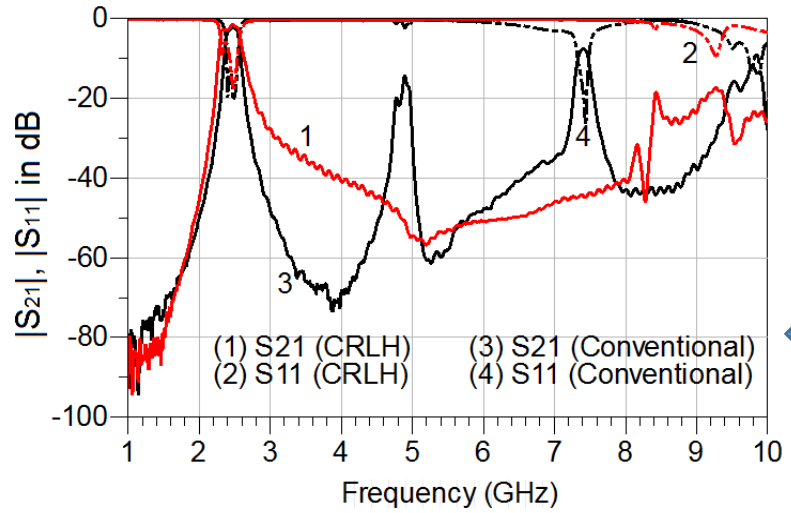

Measured performance Ch.

FILTER PERFORMANCE COMPARISON

Property	CRLH BPF	Edge coupled BPF
Insertion Loss	**1.6dB**	2.3dB
Return Loss	15dB	18dB
Harmonics	**Suppressed up to 10GHz**	2nd , 3rd etc.
Size	**4.3cm x 3cm**	6.5cm x 6cm

Our Metamaterial Research—A Glimpse (contd …) [Patch Antenna]

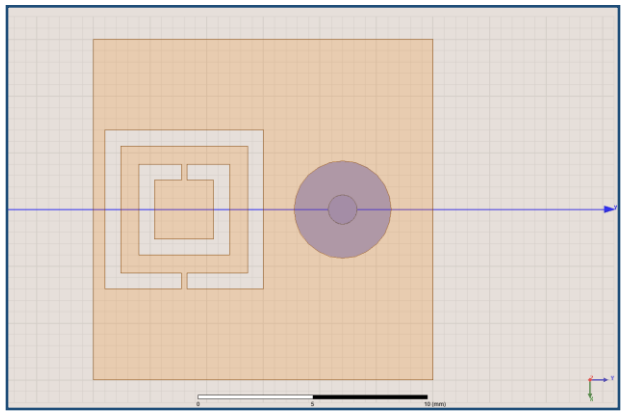

CSRR loaded patch

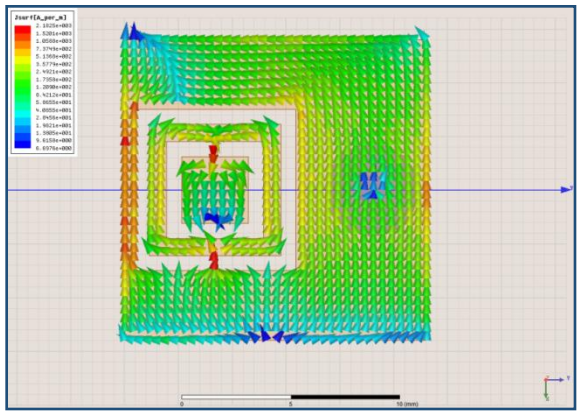

Surface current lines

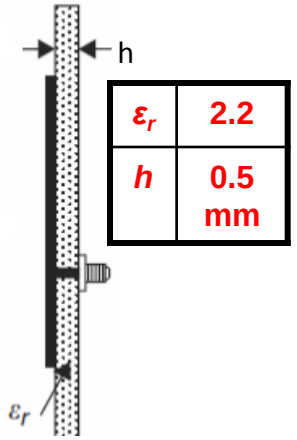

ε_r	2.2
h	0.5 mm

Fabricated structures: 24% Size Miniaturization

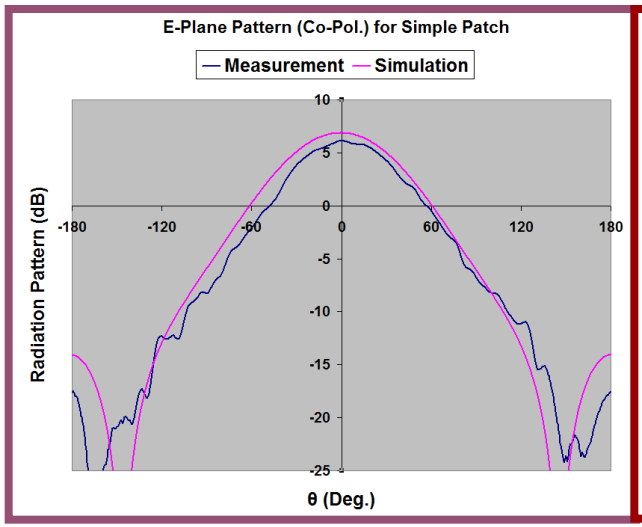

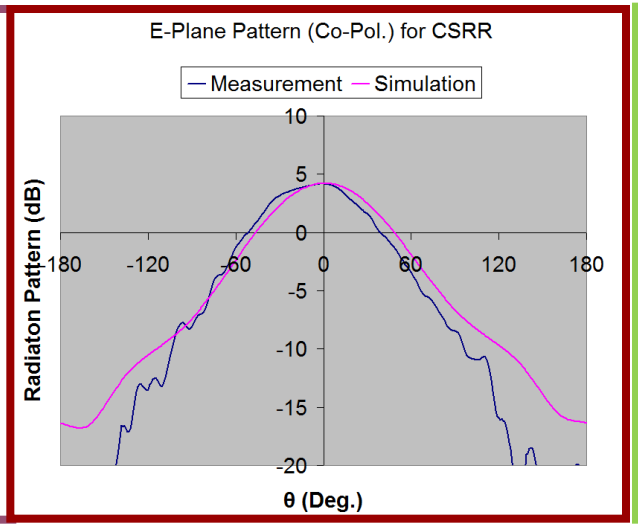

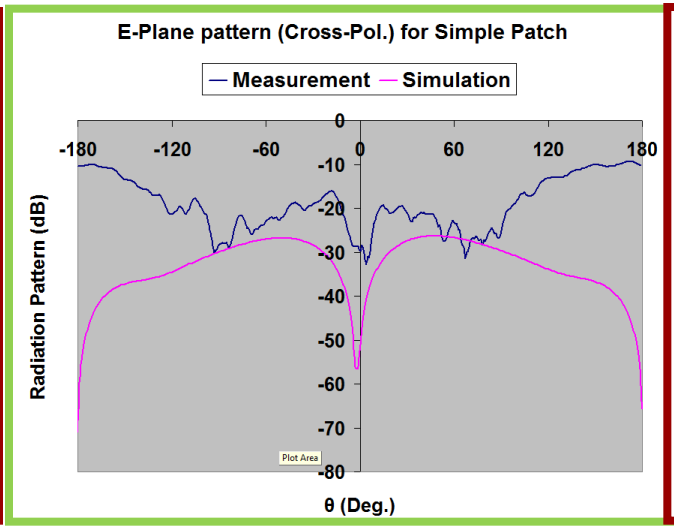

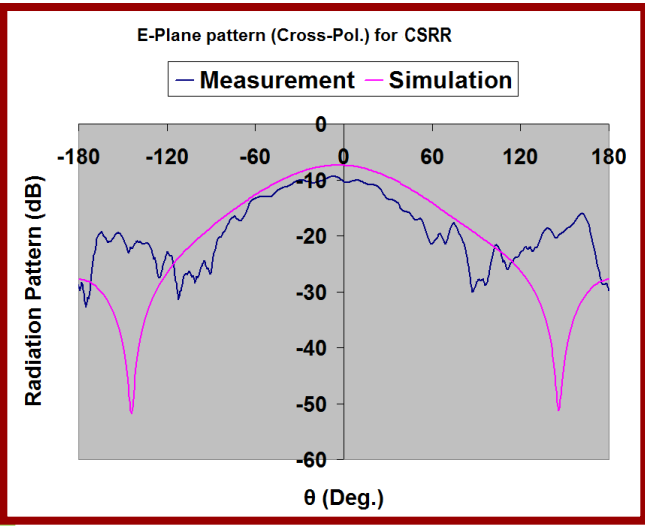

Variants of Split Ring Resonators (SRR)

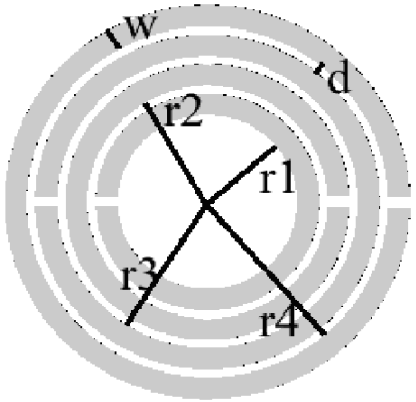

MSRR

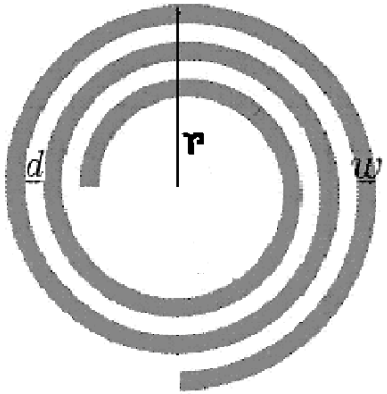

SR

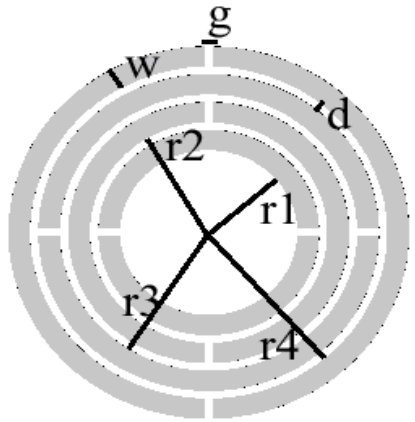

LR

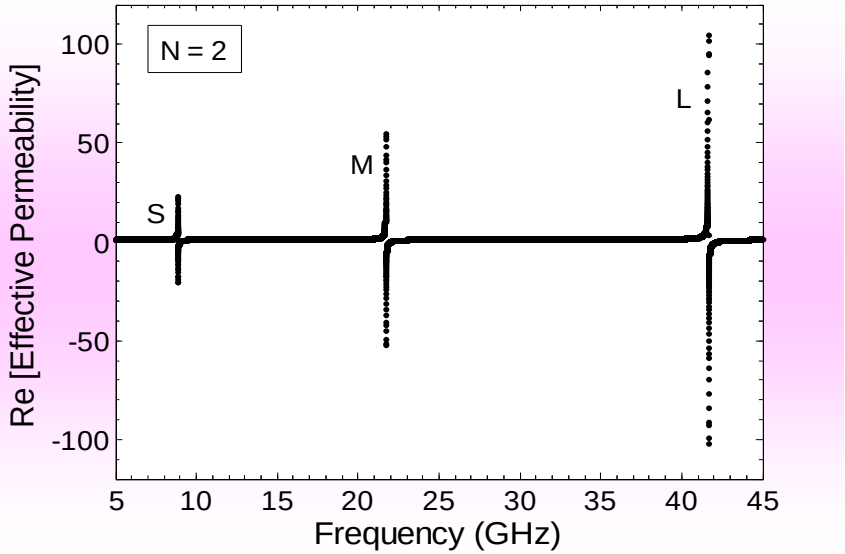

r and Δf at f_{m0} = 41.649 GHz

Structure type	r (mm)	Δf (GHz)
LR	1.000	0.670
MSRR	0.648	0.278
SR	0.357	0.081

Variants of SR: TTSR and NBSR

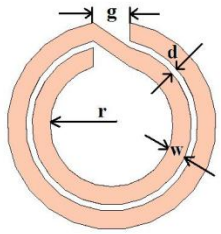

TTSR

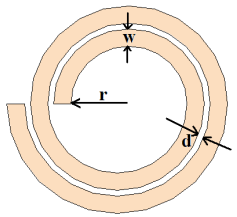

SR

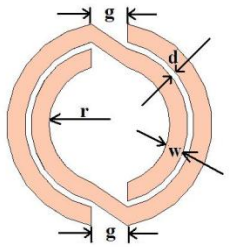

NBSR

Analytical Result ⇨

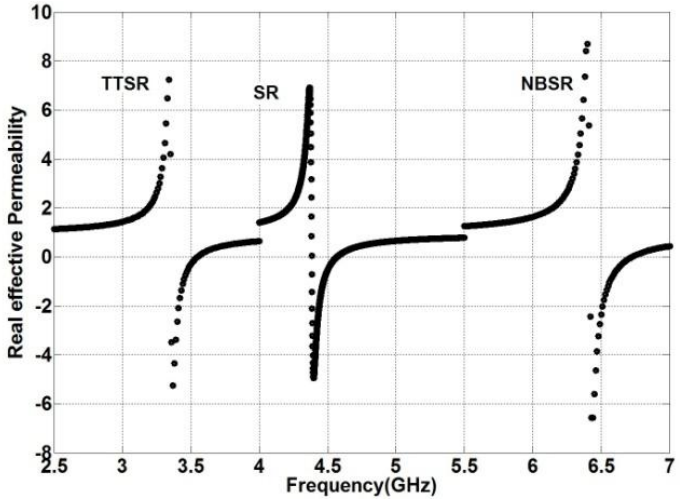

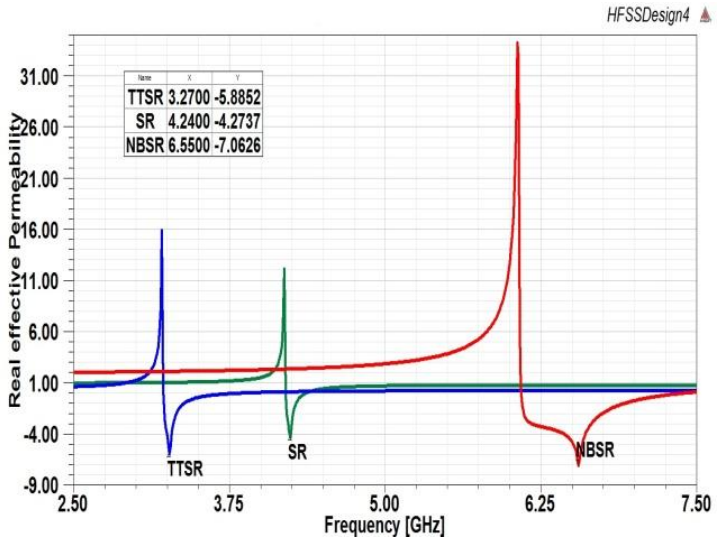

⇦ HFSS Simulation Result

TTSR ⇨

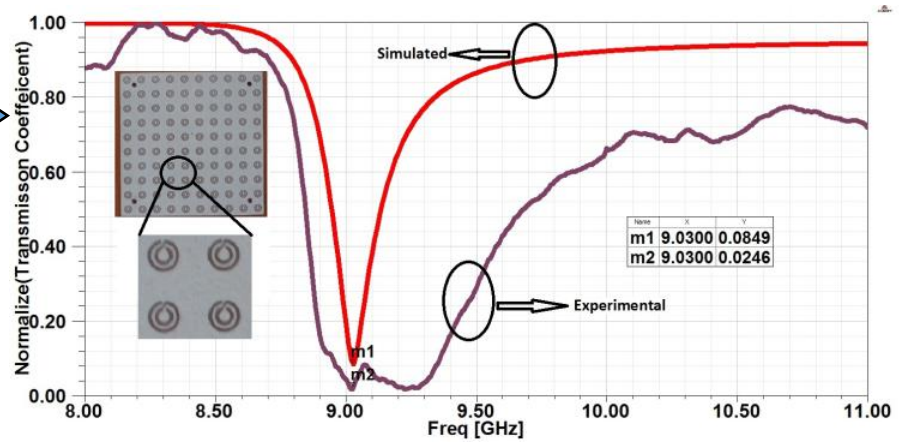

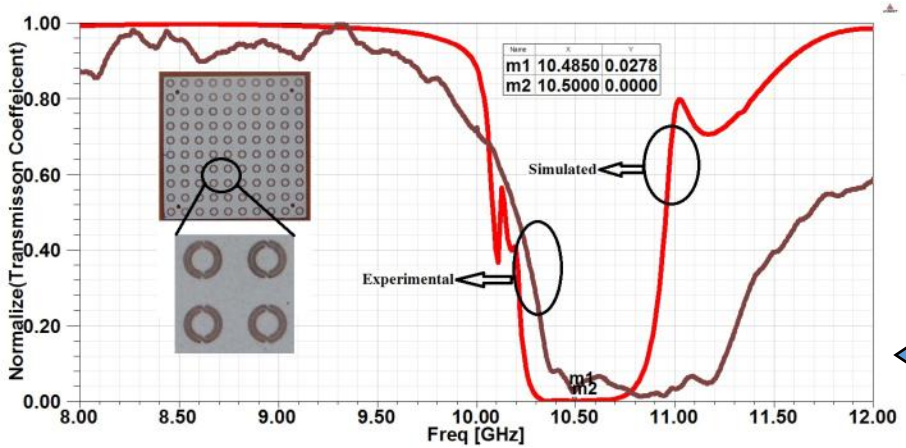

⇦ NBSR

Plasma Frequency of Wire Media

Analytical Method

$$f_p{}^2 = \frac{c_0{}^2}{2\pi sa\left[\frac{\int_0^{\frac{a}{2}} ln\left[\frac{\frac{s}{2}{}^2+y^2}{r_0(2\sqrt{\frac{s}{2}{}^2+y^2}-r_0}\right]dy}{a} + \frac{\int_0^{\frac{s}{2}} ln\left[\frac{\frac{a}{2}{}^2+y^2}{r_0(2\sqrt{\frac{a}{2}{}^2+y^2}-r_0}\right]dy}{s}\right]}$$

Loss factor Method

$$k = \frac{PowerLost}{PowerEntered} = \frac{1-|S_{11}|^2-|S_{21}|^2}{1-|S_{11}|^2}$$

$$\epsilon_{eff} = 1 - \frac{f_p{}^2}{f^2+2i\gamma f}$$

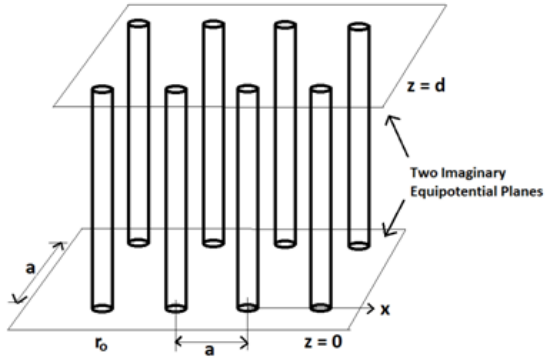

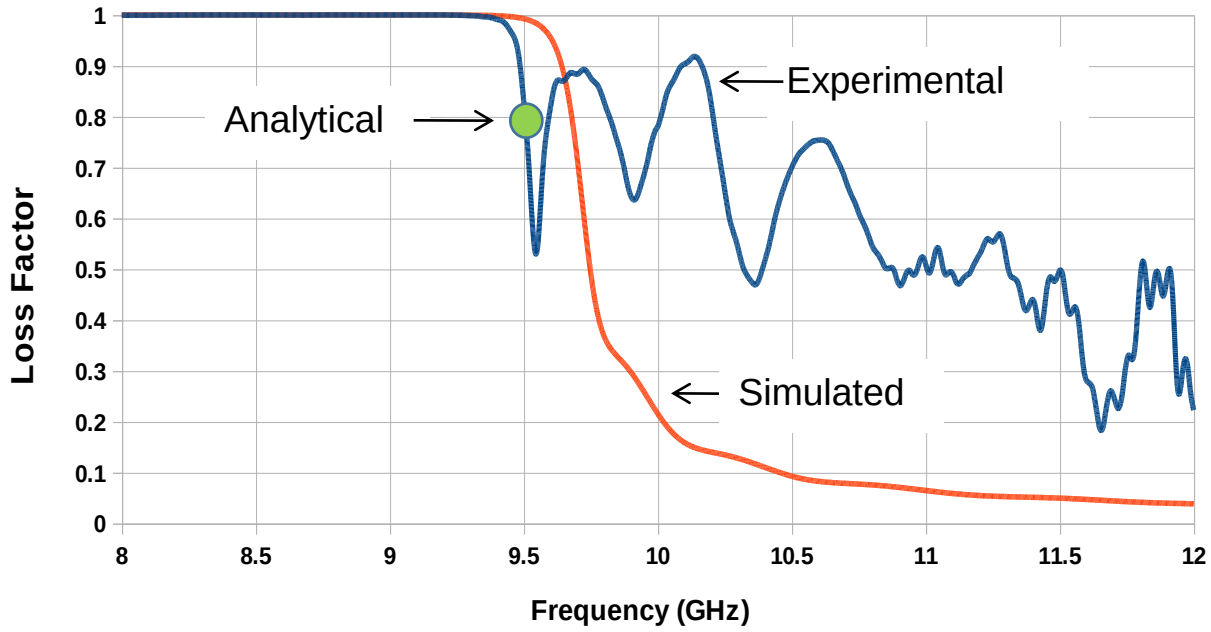

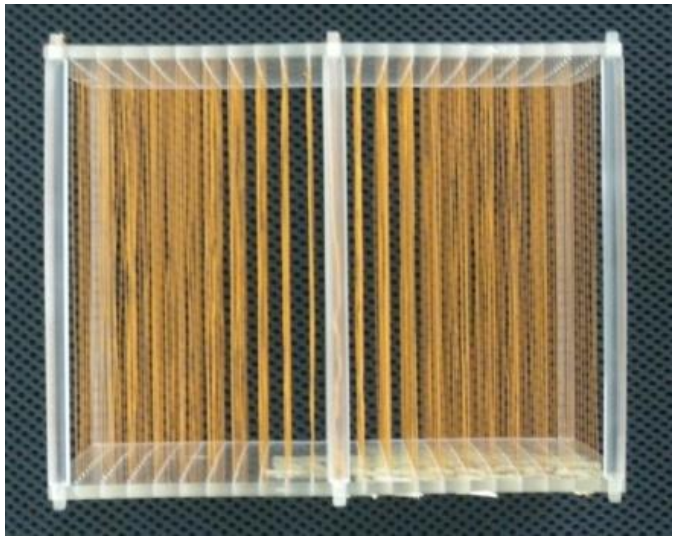

Fabricated Wire Media

Our Metamaterial Research—A Glimpse (contd …) [Assorted]

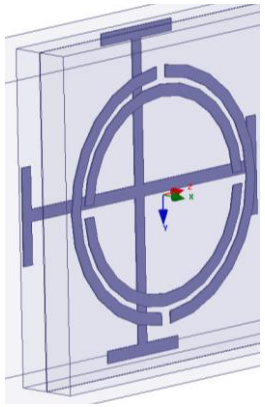

LR-CUTWIRE

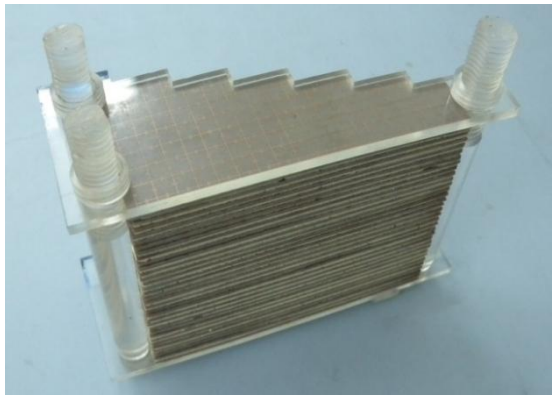

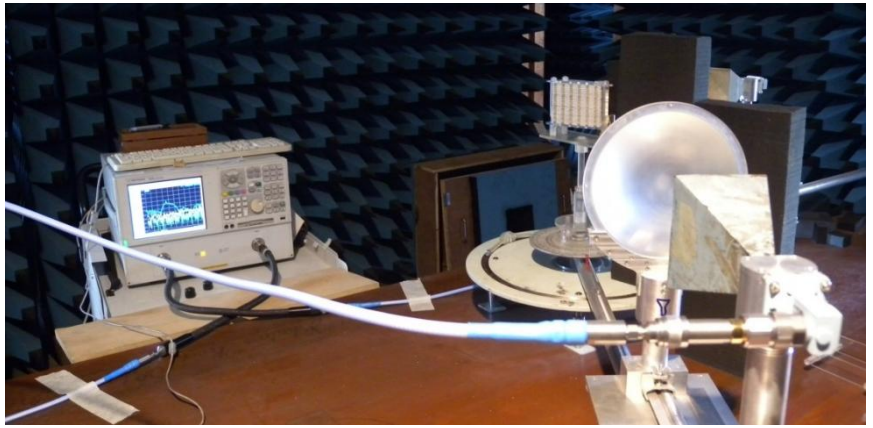

n = -1.68

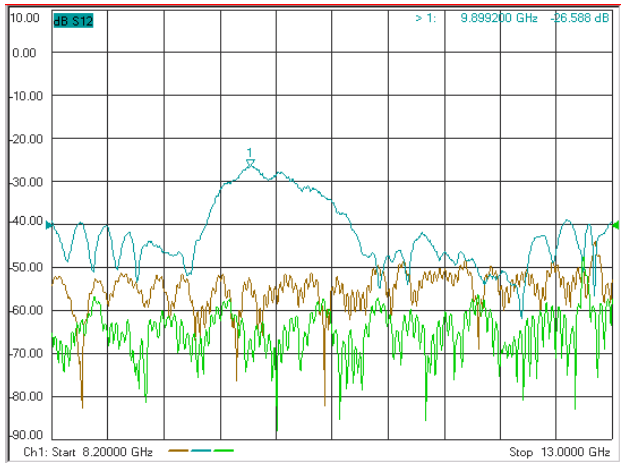

n = -1.76

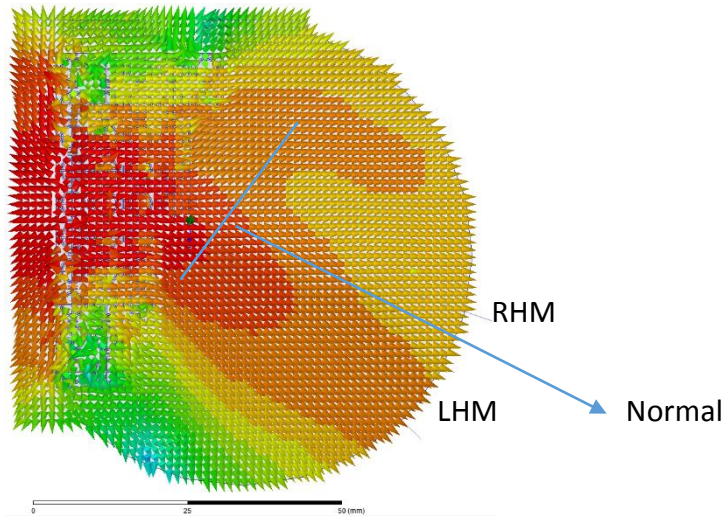

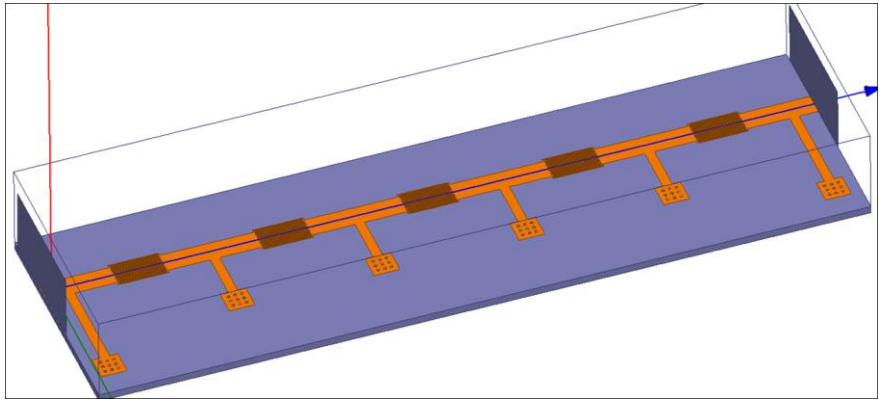

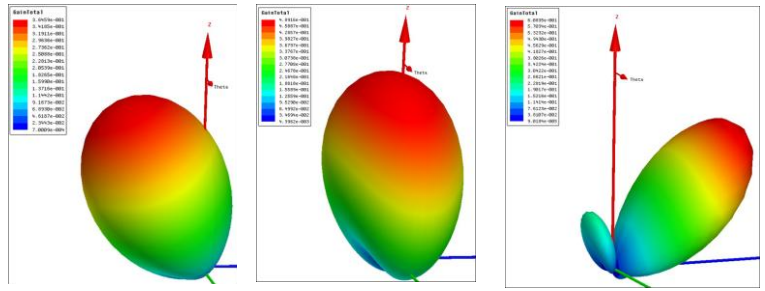

Leaky-wave PLTL Antenna

Exotic Application Potential of Metamaterial

- 'Super-lens/Sub-wavelength imaging' overcoming the well known *diffraction limit* of conventional optics supposed to be possible due to *evanescent wave growth* in LH media is gaining enough enthusiasm which might one day make it possible to image individual strands of DNA.

- 'Cloaking' of objects (may not be of the Harry Potter type at the moment) opening up the possibility of making reliable optical memories for new generation computers and showing new avenues for stealth technology.

- 'Reversed Cherencov radiation' possible with metamaterial based accelerator might revolutionize future accelerator research.

Super-lens and Sub-wavelength Imaging

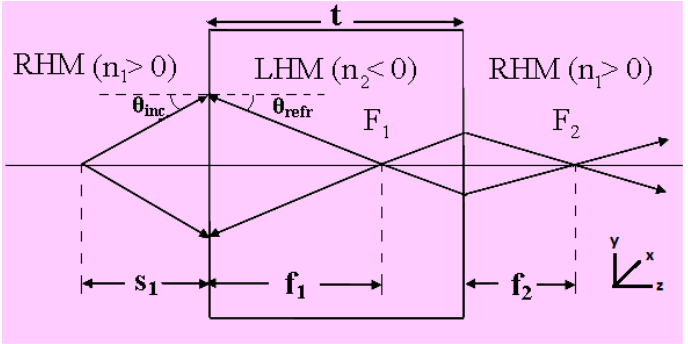

Metamaterial plane-slab can focus an object point to the image point with double focusing effect caused by negative refraction.

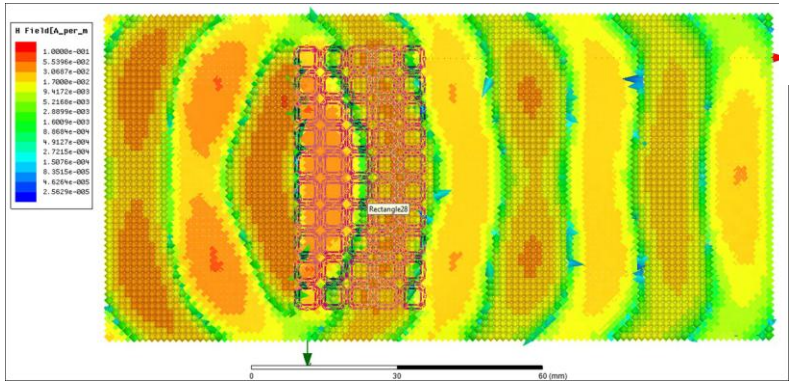

Focusing with TW-LR metamaterial

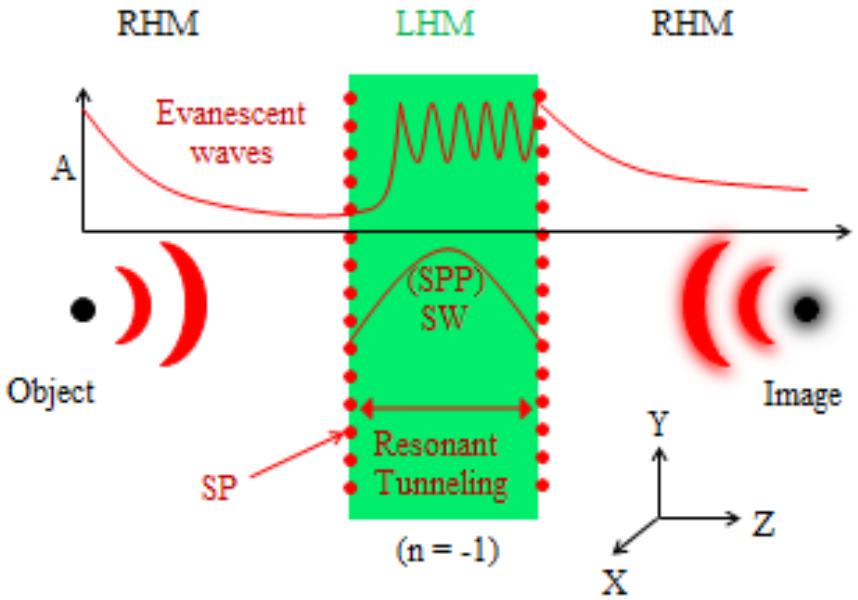

Presence and coupling of surface plasmon polariton waves in RHM-LHM interface of plasmonic metamaterial causes ***evanescent wave growth***.

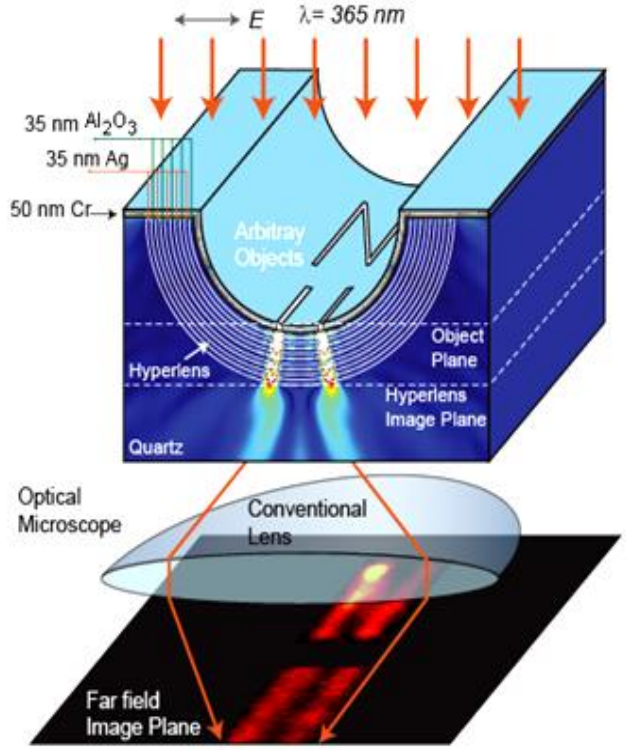

Hyper Lens based on the diffraction free super-lens capability it is able to magnify sub-diffraction limited objects and project the magnified images to the far field with conventional lens. Possible application in nanotechnology photolithography.

Cloaking and Stealth Technology

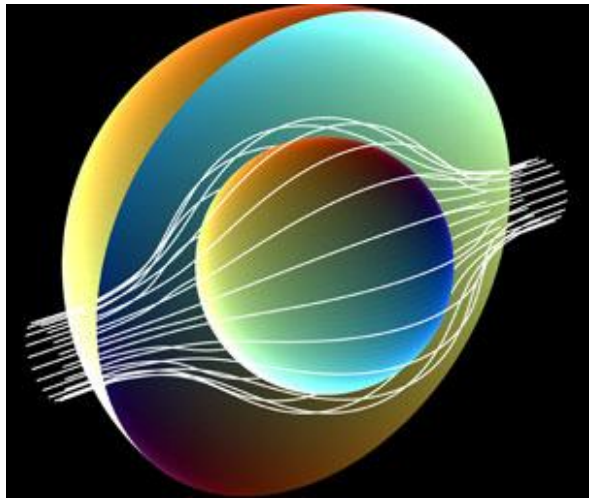

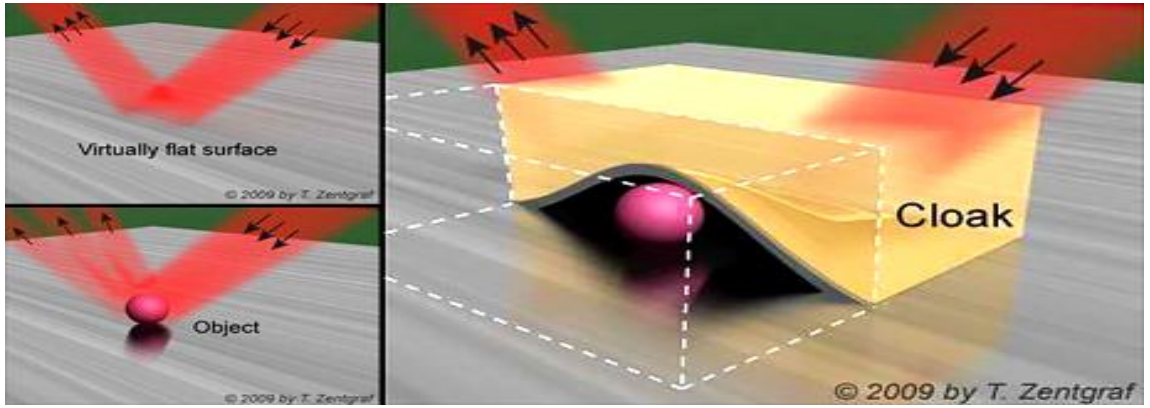

Among the many tropes found in science-fiction and fantasy, few are more popular than the cloaking device -- We are familiar with the Harry Potter's invisibility cloak. The metamaterial for cloaking was designed to have graded refractive index. **The trick is to bend the wave *subtly around the device and able to reform on the other side.***

The cloaking device ***at microwave frequency*** consisted of a group of concentric circles made of metamaterial (loops of copper wire stamped on fiber glass) with a cylindrical gap in the middle where the object to be cloaked was placed. This device could mask or make the object invisible from only one wavelength of the incident microwave signal. ***The device was not perfect causing shadowing of microwaves, i.e., distortions.***

An object covered with a piece of cloth would normally be detectable based on its telltale bump, but with metamaterial covering even the bump seems to vanish. This ***carpet cloaking*** system ***was operated in near infrared frequency and scalable to visible light -- capable of hiding microscopic objects.***

Reversed Cherencov Radiation

Argonne Wakefield Accelerator Group, Argonne, Illinois Institute of Technology, Chicago, has made experimental studies on metamaterial loaded waveguides for possible accelerator applications at X-band.

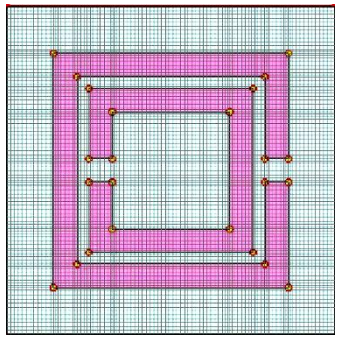

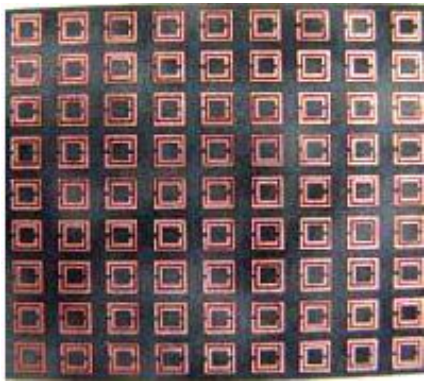

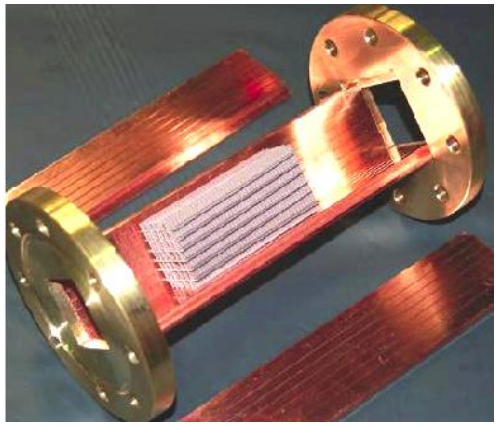

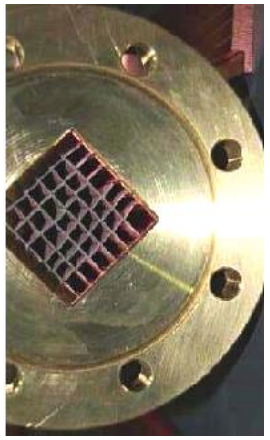

Waveguide Loaded with SRR Array

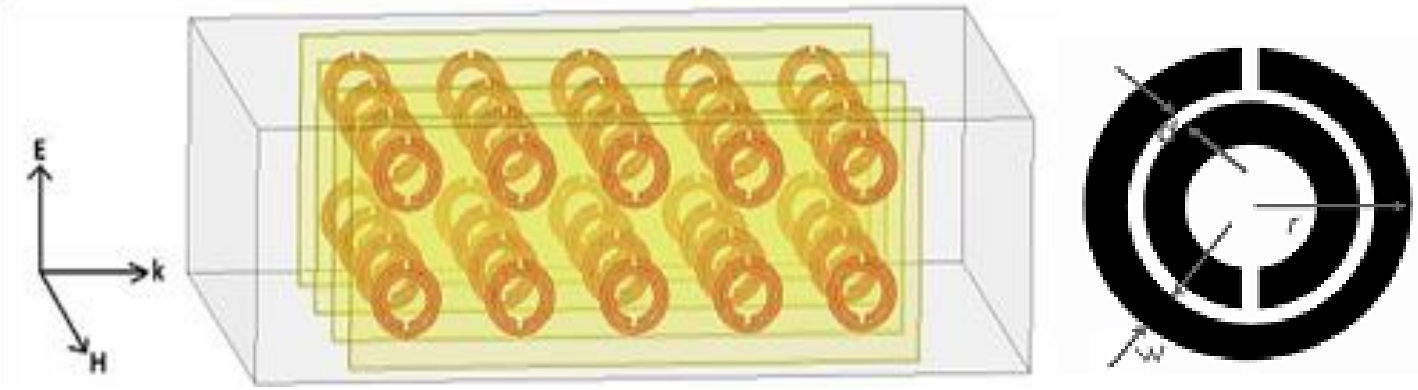

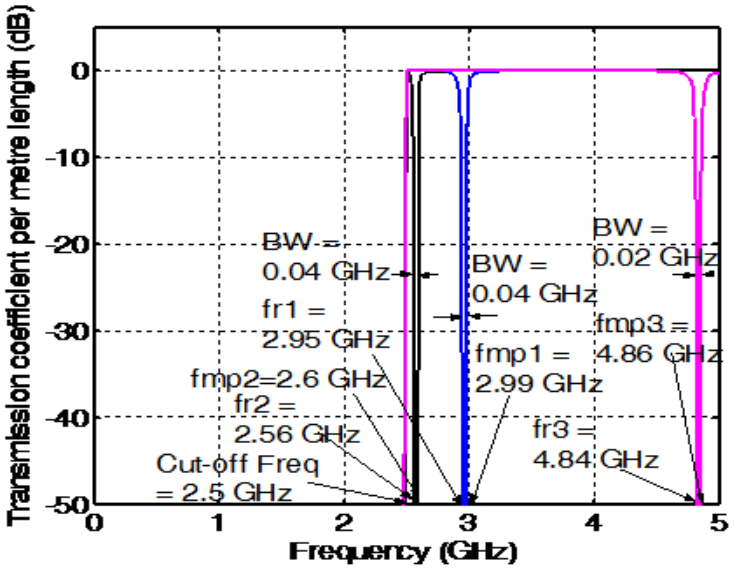

Transmission coefficient vs frequency showing LHM stop-band

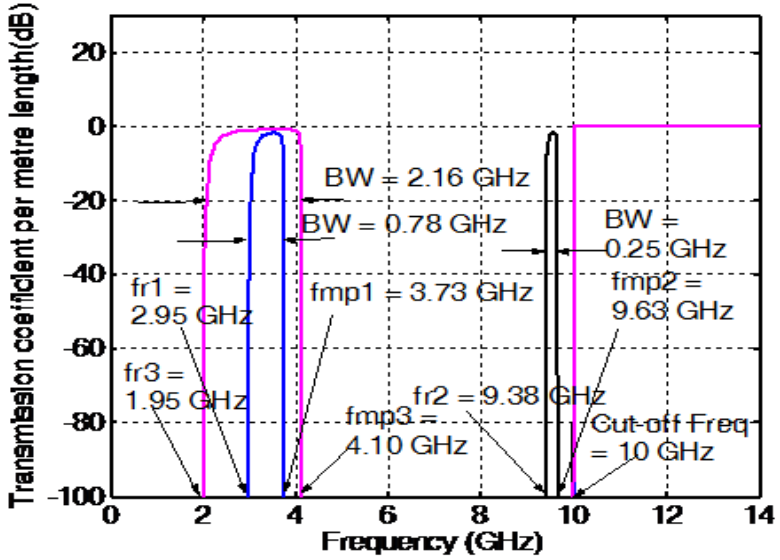

Transmission coefficient vs frequency showing LHM pass-band

Metamaterial Application for Absorbers

- Absorbers at microwave frequency are required in bolometers, anechoic chamber, stealth purposes for defense applications and so on; in solar cells such absorbers are also used to absorb solar energy. Conventional absorbers are carbon-foam or ferrite based but are either thick or bulky in nature.

- Metamaterial absorbers are designed in such a way so that it offers input impedance equal to the impedance of free space and limiting the reflections from the absorber structure. Since metamaterial absorbers are capable to offer ultra-thin thickness, conformal properties and compactness, it attracts the researchers and are practically the best suited substitute for conventional absorbers.

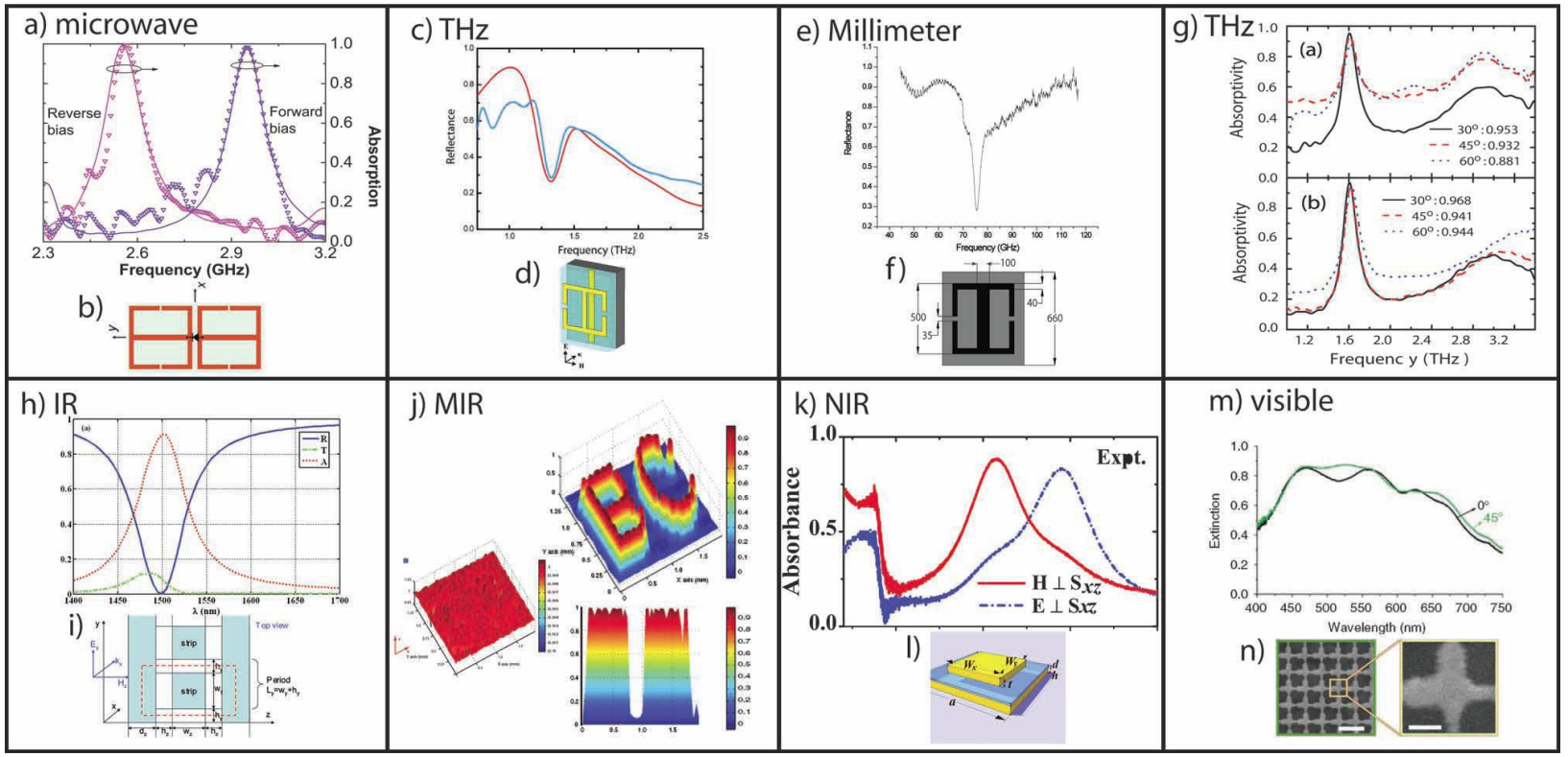

Photonic Metamaterial

- The photonic metamaterial (i.e. metamaterial designed to operate at optical frequency) demands a different set of electric and magnetic inclusions (artificial atoms) compared to those used at microwave to terahertz frequency.

- The ubiquitous Split-Ring metmolecule can be scaled down in size up to about 200 THz, but this scaling breaks down at higher frequencies as the metal does not behave any more as a conductor and becomes transparent to the radiation for wavelengths shorter than 1.5 µm i.e beyond 200 THz range. Along with this the fabrication difficulties of making nano-meter scale SRRs along with metal wires (SRR-TW combination) led to the development of alternative designs that are more suitable at optical frequencies.

- In the optical frequency regime ***cut-wire*** and ***fish-net*** structures are used to realize metamaterial property.

MHz – THz Metamaterial

21 MHz

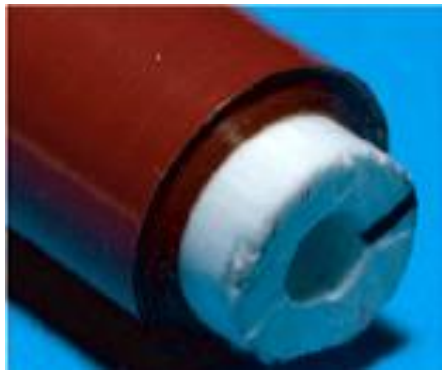

Wiltshire et. al., UK, 2001

5 GHz

Shelby et. al., USA, 2000

100 GHz

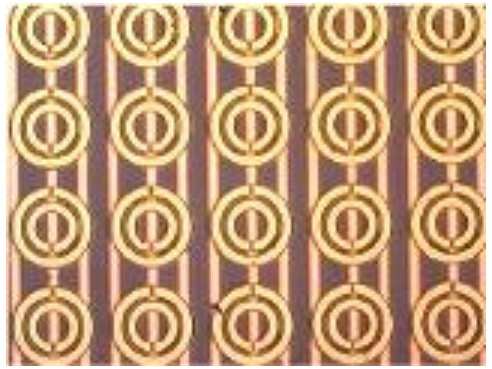

Gokkavas et. al., Turkey, 2006

1 THz

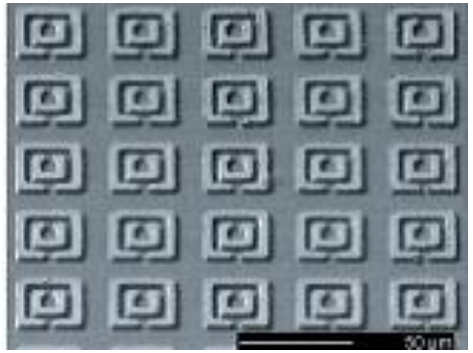

Yen et. al., USA, 2004

100 THz

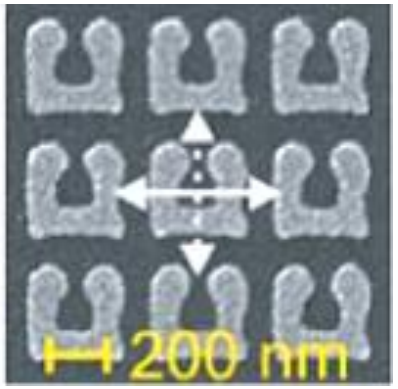

Linden et. al., Germany, 2004

200 THz

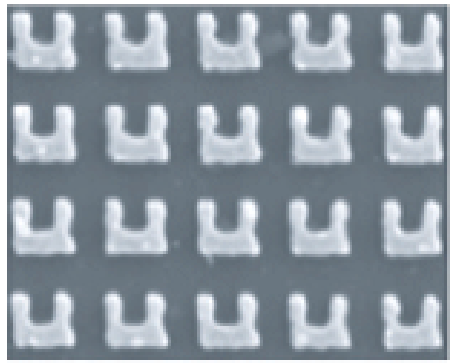

Enkrich et. al., Germany, 2005

Alternative Designs for Photonic Metamaterial

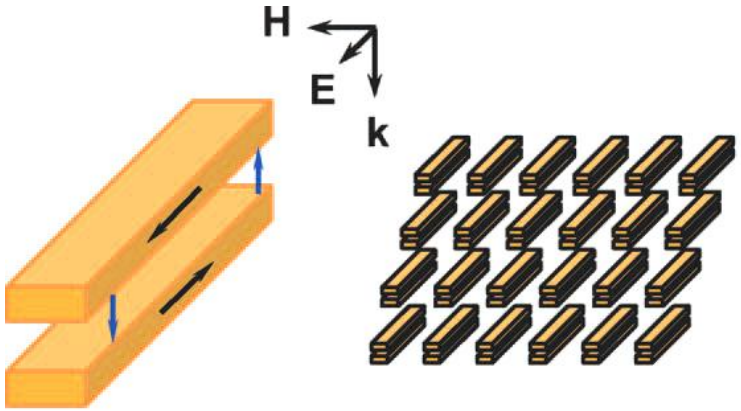

Cut-Wires: Pairs of metal nano-strips separated by dielectric spacer. Anti-parallel current flow in the pair results in magnetic resonance. Parallel current flow in the same strip causes electric resonance. Difficult to get overlapping ε<0 and μ<0 zones.

[Shalaev et. al., USA, 2005]

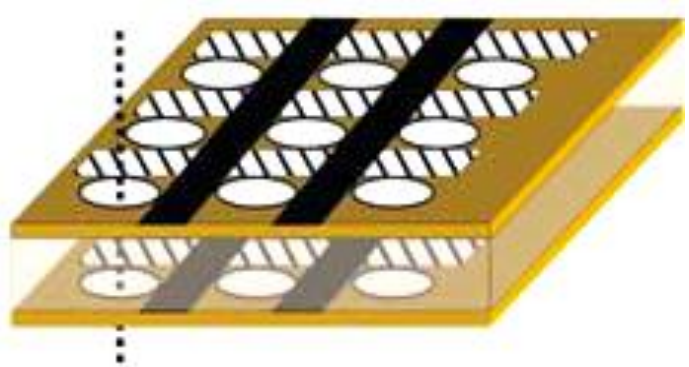

Fishnet: Combines magnetic coupled strips (to provide μ<0) with continuous electric strips (to provide ε<0) over a broad spectrum. Hence overlapping frequency zone for simultaneously negative ε and μ is easily obtained at optical frequency.

[S. Zhang et. al., USA, 2005]

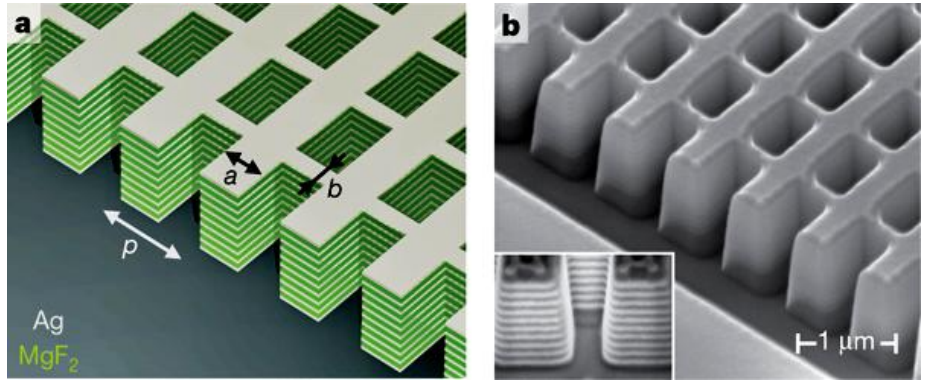

August 2008 the University of California, Berkeley engineered 3-D optical fishnet metamaterial by using *focused ion-beam* (FIB) milling.The RI varies from $n \approx 0.63$ at 1,200 nm to $n \approx -1.23$ at 1,775 nm.

Alternating layers of 30 nm Ag and 50 nm MgF_2 were stacked together nanoscale-sized fishnet patterns were cut into the layers.

METAMATERIAL
IN PHOTONIC DEVELOPMENTS

Metamaterial in Photonic Developments

- Metamaterial was considered to be 'material like' (i.e. one with tailorable constitutive properties), during the initial phase of metamaterial research.

- A paradigm shift in metamaterial research philosophy has taken place subsequently and metamaterial is now considered as a 'device': where the hybridization with functional agents brings new functionality and the response becomes gain-assisted, non-linear, switchable and so forth.

- Thus we now have '***metamaterial-fueled lasing spaser':*** in which the emission in a spaser is fueled with the plasmonic excitations in an array of coherently emitting metamolecules. '***Metamaterial based carbon nanotube' :*** that exhibits an order-of-magnitude higher non-linearity compared to bare CNT leading to high speed switching possible at optical frequency. '***Transparent metamaterial':*** made entirely of dielectric materials, might make possible for interconnecting circuits using photon instead of electrons to process and transmit data and also paving way for light sources at the single photon level.

Metamaterial-fueled Lasing Spaser

- The invention of the spaser (Surface Plasmon Amplification Stimulated Emission of Radiation), also called plasmonic laser, led to the development of thinnest possible laser. Here the light quanta—photons—of the laser is being replaced with electronic excitations at the surface of metals called surface plasmons, which can have atomic-scale dimensions. However, a spaser produces very little light and that light is not collimated into a narrow beam.

- But if the emission can be fueled by plasmonic excitations in an array of coherently emitting metamolecules (SRRs) supported by a gain medium (quantum-dot-doped dielectric), which can overcome the radiation losses and Joule losses in the metal structure of the metamolecules , we have the "lasing spaser". In contrast to conventional lasers that operate at wavelengths of suitable natural atomic or molecular transitions, the lasing spaser's emission wavelength can be controlled by metamolecule design.

- Being the thinnest (~100 nm) laser, the lasing spaser promises new applications ranging from displays to high speed communications and beyond.

Metamaterial-Feuled Lasing Spaser (contd …)

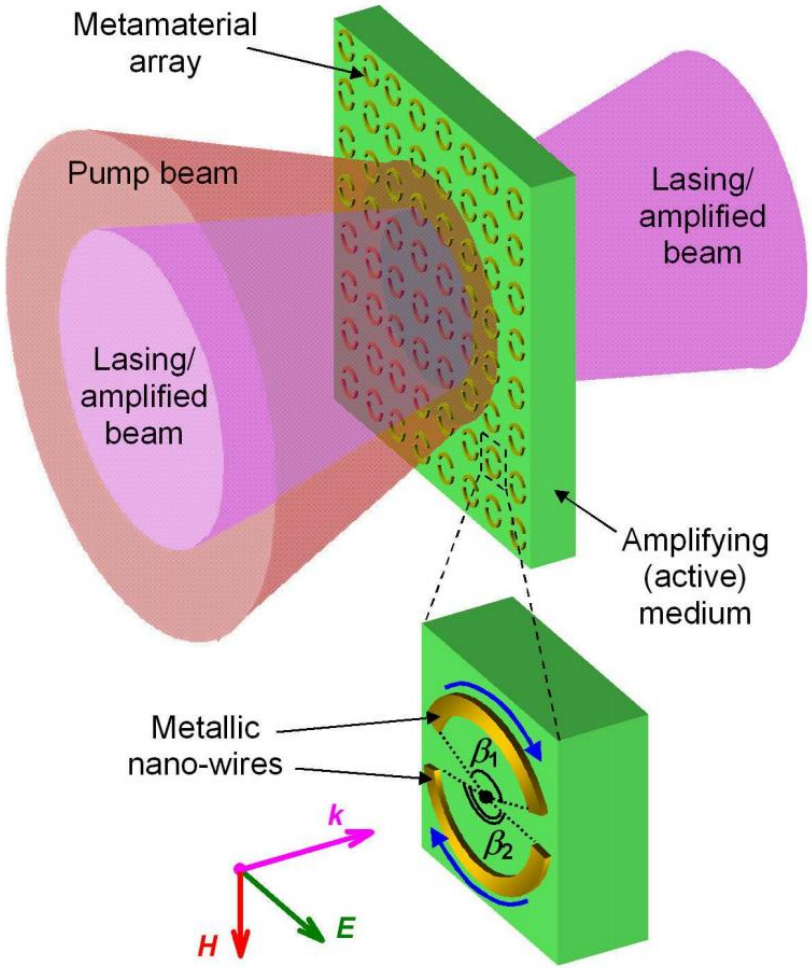

Lasing Spaser

- In the lasing spaser, identical plasmonic resonators (forming the metamaterial array) impose the frequency at which the device will lase; drawing energy from a supporting gain substrate.
- This combination of artificial classical electromagnetic resonators plays the role of the active medium in the lasing spaser, just as an assembly of essentially quantum inversely populated atoms plays the same role in a conventional laser.
- In a conventional laser the direction of emission is dictated by the external resonator, and its coherence is underpinned by the stimulated emission of atoms in the gain medium.
- In the lasing spaser the direction of emission is normal to the plane of the array, where strong trapped-mode currents in the plasmonic resonators oscillate in phase.

Metamaterial-based Carbon nanotube (CNT)

- CNTs are one-dimensional systems, with diameter of a few nanometers and length on the micron scale with unique non-linear optical properties. Single-walled CNTs rolled from a graphene sheet are direct gap semiconductors with absorption spectra dominated by exciton lines. Possible technological uses include nanoscale light sources, photodetectors, and photovoltaic devices.

- Indeed, the development of nanophotonic all-optical data processing circuits depends on the availability of fast and highly responsive nonlinear media that react to light by changing their refractive index and absorption. This is difficult to deliver in nanoscale size devices using electronic or molecular nonlinearities, where stronger responses often come at the expense of longer reaction times and where the optical path through the nonlinear medium is shorter than the wavelength of light.

- Recent experiments show that the nonlinear response of CNT can be strongly enhanced by adding a metamaterial layer. Single-wall semiconductor carbon nanotubes deposited on metamaterials exhibit an order-of-magnitude higher nonlinearity than the existing strong non-linear response of the nanotubes themselves, due to a resonant plasmon-exciton interaction making ultra-high speed switching possible at optical frequency. Also, the metamaterial environment allows one to spectrally tailor the nonlinear response.

Metamaterial-based Carbon nanotube (CNT)

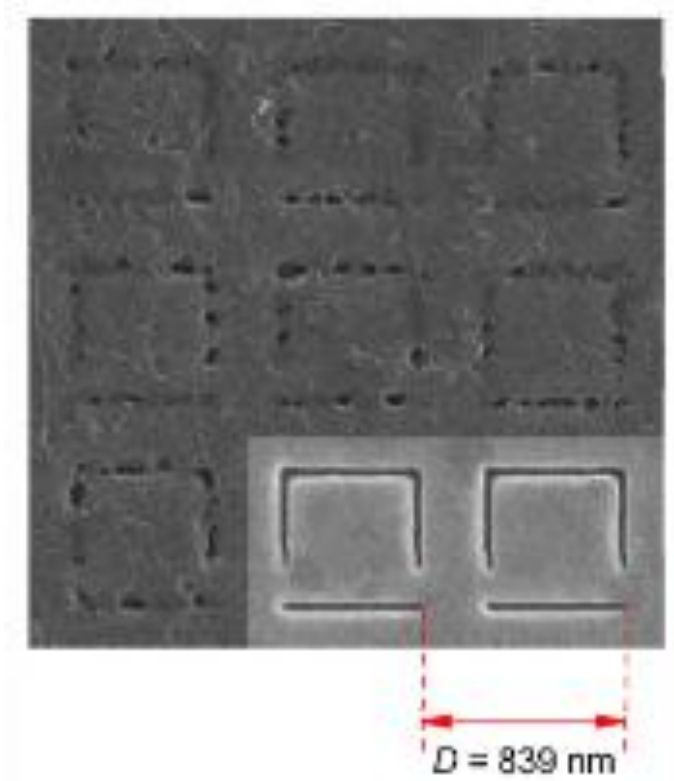

Plasmonic metamaterial covered by CNTs. Inset shows image of two unit cells of uncovered metamaterial

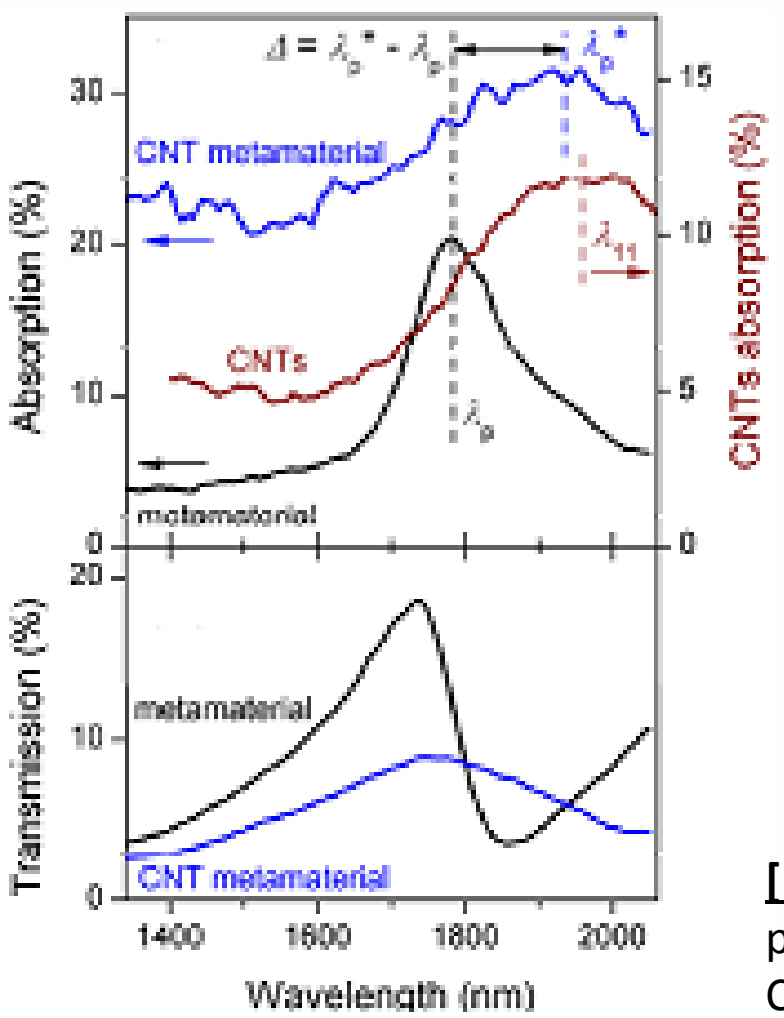

- **Top figure**: (*Left scale*)—Plasmonic absorption resonances of uncovered metamaterial (black), and metamaterial covered by CNTs (blue); (*right scale*)—Excitonic absorption spectra of bare CNT layer (wine).

- **Bottom figure**: Transmission spectra of uncovered metamaterial (black), and metamaterial covered by CNTs (blue).

[**NOTE**: The Redshift ($\Delta = \lambda_p^* - \lambda_p$) in plasmon absorption resonance in the CNT-functionalized metamaterial.]

Transparent Metamaterial

- 'Transparent metamaterials' under development can make possible computer chips and interconnecting circuits to use photonics instead of electronics to process and transmit data, representing a potential leap in performance.

- Unlike conventional metamaterial (that use noble metals like gold or silver) these new metamaterials are made entirely of dielectric materials, or insulators and non-metals. In fact, everything will be in silicon platform making integration of electronic and photonic devices on the same chip. The absence of metal in the metamaterial design will save light from getting unnecessarily lost as heat in the photonic device and interconnections.

- In computers and consumer electronics we still use copper wires between different parts of the chip. But if we can confine light to the same size as a nanoscale copper wire then we can have much faster clock speed and hence enormously fast data processing—the transparent metamaterial can make this precisely possible.

Transparent Metamaterial (contd …)

- The innovation in transparent metamaterial (TMTM) lies in modifying the phenomenon of "total internal reflection," the principle normally used to guide light in optical fibre.

- Here the optical momentum of evanescent waves is controlled as opposed to conventional photonic devices, which manipulate propagating waves. This dramatically reduces the cross-talk (mutual coupling), the figure of merit of photonic integration, among close by devices compared to any dielectric waveguide (slot, photonic crystal etc.); allowing dense photonic integration possible.

Conventional TIR; most power is in cladding that decays slowly.

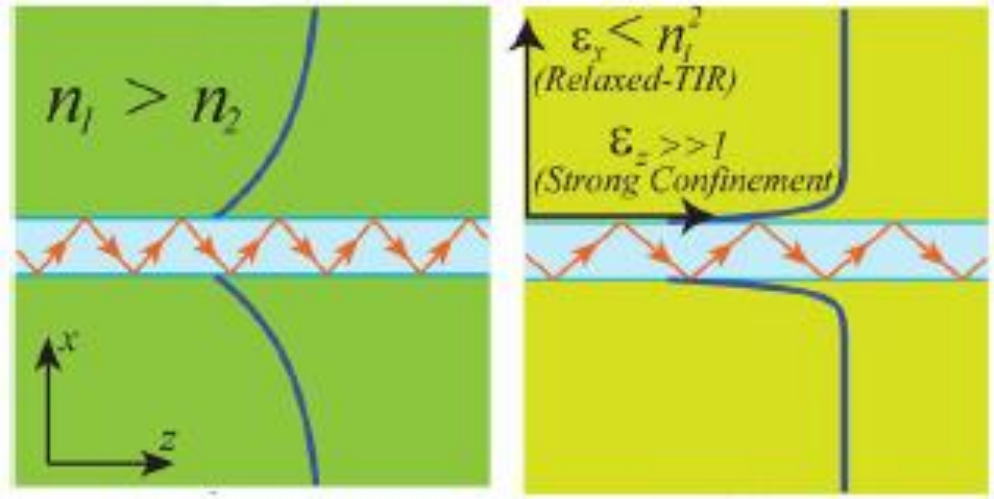

Relaxed-TIR in TMTM; light decays fast in cladding.

- The introduction of engineered anisotropy in permittivity tensor (ε_x = 4.8 and ε_z = 11.9) in the momentum of the cladding [realizable with transparent metamaterial (TMTM)] brings about the phenomena of relaxed-TIR.

Transparent Metamaterial (contd …)

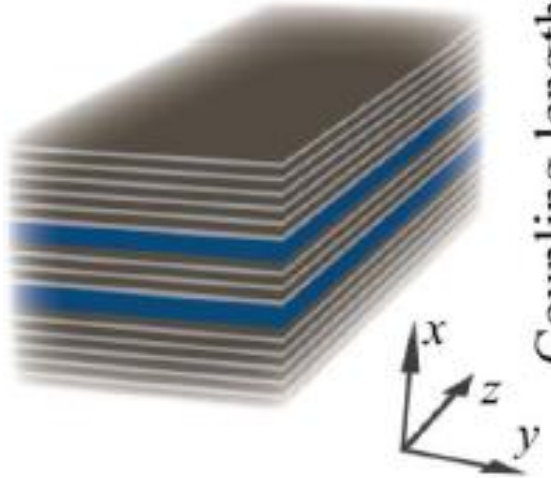

Multilayer TMTM consisting of alternate layers of sub-wavelength layers of germanium (26 nm) and silica (14 nm) acts as cladding to waveguide cores (thick blue layers, made of silicon with 0.5 λ separation between centre-to-centre of the waveguide) to realize dense photonic integration at optical telecommunication wavelength (λ =1550 nm).

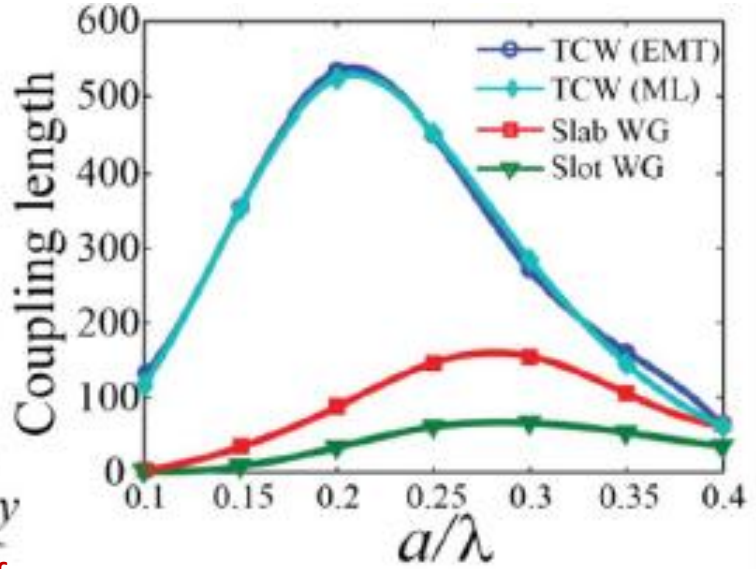

Comparison of coupling length (cross-talk) for conventional slab waveguide, slot waveguide and TCWs; is seen to outperform the state-of-the-art structures approximately by an order of magnitude improvement of cross-talk.

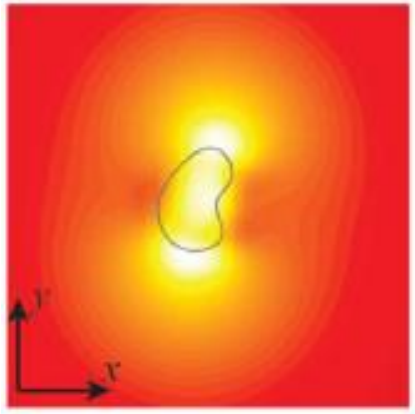

Waveguide without cladding

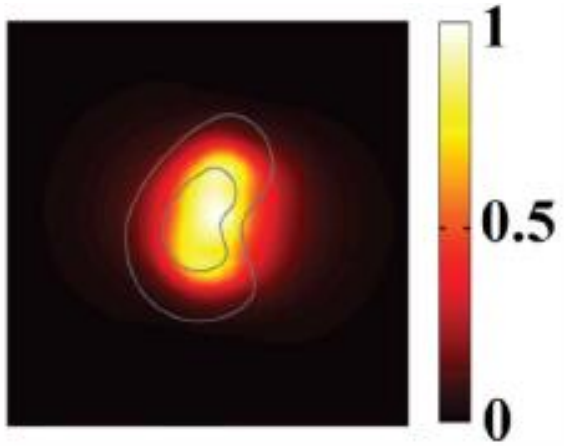

Waveguide with all-dielectric metamaterial cladding

NOTE: When the anisotropic cladding is added, the mode area of the waveguide is decreased from about 80A to 0.7A and the fraction of power inside the core to the total power is increased from 1% to approximately 36%.

Transparent Metamaterial (contd …)

- Quantum information technologies such as quantum cryptography, quantum information storage and optical quantum computing demand effective stable sources of single photons and the nanostructures to control the quantum dynamics of these photons.

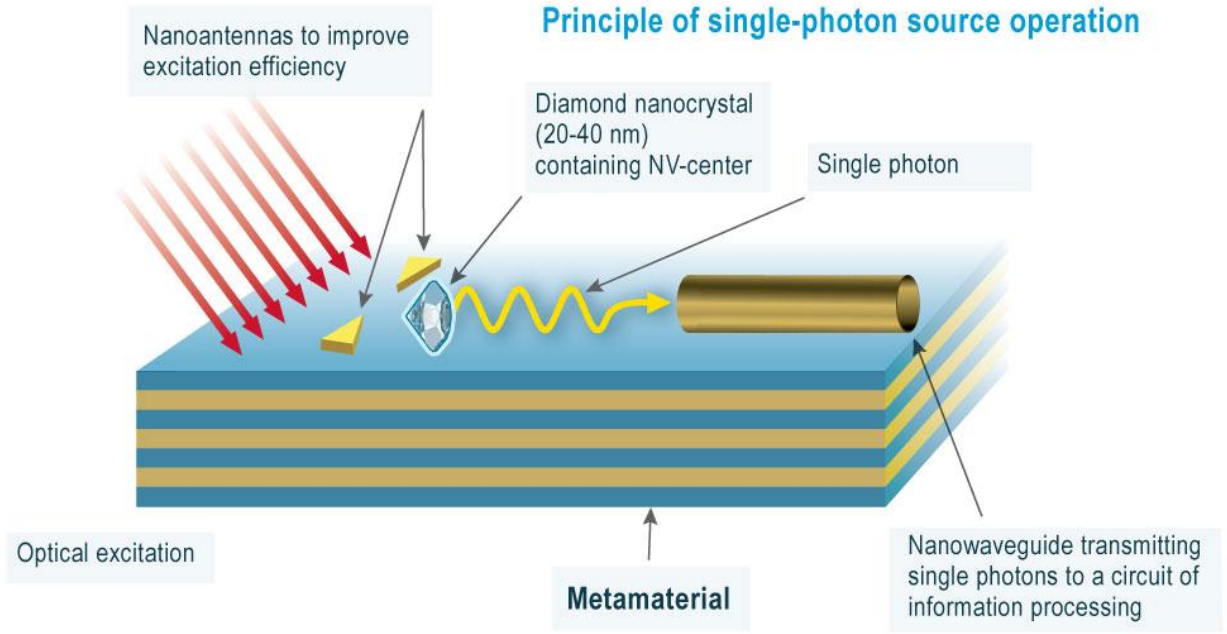

Transparent metamaterial can aid in enhancing the single photon radiation over a broad spectral range. Here single-photon generation is based on coupling diamond nitrogen-vacancy centres (or silicon-vacancy centres) with a metamaterial having hyperbolic dispersion characteristics in which the enhancement of single-photon emission is resulted due to the presence of the metamaterial (may be two orders of magnitude or so).

- Such single photon source may also have applications in nanochemistry to control chemical reactions at the level of individual molecules; biochemical analysis to determine dynamics of molecular configuration, decoding DNA an so on.


Thank You

Power Klystrons for Charged Particle Accelerators

LM Joshi
Ex- Scientist & Professor AcSIR
CSIR-CEERI, Pilani

lmj1953@gmail.com

Central Electronics Engineering Research Institute (CEERI), Pilani

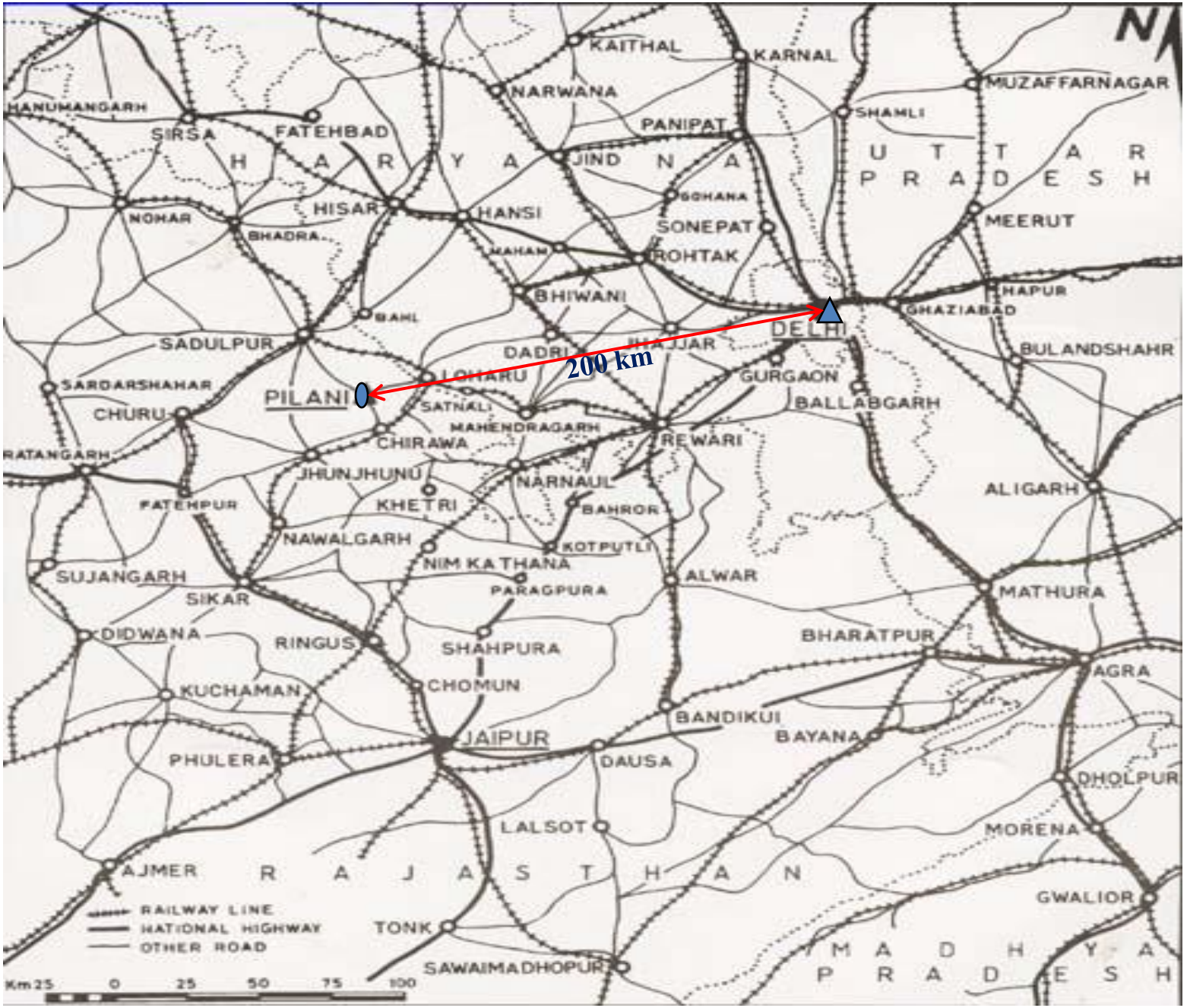
N
KAITHAL
KARNAL
MUZAFFARNAGAR
NARWANA
SHAMLI
HANUMANGARH
SIRSA
FATEHBAD
PANIPAT
H A R Y A
JIND N A
U T T A R
P R A D E S H
GOHANA
HISAR
HANSI
SONEPAT
MEERUT
NOHAR
BHADRA
MAHAM
ROHTAK
BHIWANI
HAPUR
GHAZIABAD
BAHL
DELHI
SADULPUR
DADRI
JHAJJAR
BULANDSHAHR
200 km
SARDARSHAHAR
LOHARU
GURGAON
PILANI
SATNALI
BALLABGARH
CHURU
MAHENDRAGARH
REWARI
CHIRAWA
RATANGARH
JHUNJHUNU
NARNAUL
ALIGARH
FATEHPUR
KHETRI
BAHROR
NAWALGARH
KOTPUTLI
NIM KA THANA
SUJANGARH
ALWAR
PARAGPURA
MATHURA
SIKAR
DIDWANA
RINGUS
SHAHPURA
BHARATPUR
AGRA
KUCHAMAN
CHOMUN
BANDIKUI
JAIPUR
BAYANA
PHULERA
DAUSA
DHOLPUR
LALSOT
MORENA
AJMER
R A J A S T H A N
GWALIOR
RAILWAY LINE
NATIONAL HIGHWAY
OTHER ROAD
TONK
M A D H Y A
P R A D E S H
SAWAIMADHOPUR
Km 25 0 25 50 75 100

Particle Accelerators

A particle accelerator is a machine that accelerates the sub-atomic particles, such as electron or proton, to very high velocities, close to velocity of light, using electric or electromagnetic fields.

Types of particle accelerators:

Cyclotrons, Pelletron, Synchrotron, RF linear accelerator [linac]….

RF linacs : Particles accelerated on a linear path with RF cavities.

- **Advantages**
  High current, high duty-cycle, low synchrotron radiation losses.
- **Drawbacks**
  High room & cavities consumption, no synchrotron radiation damping

Main use of linacs Low energy injectors, high intensity protons beam, high energy lepton colliders.

Linacs : Main Applications

Electrons

- High energy collider : No synchrotron losses
- Medical/Industrial irradiation : Low energy
- High-quality e- beam for FEL : Strong focusing
- Neutron sources : Material study

Protons

- Synchrotron injectors : High intensity, high duty-cycle
- Neutron sources : High Power. Material study, transmutation, nuclear fuel production, irradiation tools, exotic nucleus production

Heavy ions

- Nuclear physics research High intensity, high duty-cycle
- Implantation Semi-conductors
- Driver for inertial-confinement fusion

Medicine

- ~9000 medical accelerators in operation worldwide
- 10's of millions of patients treated/yr
- 50 medical isotopes, routinely produced with accelerators

Industry

- ~20,000 industrial accelerators in use
  - Semiconductor manufacturing
  - cross-linking/ polymerization
  - Sterilization/ irradiation
  - Welding/cutting
- Annual value of all products that use accel. Tech.: $500B

National Security

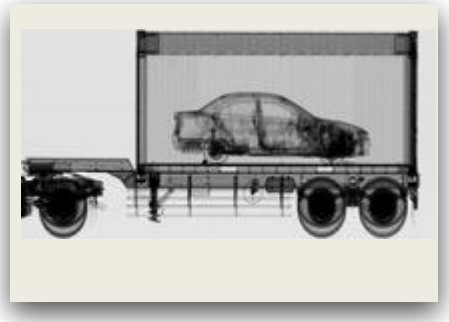

- Cargo scanning
- Active interrogation
- Stockpile stewardship: materials characterization, radiography, support of non-proliferation

Discovery Science

- ~30% of Nobel Prizes in Physics since 1939 enabled by accelerators
- 4 of last 14 Nobel Prizes in Chemistry for research utilizing accelerator facilities

There are 30,000 Particle Accelerators Making an Impact on Our Lives

1st term of Lorentz equation

$$\vec{F} = q\vec{E} + q(\vec{v} \times \vec{B})$$

linear acceleration

Problematic:

- High Electric fields require high voltages, Vg;
- Voltage generator construction limitations;
- Limitations on electrical insulation of the system;

Example:

- To reach an energy of 1MeV, a voltage generator rated for 1MV is required -> very difficult
- Most of accelerators today can reach energies in the range of several GeV !

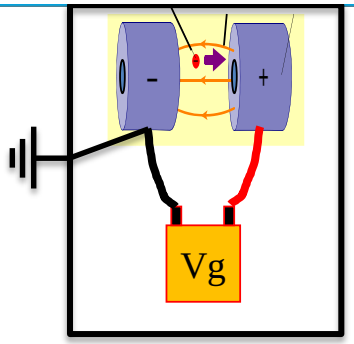

idea 1: works but the generator and insulation is a strong limiting factor

Energy gain, for 1 electron:
ΔW = Vg [eV]

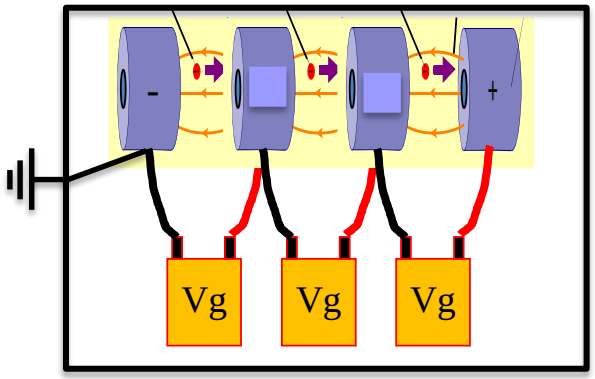

idea 2: works but insulation is still a strong limiting factor

Energy gain, for 1 electron:
ΔW = 3 x Vg [eV]

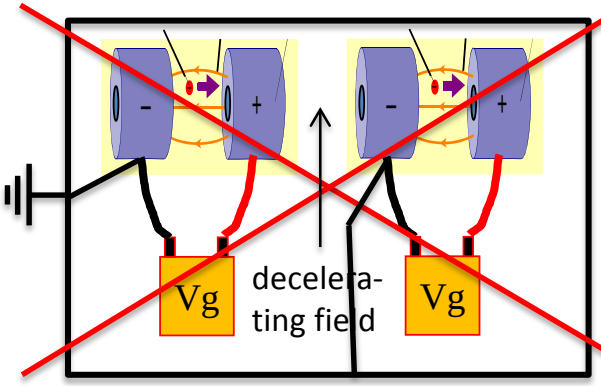

idea 3: does not work (total energy gain is still **ΔW = Vg [eV]**, due to decelerating field)

$F = qE + q(v \times B)$

1st term of Lorentz equation

$\vec{F} = q\vec{E} + q(\vec{v} \times \vec{B})$

linear acceleration

Principle:

- The AC voltage applied between multiple electrodes by a single generator creates electrical fields with the right polarity in those gaps where particles are to be accelerated;
- The generator reverses polarity when the particles are inside the drift tubes (i.e. subject to zero electric field)

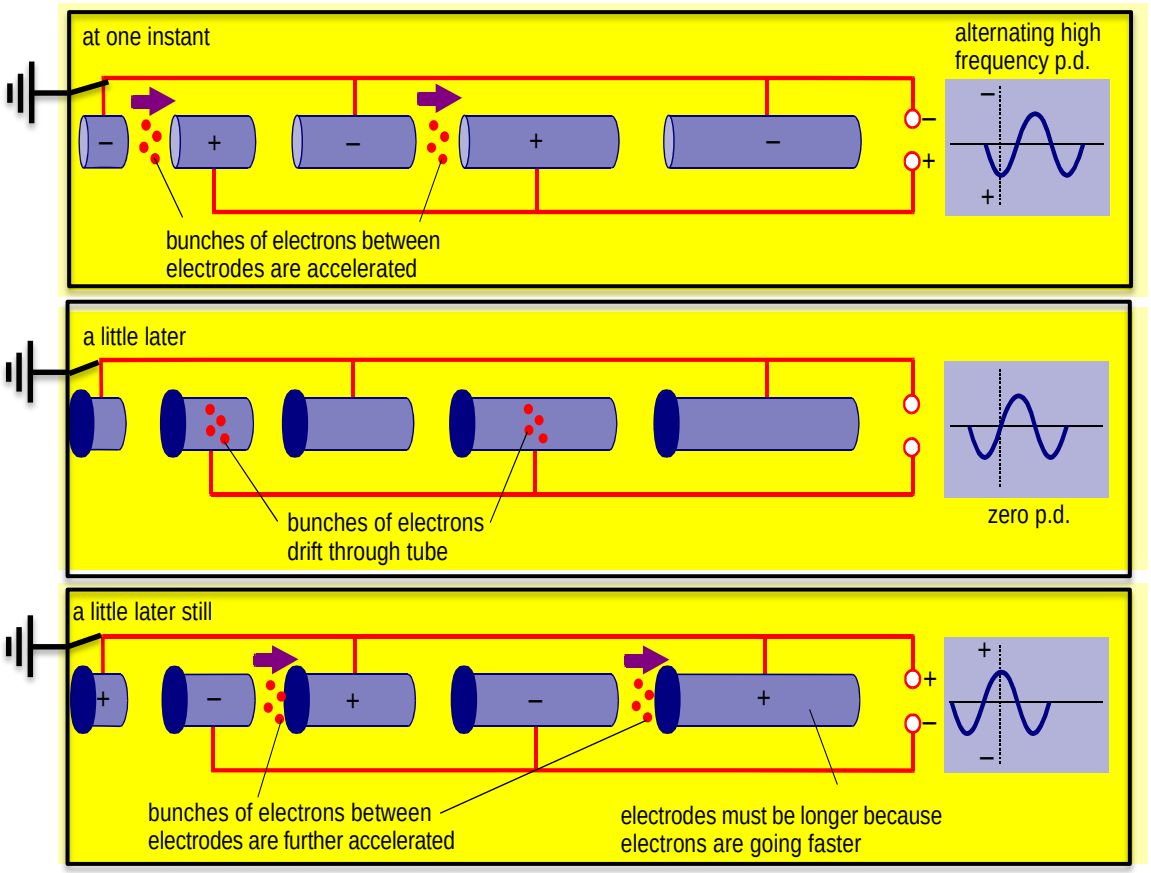

Limitations:

- For higher speeds, the frequency of the generator must increase;
- For high acceleration power, the power of the generator must increase.
- **How to generate intense AC fields (tens MV/m) at high frequencies (tens/hundreds MHz)?**

8

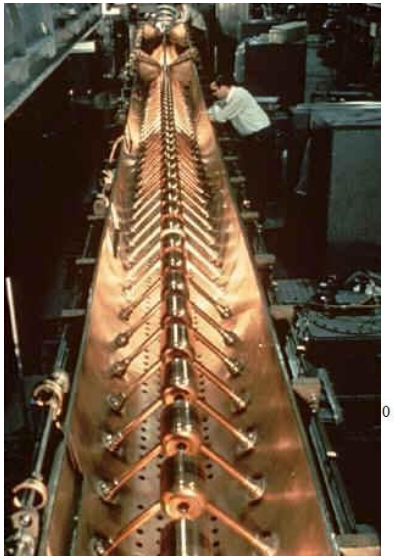

Drift Tube Linac (DTL)

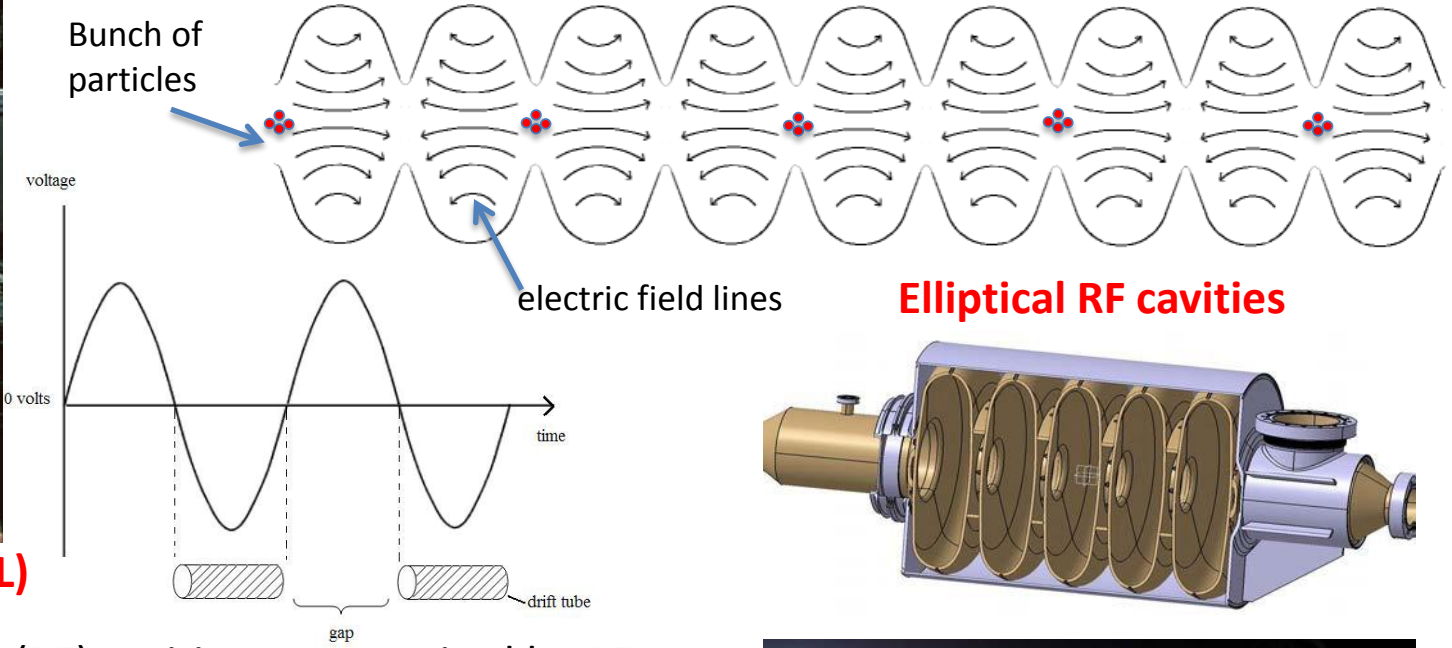

Elliptical RF cavities

- Radio Frequency (RF) cavities, once excited by RF power, produce high intensity AC electric fields that accelerate the particle beam bunches longitudinally

- RF sources are systems that generate the required RF power and transmit this power down into the RF cavities where the particle beam circulates and will be accelerated

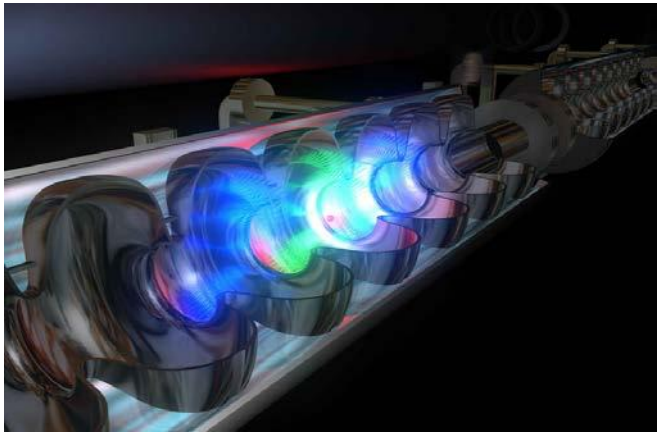

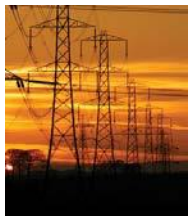

Electrical network

Modulators are HV power supplies that feed the RF sources.
- RF sources are therefore the loads of modulators

1- Modulator (HV power supply)

- Converts the electric power from a standard AC network into High Voltage (HV), either DC (Direct Current) or pulsed, depending on the accelerator duty-cycle (i.e. beam "on" versus beam "off" time) ;

2- RF source

- Converts electrical power into RF power, by amplifying a low power input RF signal (RF signal in) into a large power electromagnetic wave (RF power out);

3- Waveguides; 4- circulator; 5- RF load; 6- power coupler;

Features of RF Sources for Accelerators

- Usually an amplifier : to meet frequency and phase stability requirements
  - Frequency range 50 MHz - 50 GHz
  - Power 10 kW- 2 MW CW or more
    up to 150 MW peak

Power conversion efficiency, reliability and bandwidth are other important considerations

Type of RF Sources

1. Solid State Devices

2. Electron Tubes

- Solid State
  - Silicon bipolar transistors
  - Silicon MOS-FETs
  - Silicon carbide Static Induction Transistor (SIT)

  Can only yield low power levels and large numbers must be operated in parallel to reach even the lowest power levels required for accelerators

  Typically 576 silicon bipolar transistors each of 110 W would be needed to make a 30 kW power module.

Solid state RF Sources

- Reliability is more by a factor of 2.5 compared to electron tube devices
- Many numbers operated in parallel, so failure of one does not affect overall performance
- High stability
- Low maintenance
- Low voltage operation
- Absence of warm-up time
- Large DC Current requirement: 30 kW amplifier draws about 2000 A current
  - Require large bus bars which will have high Ohmic losses
  - Conversion efficiency ~ 40%

Table 1: State-of-the-art r.f. power transistors

	LR 301[a]	TGF2023-20		TGF4240-SCC
Manufacturer	Polyfet	TriQuint		TriQuint
Material	Si LDMOS	GaN		GaAs
Frequency	350 MHz	3.0 GHz	14 GHz	8.5 GHz
Mean r.f. power	300 W	90 W	50 W	14 W
Operating voltage	28 V	30 V	30 V	8 V
Gain	13 dB	17 dB	5 dB	10 dB
Maximum junction temperature	200 °C	200 °C	200 °C	150 °C

a. Two transistors in push-pull.

Electron Tubes

- Particle accelerators have been the main driving force for development of high and super power microwave tubes
- Microwave tubes can be seen as decelerators where kinetic energy of accelerated electron beam is extracted to amplify microwave power
- Accelerator uses microwave power to increase kinetic energy of charged particles.
- They are functionally complementary to each other. Many of the fabrication techniques are common
- Main electron tubes used for particle acceleration are
  - Tetrode
  - Inductive Output Tube
  - Magnetron
  - *Klystron*
  - Gyrotron

Major Applications

- Communication
- Radar
- Particle Accelerators
- Thermonuclear Reactors
- Industrial Microwave Heating

Schemetic Diagram

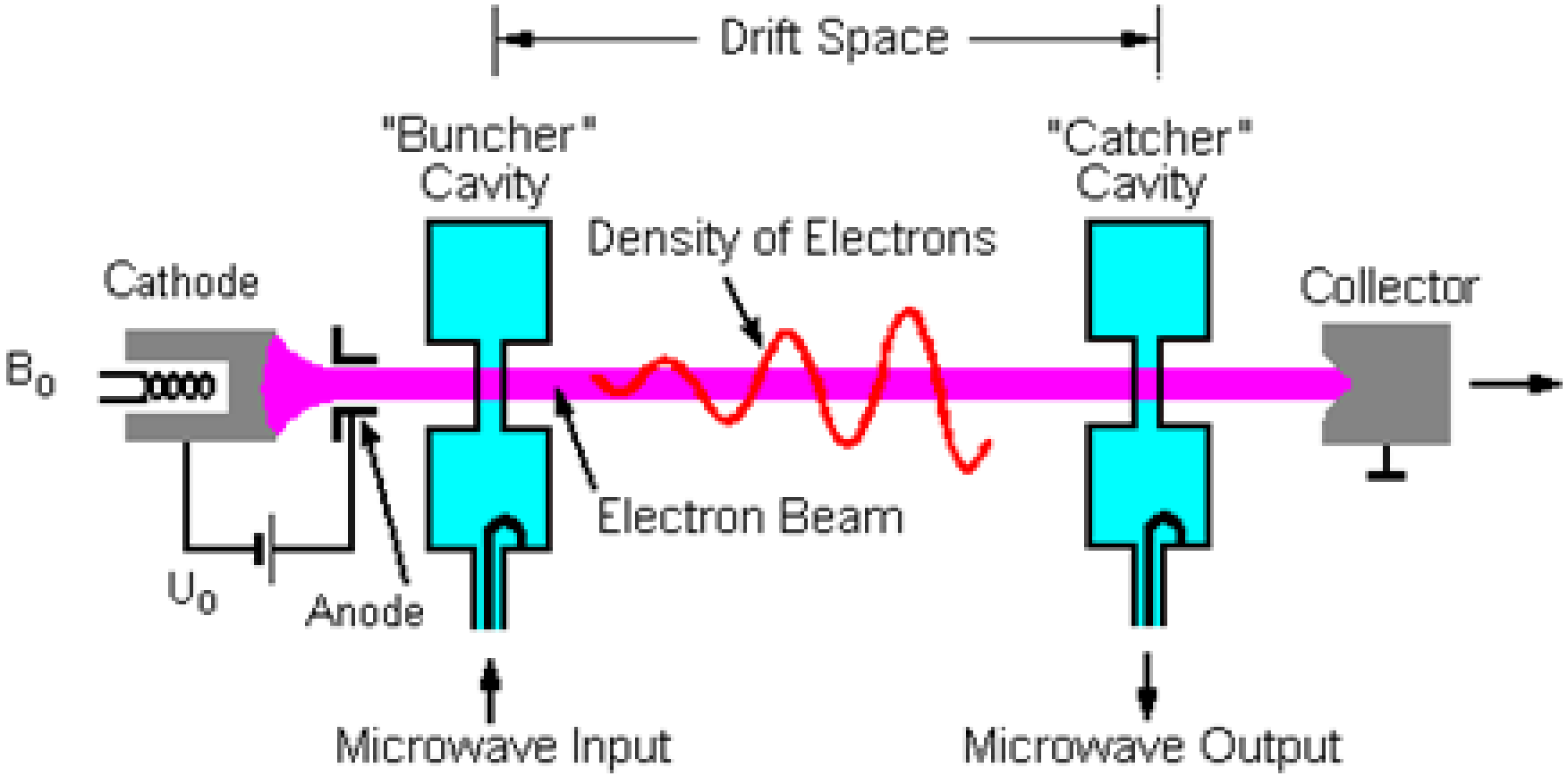

Basic Principle

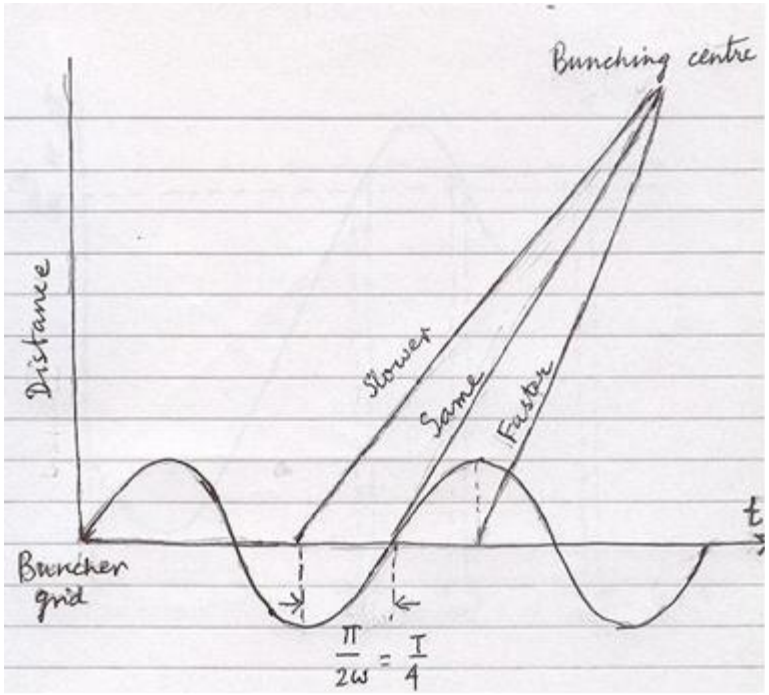

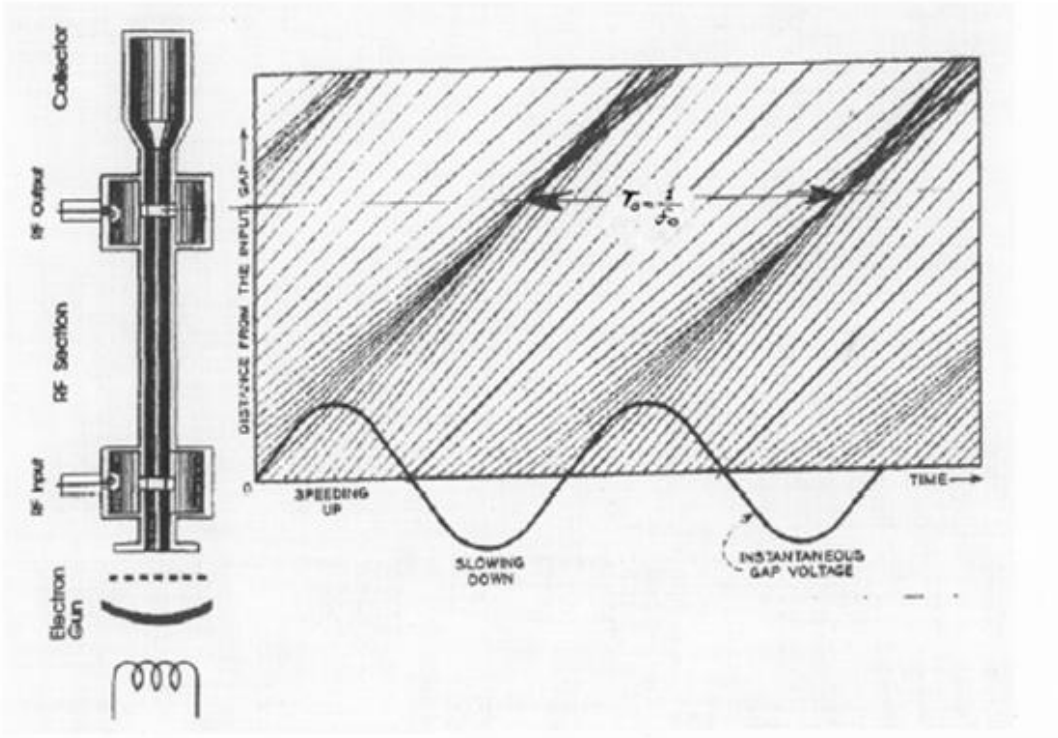

Schematic Diagram of a Multi-cavity Klystron

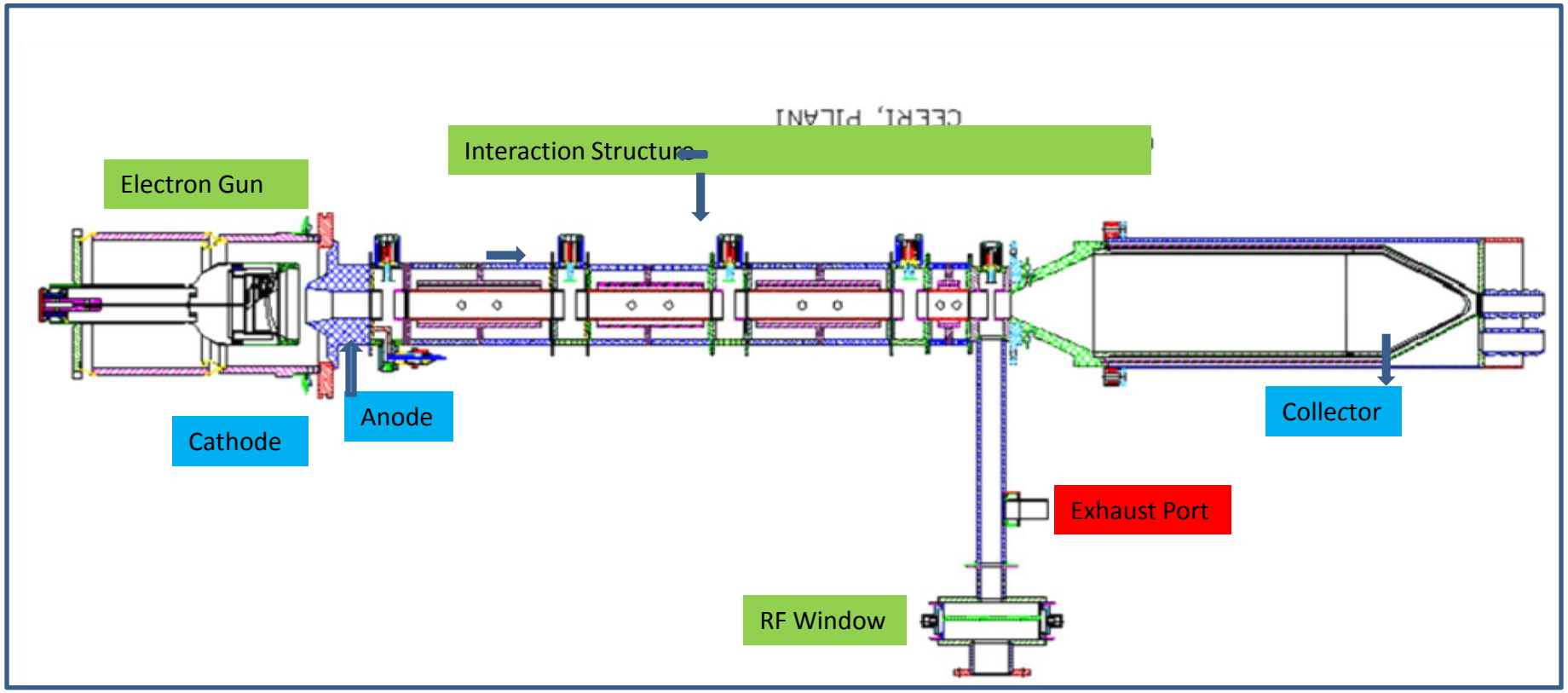

Design Considerations

Bottom-up Design Approach

- **Basic analytical design calculations**
- **Small signal modeling**
- **Large signal modeling: Mainly to design output RF section**
- **Realization of cavity or circuit properties through cavity simulation programs**
- **Design of electron gun and focusing section for desired beam optics.**
- **Thermo-mechanical design**
- **Lay out design of assemblies and piece parts**

Challenges

- Improved performance and reliability
- Reduced lifetime cost of ownership
- Reduced environmental hazards
  - Alternative materials
  - Low voltage operation
  - Spurious emissions
- Improved systems integration

APPROACH

- Improved computer modelling
- Improved understanding of device operation
- Improved understanding of breakdown phenomena
- Better characterisation of materials
  - Dielectric properties
  - Surface physics (secondary electron emission, cold cathodes)
- Novel tube types

Klystron problem areas

- • Reliability (including rate of RF trips)
- – Voltage breakdown in gun and output cavity
- – Window failure
- – Waveguide arcs
- • Efficiency
- – Electronic efficiency
- – Solenoid power consumption
- • Cost
- • Industrial capacity

Design issues:

High peak power

High voltage and current

High efficiency

High voltage and low current

Low solenoid power

High reliability

Low voltage – to avoid gun and output cavity breakdown

Low cathode loading – for long cathode life

Low peak power – to avoid output window failure and wave guide arcs

High Voltage Breakdown

- Along the insulators
- Between electrodes of the gun
- Cavity gaps with high RF fields
- Window surface

Klystron Efficiency

Perveance, P = I / V3/2

η (%)= 90-20 X P (μperv.)

For a given perveance improves with

- Shorter length of interaction region
- Use of second Harmonic cavity

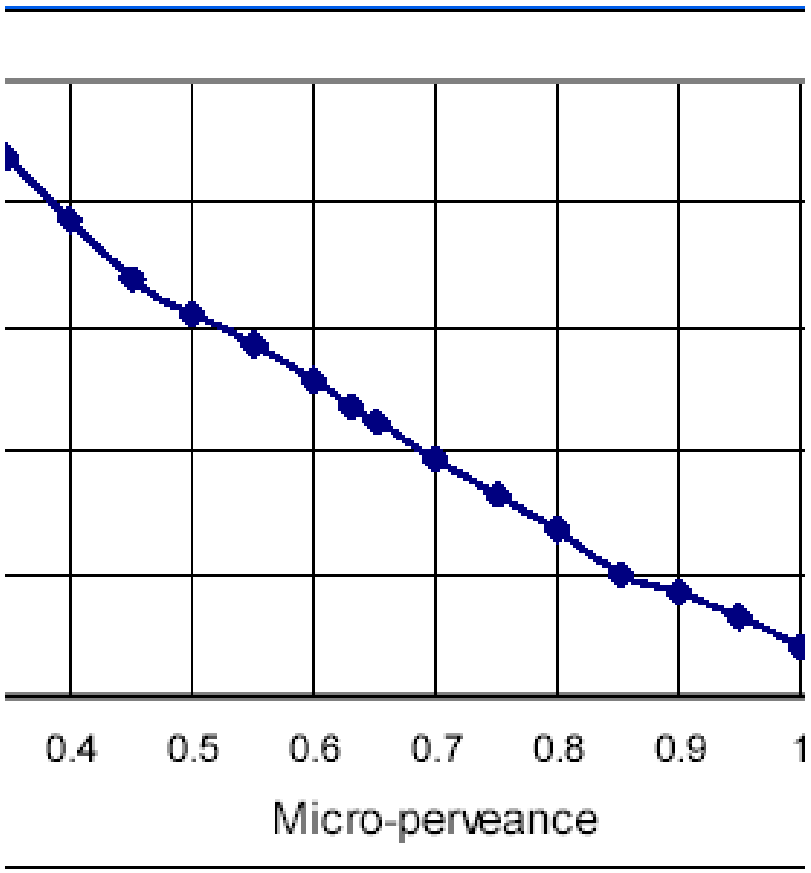

How to make a Klystron?

- Major steps involved in klystron development
  - Analytical calculations to estimate design parameters to achieve desired specifications
  - Use CAD tools to finalize electrical design
  - Convert electrical design into engineering design
    - Prepare engineering drawings of piece parts
    - Choose appropriate materials
    - Machining of parts in workshop; chemical cleaning, storage
    - Plan, fabricate and characterize subassemblies
    - Leak testing, high voltage breakdown testing, cold testing of cavities.
  - Integration of subassemblies into complete tube
  - Vacuum Processing
    - Cathode activation, pinch-off .
  - Hot testing and conditioning

Major CAD Tools

EGUN, TRAK, OPERA *for electron optics design*

POISSON, FEMAG, OPERA ***for focusing field design***

KL1D, MAGIC 2D/3D, CST PARTICLE STUDIO *for beam-wave interaction simulation*

MAFIA, CST MW Studio, HFSS *for RF circuit design*

AUTOMDC *for Depressed Collector design*

ANSYS, SOLID WORKS *for thermal and structural design*

Typical Tube Development Cycle

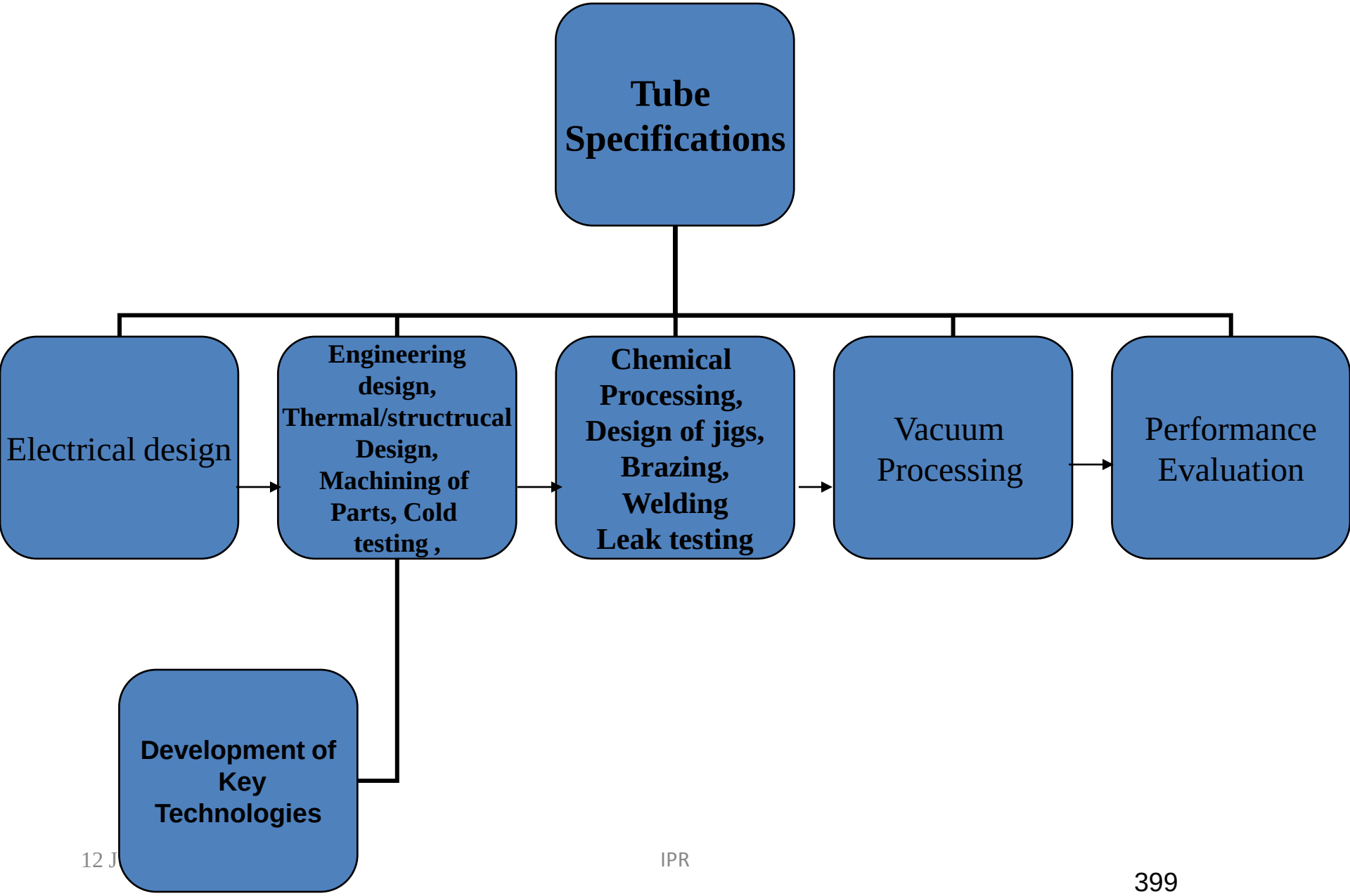

Synthesis of Gun Parameters

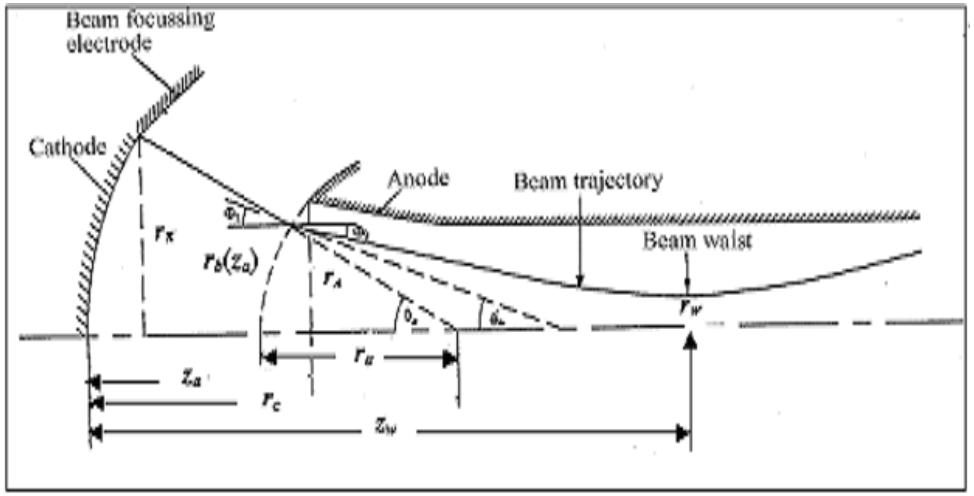

Parameters	Value
Beam voltage (V_0)	130 KV
Beam current (I_0)	94 A
Beam perveance	2 μP
Beam waist radius	8.0 mm

S. No.	Design parameters	Synthesized data
1.	Beam voltage (Volts)	130,000
2.	Beam current (Amps)	94
3.	Beam perveance (μP)	2.02678
4.	Emission current density (J_c)	5 A/cm^2
5.	Beam waist radius (r_a)	8.0 mm
6.	Cathode disk radius (r_c)	24.59245 mm
7.	BFE angle	67.5
8.	Half cone angle (θ)	24.9 ^{0}
9.	Cathode spherical radius (R_c)	~50.0 mm
10.	Cathode anode distance (Z_{ca})	31.109 mm
11.	Beam radius at anode plane r_b (Z_a)	11.51215 mm
12.	Anode aperture radius (r_a)	13.81458 mm
13.	Axial location of beam waist w.r.t cathode (Z_w)	70.8 mm

Optimization using Analytical codes

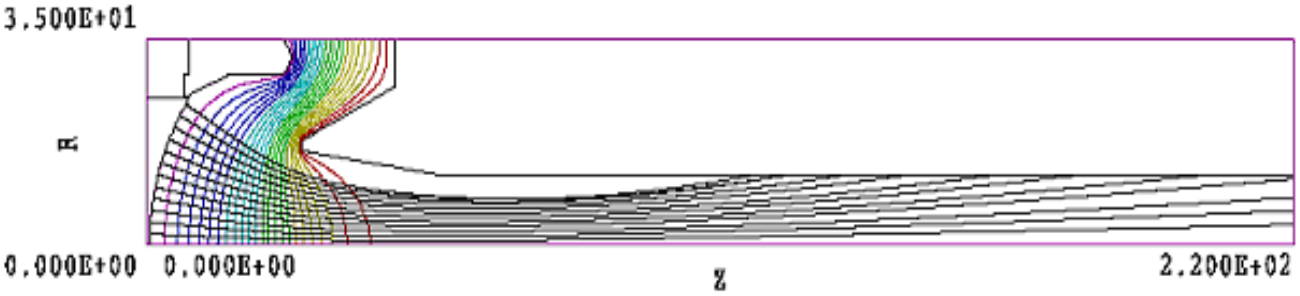

Sl. No.	Design parameters	Synthesized data	Simulated data	
			TRAK	MAGIC
1.	Beam voltage (V_0)	130,000	130,000	130,000
2.	Beam current (Amps)	94	89	90
3.	Beam perveance (μP)	2.02678	1.97	1.998
4.	Emission current density (J_c)	5 A/cm^2	5A/cm^2	5A/cm^2
5.	Beam waist radius (r_a)	8.0 mm	8.1 mm	8.0 mm
6.	Cathode disk radius (r_c)	24.59245 mm	25.00	25.00
7.	BFE angle	67.5	60.5	60.5
8.	Half cone angle (θ)	24.9 ^{0}	33.49	33.49
9.	Cathode spherical radius (R_c)	~50.0 mm	50.0 mm	50.0mm
10.	Cathode anode distance (Z_{ca})	31.109 mm	30.0mm	30.0mm
11.	Beam radius at anode plane r_b (Z_a)	11.51215 mm	12.89mm	12.76mm
12.	Anode aperture radius (r_a)	13.81458 mm	16.348mm	16.348mm
13.	Axial location of beam waist w.r.t cathode (Z_w)	70.8 mm	74.8mm	75.0mm

Focussing structure design

- Linear collider installations use thousands of klystrons
- The power consumed by solenoids is of the same order as is needed for running rest of the system
- Major design emphasis is on

  Super conducting magnets

  Permanent Magnets

  PPM

Electron Gun Simulation

- Beam Radius = 8.0mm
- Perveance = 2 micro
- Beam Current = 94A
- Beam Voltage =130KV

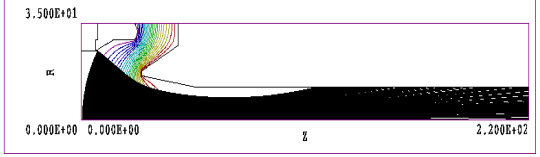


```
Total orbits: 189
Plotted range
   NOrbMin:   1
   NOrbMax: 189
Plot mode: ZR
Magnification: OFF
Orbit range
   XMin:   1.751E-02
   XMax:   2.491E+01
   YMin:   0.000E+00
   YMax:   0.000E+00
   ZMin:   4.703E-01
   ZMax:   2.200E+02
   RMin:   1.751E-02
   RMax:   2.491E+01

Plot type: Contour
Quantity: Phi

Minimum value:  -1.300E+05
Maximum value:   5.656E-02
   -1.191E+05
   -1.083E+05
   -9.748E+04
   -8.665E+04
   -7.582E+04
   -6.499E+04
   -5.416E+04
   -4.332E+04
   -3.249E+04
   -2.166E+04
   -1.083E+04
    5.656E-02
```

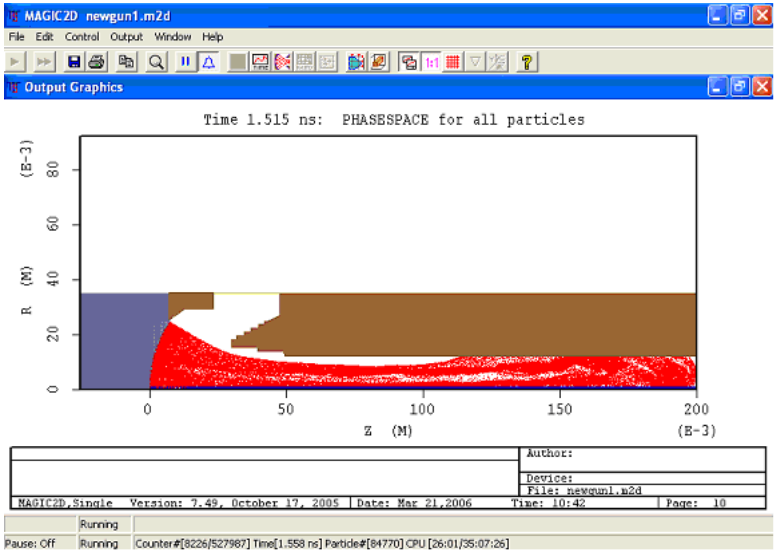

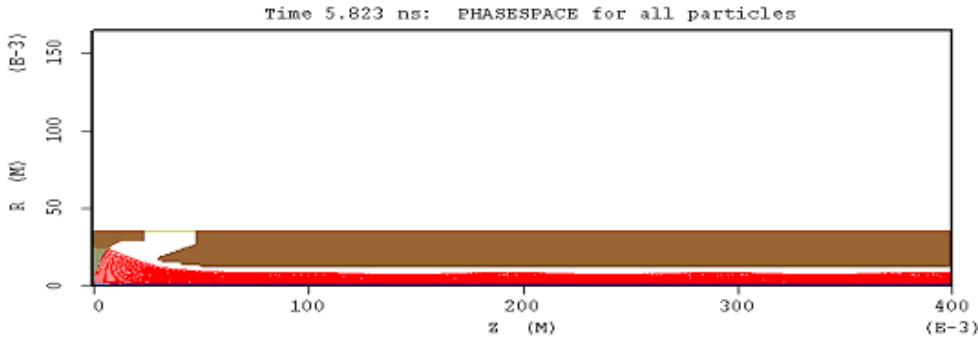

Magnetic Focusing Field

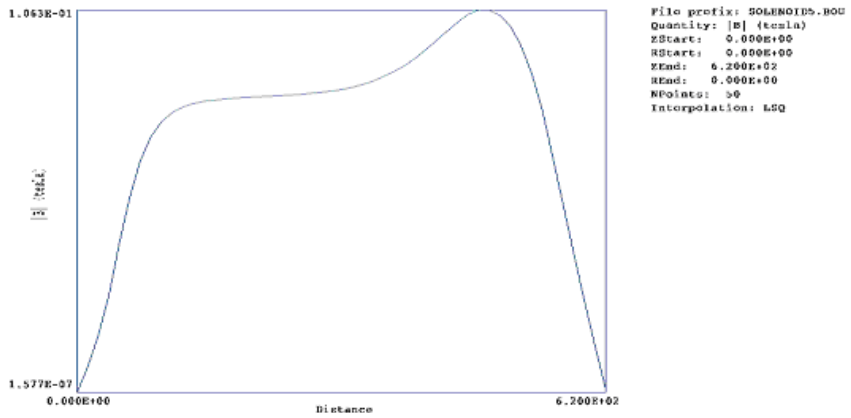

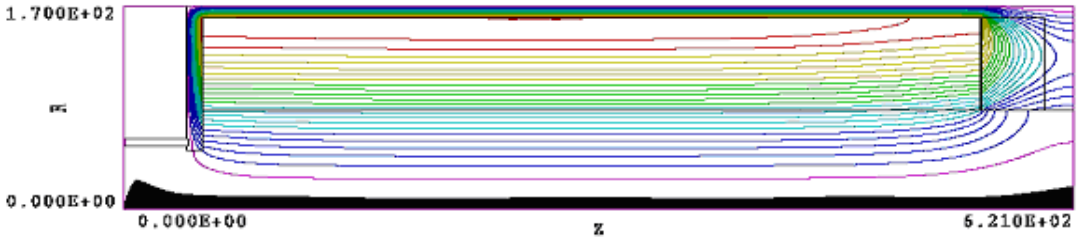

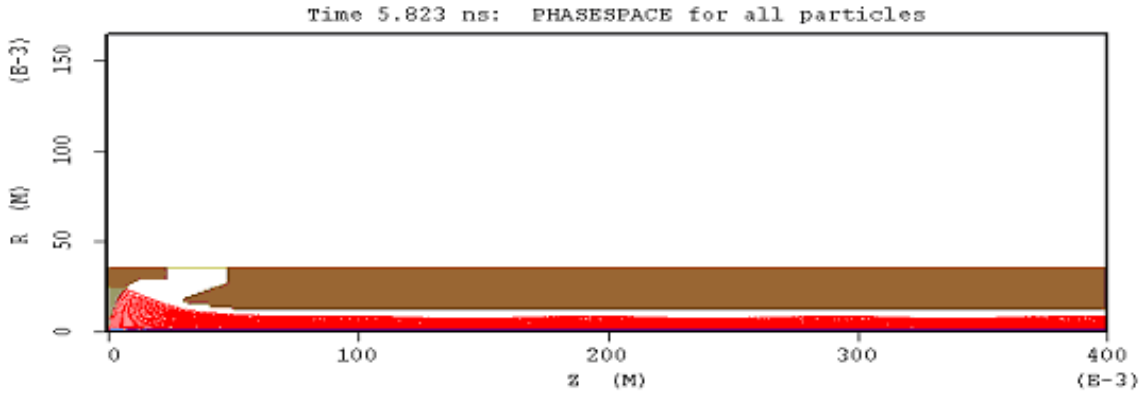

Klystron with Electromagnet

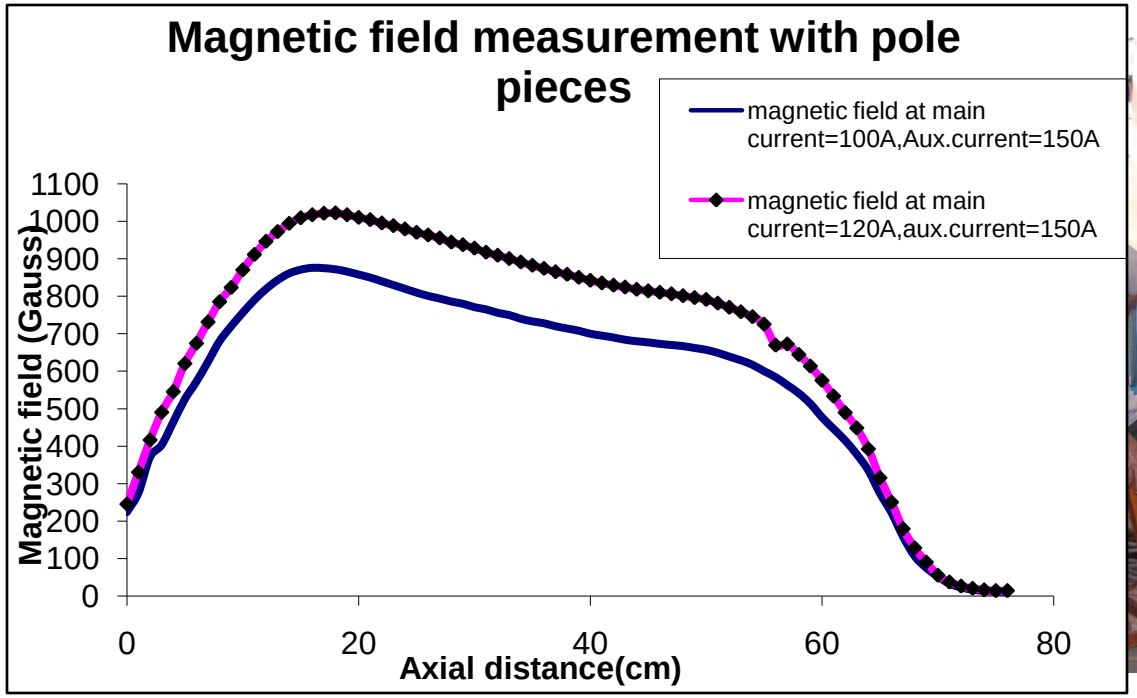

Cavity Parameters

$$Q = \frac{\omega_0 \times \text{Stored Energy}}{\text{Dissipation}}$$

$$\text{Dissipation} = V_g^2/2R$$

$$\frac{R}{Q} = \frac{V_g^2}{2\omega_0 U}$$

Power Coupling

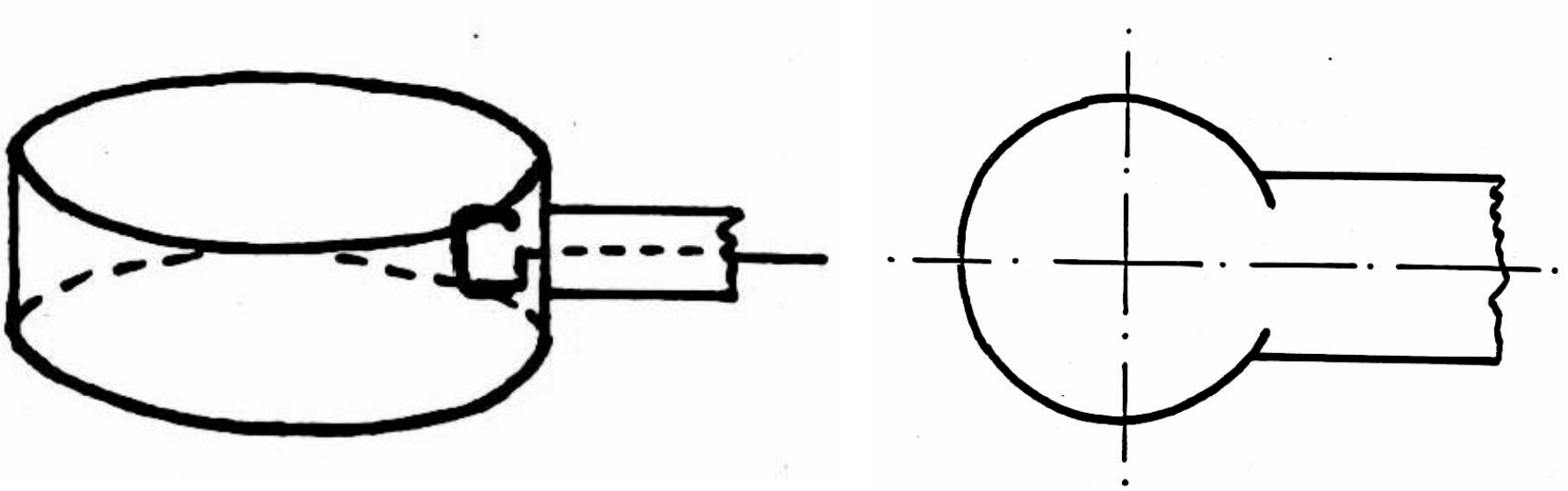

Cavity Tuning

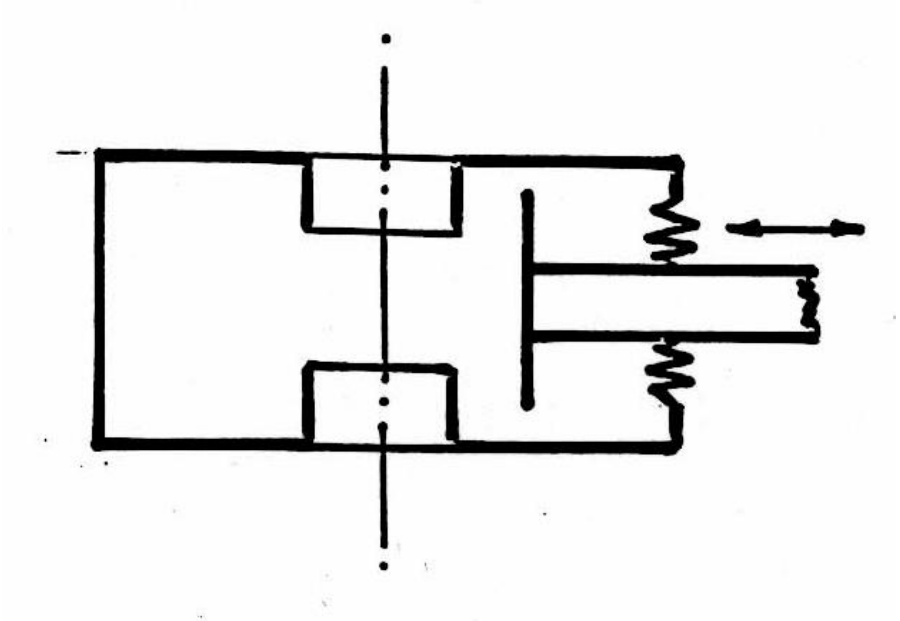

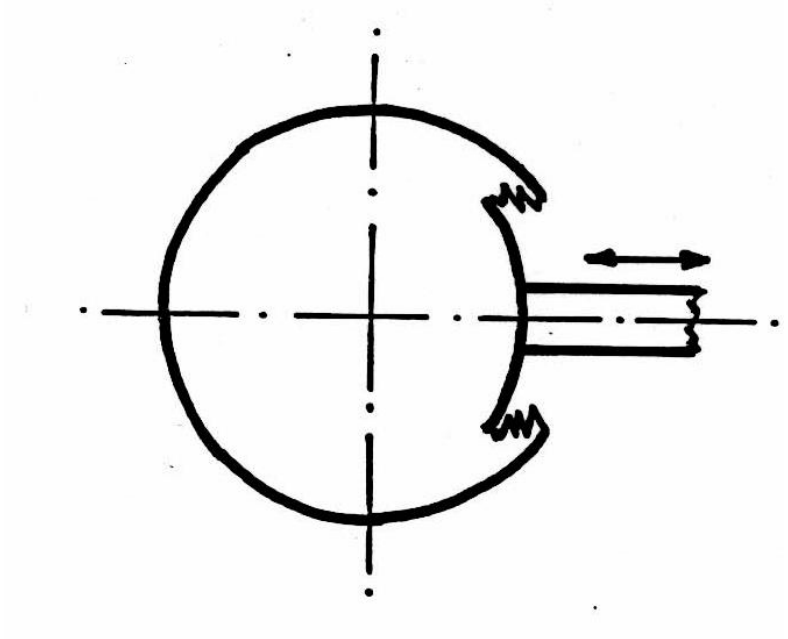

Cavity Simulation

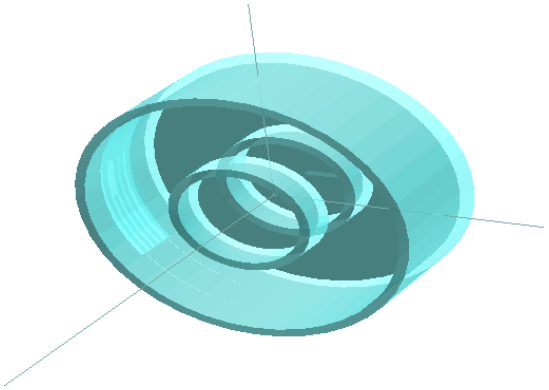

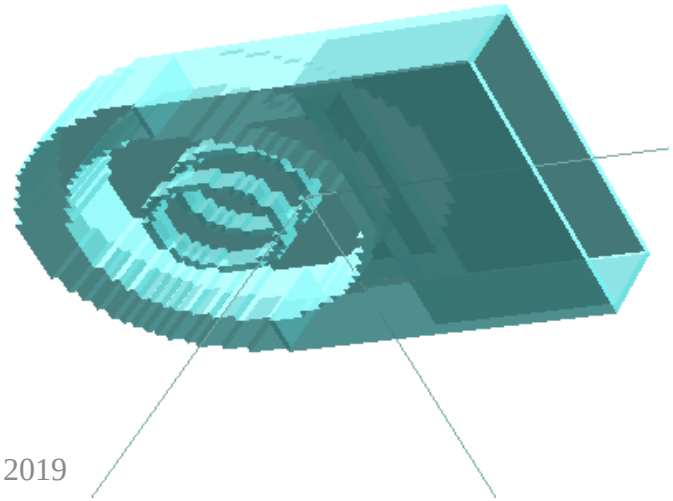

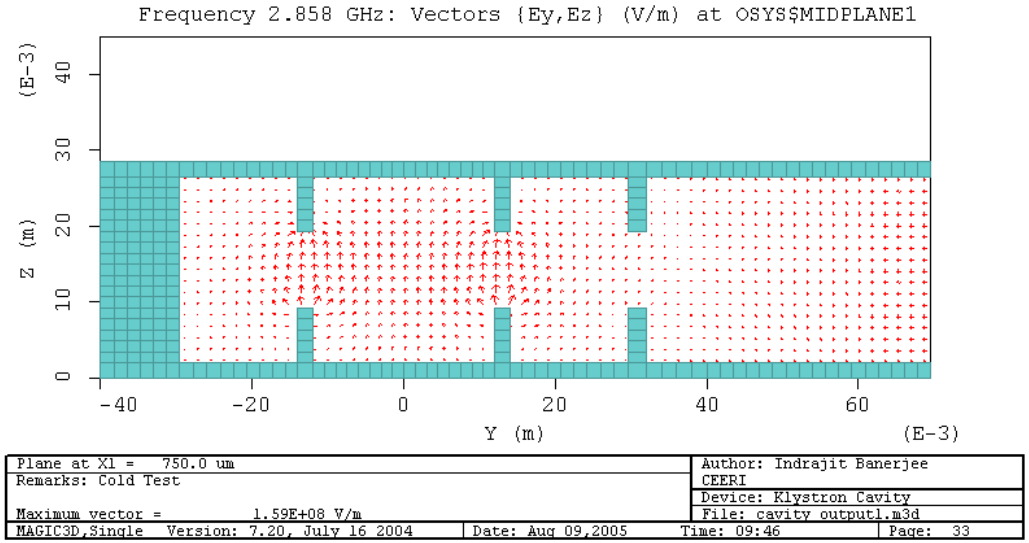

Computation of Input cavity Parameters

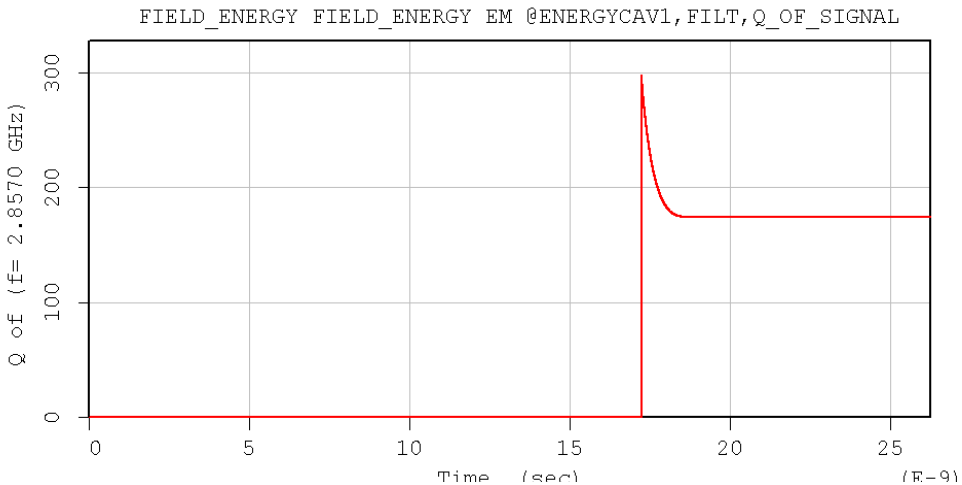

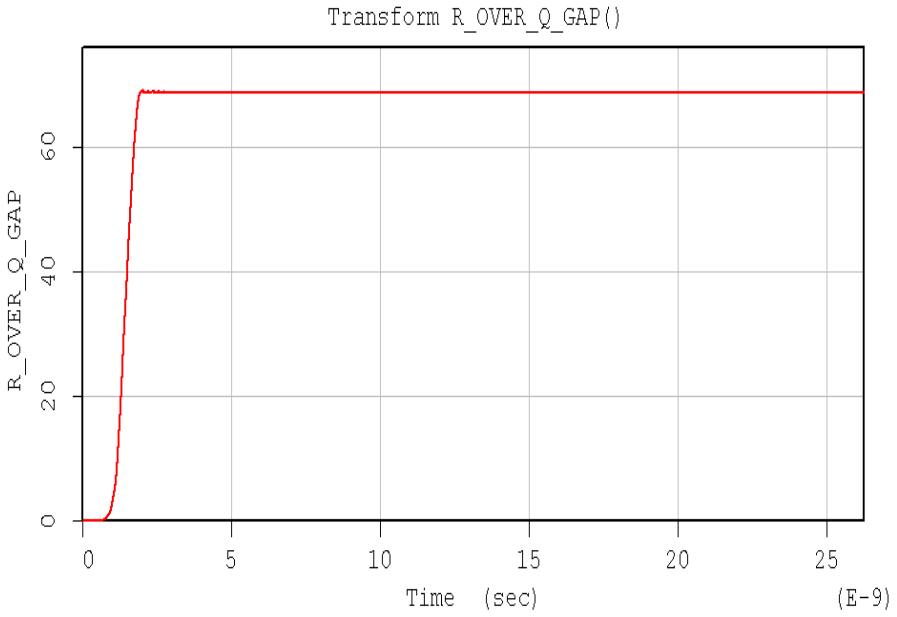

Simulated Cavity Parameters

S.No.	Resonant frequency f_o (MHz)	Q_o(unloaded quality factor)	Q_e(external quality factor)	Q_L(loaded quality factor)	R/Q
1	2856.0	6000	175.0	174.0	71.0
2	2861.0	6000	10,000	6000	71.0
3	2878.0	6000	10,000	6000	71.0
4	2920.0	6000	10,000	6000	71.0
5	2856.0	4000	30.8	30.5	68.9

high power klystron

Vo	= 30.000 kV	z(m)	0.0000	0.3000	0.5900	1.1400	1.3800
Io	= 7.000 A	f(MHz)	350.05	353.80	354.97	358.50	350.05
f	= 0.350 GHz	Qe	200.000	9000.000	9000.000	9000.000	40.000
a	= 32.000 mm	Qo	9000.000	9000.000	9000.000	9000.000	9000.000
b	= 20.000 mm	R/Q	136.790	136.500	136.700	136.200	136.790
Pin	= 3.200 W	k	30.83	30.82	30.83	30.82	30.83
Pout	= 100.191 kW	d(m)	0.03000	0.03000	0.03000	0.03000	0.03000
Gain	= 44.957 dB	V(kV)	0.4157	1.7059	6.6239	16.8893	33.1114

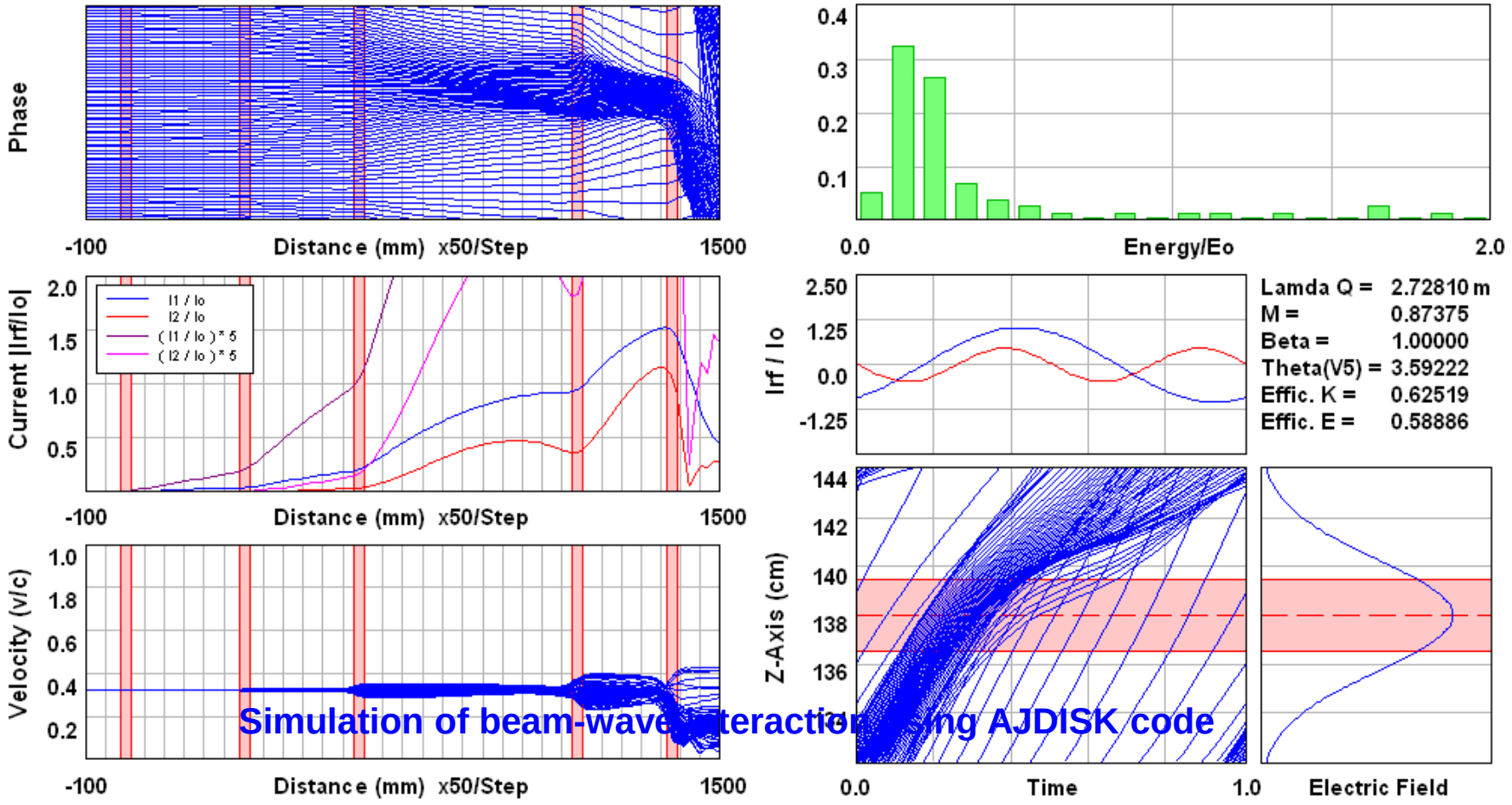

Simulation of beam-wave interaction using AJDISK code

Electron Bunching

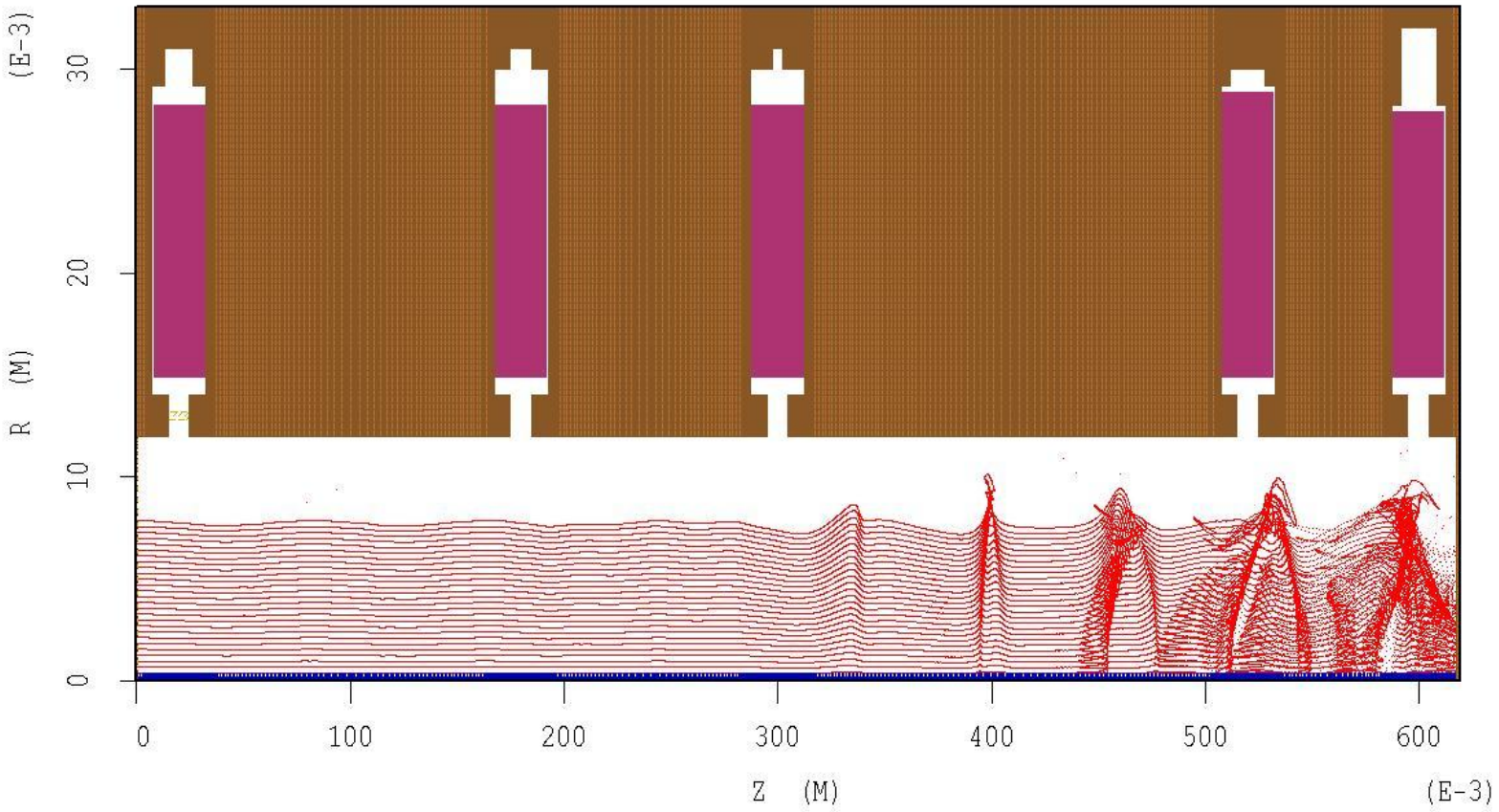

Author:

Particle Energy along Axial Direction

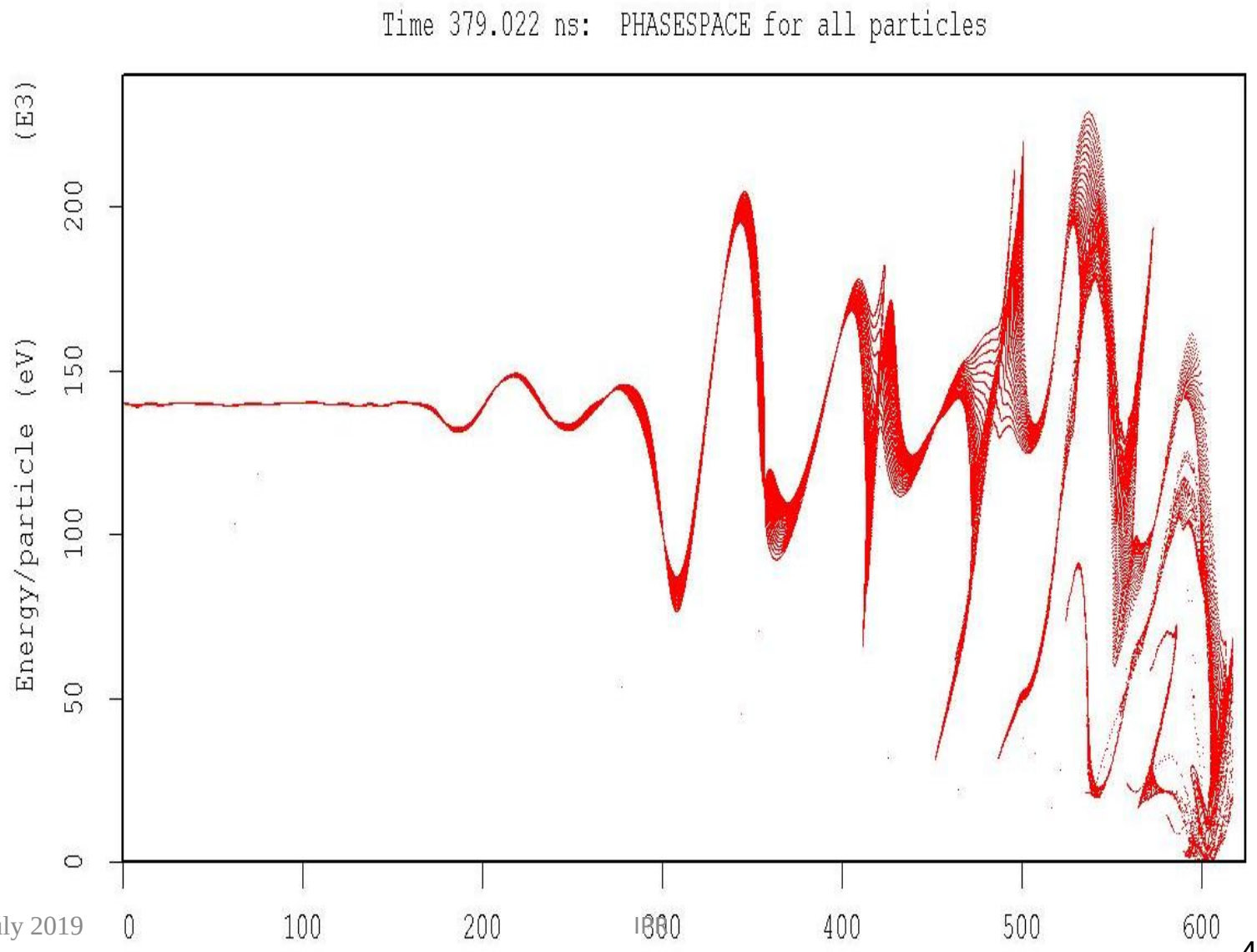

Output Power Computation

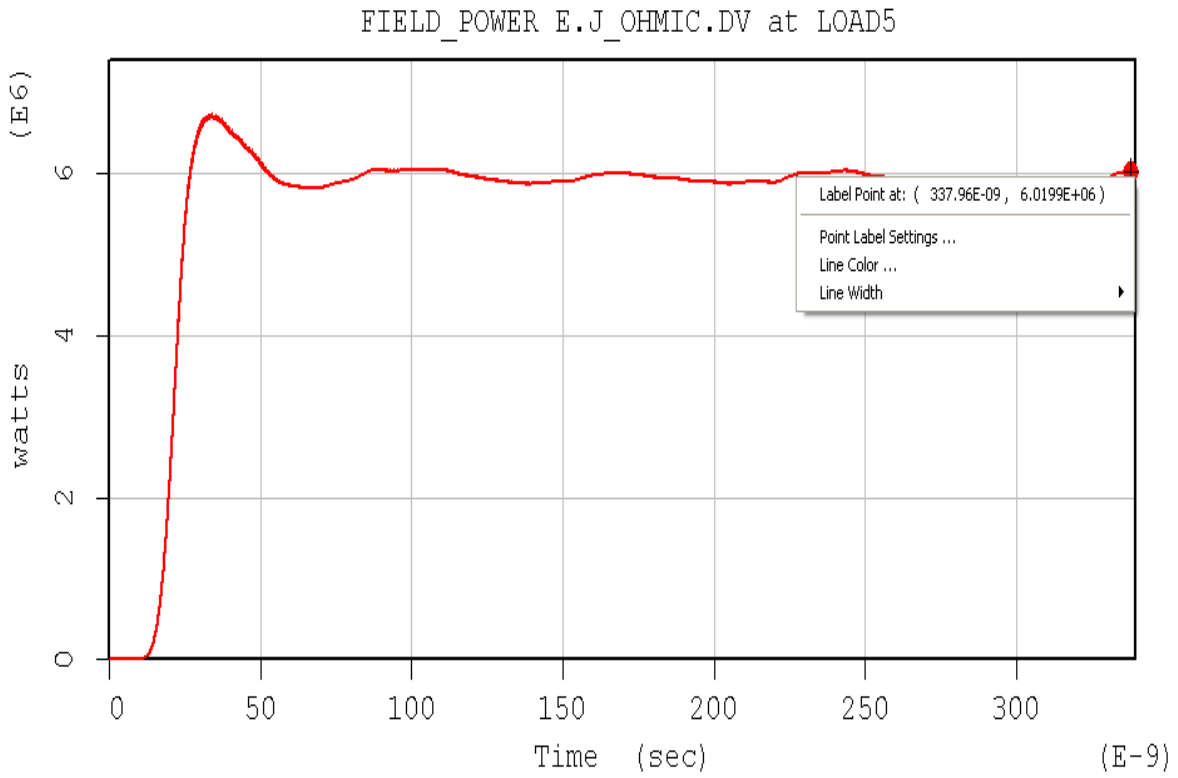

Parameters	Desired Values	Simulated values
Efficiency (%)	45(nominal)	41
Gain (dB)	45(nominal)	49
Output Power (MW)	6.0	6.0

Collector Design

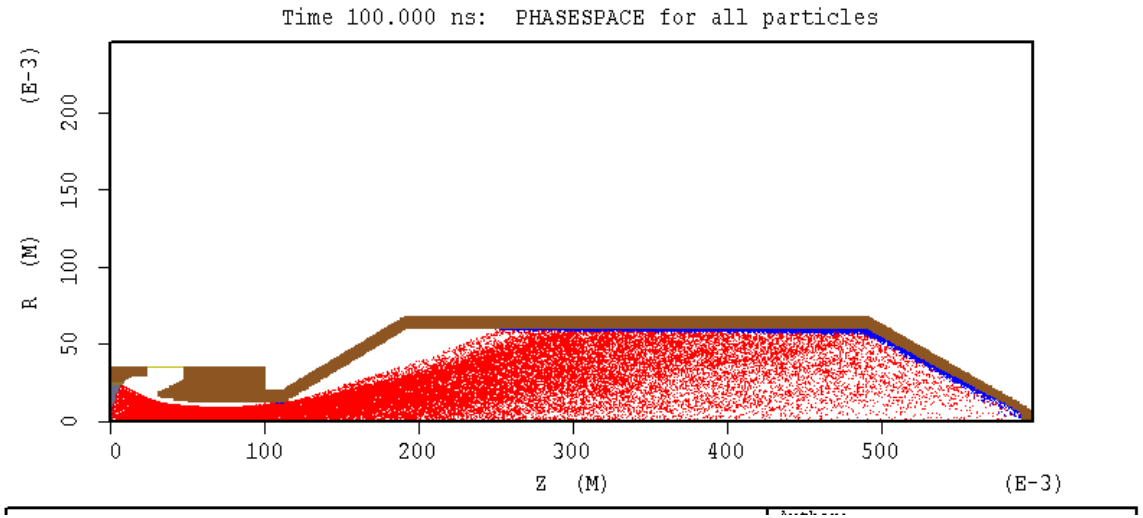

Thermal Design of Collector

Simulation for a smooth collector with full geometry

Heat dissipation = 52KW

Water inlet = 15 deg.

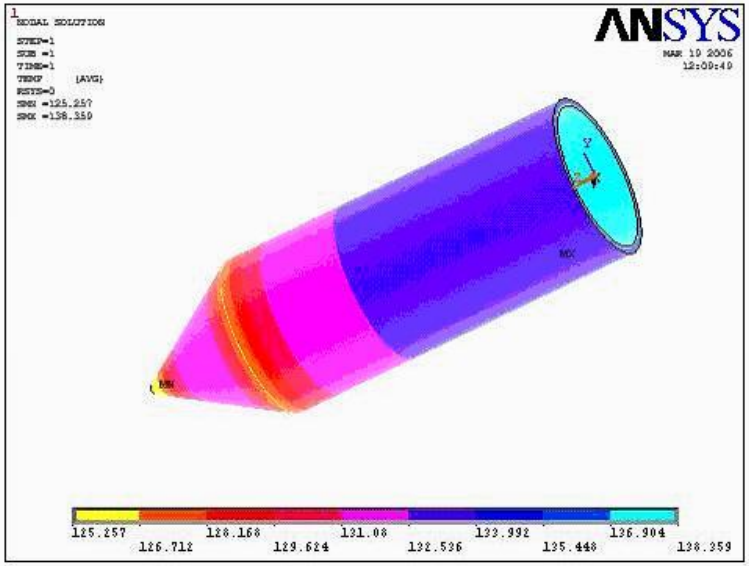

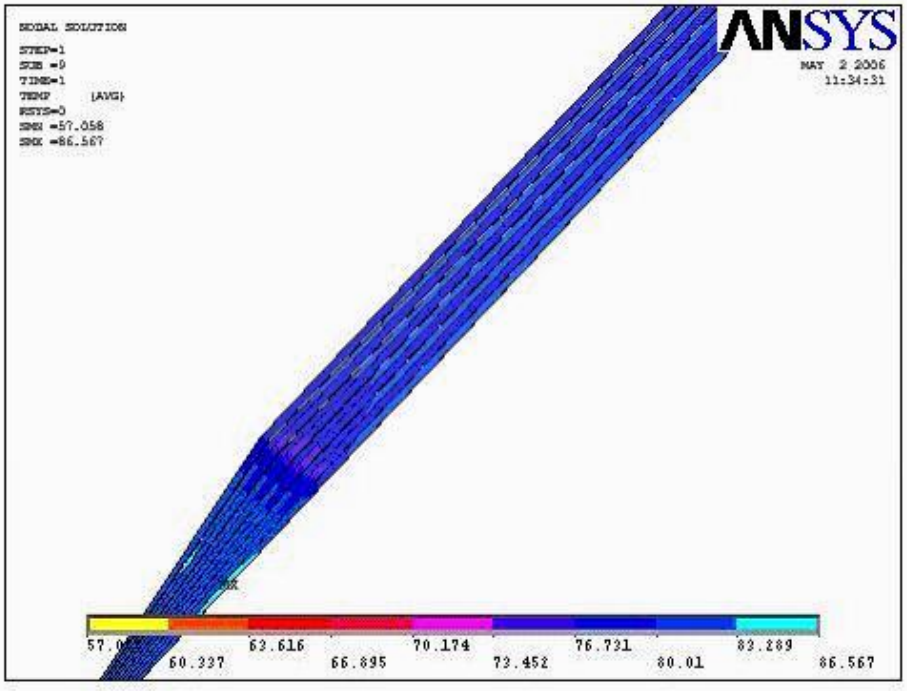

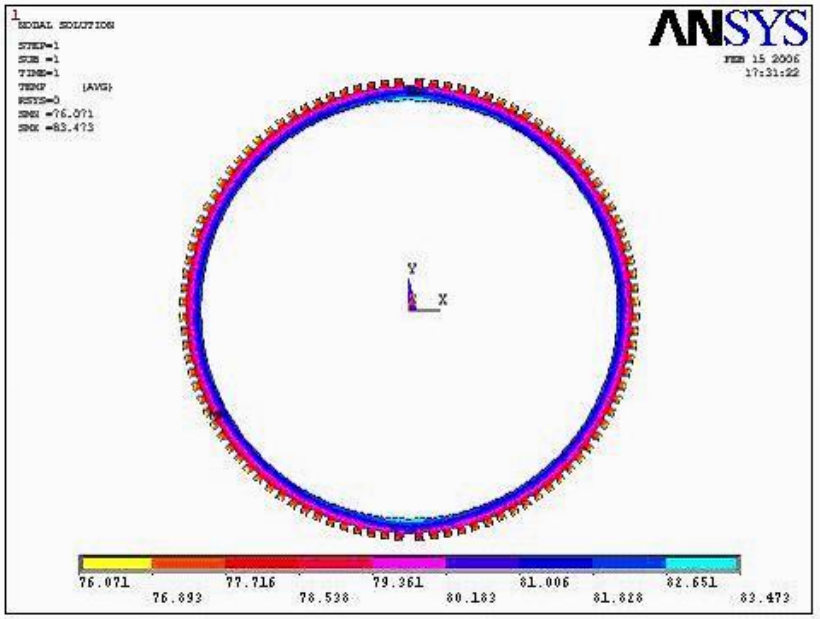

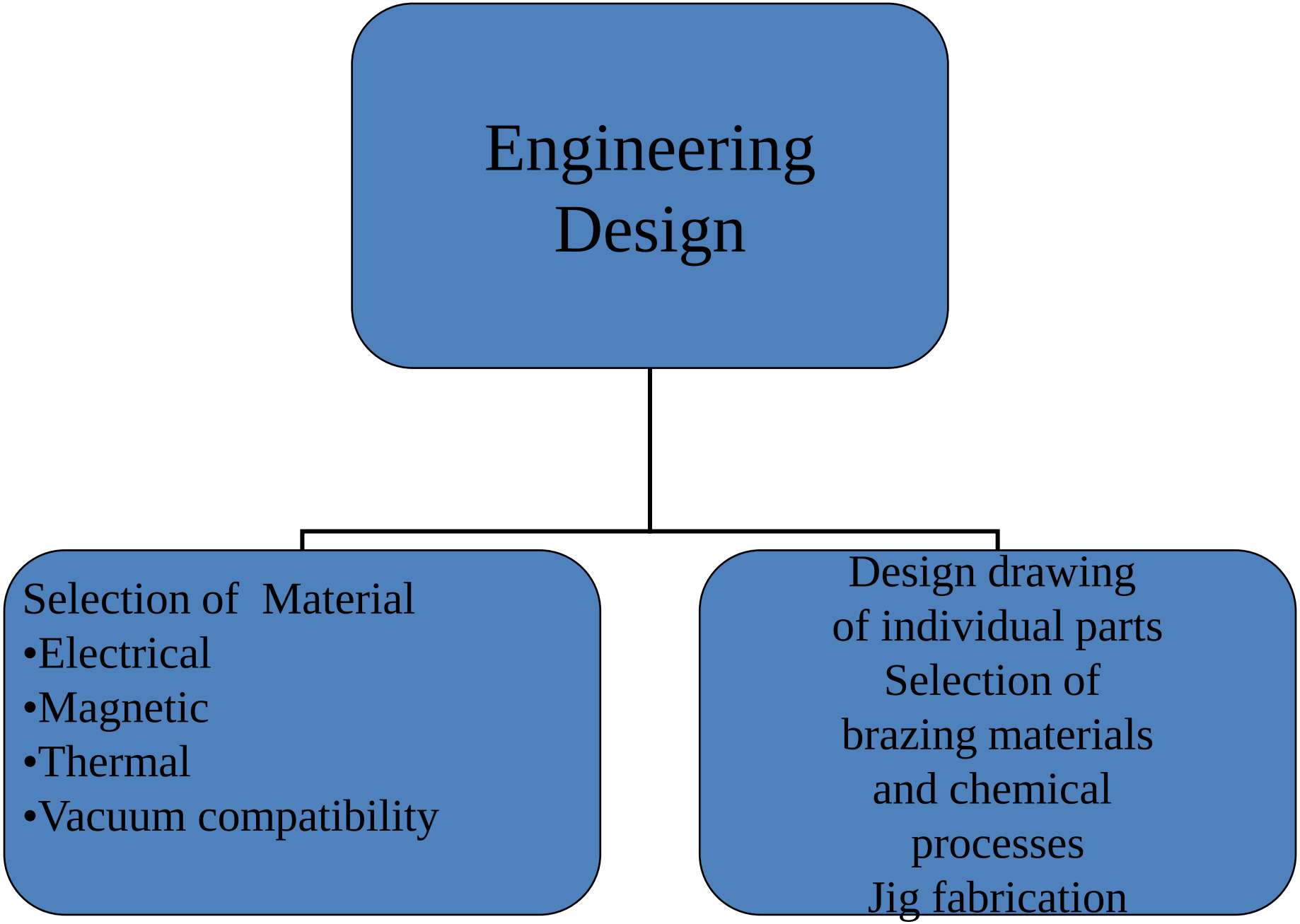
Engineering Design
Selection of Material
•Electrical
•Magnetic
•Thermal
•Vacuum compatibility
Design drawing of individual parts
Selection of brazing materials and chemical processes
Jig fabrication

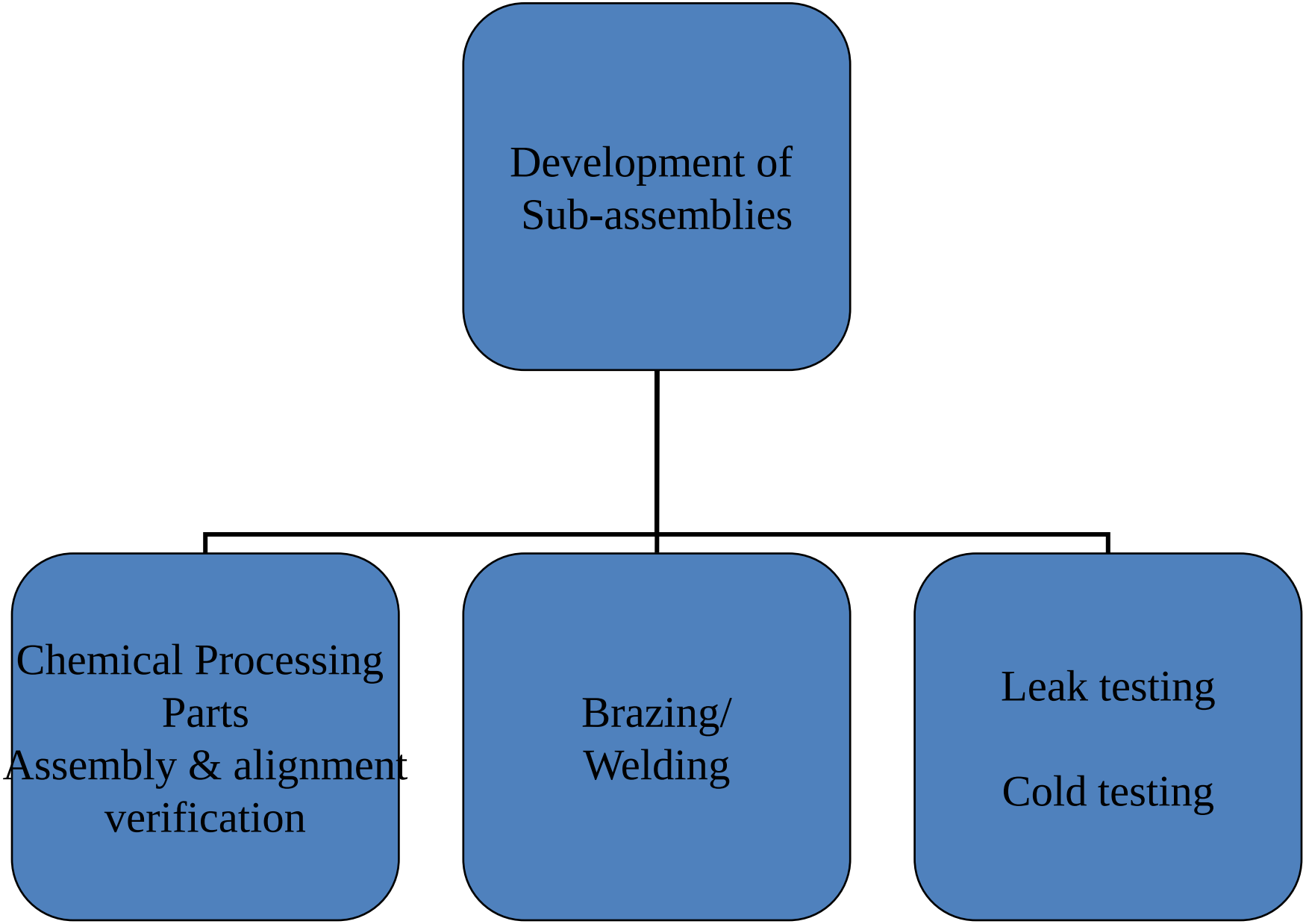
Development of Sub-assemblies
Chemical Processing Parts Assembly & alignment verification
Brazing/ Welding
Leak testing
Cold testing

Processes Involved

- All components must be hermetically sealed. Joining techniques must be suitable for high temperature processing
- • All materials must be ultra-pure and clean.
- Brazing, up to 1100C in H2, N2
- • Vacuum firing up to 1100C, 10^{-7} torr
- • TIG welding
- • Laser beam welding
- • Acid and alkali cleaning
- • Clean room assembly
- • Klystron evacuation to 10^{-9} torr

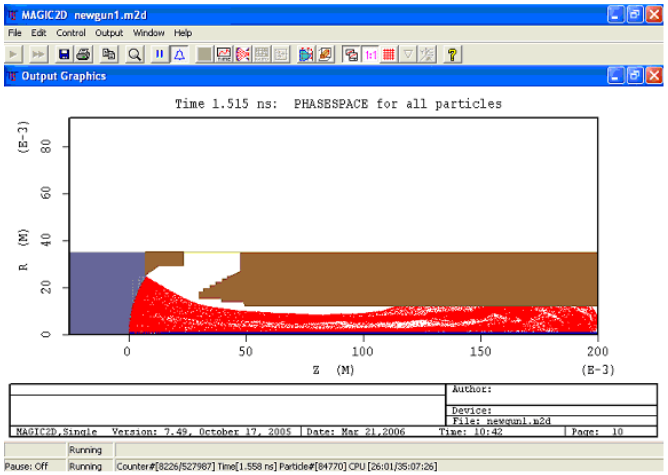
MAGIC2D newgun1.m2d
File Edit Control Output Window Help
Output Graphics
Time 1.515 ns: PHASESPACE for all particles
R (M) (E-3)
Z (M) (E-3)
Author:
Device:
File: newgun1.m2d
MAGIC2D,Single Version: 7.49, October 17, 2005 Date: Mar 21,2006 Time: 10:42 Page: 10
Running
Pause: Off
Running
Counter#[8226/527987] Time[1.558 ns] Particle#[84770] CPU [26:01/35:07:26]

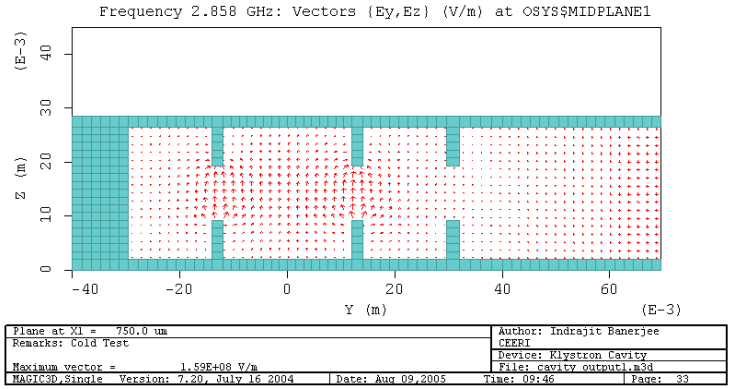
Frequency 2.858 GHz: Vectors (Ey,Ez) (V/m) at OSYS$MIDPLANE1
Z (m) (E-3)
Y (m) (E-3)
Plane at X1 = 750.0 um
Remarks: Cold Test
Maximum vector = 1.59E+08 V/m
Author: Indrajit Banerjee
CEERI
Device: Klystron Cavity
File: cavity output1.m3d
MAGIC3D,Single Version: 7.20, July 16 2004 Date: Aug 09,2005 Time: 09:46 Page: 33


5.1 10-9
SmartTes

Cleaning

- Ultrasonic degreasing,
- Chemical cleaning using
  - acetone
  - trichloroethylene
  - methyl alcohol
  - sulphuric acid
  - hydrochloric acid
  - nitric acid
  - phosphoric acid
  - sodium carbonate
  - sodium hydroxide
  - sodium nitrate
  - distilled water
- Electroplating

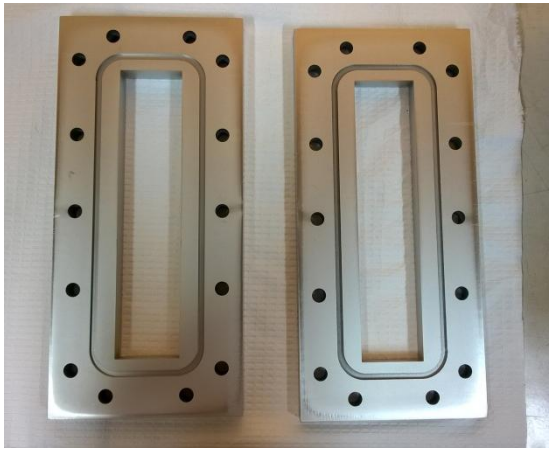

Storage and Handling

- The cleaned parts of the tube require utmost care in handling to avoid any contamination
- Parts are handled using lint free gloves
- Parts and sub-assemblies are stored in hot air boxes or vacuum desiccators

Assembly

- The cleaned parts are assembled into different subassemblies through brazing or TIG welding

- The assembly is done in clean rooms equipped with laminar air flow benches to avoid sitting of dust particles on the cleaned parts.

- Suitable jigs and fixtures are used to fabricate subassemblies so that their dimensional tolerances are maintained after joining operations

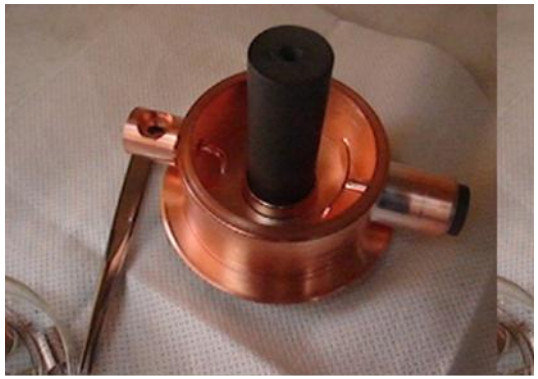

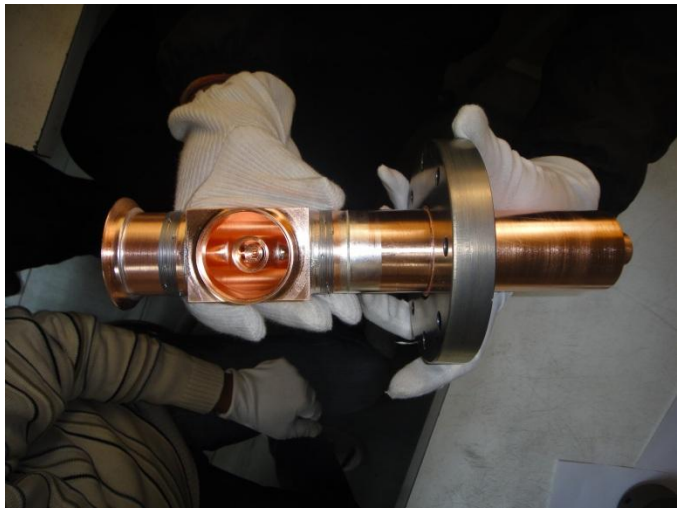

Thermal characterization of the cathode

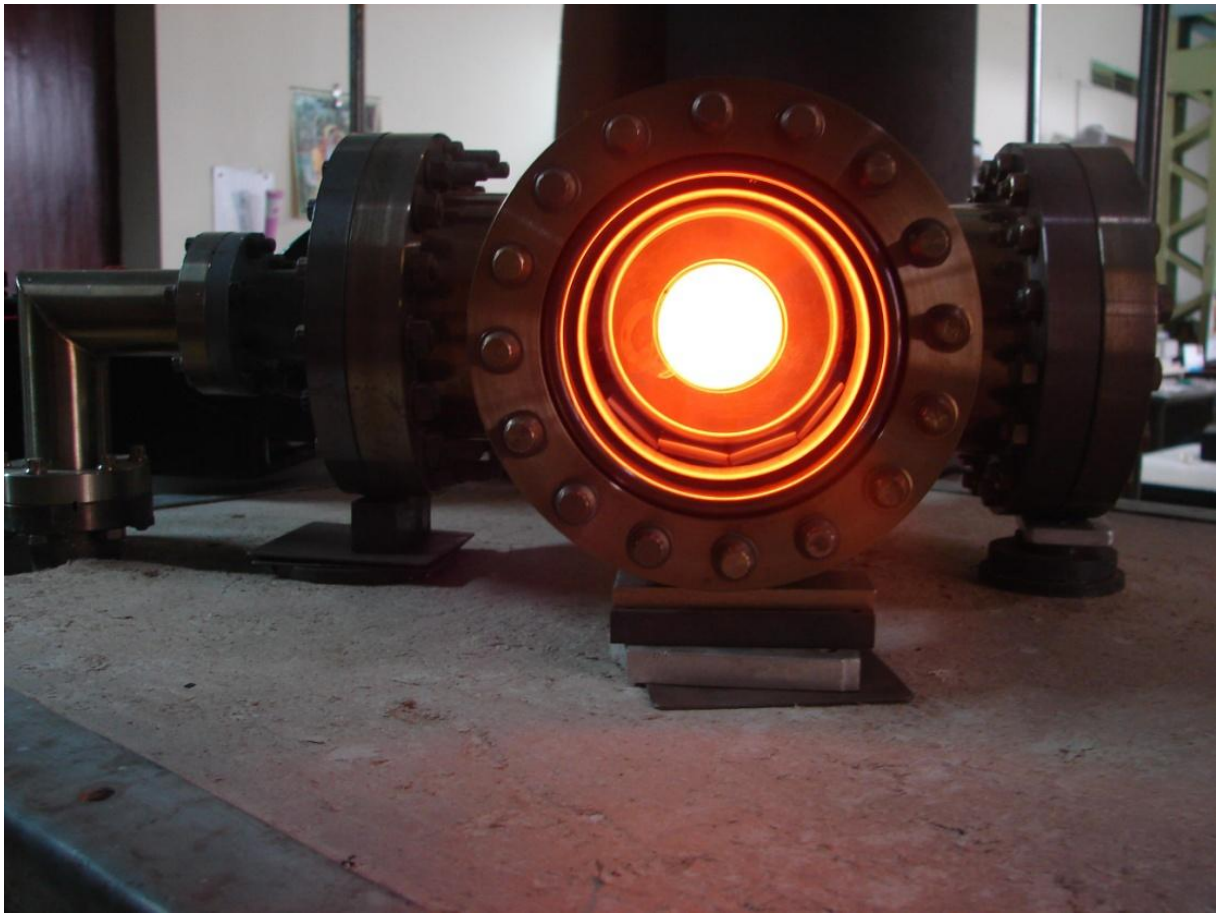

Sub-assembly Fabrication

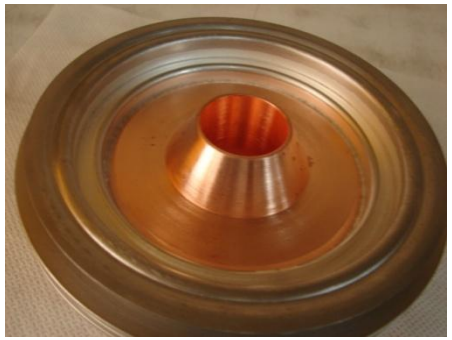

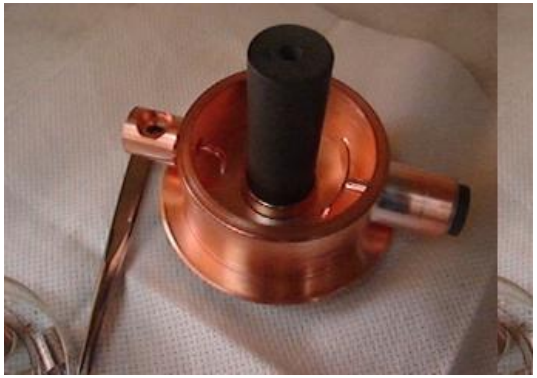

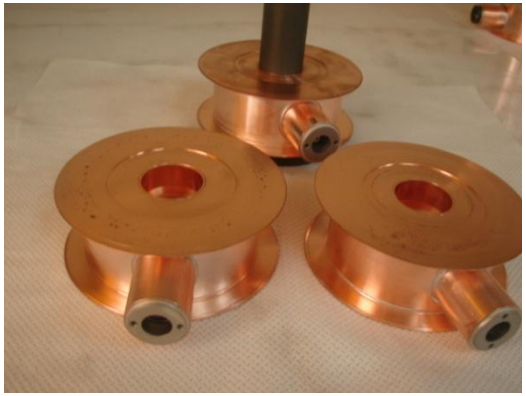

Cold testing of RF Section

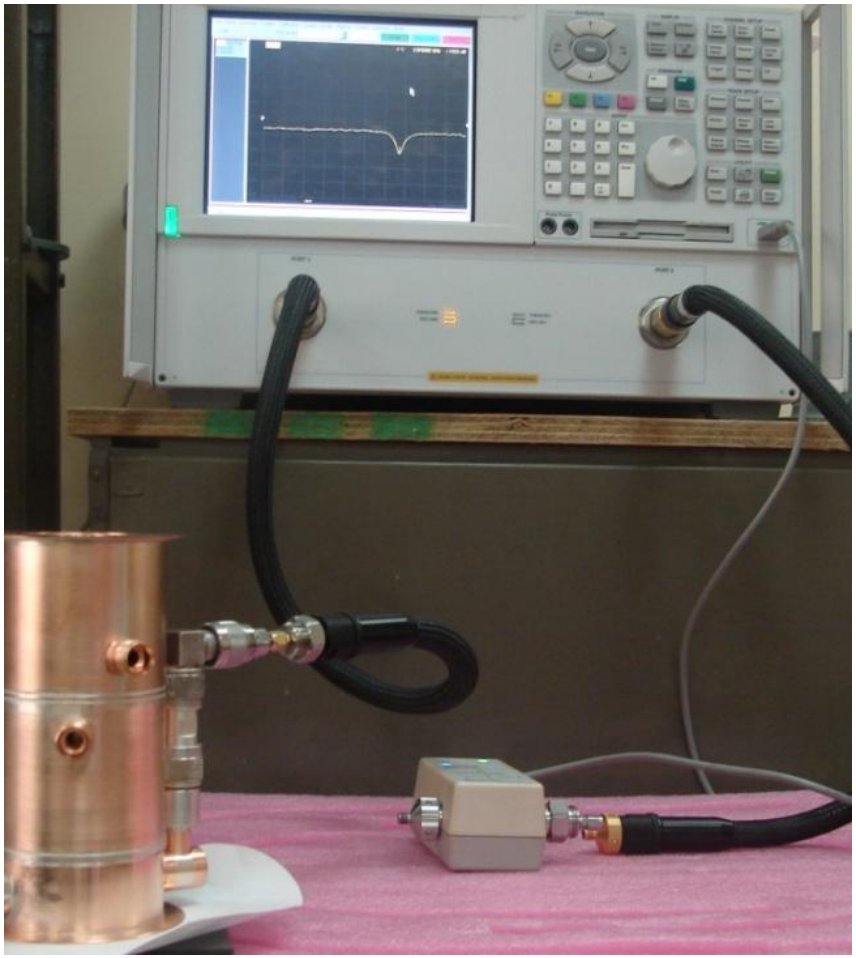

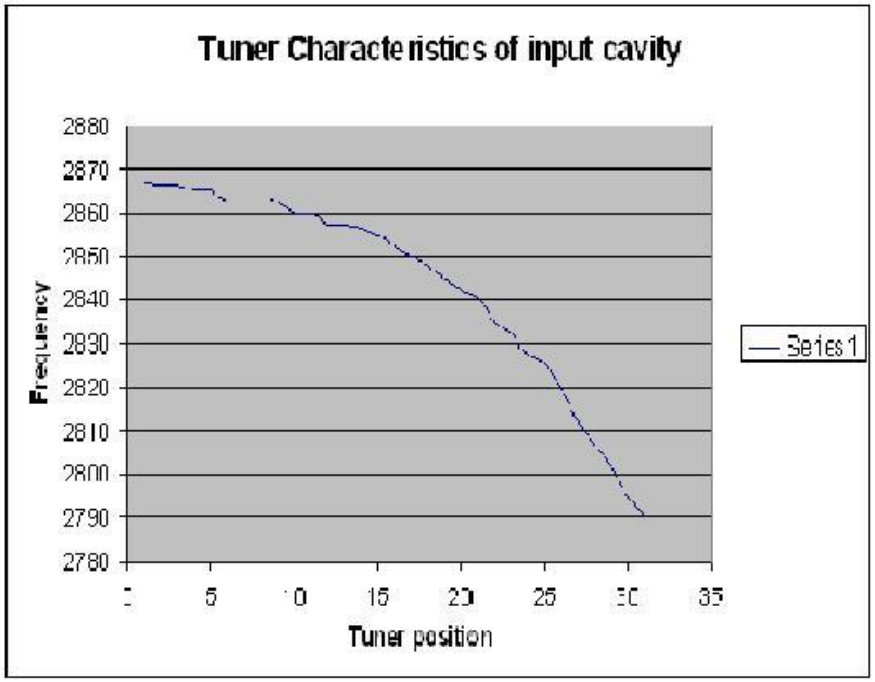

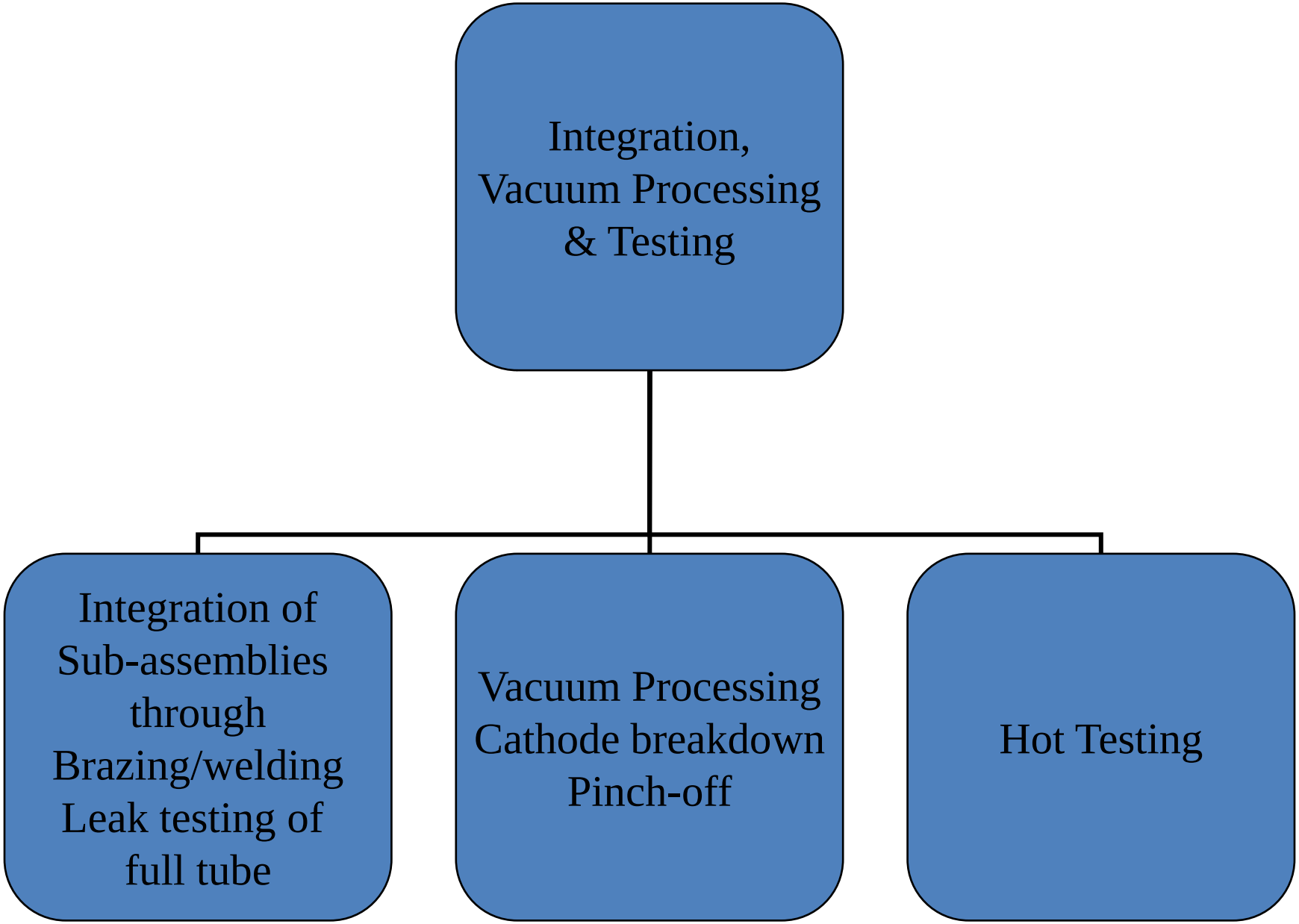
Integration, Vacuum Processing & Testing
Integration of Sub-assemblies through Brazing/welding Leak testing of full tube
Vacuum Processing Cathode breakdown Pinch-off
Hot Testing

Vertical Retort Furnace Brazing

TIG Welding

6 MW Pulse, 24 kW Average Power S-Band Klystron for BARC

Application

As Microwave source for use in 10 MeV Industrial RF Linear Accelerator developed by BARC

S-Band Klystron developed by CSIR-CEERI

User qualification of the Klystron by BARC

Frequency, Power v/s Size

Problems still to be solved

- Bringing down the manufacturing cost
- Necessity of high voltages for high power operations.
- *Higher beam voltage causes not only higher costs for the devices themselves, but also for many things in their periphery like power supplies and modulators, high voltage insulation, X-ray shielding, size of building* and environmental protection measures.

Multi Beam Klystron

- The Multibeam Klystron uses several electron beams and each beam propagates along its own individual transit time path through a resonator unit.
- The current and perveance of the individual beam are not high but the total current and perveance of the entire multibeam stream can be high.
- The operating voltage is significantly reduced (2 to 10 times) with a consequent reduction in the dimensions and weight of the devices and their power supplies.
- At the same time, the individual low perveance beams are better focused and bunched and give up their energies to the field of the resonator in an efficient manner resulting in an excellent performance

Design Issues

- The major challenge is to focus the off-axis electron beams. This requires substantial threading of the focusing magnetic field to each cathode with flux tubes shaped in a manner so as to have symmetrical convergence about each beam centerline.
- The transverse field should be negligible.
- One of the critical issues for gun design using off-axis electron beams is actual dimensions of the gun at operating temperature.
- The transverse field affects the beam transmission and some times is responsible for parasitic oscillations also.
- Magnetic screens are employed near the beam trajectories to suppress the transverse field and to restore the local cylindrical symmetry of the field.
- Values of $B1/Bn < 0.01\text{-}0.02$ have been practically achieved.

5: Multi beam Klystrons

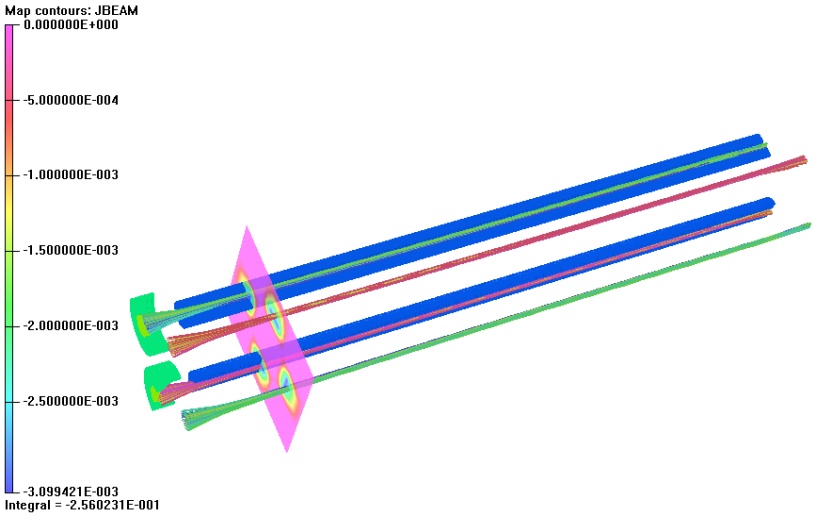

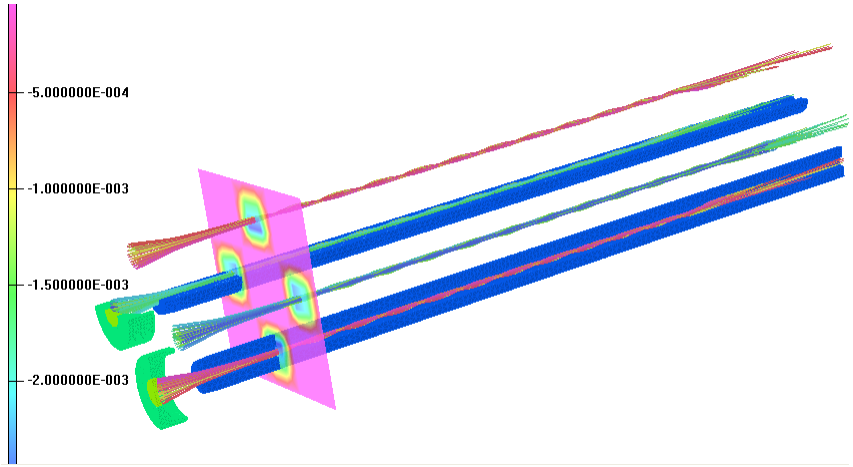

Electron trajectories through square aperture

Electron trajectories through circular aperture

Electron trajectories from OPERA 3-D simulations of a four beam electron gun with different apertures

Multi Beam Gun Simulation using MAGIC

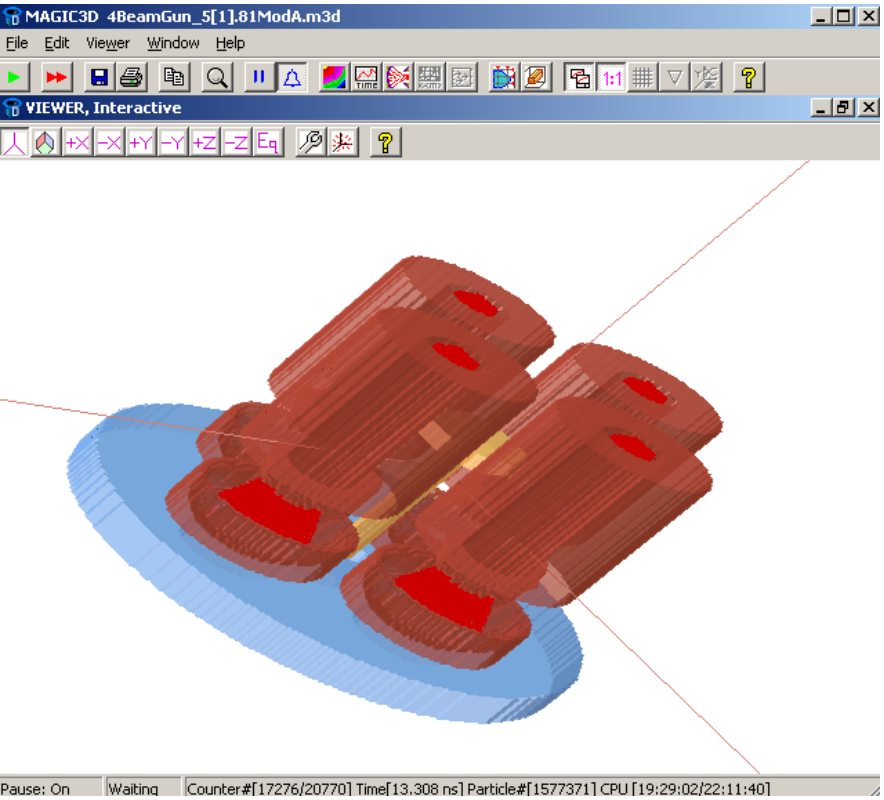

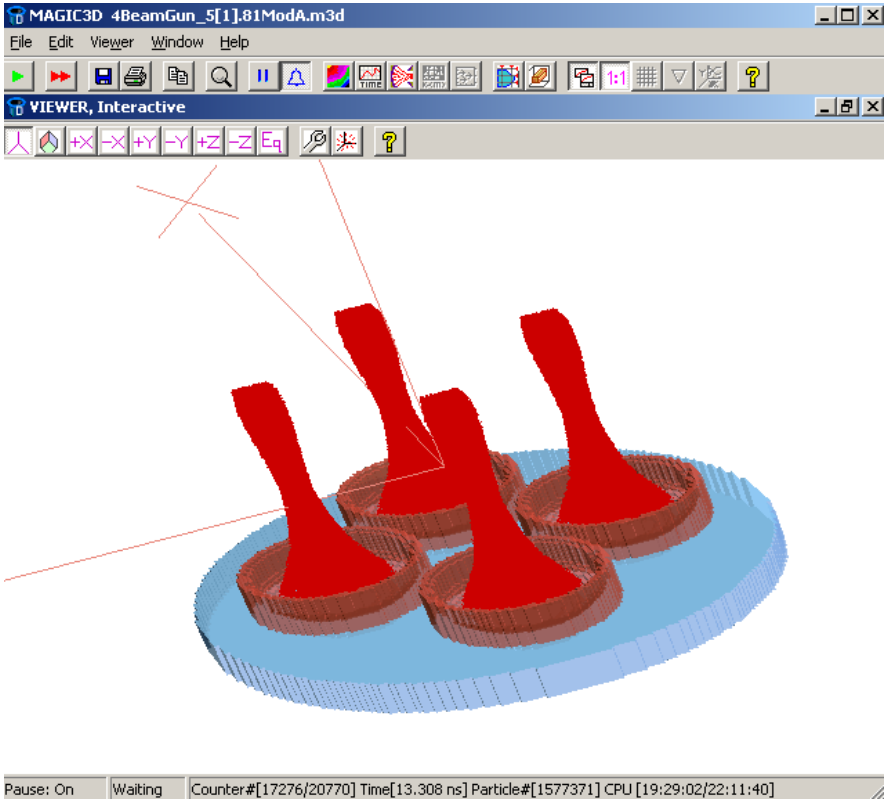

Different Parts of MBG

Parts of Multibeam RF Cavity

Available RF Sources –states of art

	Efficiency (%)	Bandwidth(%)	Gain (dB)	Relative Op Vol. Rel. Complexity of Op.
Gridded Tube/Diacrode	10-50	1-10	6-15	Low 3
Klystron	30-70	1-5	40-60	High 2
Magnetron	40-80			High 3
Helix TWT	20-40	30-120	30-50	High 3
Coupled Cavity TWT	20-40	5-40	30-50	High 3
Gyrotron	10-40	1	30-40	High 5
IOT	10-70	1-5	20-25	3

Out of most of available RF sources for accelerator use, *klystron* is the best device for average and peak power capability.

Characteristics of typical CW Super Power Klystrons

	TH 2089	VKP-7952	TH 2103C[a]
Manufacturer	Thales	CPI	Thales
Frequency (MHz)	352	700	3700
Beam voltage (kV)	100	95	73
Beam current (A)	20	21	22
RF output power (MW)	1.1	1.0	0.7
Gain (dB)	40	40	50
Efficiency (%)	65	65	44

Table 1 Specifications of Typical S-band High Peak Power Klystrons

Type		E3712	5045	PV3050
Institution	SLAC	Toshiba	SLAC	KEK
Frequency (MHz)	2998	2856	2856	2856
Peak Power (MW)	150	101	67	50
Efficiency (%)	>40	46	46	45
Voltage (kV)	535	422	350	308
Current (A)	700	522	414	359

Klystrons @ Stanford

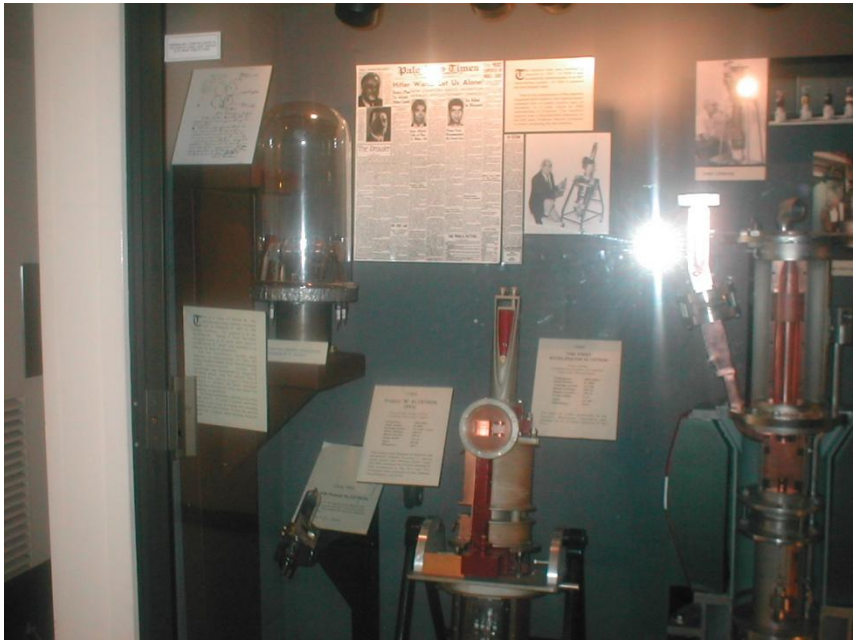

Klystrons @ Stanford

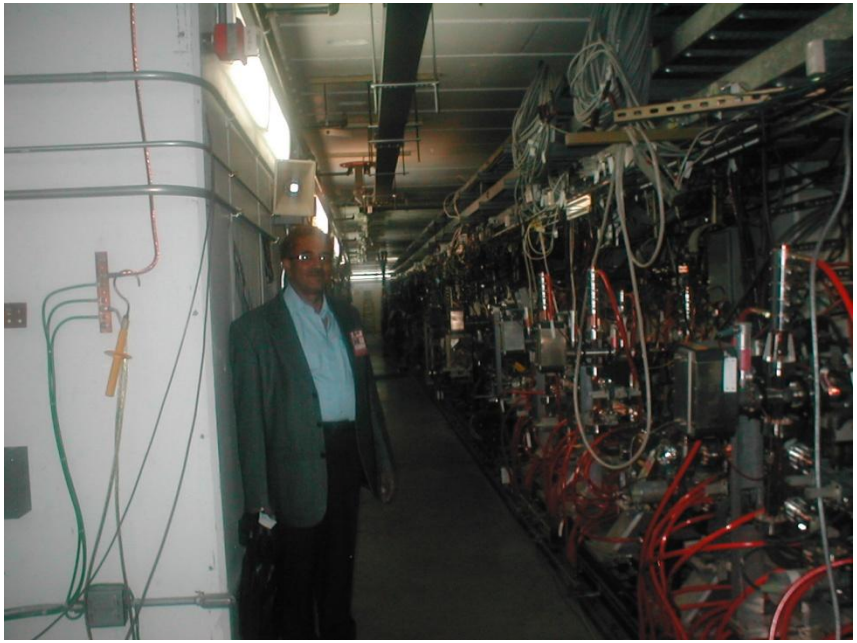

Linear Collider

- The ILC will be a high-energy e+ e- collider with a centre-of-mass energy reach up to 500 GeV, up-gradable to the 1 TeV range.
- International Technology Recommendation Panel decided that the International Linear Collider should be based on the 1.3 GHz superconducting RF technology developed by the TESLA Collaboration. Laboratories and research groups around the world are now committed to the ILC as their next big project.

Accelerator Modules

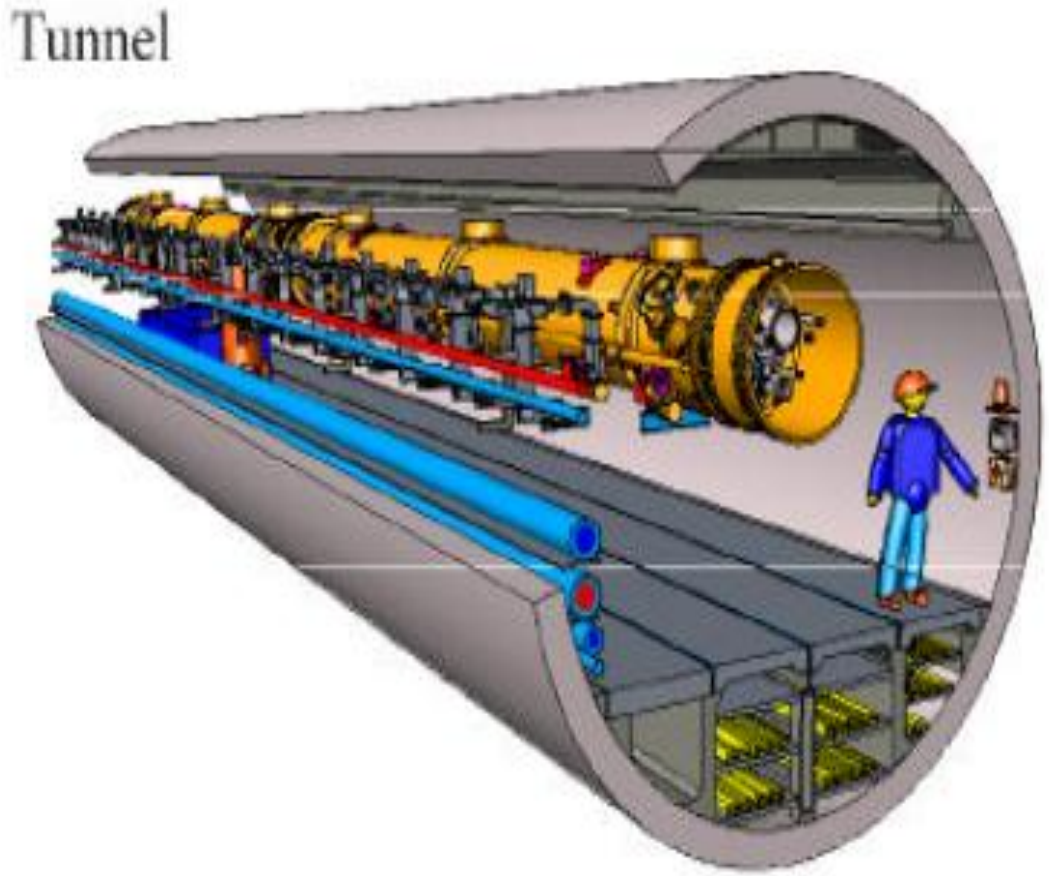

XFEL

The RF system of the European XFEL under construction at DESY in Hamburg, Germany, consists of 27 RF stations to be increased to 31.

The RF system provides RF power at 1.3 GHz for the superconducting cavities of the main linear accelerator, the cavities of the injector and the RF gun.

Each station consists of a 10MW multiple beam klystron as source of RF power

FEL Applications

- U.S. Navy has interest in material science applications such as surface hardening of propellers.
- FEL light can be used to produce carbon nanotubes on a graphite target. Transition Electron Microscopy at JLab indicates tube dia. (~1.4 nm) and small bundle size (~12 nm) can be produced.
- FEL light can produce amorphized steel surfaces providing 3x improvement in corrosion resistance.
- FEL light can create nitride coatings on metal surfaces. Commercial plasma method requires vacuum to work. Competing laser methods do not produce the same quality coatings

Main Users for Accelerators in India

- BARC
- RRCAT
- SAMEER
- IPR
- IUAC

BARC, Mumbai

X Rays Radiography for Cargo Inspection & Security Systems

This utility has immense potential in the industry and can play a vital role in strengthening the security of a nation, too. Many countries are now employing the X rays cargo scanning systems for checking the inflow of illegal arms, drugs, narcotics, ammunitions, explosives etc. By installing these devices flow of such goods can be stopped

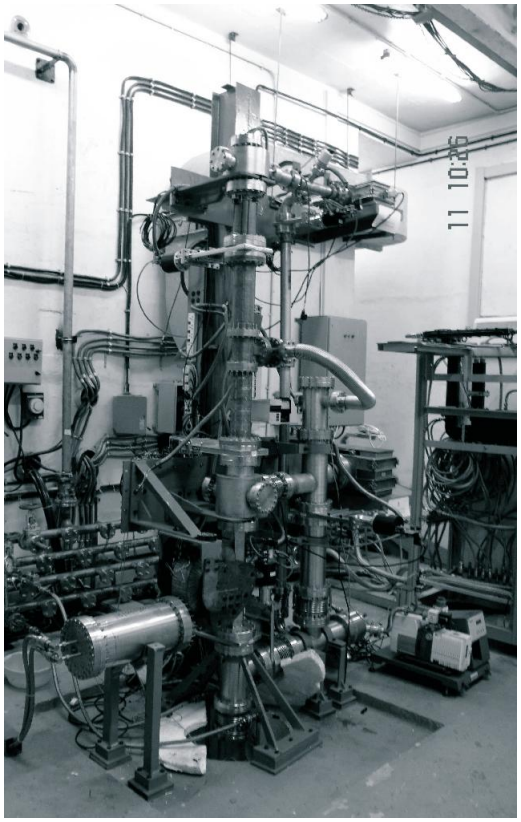

Industrial Linear Accelerator

Electrons have mass and an electric charge and therefore, are absorbed fairly quickly as they penetrate dense materials. For food products with densities similar to water (1 g/cm3), 2-sided treatment with e-beam will penetrate through approximately 3.5 inches (9 cm). However, in reality, packages with depths much greater than 3.5 inches can be decontaminated or disinfested with e-beam because most commercially packaged foods have a lower overall density

RF Source: 6 MW peak, 24 kW av. S-band Klystron

Proton Accelerator

- 350 MHz/700 MHz MW CW Klystrons are used to accelerate proton beam to GeV energy level. This is then made to hit a target to produce neutrons

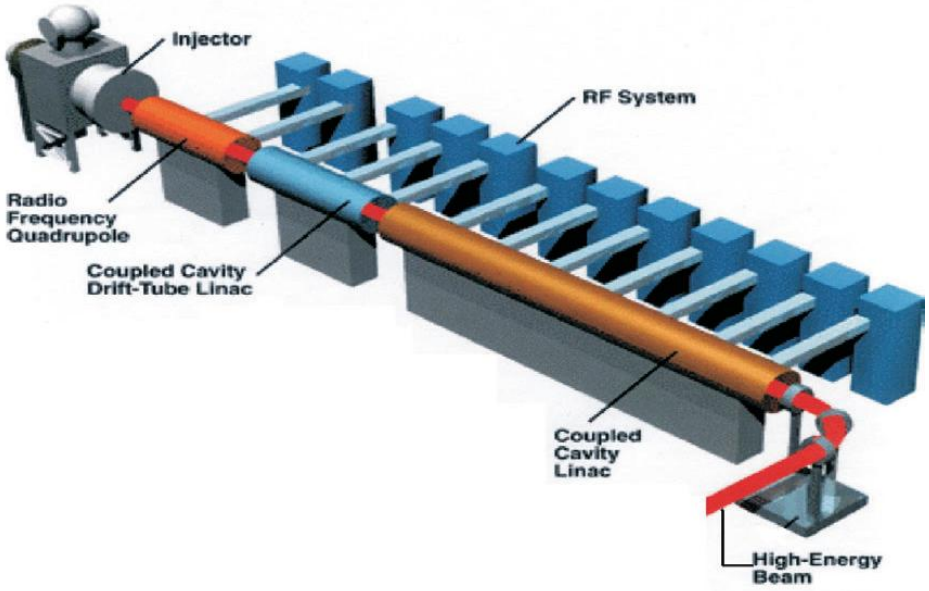

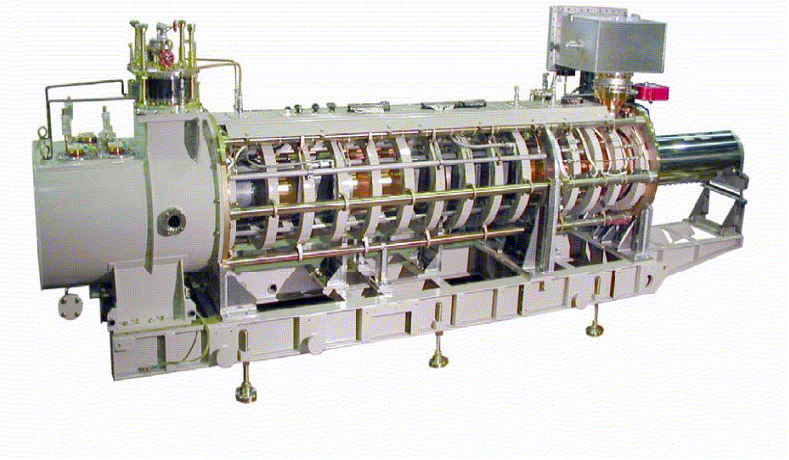

ADSS

A **subcritical reactor** is a nuclear fission reactor that produces fission without achieving criticality. Instead of a sustaining chain reaction, a subcritical reactor uses additional neutrons from an outside source. A reactor coupled to a particle accelerator to produce neutrons by spallation is called an **Accelerator-Driven System** (**ADS**).

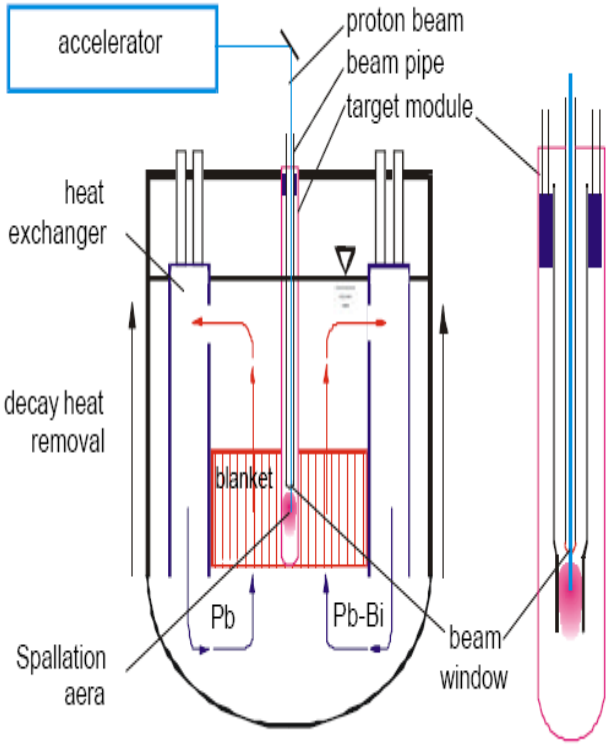

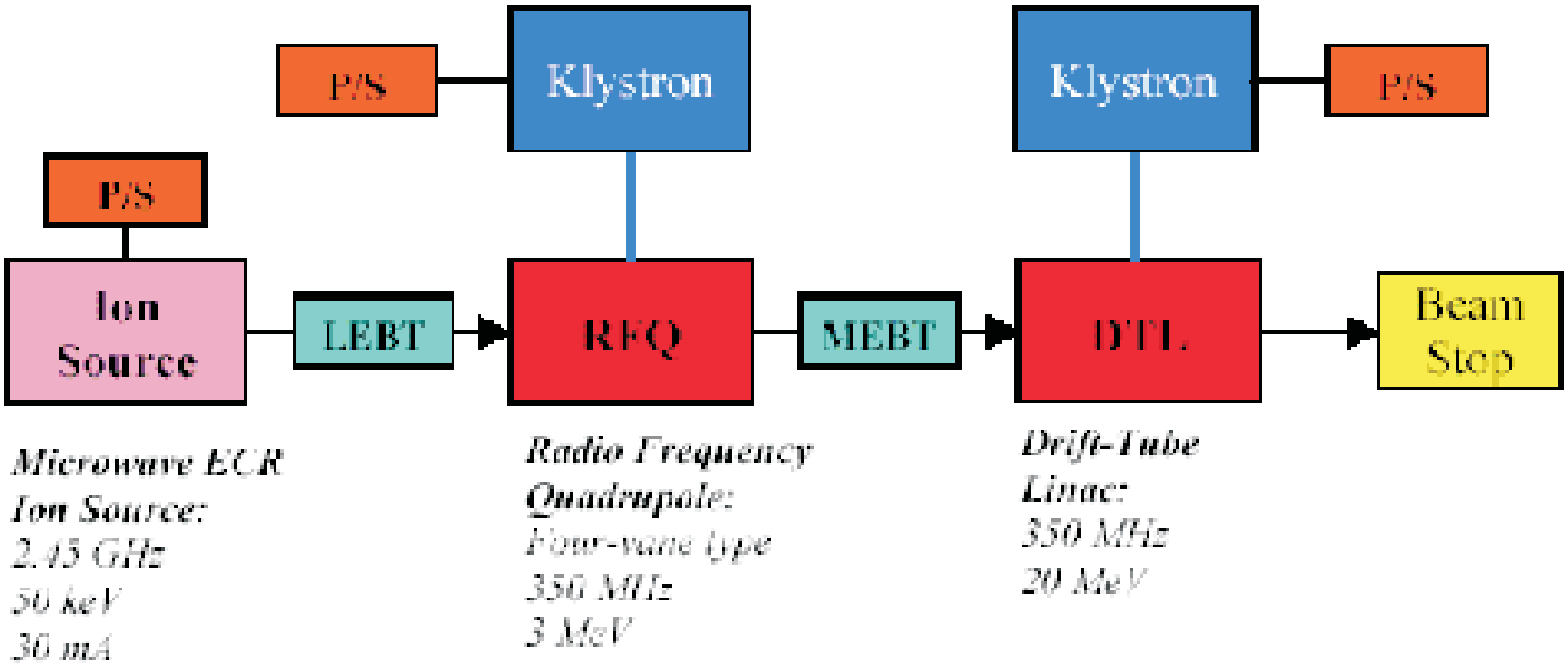
P/S
Klystron
Klystron
P/S
P/S
Ion Source
LEBT
RFQ
MEBT
DTL
Beam Stop
Microwave ECR Ion Source:
2.45 GHz
50 keV
30 mA
Radio Frequency Quadrupole:
Four-vane type
350 MHz
3 MeV
Drift-Tube Linac:
350 MHz
20 MeV

RRCAT, Indore

A 10 MeV, 10 kW Linear accelerator based electron beam radiation processing facility is being set up at RRCAT

Foods and agricultural products are treated with ionizing radiation to accomplish different objectives like reduction of pathogenic bacteria and parasites that cause food borne diseases; or lengthening the shelf-life of fresh fruits, vegetables by decreasing the normal biological changes associated with growth and maturation processes, such as ripening or sprouting. Radiation processing of food has become important due to mounting concern over food born diseases, and growing international trade in food products that must meet stiff import standards of quality and quarantine.

RF Source: 6 MW peak, 24 kW av. Power S-band Klystron

They have taken-up R&D activity on development of various subsystems for a 100 MeV 350 MHz (pulse and high duty) Proton Linear Accelerator.

RF source: 350 MHz & 700 MHz, 250/500/1 MW CW Klystrons

INDUS-2

The injection energy for Indus-2 is 700 MeV and the electrons in this energy will be injected into it from the 700 MeV synchrotron After injection, the energy of the beam will be raised to 2.5 GeV within a few minutes. The beam half lifetime at 2.5 GeV is expected to be about 24 hours. This will be achieved using six RF cavities operating at a total voltage of 1.5 MV at a frequency of 505.812 MHz

The RF system employs four numbers of elliptical cavities to generate 1500 kV accelerating RF voltage. Each RF cavity is powered by 64 kW RF amplifier through 6 1/8" co-axial transmission line. Modular in nature, four numbers of 64 kW RF transmitters have been installed to energize these cavities. Each RF module comprises of a 64 kW klystron amplifier including 20 kV HV power supply, a 10 W solid state driver amplifier, and low level control loops

The RF amplifiers are based on 64 kW multi-beam, integral-cavity klystrons, KY400, with dispenser type of cathode

SAMEER

- **4 MeV Linear accelerator**
- **For cancer treatment.**

Replaces cobalt-60 machine which is being phased out in many countries

Three machines installed, at

i) PGI, Chandigarh
ii) CCWH, Thakurpukur, Calcutta
iii) GMCH, Chandigarh
Fourth machine awaiting commissioning at Wardha, Maharashtra

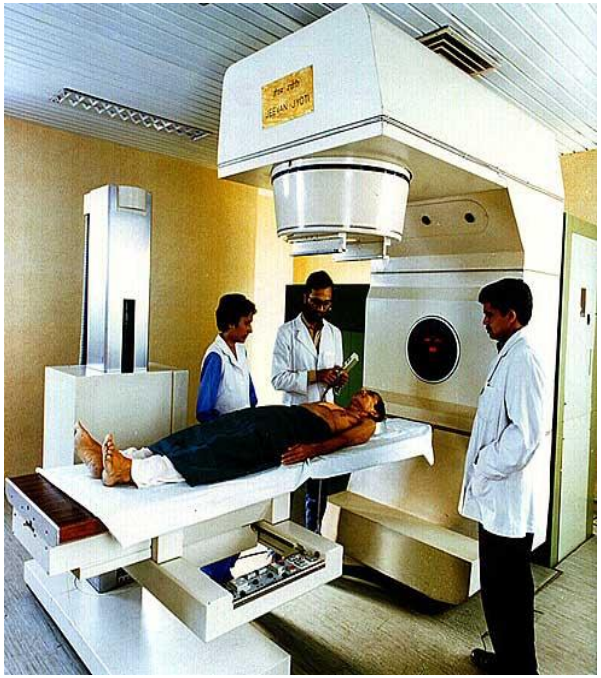

15 MeV medical LINAC Machine.

For cancer therapy.

Higher capability than 4MeV machine.

RF Source: 6 MW peak, 12 kW av. S-band Klystron

Plasma Heating Methods

- **Ohmic Heating and Current Drive**

  Currents up to several million amperes are induced in the plasma typically via the transformer or solenoid. The current inherently heats the plasma – by energizing plasma electrons and ions in a particular toroidal direction. A few megawatts of heating power is provided in this way.

- **Neutral Beam Heating**

  Beams of high energy, neutral deuterium or tritium atoms are injected into the plasma, transferring their energy to the plasma via collisions with the plasma ions. Tens of MW of additional power is available from the NBI heating systems.

- **Radio-Frequency Heating**

  The plasma ions and electrons are confined to rotating around the magnetic field lines in the tokamak, electromagnetic waves of a frequency matched to the Cyclotron frequencies of ions or electrons are able to resonate – or damp its wave power into the plasma particles.

  Waves can also be used to drive current in the plasma – by providing a "push" to electrons travelling in one particular direction. These so-called Lower Hybrid microwaves accelerate the plasma electrons to generate a plasma current of up to 3 mega amperes.

Plasma Heating Methods

- Waves have been launched in plasma in wide ranges of RF frequencies:

Ion Cyclotron Waves 20 – 120 MHz

Lower Hybrid Waves 1 – 10 GHz

Electron Cyclotron Waves 30-200 GHz

- Very effective heating has been achieved with ICRH, LHCD and ECRH with electron temperatures in excess of 10 keV achieved in Joint Europian Torus (JET)

LHCD Heating

- Main role of LHCD system is
  - ❖To provide off-axis current drive
  - ❖To assist ramp-up of plasma current
  - ❖ To provide control on the plasma current profile

Klystron: The RF Source for LHCD

- Conventional Klystrons have been used as RF source for LHCD
- They are robust and reliable with good efficiencies (45-60%)
- Can be easily controlled in phase which is quite important for current drive applications.

System	Power	Freq	Pulse length	Numbers
Tore_Supra	0.5 MW/0.7 MW	3.7 GHz	30 s	16
JT-60	1 MW	2 GHz	10 s	24
JET	0.6 MW	3.7 GHz	10-20 s	24

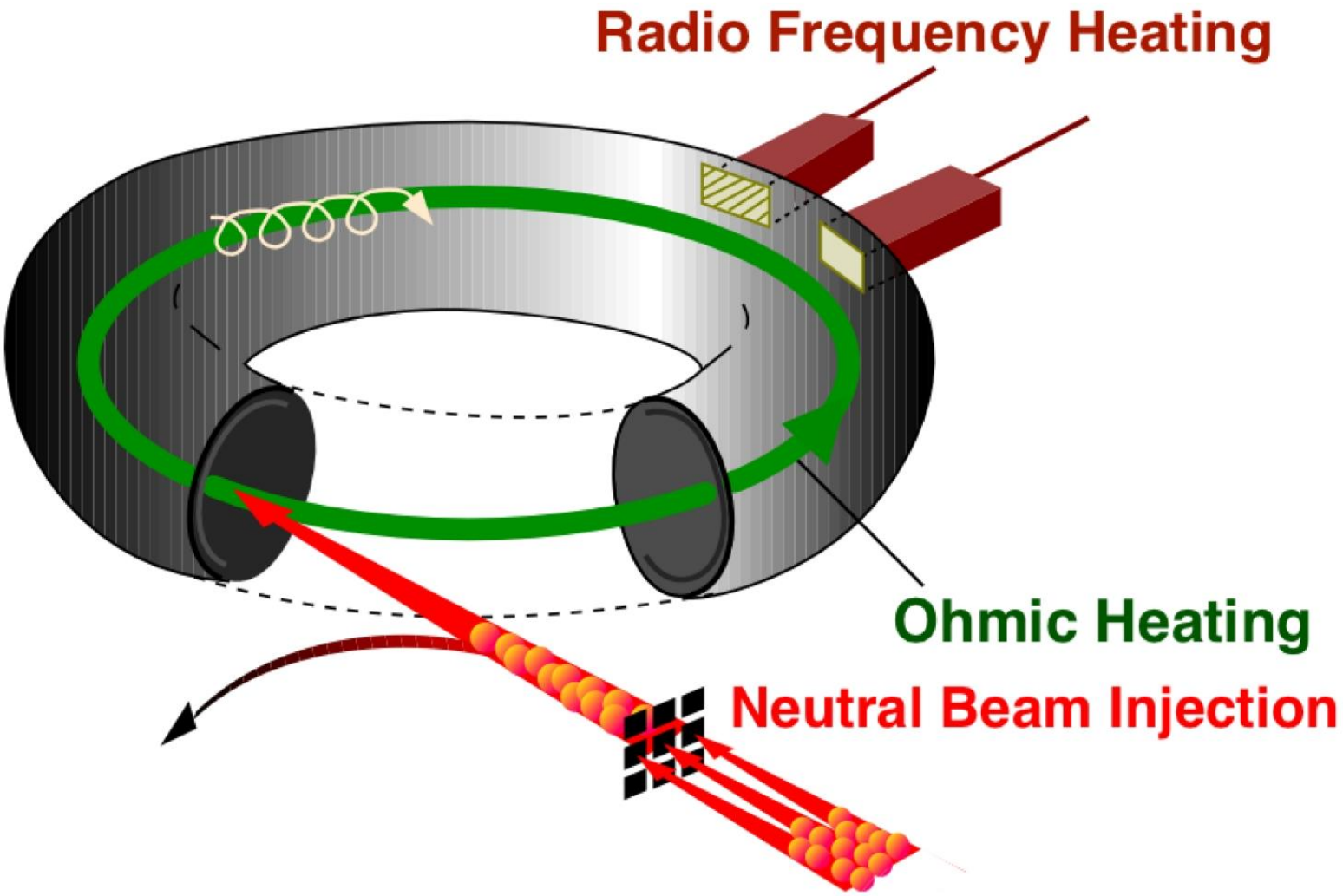
Radio Frequency Heating
Ohmic Heating
Neutral Beam Injection

Institute for Plasma Research

Steady State Superconducting Tokamak

The objectives of SST-1 include studying the physics of the plasma processes in tokamak under steady state conditions and learning technologies related to the steady state operation of the tokamak.

Hydrogen gas will be used and plasma discharge; duration will be 1000 s. Auxiliary current drive will be based mainly on 1.0 MW of Lower Hybrid current drive (LHCD) at 3.7 GHz. Auxiliary heating systems include 1 MW of Ion Cyclotron Resonance Heating (ICRH) at 22 MHz to 91 MHz, 0.2 MW of Electron Cyclotron Resonance heating (ECRH) at 84 GHz

RF Source :

2 nos. of TH2103D klystron, each rated for 500 kW, CW operation at 3.7 GHz. High power operation of klystron into water dummy load for more than 1000 seconds.

352.2 MHz, 100 kW CW Klystron development

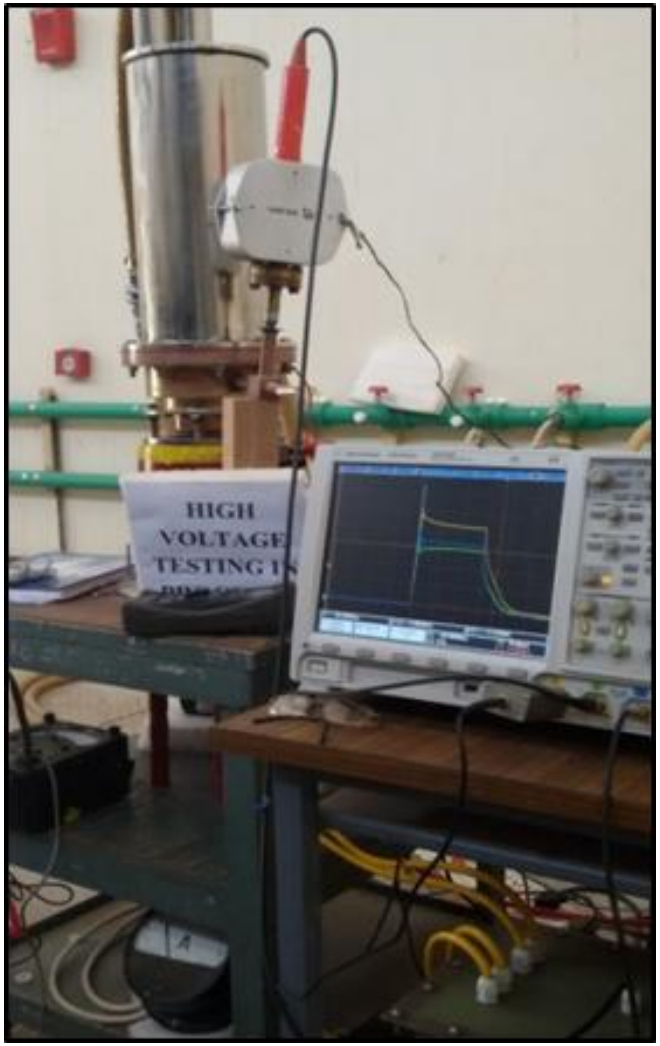

Fabrication of Cavity Parts

5 GHz, 250 kW CW Klystron

Beam profile in RF section showing plots of power & voltage in output cavity

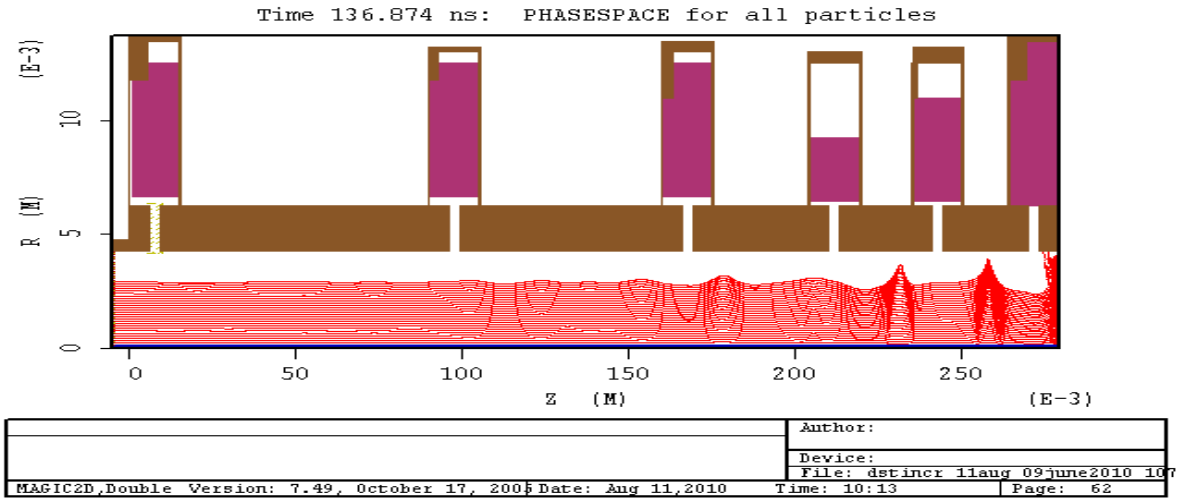

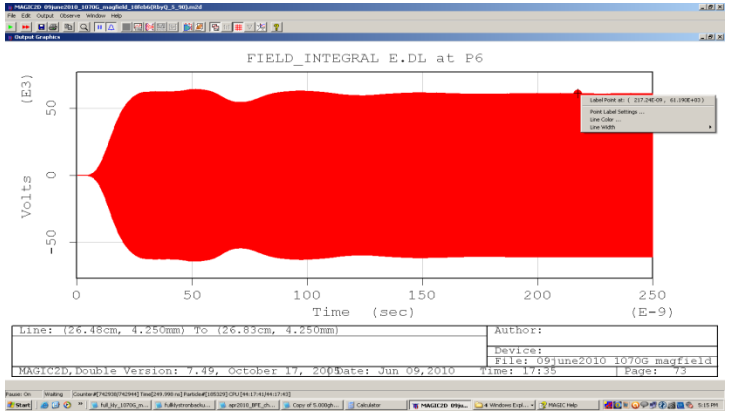

Voltage in output cavity ~ 61 kV

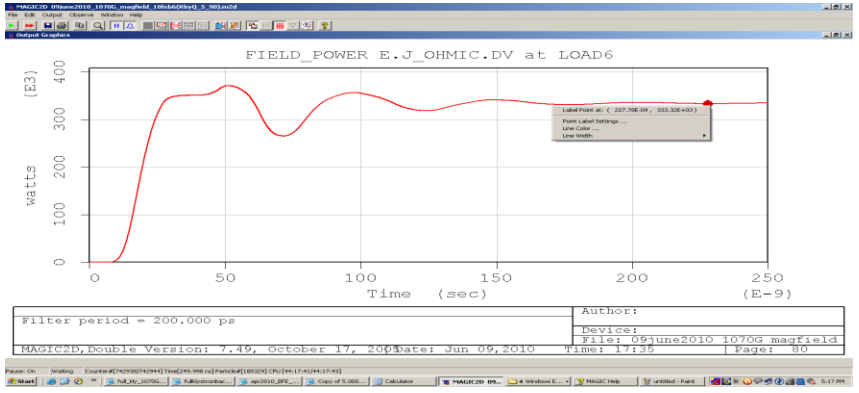

Efficiency = 53%

Output Power = 333 kW

2.6 MW S-Band Tunable Pulse Magnetron Recently Developed at CSIR-CEERI

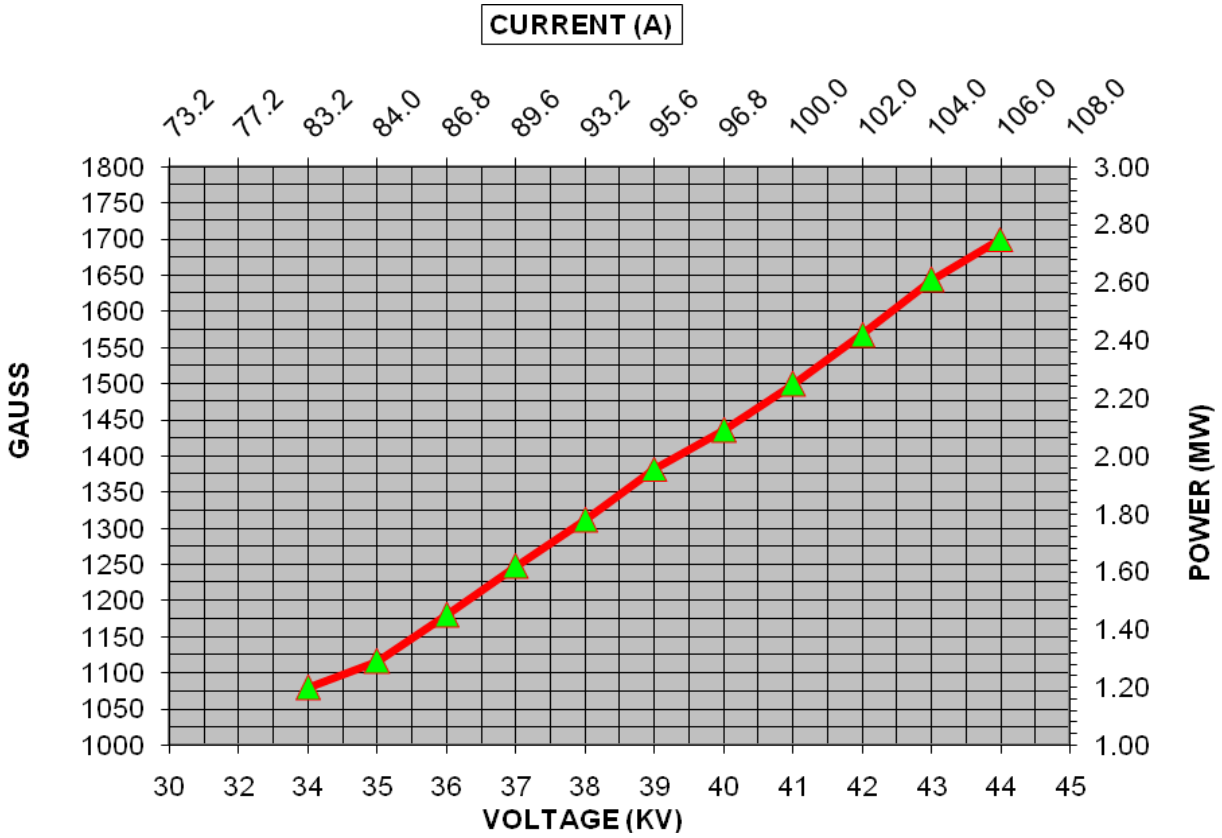

Recommended Parameters for Various Power Levels

Design & Development of 3.0 S-Band Tunable Pulse Magnetron (On-going Project)

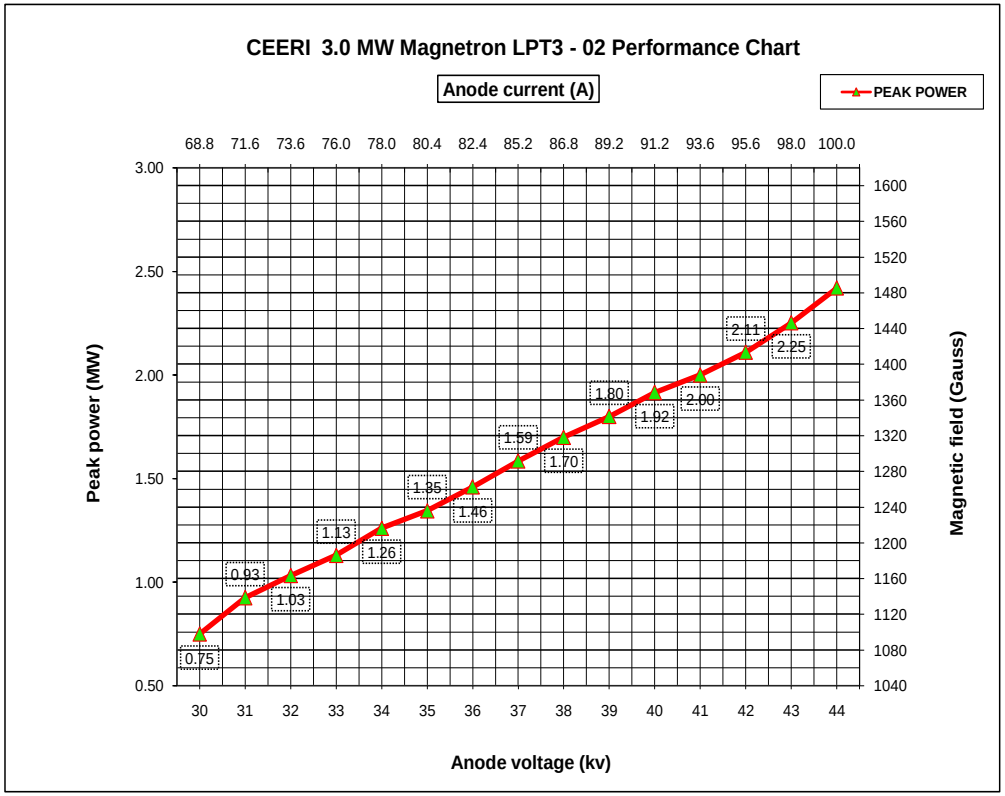

Measured Parameters for Various Power Levels

High Power Coaxial RF Coupler for BARC

Application

For coupling 50 kW RF Power at 352.2 MHz from a microwave source to Low Energy High Intensity Proton Accelerator (LEHIPA)

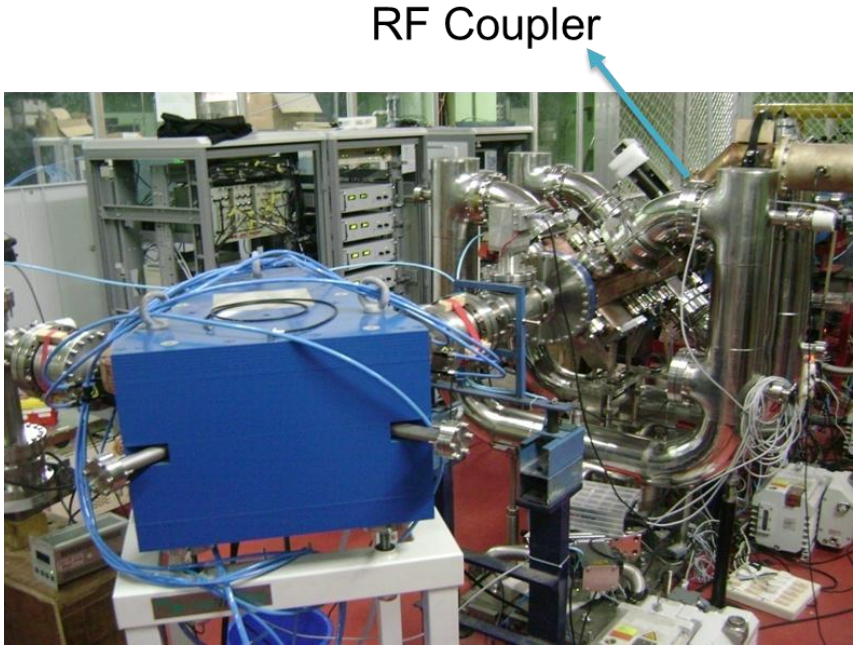

High Power Coaxial RF Coupler developed at CSIR-CEERI, Pilani

Coupler in use at BARC in LEHIPA System

Coaxial RF Couplers for Proton Accelerator

50 kW Coupler

250 kW Coupler

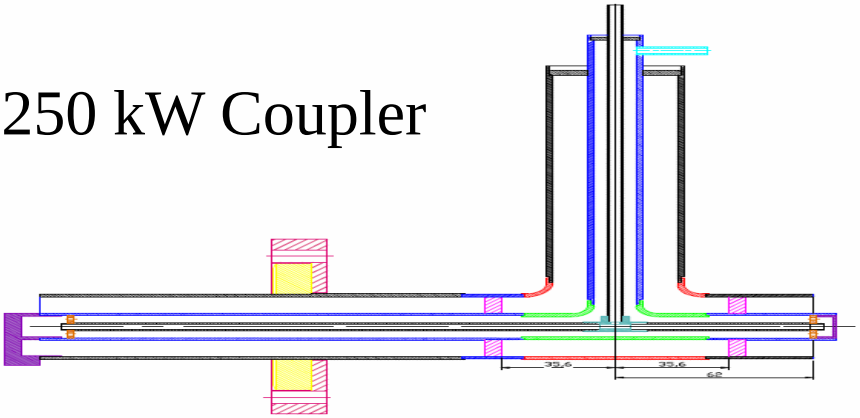

Engineering design of the coupler

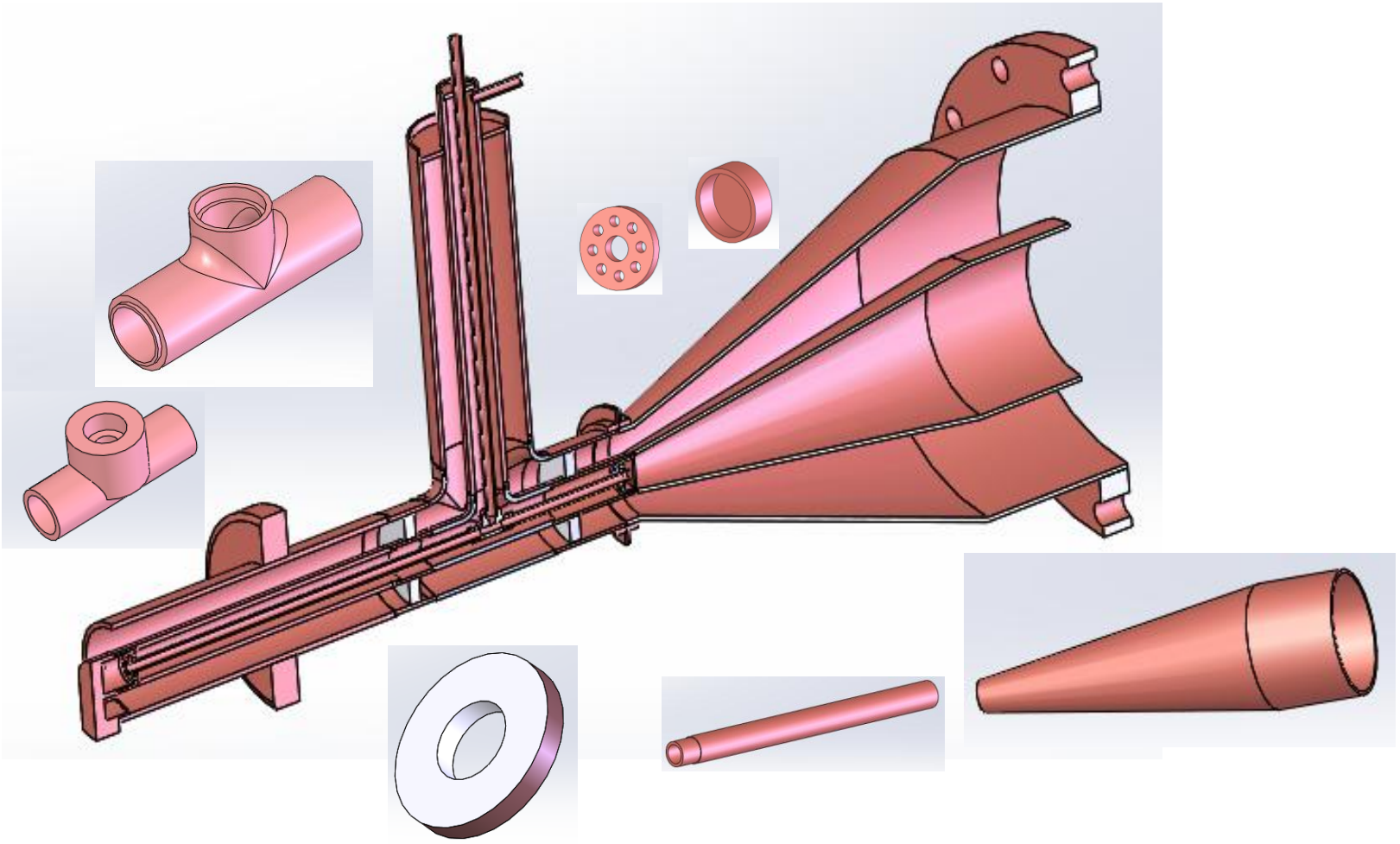

Iris Coupler for LEHIPA

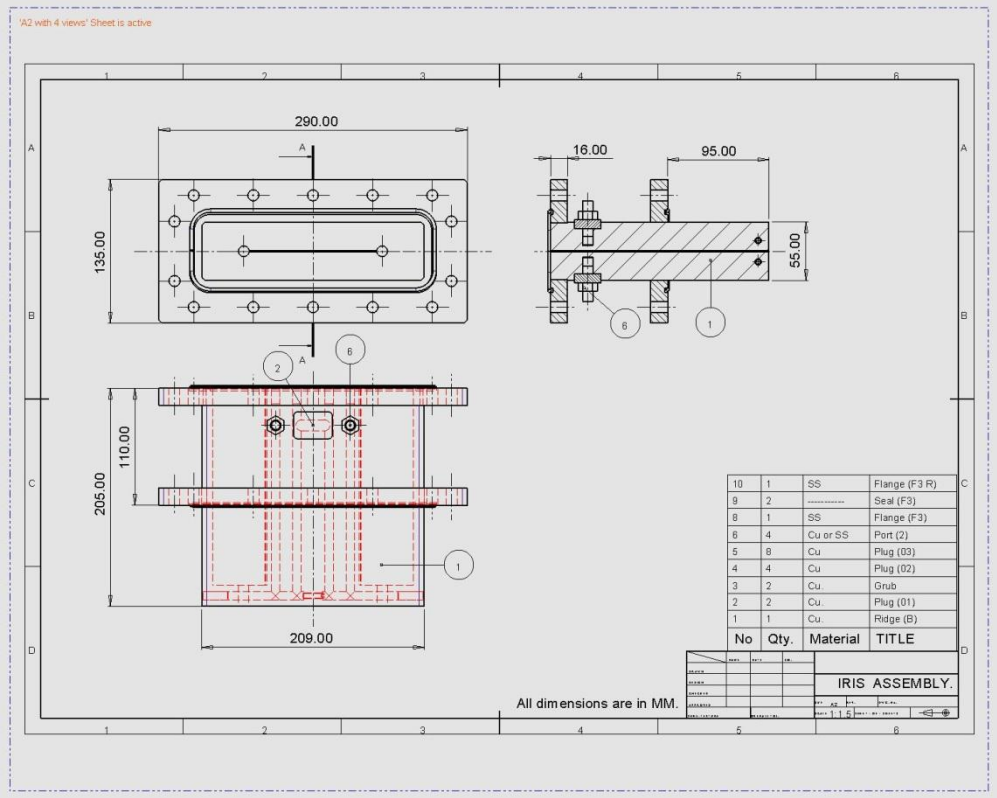

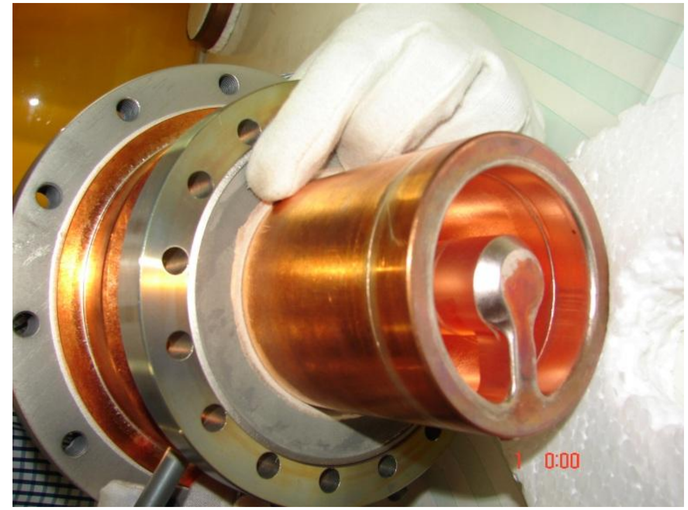

Coupler developed at CSIR-CEERI

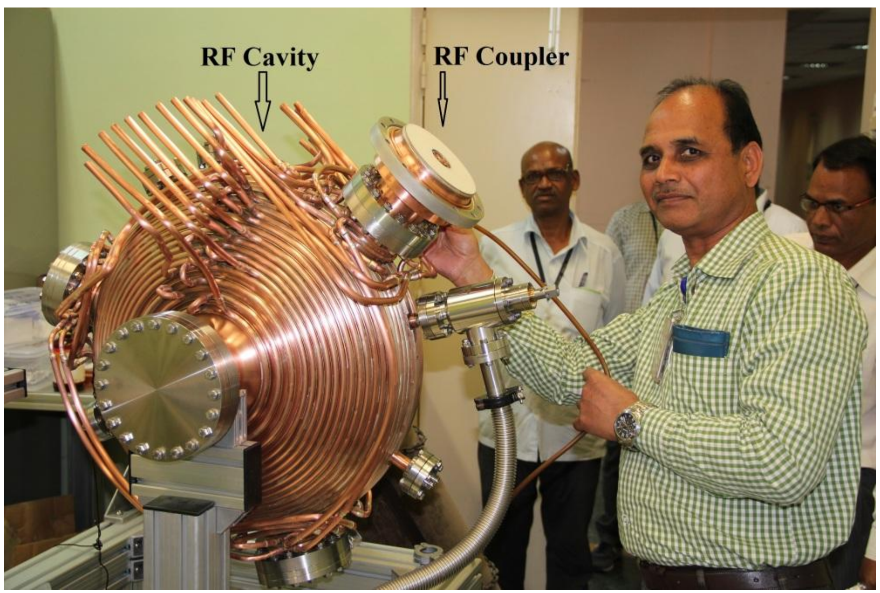

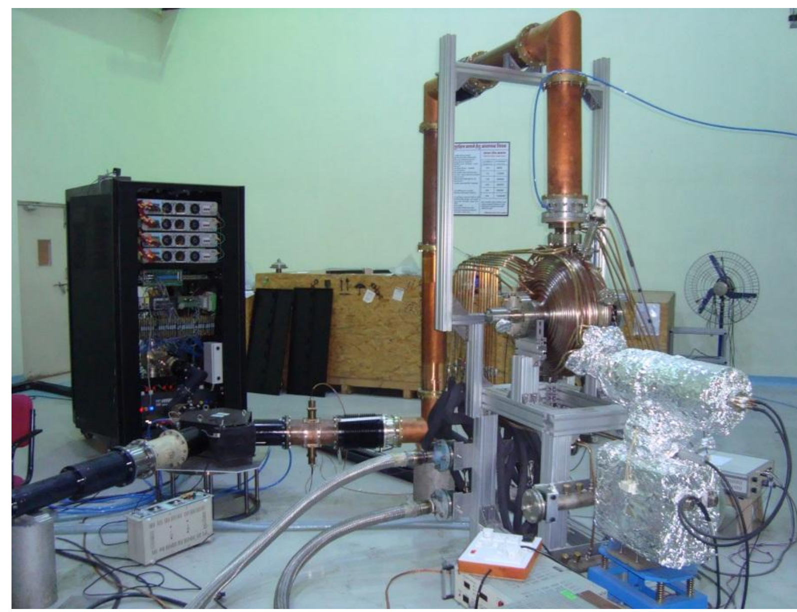

Coupler connected to Indus-2 cavity at RRCAT : 65 kW Power coupled successfully

Multi-Ceramic RF Window

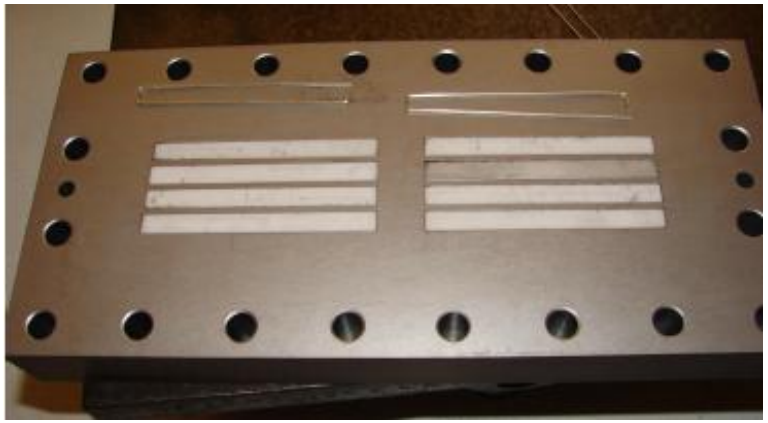

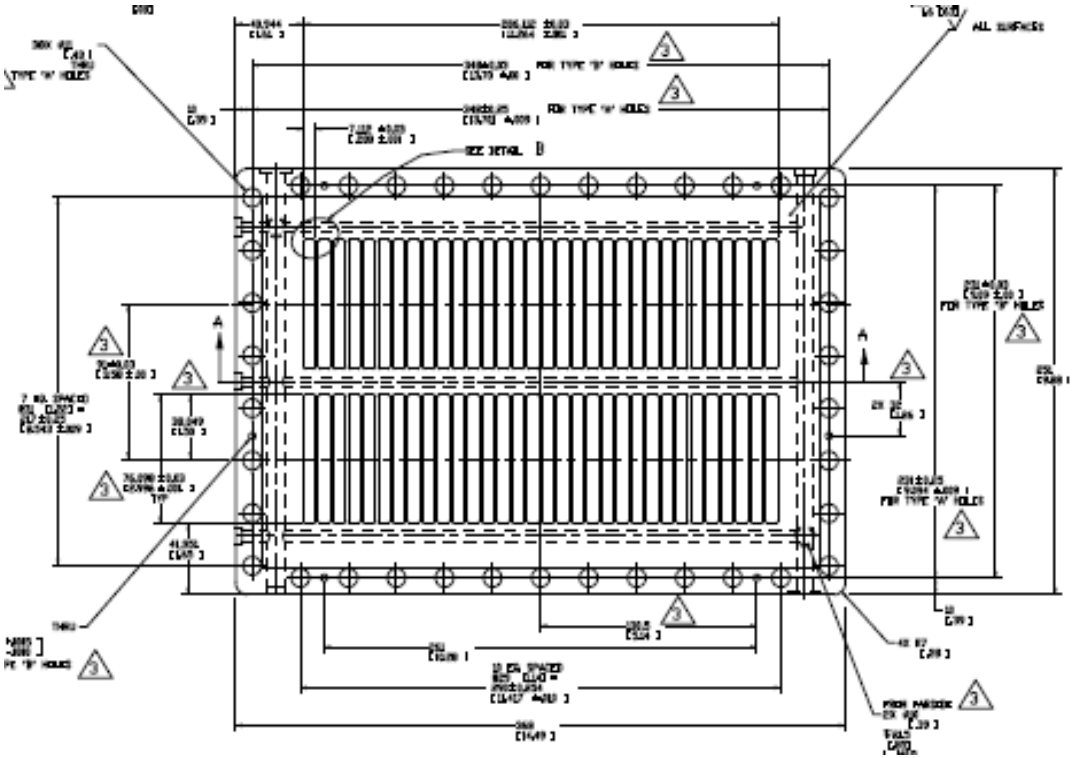

Conclusion

- Microwave tubes, particularly Klystrons, are heart of linear accelerators in laboratories and medical facilities around the globe.
- These devices are difficult to manufacture and for decades they are produced just by a few laboratories/vendors.
- India has large requirement of such devices for defense, communication, medical and advanced scientific applications
- Their demand shall grow in foreseeable future as no other category of devices have matching gain, efficiency and power performance
- Their development activities at the laboratories, academic institutes and industry should be further nurtured and supported to meet large indigenous demand.

THANKS

MICROWAVE TUBES: PROSPECT IN 21ST CENTURY

Dr AK Sinha

Gyrotron Laboratory
Central Electronics & Engineering Research Institute
(CSIR-CEERI), Pilani-333031, India

21st Century Ambition

CONTENT:

- INTRODUCTION
- GLOBAL SCENARIO
- INDIAN SCENARIO
- PROSPECT

Applications of MW Tubes

Industrial heating

Waste remediation

Electron cyclotron resonance heating (ECRH) of fusion plasmas to ~10^8 K for controlled thermonuclear reactor

Nonlinear spectroscopy

Power beaming

- Satellite power station (SPS)
- City lighting
- Showering nitrogen fertilisers on earth
- Extension of radio range
- Atmospheric purification of freons
- Ozone generation

Electronic warfare: conventional (ECM and ECCM) and directed energy weapons involving HPM

Applications

Point-to-point communication — more channels, focused radiation

Satellite communication

Deep space and specialised satellite communication

Satellite-to-home communication

High information density communication

Long-range, high resolution radar

Medical applications

Advanced high gradient RF linear accelerators

Plasma diagnostics and chemistry

Material processing (including ceramic sintering and joining)

Micro-and Millimeter Waves

Microwaves = Electromagnetic Waves

Frequency, Wavelength

($\lambda = c / f$),

Amplitude (A),

Power ($|A|^2$),

Phase, Polarisation, Reflection,Refraction,

Diffraction, Interference

300 MHz (UHF) – 300 GHz (Millimeter Waves) :

UHF (ultra high frequencies)

f = 300...3000 MHz; λ_0 = 1...0.1 m (Decimeter Waves)

SHF (super high frequencies)

f = 3...30 GHz; λ_0 = 10...1 cm (Centimeter Waves)

EHF (extremely high frequencies)

f = 30...300 GHz; λ_0 = 10...1 mm (Millimeter Waves)

Designation of frequency ranges

VLF	<30 kHz
LF	30-300 kHz
MF	0.3-3 MHz
HF	3-30 MHz
VHF	30-300 MHz
UHF	300-3000 MHz
SHF	3-30 GHz
EHF	30-300 GHz

Microwave communication/ radar	
L	1.12-1.70 GHz
S	2.60-3.95
C	3.95-5.85 GHz
X	8.20-12.40 GHz
Ku	12.40-18.00 GHz
K	18.00-26.50 GHz
Ka	26.50-40.00 GHz
V	40.00-60.00 GHz
E	60.00-90.00 GHz
F	90-140.00 GHz

(The highest frequency ever realised by a vacuum/ microwave-tube source is 1200 GHz from a Russian BWO)

Classification of Microwave Tubes

- Microwave tubes are based on the mechanism of conversion of spontaneous radiation from individual electrons into coherent radiation by bunching the electrons in a proper phase with respect to the RF wave by adjusting the beam, magnetic field and interaction structure parameters

- Accordingly, one may classify microwave tubes in different possible ways, such as (i) O-type and M-type (O-type is an abbreviation of the type TPO — tubes à propagation des ondes, and M-type is an abbreviation of the type TPOM — tubes à propagation des onde à champs magneique); (ii) slow-wave and fast-wave types; (iii) longitudinal space-charge wave, transverse space-charge wave, and cyclotron mode interaction types; (iv) kinetic and potential energy conversion types; and (v) Cerenkov, transition, and bremsstrahlung radiation types

- In an O-type microwave tube, a DC axial magnetic field constrains the electrons to move in the interaction structure as a linear beam. The device is hence also called a linear beam tube. In such a type of tube, the magnetic field does not take part in the beam-wave interaction process; the longitudinal space-charge wave interaction takes place; the axial kinetic energy of the electron beam is converted into electromagnetic waves; and a slow waveguide mode is destabilised

- On the other hand, in an M-type tube, a DC magnetic field, applied perpendicular to a DC electric field, takes part in the interaction process. In this type, the transverse space-charge wave interaction takes place and the potential energy of the electron beam is converted into electromagnetic waves
- The microwave tubes like TWT and klystron belong to the O-type, while those like magnetron and CFA belong to the M-type. In the devices like gyrotron, a fast cyclotron wave interacts with a fast waveguide mode, and the magnetic field takes a dominant role in the cyclotron resonance instability mechanism of the device

- The TWT may also be classified as a Cerenkov radiation type of microwave tube in which the electron beam velocity is greater than the phase velocity of electromagnetic waves in the interaction medium

- Klystron belongs to the family of transition radiation type of microwave tubes, in which the electrons pass through the boundary between two media with different refractive indices or pass through perturbations in a medium in the form of conducting grids or a gap between conducting surfaces

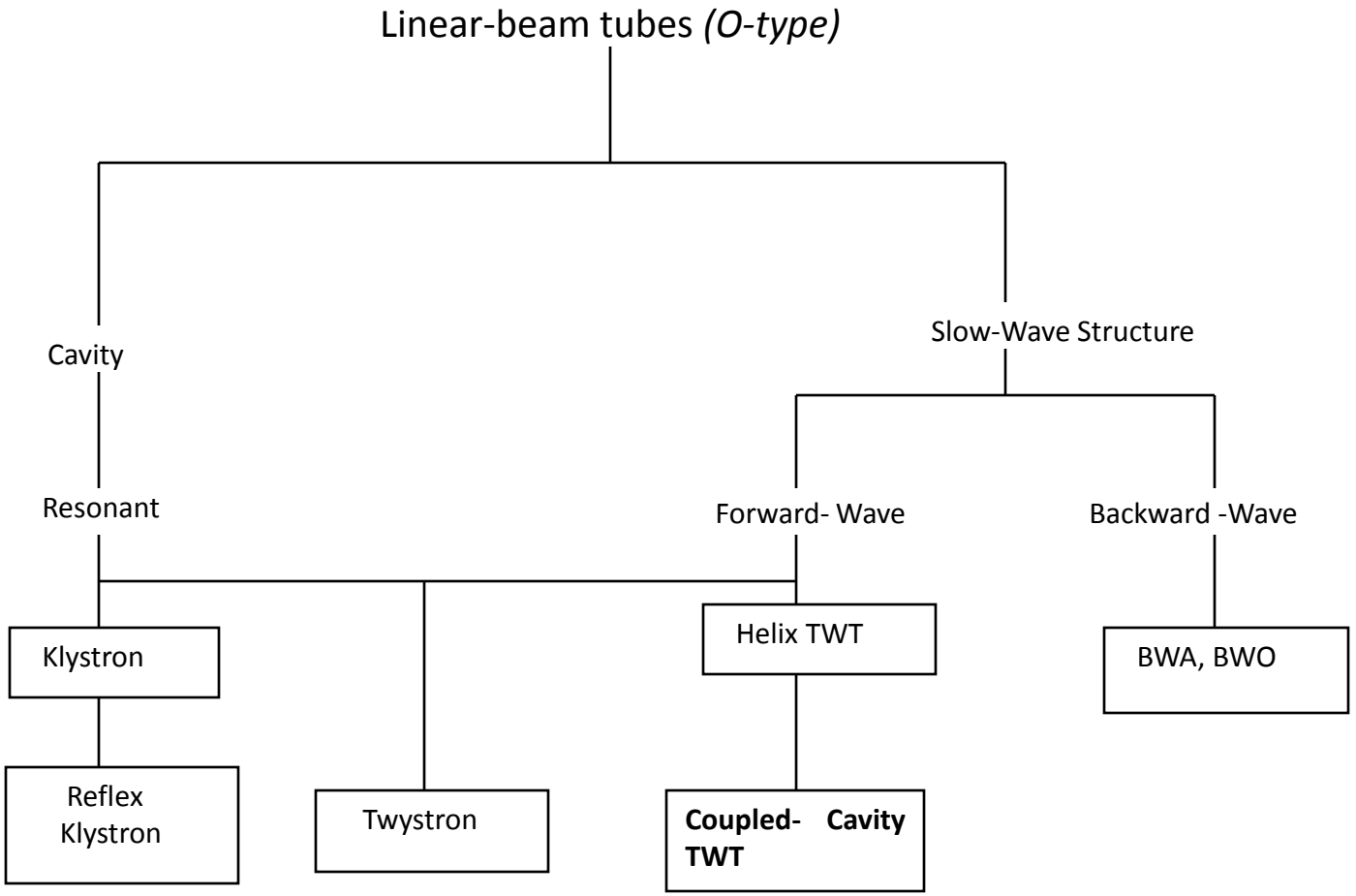

Linear Beam Tubes (O Type)

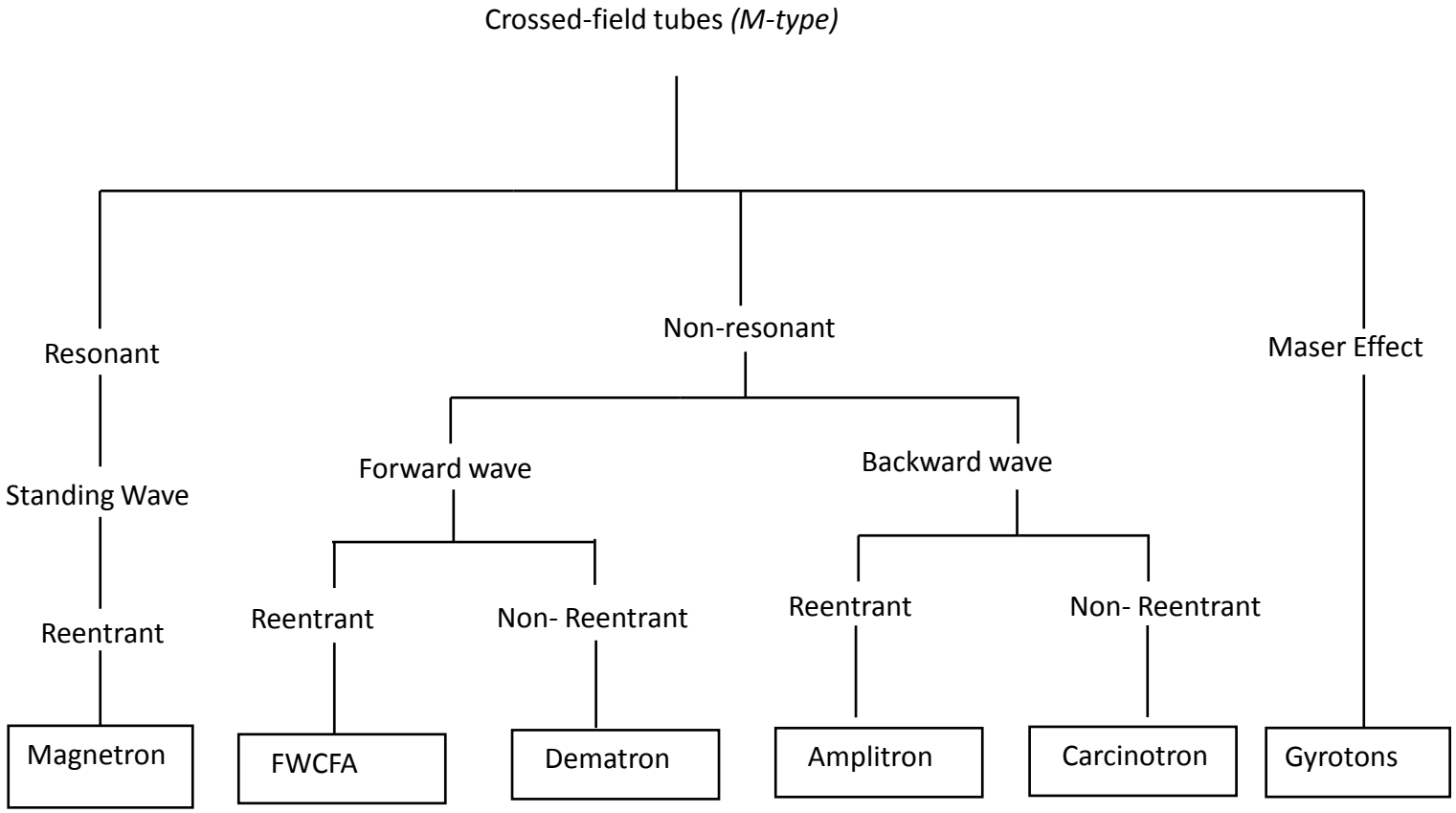

Crossed-field tubes (M type)

Classification of Microwave Tubes

- **Based on Electric and Magnetic Fields**

  (a) O- type (French TPO: tubes a propagation des ondes)

  Axes of electric and magnetic fields coincide
  Example: TWT, Klystron

  (b) M-type (French TPOM: tubes a propagation des ondes a champs magnetique)

  Axes of electric and magnetic fields are perpendicular
  Example: Magnetron, Gyrotron

- **Based on the phase velocity of rf wave**

  Slow- wave device: $v_p < c$
  Example: TWT, Klystron

  Fast wave device: $v_p > c$
  Example: Gyrotron, FEL

Helix TWT

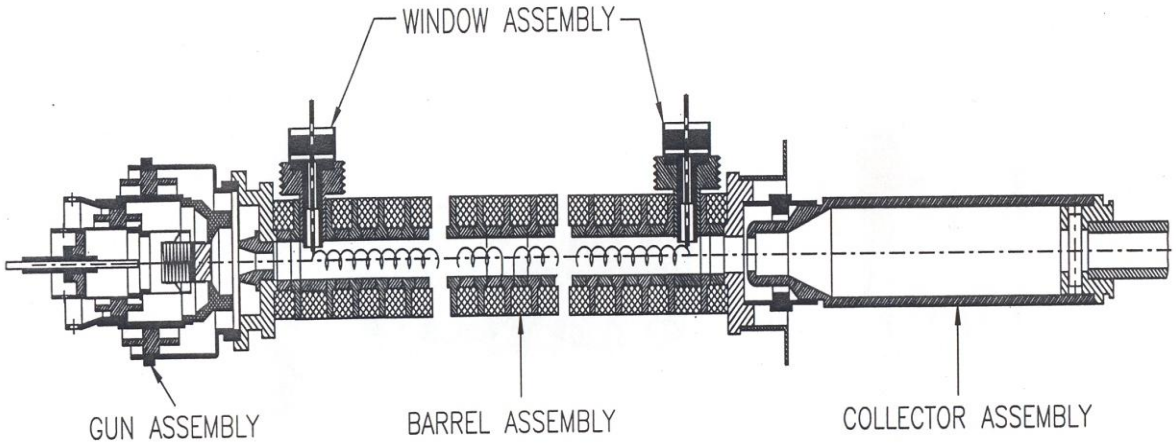
WINDOW ASSEMBLY
GUN ASSEMBLY
BARREL ASSEMBLY
COLLECTOR ASSEMBLY

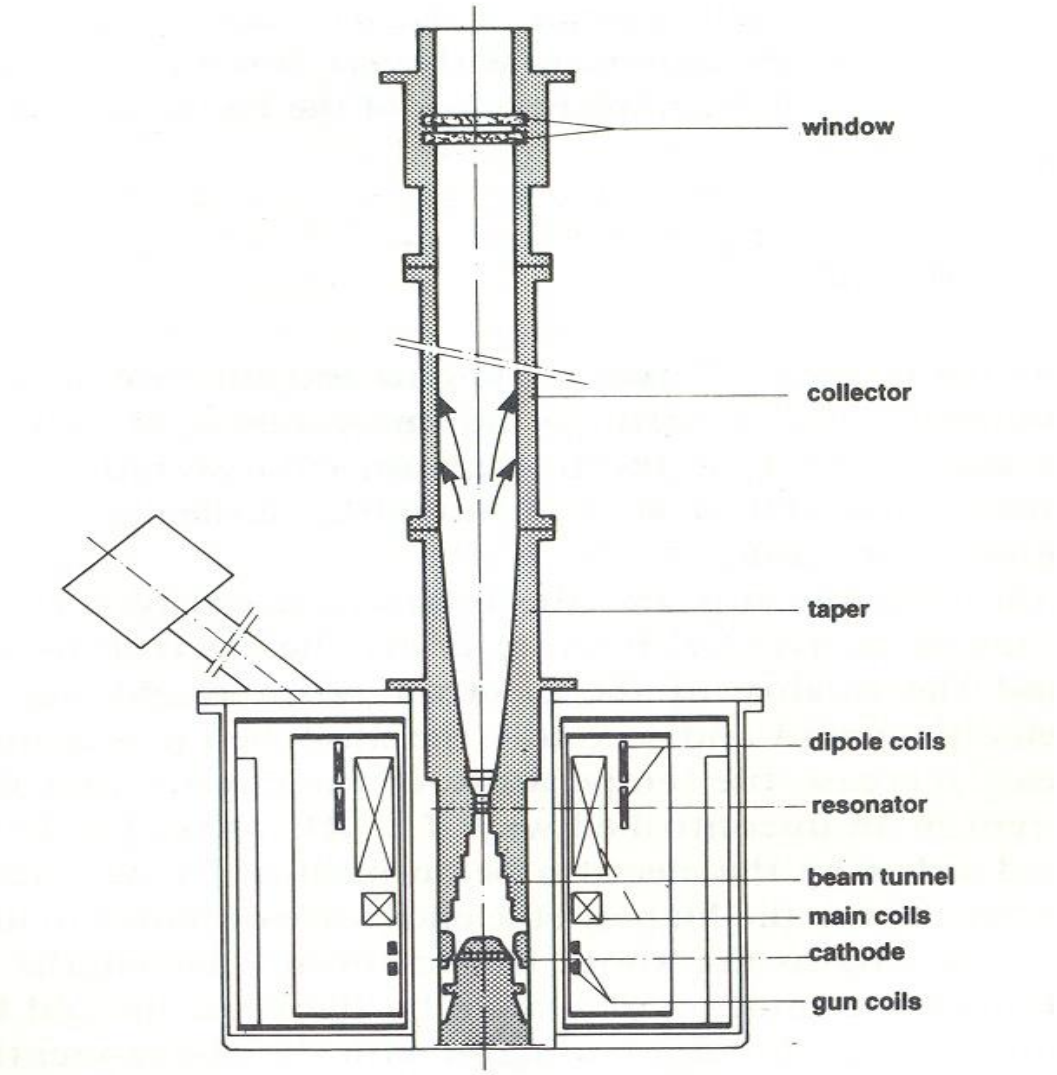
window
collector
taper
dipole coils
resonator
beam tunnel
main coils
cathode
gun coils

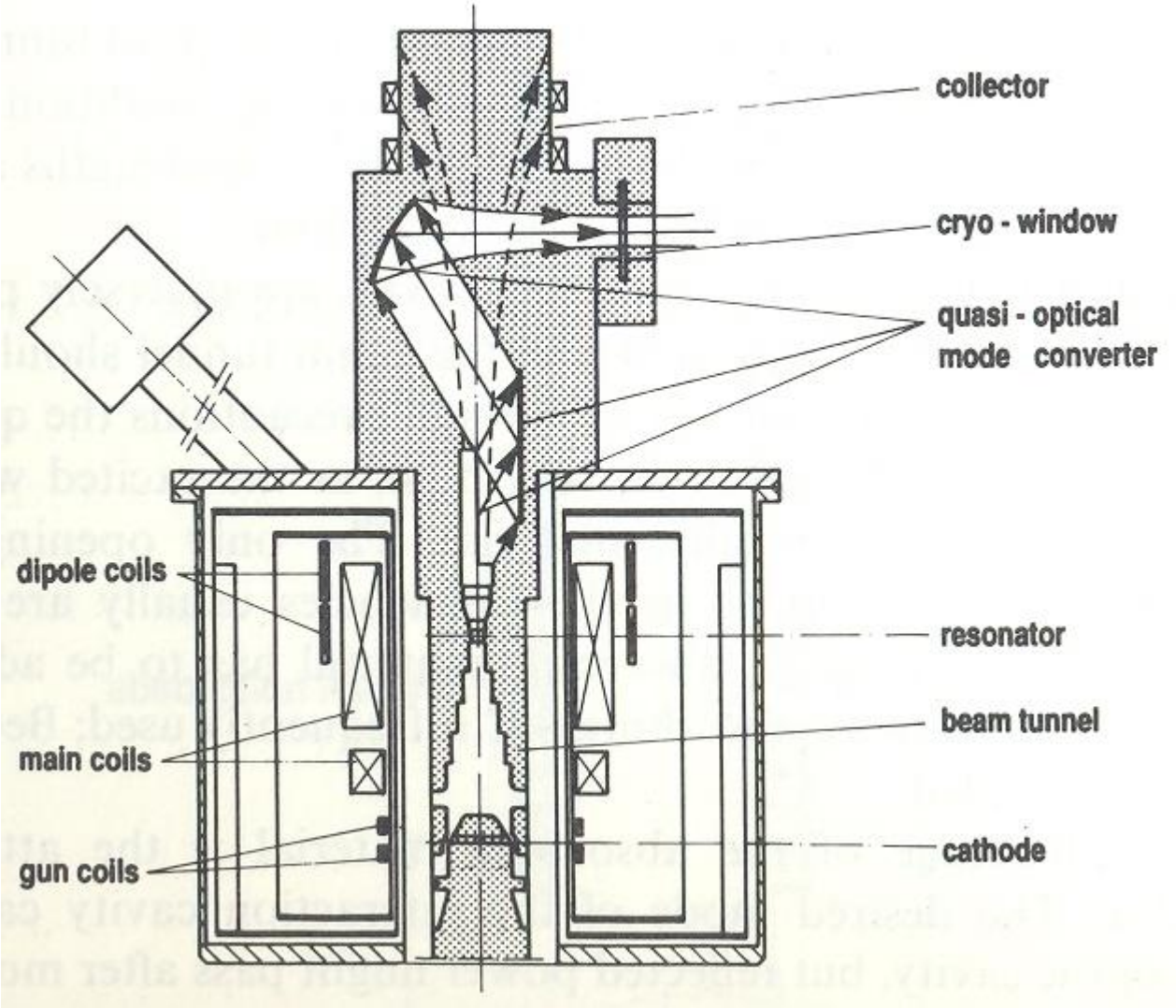
collector
cryo - window
quasi - optical
mode converter
dipole coils
resonator
beam tunnel
main coils
cathode
gun coils

Overview on Gyro-Devices and Comparison with Conventional Microwave Tubes

"0" TYP DEVICES	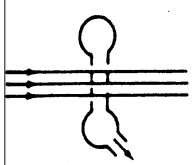 MONOTRON	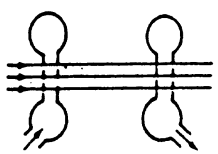 KLYSTRON	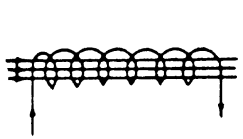 TWT	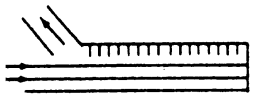 BWO	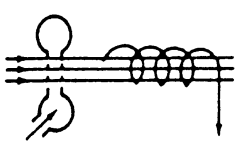 TWYSTRON
GYRO-DEVICES	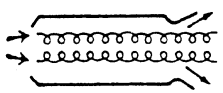 GYRO-MONOTRON	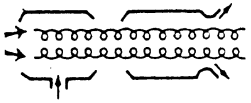 GYRO-KLYSTRON	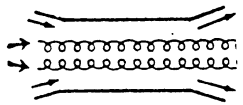 GYRO-TWT	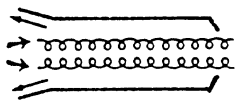 GYRO-BWO	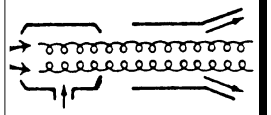 GYRO-TWYSTRON
RF-FIELD STRUCTURE	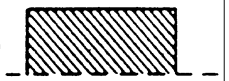		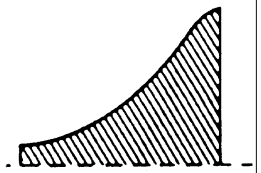		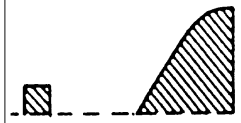
ORBITAL EFFICIENCY	0.42	0.34	0.7	0.2	0.6

Slow-wave and Fast- wave Devices

Feature	Slow-wave Device	Fast- wave Device
Wave	Slow	Fast
Phase Velocity	<c	>c
Phase synchronism	$\frac{\omega}{\beta} \geq v_0$	$\frac{\omega}{\beta_{mn}} - \frac{s\omega_c}{\gamma\beta_{mn}} \geq v_z$
bunching		
alignment	axial	transverse
force	electric	magnetic
mechanism	non-relativistic	relativistic
Field responsible for energy exchange	axial, electric	transverse, electric
Free energy	axial electron velocity	transverse electron velocity

Historical development of vacuum based amplifiers/oscillators

- **1880: Discovery of Thermionic emission by *Thomas Edison***
- **1905: First thermionic diode by *John Ambrose Fleming***
- **1907: First triode by *Lee De Forest***
- **1921: First Magnetron by *Hull***
- **1939: Klystron by *Russell Varian* and *Sigurd Varian***
- **1940: Cylindrical magnetron by *Boot* and *Randell***
- **1942: TWT by *Rudolf Kompfner***

Motivated by WW II

- **1951: Backward wave oscillator or carcinotron by *Bernard Epsztein***
- **Decade of 1970's : Invention of gyrotron by *Russian team***

Historical development of gyrotron

- **1959: Theoretical work published by *Twiss, Schneider* and *Gapanov.***
- **1964: First experiment by *Hirshfield et al* on the radiation mechanism developed in 1959.**
- **Decade of 1970's: Development of MIG and first gyrotron in the form of vacuum tube is invented by *Russian* tem.**
- **Decade of 1980's and upto 1985: Theoretical development by *Hershifield, Chu, Barnett, Read, Fliflet, Kreisher, Felich and Temkin.***
- **2007-2008: Record 1 MW CW power at 170 GHz frequency with conventional cavity by *Japanese* and *Russian* groups .**
- **2009-2010: Record 2.2 MW power at 170 GHz frequency with co-axial cavity by the *group of KIT, Germany*.**
- **2008-2010: Several experiments of THz gyrotron by *T. Idehara et al* shows record frequency in THz band (upto 3 THz).**

Gyrotron: Basics

- The name “Gyrotron” was originally used by the Russians for a single cavity oscillator, now often referred to as gyro-monotron.
- The name now refers to a class of devices including both oscillators and amplifiers.
- Gyrotron is basically a fast wave microwave tube in which the phase velocity is kept more than that of the velocity of light .

Components of gyrotron

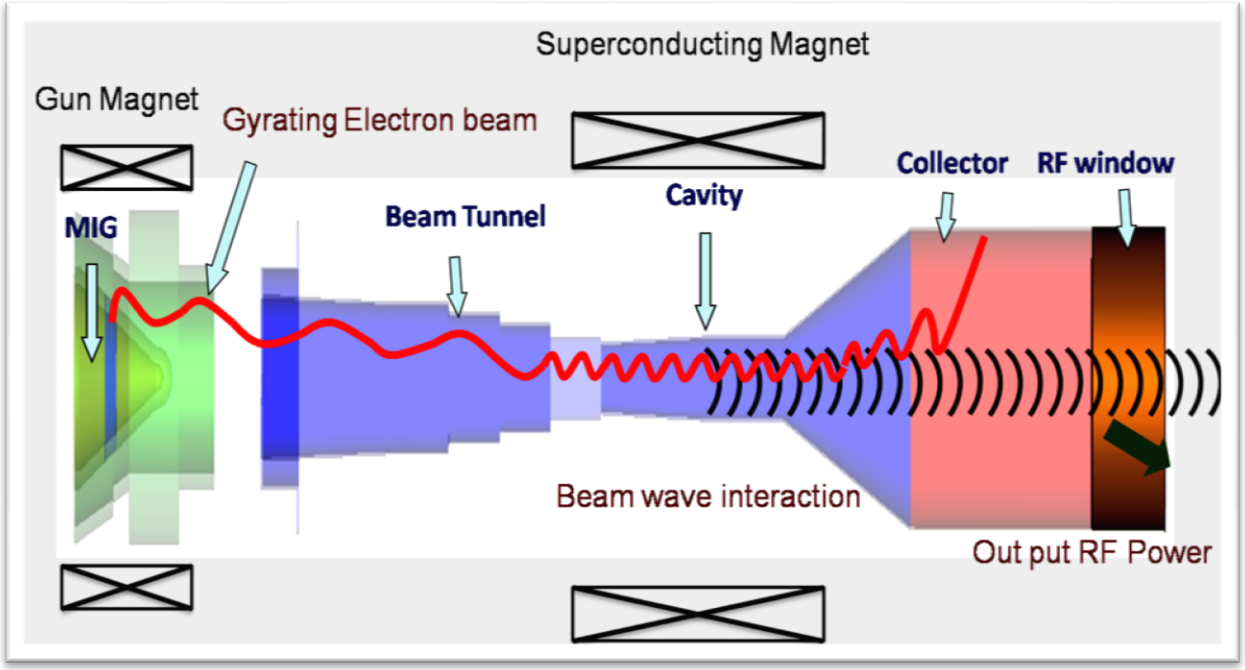

Components of gyrotron

***Electron beam source*:** In a gyrotron, the electron beam source is also called magnetron injection gun (MIG) due to the electron emission and motion occurring in a gyrotron is as happened in magnetron. The formation of gyrating electron beam with the desired parameters required at cavity center for the efficient beam-wave interaction like beam radius, transverse to axial velocity ratio of electron beam, etc, takes place in MIG. Further, MIG is a combination of various assemblies and sub-assemblies like dispenser cathode, heater, anodes, magnet system, etc. The electron emission process in MIG takes place by thermionic emission and the cross electric and magnetic fields provide the helical motion to the electron beam.

Beam tunnel: The beam tunnel is installed between the interaction cavity and MIG. The main function of this component is to prevent the backward propagation of RF, generated in the interaction cavity. The beam tunnel also provides a compression zone for the generated electron beam. This structure is made of lossy ceramic rings and high quality copper rings.

Components of gyrotron

Interaction cavity: A simple cylindrical RF interaction structure called as a resonator cavity or simply a cavity due to its resonant behaviour, is used in most of the gyrotrons from low frequency, low power to high frequency, high power. The beam-wave interaction takes place in this section. The overall performance of the gyrotron tube including the interaction cavity performance highly depends on the operating mode. A particular operating mode is selected on the basis of power and frequency requirement of a gyrotron. As the power and frequency of a gyrotron increase, the high order TE modes become more important.

Magnet system: The applied magnetic field directly depends on the required frequency of a gyrotron tube. Gyrotron is a high frequency device and thus very high magnetic field is required, which is not possible by the permanent magnets. Superconducting magnet is used to fulfill the very high magnetic field requirement and thus it makes the gyrotron more complicated than other microwave amplifiers and oscillators. A gun magnet normally of copper solenoid type is also used near the cathode to fine tune the electron emission and gyration. Another magnetic systems also made of copper solenoid type is also used around the collector to collect the spent electron beam.

Components of gyrotron

Non-linear taper: This is a tapered waveguide used in the gyrotron of axial RF output to connect the interaction cavity with the collector. The design of this waveguide should be in such a way that the generated mode in the interaction cavity cannot be converted during the propagation from cavity to collector and maximum RF transmission takes place. High quality copper is used in the fabrication of non-linear taper.

Components of gyrotron

Collector: This is a specially designed cylindrical waveguide, used for the spent electron beam collection. High quality copper is used in the fabrication of collector. In the electrical designing of collector, the electron beam spread is the main issue to eliminate the thermal spot on the collector wall. For this purpose, separate magnet system is used to spread out the spent electron beam at collector wall. Thermal and structural management of collector is also a critical issue, specially for MW power gyrotrons.

RF window: The RF window is a very sensitive part of gyrotron. This is a circular disk of high quality low loss ceramic. The ceramic disk is fitted in the cylindrical waveguide and separates the outer atmosphere from the very high order vacuum inside the gyrotron. For the window ceramic material, good dielectric, thermal and mechanical stability as well as low RF loss are very necessary. In case of high power gyrotrons, CVD diamond is used as it shows remarkable thermal and electrical properties required in the gyrotron window.

Present state of the art of Gyrotrons including agencies / Institutions working in the area

- ✓ Gyrotron was first built around 8 GHz with 10 W in Russia in 1984 just to demonstrate the principle of cyclotron resonance interaction.

- ✓ However, the progress in Gyrotron is tremendous with almost reaching 1-2 MW power at 140 and 170 GHz for plasma research and upto THz with moderate power for nuclear spectroscopy application. The activity in Gyrotron and gyro device spans the world covering Russia, China, Japan, European Counties, Australia, USA, India, etc.

Present-day scenario of Gyrotron research & development in India

- In India, research in gyro- device is about three decades back with some theoretical research in the field of gyro-TWT at CEERI and BHU with some publications.
- In India only IPR, Gandhinagar is using 28 GHz, 200kW, 42 GHz, 100 kW, 82.5 GHz, 200 kW Gyrotrons for its TOKAMAK system.
- India has started "device level" to work towards design and development of 42 GHz, 200 kW CW/ Long pulse Gyrotron for Indian TOKAMAK system with MUNGA (Multi Institutional Gyrotron Activity) approach with sponsorship from Department of Science and Technology (DST) with CEERI as nodal agency. More Institutes are now in Gyrotron Research.
- CEERI has successfully RF tested 42 GHz gyrotron upto 125 KW.
- The institutions involved in 42 GHz gyrotron are CEERI-Pilani, BHU-Varanasi, IIT- Roorkee, SAMEER-Mumbai and IPR- Gandhinagar.
- MTRDC is presently working on 95 GHz, 100 KW Gyrotron.
- BESIDES, CEERI IS ALSO WORKING ON 120/ 170 GHZ, 01 MW GYROTRON UNDER CSIR-NETWORK SCHEME.

USERS & OTHERS OF MICROWAVE TUBES IN THE COUNTRY

USER	SYSTEM	TUBE TYPE
ISRO	INSAT/ GSLV	SPACE TWT
DEFENCE AND DRDO	RADAR, EW	TWT, KLYSTRON MAGNETRON, MPM
CAT (DAE), SAMEER	PARTICLE ACCELERATORS PULSED LASER SYSTEM	MAGNETRON , KLYSTRON GDT SWITCHES (THYRATRON)
IPR	PLASMA HEATING (ECRH)	GYROTRONS, KLYSTRONS
IPR, BARC, LRDE, MTRDC	HPM	VIRCATOR
BEL, Bangalore	Industry	TWT, Magnetron, Klystron
MTRDC	R&D	TWT, Klystron, Gyrotron
CSIR-CEERI	R&D	TWT, Klystron, Magnetron, Thyratron, Gyrotron

Electricity generation (utility sector) by source in India in FY 2017-18

- Coal: 986,591 GWh (75.9%)

- Large Hydro: 126,123 GWh (9.7%)
- Small Hydro: 5,056 GWh (0.4%)

- Wind Power: 52,666 GWh (4.0%)
- Solar Power: 25,871 GWh (2.0%)
- Biomass: 15,252 GWh (1.2%)

- Nuclear: 38,346 GWh (2.9%)
- Gas: 50,208 GWh (3.9%)

Nuclear Power

- **Nuclear power** is the use of **nuclear** reactions that release **nuclear energy** to generate heat, which most frequently is then used in steam turbines to produce **electricity** in a **nuclear power plant**. As a **nuclear** technology, **nuclear power** can be obtained from **nuclear** fission, **nuclear** decay and **nuclear** fusion reactions.

Danger of Nuclear Energy

- The **Dangers** of **Nuclear Energy**. Meltdowns like the ones in Fukushima or Chernobyl released enormous amounts of radiation into the surrounding communities, forcing hundreds of thousands of people to evacuate. ... Beyond the **risks** associated with **Nuclear Power** and **Radioactive Waste**, the threat of **nuclear** weapons looms large.

Plasma ECRH, required for controlled thermonuclear fusion going to contribute largely to electric power production by the middle of the present century.

Fusion-based power plants (using abundant 'raw material') as an alternative to its fission-based counterpart, the latter being associated with the problem of disposing a large quantity of radioactive waste as well as with the danger of disastrous accidents like that occurred in Chernobyl).

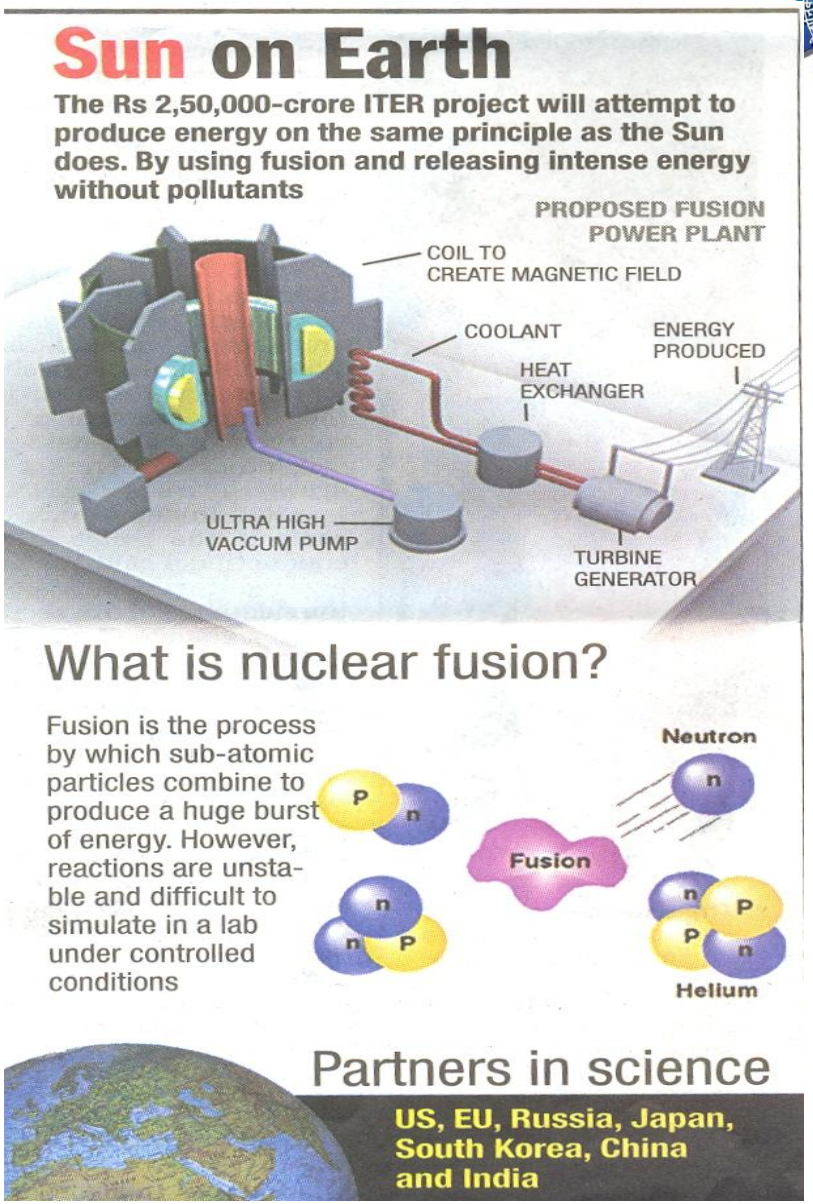

Application of microwave power in magnetic fusion devi

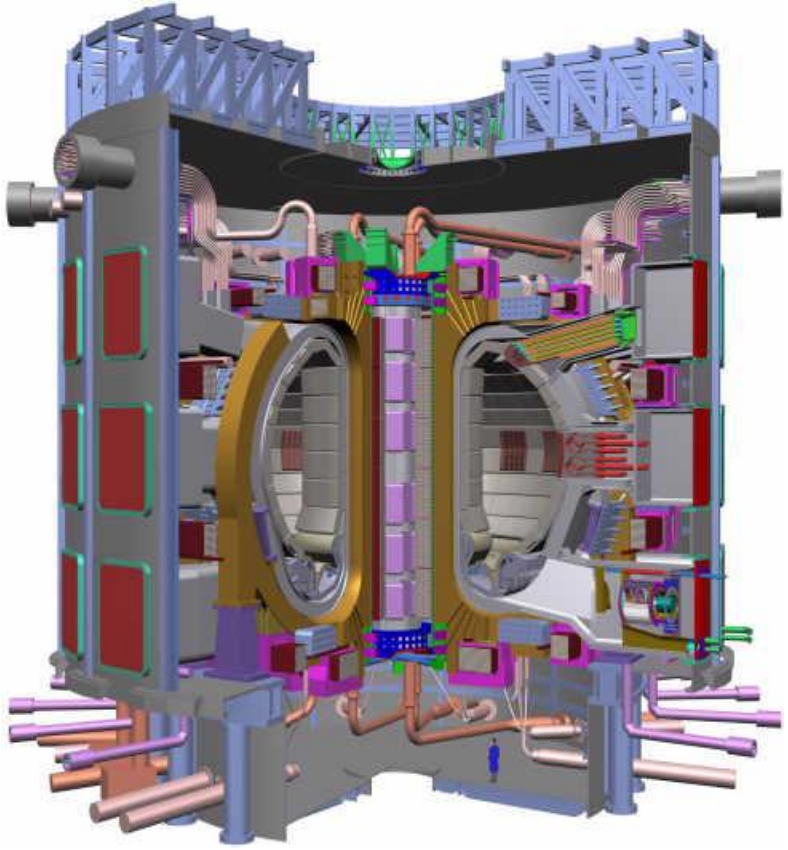

schematic view of the ITER tokamak

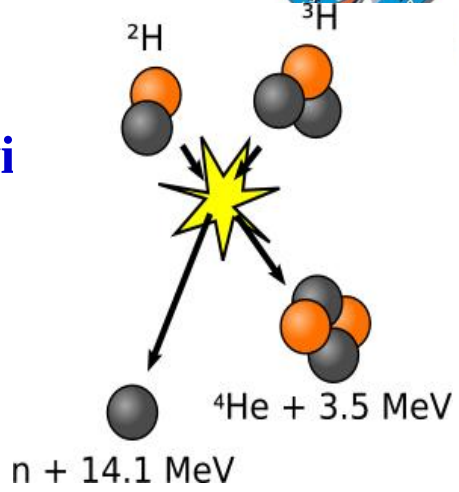

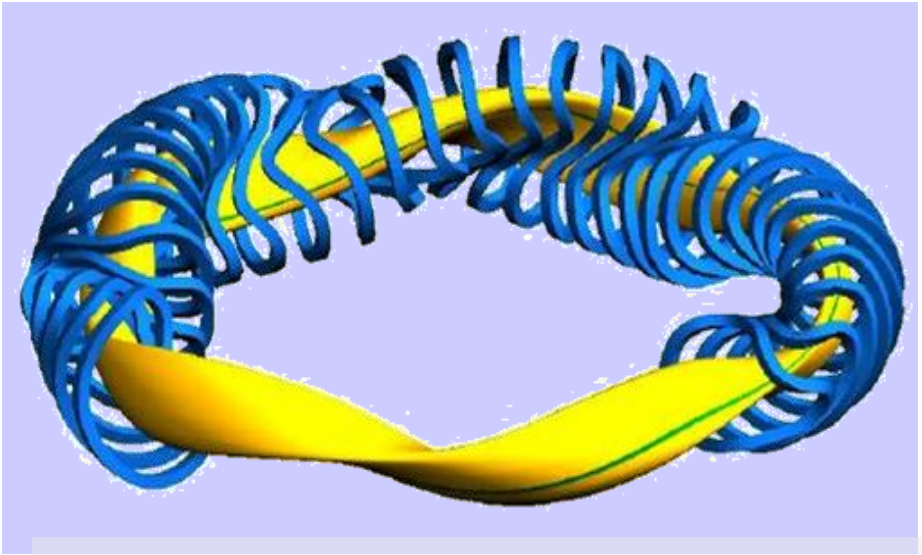

schematic view of coil arrangement and plasma shape of the W7-X stellarator

- fusion energy is one of the few (2-3) options, the mankind has, for safe, ecologically acceptable and long lasting energy source

ECW system for ITER

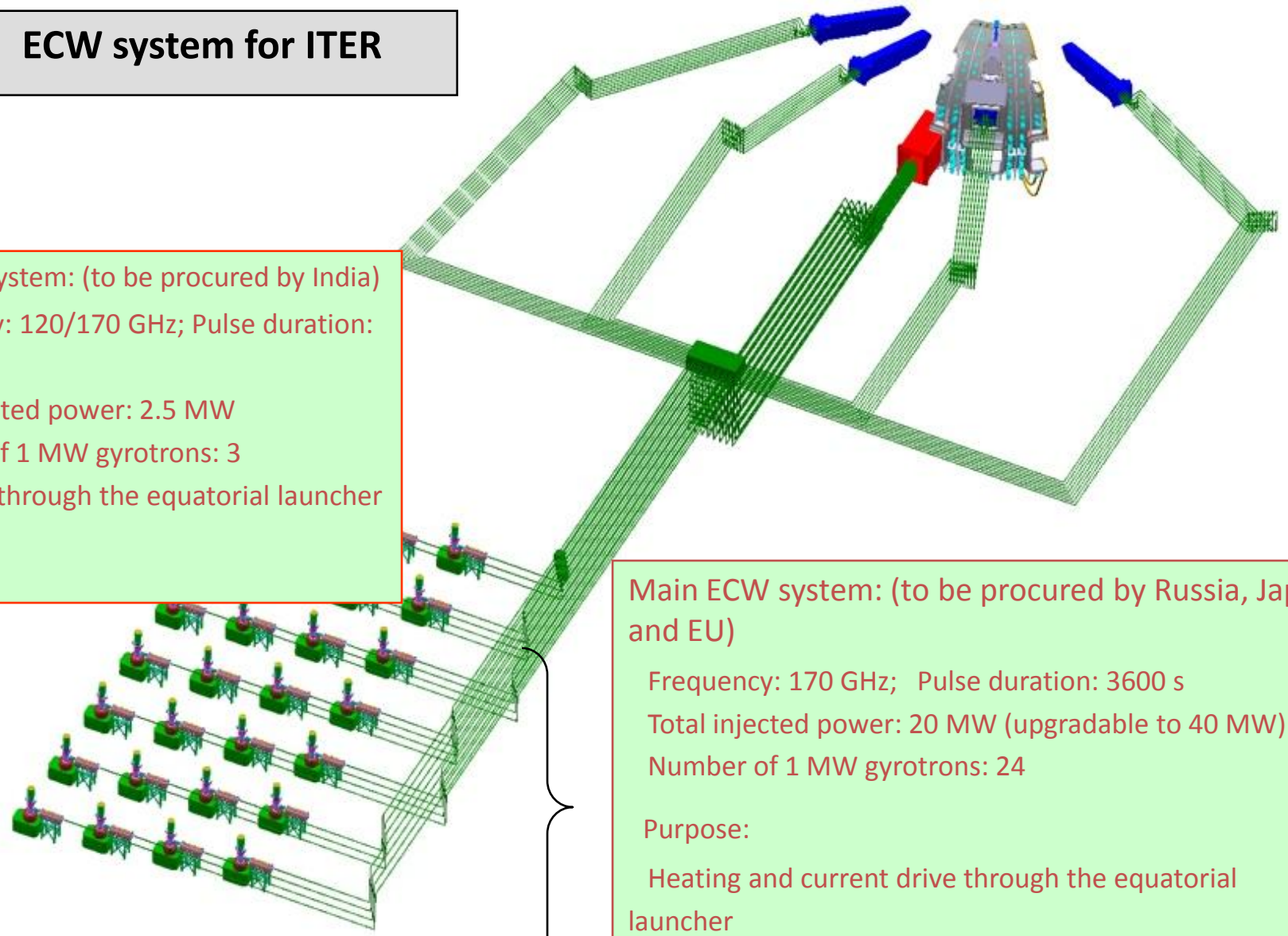

Start-up system: (to be procured by India)

Frequency: 120/170 GHz; Pulse duration: 3 s

Total injected power: 2.5 MW

Number of 1 MW gyrotrons: 3

launched through the equatorial launcher

Main ECW system: (to be procured by Russia, Japan and EU)

Frequency: 170 GHz; Pulse duration: 3600 s

Total injected power: 20 MW (upgradable to 40 MW)

Number of 1 MW gyrotrons: 24

Purpose:

Heating and current drive through the equatorial launcher

Mode control through the upper launcher

MAJOR APPLICATIONS OF GYROTRON

- PLASMA RESEARCH
- ENERGY GENERATION
- MATERIAL PROCESSING
- MEDICAL SPECTROSCOPY

Gyrotron Operating Mode

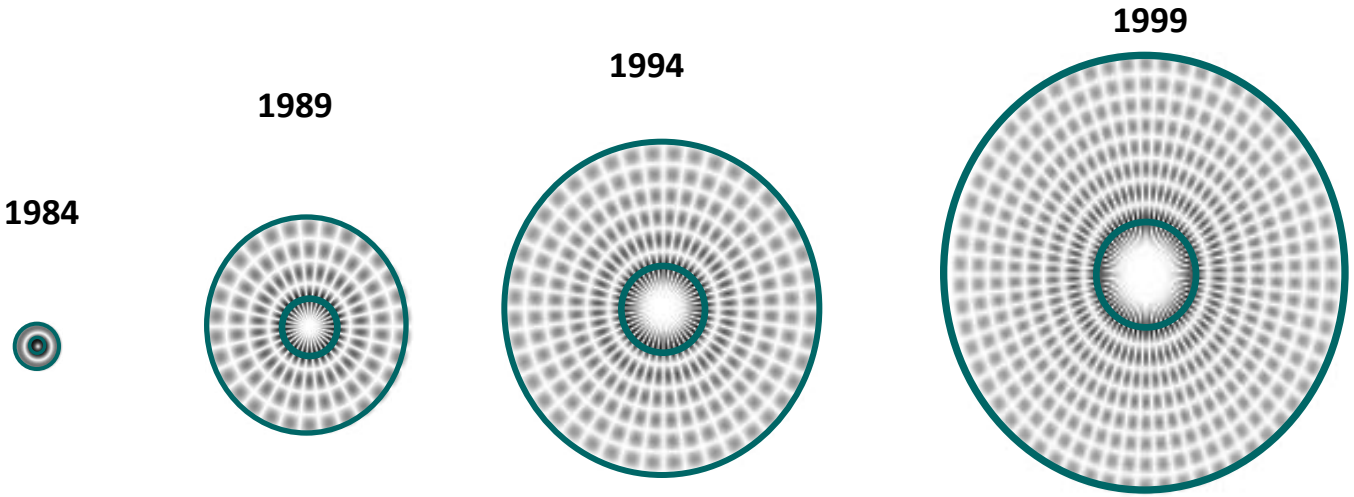

Gallery of high power long pulse gyrotrons

JAERI / TOSHIBA
170 GHz, 0.82 MW (0.6MW)
600s (1h)

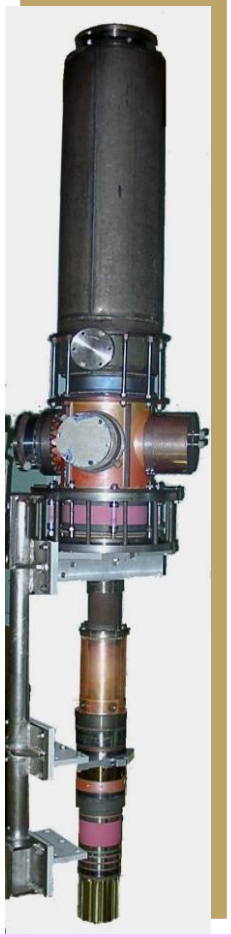

GYCOM
170 GHz, 1 MW (0.5 MW)
1.5s (80s)

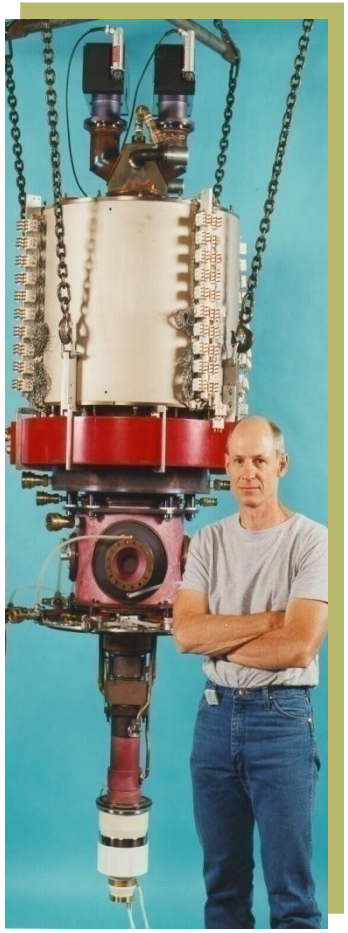

CPI
140 GHz, 0.9 MW
1800s

TED
140 GHz, 0.9 MW
1800s

DEVELOPMENT STATUS OF LONG PULSE Gyrotron FOR FUSION PLASMA APPLICATION AT 110 – 170 (GHZ)

INSTITUTION	FREQUENCY (GHz)	CAVITY MODE	OUTPUT MODE	POWER (MW)	EFFICIENCY (%)	PULSE LENGTH (S)	FUSION DEVICE
CPI Palo Alto	110	$TE_{22.6}$	TM_{00}	1.05 0.6	31 31	5.0 10.0	D III-D D III-D
	140	$TE_{28.7}$	TM_{00}	0.9	33 (SDC)	1800	W7-X
GYCOM-M (TORIY IAP), Moscow, Nizhny Novgorod	110	$TE_{19.5}$	TM_{00}	0.93 0.5 0.35	36 35 33	2.0 5.0 10.0	D III-D D III-D D III-D
	140	$TE_{22.6}$	TM_{00}	0.94 0.54	36 36	1.2 3.0	ASDEX-U W7-AS
	170	$TE_{25.10}$	TM_{00}	0.9 0.5	44 (SDC) 40 (SDC)	21 300	ITER ITER
GYCOM-N (SALUT,IAP), N. Novgorod	140	$TE_{22.6}$	TM_{00}	0.8 0.88	32 50.5 (SDC)	0.8 1.0	W7-AS W&-AS
	158.5	$TE_{28.7}$	TM_{00}	0.5	30	0.7	T 10
JAEA TOSHIBA, Naka Otawara	110	$TE_{22.6}$	TM_{00}	1.2 1.0 0.5	38 (SDC) 36 (SDC) 34 (SDC)	4.1 5.0 16.0	JT 60-U JT 60-U JT 60-U
	170	$TE_{31.8}$	TM_{00}	1.0 0.6	43.4 (SDC) 45.5 (SDC)	800 3600	ITER ITER
THALES CEA, CRPP	118	$TE_{22.6}$	TM_{00}	0.53 0.35	32 23	5.0 111	TORE SUPRA TORE SUPRA
FZK EUROPE	140	$TE_{28.8}$	TM_{00}	1.0 0.92	49 (SDC) 44 (SDC)	12 1800	W7-X W7-X

PERFORMANCE PARAMETERS OF CW Gyrotron FOR TECHNOLOGICAL APPLICATIONS

INSTITUTION	FREQUENCY (GHz)	CAVITY MODE	OUTPUT MODE	POWER (kW)	EFFICIENCY (%)	V_0 (k V)	MAGNET
CPI Palo Alto	28	TE_{02}	TE_{02}	15	38	40	Room Temp.
	28 ($2\Omega_C$)	TE_{02}	TE_{02}	10.8	33.6	30	Room Temp.
	60	TE_{02}	TE_{02}	30	38	40	Cryo Mag.
CPI NIFS GYCOM	84	$TE_{15.3}$	Tem_{00}	50	14	80	Cryo Mag.
	24.15 ($2\Omega_C$)	TE_{11}	TE_{11}	3.5	23	12	Room Temp. PM 116 Kg.
IAP, N. Novgorod	24.15	TE_{32}	TE_{32}	36	50	33	Room Temp.
	23 ($2\Omega_C$)	TE_{12}	TE_{12}	13	50	25	Room Temp.
				28	32	25	Room Temp.
	28.3 ($2\Omega_C$)	TE_{12}	TE_{12}	12	20	25	Room Temp. PM 116 Kg.
	30 ($2\Omega_C$)	TE_{02}	TE_{02}	10	42	26	Room Temp.
				30	35	26	Room Temp.
	37.5	TE_{62}	TEM_{00}	20	35	30	Cryo Mag.
	83	TE_{93}	TEM_{00}	10-40	30-40	25-30	Cryo Mag.
MITSUBISHI Amagasaki	28 ($2\Omega_C$)	TE_{02}	TE_{02}	15	38.7	21	PM, 600 Kg Tapered B
UNIV, Fukui.	300	$TE_{22.8}$	TEM_{00}	2.0	11	15	Cryo Mag.

Progress:

	8.8 GHz	42 GHz	140 GHz	1 THz
Cavity	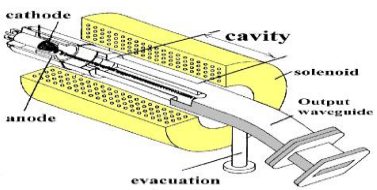	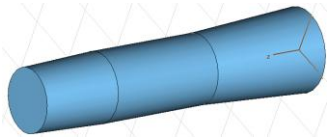	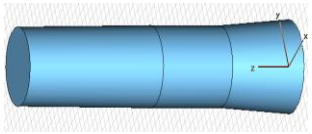	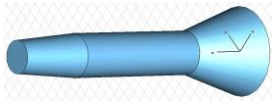
Mode	TE_{101}	$TE_{0,3}$	$TE_{28,8}$	$TE_{4,12}$
O/P Power	6W	200 kW	970kW (~1MW)	350 W
Beam parameter	10kV/ 100mA	65kV/ 10A	75kV/ 40A	30kV/ 200mA
Gun Type	MIG(Glass Triode)	MIG	MIG	MIG
Collector	Rectangular	Circular	Circular	Circular
Window	Mica type	sapphire	CVD diamond	Boron nitride
Tube length	0.6 m	2.0 m	3.5 m	2.5m
Magnetic field	0.3 T	1.65	5.0 T	20T
RF collection	Axial	Axial	Quasi-optical	Axial
Cavity	Rect.	Cir	Cir	Cir
Reference	Russia	CEERI, Pilani	FZK, Germany	Fukui, Japan

Indian Scenario

Ambitious Dream:

Development of Indian Gyrotron

CEERI, PILANI

SAMEER, MUMBAI

IPR,GANDHINAGAR

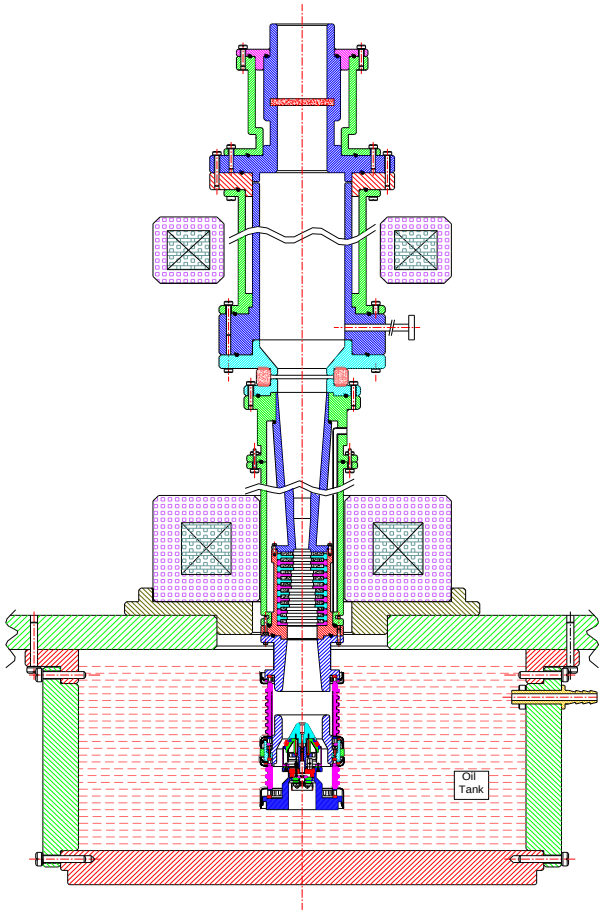

BHU, VARANASI

IIT, ROORKEE

DST, NEW DELHI (Sponsor)

Starting : 2006

Ending: 2017

Design and Development of 42GHz 200kW, CW/Long pulse Gyrotron

Participating Institute		Remarks
CEERI, Pilani (Nodal Agency)		Design Technology of MIG, Collector and Interaction Structure, Cooling Duct, Infrastructure for RF Measurement, MIG Test, **Fabrication**, **Vacuum Processing**
BHU, Varanasi		Design Technology of Interaction Structure Establishment of cold measurement set up of cavity
IPR, Gandhinagar		Design Technology of Power supply, Magnetic System, Plumbing Lines, Thermal Analysis **Infrastructure for Gyrotron Testing**
IIT, Roorkee		Design Technology of MIG and Interaction Structure
SAMEER, Mumbai		Gyrotron Window

Gyrotron: Basics

- The name “Gyrotron” was originally used by the Russians for a single cavity oscillator, now often referred to as gyro-monotron.
- The name now refers to a class of devices including both oscillators and amplifiers.
- Gyrotron is basically a fast wave microwave tube in which the phase velocity is kept more than that of the velocity of light .

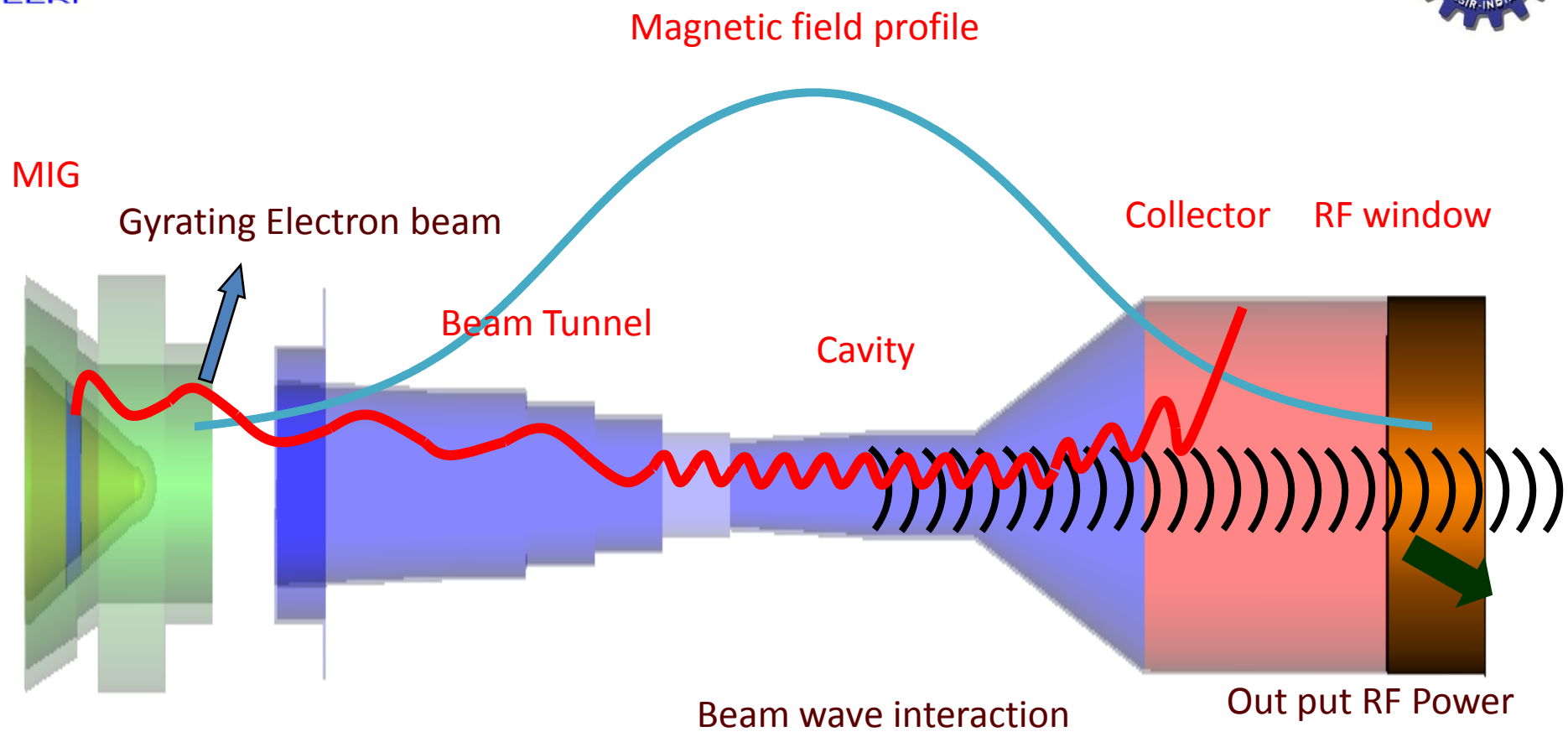

42 GHz, 200 kW Gyrotron

Operational principle for Gyrotron

- The magnetron injection gun produces an annular electron beam with the desired beam parameters.
- The beam is transported to the interaction region, where the interaction cavity converts a fraction of beam power to the RF power. In case of axial output coupling, the spent beam will be collected on the uniform output wave guide section after the out taper and the RF power in the TE mode is coupled through the output vacuum window.
- A strong externally applied magnetic field support the cyclotron motion of the electron beam.
- The magnetic field in the interaction region is so chosen such that the cyclotron frequency is close to the frequency of the RF field.

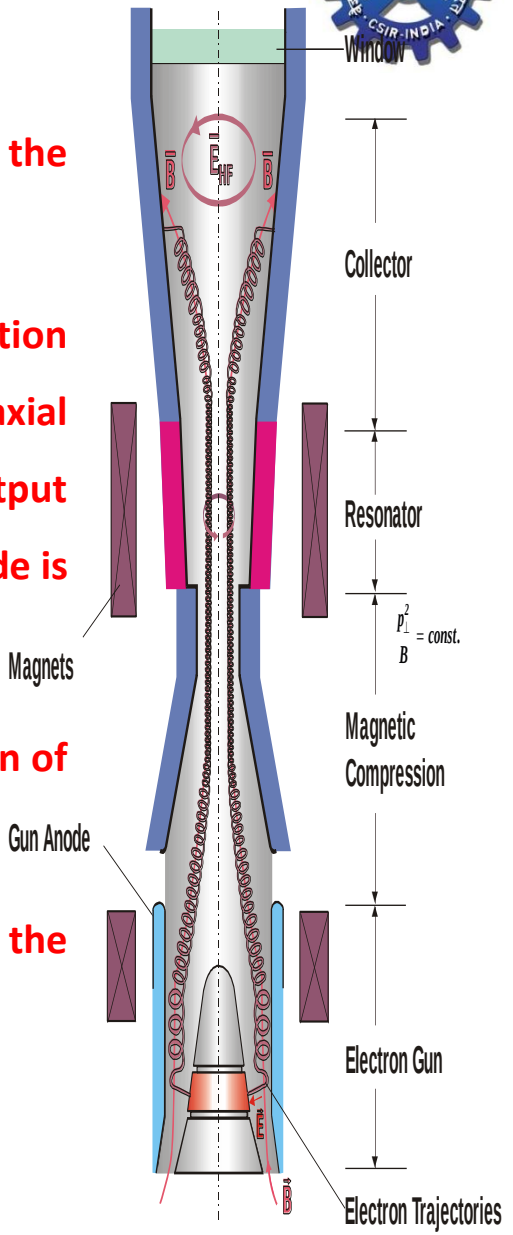

- The transverse component of the RF field in this region interacts with the electron in the annular beam and converts large part of the orbital kinetic energy into RF power output.

- The electron follows a helical path around the lines of force of the external field. In order for the net flow of energy from the transverse electron motion to the electromagnetic wave to take place, the electrons must become bunched in phase within their cyclotron orbits. Such bunching occurs due to the fact that the electron cyclotron frequency is a function of electron energy.

- To achieve bunching mechanism, a resonance condition must be satisfied between the periodic motion of electrons and the electromagnetic wave in the interaction region given as

$$\omega - k_z v_z = s\,\Omega_c$$

$$\omega - k_z v_z = s\,\Omega_c$$

Here,

ω: angular frequency, k_z: characteristic axial wave number,
v_z: electron axial velocity, s: harmonic number,

Ω_c: Cyclotron frequency of electron

$$\Omega_c = \Omega_{co} / \gamma$$

$$\Omega_{co} = eB_o / m_o$$

$$\gamma = [1 - (v_0 / c)^2]^{-1/2} = 1 + eV_o / m_o c^2$$

where,

e: electron charge, m_o: electron mass at rest, γ: relativistic factor,
B_o: magnetic field, V_o: beam voltage

- A group of relativistic electrons gyrating in a strong magnetic field will radiate due to bunching caused by the relativistic mass dependence of their gyration frequency.
- Bunching is achieved because, as an electron loses energy, its relativistic mass decreases and it thus gyrates faster.
- The consequence is that a small amplitude wave's electric field, while extracting energy from the particles, causes them to become bunched in gyration phase and reinforces the existing wave electric field.

- Because of this RF circuits are replaced in gyro devices by a simpler structure or by smooth waveguide.

- Their dimensions are not limited and thus the power handling ability increase many fold as compared to conventional tubes.

- The size depends on the operating mode. Higher the mode larger the size of the waveguide and higher is the power handled.

- The beam wave interaction produces angular velocity modulation, which in turn produces a modulation of electron energy. This can produce electron bunching of the beam.

Dispersion diagram or plots or Brillouin diagrams show the region of cyclotron interaction between TE mode and the fast electron cyclotron mode (fundamental or harmonic) as the intersection of the waveguide mode dispersion curve (hyperbola)

$$\omega^2 = k_z^2\, c^2 + k_\perp^2\, c^2$$

In the case of a device with cylindrical resonator the perpendicular wavenumber

$$k_\perp = \chi'_{mn} / R_o$$

Where

χ'_{mn}: derivative of the m^{th} root of corresponding Bessel function TE_{mn} and R_o: waveguide radius.

Dispersion Diagram

$$\omega^2 = k_z^2\, c^2 + k_\perp^2\, c^2$$

$$\omega - k_z v_z = s\,\Omega_c$$

$$k_\perp = \chi'_{mn} / R_o$$

$$\Omega_c = \Omega_{co}/\gamma$$

$$\Omega_{co} = eB_o / m_o$$

$$\gamma = [1 - (v_0 / c)^2]^{-1/2} = 1 + eV_o / m_o c^2$$

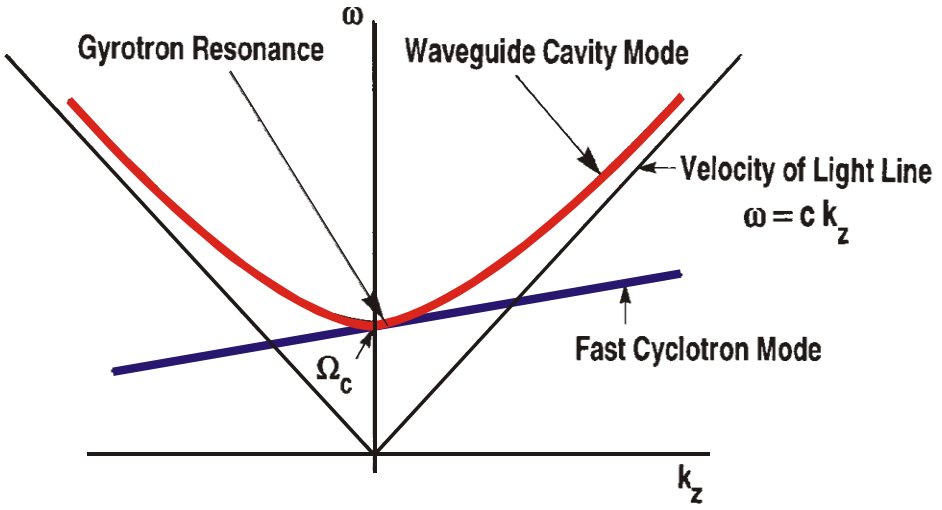

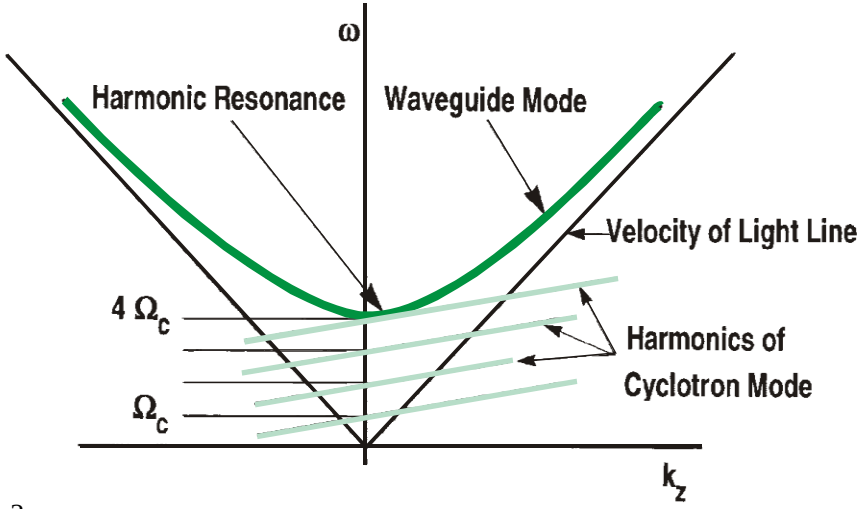

Task plan

- ✓ Creation of design base
- ✓ Design of all components/gyrotron
- ✓ Design of peripheral system
- ✓ Fabrication of all components
- ✓ Creation of infrastructure
- ✓ Development of gyrotron
- ✓ Delivery of Gyrotron

Completed

- Testing of Gyrotron

Completed

Achievements at CEERI

✓ **Design completed**

- ❖ Cathode
- ❖ Magnetron Injection Gun
- ❖ Interaction Cavity
- ❖ Beam Tunnel
- ❖ Non-linear Taper
- ❖ Collector
- ❖ Cavity Cooling duct
- ❖ Collector Cooling duct
- ❖ Magnet System

✓ **Software developed**

❖ **MIGSYN**

Synthesis of MIG

❖ **MIGANS**

Analysis of MIG

❖ **GCAVSYN**

Synthesis of interaction cavity

❖ **GCAVSOC**

SOC for gyrotron cavity

❖ **GCAVMOD**

Mode selection for gyrotron cavity

✓ **Established Design Base**

✓ **Components fabricated**

✓ **Gyrotron Developed and delivered**

✓ **Installed Design Tools**

- ➢ CST MWS TRAK, OMNI TRAK
- ➢ HFSS AUTOCAD/ SOLID WORKS
- ➢ MAGIC OPERA
- ➢ EGUN ANSYS SURF3D

➢ **First Amarjeet Singh Young Achiever VEDA Award**

Design Methodology of MIG

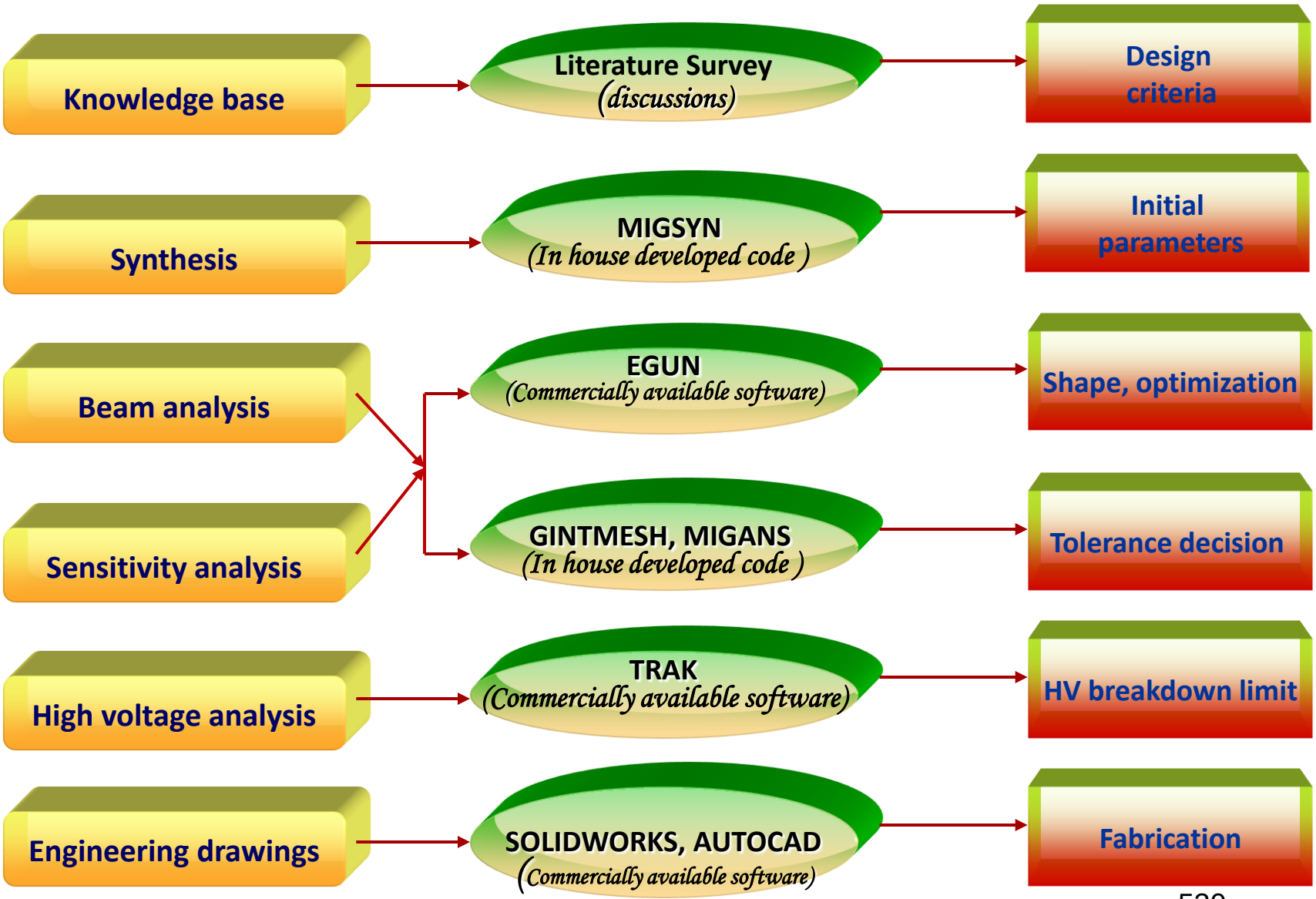

Cavity

Design flow of interaction cavity design

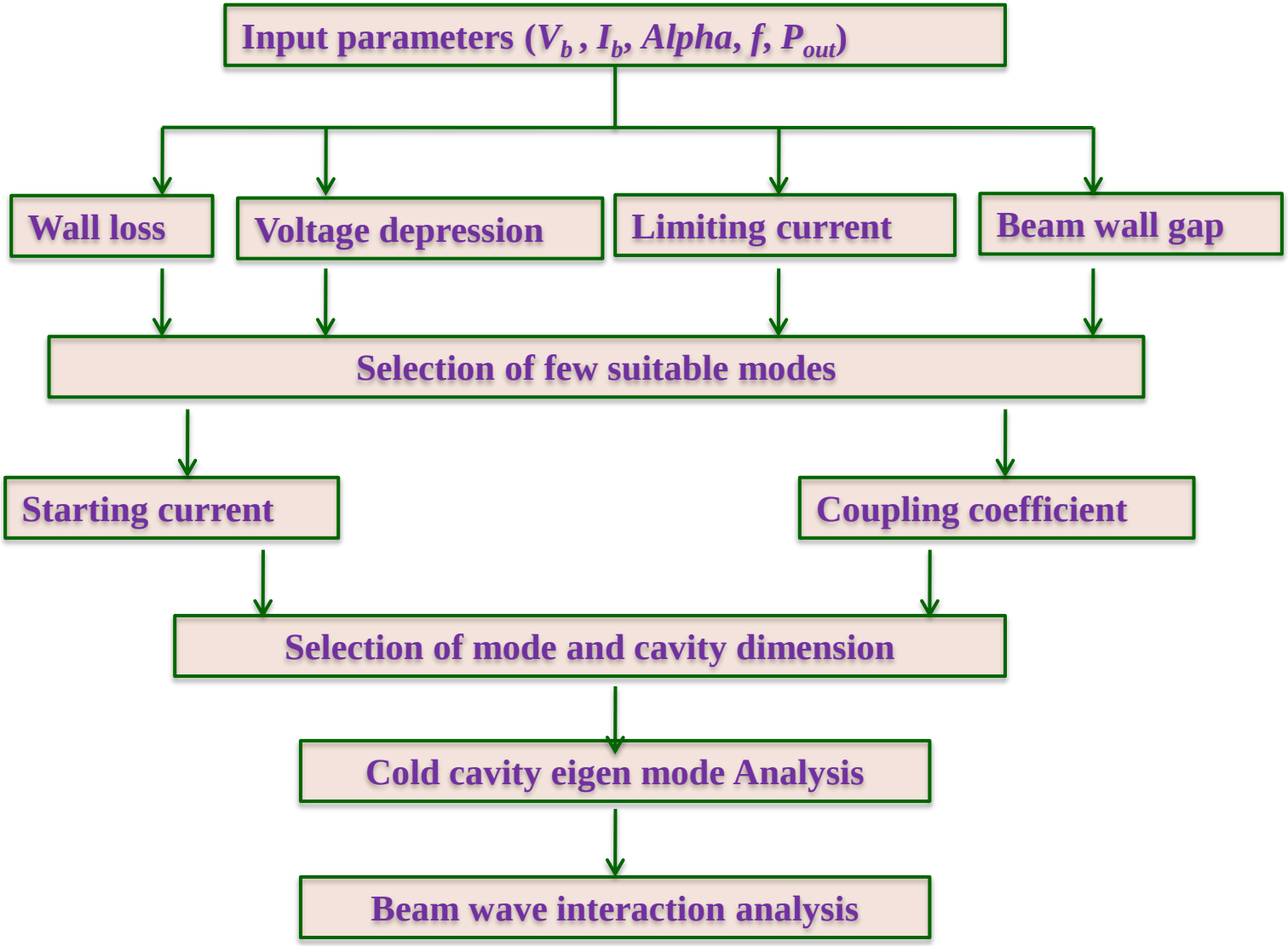

Strength: Major Simulated Tasks Completed for 42 GHz, 200 kW at CEERI

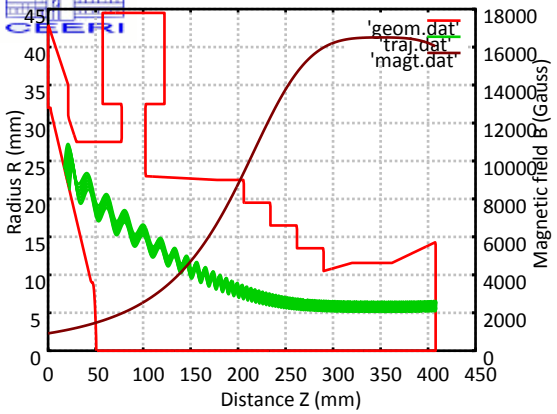

EGUN

Magnetron injection gun

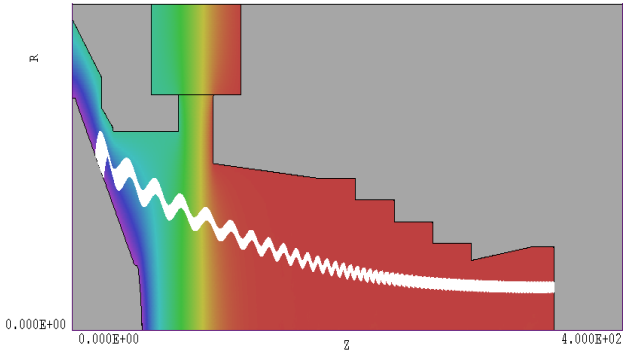

TRAK

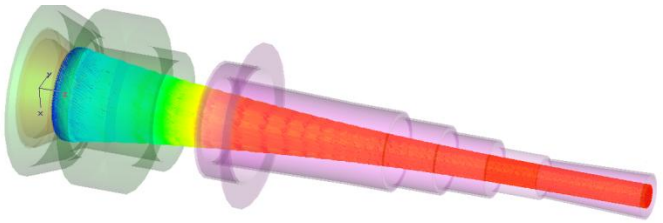

CST PS

Beam Tunnel (AlN-SiC)

Interaction cavity

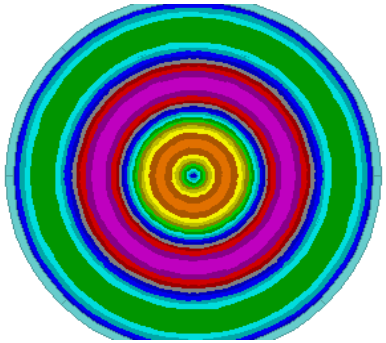

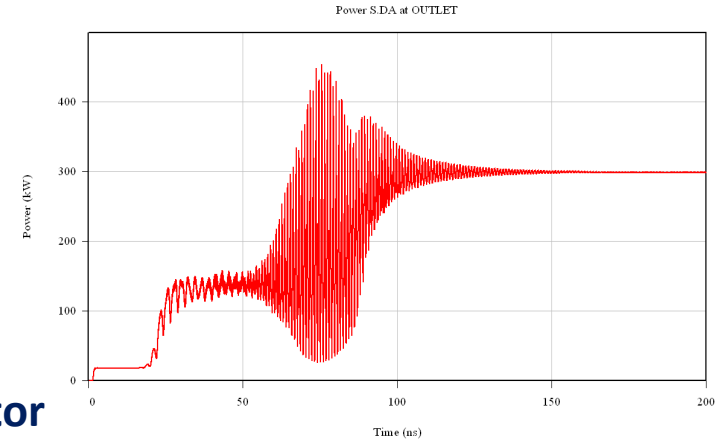

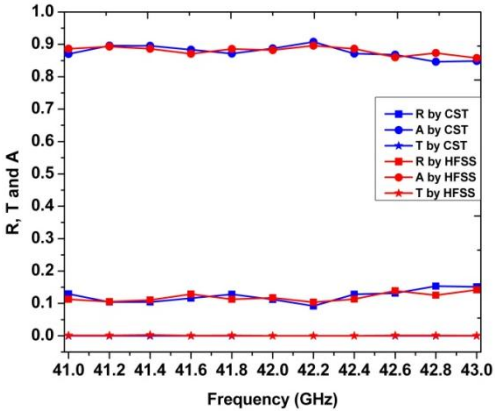

Electron beam collector

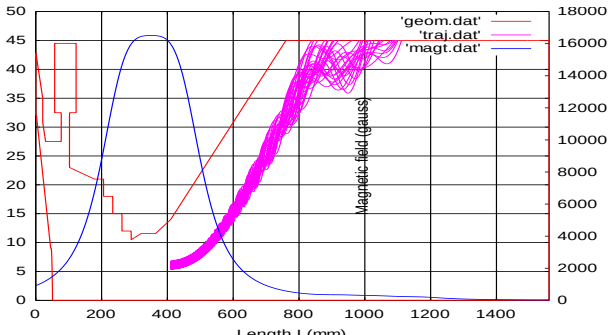

•Contribution of Student: 4-5/ year

Publications

- Invited Talk: 35
- Int/ Nat Journal -56
- Int./ National conf. – 70
- M.Tech -10
- Ph.D. Awarded – 8
- Conference Awards-06

Gyrotron Design Lab

Beam Emission Testing of 42 GHz gyrotron MIG

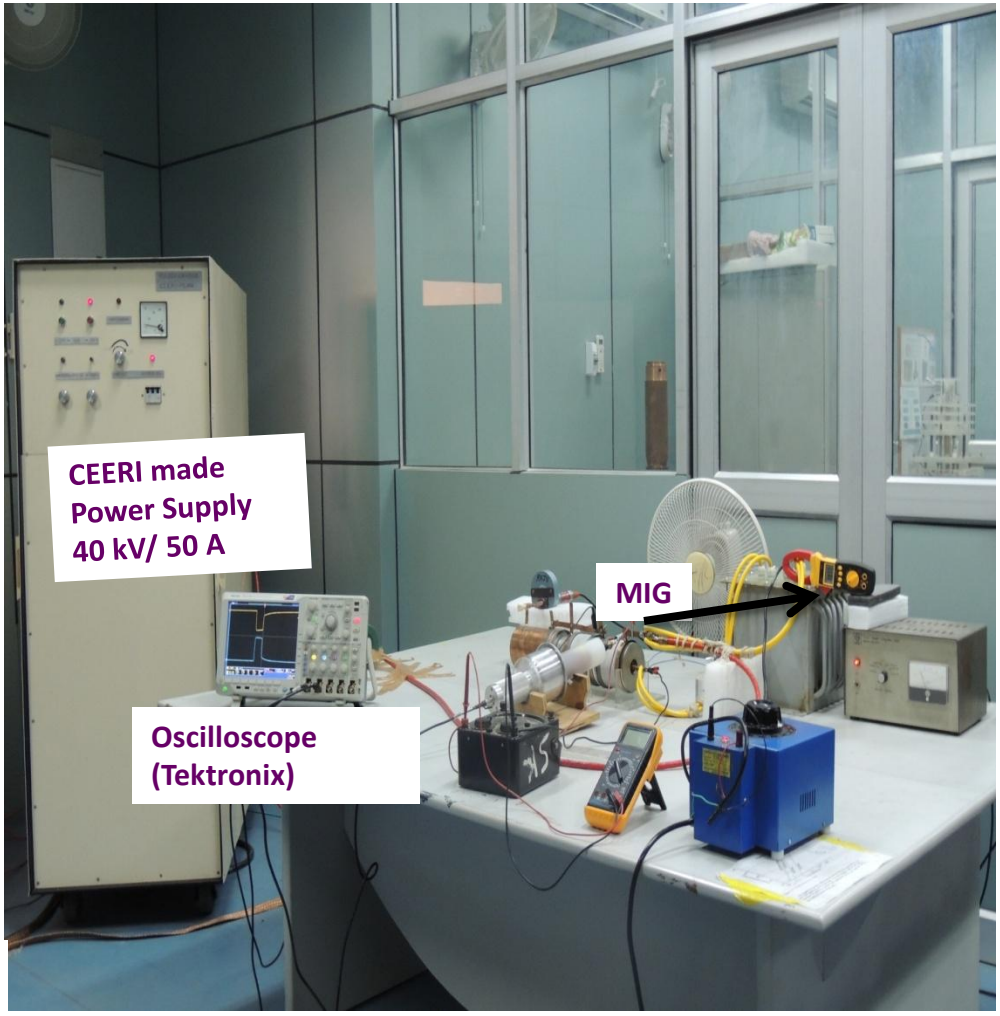

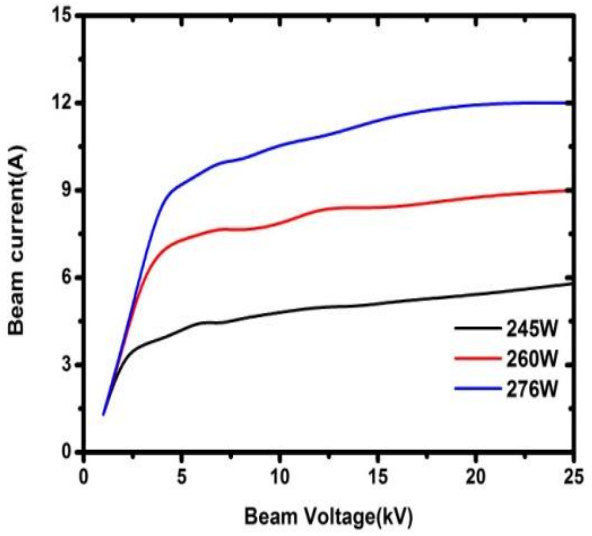

Current-voltage characteristics of the cathode

Infrastructure Developed for Measurement at CEERI

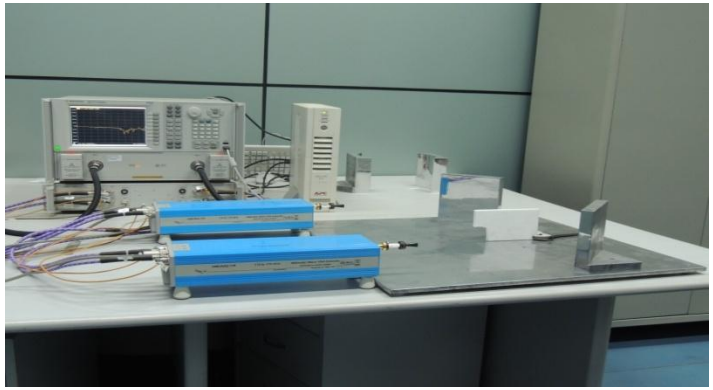

Cavity

MIG

Cooling Liquid

Cooling Duct

Vacuum Processing Unit

MIG-I testing in the presence of IPR team at CEERI Pilani

Collector cooling duct testing in the presence of IPR team at CEERI Pilani

42 GHz Gyrotron Components

Major Assemblies of 42GHz Gyrotron

MIG Assembly

Beam Tunnel + Cavity + NLT + Flange Assembly

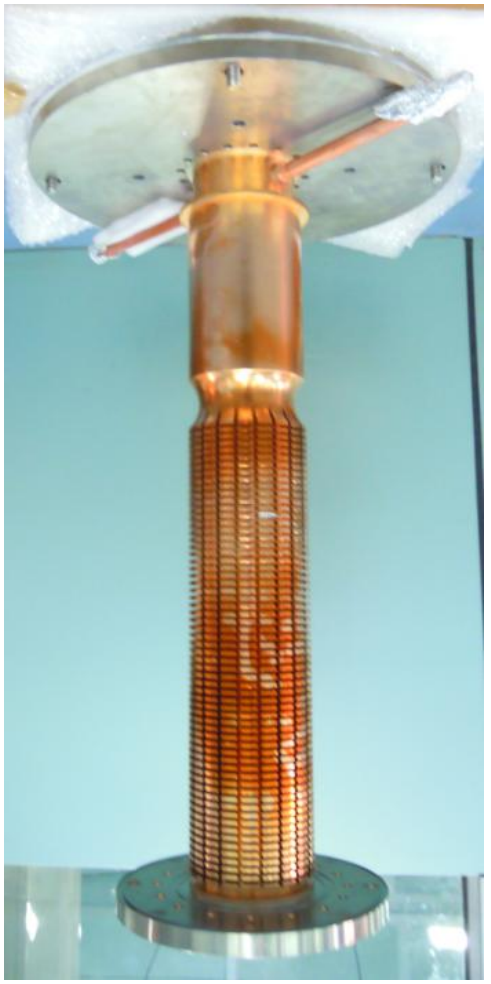

Collector + Flange Assembly

Assembling Stages of 42GHz Gyrotron

MIG Assembly

Beam Tunnel + Cavity + NLT + Flange Assembly

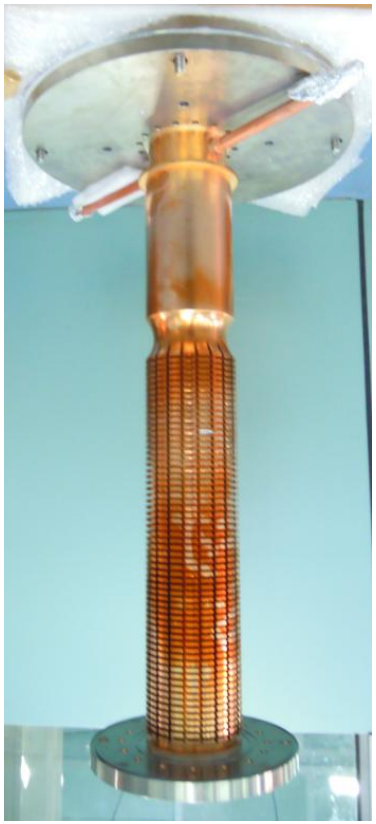

Collector + Flange Assembly

Lab Prototype Gyrotron (LPG)


VARIAN

Dr. A.K.Sinha Gyrotron Project Leader is explaining about designed Gyrotron during the Gyrotorn Lab Visit By Prof. D. Bora Director IPR Ghandinagar, Director CEERI Pilani and Dr.S.N.Joshi National Coordinator of Gyrotron

Deliverable Gyrotron: TPG

(TEST PROTOTYPE OF GYROTRON)

42 GHz 200kW-Gyrotron

Duct Mounted 42 GHz, 200 kW Gyrotron

2nd Prototype of Gyrotron

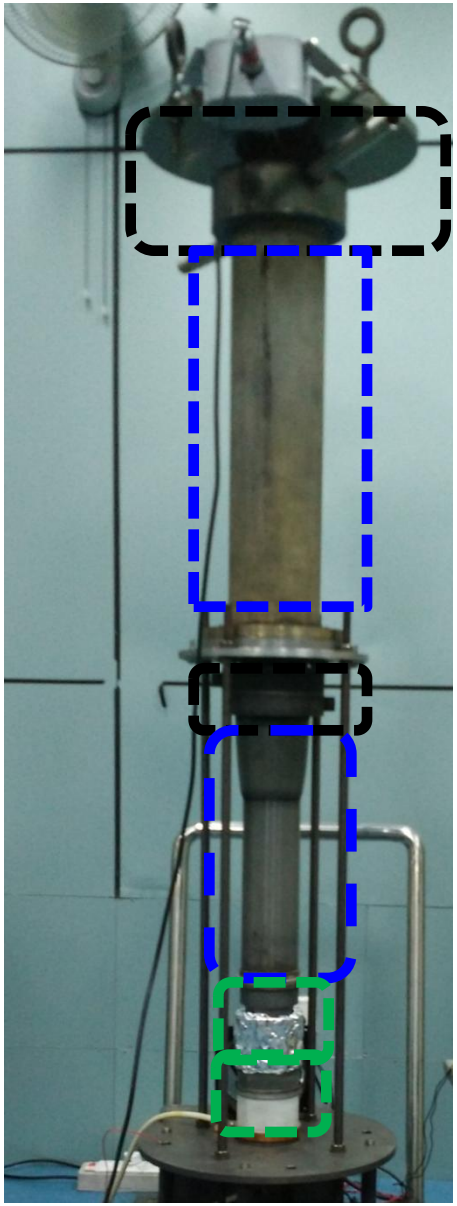

Simple to fabricate

No arc welding and cold working ⇒ Nonmagnetic

Simple to fabricate

No arc welding and cold working ⇒ Nonmagnetic

Fabrication as per design

2nd Prototype of Gyrotron…. From CSIR-CEERI to IPR

Departing from CSIR-CEERI

3 days after. safe arrival at IPR

Beam emission test

After mounting in magnet

Mounting in magnet

Gyrotron at IPR

Present

Completed

- Liquid He ⇒Magnet charging
- RF test

Development of 42GHz, 200kW Gyrotron prototypes

2014

2015

Lab prototype

For confidence building

1st prototype

2nd prototype

❖ **Electrical designs are same**

Other Gyrotrons

Frequency/Power	Applications	Recent results at CEERI
28GHz/200kW	Material Processing	Design in progress
95GHz/100kW	Active Denial System (MTRDC/DRDO Sponsored)	Design Completed
120GHz/1MW	International Thermonuclear Experimental Reactor (CSIR Network scheme)	Design (component) and development Completed
170GHz/1MW	International Thermonuclear Experimental Reactor (CSIR Network Scheme)	Design. Development and vacuum processing completed
300GHz/5 kW	Material Processing	Design in progress
670GHz/300kW	Radioactive Material Detection	Design in progress
2THz/100W	Nuclear magnetic resonance	Design in progress

Motivation: 28 GHz for material processing

Specifications

Frequency	**28 GHz**
Power	**>200 kW**
Beam Voltage	**65 kV**
Beam Current	**10 A**
Velocity ratio (α)	**1.4**
Operating mode	**TE_{03}**
Efficiency	**≤35%**

TE_{03} mode pattern

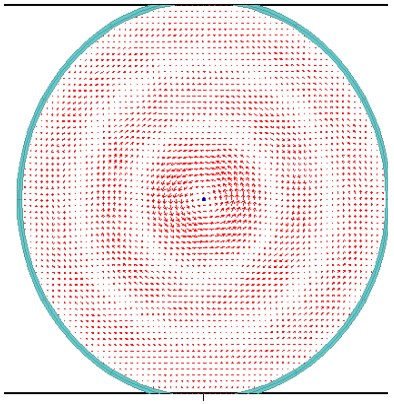

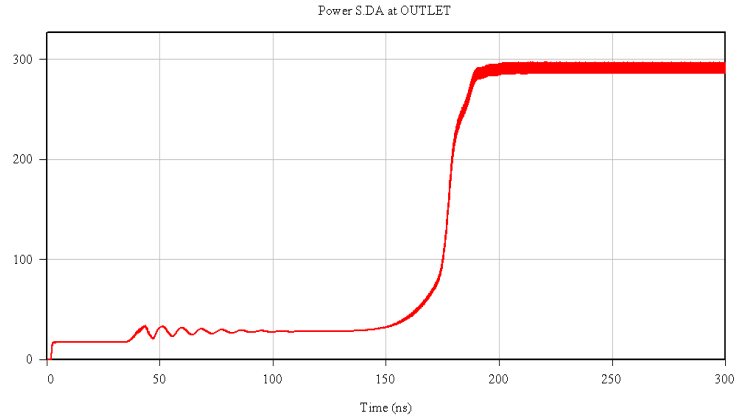

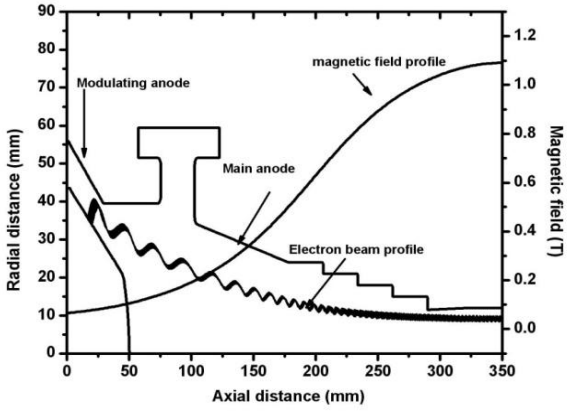

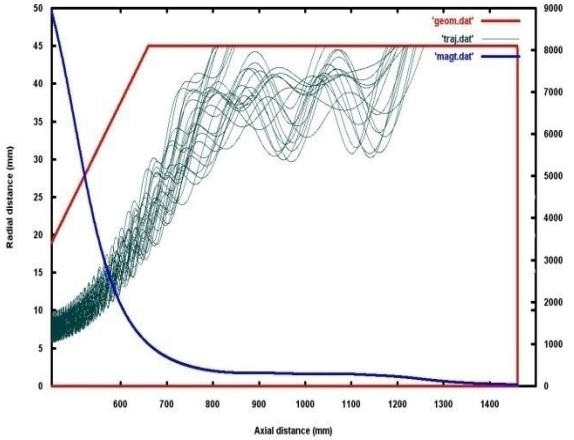

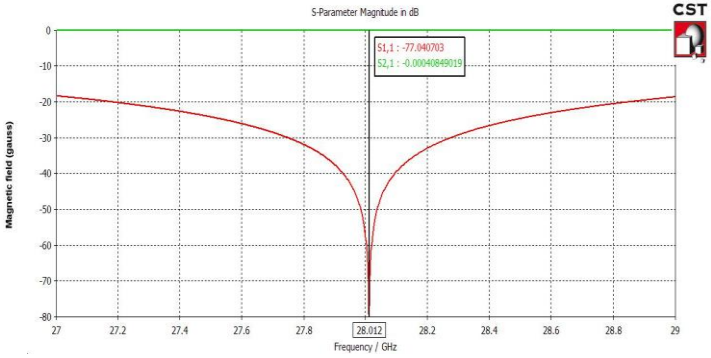

Active Denial System (ADS)

Applications of 95 GHz gyrotron

- ✓ Active Denial System
- ✓ Cloud monitoring
- ✓ ECRH

Applications of ADS

- ✓ Homeland Security (Port checkpoints, shipboard protection, port protection)
- ✓ Mob Control

ADS technology highly mobile multi wheeled vehicle

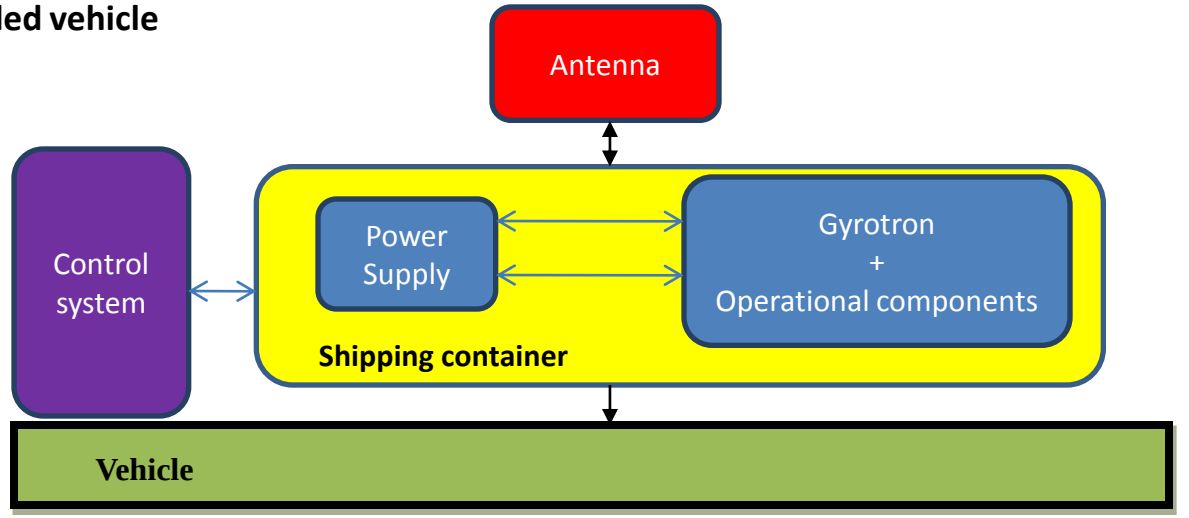

Schematic of ADS configuration.

Motivation: Mobile Energy System: 95 GHz Gyrotron

✓A novel application of gyrotron is in non lethal, counter personnel, directed energy weapon system also called Active Denial System (ADS) which can be used against human targets at a distance beyond the effective range of small arms

✓95 GHz radiation with 100 kW of power is suitable for ADS application due to the relative minimum of atmospheric absorption at 95 GHz

✓95 GHz can transmit upto several hundreds of meters (Atmospheric Window)

✓ The millimeter wave can penetrate upto 1/64 of inch of human skin

✓ Creates burning sensation but not damage the nerve system and blood vessels

✓Gyrotron is a very suitable device for the generation of 100 kW, 95 GHz radiation and is used in the current development of ADS system

✓THE DESIGN AND DEVELOPMENT OF 95 GHZ GYROTRON IS THUS INITIATED AT MTRDC, BANGALORE AND CEERI IS ALSO PARTICIPATING IN THE PROGRAM

Basic specifications of the 95 GHz gyrotron

Frequency
95GHz

Output Power
100kW

Beam voltage
50-55 kV

Beam current
6-8 A

Magnetic field at cavity center
3.55-3.57 T

Velocity ratio
1.3-1.5

Total efficiency
≈ 50 %

Wall loss
<2 kW/cm^2

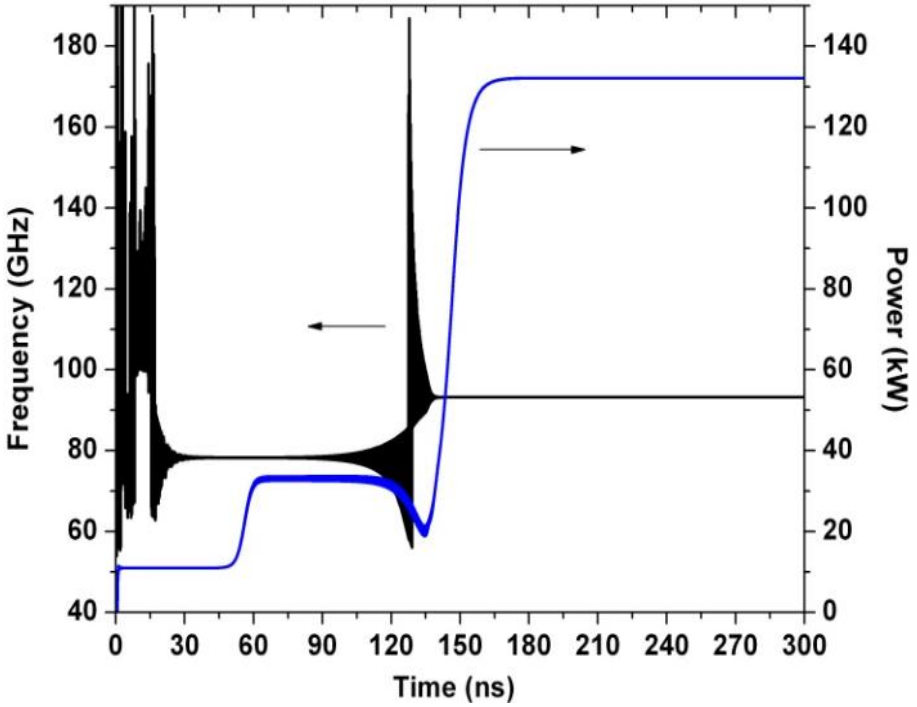

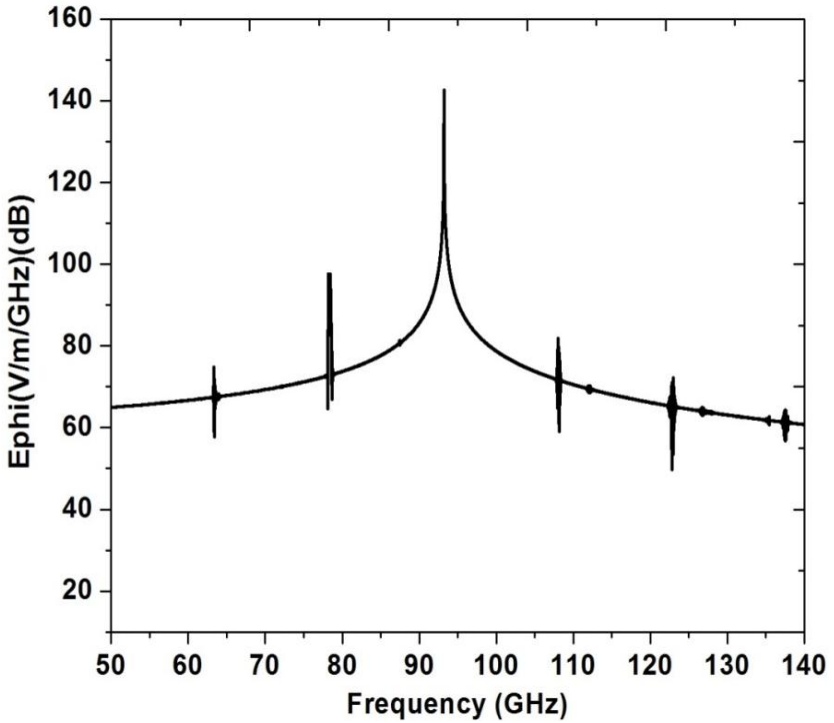

(V_b= 52 kV, I_b= 7 A, α= 1.35, B_0= 3.56 T)

Activity at CEERI

Specifications of 95 GHz gyrotron	
Frequency (f)	95 GHz
Output power (Pout)	≥ 2 MW
Efficiency (η)	≥ 40%
Beam voltage (Vb)	80–85 kV
Beam current (Ib)	45–50 A
Operating mode	TE24,8
Wall loss	< 2 kW/cm2
Diffractive Q (Q diff)	800–1000

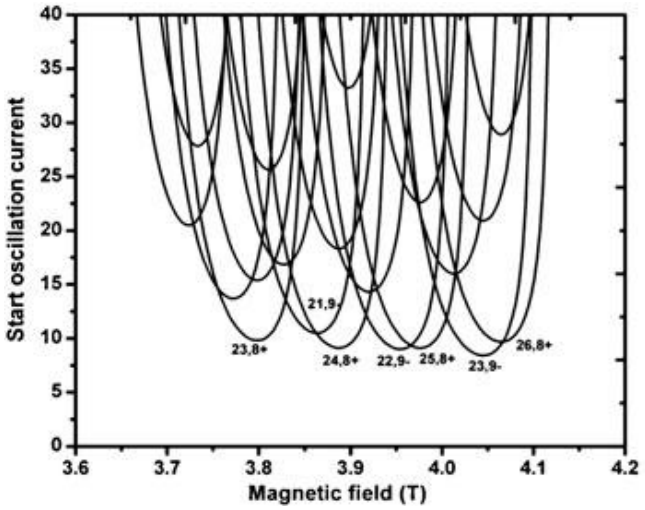

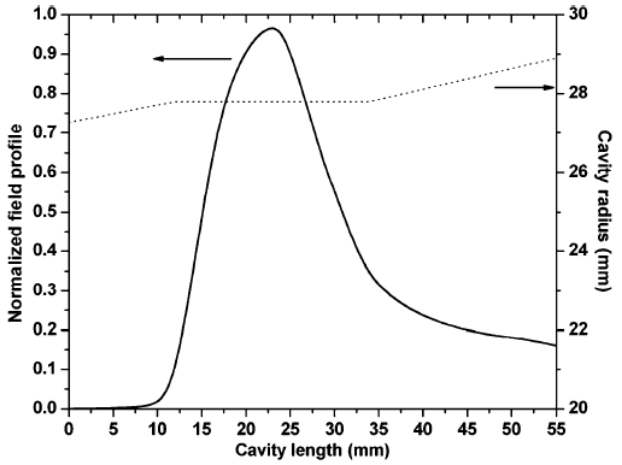

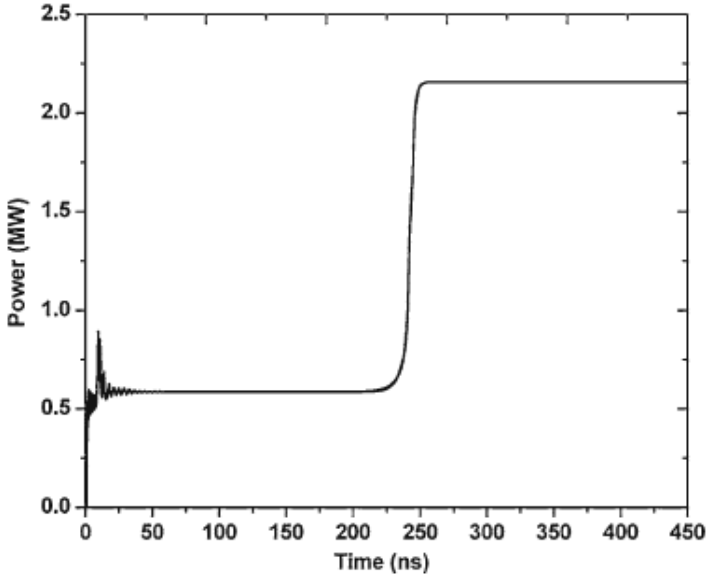

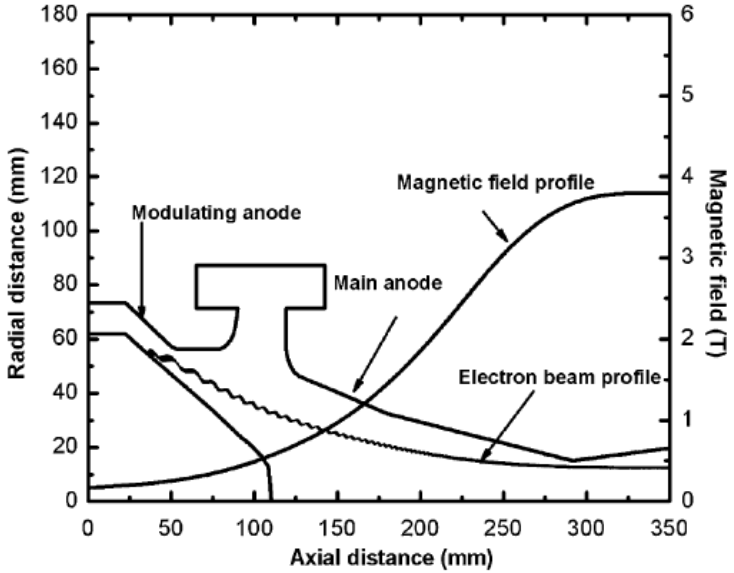

➢ *Design of 95 GHz, 2 MW Gyrotron for Communication and Security Applications*, Nitin Kumar & Udaybir Singh & T. P. Singh & A. K. Sinha, *J Infrared Milli Terahz Waves (2011)* 32:186–195

Motivation: ITER Activity

120 GHz gyrotron was initially proposed as start up gyrotron in ITER program (ITER to be built at CADARACHE, FRANCE)

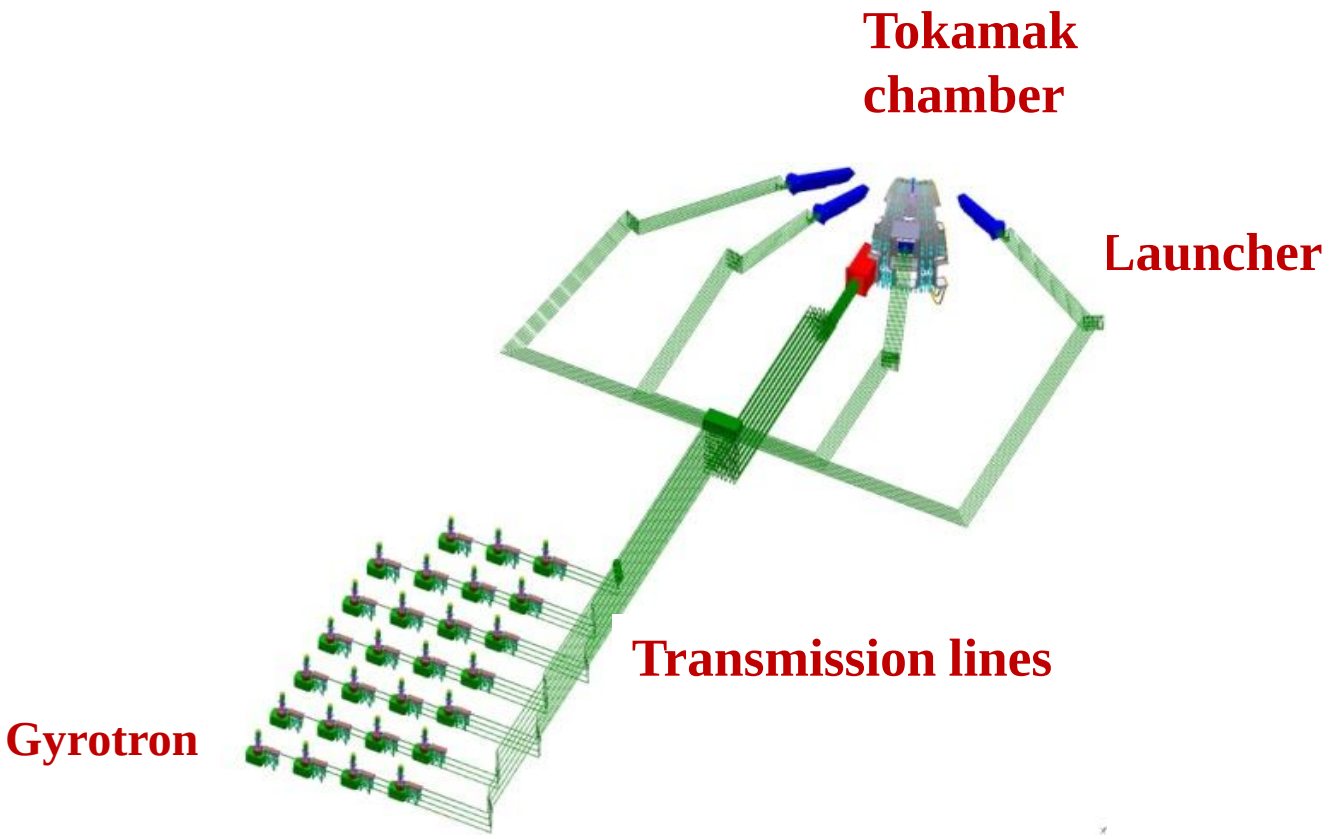

120 GHz

Motivation: ITER Activity

120 GHz gyrotron was initially proposed as start up gyrotron in ITER program (ITER to be built at CADARACHE, FRANCE) (2007-2012)

Specifications

Frequency	**120 GHz**
Power	**>1 MW**
Beam Voltage	**80 kV**
Beam Current	**40 A**
Velocity ratio (α)	**1.4**
Operating mode	**$TE_{22,6}$**
Efficiency	**≤35%**

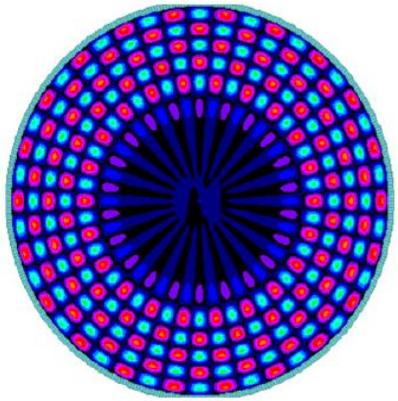

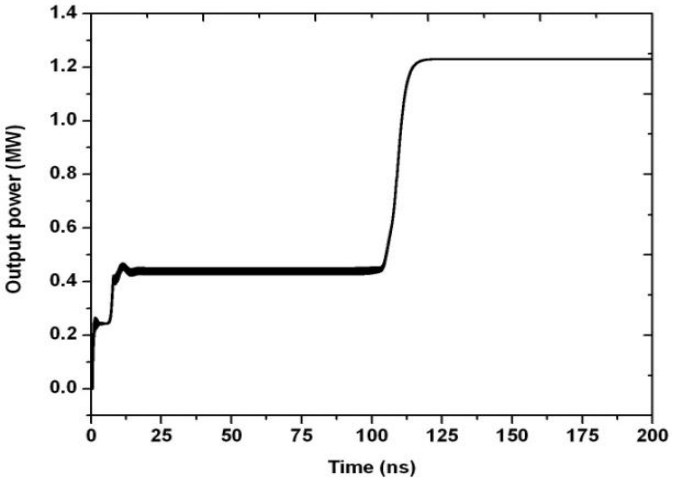

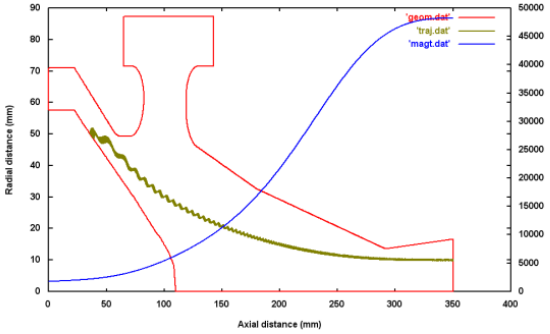

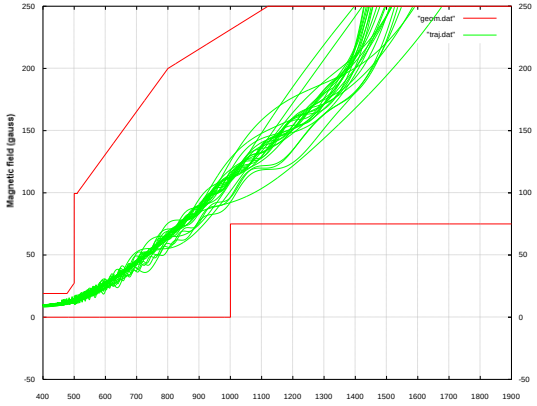

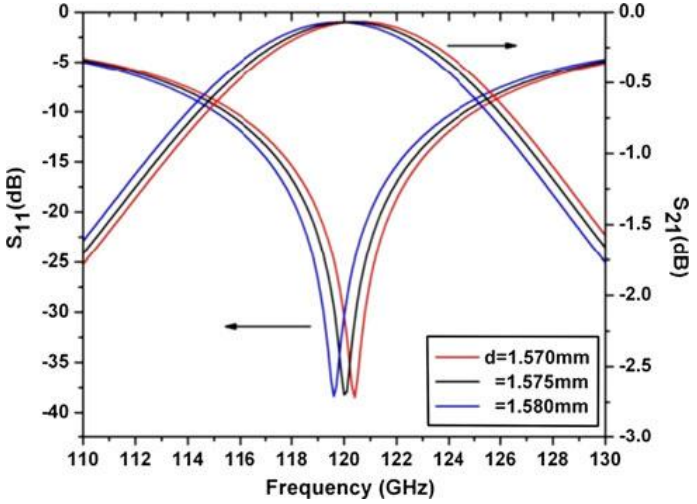

120 GHz,1MW Gyrotron

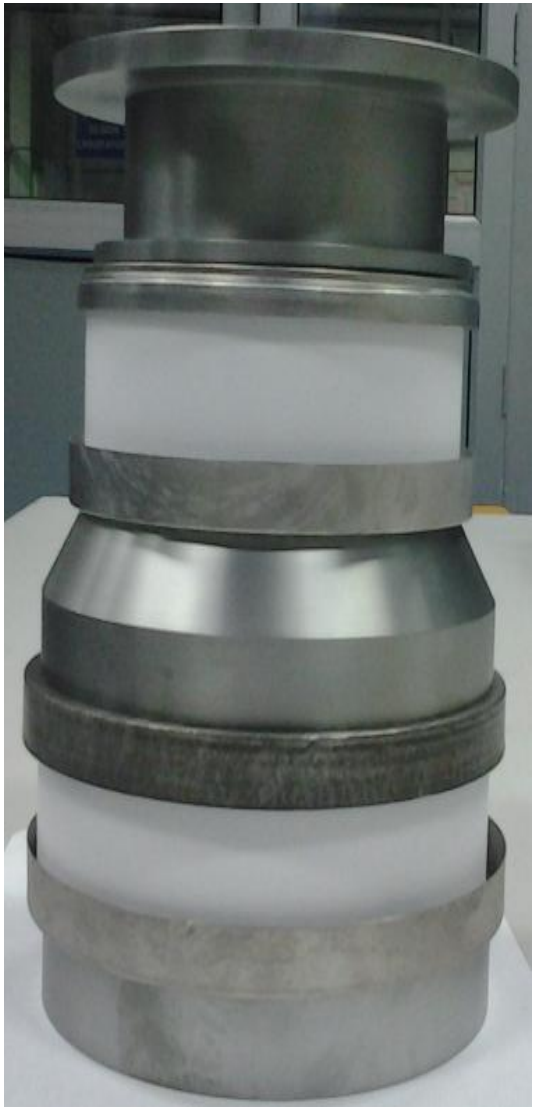

Assembly of MIG

Cavity of 120 GHz Gyrotron

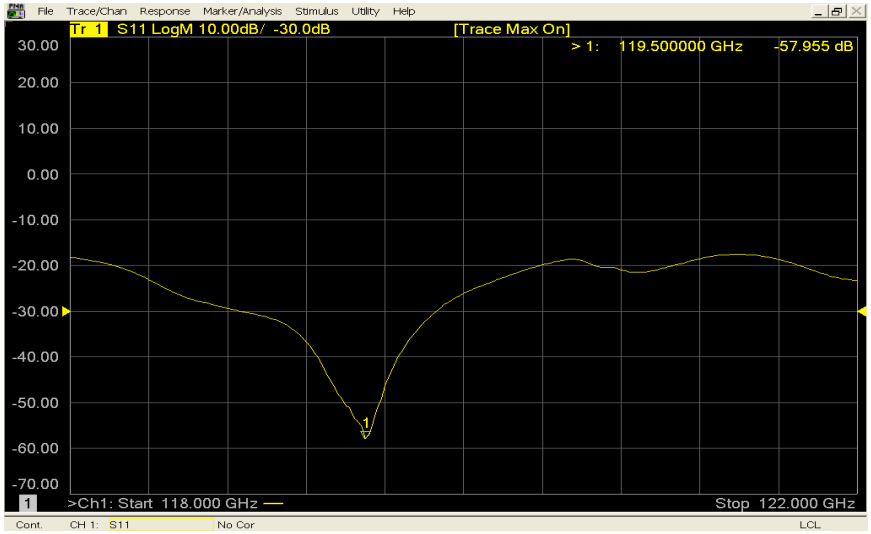

Measured results of 120 GHz Cavity

Motivation: ITER Activity

170 GHz gyrotron is finalized as start up gyrotron in ITER program (ITER to be built at CADARACHE, FRANCE) (CSIR Sponsored Project) (2012-2017)

Specifications

Frequency	170 GHz
Power	>1 MW
Beam Voltage	80 kV
Beam Current	40 A
Velocity ratio (α)	1.4
Operating mode	$TE_{34,10}$
Efficiency	≤35%

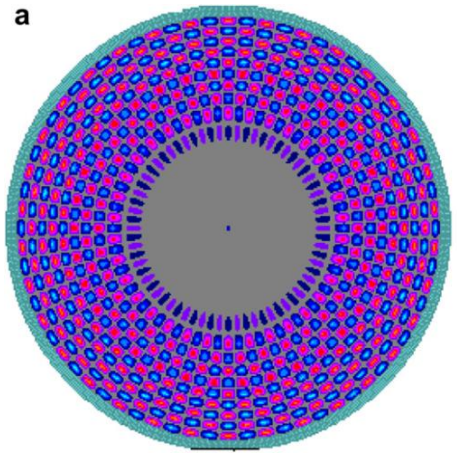

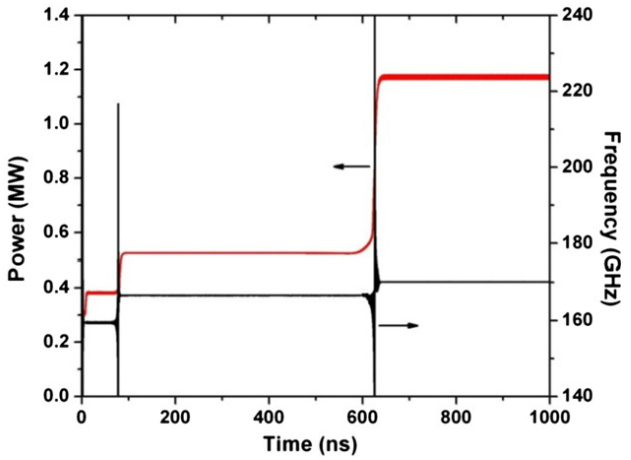

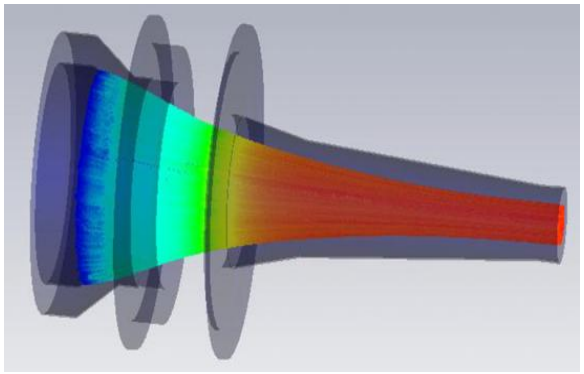

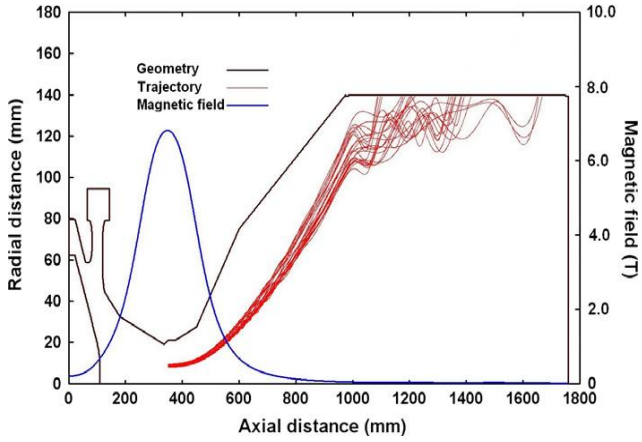

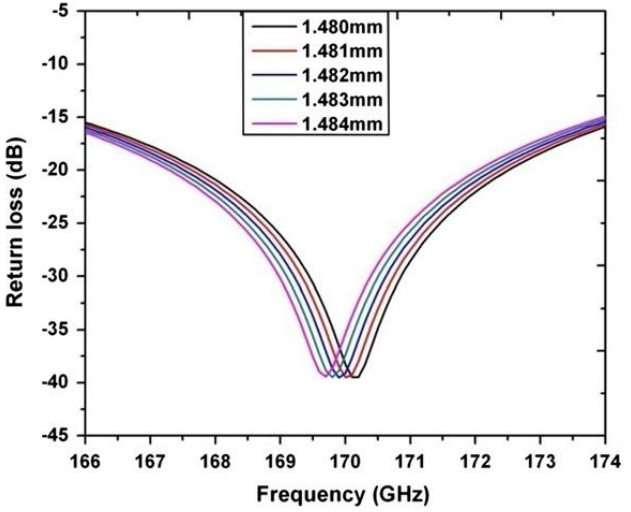

Activity : Design and Development of 170 GHz,1MW (short pulse) Gyrotron

Specifications:

Particulars	Specifications
Frequency	170 GHz
Output Power	1MW
Beam Voltage	80 kV
Beam Current	40 A
Pulse width	~ 50 µsec (Short Pulse)
Duty cycle	< 5%
Cavity Magnetic field	≈ 6.77 T (Superconducting magnet)
Output mode	TEM (Gaussian)
Mode purity	≈ 92 %
Operation	10 msec
Efficiency	≈ 30 %
RF Collection	Radial

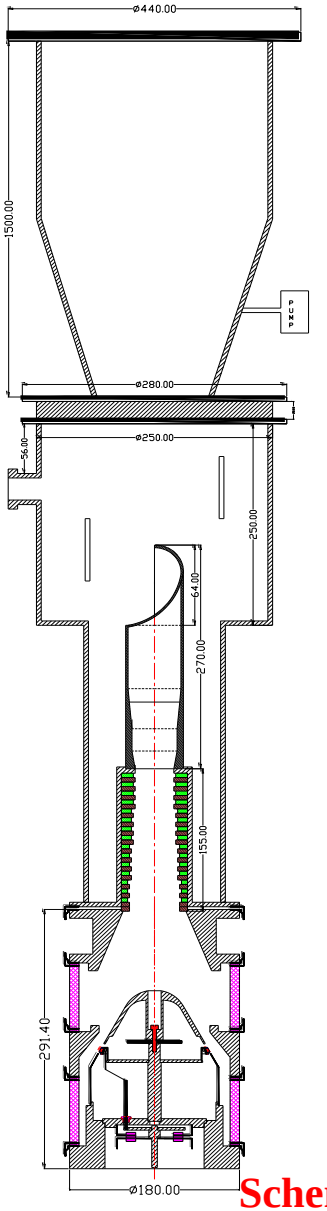

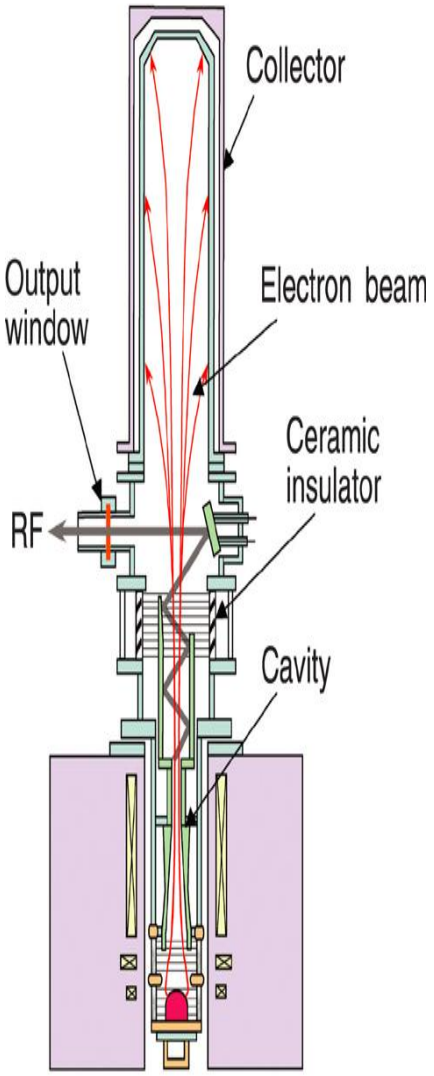

Schematic of 170GHz Gyrotron

Vacuum processing of MIG-Collector Test Module (GCTM) for 170 GHz:

(Tube vacuum = 2 x10^{-9} torr)

GCTM on vacuum processing station

Vacuum station control unit

Cathode activation of MIG-Collector Test Module for 170 GHz:

- Apply AC voltage between heater filament and cathode base to the desire rating

Cathode activation of GCTM

Operating condition:

Heater wattage	Heater Voltage (V)	Heater Current (A)
300 watt	17.0	18.1

Cavity:

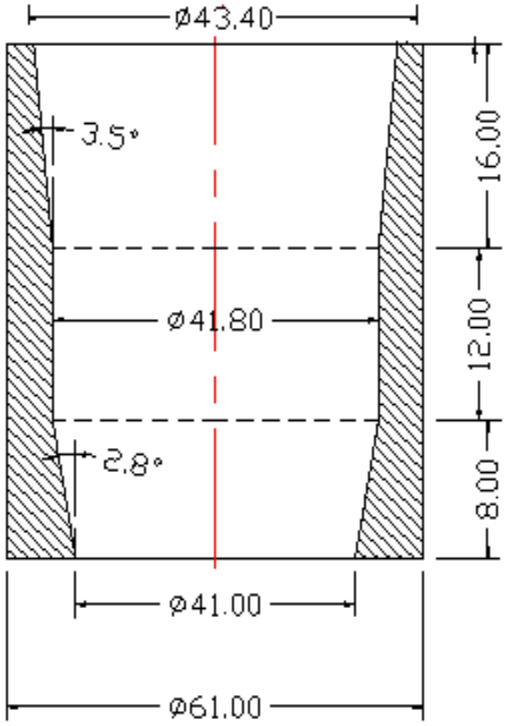

Fig. Engineering drawing of cavity

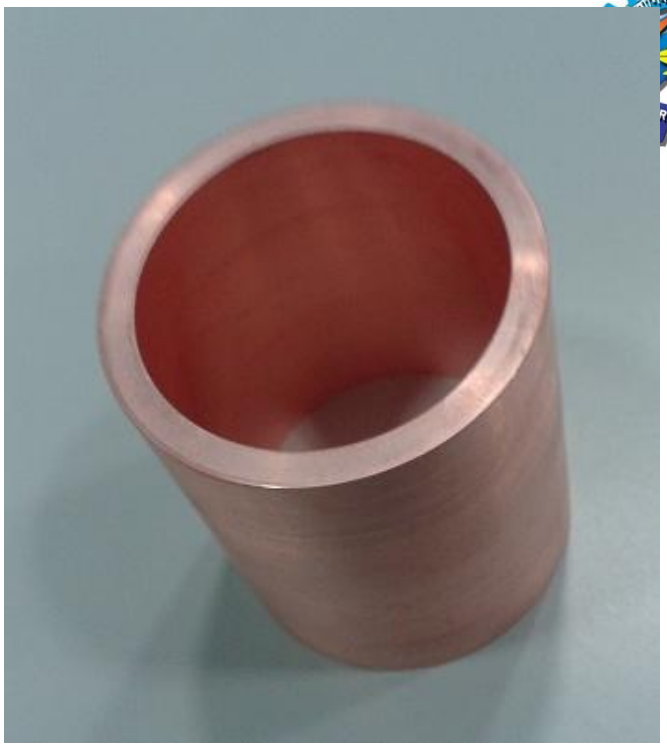

Fig. Fabricated cavity for 170 GHz

Table: Dimension measurement

Values	Length $L_1/L_2/L_3$ (mm)	Angle $\theta_1/\theta_2/\theta_3$ (degree)	Radius $R_1/R_2/R_3$(mm)
Design	36 mm	$2.8^o/0^o/3.5^o$	20.50/20.90/21.70

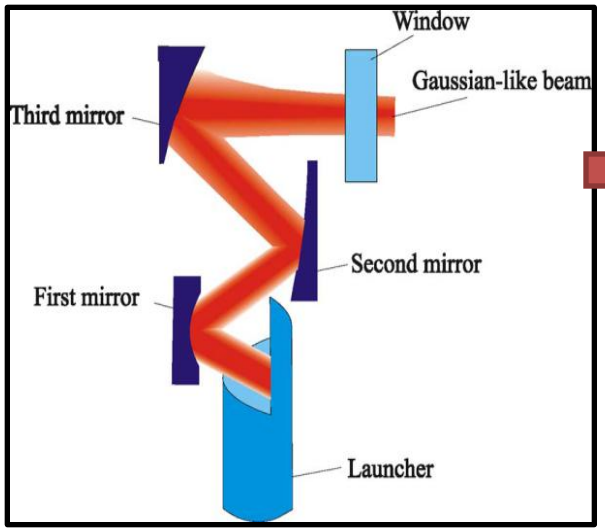

Schematic of Quasi optical mode converter

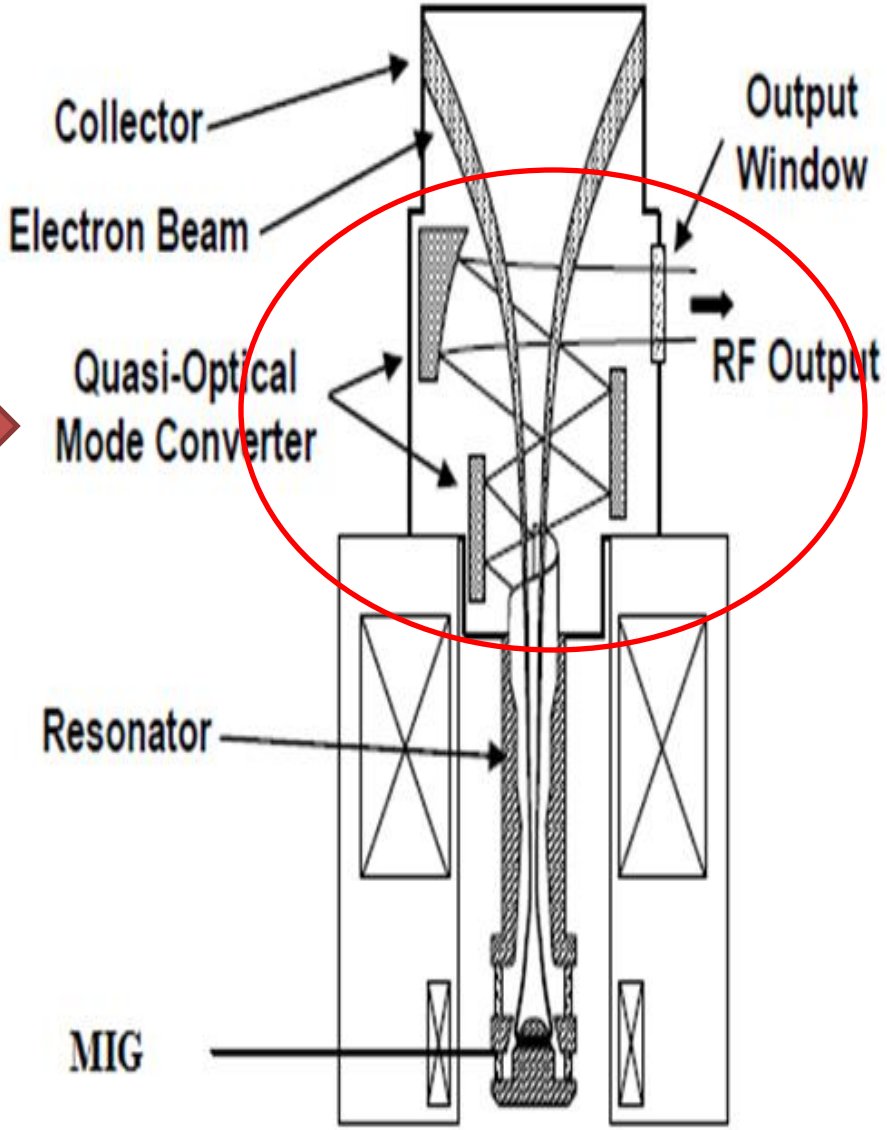

Schematic diagram of 170 GHz Gyrotron

Development of mode launcher and 3-mirrors for mode converter:

Vlasov launcher

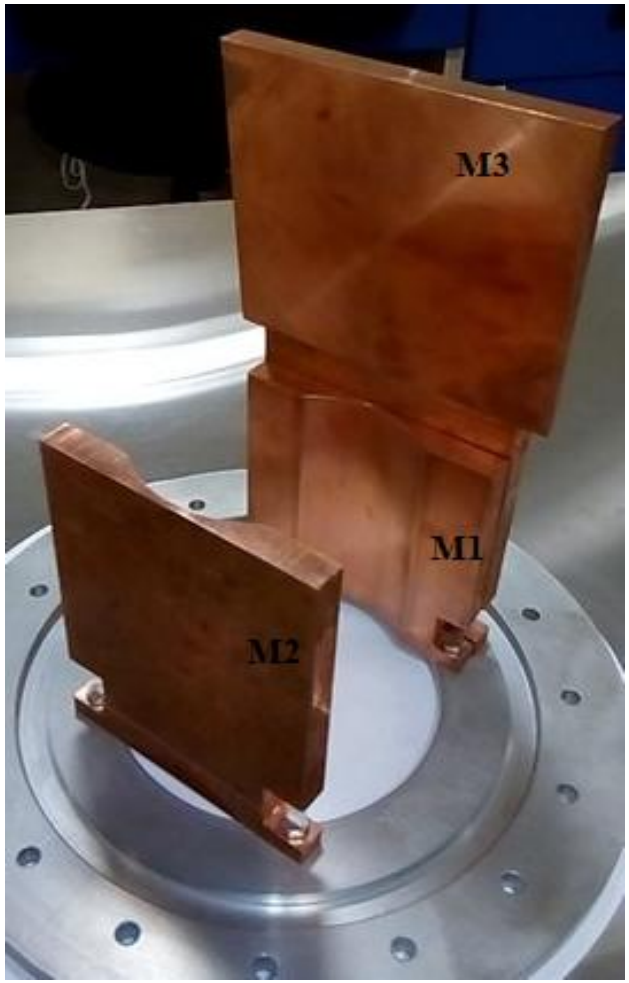

3-metal mirrors

Assembly of mode converter

Development of mirror box for Quasi optical mode converter:

SS- Tube

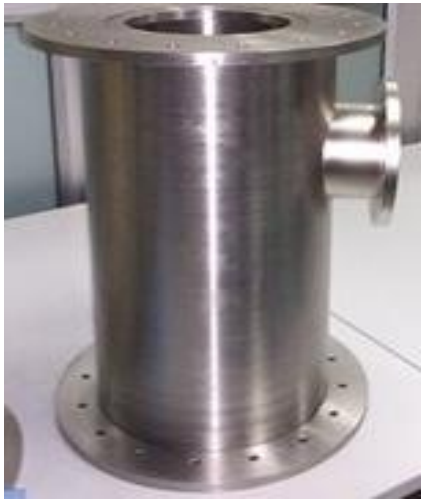

Envelope of mirrors

Assembly of mirror box with view port

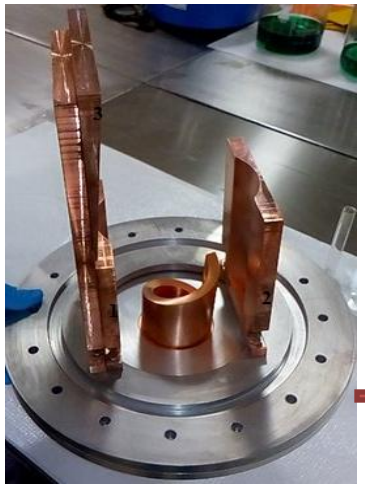

Inside Assembly

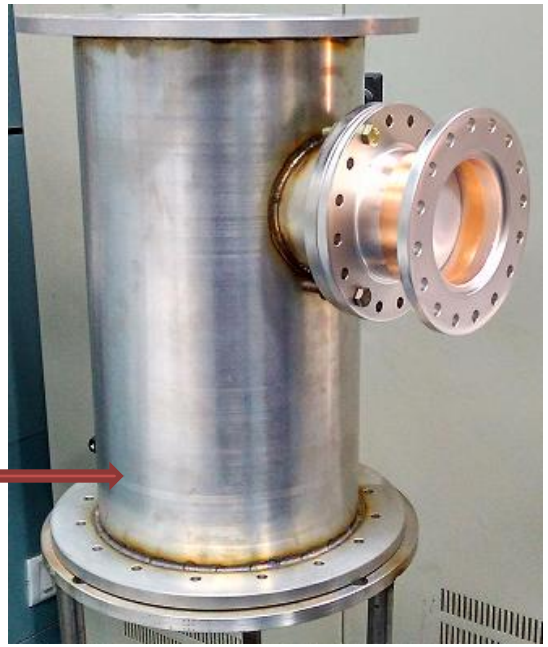

Mode converter with RF window

RF Window:

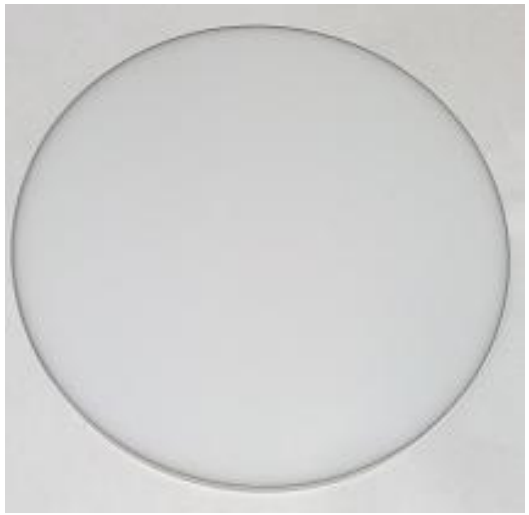

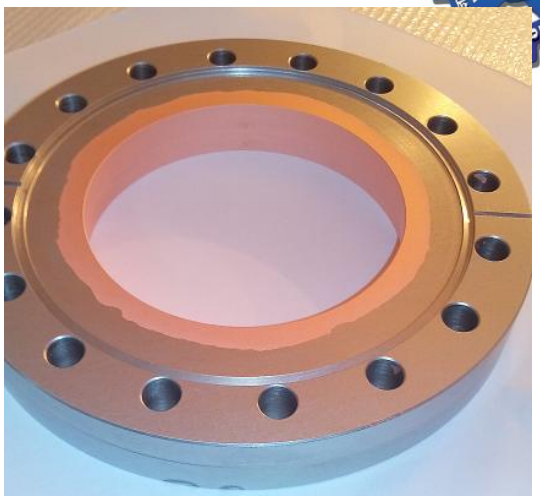

Waveguide, alumina ceramic disc and SS-flanges

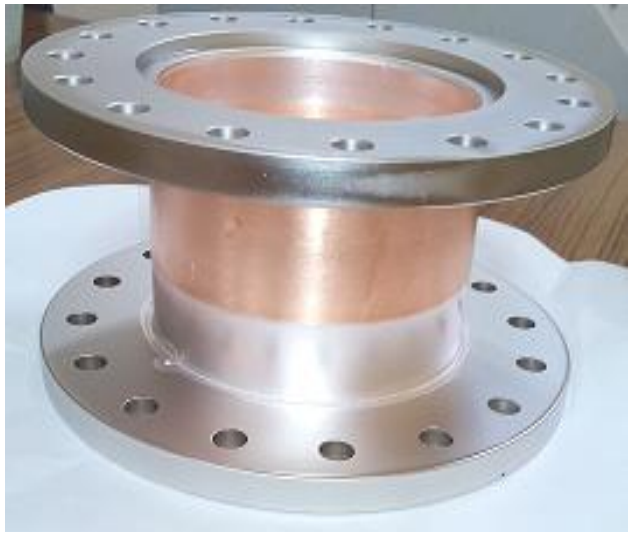

Developed single disc alumina RF window for 170GHz

Collector: in two pieces

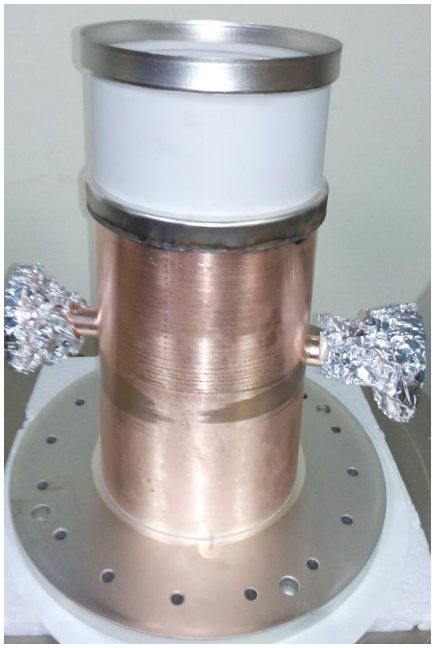

Part1(with isolation)

Part 2

Collector Assembly

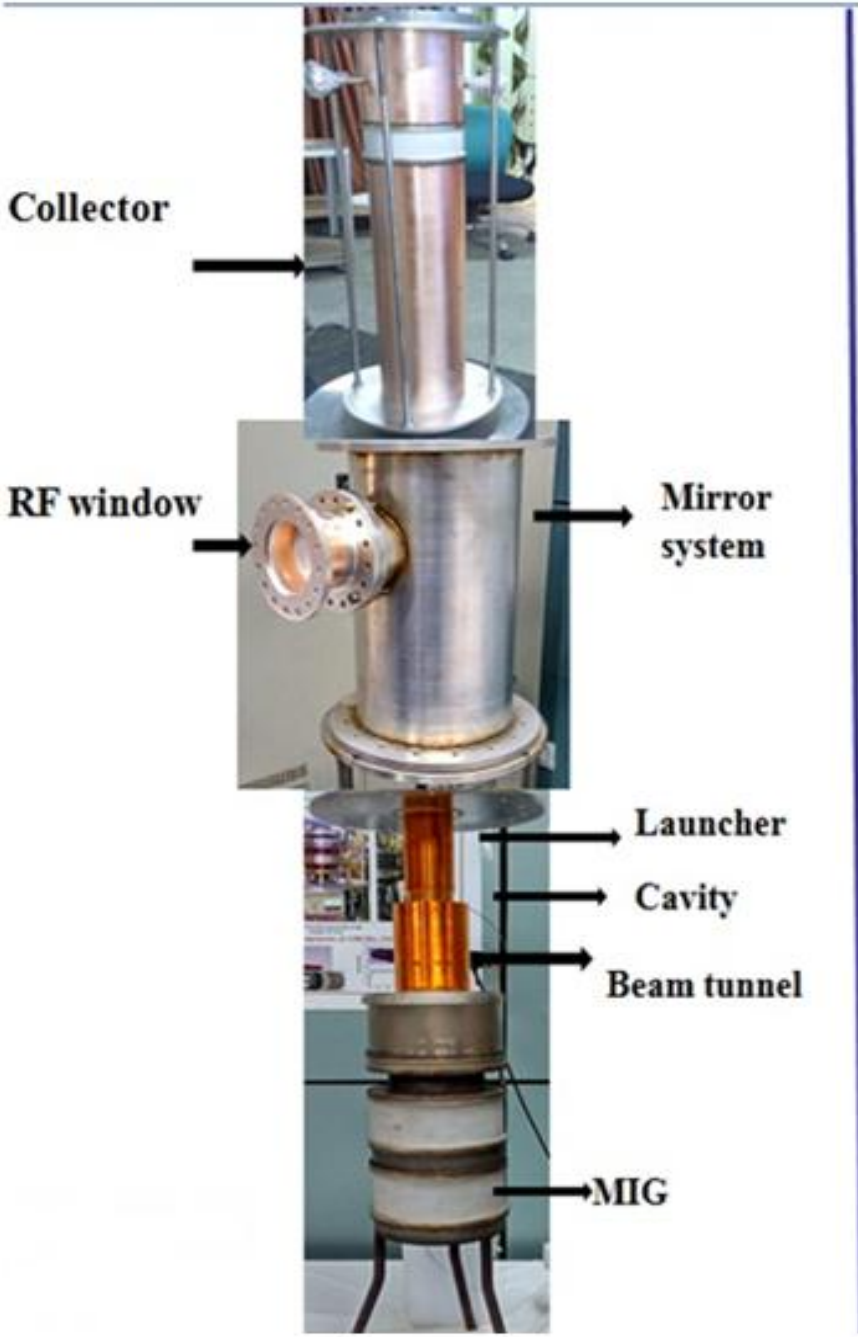

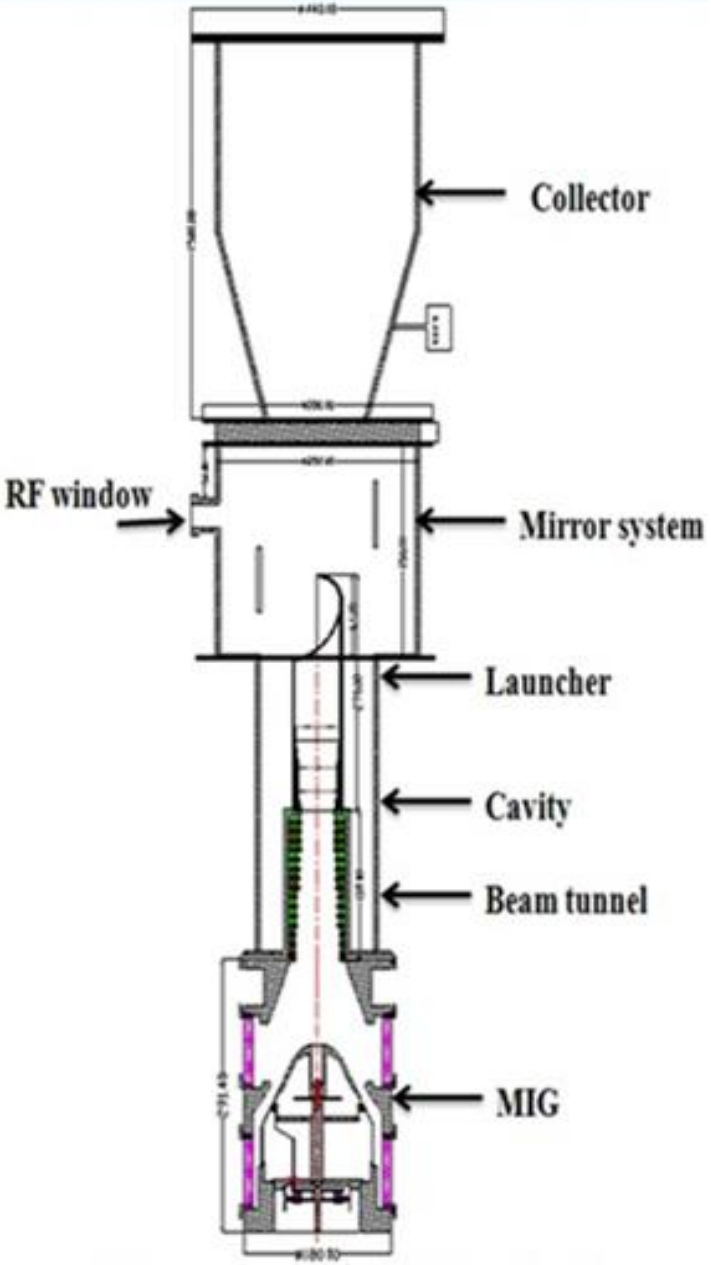

Development status vs. schematic diagram of 170 GHz short pulse Gyrotron

Complete Integration of demountable 170 GHz Gyrotron :

Leak testing of 170 GHz Gyrotron

Gyrotron on vacuum processing station

Motivation: Material Processing

300 GHz gyrotron is used in material processing applictions

Specifications

Frequency	300GHz
Power	>5 kW
Beam Voltage	20 kV
Beam Current	2A
Velocity ratio (α)	1.27
Operating mode	TE_{06}
Efficiency	≤35%

$TE_{0,6}$ mode pattern

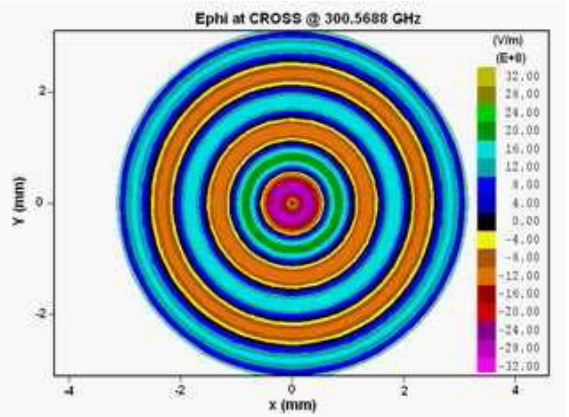

MIG design

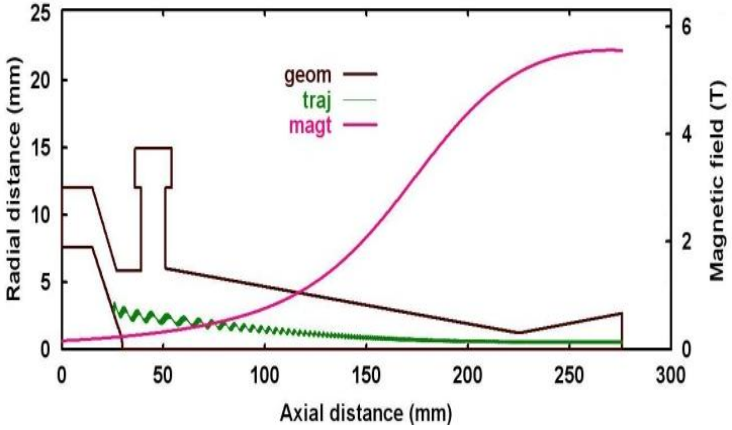

Power Growth

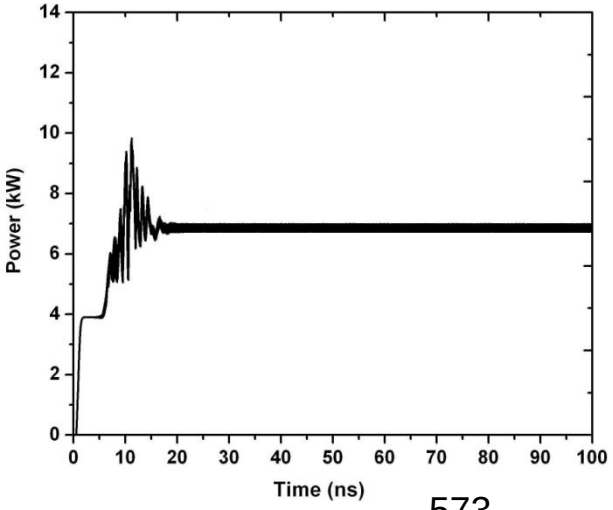

670 GHz Gyrotron

A new application of THz radiation for the concealed radioactive materials detection is proposed by Granatstein and Nusinovich in 2010 (J. Appl. Phys. 108 (2010) .

The detection of radioactive materials is based on the phenomena of air breakdown by focused terahertz radiation. In the presence of radioactive material in a container, the density of electrons increases several folds in air and initiate the breakdown in the presence of electromagnetic radiation of terahertz frequency region, which is not possible in the absence of extra electrons produced by some radioactive material.

The calculations show the electromagnetic radiation of more than 200 kW power with few μs pulse which can be focused in the area of around 10-100 μm can be used in the air breakdown in the presence of extra electrons (generated by some radioactive materials).

460 GHz and 670 GHz are two frequencies in THz band show minimum absorption in atmosphere.

670 GHz

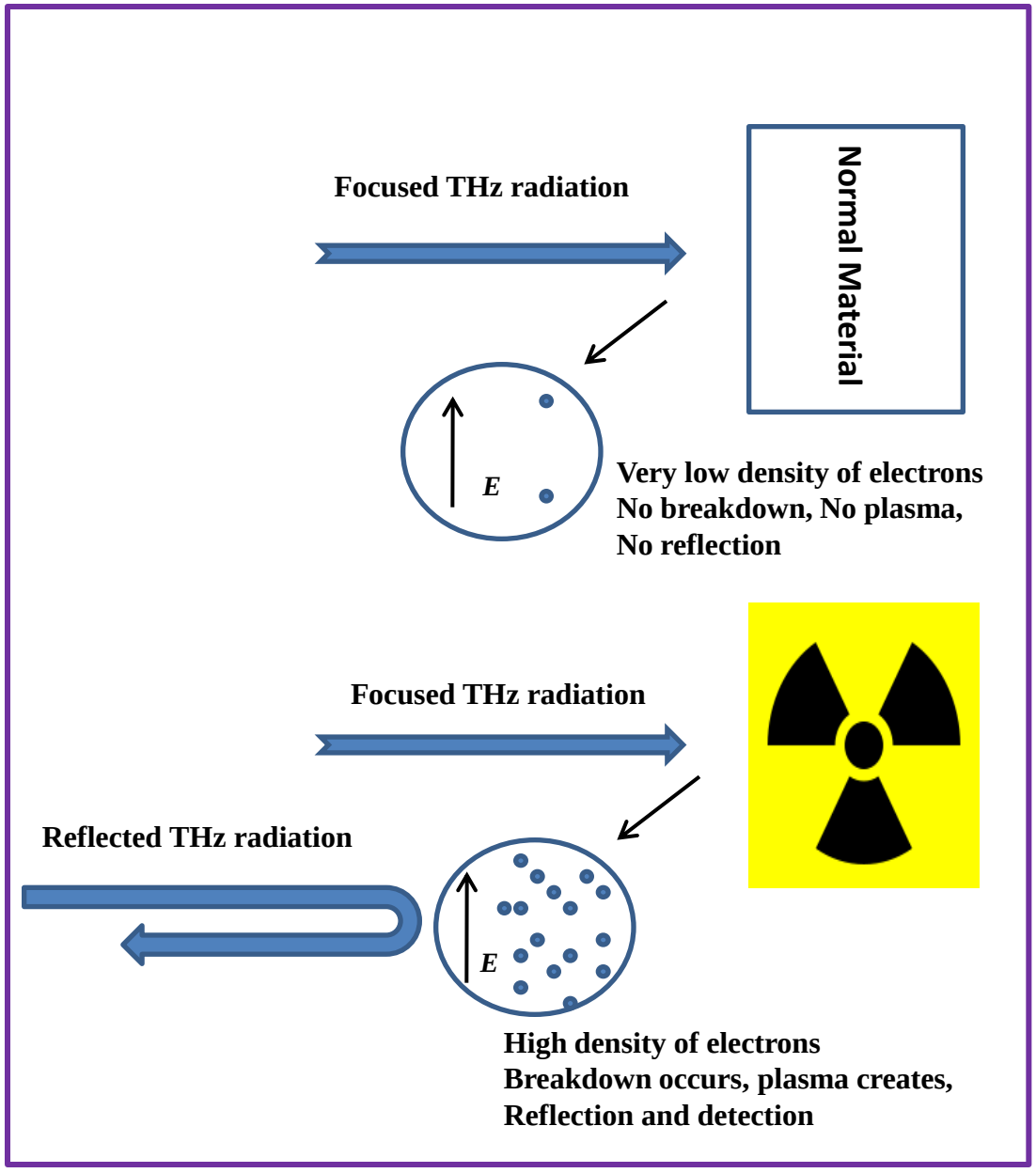

The focused THz radiation is unable for breakdown in normal air (in the absence of radioactive material)

670 GHz

Motivation: Radio active material detection

670 GHz gyrotron is used in radio active material detection

Specifications

Frequency	**670 GHz**
Power	**300 kW**
Beam Voltage	**70 kV**
Beam Current	**14A**
Velocity ratio (α)	**1.4**
Operating mode	**$TE_{25,10}$**
Efficiency	**≤ 30%**

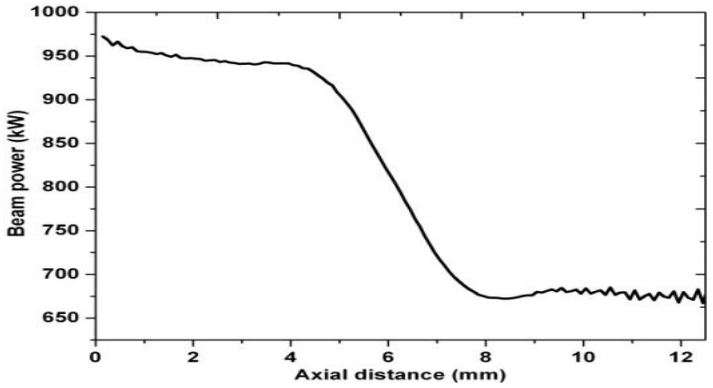

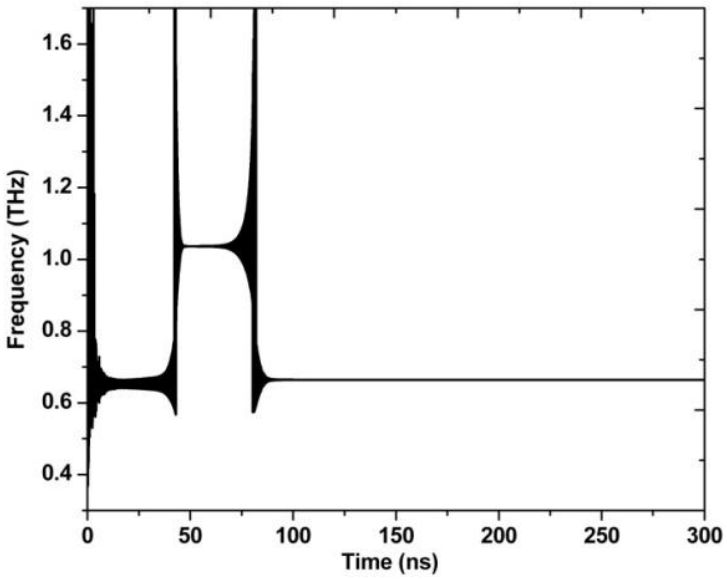

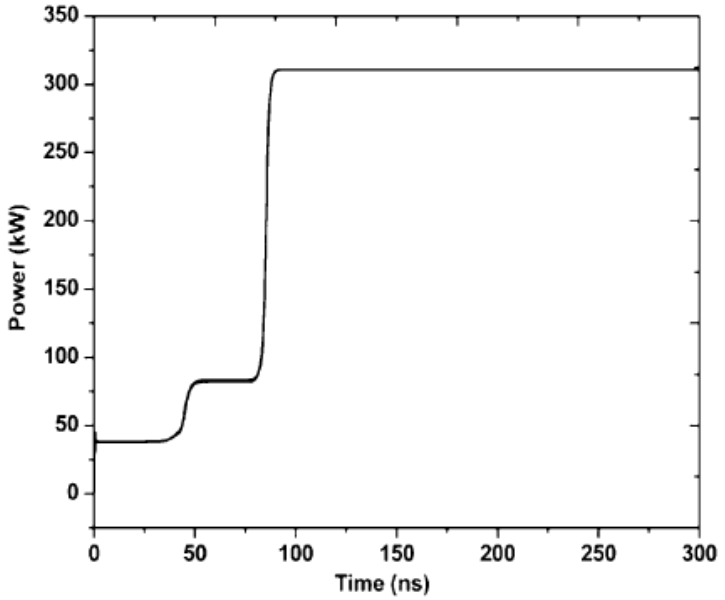

Power and frequency estimation simulations

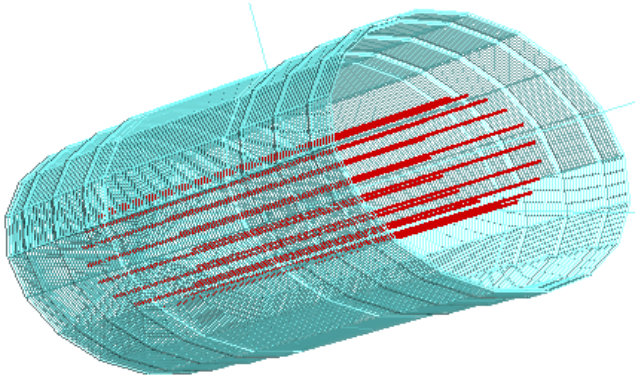

Interaction cavity with electron beam

Particle-in-Cell (PIC) algorithm is used in the Beam-wave interaction simulations (670GHz)

Interaction cavity geometrical parameters

Middle section length (L)	4.5 mm
Cavity radius (R_c)	4.5 mm
Input taper angle (θ_1)	4°
Output taper angle (θ_2)	4°
Input taper length (L_1)	4 mm
Output taper length (L_2)	4 mm

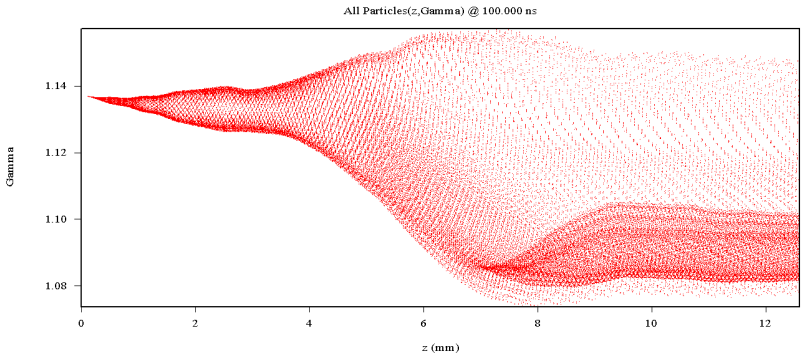

Phase space diagram

Q value and magnetic field

Diffractive Q (Q_d)	3030
Ohmic Q(Q_{ohm})	45000
Total Q	2838
Magnetic field	26.34 T

670 GHz

THz Gap

- **EM radiation is between higher frequency limit(0.3 THz) of mm waves and lower frequency limit (3THz) of far-infrared region**
- **Development of compact, simple and reliable sources of coherent terahertz (THz) radiation is important for numerous applications**

[1]

- **Compared to FELs, gyrotrons have more efficiency in this region**
- **BWO's give less power compared to gyrotrons**
- **Linacs also produce THz radiation but the structure is very huge**

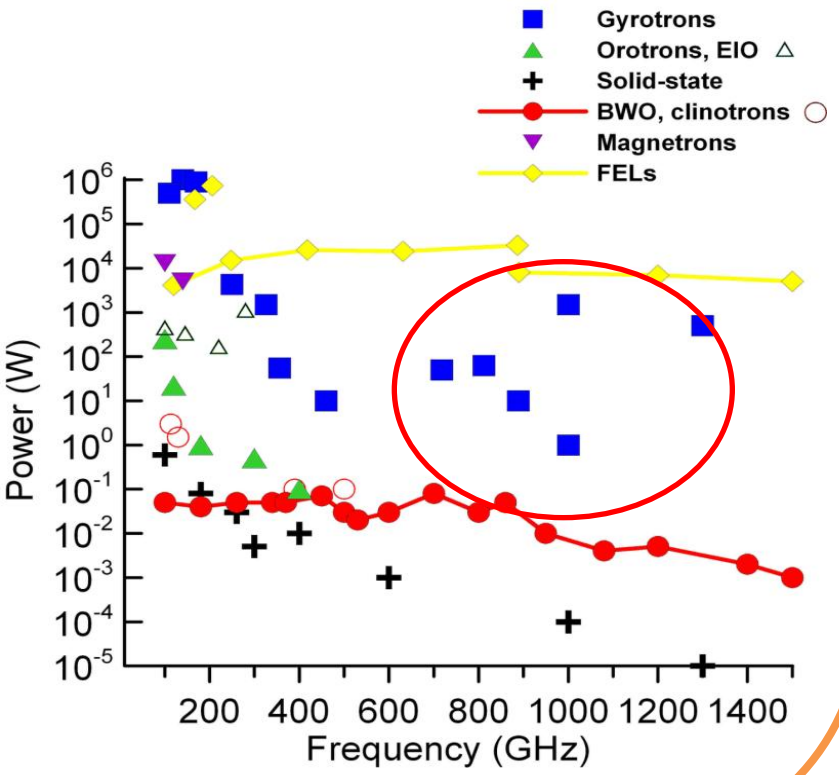

Possible Applications Of High Power THz-Gyrotrons

- **Atmosphere Sensing**
- **Radio Astronomy and Space Sciences**
- **Stand of Detection and Imaging of Explosives And Weapons**
- **THz Radars, Fast & High resolution Images and scanning's of materials are possible from more than 500m distance (KW-Power Gyrotrons)**

Present Status of THz- Gyrotron

Frequency(GHz)	Harmonic	Magnetic Field(T)	Pulse Duration(μs)	Avg Power(KW)	Operating Mode	Efficiency (%)
945	1	25.4	40	1.58	$TE_{15,4}$	-
985	1	36.86	50	1.25	$TE_{16,4}$	-
1000	2	23.6	-	1.46	$TE_{23,3}$	0.7
1002	1	37.53	40	1.75	$TE_{6,8}$	-
1014	2	20	-	0.25	$TE_{4,12}$	4.16
1024	1	38.3	40	5.3	$TE_{17,4}$	6
1300	1	48.7	20	0.57	$TE_{24,4}$	-

Institute of Applied Physics-Russia Academy Of Sciences(IAP-RAS), Russia, FUKAI University, Japan, CALABAZAS CREEK Research Inc, USA and many more Research Institutes all over World successfully developed the THz Range Gyrotrons

1THz,6KW Gyrotron

Mode Pattern of The Mode TE24,8

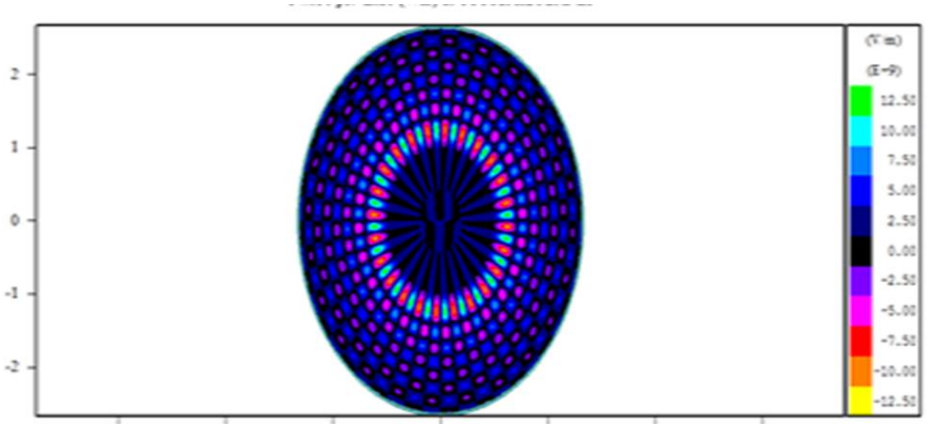

Parameters	Values
Input Voltage	45KV
Input current	2A
Output Power	6KW
Frequency(GHz)	1000
Harmonic operation	1
Mode	TE24,8

Azimuthal Electric Field Vs. Frequency(KGHz)

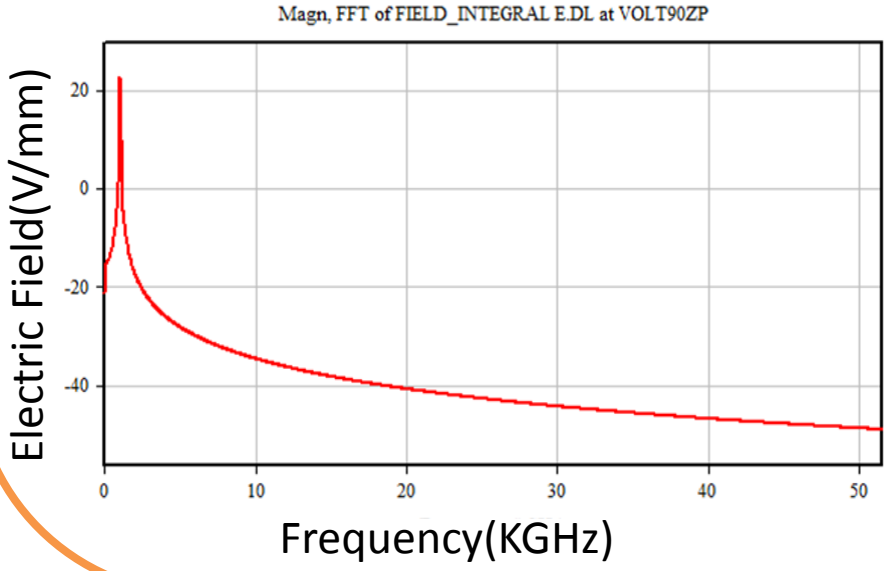

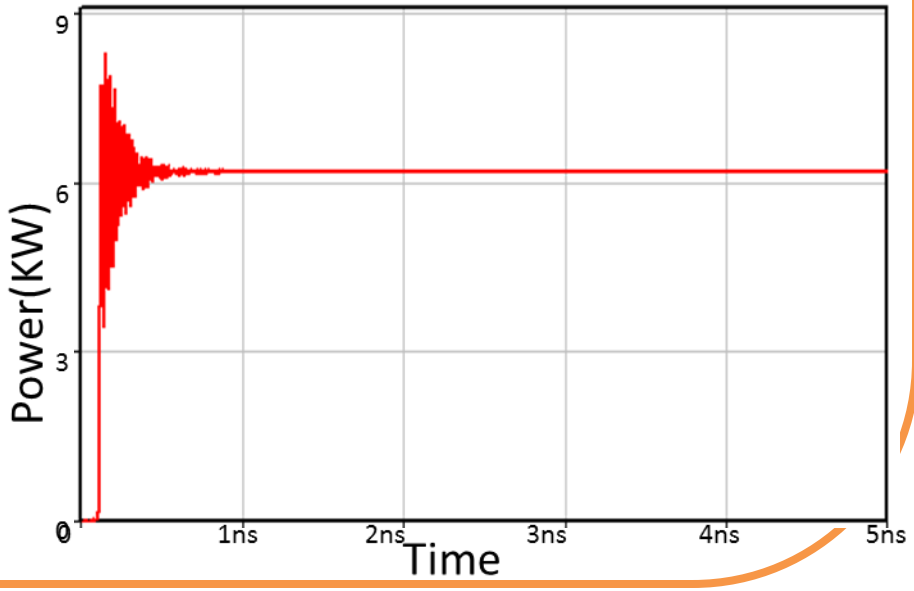

2 THz, 150W Gyrotron

Mode Pattern of TE24,4 Modes

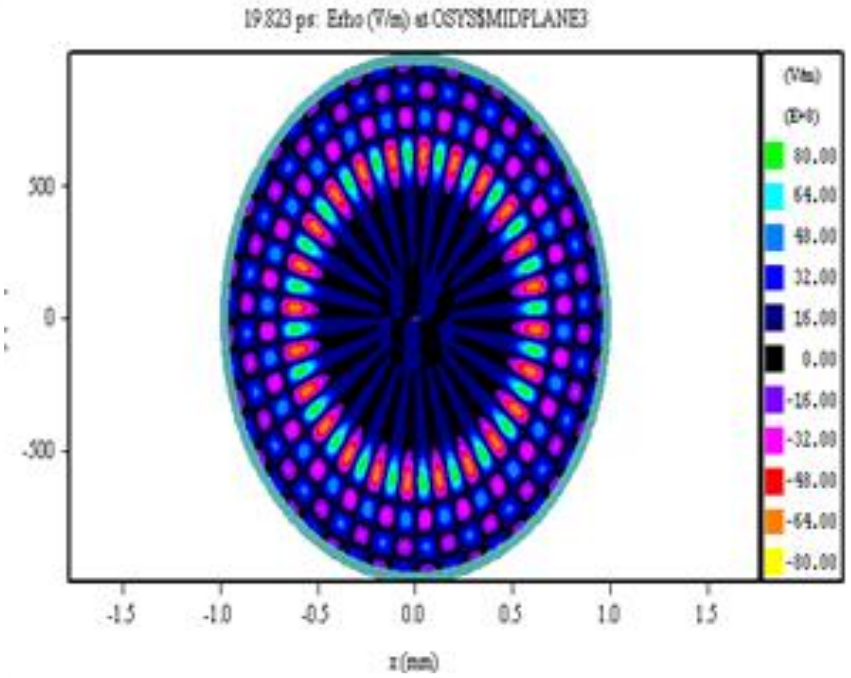

Parameters	Values
Input Voltage	12KV
Input current	0.6A
Output Power	130W
Frequency(GHz)	2016
Harmonic operation	2
Mode	TE24,4

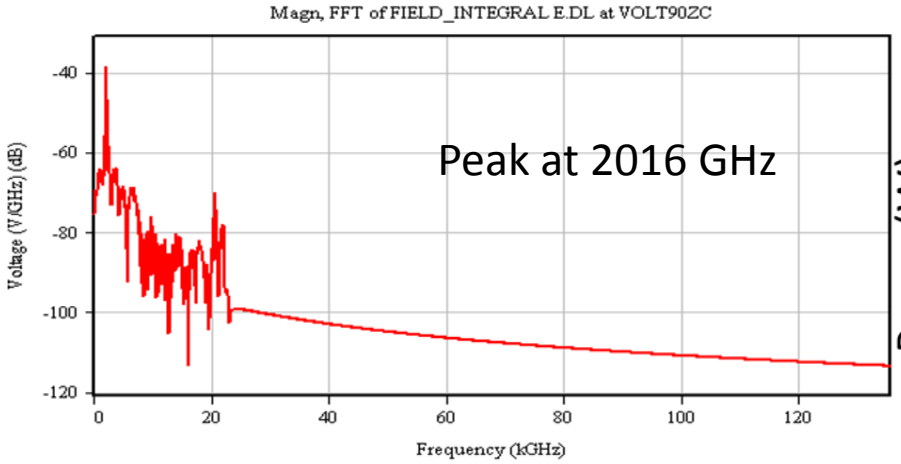

Azimuthal Electric Field Vs. Frequency(KGHz)

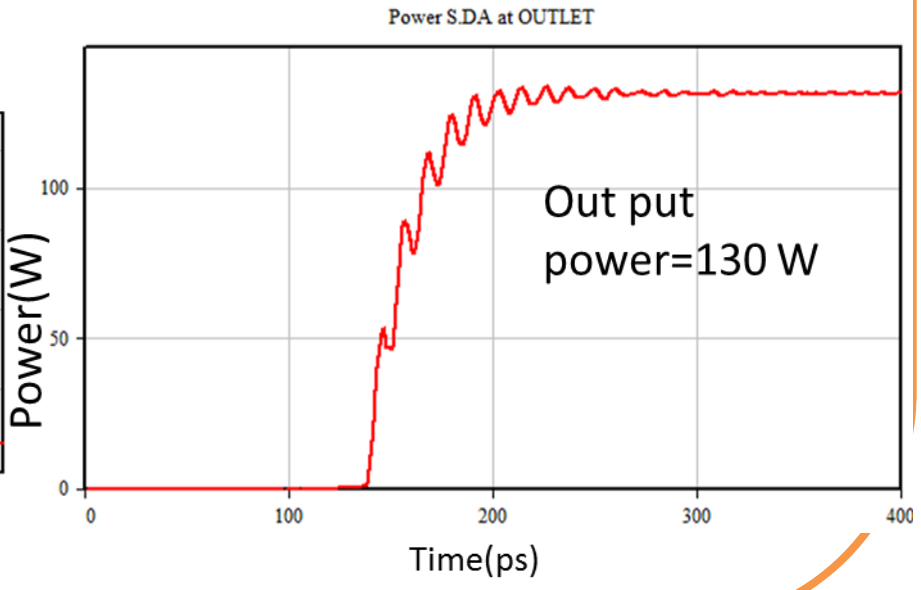

Cavity Design:

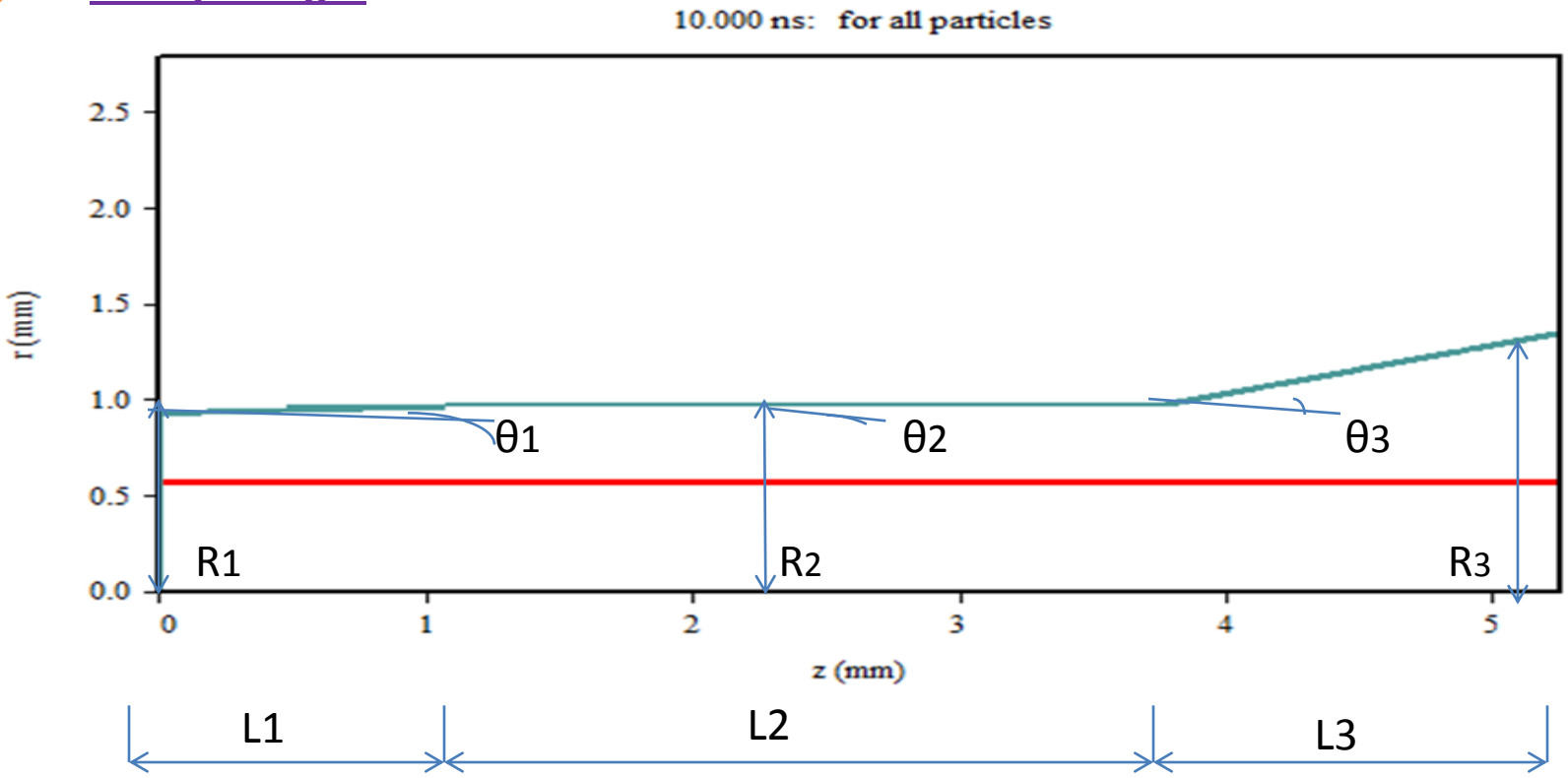

parameter	Input Taper	Middle section	Output taper
Taper angle	Θ_1=2 degree	Θ_2=0 degree	Θ_3=14 degree
Length(mm)	L_1=1.2	L_2=2.55	L_3=1.5
Radius(mm)	R_1=0.926	R_2=0.968	R_3=1.342

Summary of THz-Gyrotron Cavity Results

Frequency	Harmonics	Mode	Cavity length(mm)	Cavity Radius (mm)	Beam radius (mm)	Qd	S.O.C (A)	Magnetic field(T)	Po	Efficiency
1 THz	1	TE24,8	2.7(9λ)	2.633	1.30	8650	0.75 A	36.2	6KW	7.5%
1.3 THz	1	TE14,8	2.54(11λ)	1.56	0.62	9700	0.95 A	47.05	1KW	5.2%
1.5 THz	1	TE10,10	2.2(11λ)	1.38	0.41	11350	0.3 A	54.3	500W	3.3%
2 THz	2	TE24,4	2.55(17λ)	0.968	0.587	12300	0.14A	36.38	135W	2.1%

High Efficiency Double Beam Gyrotron: 42 GHz

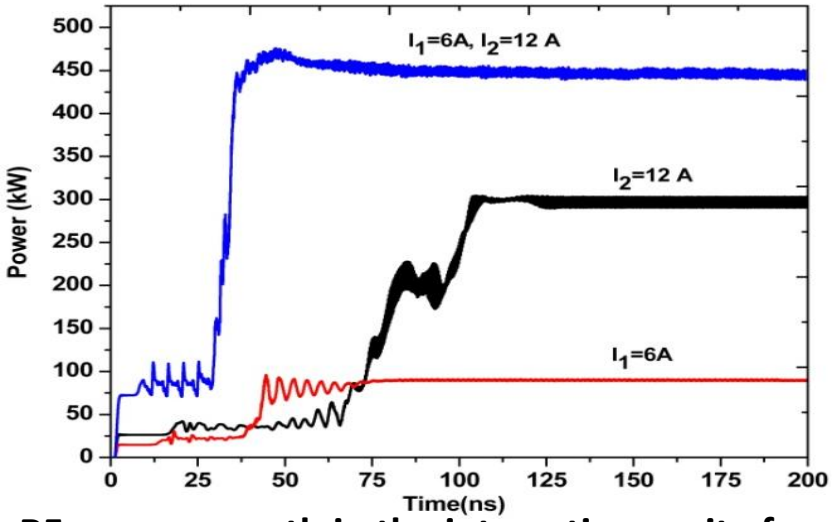

RF power growth in the interaction cavity for single bema and double beam operations

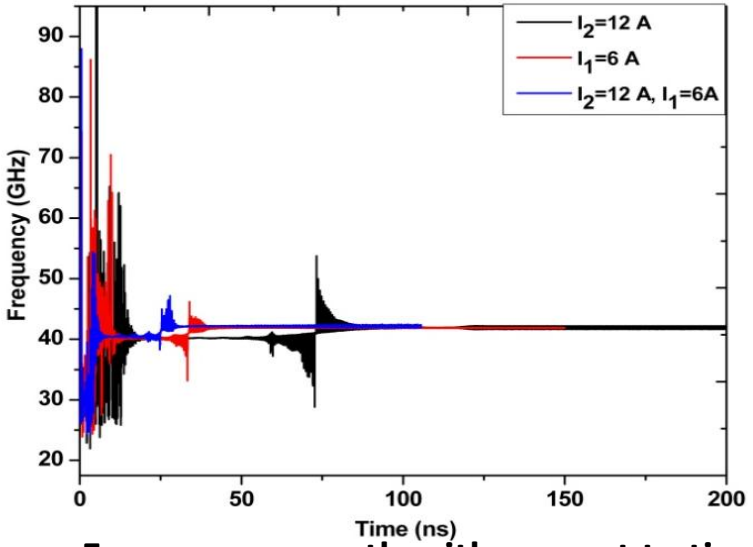

Frequency growth with respect to time

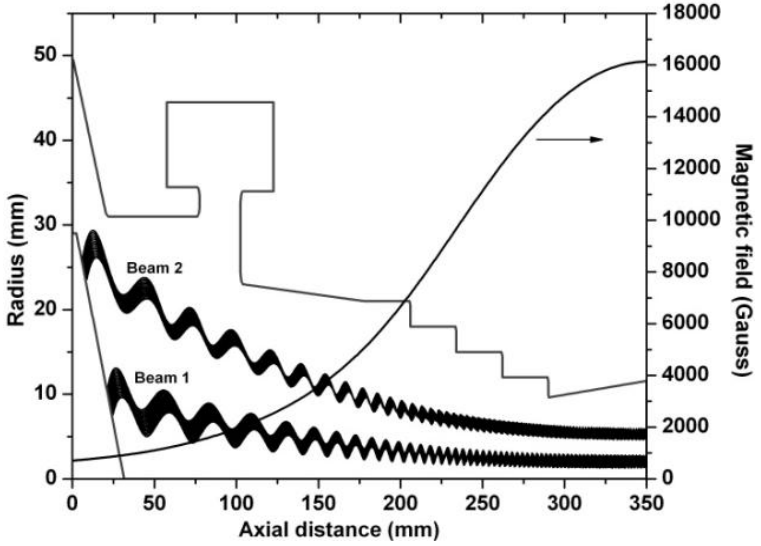

MIG with the electrode geometry, the beam profile and the magnetic field profile

OPTIMIZED MIG PARAMETERS

Parameters	Beam 1	Beam 2
Beam voltage (V_b)	65 kV	65 kV
Beam current (I_b)	6 A	12 A
Beam radius (R_b)	2.02 mm	6.05 mm
Cavity magnetic field (B_0)	1.61 T	1.61 T
Cathode magnetic field (B_{zc})	852 Gauss	740 Gauss
Larmor radius (l_r)	0.417 mm	0.43 mm
Cathode radius	8 mm	24 mm
Cathode slant angle	45°	45°
Modulating anode voltage	29 kV	29 kV
Slant length	3.4 mm	3.5 mm

Double beam gyrotron

60 GHz gyrotron

Frequency	**60 GHz**
Power	**500 kW**
Beam Voltage	**69 kV**
Beam Current	**6 A /12 A**
Velocity ratio (α)	**1.4**
Operating mode	**TE_{23}**

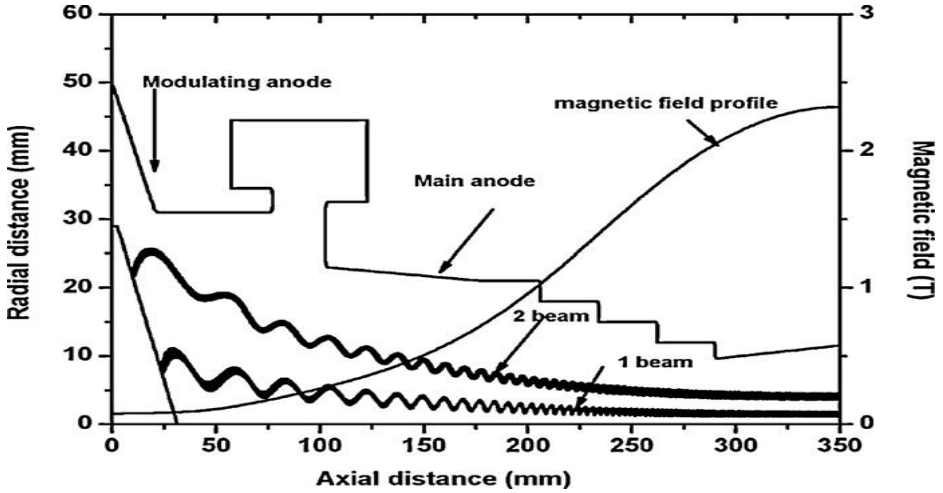

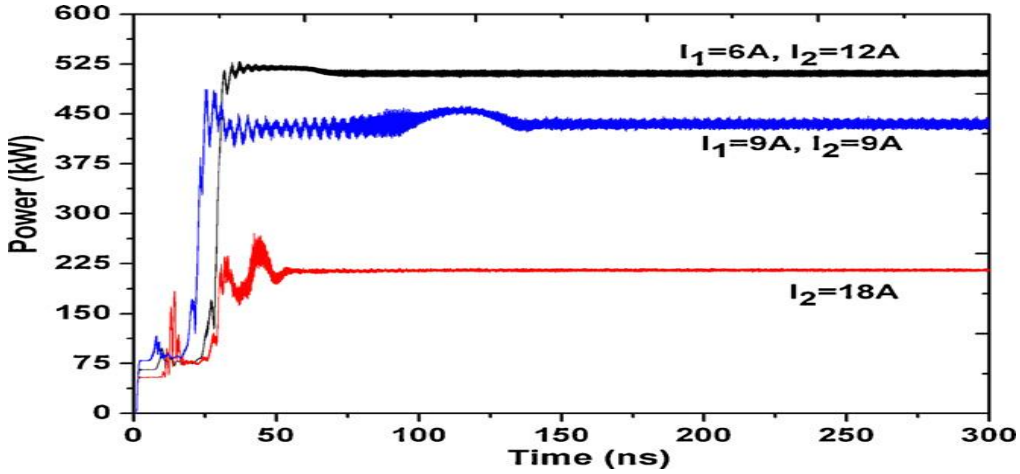

Triple Frequency Gyrotron

- Conventional gyrotrons, operate at single frequency and generate megawatt power in the millimeter wave band, are used in the plasma fusion systems.

- Two or more frequencies in millimeter wave band are used commonly in the plasma fusion machines like, SST-1 (42 GHz and 82.6 GHz), ITER (127.5 GHz and 170 GHz), ASDEX (105 GHz and 140 GHz), etc, for ECRH and start-up.

- The RF power at different frequencies is supplied by different gyrotron oscillators. This make the whole RF system more complicated as the separate power supplies, magnet system, transmission line system, etc., are required for each gyrotron, which enhance the overall cost of ECRH system.

- The ECRH RF system can be simplified if the single gyrotron device delivers MW power at two or more frequencies.

- Considering the advantages of multi frequency gyrotron, a design study is completed for three frequency generation from a single tube.

Design parameters for triple frequency gyrotron..

Frequency	170 GHz, 140 GHz & 127.5 GHz
Power	> 1 MW
Harmonic	1
Beam voltage	77-83 kV
Beam current	41-45 A
Interaction efficiency	≈ 35 %

Mode selection..

After selecting the operating mode for 170 GHz frequency, modes for 140 GHz and 127.5 GHz are searched keeping the interaction cavity geometry fixed

$$f_1 / f_2 = \chi_{m,p1} / \chi_{m,p2}$$

Here, f_1= 170 GHz and X_{mp1} = 74.56

$TE_{21,11}$ ($\chi_{m,p}$=61.56) and $TE_{22,9}$ ($\chi_{m,p}$=56.09) are selected as the operating modes for 140 GHz and 127.5 GHz, respectively.

Selected modes, cavity radius and beam radius

Mode	X_{mp}	*Theoretical resonance frequency (R_c= 21 mm)*	*Beam radius (mm)*
$TE_{34,10}$	74.56	169.86 GHz	10.00
$TE_{21,11}$	61.56	140.37 GHz	8.28
$TE_{22,9}$	56.09	127.70 GHz	8.71

Beam wave interaction computation..

Interaction cavity geometrical parameters used in beam wave interaction simulations

Parameters	170 GHz	140 GHz	127.5 GHz
Input taper length (L_1)	8 mm		
Middle section length (L)	14 mm		
Output taper length (L_2)	16 mm		
Cavity radius (R_c)	20.95 mm		
Input taper angle (θ_1)	2.8°		
Output taper angle (θ_2)	3°		
Q factor	1250	910	760
Resonant frequency in cold cavity simulations (GHz)	169.86	140.37	127.70

- ✓ Beam-wave interaction simulations are performed to optimize the beam parameters
- ✓ Particle-in-Cell code MAGIC is used in the optimization
- ✓ Mesh size: Δr=0.1 mm, $\Delta\theta$=20 degree, Δz=0.1 mm

Optimized beam parameters

Optimized beam parameters	170 GHz	140 GHz	127.5 GHz
Cavity magnetic field (B_0)	6.78 T	5.56 T	5.10 T
Beam radius (R_b)	10 mm	8.28 mm	8.71 mm
Beam voltage (V_b)	80 kV		
Beam current (I_b)	43 A		
Velocity ratio (α)	1.35		

Beam wave interaction computation:

Efficiency v/s length

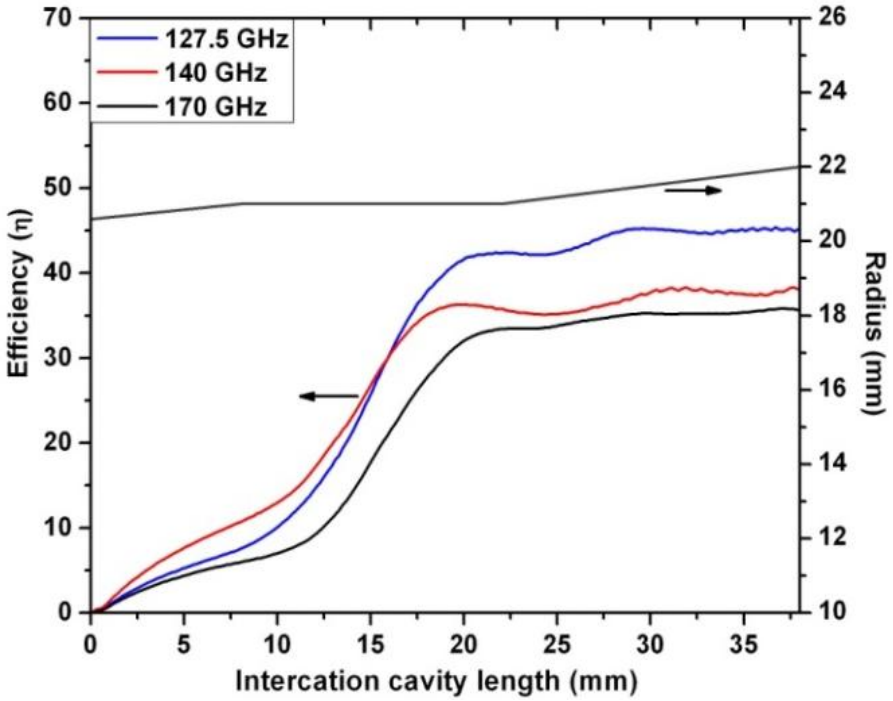

Frequency spectrum

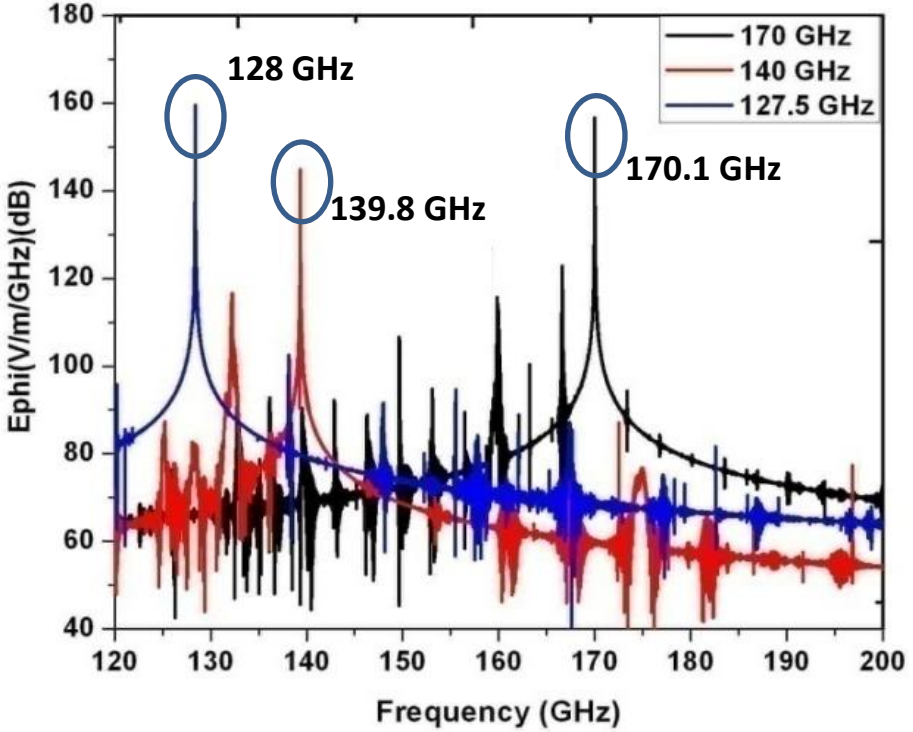

✓ **Beam wave interaction results show more than 30 % interaction efficiency for all three frequencies**

✓ **The frequency spectrum results show sharp peak of electric field gain at 128-, 139.8-, 170 GHz frequencies**

Beam wave interaction computation

Temporal growth of power and frequency

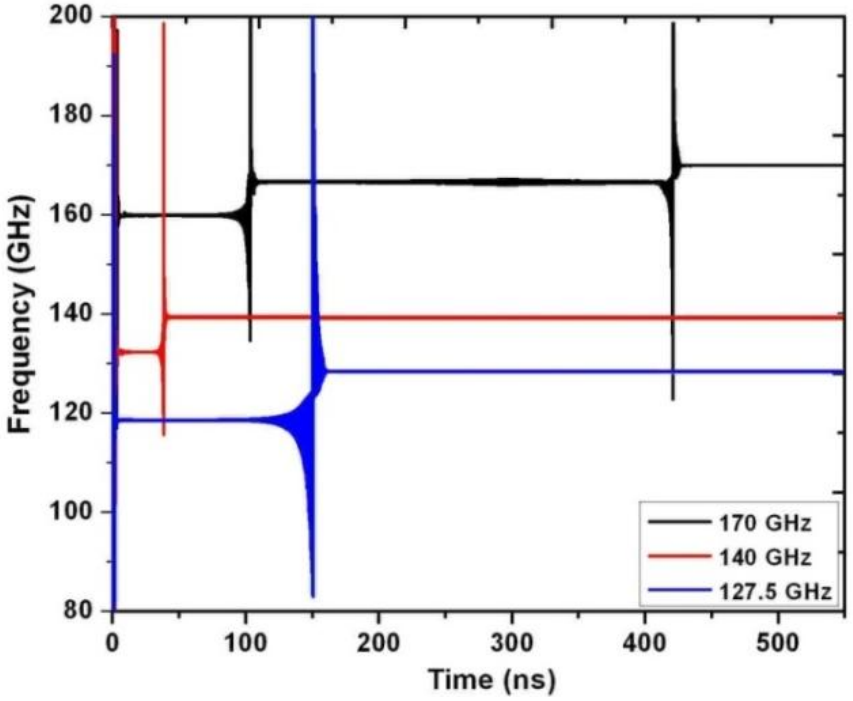

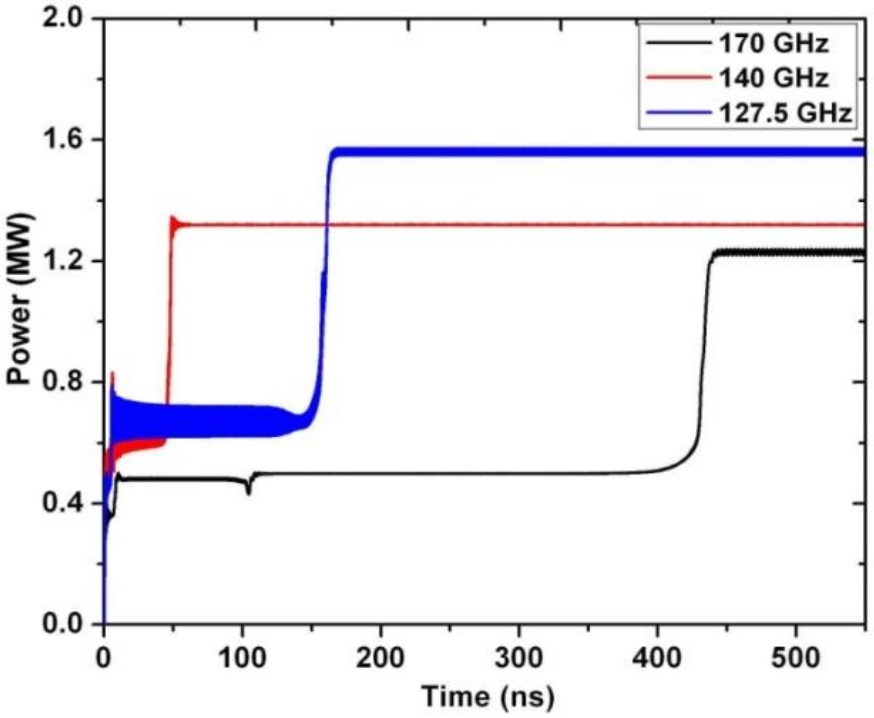

	170 GHz	140 GHz	127.5 GHz
Power (MW)	1.23	1.32	1.56
Frequency (GHz)	170.10	139.85	128.05
Efficiency (%)	35.75	38.37	45.34

Magnetron injection gun..

✓ Triode-type magnetically tunable magnetron injection gun (MT-MIG) is considered for triple frequency gyrotron

✓ The magnetic field profile and modulating anode voltage are varied to launch the electron beam at different radial maxima in the interaction cavity.

✓ EGUN , MIGANS and MIGSYN are used in the design of MIG.

Schematic view of triode MIG

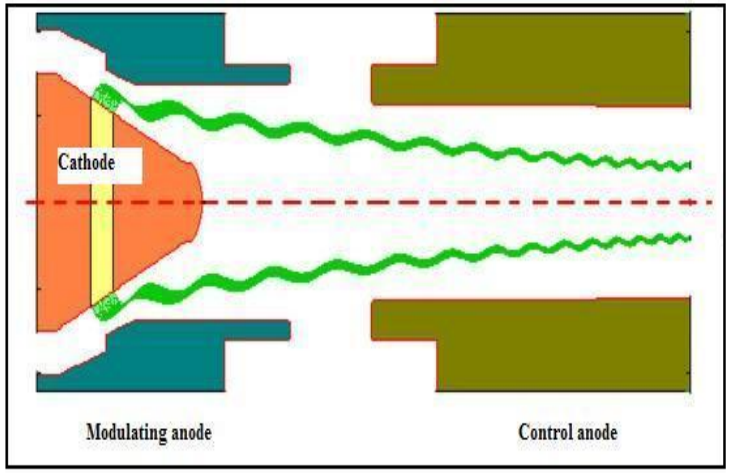

Design specifications of MIG

Frequency (f)	170 GHz	140 GHz	127.5 GHz
Beam voltage (V_0)	80 kV	80 kV	80 kV
Beam current (I_0)	43 A	43 A	43 A
Beam radius	10.00 mm	8.27 mm	8.71 mm
Cavity Magnetic filed (B_0)	6.78 T	5.56 T	5.10 T
velocity ratio (a)	1.3-1.4	1.3-1.4	1.3-1.4
Operating mode	$TE_{34,10}$	$TE_{21,11}$	$TE_{22,9}$
Cathode current density (J_c)	< 5A/cm^2	< 5A/cm^2	< 5A/cm^2
velocity spread ($db_\perp$)	< 5%	< 5%	< 5%

Magnetic field profile..

Magnetic field profile

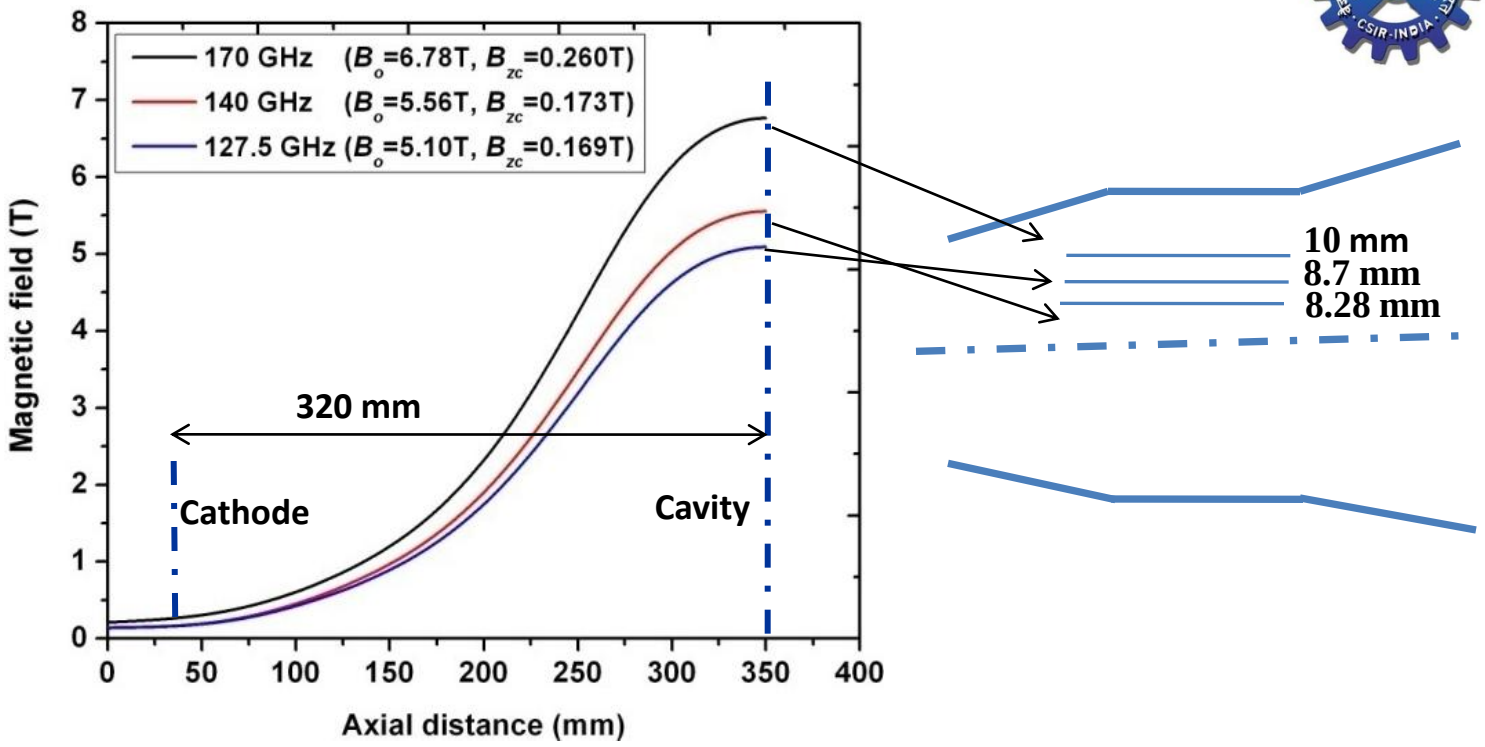

Optimized MIG parameters

Value for Frequency (GHz)	*170*	*140*	*127.5*
Mean radius of emitter (r_c)	52.8 mm	52.8 mm	52.8 mm
Slant length of emitting surface (l_s)	5.38 mm	5.38 mm	5.38 mm
Cathode-modulating anode gap	12 mm	12 mm	12 mm
Slope angle of emitter (f_c)	28^0	28^0	28^0
Magnetic field at cathode region (Bz_0)	0.260 T	0.173 T	0.169 T
Magnetic compression ratio (f_m)	25.08	32.13	30.17
Modulating anode voltage (V_a)	58 kV	30 kV	29 kV

MIG geometry and beam profile

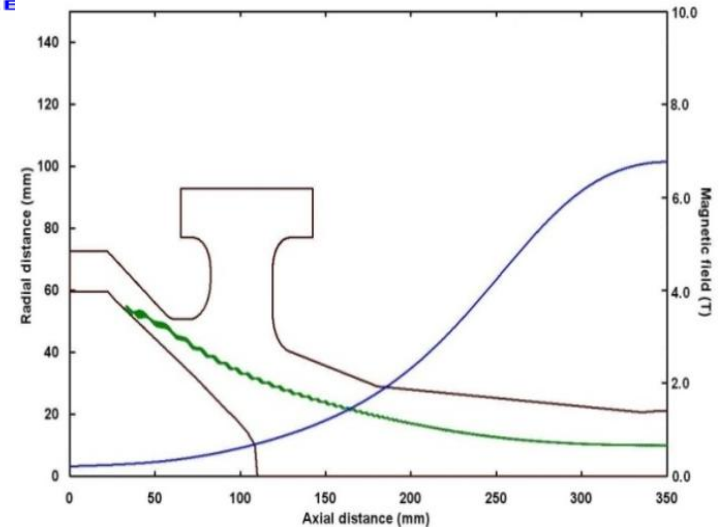

170 GHz

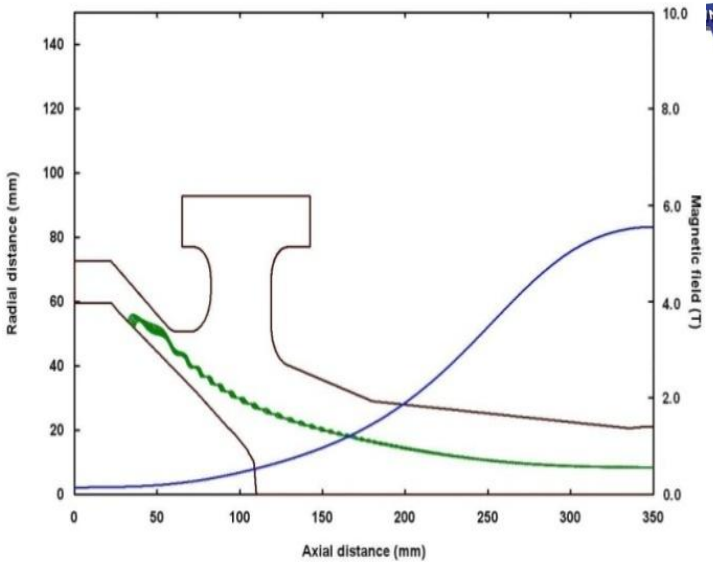

140 GHz

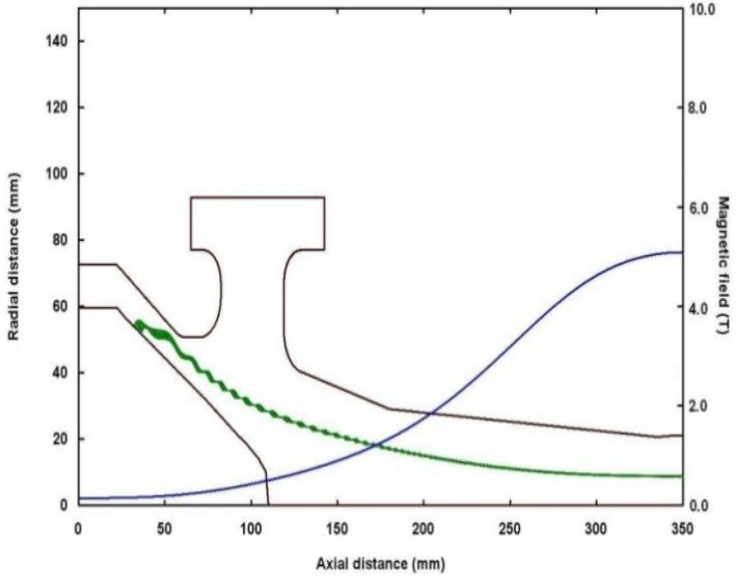

127.5 GHz

Beam quality parameters

Parameters	*170 GHz*	*140 GHz*	*127.5 GHz*
Velocity ratio (*a*)	1.38	1.30	1.32
Transverse velocity spread	2.53 %	4.81 %	4.3 %
Beam radius (mm)	9.95	8.30	8.78

Cloud Monitoring

Aerosols are the most important components in clouds and can be characterized by using millimeter wave radar system.

The cross section area of aerosols is of the order of wavelength corresponding to millimeter wave radiation.

94 GHz radiation can be used for the cloud monitoring as the absorption is minimum at this frequency.

The millimeter wave radiation is scattered by the aerosols and the scattered radiation is detected by the radar system. The scattering of radiation depends on the size and density of aerosols.

94 GHz radiation source of high power is required for this application.

Gyrotron/gyro-amplifiers are the suitable device for the generation of high power 94 GHz radiation.

The gyrotrons used in the RADAR system were developed by Navel Research laboratory (NRL).

Frequency tunable gyrotrons are much favorable in such type of RADAR system.

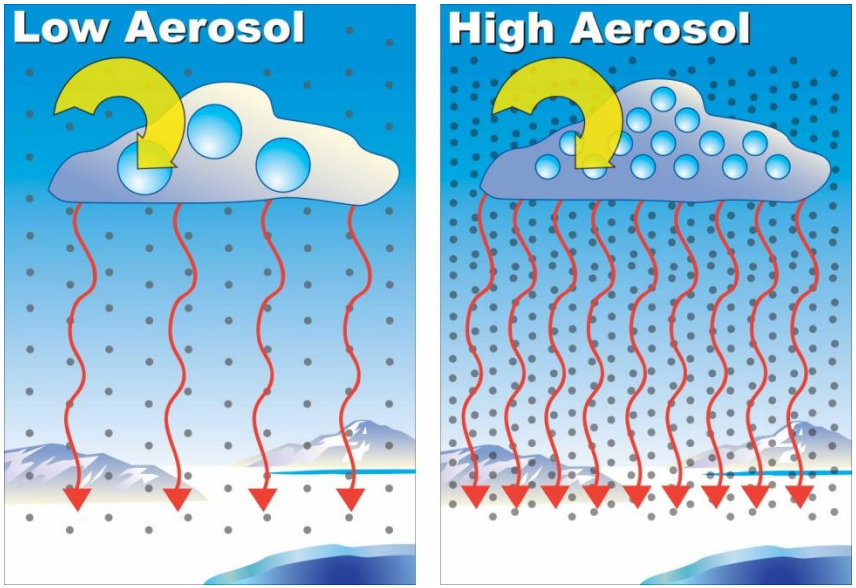

Planetary defense

- The manmade space debris is becoming a problem for the space shuttle flight as well as for the satellite movement.
- For the safe flight of space shuttles, the detection for the debris is necessary.
- To detect debris of 1 cm size at the 1000 km distance a very powerful RADAR system with very high antenna gain is required. For such system it has been predicted, 20 MW power is required with 20 meter diameter of tracking antenna.
- A earth base station including the array of several millimetre wave source or the complete RADAR system on the space station and space shuttle.
- To establish several space debris detection RADAR systems around the world nearly the equator, a full map of space debris can be collected.
- In such type of radar system 35/94 GHz gyrotron/gyro-amplifiers are required.

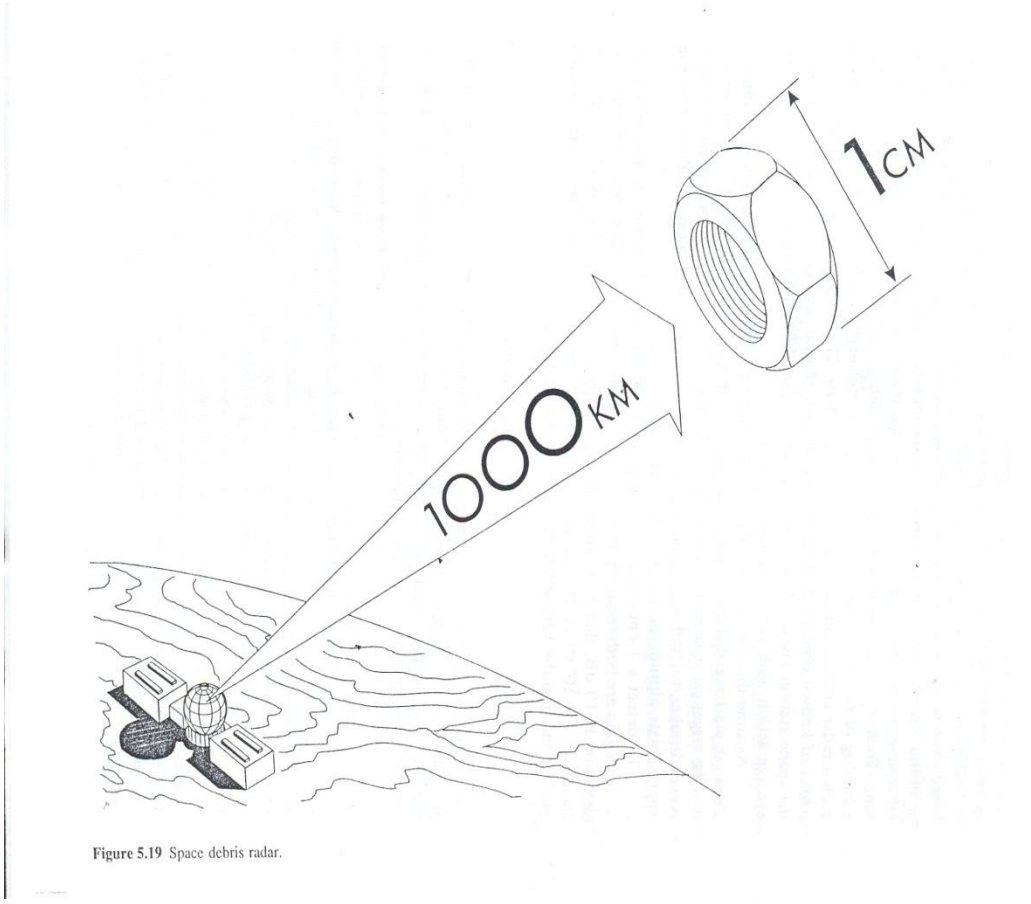

Figure 5.19 Space debris radar.

Planetary research

The planetary research is a very advance and futuristic area of the exploration of the millimetre wave RADRA system.

- To explore the surface topology and the soil characteristic of the Moon and Mares, various ambitious project has been initiated worldwide (e.g MAGIA of Italy, Chandryana of India).
- The purpose of such mission is to collect the dielectric and thermal data of the Moon/Mares soil by the backscattering of the radiation, mapping of the surface etc.
- Two type of systems are proposed for planets surface tracking:

✓ Satellite based

✓ Earth based

- **80 GHz-260 GHz (94 GHz, 150 GHz, etc.) gyrotron/gyro-amplifiers with μs pulse and 200 kW-300 kW power are proposed.**

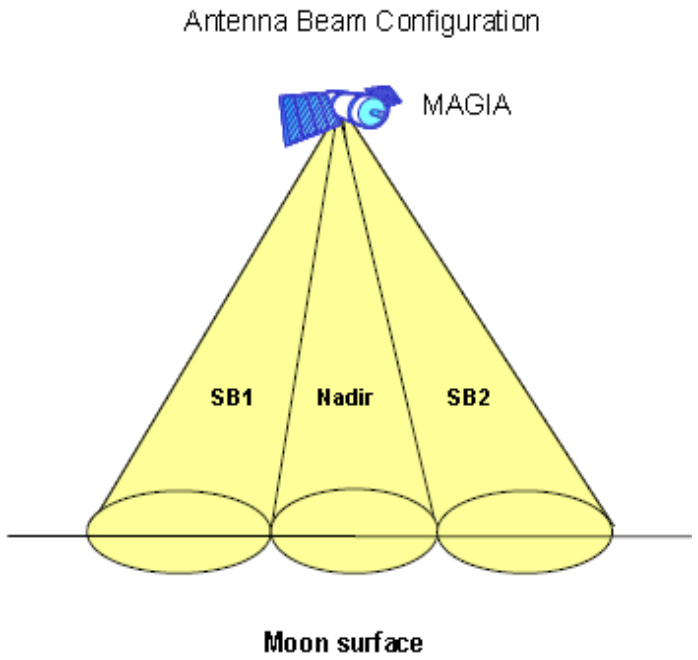

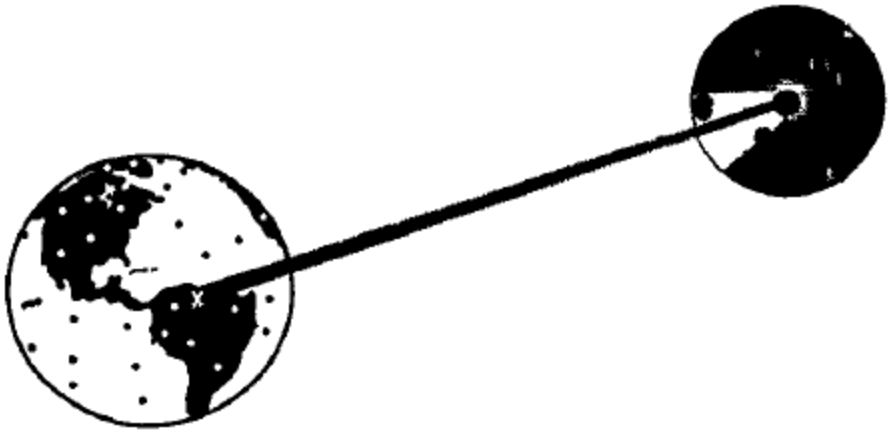

Atmospheric sensor and ozone conservation

- The absorption of the millimeter wave radiation in the atmosphere highly depends on humidity.
- On the basis of absorption, relative humidity can be measured.
- *Manheimer* proposed 100 kW power at frequencies around 100 GHz for humidity detection, which is possible by the gyrotrons/ gyro-devices .

- 4% increase in skin cancer for 1 % decrease in ozone.
- LASER can be used for the CFC molecule dissociation (vibration level increases) but it is scattered highly from the lower surface of CFC concentration and CFC at higher altitude remain same.
- Microwave energy dissociate the C-X molecule (bond energy is 3.2 eV)
- Microwave/Millimeter wave paint the sky (troposphere) and dissociated halogen rained out in the form of hydrochloric acid.
- 35 GHz atmospheric window can be used for the purpose.
- It is a very expansive geo-engineering program and under consideration.

$$CFCl_3 + hv \quad CFCl_2 + Cl$$

$$Cl + O_3 \quad ClO + O_2$$

$$ClO + O \quad Cl + 2O_2$$

Reaction of CFC molecule with radiation

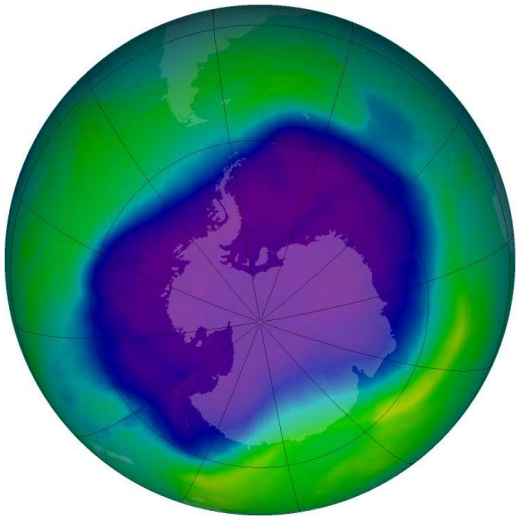

Hole in the Ozone layer over the Antarctic

CEERI Gyrotron Tree

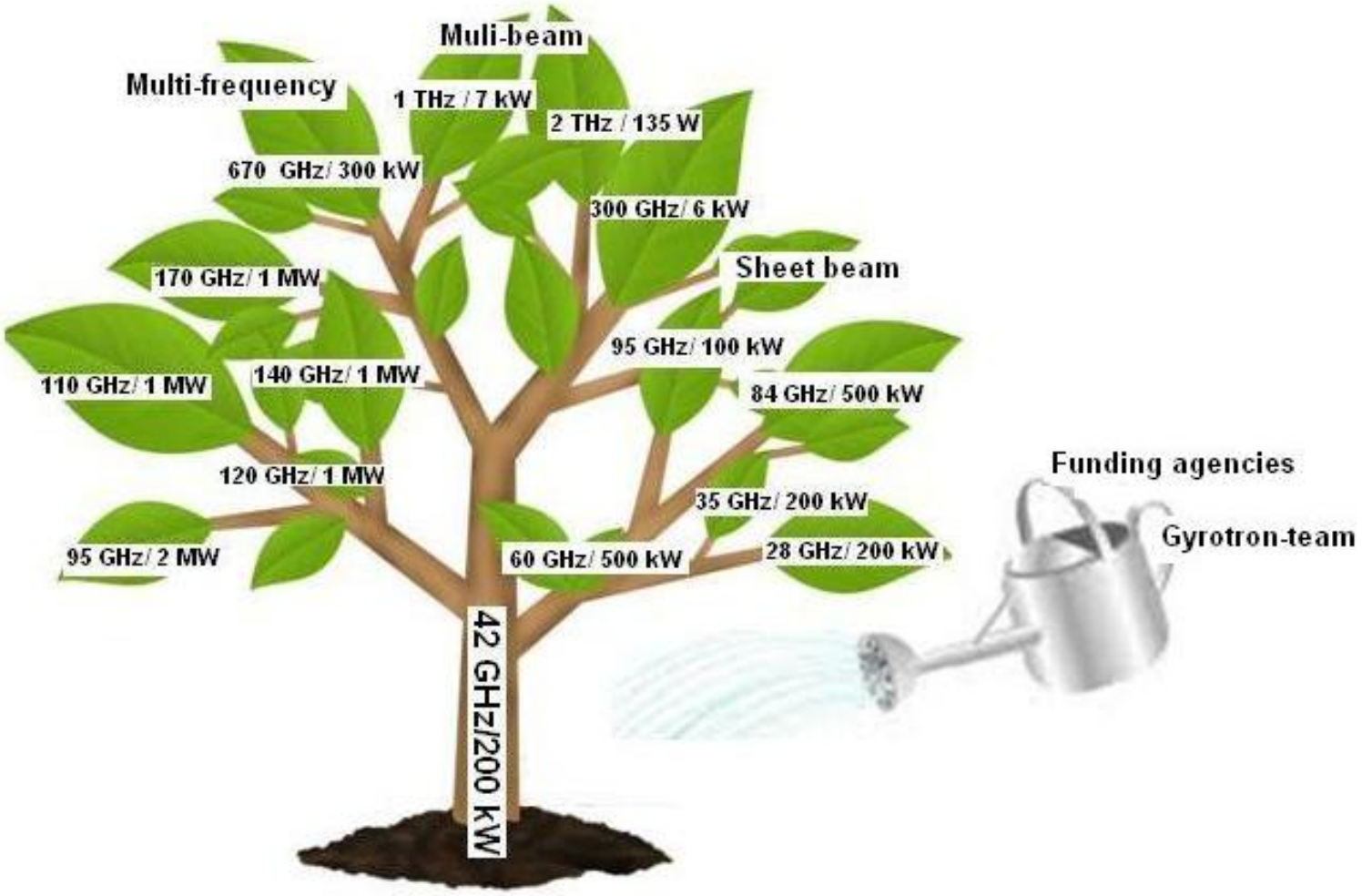

Gyrotron Project Profile

PIONEER ACTIVITY

S.No.	Particulars	Sponsor	Status
1.	Design & Development of 42GHz, 200kW Long pulse CW Gyrotron	DST	Completed
2.	Design & Development of Sub Components for 120GHz, 1MW Gyrotron	CSIR	Completed

OTHER ACTIVITY

S.No.	Particulars	Sponsor	Status
1.	Design & Development of Short pulse 170 GHz, 0.1MW Gyrotron	CSIR	Completed
2.	Development of Gyrotron Design Code	CSIR	In progress
3.	Design & Development of Sub-components of 95GHz, 100 KW Gyrotron	DRDO/MTRDC	In Progress
4.	Design & Development of Long pulse 170GHz, 1MW Gyrotron	IPR, Gandhinagar	Under Discussion
5.	THz, Multi-beam, Sheet-beam, Gyrotron, New generation Gyro-devices	-------	Under Study

Publications By CEERI

Total publications =126

International Journal Papers: 56

(Published outside India by reputed publishers)

- **IEEE Transactions: 7**
- **Springer: 19**
- **Elsevier: 10**
- **AIP(American Institute of Physics): 1**
- **Taylor & Francis: 2**
- **PIER: 2**
- **NRC Research Press: 1**
- **Frequentz: 4**

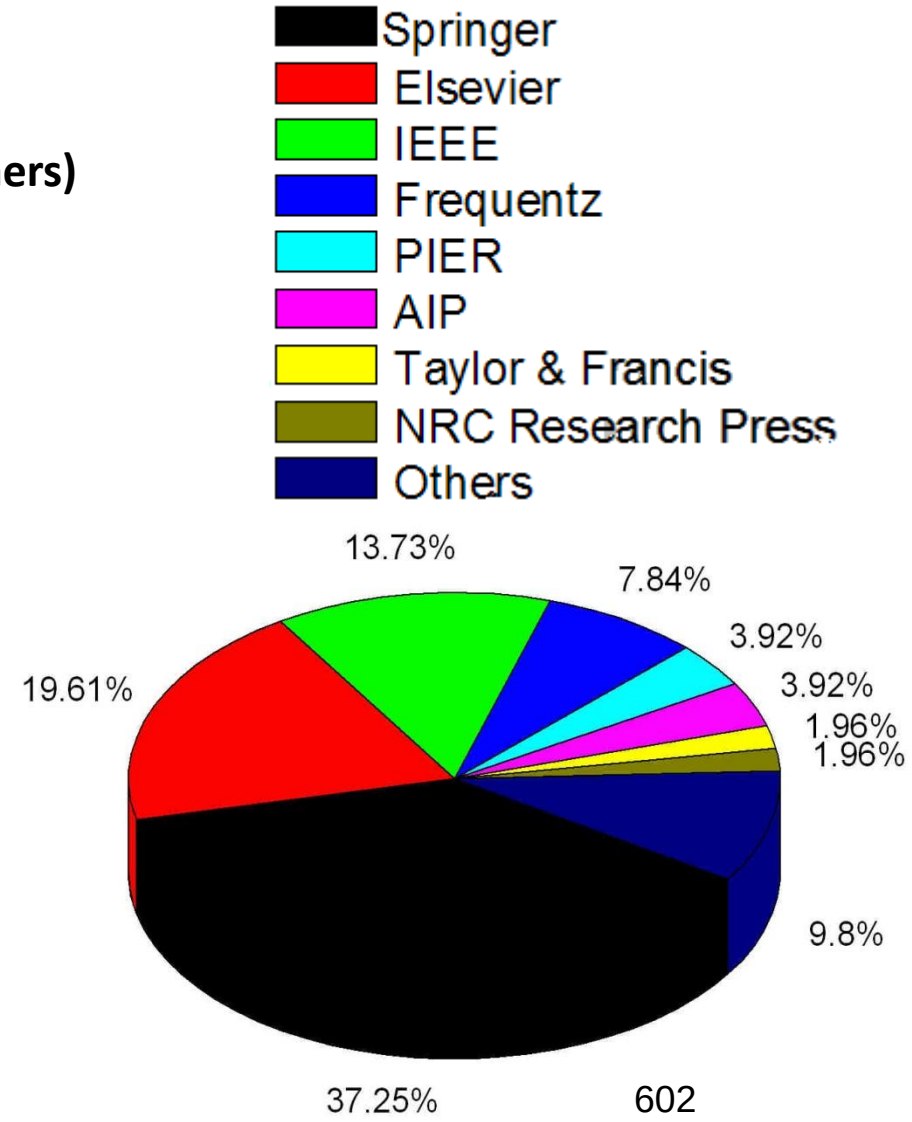

Good Development and Experimental Facilities

GYROTRON PROFILE AT CEERI

PRESENT:-
(Gyrotron lab)

FUTURE:-

- Design capability:
  Inhouse Developed Approach
- Development Capability:
  Inhouse Developed Approach

- Fabrication & Test Infrastructure

- Manpower: Around 20
  - Regular Scientist :05
  - Regular Technical Staff :05
  - Temporary Project Staff :05
  - BTech/M Tech./ Ph.D. :05
- Publication: 126
  (Journal : 56)

Gyrotron Profile at CSIR-CEERI

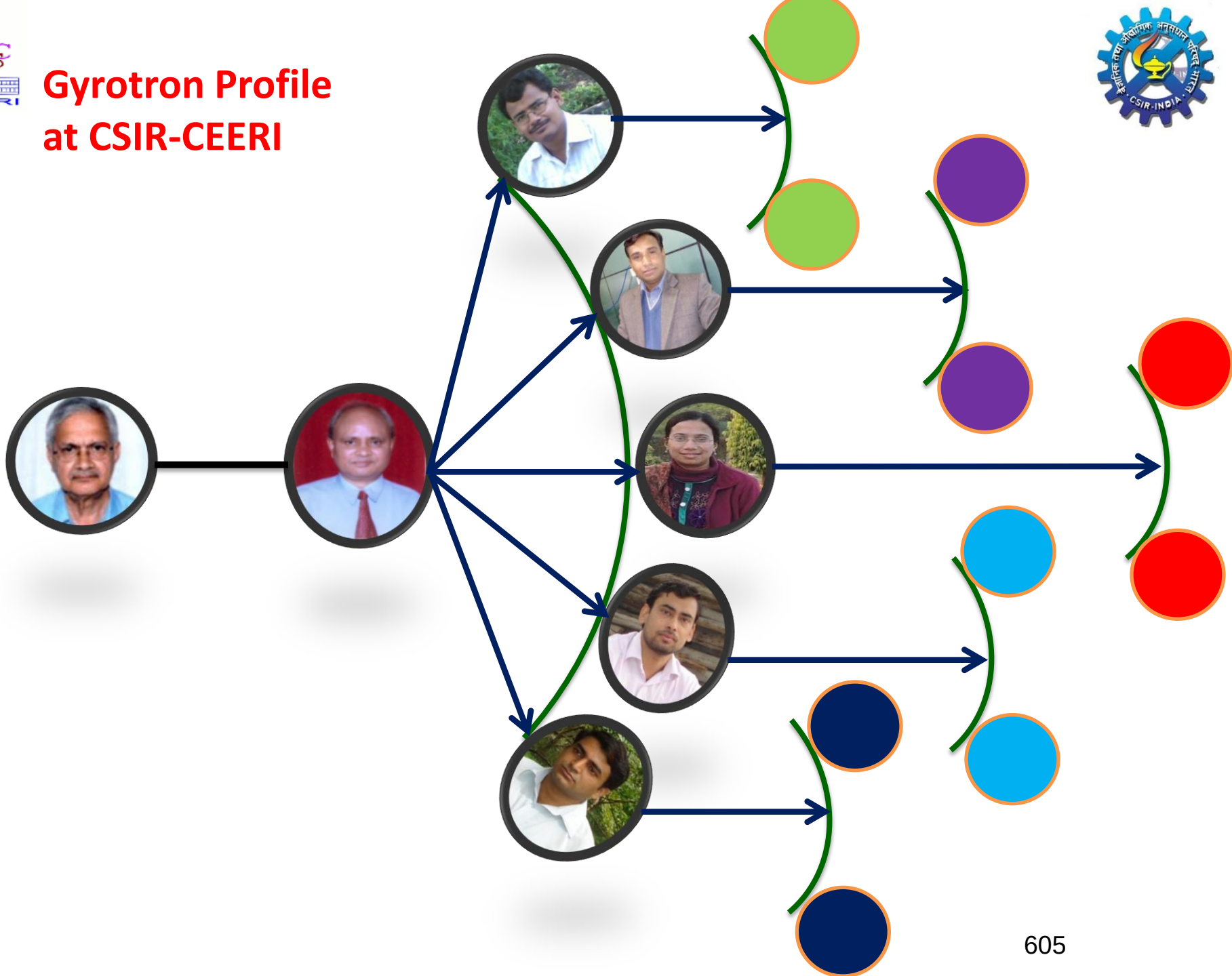

❑Indian Gyrotron: Profile

- ❑Gyrotron Design Base: Created and Applied (upto MW power and Terahertz frequency)
- ❑Gyrotron Development Base: Created and Applied
- ❑Infrastructure for Gyrotron Research: Established
- ❑Development of First Indian Gyrotron : A REALITY
- ❑First Indian Gyrotron : Delivered and RF tested
- ❑Scientific and Technical Manpower: Created
- ❑Gyrotron Research in India: Growing

INDIAN GYROTRON

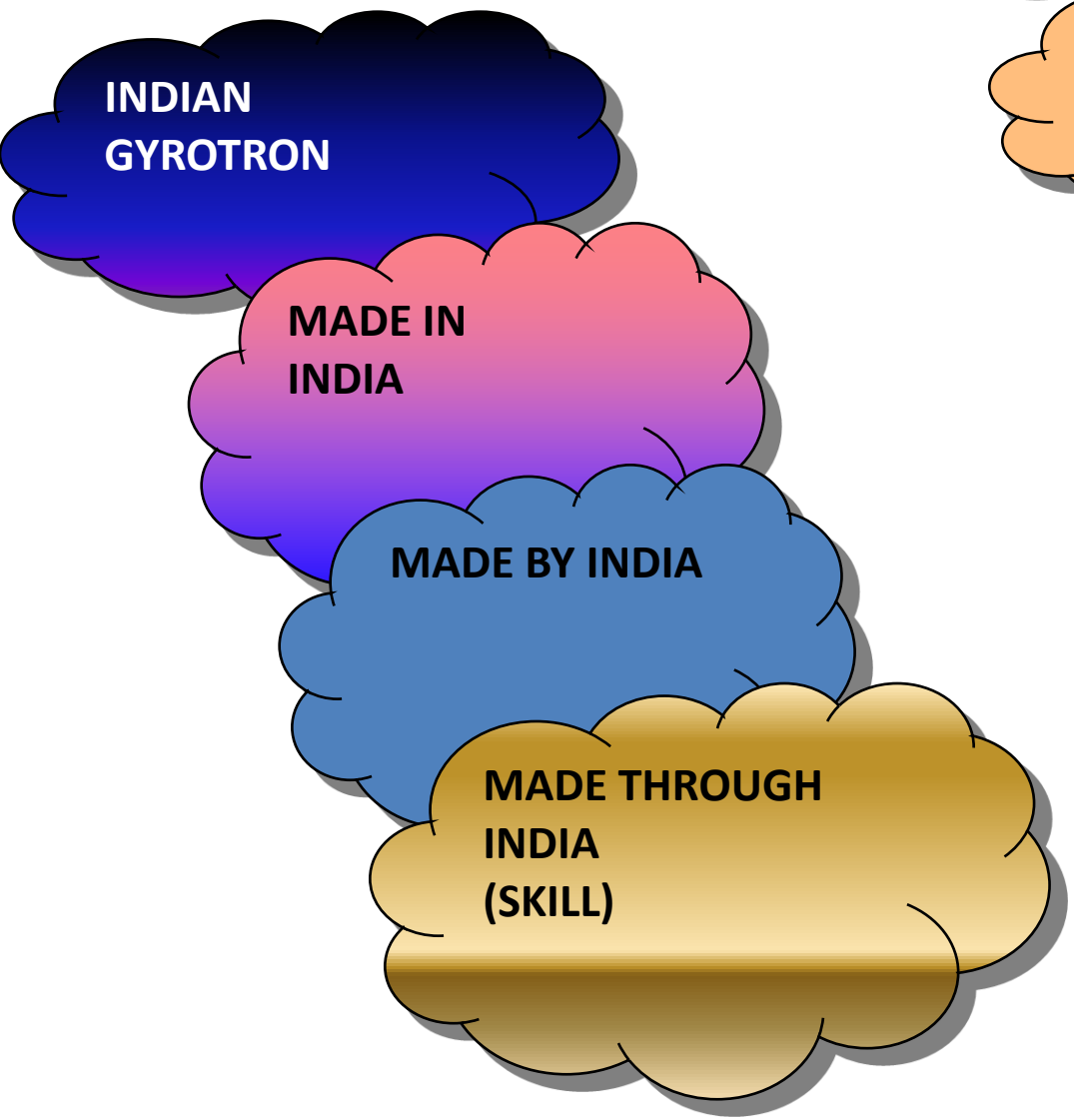

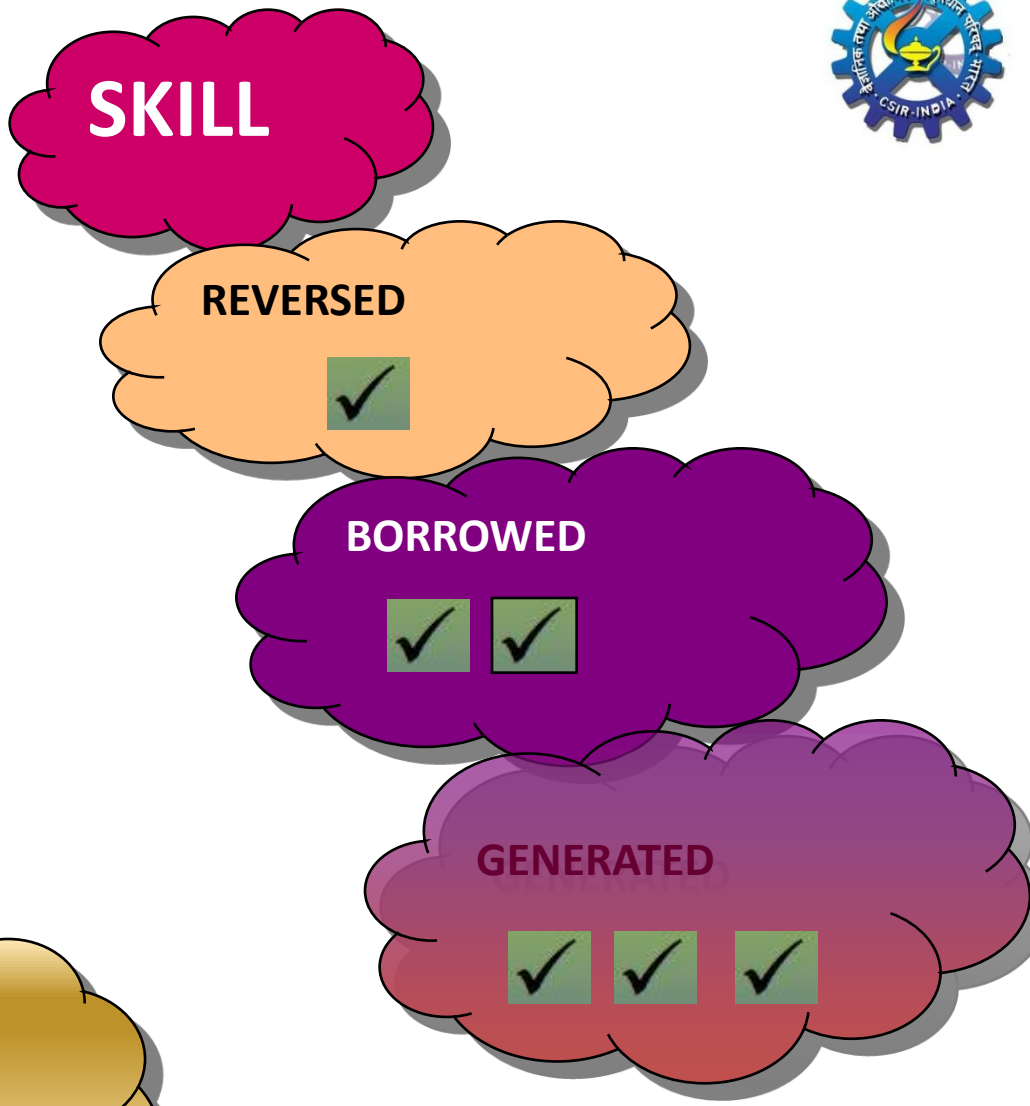

National Goal

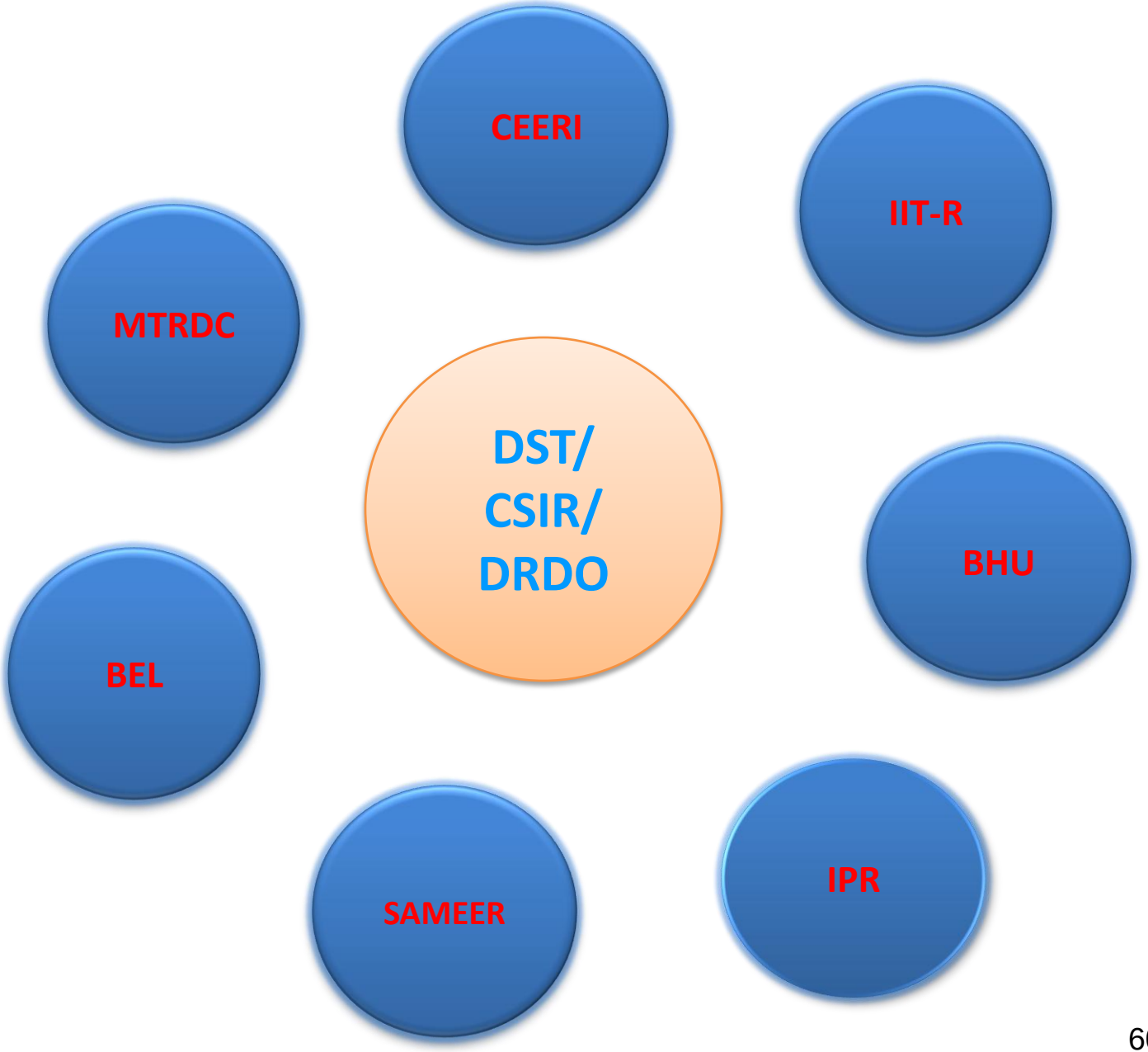

Our Mission

Successful Development of Indian Gyrotron

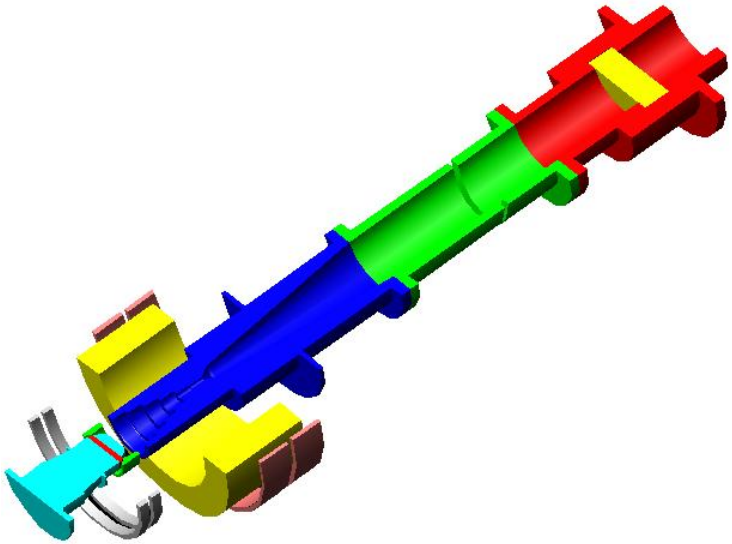

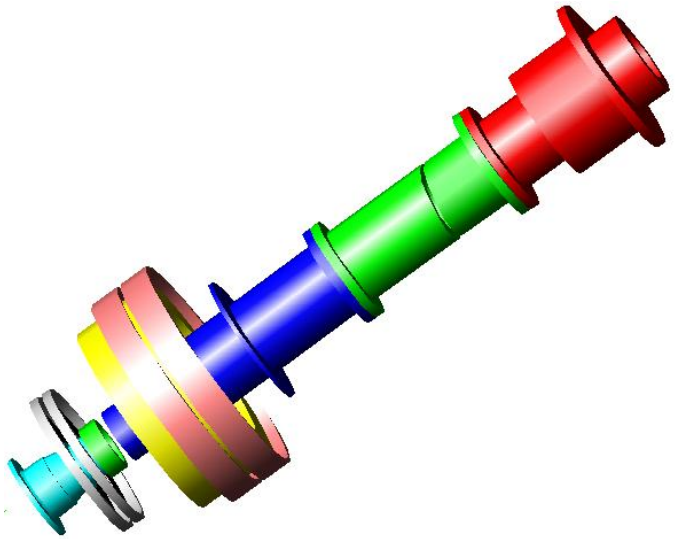

Thanks

Scientific Temperament

Dr AK Sinha

Gyrotron Laboratory
Central Electronics & Engineering Research Institute
(CSIR-CEERI), Pilani-333031, India

Successful Helix TWT>>

S-band 30 WHelix TWT

Broadband 40 W mini Helix TWT

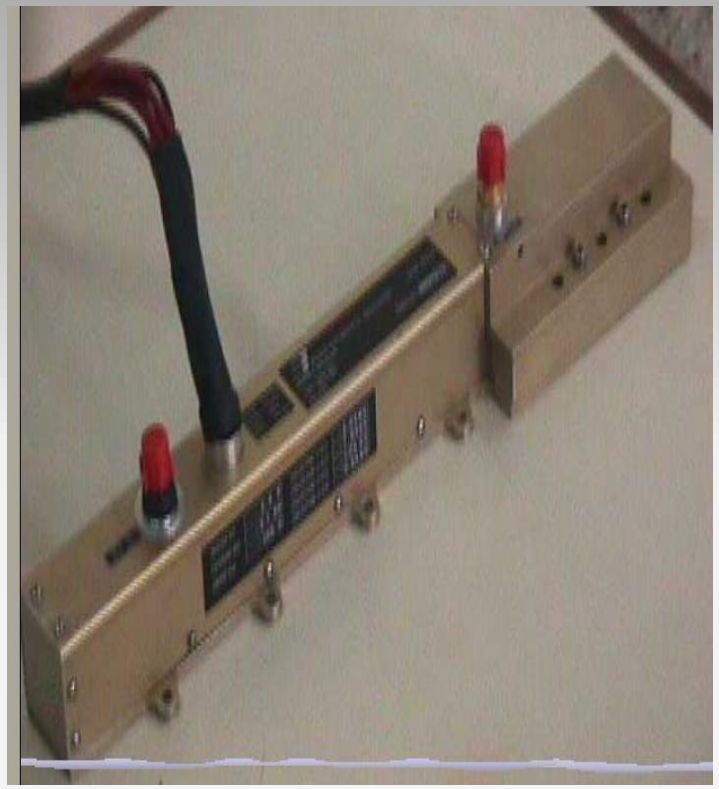

C-band 60 W Space Helix TWT

HELIX TWT

Kompfner's TWT

R Kompfner, The traveling wave tube as amplifier at microwave frequencies, Proc. IRE Vol. 35, p. 124, 1947.

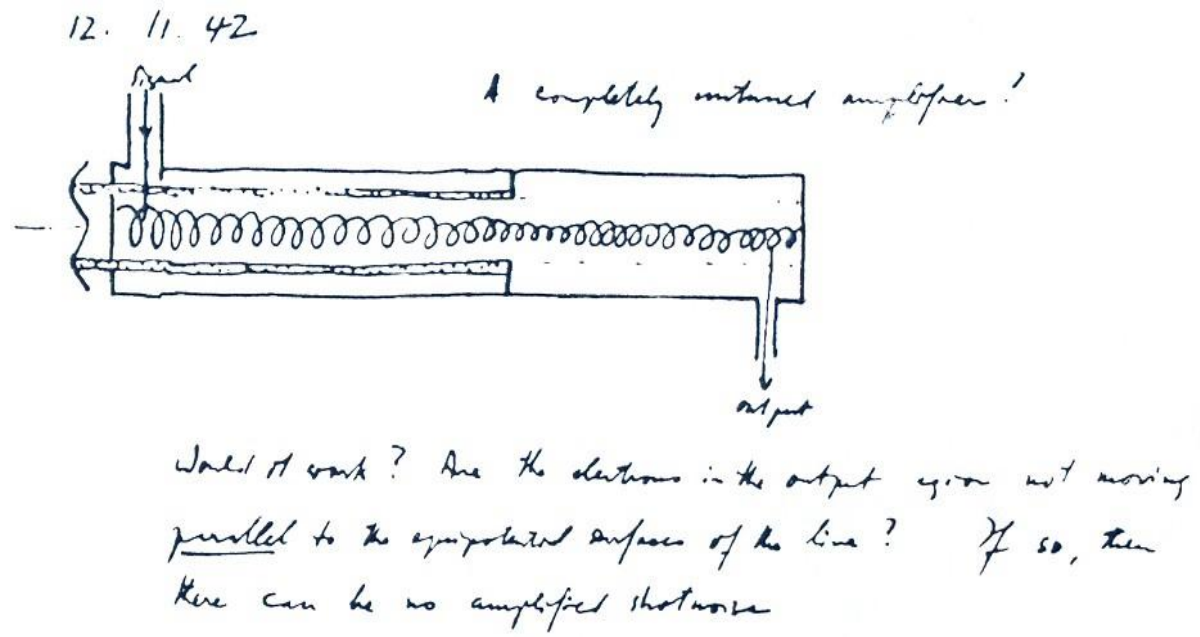

Sketch of TWT from Kompfner's notebook. From The Onvention of the TWT by R Kompfner, copyright from San Francisco Press (AS Gilmour, Principles of TWTs")

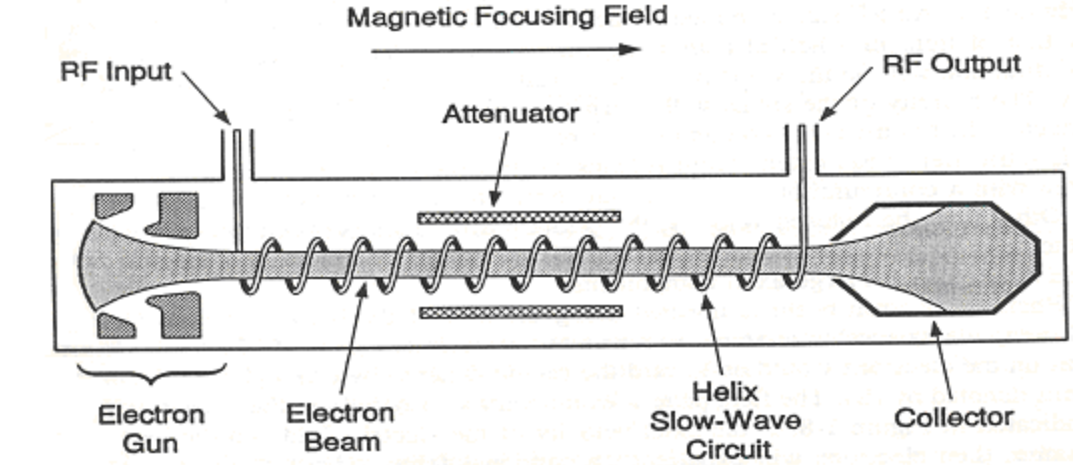

Schematic view of helix travelling –wave tube showing its different components

Some Helical Structures Used in TWTs

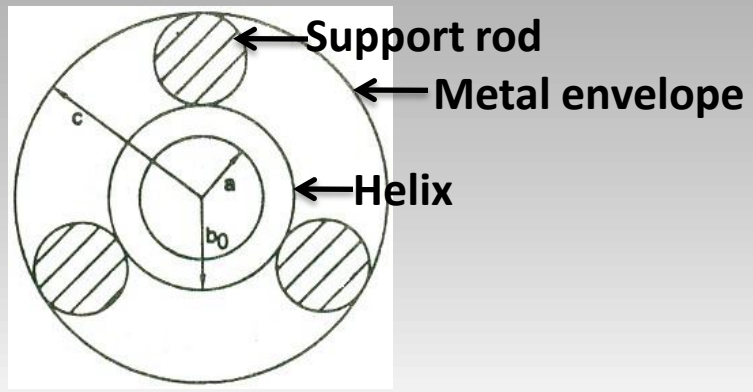

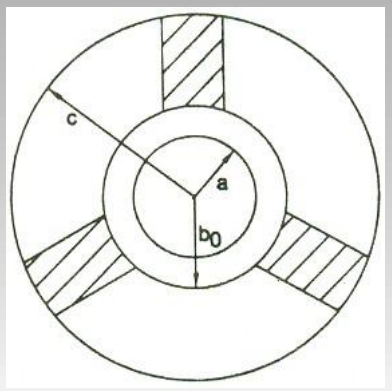

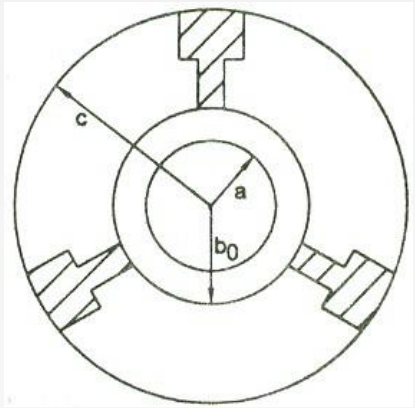

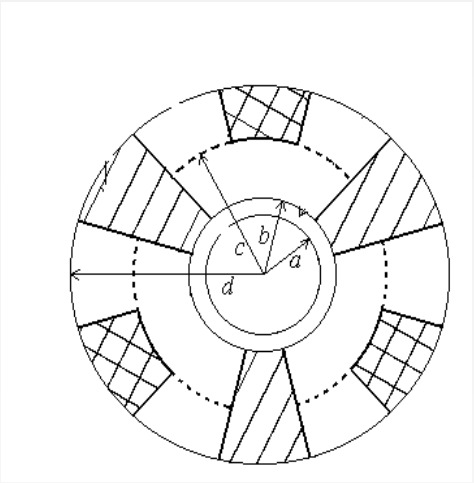

Sheath Helix Model

Part: I

(a) JR Pierce, Theory of the beam - type traveling wave tube, Proc. IRE, 35, p. 111, 1947.

(b) JR Pierce, Traveling-wave tubes, D Van Nostrand Co., Inc. , New York, 1950

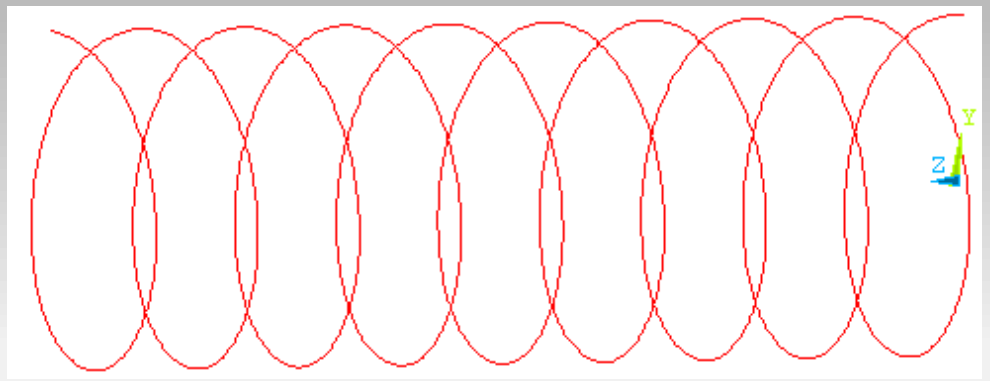

Wire helix

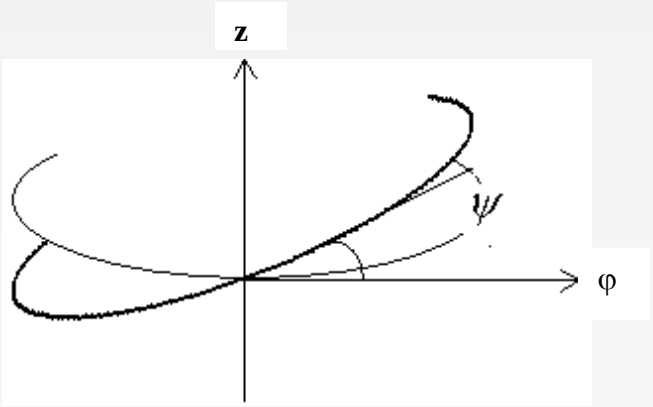

Conduction in helix winding direction and the helix pitch angle

ψ, which is the angle between the winding and azimuthal directions.

Analysis in the sheath-helix model

Steps:

- **Structure definitions and divisions into regions**
- **Write the field expressions in different regions of the structure**
- **Write proper boundary conditions and substitution of field expressions**
- **Make a determinant out of the boundary conditions**

  (the order depends upon the field constant valid for the analysis)
- **For non-trivial solution $\Delta=0$ and its solution gives the dispersion relation**

Analysis in Sheath Helix Model

Helix is modeled at its mean helix radius known as **sheath radius.**

***Structure*:**

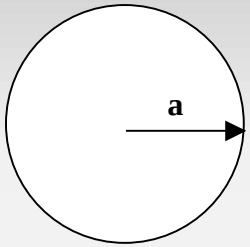

Field Analysis:

The field expressions obtained by the solution of the wave equation and their substitution into the relevant boundary conditions of the problem for the characterisation of the structure is referred to in the literature as the field analysis.

Example: Structure: Helix in free-space

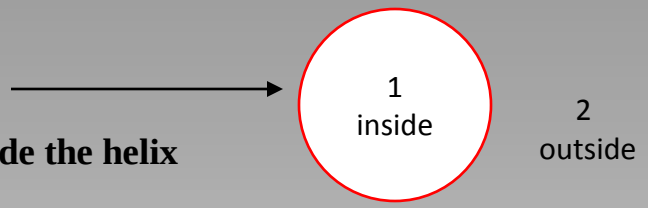

- **Regions: (1) inside the helix, (2) outside the helix**
- **Field Expressions:**

$$E_{z,p} = A_p I_0\{\gamma_p r\} + B_p K_0\{\gamma_p r\}$$
$$H_{z,p} = C_p I_0\{\gamma_p r\} + D_p K_0\{\gamma_p r\}$$

$$E_{\theta,p} = -\frac{j\omega\mu_p}{\gamma_p}\left(C_p I_1\{\gamma_p r\} - D_p K_1\{\gamma_p r\}\right)$$

$$H_{\theta,p} = \frac{j\omega\varepsilon_p}{\gamma_p}\left(A_p I_1\{\gamma_p r\} - B_p K_1\{\gamma_p r\}\right)$$

I_0 and K_0: the zeroth-order modified Bessel functions of the first and second kinds, respectively

I_1 and K_i: the corresponding first-order functions. A_p, B_p, C_p, D_p: the field constants

$\gamma_p = \gamma = (\beta^2 - k^2)^{1/2}$: the radial propagation constant, all referring to the

p^{th} region, (p = 1 and 2, inside and outside the helical sheath)

$\varepsilon_1 = \varepsilon_2 = \varepsilon_0$ and $\mu_1 = \mu_2 = \mu_0$.

Details of sheath helix model

RF dependence: $\exp\, j(\omega t - \beta z)$

The values of $I_0\{x\}$ (or $I_1\{x\}$) and $K_0\{x\}$ (or $K_1\{x\}$) each tending to infinity as the value of *x* tends to infinity and zero, respectively, makes

$$A_2 = B_1 = C_2 = D_1 = 0$$

in order to prevent the fields, from blowing up to infinity at $r = 0$ and $r = \infty$.

- **Boundary conditions**

  At $r = a$ (sheath helix that mean helix radius):

$$E_{z,1} - E_{z,2} = 0$$

$$E_{\theta,1}\cos\psi + E_{z,1}\sin\psi = 0$$

$$E_{\theta,2}\cos\psi + E_{z,2}\sin\psi = 0$$

$$(H_{\theta,1}\cos\psi + H_{z,1}\sin\psi) - (H_{\theta,2}\cos\psi + H_{z,2}\sin\psi) = 0$$

Boundary Condition

At sheath radius ($r = a$):

$$E_{z,1} = E_{z,2} \qquad \text{(a)}$$

$$E_{\theta,1} = E_{\theta,2} \qquad \text{(b)}$$

$$E_{z,1} + E_{\theta,1} \cot\psi = 0 \qquad \text{(c)}$$

$$H_{z,1} + H_{\theta,1} \cot\psi = H_{z,2} + H_{\theta,2} \cot\psi \qquad \text{(d)}$$

(a) and (b): the continuity of the axial and azimuthal components of tangential electric field intensity.

(c): the infinite conductivity of the helical sheath parallel to the winding direction $\psi\,(= \tan^{-1} p'/2\pi a)$

(d): the continuity of the tangential components of magnetic field intensity at the sheath helix arising from there being no current perpendicular to the helical direction due to infinite conductivity along the helical direction.

Dispersion Relation

(1) Finding field expressions in different regions

(2) Finding boundary conditions at the interfaces

(3) Substitutions of field expressions into boundary conditions to get a determinantal dispersion relation formed from the field coefficients. The order depends upon the number of boundary conditions. For non-trivial solution, the deteminant is equal to zero.

4×4 order determinant due to 4 boundary conditions.

$$\begin{vmatrix} I_{0a} & 0 & -K_{0a} & 0 \\ 0 & I_{1a} & 0 & K_{1a} \\ I_{0a} & -\frac{j\omega\mu_0}{\gamma} I_{1a}\cot\psi & 0 & 0 \\ \frac{j\omega\varepsilon_0}{\gamma} I_{1a}\cot\psi & I_{0a} & \frac{j\omega\varepsilon_0}{\gamma} K_{1a}\cot\psi & -K_{0a} \end{vmatrix} = 0$$

Dispersion Relation for helix in free-space:

$$\left(\frac{k\cot\psi}{\gamma}\right)^2 = \frac{I_{0a}K_{0a}}{I_{1a}K_{1a}}$$

Equivalent Circuit Analysis

JE Rowe, "Nonlinear electron wave interaction phenomena", Academic Press, New York, 1965

In this approach, the helix is considered as an equivalent transmission line with distributed parameters *L*, *C*, *R*, and *G* representing the series inductance per unit length, the shunt capacitance per unit length, the series resistance per unit length, and the shunt conductance per unit length, respectively. Considering a loss less line $(R = G = 0)$, the attenuation constant of the line is zero and the axial phase propagation constant β of the line is given by the transmission line equation

$$\beta^2 = \omega^2 LC$$

Characteristic Impedance

$$Z_0 = (L/C)^{1/2}$$

Boundary conditions:

$$H_{\theta,2} - H_{\theta,1} = \frac{I_z}{2\pi a}$$

$$H_{z,1} - H_{z,2} = \frac{I_\theta}{2\pi a}$$

due to the discontinuity of the axial and azimuthal components of tangential magnetic field intensity at the sheath helix.

$$I_\theta \sin\psi - I_z \cos\psi = 0$$

due to the condition arises from there being no current perpendicular to the helical direction due to infinite conductivity along the helical direction

Major Steps

(a) Grouping of Boundary Conditions:

$E_{z,1} = E_{z,2}$ $H_{\theta,2} - H_{\theta,1} = \frac{I_z}{2\pi a}$	$E_{\theta,1} = E_{\theta,2}$ $H_{z,1} - H_{z,2} = \frac{I_\theta}{2\pi a}$ $E_{z,1} + E_{\theta,1} \cot\psi = 0$

(b) Axial Electric Field in Terms of Scalar Potential:

Relation Between Scalar Potential (V) and Vector Potential **(*A*)**	$\boldsymbol{E} = -\nabla V - \frac{\partial \boldsymbol{A}}{\partial t}$	
Lorentz Condition	$\nabla.\boldsymbol{A} + \mu_0 \varepsilon_0 \frac{\partial V}{\partial t} = 0$	
$\exp j(\omega t - \beta z)$ RF dependence	$\frac{\partial}{\partial t} = j\omega$ $\frac{\partial}{\partial z} = -j\beta$	$\Rightarrow E_{za} = \frac{j\gamma^2}{\beta} V$
One dimensional case	$A_r = A_\theta = 0$ $A_z \neq 0$	

(c) The Telegraphist's Equation

Equation involving C	$\frac{\partial I_{za}}{\partial z} + C\frac{\partial V}{\partial t} = 0$
Equation involving L	$\frac{\partial V}{\partial z} + L\frac{\partial I_{za}}{\partial t} = 0$

(d) Combining the field expression in terms of axial current with the field expression in terms of scalar potential to write expression comparable to Telegraphist's equations

(e) Comparison with Telegraphist's equations for finding circuit parameters: axial electric field gives capacitance per unit length and azimuthal electric field inductance per unit length

Capacitance per unit length	$C_o = \frac{2\pi\varepsilon_0}{I_{0a}K_{0a}}$
Inductance per unit length	$L_o = \frac{\mu_0}{2\pi}\left(\frac{\beta}{\gamma}\right)^2 I_{1a}\, K_{1a} \cot^2\psi$

Details of Equivalent Circuit Analysis

Relation between the axial electric filed intensity with the scalar potential V (circuit potential) and the vector potential

$$\boldsymbol{E} = -\nabla V - \frac{\partial \boldsymbol{A}}{\partial z}$$

The Lorentz gauge relates the vector and scalar potentials as

$$\nabla . \boldsymbol{A} + \mu_0 \varepsilon_0 \frac{\partial V}{\partial t} = 0$$

In the one-dimensional case, ignoring variations in the transverse plane, and taking the RF dependence as $\exp j(\omega t - \beta z)$, one may write the axial electric field intensity at the helical sheath

$$E_{za} = \frac{j\gamma^2}{\beta} V \qquad \text{(i)}$$

$$\gamma (= \beta^2 - \omega^2 \mu_0 \varepsilon_0)^{1/2}$$

$$E_{z,1} - E_{z,2} = 0$$

$$H_{\theta,2} - H_{\theta,1} = J_z = \frac{I_z}{2\pi a}$$

One may express the axial component of the electric field intensity at the helical sheath *(E_{za})* in terms of the axial helix current I_{za} as

$$E_{za} = M\, I_{za} \qquad \text{(ii)}$$

Where

$$M = \frac{j\gamma^2}{2\pi\ \varepsilon_0 \omega} I_0\{\gamma a\} K_0\{\gamma a\}\ .$$

The telegraphist's equation involving *C*

$$\frac{\partial I_{za}}{\partial z} + C\frac{\partial V}{\partial t} = 0\,,$$

in view of RF dependence $\exp\, j(\omega t - \beta z)$, may be put as

$$\beta\, I_{za} = \omega CV\ . \qquad \text{(iii)}$$

Combining (i), (ii), (iii) the expression for the shunt capacitance per unit length *C* of the equivalent circuit of the helix becomes

$$C = \frac{j\gamma^2}{\omega\ M}$$

Similarly, one can find inductance per unit lemgth.

Combinational Approach for Finding C and L for Loaded Helical Structure

SF Paik, Design formulas for helix dispersion shaping, IEEE Trans Electron Devices, Vol ED-16, p. 1010 (1969)

Equivalent Circuit Parameters for Helix Loaded in Metal Shell:

Helix in free space(A)	$C_o = \frac{2\pi\varepsilon_0}{I_{0a}K_{0a}}$ $L_o = \frac{\mu_0}{2\pi}(\frac{\beta}{\gamma})^2 I_{1a} K_{1a} \cot^2\psi$ $C = C_o C_f$	--- ---
Helix surrounded by infinite dielectric (B)	$L = L_o L_f$	$C_f = [1 + (\varepsilon_r - 1)\gamma a I_{0a} K_{1a}]$ $L_f = 1$
Helix in a metal Shell (C)	$C = C_o C_f$ $L = L_o L_f$ $C = C_o C_f$	$C_f = (1 - \frac{I_{0a}K_{0d}}{K_{0a}I_{0d}})^{-1}$ $L_f = (1 - \frac{I_{1a}K_{1d}}{K_{1a}I_{1d}})$
Dielectric supported helix in a metal shell (B+C)	$L = L_o L_f$	$C_f = [1 + (\varepsilon_r - 1)\gamma a I_{0a} K_{1a}](1 - \frac{I_{0a}K_{0d}}{K_{0a}I_{0d}})^{-1}$ $L_f = (1 - \frac{I_{1a}K_{1d}}{K_{1a}I_{1d}})$

Models for Discrete Dielectric Helix-Supports

Homogeneous Supports:

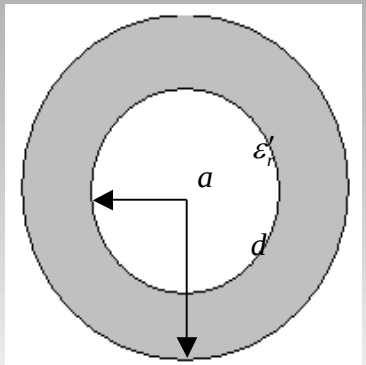

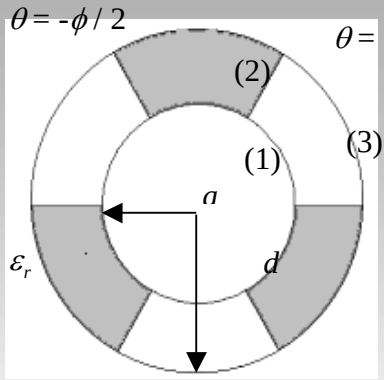

$$\theta = \frac{2\pi}{N} - \frac{\phi}{2}$$

Single continuous Dielectric Tube of effective relative permittivity ( )

$$\varepsilon_r' = 1 + \frac{\hat{A}_s}{\hat{A}}(\varepsilon_r - 1)$$

$\hat{A}_s$: cross-sectional area occupied by all the dielectric supports

ε_r: relative permittivity of support

$\hat{A}$: cross-sectional area of the total region between the helix and metal envelope

BN Basu (CEERI Period)

BN Basu and SN Joshi, "An equivalent circuit approach to the analysis of dielectric - supported helical slow-wave structures", Internal Report, Ir-01-VT/78, CEERI, Pilani, March 1978.

BN Basu, "Field analysis of dielectric supported and shielded sheath helix", Internal Report, IR-02-VT/78, CEERI, Pilani, July, 1978.

Structure: Discrete Dielectric Supported Helix in a Metal Envelope:

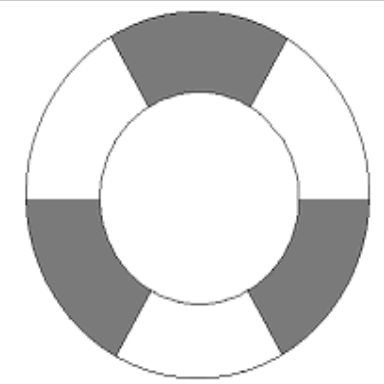

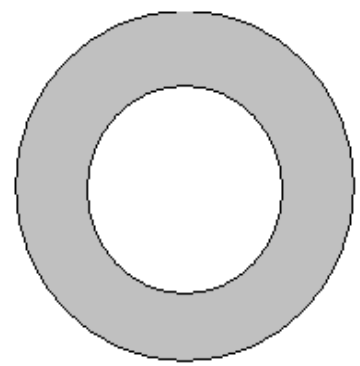

(I) Finding the expression of equivalent relative permittivity ( ) through area equivalence approach

$\varepsilon'_{r,p} = \dfrac{(\varepsilon_r)(\hat{A}_s) + (1)(\hat{A} - \hat{A}_s)}{(\hat{A}_s) + (\hat{A} - \hat{A}_s)} = 1 + (\varepsilon_r - 1)\dfrac{\hat{A}_s}{\hat{A}}$	$\varepsilon'_r == 1 + \dfrac{\phi N}{2\pi}(\varepsilon_r - 1)$

$\hat{A}$

$\hat{A}_s$:cross-sectional area occupied by the supports, : cross-sectional area of the total region between the helical sheath and the overall metal envelope, : relative permittivity of support rod

(II) Field Analysis:

$p = 1, 2$; $B_1 = D_1 = 0$; $\varepsilon_1 = \varepsilon_0$, $\varepsilon_2 = \varepsilon_0 \varepsilon_r'$

Boundary Conditions:

At helical sheath ($r = a$)	$E_{z,1} = E_{z,2}$ $E_{\theta,1} = E_{\theta,2}$ $E_{z,1} + E_{\theta,1} \cot\psi = 0$ $H_{z,1} + H_{\theta,1} \cot\psi = H_{z,2} + H_{\theta,2} \cot\psi$
At metal envelope ($r = d$)	$E_{z,2} = 0$, $E_{\theta,2} = 0$

Boundary conditions at the metal shell: arising due to perfect conductivity of the metal envelope.

Dispersion Relation from 6×6 order determinant:

$$\begin{vmatrix}
I_{0a} & 0 & -I_{0a} & -K_{0a} & 0 & 0 \\
0 & I_{1a} & 0 & 0 & -I_{1a} & K_{1a} \\
I_{0a} & -\frac{j\omega\mu_0}{\gamma} I_{1a} \cot\psi & 0 & 0 & 0 & 0 \\
\frac{j\omega\varepsilon_0}{\gamma} I_{1a} \cot\psi & I_{0a} & -\frac{j\omega\varepsilon_0\varepsilon_r'}{\gamma} I_{1a} \cot\psi & -\frac{j\omega\varepsilon_0\varepsilon_r'}{\gamma} K_{1a} \cot\psi & -I_{0a} & -K_{0a} \\
0 & 0 & I_{0d} & K_{0d} & 0 & 0 \\
0 & 0 & 0 & 0 & I_{1d} & -K_{1d}
\end{vmatrix} = 0$$

Dispersion Relation

$$\left(\frac{k \cot\psi}{\gamma}\right)^2 = \frac{I_{0a} K_{0a}}{I_{1a} K_{1a}} D^2$$

$$D = [(1 - \frac{I_{1a} K_{1d}}{K_{1a} I_{1d}})(1 - \frac{I_{0a} K_{0d}}{K_{0a} I_{0d}})^{-1}(1 + (\varepsilon_r - 1)\gamma a I_{0a} K_{1a}(1 + \frac{I_{1a} K_{0d}}{K_{1a} I_{0d}}))]^{-1/2}$$

(III)Equivalent Circuit Analysis

Grouping of Boundary Conditions:

Group I	Group II	
$E_{z,1} = E_{z,2}$ $H_{\theta,2} - H_{\theta,1} = \frac{I_z}{2\pi a}$	$E_{\theta,1} = E_{\theta,2}$ $H_{z,1} - H_{z,2} = \frac{I_\theta}{2\pi a}$ $E_{z,1} + E_{\theta,1}\cot\psi = 0$	**At helical sheath** ($r = a$)
$E_{z,2} = 0$	$E_{\theta,2} = 0$	**At metal envelope** ($r = d$)

Equivalent Circuit Parameters:

Discrete Dielectric supported helix in a metal shell	$C = C_o C_f$ $L = L_o L_f$	$C_f = [1 + (\varepsilon_r - 1)\gamma a I_{0a} K_{1a} 1 + \frac{I_{1a} K_{0d}}{K_{1a} I_{0d}}](1 - \frac{I_{0a} K_{0d}}{K_{0a} I_{0d}})^{-1}$ $L_f = (1 - \frac{I_{1a} K_{1d}}{K_{1a} I_{1d}})$

COMPARISON

Equivalent Circuit Analysis (Paik's Combinational approach)	Field Analysis of BNB Approach	Equivalent Circuit Analysis (BNB Approach
$C_f = (\chi_C)[1+G]$	---	$C_f = (\chi_C)[1+G(1+\frac{I_{1a}K_{0d}}{K_{1a}I_{0d}}]$
$D = [(\chi_L)(\chi_C)^{-1}(1+G)]$	$D = [(\chi_L)(\chi_C)^{-1}[1+G\times \times(1+\frac{I_{1a}K_{0d}}{K_{1a}I_{0d}})]^{-1/2}$	$D = [(\chi_L)(\chi_C)^{-1}[1+G\times \times(1+\frac{I_{1a}K_{1d}}{I_{1a}K_{1d}})]^{-1/2}$

$$\chi_C = 1-\frac{I_{0a}K_{0d}}{K_{0a}I_{0d}}, \quad \chi_L = 1-\frac{I_{1a}K_{1d}}{K_{1a}I_{1d}}, \quad G = \gamma a I_{0a}K_{1a}(\varepsilon_r' - 1)$$

BNB FACTOR

$$(BNB)_{factor} = 1+\frac{I_{1a}K_{0d}}{K_{1a}I_{0d}}$$

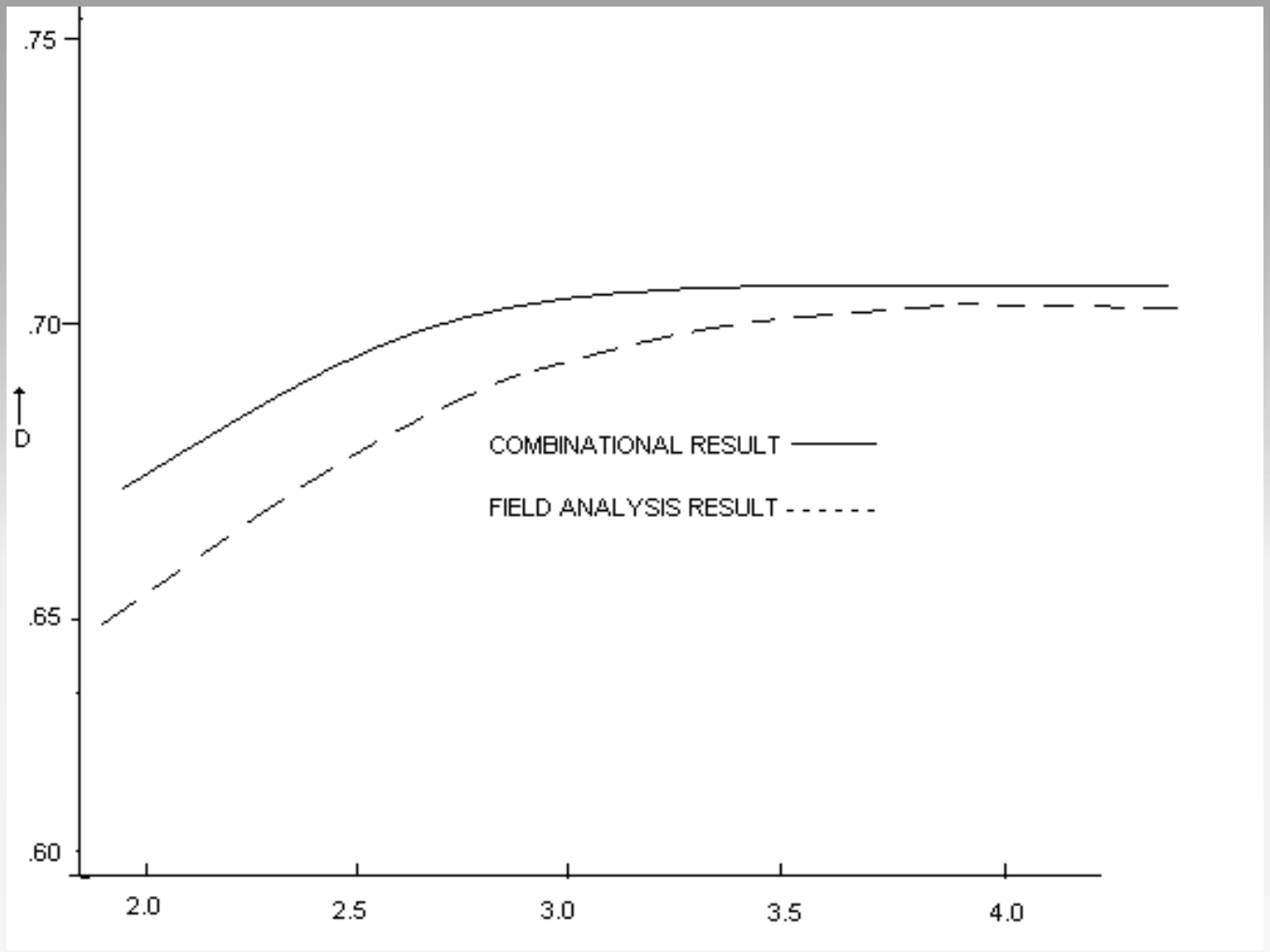

VARIATION OF DIELECTRIC LOADING FACTOR (D) WITH NORMALIZED SHELL RADIUS (γ_b) FOR CONFIGURATION V.

Inhomogeneous Loading in Helix SWS

(PART: II)

Practical Situations

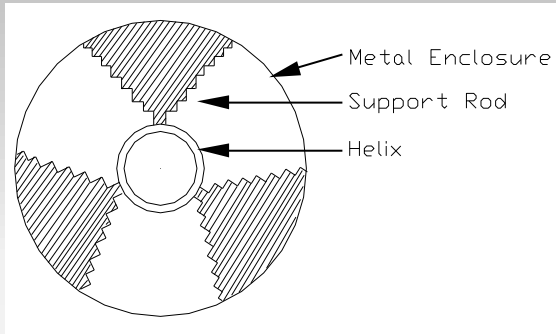

Inhomogeneous dielectric Loaded Helix SWS

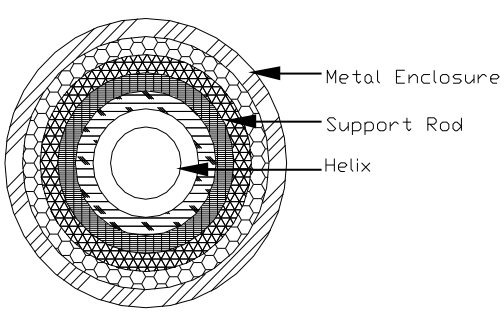

Equivalent (Multi layered Dielectric Loaded) Helix SWS

Equivalent Relative Permittivity of p^{th} dielectric tube

$$\varepsilon'_{r,p} = \frac{(\varepsilon_r)(\hat{A}_{s,p}) + (1)(\hat{A}_p - \hat{A}_{s,p})}{(\hat{A}_{s,p}) + (\hat{A}_p - \hat{A}_{s,p})} = 1 + (\varepsilon_r - 1)\frac{\hat{A}_{s,p}}{\hat{A}_p}$$

Development of Multi Layered Approach For Analysis of Inhomogeneous Dielectric Support

EFFECTIVE MODEL

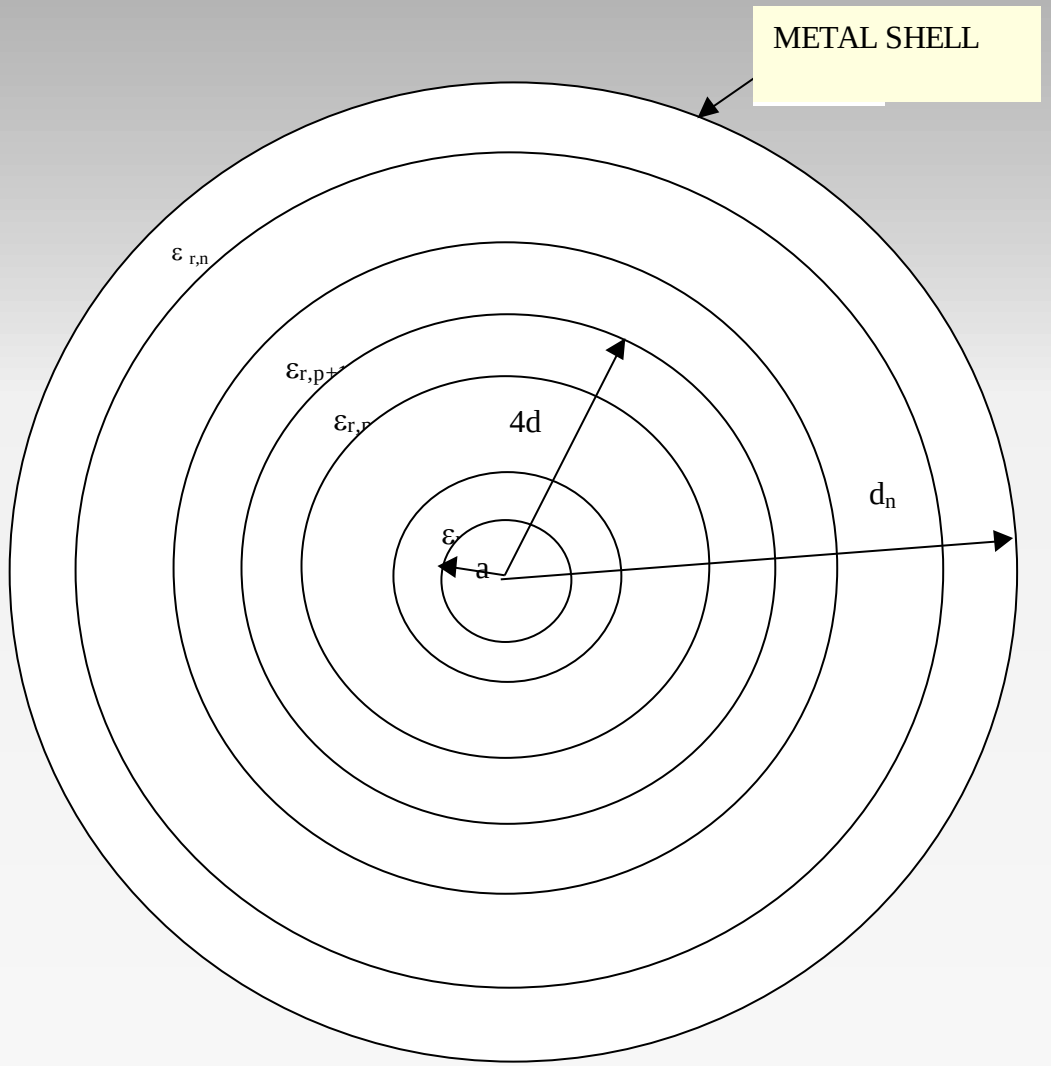

Field Expressions

$$E_{z,s} = A_s I_{0r} + B_s K_{0r}$$

$$H_{z,s} = C_s I_{0r} + D_s K_{0r}\,.$$

$$E_{\theta,s} = -\frac{j\omega\mu_0}{\gamma}\left(C_s I_{1r} - D_s K_{1r}\right)$$

$$H_{\theta,s} = \frac{j\omega\varepsilon_s}{\gamma}\left(A_s I_{1r} - B_s K_{1r}\right)$$

- s =i refer to (i) the region inside the sheath helix ($0 \le r \le a$), (ii) the free-space region between the mean helix radius and the outer helix radius to account for the finite thickness of the helix $a \le r \le b$ (ii) s=1,2,…, n: the continuous dielectric region between the helix and the metal envelope radius $a \le r \le d(=d_n)$, respectively, of effective relative permittivity ε_r'

- The functions $I_{0r}[=I_0(\gamma r)]$ and $K_{0r}[=K_0(\gamma r)]$ are the zeroth-order modified Bessel functions of the first and second kinds, respectively, and I_{1r} and K_{1r} are the corresponding first-order Bessel functions.

- A_s, B_s, C_s, and D_s are the field constants. In the field expressions, the RF dependence $\exp j(\omega t - \beta z)$ is understood, and it is implied that

$$B_1 = D_1 = 0$$

The $(4n+2)\times(4n+2)$ Determinantal Dispersion Relation (*n=10*, then 10×10 order determinant) (Helix thickness ignored)

$$\begin{vmatrix} \delta_{1,1} & \delta_{1,2} & \cdots & \delta_{1,4n+2} \\ \delta_{2,1} & \delta_{2,2} & \cdots & \delta_{2,4n+2} \\ \cdots & \cdots & \cdots & \cdots \\ \cdots & \cdots & \cdots & \cdots \\ \cdots & \cdots & \cdots & \cdots \\ \delta_{4n+2,1} & \delta_{4n+2,2} & \cdots & \delta_{4n+2,4n+2} \end{vmatrix} = 0$$

$$\delta_{1,1}=\delta_{2,2}=\delta_{3,1}=-\delta_{2,5}=-\delta_{3,3}=I_{0a}\ ;$$

$$\delta_{1,2}=-\frac{j\omega\mu_0}{\gamma}I_{1a}\cot\Psi\ ;\ \delta_{2,1}=\frac{j\omega\varepsilon_0}{\gamma}I_{1a}\cot\Psi\ ;$$

$$\delta_{2,3}=\frac{j\omega\varepsilon_0\varepsilon_{r,1}}{\gamma}I_{1a}\cot\Psi\ ;\ \delta_{2,4}=\frac{j\omega\varepsilon_0\varepsilon_{r,1}}{\gamma}K_{1a}\cot\Psi\ ;$$

$$\delta_{2,6}=\delta_{3,4}=-K_{0a}\ ;\ \delta_{4,2}=-\delta_{4,5}=I_{1a}\ ;\ \delta_{4,6}=K_{1a}\ ;$$

$$\delta_{4m+1,4p-1}=\delta_{4m+2,4p+1}=-\delta_{4m+1,4p+3}=-\delta_{4m+2,4p+5}=I_{0d_p}\ ;$$

$$\delta_{4m+1,4p}=\delta_{4m+2,4p+2}=-\delta_{4m+1,4p+4}=\delta_{4m+2,4p+6}=K_{0d_p}\ ;$$

$$\delta_{4m+3,4p+1}=-\delta_{4m+3,4p+5}=I_{1d_p}\ ;\ \delta_{4m+3,4p+2}=-\delta_{4m+3,4p+6}=-K_{1d_p}\ ;$$

$$\delta_{4m+4,4p+1}=\varepsilon_{r,p}I_{1d_p}\ ;\ \delta_{4m+4,4p}=-\varepsilon_{r,p+1}K_{1d_p}\ ;$$

$$\delta_{4m+4,4p+3}=-\varepsilon_{r,p+1}I_{1d_p}\ ;\ \delta_{4m+4,4p+4}=\varepsilon_{r,p+1}K_{1d_p}\ ;$$

$(1\le m\le n-1;1\le p\le n-1;)$ m and p being integers.

$$\delta_{4n+14n+1}=I_{0d}\ ;\ \delta_{4n+1,4n+2}=K_{0d}\ ;$$

$$\delta_{4n+2,4n+1}=I_{1c}^{0d}\ ;\ \delta_{4n+2,4n+2}=-K_{0d}\ ;$$

Simpler Approach (Formation of 2×2 order determinant):

(a) Grouping of boundary conditions into 2 groups

-----first group consists of boundary conditions not containing $\cot\psi$

----- second group consists of boundary conditions containing $\cot\psi$

(b) first group of boundary conditions are used to express all the field constants in terms of field constant A_i or C_i

(c) use of second group of boundary conditions to form 2×2 order Δ

$$\begin{vmatrix} M_{1,1} & M_{1,2} \\ M_{2,1} & M_{2,2} \end{vmatrix} = 0$$

$$M_{1,1} = I_{0a}$$

$$M_{1,2} = -\frac{j\omega\mu_0}{\gamma} I_{1a}\cot\psi$$

$$M_{2,1} = \frac{j\omega\varepsilon_0}{\gamma}\cot\psi[I_{1a} - \varepsilon_{r,1}(\frac{I_{1a}\alpha_1 - K_{1a}\beta_1}{I_{0a}\alpha_1 + K_{0a}\beta_1})I_{0a}]$$

$$M_{2,1} = I_{0a} + (\frac{\chi_L}{1-\chi_L})(I_{0a} + \frac{I_{1d}}{K_{1d}}K_{0a})$$

$$\chi_L = 1 - \frac{I_{1a}K_{1d}}{K_{1a}I_{1d}}$$

DISPERSION CHARACTERSTICS FOR VARIOUS NUMBER OF DIELECTRIC TUBES ($\varepsilon_{r,1}$ = 4, d/a=1.75) ($F = \varepsilon_{r,p} / \varepsilon_{r,p-1}$)

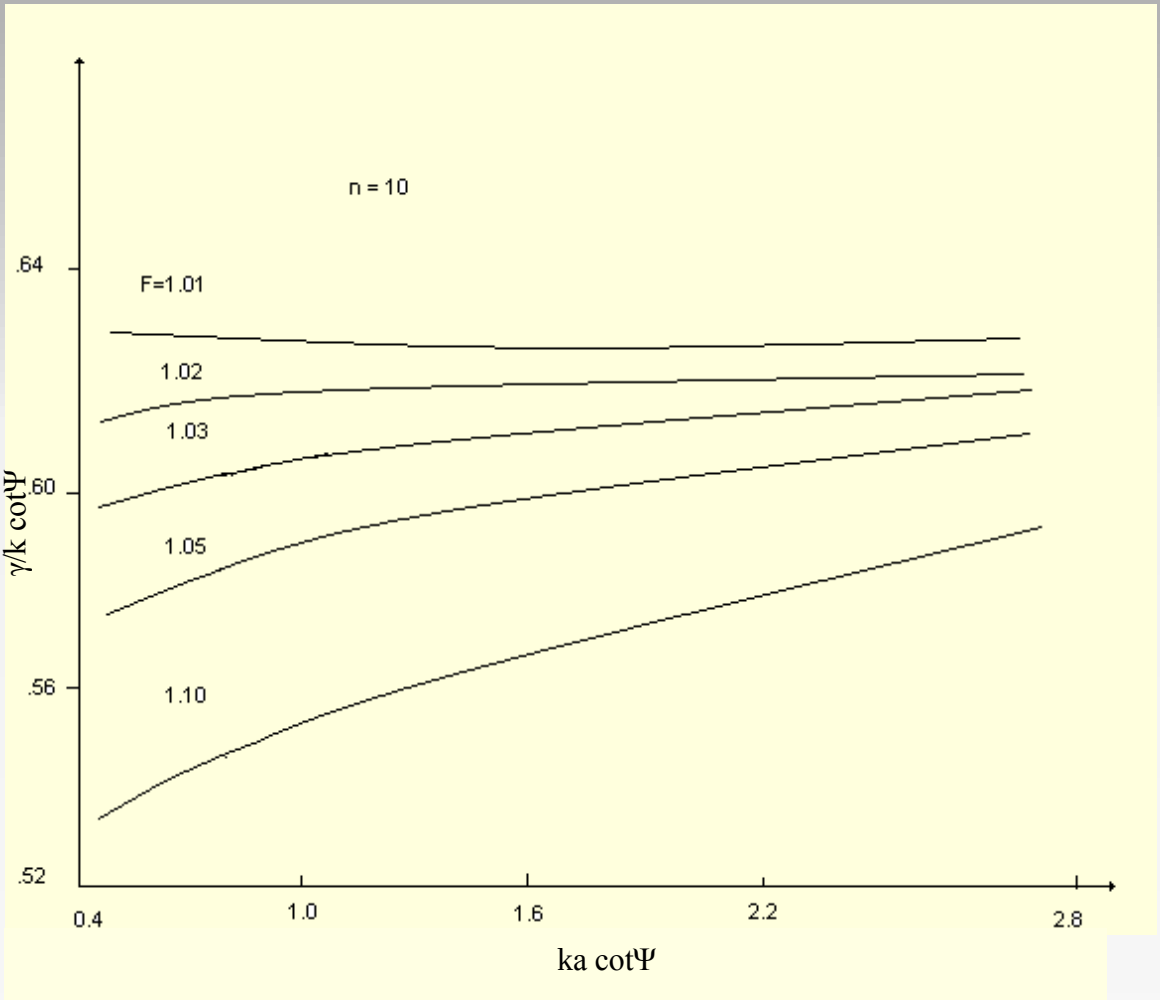

TYPICAL STAIR-CASE VARIATIONS OF THE RELATIVEPERMITTIVITY WITH THE RADIAL COORDINATE FOR THE STRUCTURE (I) $\varepsilon_{r,1}$ =2 ; F_{opt} ≈1.07 and (ii) $\varepsilon_{r,1}$ =4 ; F_{opt} ≈1.02

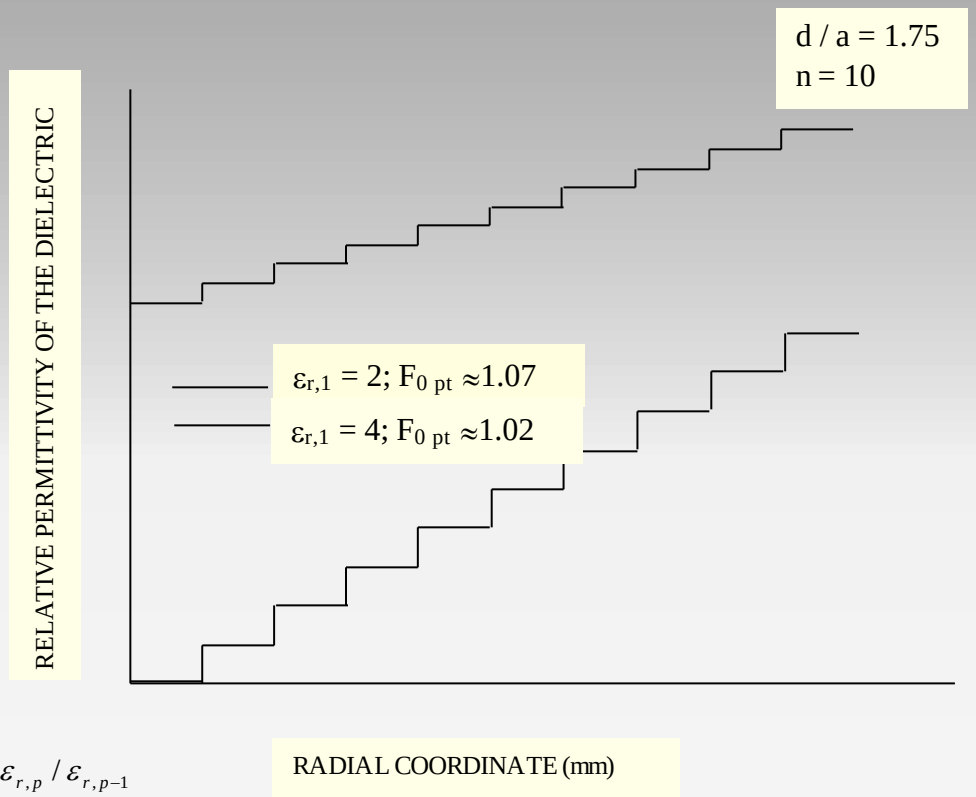

$$F = \varepsilon_{r,p} / \varepsilon_{r,p-1}$$

$$\phi_p = (\frac{2\pi}{N})(\frac{F^p - 1}{(\varepsilon_r)_w - 1} + \phi_1 F^{p-1} \qquad (p=1,2,3, \ldots..)$$

$$\phi_1 = (\frac{2\pi}{N})(\frac{\varepsilon_{r,1} - 1}{(\varepsilon_r)_w - 1} + \phi_1 F^{p-1}$$

Use of computer in Scientific journey

1980-1990

1990-2000

2000-……..

2005-…….

2010-…….

2012-…….

Future (folded system)

Part: III

Development of Simpler Approach in Tape Helix Model

Analysis on Inhomogeneous Dielectric Support

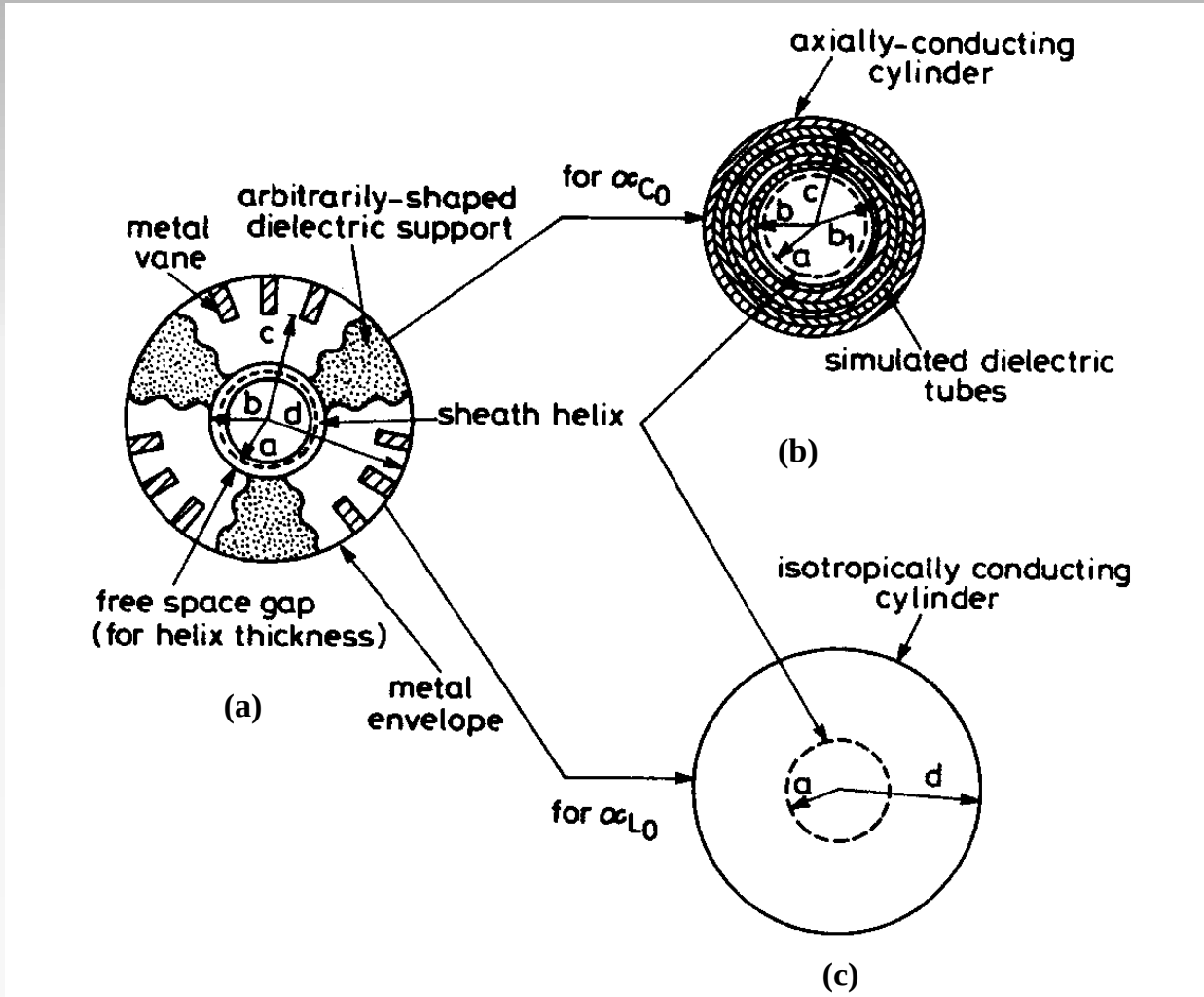

Prediction of Forbidden zone>>

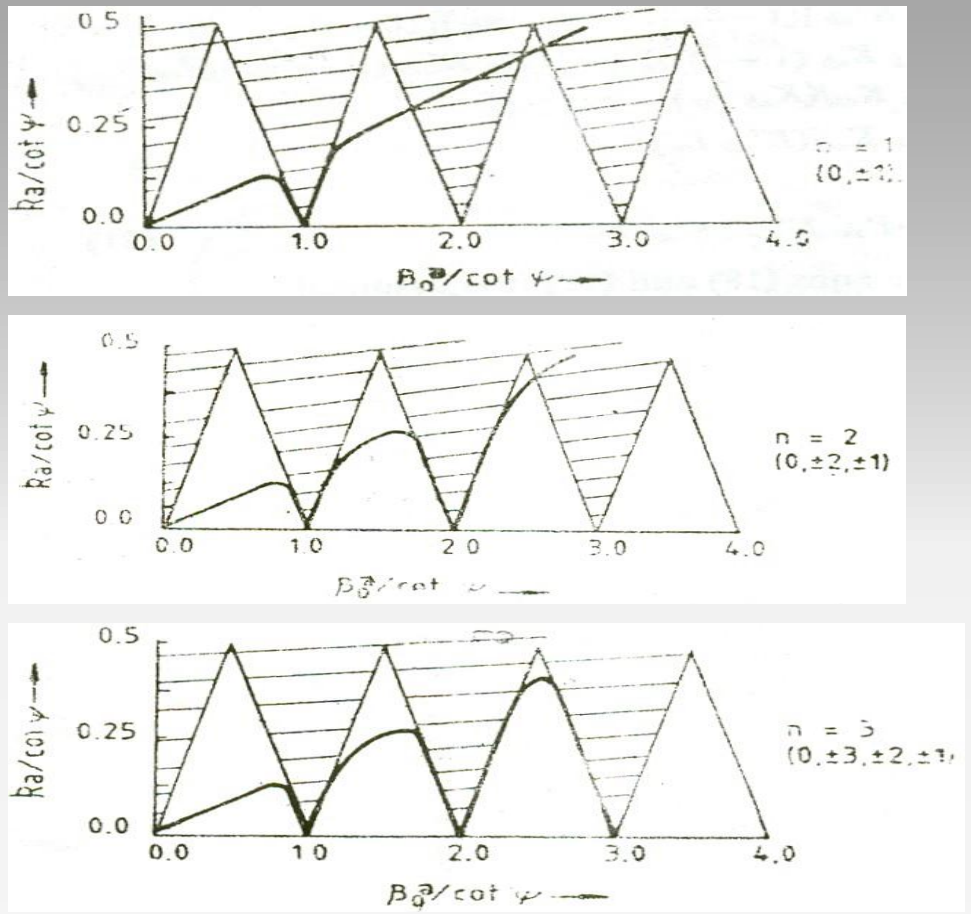

Dispersion characteristics for a tape helix in free space (--------dispersion curves; hatched portions represent for bidden zones)

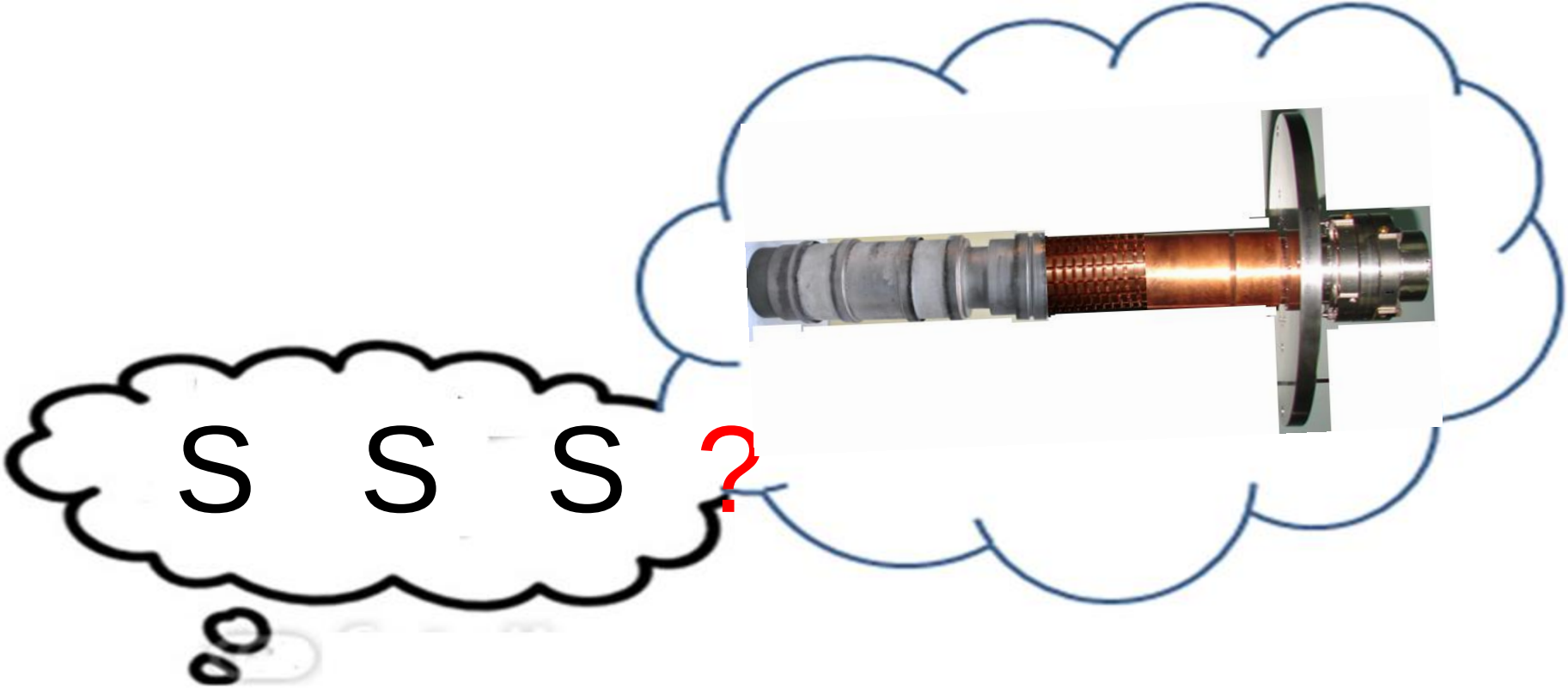

Part: IV >> Gyrotron

Challenge & Opportunity

Space

YEAR 2006

YEAR 2011

Model Space

Staff

YEAR 2006

YEAR 2011

Indian Youth

Skill

YEAR 2006

YEAR 2011

Design and Development

Indigenous

Design Methodology of MIG

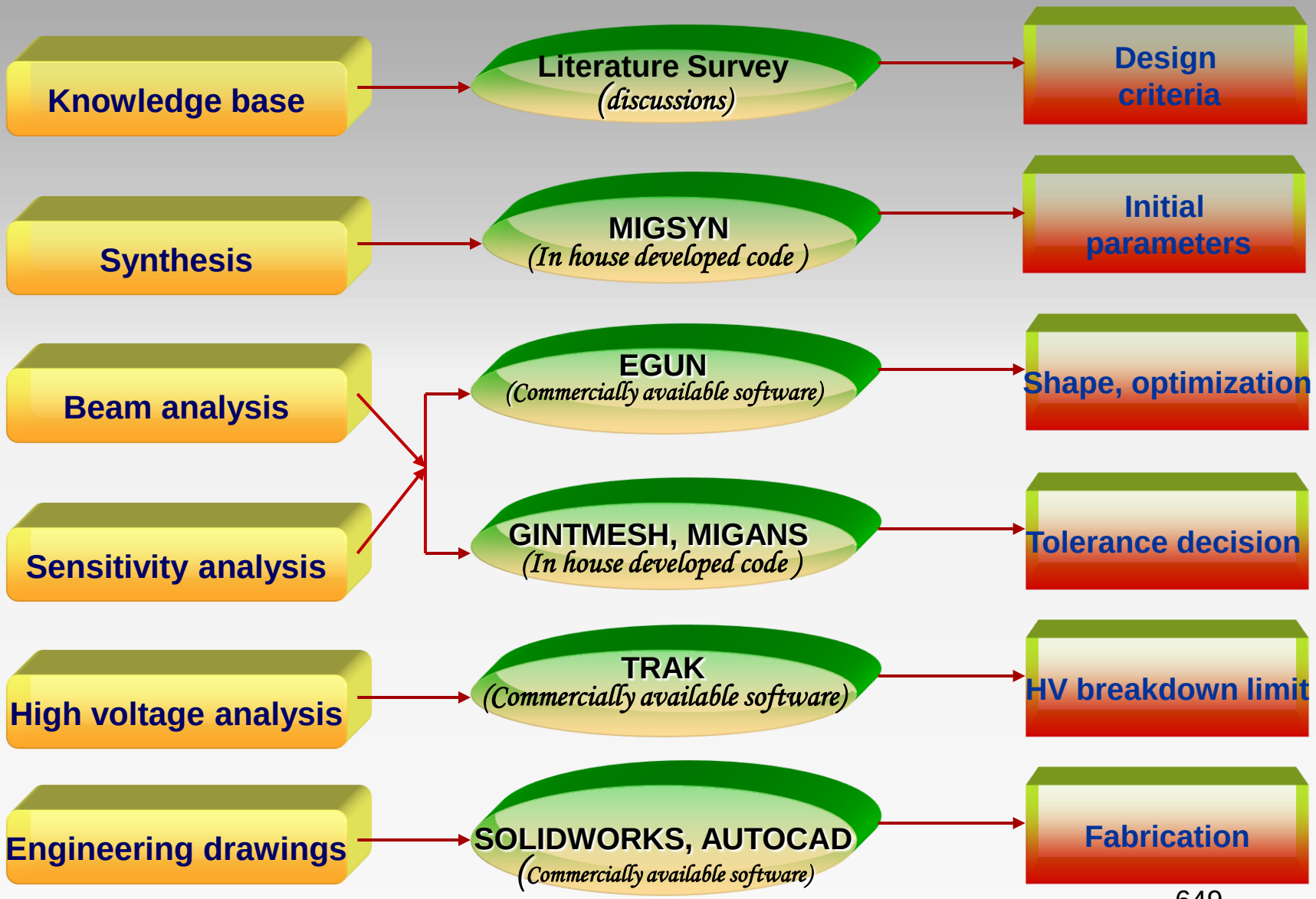

Gyrotron Gun (MIG)

Magnetron Injection Gun (MIG)

- Most Gyrotrons made use of a thermionic electron gun to provide high current annular electron beams in which electrons executes small cyclotron orbits at a frequency required for a cyclotron resonance interaction
- Shape of cathode is superficially similar to the interaction region of the magnetron
- The initial electron motion occurs in crossed electric and magnetic fields so that the electron follows helical trajectories around the magnetic field lines.

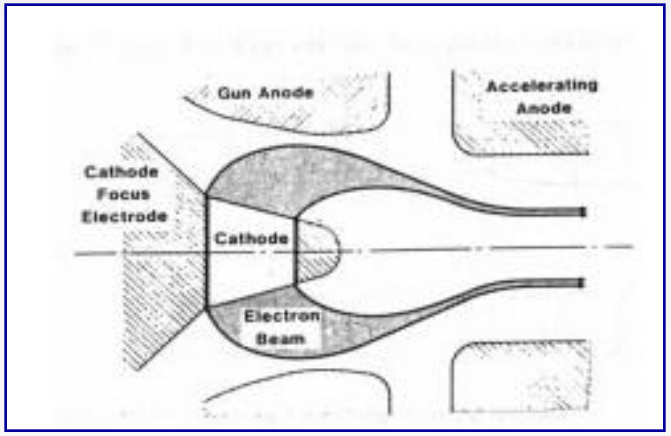

Design Equations for Synthesis of Electron Gun

Parameters	***Equation***	***Values obtained***
Relativistic mass factor γ	$\gamma = 1 + \frac{eV_B}{mc^2}$	1.127
Velocity of electron v (m/s)	$v = c\sqrt{1 - \frac{1}{\gamma^2}}$	$1.38*10^8$ m/s
Longitudinal velocity v_z (m/s)	$v_z = \frac{v}{\sqrt{\alpha^2 - 1}}$	$0.802*10^8$ m/s
Optimum magnetic field B_o (Tesla)	$B_o = \frac{2\pi f_c m\gamma}{e} = \frac{f(GHz)\gamma}{28 \times s}$	1.692 Tesla
Magnetic field at cathode B_{zc} (Tesla)	$B_{zc} = B_o \frac{\left(r_e^2 - r_c^2\right)}{r_c^2}$	0.12 Tesla
Cavity radius R_o (mm)	$R_o = \frac{\lambda}{2\pi}\chi'_{m,n}$	8 mm
Beam interaction radius R_e (mm)	$R_e = \frac{\lambda}{2\pi}\chi'_{m\pm1,n}$	6.06 mm
Larmour radius r_l (mm)	$r_l = \frac{\alpha}{\alpha^2+1}\sqrt{\gamma^2-1}\left(\frac{c}{\eta}\right)\frac{1}{B_0(T)}$	0.43 mm
Cathode radius R_c (mm)	$R_c = \sqrt{b} \cdot R_b$	22.67 mm
Larmour radius at cathode r_{lc}	$r_{lc} = r_l \cdot \sqrt{b}$	8.83 mm
Guiding Radius r_g (mm)	$r_g = \sqrt{R_b^2 - r_l^2}$	
Cylindricity parameter μ	$\mu = \frac{r_{lc}}{R_e}$	0.093

Slant length of the cathode L_s (mm)	$L_s = \frac{I_b}{2\pi R_e J_c}$	6.38 mm
Guiding centre spread Δr_g	$\frac{\Delta R_g}{R_g} = \left(\frac{\sin\phi_c}{\mu^2+1}\right)\left(\frac{I_o}{6.28 \cdot r_{L0}^2 J_c}\right)\left(\frac{1}{R_c^2}\right)$	
Voltage at first anode V_a (KV)	$V_a = \frac{mc^2}{e} \cdot \frac{\ln(1+D_f\mu)}{\ln(1+2\mu)}\left\{\left[1+\frac{4}{\mu^2}\left(\frac{1+\mu}{1+2\mu}\right)^2\left(\frac{(\gamma^2-1)r_l^2}{R_e^2\cos^2\phi_c}\right)\left(\frac{\alpha^2}{\alpha^2+1}\right)\right]^{\frac{1}{2}}-1\right\}$	31.6
Current ratio (J_c/J_l)	$\frac{J_C}{J_L} = \frac{6.28 r_{LO}^2 J_c (1+D_f\mu)\xi^2 R_c^2}{14.66x10^{-6}\left(\frac{mc^2}{e}\right)^{1.5}\cos^2\phi_c(\phi_a)^{1.5}}$ Where $\xi = \exp\left(-\frac{q}{2}\right)\left[q+\frac{q^2}{10}+\frac{5q^3}{300}+\frac{24q^4}{9900}+.....\right]$ $q = \ln(1+D_f\mu)$	0.14
Cathode Electric Field E_c (E/mm)	$E_c = \frac{V_a\cos\phi_c}{\ln(1+D_f\mu)R_e}$	29.7 KV/cm
Space charge limited Current density J_l (A/mm^2)	$J_l = \frac{14.66\times10^{-4}V_a\cos^2\phi_c}{2\pi R_e^2(1+D_f\mu)\beta^2}$	

Design Limits Obtained From Synthesis Program ***MIGSYN***

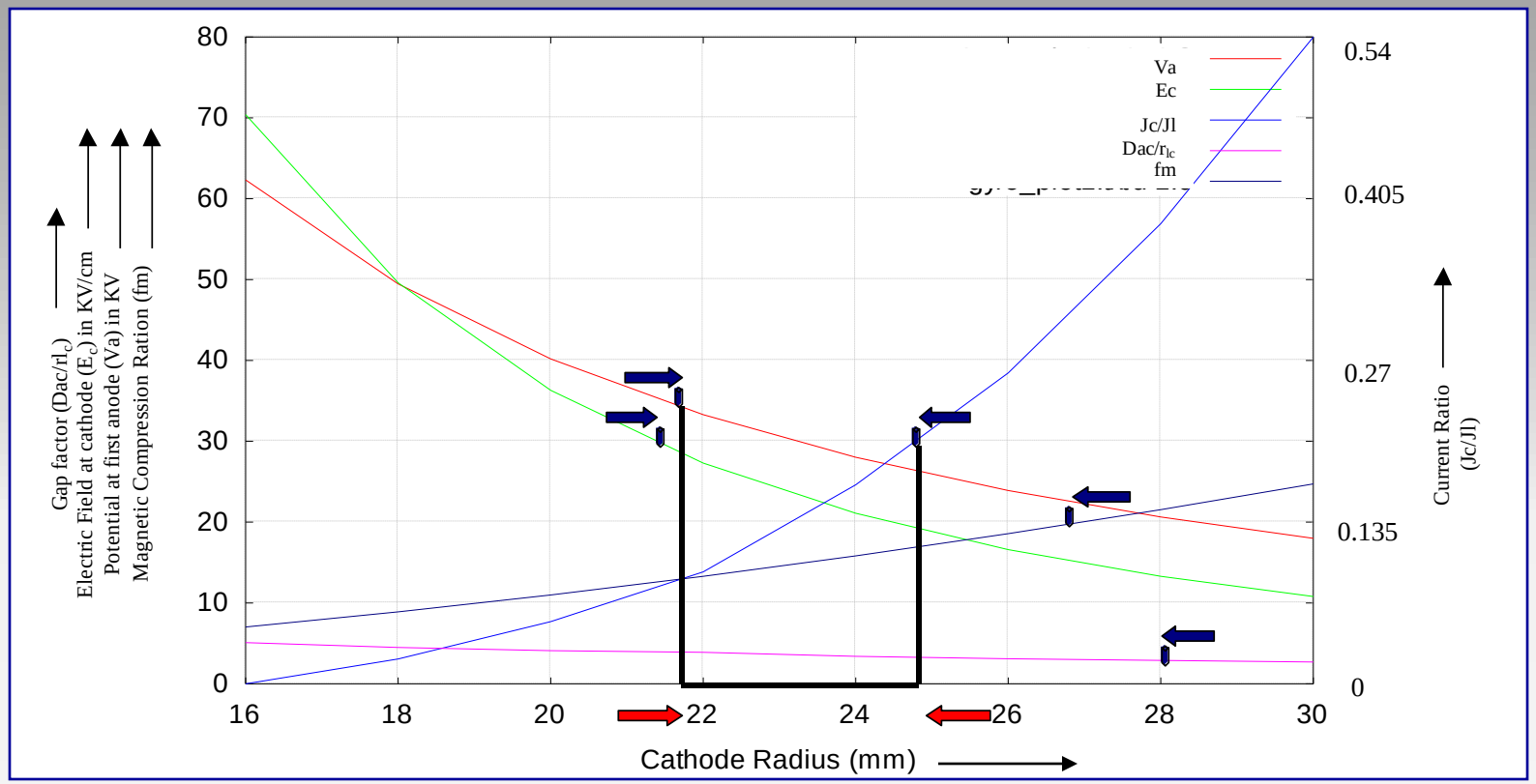

Design constrains

Electric field at cathode (Ec)	< 30 KV/cm
Potential at first anode (Va)	< 35 KV
Magnetic compression ratio (fm)	< 20
Gap Factor (D_{ac}/r_{lc})	> 3
Current Ratio (Jc/J_l)	< 0.2

Desired range cathode radius
21.8 mm to 24.8 mm

MIG with uniform magnetic field

PARAMETERS	VALUES OBTAINED
Magnetic field at cathode centre	0.11 tesla
Magnetic field at interaction region	1.65 tesla
Compression ratio	15
Variation of B field around Zcav+/-20mm	20 gauss

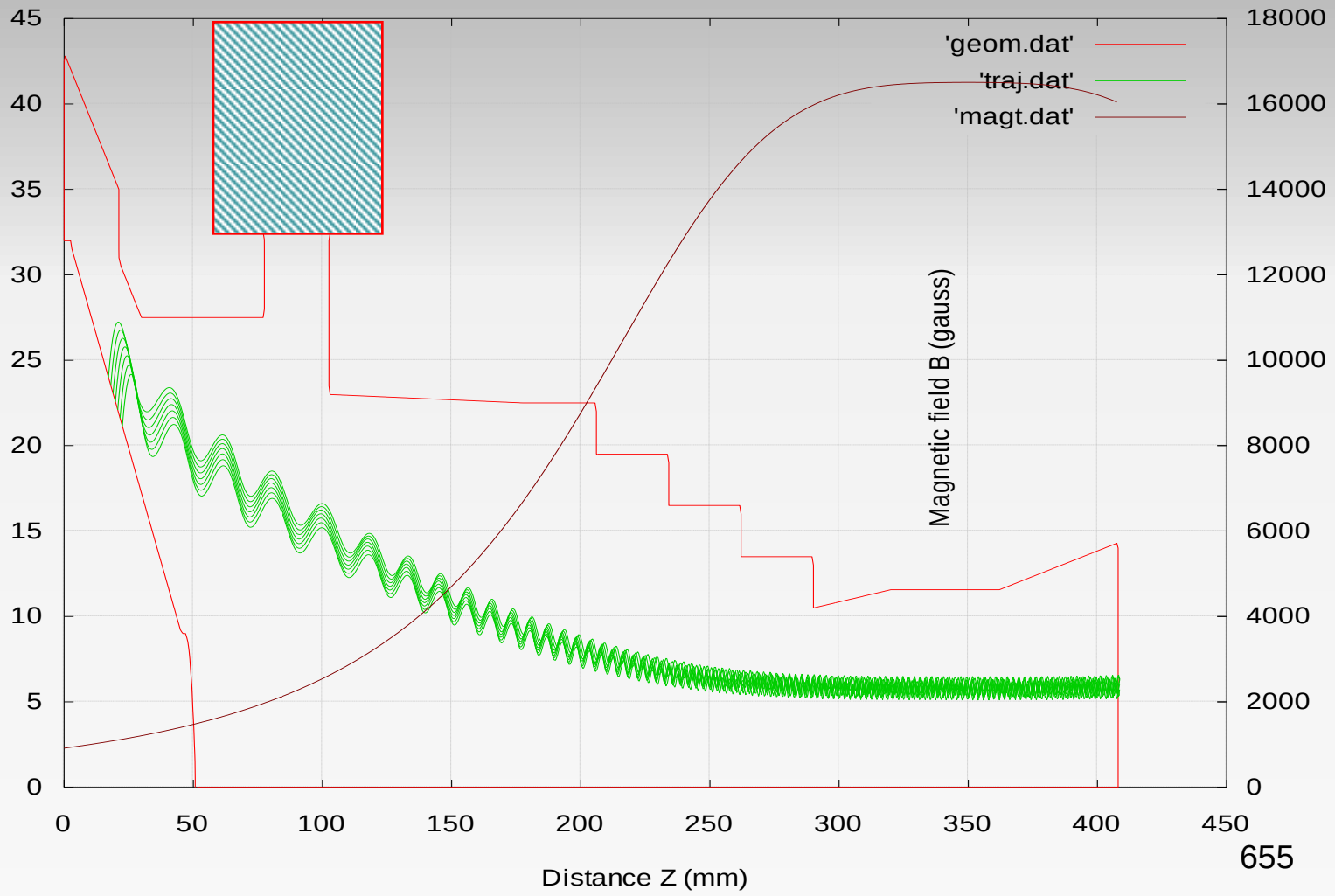

Table I: Design parameters of electron gun

SN	Electrode	Parameter
1.	Cathode	
i	Mean radius of cathode	22.65 mm
ii	Slant length of emitting surface	7.4 mm
iii	Slope angle of cathode	28^0
iv	Distance from cavity centre	330 mm
2	1st anode	
i	Voltage at 1st anode	27 KV
3	2nd anode	
i	Voltage at 2nd anode	65 KV
4	Cavity	
i	Cavity radius	11.57 mm
ii	Total length of cavity (including taper)	120 mm
iii	Length of main cavity	30 mm
iv	Down tapered angle	2.5^0
v	Up tapered angle	3.5^0
vi	Operating mode	TE_{03}
5	Beam tunnel	
i	Total length	112mm
ii	Length of each section	28 mm

Table II: Beam/magnetic field values of MIG

SN	PARAMETERS	VALUES OBTAINED
1	Electron beam	
i	Beam current	10.1 A
ii	Beam radius at interaction region	6.01 mm
iii	Minimum beam-metal gap	3 mm
iv	Beam-metal gap at cavity entrance	3 mm
2	Magnetic field	
i	Magnetic field at cathode centre	0.111 tesla
ii	Magnetic field at interaction region	1.653 tesla
iii	Compression ratio	14.84
iv	Variation of B field around Zcav +/- 20mm	15 gauss
v	$\Delta B_0/B_0$% around Z_{cav} +/- 20mm	0.09
3	Alpha	
i	Maximum value of alpha	1.38
ii	Minimum value of alpha	1.15
iii	Mean value of alpha	1.30
4	Velocity spread	
	Avg. velocity spread (%age)	1.48

Sensitivity Analysis of MIG

Effect of magnetic field

Cathode angle 28^0

With actual magnetic field value

SN	PARAMETERS	VALUES OBTAINED
1	Magnetic field	
i	**magnetic field at cathode centre**	**0.11 tesla**
ii	**Magnetic field at interaction region**	**1.65 tesla**
iii	**Compression ratio**	**15**
iv	**Variation of B field around Zcav ±20mm**	**20 gauss**

ALPHA	trans velocity	velocity spread	v.s.(rms)
1.227727	0.352812	0.009184	0.135217
1.292442	0.359713	0.010195	0.143159
1.355341	0.365996	0.027842	0.237613
1.394665	0.369628	0.038042	0.278443
1.348098	0.365254	0.025756	0.228420
1.270704	0.357652	0.004409	0.094009
1.170001	0.346121	0.027974	0.234873
1.060640	0.331482	0.069086	0.365240

avg velocity spread (percentage)=2.656107

mean value of alpha =1.26

Mean trans. Velocity (normalized) = 0.35

When magnetic field is1% less than actual value

ALPHA	trans velocity	velocity spread	v.s.(rms)
1.257010	0.356086	0.009394	0.136750
1.330793	0.363732	0.011878	0.154586
1.402060	0.370466	0.030611	0.249318
1.430456	0.372619	0.036601	0.273024
1.386174	0.369013	0.026569	0.232045
1.300437	0.360650	0.003304	0.081352
1.194378	0.349093	0.028848	0.238463
1.078665	0.334041	0.070721	0.369379

avg velocity spread(percentage)=2.724093

mean value of alpha =1.29

Mean trans. Velocity (normalized) =0.35

When magnetic field is1% more than actual value

ALPHA	transverse velocity	velocity spread	v.s.(rms)
1.200676	0.349661	0.009983	0.140950
1.263088	0.356582	0.009614	0.138998
1.322108	0.362707	0.026956	0.233748
1.358714	0.366540	0.037809	0.277574
1.317971	0.362271	0.025720	0.228257
1.242334	0.354686	0.004246	0.092250
1.147395	0.343255	0.028122	0.235484
1.047790	0.329792	0.066239	0.357898

avg velocity spread(percentage)=2.608606

mean value of alpha=1.23

Mean trans. Velocity (normalized) = 0.35

Magnetic field profile with ±1% tolerance

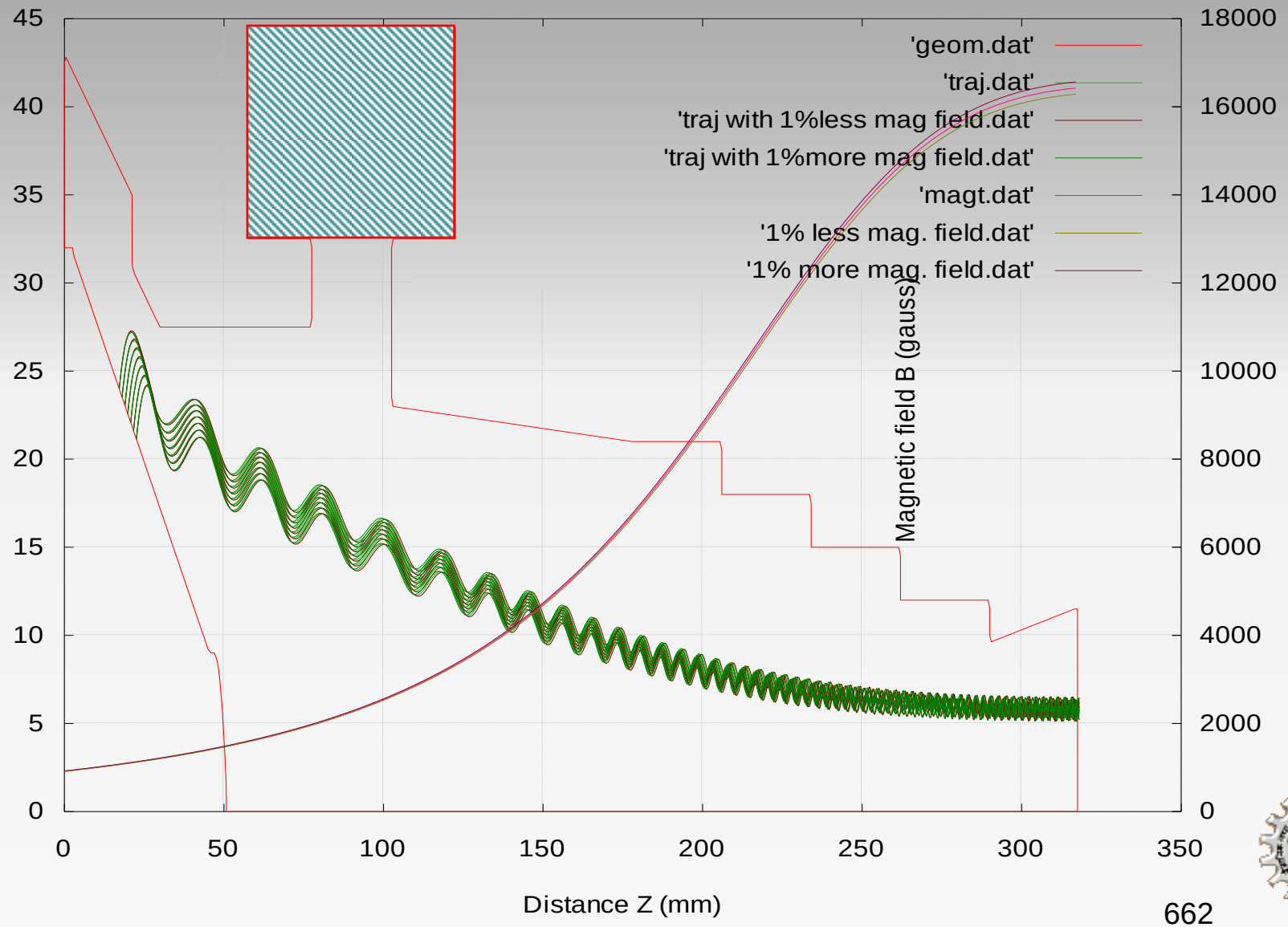

Magnetic field profile near the cathode with ±1% tolerance

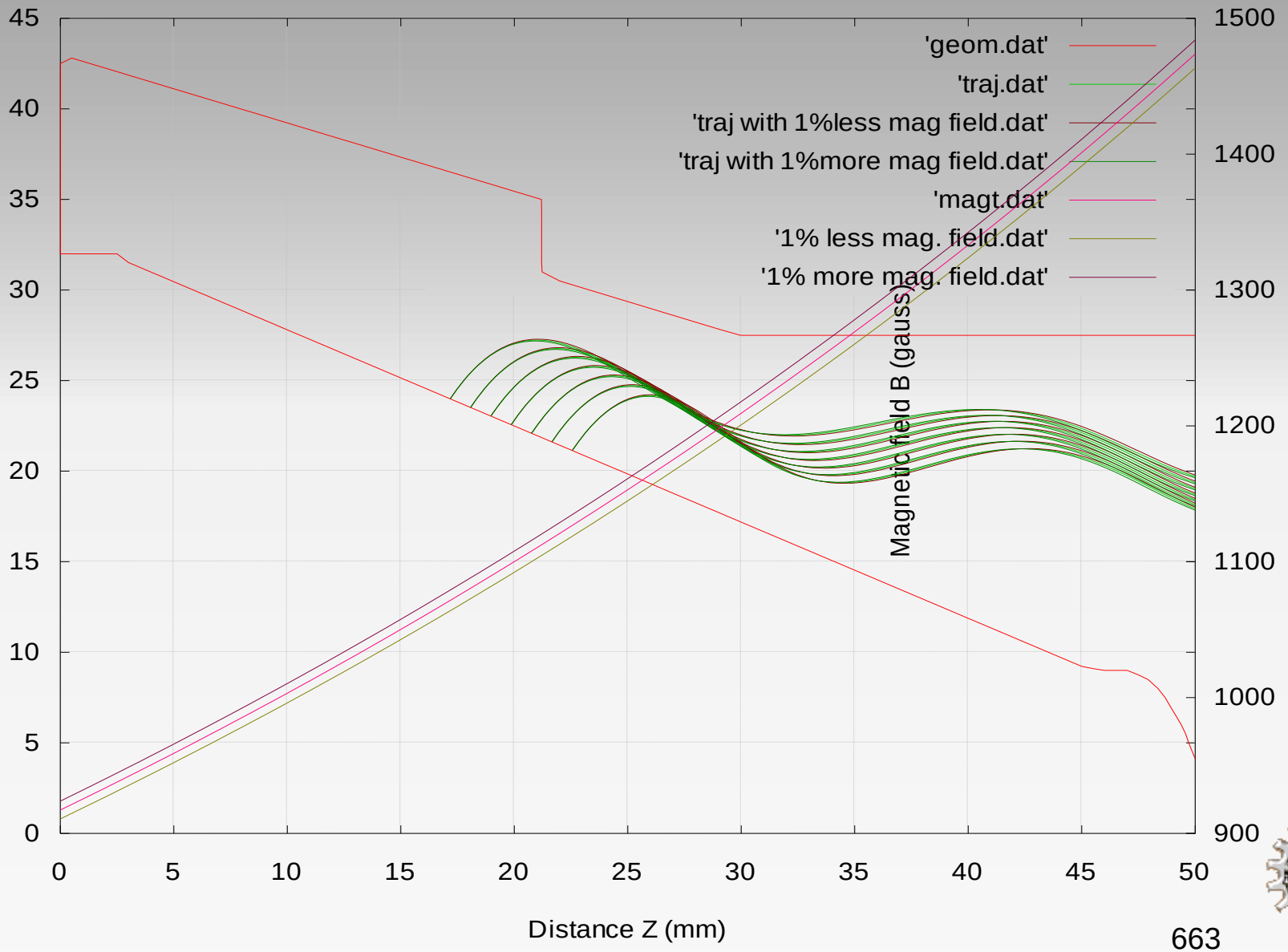

MIG with non uniform magnetic field

PARAMETERS	VALUES OBTAINED
Magnetic field at cathode centre	0.11 tesla
Magnetic field at interaction region	1.65 tesla
Compression ratio	15
Variation of B field around Zcav+/-20mm	160 gauss

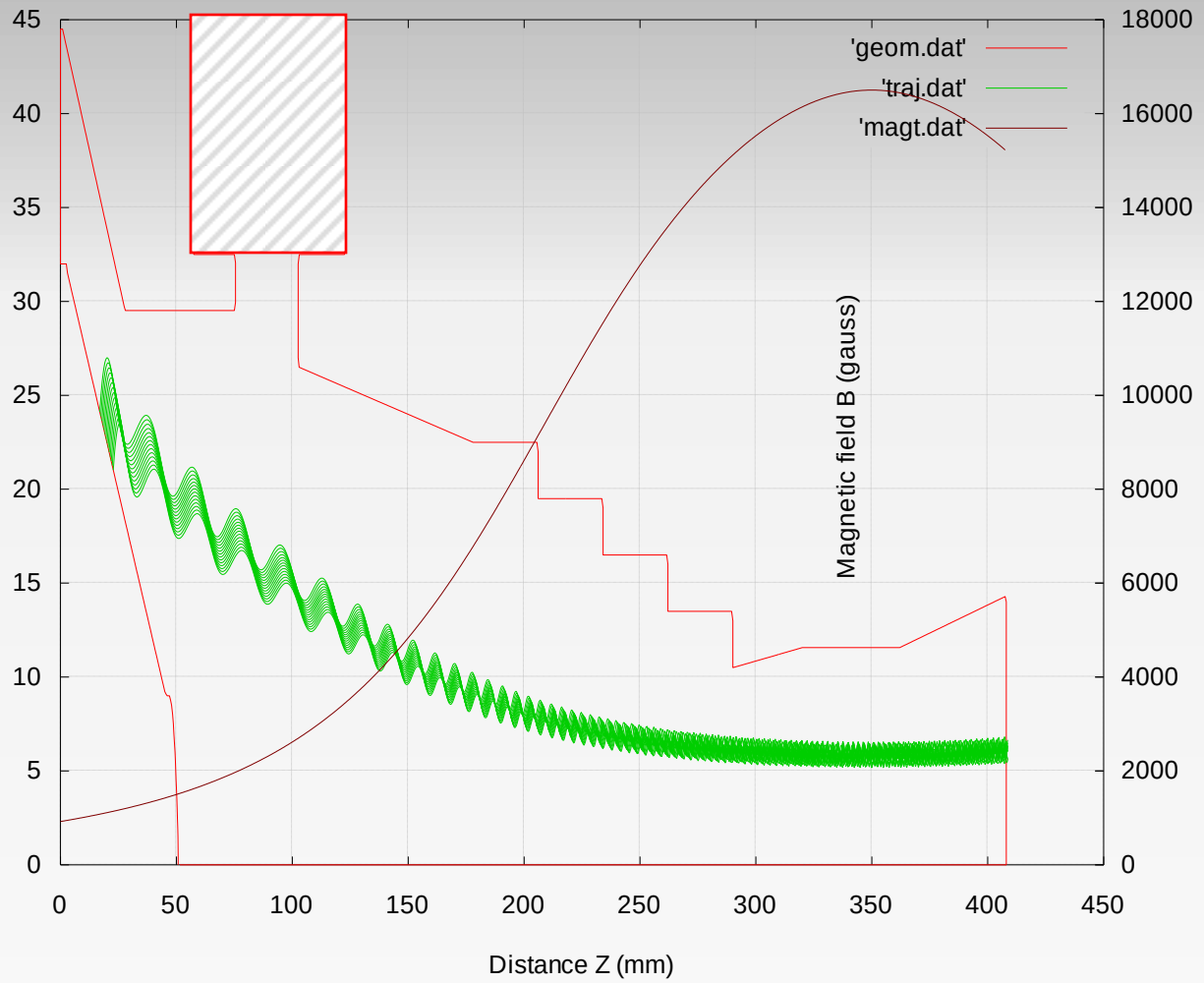

Effect of angle

Beam parameters for different cathode angles

Cathode angle	Nature of alpha	Laminarity
20^0	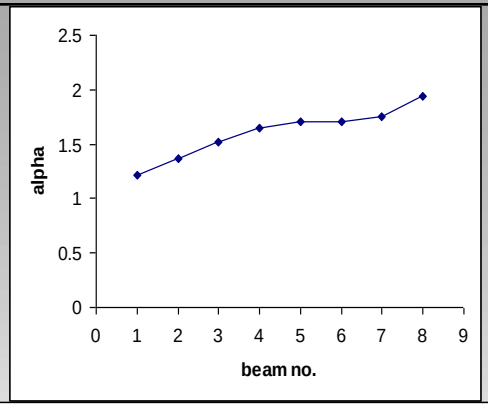	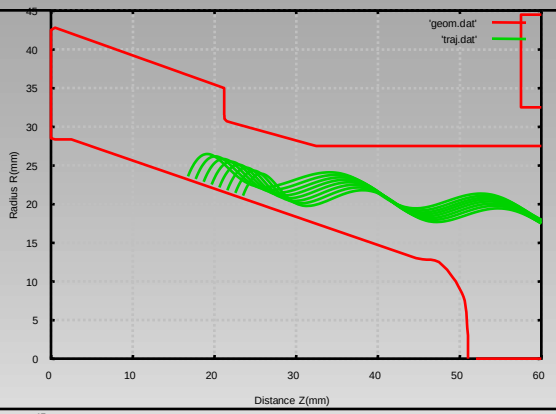
21^0	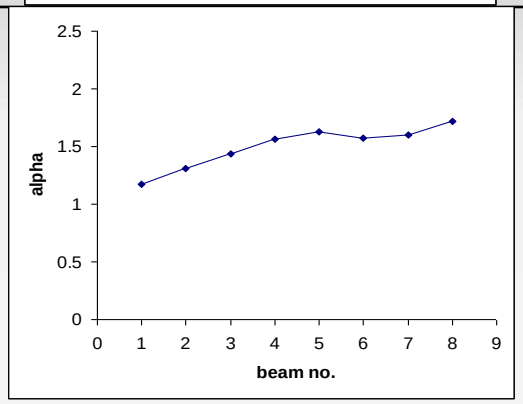	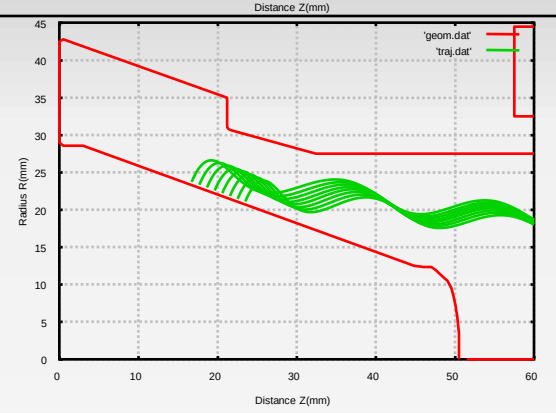
22^0	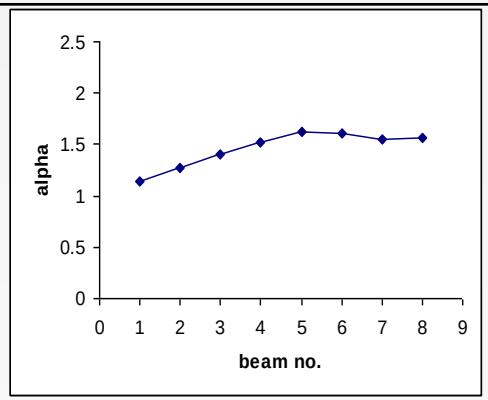	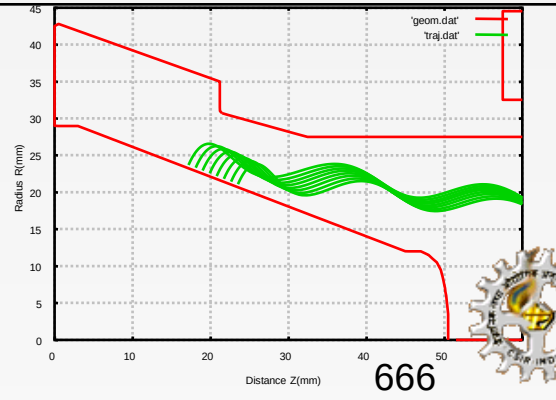

Beam parameters for different cathode angles

Cathode angle	Nature of alpha	Laminarity
23^0	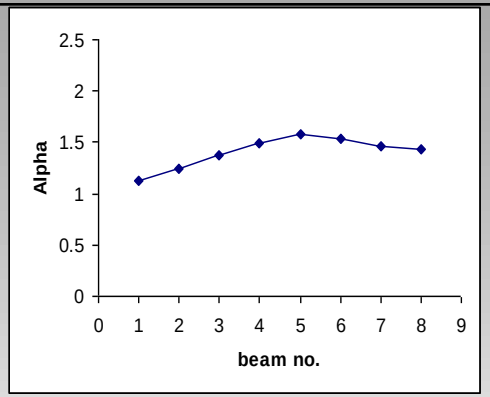	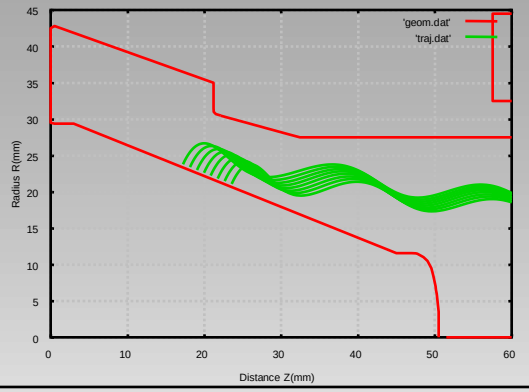
24^0	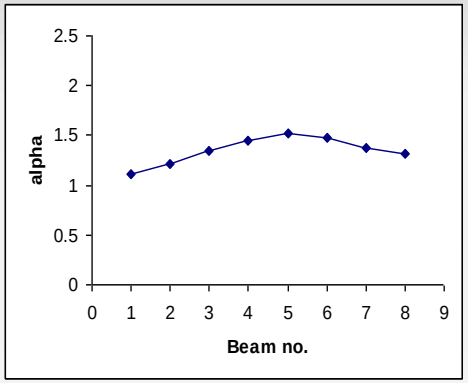	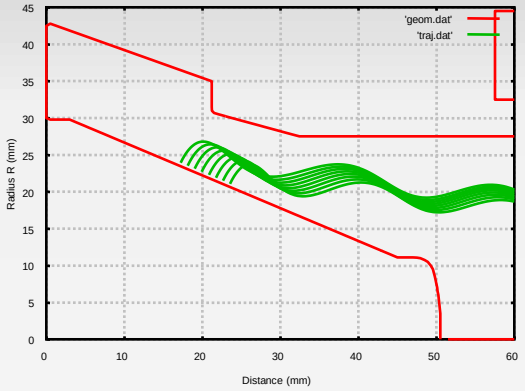
25^0	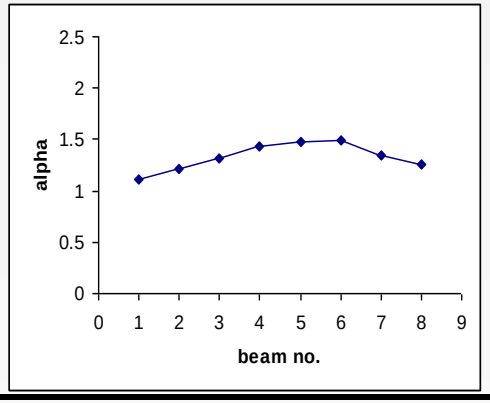	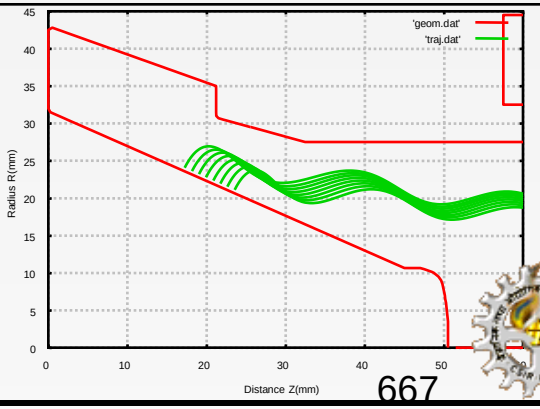

Beam parameters for different cathode angles

Cathode angle	Nature of alpha	Laminarity
26^0	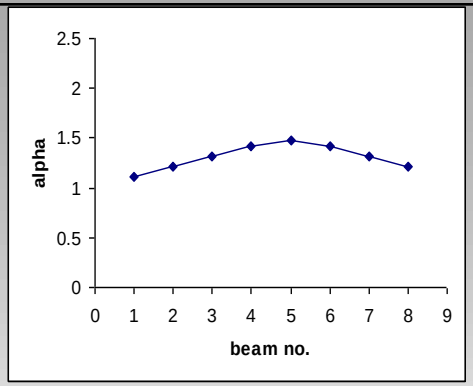	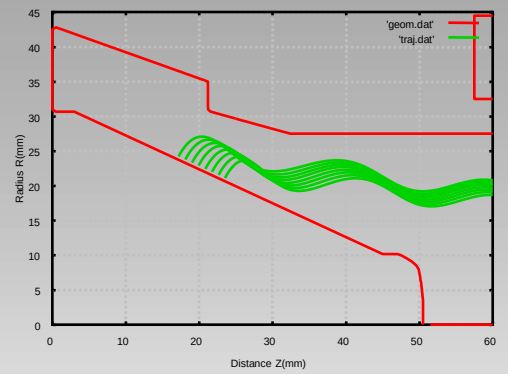
27^0	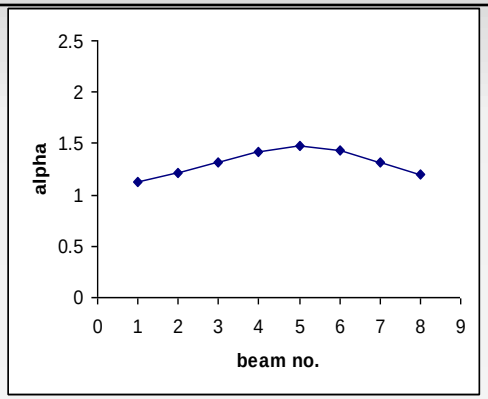	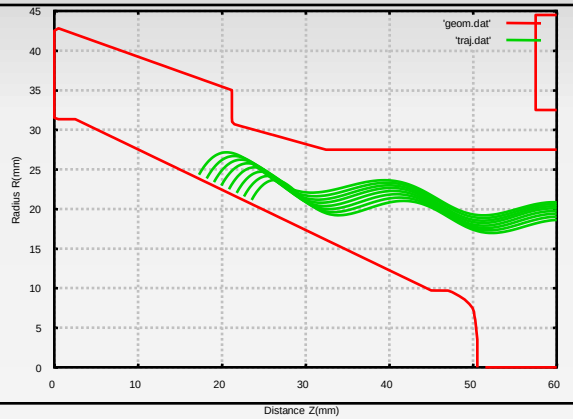
28^0	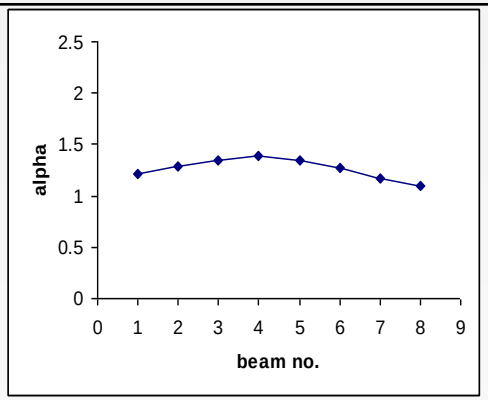	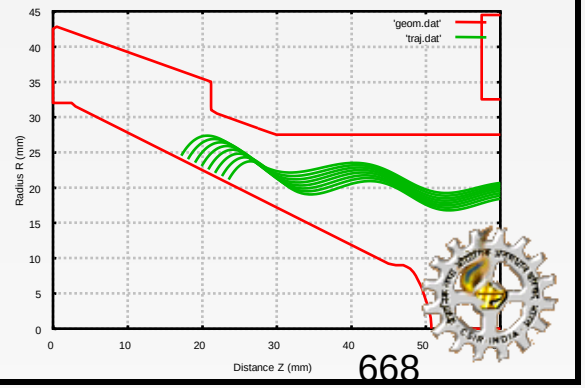

Beam parameters for different cathode angles

Cathode angle	Nature of alpha	Laminarity
29^0	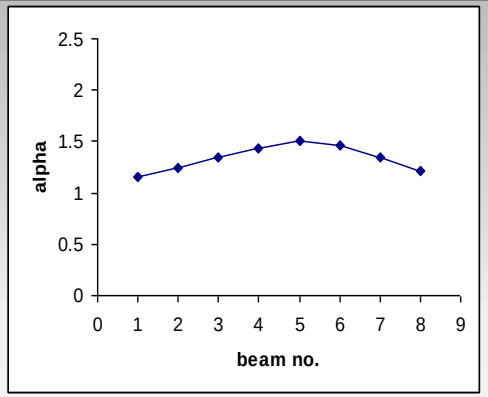	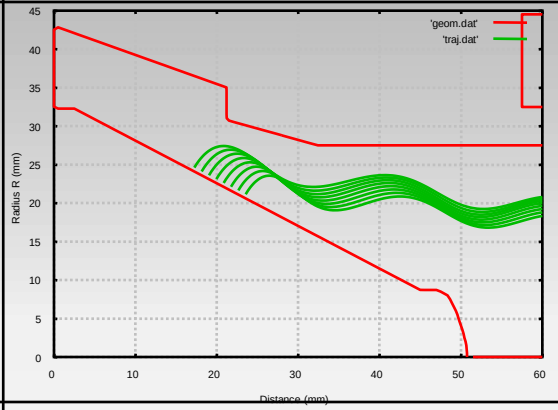
30^0	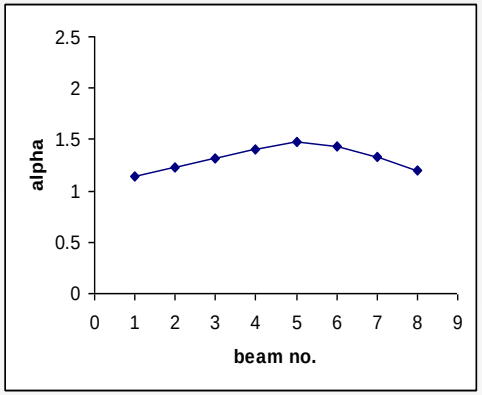	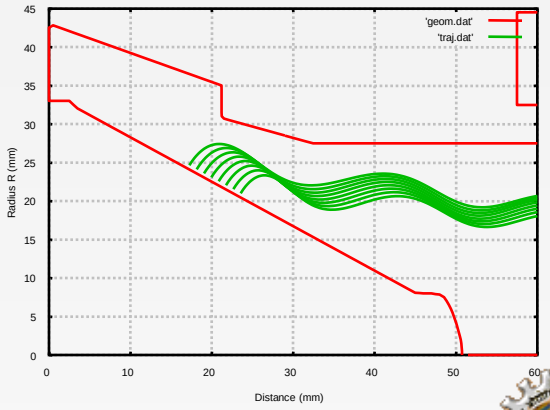

Potential Profile of MIG

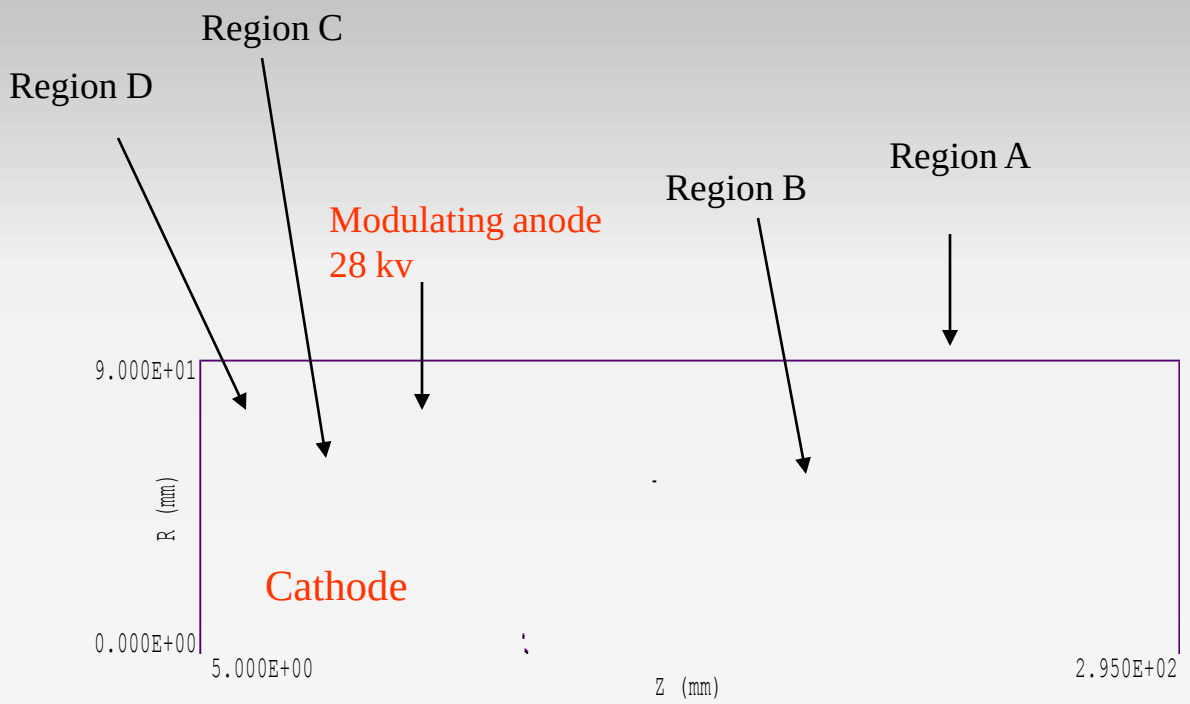

File prefix: gun1.EOU
Plot type: Contour
Quantity: Potential (V)

Minimum value: 0.000E+00
Maximum value: 6.494E+04

5.411E+03
1.082E+04
1.623E+04
2.165E+04
2.706E+04
3.247E+04
3.788E+04
4.329E+04
4.870E+04
5.411E+04
5.952E+04
6.494E+04

Controlled anode
65kv

Current view
window

Electric Field Profile

File prefix: gun1.EOU
Plot type: Contour
Quantity: |E|(V/m)

Minimum value: 0.000E+00
Maximum value: 1.545E+07

1.288E+06
2.575E+06
3.863E+06
5.151E+06
6.438E+06
7.726E+06
9.014E+06
1.030E+07
1.159E+07
1.288E+07
1.416E+07
1.545E+07

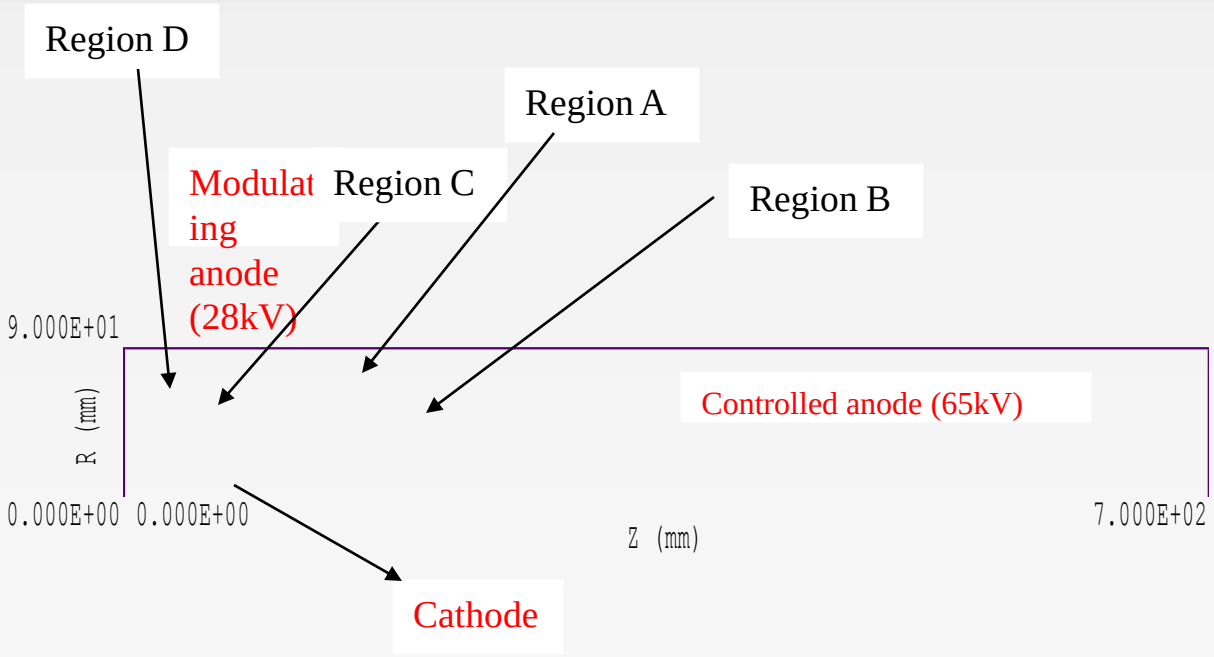

Current view window

Table: Performance parameters of MIG of 42 GHz Gyrotron
Software: TRAK

REGION No.	REGION A	REGION B	REGION C	REGION D
MEDIUM	**CERAMIC**	**AIR**	**AIR**	**AIR**
POTENTIAL (KV)	**30.28**	**48.22**	**9.04**	**11.88**
ENERGY (J)	**1.069×10^{-2}**	**1.267×10^{-3}**	**1.061×10^{-3}**	**7.824×10^{-4}**
ELECTRIC FIELD Kv/mm	**0.122**	**1.464**	**1.685**	**1.455**
CAPACITANCE (pf)	**15.61**	**1.85**	**1.55**	**1.14**

Strength: Major Simulated Tasks Completed for 42 GHz, 200 kW

at CEERI

Magnetron injection gun

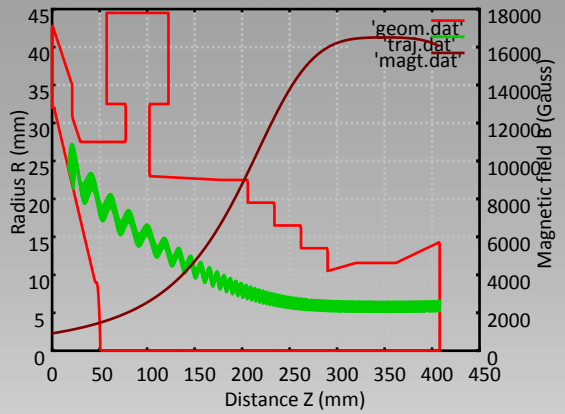

EGUN

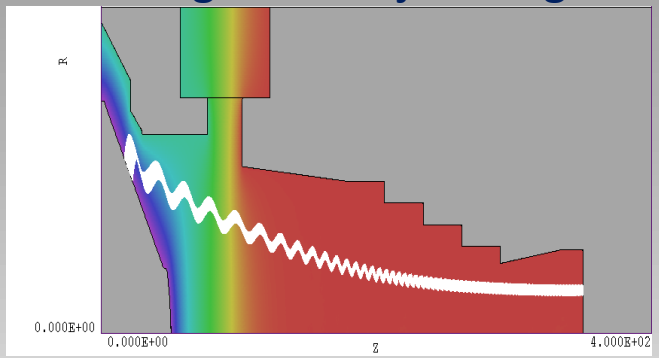

TRAK

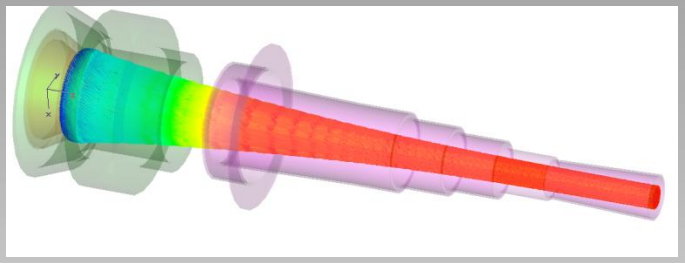

CST PS

Beam Tunnel (AlN-SiC)

Interaction cavity

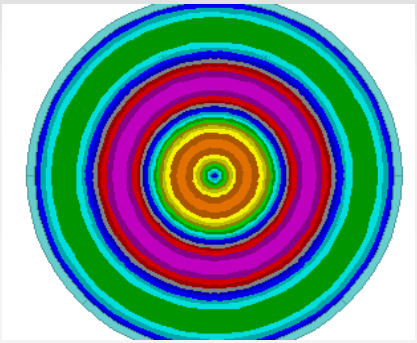

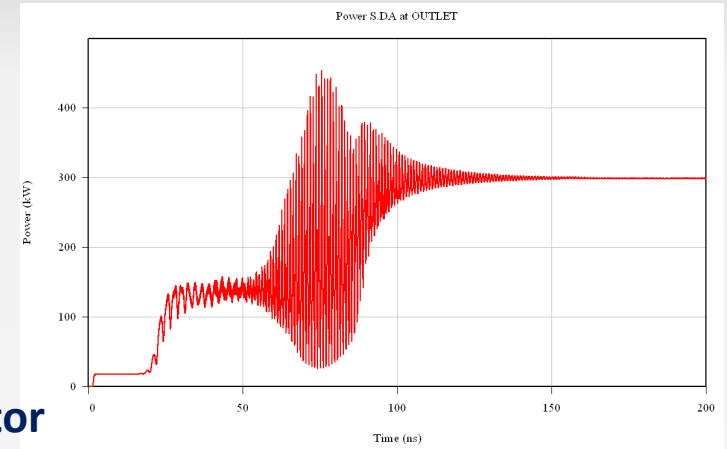

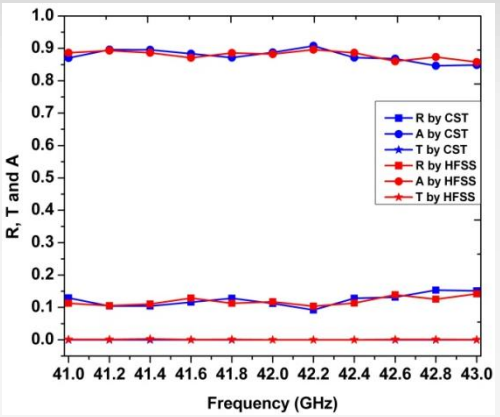

Electron beam collector

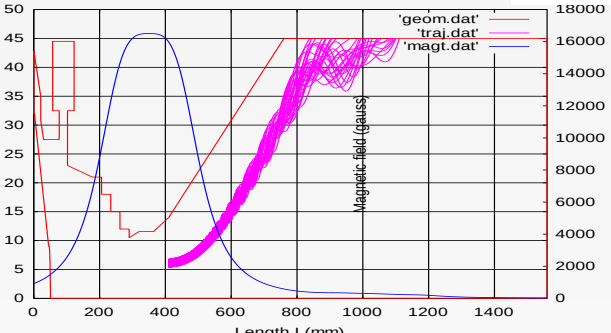

•Contribution of Student: 4-5/ year

Publications

- Invited Talk: 30
- Int/ Nat Journal -56
- Int./ National conf. – 70
- M.Tech -10
- Ph.D. Awarded – 5
- Conference Awards-06

Development of 42GHz, 200kW Gyrotron prototypes

2014

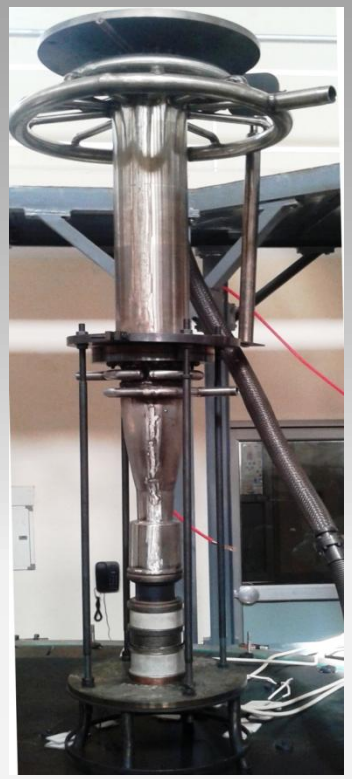

2015

Lab prototype

For confidence building

1st prototype

2nd prototype

❖ **Electrical designs are same**

Publications By CEERI

Total publications =126

International Journal Papers: 56

(Published outside India by reputed publishers)

- **IEEE Transactions: 7**
- **Springer: 19**
- **Elsevier: 10**
- **AIP(American Institute of Physics): 1**
- **Taylor & Francis: 2**
- **PIER: 2**
- **NRC Research Press: 1**
- **Frequentz: 4**

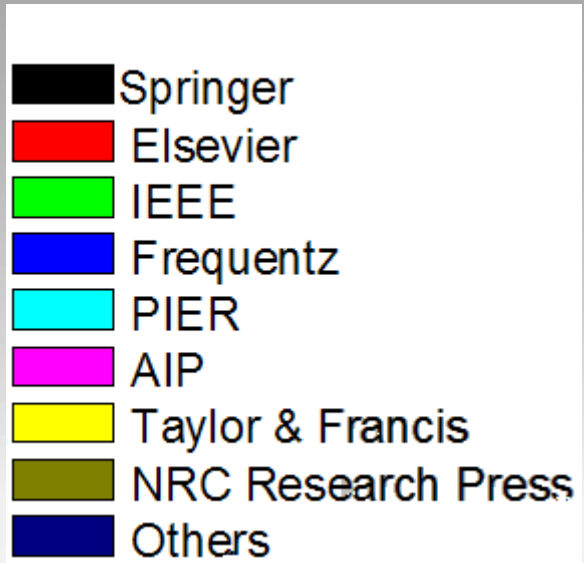

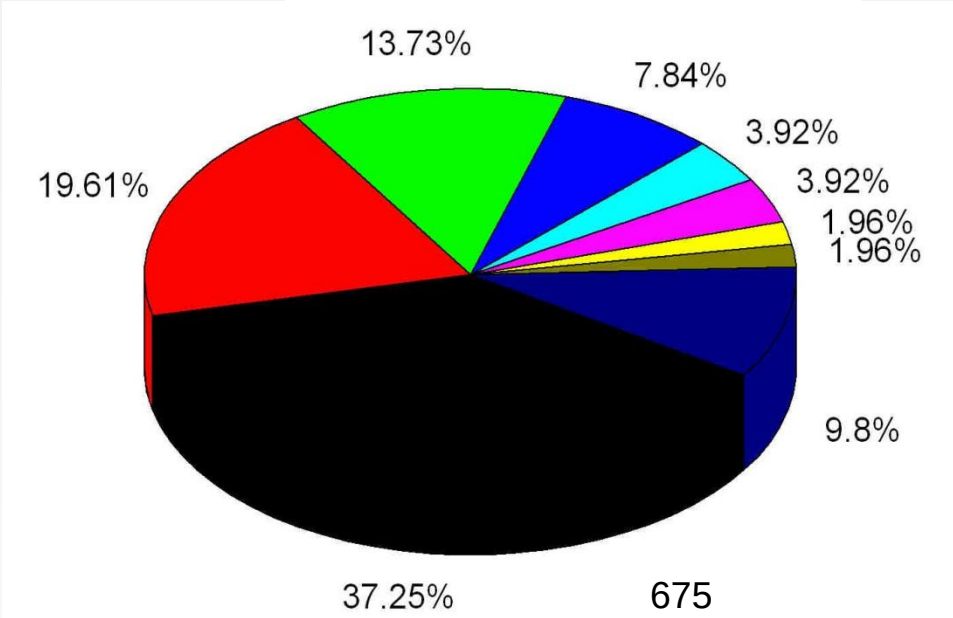

Scientific Temperament

Scientific temperament is a way of life - an individual and social process of thinking and acting - which uses a scientific method, which may include questioning, observing physical reality, testing, hypothesizing, analysing, and communicating (not necessarily in that order). Jawaharlal Nehru was one of the first people to use the term scientific temper and advocate the promotion of scientific temper.

"[What is needed] is the scientific approach, the adventurous and yet critical temper of science, the search for truth and new knowledge, the refusal to accept anything without testing and trial, the capacity to change previous conclusions in the face of new evidence, the reliance on observed fact and not on pre-conceived theory, the hard discipline of the mind—all this is necessary, not merely for the application of science but for life itself and the solution of its many problems." —Jawaharlal Nehru (1946) *The Discovery of India*, p. 512

The genesis and development of the idea of scientific temper is connected to ideas expressed earlier by Darwin when he said, "freedom of thought will best be promoted by that gradual enlightenment of human understanding which follows the progress of science ‑and by Marx Scientific temper describes an attitude which involves the application of logic. Discussion, argument and analysis are vital parts of scientific temper. Elements of fairness, equality and democracy are built into it.

"To develop scientific temper" is one of the fundamental duties of Indian citizens, according to the Constitution of India.

Ref: wikipedia.org/wiki/**Scientific_temper**

Writing is a Simple Practice

- Good writing doesn't happen overnight:
  - ***Planning***
  - ***Drafting***
  - ***Rereading***
  - ***Revisiting***
  - ***Editing***
- Learning and improvement requires:
  - ***self-review,***
  - ***peer-review,***
  - ***subject-matter***
  - ***expert feedback***
  - ***Practice***

Writing is a Practice

- There are ***no shortcuts***:

  practice makes perfect.

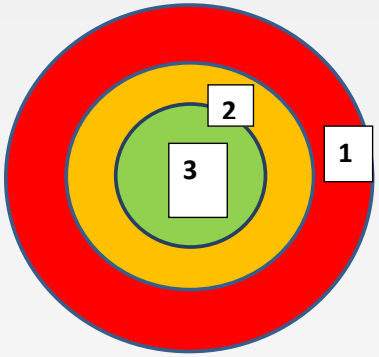

1: First Draft

2: Second Draft

3: Final Draft

Technical Writing: Steps

- Input:
  - Introduction
    - Background
      - Objective
        - Plan
- Process:
  - Theory
    - Model
      - Experiment
- Output/ Result:
  - Plot
    - Table
    - Discussion

Technical Writing: Steps

- **Others:**
  - Title
  - Authorship
  - Abstract
  - Conclusion
  - Acknowledgement
  - Reference

BASICS of Technical Writing

- Work with Belief
- Work with Target
- Work with Honesty
- Work with Discipline
- Work with Patience
- Work with Happiness
- Work within Time

BASICS of Technical Writing

- Grammar or No Grammar
- Language >> No Language
- Problem >> No Problem
- Solution >> No Solution

- Internet (Mentor/ Friend/ Critic/ Player) is there to help you.

- Have Belief and Move Forward.

- Reward (Publication/ Recognition) is Waiting for You.

Mentor is Must

SIMPDOT

" SIMpler Package for Delivery On Time "

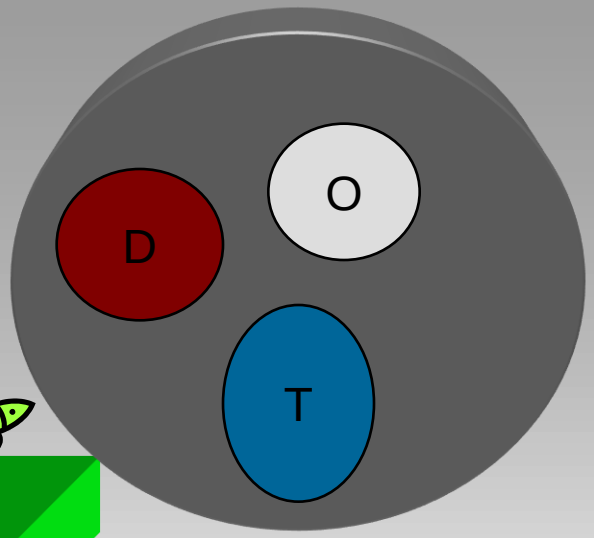

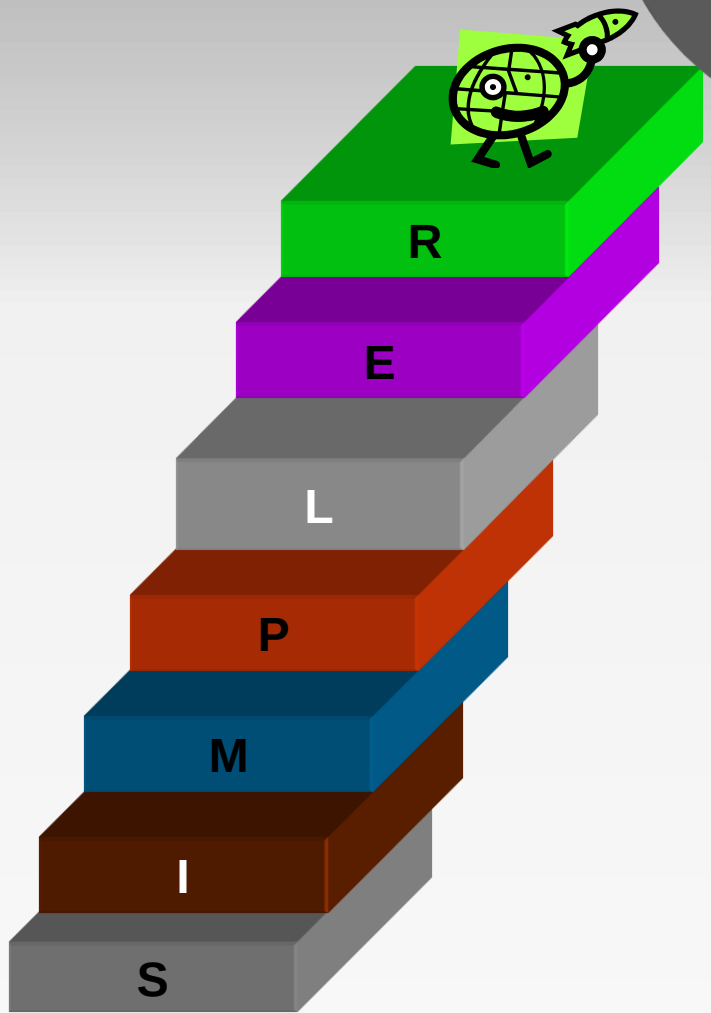

S – Self Belief

I – Interaction

M – Mentor

P – Problem Definition

L – Lovable environment

E- Execution

R - Result

HOPE

Times of india, October 21, 2014

Paralyzed man walks again after olfactory cell transplant, thanks to animal research

Today, almost 30 years after Prof. Geoffrey Raisman first identified their potential to repair nerve damage in mice, the BBC reports that olfactory ensheathing cell transplantation has been successfully used to enable Darek Fidyka, who was paralyzed from the chest down in a knife attack in 2010, to walk again.

The paper reporting the transplant, which was carried out by surgeons in Poland and led by Geoffrey Raisman of the UCL Institute of Neurology, is published today in the journal Cell Transplantation. The technique involves taking specialized cells known as olfactory ensheathing cells (OECs) from the patient's own patient's olfactory bulbs, and then grafting these cells at the site of injury, where they promote nerve cell growth to bridge the gap and restore function. An added advantage in using the patient's own cells is that it avoids the problem of rejection by their immune system

HOPE

Speaking earlier today Geoffrey Raisman described the results as

"MORE IMPRESSIVE THAN MAN WALKING ON THE MOON".

He's not to far wrong, this achievement shows what is possible for regenerative medicine, and is the result of decades of basic and translational research. Indeed, whereas only 12 people have walked on the moon, this new technique has the potential to help many thousands of people to walk again here on earth.

Darek Fidyka learns to walk again following OEC transplantation. Image BBC News.

HOPE

TIMES OF INDIA, 15 Jan, 2015

- 'No under—80 cancer deaths in UK by 2050'
- Charlier Cooper, The Independent, | Jan 15, 2015, 05.01AM IST

Deaths from cancer will be "eliminated" for all age groups except the over 80s by 2050, if recent gains in prevention and treatment carry on apace, experts have said.

Researchers from the University College, London (UCL) and the King's College London said that the UK was at a "special point in history" and could set a bold ambition to eradicate cancer—related mortality in people aged under 80 "during the course of the coming 20 to 30 years".

Falling smoking rates, speedier diagnosis and better radiological, surgical and drug treatments %have led to a 1% decline in cancer death rates every year since 1990, they said — a trend which would likely gather pace. However, the %researchers said investment in cancer care would have to increase and criticized decisions to ration innovative treatments.

Some Research Topic

- Details of Hope Topic
- Simulation
- Mobile Component
- Microwave Device
- New Application of MW Tube
- Wireless Communication
- Healthy Water
- Sewage Treatment
- Solar Power
- Embedded System
- Smart Office
- Smart House
- Smart City
- Smart Agriculture

NETWORKING

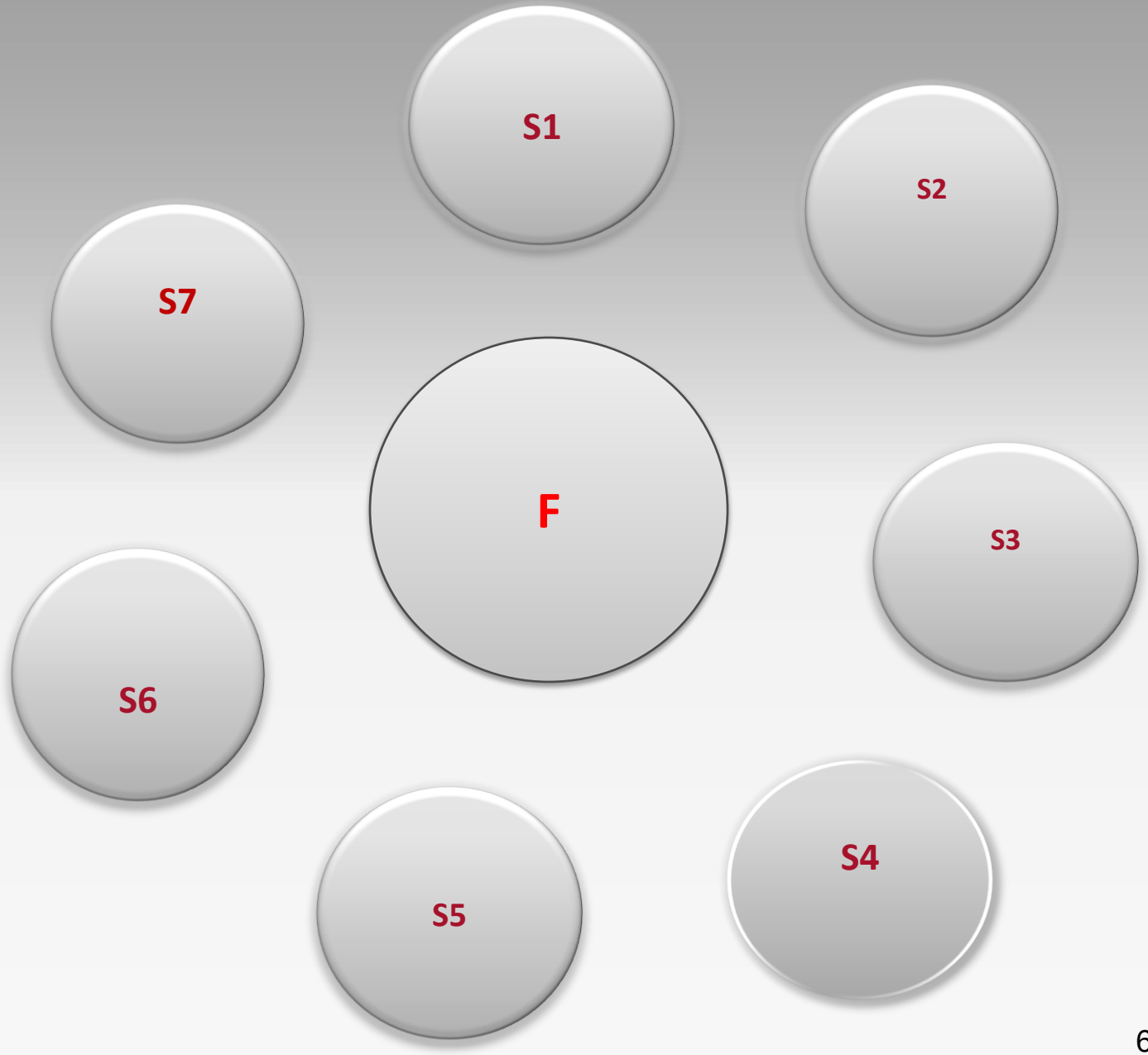

ThanKS

High Power Microwaves Sources

Dr. S. Umamaheswara Reddy

Director
Microwave Tube Research & Development Centre,
Bharat Electronics Complex, Bangalore

Introduction to HPM

Electro Magnetic Pulse (EMP):

- It is a Short Burst of Electromagnetic Energy
- At high energy levels EMP can cause damage to electronic equipment

Types of EMP:

- Natural :
  - like lightning
- Man made
  - Nuclear(NEMP) : lethal
  - High Altitude Nuclear(HEMP): Lethal
  - Non-Nuclear(NNEMP): Non-lethal

NEMP:

- NEMP is the abrupt pulse of electromagnetic radiation resulting from a nuclear explosion. The resulting rapidly changing electric fields and magnetic fields may couple with electrical/electronic systems to produce damaging current and voltage surges. Nuclear explosion produces gamma-rays which in-turn result in generation of EMP.

Detonated at an altitude of up to 30 km. Damage by explosion and radiation

HEMP:

-A nuclear warhead detonated hundreds of kilometres(500-600 km) above the Earth's surface is known as a high-altitude electromagnetic pulse (HEMP) device. Typically the HEMP device produces the EMP as its primary damage mechanism.

The energy produced travels much larger distance compared to NEMP.

(useful as anti ballistic missile, anti satellite weapon. Only US and Russia conducted such tests)

NNEMP:

-Non-nuclear electromagnetic pulse (NNEMP) is weapon-generated electromagnetic pulse without use of nuclear technology.

- Devices that can achieve this:
  - low-inductance capacitor bank discharged into a single-loop antenna,
  - a microwave generator
  - explosively pumped flux compression generator.

Systems that can produce High Power Microwave(HPM) can be classified as non-lethal weapons.

They fall under the category of Directed Energy Weapons

Need for Nonlethal Weapons

Evolution of Conventional Weapons:

Swords → Riffles → Rockets/Bombs → Missiles → Nuclear Weapons

* Lethality of weapons is increasing & Reached a stage where it can wipeout human-race & the Planet itself.
* Hence awareness increased to realize nonlethal weapons

Examples Of nonlethal Weapons:

* Tear Gas
* Plastic Bullets
* High-power Microwaves(HPM)
* Low Energy Lasers
* Acoustic Weapons etc.

Properties of Nonlethal Weapons

* Conserve Life
* Environmental Friendly
* Cost Effective

Directed Energy of weapons :

Generates High Energy through beam of concentrated EM energy or atomic or subatomic particles which will be focused on to the targets to defeat/destroy its functioning.

US DoD Explains the Directed Energy weapon as:

DE weapon is a system using DE primarily as a direct means to damage or destroy adversary equipment, facilities, and personnel. DE warfare is military action involving the use of DE weapons, devices, and countermeasures to either cause direct damage or destruction of adversary equipment, facilities, and personnel, or to determine, exploit, reduce, or prevent hostile use of the EMS through damage, destruction, and disruption.

Types of Directed Energy Weapons :

- High Energy Lasers(HEL)
- High Power Microwaves(HPM)
- Ultra Wide-band DEW

High Energy Lasers

Advantages compared to Conventional weapons:

* Attack with speed of light
  - Very difficult for targets to escape once attacked by laser weapon
  - no need to account for target movement unless attack on target is at long distance

    Example: we want to attack a cruise missile at say 100 km away.

    Laser takes 300 microsecond to reach the target.

    Cruise missile travels at speed of 1 km/sec (Typical) –MACH 3

    In 300 Micro seconds missile travels by 6 mm only.
* Limitless ammunition
* can be fired off-axis without moving the position of laser source(Steering is possible)
* No recoil (Ratio of momentum to energy is zero)
* As it produces no sound, users position is not revealed.
* Laser is not effected by gravity. Hence no trajectory compensation required.
* Focussing configuration can be changed to attack multiple targets.

Disadvantages:

* operation in line of sight
* Does not have all weather capability
  - If target exposure require longer time the speed of target, the wind speed comes into picture.
* Inflicts collateral damage to humans
* Attacks one target at a time

Definition of High Power Microwaves

Typical Parameter Range:

Frequency	: 0.1-200 GHz
Peak Power	: >100 M watts
Duty	: 0.001%-0.0001%
Pulse Width	: 30-100 n secs.
PRF	: Single Shot – 200 Hz
Pulse Energy	: > 1KJ

Applications of HPM:

- Enhanced/New Radars
- **Directed Energy Weapons**
- Mine Detection & clearing
- Riot control (Active Denial Systems)
- Power Beaming & **Pollution Control**
- Plasma Heating, Accelerators
- Materials Processing

Features of Directed Energy of weapons :

Delivers energy to target with speed of light

Types of Directed Energy Weapons :

Electromagnetic Pulse (EMP)

High Energy Lasers(HEL)

High Power Microwaves(HPM)

ADVANTAGES :

- Attacks electronic systems only
- Minimum collateral damage
- Speed-of-light
- All-weather Capability
- Area Weapon : Simplified pointing and tracking
- Requires Minimal Information Victim's Characteristics
- Graduated Effect: Deny, Disrupt, Degrade or Destroy
- Low Operating Cost , Unlimited Magazine

Disadvantages

Countermeasures

Danger of Fratricide or Suicide

Difficult Damage Assessment

New Technology yet to mature

Applications of DEW

Defensive Applications

NAVY

- Fleet defense
- Surveillance of Coastal Waters

ARMY:

- Ballistic missile (BM) and surface-to-air missile defense
- Counter-artillery and rockets
- Protection of armored vehicles
- Neutralization of explosive traps and minefield cleaning
- Critical infrastructure protection
- Stopping of Motor Vehicles

AIR FORCE:

- Air defense
- Counter-electronics against targeting and sensor systems
- Aircraft self-protection

Offensive Applications:

- Attack against ground, air and maritime targets
- Electronic suppression and disablement of C^4I
- Suppression of Enemy Air Defence (SEAD)
- Suppressing or damaging visible, IR & MW sensors
- Asymmetric strikes
- Dispersion of crowds, rioters (non-lethal attacks)
- Speedboat pursuit
- Space control and anti-satellite operations

RF-Effects Definitions

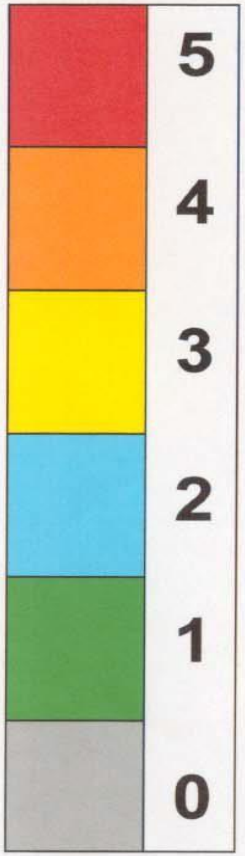

5	Damage	- Requires hardware, software, or firmware replacement
4	Upset	- Requires external intervention
3	Disturbance	- Effect present after illumination but eventually recovers
2	Interference	- Effect present only when illuminated
1	No Effect	
0	Unknown/Not Observed	

3

How HPM /DEW Effects on Electronic Systems

* Modern Electronic Systems use large number of semiconductor devices
- Once coupled into the system HPM signals generate RF/thermal effects in semiconductors
- Depending on the power level, Pulse width and PRF – different types of failures occur
  : Malfunction of the device to meltdown of the device
- HPM signal of a single pulse width less than 100 nsecs. and very high peek powers can raise the temperature of the Junction to above 600-800 degree centigrade, resulting in malfunctioning of the device.
- If there are more pulses and the gap between pulses is sufficiently large, so called thermal stacking(accumulation of energy) occurs and the heat starts to transferring from Junction to bulk of the device, even if power levels are not very high.

*PRF of about 1 KHz thermal equilibrium occurs.

HPM source Characteristics & the effect on electronics and consequences are tabulated:

Failure Mode	Power Required	Wave shape	Recovery process	Recovery time	Example
Disturb	medium	Single or Repetitive pulse	Self -recovery	Seconds	Screen of a PC
Upset	High	Short pulse, Single or repetitive	Operator intervention	Minutes	Clock of a PC
Damage	Very High	Short pulse, Single or repetitive	Maintenance	Days	Power supply of PC

Note: The actual power levels, Pulse width & PRF required depends on the enemy system We are targeting, range at which we want HPM to work, Coupling mechanism and any hardening done on enemy System.

How HPM DEW Effects Systems

•**Dielectric Heating** **High Voltage /Current Transients** **High Voltage Breakdown**

HPM Coupling to Systems

Front Door Coupling - Through Antenna, Sensor

Back Door Coupling - Power Lines, Connector cables,Windows grills, holes, Display screens

Back Door Coupling occurs when the electromagnetic field from a weapon produces large transient currents (spikes) or electrical standing waves (when produced by a HPM weapon) on fixed electrical wiring and cables interconnecting equipment, or providing connections to mains power or the telephone network

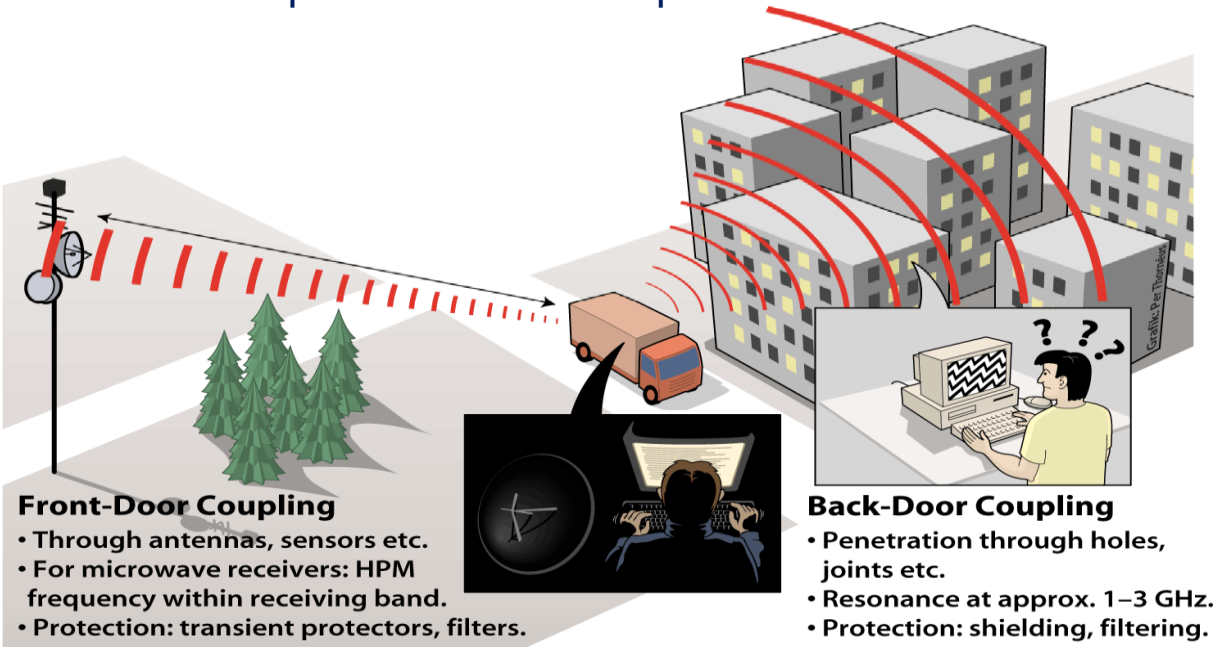

Access Possibilities for HPM

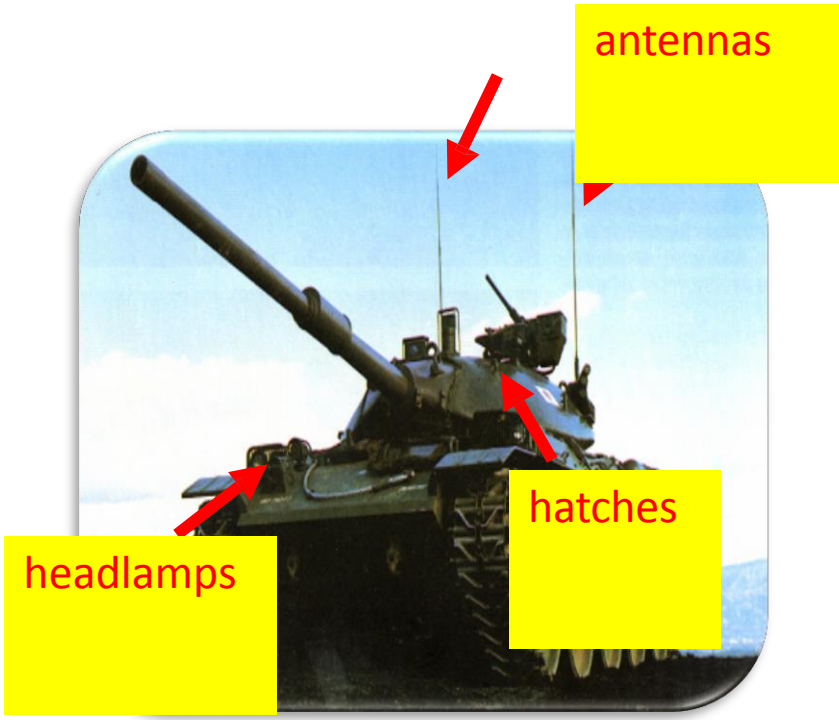

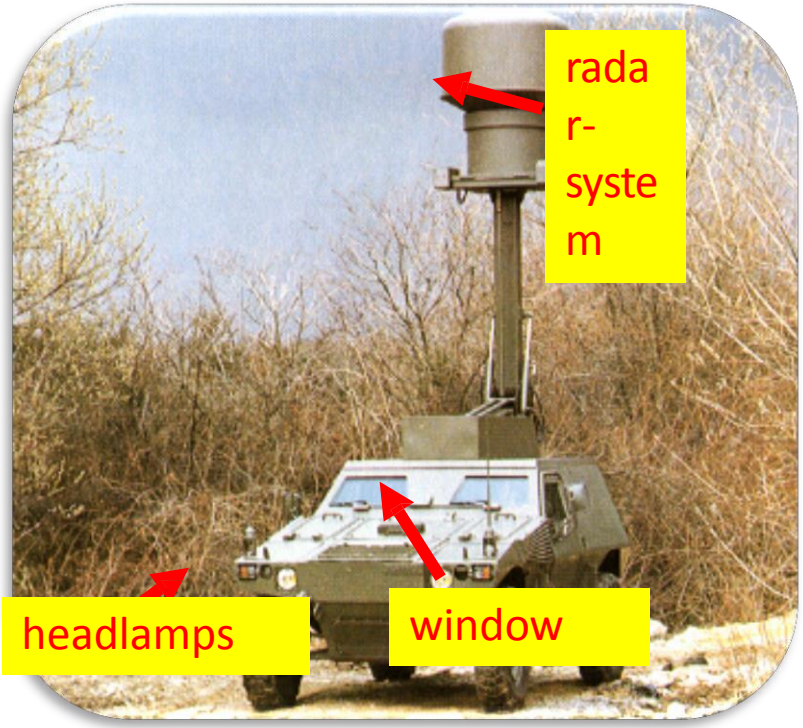

Some HPM systems that are Described in literature:

Laser DEW weapons developed by Lockheed Martin

A prototype turret developed by Lockheed Martin for the Defense Advanced Research Projects Agency and the Air Force Research Laboratory controls and compensates for air flow, paving the way for laser weapon systems on tactical aircraft. Here, a green low- power laser beam passes through the turret on a research aircraft. (Photo: Air Force Research Laboratory.)

In testing earlier this month, the Lockheed Martin laser produced a single beam of 58 kW, representing a world record for a laser of this type. The Lockheed Martin team met all contractual deliverables for the laser system and is preparing to ship it to the US Army Space and Missile Defense Command/Army Forces Strategic Command in Huntsville, Ala.

Ground Based HPM system

SHF(3-30 GHz) weapon developed by Russia

*This weapon was unveiled in the classified area of Army2015 expo, an international military forum of Russia

- It's designed to knock out aircraft, drones, guided missiles and any airborne high precision weapons using electronics.
- It creates an air-exclusion zone within a reported radius of over 10 kilometers around the defended object or installation(360 degree coverage)
- This system puts close range air defence on a whole new level.

This mobile System performs off-frequency rejection of electronics aboard low-altitude aerial targets and warheads of high precision weapons,"

Can also be used to test electronic systems of military equipment for resistance to high-power microwave radiation."

The new system is equipped with a high-power relativistic generator and reflector antenna, management and control system, and a transmission system

Anti - UAV HPM DEW system Developed by Raytheon- USA

Shooting down of drones bY narrowband HPM system

Shooting down of drones by narrowband HPM system

High Energy Laser(HEL) DEW developed by Bay systems for Navy

Shooting down of UAVs by High Energy Laser (HEL) DEW system

Raytheon

HPM for Air borne platforms

excerpt from http://www.wnd.com/2012/10/it-works-computers-fried-by-emp-like-blast/ October 25, 2012

Counter – electronics High-powered Microwave Advanced Missile Project(CHAMP), which was just tested over Utah desert.

A pre-programmed cruise missile has been proven to be capable of blasting out an EMP-type microwave that was able to destroy personal computers and electrical systems inside a building over which it was flying.

The cruise missile is equipped with a powerful magnetron that produces a Giga-watt level pulse of microwave radiation.

Experiments done by :Boeing's Phantom Works team and the U.S. Air Force Research Laboratory Directed Energy Directorate (Tested over Utah desert)

Animated video showing CHAMP capability

HPM System Developed by BAE for Navy

At the Surface Navy Association's (SNA) 2018 National Symposium held near Washington DC, BAE Systems was showcasing for the first time its High Powered Microwave. This new concept developed by BAE Systems uses radio frequency to defeat enemy targets. The company already conducted some testing (in a non maritime environment) to demonstrate it ability to defeat a wide range of threats.

HPM System – Non lethal Small vassal stopping developed for US Navy

Narrow band HPM system for stopping vehicles

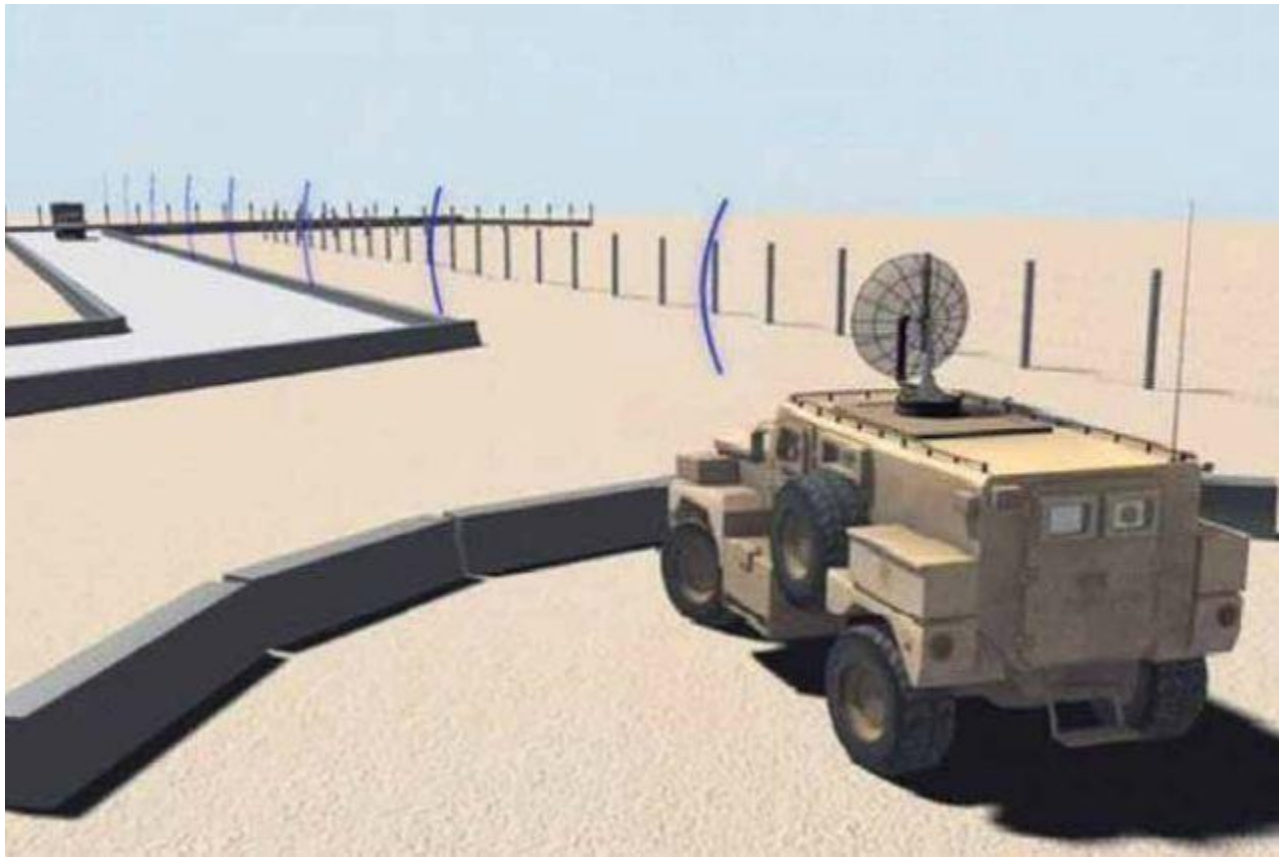

VIGILINT EAGLE AIRPORT SECURITY SYSTEM
(RAYTHEON)

Aircraft Protection against Shoulder fired Missilies (MANPAD)

- Distributed MWS
- HPM Tx
- ESA : 1° Beam width
- Command & Control

- Radiates a Tailored Pulse
- Spoofes or
- Damages Targeting System

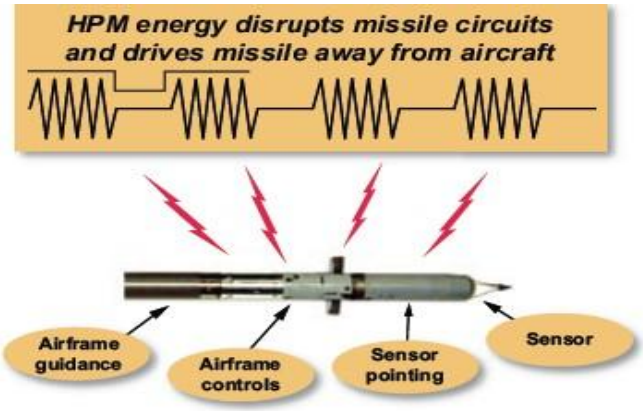

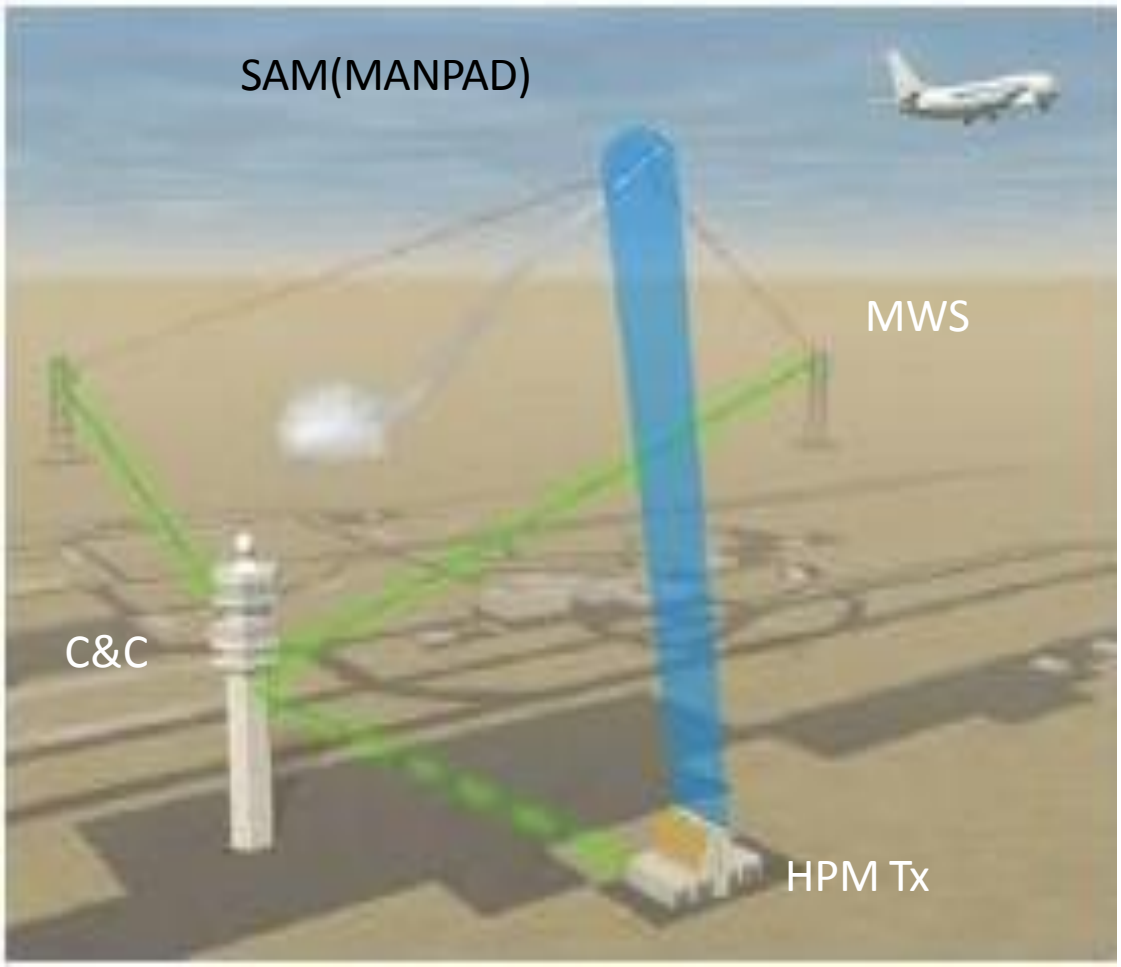

Active Denial System (ADS): Pain Ray for crowd Dispersal
Developed by Raytheon USA

"Active Denial": The Power of Persuasion

- "Active Denial" is a nonlethal weapon program designed to provide an option "between shouting and shooting".

System 1

Systems 1 & 2

Active Denial System (ADS)

Flushing out Terrorists/ Criminals

Stopping of Vehicles

Law Enforcement

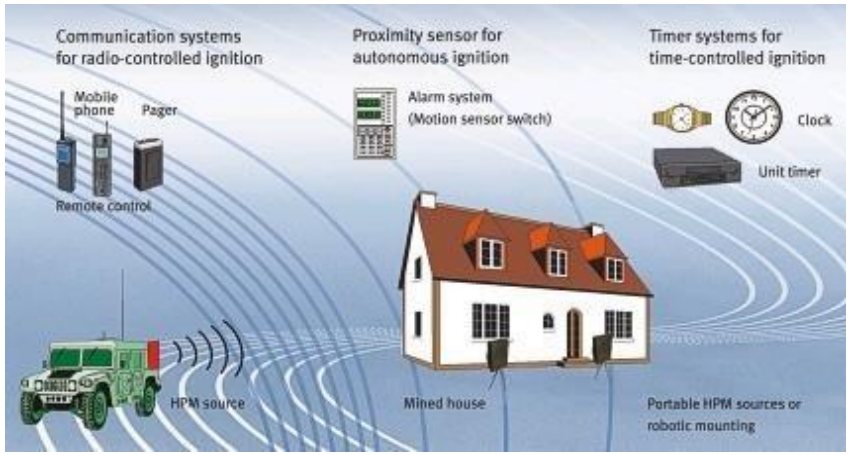

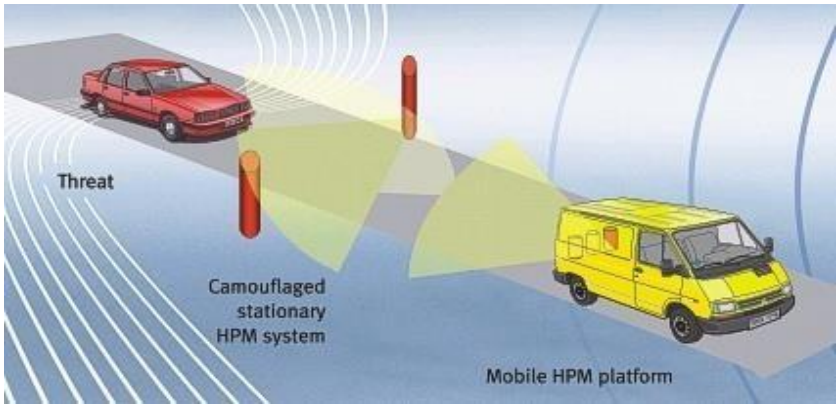

Infliction of Pain –intolerable in 5sec

(94 GHz Gyrotron) Range >750 m

Military

Vehicle-mounted Active Denial System (V-M

ADS is a safest counter personnel non lethal weapon

Moving Platform

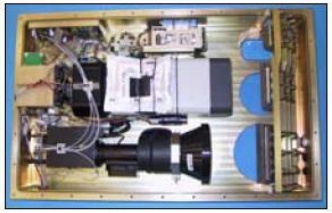

Sensors

Sevo controlled video camera FLIR
Low Light Camera
Laser Rangefinder

Operator Display
Joystick Control
Computer

ADS Complies with International Laws of Armed Conflict

Diesel Engine

High Voltage Power Conditioning

Gyrotron

Antenna System

Heat

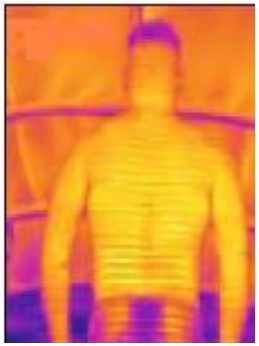

Working Principle:

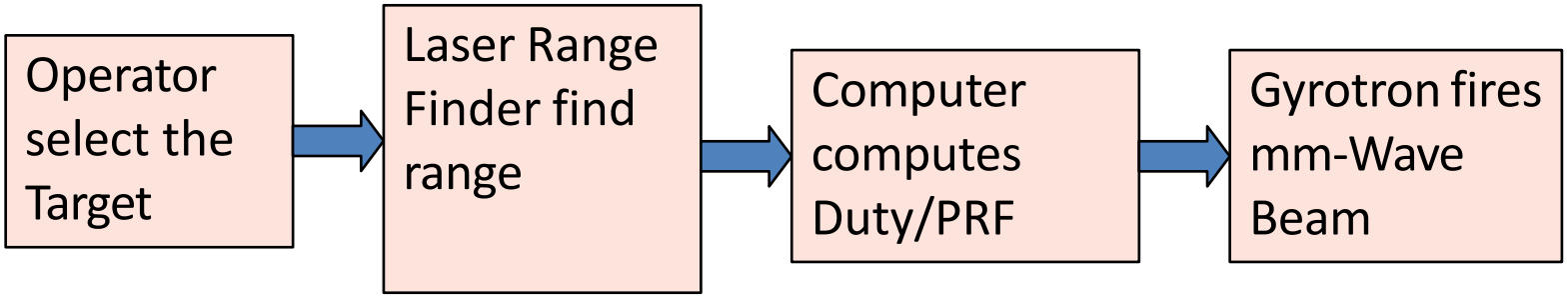

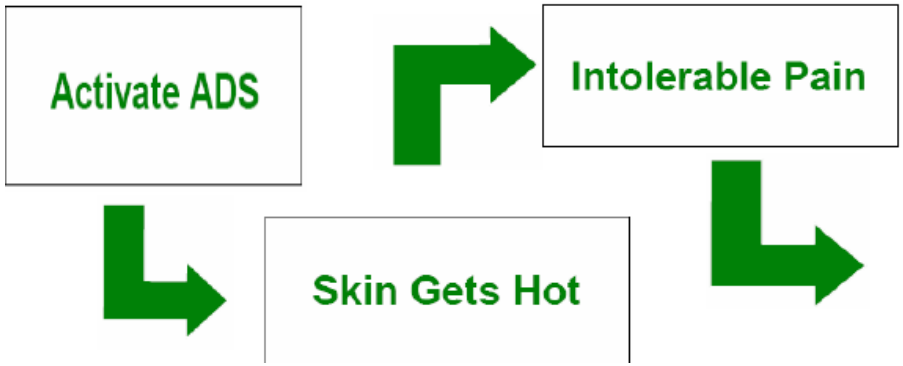

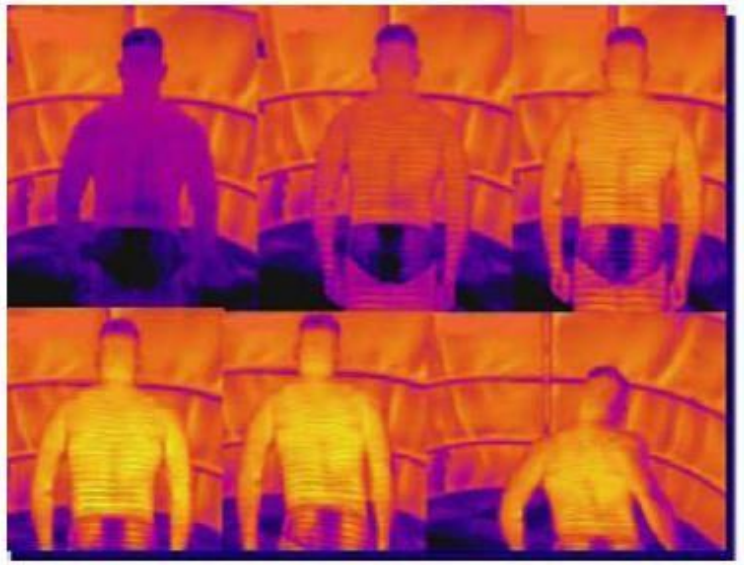

Reason for choosing 95 GHz

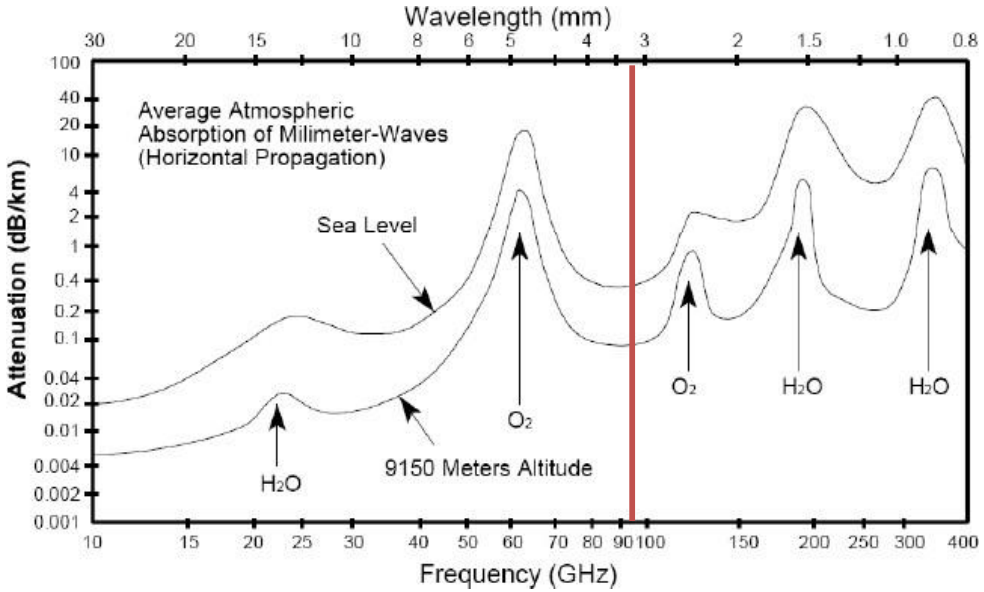

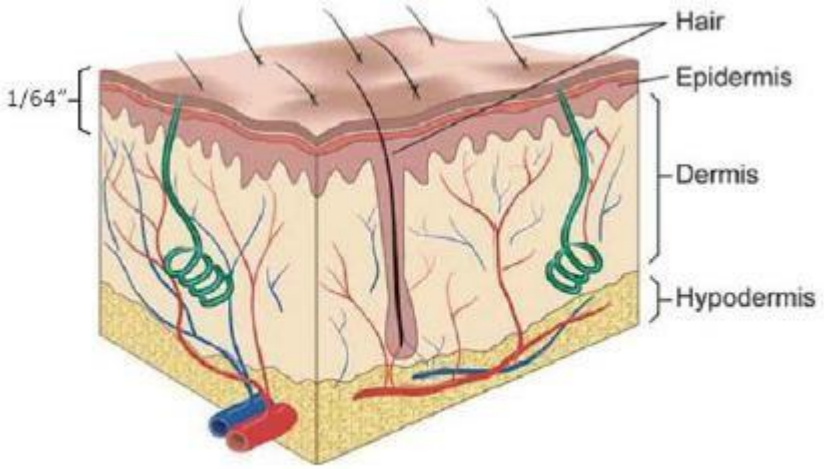

Penetrates 1/64th of an inch

At 95 GHz, skin penetration is 0.4 mm. Causes Burning sensation without permanent damage

Indian Scenario

Directed Energy Weapons

Laser DEW

CHESS

HPM - DEW

UWB DEW

RCI

Large Truck Mounted
HPRF/M Source

Electrically Driven

MTRDC

Explosively Driven

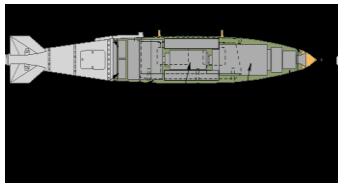

TBRL
MTRDC

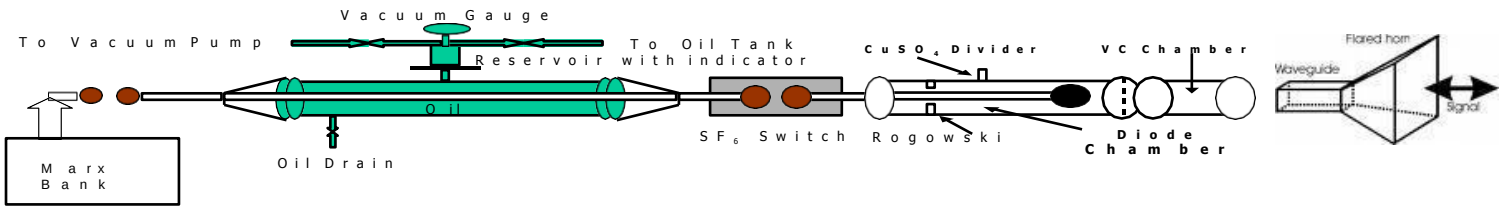

Pulse Power Source

Pulse Forming Line

High Speed Switching

HPM Devices

Radiating System

Work Done by MTRDC

Typical Block diagram of HPM SYSTEM

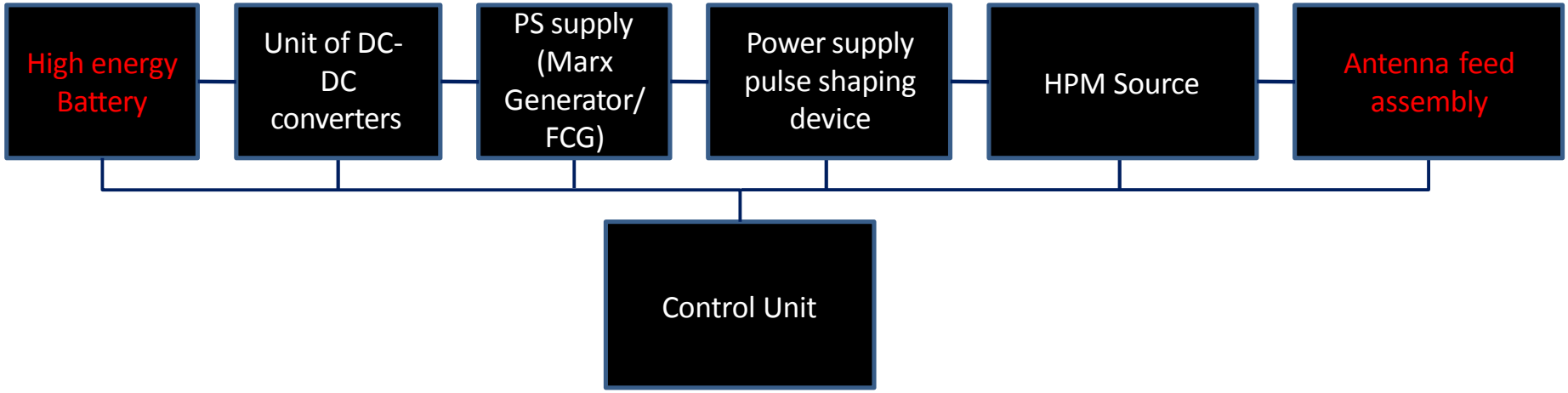

EXAMPLES OF HPM Sources

Conventional Sources	**:**	**Magnetron, Klystron**
Relativistic Electron Beam Devices	**:**	**Relativistic Magnetron, Relativistic Klystron**
		Relativistic BWO, FEL, CARM
Gyro-Devices	**:**	**Gyrotron, Gyro-Klystron, Gyro-BWO**
Slow-Wave Devices	**:**	**VIRCATOR, MILO**

Comparison of various HPM Sources

Parameter	Vircator	MILO	Reltron	Relativ. Magnetron	Relativ. BWO	Gyro-Devices
Frequecy	Upto X-band	Upto X-band	Upto X-band	Upto X-band	Upto X-band	mm- and sub-mm
Efficiency	1-5 %	10-20 %	30-40 %	20-30 %	30-40 %	30-40%
External Magnetic field	No	No	No	Yes	yes	yes
Size	Compact	Compact	Compact	Heavy	Heavy	Heavy
O/P power	> 1 GW	> 2 GW	< 500 MW	> 1GW	> 1 GW	> 1 GW
Construction Complexity	Simple	Simple	Complex	Complex	Complex	Complex
Spectral Purity	Poor	Good	Good	Good	Good	Good

Types of HPM Sources

Device Type	Features	
Vircator	Compact, Simple , No external magnetic Field Low Efficiency(1-5 %)	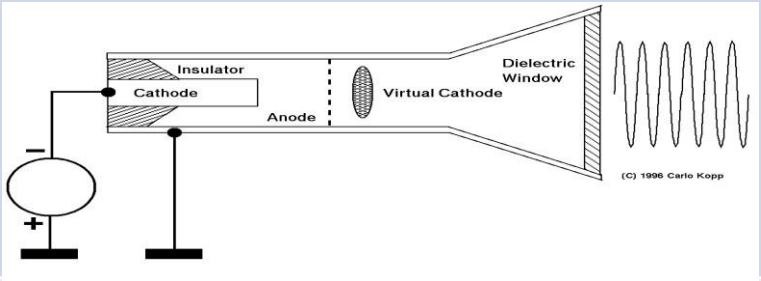
Relativistic Magnetron	Requires External Magnetic field High Efficiency (30 -40%))	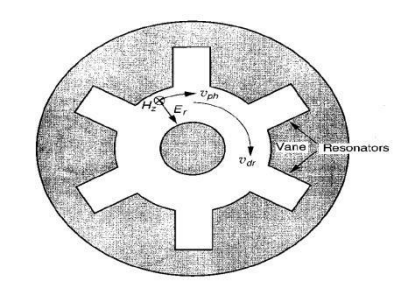
BWO	Requires External Magnetic Field High Efficiency(25-30%)	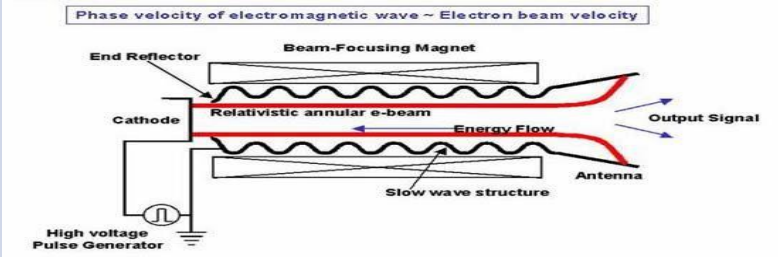

Advanced vircator integrated with KALI-200

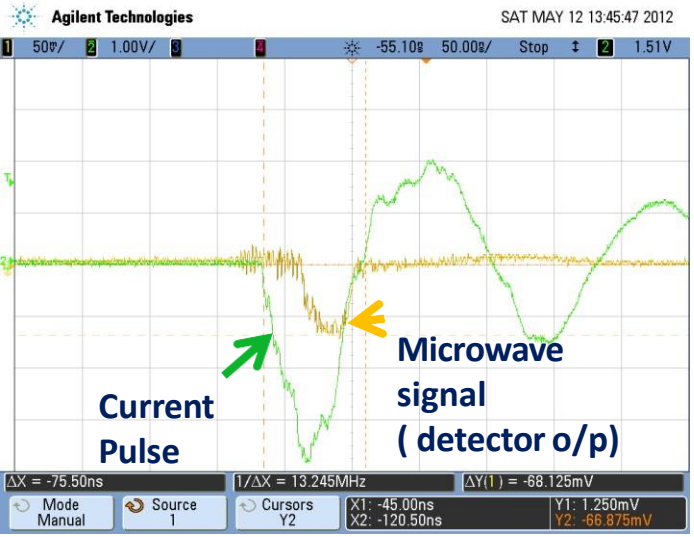

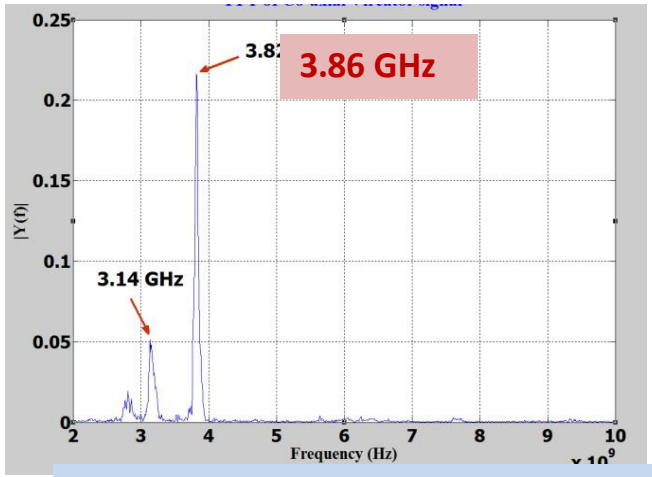

FFT of co-axial vircator signal

Parameters	Experimental
Power	180 MW
Frequency	3.86 GHz
Voltage	260 kV
Current	7 kA

Development of Relativistic Magnetron

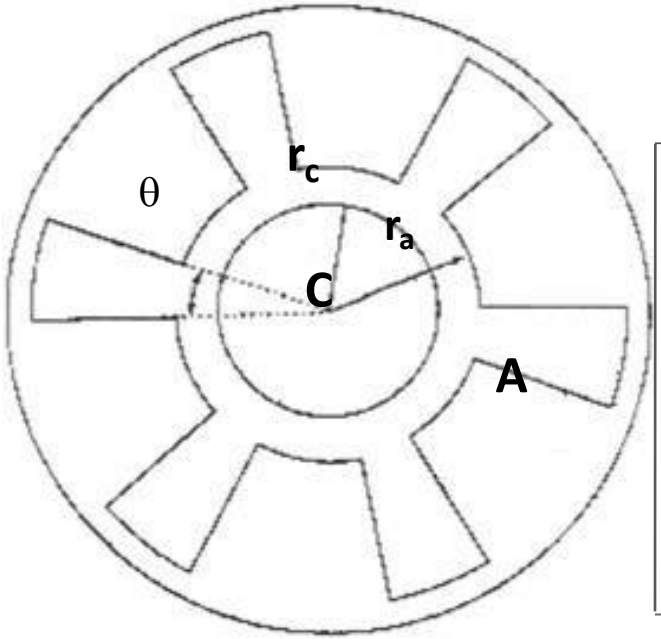

PIC simulation

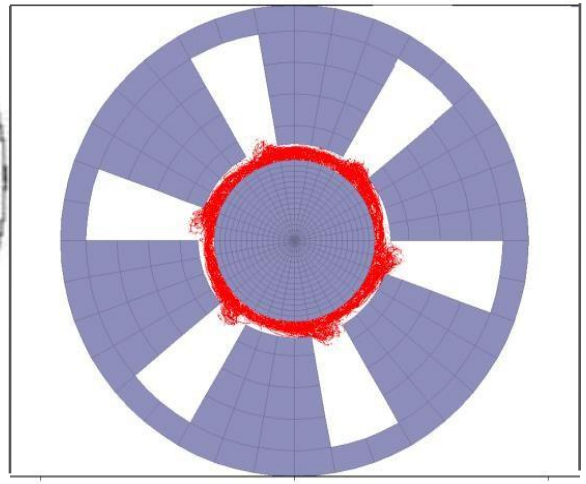

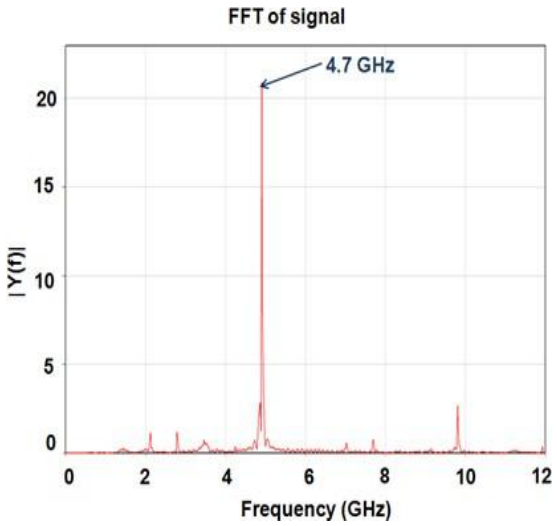

.	Parameter	Dimensions
1	Cathode radius (r_c)	1.58 cm
2	Anode radius (r_a)	2.11 cm
3	Vane radius	4.11 cm
4	Resonator length	7.20 cm
5	Vane angle (θ)	20°
6	No. of vanes	6

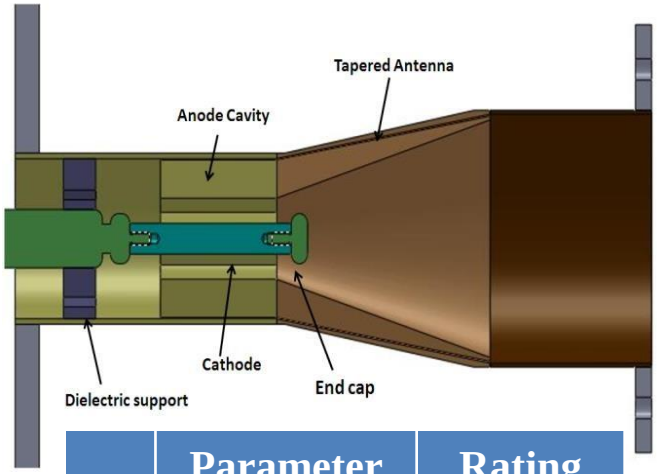

	Parameter	Rating
1.	P_{out}	~ 120MW
2.	frequency	4.6 GHz

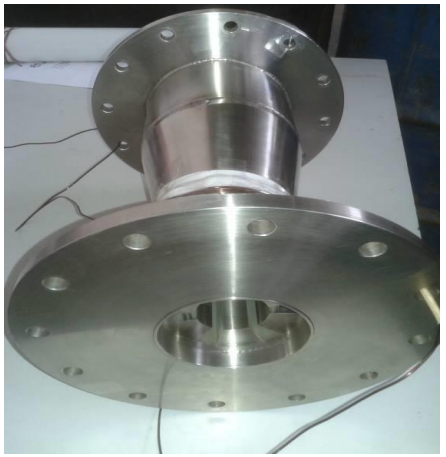

Some other Hard ware developed/available at MTRDC

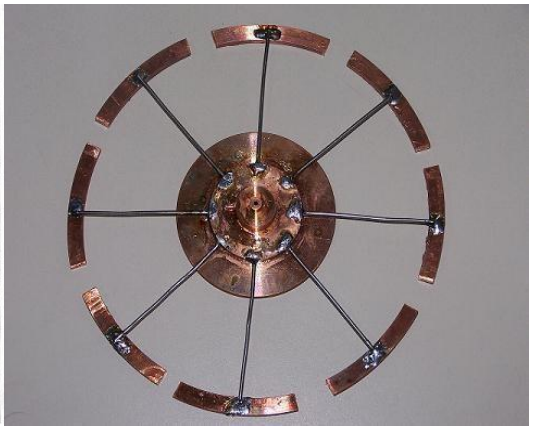

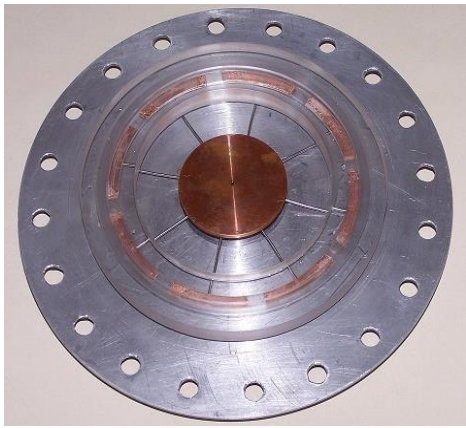

Rel. Magnetron parts

Mode Launcher Parts

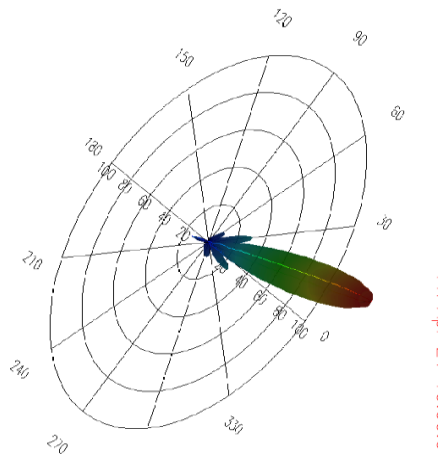

Diagnostic Components

Antenna, ts field pattern used for vulnerability

Development of 500 kV,10 KA 100 Hz Marx generator

Specifications:

Marx Voltage: 500 kV
Current : 10 kA
Pulse Width : 30 n Secs
PRF : 100 Hz

Marx Enclosure

- Dimensions: 2.5mX1.25mX1.25m
- Houses HV Protection circuit also
- Gas purging system to be attached externally
- Transformer Oil for insulation
- Compatible with Pulse Compression System and Dummy Load as well

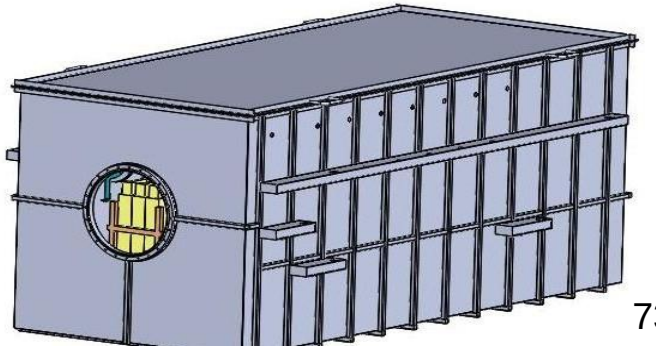

Assembly and Testing in Oil

- Single Shot to 80 Hz
- Voltage ~ 450kV
- Current ~ 9 kA

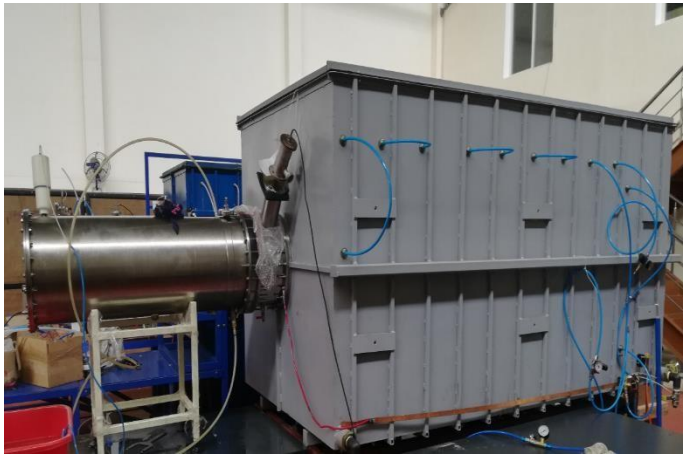

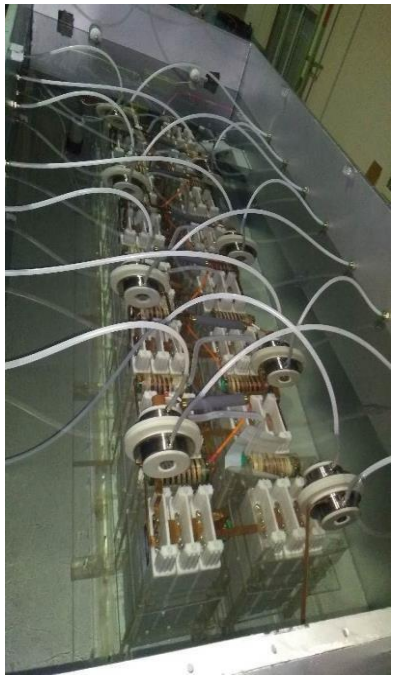

Single –Shot Waveform

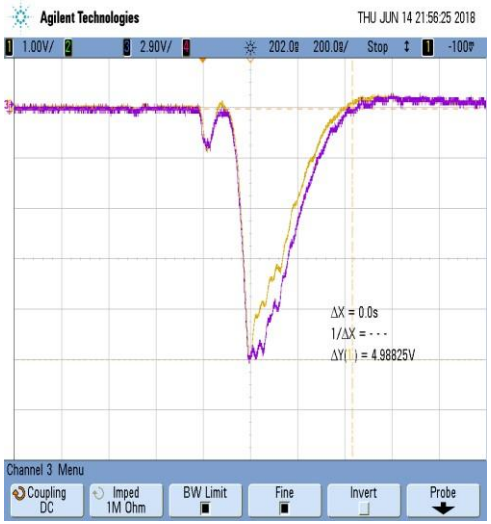

5 Hz Waveform

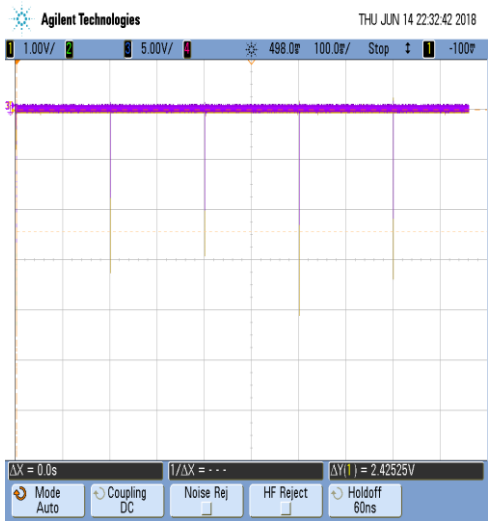

Development of of Backward Wave Oscillator

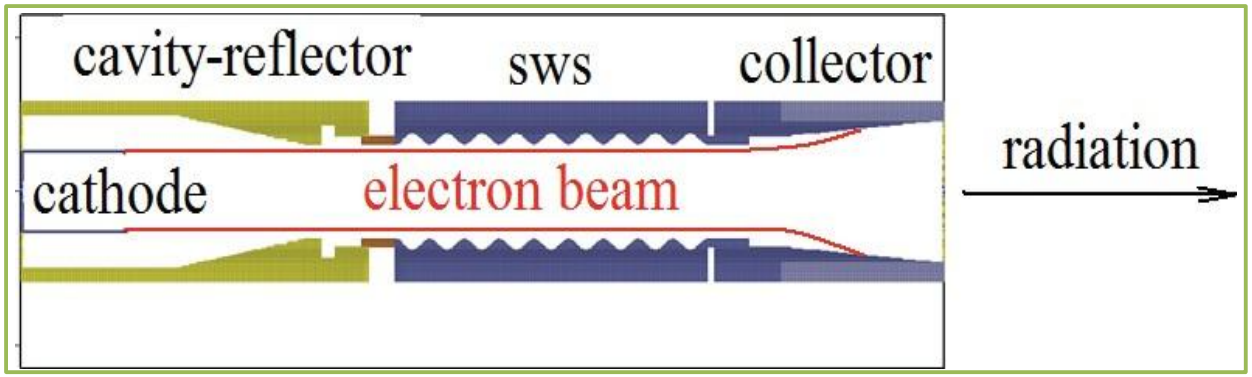

Parameter	Value
Beam Voltage (kV)	500 kV
Beam Current (kA)	8 kA
Frequency (GHz)	S-Band
Power(MW)	500 MW
Magnetic Field (T)	1.2 T
Operating Mode	TM_{01}

Process to be finalized for fabricating 12 period SWS
Initially , a 3-period SWS is fabricated and cold tested

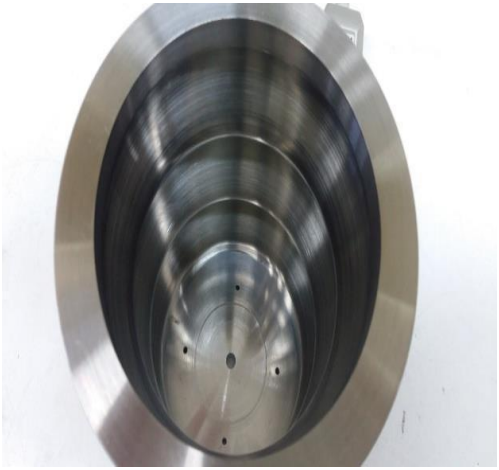

Sl. No.	Resonant Frequency (GHz)	Resonant Frequency (GHz)
1	2.31	2.30
2	2.51	2.47
3	3.62	3.68

Integrated simulation of BWO with mode converter

- Operating mode of BWO is TM_{01}
- Requirement of TE_{11} at input of antenna
- TM_{01}-TE_{11} mode converter is designed

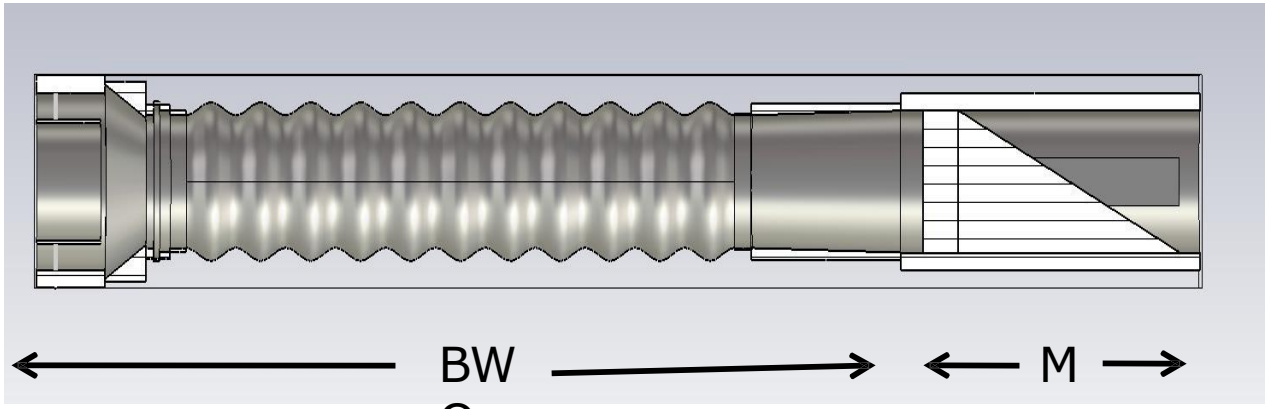

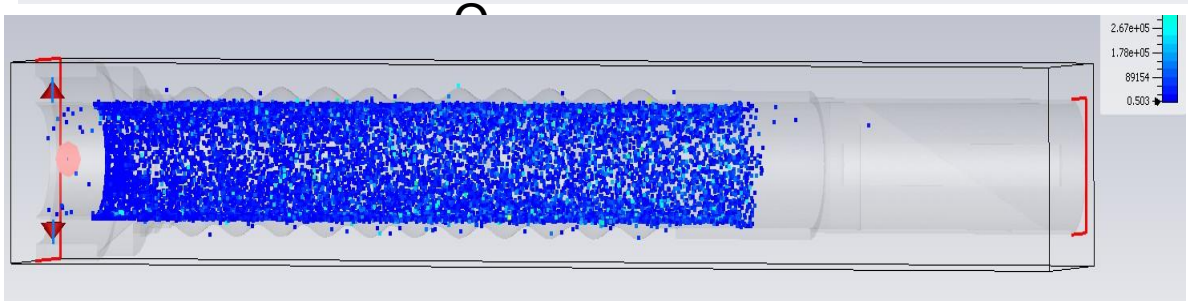

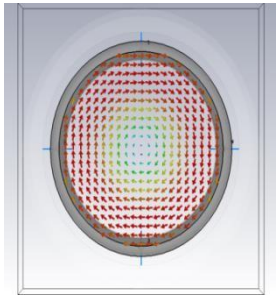

TM_{01}

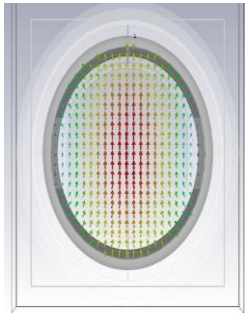

TE_{11}

MILO

Low impedance, high power

- Cross field source-applied Er, self-generated Bθ, axial electron flow
- Device is very compact (No eternal focusing magnet)•Efficiency is limited , due to power used to generate self-insulating magnetic field
- Cavity depth ~ λ/4
- Electron drift velocity ve> microwave phase velocity vϕ=2 p f, where p is the axial periodicity of the structure and f is the microwave frequency
- Microwave circuit is eroded by repeated operation

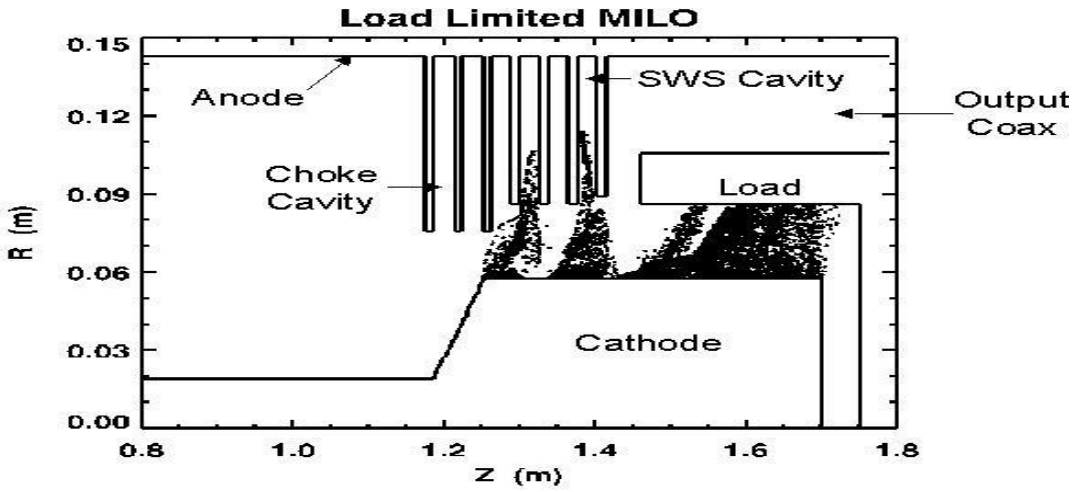

Development of of S-Band MILO

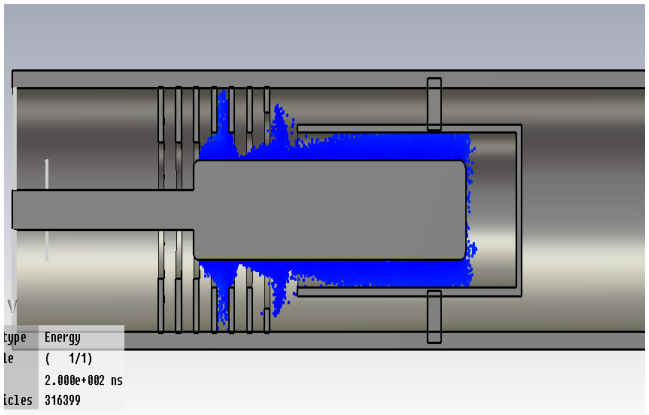

Cut view of MILO device

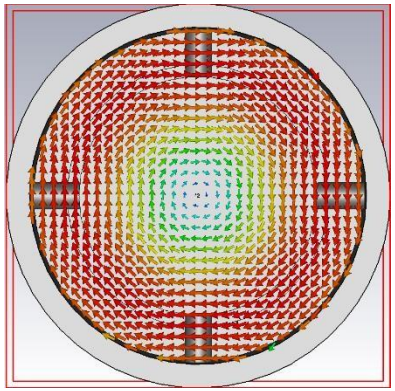

TM_{01} mode

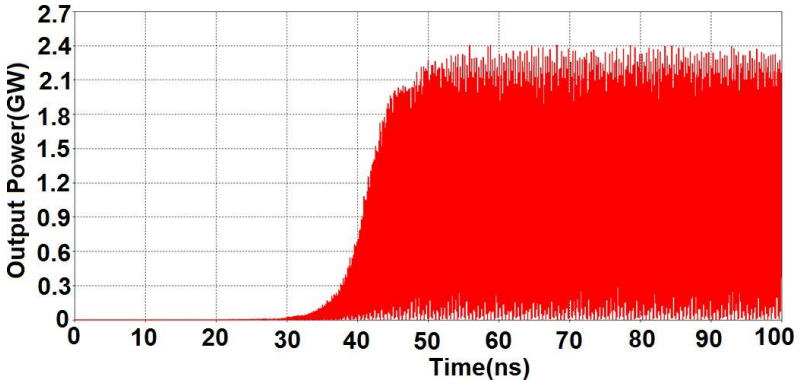

Output Power

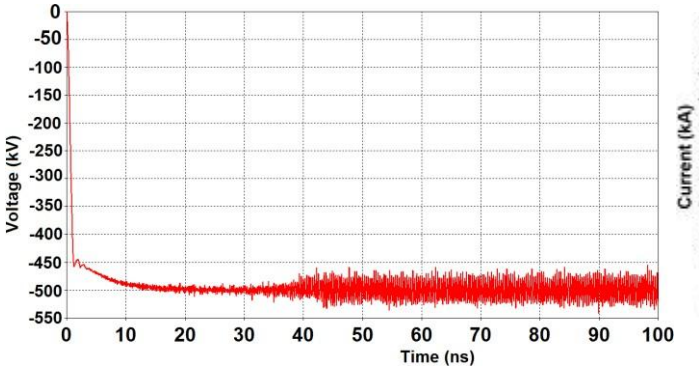

Voltage Plot

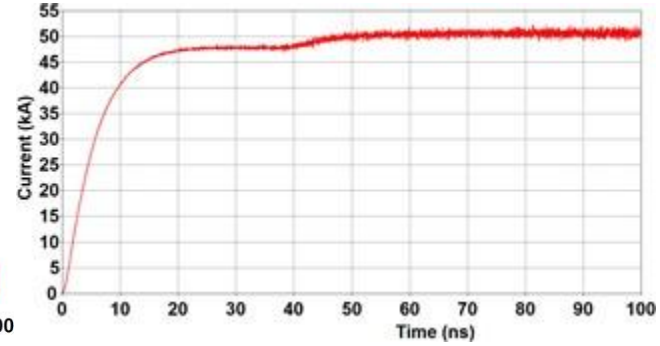

Current Plot

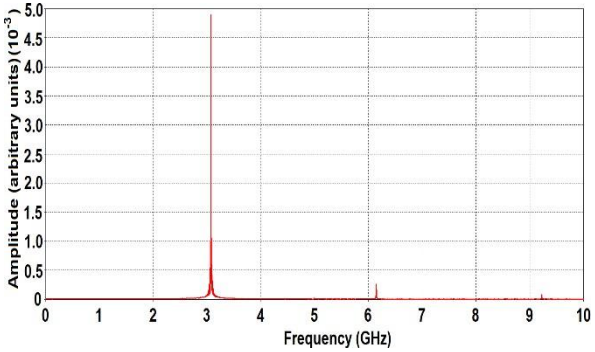

Operating frequency

Fabricated MILO Parts

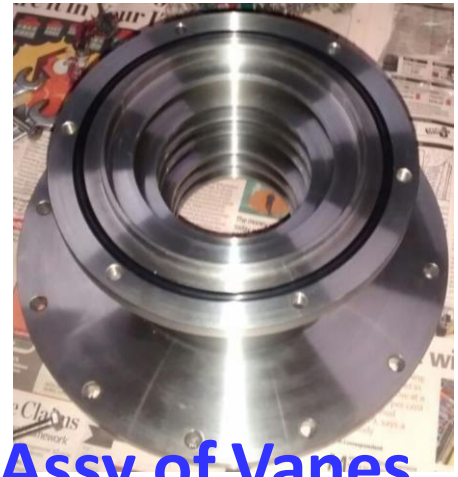

Commissioning of 600 kV and 60 kA Marx generator

- Procured from Ukraine
- Cost : 7.25 crores
- Broad specifications

Voltage: 600 kV(Max.) Current: 60 kA(Max.) Pulse width: 80-100 ns

PRF :18Hz ; Rise time: < 10 ns.

- HPM devices like MILO. Vircator, BWO, Relativistic Magnetron can be tested

* It is a work horse for developing HPM sources in the country

Test results of MILO

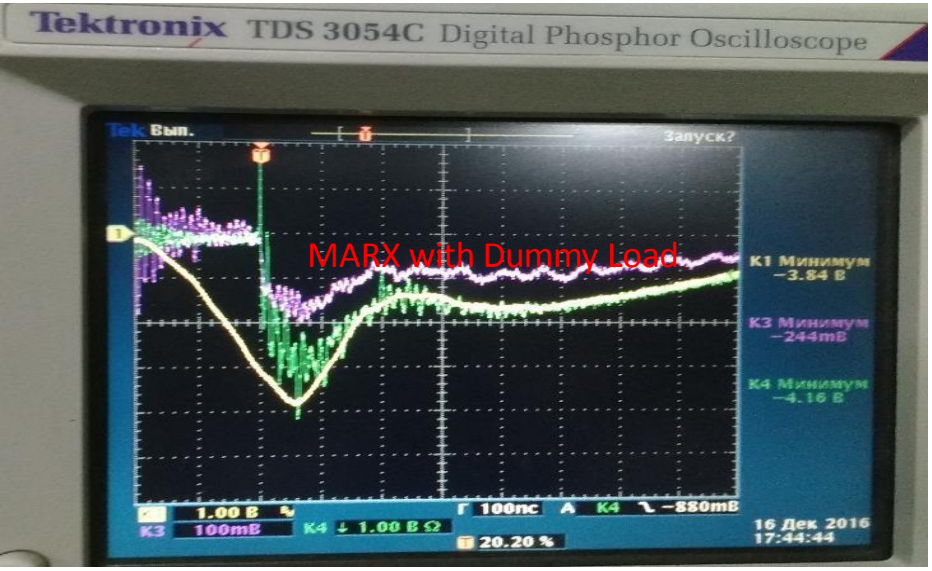

MARX with MILO

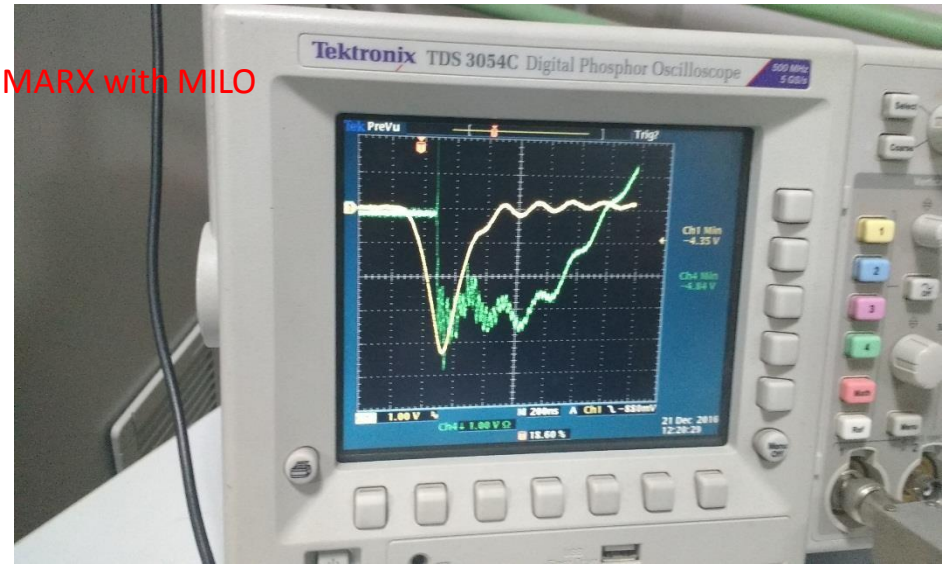

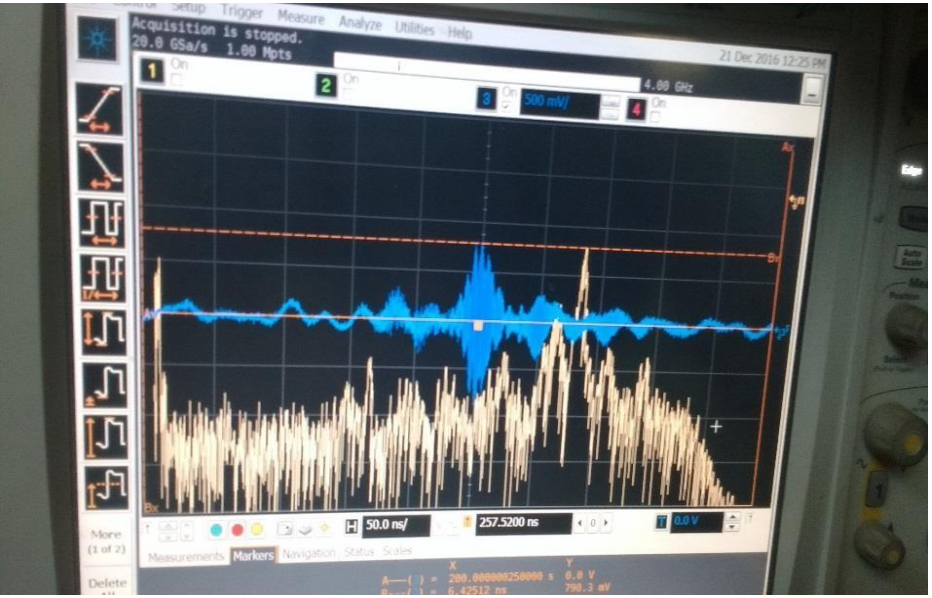

Rf output of MILO

MILO testing on 600 kV, 60 kA Marx generator	
Pulse Voltage (kV)	**Pulse Current (kA)**
324	**32.6**
377	**39.2**
438	**43.6**
485	**48.4**
560	**55.6**

Max. Measured Power -350 Mega Watts

Air-Borne single shot HPM weapon : E-Bomb

An e-bomb (electromagnetic bomb) is a weapon that uses an intense electromagnetic fieldto create a brief pulse of energy that affects electronic circuitry without harming humans or buildings

The U.S. Air Force has hit Iraqi TV with an experimental electromagetic pulse device called the "E-Bomb" in an attempt to knock it off the air and shut down Saddam Hussein's propaganda machine, **CBS News Correspondent David Martin** reports.

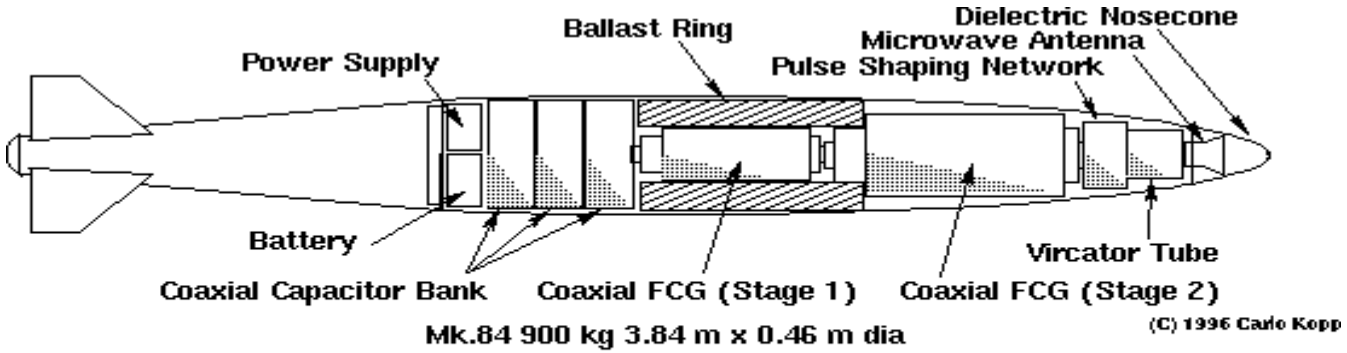

HIGH POWER MICROWAVE E-BOMB - GENERAL ARRANGMENT MK.84 PACKAGING WARHEAD USING VIRCATOR AND 2 STAGE FLUX COMPRESSION GENERATOR

FIG.6 HPM E-BOMB WARHEAD (Mk.84 FORM FACTOR)

Important Parameter

Lethal Area, Weight, Frequency, External Ballistics

Figures below show Lethal foot prints for Low frequency and HPM E-bombs:

* Low frequency: coverage area is more, coupling efficiency low and antenna size bigger
  - No HPM source required to generate RF
* High Frequency: Coverage area is less, coupling efficiency high and antenna size smaller
  - HPM source required to generate RF

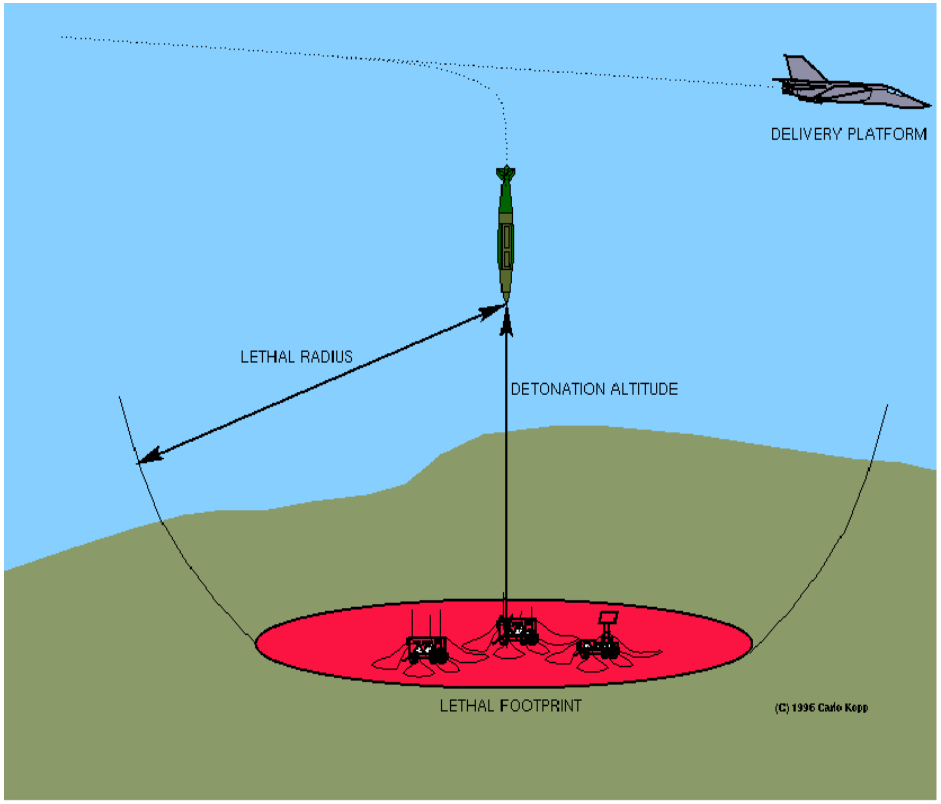

FIG.7 LETHAL FOOTPRINT OF LOW FREQUENCY E- BOMB IN RELATION TO ALTITUDE

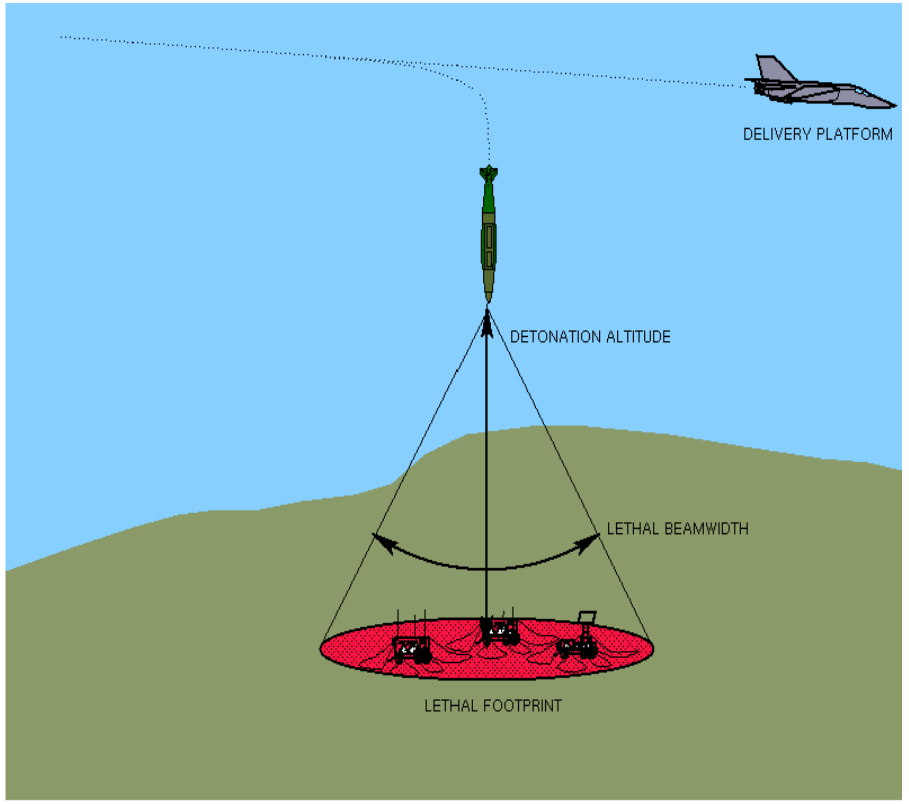

FIG.8 LETHAL FOOTPRINT OF A HPM E-BOMB IN RELATION TO ALTITUDE

Lethal Area :

Formulae for Calculation to get required field at a given distance to

E =(Sqrt(30*P*G))/R

Where

E = Electric Field in Volts/metre
P= Power in Watts
G= Absolute value of gain
R= Range in meters

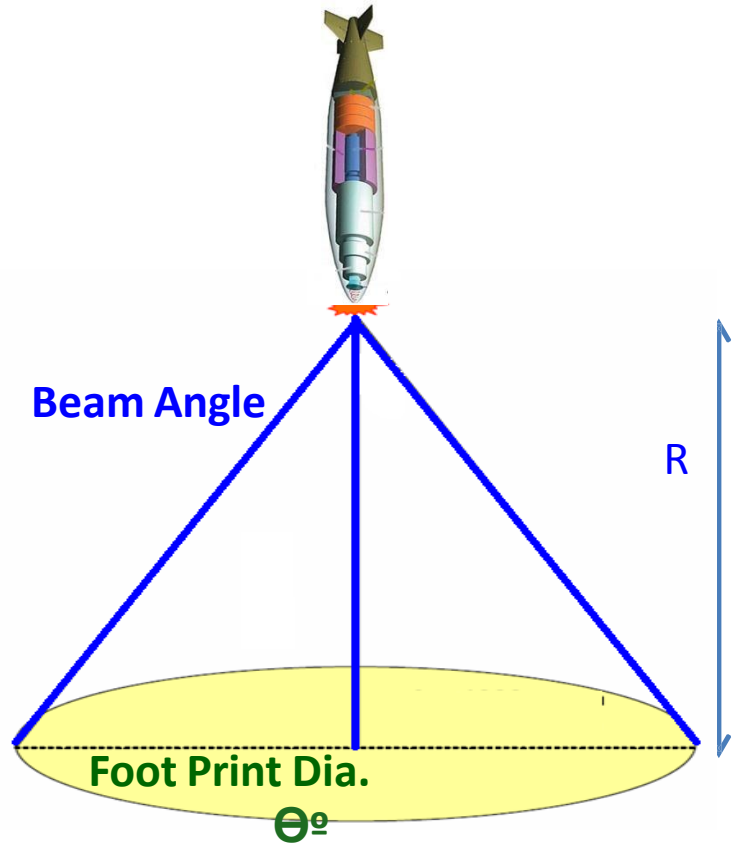

Assume:

2.5 Giga watt source and antenna Gain of 12 dB
Height(R)= 200 m
Beam width = 30 degrees

We get:

Electric field at centre of beam= 25 kV/mt
Electric field at 200 mt pheriphary= 4 kV/mt

Working Principle of FCG

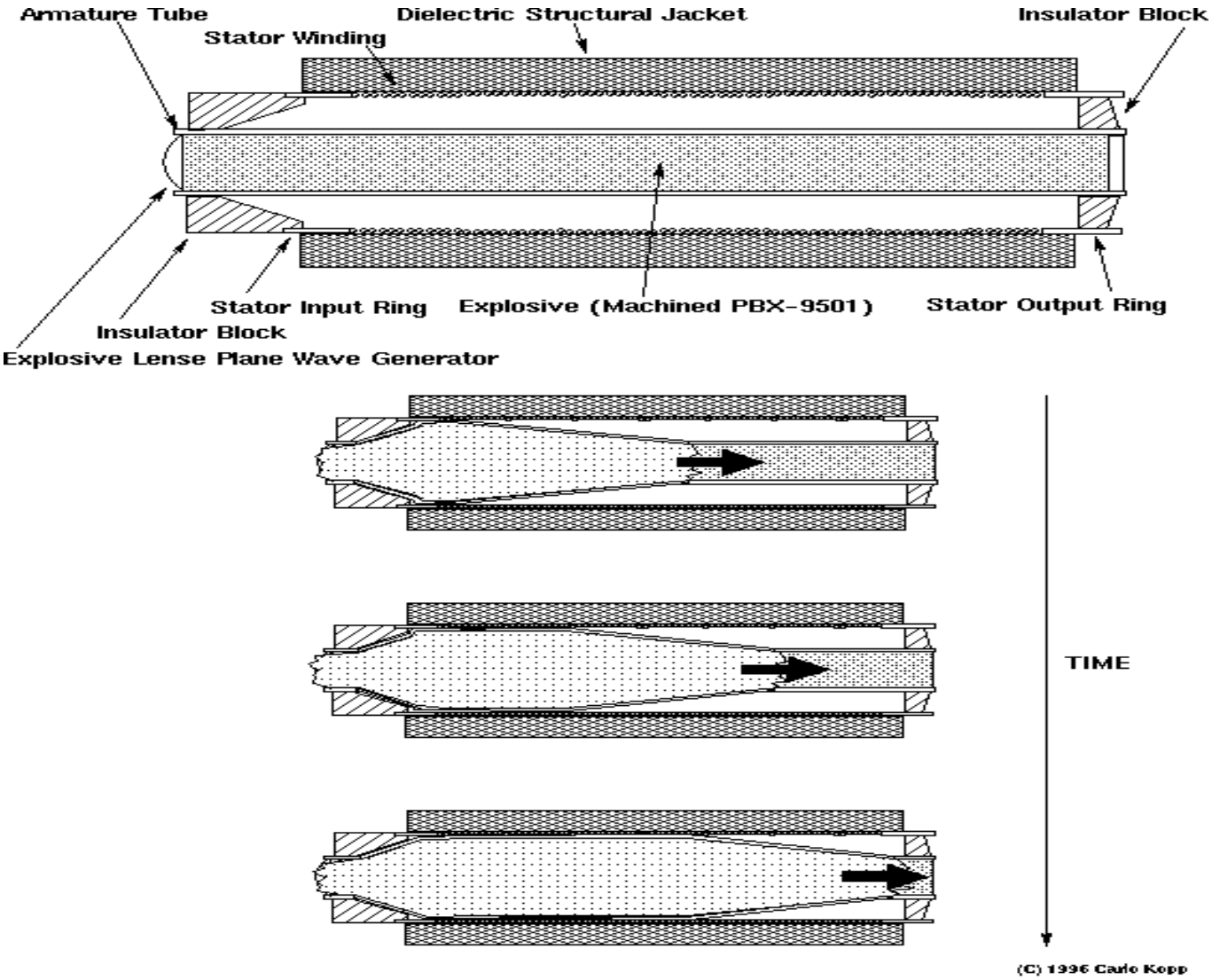

FIG.2 EXPLOSIVELY PUMPED COAXIAL FLUX COMPRESSION GENERATOR

CATHODES

cathodes should have the following properties:

a) High current densities (kA/cm^2)- Explosive emission cathodes

b) Rapid current turn on at moderate electric fields (<10 kV/cm)

c) Little or no plasma production (after conditioning or cleaning), resulting in no diode impedance collapse over microsecond pulse lengths; and

d) Survivability under intense, microsecond current generation, electron and ion back bombardment

e) Cathode which can work in UHV conditions also

Explosive Electron Emission

EEE: The emission of electrons from a plasma created on the cathode surface by the application of a strong electric field.

Field-enhancement EEE

- usually metallic surfaces
- field-enhancement at the tips of microprotrusions causes explosive vaporization
- fields at the tip are generally > 107 V/cm (enhancement factors in the range of 10-1000)
- minimum plasma temperature is few thousand degrees K.
- closure velocities generally exceed 1 cm/μsec, and can quickly short the diode.

- **Surface-flashover EEE**
- usually dielectric/metal interfaces (velvet on Al)
- plasma generated by a surface flashover mechanism at 10s of kV/cm.
- plasma can be quite cold, with closure velocities as low as 0.2cm/μsec.
- a significant amount of cathode material is liberated in the process.
- **This can limit the pulse duration and/or the pulse repetition rate.**

Cathodes for single shot devices

Field enhancement	Surface flashover
Graphite Stainless Steel	Velvet

Material	Emission Threshold kV/cm	Lifetime(#of Shots)	Outgassing(#of neutrals per electron
Sandia Red Velvet	8	~8000	10
MILO Green	10	~4000	10-14
Metal / Graphite	95	----	8
CsI-Carbon Microfibers	**<3**	**>200000**	**4-6.5**
			*** NRL data**

Explosive Emission Cathodes

Final part of cathode (diameter 5 cm) out of stainless steel covered with polyester velvet on the essence its length. [5]

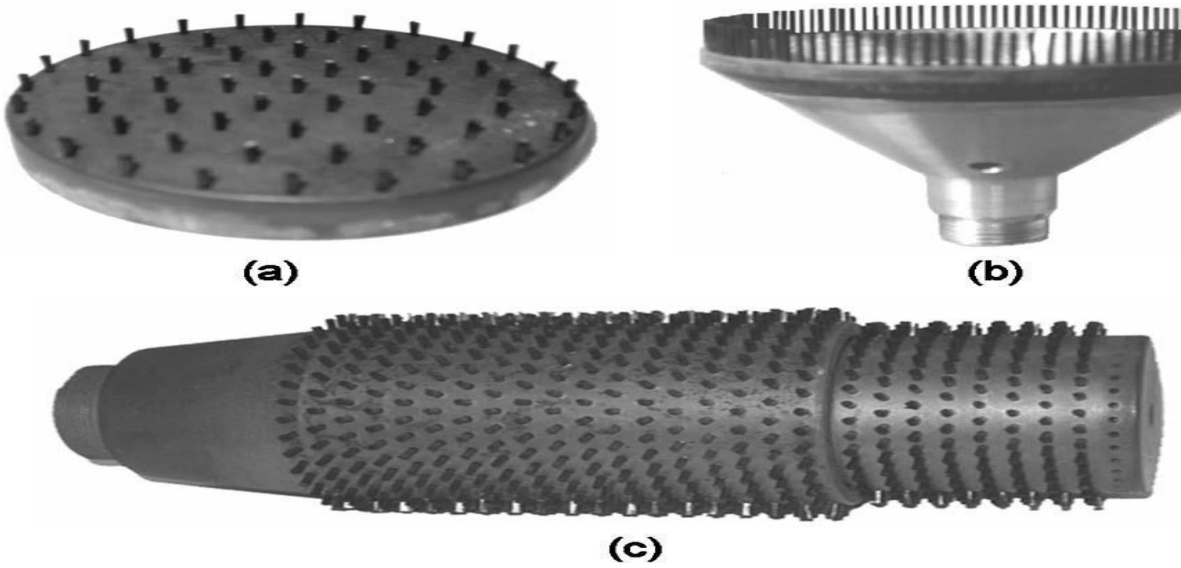

A series of tufted carbon fiber cathodes: (a) a planar tufted carbon fiber cathode,(b) an annular tufted carbon cathode, and (c) a tufted carbon fiber cathode for radial emission

HPM Cathode Summary

- The important emission mechanisms for high-power tubes include thermionic emission and explosive electron emission.
  - secondary emission may be applicable in cross-field tubes
  - true, stable field emission is difficult to realize
- Choice of cathode depends on application.
- Desirable features for HPM tubes:
  - free electron emission at the space charge limit
  - emission of no extraneous material
  - lasts forever
  - vacuum condition tolerant

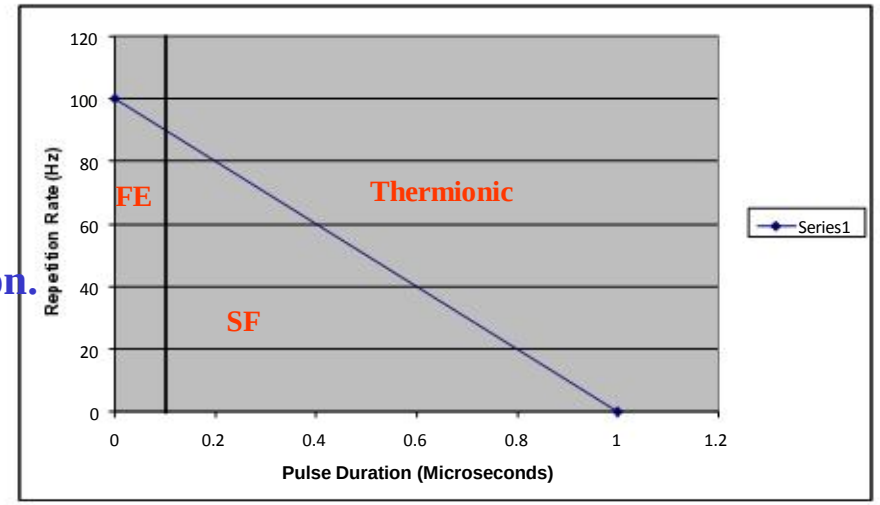

Characteristic	Thermionic	EEE - FE	EEE - SF
SCL emission	T ~ 1000 oC	E > 100 kV/cm	E > 20 kV/cm
No extra material	Ba evaporation	> 10^{14} mol/cm^2	> 10^{15} mol/cm^2
Lifetime	1000 hrs @ 10 A/cm^2	10^6 shots	10^5 shots
Vacuum conditions	< 10^{-7} torr	10^{-6} - 10^{-4} torr	10^{-6} - 10^{-4} torr

Major technological challenges :

* High density long life cathodes:
  - More than 10000 shots

* Compact Marx generator:
  - less than 400 mm dia X 1mt long to generate 500 KV, 10 KA, 10 HZ PRF
  - Compact Capacitor development is the Key

* Design Codes and subsystem design :
  - Source design, Antenna Design
  - Evaluation of HPM effects when coupled into room

* Vulnerability studies:
  - effects of HPM on Victim Systems

* Development of Efficient and compact battery sources to support the HPM System

Thank you

Microwave-Radiation Safety Standards

vis-à-vis Biological Effects of Microwave

Dr. Subrata Kumar Datta

Microwave Tube R&D Centre, Bangalore

Introduction – *The EM Spectrum*

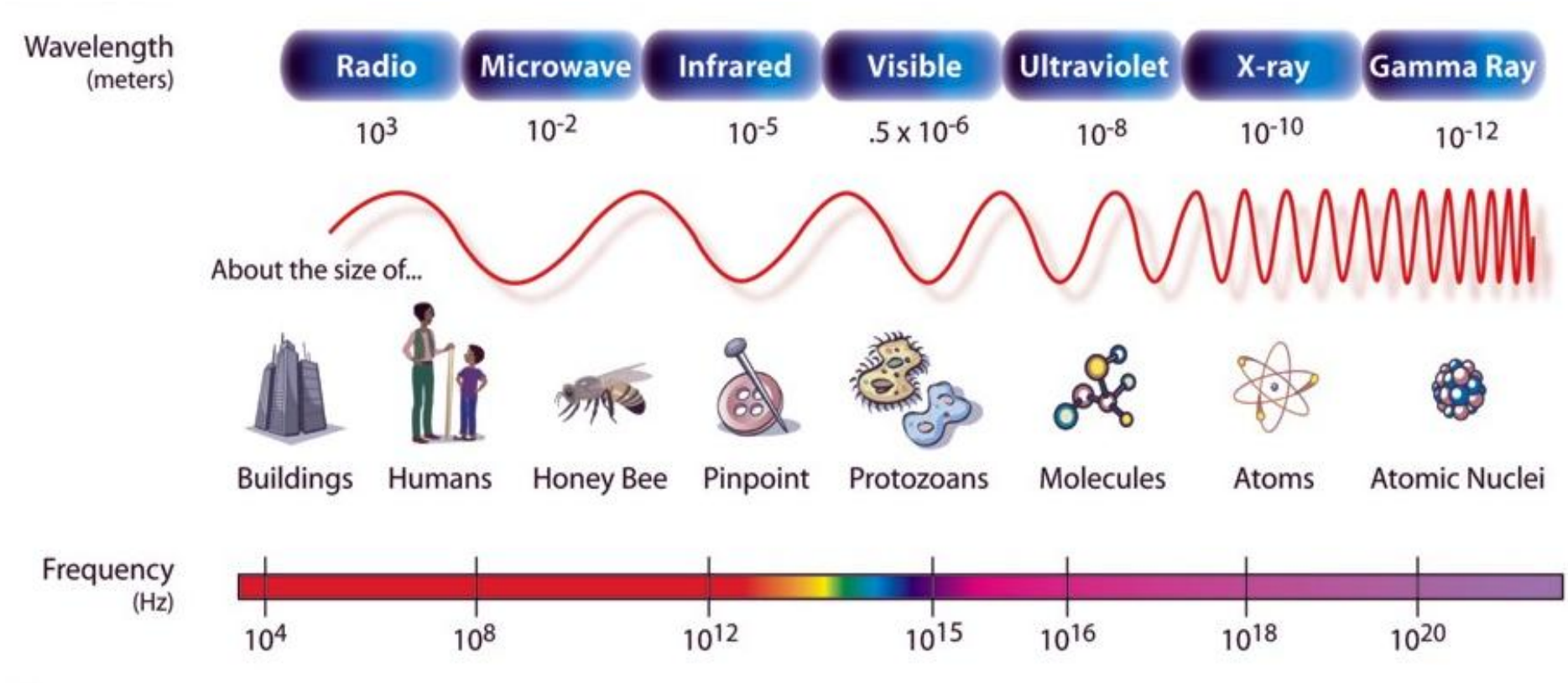

Introduction – Nature of Radiation

- **Ionizing Radiation: Quantum Energy ~ 12 eV, λ~103 nm, UV Spectrum**
  - Alpha, beta, and neutron particles, X-rays and gamma rays.
- **Non-Ionizing Radiation: Below UV Spectrum**
  - Electromagnetic radiation: Optical, Infrared, Microwave, RF, etc

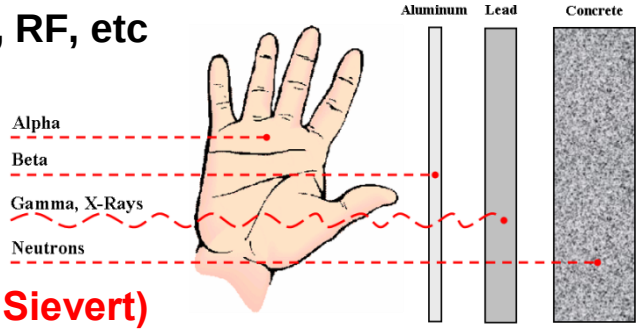

Annual Exposure Limit:

5000 mrem – Professionals
360 mrem – Common people
(rem = Roentgen Equivalent in Mammal → 100 rem = 1 J/kg = 1 Sievert)

- **Hazards of Electromagnetic Radiation to Personnel (HERP)**
  - Non-ionising radiation – RF & MW
  - Ionising X-ray radiation from RF Sources (collectors)
- **Hazards of Electromagnetic Radiation to Ordnance (HERO)**
  - Detonation of electro-explosive devices
  - Spark-ignition of flammable gases

Microwave Heating

Dielectric Loss:

- Dipole polarization
- Rotation & alignment of dipoles
- Damping of rotation due to restoring force.

Power Dissipation in watts per cubic meter:

$$P_d/V = \omega \varepsilon_0 \varepsilon_r'' E^2 = 55.6325 \times 10^{-12} f_{HZ} \varepsilon_r'' E^2$$

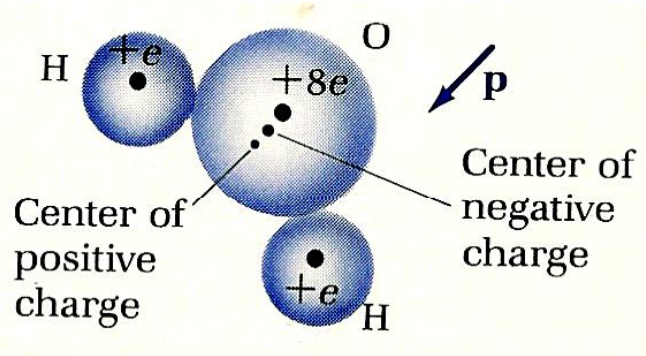

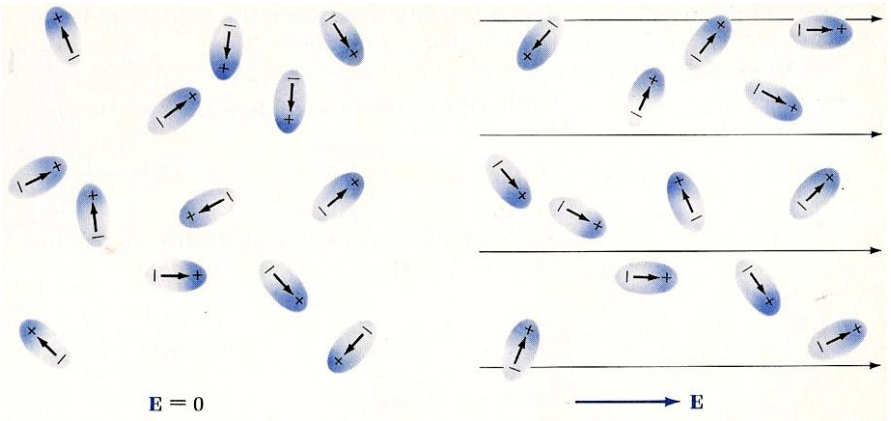

Homoeostatsis

- **Homeostasis** is the state of steady internal physical and chemical conditions maintained by Human Body.
- This dynamic state of equilibrium is the condition of optimal functioning for the body and is kept within certain pre-set limits (homeostatic range).
- Controlled solely by the Hypothalamus of the Brain.
- **Controls of variables**
  - Core temperature
  - Blood glucose
  - Iron levels, Copper regulation, blood gases, Blood oxygen content, Calcium levels, Sodium concentration, Potassium concentration
  - Arterial blood pressure and Fluid balance
  - Blood pH
  - Neuro-endocrine balance
  - **Gene regulation**
  - Energy balance

Causes of Cancer

- Cancer is a metabolic disorder leading to uncontrolled cell growth.
- The basic cause of cancer is DNA damage and genomic instability.
- A minority of cancers are due to inherited genetic mutations.
- Most cancers are related to environmental, lifestyle, or behavioral exposures.
- The term "environmental", refers to everything external that interacts with body.
- Up to 10% of cancers are related to radiation exposure (both non-ionizing radiation and ionizing radiation).
- Not all types of electromagnetic radiation are carcinogenic.
- Low-energy waves on the electromagnetic spectrum including radio waves, microwaves, infrared radiation and visible light are thought not to be because they have insufficient energey to break chemical bonds.
- However, long exposure of non-ionizing radio frequency radiation has been described as a possible carcinogen by the World Health Organization's International Agency for Research on Cancer.
- Long exposure to RF / Microwave may cause imbalance in Homoeostasis and therefore create metabolic disorders leading to cancer.

Basic Considerations – SAR & BMR

(ANSI / IEEE C95.1a-2010)

- **Specific Absorption Rate**
- **Unit: W . Kg $^{-1}$**

$$SAR = C\left(\frac{\Delta T}{\Delta t}\right)$$

C = Specific heat

ΔT = Temperature increase

Δt = Exposure duration

- **RF & MW Effects**
  - **Tissue absorption**
  - **Skin heating**
  - **RF Shock & Burn**
  - **Field Effect**

- **Basal Metabolic Rate**
- **Unit: W . Kg $^{-1}$**
- **84 Watts for a 70 Kg Human ⇒ 1.2 W/Kg**
- **BMR outward heat flux ~ 10 mW/cm^2.**
- **SAR to BMR Safety Standard: ~ 30%**
- **SAR Safety Limit Identified: ~ 0.4 W/Kg**

"Heat production of a human in a thermoneutral environment (33 ^{0}C), at rest mentally and physically, at a time exceeding 12 hours from the last meal"

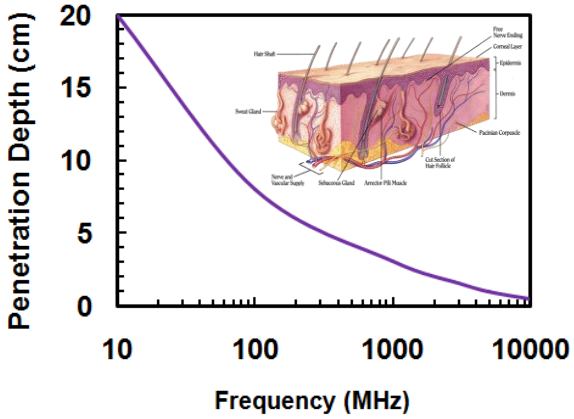

Evolution of Standards

- ANSI / IEEE C95.1-1974 →C95.1-1982 → C95.1-1991 → C95.1a-2010 (2005)
- Human body-tissues are poor conductors – dielectric heating
- Energy absorption in human tissues ~ max 50% of the incident energy.
- Human BMR outward heat flux ~ 10 mW/cm^2.
- Sunlight provides a heat flux of ~ 40 mW/cm^2.
- Rise in temperature in human tissues produced by a heat flux of 20 mW/cm^2 is about 1 ^{0}C.
  - SAR for professionals < 0.40 W/kg over 0.1 hour interval.
  - SAR for general public < 0.08 W/kg over 0.1 hour interval.
  - Recognizes the safety standards for RF shock and burn.

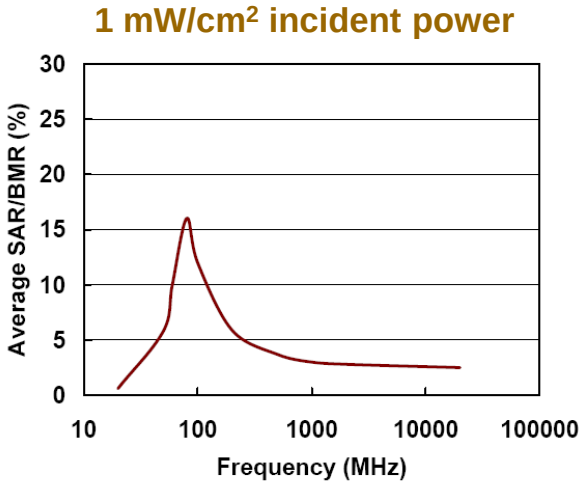

Frequency Bands

Navigation	9 KHz – 540 KHz
AM Radio	540 KHz – 1630 KHz
Shortwave radio	5 MHz – 30 MHz
TV band	54 MHz – 88 MHz
FM Radio	88 MHz – 174 MHz
TV band	174 MHz – 216 MHz
Mobile/Radio/TV	216 MHz – 600 MHz
Cell phones (CDMA)	869 MHz – 890 MHz
Cell phones (GSM 900)	935 MHz – 960 MHz
Cell phones (GSM 1800)	1805 MHz – 1880 MHz
Cell phones (3G / 4G)	2110 MHz – 2170 MHz
Microwaves	> 2000 MHz

IEEE C95.1-1974

Safety Standard

- **The incident power density limit:**
  - **10 mW/cm^2 regardless of frequency**
  - **Band: 300 KHz – 100 GHz**

IEEE C95.1-1982

Safety Standard

- **Resonance absorption**
- **Frequency dependence standard**
- **Whole body SAR < 0.4 W/kg averaged over any 0.1 hour period (6 minutes).**

30 MHz – 300 MHz : For whole body
400 MHz : For head
400 MHz – 3 GHz : Other limbs

IEEE C95.1-1991

Safety Standard

- **Expands the frequency limits up to 300 GHz.**
- **Two-tier standard for professionals and general public:**
  - **SAR for professionals < 0.40 W/kg over 0.1 hour interval.**
  - **SAR for general public < 0.08 W/kg over 0.1 hour interval.**
- **Recognizes the safety standards for RF shock and burn.**

IEEE C95.1a-2010 (2005)

Safety Standard – Professionals

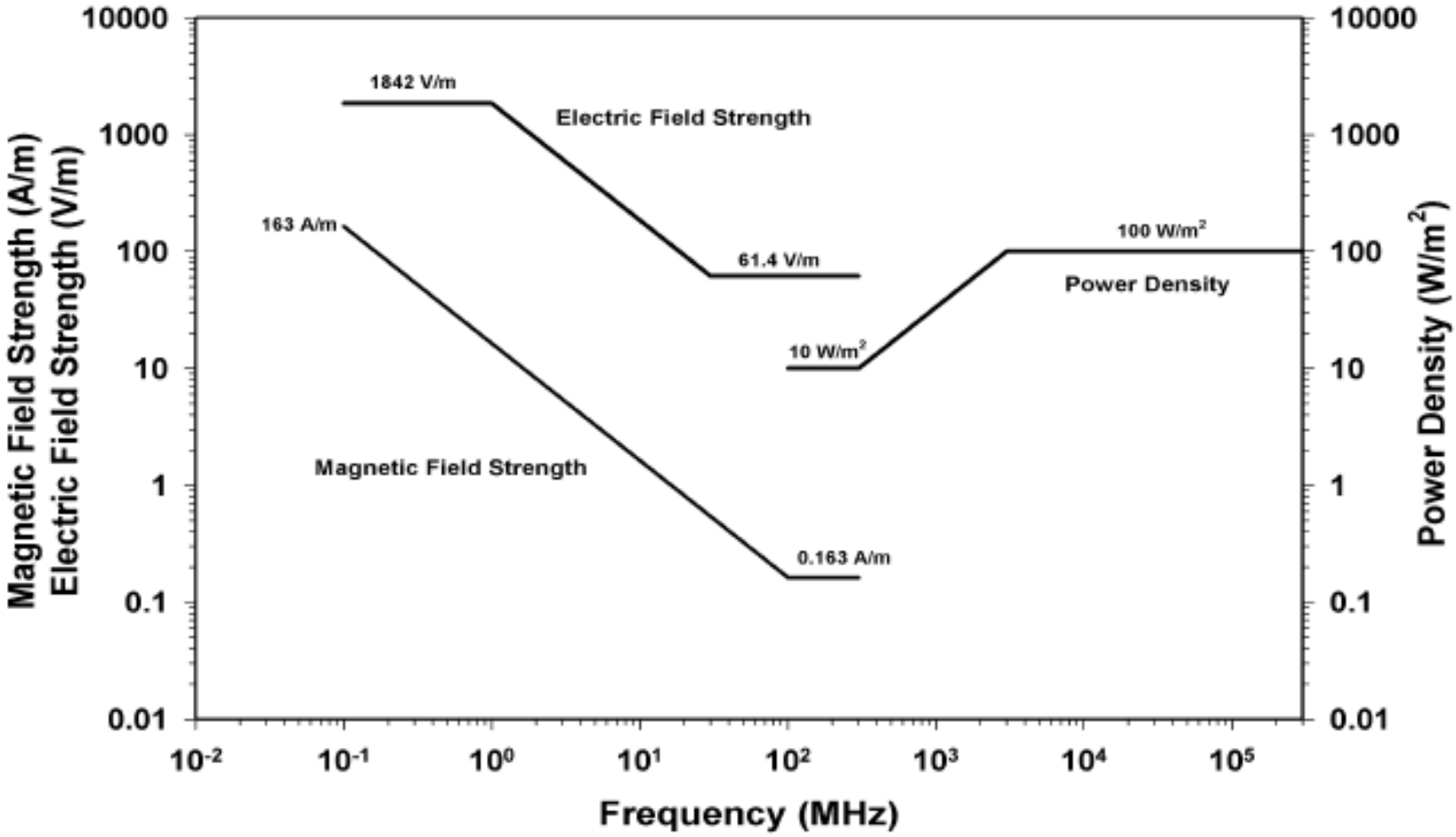

IEEE C95.1a-2010 (2005)

Safety Standard – Common People

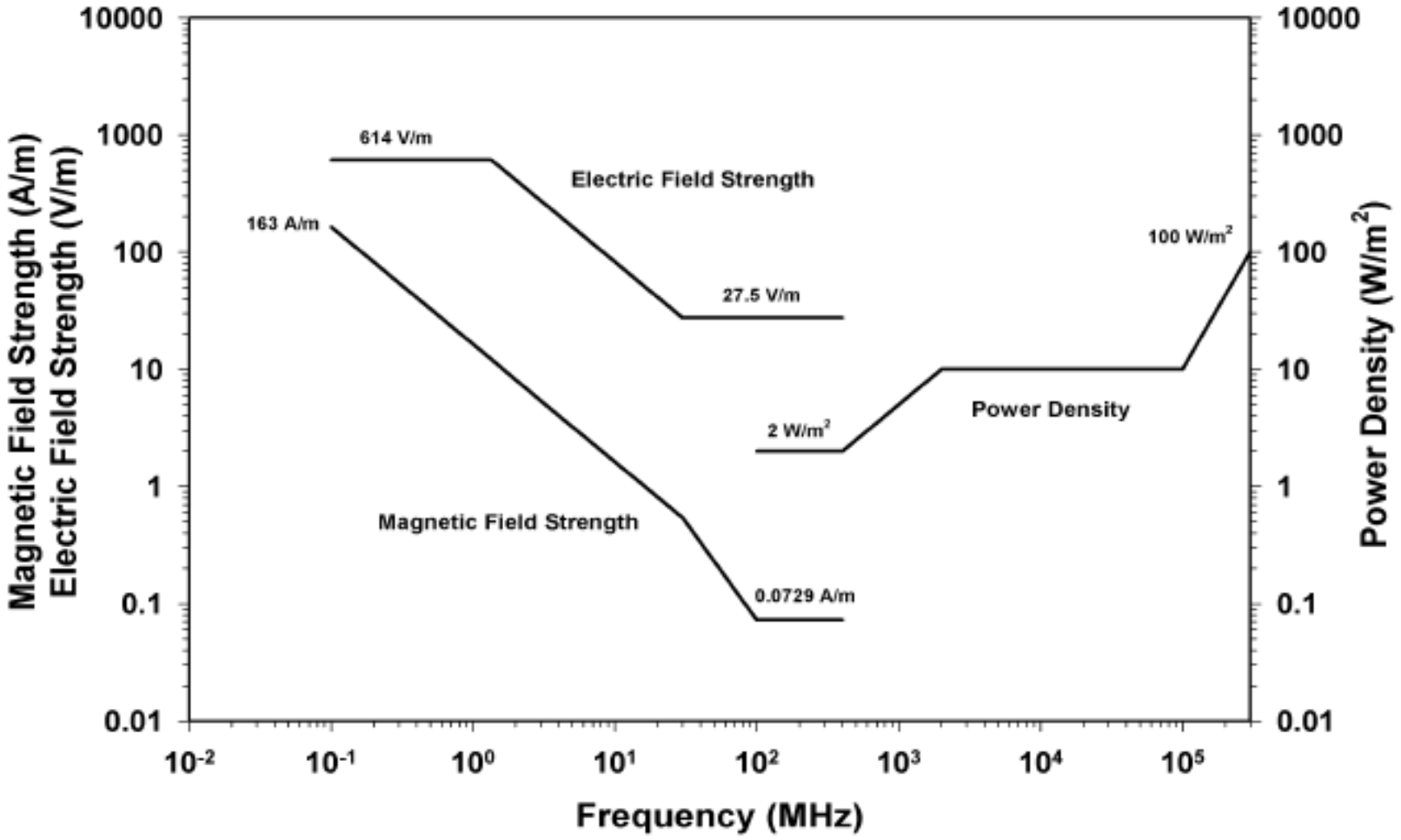

IEEE C95.1a-2010 (2005)

IEEE C95.1-2005 Safety Standard
(Amendment IEEE C95.1a-2010)

Recommendations to protect against harmful effects in human beings exposed to electromagnetic fields in the frequency range from 3 kHz to 300 GHz are provided in this standard. These recommendations are intended to apply in controlled environments and for general population exposure. The Amendment of 2010 specifies ceiling limits for induced and contact current, clarifies distinctions between localized exposure and spatial peak power density.

Dept. of Telecomm, GOI

Standards for Individual Cell Phone Towers

Frequency	Power Density (W/m^2)
400 – 2000 MHz	f_{MHz} / 2000
2 – 300 GHz	1

900 MHz Power Density ~ 0.045 mW/cm^2

0.9+ million Towers in India

The Reality:	
P_t = 20W, G_t = 17 dB	
Distance (m)	**Power Density (mW/cm^2)**
1	8
5	0.3
10	0.08
50	0.003
100	0.0008
500	0.00003

Dept. of Telecomm, GOI

Standards for Cell Phones

800+ million Phones in India

- SAR < 2 W/kg – Valid till 31-August-2013
- SAR < 1.6 W/kg
- Test facility at Telecom Engineering Centre (TEC)
- Indian Telegraph Act 1885 is amended in 2012.

- European Union : 2.0 W/kg @ 6 min / hour
- USA : 1.6 W/kg @ 6 min / hour

Samsung Galaxy Ace Duos	~ 0.3 W/kg
HTC EVO 4G	~ 1.03 W/kg
Blackberry 8110 Pearl	~ 1.13 W/kg

(www.sarshield.com)

Standard Bluetooth

50 – 100 mW/cm^2 @ 2.4 GHz

Domestic Microwave Ovens

Study	Average leakage radiation (mW/cm^2)	No of appliances Studied	Age of appliances (years)
Study [1]: Used appliances	0.41	106	0.1 – 14
Study [2] new appliances	0.08	60	0

1. A. Thansandote, D. Lecuyer, and B. Gaijda, "Radiation leakage of before-sale and used microwave ovens," Microwave World, vol. 21, pp. 4-8, 2000.
2. R. Matthes, "Radiation emission from microwave ovens," J. Radiol. Prot., vol. 12, pp. 167-172, 1992.

Microwave Cooking – The Myth vs. Truth

- Dielectric Heating – No side-effects
- Taste may differ due to lack of oxidation & roasting
- Food value is not at all spoilt
- Vitamins are better contained because of no boiling

FM Radio Stations in India

Freq (MHz)	Tx Power (kW)	Location	Station
90.4	0.05	Chandigarh	Vivek High School
90.4	0.05	New Delhi	Delhi University
90.4	0.05	Bangalore	Ramana Mahrishi Academy of the Blind
91.1	20	Mumbai	Radio City
91.9	10	Coimbatore	Gyan Vani
93.5	20	Chennai	Suryan FM
101.3	10	Bangalore	All India Radio
101.3	20	Kolkata	All India Radio

(http://www.asiawaves.net/india-fm-radio.htm)

Military Radars / Comm. Links

Air Force Station	Radar / Tropo Unit	Freq. range of operation	Location/site of measurement	Power density (mW/cm^2)
AGRA	Radar: PSM-33 MK-1	2-4 GHz	Just below RADAR	14
	ATCR-4T	1.28-1.35 GHz	Close to Klystron (1' distance)	14 - 16
	Missile Guidance RADAR	1.25-1.35 GHz	Just below RADAR	0.065 - 0.085
AGRA	TROPO UNIT	1.7-2.1 GHz	Very close to Power Amplifier	100 - 150
			At 1 ft distance from Power Amplifier	10 - 10.5
BAGDOGRA	PSM-33	2.925-3.075 GHz	Near Magnetron	12
			In working area	0.02 - 0.04
AYANAGAR	RADAR: THD-1955	2.825-3.125 GHz	In working area	0.07 - 0.09
	TROPO UNIT		In working area	0.05 - 0.07
PATIALA	INDRA Mk-I	1.25-1.35 GHz	Very close to klystron	1.40 - 1.65
	INDRA Mk-II	1.25-1.35 GHz	In working area	0.07 - 0.08
AMRITSAR	TRS 2215	2.0-4.0 GHz	Along waveguide	30 - 40
			Along coupler	6 - 7.5
			Near Travelling Wave Tube (TWT	17

US Military Radars / EW Jammers

LOCATION	FREQ. RANGE (MHz)	APPROXIMATE NEAR FIELD EM LEVELS			
		Pwr Dens (mW/cm^2)		Fld Stgth (V/m)	
		Peak	Avg	Peak	Avg
MIL-HDBK-235 Part 3 (Partial)					
Maximum EM Environmental Levels for Hostile Shipboard Emitters	< 30 30-2000 > 2000	0.4 14,500 250,000	0.4 90 450	40 7,300 30,000	40 600 1,400
Maximum EM Environment Levels for Hostile Airborne Emitters	< 30 30-2000 > 2000	– 2,510 50,000	– 4 65	– 3,100 14,000	– 125 500
Maximum EM Environment Levels for Hostile Landbased Emitters	< 30 30-2000 > 2000	4 700,000 800,000	4 7,000 275,000	120 55,000 850,000	120 5,500 33,000
Actual Hostile Jammers	< 2000 > 2000	25 35	2 30	300 360	85 320
Postulated Hostile Jammers	< 2000 > 2000	4,500 35,000	25 350	4,100 12,000	300 1,200

Typical Military Installations – Released by US Ministry of Defence (Source Internet)

High Power Microwaves (HPM)
Directed Energy Weapons

Frequency	1 – 300 GHz
Peak Power	> 100 MW
Pulse Width	~ 100 Nano-secs
PRF	Single Shots, 20-250 Hz
Pulse Energy	> 1KJ

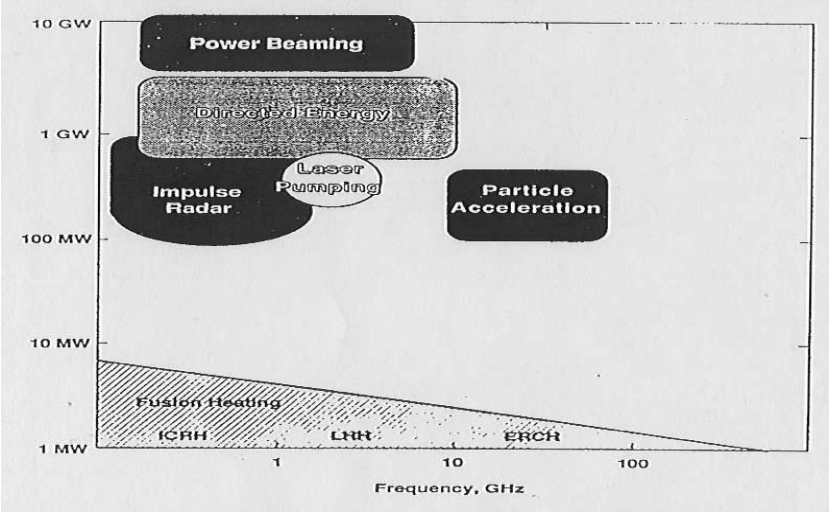

- Speed-of-light, all-weather attack
- Area coverage of multiple targets
- Surgical strike (damage, disrupt, degrade)

- Average Power quite low
- Heating effect negligible
- Electric field effect is not substantiated yet
- Further research is continued worldwide

Active Denial System (ADS)
Law Enforcement & Military

- Flushing out Terrorists/ Criminals; Stopping of Vehicles
- Infliction of Pain – intolerable in 5 sec
- 94 GHz Gyrotron, 100 kW Peak Power: Range >750 m

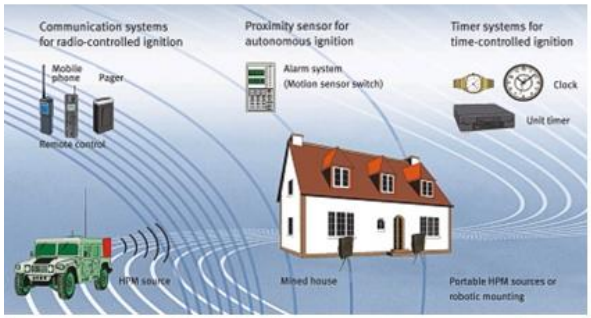

Vehicle-mounted ADS

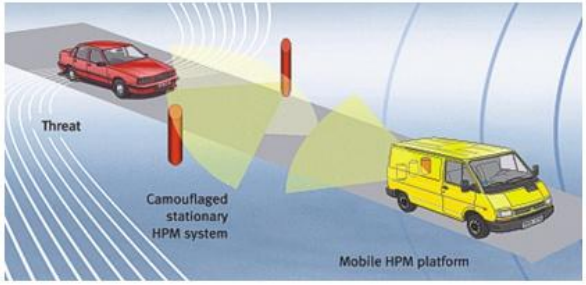

Deny Access of Vecjles to Specific Areas

No known / reported health hazard @ 94 GHz

HPM-DEW Effects

Salient Features

- Single pulse – Low PRF
- Low average power
- High electric field (V/m)
- High magnetic field (A/m)
- High short-circuit current

Possible Biological Effects

- Hyperthermia – negligible effect
- RF Shock & burn
- Ocular disorder
- Cardiac disorder
- Neurological disorder
- Effects on bodily implants
- Effects on ornaments

Typical Power Levels and Field Exposure for HPM Systems

Frequency Band	Peak Power (GW)	Pulse-width (ns)	PRF (Hz)	Average Power (kW)	E_{peak}
L-/S-band (APELC, USA)	10	200	6	12	500 kV/m @ 1 m 5 kV/m @ 100 m
X-band (RANET-E)	0.5	20	500	5	30 kV/m @ 2 km

RF Shock & Burn – IRPA Calculation

$$I_{sc}(\text{mA}) = 0.09\, h^2\, E\, f_{kHz} \qquad (h \Rightarrow m, \quad E \Rightarrow kV/m)$$

- I_{sc} is the total body short-circuit current.
- Example: 175 cm tall human exposed to 1 kV/m @ 2 GHz
- I_{sc} becomes ~ 550 A
- This will give an *Impulse-Shock* – repeated shocks for finite PRF
- > 150 mA for more than few milliseconds
  - Fibrillation of tissues causing cardiac arrest
  - Vesicular fibrillation / blockage observed in human
- > 200 V for more than few milliseconds
  - Causes inflammation of stratum corneum – burn injury
- Electro-convulsive therapy – 130V, 200 mA, PRF ~ 140, over 0.3 Sec

Risk Assessment still inconclusive – research needed

Neural Signal & Cardiac Rhythm

- Neural impulse potential typically 50 – 70 mV
- > 1 kV/m Field:
  - Temporary malfunctioning of astrocytes (non-neural glial cells)
  - Na^{+}, K^{+}, Ca^{++} ion transportation affected
  - Causes breathing troubles, nausea, headache, etc.

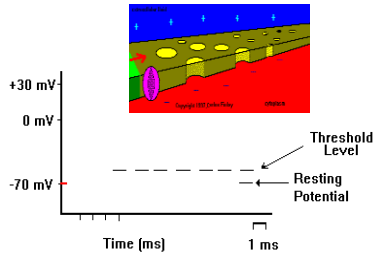

- Corneal and Retinal injury – eddy current effects in ocular fluids
  - Temporary black-out observed due to EMP burst

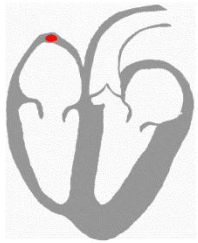

- > 10 kV/m – Pearl-Chain aligning of protein molecules in blood

- Pacemaker Cells – threshold potential typically 50 – 70 mV
- Cardio-version during open-heart surgery uses ~ 2 J/kg
- > 1 kV/m Field:
  - Irregular rhythms of Sinoatrial (SA) nodes
  - Irregular rhythms of Atrioventricular (AV) nodes
  - Interference in myocardial conduction (impulse reaches from SA to SV in 50 ms)

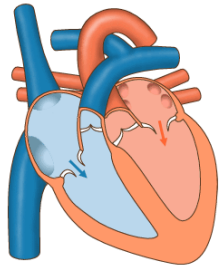

Risk Assessment still inconclusive – research needed

Implants & Ornaments

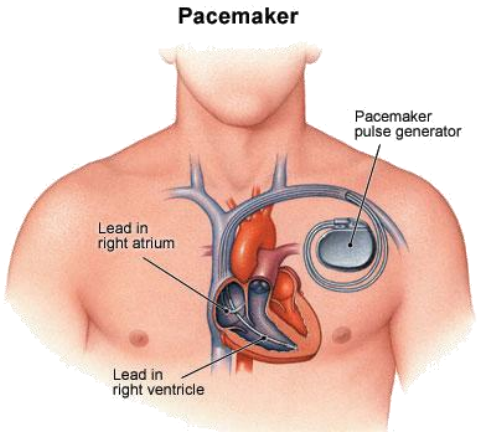

- ***Pacemaker:***
  - *Impulse potential ~ 100 mV*
- ***Hearing Aids:***
  - *Operating potential ~ 1 V*
  - *Interference observed due to EMP bursts*
- ***Vascular & Prostatic Stents:***
  - *Titanium – induced current effect – internal fibrillation of blood cells*
  - *Cobalt-Chromium – induced current impulse – permanent magnetisation*

- ***Ornaments:***
  - *Ear-rings, Finger-rings, Bangles, Wrist watch, etc – sudden shock due to induced impulse current*

Risk Assessment still inconclusive – research needed

Conclusion – Continuous RF Exposure

- Effects are mainly thermal – non-ionizing
- Homoeostasis maintains the body temperature & metabolic balance

- Radiation limit for common people < 0.2 mW/cm^2 @ 6 min/hour
- Radiation limit for professionals < 1 mW/cm^2 @ 6 min/hour
- SAR for cell phones < 1.6 W/kg – safe for user @ 6 min/hour
- Radiation limit for Telephone Towers < 0.05 mW/cm^2 @ 900 MHz

- Military radars – unsafe around the installation
- FM / AIR Towers – unsafe around the installation
- Bluetooth radiation ~ 50 – 100 mW/cm^2 @ 2.4 GHz

- IRPA/IEEE/ANSI now proposing:
  - Power density < 10 μW/cm^2 for continuous exposure for common public

Health Risk Assessment is still inconclusive – research continued

Conclusion – EMP Exposure

- Effects are mainly due to induced EMF and Current – non-ionizing
- Homoeostasis can not help

- Boeing Professional Standard: 1 kV/m

- ICNIRP Professional Standard: E ~ 1 kV/m, H ~ 5 A/m
  - 10^3 W/m^2 - 600 V/m - 1.5 A/m
  - 10^4 W/m^2 - 2 kV/m - 5 A/m

- IRPA Standard for common public:

Frequency (MHz)	E_{rms} (V/m)	Hrms (A/m)	Power Density (W/m^2)
400 – 2000	3 $f^{0.5}$	0.008 $f^{0.5}$	f/40
2000 – 300000	137	0.36	50

Risk Assessment completely inconclusive – research needed

Conclusion – EMP Exposure

- DEW uses directional antennas.
- The space enclosed by main lobe is of primary concern.
- Only the target along with the pilot are affected
- Common public is not directly exposed by the DEW beam

- Operators may get RF leakage exposure or due to side-lobe radiation
  - Safety garments / protective clothing are prescribed.

- Operators might get mild X-ray exposure
  - Shielding / protective clothing are prescribed.

Thank You

Fast-wave Electromagnetic Methods for Analysing Disc-loaded Circular Waveguides for their Prospective Application in Gyro-Travelling-Wave Tube

Invited Talk by

Vishal Kesari

Microwave Tube Research and Development Centre
Defence Research and Development Orgnisation
Bangalore – 560013, INDIA

Email: vishal_kesari@rediffmail.com
vishalkesari@mtrdc.drdo.in

Technology Gap

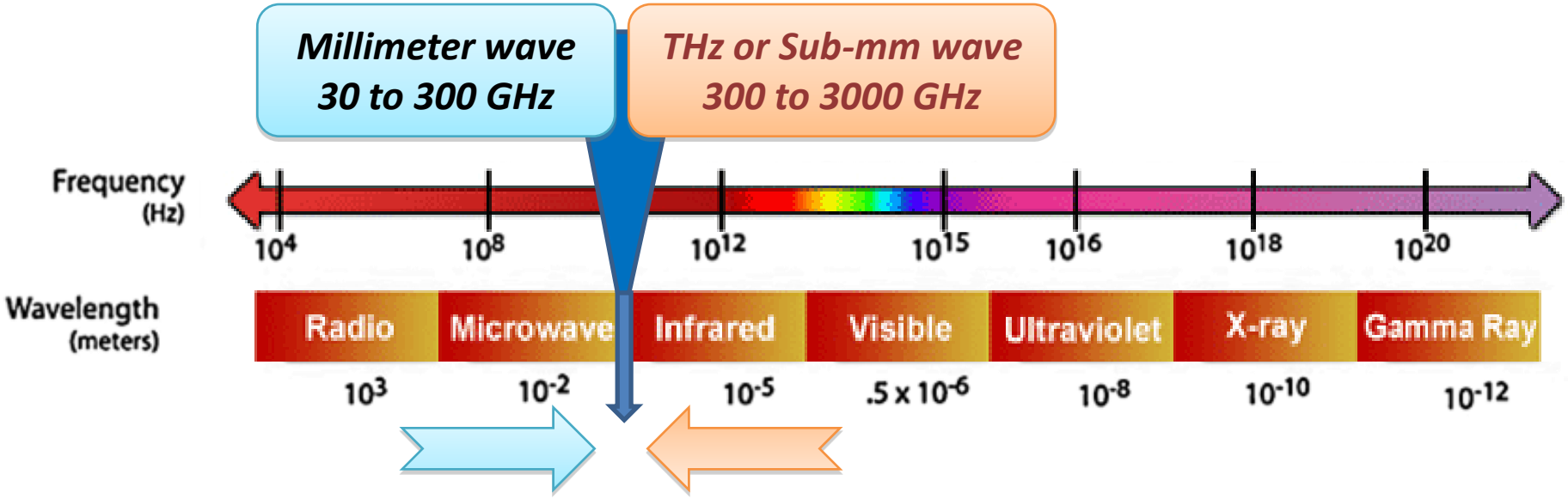

Conventional mi

- Output power
- DC power diss
- RF losses
- Attainable elec
- Heat transfer
- Material break
- Difficulty of fa

Gyro-Devices Filling Technology Gap

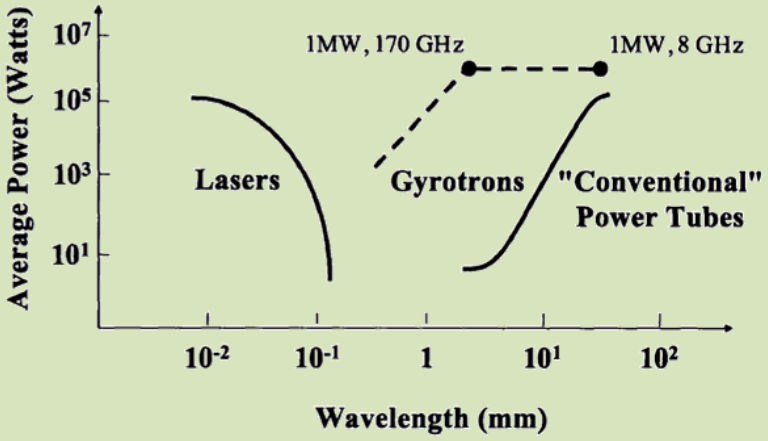

al optical devices

antum reduces and
vailable power from

in the population

Average Power Capability

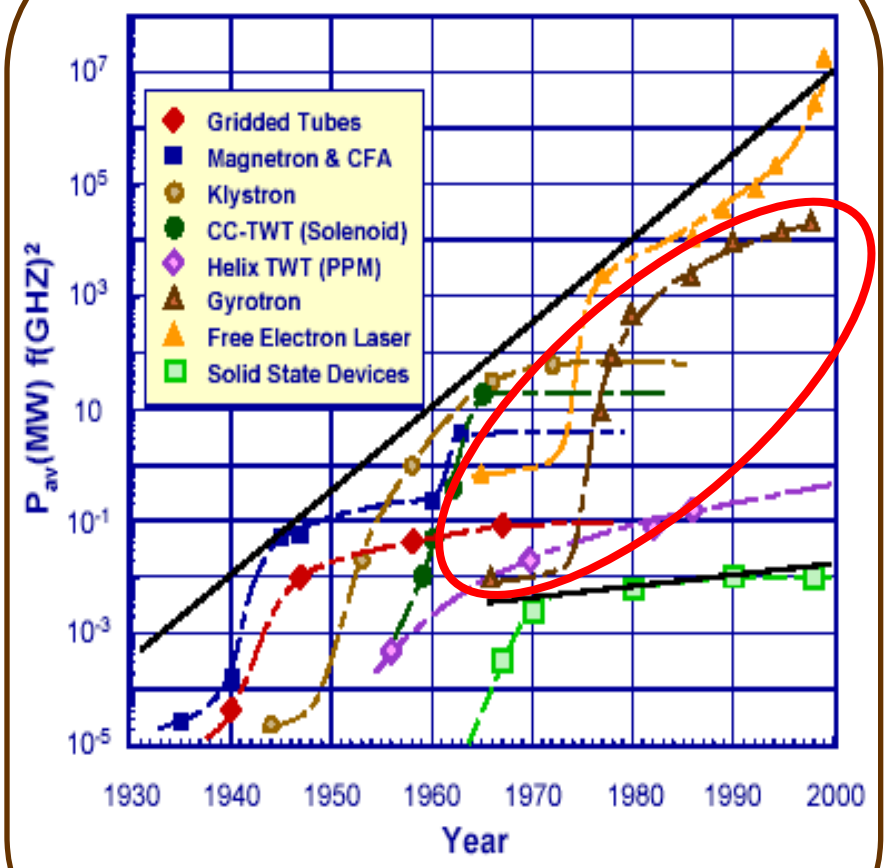

Development

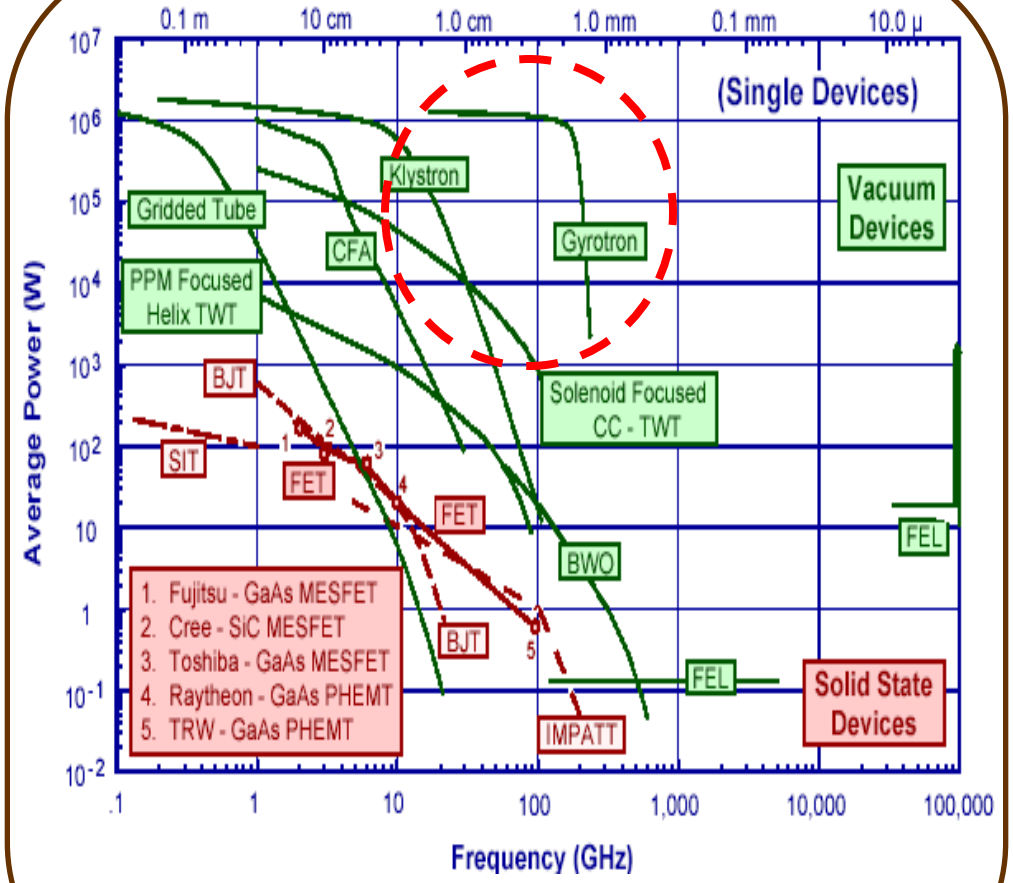

Capability

Historical Development

A Typical Gyro Travelling Wave Tube

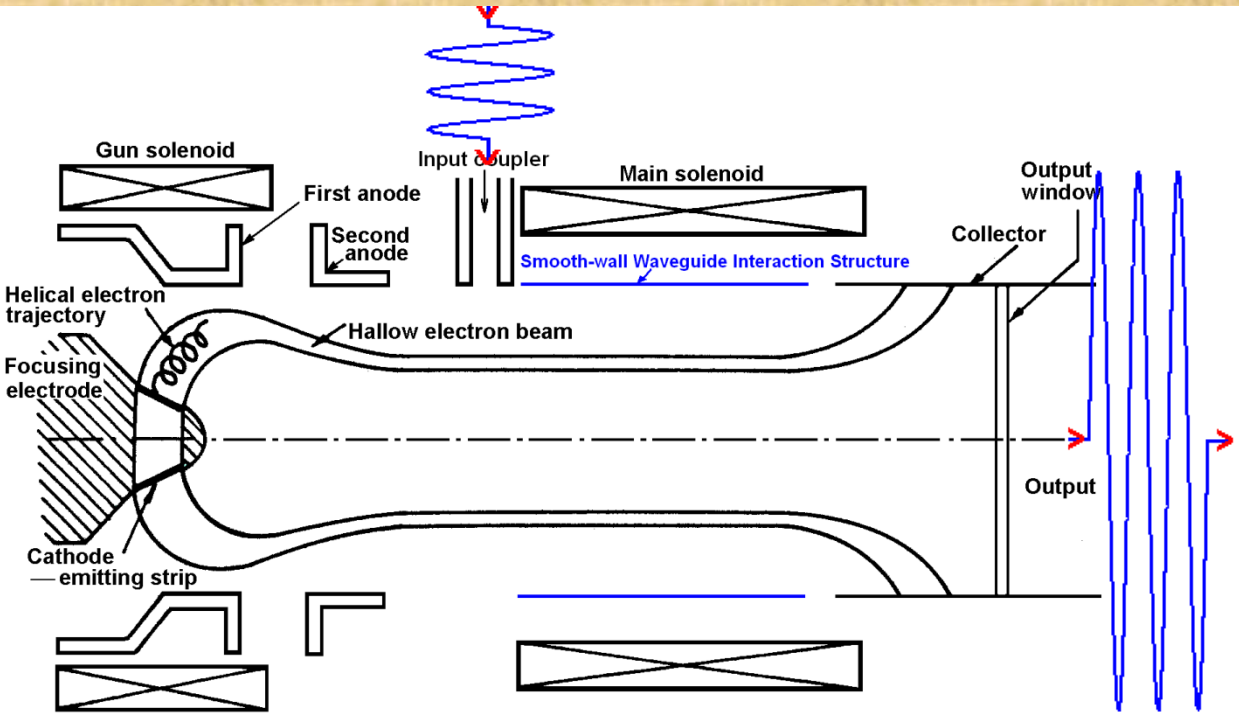

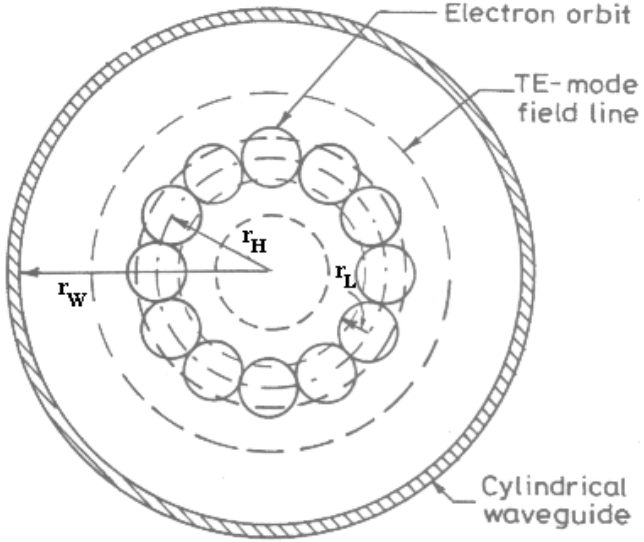

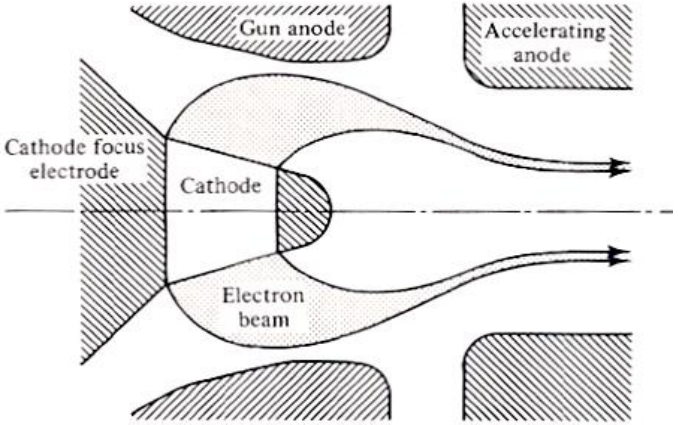

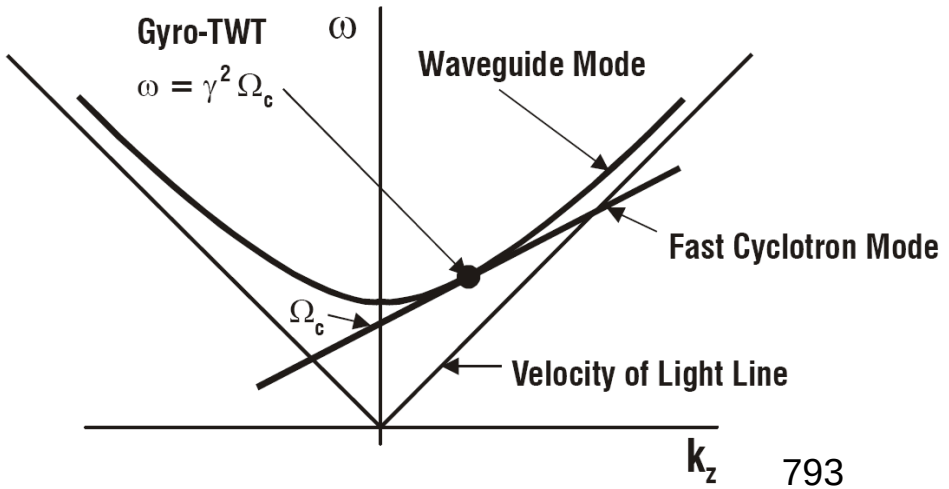

Broadbanding Technique to a Gyro-TWT (1)

Broadbanding through dispersion shaping

- Shape the dispersion characteristics of the interaction structure to coalesce it with beam-mode dispersion line over a wider frequency range, that in turn widens the device bandwidth
  - Can be achieved by different kinds of metal, dielectric, and combined loadings
- Loading the waveguide associates with a shift of waveguide cutoff frequency
  - Can be controlled by varying waveguide radius
- Loading the waveguide increases the amount of azimuthal electric field available for beam-wave interaction and thus azimuthal interaction impedance (sometimes), which increases device gain
- Increasing the beam voltage increases the slope of the beam-mode dispersion line
- Increasing the magnetic field shifts the beam-mode dispersion line up over the frequency axis

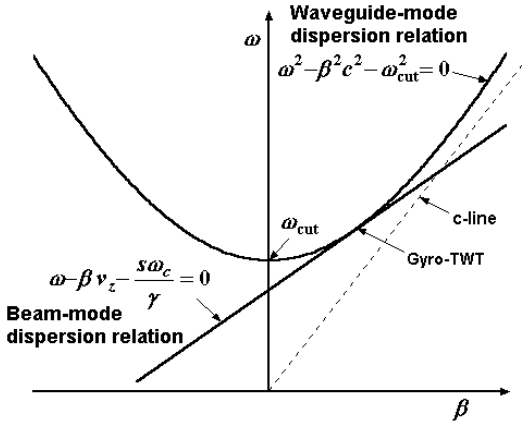

Broadbanding Technique to a Gyro-TWT (2)

Broadbanding by tapering the waveguide cross-section

- Waveguide cross-section varies along the axis
- Different waveguide cross-sections are effective for different frequency values
- Reduced the effective interaction length and thus device gain for each of the frequency
- Required profiled magnetic field for optimum beam-wave synchronism
- Beam parameters, namely, the transverse beam velocity, the Larmor radius, and the hollow-beam radius will vary over the length of the interaction structure
- Required to obey the conservation of electron magnetic moment
  the adiabatic beam-flow condition, and
  the conservation of magnetic flux

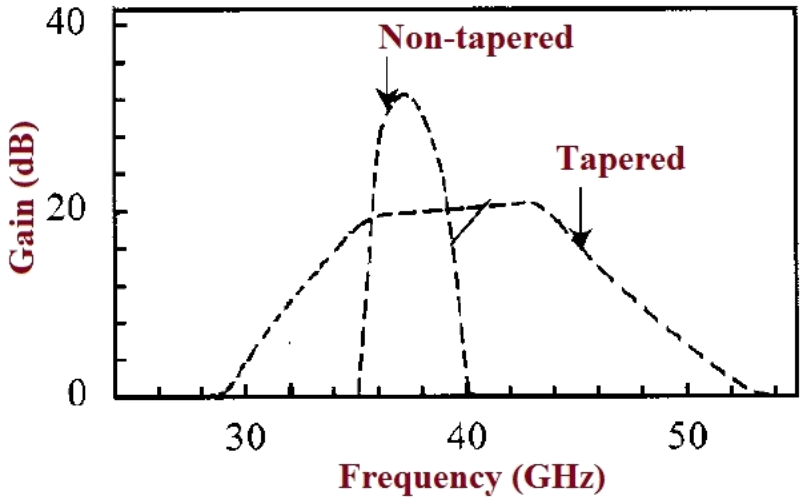

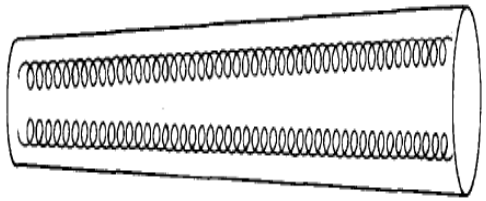

Outline of the today's discussion

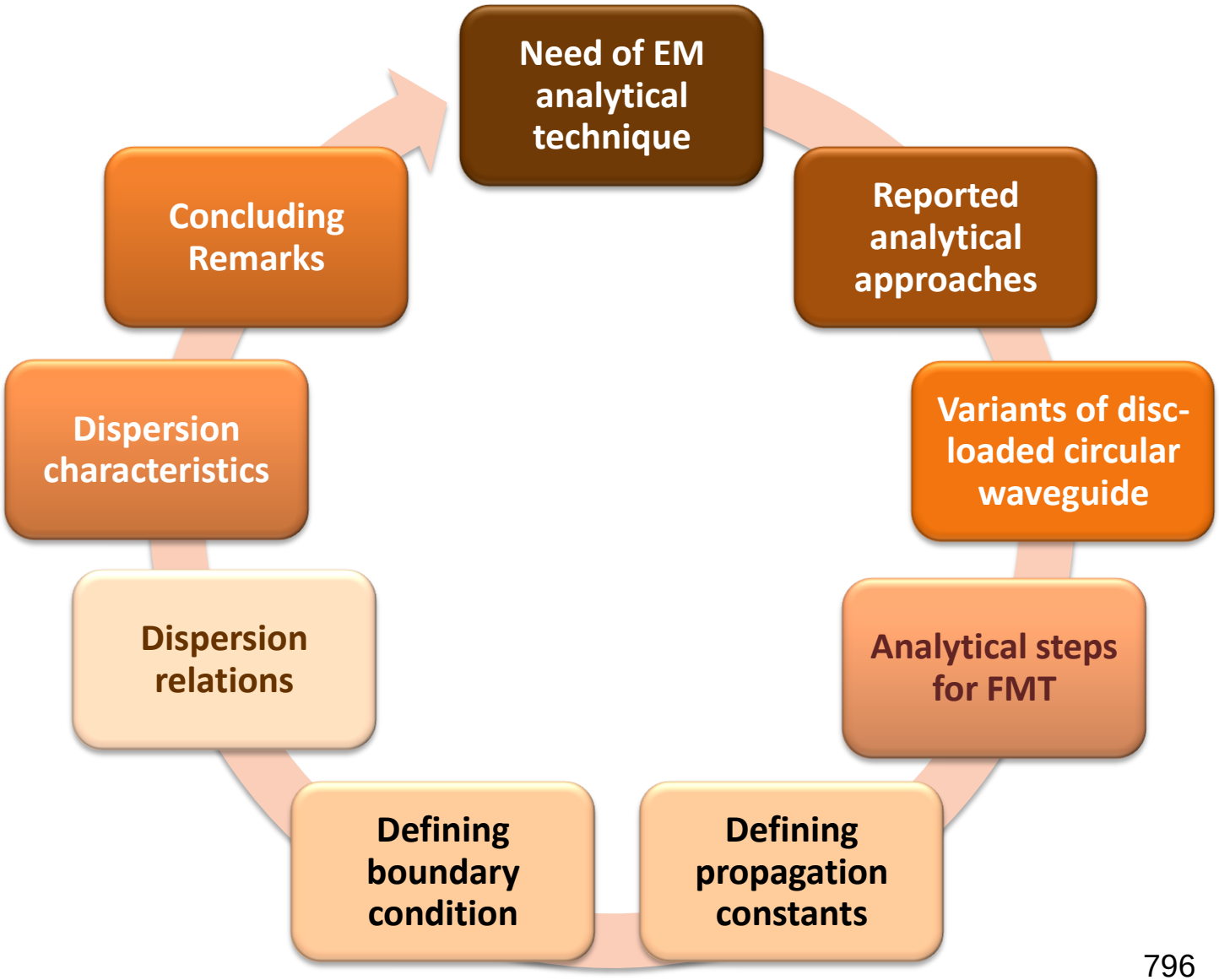

Need of Electromagnetic Analytical Techniques

- To study the behavior of electromagnetic (EM) field or structure
- Gives a straight forward understanding of EM problem
- To obtain the physical understanding of EM phenomenon
- To get closed form expression for EM field
- To explore the insight of actual physical processes
- To get the rigorous analytical solution to EM problem
- To find the precise quantity of interest over a range of parameters

Method of broadbanding a gyro-TWT

Controlling dispersion characteristics of the waveguide for wideband coalescence between the beam-mode and waveguide-mode dispersion characteristics

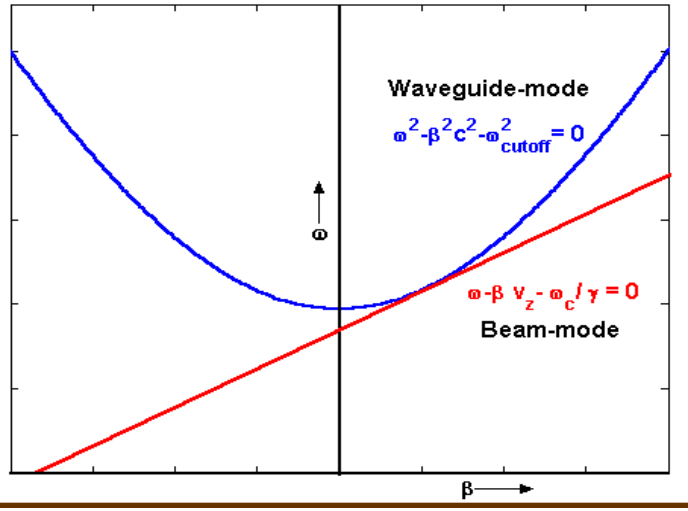

Reported Analytical Approaches for Disc-loaded Waveguide

• *Equivalent circuit approach*	• *Surface admittance model*	• *Galerkin's method*	• *Coupled integral equation approach*	• *Scattering matrix formalism*
Watkins, Slater	Clarricoats and Olver	Scharstein and Adams	Amari *et al.*	Wagner *et al.*
• *Modal field matching technique*	• *Mode matching approach*	• *Transfer matrix and half-cell formulations*	• *Variational technique*	• *Field matching technique*
Hahn	Esteban & Rebollar	Hahn *et al*	Collins, Bevensee	Field, Choe and Uhm

Field Matching Technique

One suitable technique for the problem of a disc-loaded waveguide, in particular for the analysis considering factors of practical relevance, such as higher order harmonics in both the disc-free and disc-occupied regions

Variants of Disc-loaded Circular Waveguide considered

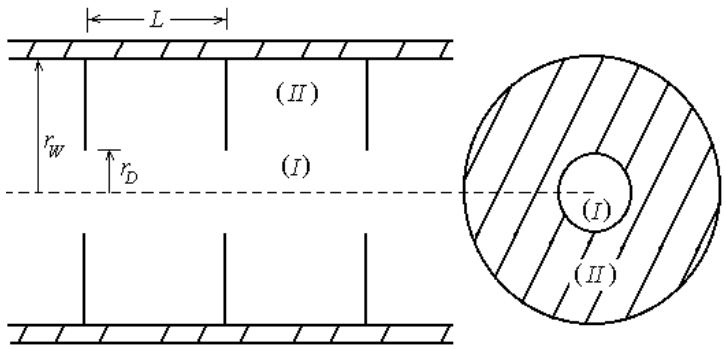

Infinitesimally thin metal disc-loaded circular waveguide

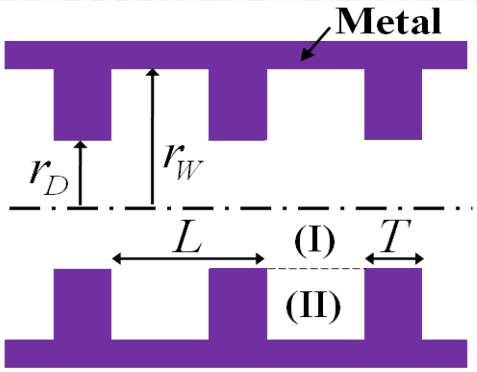

Metal disc-loaded circular waveguide of finite disc-thickness

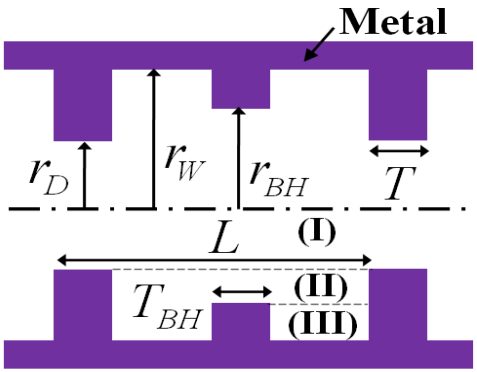

Interwoven-disc-loaded circular waveguide

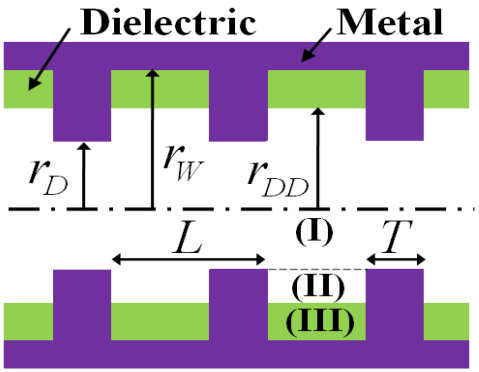

Alternate dielectric and metal disc loaded circular waveguide

Variants of Disc-loaded Circular Waveguide considered

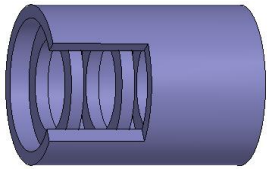

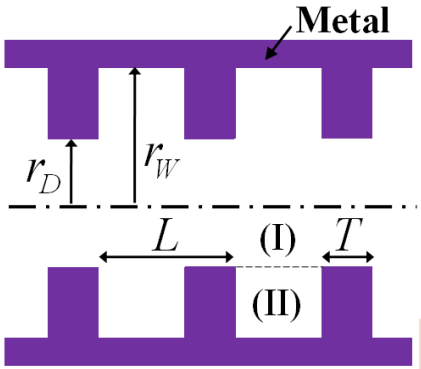

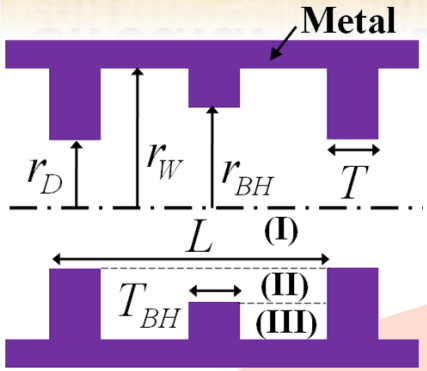

Alternate disc hole radii are varied.

Space between two consecutive metal discs is partly filled with dielectric.

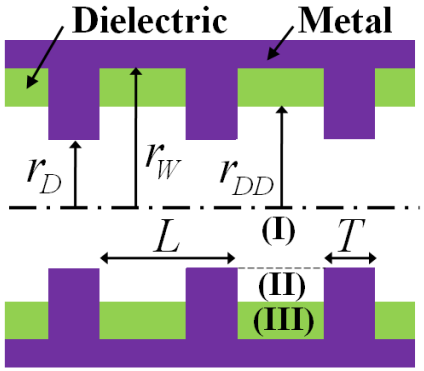

Finite disc thickness is added.

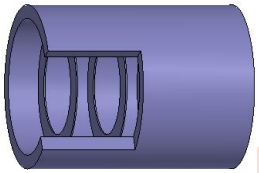

Infinitesimally thin metal disc-loaded circular waveguide

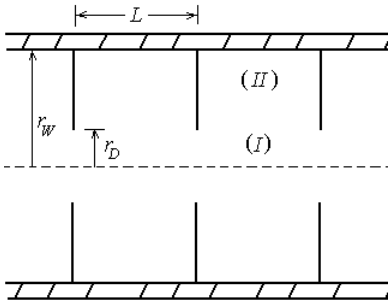

Analytical Steps for Field Matching Technique

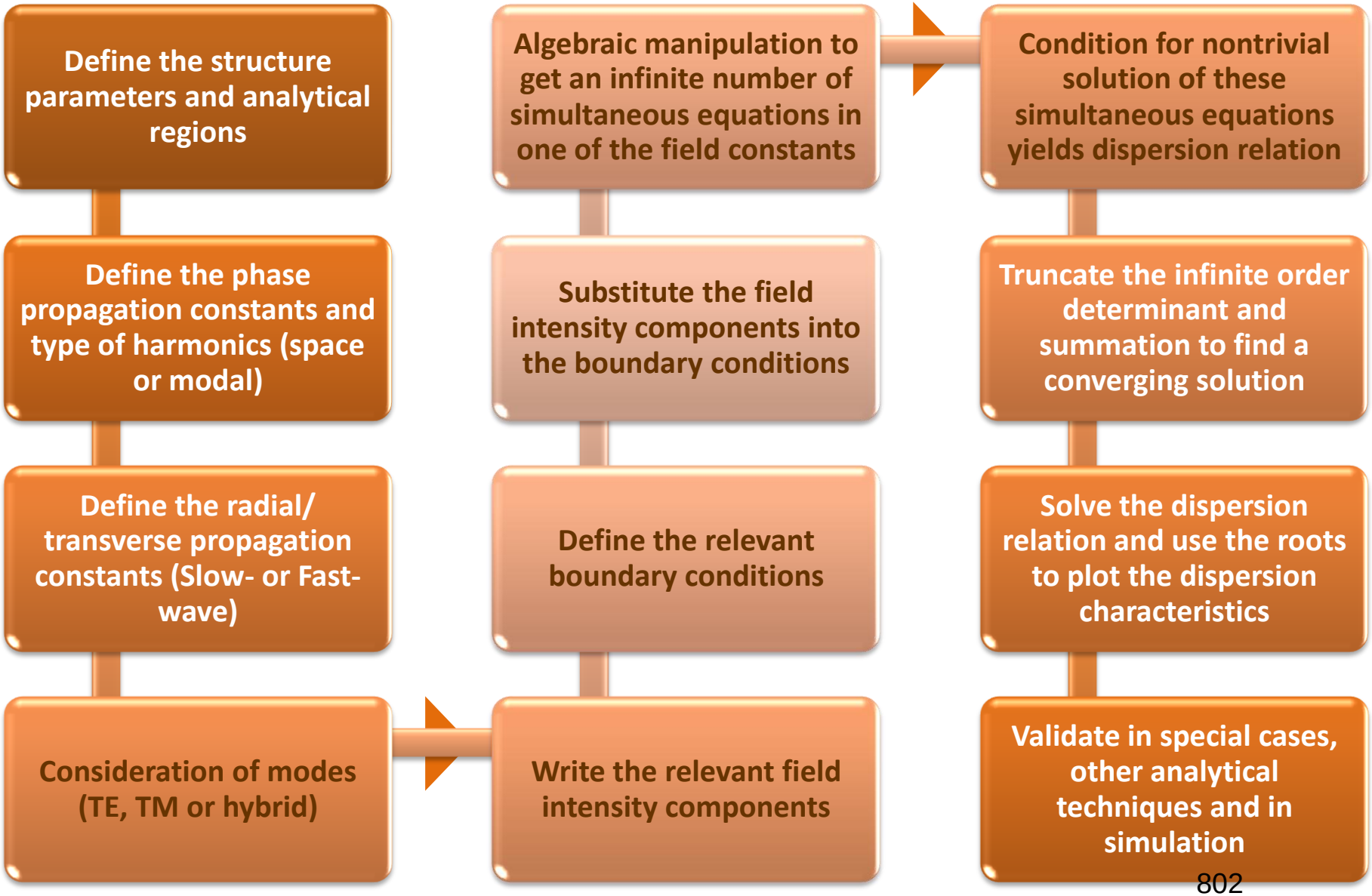

Propagation Constants

Disc-free free-space region

$$\beta_n^I = \beta_0^I + 2\pi n/L, \quad (n = 0, \pm 1, \pm 2, \ldots . \pm \infty)$$

Propagating waves

$$\gamma_n^I = [k^2 - (\beta_n^I)^2]^{1/2}$$

Disc-occupied free-space region

$$\beta_m^{II} = m\pi/(L-T), \quad (m = 1, 2, 3, \ldots . \infty)$$

Standing waves

$$\gamma_m^{II} = [k^2 - (\beta_m^{II})^2]^{1/2}$$

Disc-occupied dielectric region

$$\beta_p^{III} = p\pi/(L-T), \quad (p = 1, 2, 3, \ldots . \infty)$$

Standing waves

$$\gamma_p^{III} = [\varepsilon_r k^2 - (\beta_p^{III})^2]^{1/2}$$

Boundary Conditions

i) Vanishing tangential azimuthal component of electric field at the conducting wall of the waveguide

$$E_\theta = 0$$

ii) Continuity of the axial magnetic field between the regions I and II

$$H_z^I = H_z^{II}$$

iii) Continuity of the azimuthal electric field between the regions I and II

$$E_\theta^I = E_\theta^{II}$$

iv) Vanishing tangential azimuthal component of electric field at the conducting inner circumferential surface of the metal discs

$$E_\theta = 0$$

v) Continuity of the axial magnetic field between the regions II and III

$$H_z^{II} = H_z^{III}$$

vi) Continuity of the azimuthal electric field between the regions II and III

$$E_\theta^{II} = E_\theta^{III}$$

Relevant Field Intensity Components

In region I:

$$H_z^I = \sum_{n=-\infty}^{+\infty} A_n^I J_0\{\gamma_n^I r\} \exp\ j(\omega t - \beta_n^I z)$$

$$E_\theta^I = j\omega\mu_0 \sum_{n=-\infty}^{+\infty} \frac{1}{\gamma_n^I} A_n^I J_0'\{\gamma_n^I r\} \exp\ j(\omega t - \beta_n^I z)$$

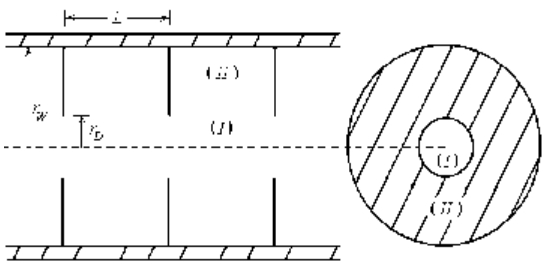

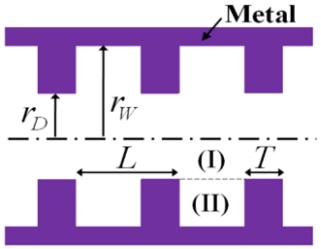

In region II:

$$H_z^{II} = \sum_{m=1}^{\infty} A_m^{II} Z_0\{\gamma_m^{II} r\} \exp(j\omega t) \sin(\beta_m z)$$

$$E_\theta^{II} = j\omega\mu_0 \sum_{m=1}^{\infty} \frac{1}{\gamma_m^{II}} A_m^{II} Z_0'\{\gamma_m^{II} r\} \exp(j\omega t) \sin(\beta_m z)$$

$$Z_0\{\gamma_m^{II} r\} = J_0\{\gamma_m^{II} r\} Y_0'\{\gamma_m^{II} r_W\} - J_0'\{\gamma_m^{II} r_W\} Y_0\{\gamma_m^{II} r\}$$

Relevant Field Intensity Components

In region II:

$$H_z^{II} = \sum_{m=1}^{\infty} [A_m^{II} J_0\{\gamma_m^{II} r\} + B_m^{II} Y_0\{\gamma_m^{II} r\}] \exp(j\omega t) \sin(\beta_m z)$$

$$E_\theta^{II} = j\omega\mu_0 \sum_{m=1}^{\infty} \frac{1}{\gamma_m^{II}} [A_m^{II} J_0'\{\gamma_m^{II} r\} + B_m^{II} Y_0'\{\gamma_m^{II} r\}] \exp(j\omega t) \sin(\beta_m z)$$

In region III:

$$H_z^{III} = \sum_{p=1}^{\infty} A_p^{III} Z_0\{\gamma_p^{III} r\} \exp(j\omega t) \sin(\beta_p z)$$

$$E_q^{III} = jw\mu_0 \sum_{p=1}^{\infty} \frac{1}{g_p^{III}} A_p^{III} Z_0'\{g_p^{III} r\} \exp(jwt) \sin(b_p z)$$

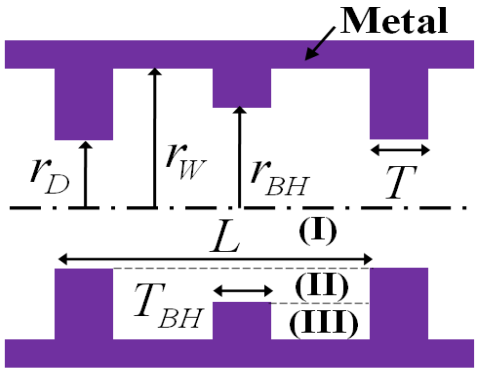

$$Z_0\{\gamma_p^{III} r\} = J_0\{\gamma_p^{III} r\} Y_0'\{\gamma_p^{III} r_W\} - J_0'\{\gamma_p^{III} r_W\} Y_0\{\gamma_p^{III} r\}$$

In region II:

$$H_z^{II} = \sum_{m=1}^{\infty} [A_m^{II} J_0\{g_m^{II} r\} + B_m^{II} Y_0\{g_m^{II} r\}] \exp(jwt) \sin(b_m z)$$

$$E_q^{II} = jw\mu_0 \sum_{m=1}^{\infty} \frac{1}{g_m^{II}} [A_m^{II} J_0'\{g_m^{II} r\} + B_m^{II} Y_0'\{g_m^{II} r\}] \exp(jwt) \sin(b_m z)$$

In region III:

$$H_z^{III} = \sum_{m=1}^{\infty} A_m^{III} Z_0\{g_m^{III} r\} \exp(jwt) \sin(b_m z)$$

$$E_q^{III} = jw\mu_0 \sum_{m=1}^{\infty} \frac{1}{g_m^{III}} A_m^{III} Z_0'\{g_m^{III} r\} \exp(jwt) \sin(b_m z)$$

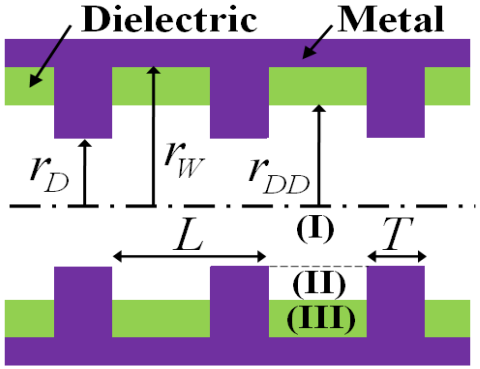

$$Z_0\{g_m^{III} r\} = J_0\{g_m^{III} r\} Y_0'\{g_m^{III} r_W\} - J_0'\{g_m^{III} r_W\} Y_0\{g_m^{III} r\}$$

Dispersion Relation for the Variants

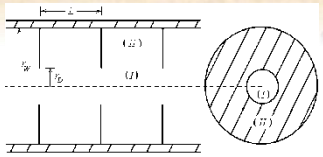

Infinitesimally thin metal disc

$$\det\left|\frac{1}{(\beta_m^{II})^2-(\beta_n^{I})^2}\left[\frac{1}{\gamma_n^{I}}\frac{J_0'\{\gamma_n^{I}r_D\}}{Z_0'\{\gamma_m^{II}r_D\}}-\frac{1}{\gamma_m^{II}}\frac{J_0\{\gamma_n^{I}r_D\}}{Z_0\{\gamma_m^{II}r_D\}}\right]\right|=0$$

$$Z_0\{g_m^{II}r\}=J_0\{g_m^{II}r\}Y_0'\{g_m^{II}r_W\}-J_0'\{g_m^{II}r_W\}Y_0\{g_m^{II}r\}$$

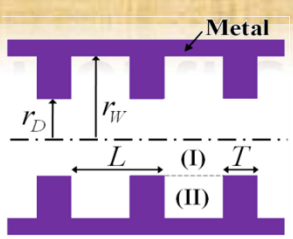

Finite disc-thickness

$$\det\left|M_{nm}J_0\{g_n^{I}r_D\}Z_0'\{g_m^{II}r_D\}-Z_0\{g_m^{II}r_D\}J_0'\{g_n^{I}r_D\}\right|=0$$

$$M_{nm}=\frac{g_n^{I}b_m^{II}\left(1-(-1)^m\exp[-jb_n^{I}(L-T)]\right)}{g_m^{II}[b_m^{II}-\exp(-jb_0^{I}L)(b_m^{II}\cos(b_m^{II}L)+jb_n^{I}\sin(b_m^{II}L))]}$$

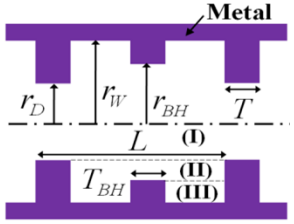

Interwoven-disc

$$\det\left|M_{nm}J_0\{\gamma_n^{I}r_D\}[J_0'\{\gamma_m^{II}r_D\}+\xi Y_0'\{\gamma_m^{II}r_D\}]-J_0'\{\gamma_n^{I}r_D\}[J_0\{\gamma_m^{II}r_D\}+\xi Y_0\{\gamma_m^{II}r_D\}]\right|=0$$

$$x=\frac{g_p^{III}J_0'\{g_m^{II}r_{BH}\}Z_0\{g_m^{III}r_{BH}\}-g_m^{II}J_0\{g_m^{II}r_{BH}\}Z_0'\{g_m^{III}r_{BH}\}}{g_m^{II}Y_0\{g_m^{II}r_{BH}\}Z_0'\{g_m^{III}r_{BH}\}-g_m^{III}Y_0'\{g_m^{II}r_{BH}\}Z_0\{g_m^{III}r_{BH}\}}$$

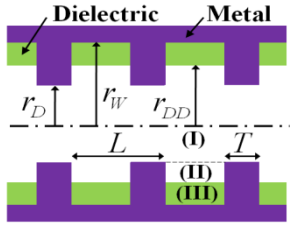

Alternate dielectric and metal disc

$$\det\left|M_{nm}J_0\{\gamma_n^{I}r_D\}[J_0'\{\gamma_m^{II}r_D\}+\xi Y_0'\{\gamma_m^{II}r_D\}]-J_0'\{\gamma_n^{I}r_D\}[J_0\{\gamma_m^{II}r_D\}+\xi Y_0\{\gamma_m^{II}r_D\}]\right|=0$$

$$x=\frac{g_m^{III}J_0'\{g_m^{II}r_{DD}\}Z_0\{g_m^{III}r_{DD}\}-g_m^{II}J_0\{g_m^{II}r_{DD}\}Z_0'\{g_m^{III}r_{DD}\}}{g_m^{II}Y_0\{g_m^{II}r_{DD}\}Z_0'\{g_m^{III}r_{DD}\}-g_m^{III}Y_0'\{g_m^{II}r_{DD}\}Z_0\{g_m^{III}r_{DD}\}}$$

Dispersion Characteristics of Variant-1

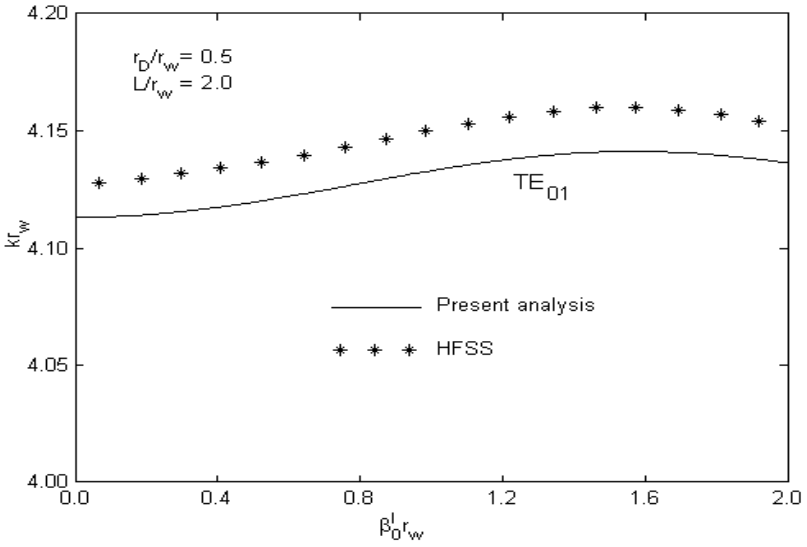

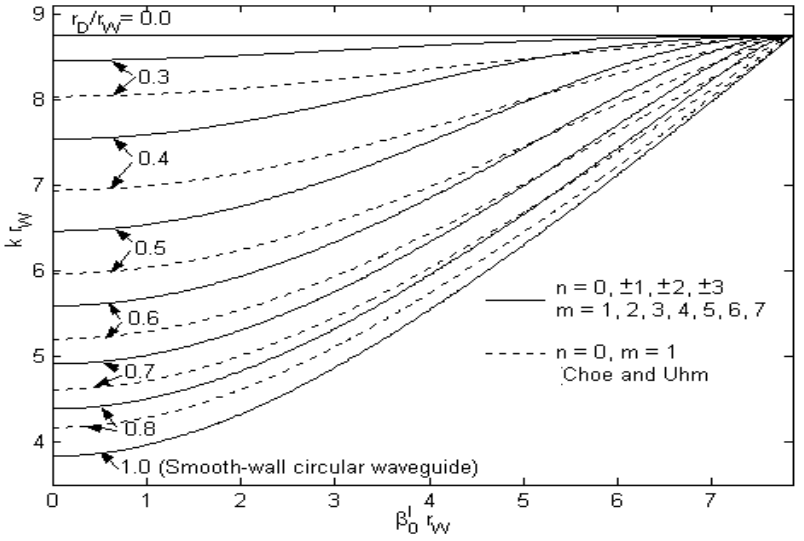

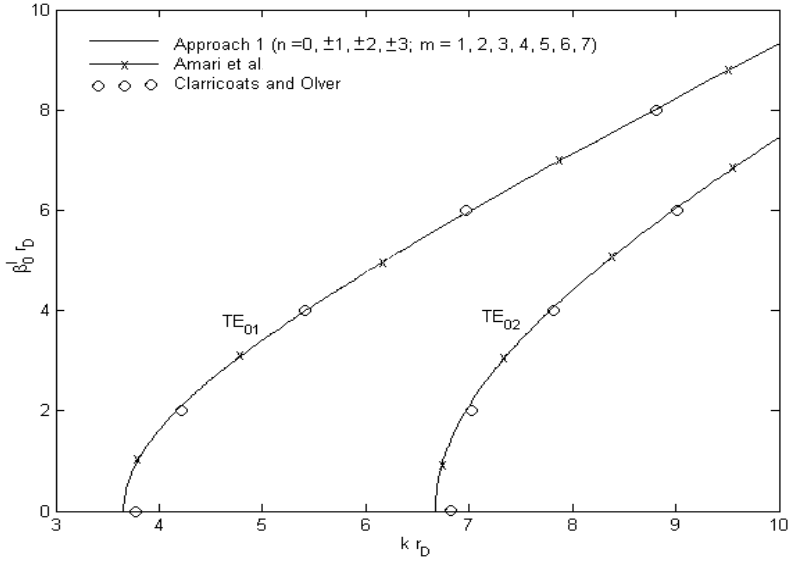

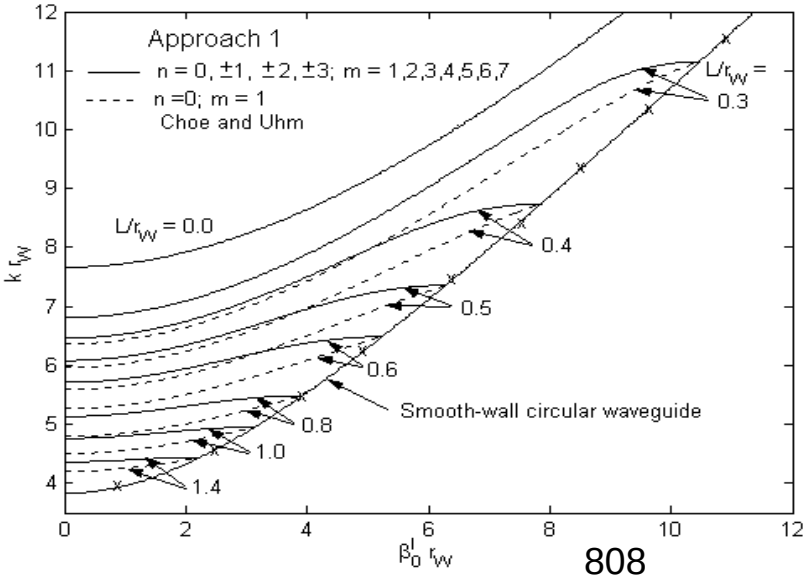

Dispersion Characteristics of Variant-2

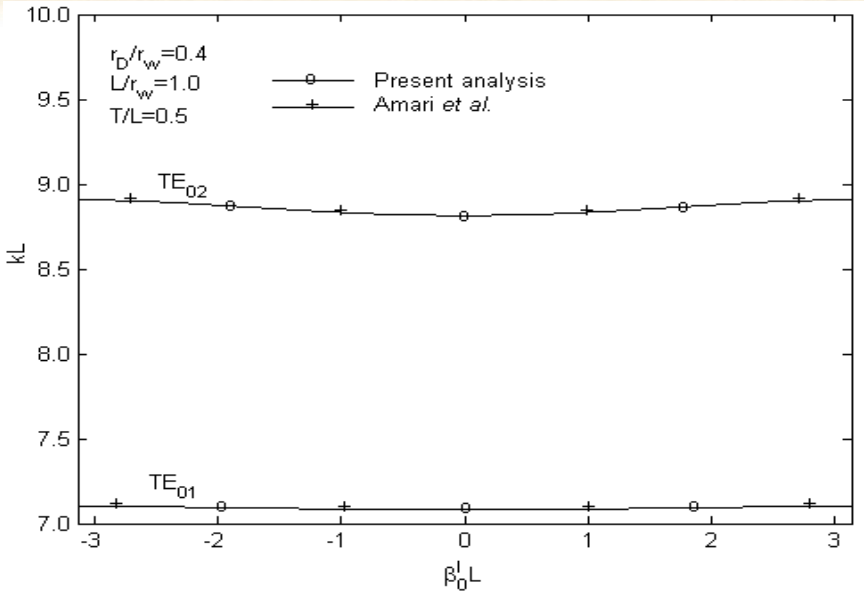

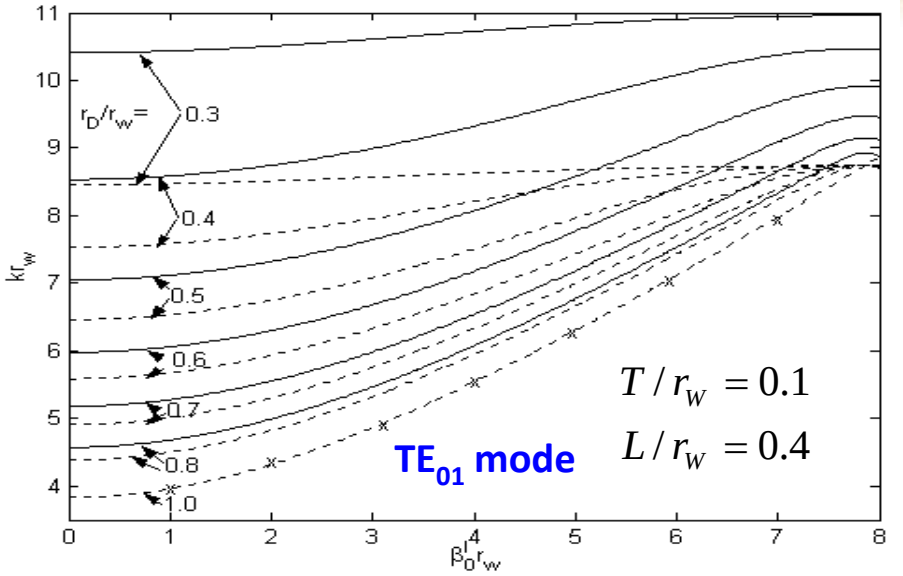

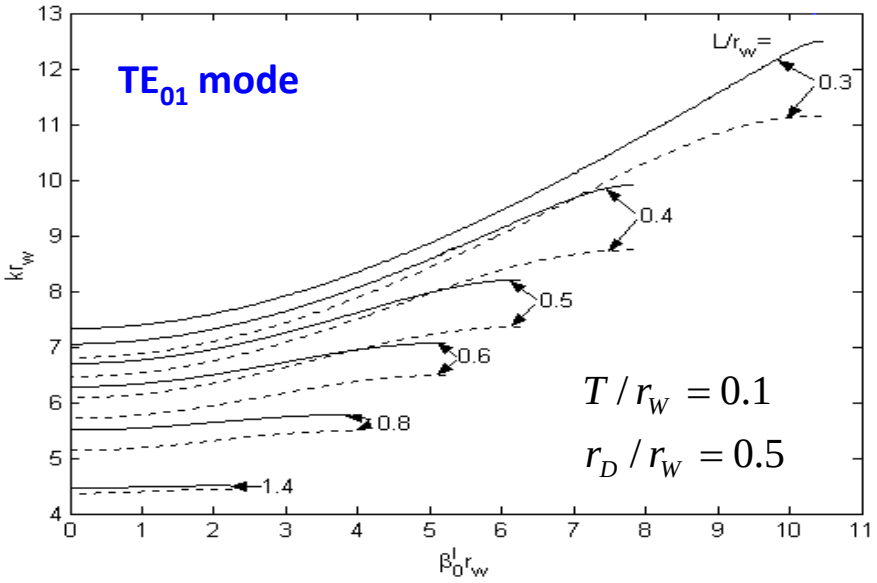

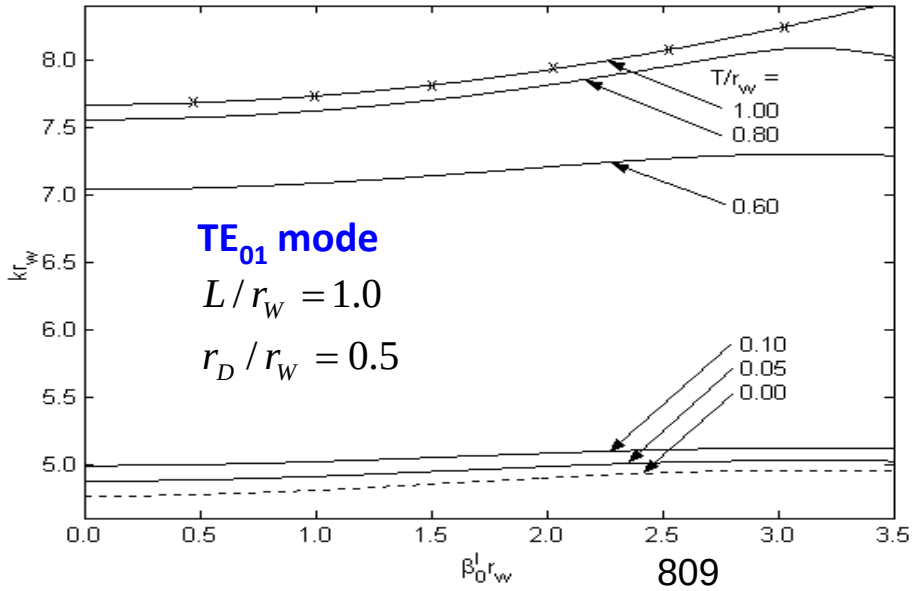

Dispersion Characteristics of Variant-3

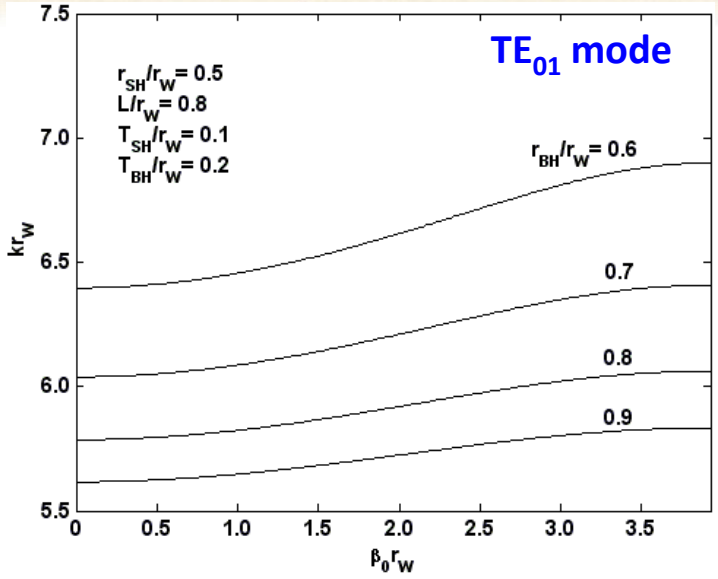

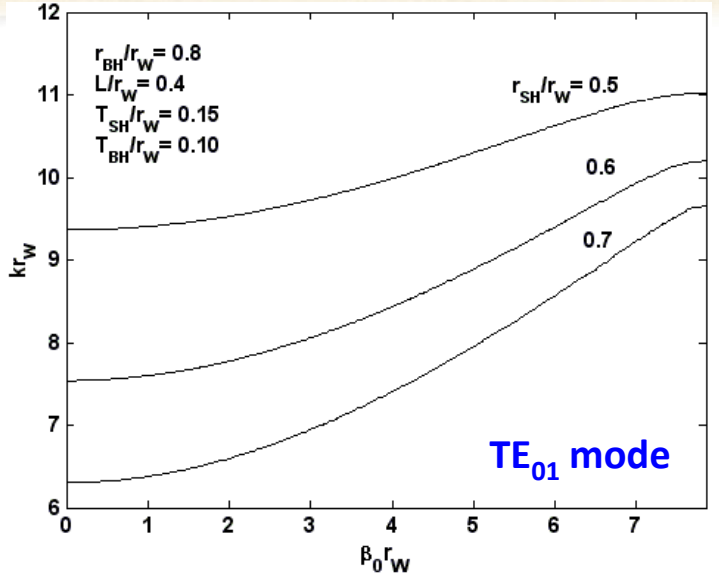

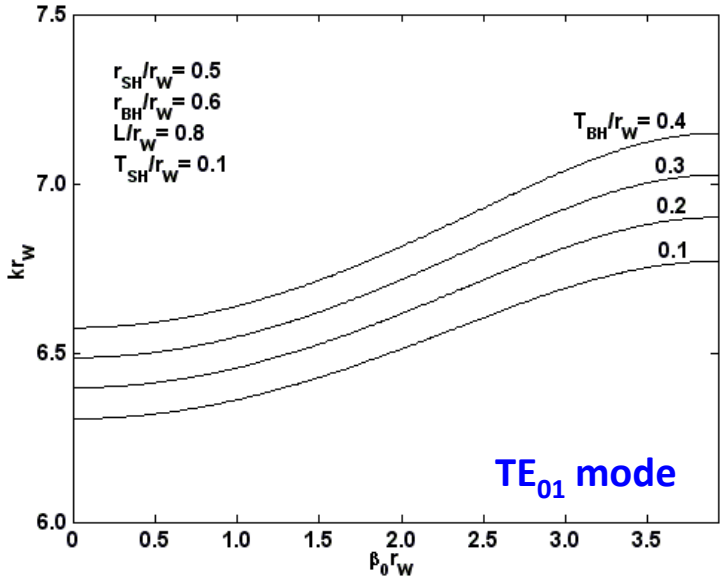

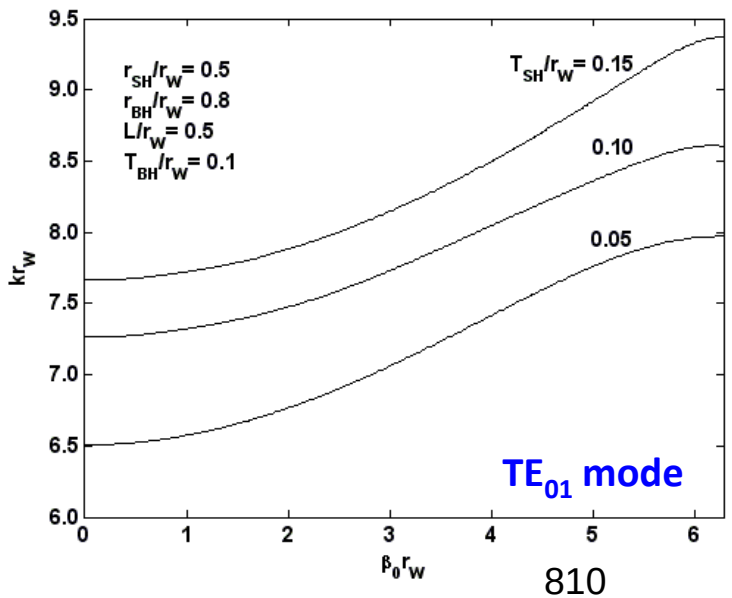

Dispersion Characteristics of Variant-3

Contd…

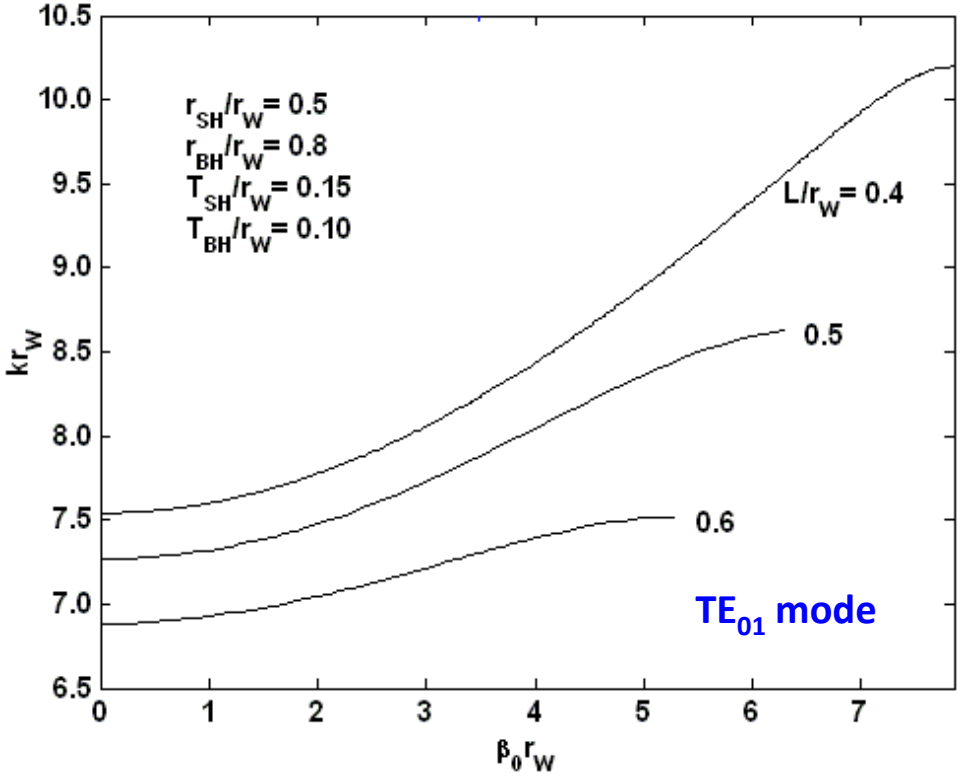

Dispersion Characteristics of Variant-4

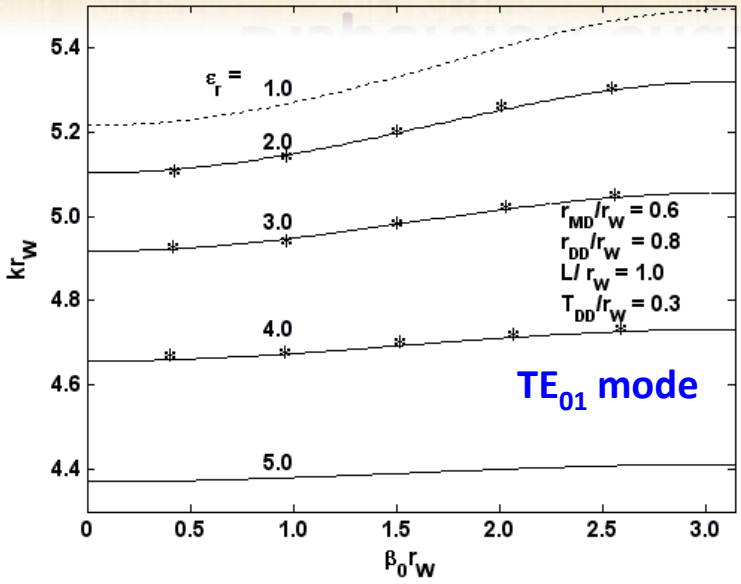

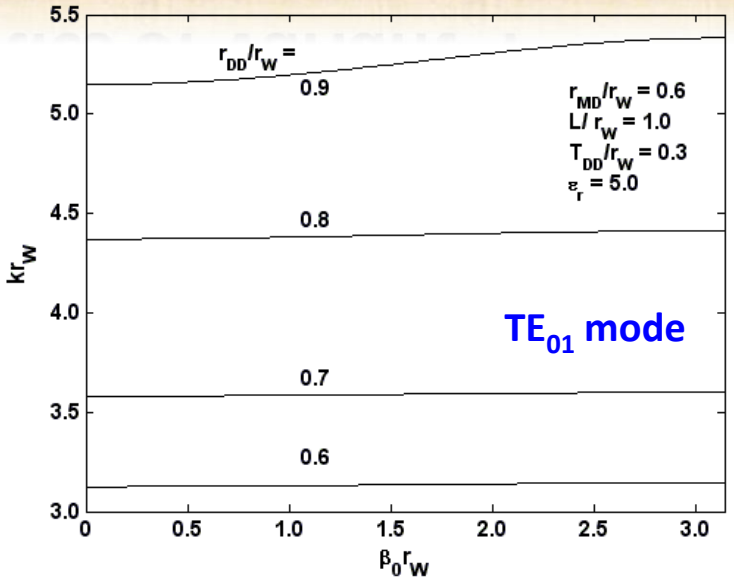

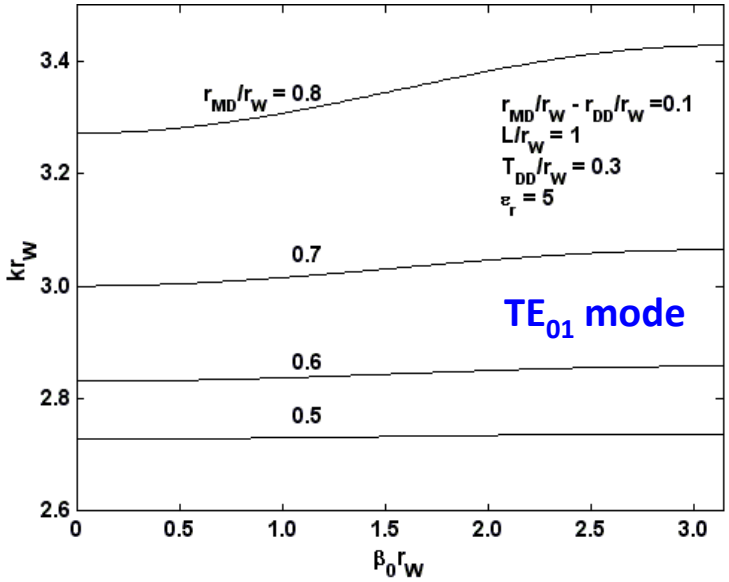

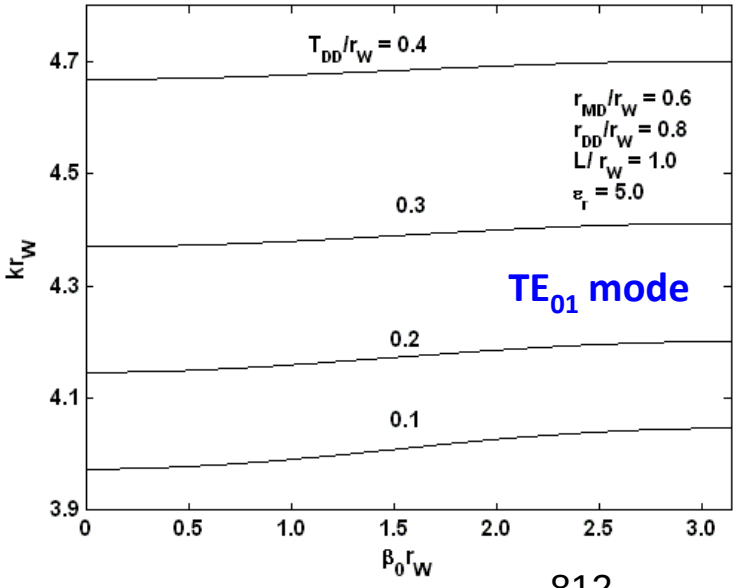

Dispersion Characteristics of Variant-4

Contd…

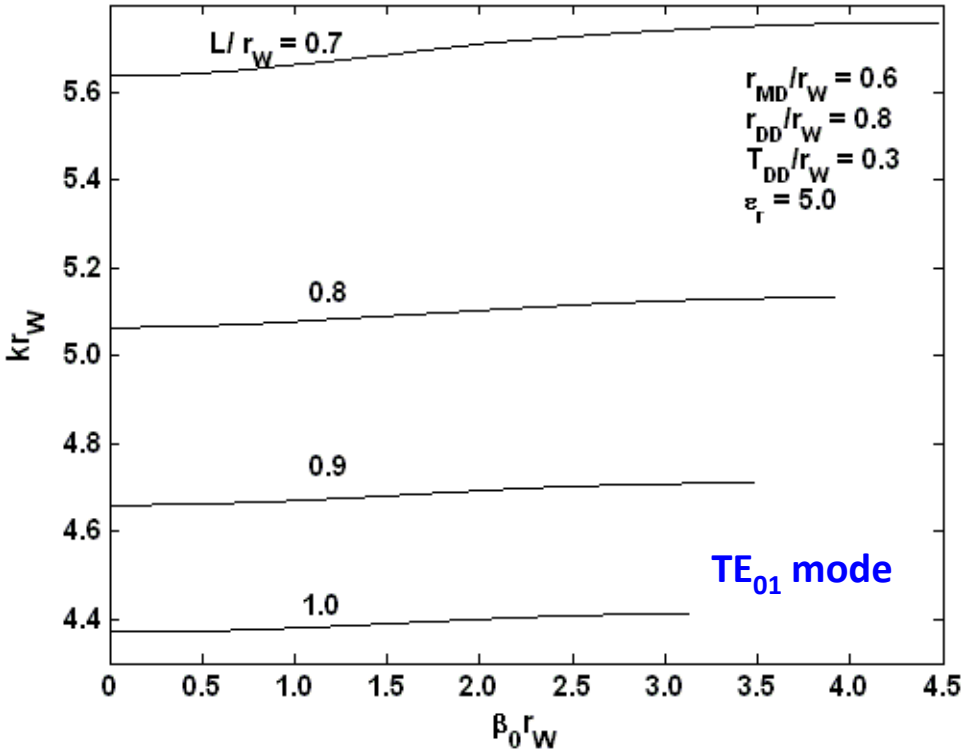

Conclusion

- Field matching technique was discussed for four variants of the disc-loaded circular waveguide.
- Technique includes the effect of higher order space harmonics.
- Dispersion relations were obtained.
- Dispersion relations are solved numerically for their solutions.
- Dispersion characteristics were plotted.
- Effect of structure parameters on dispersion characteristics were studied.
- For each variant of the disc-loaded waveguide the structure periodicity is the most sensitive parameter for dispersion shaping.
- Dispersion shaping may be utilized to obtain a wideband coalescence between waveguide- and beam-mode dispersion characteristics that would result in wideband gyro-TWT performance.

Acknowledgement

- Vice Chancellor, Dr. A.P.J. Abdul Kalam Technical University Uttar Pradesh for guest lecture invitation
- Professor BN Basu for planning and coordinating Faculty Development Programme on Advances in Microwave Engineering
- Dr. Rajiv Kumar Singh for his liaising efforts

Thanks!

http://vishalkesari.webnode.com

vishal_kesari@rediffmail.com

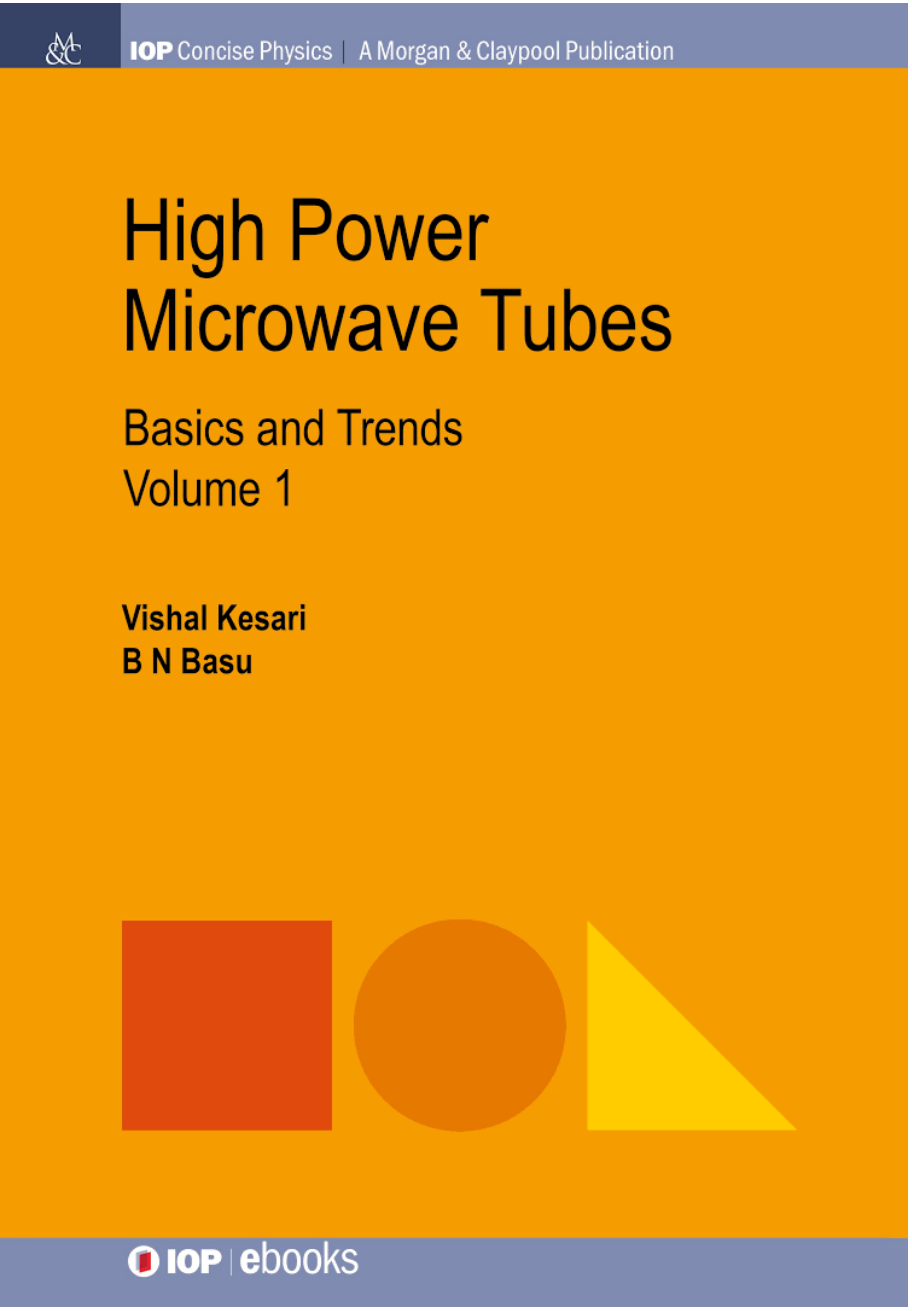
IOP Concise Physics | A Morgan & Claypool Publication
High Power Microwave Tubes
Basics and Trends
Volume 1
Vishal Kesari
B N Basu
IOP | ebooks

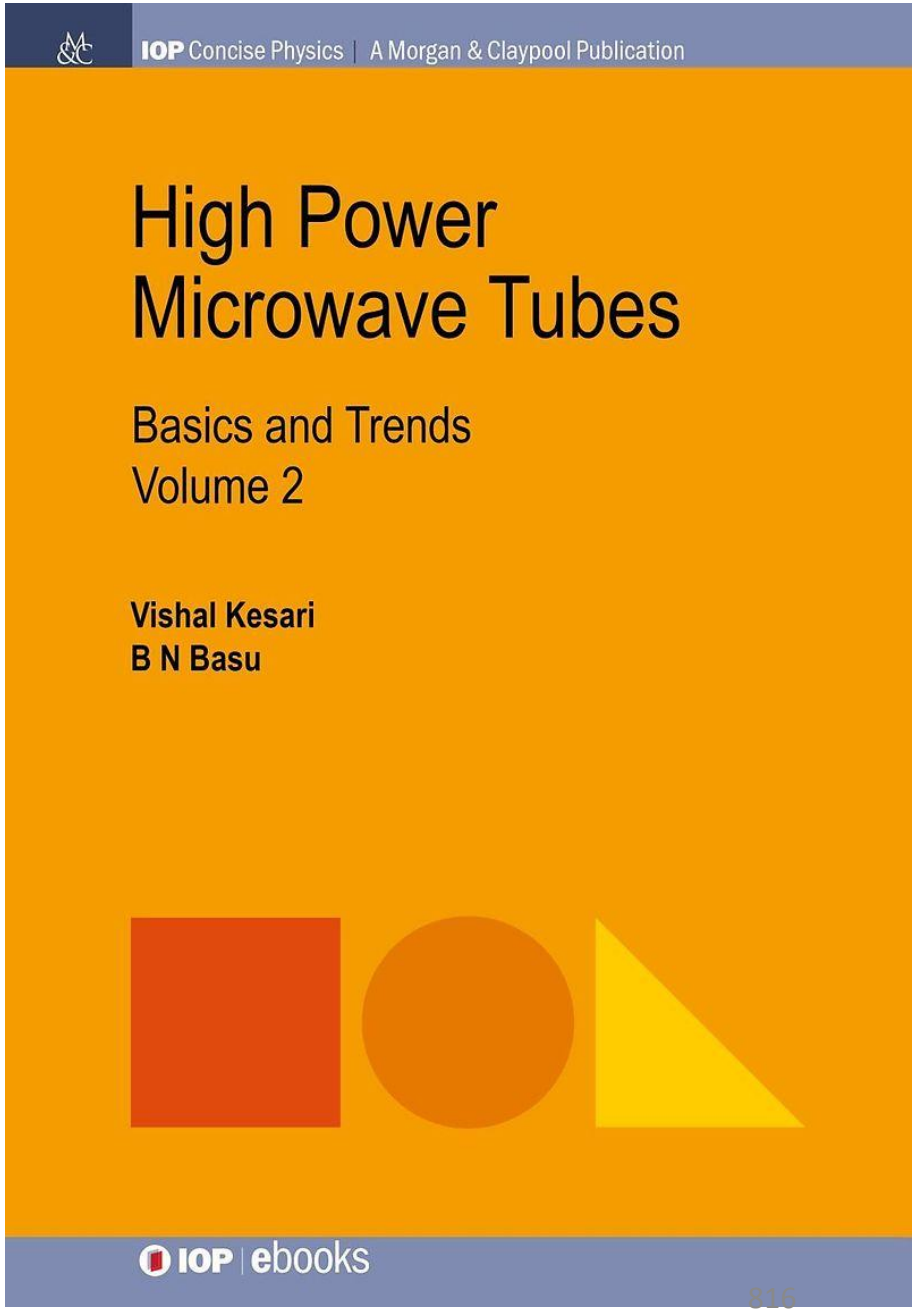
IOP Concise Physics | A Morgan & Claypool Publication
High Power Microwave Tubes
Basics and Trends
Volume 2
Vishal Kesari
B N Basu
IOP | ebooks

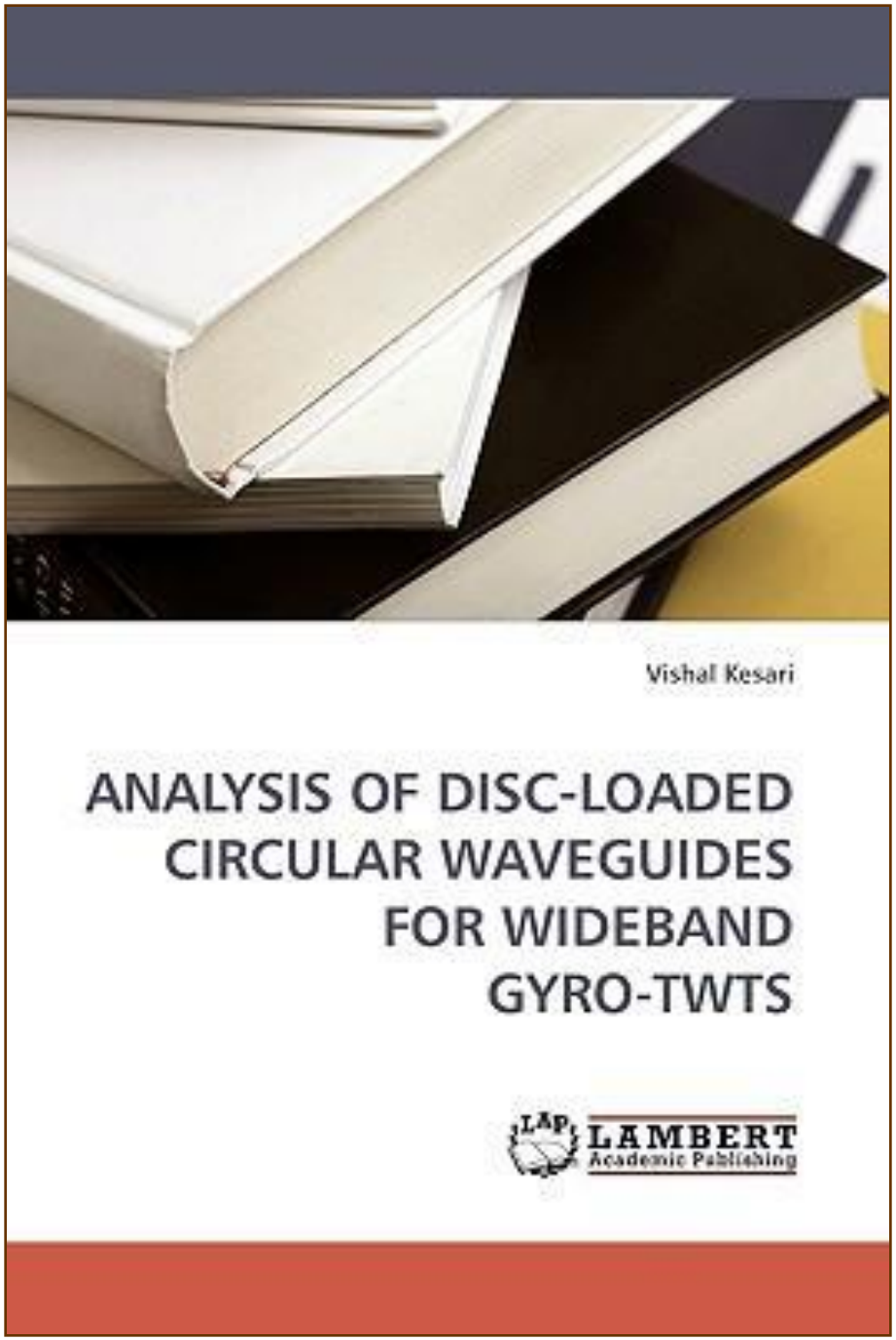
Vishal Kesari
ANALYSIS OF DISC-LOADED CIRCULAR WAVEGUIDES FOR WIDEBAND GYRO-TWTS
LAP LAMBERT Academic Publishing

THERMAL MANAGEMENT OF MICROWAVE TUBES SHARING THE ANSYS SIMULATION EXPERIENCE

By:
Dr. VISHANT GAHLAUT
Assistant Professor
Banasthali Vidyapith
Banasthali, Rajasthan-304022

OUTLINES

- Introduction
  - Microwave tubes (TWT)
  - Applications, Features of Space TWTs
- Thermal Management for TWTs
  - Need for Thermal Analysis
  - Importance of Thermal-Structural Analysis
- Thermal-Structural Analysis of Sub-Assemblies of TWTs
  - Electron Gun
  - Slow Wave Structure
  - Coupler
  - Collector
- Thermal Management for Gyrotron
  - Importance of Thermal-Structural Analysis
- Thermal-Structural Analysis of Components of Gyrotron
  - Cavity
  - Collector
- Conclusion
- References

TRAVELLING WAVE TUBE (TWT)

- **Used as a high frequency, high gain microwave amplifier in satellite transponders**
- **Advantages : Wide bandwidth, high linearity and reliability**

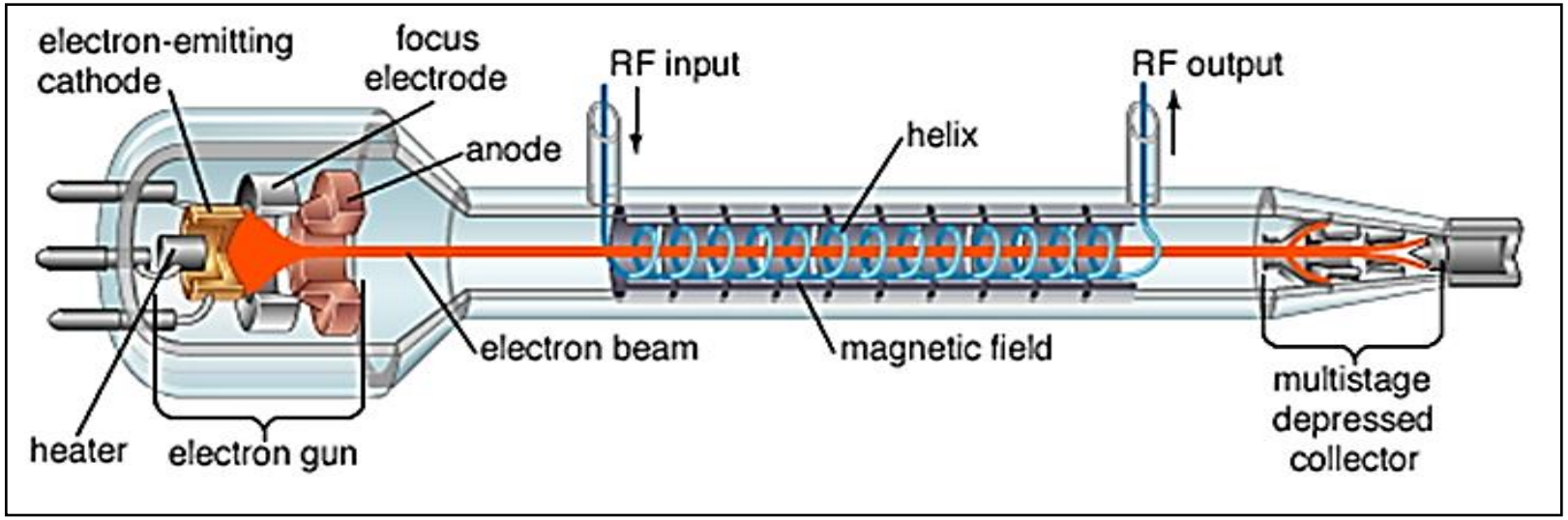

MAJOR APPLICATION AREAS OF TWTs

- **Space**
- Radar
- Electronic Counter Measure
- Driver for other high power RF amplifiers

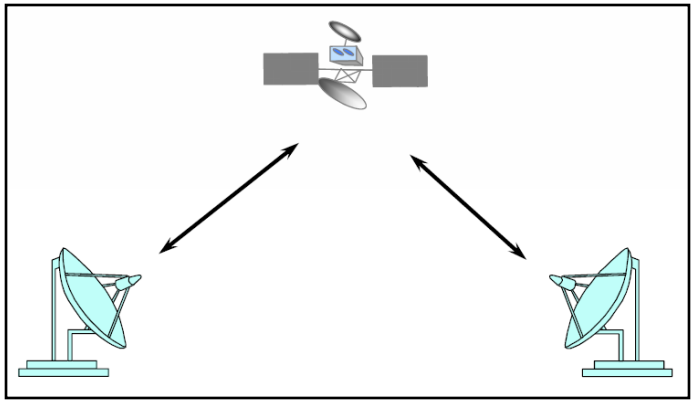

FEATURES OF SPACE TWTs

Size & weight

- Reduction in size and weight reduces launching cost

Life & reliability

- Expected to work for more than 10 years without any deterioration in performance or failure
- For long life, cathode needs to emit required current density throughout the life

Efficiency

- Very high efficiency requirement of space TWT also has direct relevance with the size and weight of the TWT

NEED OF THERMAL MANAGEMENT

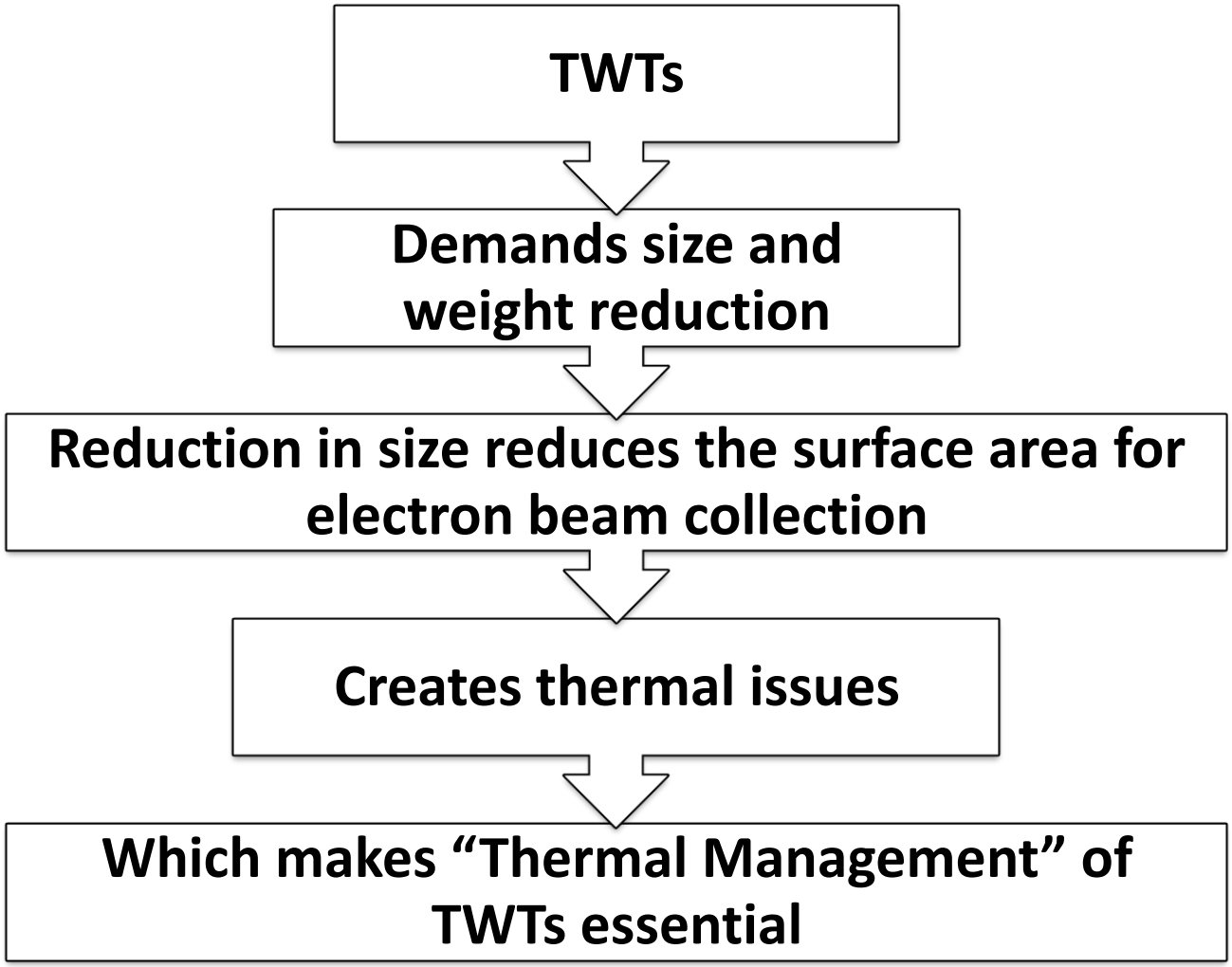

IMPORTANCE OF THERMAL-STRUCTURAL ANALYSIS

Thermal analysis : Temperature distribution

- Cooling arrangement is restricted due to restriction of weight
- Needs proper thermal management of constituent elements, such that there would not be any deformation in structure which leads to destruction of TWT

Structural analysis : Deformations and Stresses in structure

- TWT consists of several brazing joints between metal to metal and metal to ceramic insulators
- Stresses at different brazing joints are important factors to study

TWTs for space application, needs thorough analysis before putting into the space. Unlike TWTs for ground application, it can not be replaced, in case of any failure. This motivates me to select it as the topic for research.

THERMAL-STRUCTURAL ANALYSIS OF DIFFERENT SUB-ASSEMBLIES OF TWTs

ELECTRON GUN

Cathode, when heated, emits continuous electron beam.

Cathode has to give uniform current density throughout the life of the TWT.

For long life and reliable TWT, a cathode needs to be operated at lower temperature and, hence, proper heat shielding from cathode is important.

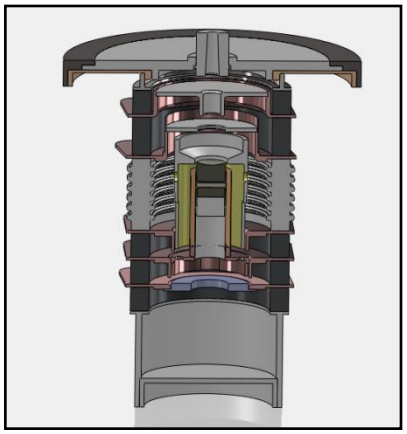

Heat shield for cathode plays most important role in minimizing drainage of cathode power.

Electron gun consisting of several brazing joints, hence, demand for proper thermal and structural analysis.

Hence, attention has been given to study the effect of heat shield on thermal management for different material properties, different thickness, etc.

THERMAL MODELING OF ELECTRON GUN

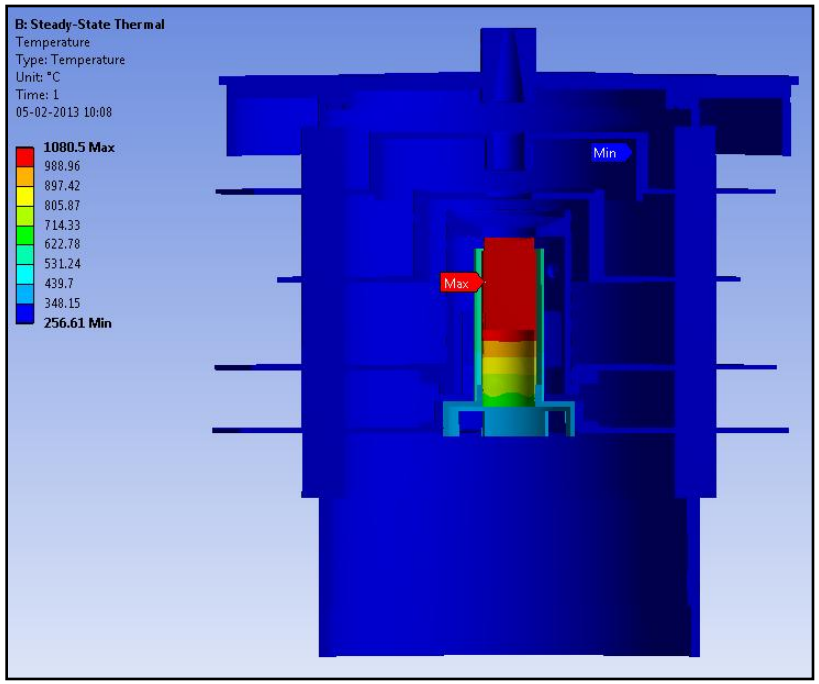

Temperature distribution in Electron Gun assembly

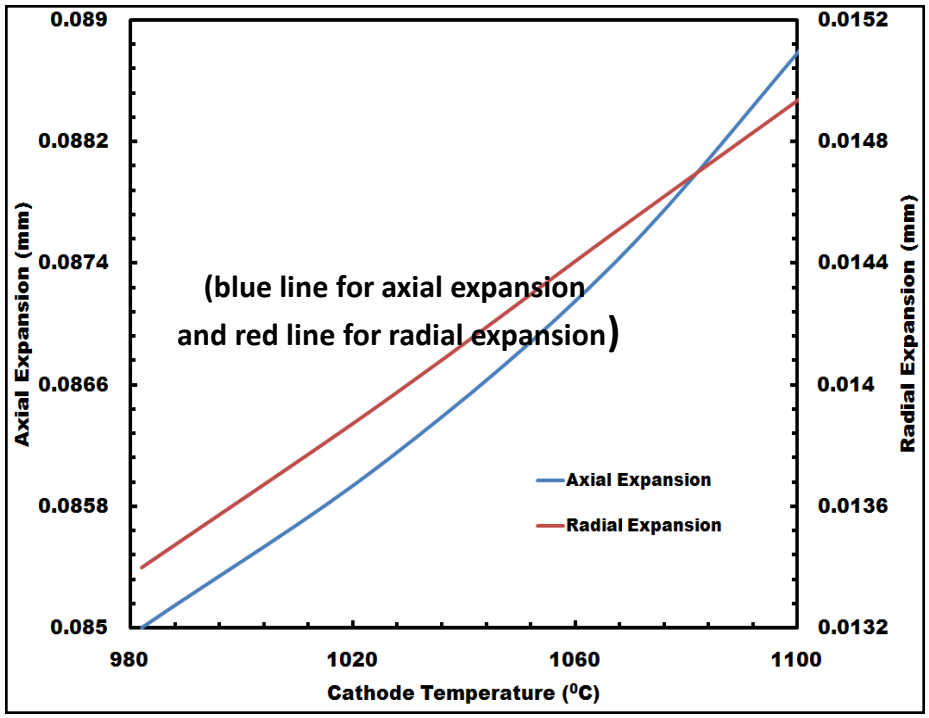

Expansion of Cathode Surface With the Increase in Temperature

COMPARISON OF EXPERIMENTAL AND SIMULATED CATHODE TEMPERATURE

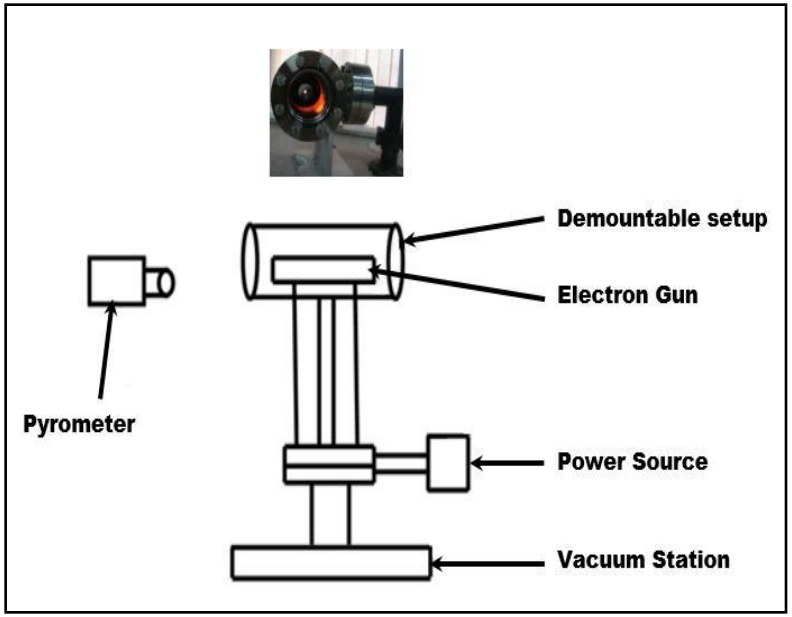

Experimental setup for temperature measurement

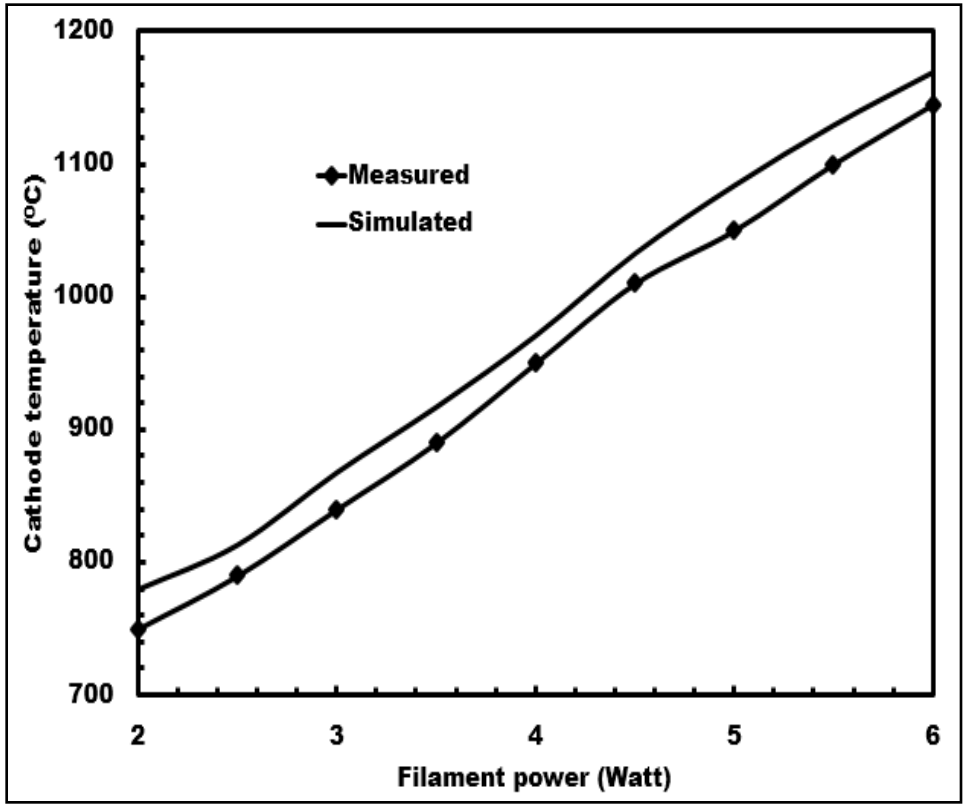

Comparative results

SLOW-WAVE STRUCTURE

Interaction structure of a TWT decides power, gain, efficiency, etc

In interaction structure, high energy electron beam and RF signal (fed through input coupler) interacts

Interaction structure consists of helix, APBN support rods and barrel envelope in TWTs

Thermal management of helix enhances the average power handling capability of a TWT

Proper thermal management of helix SWS is essential while designing a TWT for high power and high efficiency applications

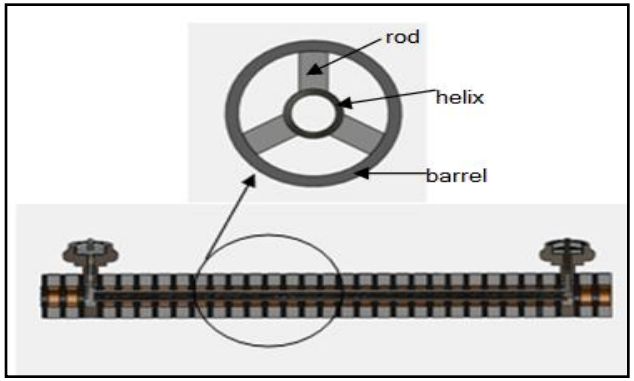

SLOW-WAVE STRUCTURE CONTINUED…

- Geometry and material property of dielectric support have effect on thermal management

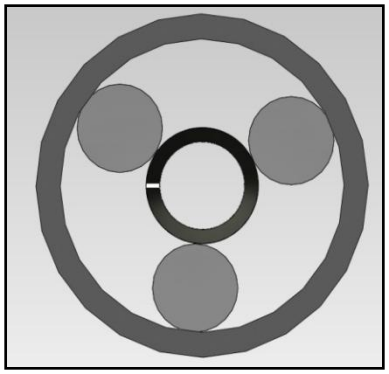

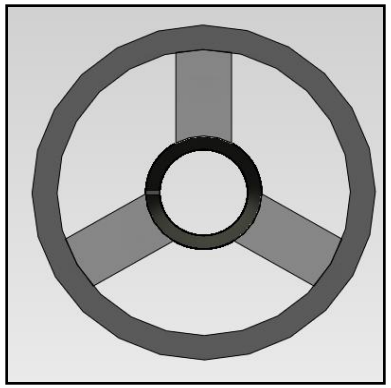

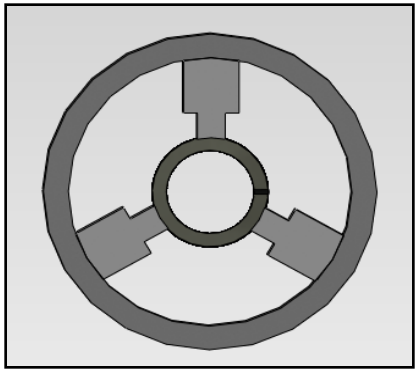

EFFECT OF MATERIAL AND SHAPE OF SUPPORT ROD ON HEAT DISSIPATION

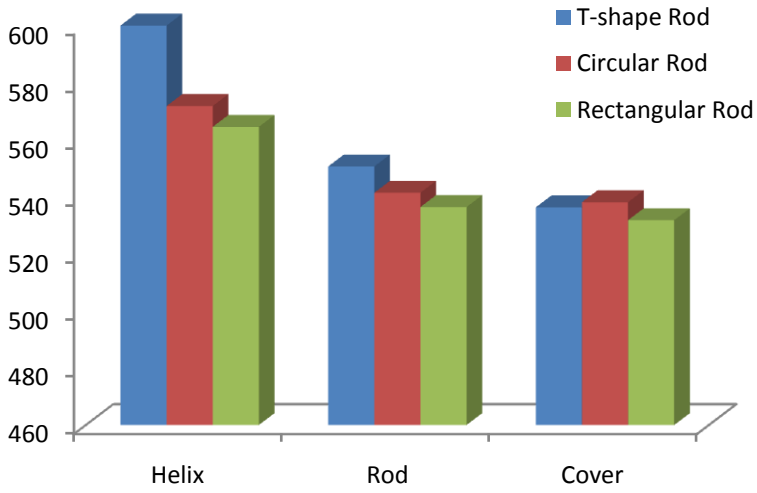

Effect of support geometry on heat dissipation, taking APBN as support material

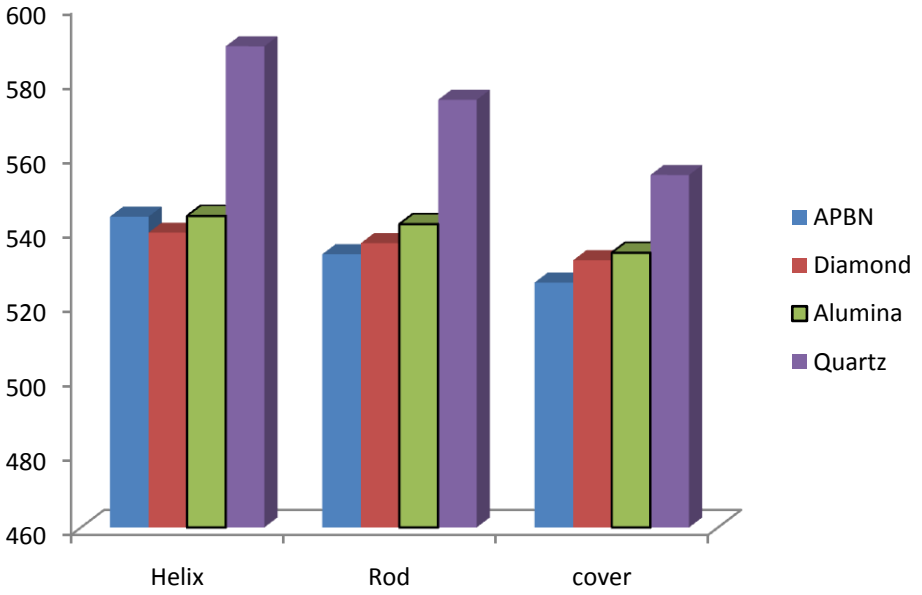

Effect of support material (permittivity) on heat dissipation, for constant support geometry (rectangular)

ANSYS THERMAL MODEL OF SLOW WAVE STRUCTURE

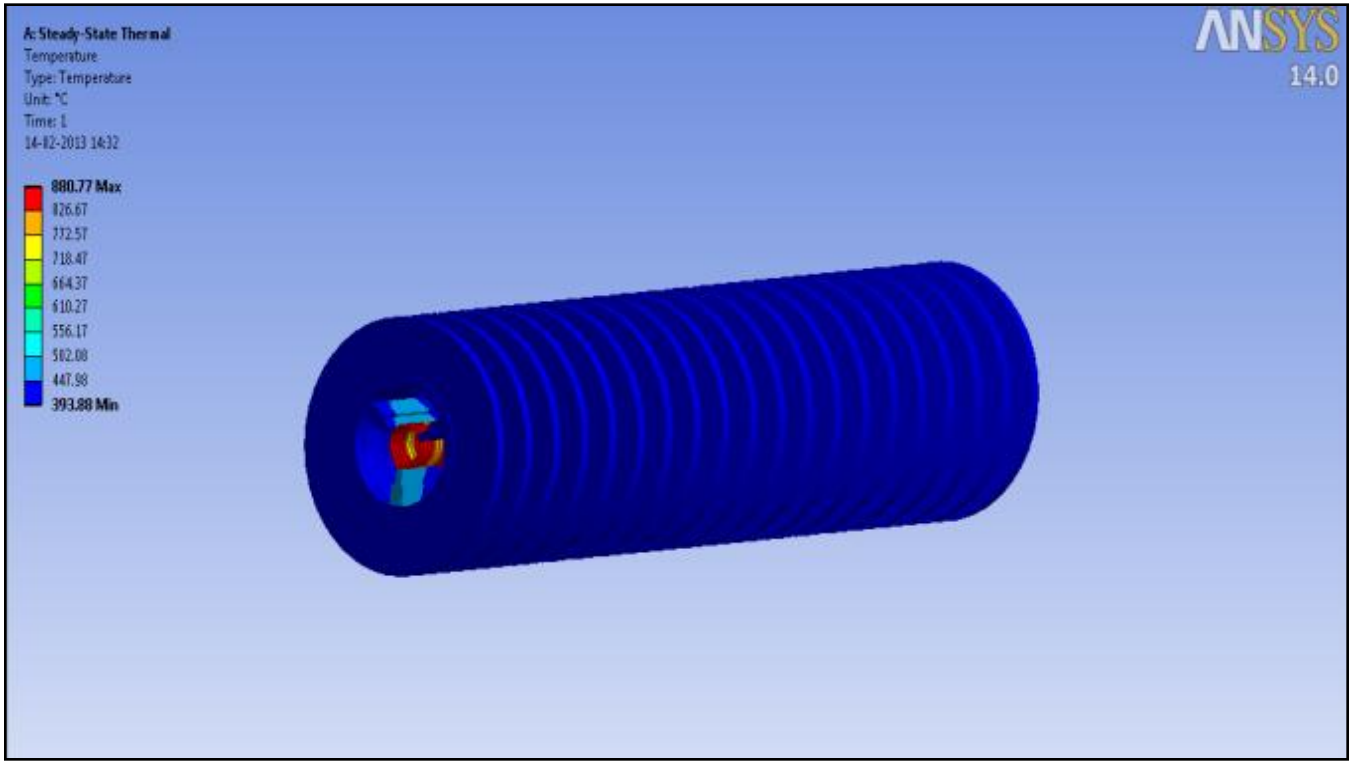

Thermal model of the structure (10 watts helix power)

COAXIAL COUPLER

Used for coupling milliwatt (mW) to hundreds of watts average power

Transform helix characteristic impedance to the standard connector

Heat gets generated due to power propagation, the coupler gets deformed affecting VSWR and enhancement of thermal load

Due to impedance mismatch, reflectio n of RF signal occurs from the couplers causing oscillation and finally damages the TWT

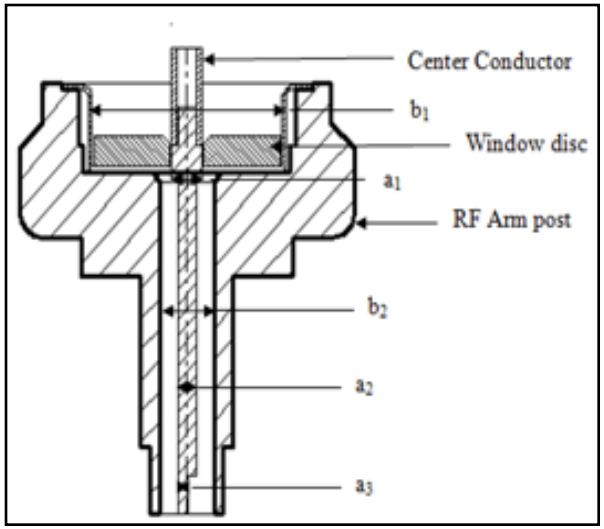

TEMPERATURE DISTRIBUTION AT DIFFERENT PARTS IN THE CO-AXIAL COUPLER ASSEMBLY

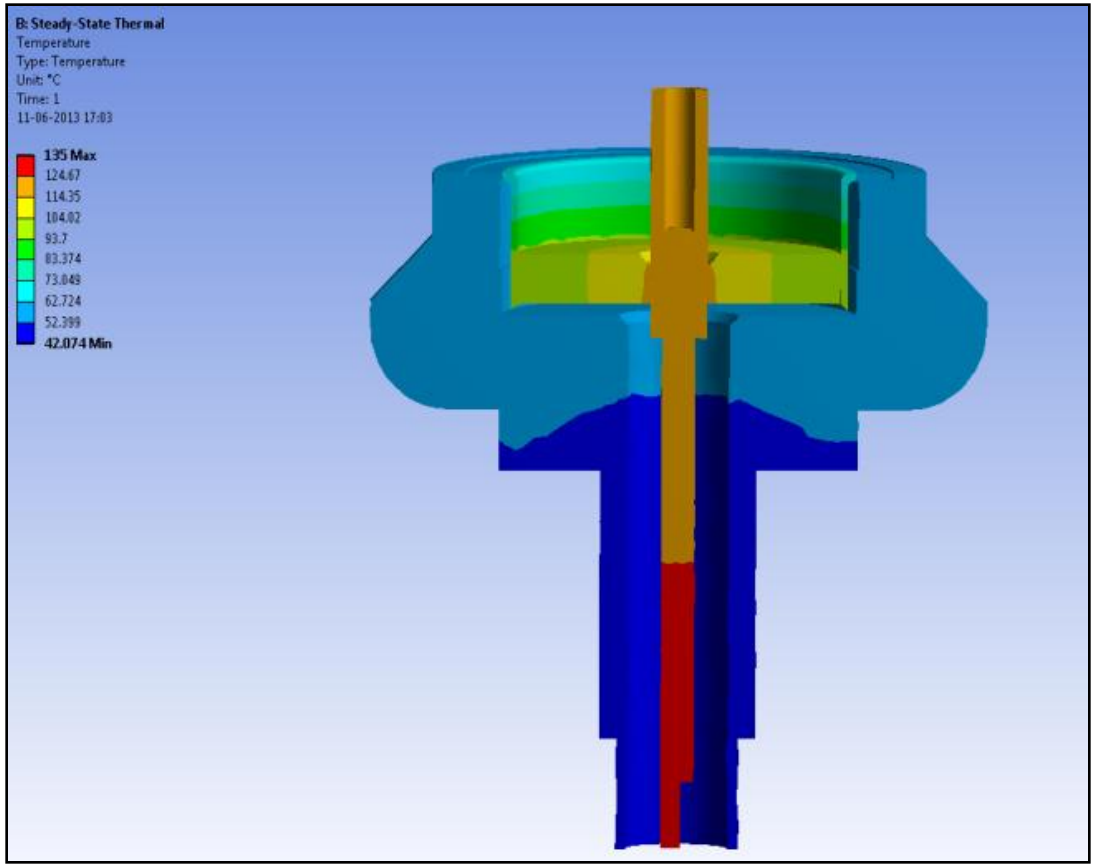

Parts	Maximum Temperature distribution (^{0}C)
Center Pin	135
Tubing	107
Window Ceramic	91
Window Cup	83
RF-arm post	61

DISPLACEMENTS OF DIFFERENT PARTS

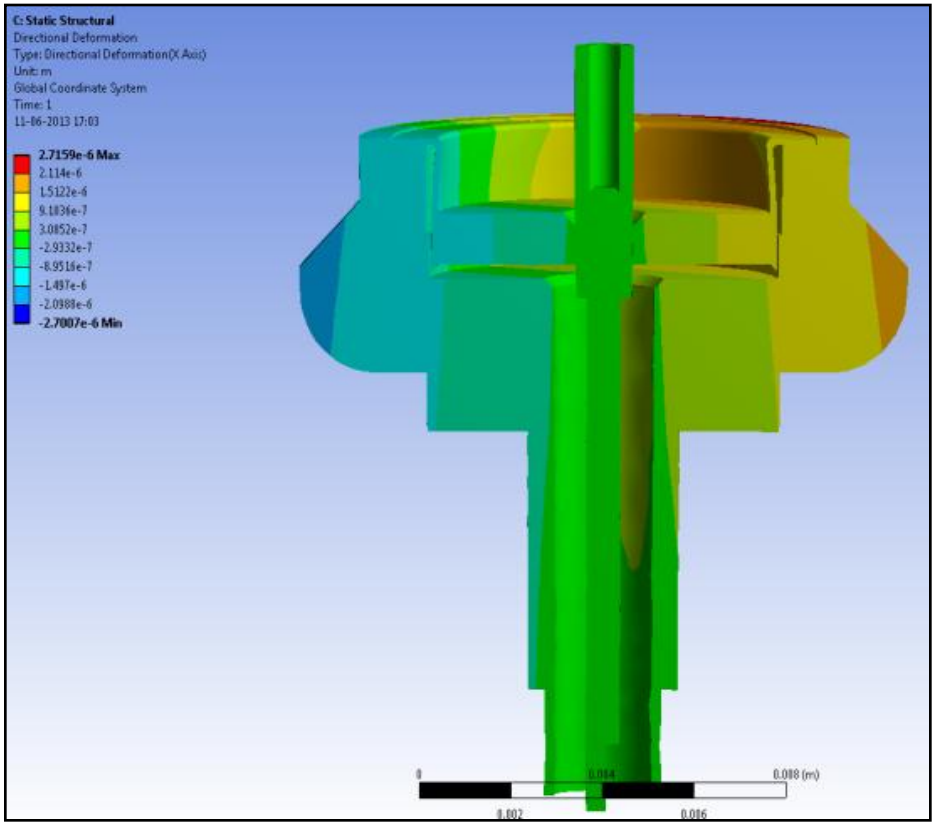

Parts	Axial Expansion (mm) in ANSYS	Radial Expansion (mm) in ANSYS
Center pin	0.00910	0.00027
Tubing	0.00326	0.00023
Ceramic window	0.00057	0.00072
Window cup	0.00095	0.00074
RF Arm post	0.00024	0.00012

EFFECT OF WINDOW DISC MATERIAL ON S-PARAMETER (RETURN LOSS)

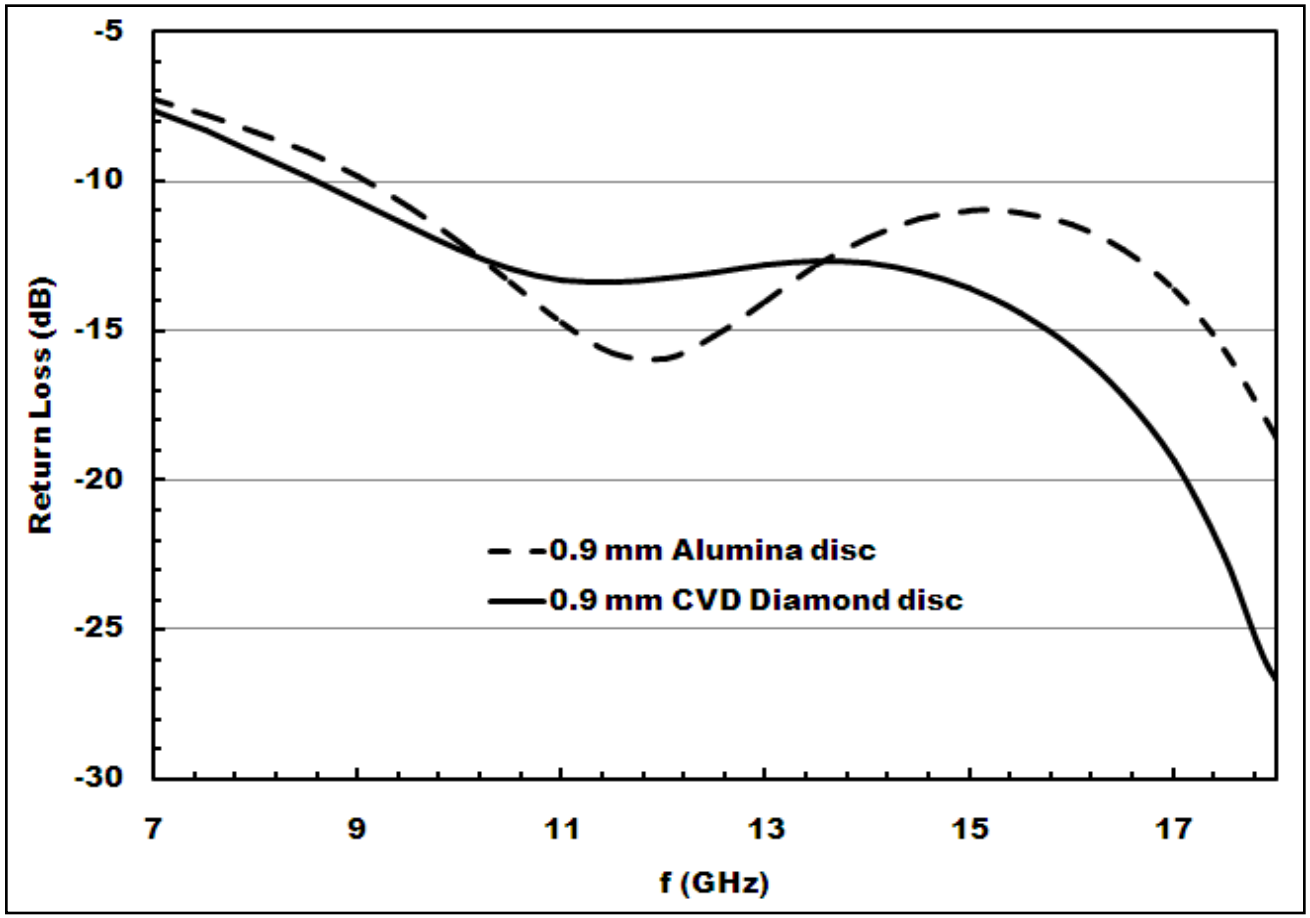

COLLECTOR

After beam-wave interaction in the interaction structure, the spent electron beam gets collected in the collector

Efficiency of a TWT mainly depends on the efficiency of collector

To increase collector efficiency, spent electron beam is collected at different depressed potentials stages

Heat dissipation is reduced by recovering spent beam power which in turn enhances efficiency of the collector and hence of the TWT

Due to different temperature distribution in collector electrodes, stresses gets developed at different joints

MULTI-STAGE DEPRESSED COLLECTOR (MDC) AND ITS TEMPERATURE DISTRIBUTION

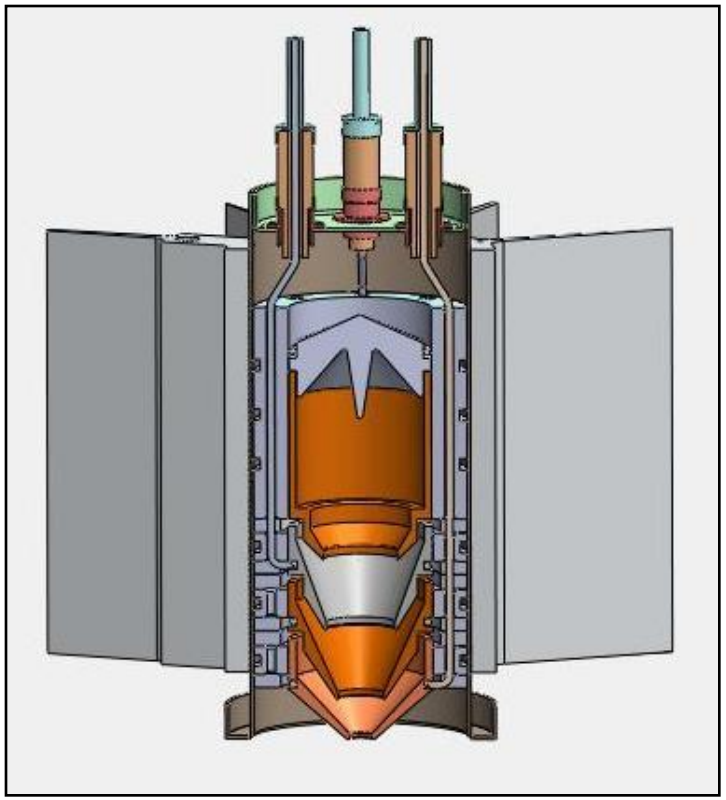

Cross-sectional view of radiation cooled four-stage collector

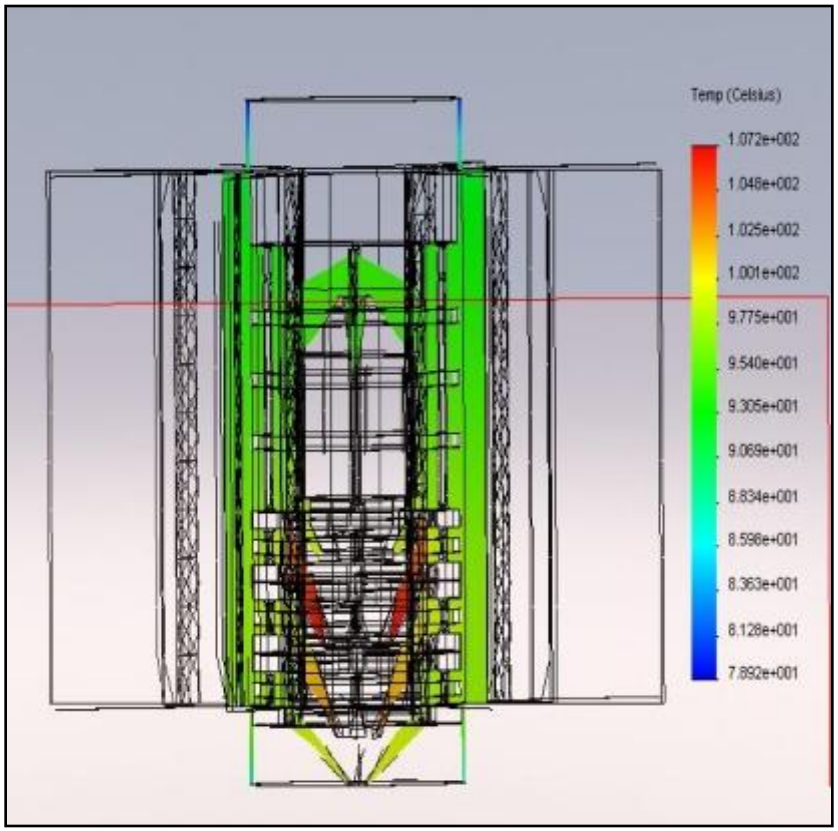

Temperature distribution in Collector

EFFECT OF CERAMIC SUPPORT MATERIAL AND ELECTRODE MATERIAL

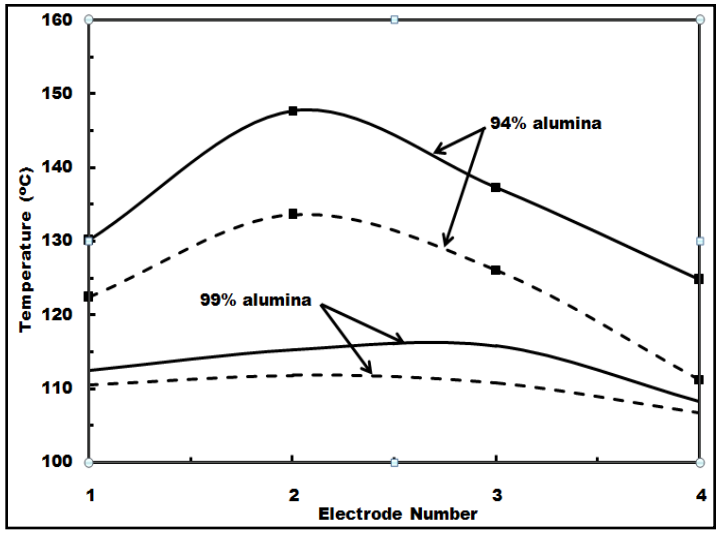

copper electrodes (solid lines)
ceramic insulators (broken lines)

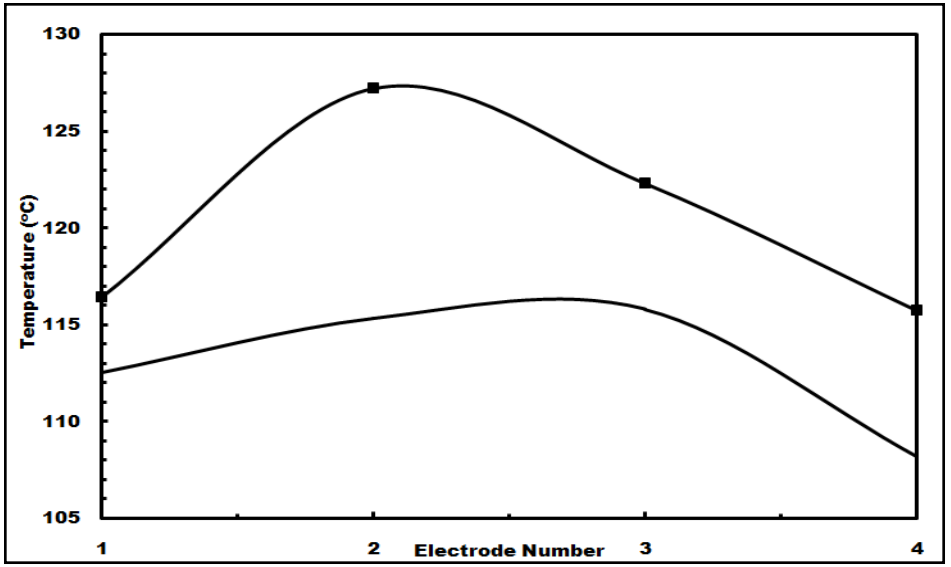

copper (solid line)
graphite (line with symbol)

COMPLETE TWT

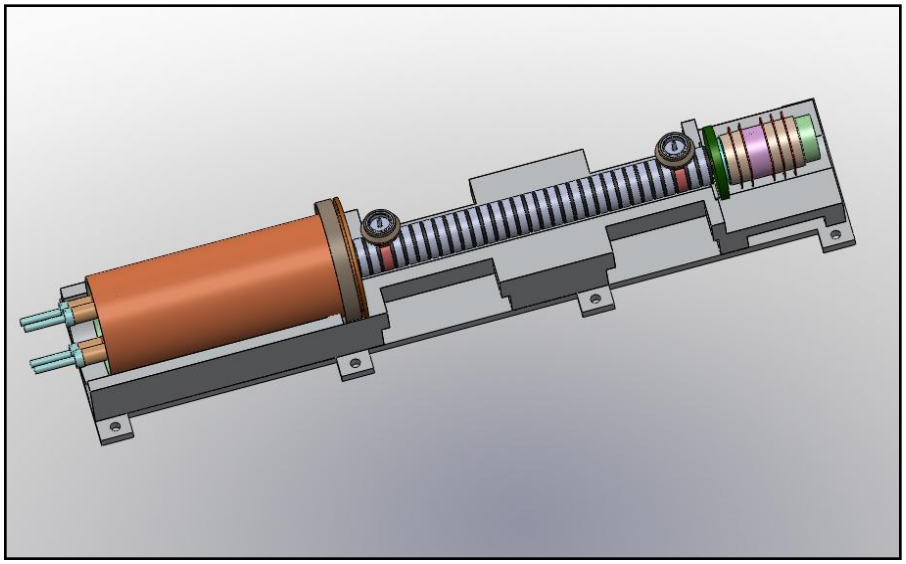

With base plate

Fully Packaged TWT

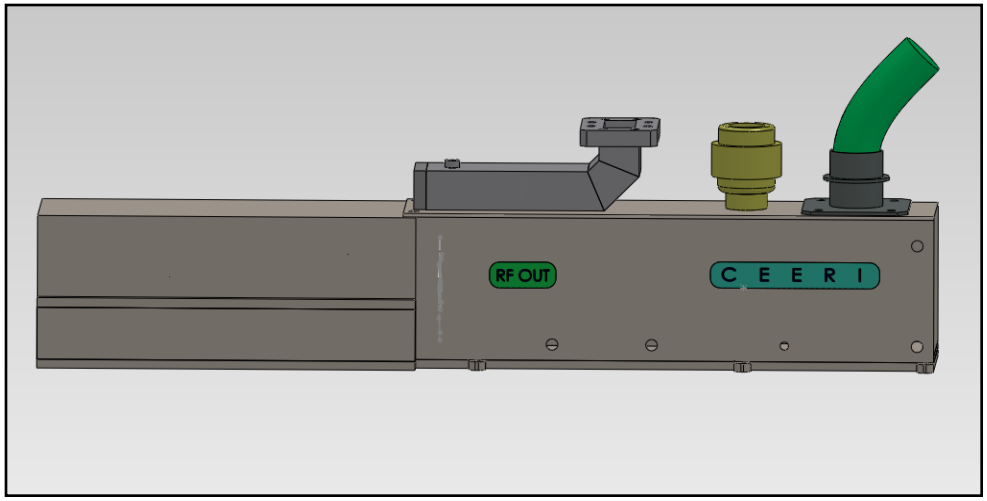

TEMPERATURE CYCLING TRAVELLING WAVE TUBES (TWTS)

Thermal Solutions has designed a multi-zone thermal plate for hot/cold temperature cycling of microwave signal amplifiers used in satellite data communications. The heart of the amplifier is a travelling wave tube (TWT) and power supply.

In their space-borne environment, TWTs are exposed to extreme temperatures that influence the strength and stability of their magnetic field and can adversely affect RF signal outputs. Rigorous thermal stressing of TWTs is required to characterize RF signal outputs and ensure trouble-free operation after deployment.

The two-zone thermal plate is both a thermal cycler to test the TWT and a heat sink to cool the power supply. With a ±1°C stability through the full -100 to 250°C temperature range, the plate can be programmed to replicate the gradual and rapid temperature changes experienced in orbit. Data logging records each test, allowing for accurate analysis of the TWT During temperature cycling.

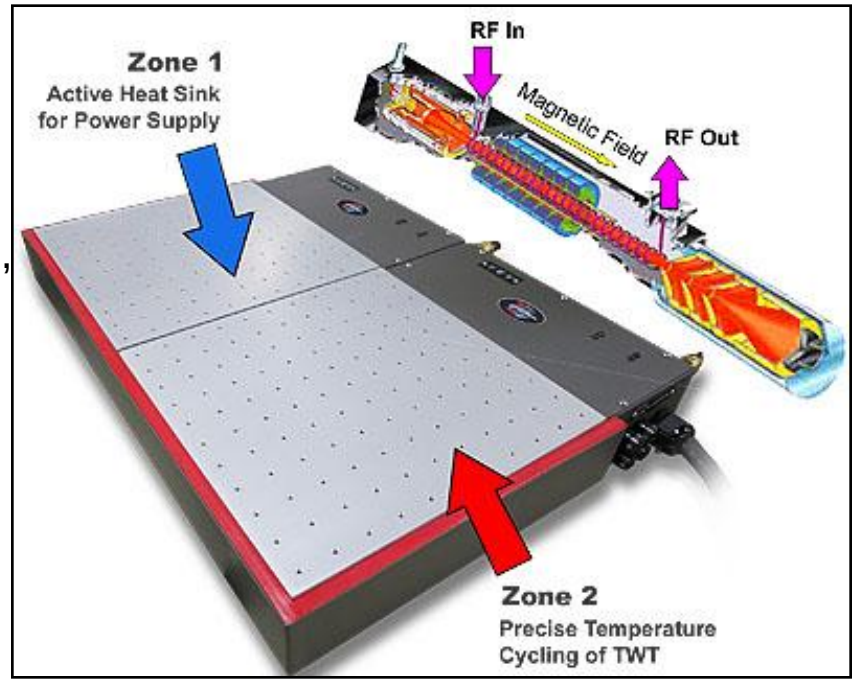

GYROTRON- A FAST WAVE DEVICE

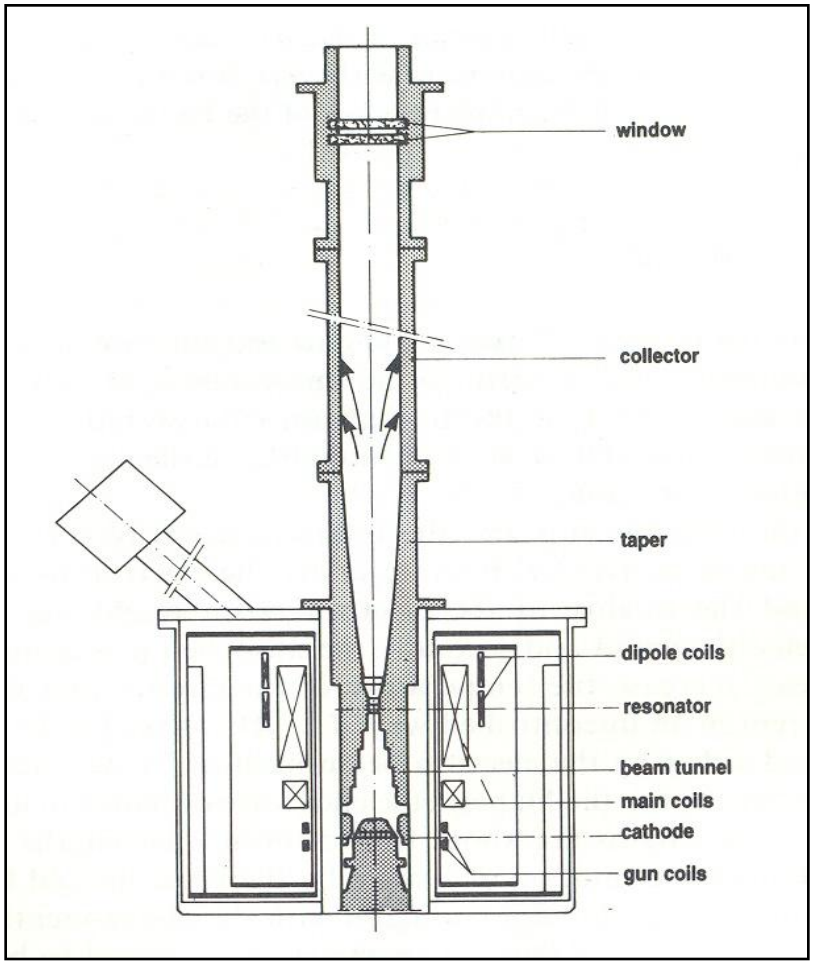

Schematic diagram of Gyrotron

Gyrotron

THERMAL-STRUCTURAL ANALYSIS OF DIFFERENT COMPONENTS OF GYROTRON

IMPORTANCE OF THERMAL-STRUCTURAL ANALYSIS FOR GYROTRON

Thermal : Temperature analysis distribution

- Multi megawatt RF power is required in millimetre wave band at high frequency for electron cyclotron resonance heating to suppress instabilities. As this device deals with very high thermal loading hence, efficient thermal management of gyrotron and its constituent parts is very important.

Structural analysis : Deformations and Stresses in structure

- Higher order mode is selected in high power gyrotron so that heat load can be managed due to the large size of cavity, but still it requires proper heat management

THERMAL ANALYSIS AND ITS EFFECT ON THE BEAM-WAVE INTERACTION OF GYROTRON

In heat transfer analysis, ANSYS was used, in which Fluent simulates the thermal analysis, and Static Structural simulates cavity mechanics.

For the cavity cooling system, 50 uniform axial wedge grooves in the outside surface of the cavity were considered, in which the total external loaded coolant flow rate is 40 L/min.

Thermal analysis result shows that maximum temperature is about 260 °C in the center section of the cavity. The deformed cavity was obtained by the structural analysis.

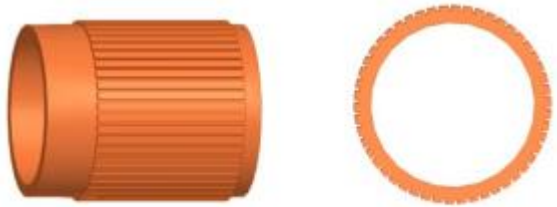

I. Cavity with the external heat radiation structure.

Simulation domain used in the ANSYS with the flow of water (blue region).

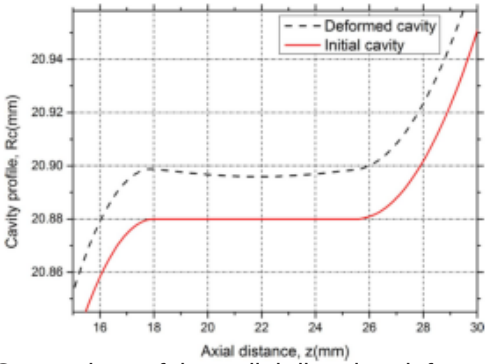

Comparison of the radial direction deformation of the cavity and the initial cavity

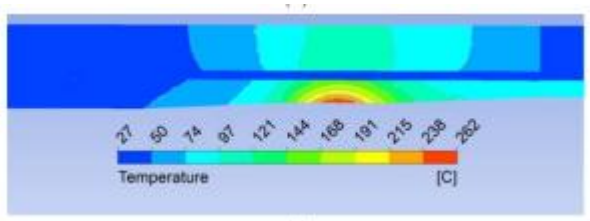

Temperature on the longitudinal section, where the observation surface is the symmetry plane of the simulation

*Qiao Liu et al, "Thermoanalysis and Its Effect on the Multimode Beam-Wave Interaction for a 0.24-THz, Megawatt-Class Gyrotron", IEEE Transactions on Electron Devices, 035349 (2019), doi.org/10.1109/TED.2017.2783927, 2018.

THERMAL SIMULATION OF COLLECTOR FOR HIGH POWER GYROTRON

The convective heat transfer coefficient of copper with different water flow rate has been used for collector cooling.

The maximum temperature in the collector changes from 419°C to 245°C, which is achieved respectively at the water flow rates from 5m/s to 15m/s.

The thermal deformation caused by different temperature distribution in the collector changes from 0.551 mm to 0.253 mm.

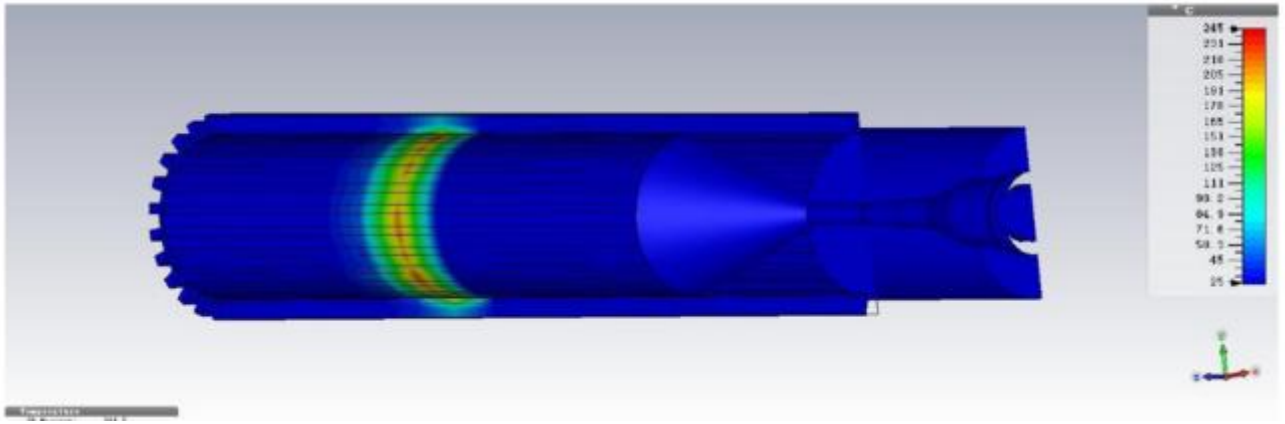

Temperature distribution with the water flow rate of 15m/s in the collector with the diameter of 282mm.

*Guo Guo et al, "Thermal design and simulation of the collector for 140GHz megawatt-class gyrotron on ITER", AIP Advances, , 035349 (2019), doi.org/10.1063/1.5091458, 26 March 2019.

Conti…

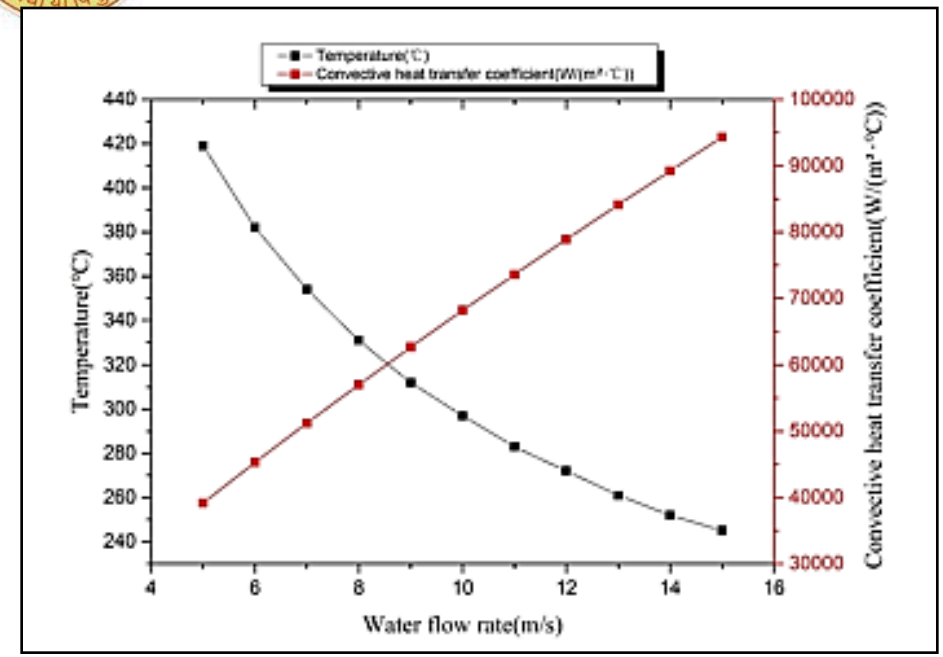

Collector temperature and heat transfer coefficient with respect to water flow rate. (collector diameter: 282mm)

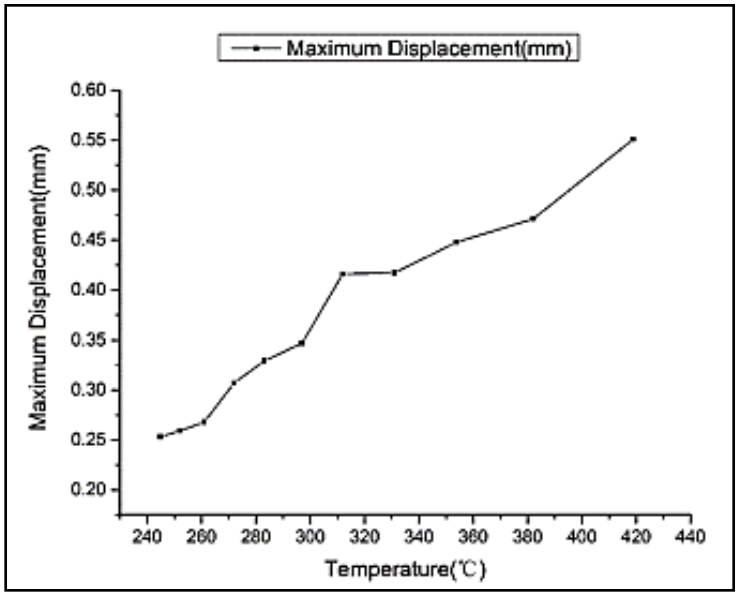

Variation of the maximum displacement with respect to temperature

CONCLUSION

THERMAL ASPECTS OF ELECTRON GUN:

- Thickness and material property of heat shield plays an important role in controlling cathode temperature.
- At operating temperature, both axial and radial expansions of cathode are very less and has no significant effect of electron beam trajectory.
- These findings are potentially helpful in microwave tube technology for design and development of thermally efficient TWTs for long life applications.

THERMAL ASPECTS OF SWS:

- For proper thermal management, rectangular support is more effective as it has larger contact area with the helix.
- For cost effectiveness and fabrication simplicity, APBN/Beryllia support rod with rectangular geometry is a suitable choice for helix support.
- Material property of supports and contact resistance has great effect on thermal management.

THERMAL ASPECTS OF COAXIAL COUPLER:

- The estimation of dimensional deformations and stress generated in critical sensitive dimensions helps in keeping the proper dimensions in cold conditions so that desired dimensions are achieved in the operating hot conditions.
- CVD diamond is found as a better choice as stress developed is lesser as compared to alumina disc. However, CVD diamond is costlier hence for low to medium power level, alumina is a better choice.

THERMAL ASPECTS OF COLLECTOR:

- Improper shape, size and material property of collector electrode affect the thermal management of collector.
- Graphite has low secondary electron emission coefficient and is light weight. But it is very difficult to fabricate and to braze with ceramic insulators. Hence, copper is selected due to high thermal conductivity and fabrication simplicity.
- Material property of ceramic insulator also has great impact on thermal management.

REFERENCES

- V. Gahlaut, et al, “Electrostatics and Thermal Analysis of a Dual-Anode Electron Gun”, Journal of Electromagnetic Waves and Applications, Taylor & Francis,Vol. 28, no. 16, pp. 2005-2013, August 2014.

- V. Gahlaut, et al, “Multi-stage Depressed Collector with Improved Thermal Management for High Efficiency Traveling Wave Tubes”, IEEE Trans. on Electron Devices, Vol 61, No. 5, pp. 1536-1540, May, 2014.

- V. Gahlaut et al, “Thermal and Structural Analysis of Co-axial Coupler used in High Power Helix Traveling-Wave Tube”, Frequenz-Journal of RF-Engineering and Telecommunications, Vol. 68, no. 7-8, pp. 329-333, May 2014.

- V Gahlaut, et al, “Thermal behavior of a periodic structure supported by dielectric rods in vacuum”, Heat and Mass Transfer, Springer, Vol. 50, pp. 821-826, Jan. 2014.

- V. Gahlaut et al, “Thermal Impact on the Performance of Highly Efficient Multi-Stage Depressed Collector for Space TWT”, Frequenz-Journal of RF-Engineering and Telecommunications, Vol.68, no. 1-2, pp. 83-87, Jan. 2014.

Conti…

- V. Gahlaut et al, “Thermal Management of Helix Used in High Power High Efficiency Traveling-Wave Tubes”, Journal of Electromagnetic wave and applications, Taylor & Francis, Vol.27, no.15, 1861-1868, 2013.

- V. Gahlaut et al, “Effect of ceramic material on heat dissipation from multi-stage depressed collector used in high efficiency traveling-wave tubes”, Indian Journal of Pure and Applied Physics, Vol.51, 657-660, Sept. 2013.

- Qiao Liu et al, “Thermoanalysis and Its Effect on the Multimode Beam-Wave Interaction for a 0.24-THz, Megawatt-Class Gyrotron”, IEEE Transactions on Electron Devices, 035349 (2019), doi.org/10.1109/TED.2017.2783927, 2018.

- Guo Guo et al, “Thermal design and simulation of the collector for 140GHz megawatt-class gyrotron on ITER”, AIP Advances, , 035349 (2019), doi.org/10.1063/1.5091458, 26 March 2019.

THANK YOU

Metamaterials and metamaterial-based vacuum microwave devices - A Design Perspective

- Purushothaman Narasimhan,
CSIR-CEERI, Pilani – 333031, Rajasthan.
Email: purushothaman.n@gmail.com

Overview

- EM metamaterials (MTMs) – general design studies
- Case studies – SRRs and fishnet structures
- Thin wire MTM based backward interaction structure
- Use of optimization methods in designing metamaterial-based devices

Metamaterials (MTMs)

- Coinage by Walser in 1999
- Engineered composites exhibiting properties not found in nature or in the constituent materials
- Electromagnetic MTMs – permittivity and permeability can be controlled
- Size of the unit cell smaller than the wavelength

Material parameter space

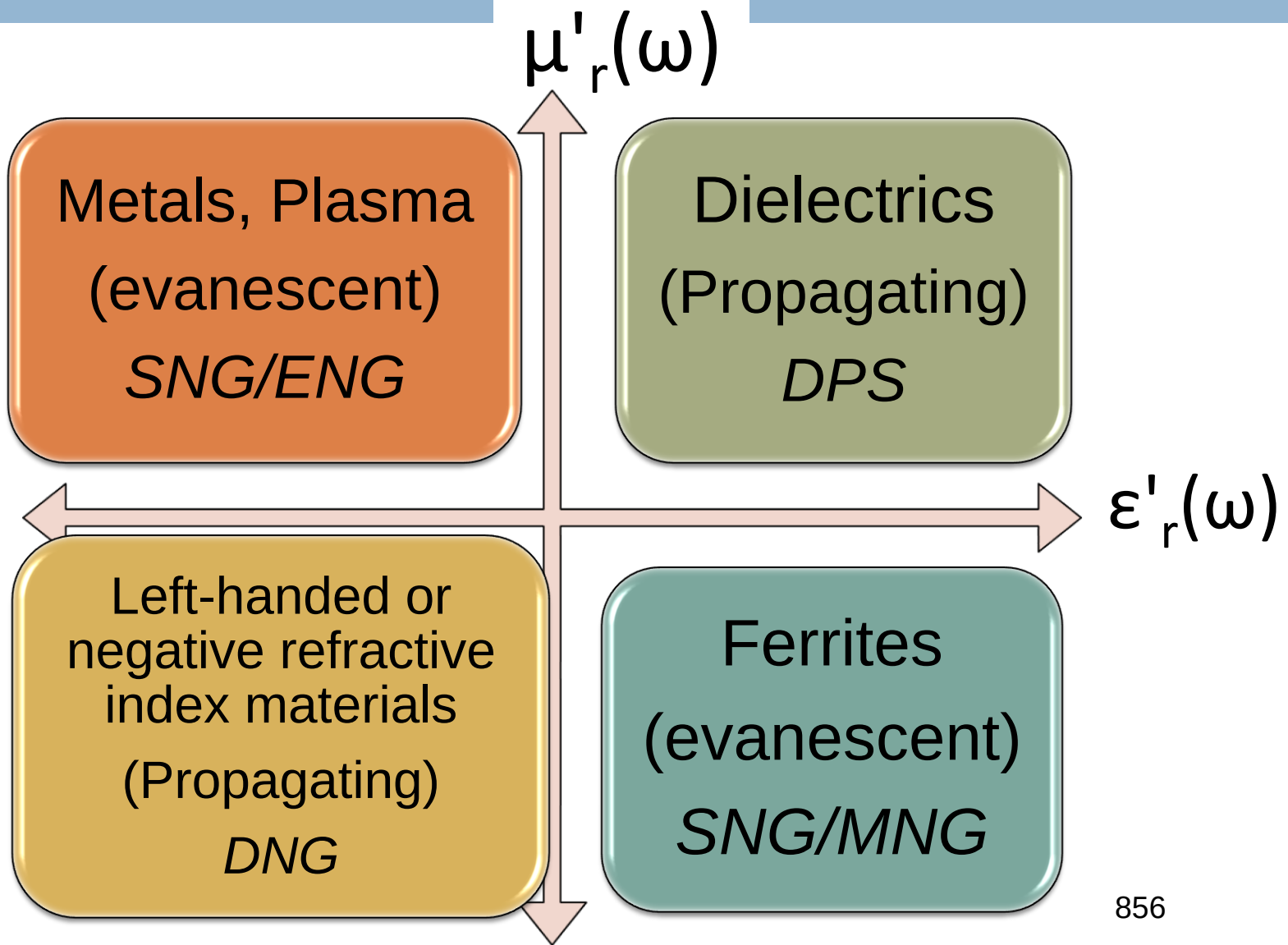

Conditions for permittivity and permeability values

- $\epsilon_r(\omega)$ and $\mu_r(\omega)$ tend to unity for large values of ω

- $\frac{d(\omega\epsilon)}{d\omega} > 0$ and $\frac{d(\omega\mu)}{d\omega} > 0$ => entropy condition

Split Ring Resonator (SRR) + Thin Wire (TW) MTM

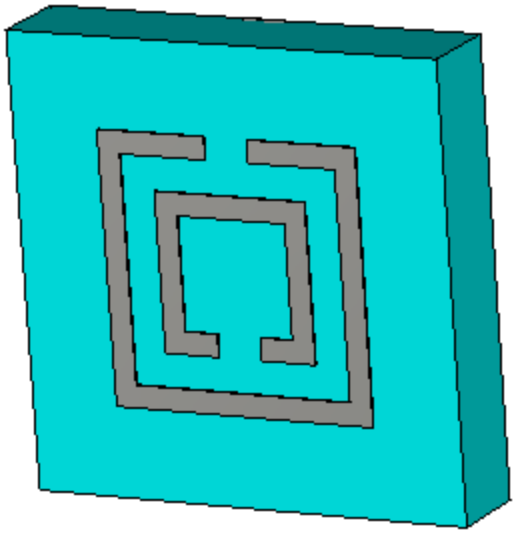

Edge-coupled SRR

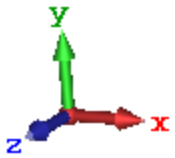

SRR – negative permeability medium -
Requires H_z component, or E_x component.

Bianisotropic structures:

$$\vec{D} = \bar{\bar{\epsilon}}\vec{E} + \bar{\bar{\xi}}\vec{H}$$
$$\vec{B} = \bar{\bar{\mu}}\vec{H} + \bar{\bar{\zeta}}\vec{E}$$

Broad-side coupled SRR with rings on both the sides of the substrate is used to reduce bianisotropy

Split Ring Resonator (SRR) + Thin Wire (TW) MTM

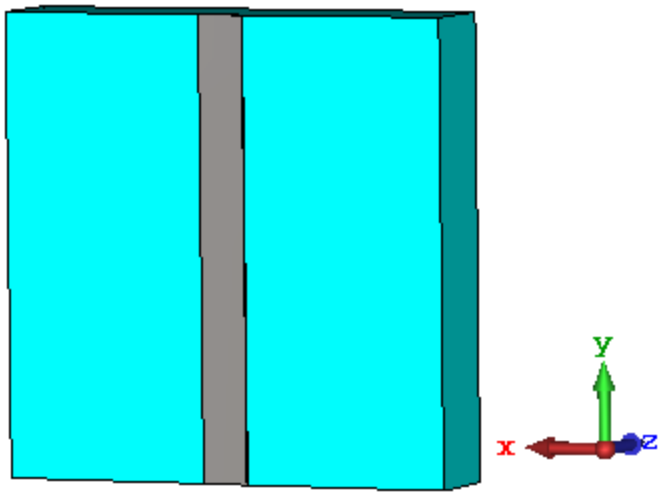

TW – negative permittivity medium - Requires E_y component

$$\omega_p = \frac{Ne^2}{\epsilon_0 m}$$

N – number density,

m – effective mass, e – charge,

ϵ_0 - free space permittivity

Decrease in number density and increase in effective mass.

For periodicity, a = 3 mm, wire radius = 1 μm, plasma frequency $\approx$ 14 GHz

SRR+TW MTM

Parameter	Value
Substrate relative permittivity	3.84 (FR4)
Substrate loss tangent	0.018
Unit cell size	5 mm X 5 mm X 1mm
Ring width/thin wire width	0.25 mm
Inter ring gap	0.375 mm
Intra ring gap	0.5 mm
Metallic inclusion thickness	17 μm

SRR+TW simulation

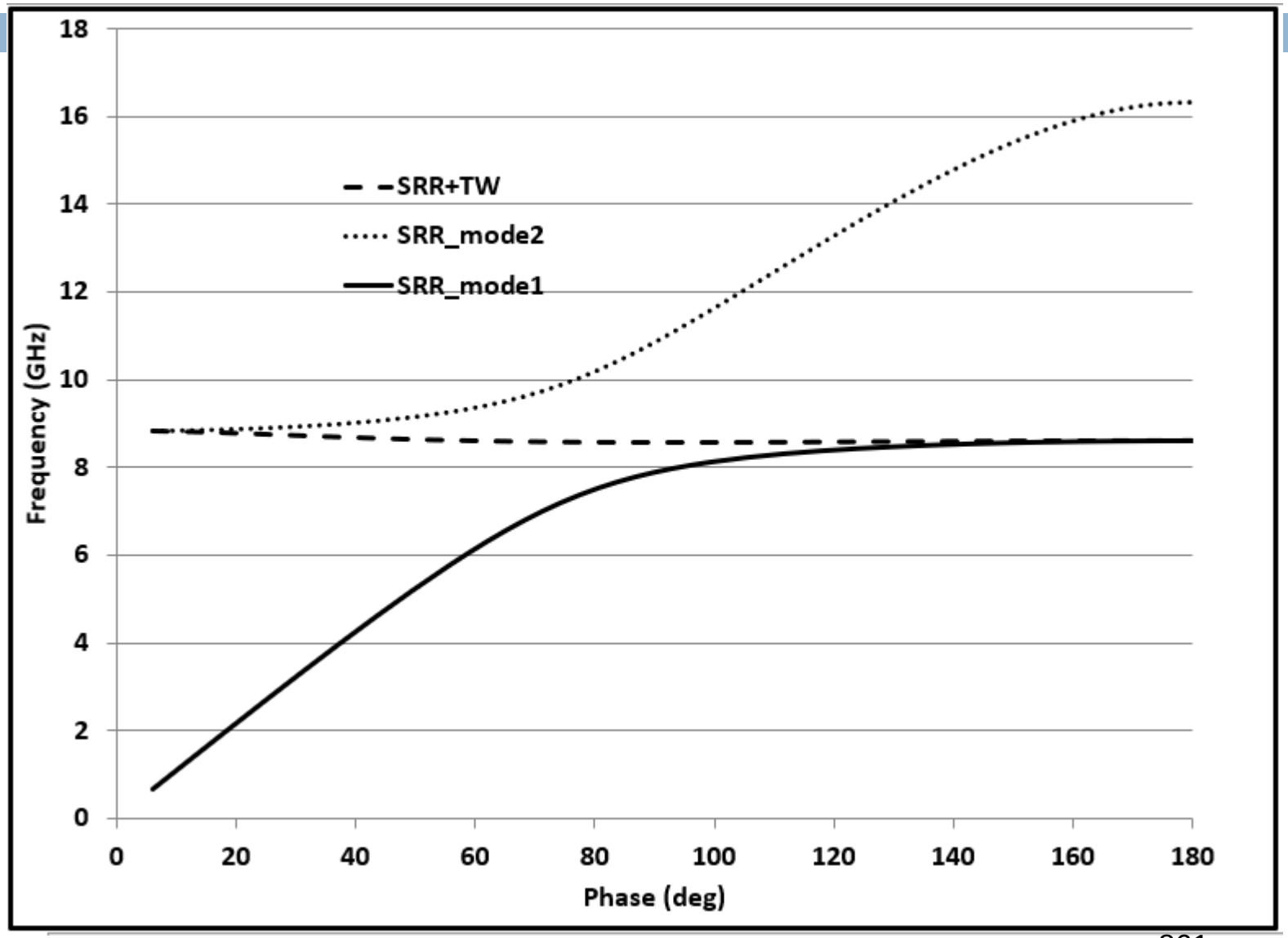

SRR+TW simulation

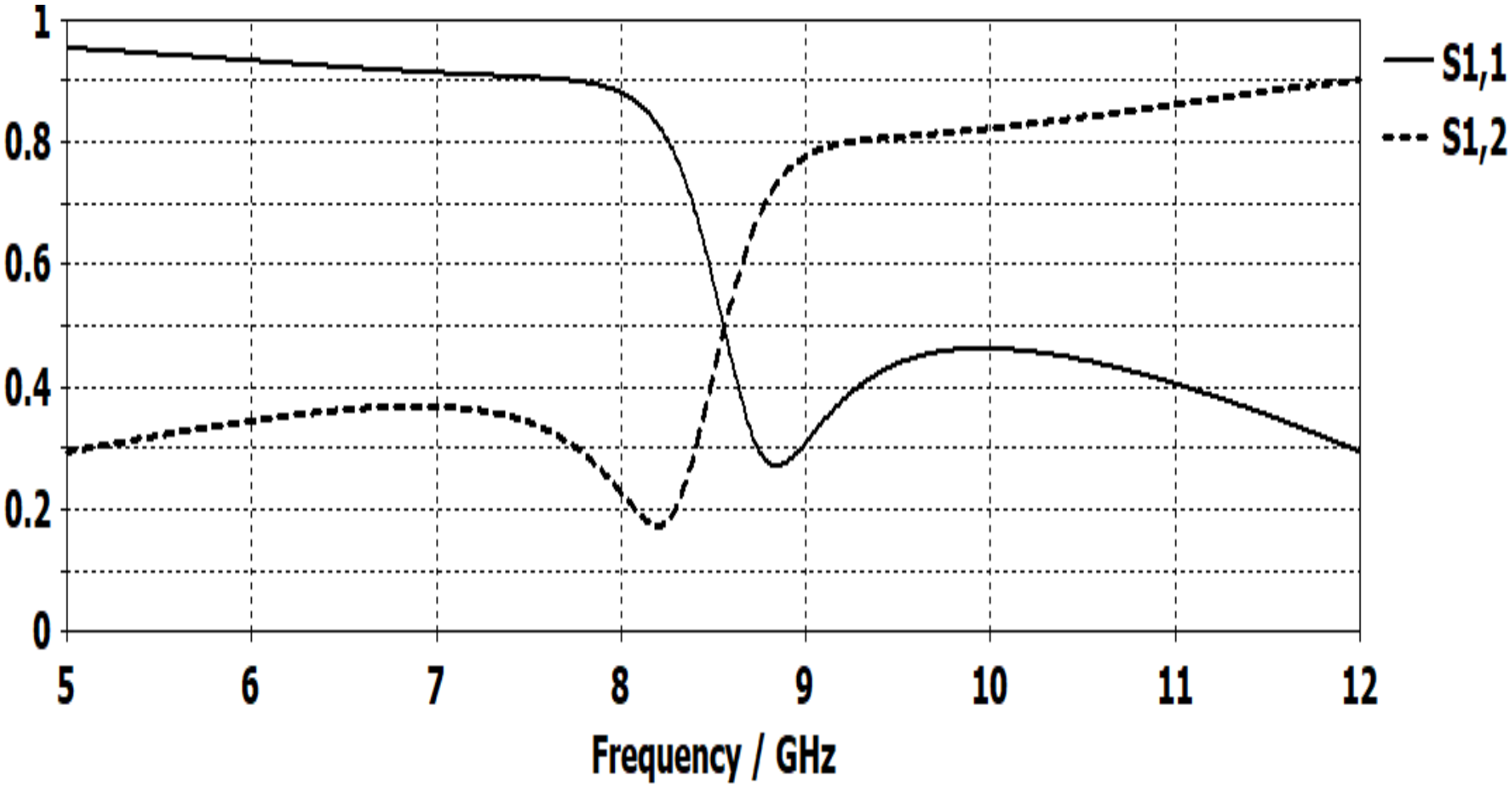

Extraction procedure

$$z = \pm\sqrt{\left(\frac{(1+S_{11})^2 - S_{21}^2}{(1-S_{11})^2 - S_{21}^2}\right)}$$

$$e^{ink_0 d} = X \pm i\sqrt{1-X^2}$$

$$\text{where, } X = \frac{1-S_{11}^2+S_{21}^2}{2S_{21}}$$

Sign of Z_{eff} is determined by,
$Re(Z_{eff})>=0$ and $Im(N_{eff})>=0$

The Branching Problem

$$N_{eff} = n_{eff}(\omega) + i\kappa_{eff}(\omega)$$

$$n_{eff} = \frac{1}{k_0 d}\{\mathrm{Im}\left[\ln\left(e^{iN_{eff}k_0 d}\right)\right] + 2m\pi\}$$

$$= n_{eff}^{0} + \frac{2m\pi}{k_0 d}$$

$$\kappa_{eff} = -\frac{\mathrm{Re}\left[\ln\left(e^{iN_{eff}k_0 d}\right)\right]}{k_0 d}$$

m – branch index (Source of ambiguity)

n_{eff}^{0} → corresponds to principal branch of the logarithmic function

Method #1: Extraction through Kramers-Kronig (K-K) Relation

$$n^{kk}(\omega') = 1 + \frac{2}{\pi} \mathrm{P} \int_0^{\infty} \frac{\omega \kappa_{eff}(\omega)}{\omega^2 - \omega'^2} d\omega$$

- Avoiding singularity
- Truncated integral
  - Leads to numerical error
  - Frequency range trade-off

Method #1: Extraction through Kramers-Kronig (K-K) Relation

$$m = \text{round}\left[\left(n^{kk} - n_{eff}^{0}\right)\frac{k_0 d_{eff}}{2\pi}\right]$$

- Branch number is substituted back into N_{eff}

$$\epsilon_{eff} = \frac{N_{eff}}{Z_{eff}}$$

$$\mu_{eff} = N_{eff} Z_{eff}$$

Method #1: Extraction through Kramers-Kronig Relation

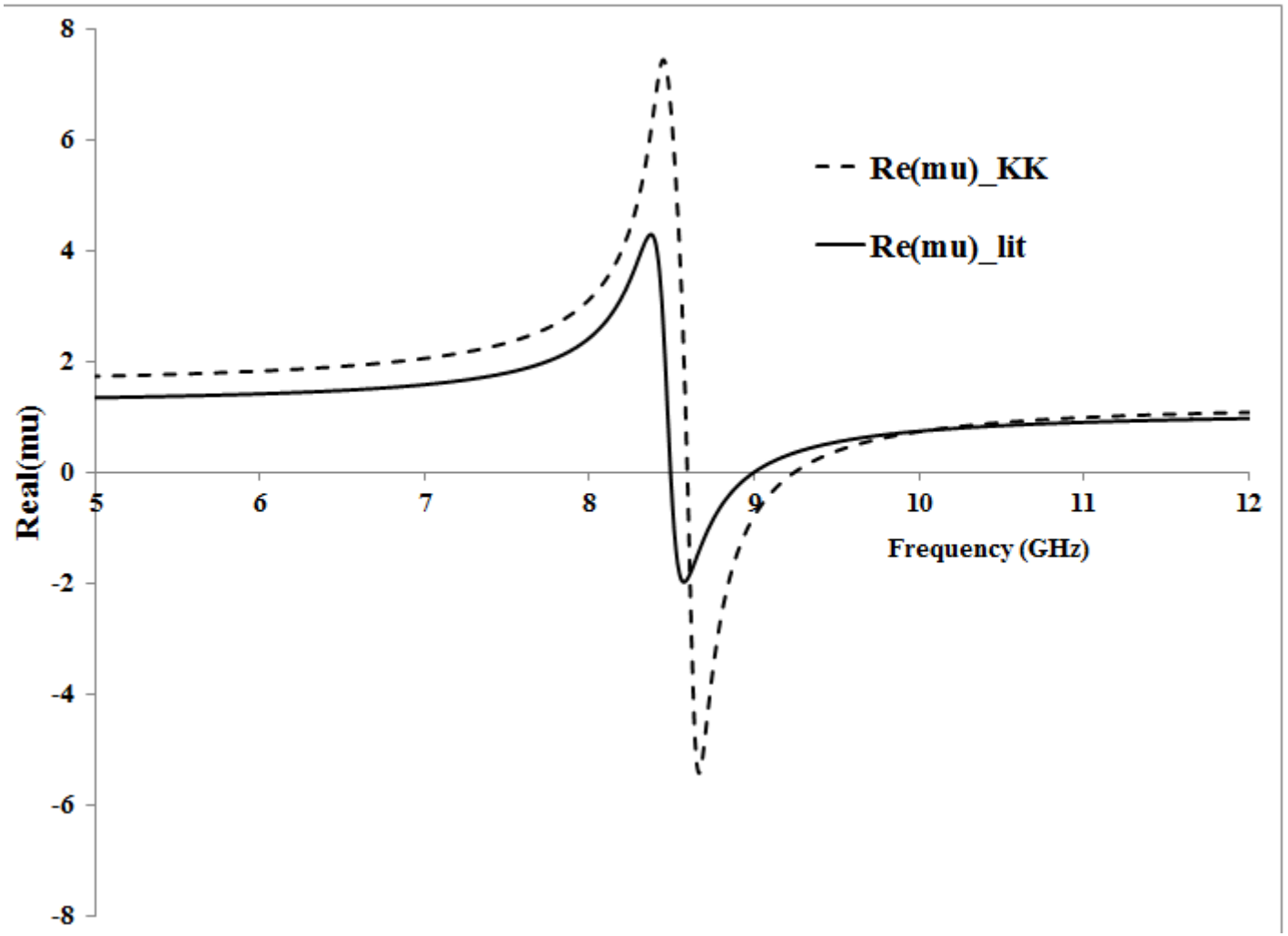

Method #1: Extraction through KK Relation

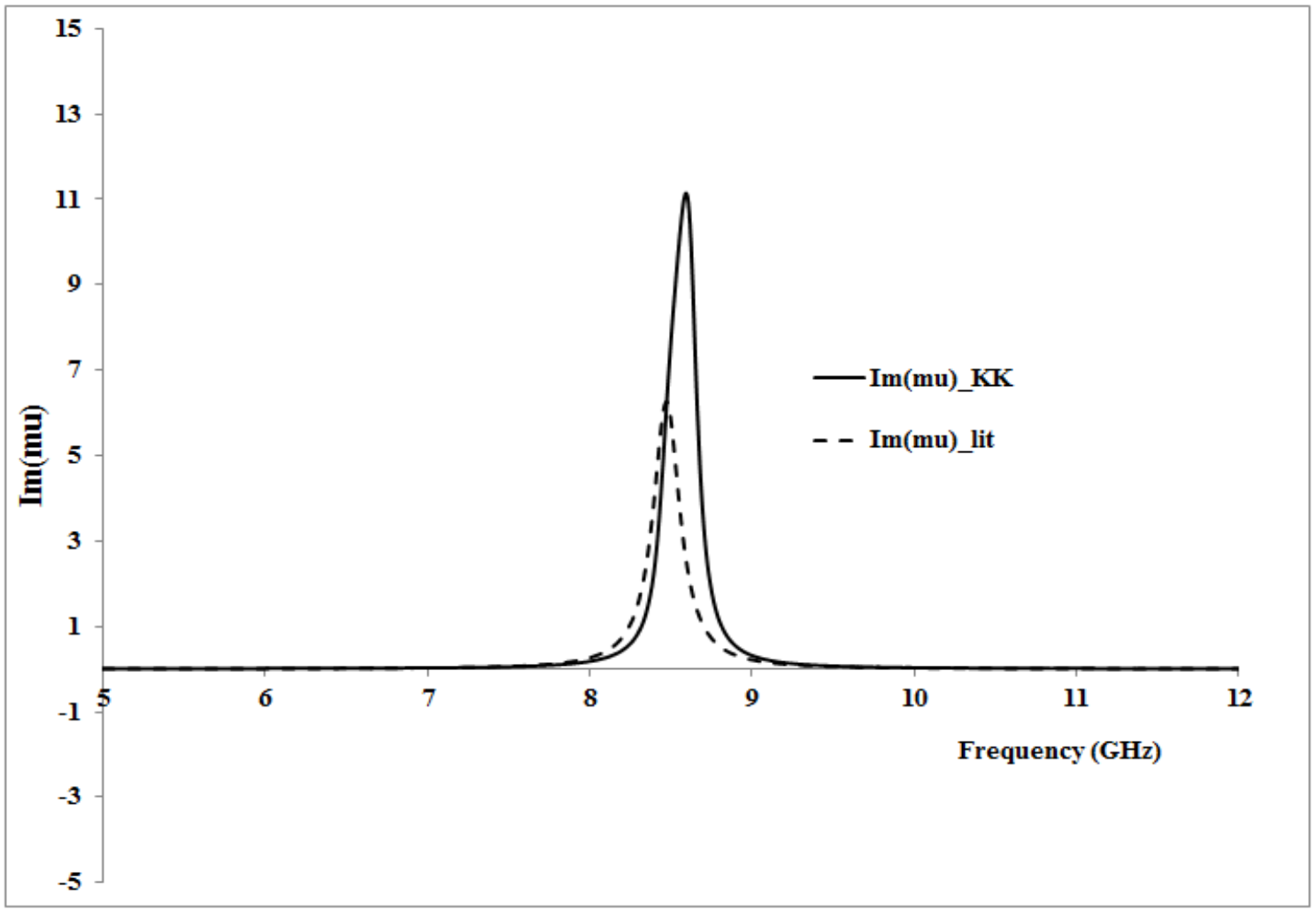

Method #1: Extraction through KK Relation

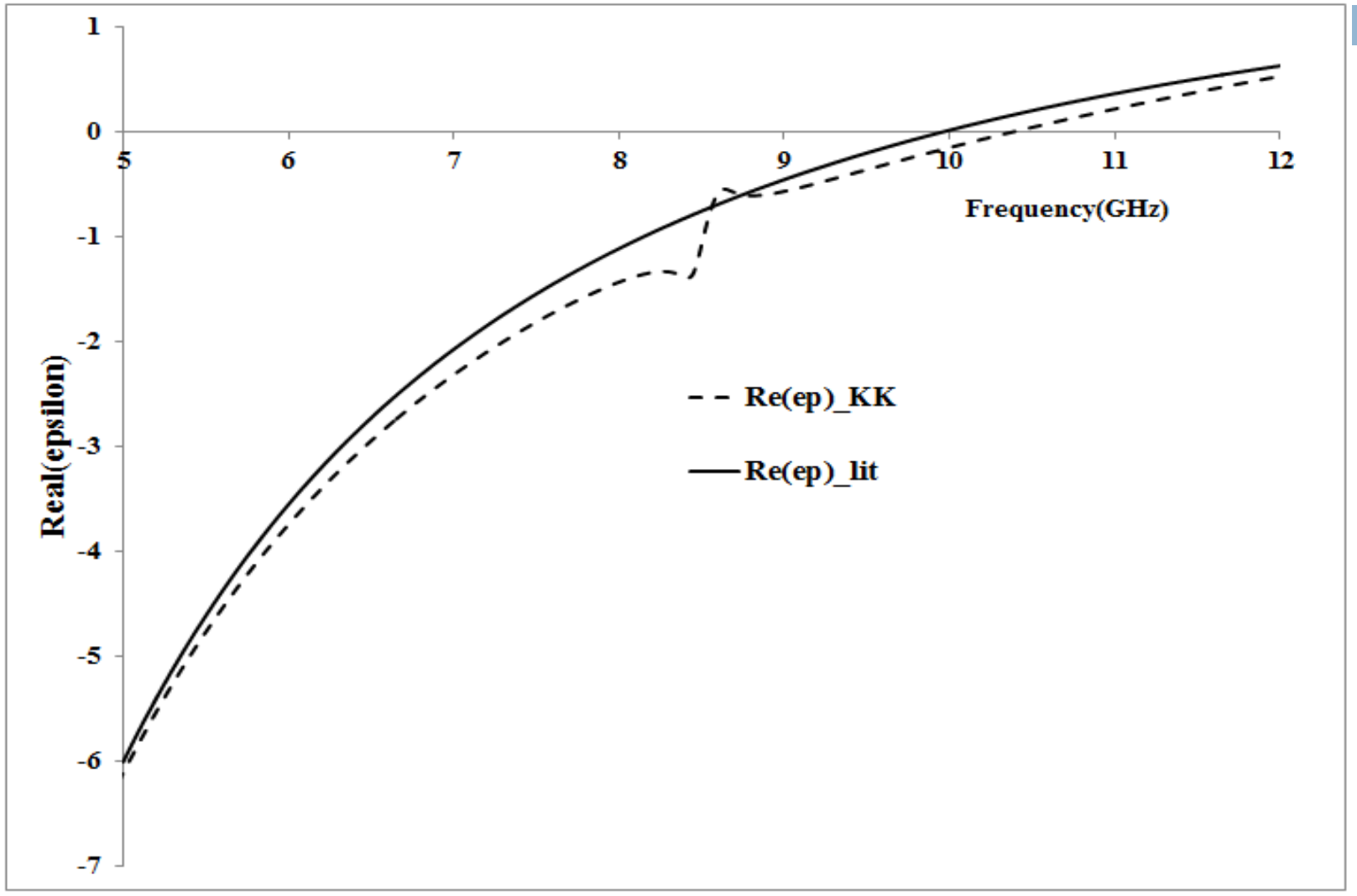

Method #1: Extraction through KK Relation

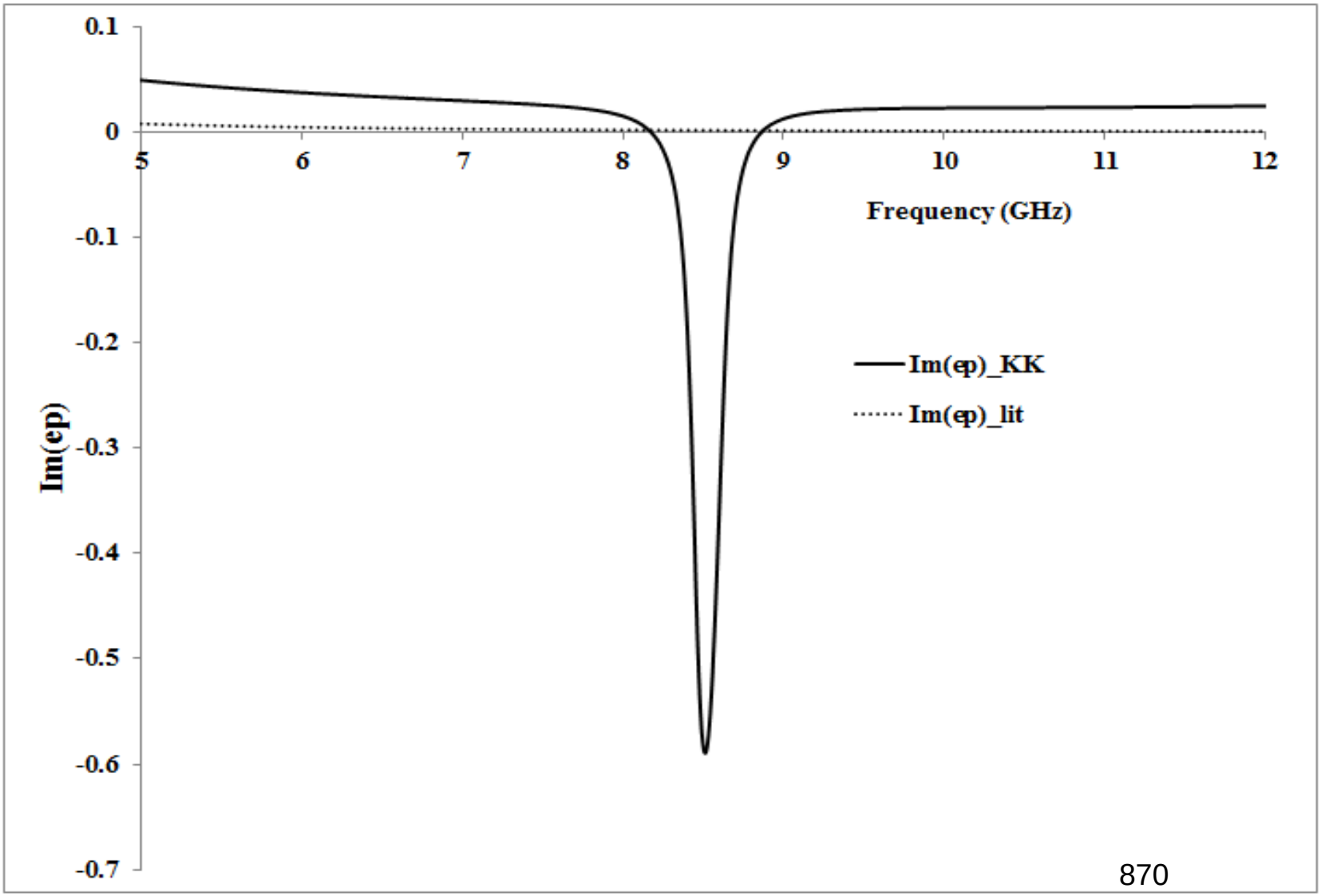

Unit Cell to bulk medium model

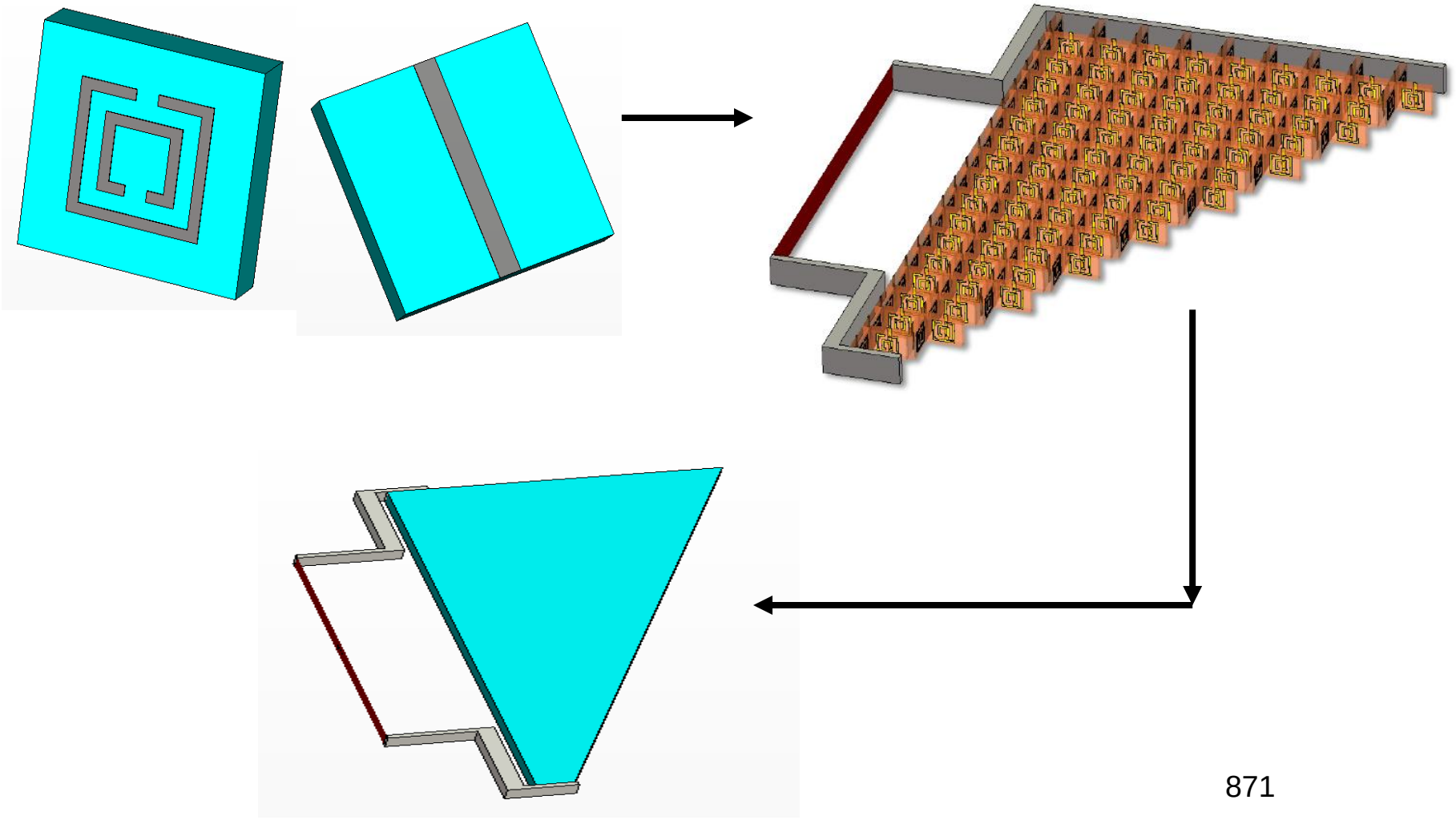

Method #2: Parameter Fitting of Dispersive Models (PFDM)

Drude Model:

$$\epsilon_{eff}(\omega) = \epsilon_\infty - \frac{\omega_p^2}{\omega(\omega - i\nu_c)}$$

$\epsilon_\infty \Rightarrow$ Higher frequency limit of permittivity

$\omega_p \Rightarrow$ Radial plasma frequency

$\nu_c \Rightarrow$ Collision frequency

Method #2: PFDM

Lorentz Model:

$$\mu_{eff}(\omega) = \mu_\infty + \frac{(\mu_s - \mu_\infty)\omega_0^2}{\omega_0^2 + i\omega\delta - \omega^2}$$

$\mu_s, \mu_\infty \Rightarrow$ lower and higher frequency permeability limit respectively

$\omega_0 \Rightarrow$ radial resonant frequncy

$\delta \Rightarrow$ damping frequency

Method #2: PFDM

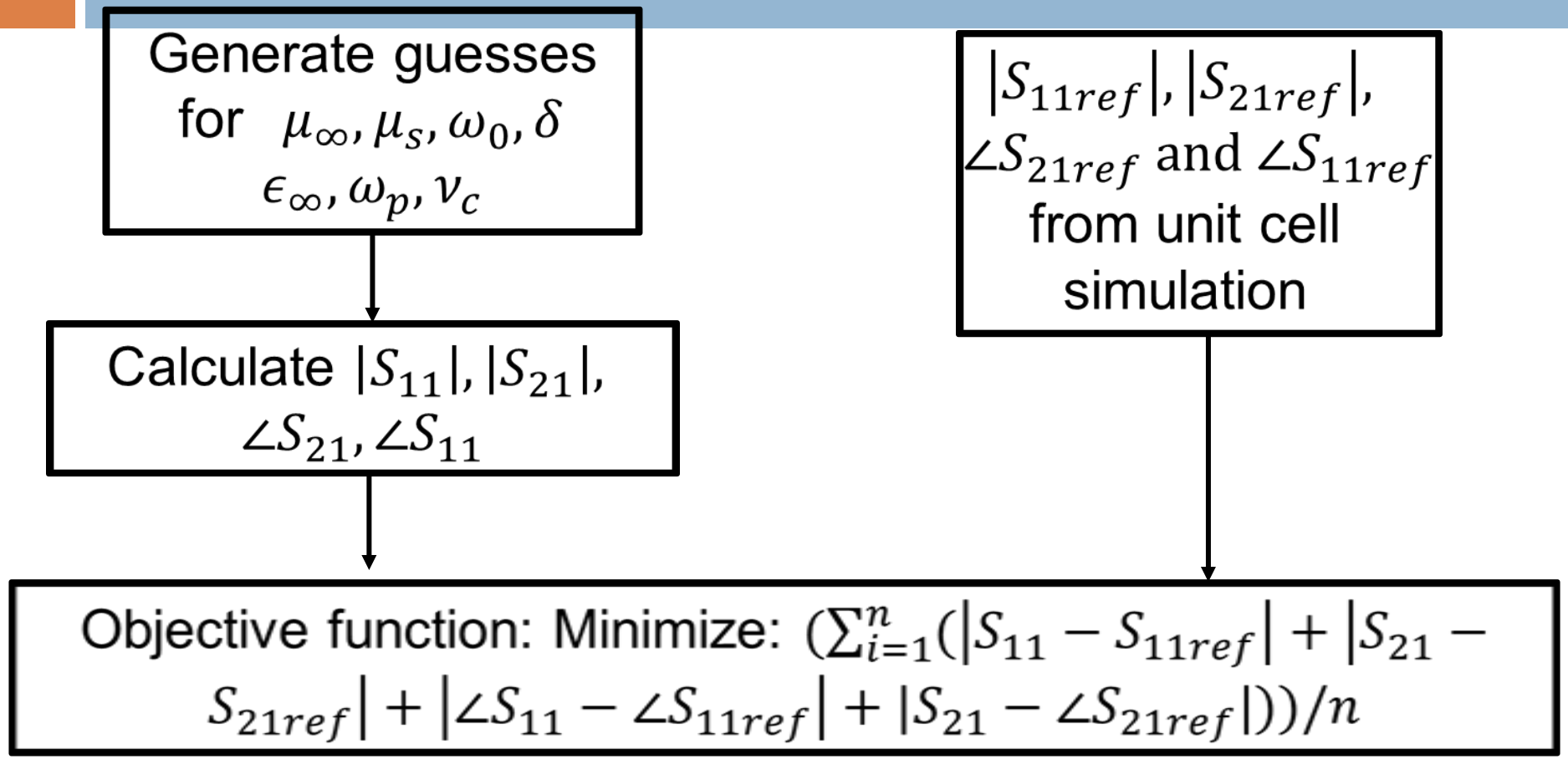

n is the number of points

Method #2: PFDM

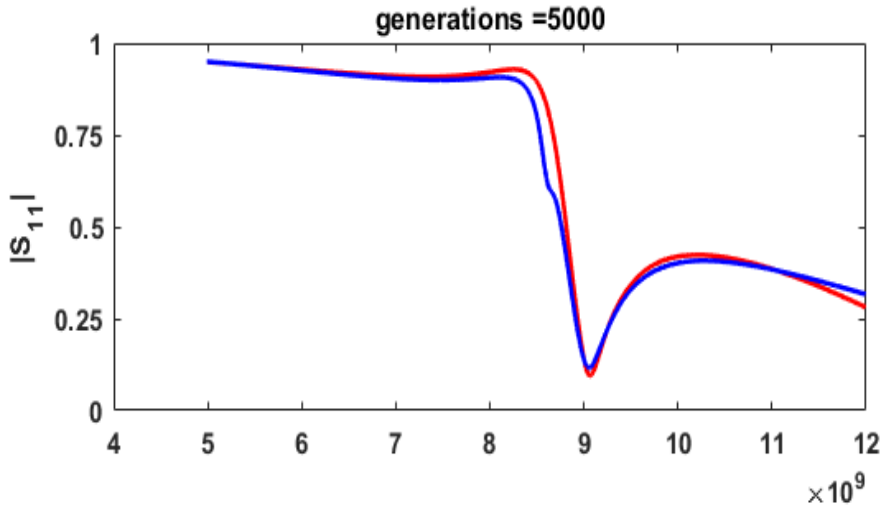

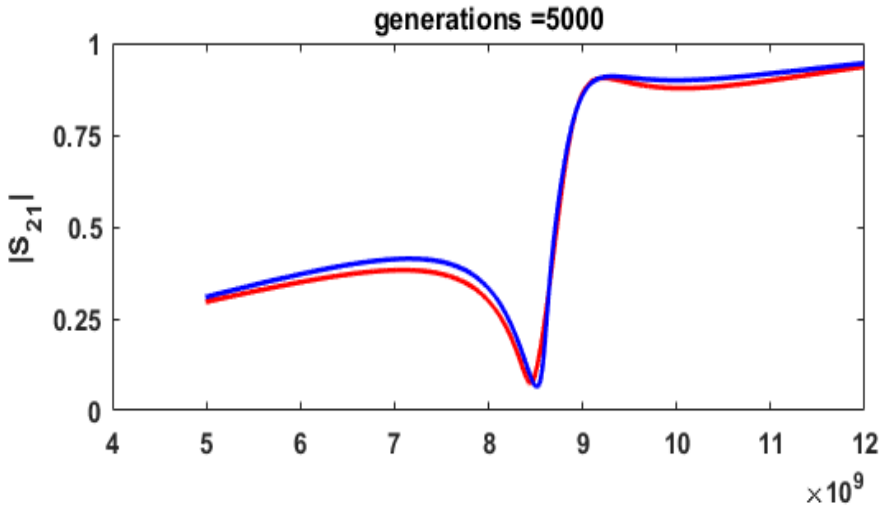

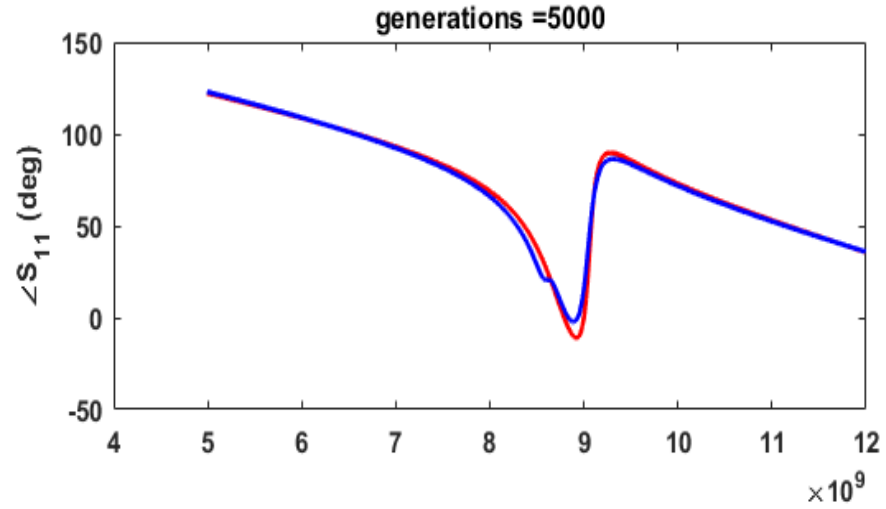

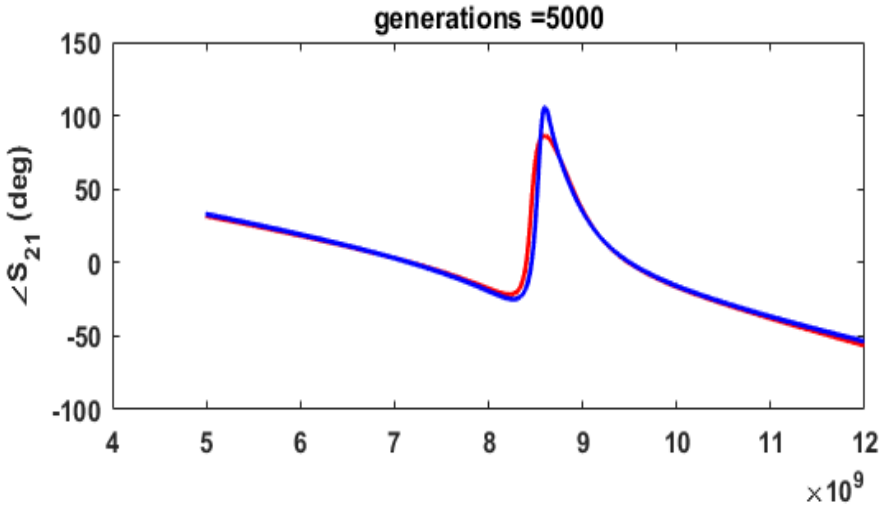

Abscissa: Frequency (Hz), red: from unit cell simulation, blue: PFDM

Method #2: PFDM

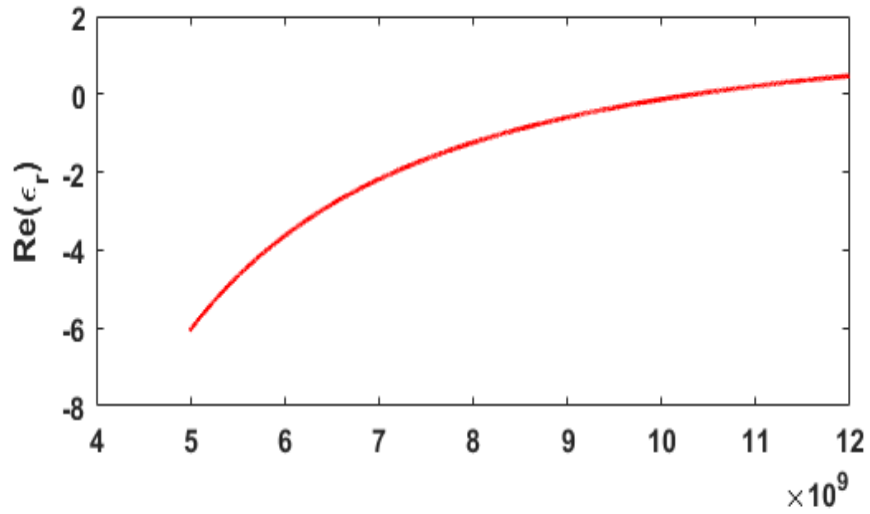

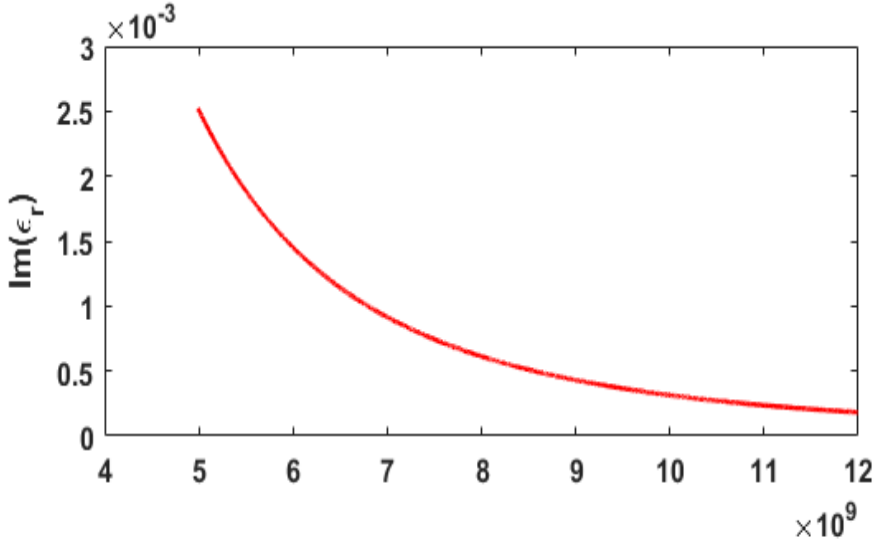

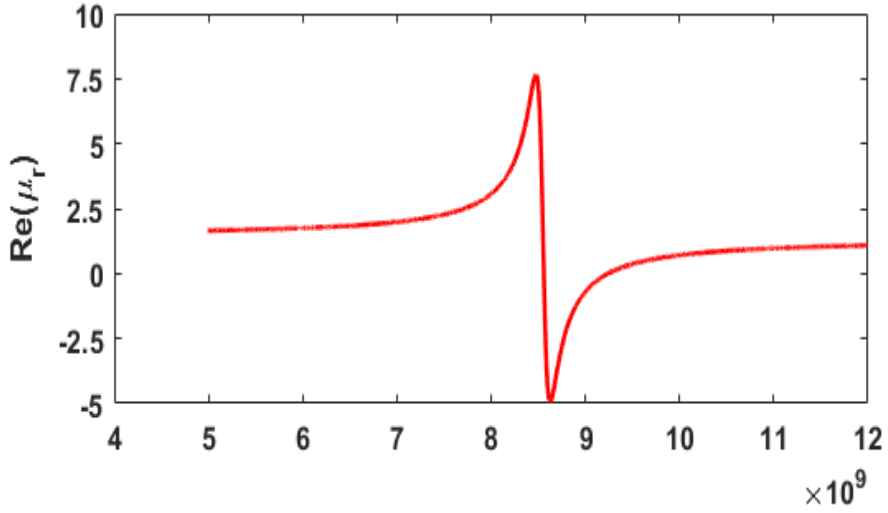

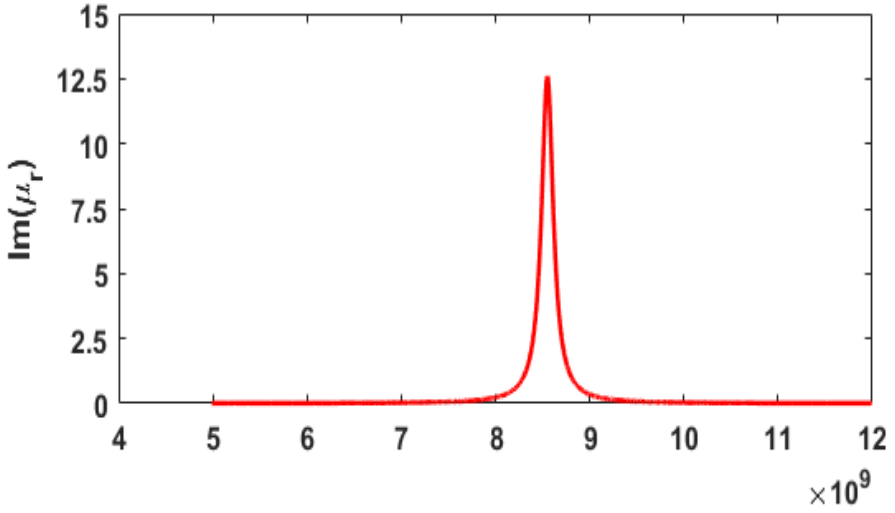

Abscissa: Frequency (Hz)

Fabricated samples

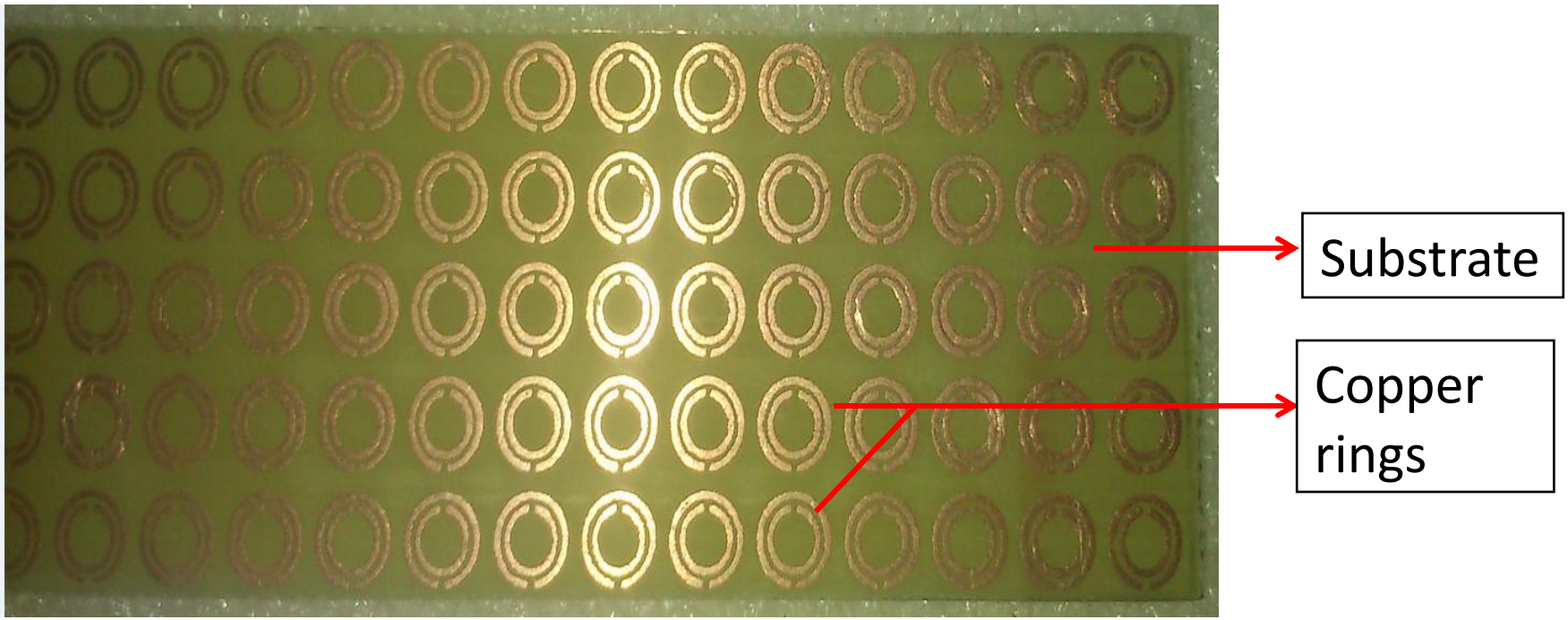

Fabricated samples

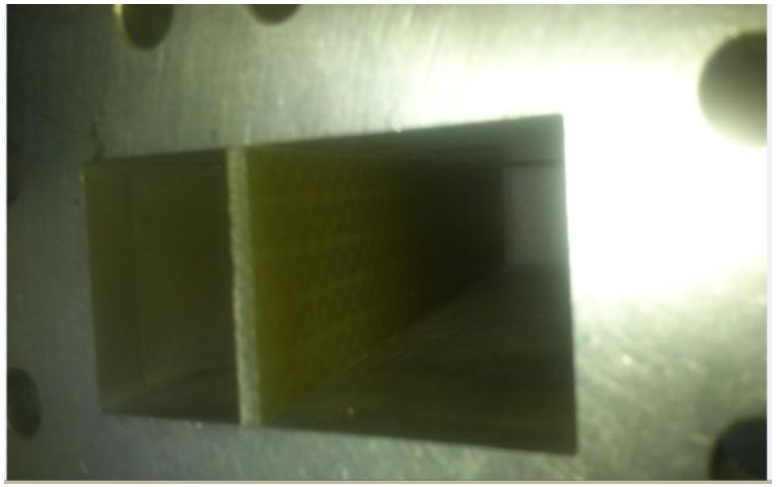

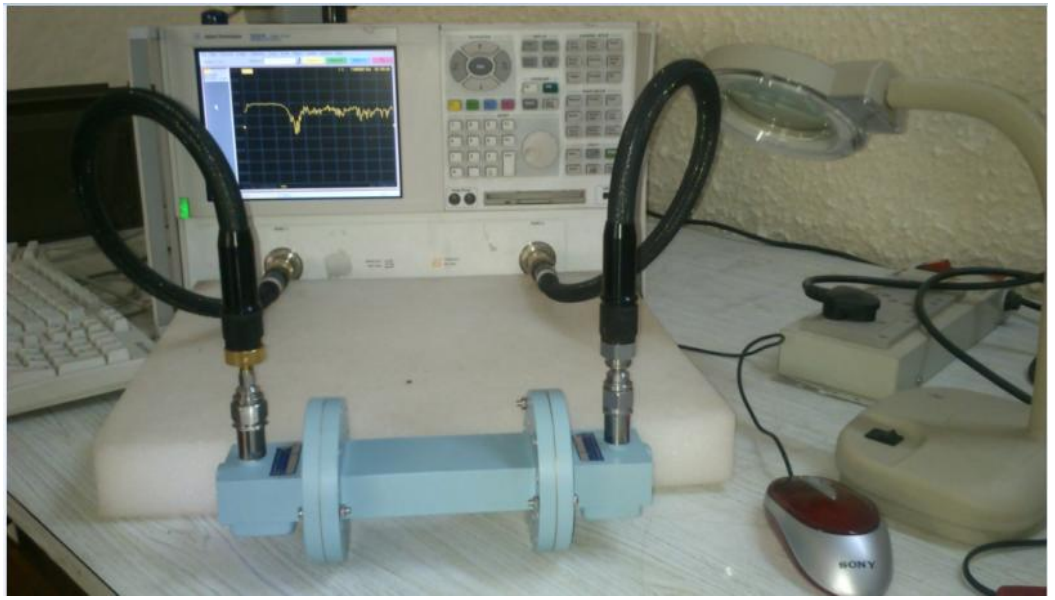

Fabricated samples

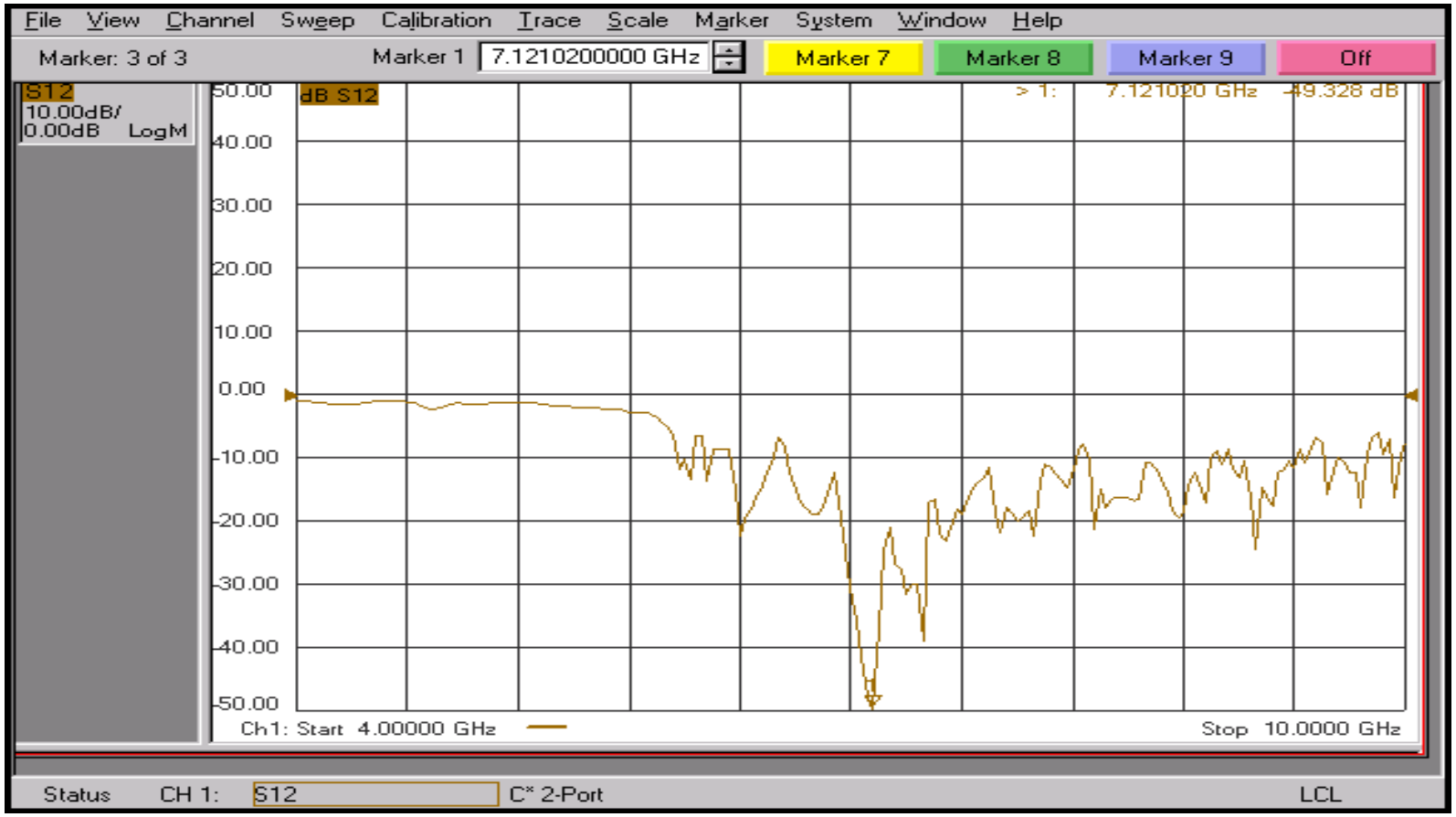

Fabricated samples

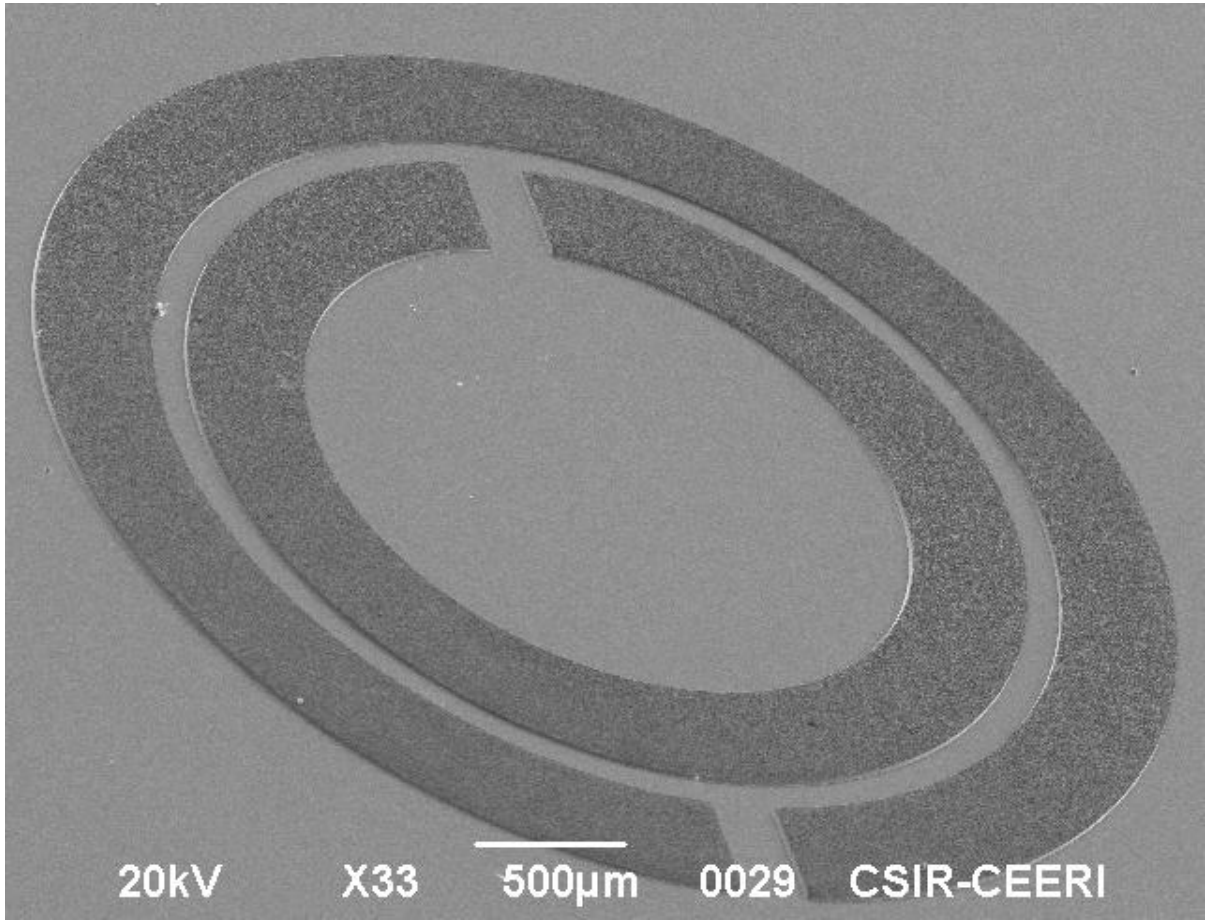

Fabricated samples

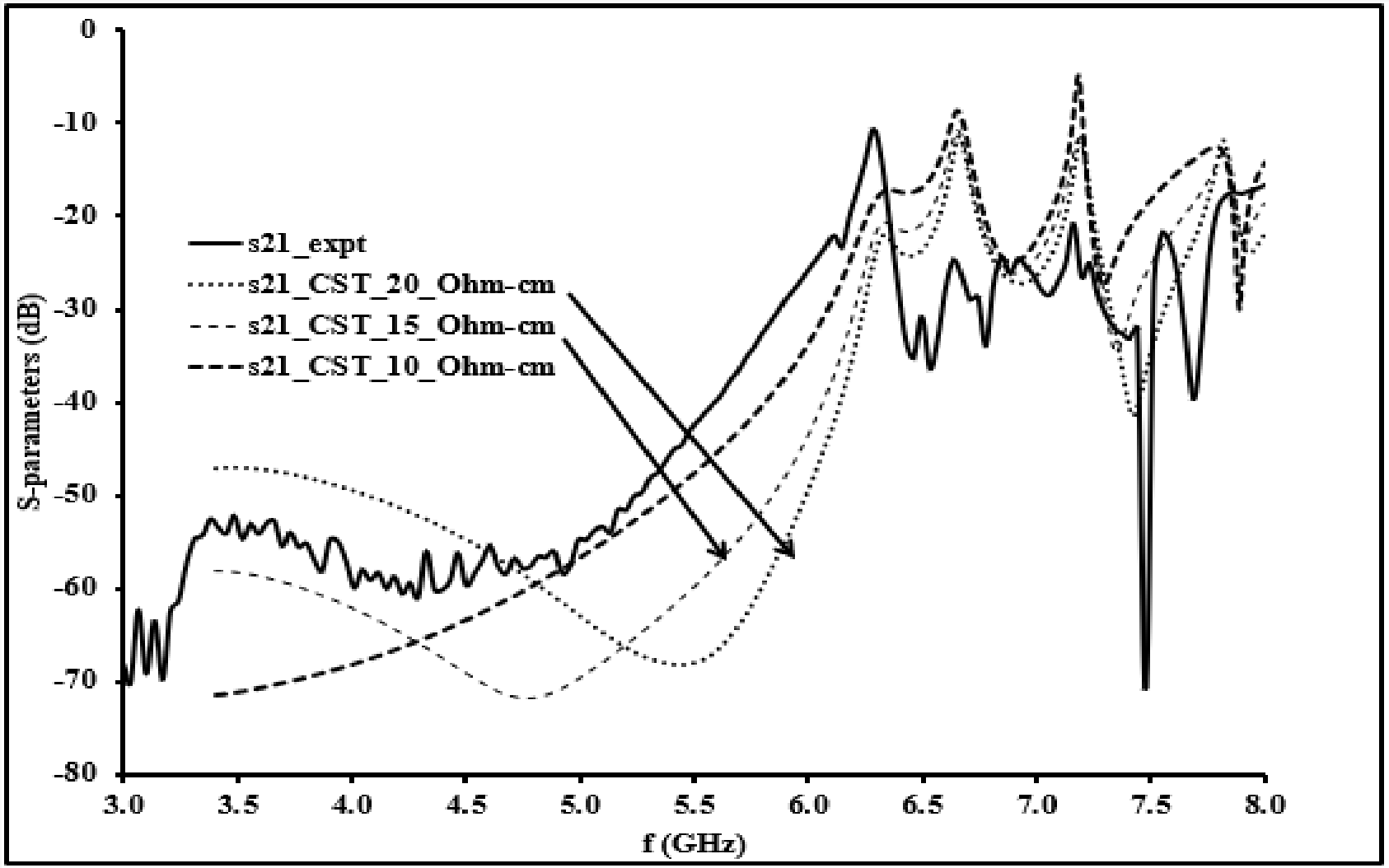

Fishnet MTMs - evolution

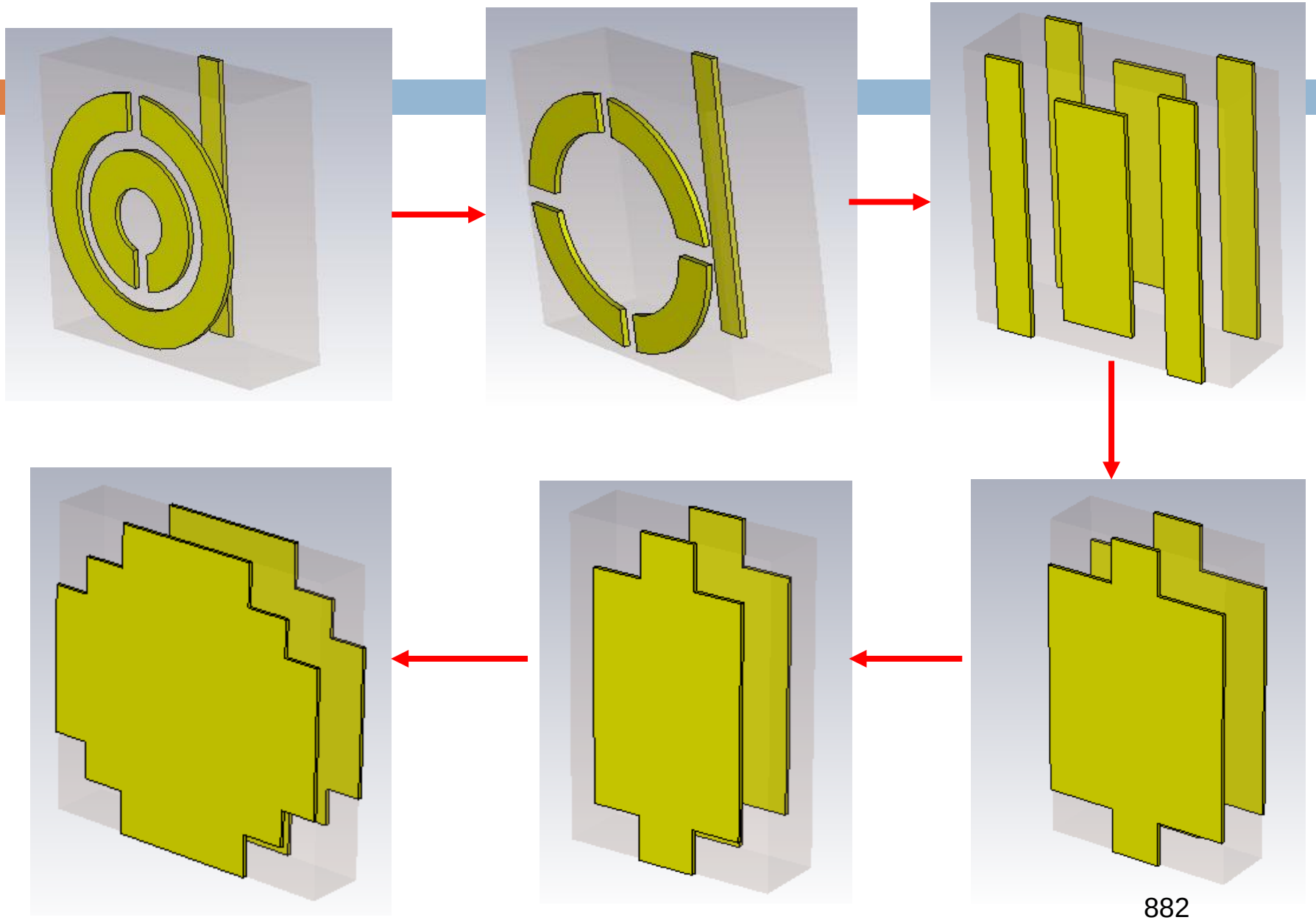

Vane-type fishnet MTM

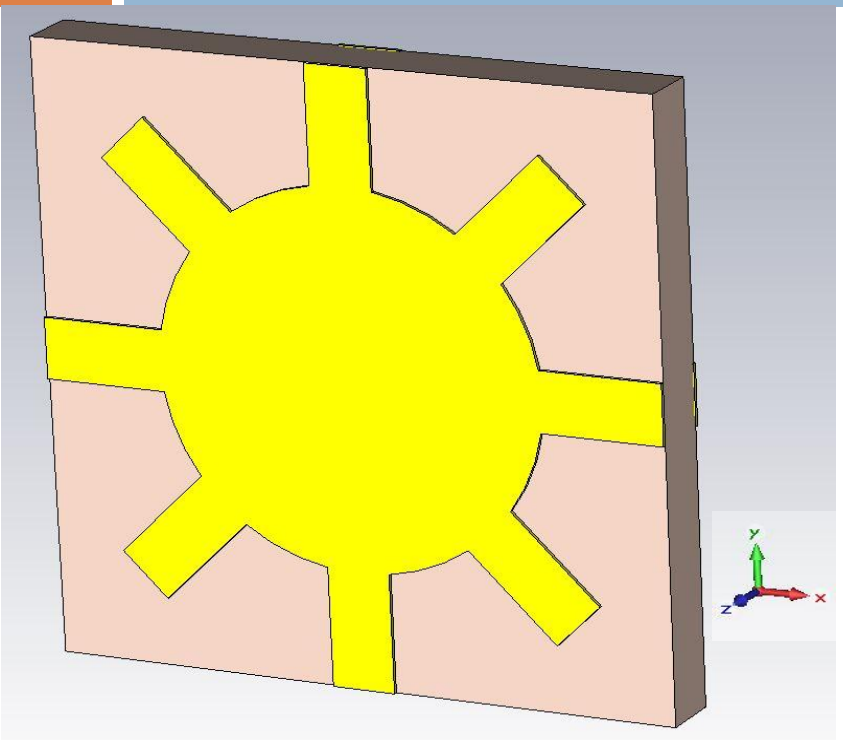

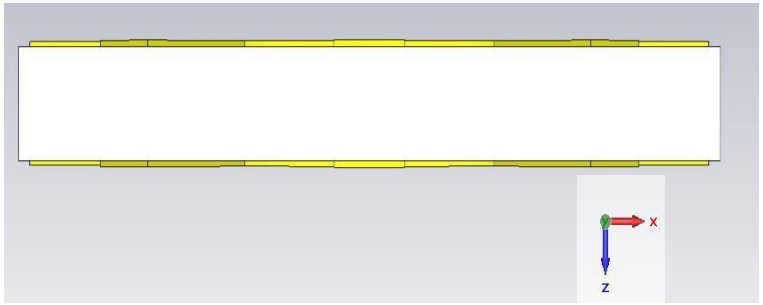

Orthogonal incidence and TE/TM polarization

Vane-type fishnet MTM

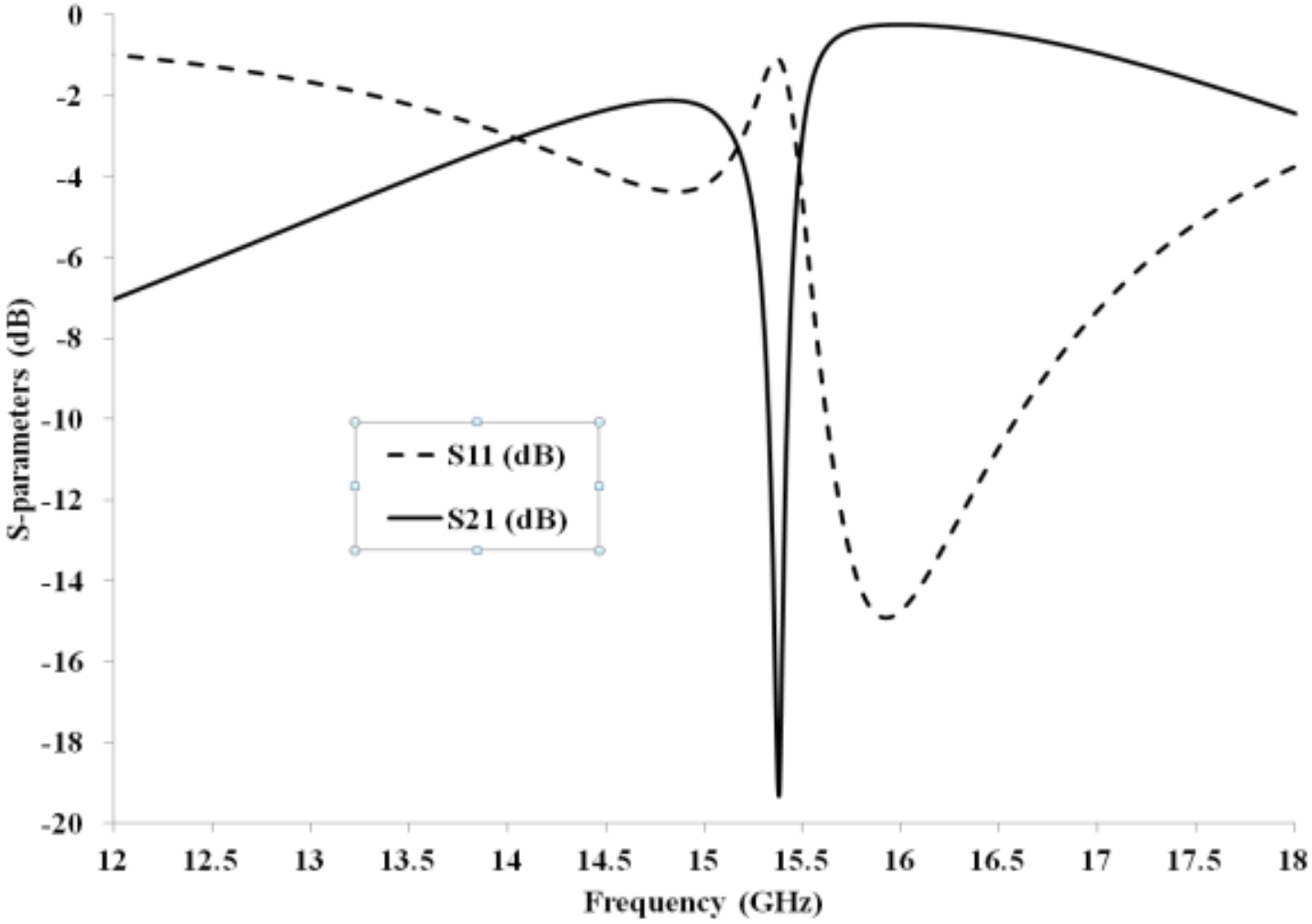

Vane-type fishnet MTM

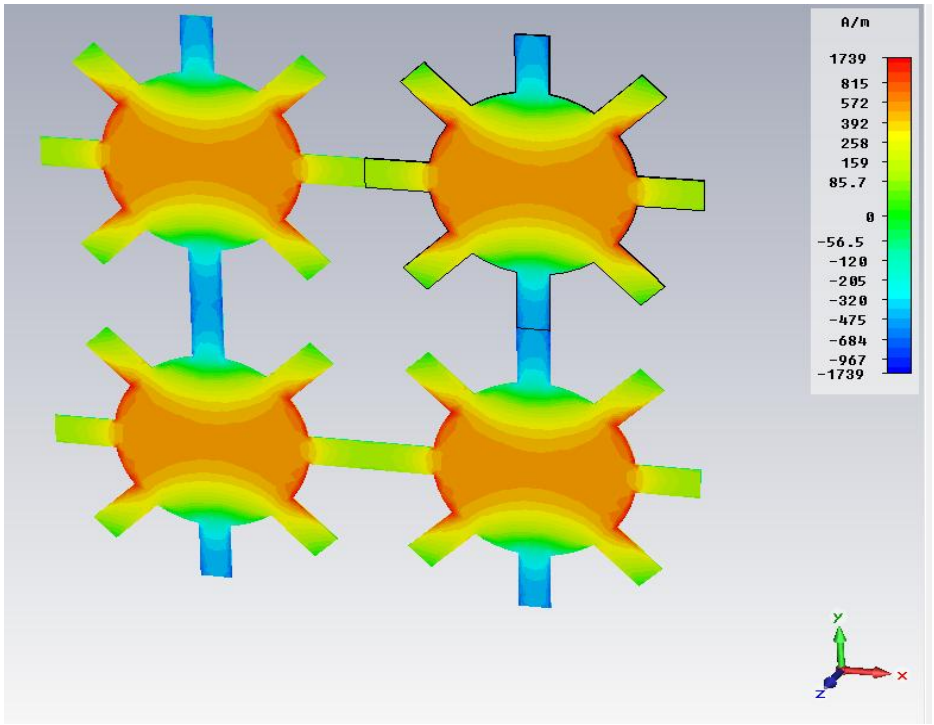

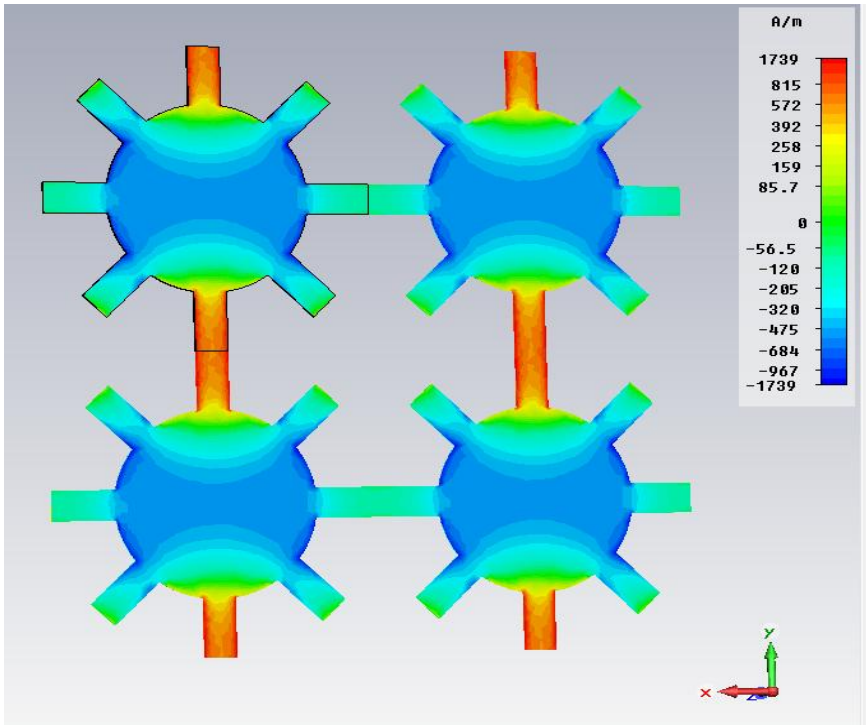

Surface current on both the sides of the structure

Vane-type fishnet MTM

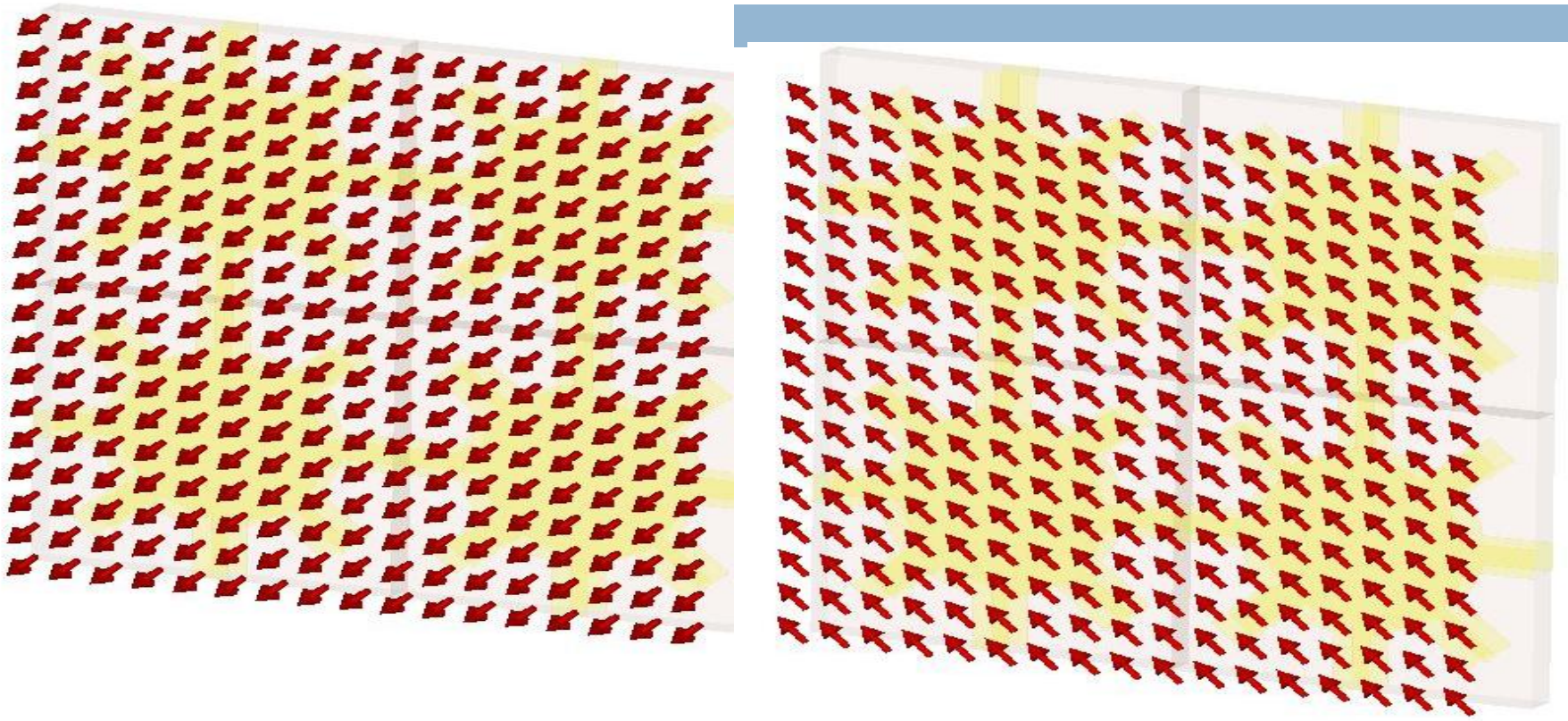

TE polarized plane wave excitation of the vane-type fishnet structure polarized at 135^0. E-field (left) and H-field (right). The unit cells in the background.

Vane-type fishnet MTM

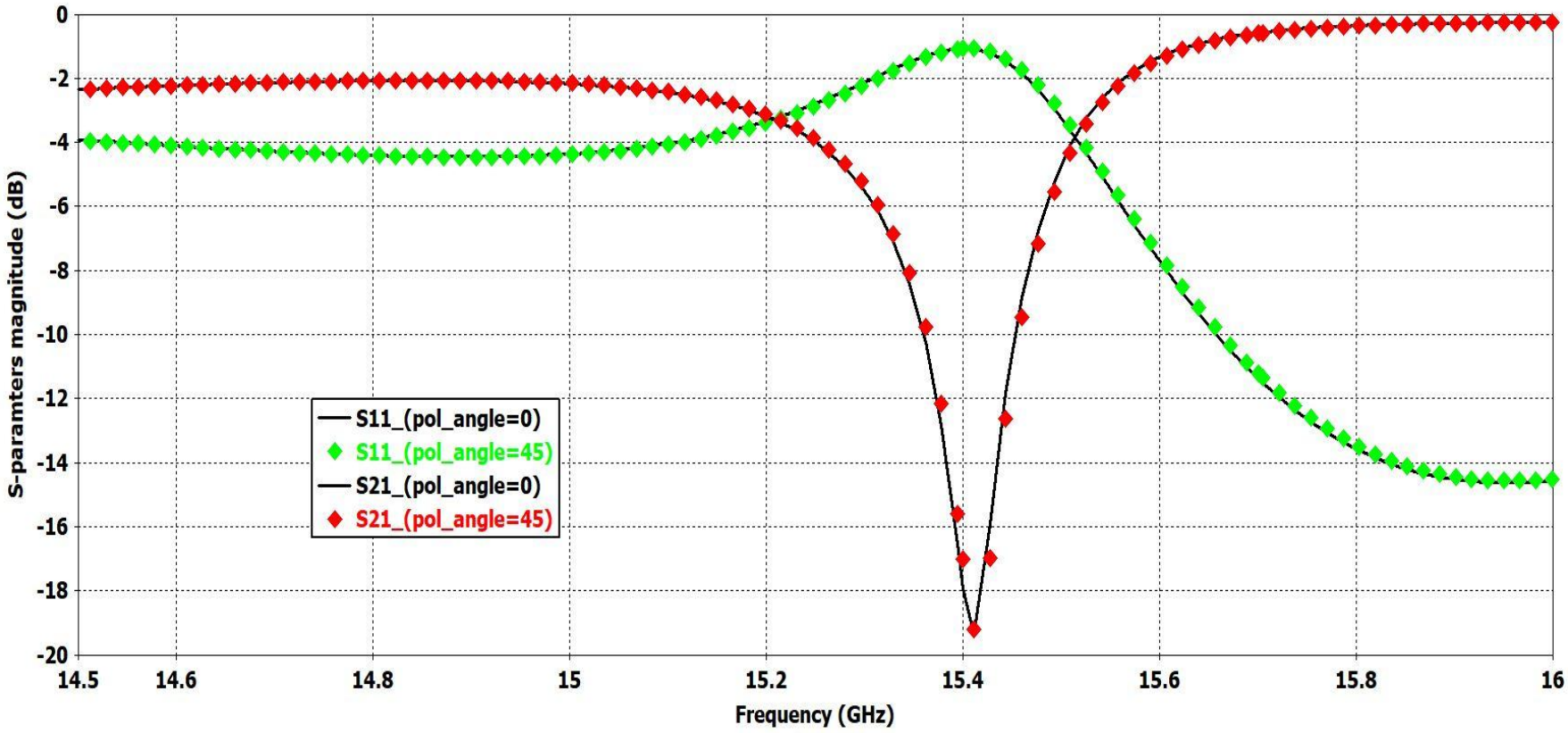

S_{11} and S_{21} response of the vane-type fishnet structure for 0 and 45degree polarization angles

Vane-type fishnet MTM

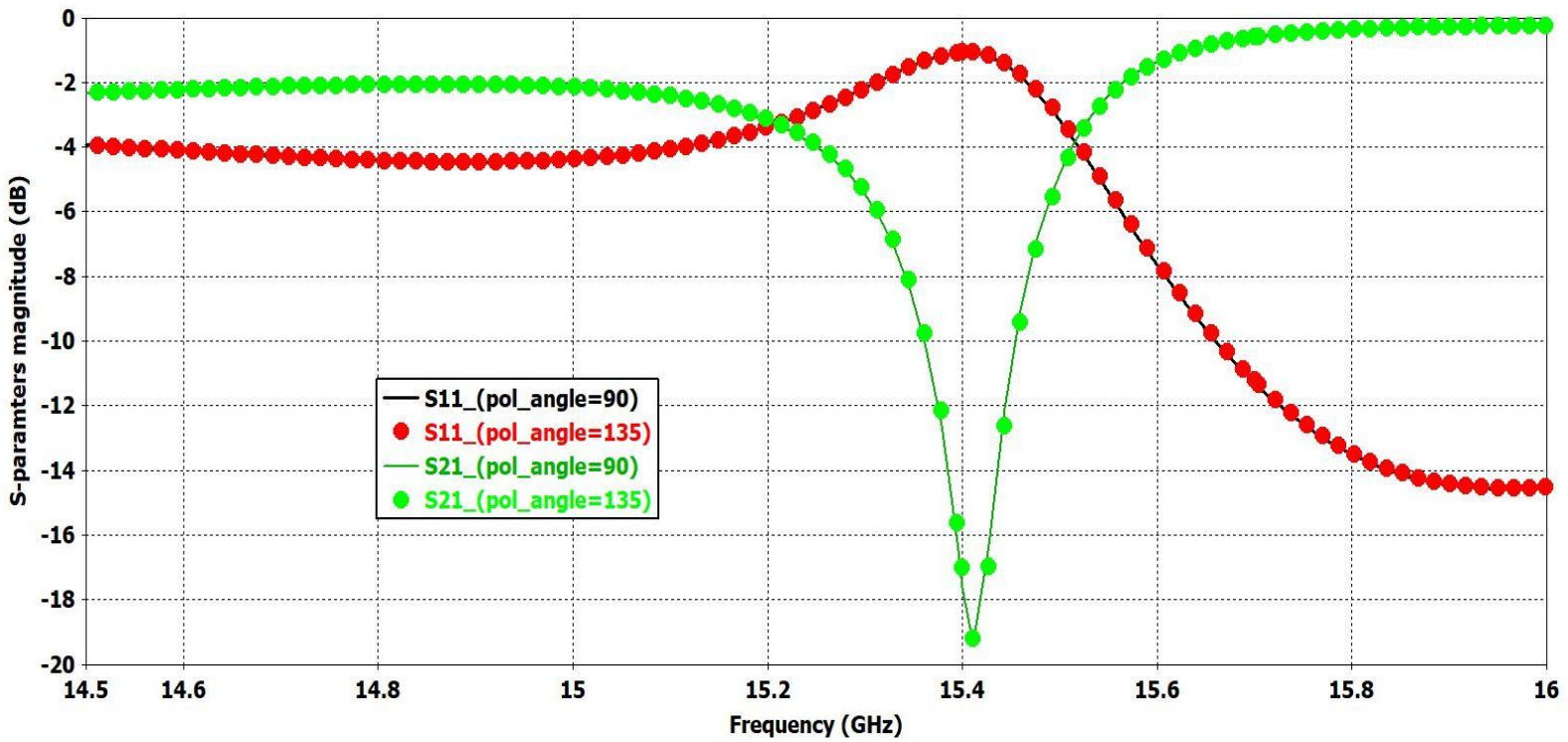

S_{11} and S_{21} response of the vane-type fishnet structure for 90 and 135 degree polarization angles

Vane-type fishnet MTM

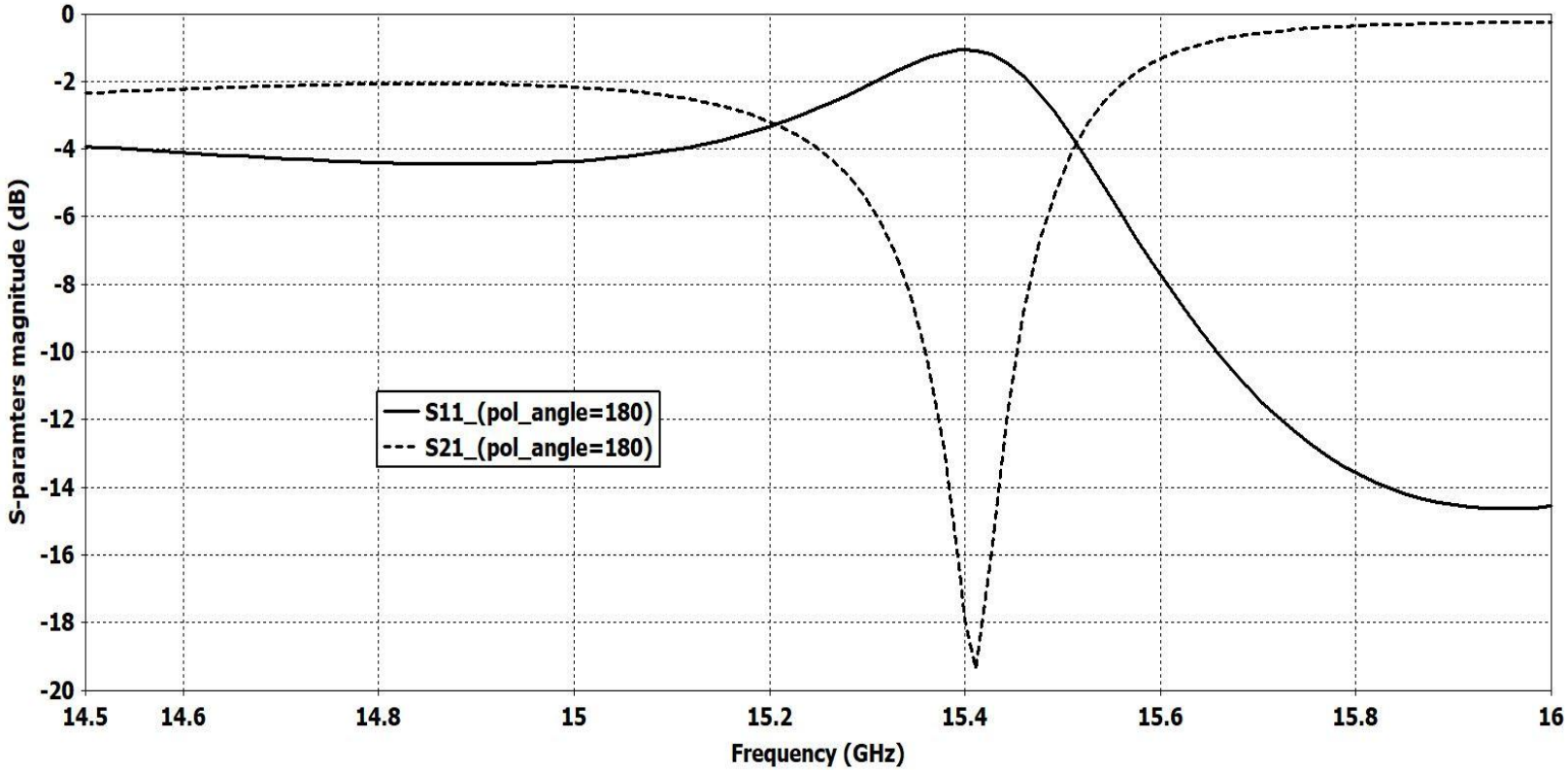

S_{11} and S_{21} response of the vane-type fishnet structure for 180 degree polarization angle

Negative refraction experiment

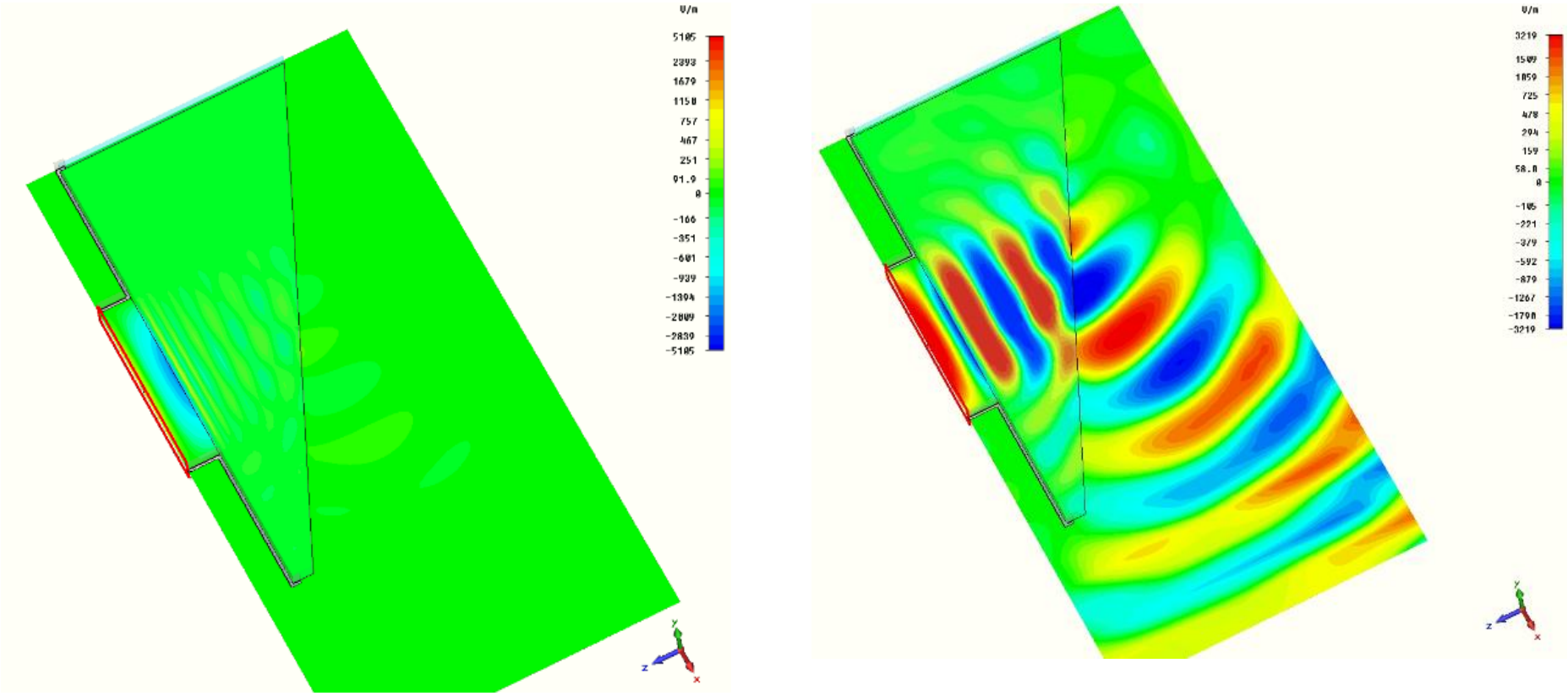

Negative refraction observed at 15.4 GHz (left) and 15.7 GHz (right);

Comparison with other structures

Parameter	W. S. Zaoui et. al., Phot. Nanost. – Fund. Applns, 10, 2012	B. Kante et. al. Phys. Rev. B., 79, 075121, 2009	Y. Z. Cheng et. al. Eur. Phys. J. B, 85:62, 2012	C. Sabah, J. Mater. Sci: Mater Elect. 2016	M. Choi et. al. Nature, 470, 2011	Present work
Frequency	40 GHz	11.5 GHz	8.5 GHz	10.8 GHz	0.851 THz	15.66 GHz
MTM type	Cross-circle fishnet	Cut-wire pair	3D fishnet	Octogon-shaped	I-shaped patch	Vane-type fishnet
Refractive index	-0.93	~-3	-4.5	>-1	+33.22	-2.22
FoM	42	42	55.1	80	> 10	17.65

Vane-type fishnet fabrication

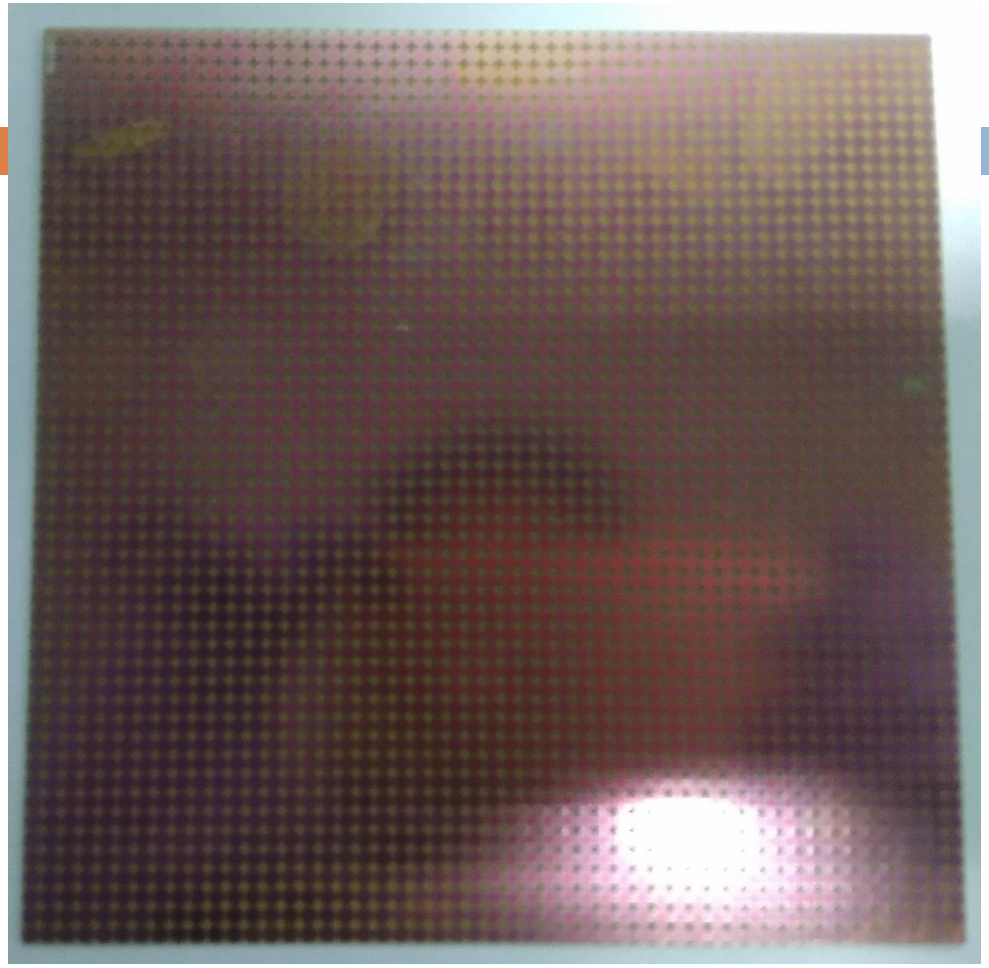

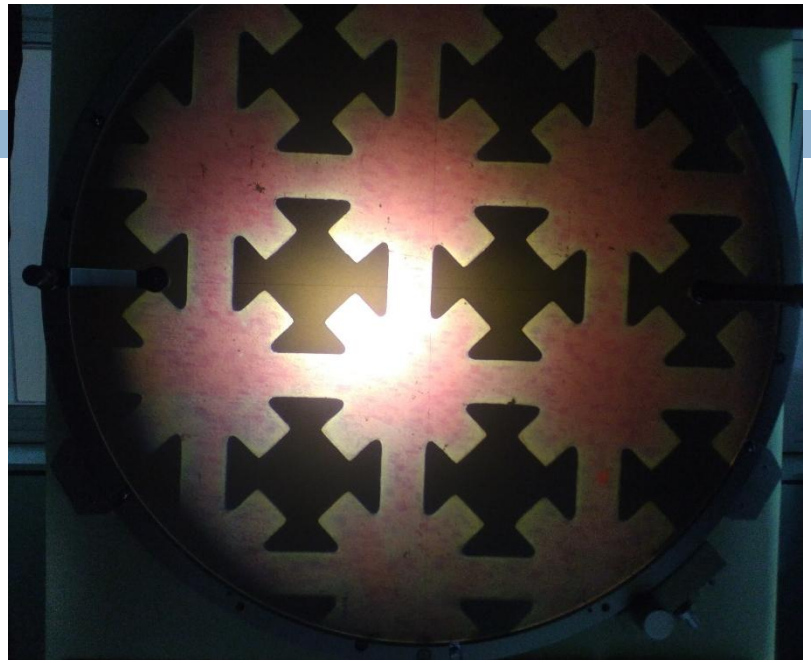

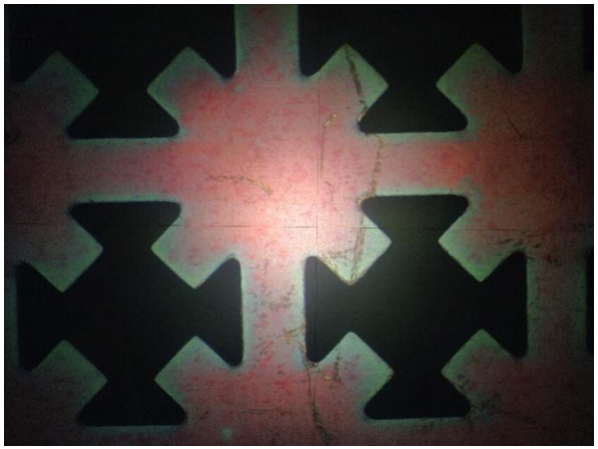

Fabricated array (51X51 unit cells) on FR4 substrate and close-up shots from profile projector

ε-negative MTM based interaction structures

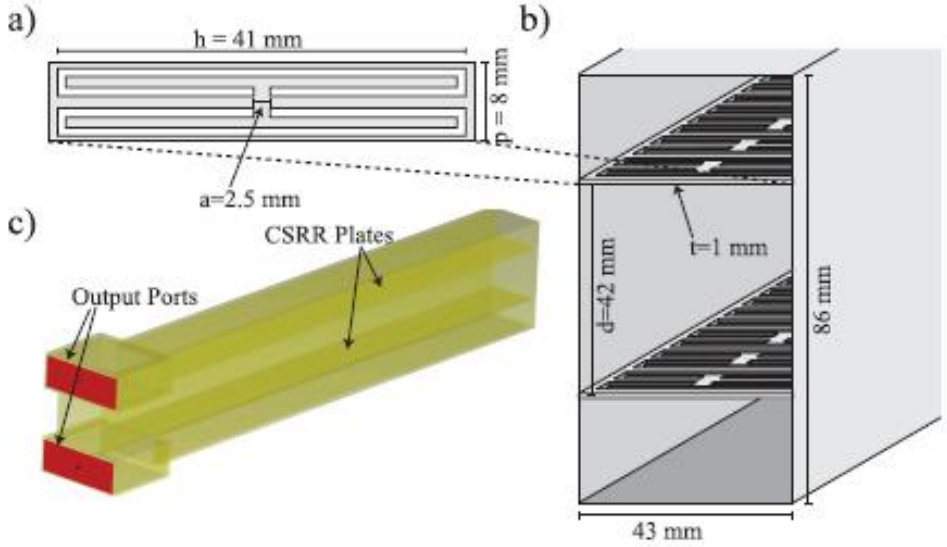

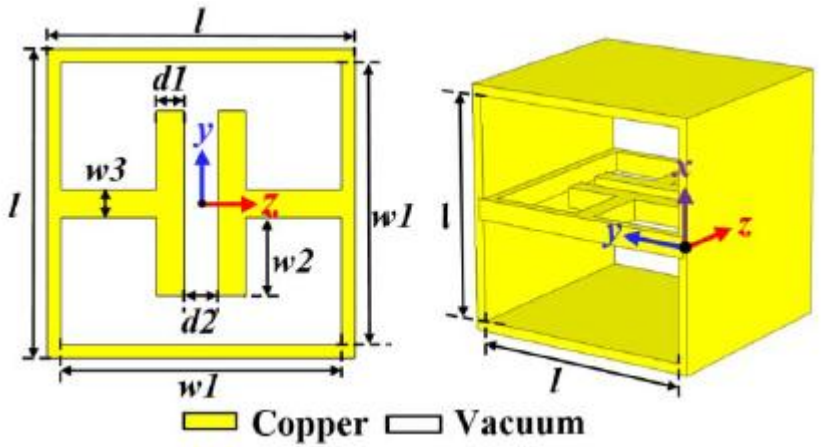

Hummelt et. al., IEEE Trans. Plas. Sci., 42, 4, pp. 930-936, 2014

Wu et. al., IEEE Trans. Elect. Dev. 65, 3,pp. 1171-1178, 2018

TW MTM based Interaction Structure

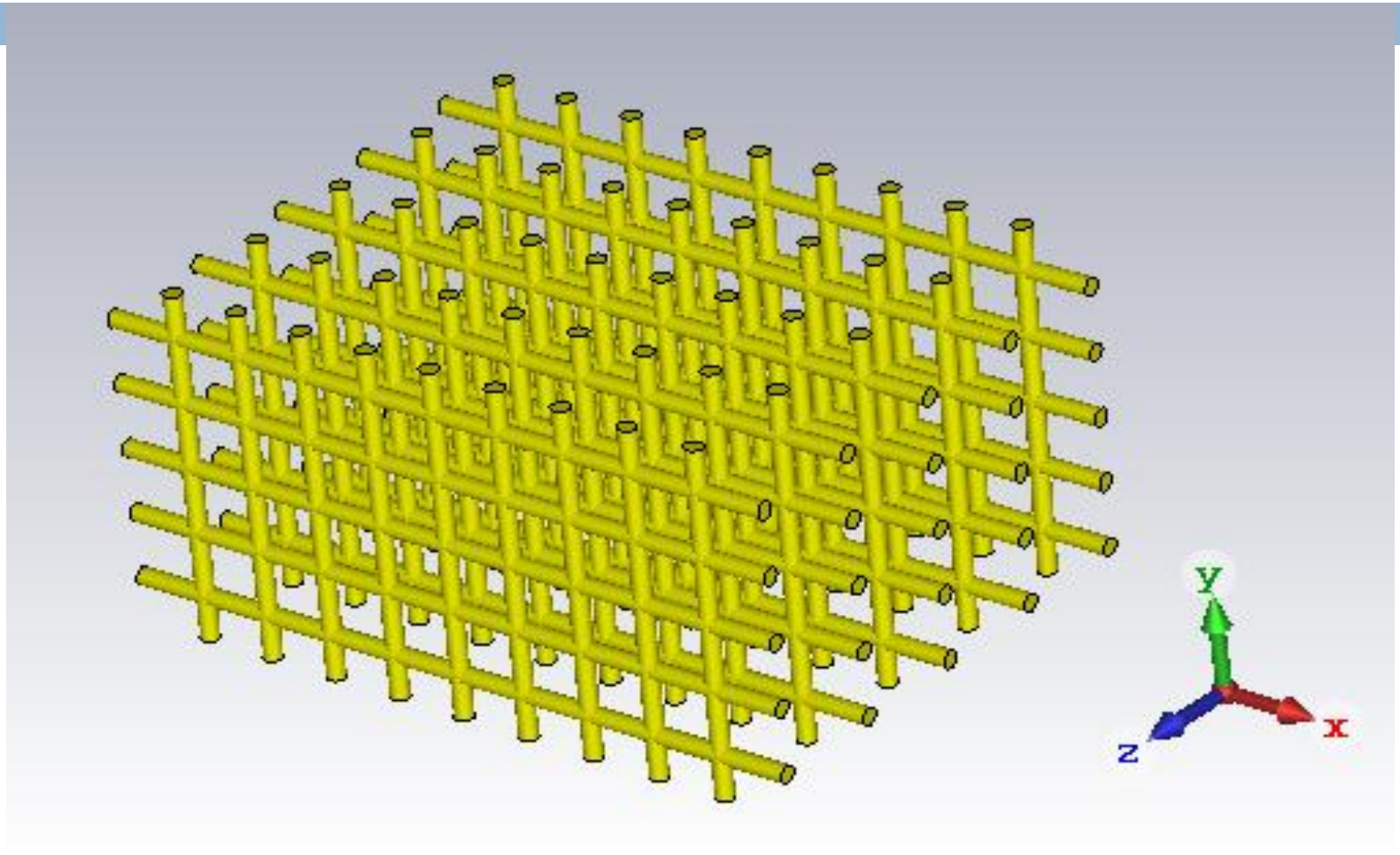

$$\bar{\bar{\epsilon}} = \epsilon_h u_z u_z + \epsilon_t (u_x u_x + u_y u_y)$$

TW MTM based Interaction Structure

$$\epsilon_t = \epsilon_h \left(1 - \frac{k_p^2}{k^2 - k_z^2}\right)$$

$$k_p = \sqrt{\frac{2\pi}{d^2\left(\ln\left(\frac{d}{2\pi r}\right) + 0.5275\right)}}$$

ε_t – transverse permittivity, ε_h – permittivity of the host medium, r – radius of the wire, d - period

TW MTM based Interaction Structure

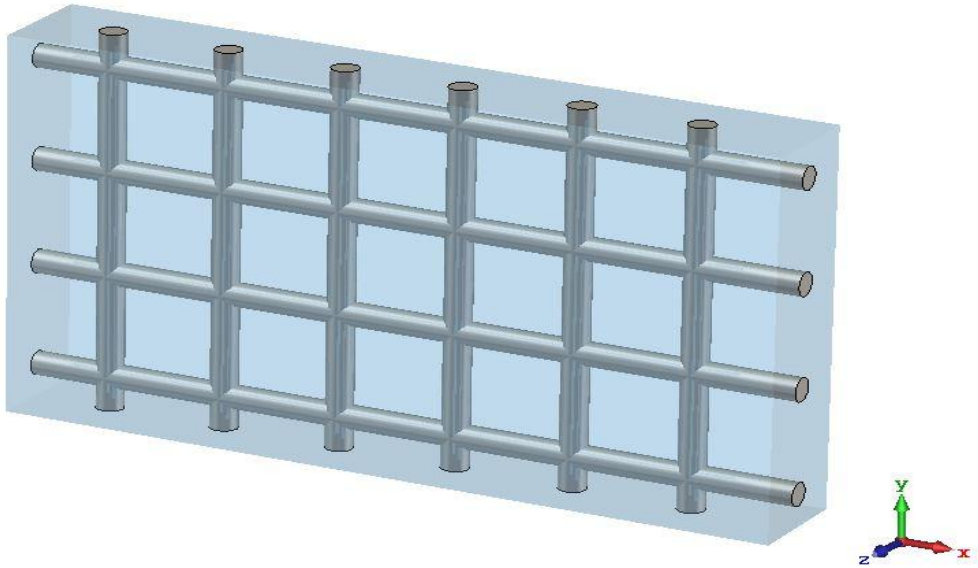

- Periodic in Z-direction

TW MTM based Interaction Structure

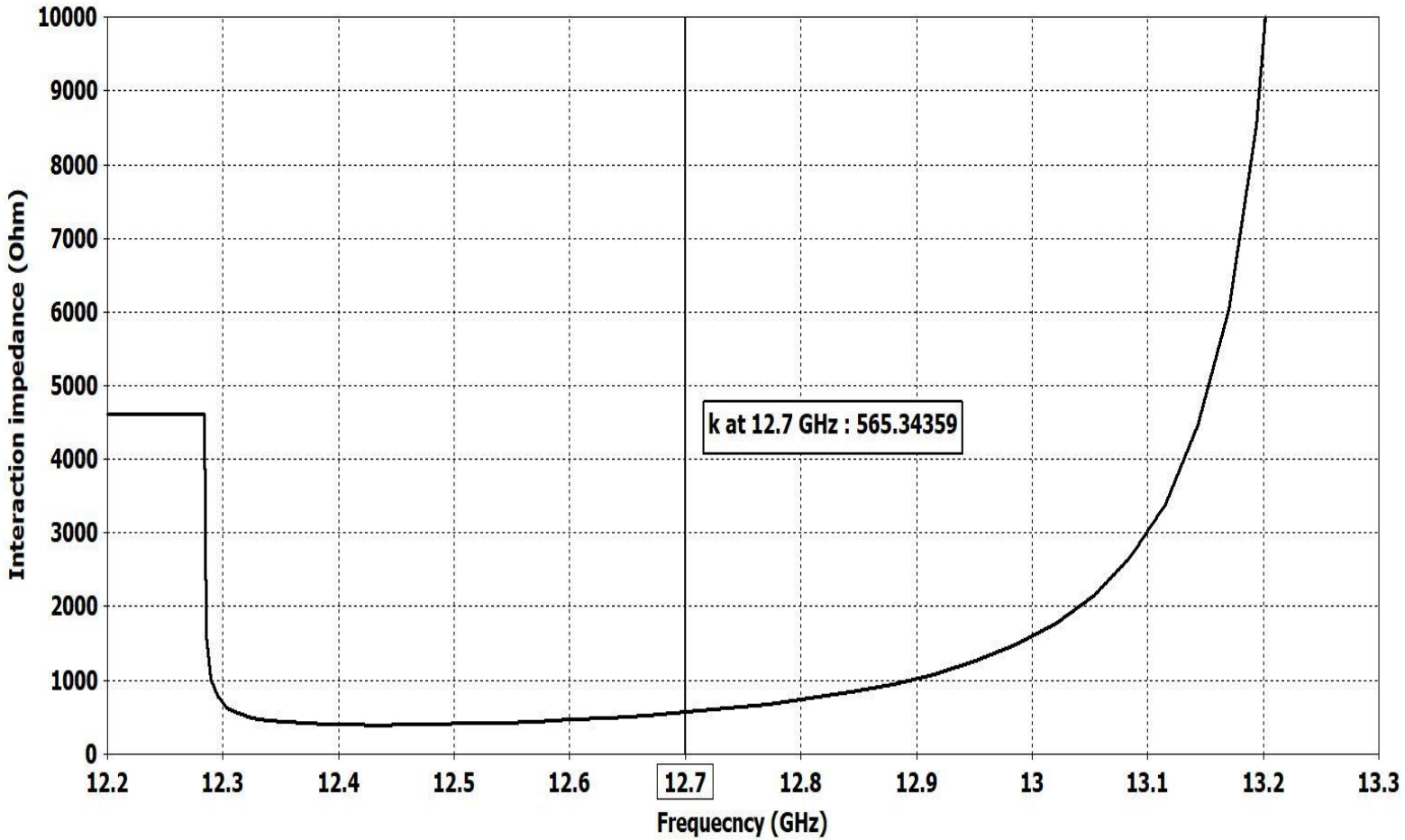

Interaction impedance of the first backward mode

TW MTM based Interaction Structure

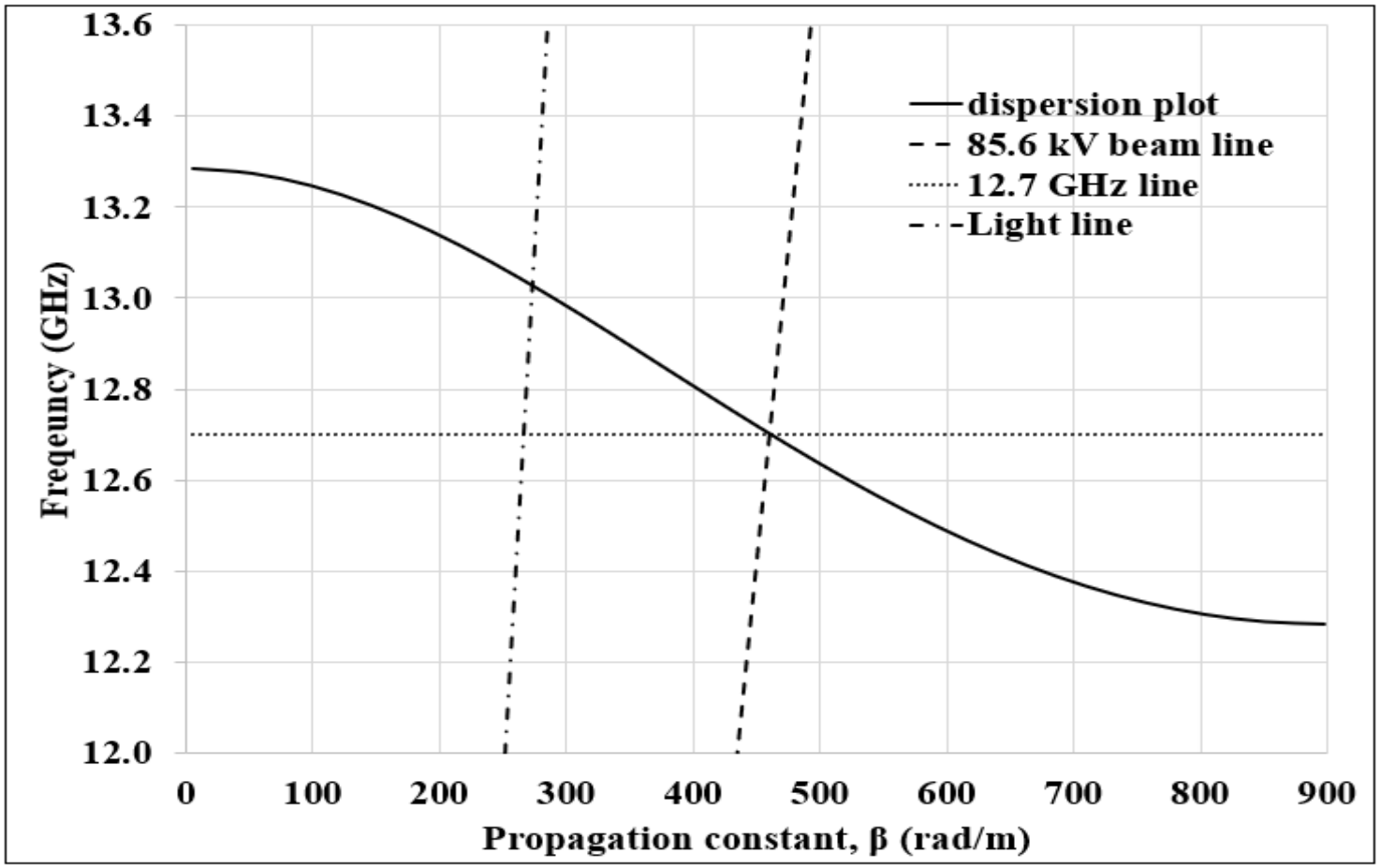

Operating point of the first mode

TW MTM based Interaction Structure

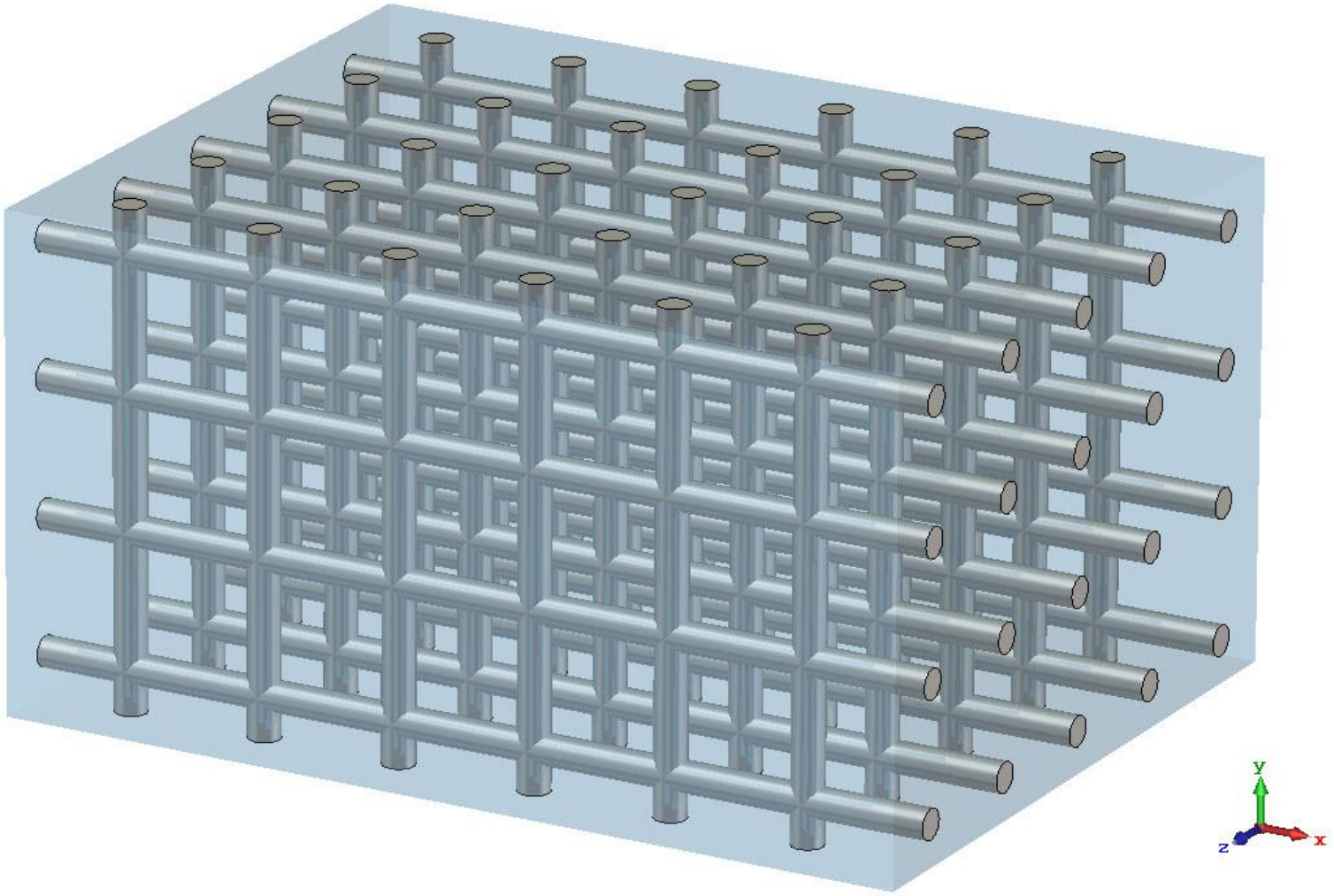

TW MTM based Interaction Structure

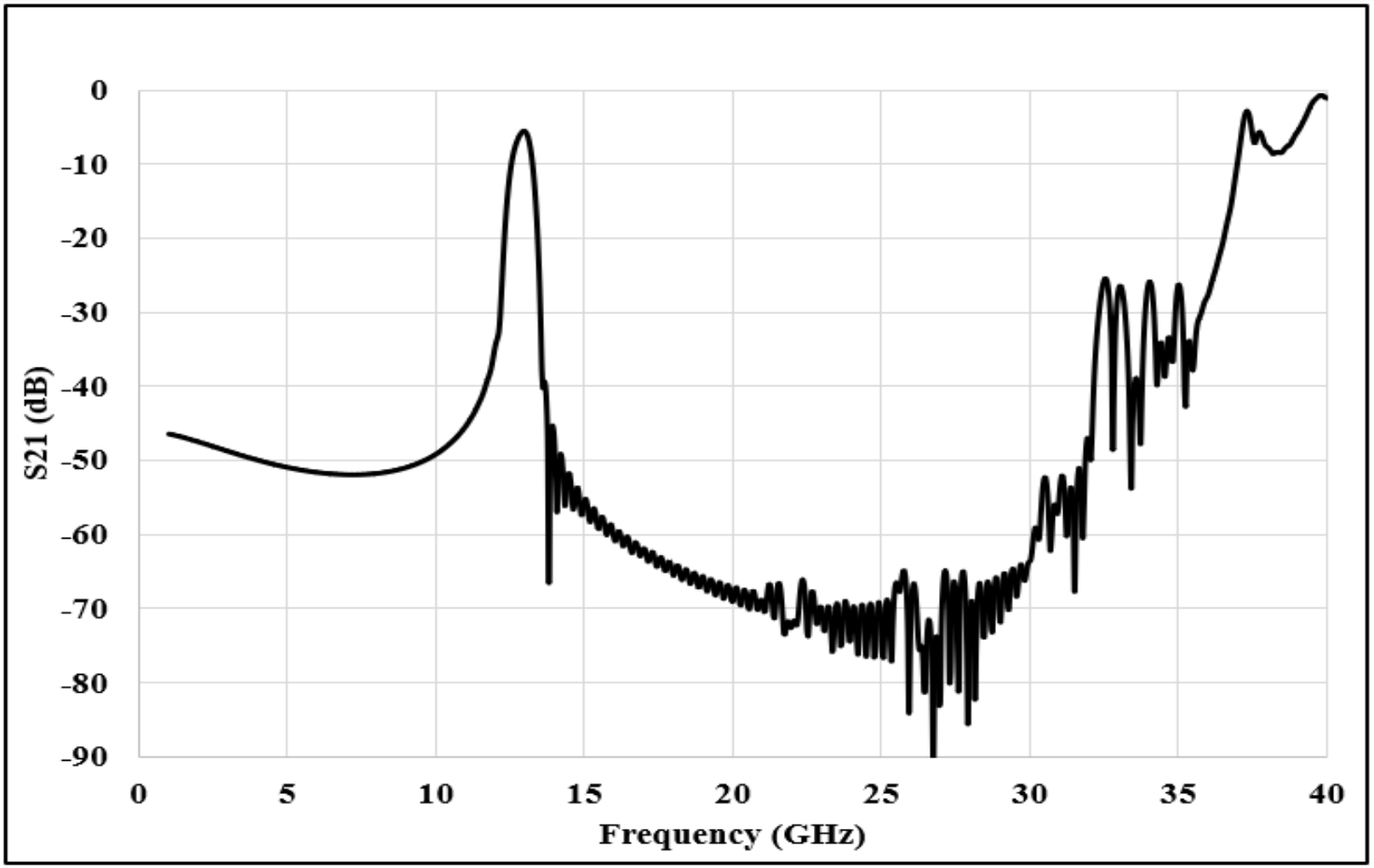

S-parameter response showing the first backward mode

TW MTM based Interaction Structure

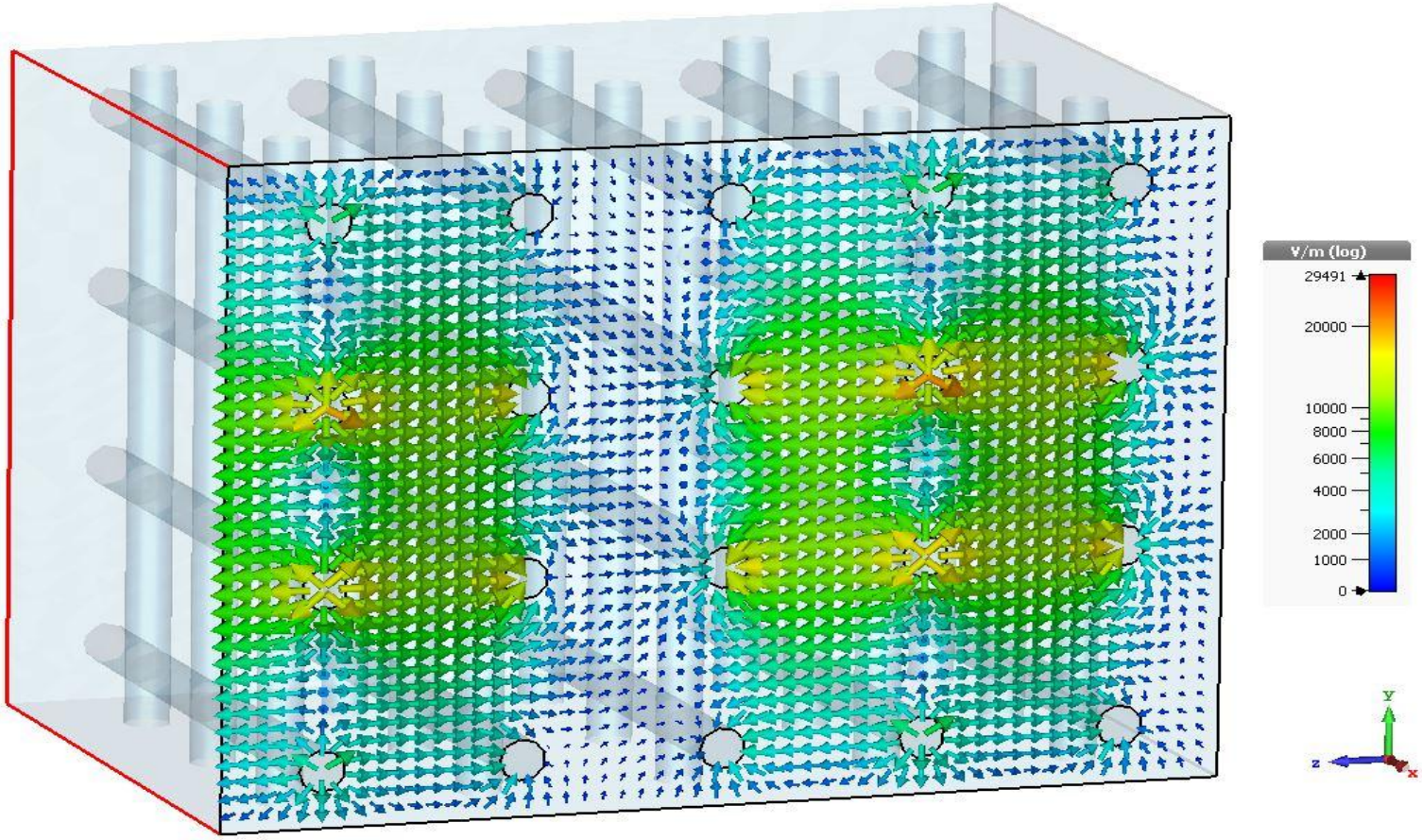

Axial electric field (E_z) of the first backward mode

TW MTM based Interaction Structure

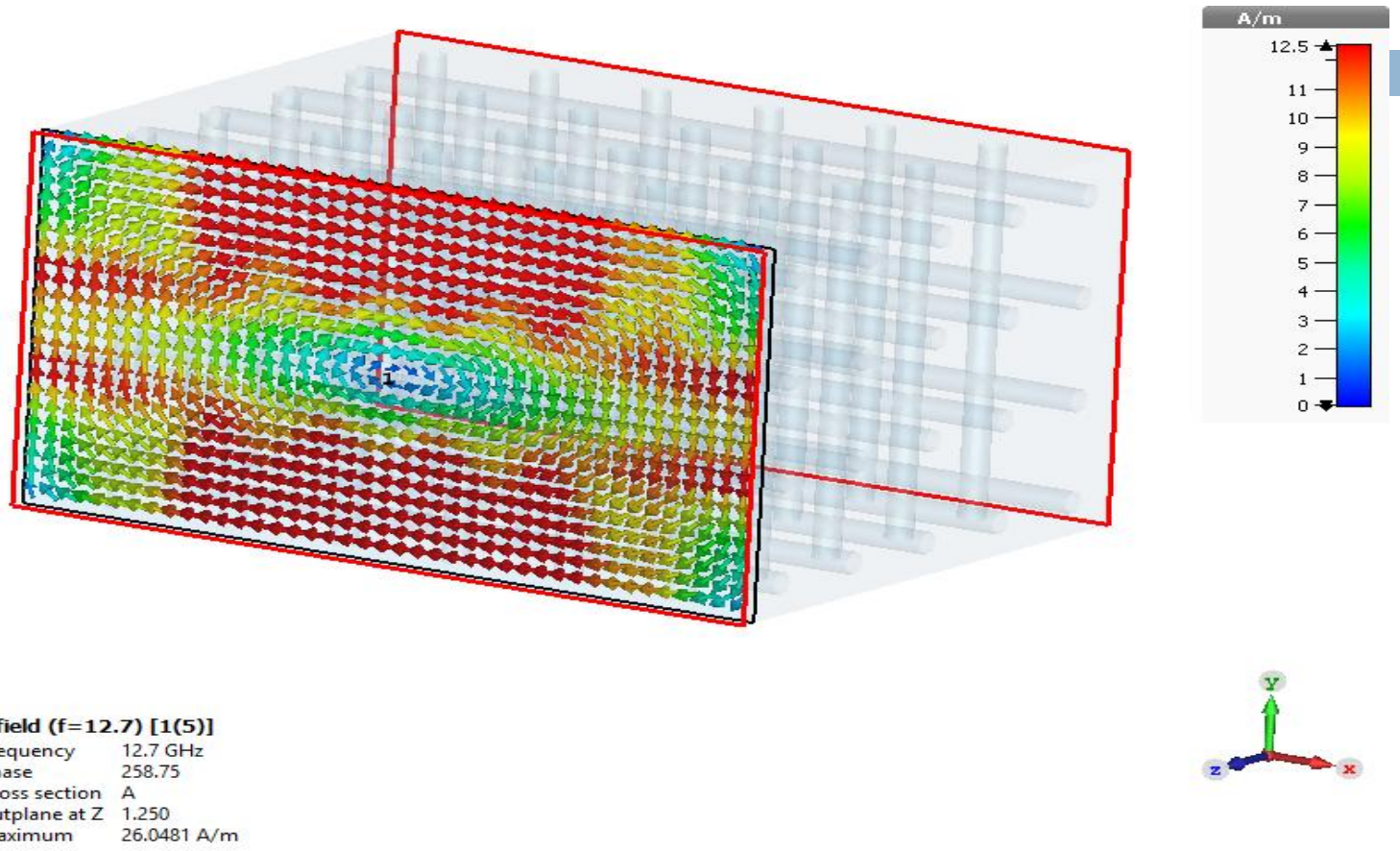

Magnetic field profile observed at +Z end of the interaction structure

Fabricated square TW array and waveguide

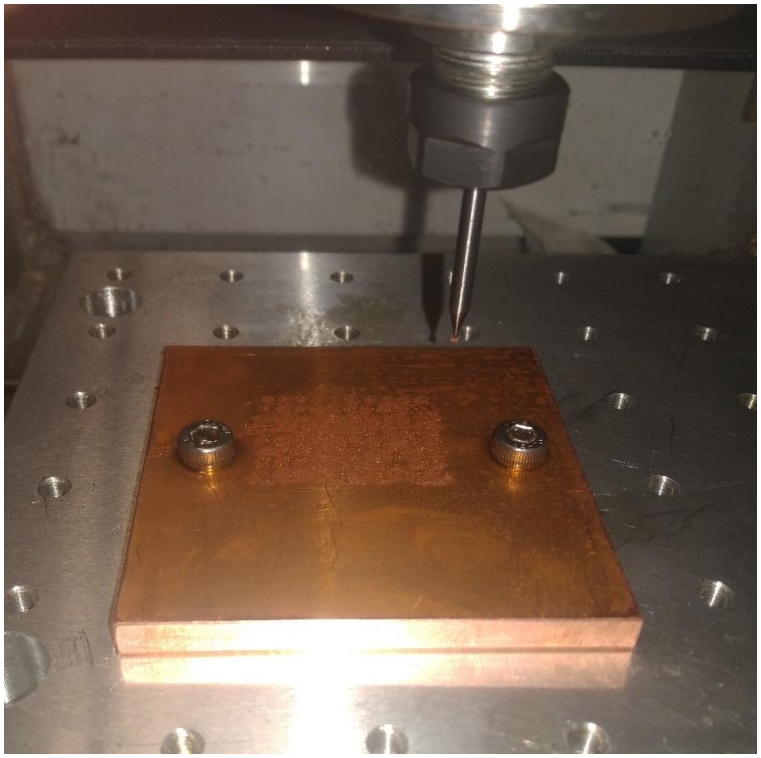

Grooves being made using Micro-EDM

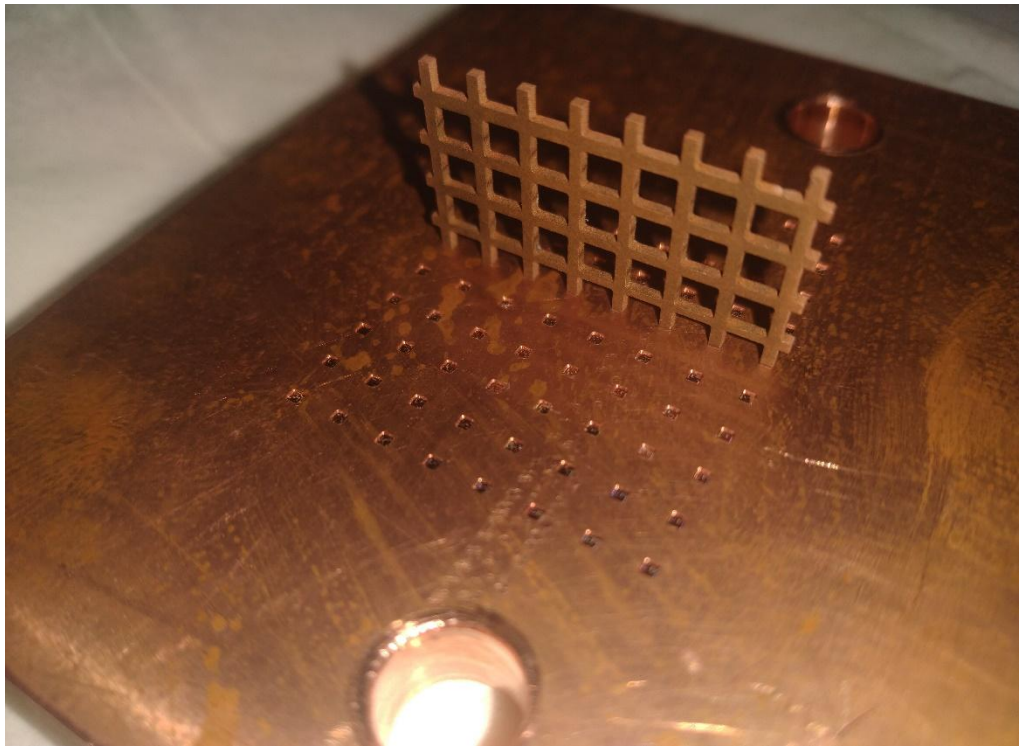

A TW array fitted in the grooves

MTM based helix SWS

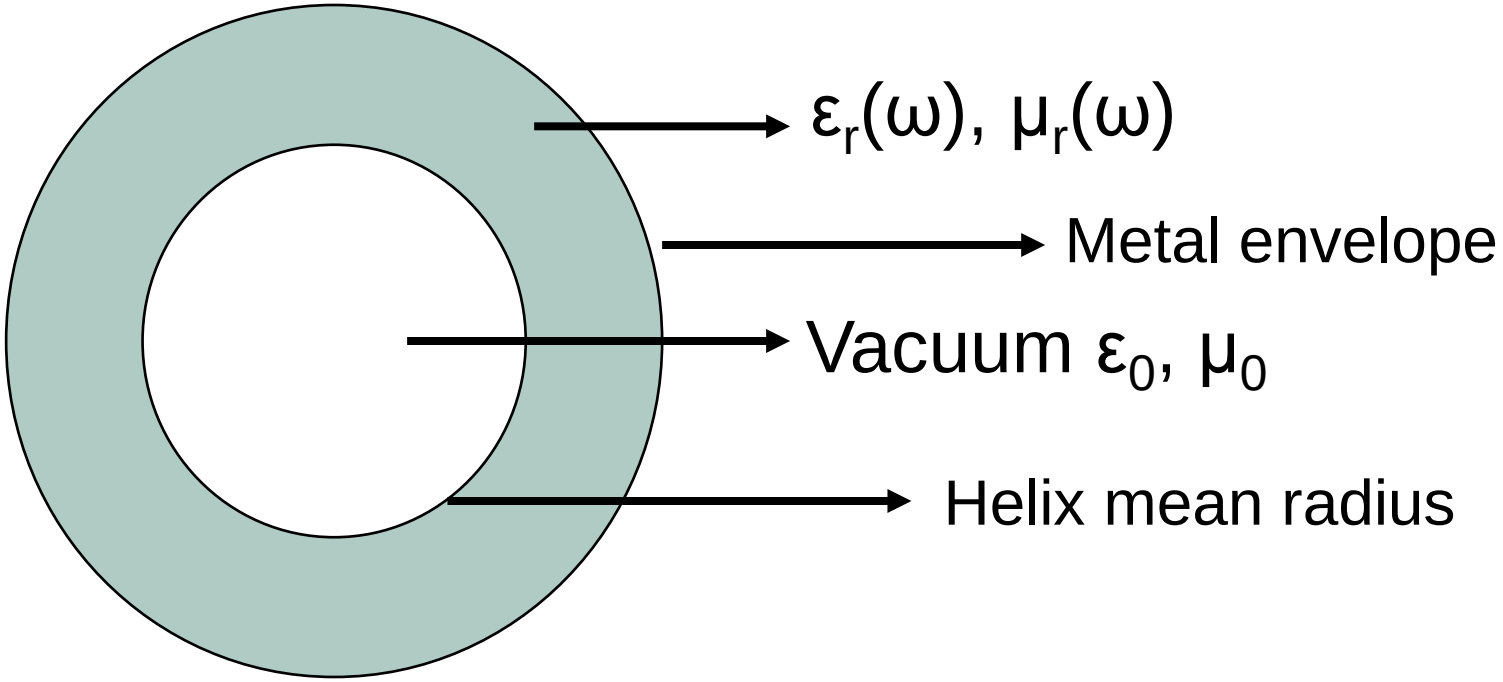

ϵ_0 and μ_0 - permittivity and permeability of free space respectively. $\epsilon_r(\omega)$ and $\mu_r(\omega)$ - relative permittivity and relative permeability of the support region respectively.

Flowchart showing the process of generating ϵ_r/μ_r dataset

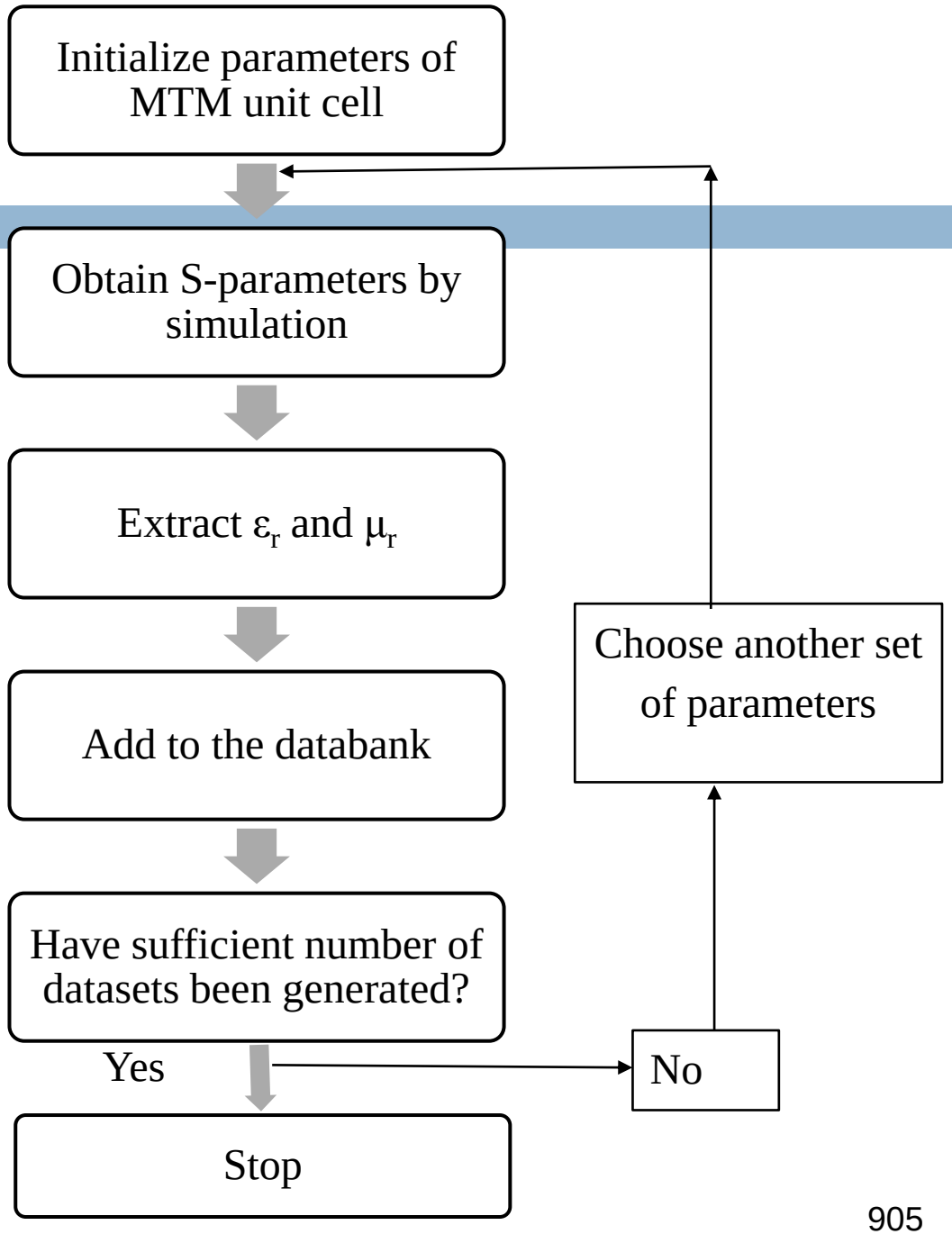

Flowchart showing overall optimization methodology

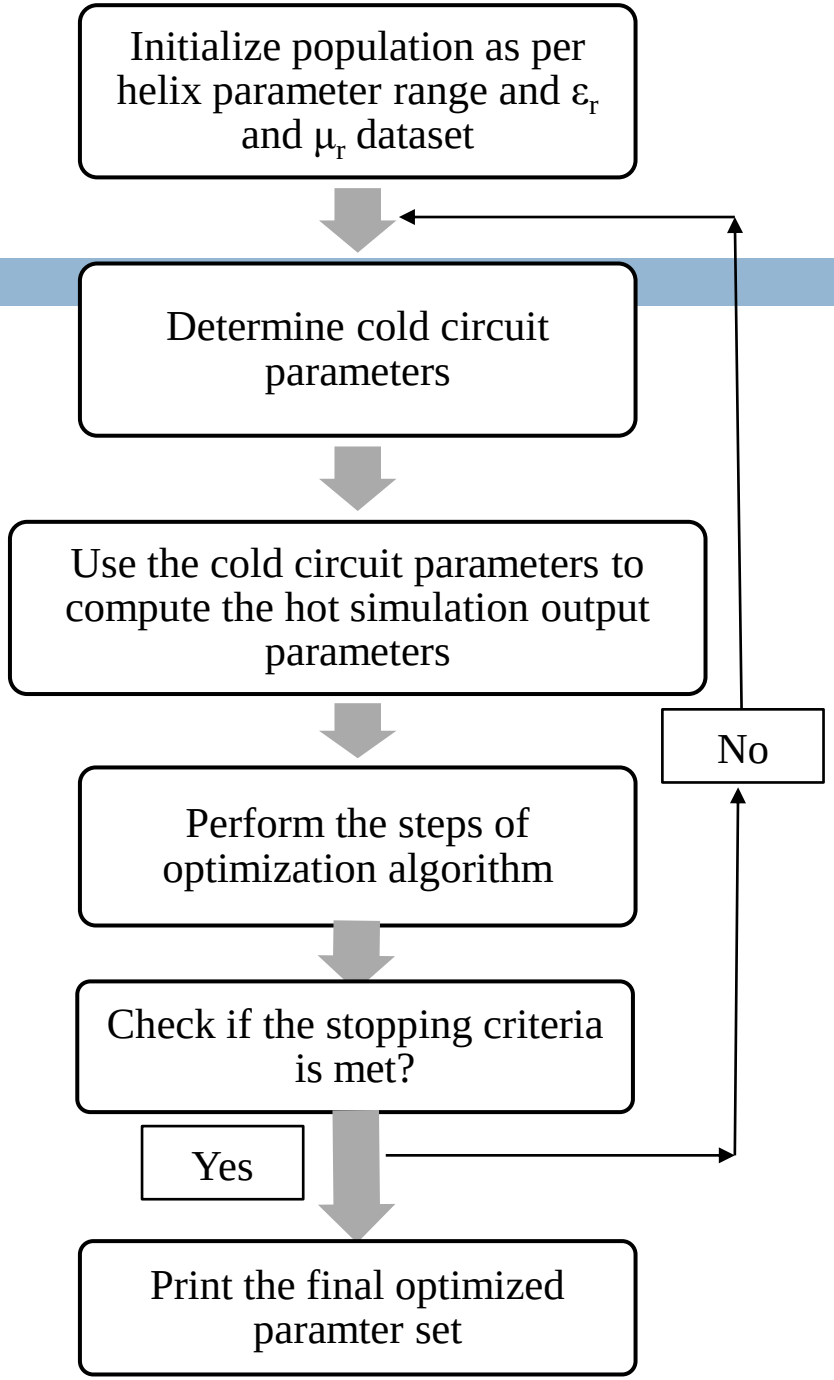

Final thoughts!!!

- Design of MTMs bring together multi-disciplinary skills
- MTM-based/inspired vacuum microwave tubes have potential to improve performance of conventional vacuum tubes
- TWMTM based BWO – coupling system and hot simulation and realization → critical
- MTM based Helix SWS – need for improved analytical exploration

Thank you!!!

Basics of Antennas and Some Concepts of Microstrip Antennas

Subhradeep Chakraborty
Scientist
Device Technology Group
Microwave Devices Area
CSIR-CEERI, Pilani
E-mail: subhradeep@ceeri.res.in, s.c.in@ieee.org

Acknowledgements

- Director, CSIR-CEERI, Pilani
- Dr. R. K. Sharma, Area-Coordinator, MWD Area
- Dr. S. K. Ghosh, Group Head, DTG Group
- Prof. B. N. Basu, SKFGI, Mankundu, India
- Prof. P. K. Saha, Ex- University of Calcutta, India
- Prof. D. Guha, University of Calcutta, India
- Prof. S. Chattopadhyay, Mizoram University, India
- Prof. J. Y. Siddiqui, University of Calcutta, India

Part-A

What is an Antenna?

- An antenna is a device for radiating or receiving EM waves and is the transitional structure between free space and wave-guiding structure.
- *The IEEE Standards Definitions of Terms for Antennas* defines Antennas as "a means for radiating or receiving radio waves".
- Broadly speaking, an antenna can be looked upon from four perspectives:

➢ Antennas as Transducers

➢ Antennas as Transformers

➢ Antennas as Radiators

➢ Antennas as Energy Converters

Antennas as Transducers

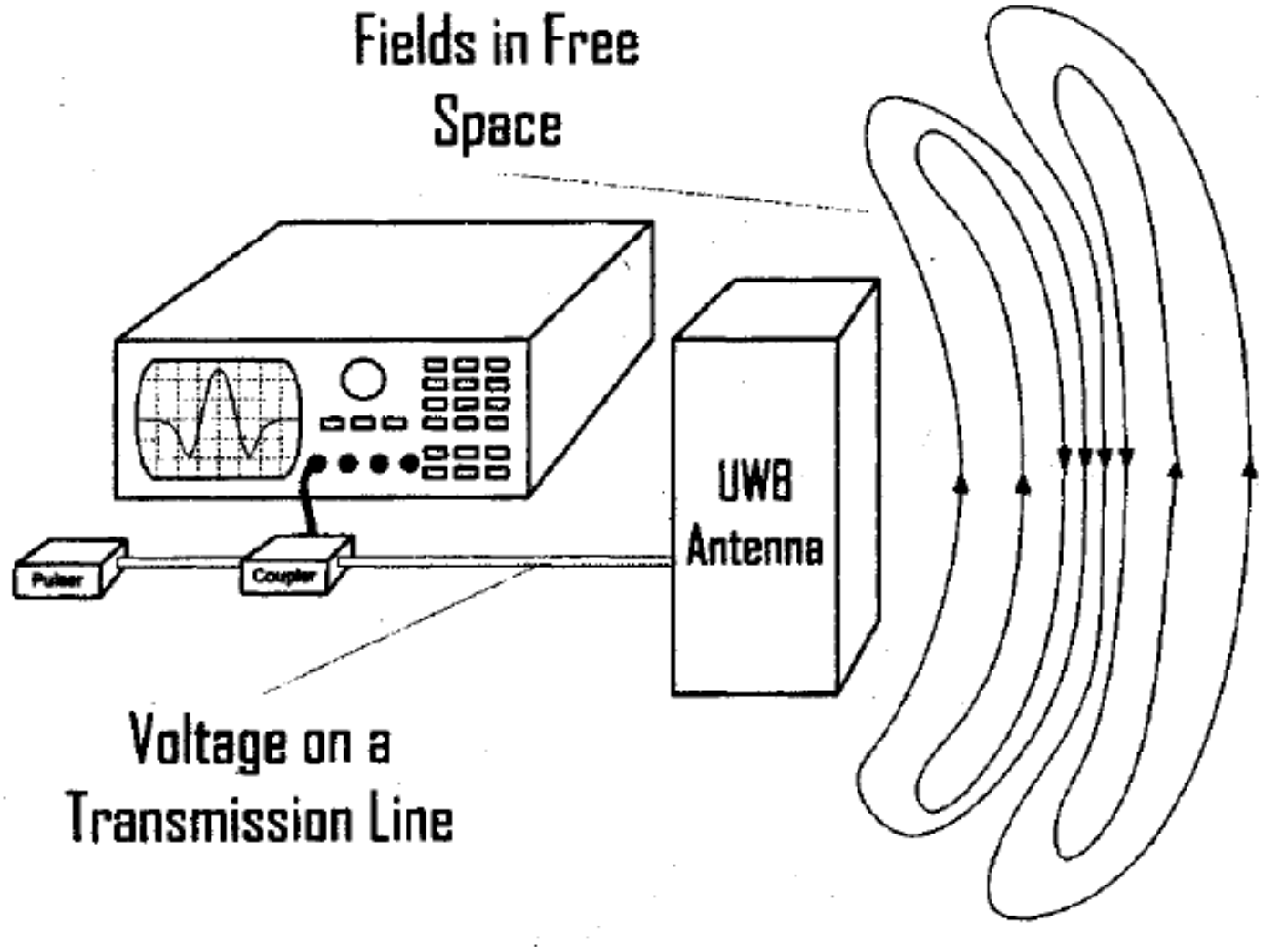

Source: Lectures of Prof. P. K. Saha

Antenna as Transformers

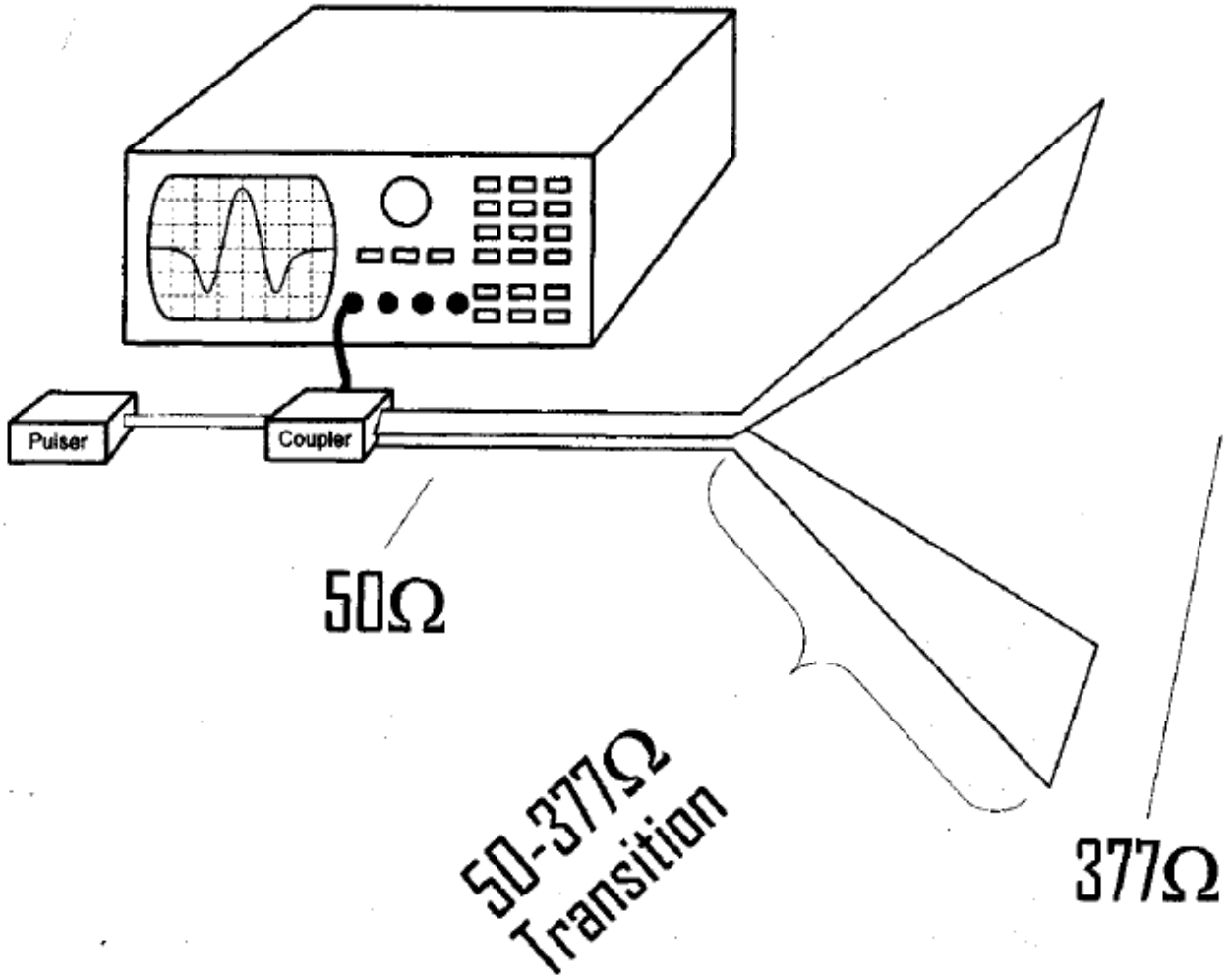

Source: Lectures of Prof. P. K. Saha

Antenna as Radiators

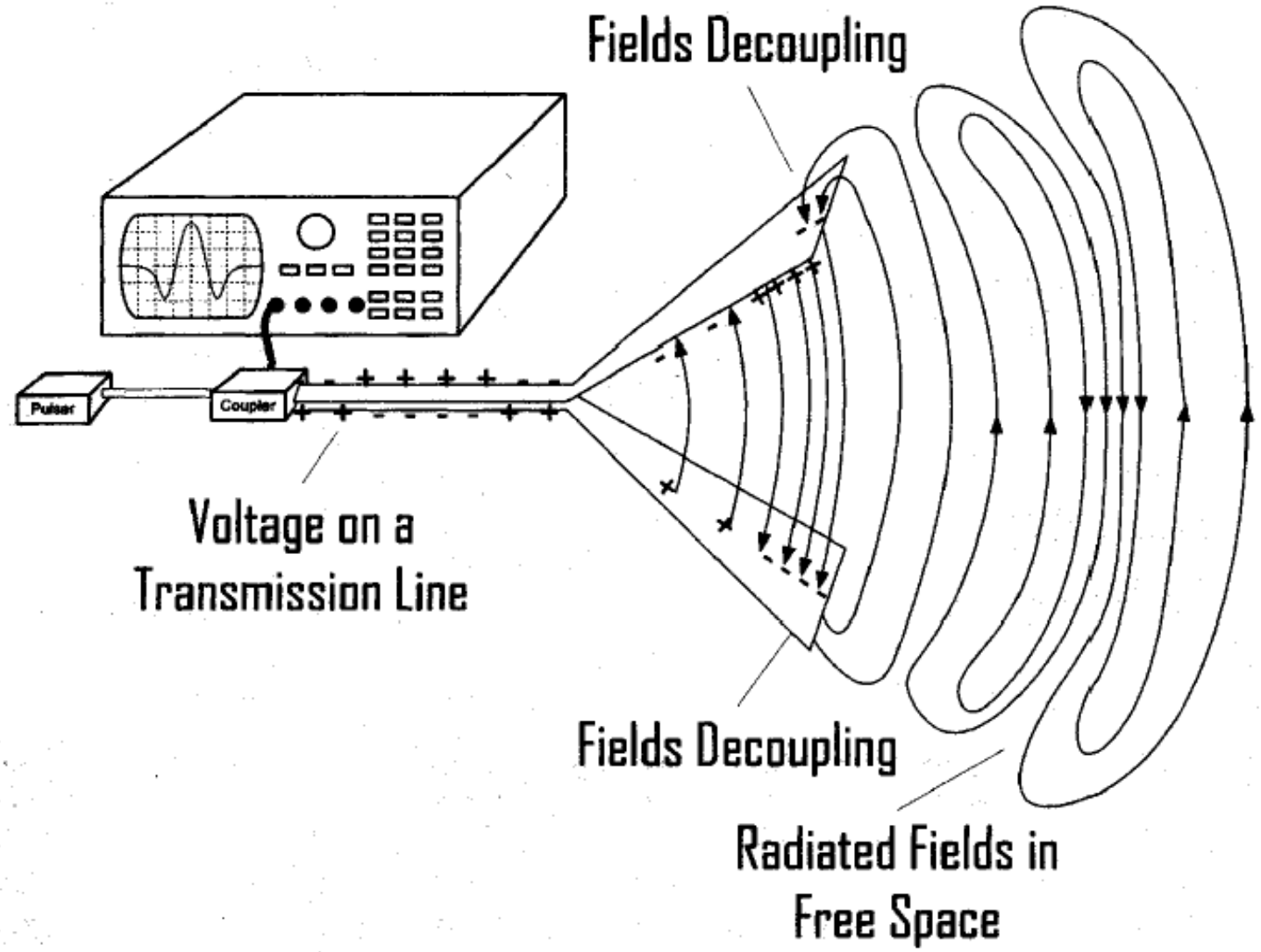

Source: Lectures of Prof. P. K. Saha

Antenna as Radiators

“This classical view of antennas interprets them as current-bearing structures that radiate in a pattern governed by the current geometry. Voltages induce and accelerate charge distributions giving rise to currents. These time varying currents generate radiation fields.”

Source: Lectures of Prof. P. K. Saha

Antennas as Energy Converters

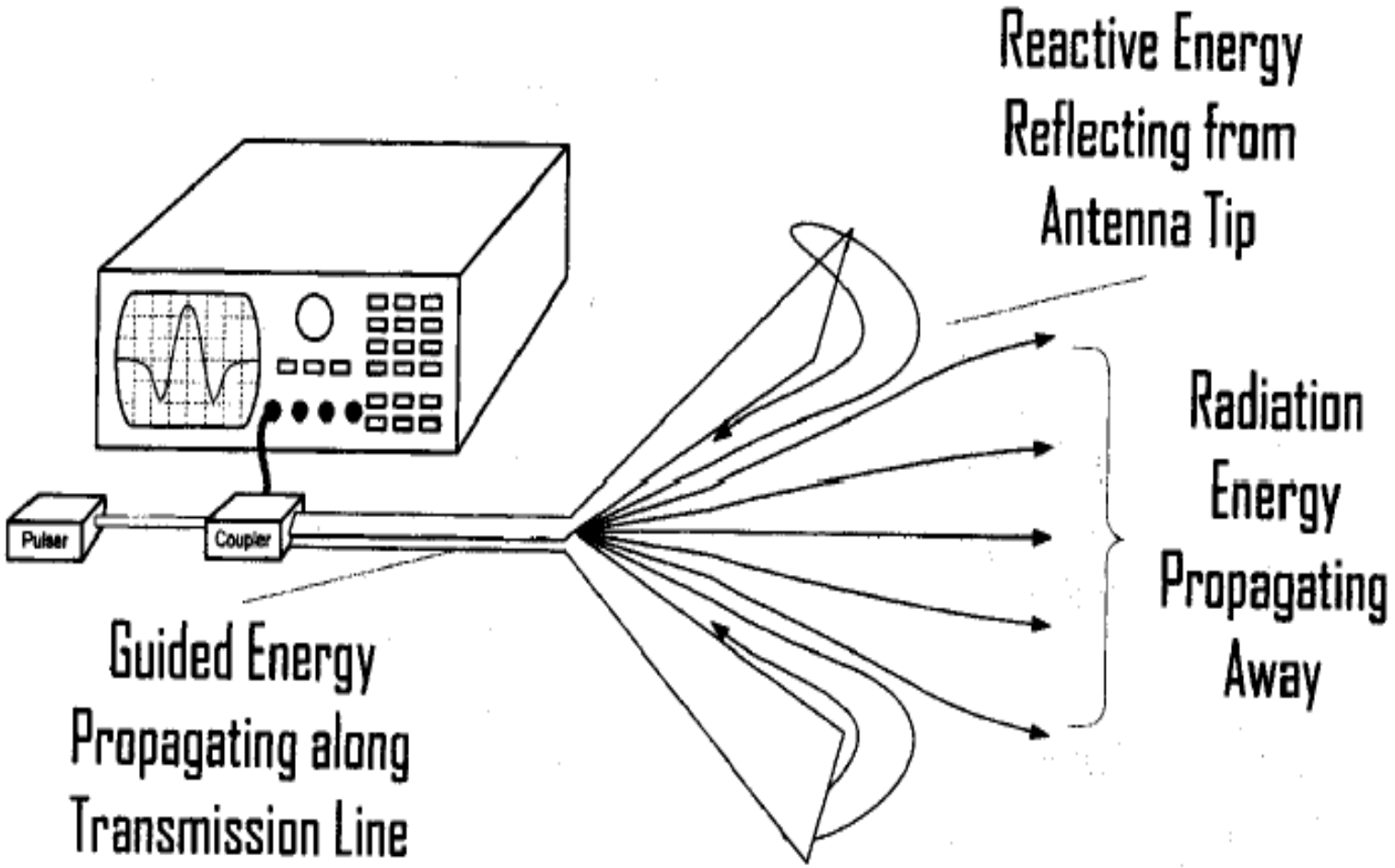

Source: Lectures of Prof. P. K. Saha

The First Aerial

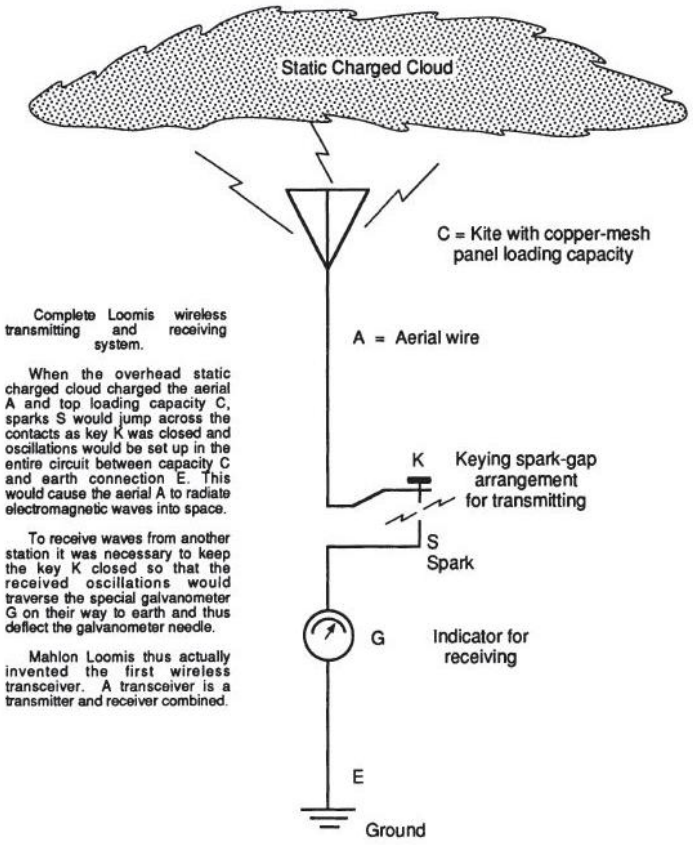

Complete Loomis wireless transmitting and receiving system.

When the overhead static charged cloud charged the aerial A and top loading capacity C, sparks S would jump across the contacts as key K was closed and oscillations would be set up in the entire circuit between capacity C and earth connection E. This would cause the aerial A to radiate electromagnetic waves into space.

To receive waves from another station it was necessary to keep the key K closed so that the received oscillations would traverse the special galvanometer G on their way to earth and thus deflect the galvanometer needle.

Mahlon Loomis thus actually invented the first wireless transceiver. A transceiver is a transmitter and receiver combined.

- The first aerial (antenna) was proposed by Dr. Mahlon Loomis on 21st July, 1864 in USA.

Heinrich Hertz's Experiment

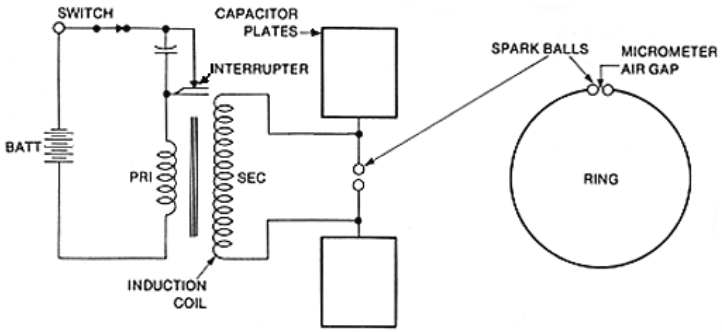

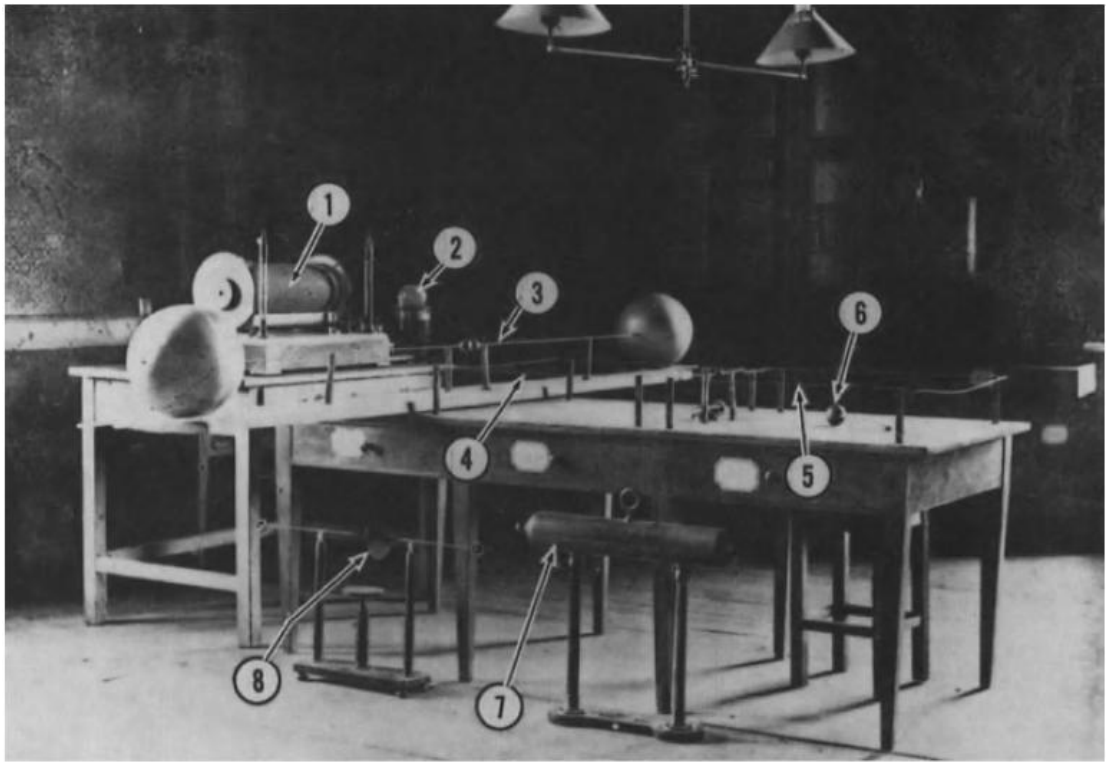

- In 1886, Prof. Hertz used a loop of wire held near the oscillating spark and observed that there was a spark jump across the air gap between the ends of the wire whenever there was a spark jump across the high voltage (induction coil) spark gap. This wave length around 5 meters.

Davis Baird et al, Heinrich Hertz:classical physicist, modern philosopher, Springer, 1998.

Sir J C Bose

IEEE Milestone Plaque for Sir JC Bose

By 1895, Sir. J. C. Bose made the first public demonstration of radio waves in the Kolkata town hall. Details of the apparatus used are vague, but at a distance of 75 feet, he remotely rang an electric bell and ignited a small charge of gunpowder. He called it *Adrisya Alok,* or "Invisible Light". The frequency of operation is nearly 60 GHz. He termed horn antenna as collecting funnel.

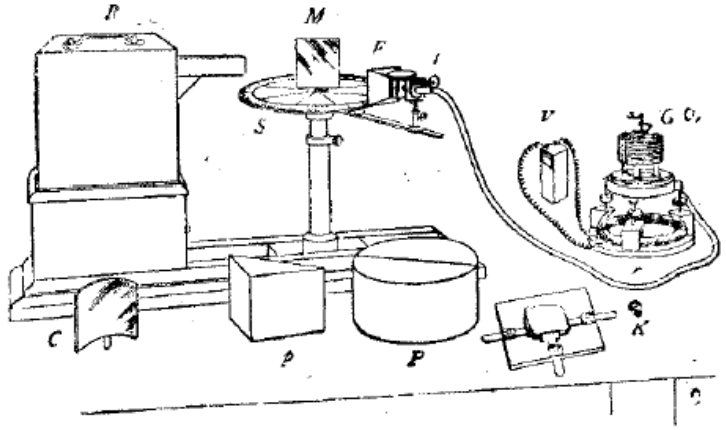

R, radiator ; S, spectrometer-circle ; M, plane mirror ; C, cylindrical mirror ; *p*, totally reflecting prism ; P, semi-cylinders ; K, crystal-holder ; F, collecting funnel attached to the spiral spring receiver ; *t*, tangent screw, by which the receiver is rotated ; V, voltaic cell ; *r*, circular rheostat ; G, galvanometer.

First Research Paper in Antenna from INDIA

in Fig. 3. The integral in Eq. (24) can be reduced to real integrals, and actual integration carried out numerically. Care must be taken to maintain the proper phase of the radicals.

An interesting check of the solution can be obtained by letting $a=0$, $b>0$ in either the transform solution or the far field solution. This is the situation for which the current element lies on the surface of the conductor. Now the branch point at $\gamma=-j\beta$ is no longer present, and the path of integration can be closed at infinity to the left. Evaluation by the theory of residues shows the field to be everywhere zero, which is the expected result.

The far field pattern given by Eq. (23) is also the pattern of a stub antenna (or finite length line source) in the plane perpendicular to its axis. That this is so can be seen as follows. The far field from an infinite line source is characterized mathematically by the assumption that each differential element of length sees the field point at right angles to its axis. Thus, by superposition, the pattern is also that from a single differential dipole, in the plane perpendicular to its axis.

A pattern has been calculated by numerical integration for the case where the source was a distance $\lambda/4$ from the plane reflector and $\lambda/4$ back from the edge, that is, $\beta a=\lambda/4$, $\beta b=\lambda/4$. Experimental measurements were taken on a model for the same conditions, using a stub antenna for the source. The results are given in Fig. 4. The experimental and theoretical patterns are in good agreement within the experimental accuracy.

JOURNAL OF APPLIED PHYSICS VOLUME 24, NUMBER 5 MAY, 1953

Radiation Field of a Conical Helix

J. S. CHATTERJEE
Institute of Radio Physics and Electronics, Calcutta University, Calcutta, India
(Received November 5, 1952)

It is now well known that a cylindrical helix, when excited at frequencies corresponding to wavelengths comparable to the length of one turn of the helix, can radiate a sharp beam along the axis over a wide frequency range (about one octave). It is shown in the present communication that if the helix be conical instead of cylindrical (the diameter varying along the length of helix), then the axial mode of radiation can be maintained over a much wider band of frequencies. The radiation pattern of a conical helix, 60 cm diameter at the base, tapering linearly to 20 cm at the top in 10 turns within a height of 112 cm (with the "ground" provided by brass disk of 100 cm in diameter) has been studied experimentally. It is found that the axial mode of radiation is maintained from 150 Mc/sec to 450 Mc/sec. By increasing the number of turns, the band width can be considerably increased. Assuming a linear current distribution, theoretical expressions have also been deduced for E_ϕ and E_θ for a conical helix. Some modifications of the simple conical helix, such as may have special applications, are indicated.

I. INTRODUCTION

A CYLINDRICAL helix is a well-known circuit element having many uses. It is widely used, for example, as an inductance; in a traveling wave tube it is used to guide the wave along the axis with a velocity smaller than that of light. In all such applications, the helix diameter is a small fraction of the free space wavelength corresponding to the frequencies concerned. Uses have also been found in recent years of a helix, the diameter of which is of the same order as the free space wavelength. It has been shown by Kraus[1] that for such wavelengths, the circular helix can be an efficient radiator. Depending upon the pitch angle and upon the ratio of the wavelength to the helix diameter, the helix can radiate in three modes. For example, for the pitch angle of 12.6° the so-called "normal" radiation mode (resulting from the T_0 mode of current) is observed when the length of one turn of the helix is smaller than 0.8λ; when this length is between $0.8\lambda-1.3\lambda$, the "axial" radiation mode, due to the T_1 mode of current distribution along the helix, is obtained; and, when the length is more than 1.3λ, energy is radiated in the "conical" mode due also to T_2 mode of current distribution.[2,3] Further, for the axial mode of radiation, a sharp beam is maintained along the axis over the large frequency band of nearly one octave. The three modes[2] of radiation are illustrated in Fig. 1.

It is interesting to inquire how the radiation characteristic of the helix will be altered, if the diameter instead of remaining constant varies along the length of the helix. This problem has been investigated both experimentally and theoretically by the author of the paper for the case of a simple conical helix, the radius of which varies along the length of the axis and the pitch angle remaining constant. It has been found that for such a helix there exists in general all the three modes of radiation as in the case of the cylindrical helix. The normal radiation mode is present when the frequency is

[1] J. D. Kraus, Electronics **20**, No. 4, 109 (1947).

[2] J. D. Kraus and J. C. Williamson, J. Appl. Phys. **19**, 87 (1948).
[3] J. A. Marsh, Proc. Inst. Radio Engrs. **39**, 668 (1951).

Prof. J. S. Chatterjee, Calcutta University, Kolkata, India, then he joined Jadavpur University

Antenna Radiation Pattern in 3D

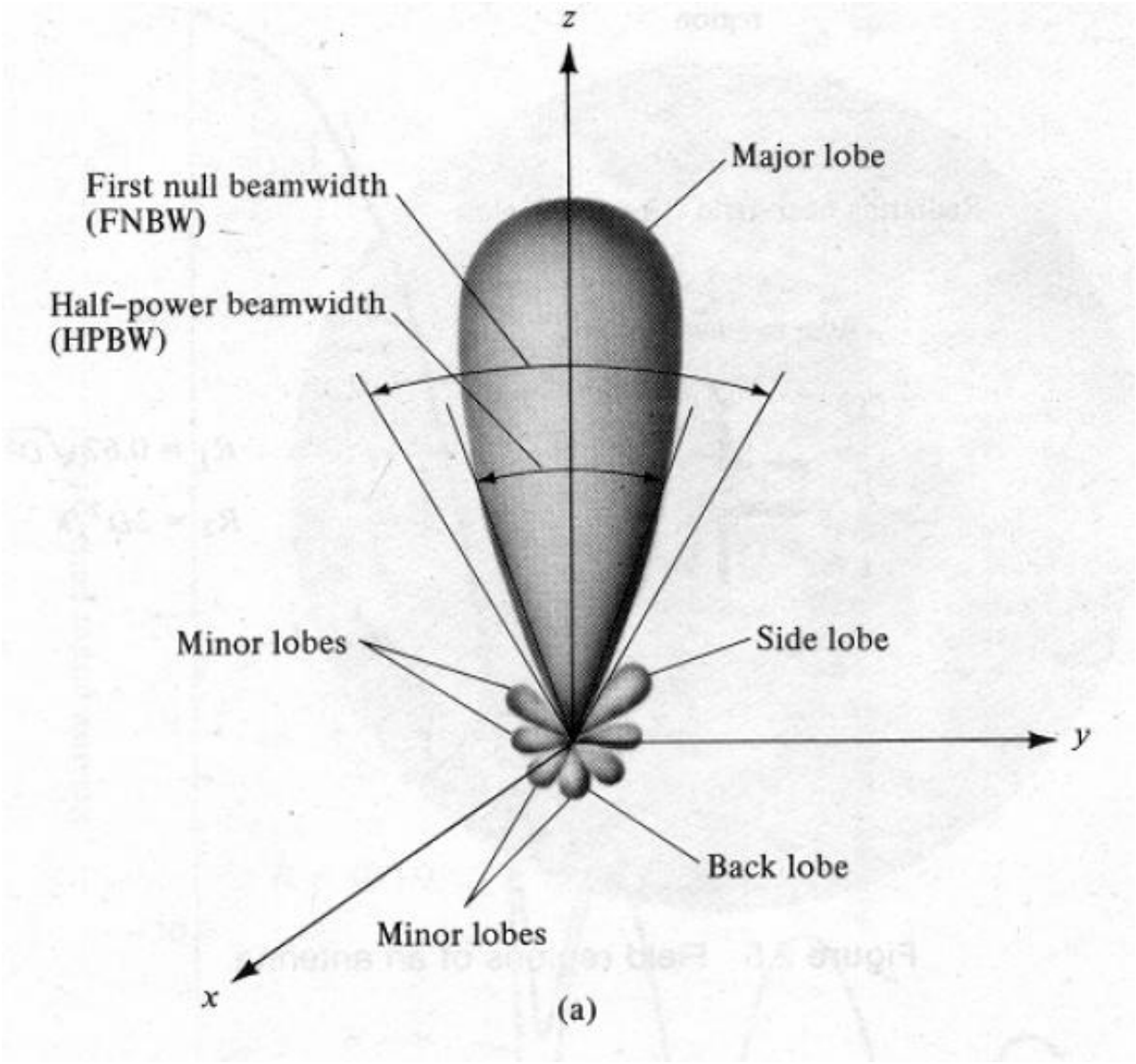

Active Denial System: The Pain Ray

The Active Denial System (ADS) is a less-lethal, directed-energy weapon developed by the U.S. military. It is a strong millimeter-wave transmitter primarily used for crowd control (the "goodbye effect”). Some ADS such as HPEM ADS are also used to disable vehicles. Informally, the weapon is also called pain ray.

Part-B

Microstrip Patch Antenna

•Microstrip Patch Antenna (MPA) consists of a radiating patch on one side of a dielectric substrate and one ground plane on the other side.

•Concept of MPA was proposed firstly by G. Deschamp and W. Sichak at 3rd Symposium of the US Air Force Antenna Research and Development Program in 1953.

•The main curiosity of the authors of the paper was to explore the radiation characteristics of a microstrip – planar variant of a “wire above ground” transmission line, for the development of an X band antenna.

•The “MPA” to which all the researchers associated to Antenna Theory are familiar with, was theoretically analyzed by Howell in 1972.

•MPA was realized experimentally by Munson in 1974.

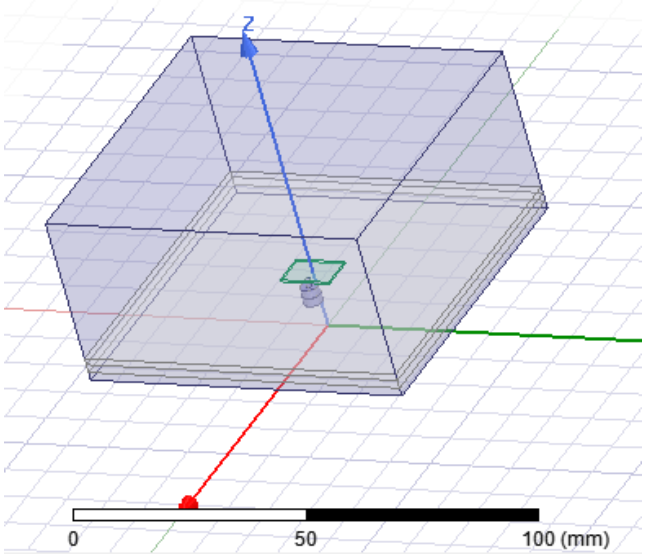

Advantages

- Light Weight /planer configuration.
- Easy to fabricate/Low fabrication cost.
- Easy to feed (coaxial cable, microstrip line, etc.).
- Easy to use in an array. Feedlines and matching networks can be fabricated simultaneously with the antenna structure.
- Easily integrated with Monolithic Microwave Integrated Circuits (MMICs).

Disadvantages

- Narrow bandwidth
- Poor Polarization Purity/Co-polar to Cross polar isolation-CP-XP isolation
- Low gain.
- Large ohmic loss in the feed structures of arrays.
- Most microstrip antennas radiate into half-space.
- Complex feed structures required for high performance arrays.

Rectangular Microstrip Antennas (RMA)

- RMA resonates at its dominant TM_{10} mode.
- In general, gain of a RMA is around 4-6 dBi and impedance bandwidth is 2-6%
- In TM_{10} mode, polarization is linear and directed towards the broadside.
- However, few degree of orthogonally polarized radiation is always present.
- Orthogonal polarization is also known as Cross Polarization (XP).

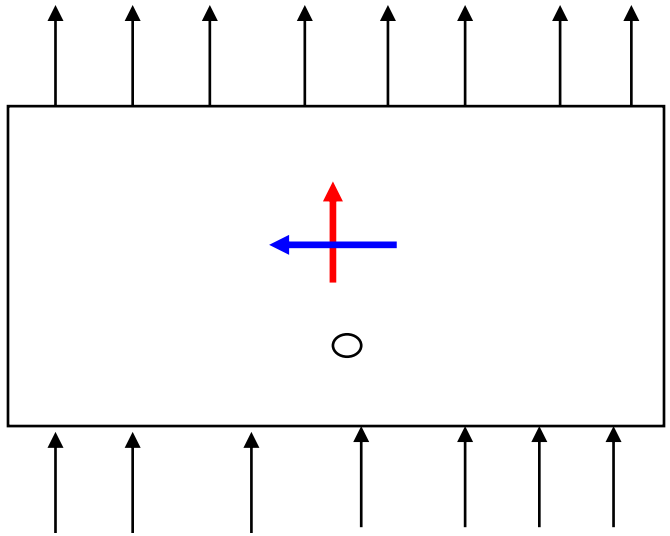

Rectangular Microstrip Antenna (RMA)

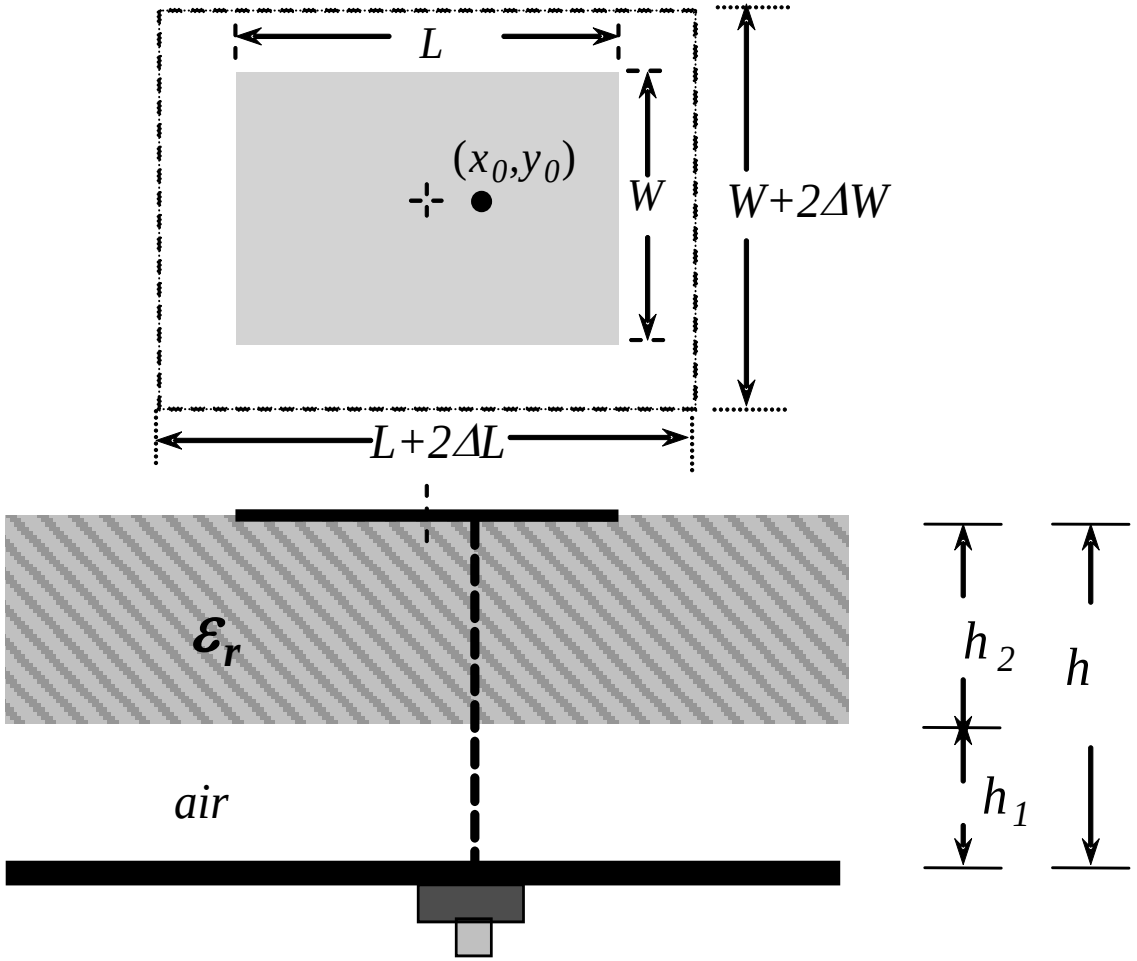

Chattopadhyay S, Biswas M, SiddiquiJ Y,Guha D.Rectangular microstrip antenna with variable air gap and varying aspect ratio: improved formulations and experiments.Microwave Opt. Technol. Lett. 2009, Volume **51**, pp. 169–173, DOI:10.1002/mop.24025

Design Approach

- Here, an equivalent circular patch is considered with radius a, effective radius a_{eff} and same resonant frequency as that of the RMA. This helps to establish a relationship amongst the fringing parameters ΔL, ΔW and a_{eff} by equating the zero order resonant frequencies of both the patches.The resonant frequency (f_{0r}) of the dominant mode of RMA can be expressed as

$$f_{0,r} = \frac{c}{2L\sqrt{\varepsilon_r}} = \frac{c\alpha}{2\pi a\sqrt{\varepsilon_r}}$$

• We can assume that both the antennas of same resonant frequencies have same circumference. Therefore, we can write

$$(W + L) = \pi a$$

$$(L + 2\Delta L) + (W + 2\Delta W) = \pi a_{eff}$$

•c is the velocity of light in free space, a is the first zero of the derivative of the Bessel function of order n =1 and a_{eff} is the effective radius of a circular patch due to fringing electric fields.

Design Approach

$$a_{eff} = a\sqrt{(1+q)}$$

where, q is the fringing factor

$$q = u + v + uv$$

where,

$$u = \left(1 + \varepsilon_{re}^{-1}\right)\frac{4}{\pi a/h}$$

$$v = \frac{2}{3t} \times \frac{\ln(p)}{\left(8 + \pi a/h\right)} + \frac{\left(1/t - 1\right)}{\left(4 + 2.6\,a/h + 2.9\,h/a\right)}$$

$$p = \frac{1 + 0.8\left(a/h\right)^2 + \left(0.31\,a/h\right)^4}{1 + 0.9\,a/h}$$

$$t = 0.37 + 0.63\varepsilon_{re}$$

u, v, t, p all are dummy variables.

Chattopadhyay S, Biswas M, SiddiquiJ Y,Guha D. Rectangular microstrip antenna with variable air gap and varying aspect ratio: improved formulations and experiments.Microwave Opt. Technol. Lett. 2009, Volume **51**, pp. 169–173, DOI:10.1002/mop.24025

Design Approach

$$\varepsilon_{re} = \frac{\varepsilon_r (1 + h_1 / h_2)}{(1 + \varepsilon_r h_1 / h_2)}$$

where, ε_{re} is the equivalent permittivity of the two-layer dielectric medium (Fig.1) having total thickness $h = (h_1 + h_2)$.
Solving (1.1)-(1.4) we can write the relations:

$$L = 1.7a$$

$$W = 1.44a$$

$$\Delta L + \Delta W = \frac{\pi a[\sqrt{(1+q)} - 1]}{2}$$

An empirical relation is used in to determine ΔW in terms of ΔL for a wide range of W/L values: $2 > W/L > 0.5$ as

$$\Delta W = \Delta L(1.5 - p),$$

$$p = W/2L$$

Chattopadhyay S, Biswas M, SiddiquiJ Y,Guha D.Rectangular microstrip antenna with variable air gap and varying aspect ratio: improved formulations and experiments.Microwave Opt. Technol. Lett. 2009, Volume **51**, pp. 169–173, DOI:10.1002/mop.24025

Design Approach

and subsequently ΔL can be written as,

$$\Delta L = \frac{\pi a[\sqrt{(1+q)}-1]}{2[2.5-0.5(W/L)]}$$

The resonant frequency of a RMA with a variable air-gap h_1 is found as

$$f_{r,nm} = \frac{c}{2\sqrt{\varepsilon_{r,eff}}}\left[\left(\frac{n}{L+2\Delta L}\right)^2 + \left(\frac{m}{W+2\Delta W}\right)^2\right]^{1/2}$$

where, $\varepsilon_{r,eff}$ is the effective relative permittivity of the medium.

$$\varepsilon_{r,eff} = \frac{4\varepsilon_{re}\varepsilon_{r,dyn}}{(\sqrt{\varepsilon_{re}}+\sqrt{\varepsilon_{r,dyn}})^2}$$

$$\varepsilon_{r,dyn} = \frac{C_{dyn}(\varepsilon = \varepsilon_0\varepsilon_{re})}{C_{dyn}(\varepsilon = \varepsilon_0)}$$

Chattopadhyay S, Biswas M, SiddiquiJ Y,Guha D.Rectangular microstrip antenna with variable air gap and varying aspect ratio: improved formulations and experiments.Microwave Opt. Technol. Lett. 2009, Volume **51**, pp. 169–173, DOI:10.1002/mop.24025

Design Approach

$$C_{dyn} = C_{0,dyn} + C_{e,dyn}$$

where, C_{dyn} is the total dynamic capacitance of the microstrip patch and suffixes *0* and *e* denote the main and fringing components, respectively.

$$C_{0,dyn} = \gamma_n C_{0,stat}$$

$$C_{e,dyn} = \frac{1}{\delta} C_{e,stat}$$

$$\gamma_n = 1.0 \quad \text{for} \quad n = 0$$
$$= 0.3525 \quad = 1$$
$$= 0.2865 \quad = 2$$
$$= 0.2450 \quad = 3$$

$$\delta = 1.0 \quad \text{for} \quad n = 0$$
$$= 2.0 \quad \neq 0$$

$$C_{0,stat} = \varepsilon_0 \varepsilon_{re} \frac{\pi a^2}{h}$$

$$C_{e,stat} = C_{0,stat}.q$$

Chattopadhyay S, Biswas M, SiddiquiJ Y,Guha D.Rectangular microstrip antenna with variable air gap and varying aspect ratio: improved formulations and experiments.Microwave Opt. Technol. Lett. 2009, Volume **51**, pp. 169–173, DOI:10.1002/mop.24025

Example

Find out the resonant frequency of a RMA with length 18.2 mm, width 28 mm, etched on a PTFE substrate of height 1.575 mm with dielectric constant 2.33.

The resonant frequency of the RMA is

$$f_{r,nm} = \frac{c}{2\sqrt{\varepsilon_{r,eff}}}\left[\left(\frac{n}{L+2\Delta L}\right)^2 + \left(\frac{m}{W+2\Delta W}\right)^2\right]^{1/2}$$

As the dominant mode is TM_{10}; n=1 and m=0 and therefore

$$f_r = \frac{c}{2(L+2\Delta L)\sqrt{\varepsilon_{r,eff}}}$$

Example

Now,

$$\varepsilon_{r,eff} = \frac{4\varepsilon_{re}\varepsilon_{r,dyn}}{(\sqrt{\varepsilon_{re}} + \sqrt{\varepsilon_{r,dyn}})^2}$$

$$\varepsilon_{re} = \frac{\varepsilon_r (1 + h_1 / h_2)}{(1 + \varepsilon_r h_1 / h_2)}$$

As air-gap height h_2 =0;

$$\varepsilon_{re} = \varepsilon_r = 2.33$$

$\varepsilon_{r.dyn}$=1.94

Example

Therefore,

$\varepsilon_{r.eff}$=2.12

The fringing length ΔL may be computed as

$$\Delta L = \frac{\pi\, a[\sqrt{(1+q)}-1]}{2[2.5-0.5(W/L)]}$$

$$a = W/1.44 = 19.44$$

The fringing factor q is $q = u + v + uv$

$$u = \left(1+\varepsilon_{re}^{-1}\right)\frac{4}{\pi\, a/h} \quad =0.147 \qquad t = 0.37 + 0.63\varepsilon_{re} \quad =1.83$$

$$p = \frac{1+0.8\left(a/h\right)^2+\left(0.31\, a/h\right)^4}{1+0.9\, a/h} \quad =27.83$$

Example

Hence,

$$v = \frac{2}{3t} \times \frac{\ln(p)}{\left(8 + \pi a/h\right)} + \frac{\left(1/t - 1\right)}{\left(4 + 2.6\,a/h + 2.9\,h/a\right)} \quad = 0.013$$

Therefore,

$$q = u + v + uv = 0.162$$

$$\Delta L = \frac{\pi\, a[\sqrt{(1+q)} - 1]}{2[2.5 - 0.5(W/L)]} = 1.365$$

$$f_r = \frac{c}{2(L + 2\Delta L)\sqrt{\varepsilon_{r,eff}}} = 4.91 \text{ GHz}$$

Input Impedance of RMA

Input impedance for a RMA at the dominant mode near resonance

$$Z_{in}(f,x_0)=\frac{R_r}{1+Q_T^2\left(\overline{f}-\overline{f}^{-1}\right)^2}+j\left[X_f-\frac{R_rQ_T\left(\overline{f}-\overline{f}^{-1}\right)}{1+Q_T^2\left(\overline{f}-\overline{f}^{-1}\right)^2}\right]$$

R_r is the input resistance at resonance

$$R_r=\frac{4h}{\pi\lambda_0}\mu\eta_0Q_T\left(\frac{L+2\Delta L}{W+2\Delta W}\right)\cos^2\left(\frac{\pi(0.5L-x_0)}{L+2\Delta L}\right)$$

$$Q_T=\left[\frac{1}{Q_r}+\frac{1}{Q_d}+\frac{1}{Q_c}\right]^{-1}$$

$$\varepsilon_{r,n}=\frac{\varepsilon_{reff}+1}{2}$$

$$Q_r=\frac{\pi}{4G_rZ_r}$$

Chattopadhyay, S. Biswas M, Siddiqui J Y, Guha D. Input Impedance of Probe fed Rectangular Microstrip Antenna with Air gap and Aspect Ratio. IET Microwaves, Antennas Propagat. 2009, Volume **3**, pp. 1151-1156. DOI: 10.1049/iet-map.2008.0320.

Input Impedance of RMA

$$Q_d = \frac{\pi(\varepsilon_r - 1)\sqrt{\varepsilon_{r,n}}}{27.3(\varepsilon_{r,n} - 1)\sqrt{2\varepsilon_{r,n} - 1}} \frac{1}{\tan\delta}$$

$$Q_c = h\sqrt{\pi f \mu_0 \sigma}$$

$$G_r = \frac{W^2}{90\lambda_0^2} \quad \text{when} \quad W \le 0.35\lambda_0$$

$$= \frac{W}{120\lambda_0} - \frac{1}{60\pi^2} \quad \text{when} \quad 0.35\lambda_0 \le W \le 2\lambda_0$$

$$= \frac{W}{120\lambda_0} \quad \text{when} \quad 2\lambda_0 < W$$

$$Z_r = \frac{120\pi\left[\frac{W}{h} + 1.393 + 0.667\ln\left(\frac{W}{h} + 1.444\right)\right]^{-1}}{\sqrt{\varepsilon_{r,n}}}$$

Example

Find out the input resonant resistance at the edge of a square microstrip antenna with length 30 mm, width 30 mm, etched on a PTFE substrate of height 1.575 mm with dielectric constant 2.33.

$$Z_{in}(f,x_0)=\frac{R_r}{1+Q_T^2\left(\overline{f}-\overline{f}^{-1}\right)^2}+j\left[X_f-\frac{R_rQ_T\left(\overline{f}-\overline{f}^{-1}\right)}{1+Q_T^2\left(\overline{f}-\overline{f}^{-1}\right)^2}\right]$$

Now, f_r can be obtained as done in earlier example and it is found to be f_r = 3.13 GHz.

$$R_r=\frac{4h}{\pi\lambda_0}\mu\eta_0Q_T\left(\frac{L+2\Delta L}{W+2\Delta W}\right)\cos^2\left(\frac{\pi(0.5L-x_0)}{L+2\Delta L}\right)$$

ΔL and ΔW can be obtained as done in earlier example and ΔL = 1.381 mm, ΔW = 1.381 mm.

$$\lambda_0=c/f_r=95.84\text{ mm}$$

$$G_r=\frac{W^2}{90\lambda_0^2}=0.001\text{mm}$$

Example

$$\varepsilon_{r,n} = \frac{\varepsilon_{reff} + 1}{2} = 1.165$$

$$Q_T = 42.27$$

$$Z_r = \frac{120\pi\left[\frac{W}{h} + 1.393 + 0.667\ln\left(\frac{W}{h} + 1.444\right)\right]^{-1}}{\sqrt{\varepsilon_{r,n}}} = 13.41\ \Omega$$

Therefore, the resonant resistance at edge ($x_0 = 0.5L$) is

$$R_r = \frac{4h}{\pi\lambda_0}\mu\eta_0 Q_T\left(\frac{L + 2\Delta L}{W + 2\Delta W}\right)\cos^2\left(\frac{\pi(0.5L - x_0)}{L + 2\Delta L}\right)$$

$$= 333.43\ \Omega$$

XP Sources

- The XP radiation becomes significantly prominent in probe-fed design.
- Unwanted radiation from probe contributes in cross polarized radiation XP.
- Matching is an important issue and improper matching causes XP radiation
- Another source of XP is the fringing field along the non-radiating edges.
- Radiations from orthogonal component of dominant mode are primarily responsible for XP radiation.
- XP level increases when substrate thickness increases as well the value of dielectric constant of substrate decreases.

XP Sources

- The cross polarized radiation (XP) fields are more noteworthy in H plane compared to its E plane.
- In E plane, XP is usually low and the CP-XP isolation in that plane is around 35 dB; while the same in H plane is around 10 dB in X band.
- XP is a restriction to the applications, where polarization purity is the key issue.
- Therefore, scientist and researchers have started to address this issue of lowering XP radiation, particularly in H plane during last few years

Simulated Radiation Characteristics of RMA

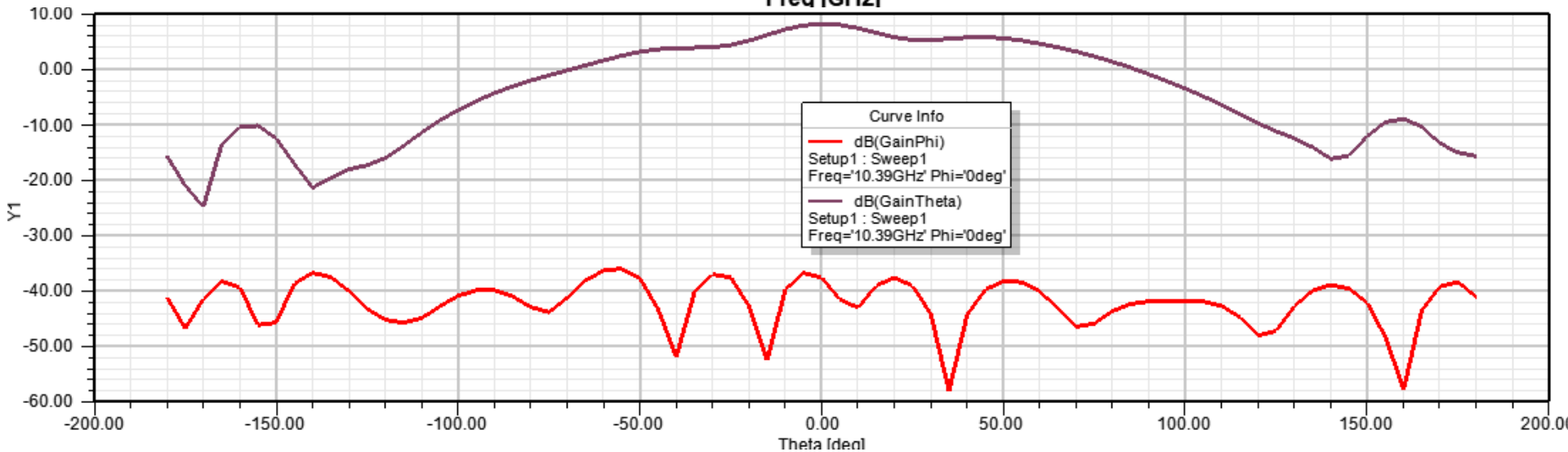

Simulated Radiation Characteristics of RMA

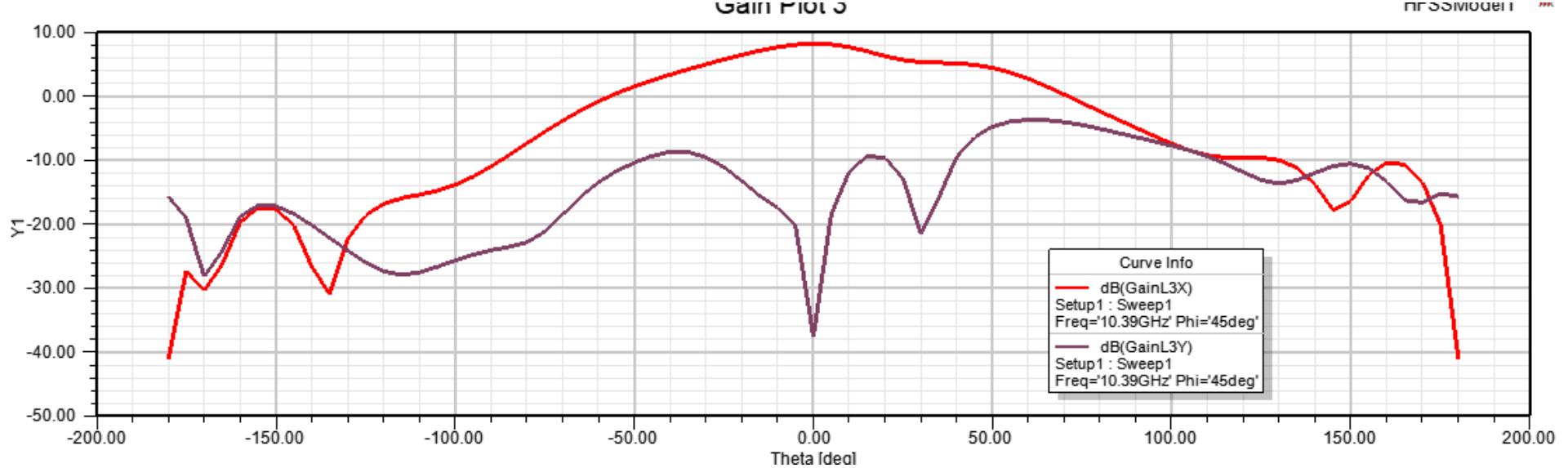

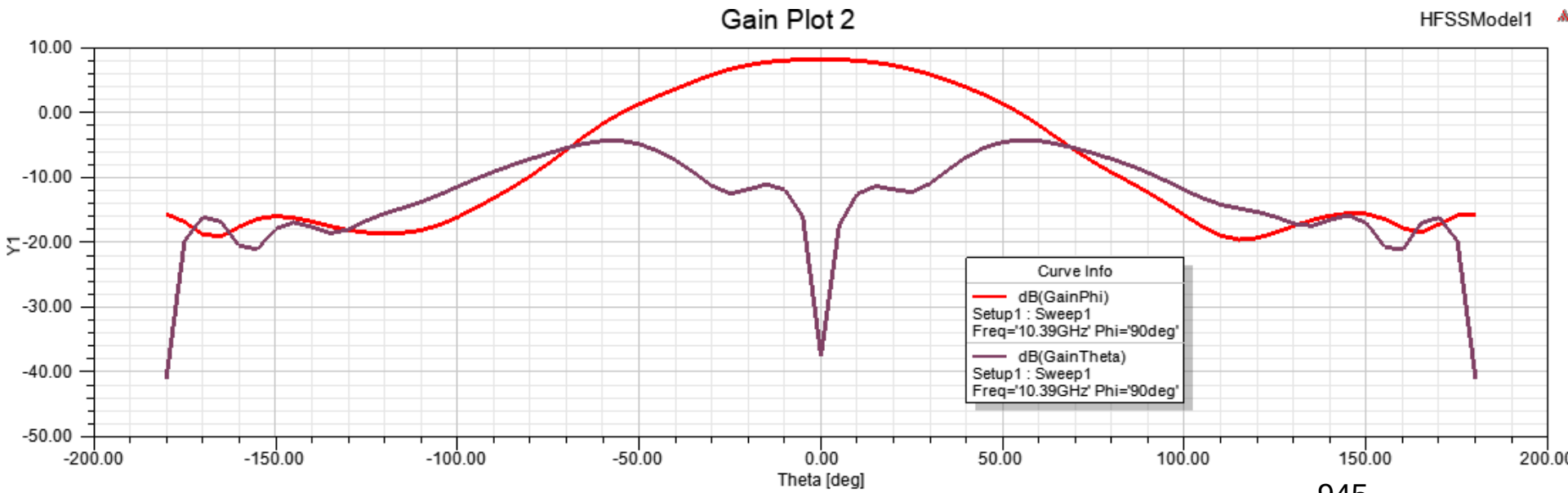

Orthogonal Component of Dominant Mode

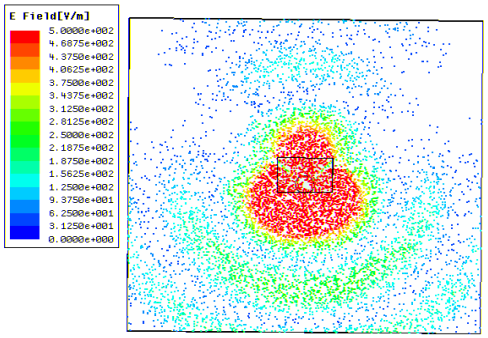

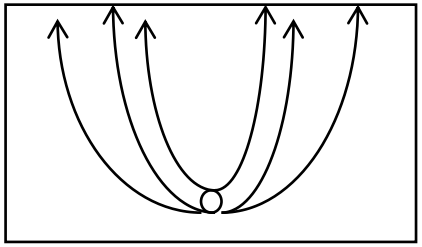

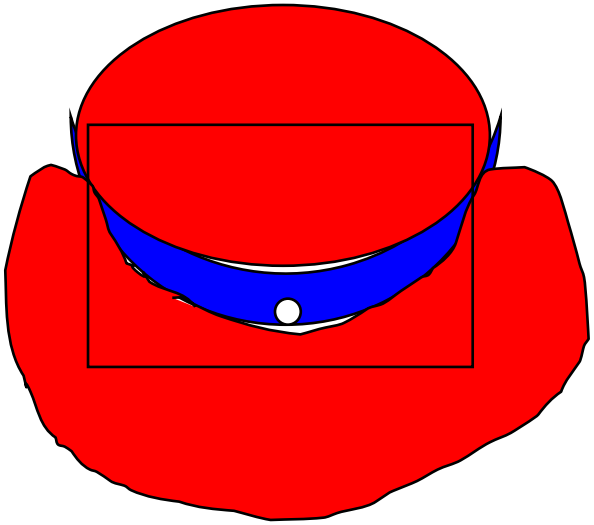

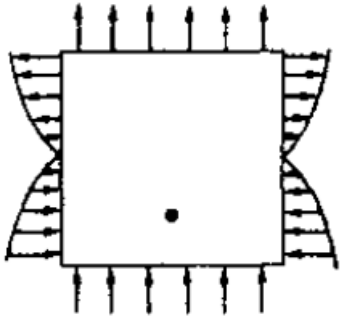

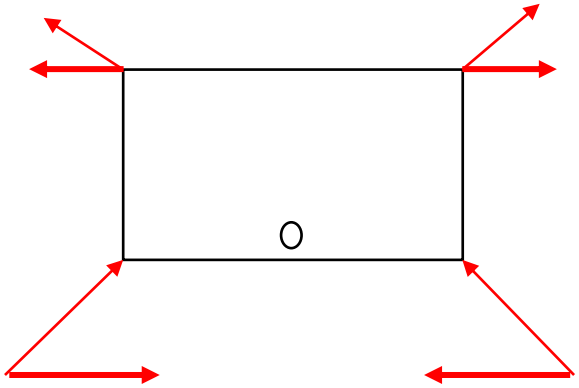

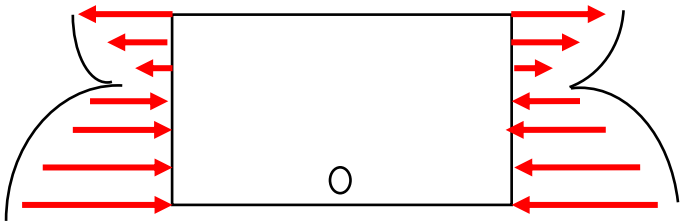

XP fields are oriented 90^0 with respect to the field at radiating edges

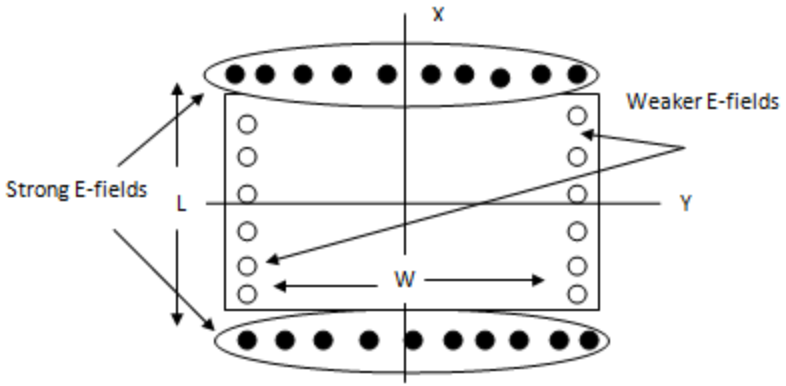

Radiated Electric field a patch edges for TM_{10}

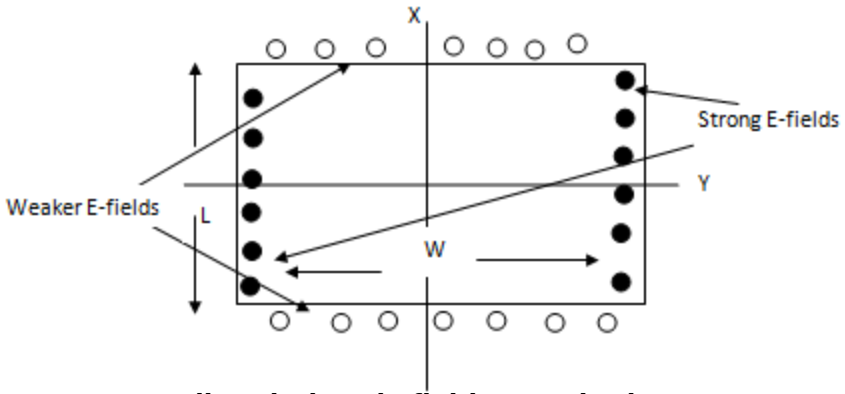

Radiated Electric field a patch due to orthogonal component of TM_{10}

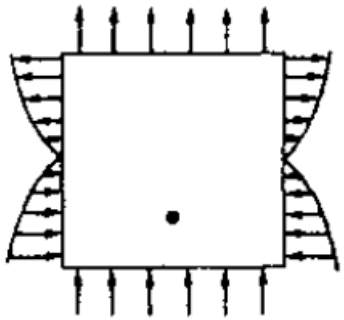

Electric field orientation at patch edges for TM_{10}

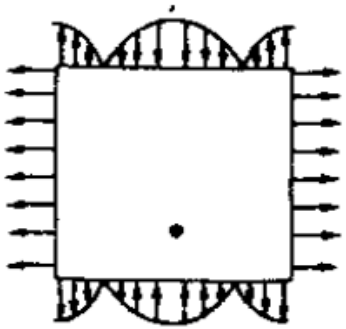

Electric field orientation at patch edges for orthogonal component of TM_{10}

Circular Microstrip Antennas (CMA)

- The conventional CMA resonates at its fundamental TM_{11} mode produces linearly polarized field along its broadside (E plane).
- Some extent of orthogonally polarized field (orthogonal to E plane) is always evident which is referred to as cross-polarized (XP) radiation.

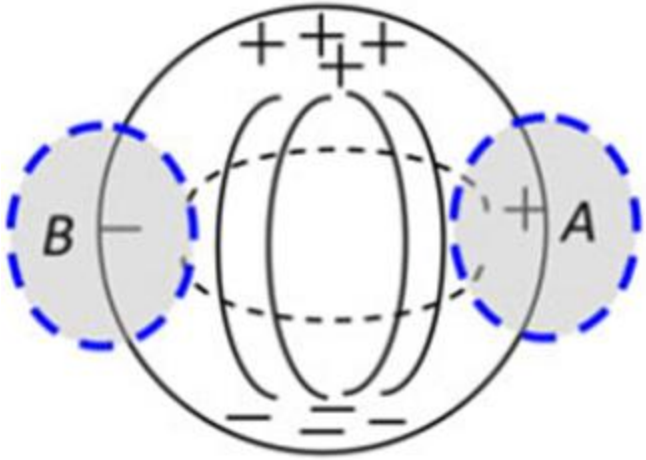

Electric field and current distribution over patch for TM_{11}

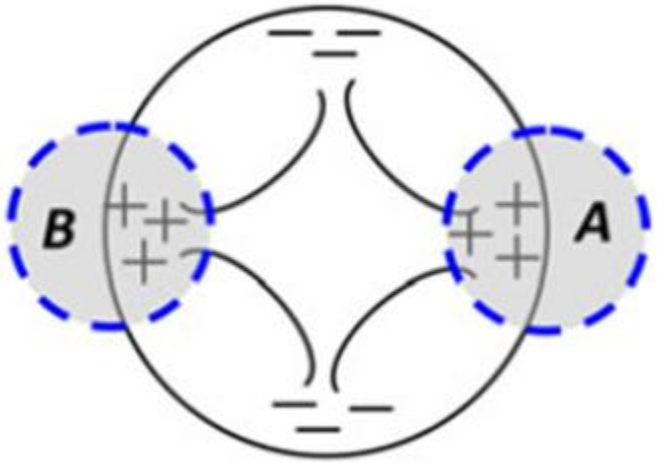

Electric field and current distribution over patch for orthogonal component of TM_{11}

Dominant Mode Resonant Frequency Computation of CSMA

The vector potential equation can be written as

$$\nabla^2 A_z(\rho,\phi,z) + k^2 A_z(\rho,\phi,z) = 0$$

$$A_z = B_{mnp} J_m(k_\rho \rho)[A\cos(m\phi) + B\sin(m\phi)][\cos(k_z z)]$$

Therefore the fields within the CSMA structure can be written as

$$E_\rho = -\frac{j}{\omega\mu\varepsilon}\frac{\partial^2 A_z}{\partial\rho\partial z} \quad H_\rho = \frac{1}{\mu}\frac{1}{\rho}\frac{\partial A_z}{\partial\phi} \quad E_\phi = -\frac{j}{\omega\mu\varepsilon}\frac{1}{\rho}\frac{\partial^2 A_z}{\partial\phi\partial z} \quad H_\phi = -\frac{1}{\mu}\frac{1}{\rho}\frac{\partial A_z}{\partial\rho} \quad E_z = -\frac{j}{\omega\mu\varepsilon}\left(\frac{\partial^2}{\partial z^2} + k^2\right)A_z$$

$$H_z = 0$$

Now, for the CSMA with arbitrary sector angle $\phi_0{}^0$

$$H_\phi = 0; \left(\rho = a, 0 \le \phi \le \phi_0^0; 0 \le z \le h\right)$$

$$H_\phi(\rho = a) = -\frac{1}{\mu}\frac{\partial A_z}{\partial\rho} = -\frac{1}{\mu} B_{mnp} J'_m\left(k_\rho a\right)[A\cos m\phi + B\sin m\phi][\cos\left(k_z z\right)] = 0$$

$$J'_m\left(k_\rho a\right) = 0 \Rightarrow k_\rho a = \chi'_{mn} \Rightarrow k_\rho = \chi'_{mn}/a$$

χ'_{mn} is the n th zero of derivative of Bessel function of order m.

Sudip Kumar Ghosh, Subhradeep Chakraborty, L. Lolit Kumar Singh and Sudipta Chattopadhyay, "Modal Analysis of Probe Fed Circular Sector Microstrip Antenna with and without Variable Air Gap: Investigations with Modified Cavity Model," International journal of RF and Microwave Computer Aided Engineering, Vol. 28, No. 1, pp. 1-14, 2018, DOI: 10.1002/mmce.21172.

Dominant Mode Resonant Frequency Computation of CSMA

Again, the vanishing radial magnetic field boundary condition requires

$$H_\rho = 0; \left(\phi = 0, 0 \le \rho \le a; 0 \le z \le h\right)$$

$$H_\rho = 0; \left(\phi = \phi_0^0, 0 \le \rho \le a; 0 \le z \le h\right)$$

Thus,

$$H_\rho(\phi = 0) = \frac{1}{\mu}\frac{1}{\rho}\frac{\partial A_z}{\partial \phi} = \frac{1}{\mu}\frac{1}{\rho} B_{mnp} J_m(k_\rho \rho)[-mA\sin m\phi + mB\cos m\phi][\cos(k_z z)] = 0$$

If, $B = 0$

$$H_\rho(\phi = \phi_0^0) = \frac{1}{\mu}\frac{1}{\rho} B_{mnp} J_m\left(k_\rho \rho\right)[-mA\sin m\phi_0][\cos\left(k_z z\right)] = 0$$

It is possible if, $m\phi_0 = q\pi$

Again, the tangential electric field boundary condition requires

$$E_\phi = 0; \left(z = 0, 0 \le \rho \le a; 0 \le \phi \le \phi_0^0\right)$$

$$E_\phi = 0; \left(z = h, 0 \le \rho \le a; 0 \le \phi \le \phi_0^0\right)$$

$$E_\phi\left(z = h\right) = \frac{j}{\omega\mu\varepsilon}\frac{1}{\rho} B_{mnp} J_m\left(k_\rho \rho\right) k_z\left(-mA\sin m\phi\right)\sin\left(k_z h\right) = 0$$

Dominant Mode Resonant Frequency Computation of CSMA

It is possible if,

$$k_z = \frac{p\pi}{h}$$

$$k^2 = k_\rho^2 + k_z^2$$

Considering the patch is on thin substrate; the zeroth order resonance frequency f_r is

$$f_r = \frac{\chi'_{mn} c}{2\pi a_{eff}\sqrt{\varepsilon_{reff}}}$$

For 90^0 circular sector,

$$\phi_0 = \pi/2$$

$$m = 2q$$

The lowest value of $\chi'_{mn} = 3.05$ occurs when m = 2, n =1. So, dominant mode is TM_{21}.

$$f_r = \frac{\chi'_{21} c}{2\pi a_{eff}\sqrt{\varepsilon_{reff}}} = \frac{3.05c}{2\pi a_{eff}\sqrt{\varepsilon_{reff}}}$$

The number of variations in electric field along the radial direction (along ρ direction) is n and that along the circumferential direction (along φ direction) is q ($m = 3q$).

Feed Position Influence on 90^0 CSMA

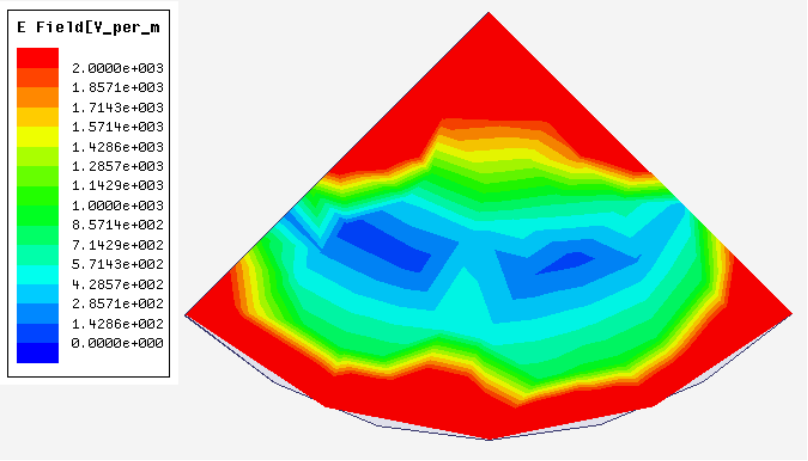

The magnitude of simulated electric field distribution over patch surface of CSMA with ϕ_0 = 90^0 fed along ϕ= $\phi_0/2$ line. (CSMA parameters: radius a = 10 mm, ε_r=2.33, substrate height h= 1.575 mm.)

The magnitude of simulated electric field distribution over patch surface of CSMA with ϕ_0 =90^0 fed along ϕ= 0^0 line. (CSMA parameters: radius a = 10 mm, ε_r=2.33, substrate height h= 1.575 mm.)

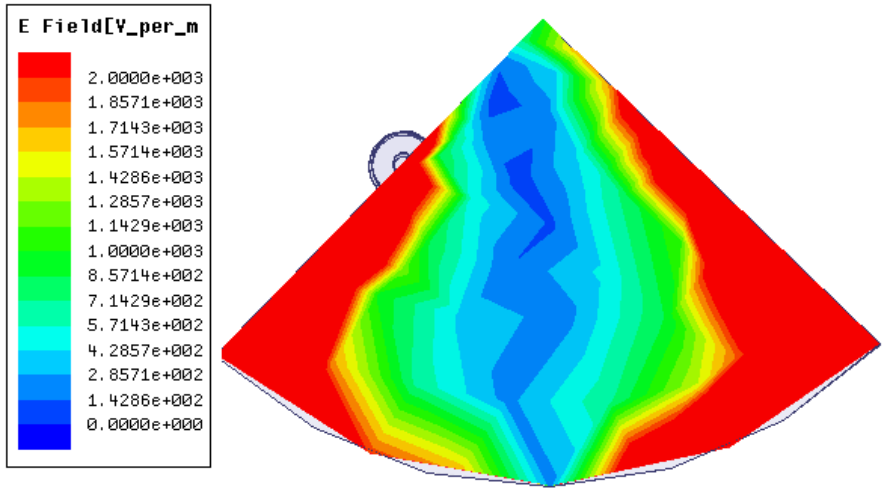

Feed Position Influence on 90^0 CSMA

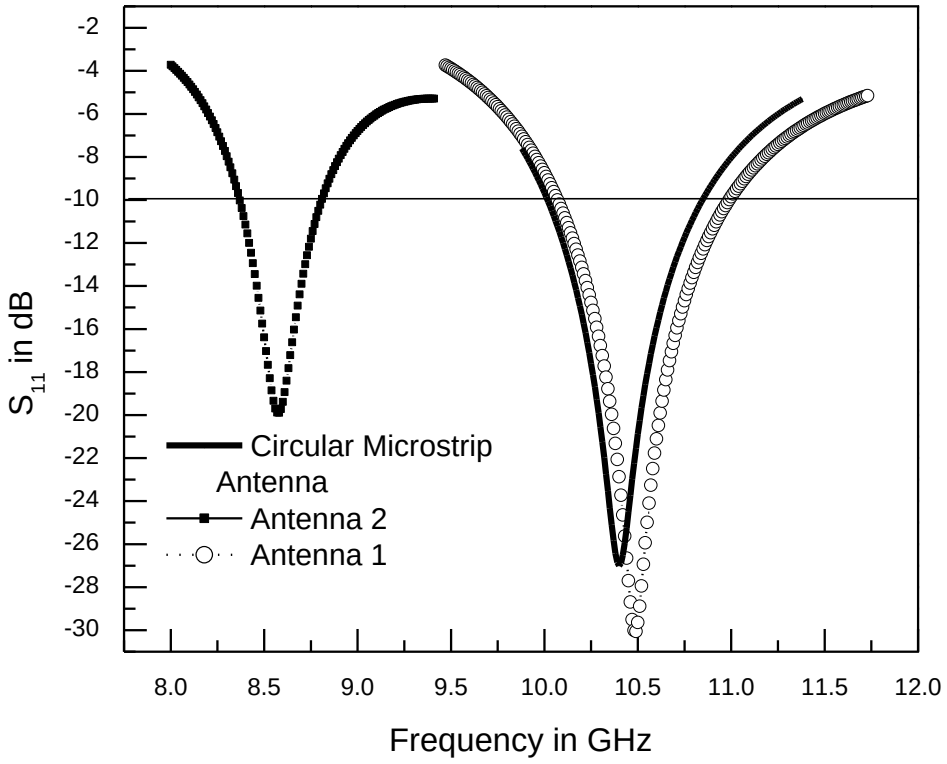

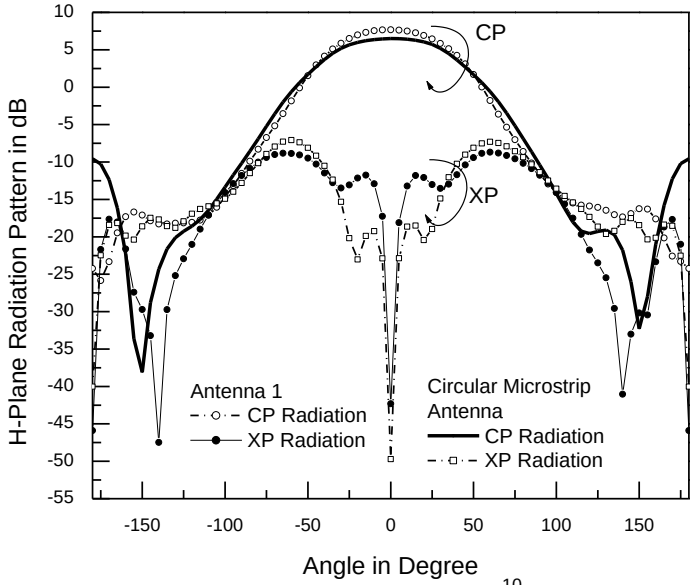

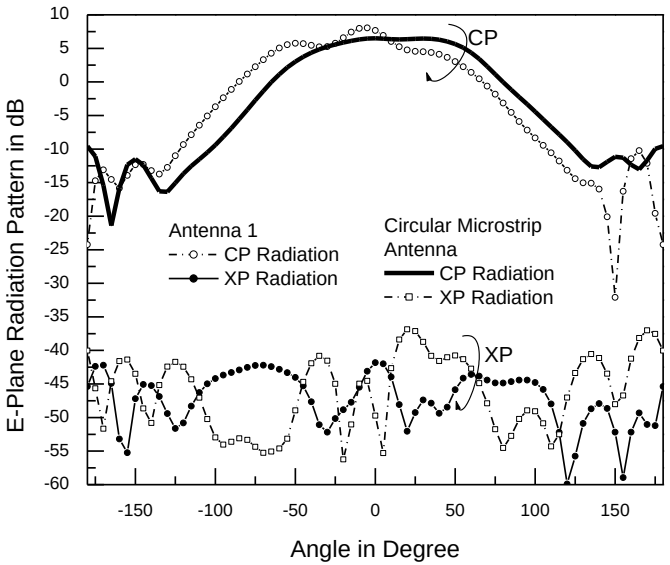

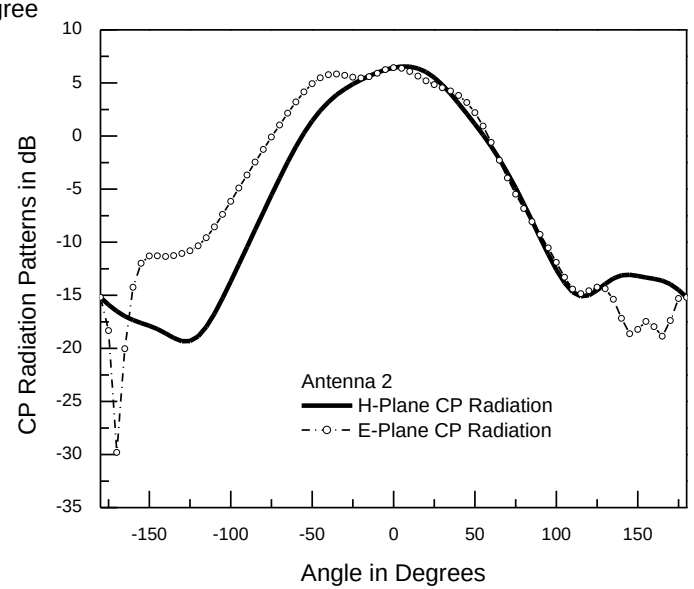

Radiation patterns for (a) antenna 1 at higher order TM_{01} mode (*f= 10.5 GHz*) and (b) circular microstrip antenna at dominant TM_{11} mode (*f= 10.38 GHz*), (c) H and E plane radiation patterns for antenna 2 at dominant mode frequency (*f= 8.56 GHz*).

.

Parameters	Antenna 1	Antenna 2	Reference Circular Microstrip Antenna
Electromagnetic Modes	TM_{01} (higher order)	TM_{21} (dominant)	TM_{11} (dominant)
Frequency (GHz)	10.5	8.56	10.38
S_{11} in dB	-30.5	-21	-27
Bandwidth (%)	8.91	4.6	6.3
Gain	7.72	6.7	7.1
CP-XP isolation	15.1	10.1	12

Feed Position Influence on 90^0 CSMA

- Feed-probe position has a strong impacton the radiation characteristics of 90^0 CSMA.
- When the CSMA is fed by feed-probe along edge ($\phi=0^0$ line) and central symmetrical $\phi=\phi_0/2$ line, dominant TM_{21} mode and higher order TM_{01} mode get excited.
- A 90^0 CSMA resonating at higher order TM_{01} mode has nearly equivalent radiation characteristics with a circular microstrip antenna resonating nearly at same frequency at dominant TM_{11} mode.
- Therefore, 90^0 CSMA can be a suitable alternative to circular microstrip antenna.
- It will be very much useful in compact array configurations.

Received: 8 August 2017 | Revised: 24 August 2017 | Accepted: 24 August 2017

DOI: 10.1002/mmce.21172

RESEARCH ARTICLE

WILEY INTERNATIONAL JOURNAL OF RF AND MICROWAVE COMPUTER-AIDED ENGINEERING

Modal analysis of probe-fed circular sector microstrip antenna with and without variable air gap: Investigation with modified cavity model

Sudip Kumar Ghosh[1] | **Subhradeep Chakraborty**[2] | **L. Lolit Kumar Singh**[3] | **Sudipta Chattopadhyay**[3]

[1] Siliguri Institute of Technology, Siliguri, West Bengal, India

[2] CSIR-Central Electronics Engineering Research Institute, Pilani, Rajasthan, India

[3] Department of Electronics and Communication Engineering, Mizoram University, Aizawl, Mizoram, India

Correspondence
Sudipta Chattopadhyay, Department of Electronics and Communication Engineering, Mizoram University, Aizawl, Mizoram, India.
Email: sudipta_tutun@yahoo.co.in

Abstract

Determination of accurate modal fields is one of the most crucial issues to understand the proper behavior of circular sector microstrip antennas (CSMAs) to achieve the best performance. In this article, dominant and higher order modal characteristics have been rigorously studied which germinate an improved, accurate, and efficient computer-aided design (CAD) formulation to estimate the resonant frequency of CSMA with and without air gap between substrate and ground plane. The proposed formulation can address the wide variety of issues (such as substrate height, substrate permittivity, air gap height, higher order modes, etc.). The computed results were validated against the results obtained from high-frequency structure simulator (HFSS) and our own experiments, while they have been also justified through the results obtained from the available literature.

KEYWORDS

antenna parameters, circular sector, microstrip antenna, resonant frequency

1 | INTRODUCTION

IN the modern era of microwave communications, the design and analysis of miniaturized and multifunctional antennas of different geometries continue to be the focus of state-of-the-art research. In this scenario, microstrip patch antennas (MPAs) are extremely useful and are the obvious choice of the designers because of their light weight, small size, and excellent compatibility with monolithic microwave integrated circuits. The most common geometries of MPAs, such as rectangular and circular, have been extensively studied, analyzed, and implemented for at least the last three decades. In fact, a significant number of analyses[1–6] and applications[7–12] of common MPA geometries have been reported during the last two decades. However, in various practical wireless applications, radiators should be conformally mounted onto the previously existing structures, where space limitation is a crucial problem. In such applications, a circular sector microstrip antenna (CSMA) is highly advantageous because it requires less space than a conventional patch antenna of common geometries. Approximately 30% and 35% patch area reductions can be achieved with a CSMA using 60° and 90° sector angles, respectively, compared with a conventional circular MPA. Therefore, an accurate analysis of CSMA is a priority in the present scenario of printed antenna research. In this context, we have found a limited number of analyses,[13–17] in which the computation of the accurate resonant frequency of CSMA with arbitrary sector angles has been dealt with.

The formulation of the resonant frequency of a CSMA based on the cavity model was first reported in ref. 13. The electric field beneath the patch and the eigen functions of those antennas were also presented in ref. 13. In ref. 14, a generalized transmission line modeling was used for computing the resonant frequency of a CSMA. However, the effect of fringing fields, which should be considered for the accurate estimation of the resonant frequency of a CSMA, was not included in refs. 13 and 14.

Recent Reported Techniques for XP Minimisation

- Use of Defected Ground Structure (DGS): It may be of different geometry:
  - 1. Simple Slot DGS/ Bracketed DGS
  - 2. Dumbbell DGS:
    - (A) Rectangular Headed Dumbbell
    - (B) Circular Headed Dumbbell

- Use of Defected Patch Surface :
- Shorted patch concept:
  - 1. Fully shorted Patch
  - 2. Discrete shorted patch

DGS – A Easy Solution

- Recently, there has been an increasing interest in using Defected Ground Structures (DGS) to reduce XP radiation from a RMA.

- First concept of DGS for minimizing XP radiation for a patch antenna was proposed by applying a dot shaped DGS with 5-8dB XP suppression in broad side direction for CMA.

- H plane XP radiation minimized by 10-12 dB compared to conventional CMA by using arc shaped DGS has been reported by Guha et. Al.[D. Guha et. Al, *IEEE Antenna and Wireless Propagat. Letters*, Vol. 8, 2009]

Problems with DGS

- The DGS structures, either in circular or rectangular patch geometry enhances the back radiation from the antenna structure.

- The XP radiation suppression is mainly in the broadside region of radiation. Application like Mobile phone, Wi-Fi, WiMax etc. requires wide coverage with good polarization purity. Good polarization purity requires high CP-XP separation in wide angular region.

- Narrow band width is limiting factor for MPA integrated with DGS.

- In almost all cases, defect is extended beyond the patch periphery. This is evidently a restriction for an array structure.

Dumbbell DGS: Effort to Reduce Size of The Defect

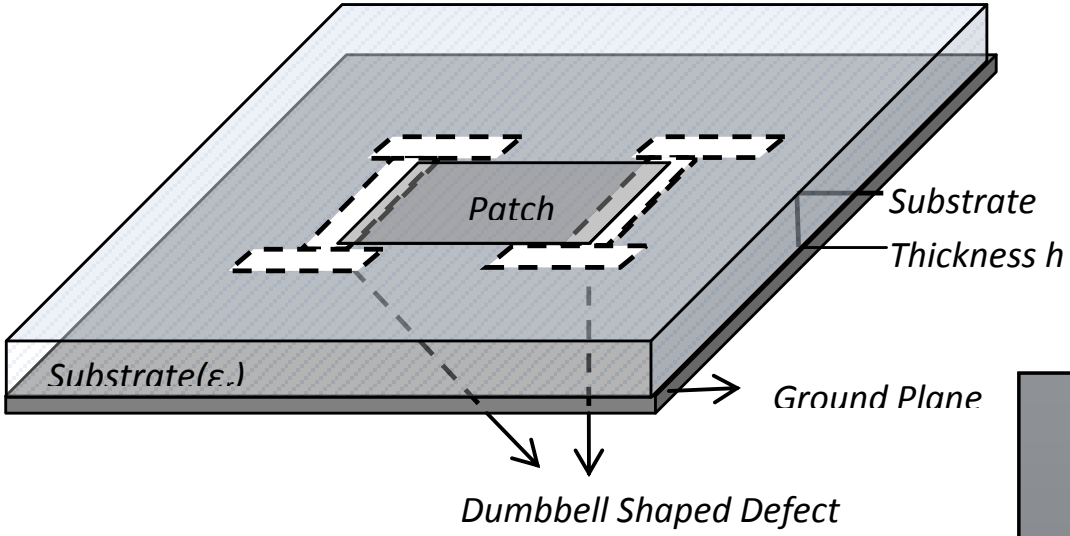

(a)

[Ghosh *et. al*, *IET Microwaves, Antenna and Propagat.*, Vol. 10, 2016] .

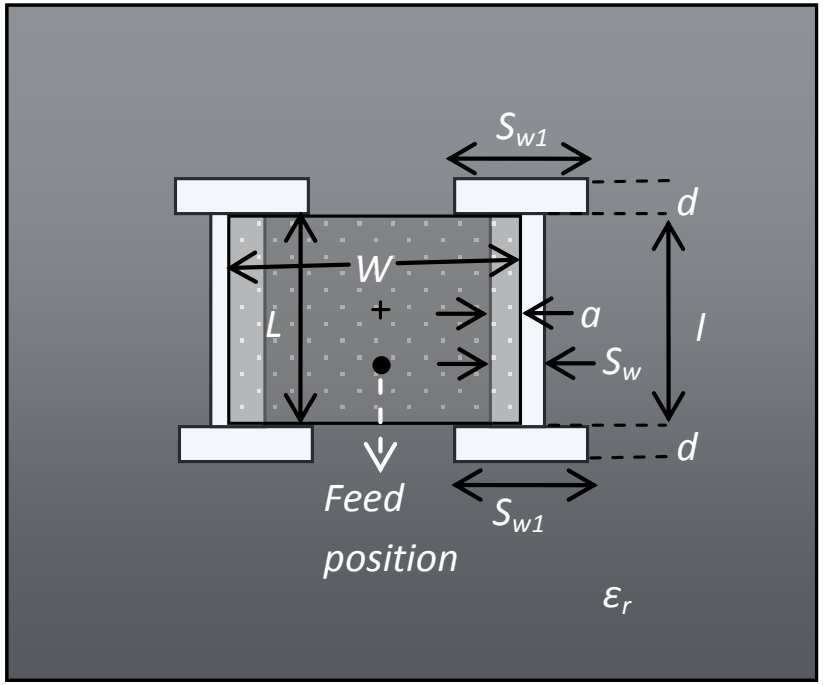

(b)

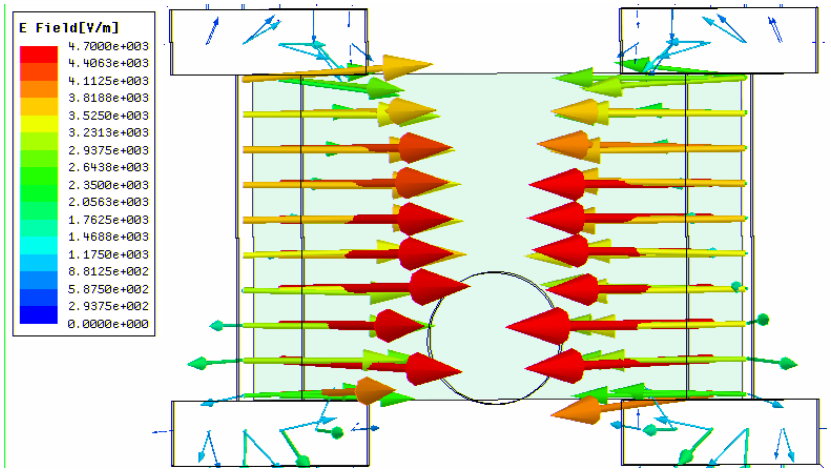

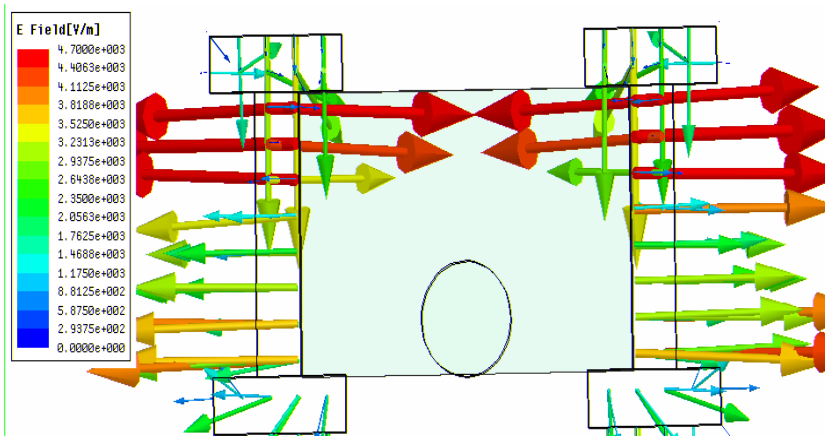

The heads of the dumbbell, is quarter wave resonant at TM_{10} mode frequency and taking care of corner fields.

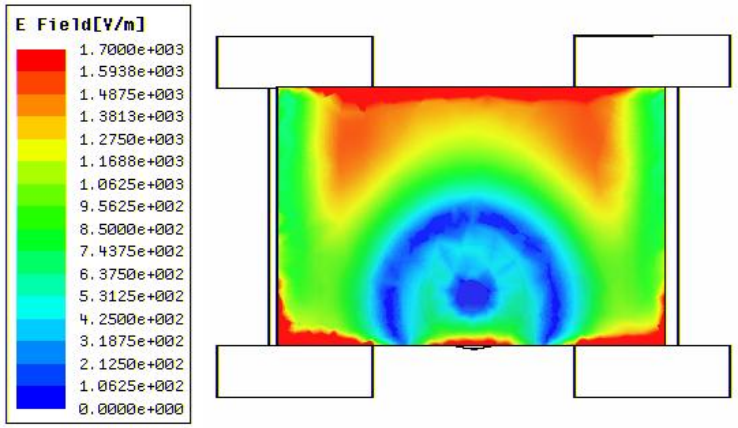

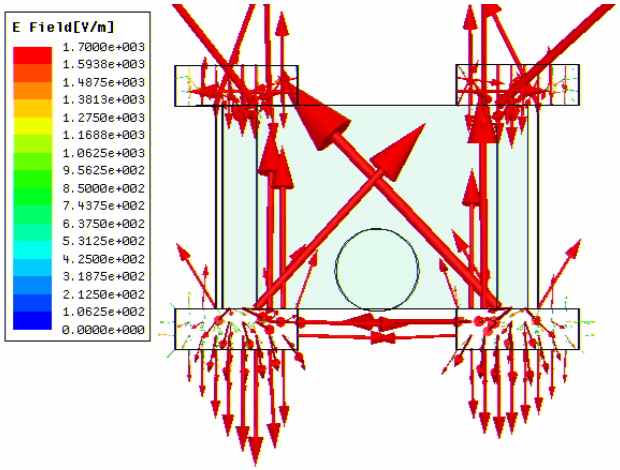

8 X 12 RMA: f=10.02 GHz, a= 1.47 mm Gain 6.53 dBi, CP-XP isolation: 25 dB

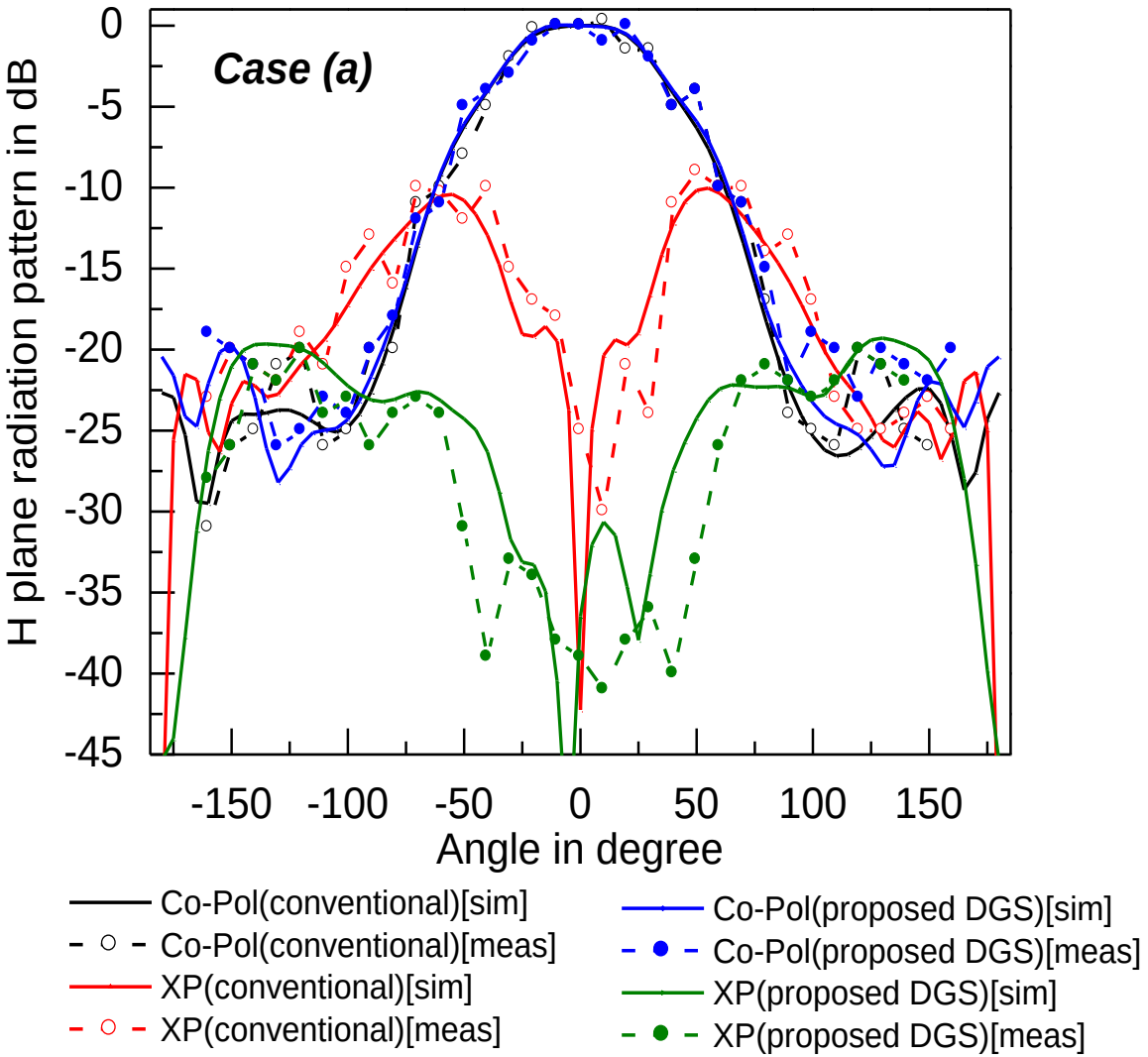

10 X 15 RMA: a= 1.66 mm f=8.5 GHz Gain 7.02 dBi, CP-XP isolation: 24 dB

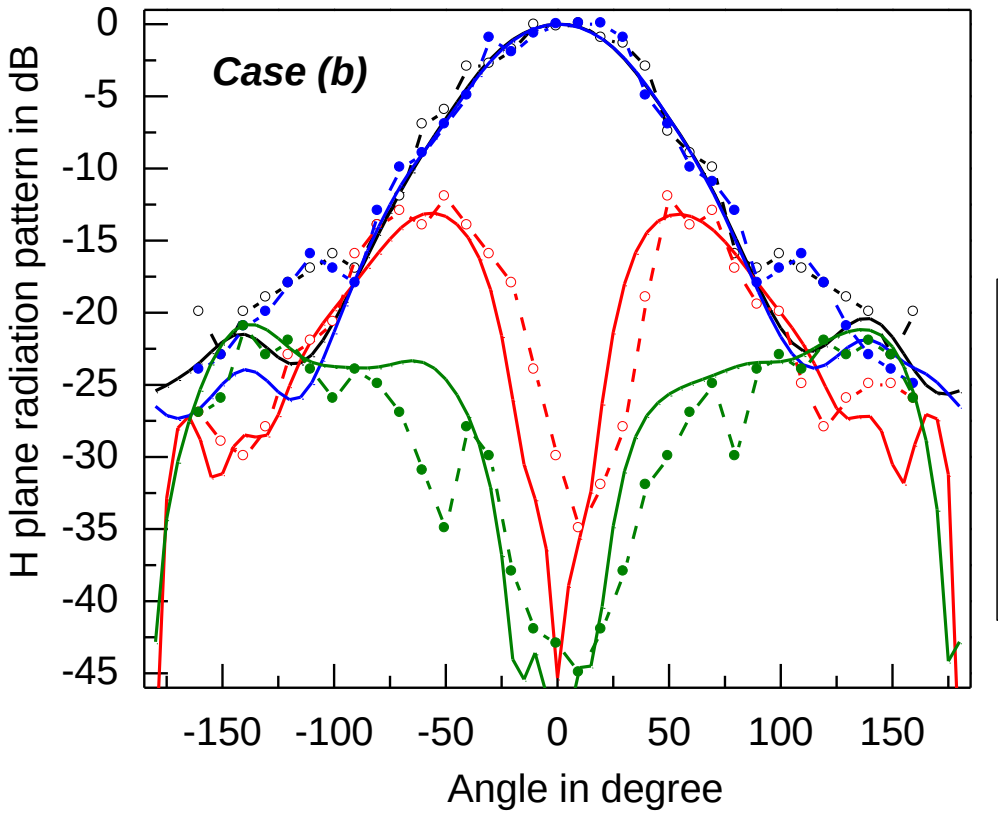

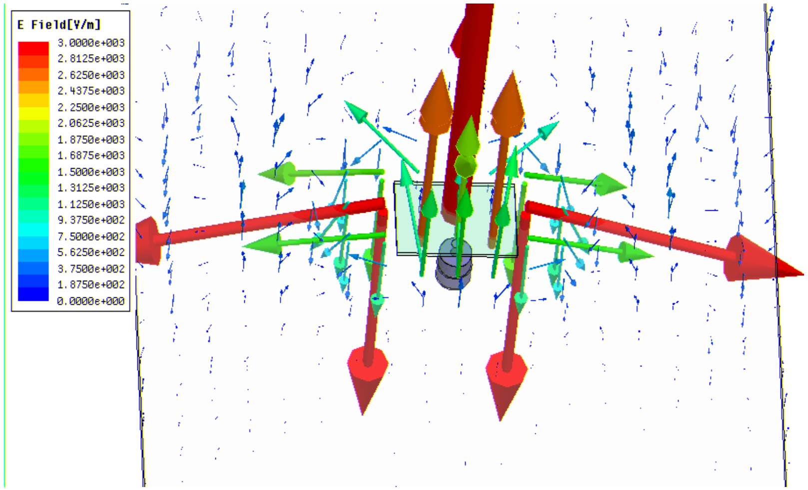

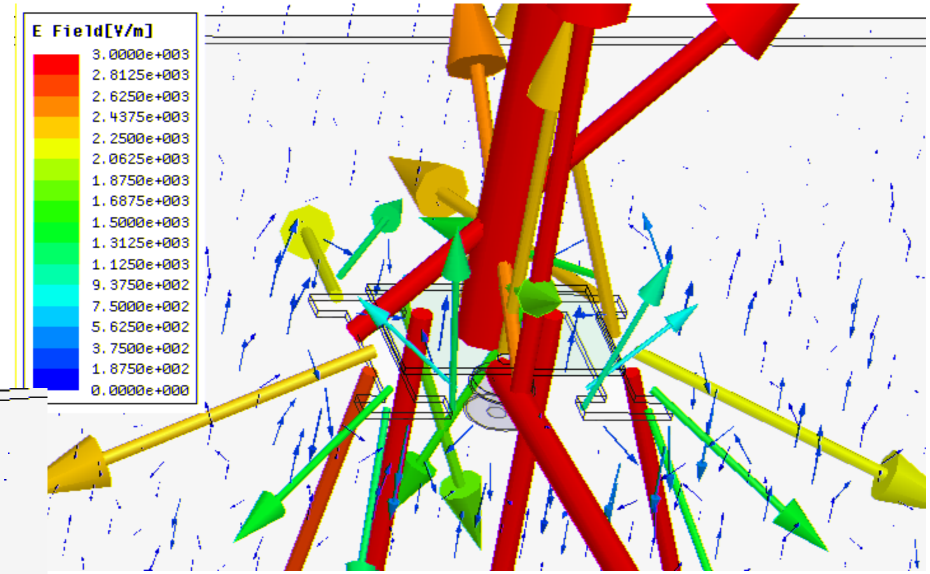

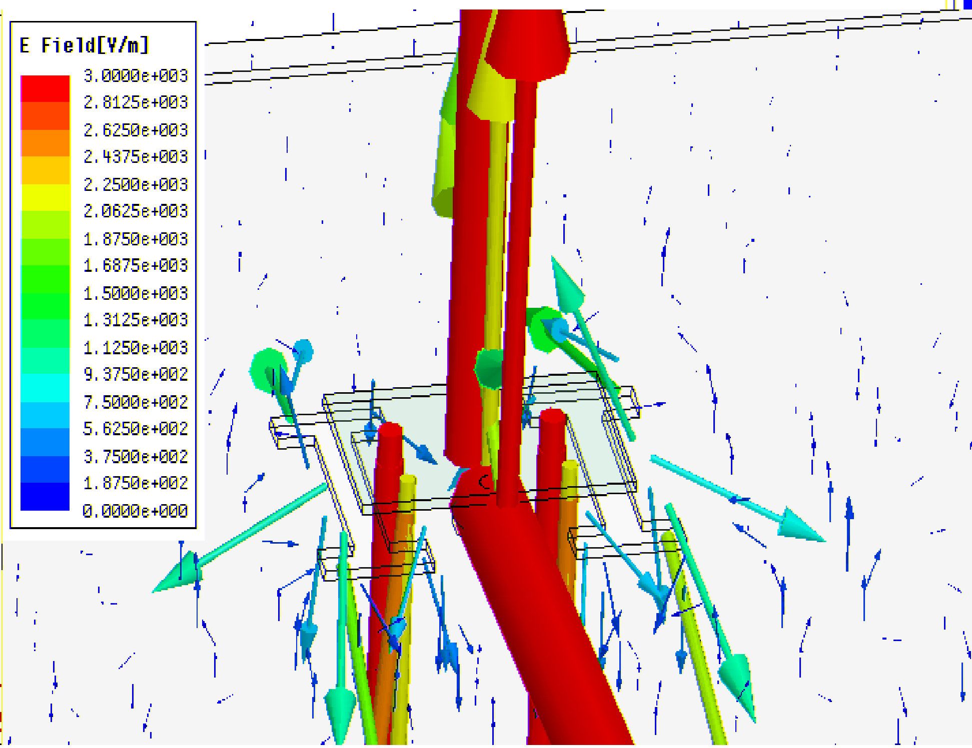

As the defect is moved beneath the patch orthogonal component of TM_{10} fields become profoundly coupled to the slot…… Radiation from non radiating edge of the patch decreases.

"Better than a thousand days of diligent study is one day with a great teacher"

- A Japanese Proverb

Thank You

Some Glimpses of New Techniques for Generation of Flat-Top Radiation Patterns from Antenna Arrays and Antennas

Subhradeep Chakraborty
Scientist
Device Technology Group
Microwave Devices Area
CSIR-CEERI, Pilani
E-mail: subhradeep@ceeri.res.in, s.c.in@ieee.org

Acknowledgements

- Director, CSIR-CEERI, Pilani
- Dr. R. K. Sharma, Area-Coordinator, MWD Area
- Dr. S. K. Ghosh, Group Head, DTG Group
- Prof. B. N. Basu, SKFGI, Mankundu, India
- Prof. P. K. Saha, Ex- University of Calcutta, India
- Dr. A. K. Bhattacharyya, Lockhead Martin, USA
- Prof. D. Guha, University of Calcutta, India
- Prof. S. Chattopadhyay, Mizoram University, India
- Prof. J. Y. Siddiqui, University of Calcutta, India

Outline

- Radiation Patterns of Conventional Antennas
- Antenna Arrays
- Flat-Top Radiation Pattern
- Beam Synthesis Methods
- Flat-Top Radiation from Arrays
- Can We Get a Flat-Top Radiation Pattern from Unit Antenna?
- QPCMA
- Conclusions
- References

Antenna Radiation Pattern in 3D

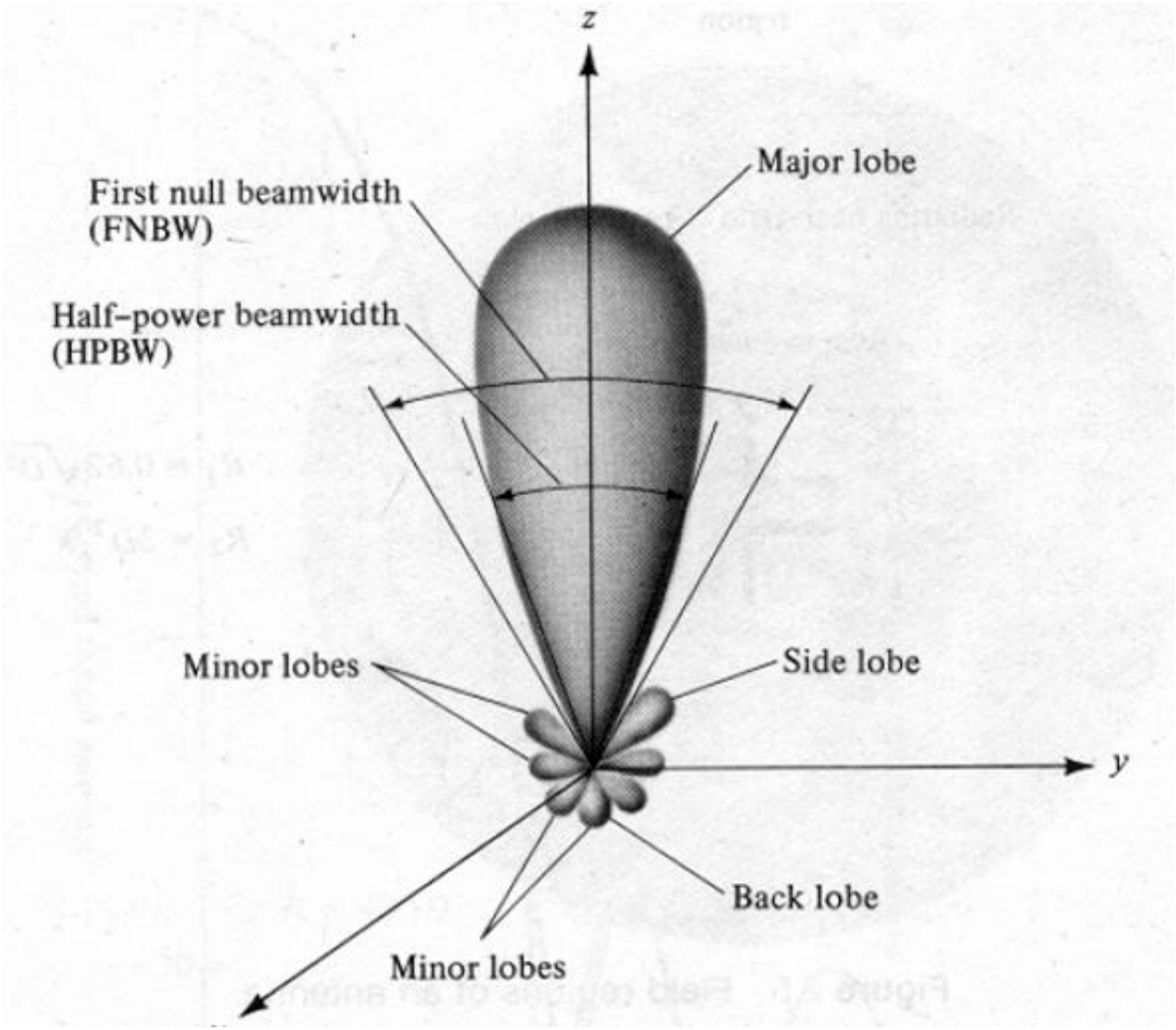

Antenna Radiation Pattern in 2D Polar Plot (ϕ=const. plane)

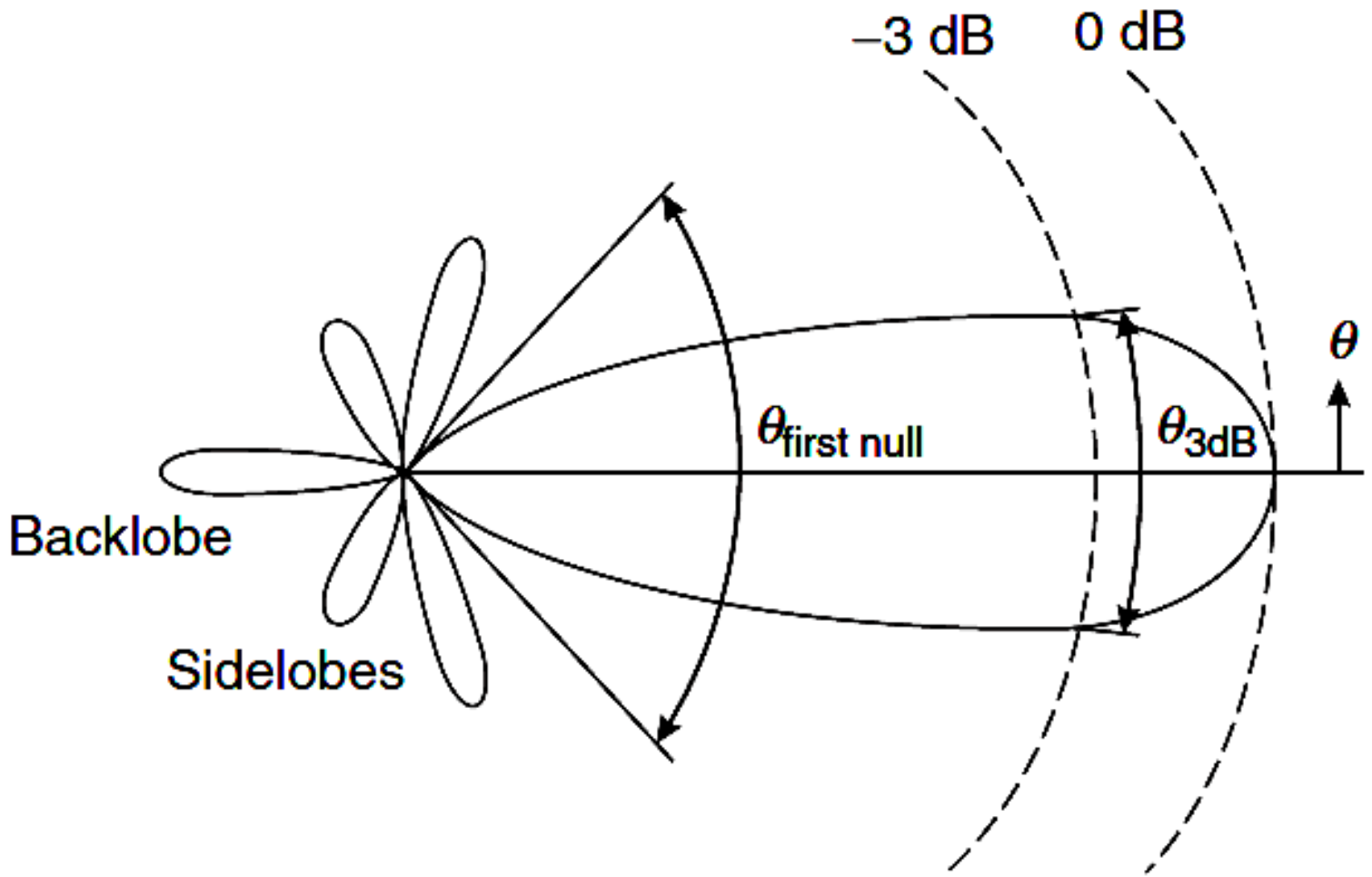

Antenna Radiation Pattern in 2D: Cartesian Plot (ϕ=const. plane)

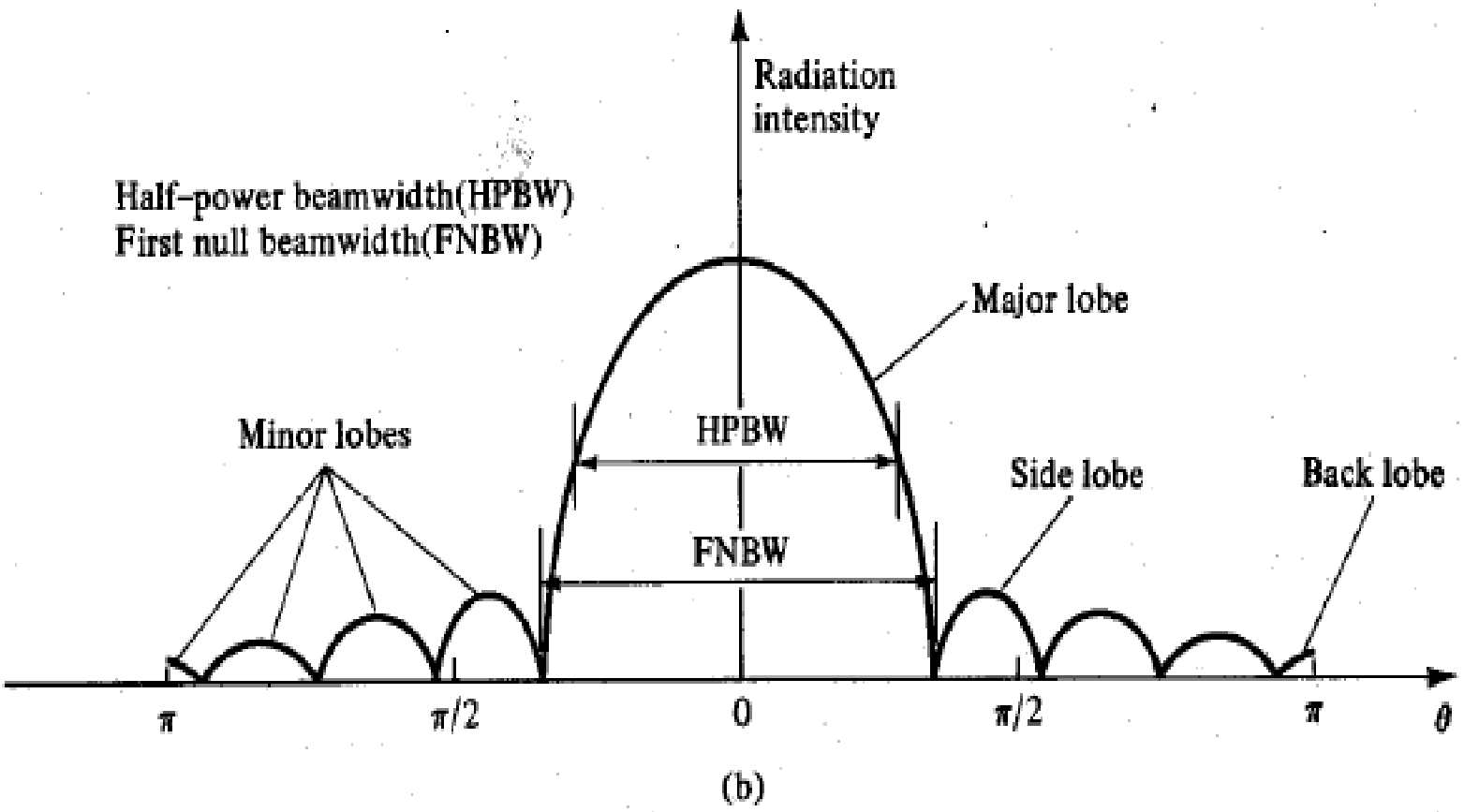

(b)

Flat-top Radiation Patterns

- Beyond a certain angular region, the power intensity decays rapidly to a very low level to avoid the same frequency interference with other antennas operating at the same time.
- Provides stable maximum gain along bore sight to improve signal strength within service coverage area.
- First, explored in antenna arrays to achieve a flat sector beam.
- Useful in ubiquitous wireless communication services, in base station for mobile communication and as efficient feeds for parabolic reflectors for the sake of uniform aperture illumination.
- To the best of our knowledge, around 10-15 papers are available in SCI Journals.

Some Published Papers on Flat-Top Radiation Patterns

- A Ngoc Tinh, R. Sauleau, and L. Le Coq, “Reduced-size double shell lens antenna with flat-top radiation pattern for indoor communications at millimeter waves,” *IEEE Transactions Antenn. Propag*., vol. 59, no. 6, pp. 2424–2429, 2011
- Han Wang, Zhijun Zhang, Yue Li, Magdy F. Iskander, “A Switched Beam Antenna With Shaped Radiation Pattern and Interleaving Array Architecture,” *IEEE Transactions Antenn. Propag*., vol. 63, no. 7, pp. 2914–2921, 2015.
- H. J. Zhou, B. H. Sun, J. F. Li, and Q. Z. Liu, “Efficient Optimization and Realization of A Shaped Beam Planar Array for Very Large Array Application,” *Progress In Electromagnetics Research, PIER* 89, 1–10, 2009
- R. Eirey-Pérez, A. A. Salas-Sánchez, J. A. Rodríguez-González, and F. J. Ares-Pena, “Pencil beams and flat-topped beams with asymmetric sidelobes from circular arrays,” *IEEE Trans Antennas Propag.,* vol. 56, no. 6, pp. 153–161, 2014.
- Z. Zhang, N. Liu, S. Zuo, Y. Li, and G. Fu, “Wideband circularly polarised array antenna with flat-top beam pattern,” *IET Microwaves Antennas Propag*., vol. 9, no. 8, pp. 755–761, 2015.

Some Published Papers on Flat-Top Radiation Patterns

- Chunmei Meng, Jin Shi and Jian-Xin Chen, “Flat-gain dual-patch antenna with multi-radiation nulls and low cross-polarisation, *Electronic Letters*, Vol. 54 No. 3 pp. 114–116, 2018
- H. Wang, Z. Zhang, and Z. Feng, “A beam-switching antenna array with shaped radiation patterns,” *IEEE Antennas Wireless Propag. Lett.,* vol. 11, pp. 818–821, 2012.
- Xiao Cai and Wen Geyi , “An Optimization Method for the Synthesis of Flat-Top Radiation Patterns in the Near- and Far-Field Regions” *IEEE Transactions Antenn. Propag*., vol. 67, no. 2, pp. 980–988, 2019
- J. Wang, Y. Yao, J. Yu and X. Chen, “Broadband compact smooth horn with flat-top radiation pattern,” *Electron. Lett*., vol. 55, no. 3, pp. 119-120, 2019
- Umesh Ankush Pawar, Subhradeep Chakraborty, Tanmoy Sarkar, Abhijyoti Ghosh, LLK Singh, Sudipta Chattopadhyay, “Quasi-planar Composite Microstrip Antenna: Symmetrical Flat-Top Radiation with High Gain and Low Cross Polarization, ” *IEEE Access*, USA, (accepted).

Flat-Top Radiation from Antenna Arrays

Interleaving Array Architecture

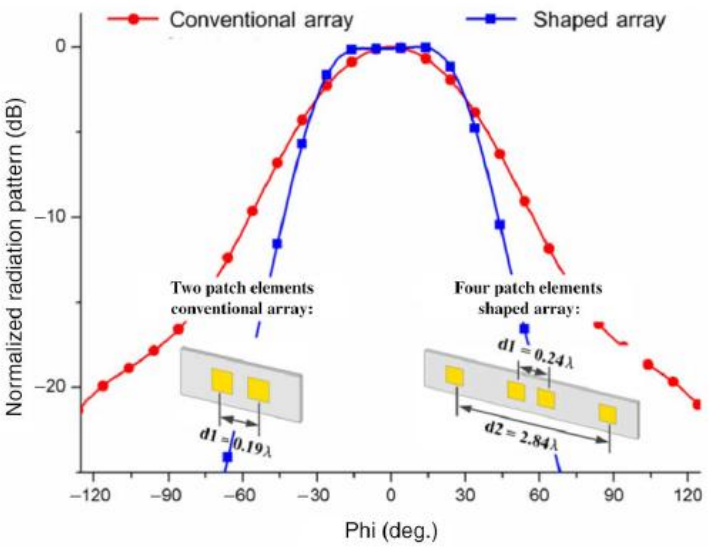

Fig. 2. Beam pattern and structure comparison between the conventional array and the shaped array.

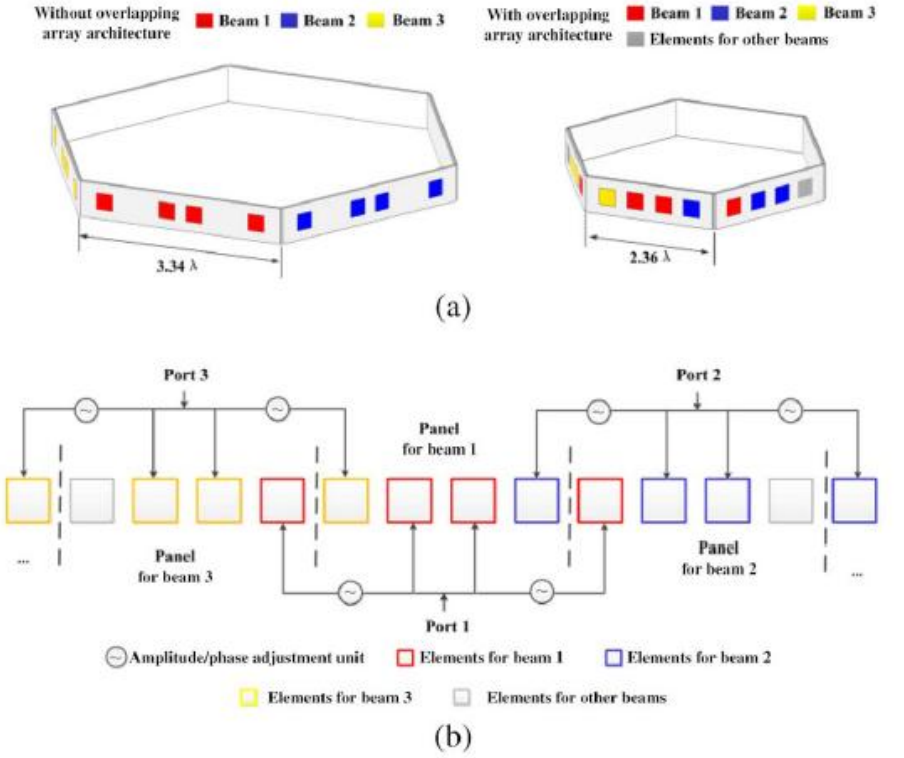

Fig. 3. Interleaving array architecture. (a) Size comparison between the array panel and the SBA with/without interleaving architecture. (b) Proposed interleaving array architecture.

• Han Wang, Zhijun Zhang, Yue Li, Magdy F. Iskander, "A Switched Beam Antenna With Shaped Radiation Pattern and Interleaving Array Architecture," *IEEE Transactions Antenn. Propag.*, vol. 63, no. 7, pp. 2914–2921, 2015

Interleaving Array Architecture

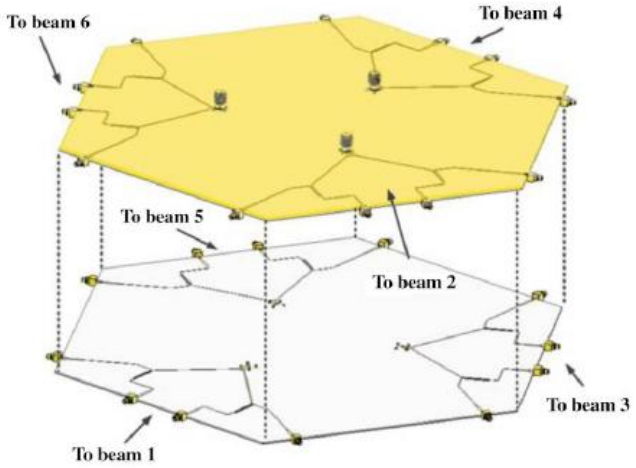

Fig. 7. Double-layer feeding structure designed for interleaving array architecture.

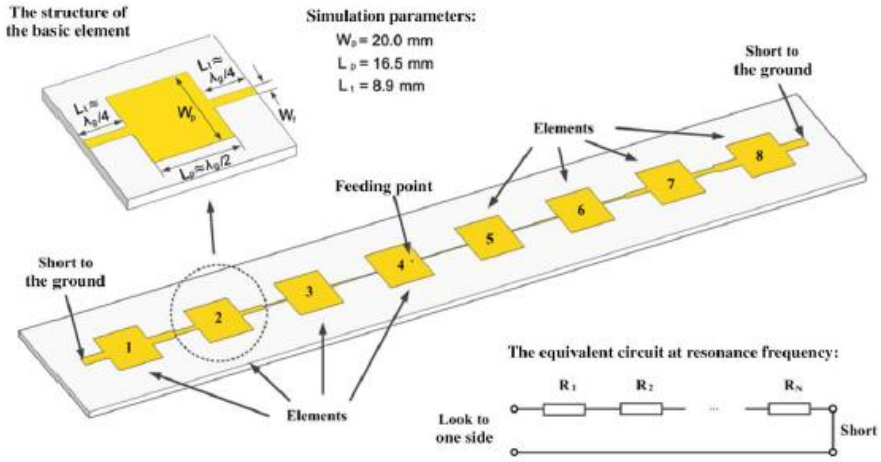

Fig. 8. Structure of the array and its basic element in elevation plane.

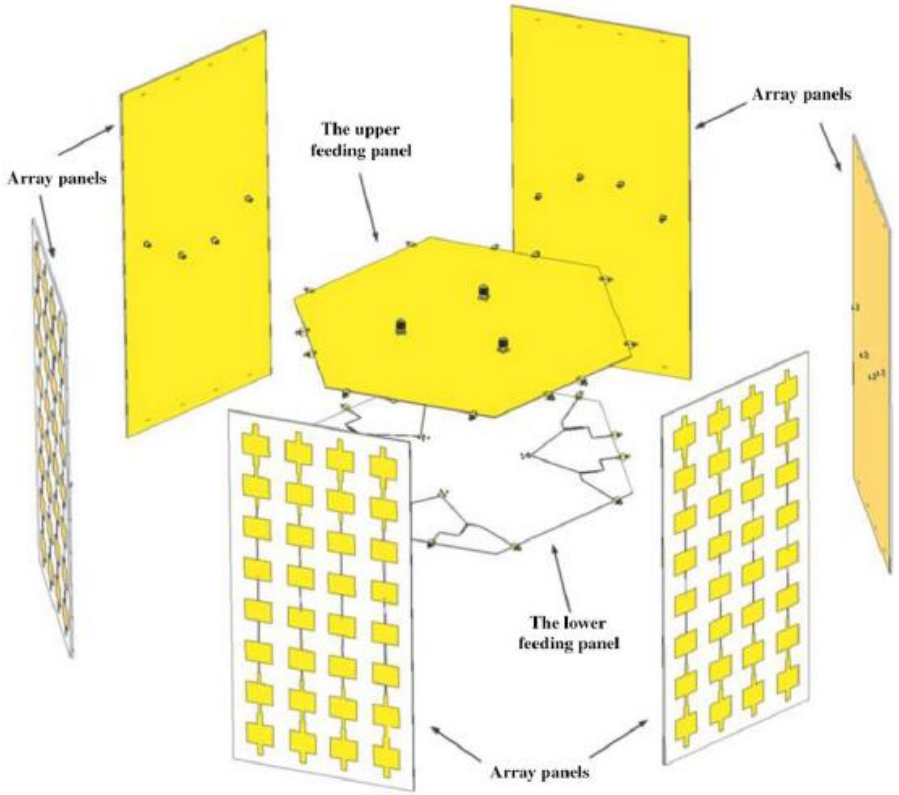

Fig. 12. Explosive view of the proposed SBA.

• Han Wang, Zhijun Zhang, Yue Li, Magdy F. Iskander, "A Switched Beam Antenna With Shaped Radiation Pattern and Interleaving Array Architecture," *IEEE Transactions Antenn. Propag.*, vol. 63, no. 7, pp. 2914–2921, 2015

Interleaving Array Architecture

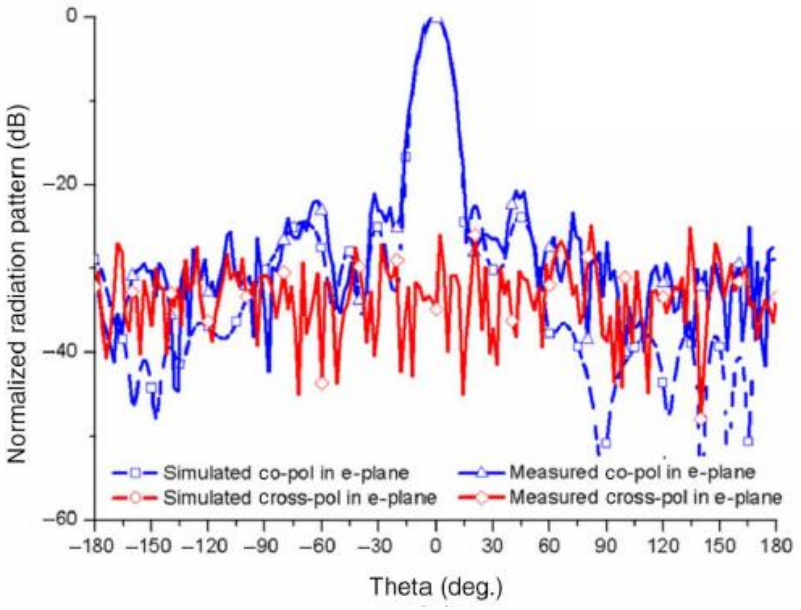

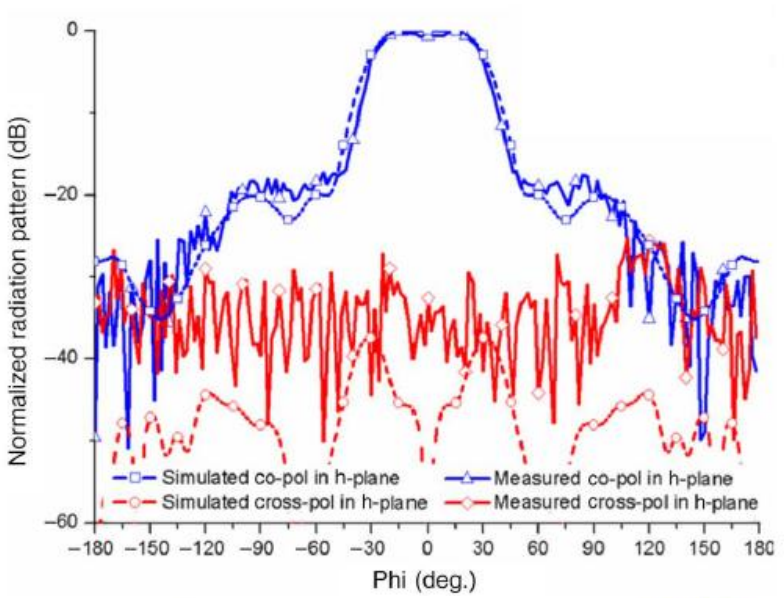

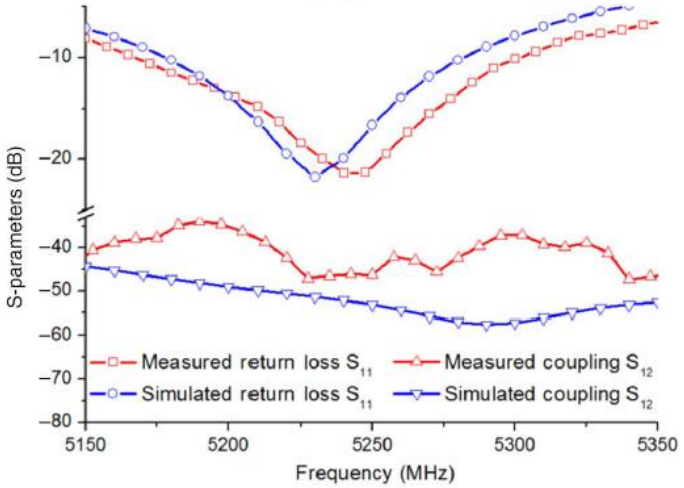

Fig. 14. Simulated and measured S-parameters of the proposed SBA.

• Han Wang, Zhijun Zhang, Yue Li, Magdy F. Iskander, "A Switched Beam Antenna With Shaped Radiation Pattern and Interleaving Array Architecture," *IEEE Transactions Antenn. Propag.*, vol. 63, no. 7, pp. 2914–2921, 2015

Beam-Switching Antenna Array

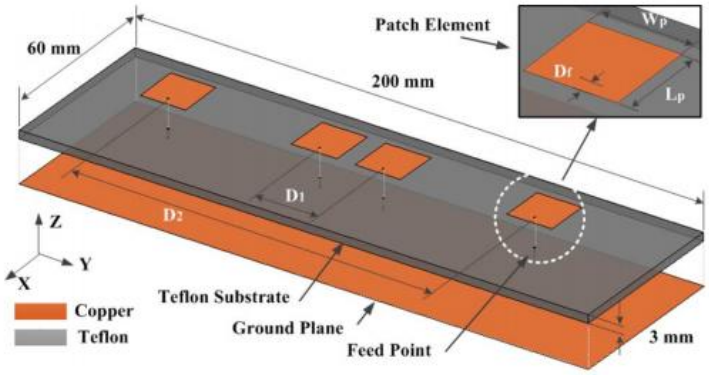

Fig. 3. Structure of proposed array.

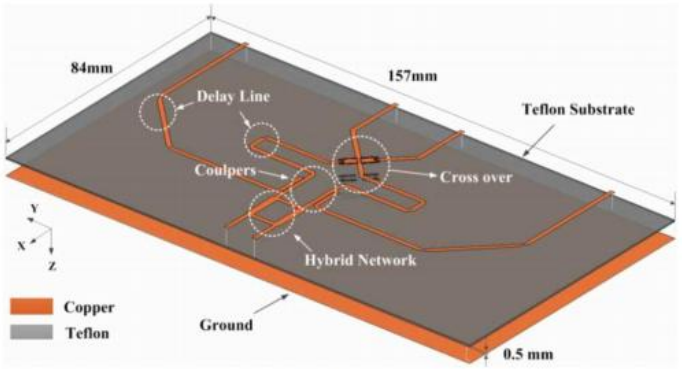

Fig. 4. Structure of feeding network.

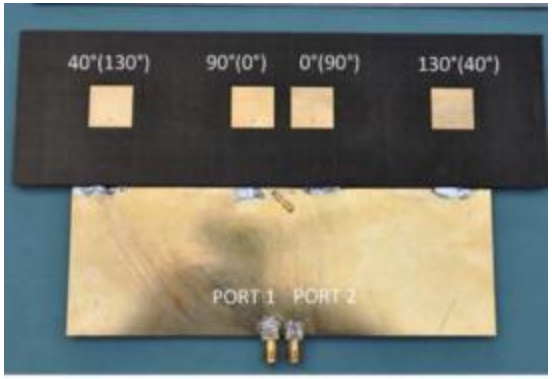

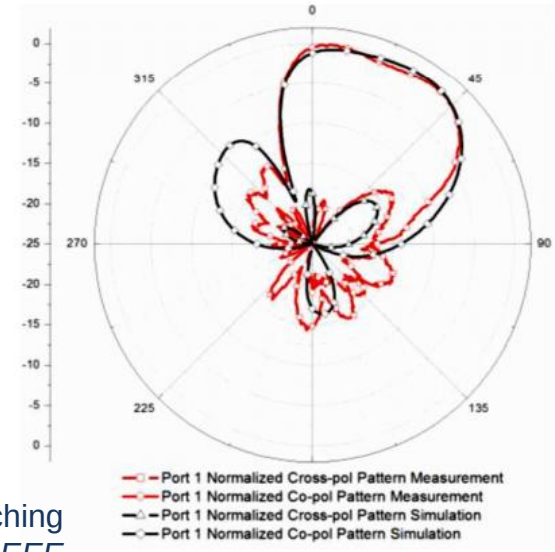

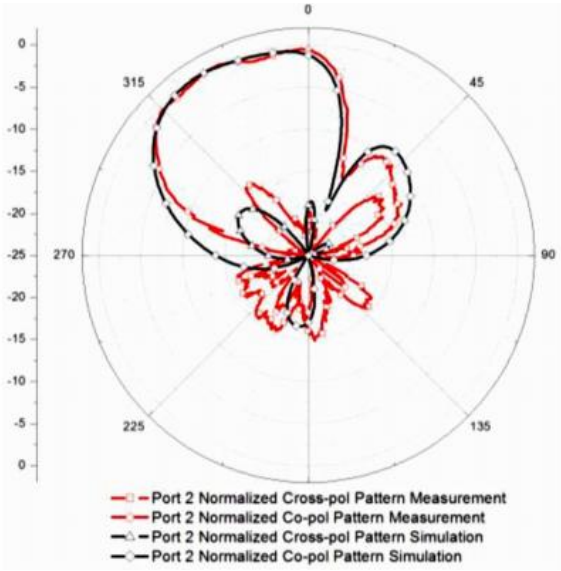

• H. Wang, Z. Zhang, and Z. Feng, “A beam-switching antenna array with shaped radiation patterns,” *IEEE Antennas Wireless Propag. Lett.,* vol. 11, pp. 818–821, 2012.

MMPTE Approach for Synthesis of Flat-Top Radiation Patterns

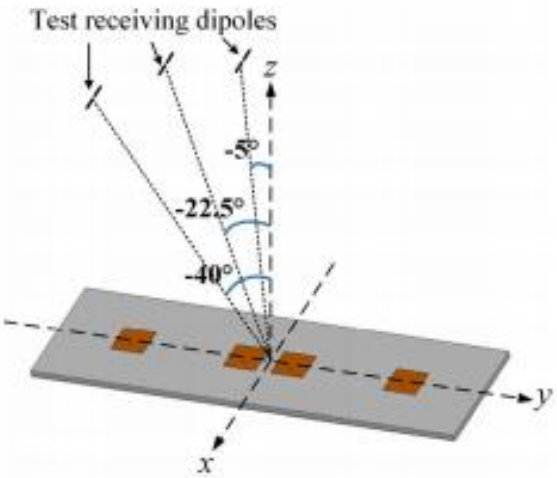

Fig. 4. Diagram for the far-field power transmission system.

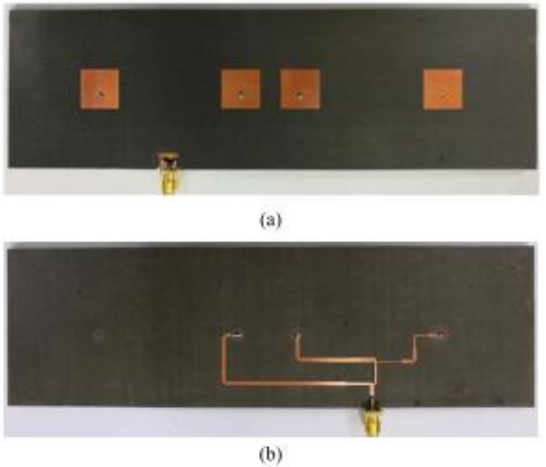

Fig. 5. Photograph of the shaped beam array antenna. (a) Top view. (b) Back view.

DISTRIBUTIONS OF EXCITATIONS

Port No.	Literature [19]	Optimized excitations (proposed)	Excitations of feeding network (proposed)
1	0.12∠130	0.17∠179.3	0.16∠179.7
2	0.70∠0	0.58∠130.0	0.58∠130.8
3	0.70∠90	0.79∠−153.3	0.79∠−153.3
4	0.12∠40	0.01∠99.5	—

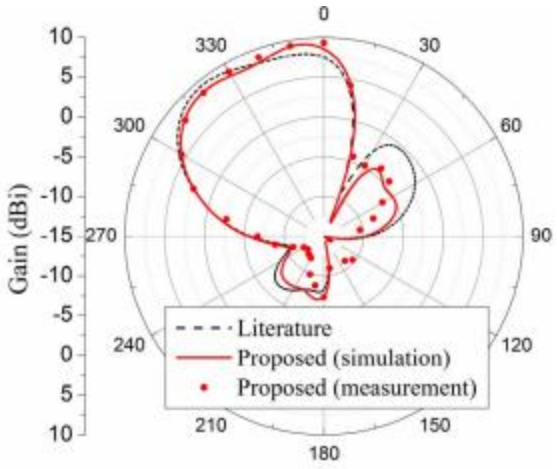

Fig. 7. Radiation patterns of the proposed array at 5.4 GHz on the yz plane.

• Xiao Cai and Wen Geyi , “An Optimization Method for the Synthesis of Flat-Top Radiation Patterns in the Near- and Far-Field Regions” *IEEE Transactions Antenn. Propag*., vol. 67, no. 2, pp. 980–988, 2019

MMPTE Approach for Synthesis of Flat-Top Radiation Patterns

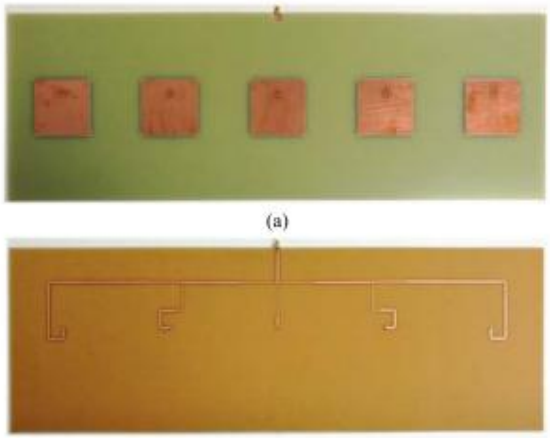

Fig. 11. Photograph of the five-element RFID reader antenna. (a) Top view. (b) Back view.

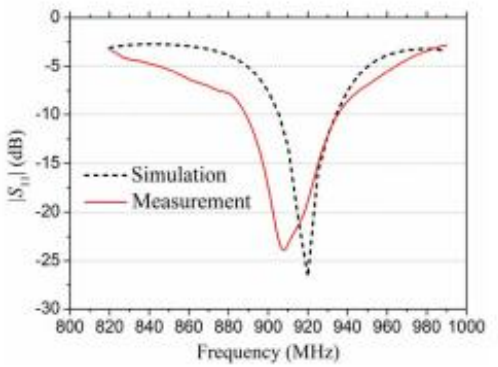

Fig. 12. Reflection coefficients of the RFID reader antenna array

Fig. 15. Test scenario for reader antenna measurements.

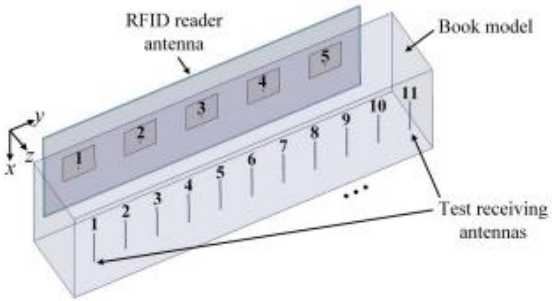

Fig. 9. Diagram for the near-field power transmission system.

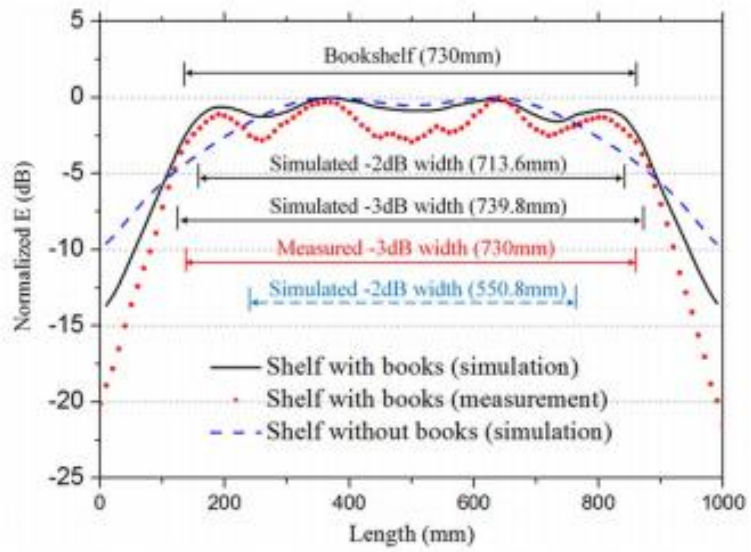

Fig. 13. Normalized electric field intensity in the y-direction at $z = 220$ mm.

• Xiao Cai and Wen Geyi , “An Optimization Method for the Synthesis of Flat-Top Radiation Patterns in the Near- and Far-Field Regions” *IEEE Transactions Antenn. Propag*., vol. 67, no. 2, pp. 980–988, 2019

Can We Get Flat-Top Radiation Patterns from Unit Antenna?

Reduced-Size Double-Shell Lens Antenna

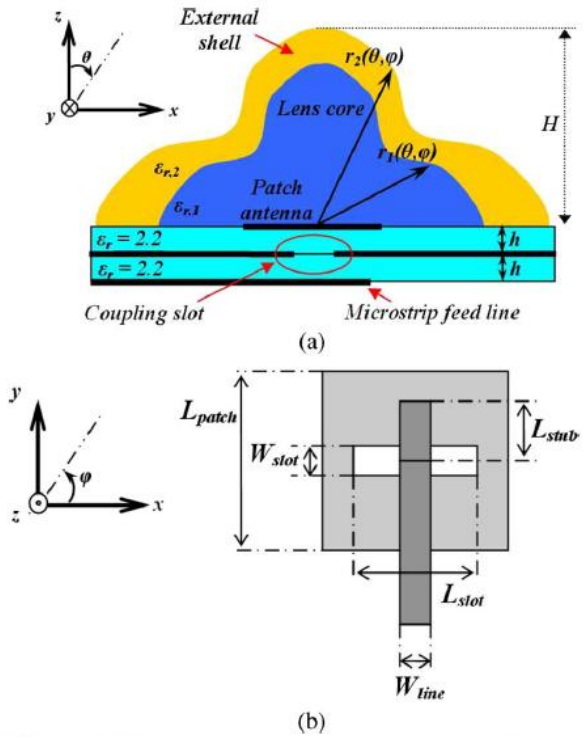

Fig. 1. Double-shell lens antenna. (a) Cross-section view. (b) Geometry of the primary feed (bottom view). The unknown lens profiles are denoted by $r_1(\theta,\varphi)$ and $r_2(\theta,\varphi)$. Dimensions of the feed: $L_{patch} = 2.45$ mm, $W_{slot} = 0.32$ mm, $L_{slot} = 1.78$ mm, $W_{line} = 0.74$ mm, $L_{stub} = 0.58$ mm.

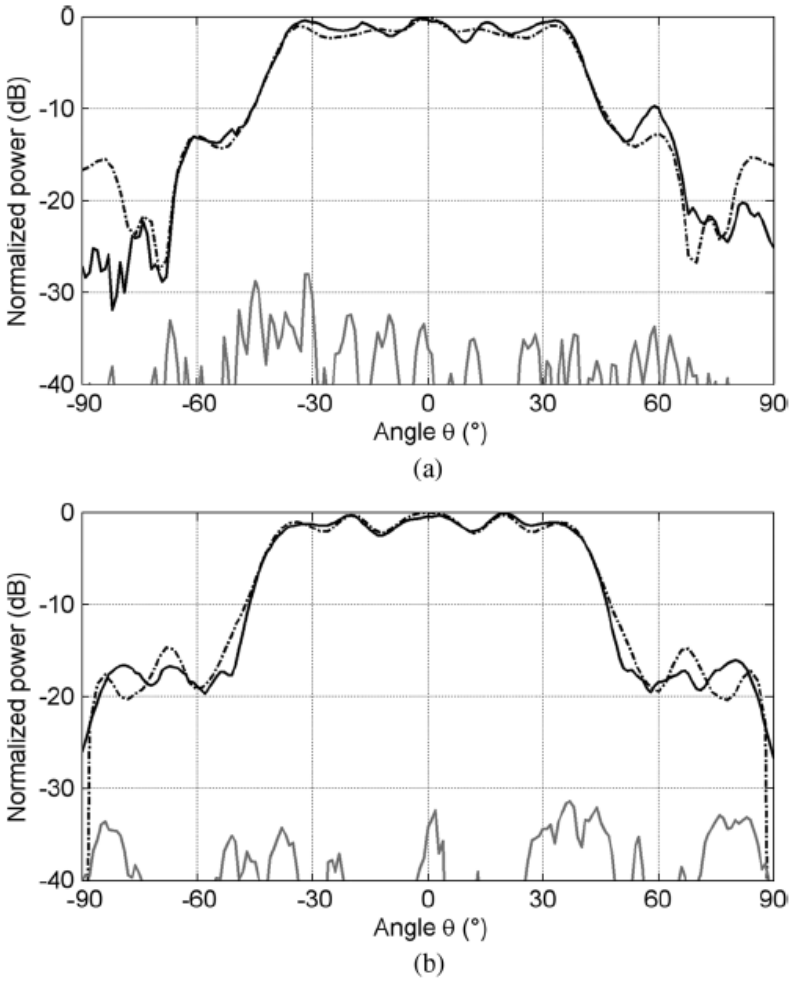

Fig. 9. Radiation patterns of the double-shell lens antenna at 28 GHz. ——: Measured co-polarization component. – – –: Computed co-polarization component (FDTD). ——: Measured cross-polarization component. (a) E-plane; (b) H-plane.

- A Ngoc Tinh, R. Sauleau, and L. Le Coq, "Reduced-size double shell lens antenna with flat-top radiation pattern for indoor communications at millimeter waves," *IEEE Transactions Antenn. Propag*., vol. 59, no. 6, pp. 2424–2429, 2011

Broad Beamwidth Circular Polarisation Antenna: Microstrip-Monopole Antenna

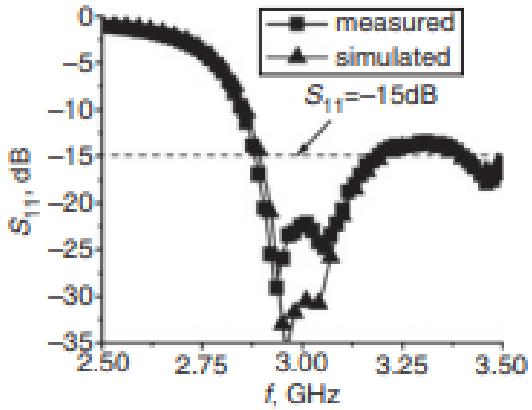

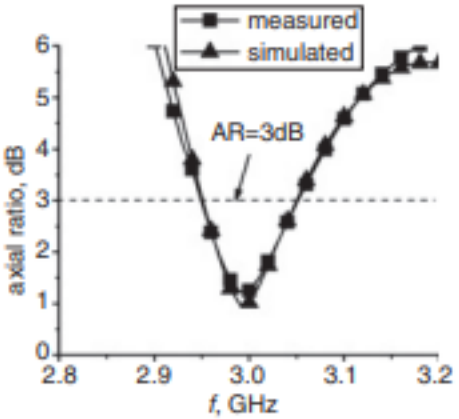

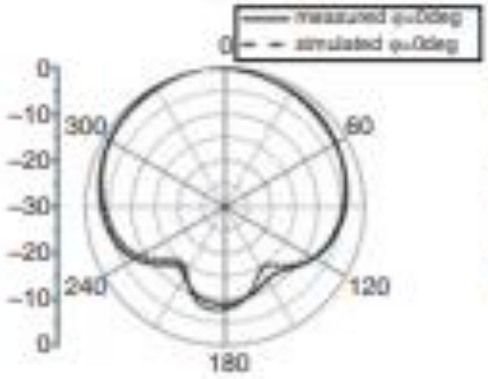

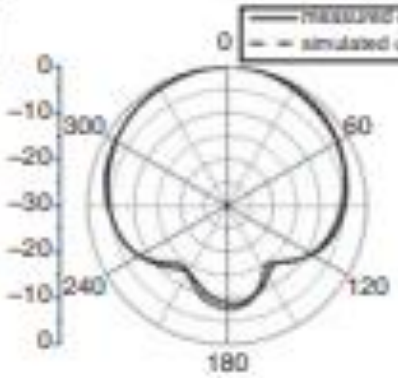

Table 2: 3 dB beamwidth at different frequencies

f	2.95 GHz	3.0 GHz	3.05 GHz
$\varphi = 0°$	140°(−67°–73°)	156°(−72°–84°)	164°(−70°–94°)
$\varphi = 90°$	117°(−57°–60°)	137°(−69°–68°)	178°(−92°–86°)

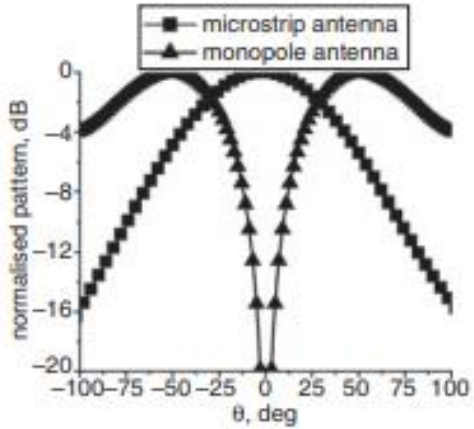

• Chuan Wu, Lei Han, Feng Yang, Liangyi Wang and Peng Yang, "Broad beamwidth circular polarisation antenna: Microstrip-monopole antenna," *Electronics Letters*, Vol. 48, Issue. 19, pp. 1176 - 1178, 2012

Flat-Gain Dual-Patch Antenna

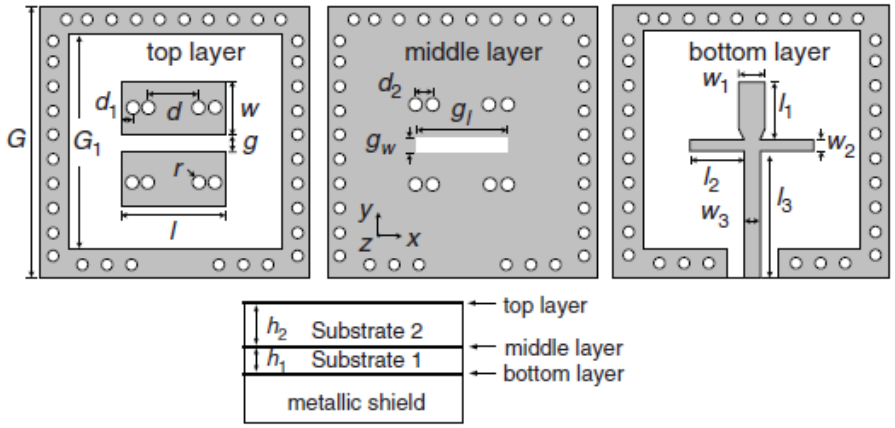

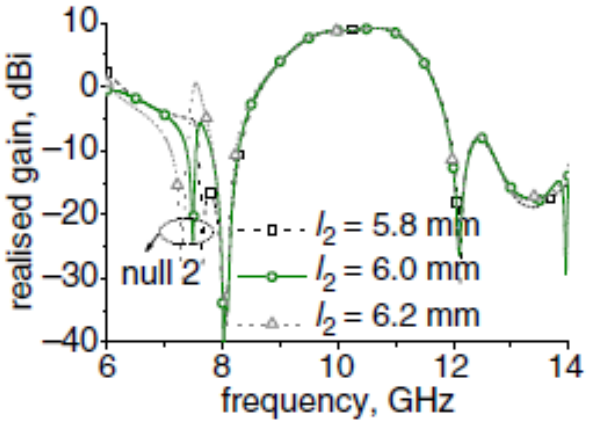

Fig. 1 *Geometry of the proposed antenna ($G = 31$ mm, $G_1 = 23$ mm, $l = 12$ mm, $l_1 = 6.6$ mm, $l_2 = 6$ mm, $l_3 = 15.15$ mm, $w = 6.4$ mm, $w_1 = 3$ mm, $w_2 = 0.4$ mm, $w_3 = 1.8$ mm, $g_w = 0.4$ mm, $g_l = 10.5$ mm, $r = 0.55$ mm, $d = 6$ mm, $d_1 = 1.6$ mm, $d_2 = 1.4$ mm, and $g = 1.7$ mm)*

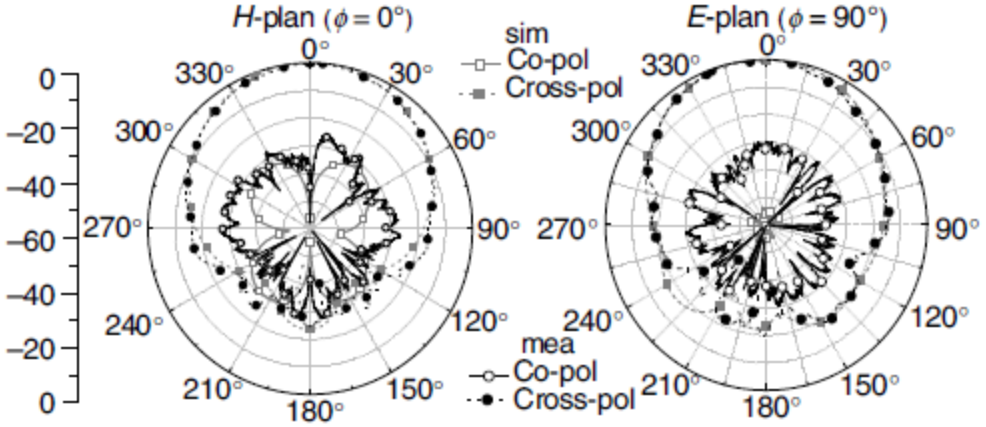

Fig. 8 *Radiation patterns of the proposed antenna*

• Chunmei Meng, Jin Shi and Jian-Xin Chen, "Flat-gain dual-patch antenna with multi-radiation nulls and low cross-polarisation, *Electronic Letters*, Vol. 54 No. 3 pp. 114–116, 2018

Broadband Compact Smooth Horn

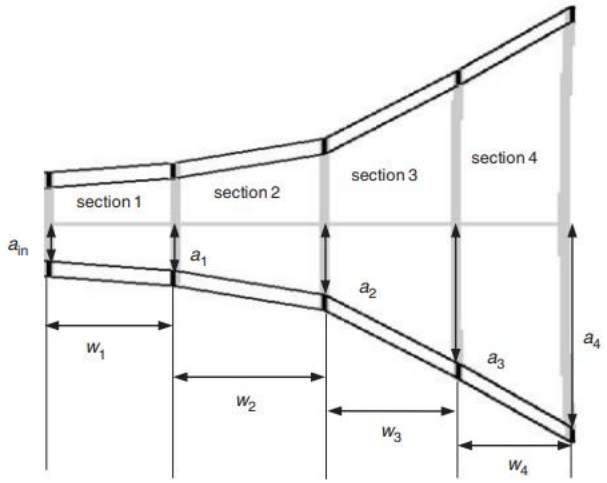

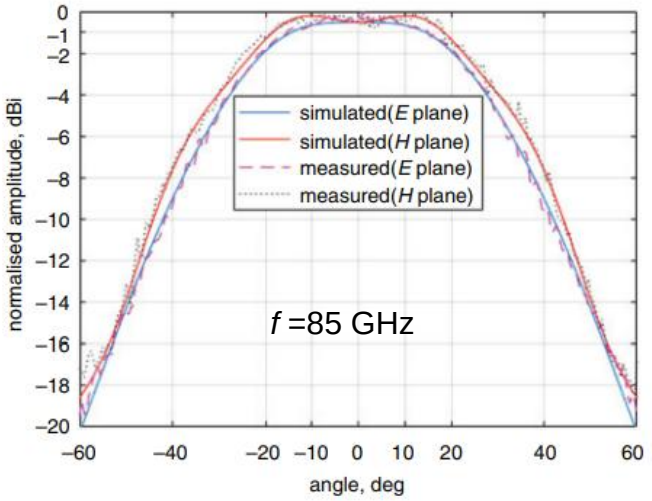

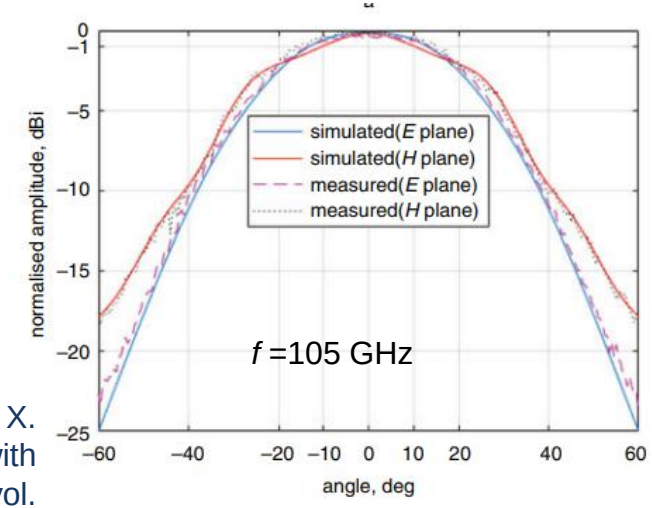

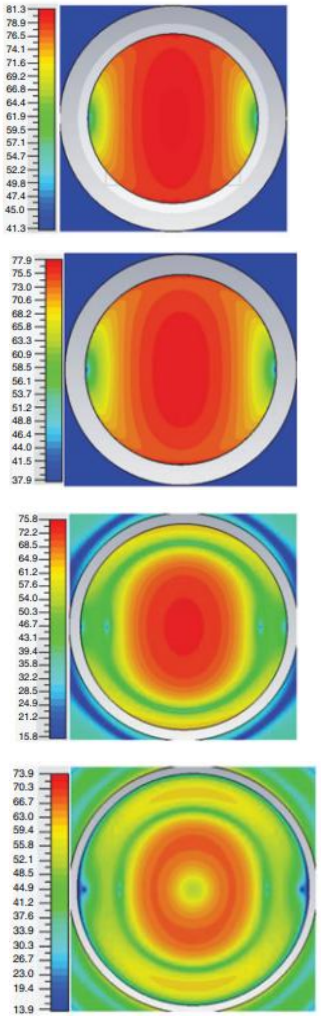

• J. Wang, Y. Yao, J. Yu and X. Chen, “Broadband compact smooth horn with flat-top radiation pattern,” *Electron. Lett.*, vol. 55, no. 3, pp. 119-120, 2019

Quasi Planar Composite Microstrip Antenna

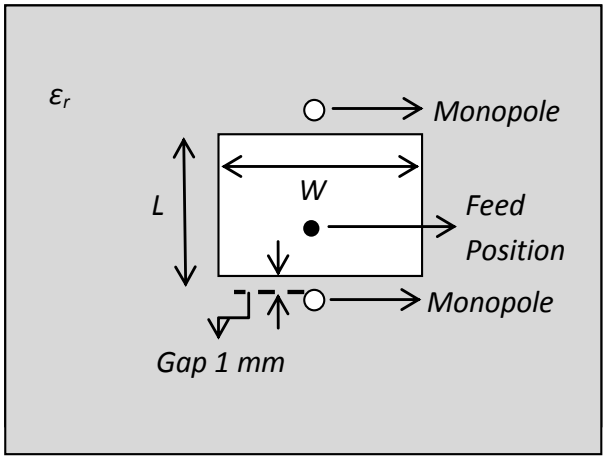

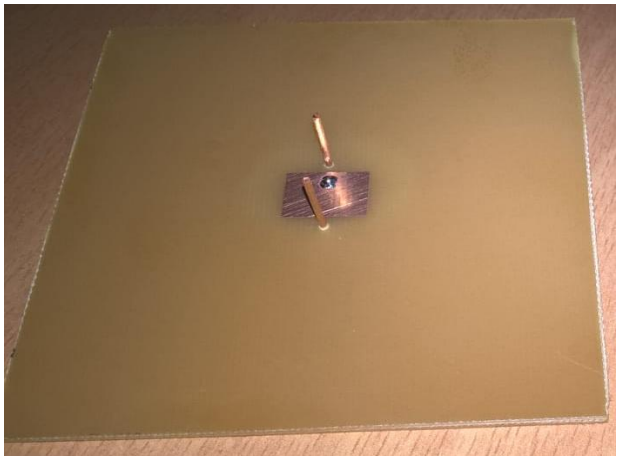

Quasi-planar composite microstrip antenna (QPCMA) consists of a single element RMA along with two metallic posts (monopoles)

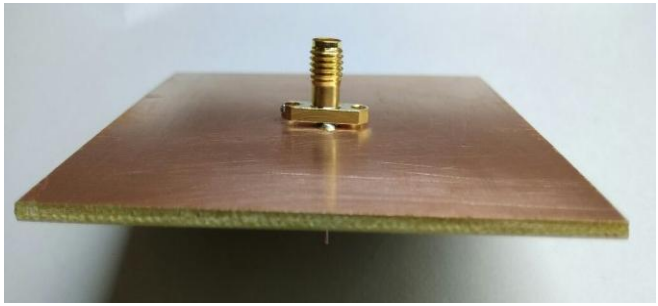

Umesh Ankush Pawar, Subhradeep Chakraborty, Tanmoy Sarkar, Abhijyoti Ghosh, LLK Singh, Sudipta Chattopadhyay, “Quasi-planar Composite Microstrip Antenna: Symmetrical Flat-Top Radiation with High Gain and Low Cross Polarization, ” *IEEE Access*, USA, (accepted).

Effect of Monopole Height on Radiation Pattern of QPCMA

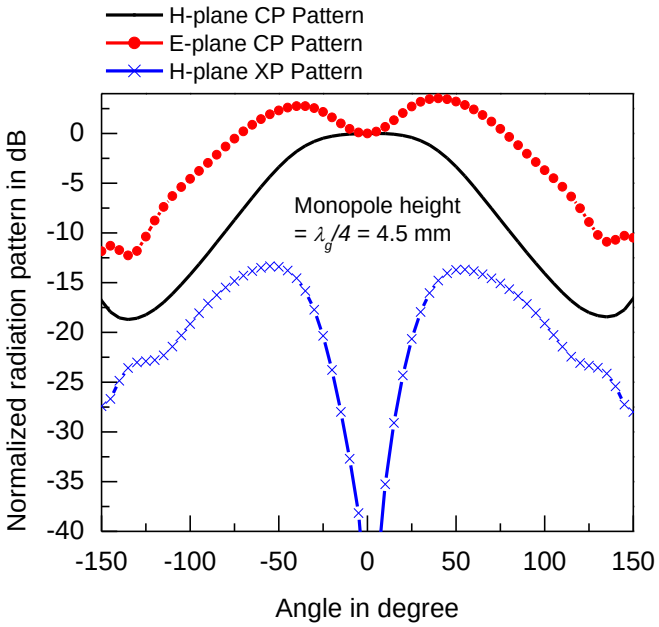

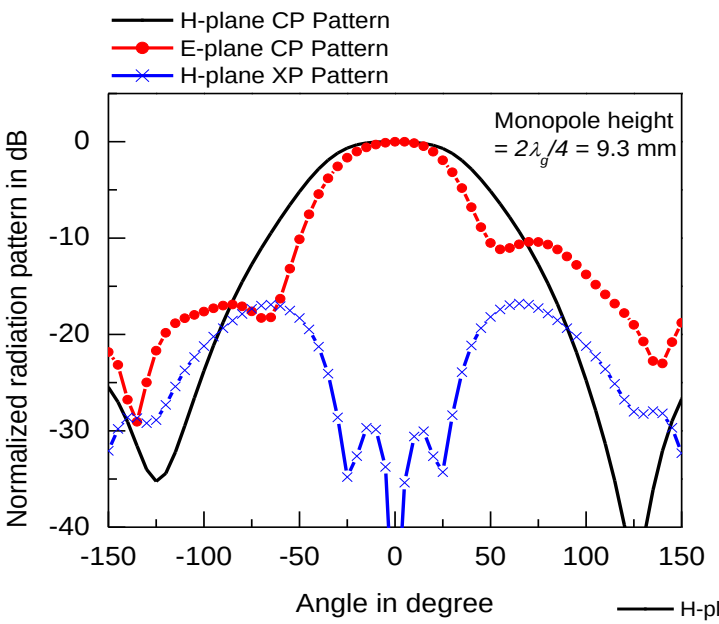

Electrical length of monopole	E-plane 3 dB beam - width	H-plane 3 dB beam - width	CP-XP isolation in dB	Symmetry in principal planes	Flat-top range in the beam
$2\lambda_g/4$	70^0	86^0	17	30^0	45^0
$2.3\lambda_g/4$	74^0	86^0	21	40^0	50^0
$2.5\lambda_g/4$	78^0	88^0	25	60^0	60^0
$2.7\lambda_g/4$	82^0	87^0	28	95^0	68^0
$3\lambda_g/4$	90^0	90^0	26	145^0	72^0

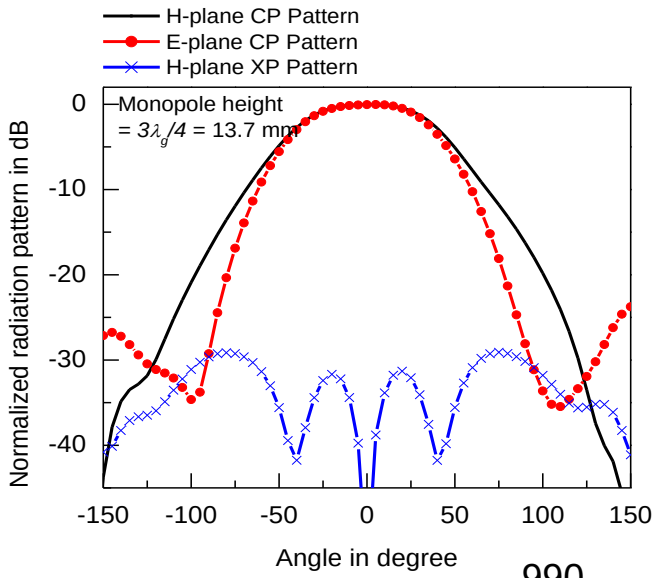

Effect of Monopole Spacing on CP and XP Radiation Patterns of QPCMA

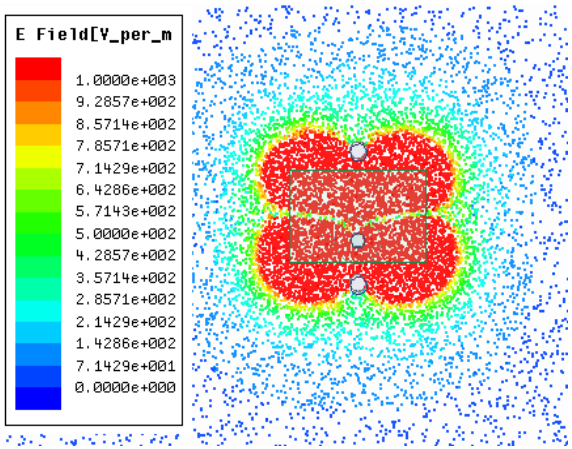

(a)

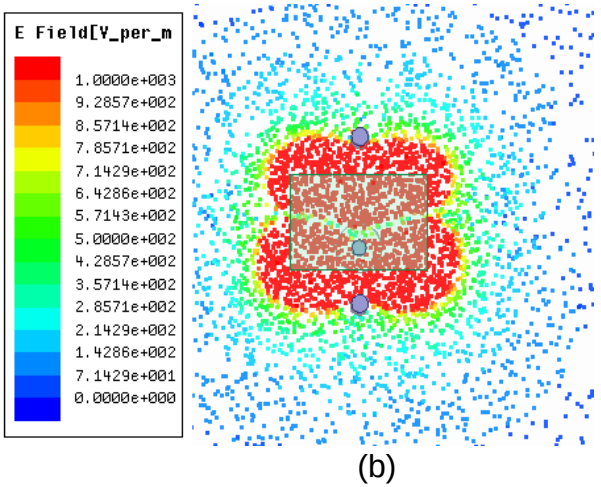

(b)

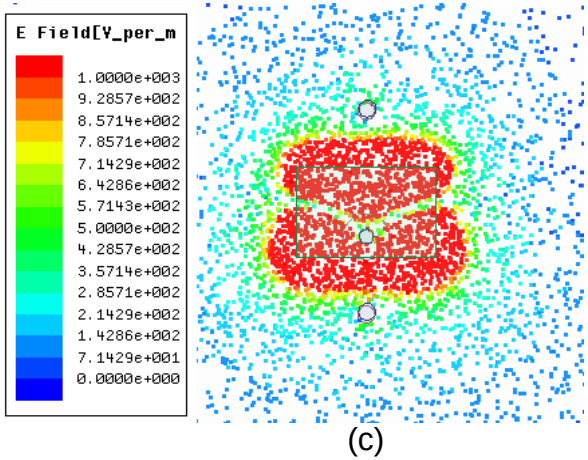

(c)

Simulated Field distribution over the substrate for QPCMA with (a) *a* =2.5 mm, (b) *a* =4 mm, (c) *a* =5.5 mm.

Flat-Top Radiation: A Classical Antenna Theory Approach

- The $3\lambda_g/4$ monopole has a critical influence in the overall E-plane radiation pattern of QPCMA.
- On the contrary, the H-plane beam-width of QPCMA is already wide due to non-uniform electric field variation at slot aperture.
- For a conventional RMA, E_θ and E_φ components of the far-field radiation pattern are

$$[E_\theta]_{RMA} = 2\cos\phi \frac{\sin\left(k_0 W \sin\theta \sin\phi / 2\right)}{\left(k_0 W \sin\theta \sin\phi / 2\right)} \cos\left(\frac{k_0 L \sin\theta \cos\phi}{2}\right)$$

$$[E_\phi]_{RMA} = 2\cos\theta\sin\phi \frac{\sin\left(k_0 W \sin\theta \sin\phi / 2\right)}{\left(k_0 W \sin\theta \sin\phi / 2\right)} \cos\left(\frac{k_0 L \sin\theta \cos\phi}{2}\right)$$

$$W = 1.5L, \quad L = \lambda_g/2, \quad k_0 = 2\pi/\lambda_g$$

Flat-Top Radiation: A Classical Antenna Theory Approach

- For a simple metallic post or monopole antenna of length l, E_θ component of the far-field radiation pattern is

$$[E_\theta]_{single\_monopole} = \frac{\cos(kl\cos\theta) - \cos(kl)}{\sin\theta}$$

- Two monopoles constitute a linear array along and the array factor will be

$$F = \frac{\sin(k_0 d \sin\theta\cos\phi + \delta)}{\sin\left[\frac{1}{2}(k_0 d \sin\theta\cos\phi + \delta)\right]} \quad \text{where } \delta = \pi$$

$$d \cong \lambda_g / 2$$

$$= 2\sin\left(\frac{\pi}{2}\sin\theta\cos\phi\right)$$

- Hence, contribution from monopoles can be computed as

$$[E_\theta]_{monopole} = \left[\frac{\cos(kl\cos\theta) - \cos(kl)}{\sin\theta}\right]\left[2\sin\left(\frac{\pi}{2}\sin\theta\cos\phi\right)\right]$$

Flat-Top Radiation: A Classical Antenna Theory Approach

- In case of array of two dissimilar sources, the total field pattern factor may be written as for E-plane,

$$[E_\theta]_{TOTAL} = [E_\theta]_{monopole} + [E_\theta]_{RMA}$$

- In H-plane,

$$[E_\theta]_{TOTAL} = [E_\theta]_{monopole} + [E_\phi]_{RMA}$$

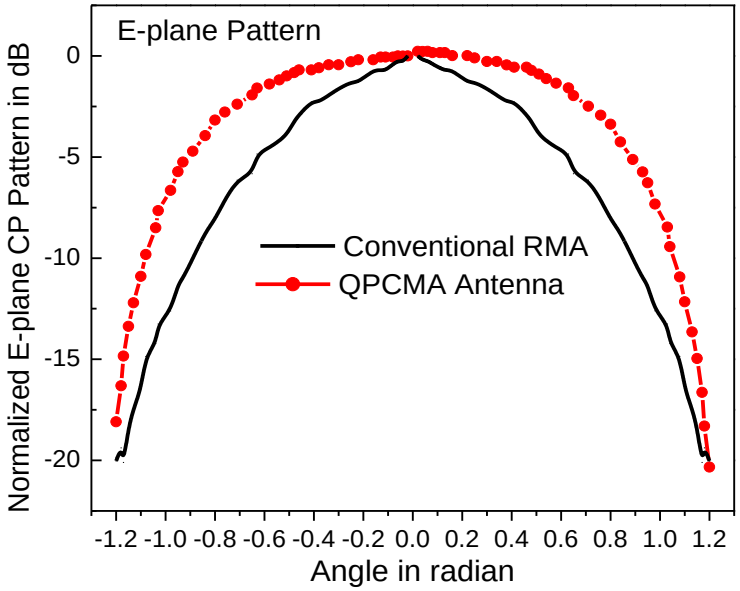

- The length of monopoles is greater than $3\lambda_g/4$, it develops higher elevation lobes which is superposed with the radiation pattern of conventional RMA and hence, the proposed QPCMA develops wide flat-top radiation pattern.

From Principle of Pattern Multiplication

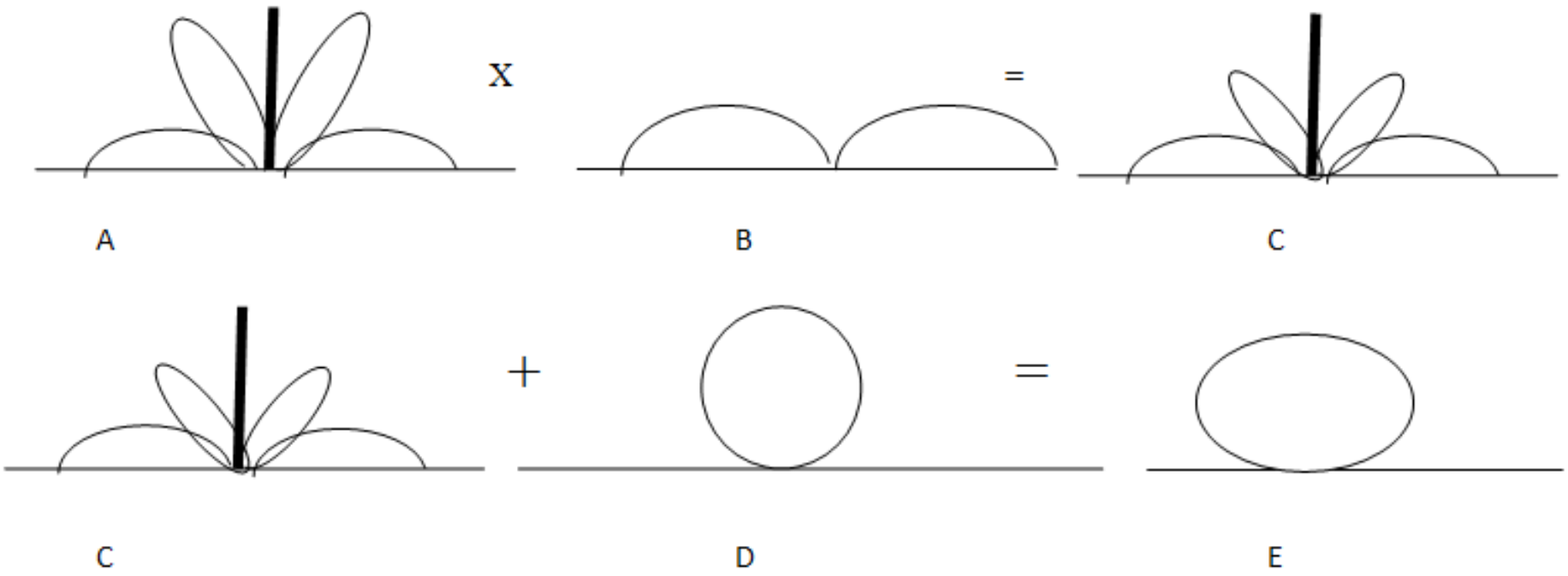

- Pattern of simple RMA is depicted as Fig. D. And the resultant pattern constituted by binary monopole array pattern (C) and single patch pattern (D) is presented as Fig. E. It is observed that the resultant pattern E is bit wider than single RMA pattern D. This is because of merging of high elevation lobes of C with the patch pattern D. This is true in E plane of patch antenna.

QPCMA in Low-Loss Substrate

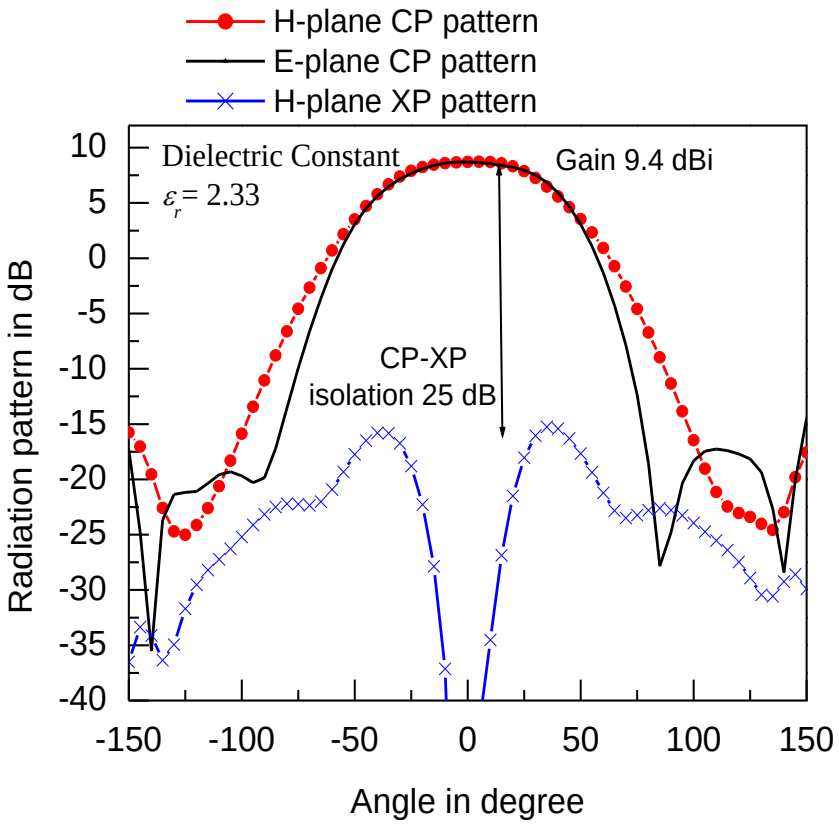

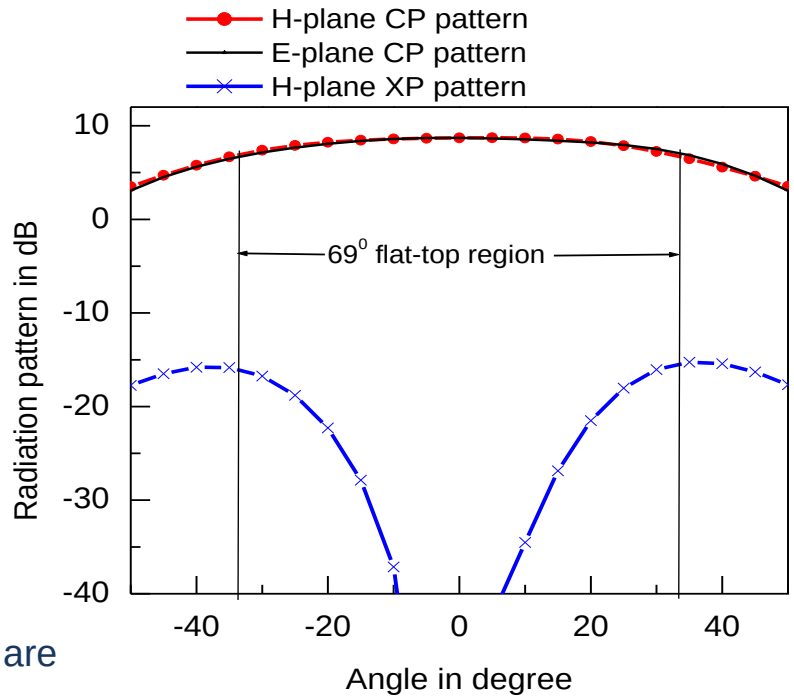

- In lower dielectric constant substrate, the E-fields are loosely bound to the substrate.
- This may be attributed for higher gain of QPCMA.
- XP radiation is also high in lower dielectric constant substrate, however, CP-XP isolation is 25 dB.

Measured Results

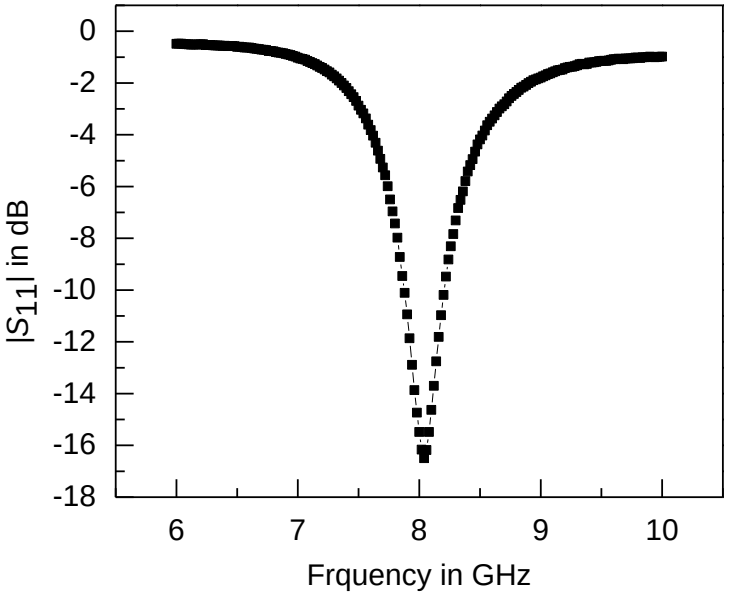

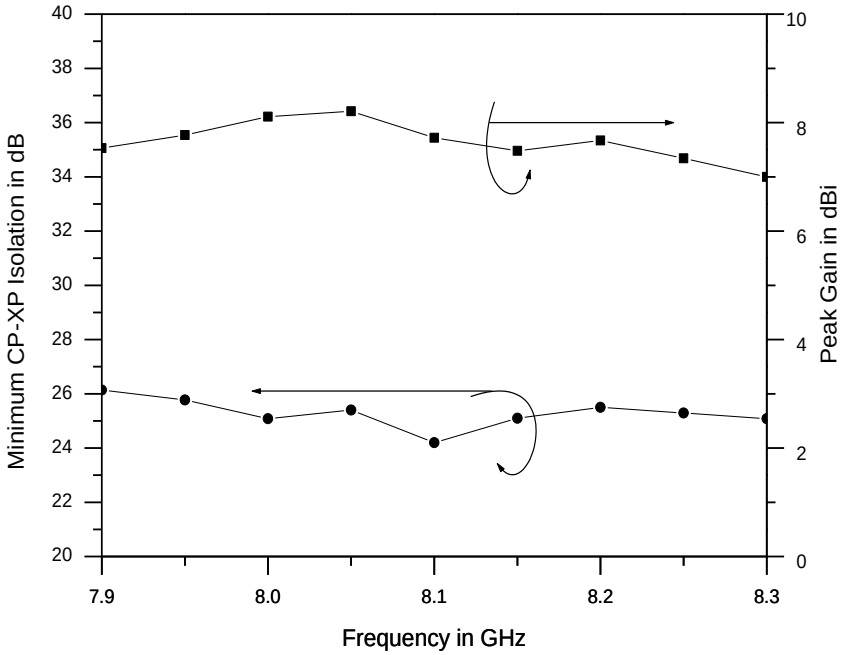

Umesh Ankush Pawar, Subhradeep Chakraborty, Tanmoy Sarkar, Abhijyoti Ghosh, LLK Singh, Sudipta Chattopadhyay, “Quasi-planar Composite Microstrip Antenna: Symmetrical Flat-Top Radiation with High Gain and Low Cross Polarization, ” *IEEE Access*, USA, (accepted).

Measured Results

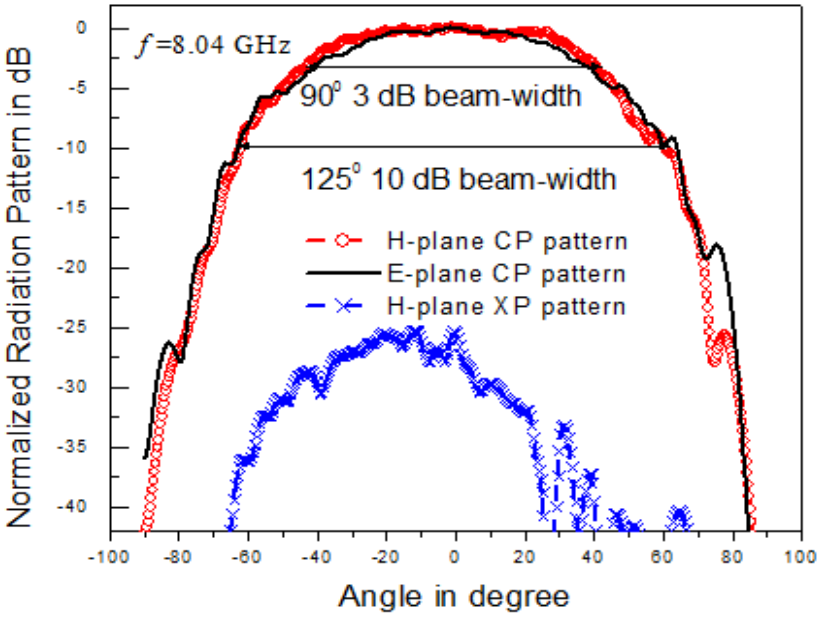

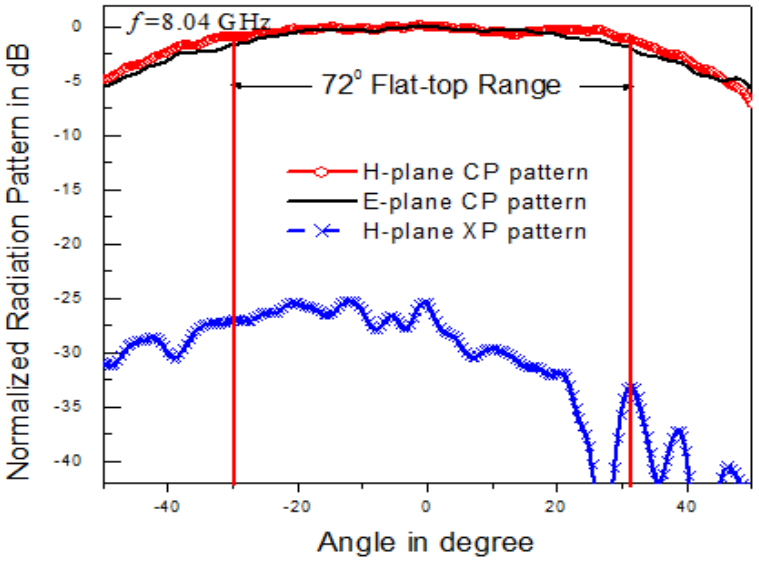

Umesh Ankush Pawar, Subhradeep Chakraborty, Tanmoy Sarkar, Abhijyoti Ghosh, LLK Singh, Sudipta Chattopadhyay, "Quasi-planar Composite Microstrip Antenna: Symmetrical Flat-Top Radiation with High Gain and Low Cross Polarization, " *IEEE Access*, USA, (accepted).

Measured Results

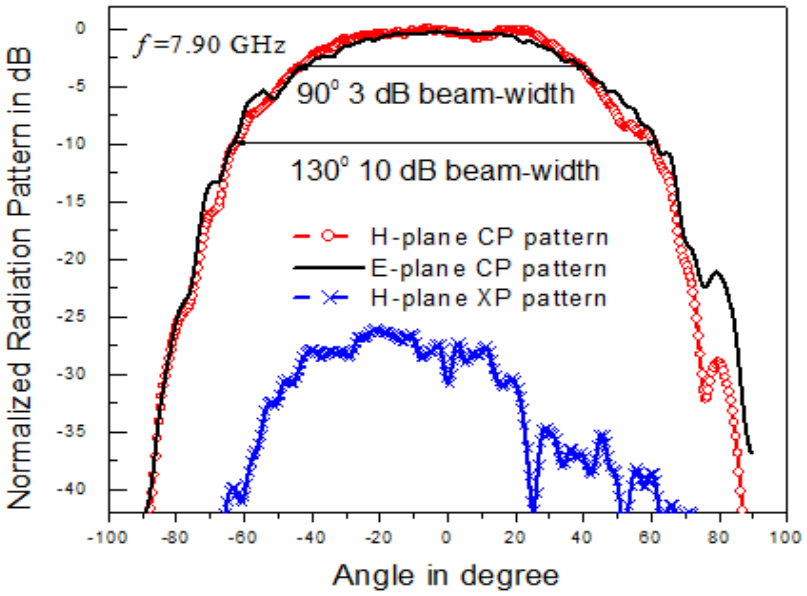

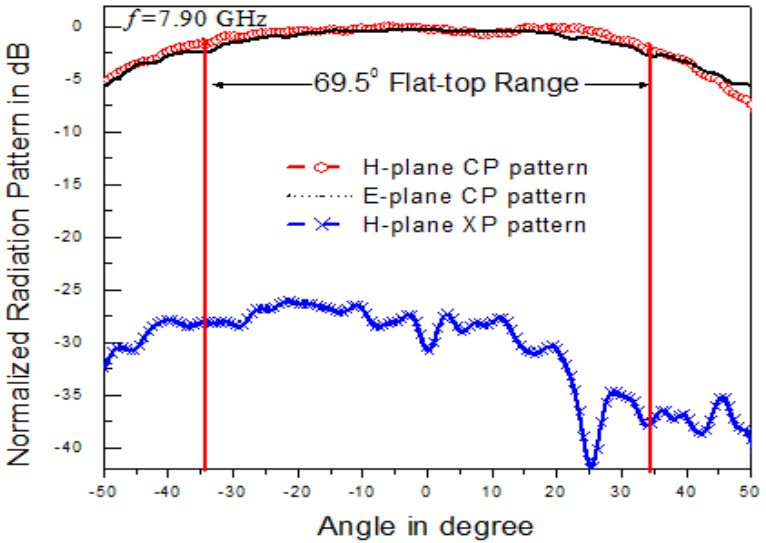

Umesh Ankush Pawar, Subhradeep Chakraborty, Tanmoy Sarkar, Abhijyoti Ghosh, LLK Singh, Sudipta Chattopadhyay, “Quasi-planar Composite Microstrip Antenna: Symmetrical Flat-Top Radiation with High Gain and Low Cross Polarization, ” *IEEE Access*, USA, (accepted).

Comparison between radiation properties of the QPCMA with conventional RMA and earlier reported works

References	Antenna type	Gain (dBi)	H-plane 3 dB beam width	E-plane 3 dB beam width	Symmetry between radiation patterns in principal planes	Peak CP-XP isolation in dB	Flat-top range in the radiation patterns	Remarks
-	Conventional RMA ($\varepsilon_r = 4.4$)	4.5	65°	70°	-	16	-	Planar structure
[1]	Double shell lens antenna fed by aperture coupled microstrip antenna		80		-	28	80° in H-plane, 60° in E-plane,	Volumetric antenna, ripple in flat-top region
[2]	Switched beam microstrip antenna array	16.6	56°	5°		25	46°	Quasi planar antenna array
[5]	Circularly polarised bow tie array	>11.8	60°	30°		25	30° in E-plane	Quasi planar antenna array
[9]	Composite dielectric loaded RMA	7	64°	88°	-	17	-	Quasi planar structure
[12]	Circularly polarised microstrip monopole antenna	3.5	137°	156°	130°	-	-	Quasi planar structure
[15]	Slot type DGS integrated RMA	-	55°	60°	-	25	-	Planar structure
[17]	Shorted RMA	7.5	60°	70°	-	27	-	Planar structure
[29]	T-shaped microstrip antenna	6.11	56°	-	-	21	-	Planar structure
-	Present QPCMA	8.2	90°	90°	145°	26	72° in both E and H-plane	Quasi planar structure

IEEE Access
Multidisciplinary | Rapid Review | Open Access Journal

Received May 2, 2019, accepted May 15, 2019, date of publication May 23, 2019, date of current version June 7, 2019.

Digital Object Identifier 10.1109/ACCESS.2019.2918580

Quasi-Planar Composite Microstrip Antenna: Symmetrical Flat-Top Radiation With High Gain and Low Cross Polarization

UMESH ANKUSH PAWAR[1,4], SUBHRADEEP CHAKRABORTY[2], (Member, IEEE), TANMOY SARKAR[3,4], (Student Member, IEEE), ABHIJYOTI GHOSH[4], L. LOLIT KUMAR SINGH[4], AND SUDIPTA CHATTOPADHYAY[4], (Member, IEEE)

[1] Indian Army, India
[2]MWD Area, CSIR-CEERI, Pilani 333031, India
[3]Radionics Lab, The University of Burdwan, Burdwan 713104, India
[4]Electronics and Communication Engineering Department, Mizoram University, Aizawl 796004, India

Corresponding author: Tanmoy Sarkar (2005.tanmoy@gmail.com)

ABSTRACT In this paper, a quasi-planar composite microstrip antenna consisting of a single layer rectangular microstrip antenna along with two metallic posts (monopoles) has been studied theoretically and experimentally. The proposed antenna exhibits wide, symmetrical radiation (around 145°) in both principle planes, along with flat-top radiation in the entire bore sight region (72° along with bore sight) with high gain (8.5 dBi) and significantly low cross polarized radiation. More than 26 dB co-cross polarization isolation over an entire broadside direction is obtained. The present structure is very simple and easy to manufacture. The present investigation provides an insightful, visualization-based understanding of concurrent improvement of the radiation characteristics.

“Research is passion, a 24×7 obsession.”

-Prof. S. C. Dutta Roy
Ex-Professor, IIT Delhi
IETE Journal of Education, 2019.

RECENT ADVANCES IN METAMATERIAL ASSISTANCE IN MICROWAVE TUBES

Faculty Development Program (FDP) on "Advances in Microwave Engineering"

Dr. A.P J. Abdul Kalam Technical University (AKTU), Lucknow, Uttar Pradesh, India

Raktim Guha

Senior Project Assistant, MWD area
CSIR-CEERI, Pilani, Rajasthan, India

Date: 11th June 2019

Dedicated to.....

my parents

Mr. Shibanth Guha
Mrs. Rita Guha

and

my teachers/mentors

Prof. B. N. Basu
Mrs. Manikuntala Basu

Outlines

- Pioneers of metamaterials
- Metamaterial: a general definition
- Metamaterial properties
- Application areas of Metamaterials in Microwaves Engineering
- Quadrant classification of materials
- Lorentz Oscillator Model for Dielectrics
- Drude model for metals
- Negative permittivity
- Negative permeability
- The Complementry Split Ring Resonator (CSRR)
- Classification of Metamaterials
- What happens when both ε and μ are negative?

Outlines (contd..)

- How to Realize a Left-Handed Metamaterial
- Waveguide loaded with SRRs and CSRRs
- Origin of Bianisotropy
- Parameter Retrieval of metamaterial
- Metamaterial design using CST
- Metamaterial parameter retrieved using CST and MATLAB
- Fabrication Techniques of metamaterials
- Demerits of conventional linear electron beam MWTs
- Metamaterial Slow-wave Structures
- Contribution of Researchers in India on MTM-VEDs
- Researchers of Metamaterial assisted Microwave Tubes
- References

Pioneers of metamaterials

Victor G. Veselago
Moscow Institute of Physics and technology

Investigate theoretically the effect of negative permittivity and permeability of material (1967).

after ~ 30 years

Sir John B. Pendry
Imperial college London, UK

1) Practical insight of negative permittivity (roded medium) (1996) and permeability (SRR) (1999).
2) Perfect lens, theoretical demonstration (2000).

Prof. David R. Smith
Duke University, Durham, UK

1) Experimentally verified negative index of refraction (2001).
2) MTenna (2017).

Fabricated and tested invisibility cloak at microwave frequency (2006).

Dr. Andrea Alù
The University of Texas, Austin

1) Optical and acoustic metamaterials and metasurfaces.
2) Plasmonics, non-linearities and non-reciprocity.
3) Cloaking and scattering.
4) Optical nano-circuits and nano-antennas.

Post doctoral fellow

Prof. Nader Engheta
University of Pennsylvania, USA

1) Near-zero-index metamaterials.
2) Sub-wavelength Cavity Resonators.
3) Epsilon-near-zero metamaterials.

Prof. Richard W. Ziolkowski
University of Technology Sydney, Australia

1) Metamaterial-inspired antennas.
2) Effective parameter retrieved process of metamaterials.

Metamaterials: Physics and Engineering Explorations

Pioneer of metamaterials in India

Prof. Subal Kar
University of Calcutta
Institute of Radio Physics and Electronics

A joint research team from Institute of Radio Physics and Electronics of Calcutta University (CU) and SAMEER, Kolkata has designed and fabricated the crystal.

The crystal was on display at a national meet on metamaterials at the Bhaba Atomic Research Centre (BARC) on August 17 2009.

T. Roy, D. Banerjee, and S. Kar, "Studies on Multiple Inclusion Magnetic Structures Useful for Millimeter-wave Left Handed Metamaterial Applications", *IETE J. Res*. vol.55, pp.83-89, Mar. 2009.

D. Banerjee, T. Roy and S. Kar, "A Computer-Aided Analytical Study on the Characteristics of Left Handed Material Structures at Microwave Frequencies", *IETE J. Res*. vol. 55, pp.112-117, May 2009.

Metamaterial: a general definition

Artificial media with unusual
Electromagnetic properties

Metamaterial: a general definition

Man-made,
Structures < wavelength,
Homogenization regime

Artificial media with unusual
Electromagnetic properties

Metamaterial: a general definition

Man-made,
Structures < wavelength,
Homogenization regime

Artificial media with unusual
Electromagnetic properties

Permittivity/permeability,
Refraction index,
Refraction/reflection
Propagation....

Metamaterial: a general definition

Man-made,
Structures < wavelength,
Homogenization regime

Material properties that can not be found in nature.

Is it true??

Artificial media with unusual Electromagnetic properties

1) Superconductors at microwave frequencies (very large negative permittivity)
2) Metals Au, Ag at optical frequencies (well known phenomena associated with plasmons)
3) Ferrimagnetics at microwave frequencies (very large negative permeability).

Permittivity/permeability,
Refraction index,
Refraction/reflection
Propagation....

Then why we are interested in metamaterials ???

Metamaterials: a general definition (contd…)

- According to Dr. David R. Smith, **any material composed of periodic, macroscopic structures so as to achieve a desired electromagnetic response** can be referred to as a *Metamaterial*

Altered/changed/beyond

Large enough to be visible with the naked eye

- Metamaterials can have their electromagnetic properties ***altered*** to something ***beyond*** what can be found in nature

Metamaterial properties

- Negative refractive index
- reverse Snell's law
- reverse Cherenkov radiation
- reverse Doppler effect

Application areas of Metamaterials in Microwaves Engineering

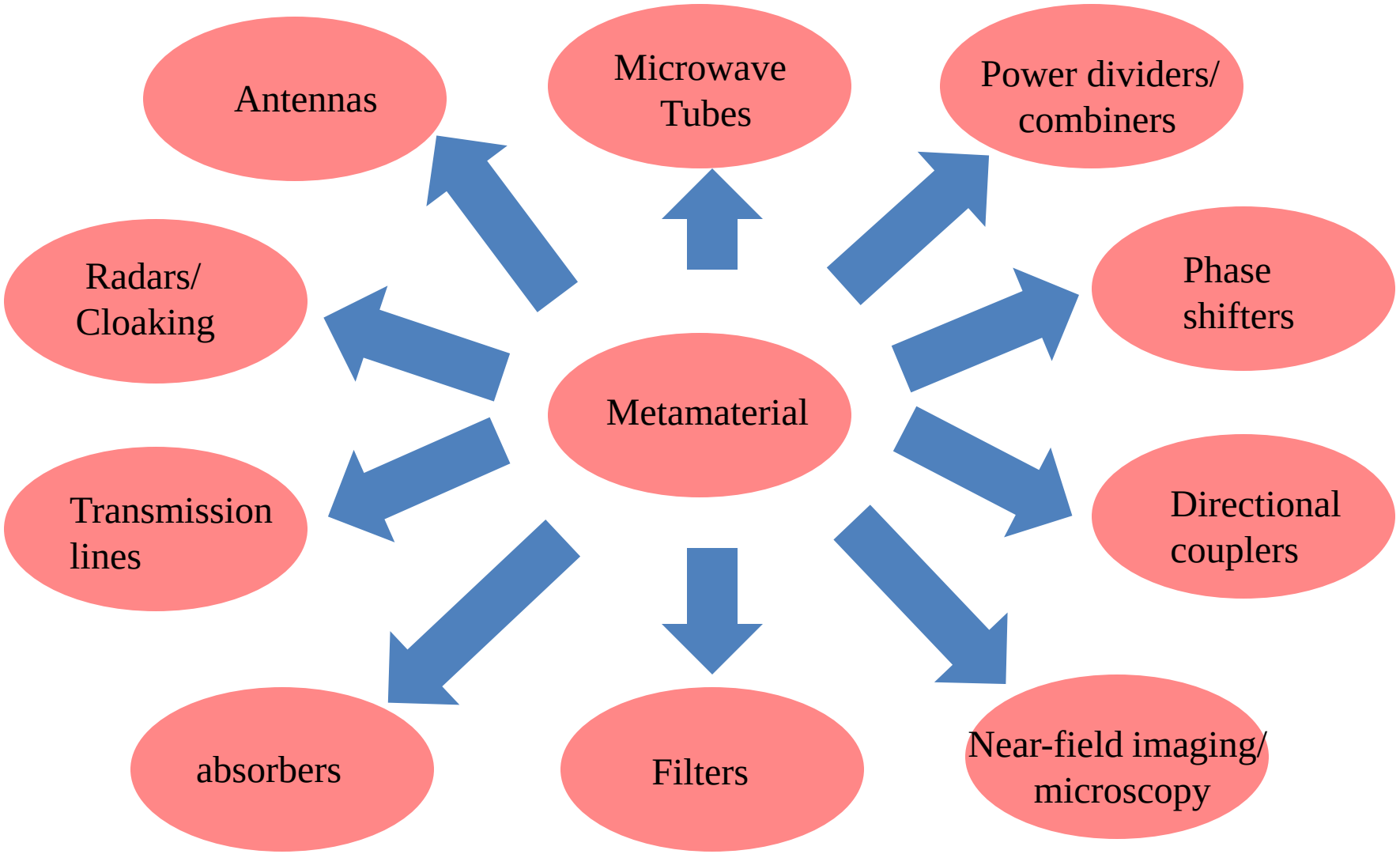

Application areas of Metamaterials in Microwaves Engineering

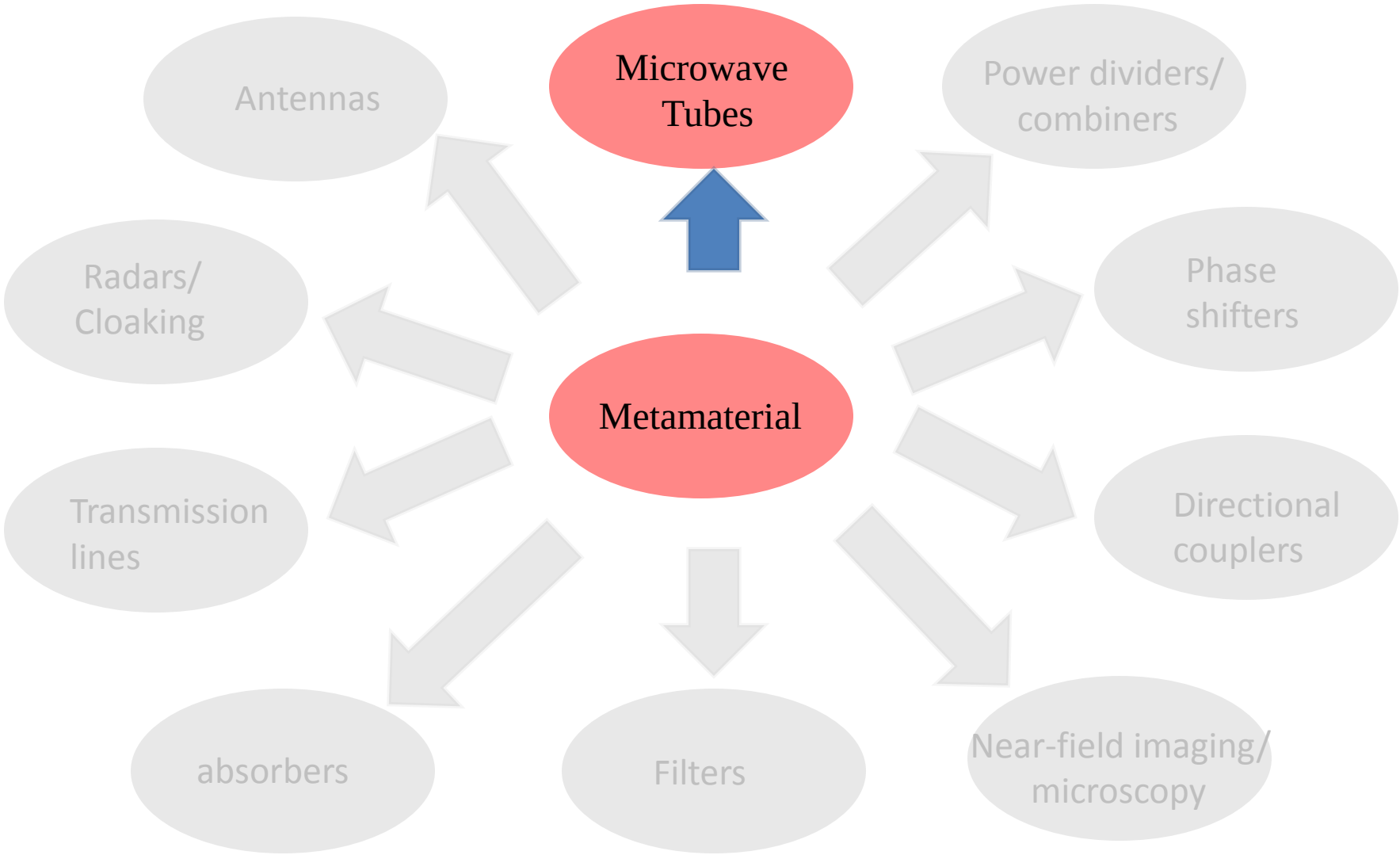

Quadrant classification of materials

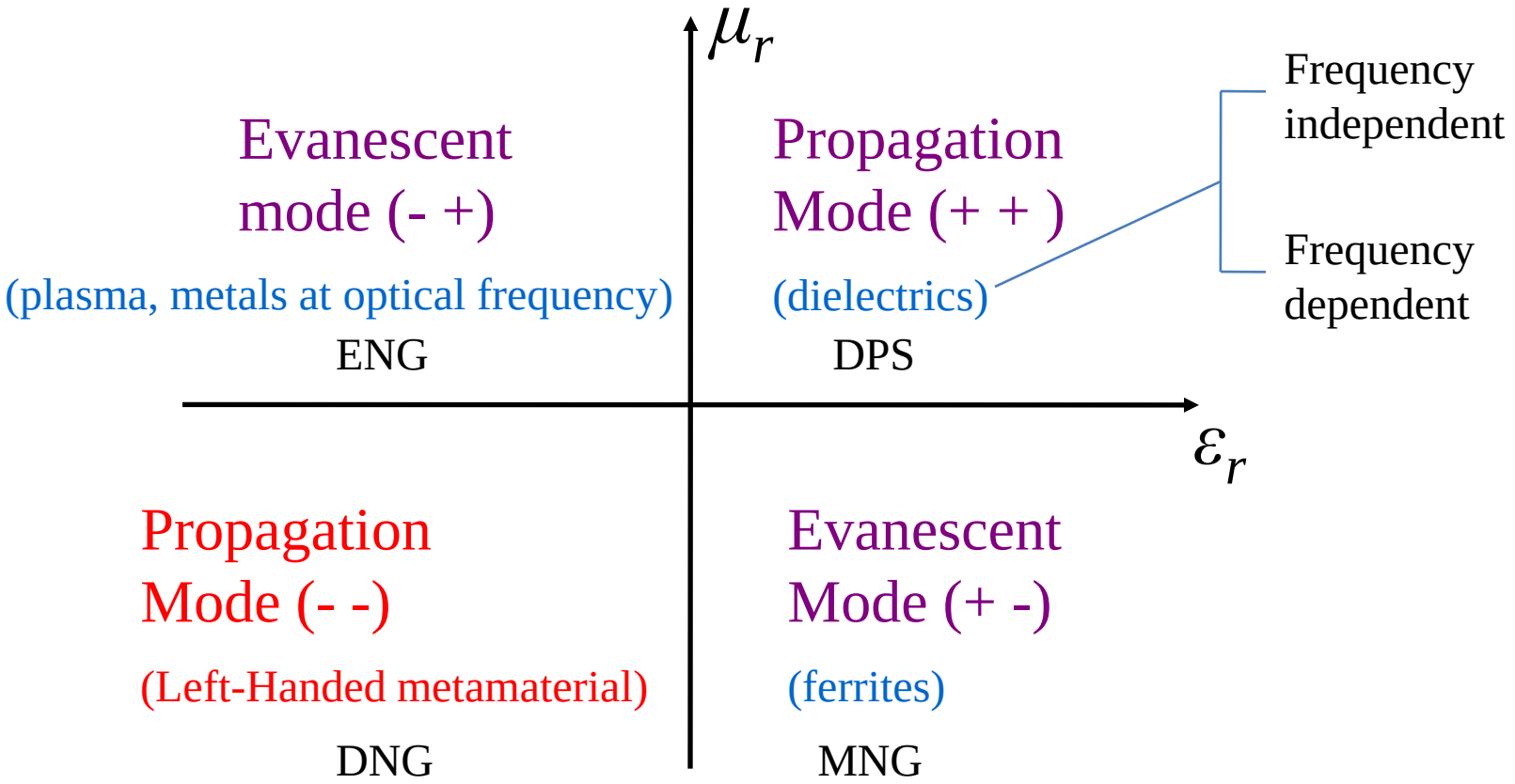

Lorentz Oscillator Model for Dielectrics

Governing Equation

$$m\frac{\partial^2\vec{r}}{\partial t^2}+m\Gamma\frac{\partial\vec{r}}{\partial t}+m\omega_0^2\vec{r}=-q\vec{E}$$

- $m\frac{\partial^2\vec{r}}{\partial t^2}$: acceleration force; $m \Rightarrow m_e$ mass of an electron
- $m\Gamma\frac{\partial\vec{r}}{\partial t}$: frictional force; Γ damping rate (loss/sec)
- $m\omega_0^2\vec{r}$: restoring force; $\omega_0=\sqrt{\frac{K}{m}}$ natural frequency
- $-q\vec{E}$: electric force

Resulting Dielectric Function

$$\varepsilon_r=1+\frac{\omega_p^2}{\omega_0^2-\omega^2-j\omega\Gamma}$$

$$\omega_p^2=\frac{Nq^2}{\varepsilon_0 m}$$

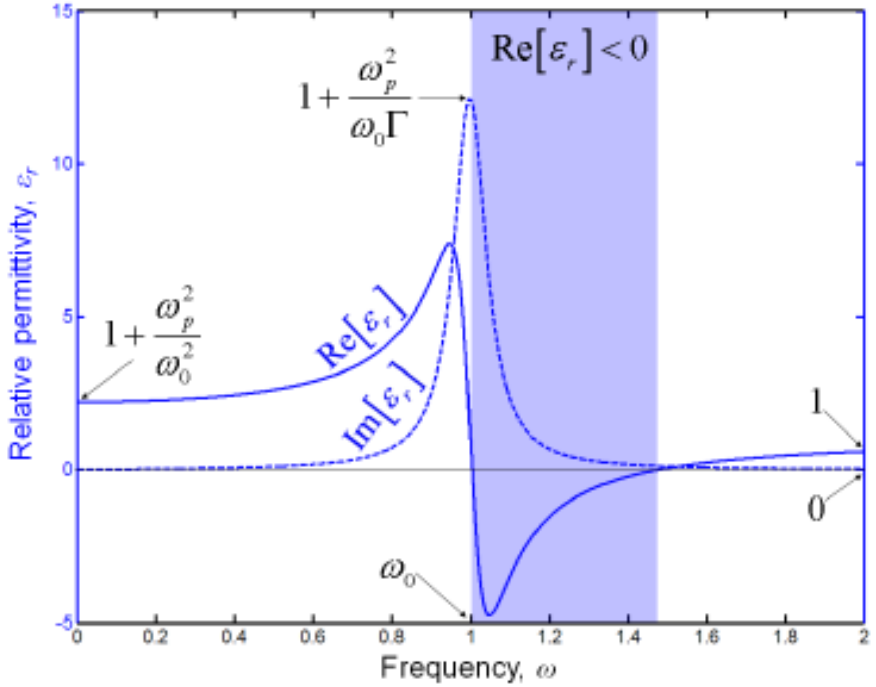

Drude Model for Metals

In metals, most electrons are free because they are not bound to a nucleus. For this reason, the restoring force is negligible and there is no natural frequency.

Governing Equation

$$m\frac{\partial^2\vec{r}}{\partial t^2}+m\Gamma\frac{\partial\vec{r}}{\partial t}+\cancel{m\omega_0^2\vec{r}}=-q\vec{E}$$

Electrons are not bound so restoring force is zero.

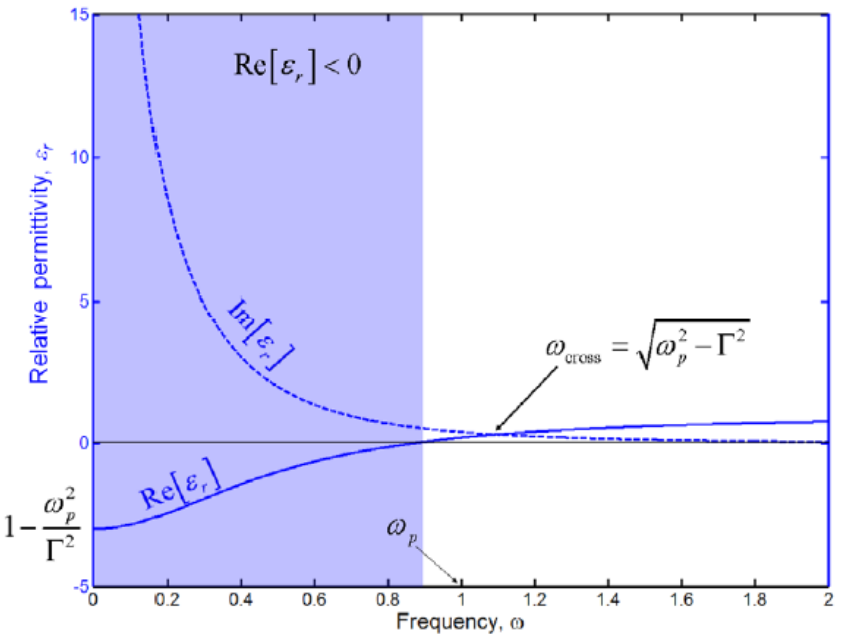

Resulting Dielectric Function

$$\varepsilon_r=1-\frac{\omega_p^2}{\omega^2+j\omega\Gamma}$$

$$\omega_p^2=\frac{Nq^2}{\varepsilon_0 m}$$

Negative Permittivity

The permittivity of metal is given by

$$\varepsilon(\omega) = 1 - \frac{\omega_{ep}^2}{\omega(\omega + i\gamma)}$$

Plasma frequency: $\omega_{ep}^2 = \frac{ne^2}{\varepsilon_0 m_e}$ (typically in the UV region)

where n is the electron density, and m_e is the electron mass

Damping factor: $\gamma = \frac{\varepsilon_0}{\sigma}$

where σ is the electric conductivity

In the visible region, $\varepsilon(\omega)$ is negative for most metals. At lower frequencies, permittivity is imaginary.

J. B.Pendry, A. J. Holden and W. J. Stewart, I. Youngs, "Extremely Low Frequency Plasmons in Metallic Mesostructures" *et al., Phys. Rev. Lett.* vol. 76, no. 25, pp. 4773-4776, June 1996.

Negative Permittivity (contd…)

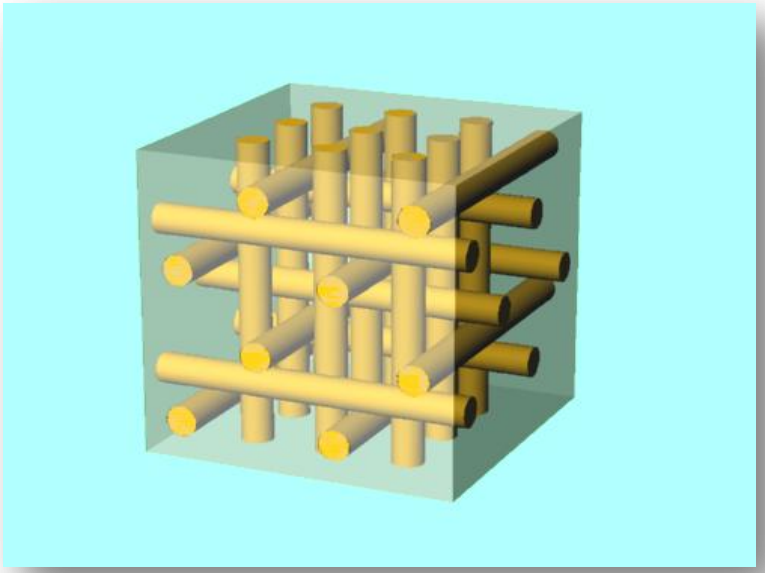

Effective electron density

Effective mass of electron

$$n_{eff} = n\frac{\pi r^2}{a^2}, \qquad m_{eff} = \frac{\mu_0 n e^2}{2\pi}\ln(a/r)$$

$$\omega_{ep}^2 = \frac{n_{eff}e^2}{\varepsilon_0 m_{eff}}$$

radius of wire: $r = 1.0\times10^{-6}m,$

lattice constant: $a = 5.0\times10^{-3}m,$

$$n = 5.675\times10^{17}m^{-3}$$

$$\omega_{ep} \approx 8.2GHz!!$$

$$\varepsilon_{eff} = 1 - \frac{\omega_{ep}^2}{\omega(\omega + i\times0.1\omega_{ep})}$$

Negative ε with small loss in low frequencies can be achieved by metallic wire lattice

J. B.Pendry, A. J. Holden and W. J. Stewart, I. Youngs, "Extremely Low Frequency Plasmons in Metallic Mesostructures" *et al., Phys. Rev. Lett.* vol. 76, no. 25, pp. 4773-4776, June 1996.

Negative Permeability

The Split Ring Resonator (SRR)

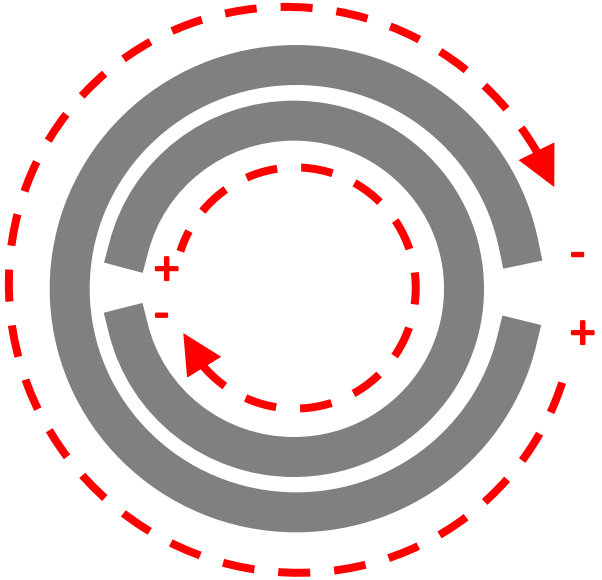

External magnetic field penetrates through the rings and currents are induced.

Gap prevents currents from flowing around the ring, which considerably increases the resonance frequency of the structure.

SRR provides a resonant structure which is much smaller than the resonance wavelength.

Metamaterial, which response should be homogeneous on the scale of the wavelength.

J. B. Pendry, A. J. Holden, D. J. Robbins, and W. J. Stewart, "Magnetism from conductors and enhanced nonlinear phenomena," *IEEE Trans. Microw. Theory Techn.*, vol. 47, no. 11, pp. 2075–2084, Nov. 1999.

The Complementry Split Ring Resonator (CSRR)

Equivalent circuit

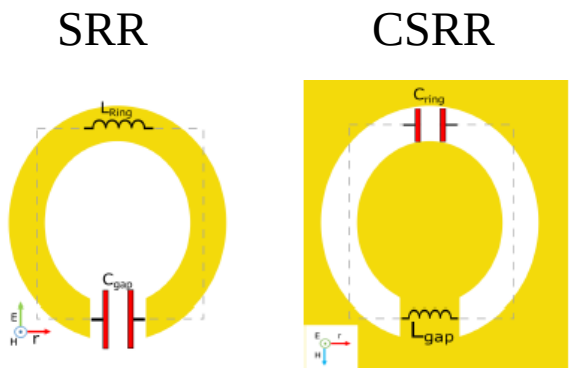

Fig. 1. Equivalent of single SRR and CSRR.

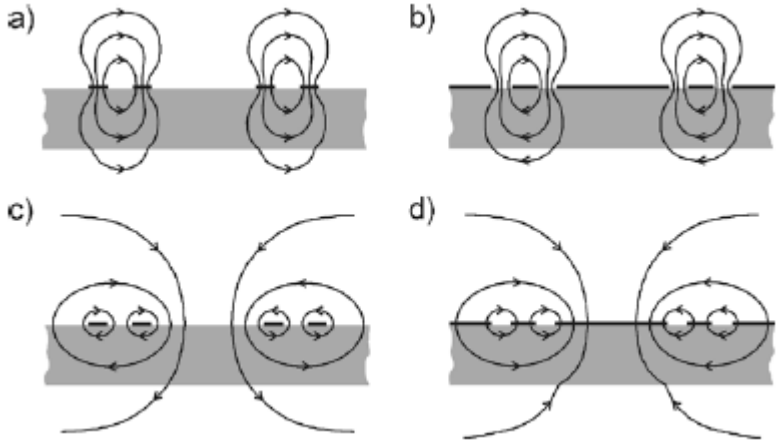

Fig. 2. Sketch of the: (a) electric- and (c) magnetic-field lines of an SRR on a dielectric substrate. (b) Magnetic- and (d) electric-field lines of a similar CSRR on the same dielectric substrate are also sketched.

F. Falcone *et al*., "Babinet principle applied to the design of metasurfaces and metamaterials," *Phys. Rev. Lett*., vol. 93, p. 197401, Nov. 2004.

J. D. Baena *et al*., "Equivalent-Circuit Models for Split-Ring Resonators and Complementary Split-Ring Resonators Coupled to Planar Transmission Lines," *IEEE Tran. on Micro. Theo. and Tech*., vol. 53, no. 4, pp. 1451-1461, Apr. 2005.

Classification of Metamaterials

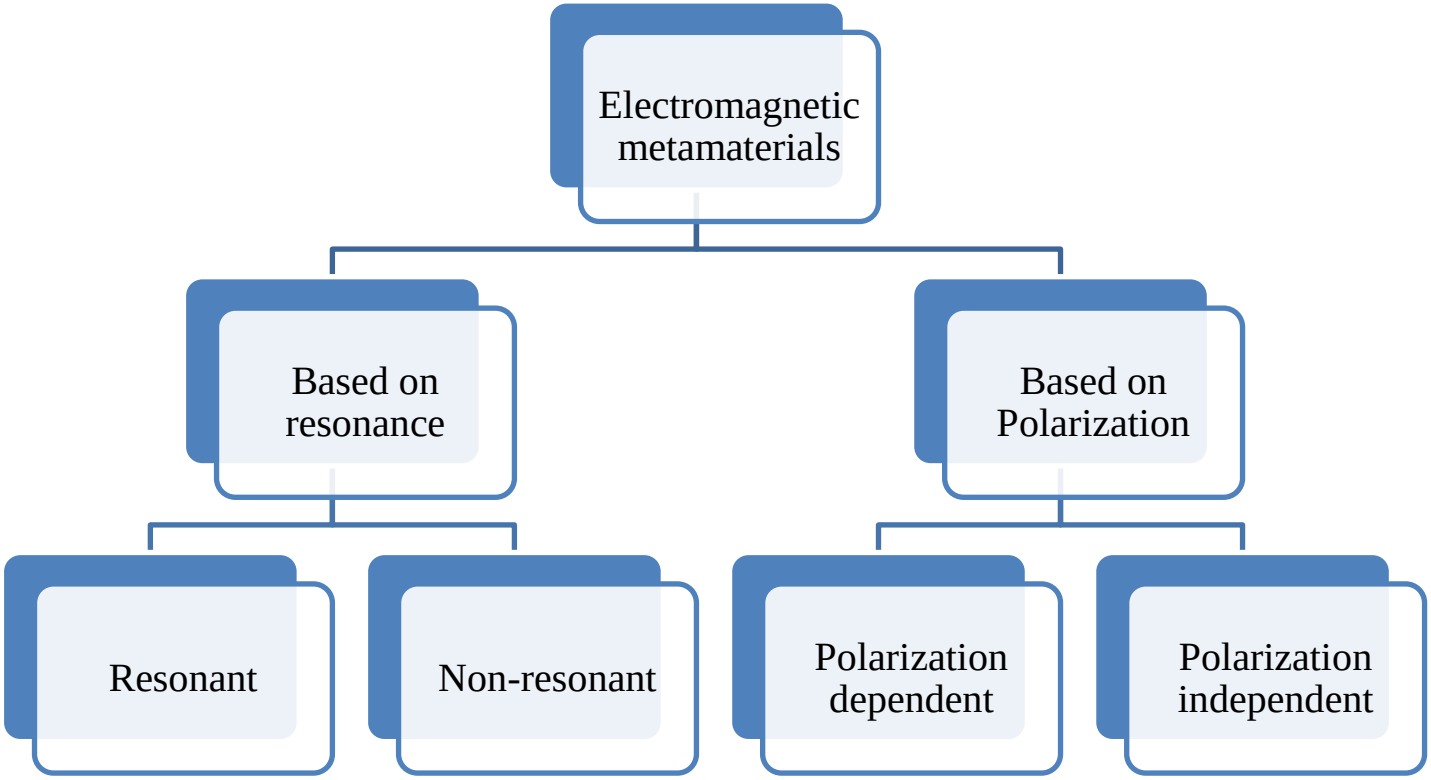

What happens when both ε and μ are negative?

$$\nabla \times \vec{E} = -j\omega(-\tilde{\mu})\vec{H} \qquad \nabla \times \vec{E} = -j\omega\tilde{\mu}(-\vec{H})$$

$$\nabla \times \vec{H} = j\omega(-\tilde{\varepsilon})\vec{E} \qquad \nabla \times (-\vec{H}) = j\omega\tilde{\varepsilon}\vec{E}$$

The system is left handed!

$$\vec{k} \perp \vec{E} \perp (-\vec{H}) \quad \Rightarrow \quad -\vec{k} \perp \vec{E} \perp \vec{H}$$

E, H, and k form a "left-handed" system

V. G. Veselago, "The electrodynamics of substances with simultaneously negative values of ε *and* μ," *Sov. Phys. Uspekhi*, vol. 47, pp. 509–514, Jan. 1968.

What happens when both ε and μ are negative? (contd..)

Example: How to achieve negative index of refraction

- $n = \sqrt{\mu_r \varepsilon_r}$

- negative refraction can be achieved when both μ_r and ε_r are negative

$$\sqrt{\mu_r \varepsilon_r} = \left((e^{-j\pi})(e^{-j\pi})\right)^{1/2} = (e^{-j\pi/2})(e^{-j\pi/2}) = e^{-j\pi} = -1$$

- negative μ_r and ε_r occur in nature, but not simultaneously

  -silver, gold, and aluminum display negative ε_r at optical frequencies

  -resonant ferromagnetic systems display negative μ_r at resonance

V. G. Veselago, "The electrodynamics of substances with simultaneously negative values of *ε and μ*," *Sov. Phys. Uspekhi*, vol. 47, pp. 509–514, Jan. 1968.

How to Realize a Left-Handed Metamaterial

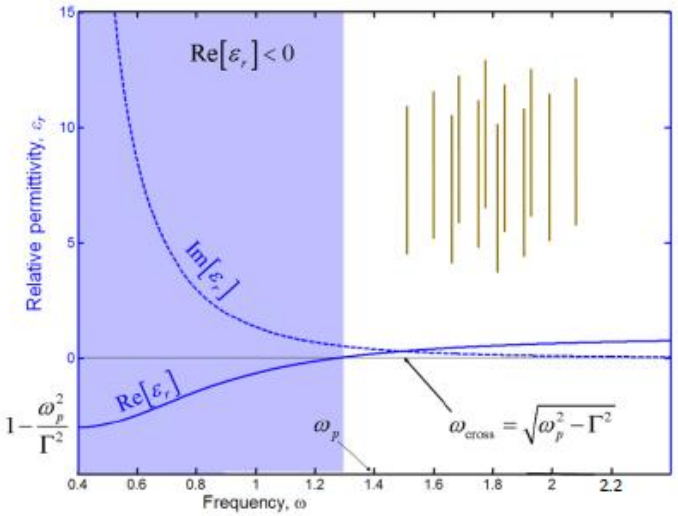

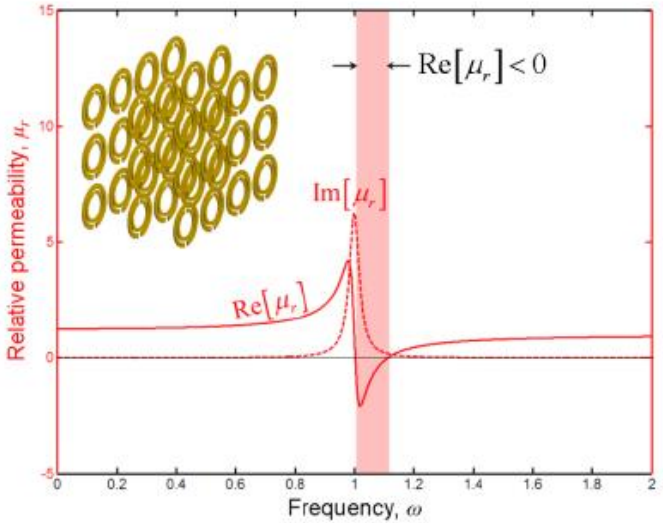

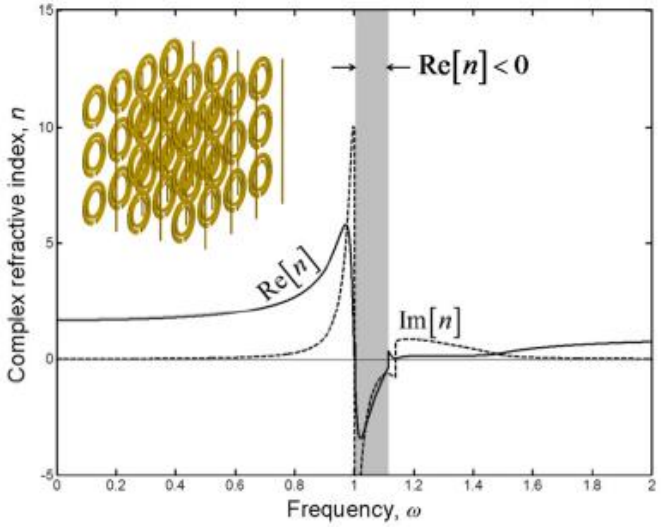

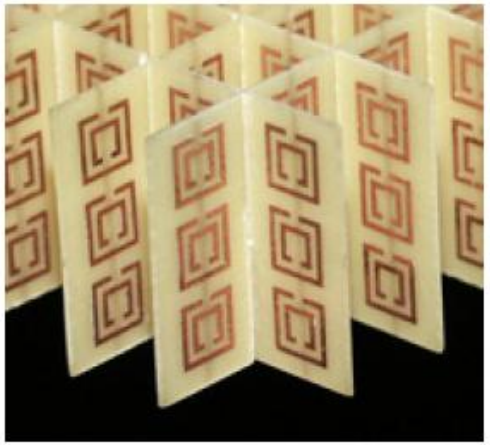

Smith et al., Phys. Rev. Lett. **84**, 4184–4187 (2000).

D. R. Smith, W. J. Padilla, D. C. Vier, S. C. Nemat-Nasser, and S. Schultz, "Composite medium with simultaneously negative permeability and permittivity," *Phys. Rev. Lett., vol. 84, pp. 4184–4187,* May 2000.

Waveguide loaded with SRRs and CSRRs

TE mode waveguide (below cut-off)

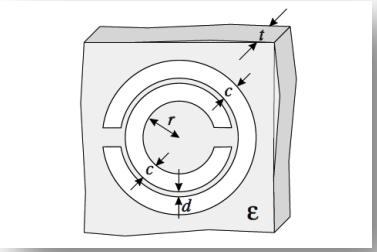

FIG. 1. The split ring resonator (SRR) used in this work. Structural parameters are r = 1:4 mm, c = 0.5 mm, d = 0.2 mm, t = 0.49 mm, and $\varepsilon = 2.43\varepsilon_0$.

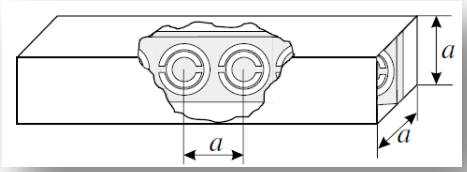

FIG. 2. The SRR-loaded square waveguide (a = 6 mm) used for simulating the left-handed metamaterial.

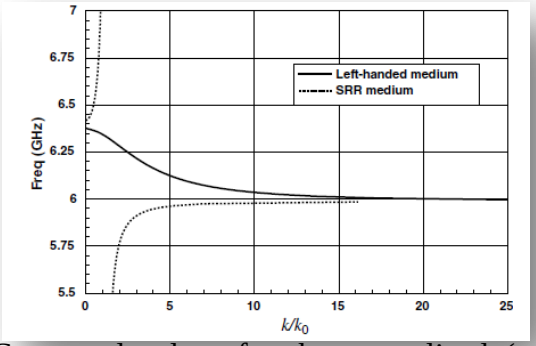

FIG. 3. Computed values for the normalized (to the freespace wave number, k_0) phase constants of the simulated left-handed and the SRR media. The plasma frequency is the cutoff frequency of the dominant TE10 mode of the square hollow waveguide in Fig. 2.

TM mode waveguide (below cut-off)

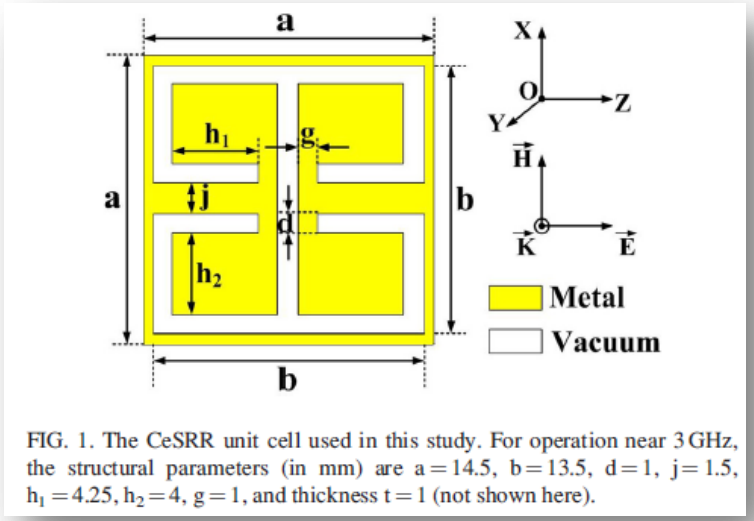

FIG. 1. The CeSRR unit cell used in this study. For operation near 3 GHz, the structural parameters (in mm) are a = 14.5, b = 13.5, d = 1, j = 1.5, h_1 = 4.25, h_2 = 4, g = 1, and thickness t = 1 (not shown here).

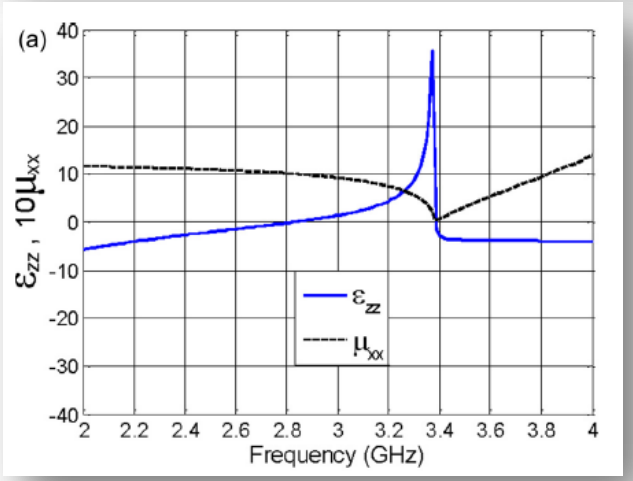

Waveguide loaded with SRRs and CSRRs (contd..)

TE mode waveguide (below cut-off)

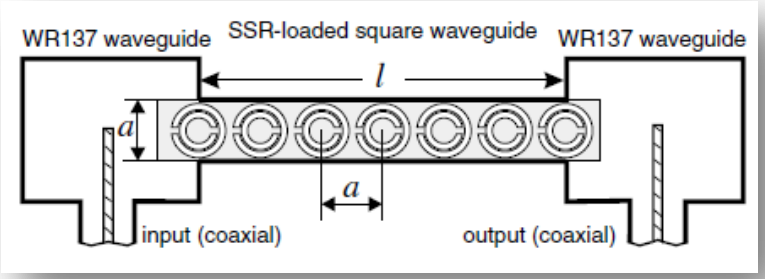

FIG. 4. Sketch of the experimental setup.

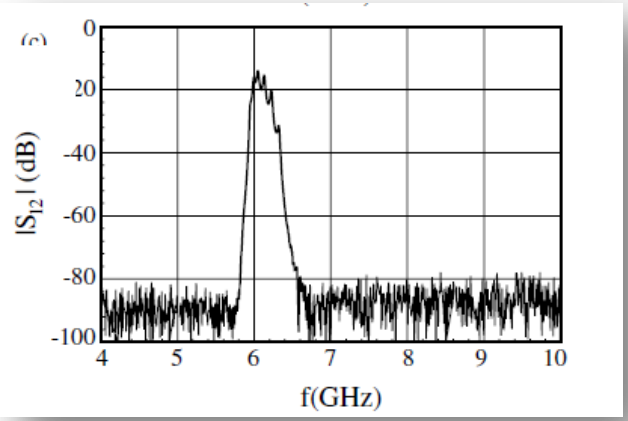

FIG. 5. Measured transmission coefficient (|S12|) for the experimental setup in Fig. 4. Three different lengths of the SRR loaded square waveguide are studied: l = 36 mm.

R. Marques, J. Martel, F. Mesa, and F. Medina, "Left-Handed-Media Simulation and Transmission of EM Waves in Sub-wavelength Split-Ring-Resonator-Loaded Metallic Waveguides", *Phys. Rev. Lett.* Vol. 89, no. 18, pp. 183901-1: 183901-1, Oct. 2002.

TM mode waveguide (below cut-off)

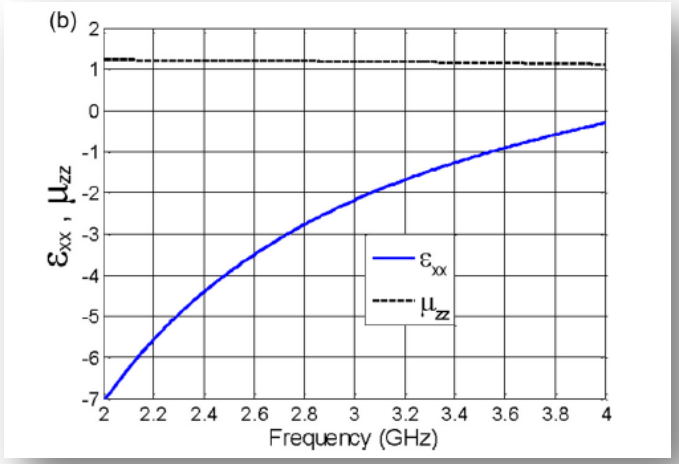

FIG. 2. Retrieved permittivities and permeabilities of the CeSRRs as functions of frequency for *z* (a) and *x* (b) polarizations, respectively.

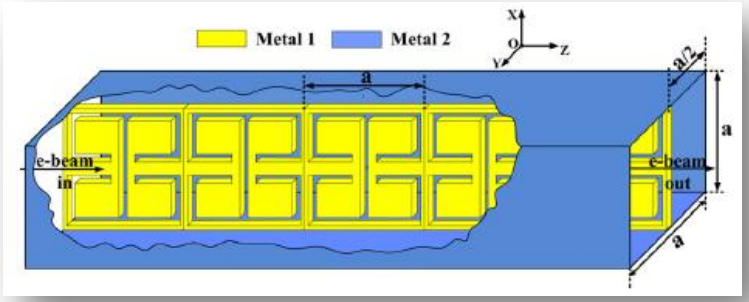

FIG. 3. The square metallic waveguide loaded with the CeSRR plate in the middle. Here, *a* = 14.5 mm.

Z. Duan, J. S. Hummelt, M. A. Shapiro, and R. J. Temkin, "Sub-wavelength waveguide loaded by a complementary electric metamaterial for vacuum electron devices," *Phys. Plasmas*, vol. 21, no. 10, pp. 103301-1–103301-6, Oct. 2014.

Origin of Bianisotropy

Bi-anisotropy occurs whenever a metamaterial lacks a centre of inversion symmetry along the direction of propagation.

If this SRR had a split at the bottom and top, it would exhibit ordinary anisotropy.

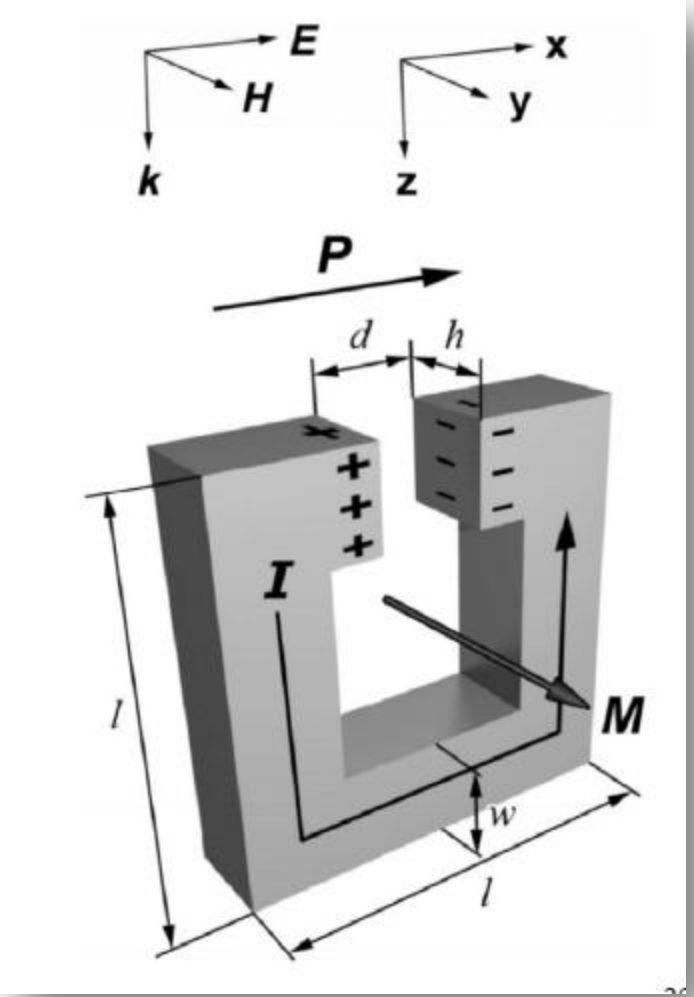

Origin of Bianisotropy

A helix is one of the most basic and easiest to understand elements that produces a bi-anisotropic response.

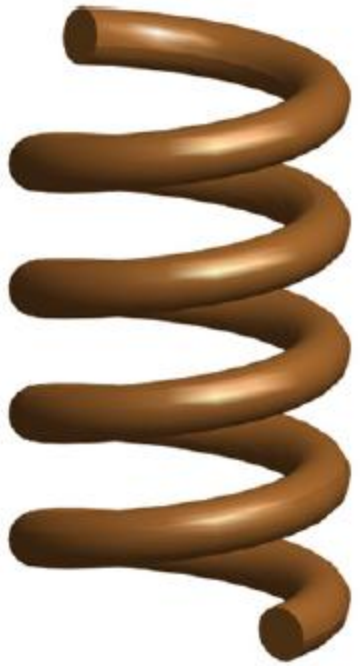

Origin of Bianisotropy

Suppose an electric field is applied to the helix.

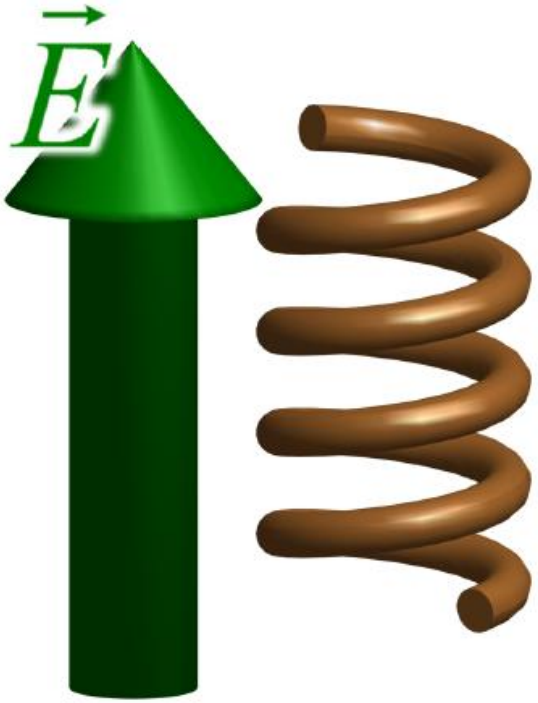

Origin of Bianisotropy

Charge along the wire will be displaced due to the electric field.

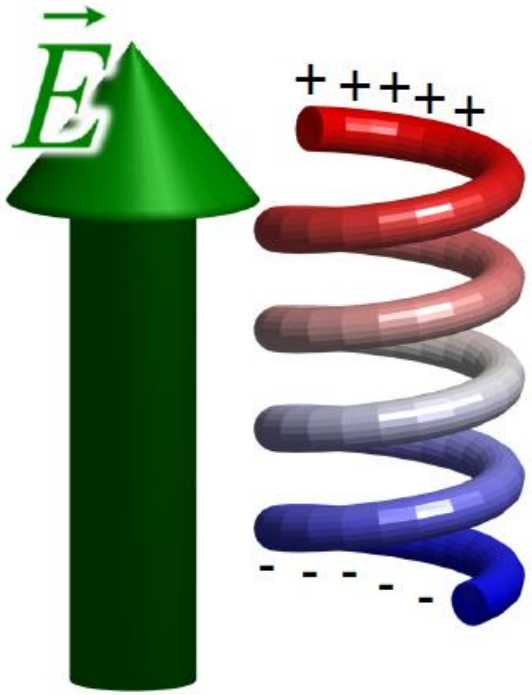

Origin of Bianisotropy

The displaced charge induces an electric dipole *D*, while the current produced by the displaced charge induces a magnetic dipole *B*.
An *E* has induced a *B*!

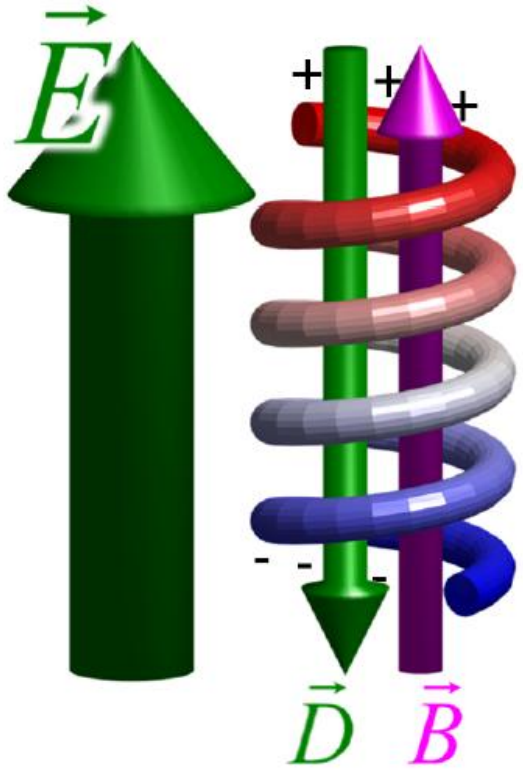

Parameter Retrieval of metamaterial

According to the effective medium concept, the metamaterial slab can be equivalent to a homogenous material slab with same electromagnetic responses.

$$n = \frac{1}{kd}\cos^{-1}\left[\frac{1}{2S_{21}}(1 - S_{11}^2 + S_{21}^2)\right],$$

$$z = \sqrt{\frac{(1+S_{11})^2 - S_{21}^2}{(1-S_{11})^2 - S_{21}^2}},$$

$$\varepsilon = n/z, \quad \mu = nz.$$

D. R. Smith, D. C. Vier, T. Koschny, and C. M. Soukoulis, "Electromagnetic parameter retrieval from inhomogeneous metamaterials," *Phys. Rev. E, Stat. Phys. Plasmas Fluids Relat. Interdiscip. Top.*, vol. 71, pp. 036617-1–036617-11, Mar. 2005.

Metamaterial design using CST

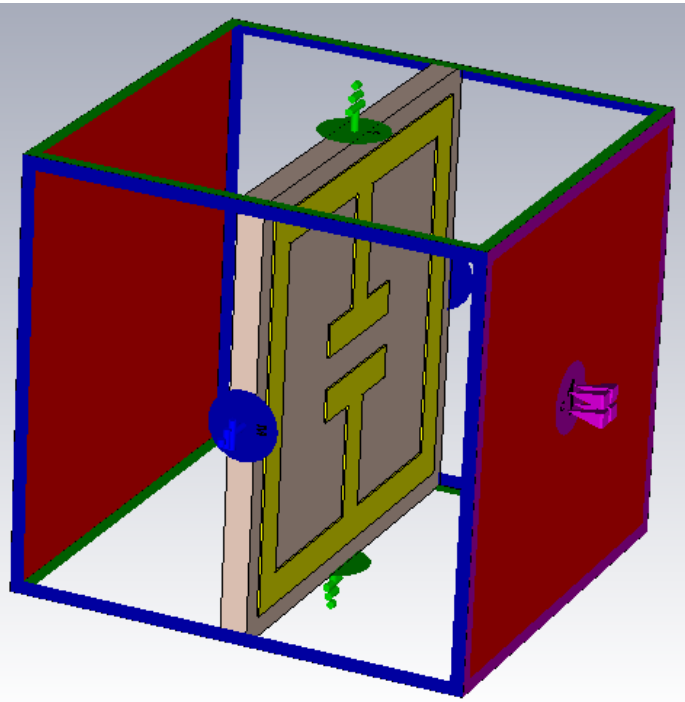

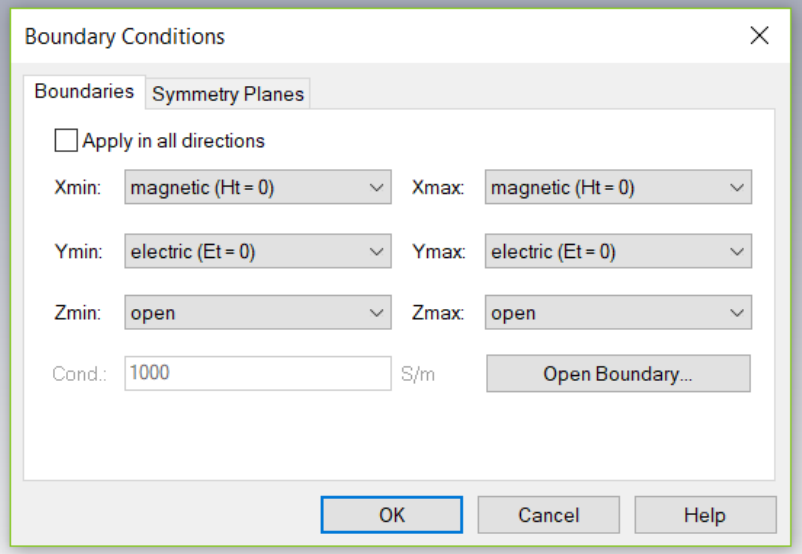

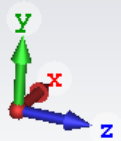

D. Schurig, J. J. Mock, anda D. R. Smith, “Electric-field-coupled resonators for negative permittivity metamaterials,” *Appl. Phys. Lett.* Vol. 88, p. 041109, Jan. 2006.

Metamaterial design using CST (cont'd)

Meshing style:
Tetrahedral

Before adaptive meshing

After adaptive meshing

Poor meshing

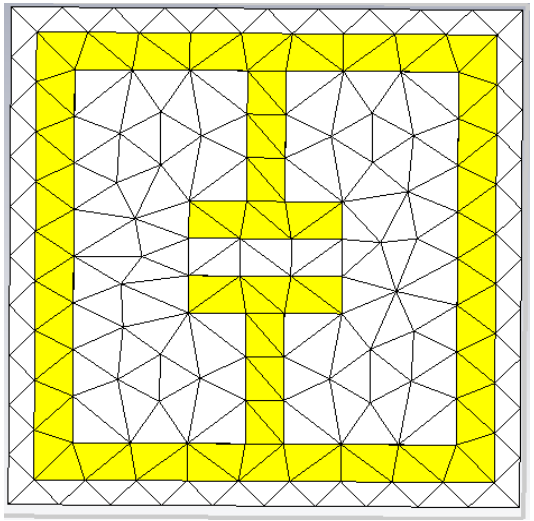

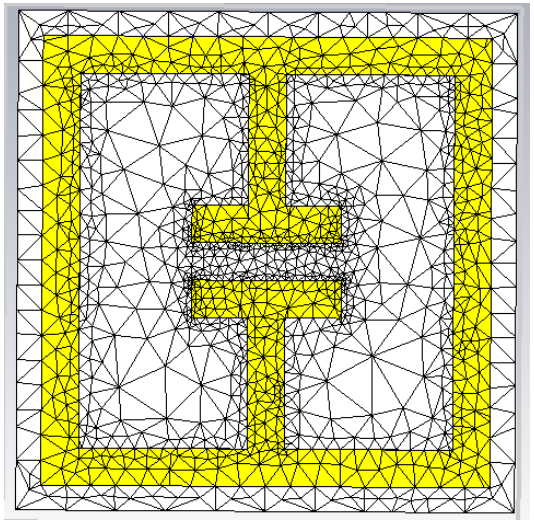

Very good meshing

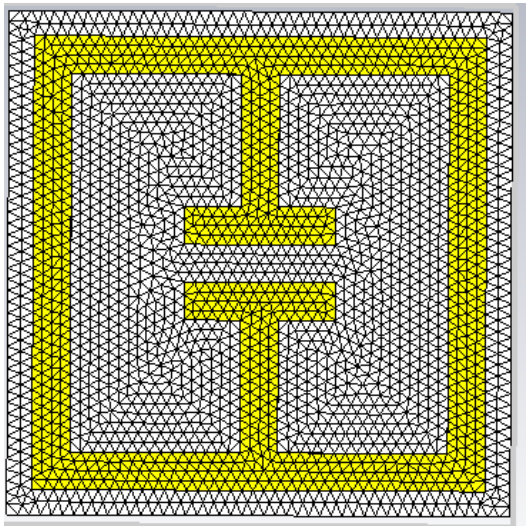

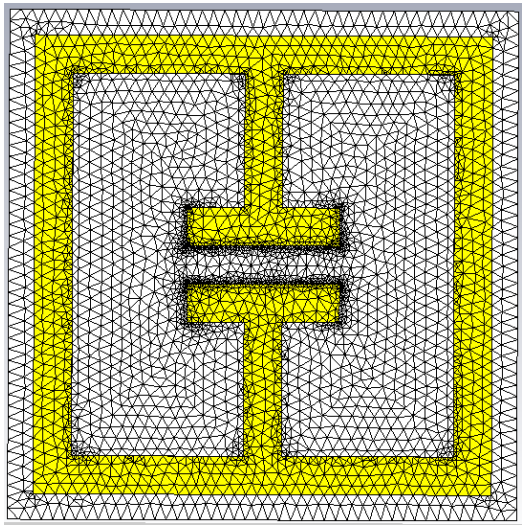

Metamaterial design using CST (cont'd)

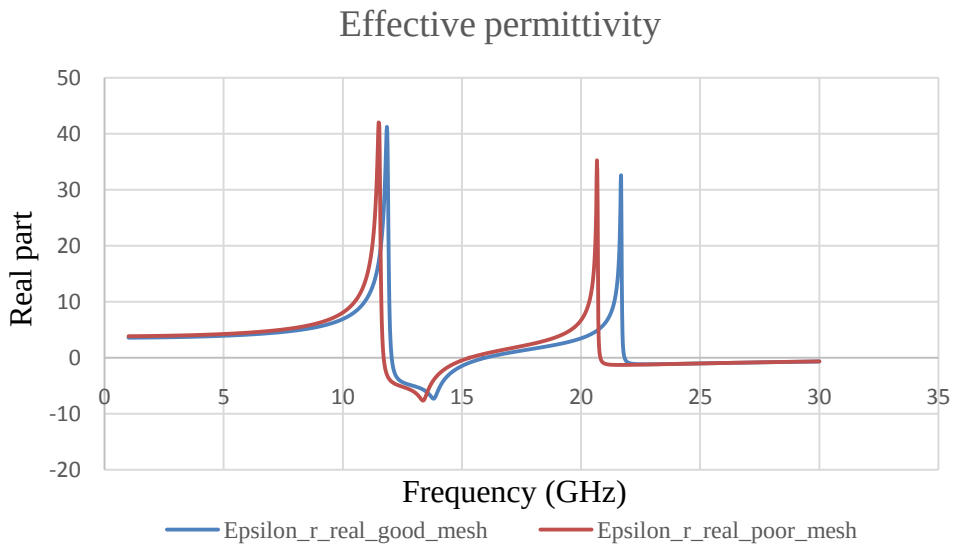

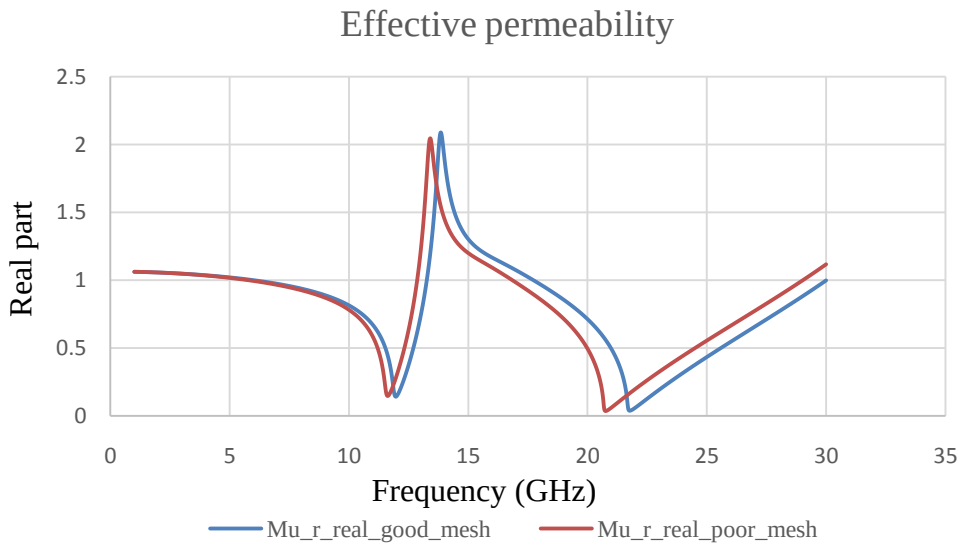

Metamaterial parameter retrieved using CST and MATLAB

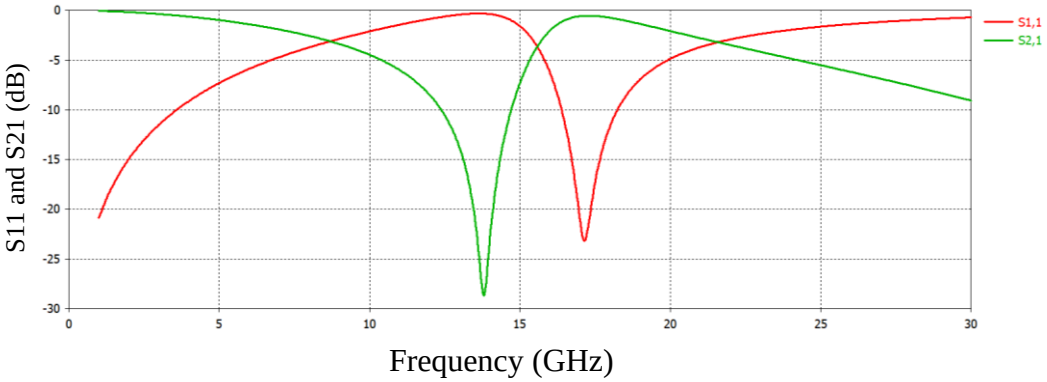

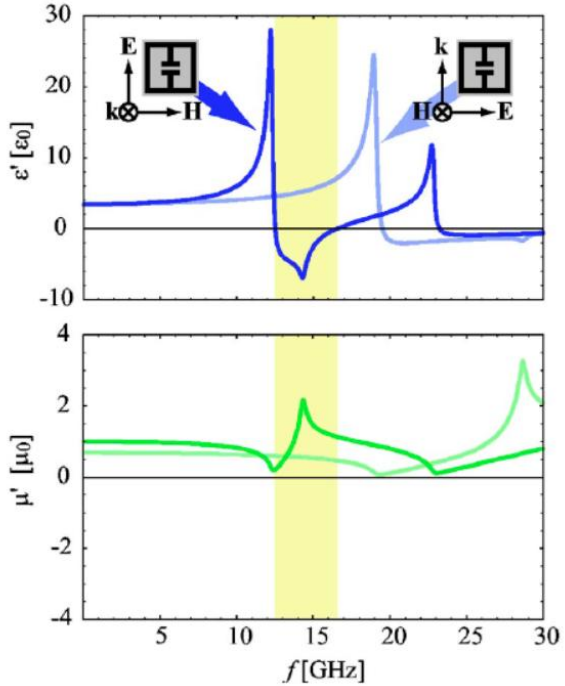

Effective permittivity

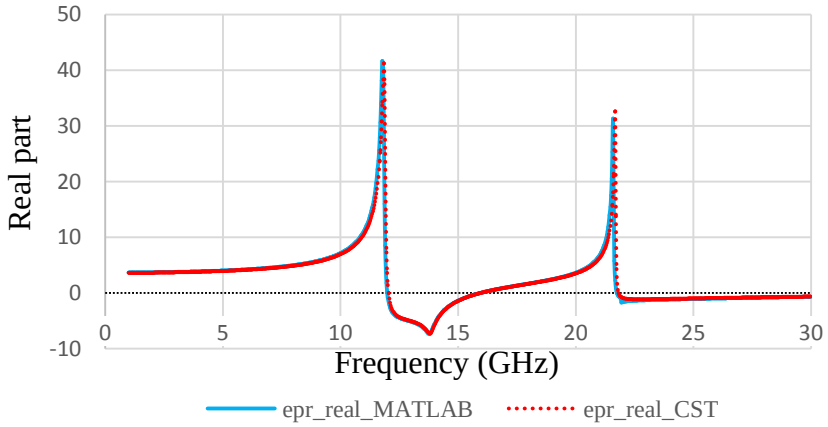

Effective permeability

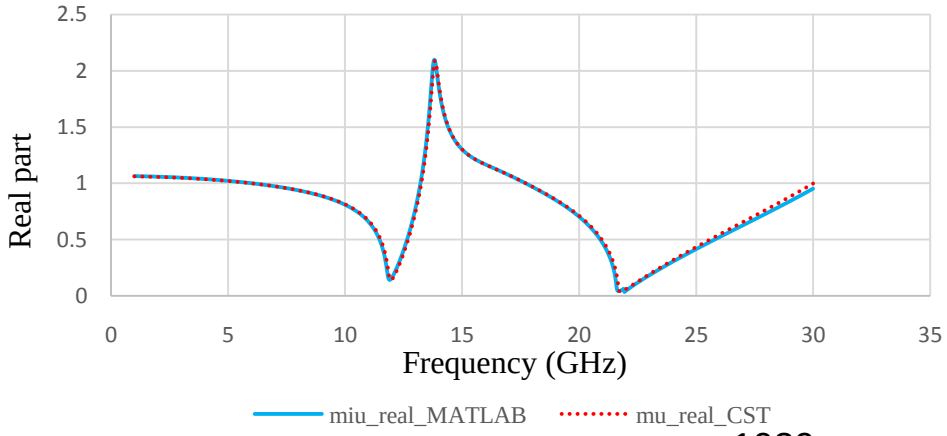

Fabrication Techniques of metamaterials

- PCB printing technique.
- UV-LIGA technique.
- 3-D printing technique.

Demerits of conventional linear electron beam MWTs

Parameters	TWTs	Klystrons	BWOs
Interaction impedance	low	—	medium
Efficiency	medium	low	medium
RF Output power	low	high	medium
Bandwidth	medium	very low	low
Design complexity at high frequency	high	high	high
Multi-band operation	—	—	yes

Metamaterial Slow-wave Structures

#

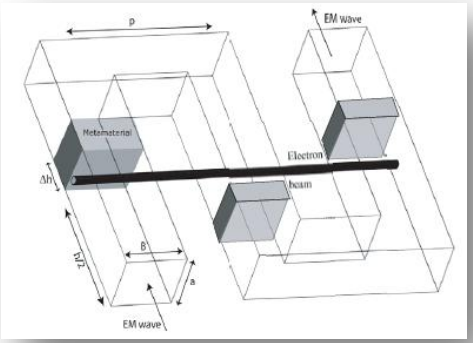

Fig. 1: The traveling wave structure considered here, consisting of a folded waveguide with a metamaterial insert, the electron beam passes through the middle of the structure.

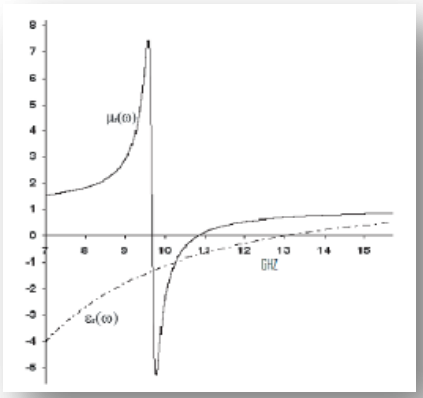

Fig. 2: The real component of eqs. (6) and (7), with the parameters ε_∞ = 1.62, μ_∞ = 1.12, μ_s = 1.26, ω_p = 2π14.62 GHz, ω_0 = 2π9.56 GHz, v_c = 3.07·10^7 GHz, and δ = 1.24·10^9.

##

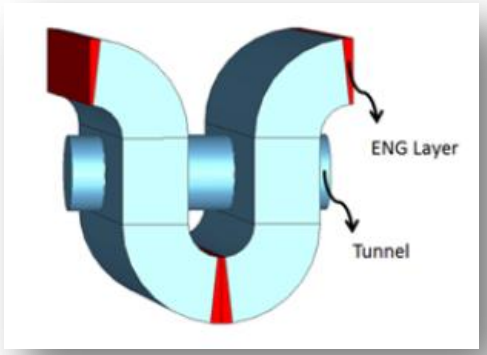

Fig. 1. Unit cell of the ENG loaded TWT.

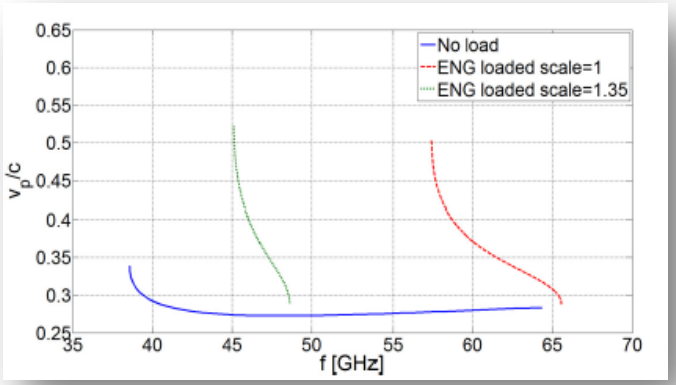

Fig. 2. Phase velocities for the zeroth order spatial harmonic for the unloaded, ENG loaded, and scaled ENG loaded cases.

###

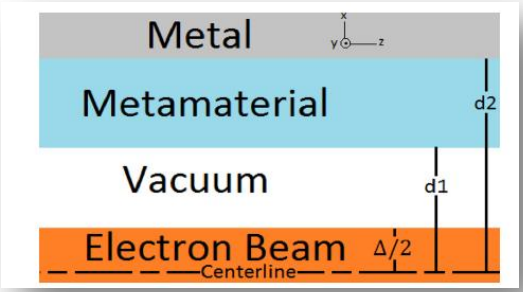

FIG. 1. Geometry considered in the article, showing the extent of the electron beam and the metamaterial boundaries.

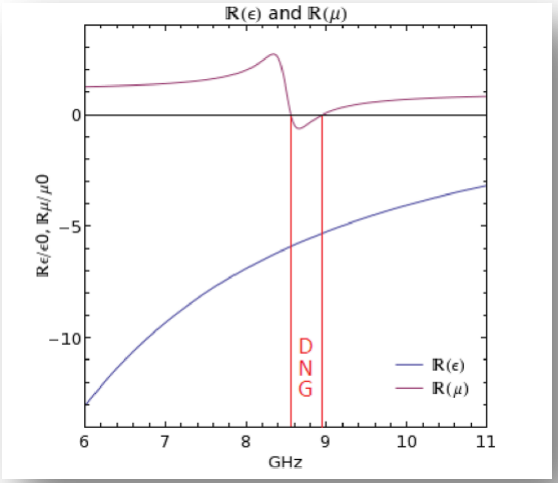

FIG. 2. Real part of ε and μ for the SRR and metallic wire metamaterial with the DNG region indicated.

Y. S. Tan and R. Seviour, "Wave energy amplification in a metamaterial based traveling-wave structure," *Europhys. Lett.*, vol. 87, no. 3, p. 34005, Aug. 2009,.

A. Rashidi and N. Behdad, "Metamaterial-enhanced traveling wave tubes," in *Proc. IEEE Int. Vac. Electron. Conf. (IVEC)*, Monterey, CA, USA, Apr. 2014, pp. 199–200,.

D. M. French , D. Shiffler, and K. Cartwright "Electron beam coupling to a metamaterial structure," *Phys. Plasmas*, vol. 20, no. 5, p. 083116, Aug. 2013.

Metamaterial Slow-wave Structures (contd..)

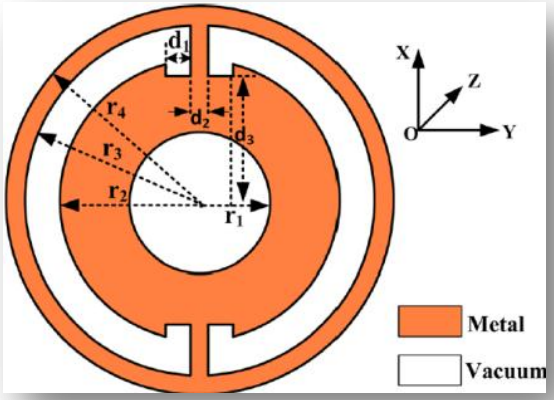

Fig. 1. Schematic of a MTM unit cell.

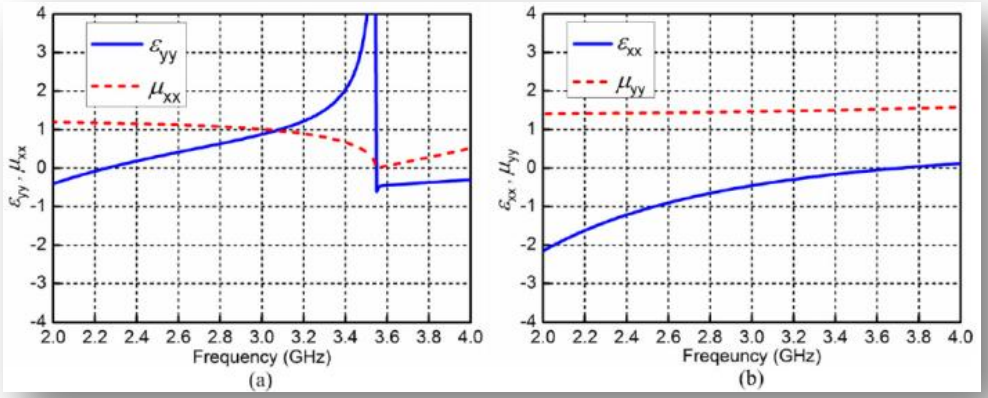

Fig. 2. Retrieved permittivities and permeabilities of the MTM as functions of frequency for *y* (a) and *x* (b) polarizations, respectively.

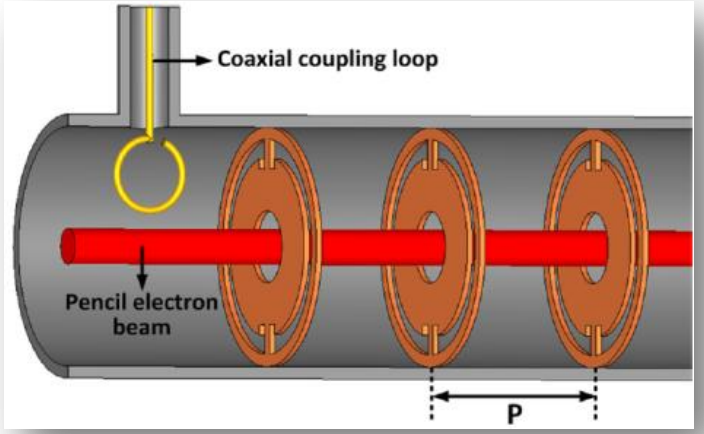

Fig.3. Sketch of the PIC simulation model.

Y. Wang *et al.*, "All-metal metamaterial slow-wave structure for high power sources with high efficiency," *Appl. Phys. Lett.*, vol. 107, no. 15, pp. 153502-1–153502-4, Oct. 2015.

Metamaterial Slow-wave Structures (contd..)

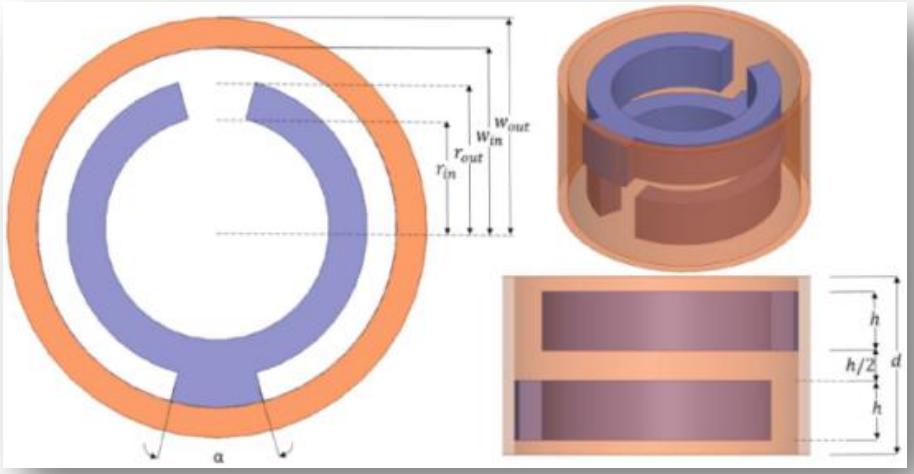

Fig. 1. Geometry of the O-Type MSWS in different angles of view for a single unit cell comprising two oppositely oriented SRRs.

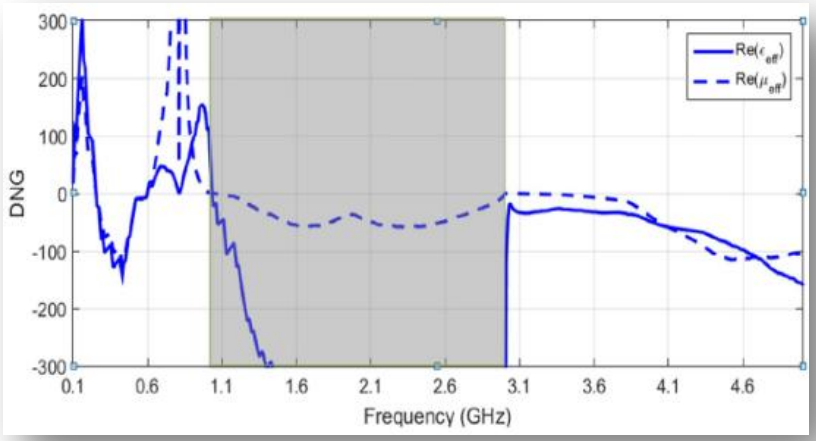

Fig. 2. Retrieved material parameters using a stepwise extraction technique.

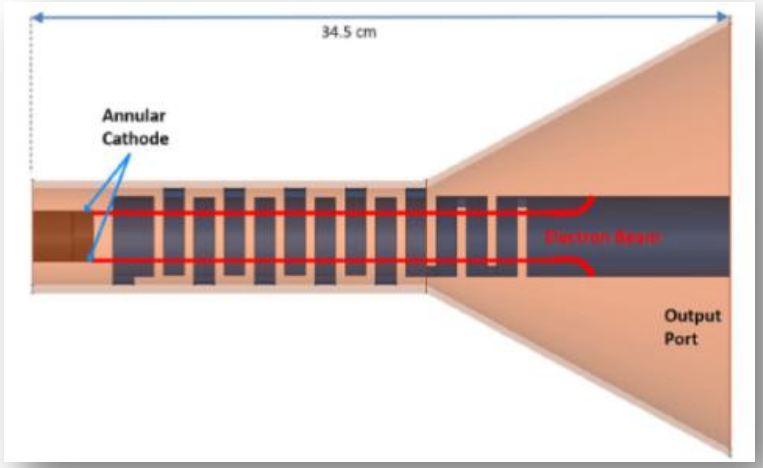

Fig. 3. Illustration of entire SWS and extraction geometry.

S. C. Yurt, M. I. Fuks, S. Prasad, and E. Schamiloglu, "Design of a metamaterial slow wave structure for an O-type high power microwave generator," *Phys. Plasmas*, vol. 23, no. 12, p. 123115, Dec. 2016.

Metamaterial Slow-wave Structures (contd..)

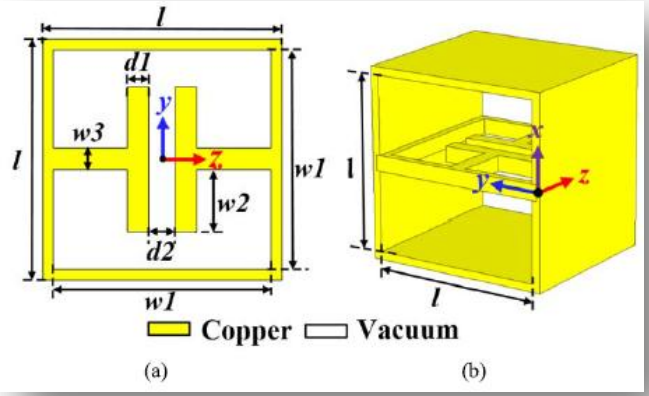

Fig. 1. (a) Schematic of a CESRR unit cell. (b) Simplified schematic of one period of SWS.

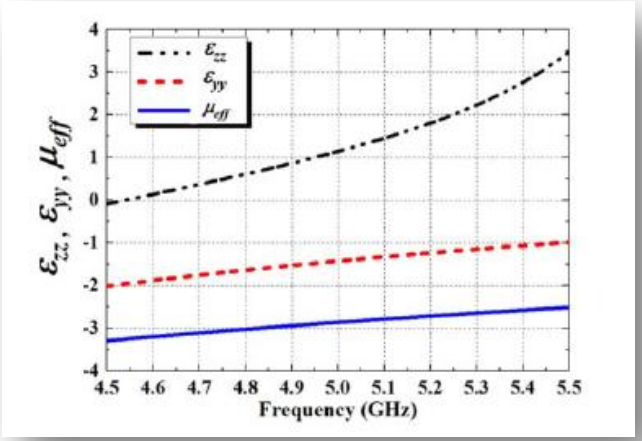

(a)

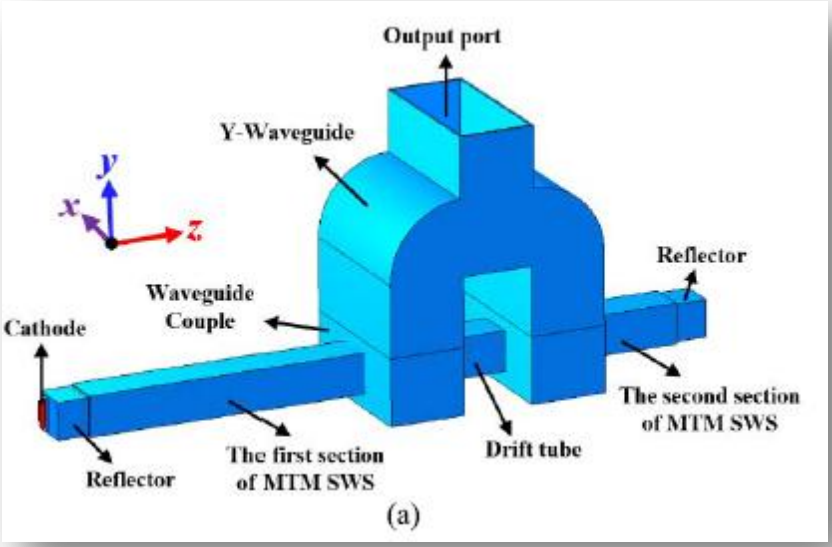

Fig. 3. Sketch of the PIC simulation model.

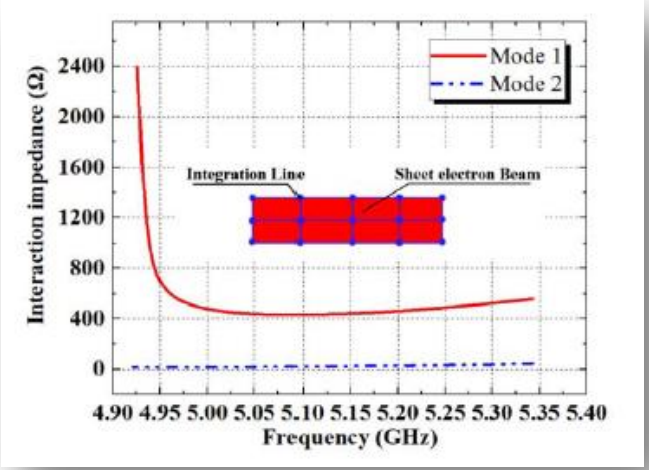

(b)

Fig. 2. (a) Effective constitutive parameters of MSWS and (b) interaction impedance of Mode 1 and Mode 2.

G. Wu, Q. Li , X. Lei, C. Ding , X. Jiang, S.u Fang, R. Yang, F. Wang, L. Yue, Y. Gong, and Y. Wei, "Design of a Cascade Backward-Wave Oscillator Based on Metamaterial Slow-Wave Structure," *IEEE Trans. Electron Devices*, vol. 65, no. 3, pp. 1172–1178, March 2018.

Contribution of Researchers in India on MTM-VEDs

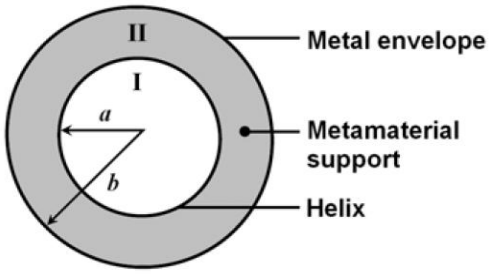

Figure 1. Schematic of the metamaterial supported helical slow-wave structure.

Sheath helix model (equi. ckt. analysis)

$$
\begin{aligned}
E_{z1}\{\gamma r\} &= A_1 I_0\{\gamma r\} \\
H_{\theta 1}\{\gamma r\} &= (j\omega\varepsilon_0/\gamma) A_1 I_1\{\gamma r\} \\
E_{z2}\{\gamma r\} &= A_2 I_0\{\gamma r\} + B_2 K_0\{\gamma r\} \\
H_{\theta 2}\{\gamma r\} &= (j\omega\varepsilon_m/\gamma)(A_2 I_1\{\gamma r\} - B_2 K_1\{\gamma r\} \\
H_{z1}\{\gamma r\} &= C_1 I_0\{\gamma r\} \qquad) \\
E_{\theta 1}\{\gamma r\} &= -(j\omega\mu_0/\gamma) C_1 I_1\{\gamma r\} \\
H_{z2}\{\gamma r\} &= C_2 I_0\{\gamma r\} + D_2 K_0\{\gamma r\} \\
E_{\theta 2}\{\gamma r\} &= -(j\omega\mu_m/\gamma)(C_2 I_1\{\gamma r\} - D_2 K_1\{\gamma r\} \\
& \qquad) \qquad (1)
\end{aligned}
$$

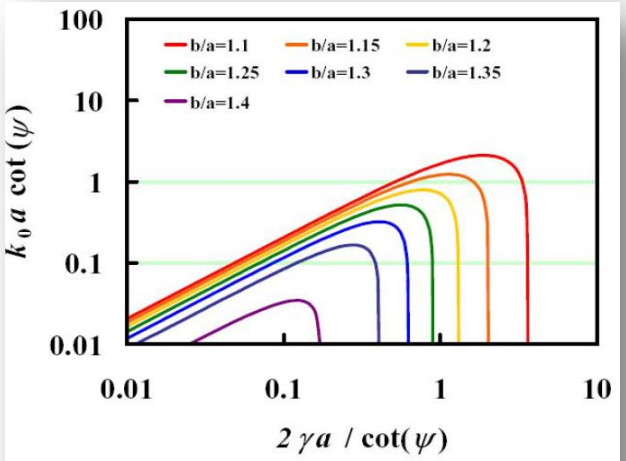

Figure 2. Dispersion characteristics of the metamaterial supported SWS with b/a as the parameter.

$$\varepsilon_m = \varepsilon_0 \varepsilon_{mr} \qquad \mu_m = \mu_0 \mu_{mr}$$

Dispersion relation

$$
k_0 \cot(\psi)/\gamma = \left(\frac{I_{0a} K_{0a}}{I_{1a} K_{1a}}\right)^{\frac{1}{2}} \left(\frac{(1+(\mu_{mr}-1)\gamma a I_{0a} K_{1a} X_L) Y_C}{(1+(\varepsilon_{mr}-1)\gamma a I_{0a} K_{1a} X_C) X_L \mu_{mr}}\right)^{\frac{1}{2}} \qquad (2)
$$

with

$$X_L = 1 - I_{1a} K_{1b}/(I_{1b} K_{1a}), \qquad X_C = 1 + I_{1a} K_{0b}/(I_{0b} K_{1a})$$

$$Y_C = 1 - I_{0a} K_{0b}/(I_{0b} K_{0a})$$

Where $I_{\nu r} = I_\nu\{\gamma r\}$ $(\nu = 1, 2)$ and $K_{\nu r} = K_\nu\{\gamma r\}$ **(ν=1, 2).**

$k_0 a \cot(\psi)$ ⟶ normalized frequency

$2\gamma a / \cot(\psi)$ ⟶ normalized phase shift per period

$\varepsilon_{mr} = -4.2 \quad \mu_{mr} = -1 \quad \cot(\psi) = 10 \rightarrow 5.71°$

S. K. Datta, L. Kumar, and B. N. Basu, "Investigation into a metamaterial supported helix slow-wave structure," in *Proc. IEEE Int. Vac. Electron. Conf. (IVEC)*, Bangalore, India, Feb. 2011, pp. 211–212.

Contribution of Researchers in India on MTM-VEDs (contd..)

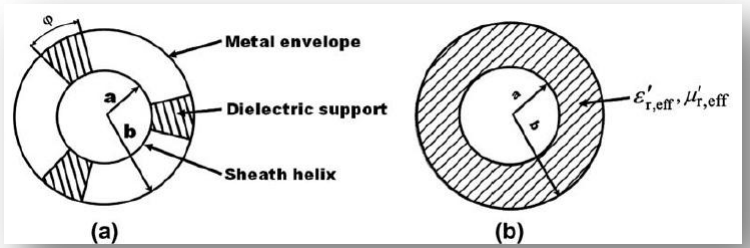

Tape helix model

Dispersion relation

$$\sum_{m=-\infty}^{+\infty}\left\{\frac{k^2\mathrm{Cot}^2\psi}{\gamma_m^2}+\frac{I_{ma}K_{ma}}{I'_{ma}K'_{ma}}\left(1-\frac{m\beta_m\mathrm{Cot}\psi}{\gamma_m^2 a}\right)^2\times\alpha\right\}\frac{\mathrm{Sin}(\beta_m\delta/2)}{\beta_m\delta/2}=0$$

where

$$\alpha=\left[\frac{(1-I_{ma}K'_{ma}\gamma_m a(\mu'_{r,\mathrm{eff}}-1))X_{1m}}{(1-I_{ma}K'_{ma}X_{2m}\gamma_m a(\varepsilon'_{r,\mathrm{eff}}-1))X_{3m}\mu'_{r,\mathrm{eff}}}\right]$$

with

$$\varepsilon'_{r,\mathrm{eff}}=1+(N\varphi/2\pi)(\varepsilon_r-1)$$

$$\mu'_{r,\mathrm{eff}}=1+(N\varphi/2)(\mu_r-1)$$

$$X_{1m}=1-\frac{I_{ma}K_{mb}}{K_{ma}I_{mb}},\quad X_{2m}=1-\frac{I'_{ma}K_{mb}}{K'_{ma}I_{mb}},\quad X_{3m}=1-\frac{I'_{ma}K'_{mb}}{K'_{ma}I'_{mb}}$$

Fig. 1. (a) Cross-sectional view of the homogeneously loaded helix in a metal envelope and (b) its equivalent model.

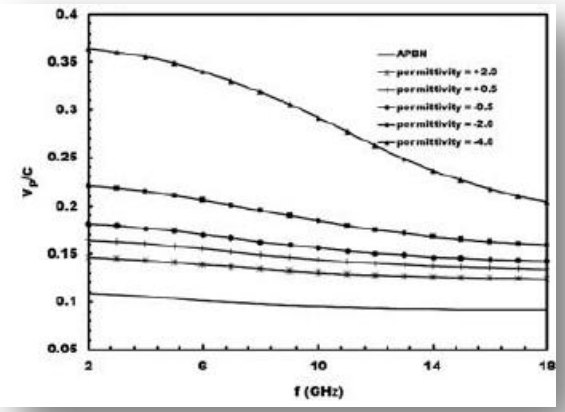

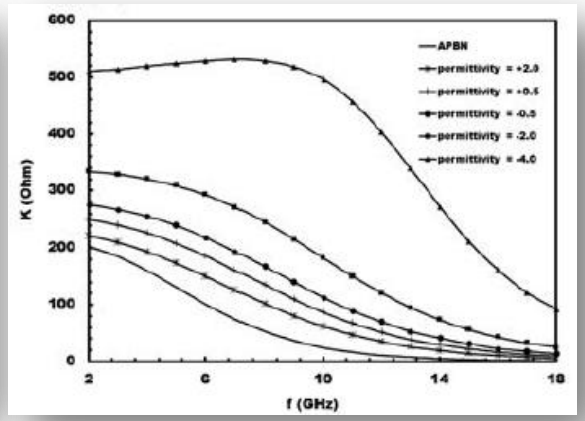

Interaction impedance

$$K_m=\frac{E_{z,m}^2}{2\beta_m^2\sum_{m=-\infty}^{+\infty}P_m}$$

Fig. 2. (a) Dispersion and (b) interaction impedance versus frequency characteristics taking permittivity as the parameter with $\mu_r=-2$.

N. Purushothaman and S. K. Ghosh, "Performance improvement of helix TWT using metamaterial helix-support structure," *J. Electromagn. Waves Appl.*, vol. 27, no. 7, pp. 890–900, Apr. 2013.

Contribution of Researchers in India on MTM-VEDs (contd..)

Table 1 List of optimized design parameters

Parameter	Value
Substrate	FR4 with $\varepsilon_r = 4.3$
Substrate thickness (t)	1.6 mm
Inclusion material	Copper
Inclusion material thickness	0.05 mm
Ring width (rw)	0.4 mm
Intra ring gap (g)	0.2 mm
Outer radius of outer ring (r)	1.9 mm
Inter ring gap (d)	0.1 mm
Periodicity (a)	4.4 mm

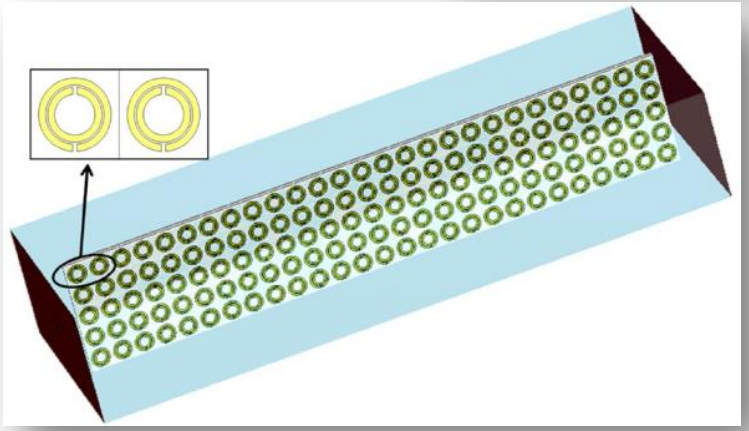

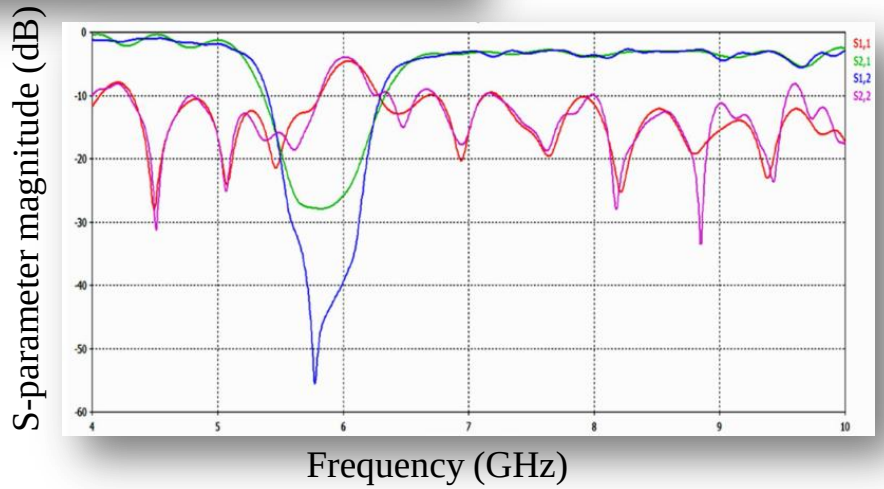

Fig. 1 a) Modeled SRR array with 135 unit cells, b) Simulated S-parameter response of (a). Blue and green curves show transmission parameters (S21, S12), and red and pink curves show reflection parameters (S11, S22) .

N. Purushothaman , A. Jain, W. R. Taube, R. Gopal, S. K. Ghosh, "Modeling and fabrication studies of negative permeability metamaterial for use in waveguide applications", *Microsyst Technol*, Volume 21, issue 11, pp 2415–2424, Nov. 2015.

Contribution of Researchers in India on MTM-VEDs (contd..)

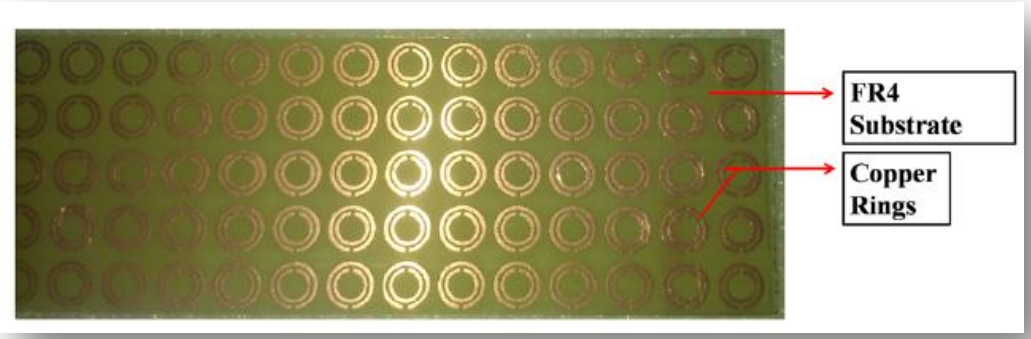

(a)

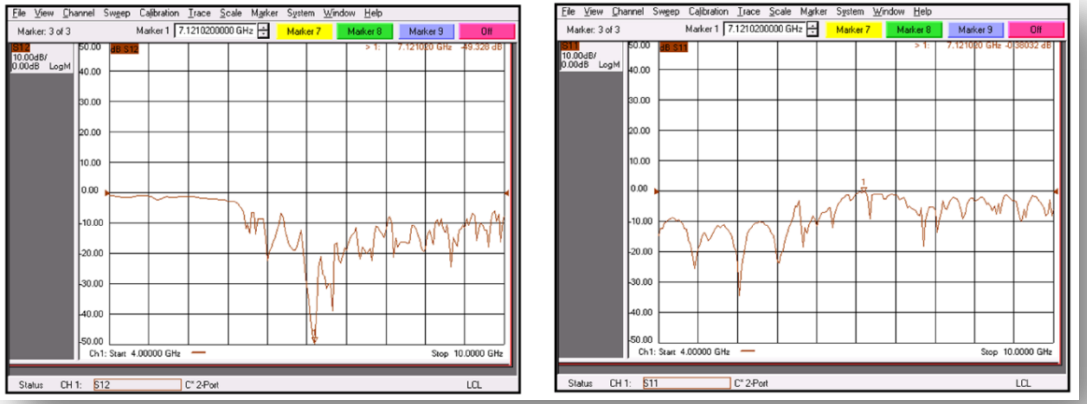

(b) (c)

Fig. 2. a) SRR array fabricated on the FR4 substrate, b) Experimental S12 parameters, c) Experimental S11 parameters.

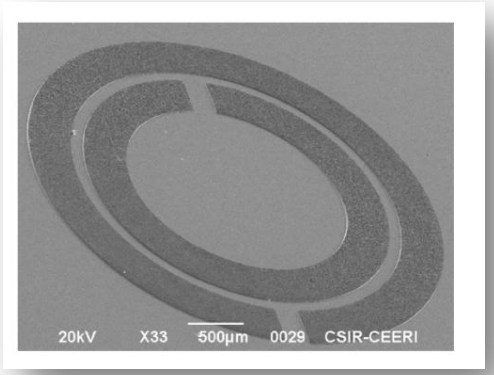

Fig. 3. SEM image of one of the fabricated SRR unit cells.

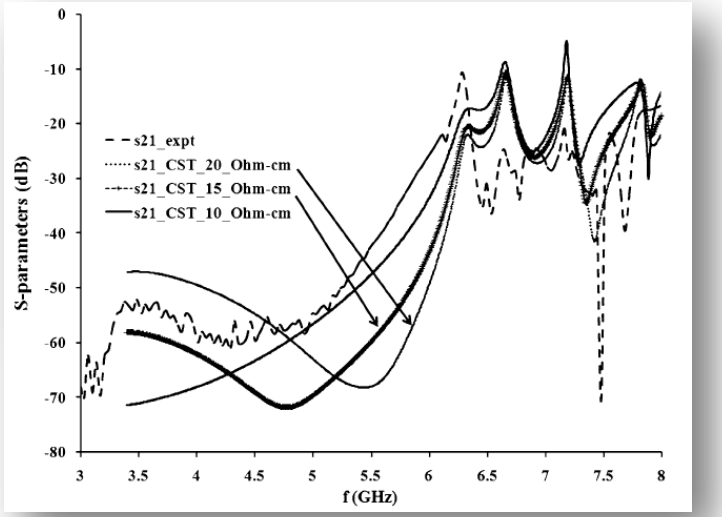

Fig. 4. Comparison of the simulated and the measured S21 parameters with the SRR array fabricated on silicon substrate.

N. Purushothaman , A. Jain, W. R. Taube, R. Gopal, S. K. Ghosh, "Modeling and fabrication studies of negative permeability metamaterial for use in waveguide applications", *Microsyst Technol*, Volume 21, issue 11, pp 2415–2424, Nov. 2015.

Contribution of Researchers in India on MTM-VEDs (contd..)

Sheath helix model
(EM analysis)

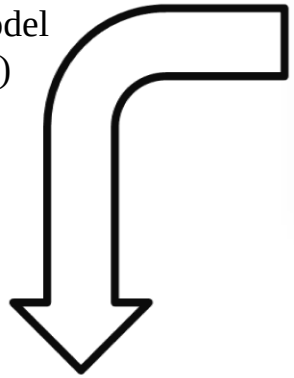

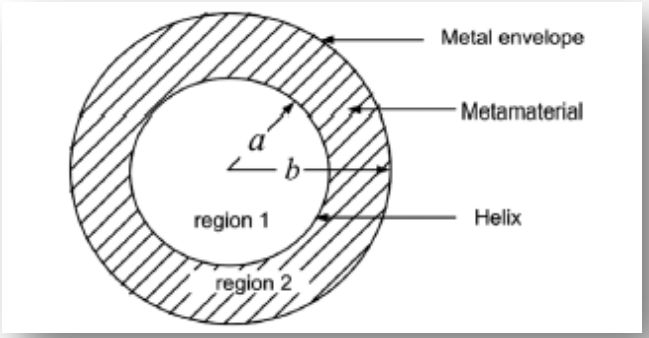

Fig. 1. Cross section of a helix supported by a DNG-MMT surrounding it in a metal envelope.

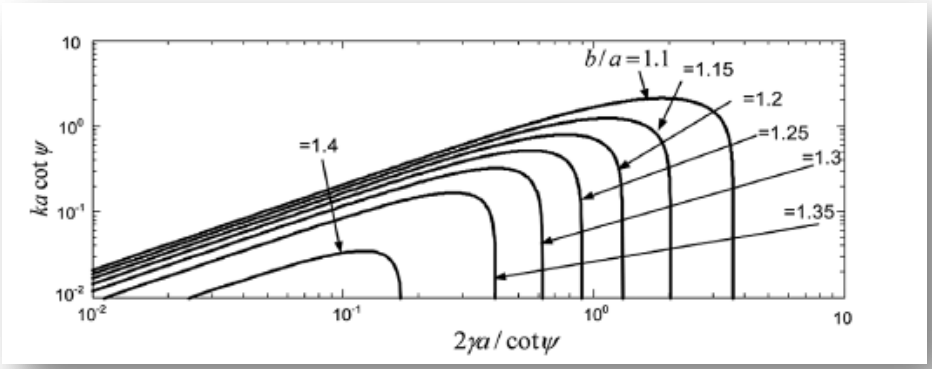

Fig. 2. Normalized $\omega - \beta$ dispersion characteristics taking *b/a* as the parameter.

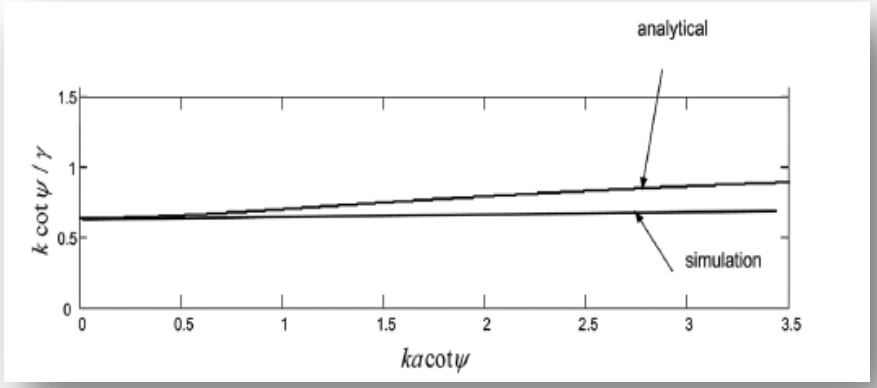

Fig. 3. Comparison of the results of electromagnetic analysis with those of simulation obtained by CST Microwave Studio with respect to the dispersion characteristics of the structure.

$$\varepsilon_{mr} = -2 \qquad \mu_{mr} = -0.4 \qquad b/a = 1.5$$

A. K. Varshney, R. Guha, S. K. Datta, and B. N. Basu, "Dispersion control of helical slow-wave structure by double-negative metamaterial loading," *J. Electromagn. Waves Appl.*, vol. 30, no. 10, pp. 1308–1320, Jun. 2016.

Contribution of Researchers in India on MTM-VEDs (contd..)

Tape helix model

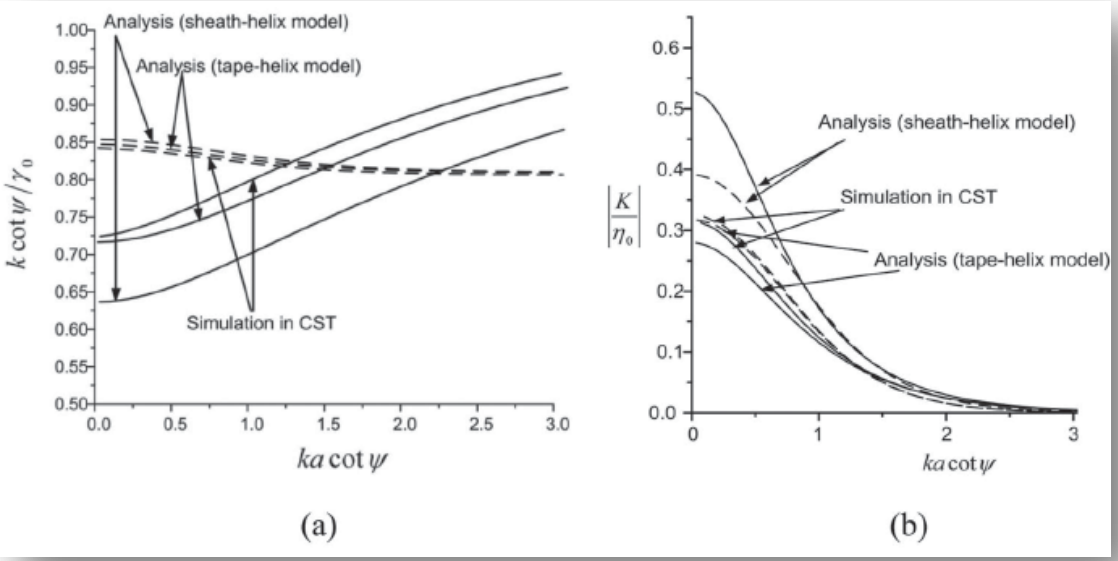

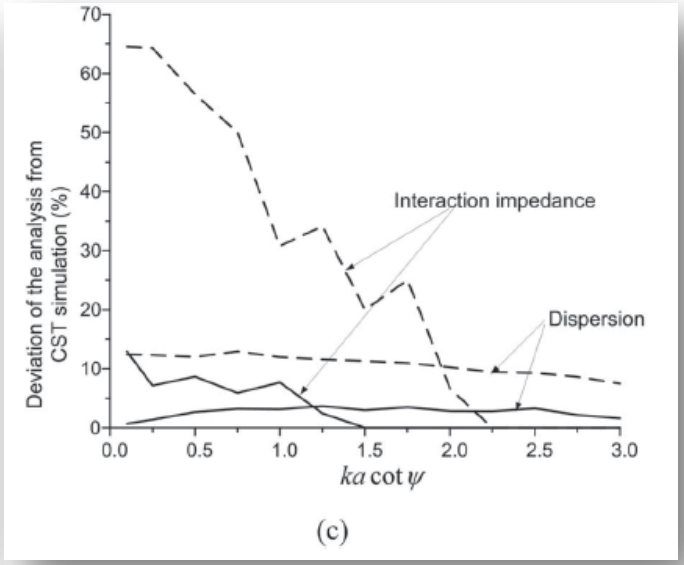

Fig. 1. Dispersion (a) and interaction impedance (b) characteristics of a helix surrounded by (i) a DNG-MTM tube ($\varepsilon_{r2} = -2$, $\mu_{r2} = -0.4$) (solid line), and (ii) a conventional dielectric tube ($\varepsilon_{r2} = 2$, $\mu_{r2} = 1$) (broken line), the whole enclosed in a metal envelope, taking $b/a = 1.5$, pitch $p' = 0.6$mm, tape width $\delta = 0.2$ mm—obtained by the tape-helix model and compared with the sheath-helix model and CST simulation, tape-helix model (solid line) and sheath-helix model (broken line); and the percentage deviation of the dispersion and interaction impedance of the DNG-MTM-supported SWS using tape-helix model (solid line) and sheath-helix model (broken line) against CST simulation (c).

A. K. Varshney, R. Guha, S. Biswas, P. P. Sarkar, S. K. Datta, and B. N. Basu, "Tape-helix model of analysis for the dispersion and interaction impedance characteristics of a helix loaded with a double-negative metamaterial for potential application in vacuum electron devices", *J. Electromagn. Waves Appl.*, vol. 33, no. 2, pp. 138-150, Oct. 2018.

Contribution of Researchers in India on MTM-VEDs (contd..)

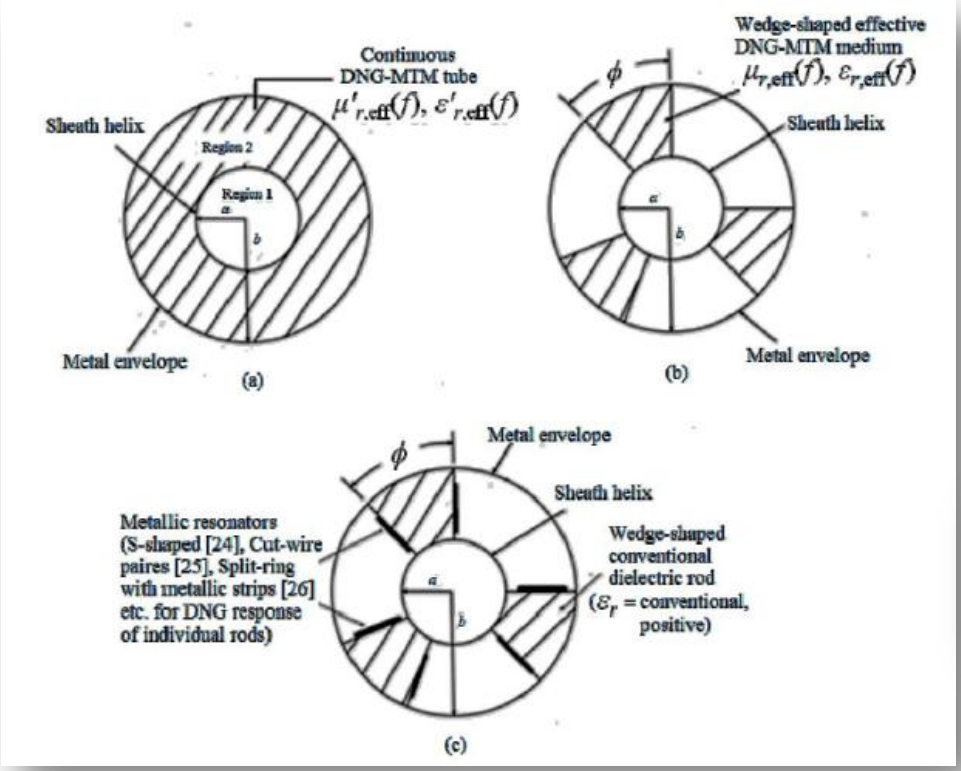

$$\mu_{r,\text{eff}}(f) = 1 - \frac{f_{\text{mp}}^2 - f_{m0}^2}{f^2 + j\Gamma_m f/(2\pi) - f_{m0}^2} \quad \text{(Lorentz model)} \tag{1}$$

$$\varepsilon_{r,\text{eff}}(f) = 1 - \frac{f_{\text{ep}}^2}{f^2 + j\Gamma_e f/(2\pi)} \quad \text{(Drude model)} \tag{2}$$

$$\mu'_{r,\text{eff}}(f) = 1 + (\phi N/2\pi)[\mu_{r,\text{eff}}(f) - 1] \tag{3}$$

$$\varepsilon'_{r,\text{eff}}(f) = 1 + (\phi N/2\pi)[\varepsilon_{r,\text{eff}}(f) - 1] \tag{4}$$

Fig. 1. (a) Analytical structure model consisting of a helix surrounded by a DNG-MTM tube. (b) Identical discrete DNG-MTM helix-support rods, typically shown as wedge-shaped, from which to derive the structure model in (a) by smoothing out the support rods. (c) Metallic MTM layering of the radial surfaces of dielectric helix supports—the dielectric supports and the metallic MTM layer collectively expressing the DNG-MTM response [24]–[26] of each rod in (b).

R. Guha, A. K. Bandyopadhyay, A. K. Varshney, S. K. Datta, and B. N. Basu, "Investigations into helix slow-wave structure assisted by double-negative metamaterial," *IEEE Trans. Electron Devices*, vol. 65, no. 11, pp. 5082–5088, Nov. 2018.

Contribution of Researchers in India on MTM-VEDs (contd..)

Dispersion relation

$$\frac{k\cot\psi}{\gamma} \cong \frac{v_p}{c}\cot\psi = \left[\frac{I_0(\gamma a)K_0(\gamma a)}{I_1(\gamma a)K_1(\gamma a)}\right]^{1/2} M_{lf} \qquad (5)$$

$$M_{lf} = \left[\left\{1-\frac{I_0(\gamma a)K_0(\gamma b)}{I_0(\gamma b)K_0(\gamma a)}\right\}\left\{1-\frac{I_1(\gamma a)K_1(\gamma b)}{I_1(\gamma b)K_1(\gamma a)}\right\}^{-1} \times\left\{\frac{I_0(\gamma a)K_1(\gamma a)X_1+(1/\mu'_{r,\mathrm{eff}}(f))I_1(\gamma a)K_0(\gamma a)X_2}{I_1(\gamma a)K_0(\gamma a)X_3+\varepsilon'_{r,\mathrm{eff}}(f)I_0(\gamma a)K_1(\gamma a)X_4}\right\}\right]^{1/2}$$

with

$$X_1 = \left(1-\frac{I_1(\gamma a)K_1(\gamma b)}{I_1(\gamma b)K_1(\gamma a)}\right), \quad X_2 = \left(1+\frac{I_0(\gamma a)K_1(\gamma b)}{I_1(\gamma b)K_0(\gamma a)}\right)$$

$$X_3 = \left(1-\frac{I_0(\gamma a)K_0(\gamma b)}{I_0(\gamma b)K_0(\gamma a)}\right), \quad X_4 = \left(1+\frac{I_1(\gamma a)K_0(\gamma b)}{I_0(\gamma b)K_1(\gamma a)}\right).$$

Interaction impedance

$$K = \frac{E_z^2(0)}{2\beta^2 P} \qquad (6)$$

$$P = 1/2\mathrm{Re}\int_0^a \left(E_{r1}H^*_{\theta 1} - E_{\theta 1}H^*_{r1}\right)2\pi r\,dr + 1/2\mathrm{Re}\int_a^b \left(E_{r2}H^*_{\theta 2} - E_{\theta 2}H^*_{r2}\right)2\pi r\,dr$$

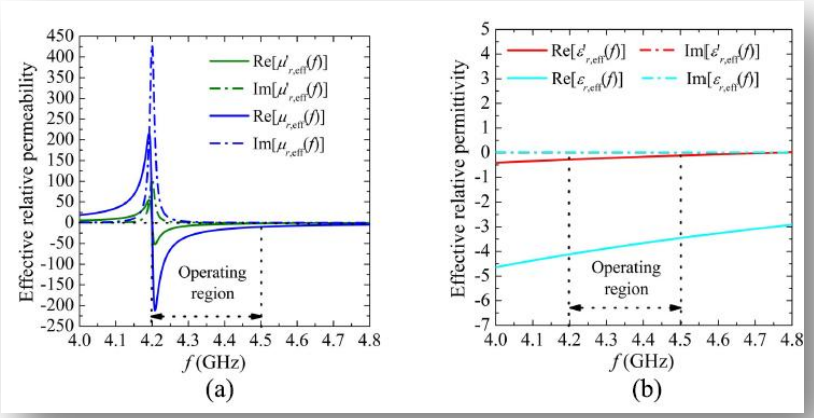

Fig. 2. (a) Effective relative permeability quantities and (b) effective relative permittivity quantities plotted against frequency f to identify the common frequency region of MNG-MTM and ENG-MTM, i.e., the operating frequency region of DNG-MTM (4.2–4.5 GHz).

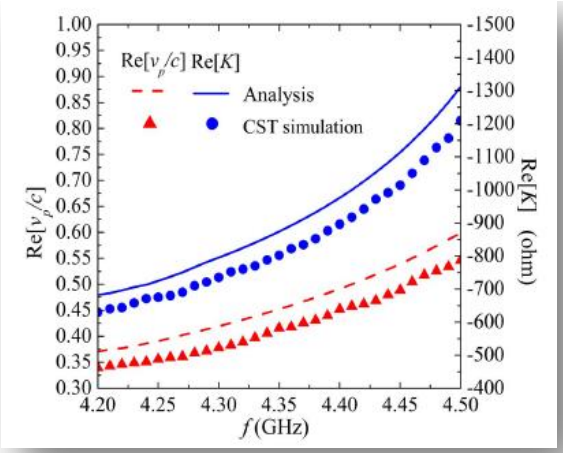

Fig. 3. Validation of the dispersion and interaction impedance versus frequency characteristics of the DNG-MTM-supported helical SWS [Fig. 1(a)], derivable from the structure configurations in Fig. 1(a) and (b), obtained by the present analysis against CST simulation [27].

R. Guha, A. K. Bandyopadhyay, A. K. Varshney, S. K. Datta, and B. N. Basu, "Investigations into helix slow-wave structure assisted by double-negative metamaterial," *IEEE Trans. Electron Devices*, vol. 65, no. 11, pp. 5082–5088, Nov. 2018.

Contribution of Researchers in India on MTM-VEDs (contd..)

Parametric study

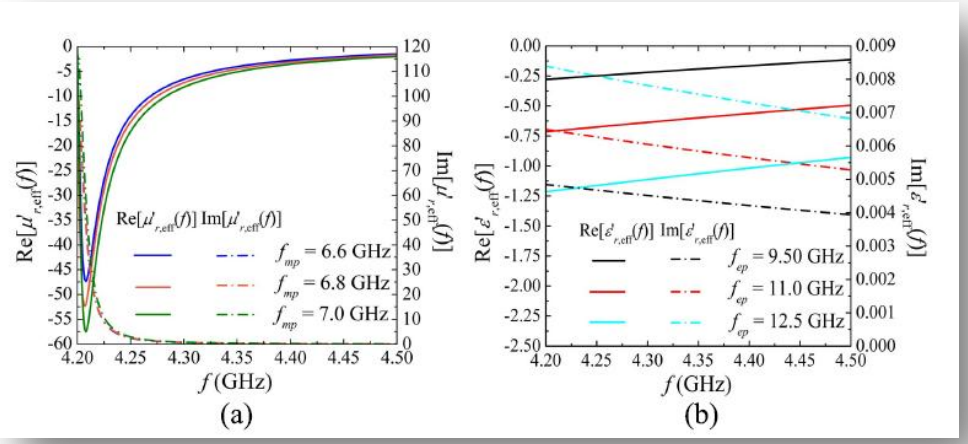

Fig. 4. (a) Real part Re[$\mu'_{r,\mathrm{eff}}(f)$] and imaginary part Im[$\mu'_{r,\mathrm{eff}}(f)$] of the effective permittivity $\mu'_{r,\mathrm{eff}}$ versus frequency characteristics, taking f_{mp} as the parameter, with $f_{m0} = 4.2$ GHz and $\Gamma_m = 0.1$ GHz. (b) Real part Re[$\varepsilon'_{r,\mathrm{eff}}(f)$] and imaginary part Im[$\varepsilon'_{r,\mathrm{eff}}(f)$] of the effective permittivity $\varepsilon'_{r,\mathrm{eff}}$ versus frequency characteristics taking f_{ep} as the parameter, with $\Gamma_e = 0.1$ GHz.

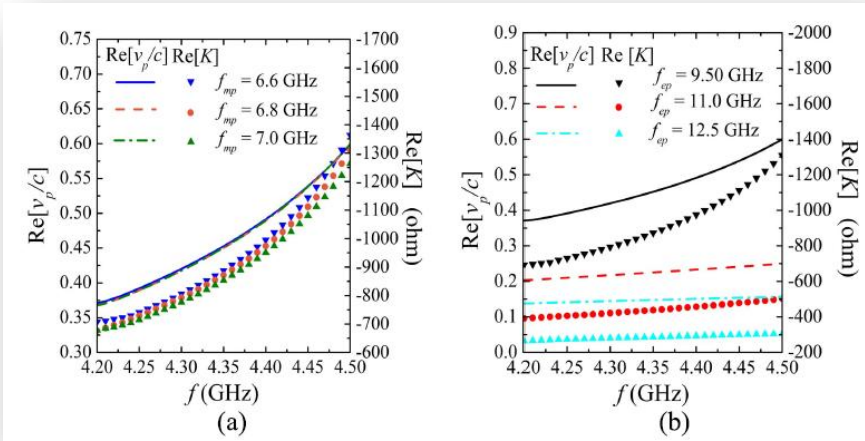

Fig. 5. Dispersion and interaction impedance versus frequency characteristics taking (a) f_{mp} as the parameter, with $f_{m0} = 4.2$ GHz and $\Gamma_m = 0.1$ GHz, and $f_{\mathrm{ep}} = 9.5$ GHz and $\Gamma_e = 0.1$ GHz and (b) f_{ep} as the parameter with $\Gamma_e = 0.1$ GHz, and $f_{m0} = 4.2$ GHz, $f_{\mathrm{mp}} = 6.8$ GHz, and $\Gamma_m = 0.1$ GHz; corresponding to the values of $\mu'_{r,\mathrm{eff}}(f)$ and $\varepsilon'_{r,\mathrm{eff}}(f)$ obtainable from Fig. 4(a) and (b), respectively, for the operating frequency f ranging between 4.2 and 4.5 GHz for the structure dimensions $a = 1.2$ mm, $b/a = 4$, and $\psi = 6.8°$.

R. Guha, A. K. Bandyopadhyay, A. K. Varshney, S. K. Datta, and B. N. Basu, "Investigations into helix slow-wave structure assisted by double-negative metamaterial," *IEEE Trans. Electron Devices*, vol. 65, no. 11, pp. 5082–5088, Nov. 2018.

Contribution of Researchers in India on MTM-VEDs (contd..)

TABLE I
SWSs IN DIFFERENT INDIVIDUAL BANDS REPORTED IN THE LITERATURE AND THE EFFECTIVE DNG-MTM PARAMETERS OF DISCRETE HELIX-SUPPORT RODS OF THE PROPOSED SINGLE SWS RESPONSIVE TO MULTIPLE BANDS OF FREQUENCIES

Reported SWSs in L-, S- and C-bands	Basic dimensions of the structures reported in literature	DNG-MTM helix support parameters of the proposed SWS
L band [30]: Helix SWS for PASOTRON	Helix radius = 25 mm, Axial periodicity = 22.8 mm, Outer envelope radius = 50 mm	f_{m0} = 1.22GHz f_{mp} = 2.0 GHz Γ_m = 0.1 GHz f_{ep} = 2.8 GHz Γ_e = 0.1 GHz
S band [11]: Periodic array of CeSRR loaded with below cut-off waveguide	Inner radius = 6 mm, Width of inner ring = 9 mm, Width of outer ring = 2 mm, Outer radius = 20 mm, Axial periodicity = 25 mm, Thickness = 1 mm	f_{m0} = 2.4GHz f_{mp} = 4.0 GHz Γ_m = 0.1 GHz f_{ep} = 6 GHz Γ_e = 0.1 GHz
S band [12]: Rectangular waveguide, operating below cutoff, loaded with two CSRR metamaterial plates	Plate width = 41 mm, Thickness = 1 mm, Axial periodicity = 8 mm, Vertical separation = 42 mm	
S band [13]: Coaxial NRI-TL	Capacitive sheet radius = 2 mm, Outer conductor radius = 5 mm, Axial periodicity = 5 mm	
S band [31]: Cylindrical deeply corrugated waveguide with cavity recessions and metallic ring inclusions as SWS	External radius = 45 mm, Internal radius = 30 mm, Cavity radius = 35 mm, Axial periodicity = 45 mm	
C band [32]: SWS same as that of S-band structure of [31] scaled at C band	External radius = 30 mm, Internal radius = 20 mm, Cavity radius = 24 mm, Axial periodicity = 36 mm	f_{m0} = 4.8GHz f_{mp} = 7.0 GHz Γ_m = 0.1 GHz f_{ep} = 11 GHz Γ_e = 0.1 GHz

Multi-band operation

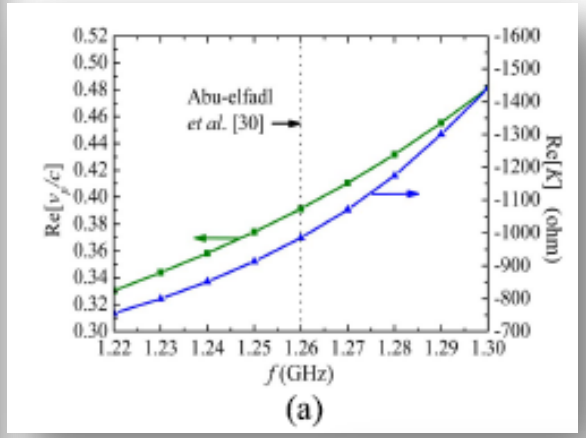

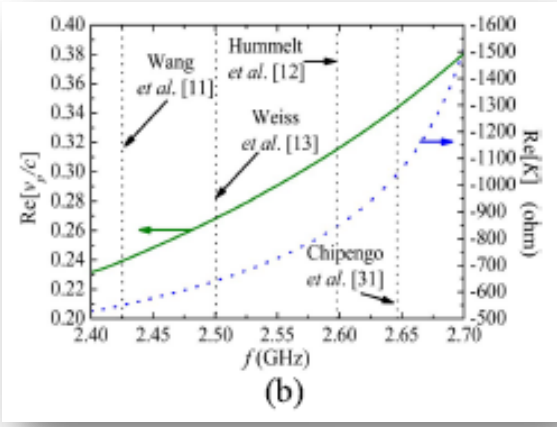

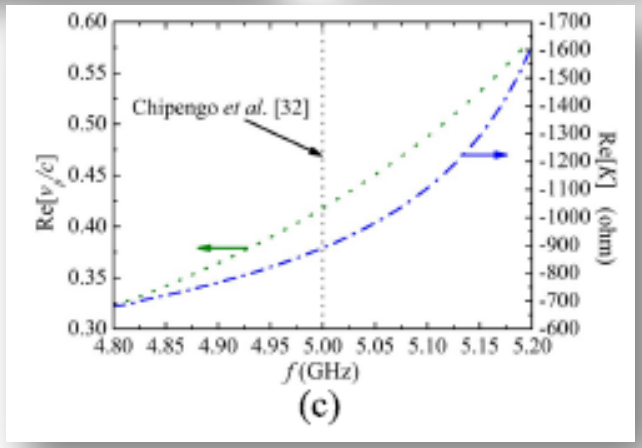

Fig. 6. Dispersion and interaction impedance versus frequency characteristics of the DNG-MTM-loaded helix SWS in (a) *L*-band, (b) *S*-band, and (c) *C*-band, corresponding to DNG-MTM parameters given in Table I, taking the structure dimensions $a = 1.2$ mm, $b = 5.0$ mm, and $\psi = 6.8°$.

R. Guha, A. K. Bandyopadhyay, A. K. Varshney, S. K. Datta, and B. N. Basu, "Investigations into helix slow-wave structure assisted by double-negative metamaterial," *IEEE Trans. Electron Devices*, vol. 65, no. 11, pp. 5082–5088, Nov. 2018.

Contribution of Researchers in India on MTM-VEDs (contd..)

Realization of DNG-MTM on Actual Discrete Helix Supports

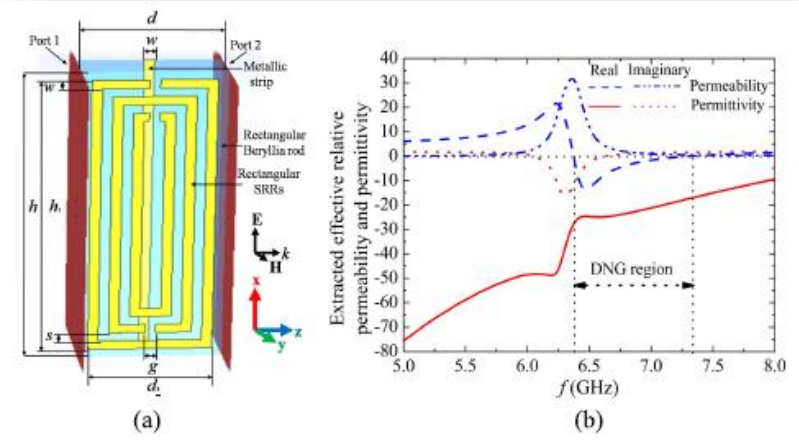

Fig. 7. (a) Unit cell of rectangular SRRs printed on the substrate of one of the radial edges of a rectangular dielectric support (Beryllia, $\varepsilon_r = 6.3$) of the helix and a metallic strip on the substrate on its other radial edge [26] ($d = 1.4$ mm, $d_1 = 1.2$ mm, $h = 3.5$ mm, $h_1 = 3.3$ mm, $w = 0.1$ mm, $s = 0.1$ mm, $g = 0.1$ mm, dielectric substrate thickness = 0.55 mm, and metallic strip thickness = 0.035 mm). (b) Extracted effective relative permeability and relative permittivity versus frequency response.

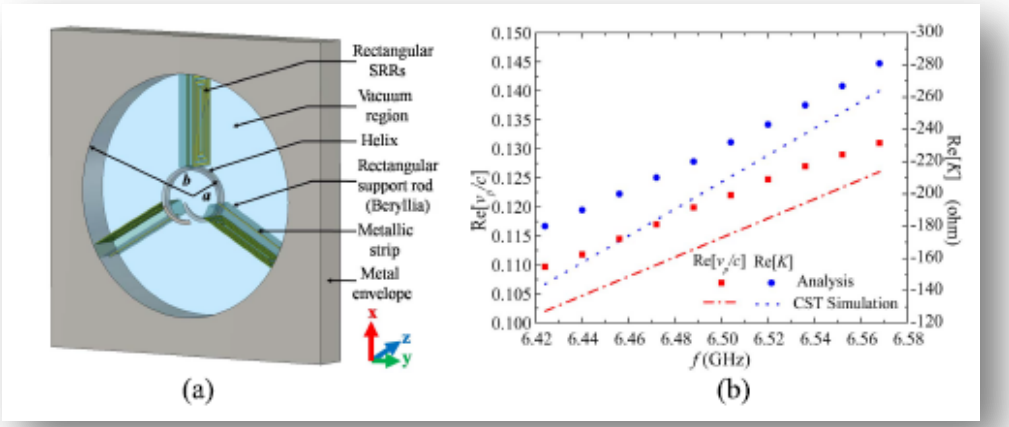

Fig. 8. (a) CST model of a single turn of the helix supported by three rectangular support rods with SRRs and metallic strip printed on each of them, as described in Fig. 7(a), (b) Dispersion and interaction impedance versus frequency characteristics of the structure, taking the typical structure dimensions $a = 1.0$ mm, $b = 4.575$ mm, and $\psi = 12.56°$, in the DNG frequency range reduced to 6.42–6.57 GHz due to smoothing out of the discrete supports into a continuous medium (as shown in Fig. 2, Section III-A).

R. Guha, A. K. Bandyopadhyay, A. K. Varshney, S. K. Datta, and B. N. Basu, "Investigations into helix slow-wave structure assisted by double-negative metamaterial," *IEEE Trans. Electron Devices*, vol. 65, no. 11, pp. 5082–5088, Nov. 2018.

Researchers of Metamaterial assisted Microwave Tubes

Prof. B. N. Basu
Ex-Professor and -Head, Electronics Engineering Department, and Ex-Coordinator
IIT-BHU, UP, India

Dr. Subrata. K. Datta
Associate Director
MTRDC-DRDO, Bangalore, India

Dr. Sanjay K. Ghosh
Senior Principal Scientist, MWD area
CSIR-CEERI, Pilani, Rajasthan, India

Dr. Ayan K. Bandyopadhyay
Principal Scientist, MWD area
CSIR-CEERI, Pilani, Rajasthan, India

Dr. Anirban Bera
Principal Scientist, MWD area
CSIR-CEERI, Pilani, Rajasthan, India

Dr. Purushothaman N
Scientist, MWD area
CSIR-CEERI, Pilani, Rajasthan, India

Mr. Amit K. Varshney
Assistant Professor of E.C.E
SKFGI, Mankundu, Hooghly, India

Mr. Raktim Guha
Senior Project Assistant, MWD area
CSIR-CEERI, Pilani, Rajasthan, India

References

1) T. Roy, D. Banerjee, and S. Kar, "Studies on Multiple Inclusion Magnetic Structures Useful for Millimeter-wave Left Handed Metamaterial Applications", *IETE J. Res*. vol.55, pp.83-89, Mar. 2009.
2) D. Banerjee, T. Roy and S. Kar, "A Computer-Aided Analytical Study on the Characteristics of Left Handed Material Structures at Microwave Frequencies", *IETE J. Res*. vol. 55, pp.112-117, May 2009.
3) J. B.Pendry, A. J. Holden and W. J. Stewart, I. Youngs, "Extremely Low Frequency Plasmons in Metallic Mesostructures" *et al.*, *Phys. Rev. Lett.* vol. 76, no. 25, pp. 4773-4776, June 1996.
4) J. B. Pendry, A. J. Holden, D. J. Robbins, and W. J. Stewart, "Magnetism from conductors and enhanced nonlinear phenomena," *IEEE Trans. Microw. Theory Techn.*, vol. 47, no. 11, pp. 2075–2084, Nov. 1999.
5) J. D. Baena *et al*., "Equivalent-Circuit Models for Split-Ring Resonators and Complementary Split-Ring Resonators Coupled to Planar Transmission Lines," *IEEE Tran. on Micro. Theo. and Tech*., vol. 53, no. 4, pp. 1451-1461, Apr. 2005.
6) F. Falcone *et al*., "Babinet principle applied to the design of metasurfaces and metamaterials," *Phys. Rev. Lett*., vol. 93, p. 197401, Nov. 2004.
7) V. G. Veselago, "The electrodynamics of substances with simultaneously negative values of ε *and* μ," *Sov. Phys. Uspekhi*, vol. 47, pp. 509–514, Jan. 1968.
8) D. R. Smith, W. J. Padilla, D. C. Vier, S. C. Nemat-Nasser, and S. Schultz, "Composite medium with simultaneously negative permeability and permittivity," *Phys. Rev. Lett., vol. 84, pp. 4184–4187*, May 2000.
9) R. Marques, J. Martel, F. Mesa, and F. Medina, "Left-Handed-Media Simulation and Transmission of EM Waves in Sub-wavelength Split-Ring-Resonator-Loaded Metallic Waveguides", *Phys. Rev. Lett*. Vol. 89, no. 18, pp. 183901-1: 183901-1, Oct. 2002.
10) Z. Duan, J. S. Hummelt, M. A. Shapiro, and R. J. Temkin, "Sub-wavelength waveguide loaded by a complementary electric metamaterial for vacuum electron devices," *Phys. Plasmas*, vol. 21, no. 10, pp. 103301-1–103301-6, Oct. 2014.

References

11) D. R. Smith, D. C. Vier, T. Koschny, and C. M. Soukoulis, "Electromagnetic parameter retrieval from inhomogeneous metamaterials," *Phys. Rev. E, Stat. Phys. Plasmas Fluids Relat. Interdiscip. Top.*, vol. 71, pp. 036617-1–036617-11, Mar. 2005.

12) D. Schurig, J. J. Mock, anda D. R. Smith, "Electric-field-coupled resonators for negative permittivity metamaterials," *Appl. Phys. Lett.* Vol. 88, p. 041109, Jan. 2006.

13) Y. S. Tan and R. Seviour, "Wave energy amplification in a metamaterial based traveling-wave structure," *Europhys. Lett.*, vol. 87, no. 3, p. 34005, Aug. 2009.

14) A. Rashidi and N. Behdad, "Metamaterial-enhanced traveling wave tubes," in *Proc. IEEE Int. Vac. Electron. Conf. (IVEC)*, Monterey, CA, USA, Apr. 2014, pp. 199–200,.

15) D. M. French , D. Shiffler, and K. Cartwright "Electron beam coupling to a metamaterial structure," *Phys. Plasmas*, vol. 20, no. 5, p. 083116, Aug. 2013.

16) Y. Wang *et al.*, "All-metal metamaterial slow-wave structure for high power sources with high efficiency," *Appl. Phys. Lett.*, vol. 107, no. 15, pp. 153502-1–153502-4, Oct. 2015.

17) S. C. Yurt, M. I. Fuks, S. Prasad, and E. Schamiloglu, "Design of a metamaterial slow wave structure for an O-type high power microwave generator," *Phys. Plasmas*, vol. 23, no. 12, p. 123115, Dec. 2016.

18) G. Wu, Q. Li , X. Lei, C. Ding , X. Jiang, S.u Fang, R. Yang, F. Wang, L. Yue, Y. Gong, and Y. Wei, "Design of a Cascade Backward-Wave Oscillator Based on Metamaterial Slow-Wave Structure," *IEEE Trans. Electron Devices*, vol. 65, no. 3, pp. 1172–1178, March 2018.

19) S. K. Datta, L. Kumar, and B. N. Basu, "Investigation into a metamaterial supported helix slow-wave structure," in *Proc. IEEE Int. Vac. Electron. Conf. (IVEC)*, Bangalore, India, Feb. 2011, pp. 211–212.

20) N. Purushothaman and S. K. Ghosh, "Performance improvement of helix TWT using metamaterial helix-support structure," *J. Electromagn. Waves Appl.*, vol. 27, no. 7, pp. 890–900, Apr. 2013.

21) N. Purushothaman , A. Jain, W. R. Taube, R. Gopal, S. K. Ghosh, "Modeling and fabrication studies of negative permeability metamaterial for use in waveguide applications", *Microsyst Technol*, Volume 21, issue 11, pp 2415–2424, Nov. 2015.

References

22) A. K. Varshney, R. Guha, S. K. Datta, and B. N. Basu, "Dispersion control of helical slow-wave structure by double-negative metamaterial loading," *J. Electromagn. Waves Appl.*, vol. 30, no. 10, pp. 1308–1320, Jun. 2016.

23) A. K. Varshney, R. Guha, S. Biswas, P. P. Sarkar, S. K. Datta, and B. N. Basu, "Tape-helix model of analysis for the dispersion and interaction impedance characteristics of a helix loaded with a double-negative metamaterial for potential application in vacuum electron devices", *J. Electromagn. Waves Appl.*, vol. 33, no. 2, pp. 138-150, Oct. 2018.

24) R. Guha, A. K. Bandyopadhyay, A. K. Varshney, S. K. Datta, and B. N. Basu, "Investigations into helix slow-wave structure assisted by double-negative metamaterial," *IEEE Trans. Electron Devices*, vol. 65, no. 11, pp. 5082–5088, Nov. 2018.


Thank You!

EM Analysis of RF Interaction Structures for Their Potential Application in Gyro-Devices

Presented by

Dr. Rajiv Kumar Singh

Department of Electronics Engineering
Institute of Engineering & Technology, Lucknow 226 021, India

Contents

- **INTRODUCTION**
- **EM ANALYSIS RF STRUCTURES**
  - ***Tapered Structure***
  - ***Vane-Loaded Structure***
  - ***Disc-Loaded Structure***
- **RESULT AND DISCUSSION**
- **CONCLUSION**
- **REFERENCES**

Gyro-Travelling Wave Tube Amplifier

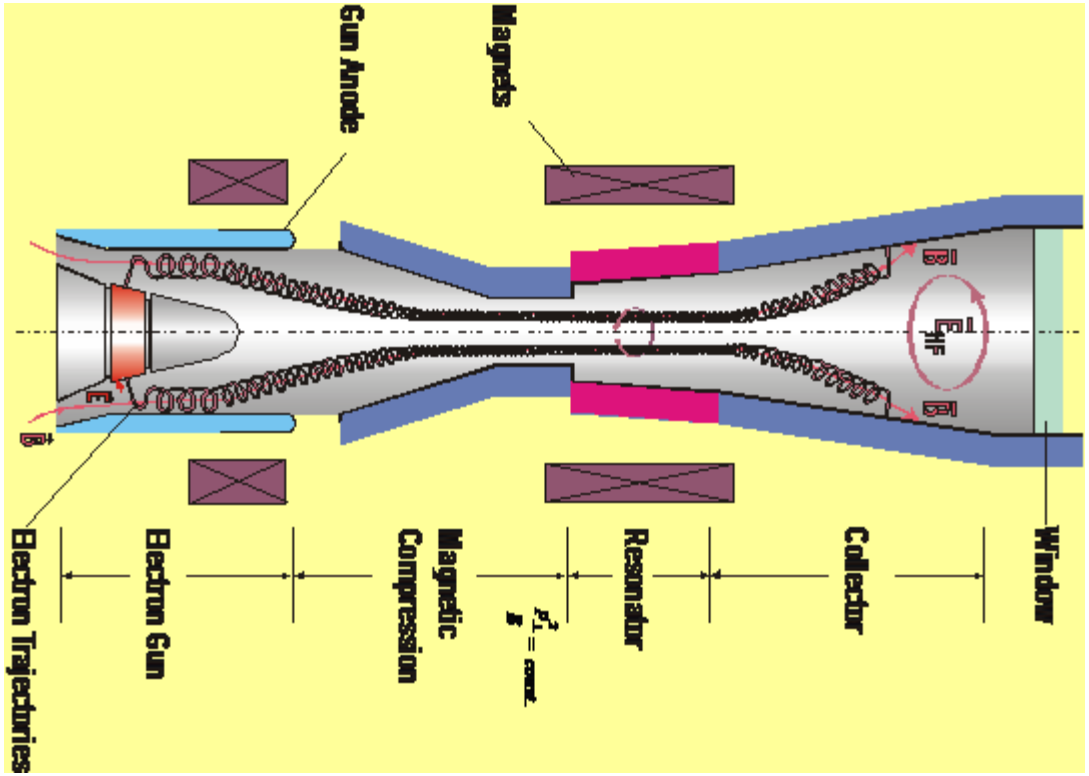

Fig. 1: Gyro-TWT Amplifier [1]

An annular e-beam is produced in a magnetron Injection gun (MIG). The electrons perform helical motions along the magnetic field lines with the cyclotron frequency $\Omega c = (eB)/(m0\gamma)$.

In the interaction region , the e-beam interacts with RF fields. Energy from the e-beam is transferred to the RF fields.

The spent e-beam is dissipated on the collector surface and the generated microwave is extracted through an output window.

Applications

- **Point-to-point communication — more channels, focused radiation**
- **High information density communication**
- **Long-range, high resolution radar**
- **Medical applications: Hyperthermia**
- **Industrial heating**
- **Material processing**

Bandwidth: Limitations & Solutions

- Smooth wall Gyro-TWTs are not capable of providing fairly wide bandwidths due to rapid increase in the group velocity with frequency

✓Suitable selection of beam and magnetic field parameters reported 3-dB bandwidth upto 8%

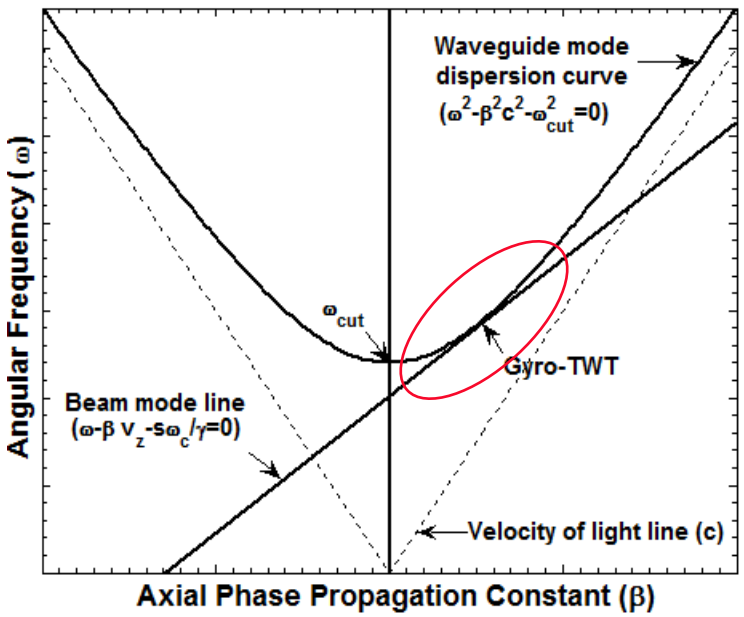

Fig. 2: Dispersion Curve

✓Controlling dispersion characteristics of the waveguide for wideband coalescence between the beam-mode and waveguide-mode dispersion characteristics

Methods of Broadbanding Gyro-TWT

i) By helix loading

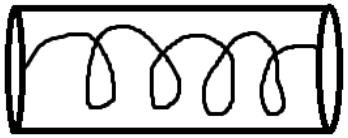

Problem of mode competition

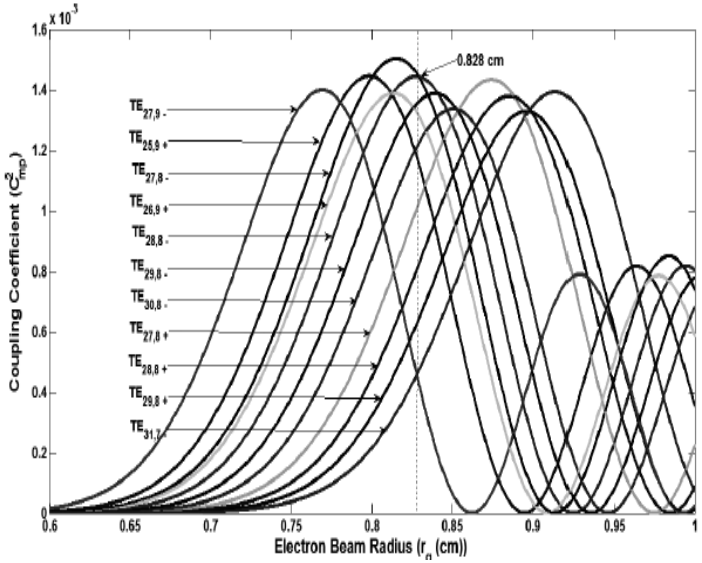

Fig. 3: Mode density in helix loaded Structure [10]

ii) By dielectric lining the metal wall

iii) By placing a dielectric rod at the axis of the guide

iv) Two stage dielectric loading

Entails the risk of dielectric charging that results into heating if the dielectric is lossy

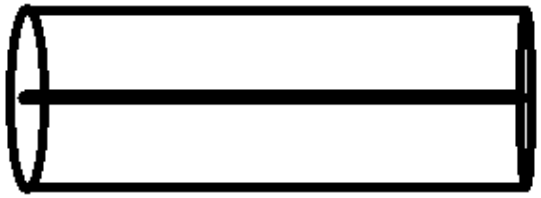

Fig. 4: Central Dielectric Loaded [8]

EM Analysis of Some RF Structure

- **Tapered Structure**
- **Vane-Loaded Structure**
- **Disc-Loaded Structure**

Tapered Structure

- The tapered waveguide is similar to the normal waveguide but with an addition of the parameter tapering angle θ.
- Length of the structure(L).
- Initial radius(r_o).
- Taper angle
- The relation between the tapered waveguide radius and tapering angle is
- $\frac{r(z)}{r(0)} = 1 + \frac{z \tan\theta}{r\left(\frac{l}{2}\right) - \frac{l}{2}\tan\theta}$

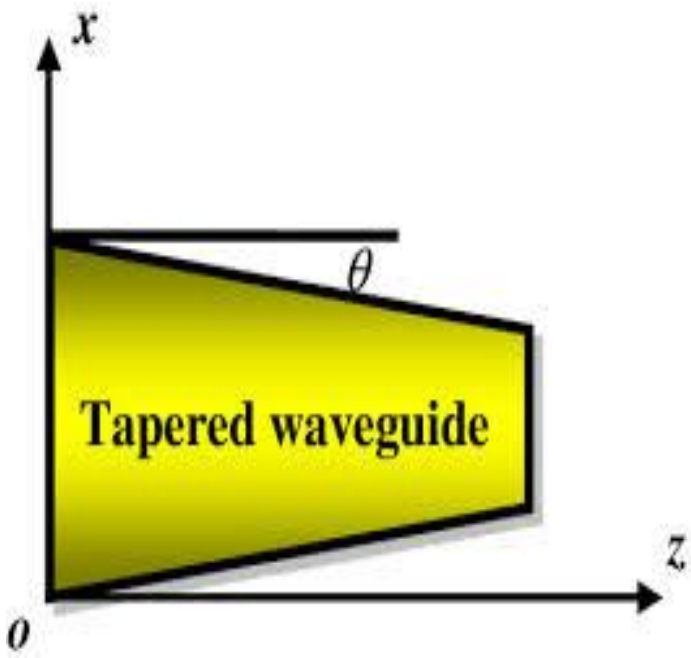

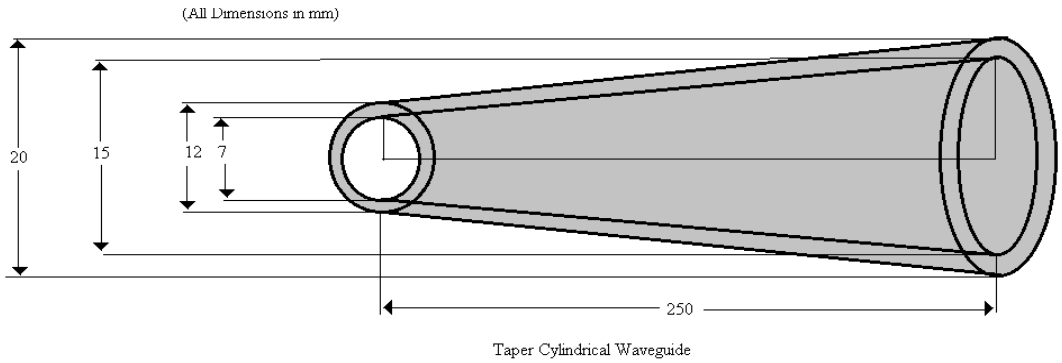

Fig. 5: Tapered RF Structure

Analysis of Tapered RF Structure

Commensurate with the taper of the waveguide cross section, In order to maintain the condition of cyclotron resonance throughout the length of the waveguide. Let us choose to taper $B_o\{z\}$ along the taper:

$$\frac{B_o}{B_g} = constant$$

$$\frac{B_o\{z\}}{B_o\{0\}} = \frac{\gamma_z^2\{0\}\left(\frac{v_t\{0\}}{c}\right)^2 + \left(\left(\gamma_z^2\{0\}\left(\frac{v_t\{0\}}{c}\right)^2\right)^2 + 4\left(\frac{r_W\{z\}}{r_w\{0\}}\right)^2(\gamma_z\{0\}/\gamma)^2\right)^{1/2}}{2\left(\frac{r_W\{z\}}{r_w\{0\}}\right)^2}$$

- The dispersion relation for a tapered waveguide is given by

- **Dispersion Relation**
- $$\left(k_o{}^2 - \beta^2 - k_c{}^2\right)\left(\omega - \beta v_t - \frac{s\omega_c}{\gamma}\right)^2 = -\frac{\mu_o|c|^2 N_o (v_t/c)^2(\omega^2-\beta^2c^2)J_{x-m}^2\{k_c r_H\}J_S'^2\{k_c r_L\}}{\gamma m_{eo}\pi r_W^2\left[1-\left(\frac{m}{k_c r_W)^2}\right]J_m'^2\{k_c r_W\}\right.}$$

Analysis of Vane-Loaded RF Structure

The Structure

r_W is the waveguide wall radius
r_v is the vane radius
N is the number of vanes
Ø is the vane angle

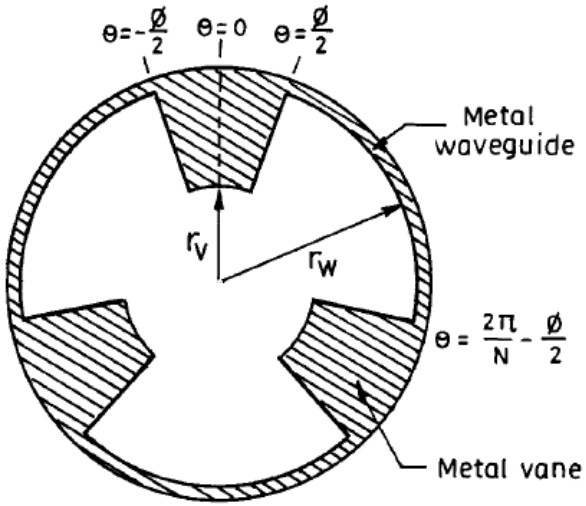

Fig. 6: Vane-Loaded RF Structure

Vane-free Free-space region, Labelled as region-I

$$0 \le r < r_v$$

Propagating waves

Vane-occupied Free-space, Labelled as region-II

$$r_v \le r < r_W$$

Propagating waves

Field Expressions in Vane-Loaded Structure

Vane-Free Region

$$E_{z,1} = 0$$

$$H_{z,1} = \sum_{m=-\infty}^{\infty} \left(A_{m,1} J_{mN}\left\{k_c r\right\} + B_{m,1} Y_{mN}\left\{k_c r\right\} \right)$$

$$E_{r,1} = \sum_{m=-\infty}^{\infty} -\left(mN\omega\mu_o / \left(k_c^2 r \right) \right) \left(A_{m,1} J_{mN}\left\{k_c r\right\} + B_{m,1} Y_{mN}\left\{k_c r\right\} \right)$$

$$H_{r,1} = \sum_{m=-\infty}^{\infty} -\left(j\beta / \left(k_c \right) \right) \left(A_{m,1} J'_{mN}\left\{k_c r\right\} + B_{m,1} Y'_{mN}\left\{k_c r\right\} \right)$$

$$E_{\theta,1} = \sum_{m=-\infty}^{\infty} -\left(j\omega\mu_o / \left(k_c \right) \right) \left(A_{m,1} J'_{mN}\left\{k_c r\right\} + B_{m,1} Y'_{mN}\left\{k_c r\right\} \right)$$

$$H_{\theta,1} = \sum_{m=-\infty}^{\infty} -\left(mN\beta / \left(k_c^2 r \right) \right) \left(A_{m,1} J_{mN}\left\{k_c r\right\} + B_{m,1} Y_{mN}\left\{k_c r\right\} \right)$$

Vane-Occupied Region

$$E_{z,2} = 0$$

$$H_{z,2} = \sum_{m=-\infty}^{\infty} \left(A_{m,2} J_{mN}\left\{k_c r\right\} + B_{m,2} Y_{mN}\left\{k_c r\right\} \right)$$

$$E_{r,2} = \sum_{m=-\infty}^{\infty} -\left(mN\omega\mu_o / \left(k_c^2 r \right) \right) \left(A_{m,2} J_{mN}\left\{k_c r\right\} + B_{m,2} Y_{mN}\left\{k_c r\right\} \right)$$

$$H_{r,2} = \sum_{m=-\infty}^{\infty} -\left(j\beta / \left(k_c \right) \right) \left(A_{m,2} J'_{mN}\left\{k_c r\right\} + B_{m,2} Y'_{mN}\left\{k_c r\right\} \right)$$

$$E_{\theta,2} = \sum_{m=-\infty}^{\infty} -\left(j\omega\mu_o / \left(k_c \right) \right) \left(A_{m,2} J'_{mN}\left\{k_c r\right\} + B_{m,2} Y'_{mN}\left\{k_c r\right\} \right)$$

$$H_{\theta,2} = \sum_{m=-\infty}^{\infty} -\left(mN\beta / \left(k_c^2 r \right) \right) \left(A_{m,2} J_{mN}\left\{k_c r\right\} + B_{m,2} Y_{mN}\left\{k_c r\right\} \right)$$

Field expressions

Boundary conditions

Integration within limits of validity

Elimination of field constants

Dispersion relation

Boundary Conditions in Vane-Loaded

$$E_{\theta,1} = E_{\theta,2}\Big|_{r=r_V} \qquad (\phi/2 \le \theta \le 2\pi/N - \phi/2)$$

$$E_{\theta,2} = 0\Big|_{r=r_W} \qquad (\phi/2 \le \theta \le 2\pi/N - \phi/2)$$

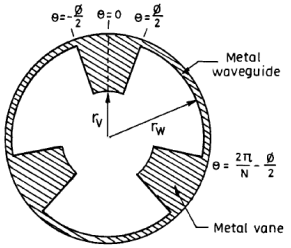

$$H_{\theta,1} = H_{\theta,2}\Big|_{r=r_V} \qquad (\phi/2 \le \theta \le 2\pi/N - \phi/2)$$

$$H_{r,1} = 0\Big|_{r=r_V} \qquad (-\phi/2 \le \theta \le \phi/2)$$

Dispersion Relation of Vane-Loaded RF Structure

$$\alpha_q A_{q,1} + \sum_{\substack{m=-\infty \\ m\neq q}}^{\infty} \delta_{m,q} A_{m,1} = 0$$

$$\alpha_q = J'_{qN}\{k_C r_V\}\varphi + \left((1+\eta_q) J_{qN}\{k_C r_V\} - \eta_q \frac{J'_{qN}\{k_C r_V\}}{Y'_{qN}\{k_C r_V\}} Y_{qN}\{k_C r_V\} \right)(2\pi/N - \varphi)$$

Where, $\delta_{m,q} = \dfrac{2\sin\left((m-q)(N\phi/2)\right)}{(m-q)N} \times \left(J'_{mN}\{k_c r_V\} - \left((1+\eta_m) J_{mN}\{k_c r_V\} + \eta_m \dfrac{J'_{mN}\{k_c r_V\}}{Y'_{mN}\{k_c r_V\}} Y_{mN}\{k_c r_V\} \right) \right)$

$$\eta_{m \text{ or } q} = \frac{J'_{mN}\{k_c r_V\} Y'_{mN}\{k_c r_W\}}{J'_{mN}\{k_c r_W\} Y'_{mN}\{k_c r_V\} - J'_{mN}\{k_c r_V\} Y'_{mN}\{k_c r_W\}}$$

Analysis of Disc-Loaded Cylindrical Waveguide

The Structure

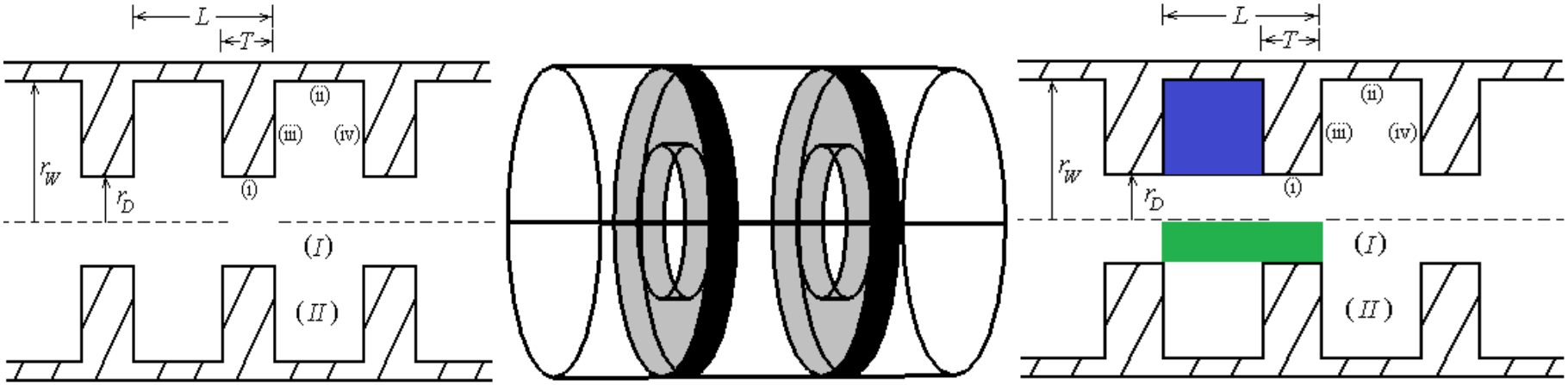

Fig. 7: Disc-Loaded Structure

Disc-free region, Labelled as region-I

$$0 \le r < r_D, \qquad 0 < z < L$$

$$\beta_n^I = \beta_0^I + 2\pi n / L, \quad (n = 0, \pm 1, \pm 2, \ldots \pm \infty)$$

$$\gamma_n^I = [k^2 - (\beta_n^I)^2]^{1/2}$$

Propagating waves

Disc-occupied region, Labelled as region-II

$$r_D \le r < r_W, \qquad 0 < z < L - T$$

$$\beta_m^{II} = m\pi / L - T, \quad (m = 1, 2, 3, \ldots \infty)$$

$$\gamma_m^{II} = [k^2 - (\beta_m^{II})^2]^{1/2}$$

Standing waves

Field Expressions in Disc-Loaded RF Structure

Disc-Free Region

$$H_z^I = \sum_{n=-\infty}^{+\infty} A_n^I J_0\{\gamma_n^I r\} exp\, j(\omega t - \beta_n^I z)$$

$$E_\theta^I = j\omega\mu_0 \sum_{n=-\infty}^{+\infty} \frac{1}{\gamma_n^I} A_n^I J_0'\{\gamma_n^I r\} exp\, j(\omega t - \beta_n^I z)$$

$$H_r^I = -j \sum_{n=-\infty}^{+\infty} \frac{\beta_n^I}{\gamma_n^I} A_n^I J_0'\{\gamma_n^I r\} exp\, j(\omega t - \beta_n^I z)$$

$$E_z^I = 0$$

$$H_\theta^I = 0$$

where $\beta_n = \beta_0 + \dfrac{2n\pi}{L}$

$(n = 0, \pm 1, \pm 2, ...)$

Disc-Occupied Region

$$H_z^{II} = \sum_{m=1}^{\infty} A_m^{II} Z_0\{\gamma_m^{II} r\} exp(j\omega t)\, sin(\beta_m^{II} z)$$

$$E_\theta^{II} = j\omega\mu_0 \sum_{m=1}^{\infty} \frac{1}{\gamma_m^{II}} A_m^{II} Z_0'\{\gamma_m^{II} r\} exp(j\omega t)\, sin(\beta_m^{II} z)$$

$$H_r^{II} = -\frac{j\beta_m^{II}}{\gamma_m^{II}} \sum_{m=1}^{\infty} A_m^{II} Z_o'\{\gamma_m^{II} r\} exp(j\omega t) sin(\beta_m^{II} z)$$

$$H_\theta^{II} = 0$$

$$E_r^{II} = 0$$

where

$$Z_o\{\gamma_m^{II} r\} = J_o\{\gamma_m^{II} r\} Y_0'\{\gamma_m^{II} r_W\} - J_0'\{\gamma_m^{II} r_W\} Y_o\{\gamma_m^{II} r\}$$

$$\beta_m^{II} = \frac{m\pi}{L - T} \qquad (m = 1,2,3,...)$$

Boundary Conditions in Disc-Loaded Structure

$$E_\theta^I = \begin{cases} E_\theta^{II} & 0 < z < (L-T) \\ 0 & (L-T) \le z \le L \end{cases} \qquad (r = r_D)$$

$$H_z^I = H_z^{II} \qquad 0 < z < (L-T) \qquad (r = r_D)$$

$$E_\theta^{II} = 0 \qquad 0 \le z < \infty \qquad (r = r_W)$$

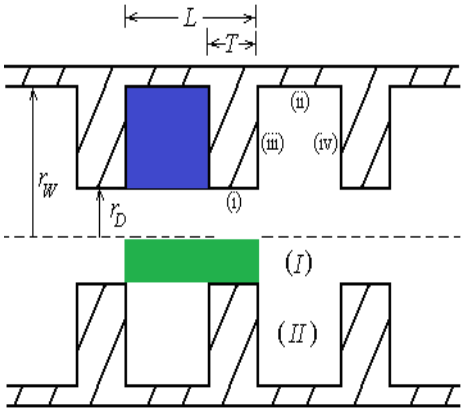

Dispersion Relation of Disc-Loaded Structure

$$det\left| \Im_{n\,m}\, J_0\{\gamma_n^I r_D\}\, Z_0'\{\gamma_m^{II} r_D\} - Z_0\{\gamma_m^{II} r_D\}\, J_0'\{\gamma_n^I r_D\} \right| = 0$$

$$(-\infty < n < +\infty,\ 1 \le m < \infty),$$

where $$\Im_{nm} = \frac{\gamma_n^I \beta_m^{II}\left(1-(-1)^m exp[-j\beta_n^I(L-T)]\right)}{\gamma_m^{II}\left[\beta_m^{II} - exp(-j\beta_0^I L)\left(\beta_m^{II} cos(\beta_m^{II} L) + j\beta_n^I sin(\beta_m^{II} L)\right)\right]}$$

Field expressions

Boundary conditions

Integration within limits of validity

Elimination of field constants

Dispersion relation

Results
(Simulation and Analytical)

Dispersion Characteristics of Tapered RF Structure

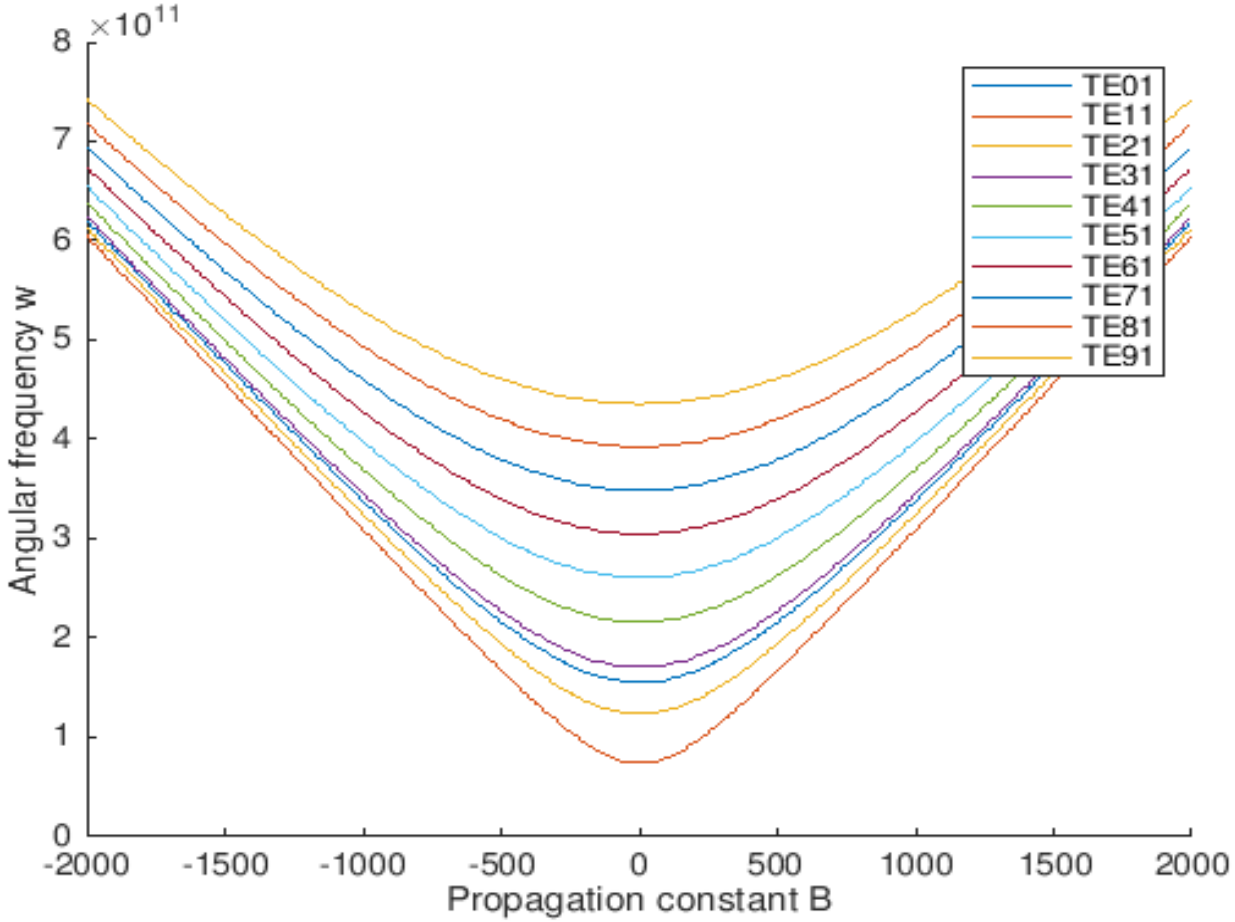

Fig. 8. Dispersion plot for the tapered structure in TEm1 mode.

Dispersion Characteristics of Tapered RF Structure

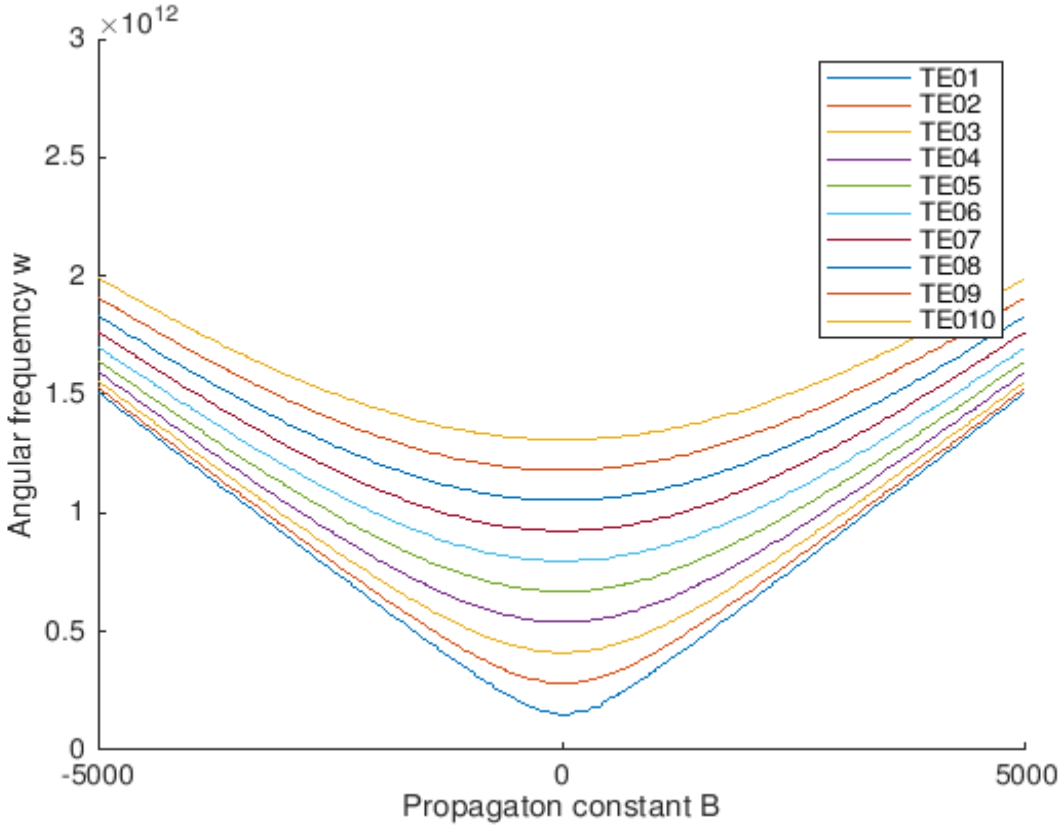

Fig. 9. Dispersion plot for tapered structure in TE0p mode.

Dispersion Characteristics of Vane-Loaded RF Structure

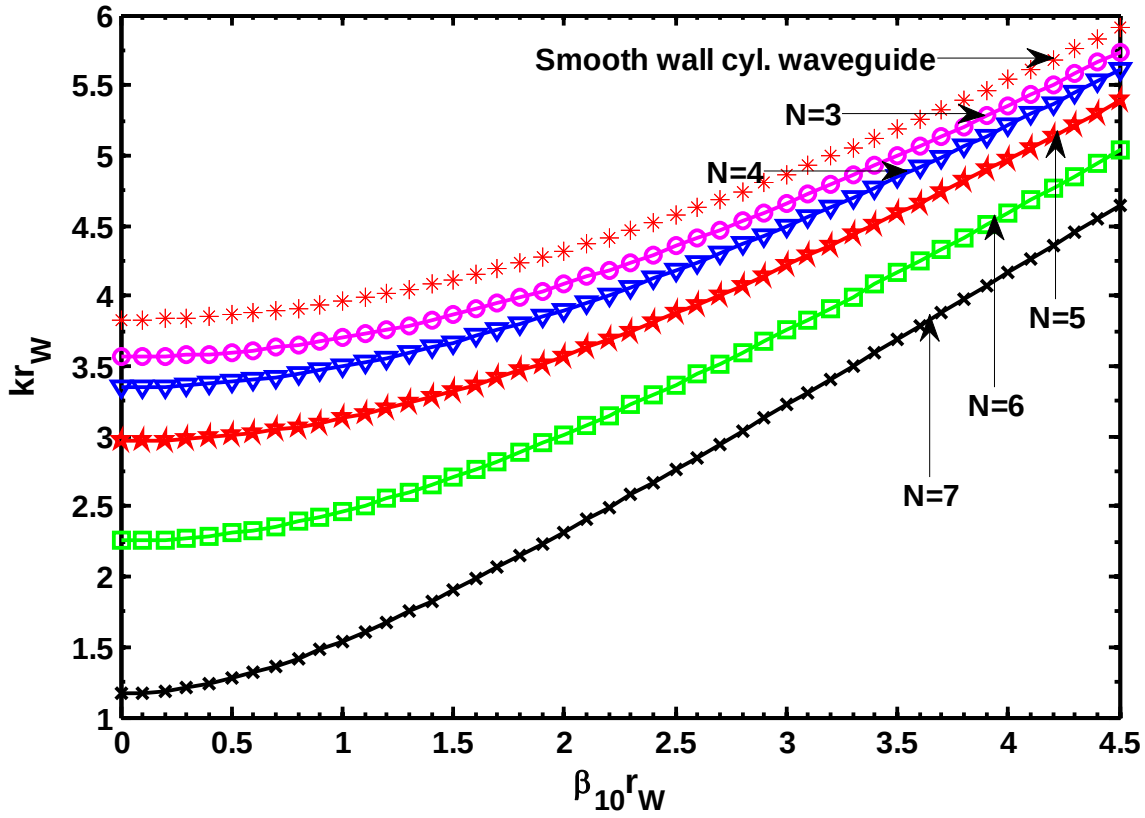

Fig. 10 Dispersion characteristics of a vane-loaded cylindrical waveguide excited in TE_{01} mode, taking number of vanes as a parameter.

Dispersion Characteristics of Vane-Loaded RF Structure

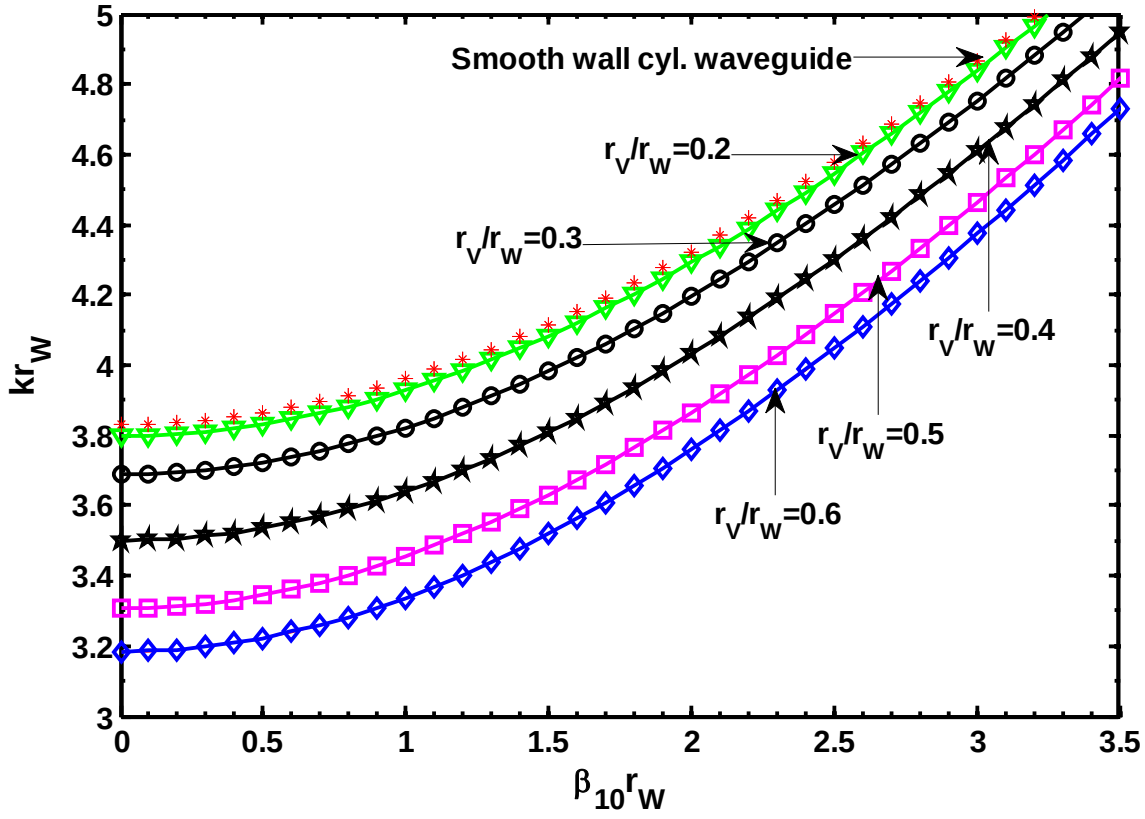

Fig. 11 Dispersion characteristics of a vane-loaded cylindrical waveguide excited in TE_{01} mode, taking vane-depth as a parameter.

Dispersion Characteristics of Vane-Loaded RF Structure

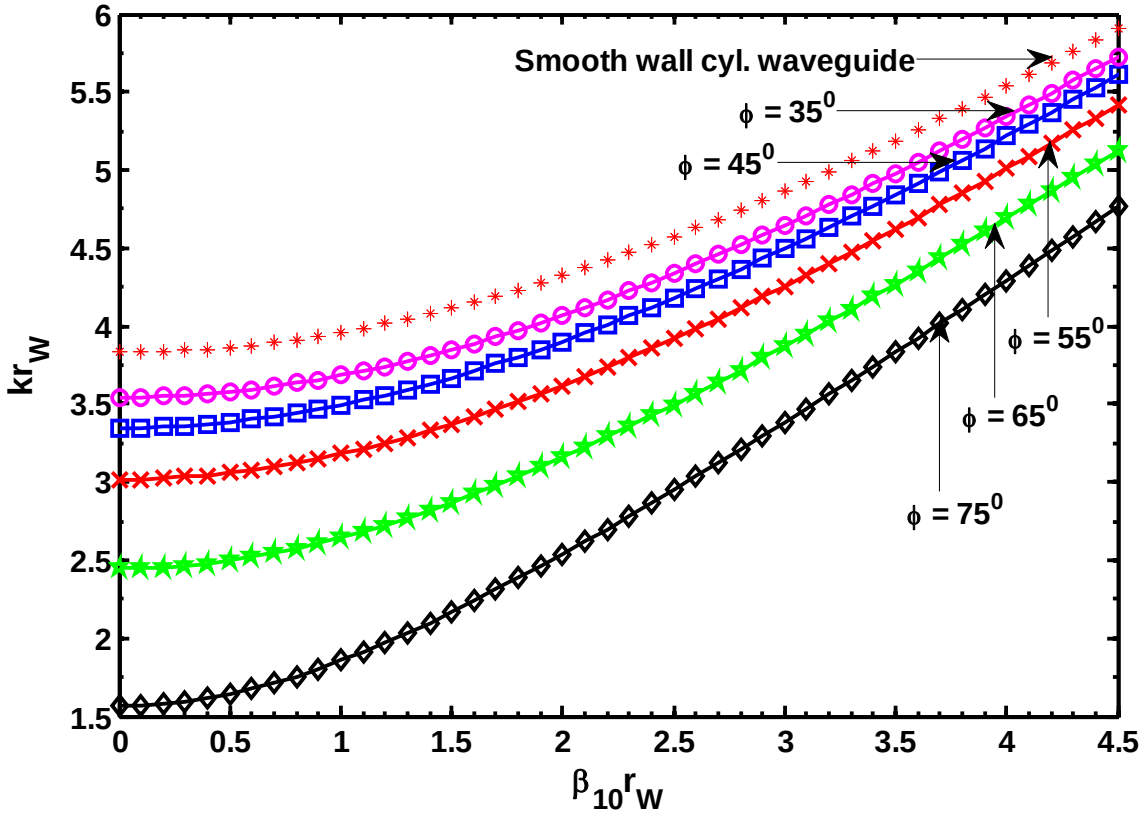

Fig. 12 Dispersion characteristics of a vane-loaded cylindrical waveguide excited in TE_{01} mode, taking vane-angle as a parameter.

EIGENMODE ANALYSIS OF DISC-LOADED CYLINDRICAL WAVEGUIDE

TE_{01}

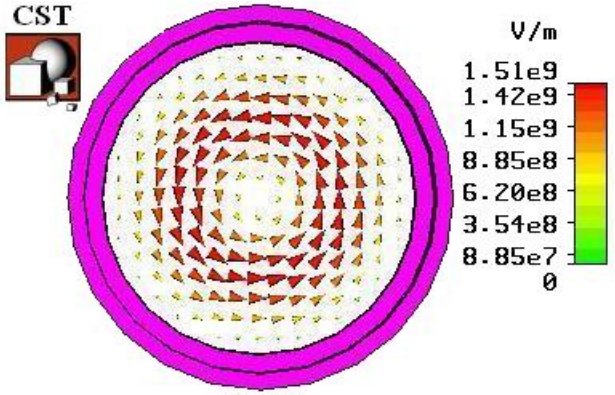

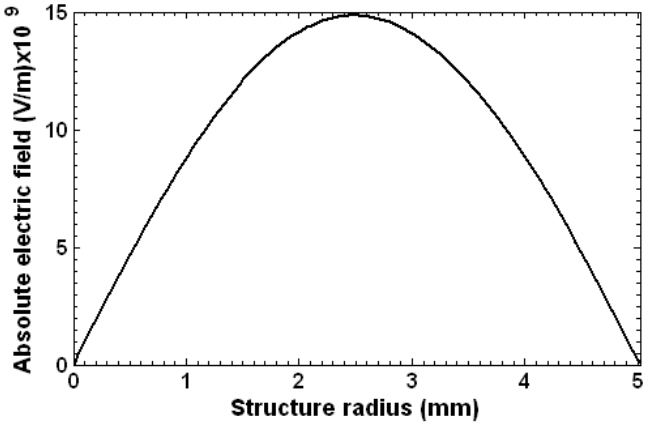

TE_{02}

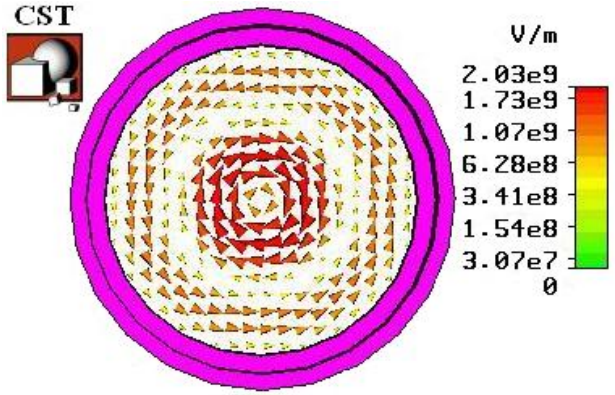

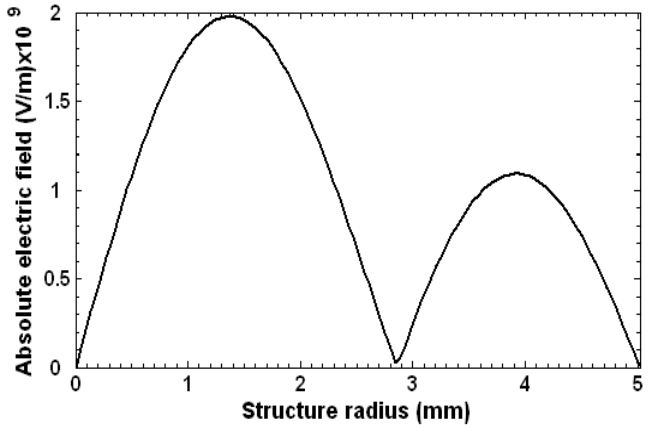

TE_{03}

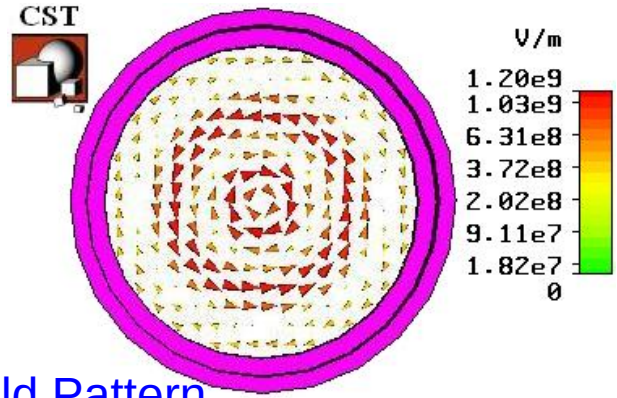

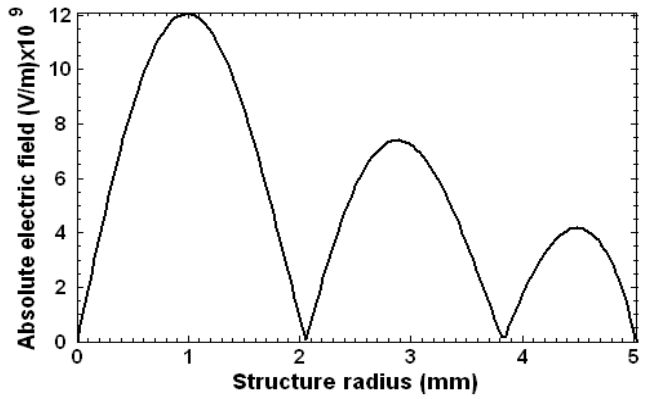

Fig. 13 Field Pattern

PROPAGATION OF ELECTRIC FIELD IN A DISC-LOADED WAVEGUIDE

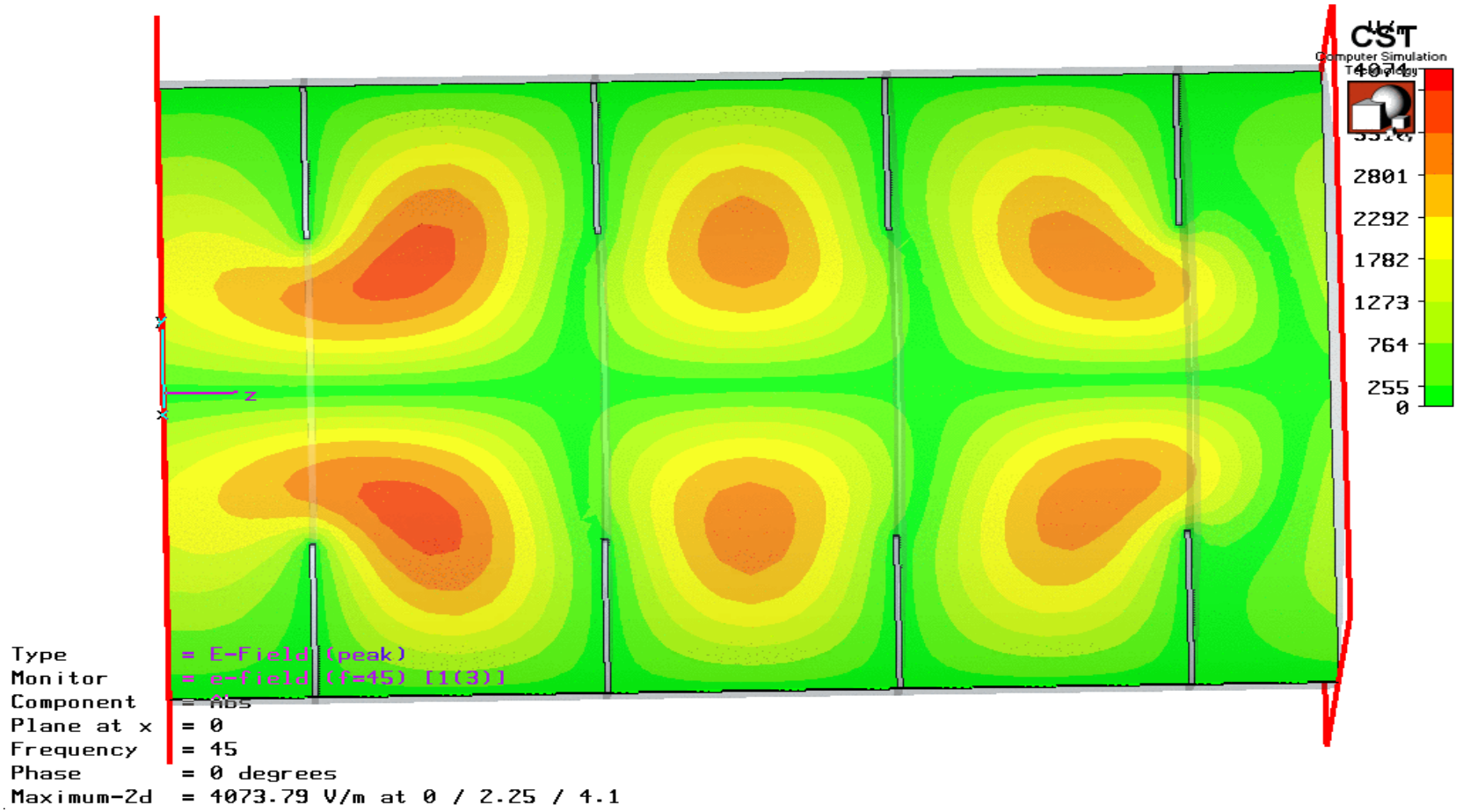

Fig. 14: E-Field propagation in Disc-Loaded Structure

Dispersion Characteristics of Disc-Loaded

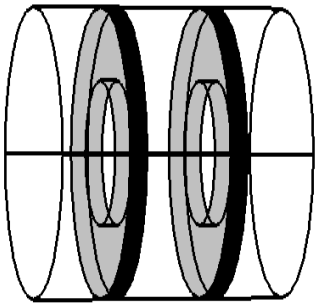

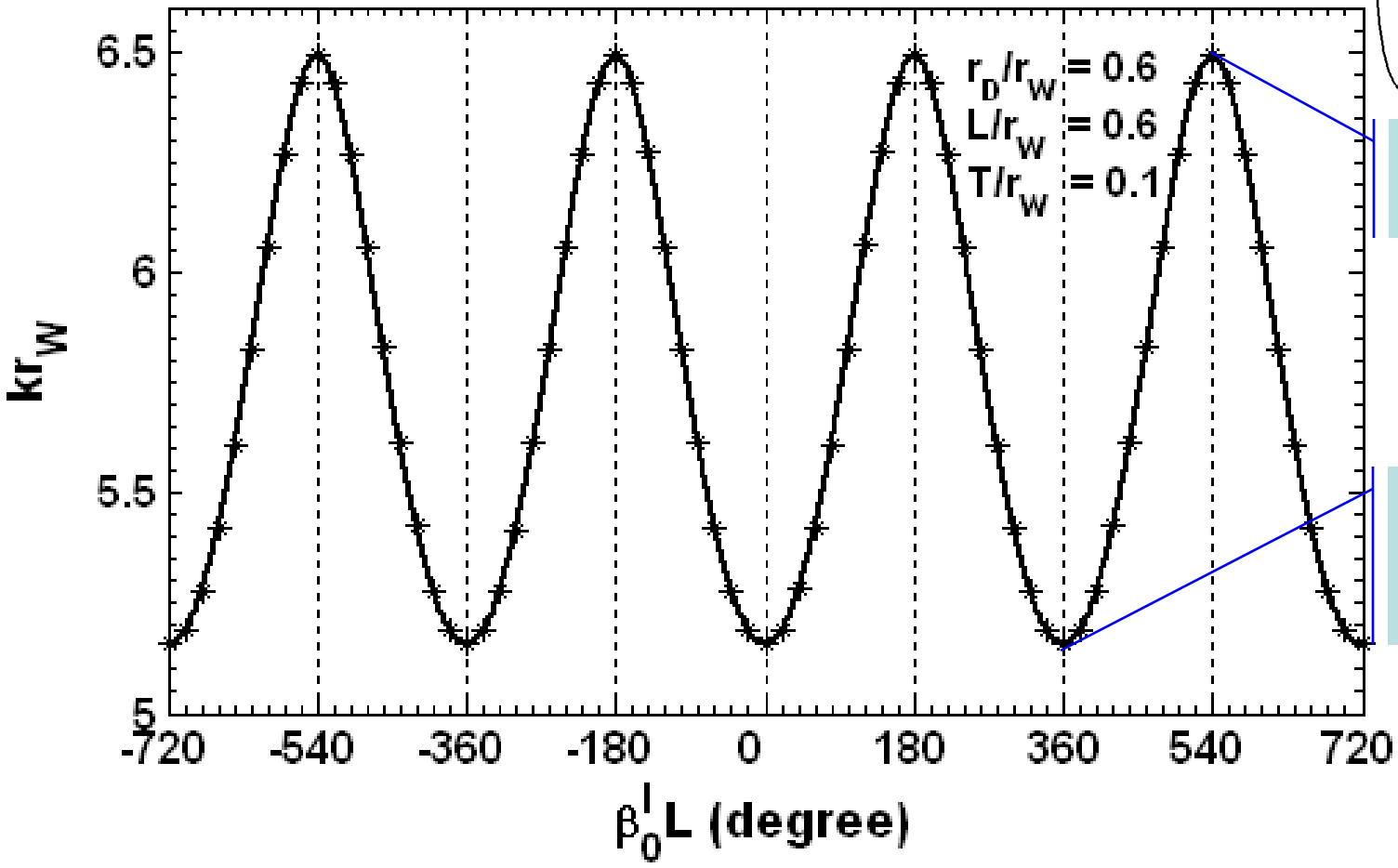

Upper cut-off due to discs

Lower cut-off due to waveguide wall radius

Fig. 15: Band pass characteristics of a disc-loaded cylindrical waveguide excited in TE_{01} mode (solid curve) validated against those obtained from CST Microwave Studio (asterisk). Results agree <1%.

Dispersion Characteristics of Disc-Loaded

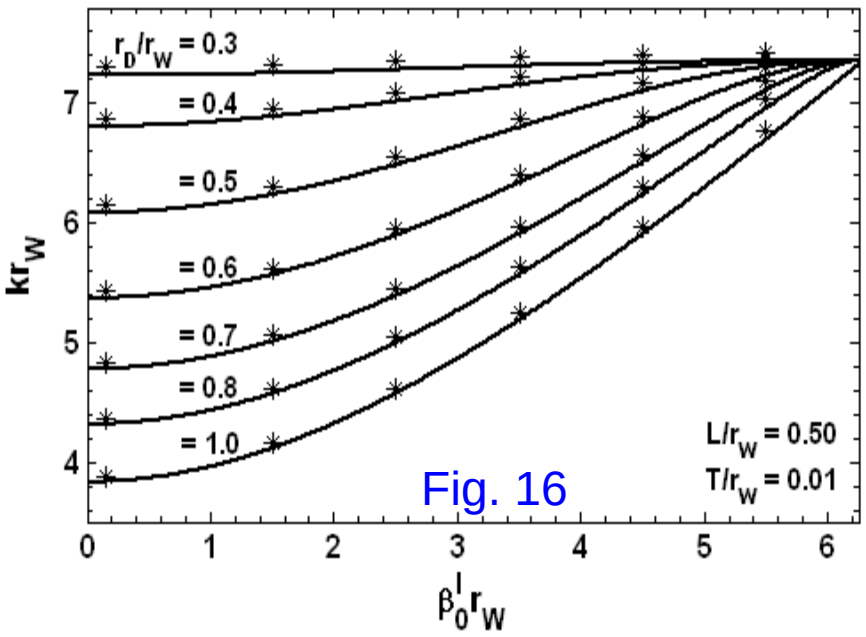

Fig. 16

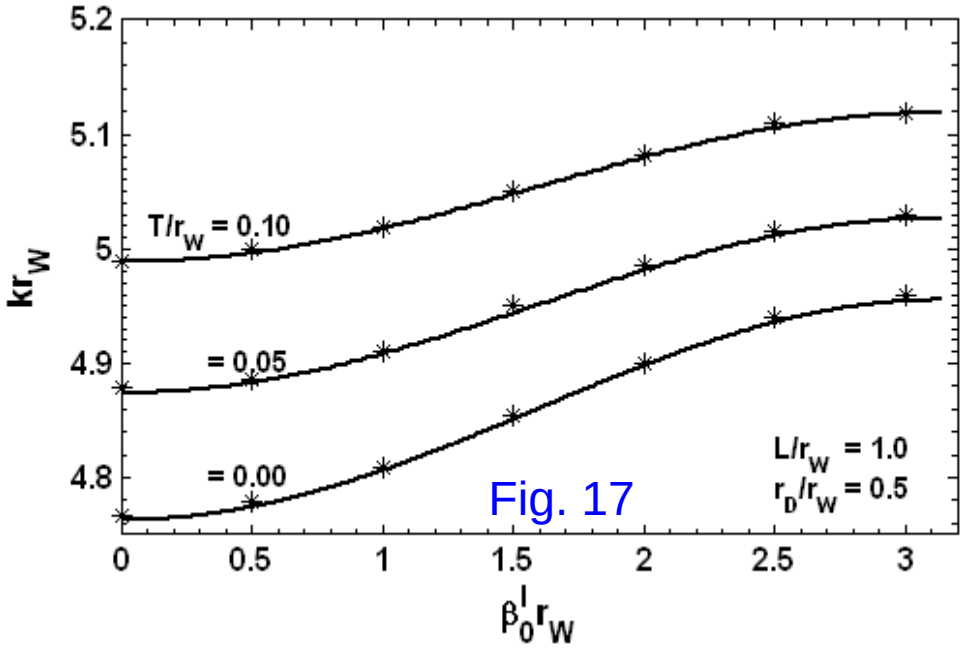

Fig. 17

Dispersion characteristics of a disc-loaded cylindrical waveguide excited in TE_{01} mode (solid curve) validated against those obtained from CST Microwave Studio (asterisk).

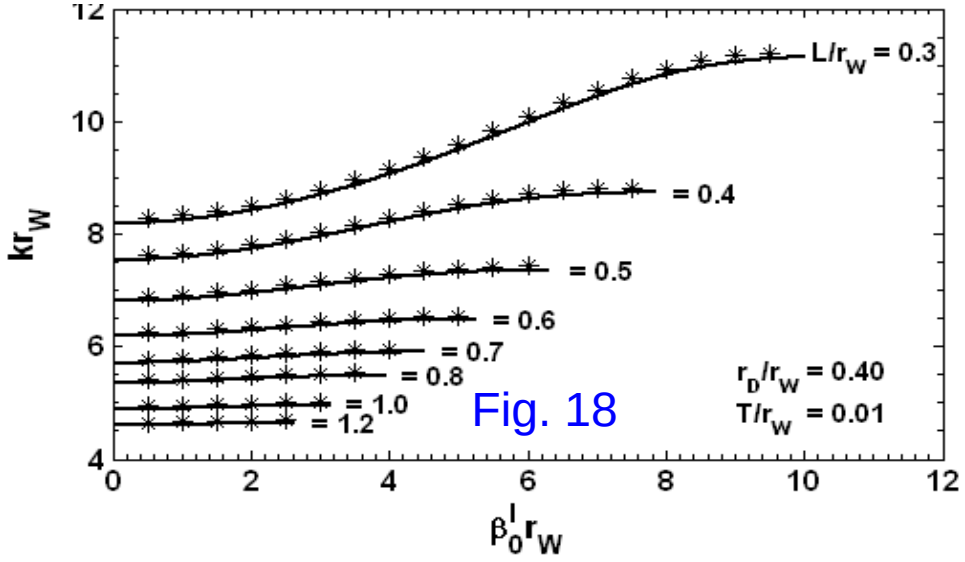

Fig. 18

SUMMARY & CONCLUSION

- **Tapering the structure resulted in large bandwidths.** Increasing the taper angle results in larger bandwidth and Increasing the taper length reduces the cutoff frequency.
- **It has been found that in vane-loaded structure the vane-angle is more effective than the vane-depth and number of vanes in flattening the dispersion curves.**
- **It has been shown that the dispersion characteristic of a disc-loaded structure has characteristics like a band-pass filter. The bandwidth of the gyro-TWT employing such a structure will depend upon the pass-band of the structure which ultimately depends upon the structure parameters.**
- **It has been found that the disc-periodicity is more effective than the disc-hole radius in flattening the dispersion curves.**

References

1. Granatstein, V. L., Parker, R. K., Armstrong, C. M.: Vacuum electronics at the dawn of the twenty-first century. Proc. IEEE 187, 702-716 (1999).
2. Basu, B. N.: Electromagnetic Theory and Applications in Beam-Wave Electronics. World Scientific, Singapore (1996).
3. Kartikeyan, M. V., Borie, E., Thumm, M. K. A.: Gyrotrons High-Power Microwave and Millimeter Wave Technology. Springer, Germany (2004).
4. Sakamoto, K.: Gyrotron and millimeter wave technology. IEEE Trans. Plasma Sc. 34, 635-639 (2006).
5. Thumm, M.: History, Present and Future of Gyrotrons. International Vacuum Electronics Conference (IVEC – 2009), Rome, Italy (2009).
6. Park, G.S., Park, S.Y., Kyser, R.H., Armstrong, C.M., Ganguly, A.K.: Investigation of the Stability of a Tapered Gyro-TWT Amplifier. International Electron Devices Meeting, IEDM'91, Technical Digest, 779-781 (1991).
7. Park, G.S., Park, S.Y., Kyser, R.H., Armstrong, C.M., Ganguly, A.K., Parker, R.K.: Broadband Operation of a Ka-Band Tapered Gyro-Traveling Wave Amplifier. IEEE Tran. Plasma Sci. 22(5), 536-543 (1994).
8. Leou, K.C., McDermott, D.B., Luhmann, N.C.: Dielectric-Loaded Wideband Gyro-TWT. IEEE Trans.Plasma Sci. 20(3), 188-196 (1992).
9. Bratman, V. L., Gross, A. W., Denisov, G. G., He, W., Phelps, A. D. R., Ronald, K., Samsonov, S. V., Whyte, C. G., Young, A. R.: High-gain wide-band gyrotron travelling wave amplifier with a helically corrugated waveguide. Phys. Rev. Lett. 84, 2746-2749 (2000).
10. Choe, J. Y., Uhm, H. S.: Theory of gyrotron amplifiers in disc or helix-loaded waveguides. Int. J. Electronics 53, 729-741 (1982).
11. Cooke, S. J., Denisov, G. G.: Linear theory of wide-band gyro-TWT amplifier using spiral waveguide. IEEE Trans. Plasma Sci. 26, 519-530 (1998).
12. Denisov, G. G., Bratman, V. L., Cross, A. W., He, W., Phelps, A. D. R., Ronald, K., Samsonov, S. V., Whyte, C. G.: Gyrotron travelling wave amplifier with a helical interaction waveguide. Phys. Rev. Lett. 81, 5680-5683 (1998).
13. Uhm H. S., Choe, J. Y.: Theory of gyrotron amplifier in a tape helix loaded waveguide. J. Appl. Phys. 54, 4889-4894 (1983).
14. Takukdar, I., Tripathi, V. K.: Excitation of whistler modes in a sheath-helix loaded waveguide. J. Appl. Phys. 65, 1479-1483 (1989).
15. Yue, L., Wang, W., Gong, Y., Zhang, K.: Analysis of coaxial ridged disk-loaded slow-wave structures for relativistic travelling wave tubes. IEEE Trans. Plasma Sci. 32, 1086-1092 (2004).
16. Zhang, Y., Mo, Y., Zhou, X.: “Rigorous analysis of the disk-loaded waveguide slow-wave structures. Int. J. Infrared and Millimeter Waves 24, 525-535 (2003).
17. Amari, S., Vahldieck, R., Bornemann, J.: Analysis of propagation in periodically loaded circular waveguides. IEE Proc. Microw. Antennas Propag., 146, 50-54 (1999).
18. Rekiouak, A., Cheo, B. R., Wurthman, G., Bates, C.: A slow wave structure for gyro-TWA H_{11} operation. IEEE Trans. Microwave Theory Tech. 42, 1091-1094 (1994).
19. Barroso, J. J., Correa, R. A., Castro, P. J. de: Gyrotron coaxial cylindrical resonators with corrugated inner conductor: Theory and experiment. IEEE Trans. Microwave Theory Tech. 46, 1221-1230 (1998).
20. Zaginaylov, G.I., Iaremenko, S.S.: Efficient Method for Analysis of Coaxial Gyrotron Cavity with Corrugated Inner Insert. Proc. of 41th EUMW, 183-186 (2011).
21. Singh, S., Kartikeyan, M.V.: Analysis of a Triangular Corrugated Coaxial Cavity for Megawatt-Class Gyrotron. IEEE Trans. Electron Devices 62(7), 2333-2338 (2015).
22. Singh, S., Kartikeyan, M.V.: Analysis of Plasma-Loaded Noncorrugated and Triangular Corrugated Coaxial Cavity. IEEE Trans. Electron Devices, 63(10), 4060-4066 (2016).
23. Singh, S., Kartikeyan, M.V.: Full Wave Analysis of Coaxial Gyrotron Cavity with Triangular Corrugations on the Insert. IEEE Trans. Electron Devices 64(4), 1756-1762 (2017).

THANK YOU !

APPENDIX

The organiser of the present faculty development programme on ‘Advances in Microwave Engineering’ was fortunate to have a resource person in Professor P. K. Saha who, however, could not reach the venue due to unforeseen reasons. Professor Saha, nevertheless, sent his encouraging message to the organisers and participants of the programme which we have put at the outset of this compendium.

Professor Saha is a teacher par excellence in the area of microwave engineering. His research contribution in the area of corrugated horn is internationally acclaimed.

The present appendix is a tribute to Professor Saha by his students who themselves are globally renowned for their contribution in the area of microwave engineering.

The editors of the present compendium through this motivating appendix not only salute Professor Saha but also express their appreciation to the cause of microwave engineering—the theme of the present faculty development programme—which Professor Saha served throughout his life.

SAHA in the eyes of Antenna Industry Leaders:

Prepared by Debatosh Guha

ARUN BHATTACHARYYA, IEEE FELLOW
Principal Scientist, Lockheed Martin Space Division, Colorado.
involved in the R&D for Satellite payload systems

Professor P.K. Saha
a pioneer contributor to the development of corrugated horns

Professor Saha

I became familiar with Professor Saha's work on corrugated horns during my graduate studies at IIT, Kharagpur. His name became more relevant to me when I joined Hughes Space and Communications Company and became very involved in designing corrugated horns for shaped Reflector feeds. I was highly motivated by his pioneering work that was published in Proceedings of Institute of Electrical Engineers (IEE), UK, one of the most prestigious journal in the academic world.

Corrugated Horn and Professor Saha

Propagation and radiation behaviour of corrugated feeds
Part 1-Corrugated-waveguide feed

Prof. P. J. B. Clarricoats, D.Sc.(Eng.), F.Inst.P., Fel.I.E.E.E., C.Eng., F.I.E.E., and P. K. Saha, B.Sc, M.Tech., Ph.D.

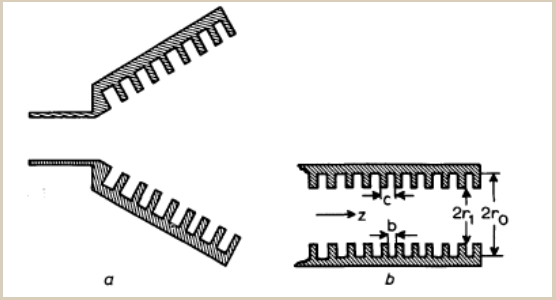

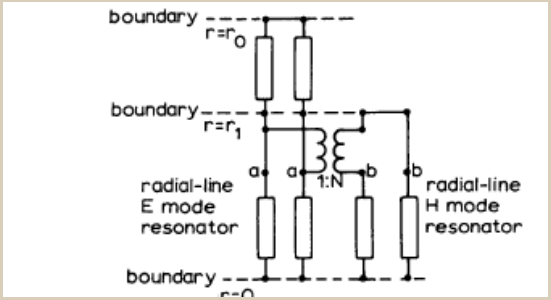

Professor Saha's contributions to corrugated horn design is **outstanding.** His works revealed many interesting properties of corrugated waveguides and horns, which were not known before. In particular, he and his colleague, for the first time, modeled the groove of a corrugated wall as a "parallel resonant circuit" that identify a clear mechanism of the "soft and hard" boundaries that produce symmetrical patterns with negligible cross polarizations. The model **facilitated a proper design direction**, including optimum groove depth to create a balanced hybrid mode, slot-to-tooth ratio, and other important parameters. His treatment of the problem with **high-level mathematics** is very elegant and illuminating for engineers. Today, when most of the design engineers rely on commercial software, Professor Saha's work provides direction for obtaining an initial structure, which is **invaluable** for a fast design process.

My Tribute to Professor Saha

Professor Saha's works enable the modern communication industry to develop high quality antenna systems. In a reflector system, wide-band high level cross-polar isolation is impossible without a corrugated horn feed. For today's satellite industry, the corrugated horn is the primary feed component for a reflector system. Although corrugated horns have evolved over the past several decades, the basic principle of operation that Professor Saha elegantly illustrated in his publications is highly valued by the antenna community.

I humbly offer my sincere gratitude for the lessons I learned from his works. On his 75th birth year, I wish Professor Saha a long, healthy, and peaceful life for the years to come.

Sudhakar Rao, IEEE Fellow

Technical Fellow, Northrop Grumman Aerospace Systems, California
Formerly, Corporate Fellow and Chief Scientist at
Lockheed Martin, Boeing Satellite Systems, and Spar Aerospace Limited

Prof Saha was the "brain" behind the famous work

Thanks Debatosh for asking me to write a message on 75th birth year of Prof. Saha. I am very honored and here it is:

"Prof. P.K. Saha is the first to provide detailed hybrid-mode analysis of corrugated horns through two original papers published in the Proceedings of the IEEE. These papers were written when he was at Queen Mary College, London and were co-authored with Prof. Clarricoats.

Prof. Clarricoats visited University of Trondheim, Norway in 1981 where I was doing my post-doctoral research and privately told me that Prof Saha was the "brain" behind the famous work. Prof Saha's work was original and millions of corrugated horns are used as feeds for ground-station reflector antennas and satellite antennas because of wide bandwidth, low cross-polar radiation, and circularly symmetric radiation patterns.

I personally consider Prof. Saha as an outstanding researcher with strong analytical background and feel sometimes that he did not get the recognition that he deserved for his outstanding contributions in the field of antennas and electromagnetics. Although I never met Prof Saha personally, he was and still is an inspiration to me and several of my colleagues”

"May you live life to the fullest is what I wish wholeheartedly and happy 75th birthday!"

Sudhakar

Recognition